BEILSTEIN JOURNAL OF ORGANIC CHEMISTRY

Natural products in synthesis and biosynthesis

Edited by Jeroen S. Dickschat

Generated on 03 November 2026, 13:41

Imprint

Beilstein Journal of Organic Chemistry
www.bjoc.org
ISSN 1860-5397
Email: journals-support@beilstein-institut.de

The *Beilstein Journal of Organic Chemistry* is published by the Beilstein-Institut zur Förderung der Chemischen Wissenschaften.

Beilstein-Institut zur Förderung der Chemischen Wissenschaften
Trakehner Straße 7–9
60487 Frankfurt am Main
Germany
www.beilstein-institut.de

The copyright to this document as a whole, which is published in the *Beilstein Journal of Organic Chemistry*, is held by the Beilstein-Institut zur Förderung der Chemischen Wissenschaften. The copyright to the individual articles in this document is held by the respective authors, subject to a Creative Commons Attribution license.

Beilstein Journal of Organic Chemistry

Natural products in synthesis and biosynthesis

Jeroen S. Dickschat

Editorial

Open Access

Address:
Institut für Organische Chemie, Technische Universität Carolo-Wilhelmina zu Braunschweig, Hagenring 30, D-38106 Braunschweig, Germany

Email:
Jeroen S. Dickschat - j.dickschat@tu-bs.de

Keywords:
natural products

Beilstein J. Org. Chem. **2013,** *9,* 1897–1898.
doi:10.3762/bjoc.9.223

Received: 04 September 2013
Accepted: 11 September 2013
Published: 19 September 2013

This article is part of the Thematic Series "Natural products in synthesis and biosynthesis".

Guest Editor: J. S. Dickschat

© 2013 Dickschat; licensee Beilstein-Institut.
License and terms: see end of document.

This is the second Thematic Series in the Beilstein Journal of Organic Chemistry focused on natural products. While the first Thematic Series summarized recent research work on the biosynthesis and function of natural products [1,2], the present Thematic Series deals with synthetic and biosynthetic aspects.

Why the research interest in natural products? Natural products are structurally fascinating as is spectacularly demonstrated by the prominent examples of maitotoxin [3], the largest non-polymer secondary metabolite known to date, or calicheamycin (Figure 1), which possibly holds the record in carrying the most diverse functional groups including an enediyne subunit, a deoxysugar, an aminosugar, a hydroxylamine linkage between two sugar subunits, a carbamate, an aromatic iodide, a thioester, and a trisulfide [4]. Natural products have also been used by humankind since ancient times and are part of our traditions and culture, as is evident from the widespread consumption of coffee, tea, tobacco and cocoa, drugs that all contain alkaloids with stimulating effects. More importantly, starting from their usage in traditional medicine natural products – and today also compounds inspired by natural products – are indispensable in the treatment of various threatening infectious diseases. The

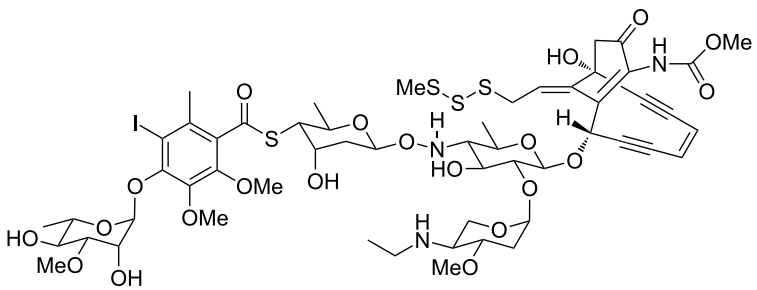


Figure 1: Calicheamycin.

rapid spreading of antibiotic resistances and the comeback of some infectious diseases already claimed to be eliminated should sharpen our minds for the beneficial roles of natural products in medicine as well as their responsible use. This should be a strong appeal upon the responsibility of both researchers and decision makers in the academic sciences and the pharmaceutical industry.

Why should we have a look at the synthetic and biosynthetic aspects of natural products in this Thematic Series? Of course, the chemistry of nature and as it is used by chemists is one and the same and makes use of the same intrinsic reactivity of molecules. It is fascinating to see that a particular chemical reaction, believed to be invented by man, is in fact already used for millions – sometimes even billions – of years by Mother Nature. An interesting example is the discovery of the Diels–Alder reaction in the 1920s and its later enhancement into an enantioselective reaction by the development of chiral catalysts. But a Diels–Alder reaction also occurs in the biosynthesis of lovastatin and is likely catalysed by a Diels–Alderase [5], a natural analogue of man-made chiral catalysts! Beyond such fascinating examples of comparing natural to artificial systems it is their interplay that may provide the best solutions to some of the most urgent problems of our time. A perfect example is artemisinin, a terpenoid natural product from *Artemisia annua*, which is highly efficient in the treatment of malaria. The problem is that the plant produces only small and variable amounts, thereby making the isolation procedure difficult and expensive. Neither biotechnology nor chemistry were able to provide a solution on their own, but the combination of the heterologous production of an advanced intermediate in yeast [6] and its further elaboration by chemical synthesis [7] procures sufficient quantities of artemisinin at a reasonable price. An impressive demonstration of the effectiveness of multi-disciplinary research.

I would like to thank the highly professional team of the Beilstein-Institut for a very pleasant cooperation on this Thematic Series. I wish you, the reader, joy and fun with this Thematic Series and – at the best – a new impetus for your own future research!

Jeroen S. Dickschat

Braunschweig, September 2013

References

1. Dickschat, J. S. *Beilstein J. Org. Chem.* **2011,** *7,* 1620–1621. doi:10.3762/bjoc.7.190
2. Biosynthesis and function of secondary metabolites. http://www.beilstein-journals.org/bjoc/browse/singleSeries.htm?sn=20 (accessed Sept 12, 2013).
3. Nicolaou, K. C.; Frederick, M. O. *Angew. Chem., Int. Ed.* **2007,** *46,* 5278–5282. doi:10.1002/anie.200604656
4. Maiese, W. M.; Lechevalier, M. P.; Lechevalier, H. A.; Korshalla, J.; Kuck, N.; Fantini, A.; Wildey, M. J.; Thomas, J.; Greenstein, M. *J. Antibiot.* **1989,** *42,* 558–563. doi:10.7164/antibiotics.42.558
5. Campbell, C. D.; Vederas, J. C. *Biopolymers* **2010,** *93,* 755–763. doi:10.1002/bip.21428
6. Ro, D.-K.; Paradise, E. M.; Ouellet, M.; Fisher, K. J.; Newman, K. L.; Ndungu, J. M.; Ho, K. A.; Eachus, R. A.; Ham, T. S.; Kirby, J.; Chang, M. C. Y.; Withers, S. T.; Shiba, Y.; Sarpong, R.; Keasling, J. D. *Nature* **2006,** *440,* 940–943. doi:10.1038/nature04640
7. Lévesque, F.; Seeberger, P. H. *Angew. Chem., Int. Ed.* **2012,** *51,* 1706–1709. doi:10.1002/anie.201107446

License and Terms

This is an Open Access article under the terms of the Creative Commons Attribution License (http://creativecommons.org/licenses/by/2.0), which permits unrestricted use, distribution, and reproduction in any medium, provided the original work is properly cited.

The license is subject to the *Beilstein Journal of Organic Chemistry* terms and conditions: (http://www.beilstein-journals.org/bjoc)

The definitive version of this article is the electronic one which can be found at: doi:10.3762/bjoc.9.223

Beilstein Journal of Organic Chemistry

Total synthesis of ochnaflavone

Monica M. Ndoile and Fanie R. van Heerden*

Full Research Paper

Open Access

Address:
School of Chemistry and Physics, University of KwaZulu-Natal, Private Bag X01, Scottsville 3209, Pietermaritzburg, South Africa

Email:
Fanie R. van Heerden* - vanheerdenf@ukzn.ac.za

* Corresponding author

Keywords:
biflavone; diaryl ether; natural products; nucleophilic aromatic substitution; ochnaflavone; tetrahydroochnaflavone

Beilstein J. Org. Chem. **2013,** *9,* 1346–1351.
doi:10.3762/bjoc.9.152

Received: 22 April 2013
Accepted: 18 June 2013
Published: 08 July 2013

This article is part of the Thematic Series "Natural products in synthesis and biosynthesis".

Guest Editor: J. S. Dickschat

© 2013 Ndoile and van Heerden; licensee Beilstein-Institut.
License and terms: see end of document.

Abstract

The first total syntheses of ochnaflavone, an asymmetric biflavone consisting of apigenin and luteolin moieties, and the permethyl ether of 2,3,2",3"-tetrahydroochnaflavone have been achieved. The key steps in the synthesis of ochnaflavone were the formation of a diaryl ether and ring cyclization of an ether-linked dimeric chalcone to assemble the two flavone nuclei. Optimal experimental conditions for the oxidative cyclization to form ochnaflavone were established.

Introduction

Biflavonoids are a class of compounds that are receiving increasing attention because of their biological activity. Biflavonoids with anti-inflammatory [1-3], antileishmanial [4,5], antiplasmodial [6-8], antiviral [9] and β-secretase inhibitory [10] activity, amongst others, have been reported. The activity of the biflavonoids is in general much higher than that of the individual monomers [11]. The flavonoid units in these compounds are joined in a symmetric or asymmetric manner and can either be identical or nonidentical. In addition, the two flavonoid units can be linked through a C–C bond or C–O–C bond. Many biflavonoids consist of an interflavonoid linkage between ring B of one moiety and the ring A of the other moiety (AB type), between two A rings (AA type) or between the two C rings (3,3"-CC type), but the most rare biflavonoids are the ones with the interflavonoid linkage between the two B rings.

Ochnaflavone (**1**) (Figure 1) is a biflavone with an ether linkage between the B-rings of the apigenin and luteolin subunits [12], which has been isolated from several members of the

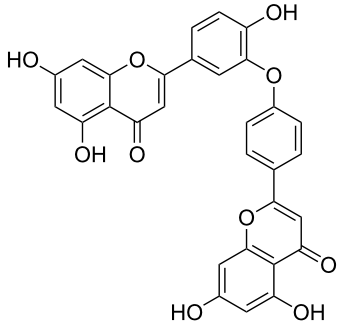


Figure 1: Structure of ochnaflavone (**1**).

Ochnaceae, a plant family that is rich in biflavonoids [13]. It is considered as the taxonomic marker for the genus *Ochna* [13]. A wide range of activities have been reported for **1**, amongst them prominent anticancer [14,15], anti-inflammatory and atherogenic activity [16,17]. The activity associated with **1** prompted us to develop an efficient synthesis of this compound.

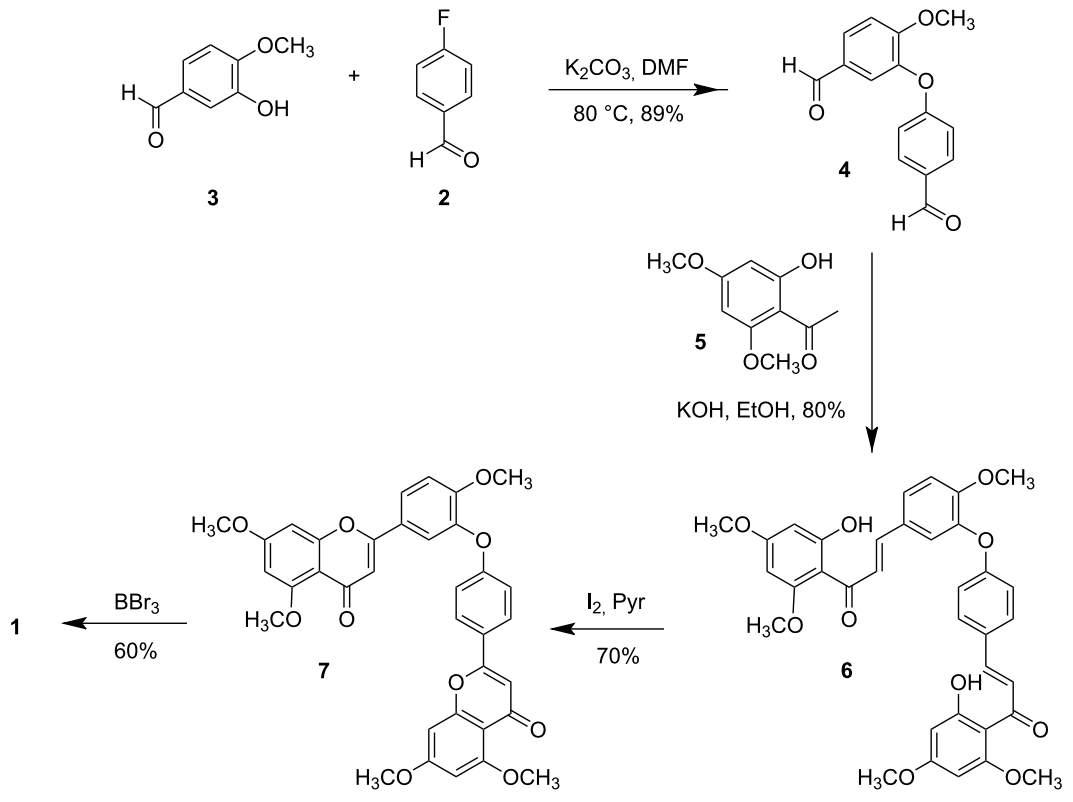
The only previous synthesis of a derivative of **1** was by Okigawa et al. [12,18]. The group synthesized the pentamethyl ether of biflavone **1** by using the Baker–Vankataraman rearrangement as the key step. The conditions used in this reaction sequence were fairly harsh, moderate yields were obtained and the authors did not synthesize the desired product, ochnaflavone (**1**). In this paper we report the synthesis of **1** with aromatic nucleophilic substitution and chalcone formation as the key steps.

Results and Discussion

Our synthesis of **1** is summarized in Scheme 1. The two most important steps in the synthesis of **1** are the formation of the diaryl ether linkage and the assembly of the flavone nuclei. The most logical approach to the synthesis of **1** would be to start with the preparation of a diaryl ether. This functionality is present in many important bioactive natural compounds [19] and it is not surprising that a great amount of effort has been focused on the development and improvement of the methods to form diaryl ethers [20,21]. The Ullman reaction is often used to prepare diaryl ethers, but this reaction has the disadvantages of high reaction temperatures and intolerance to a wide variety of functional groups, with the major weakness being the inconsistency in the products obtained by the use of different copper sources [22-24]. We have opted to prepare the diaryl ether by using an aromatic nucleophilic substitution reaction. 4-Fluorobenzaldehyde (**2**) is a readily available starting material, and under basic conditions it reacted with isovanillin (**3**) to form the diaryl ether **4** in a high yield.

The next step was the formation of the chalcone by an aldol condensation reaction with a suitably substituted acetophenone. Selective methylation of 2,4,6-trihydroxyacetophenone with methyl iodide yielded 2'-hydroxy-4',6'-dimethoxyacetophenone (**5**) in moderate yield. The Claisen–Schmidt condensation of **5** with diaryl ether **4** under basic conditions (KOH) in EtOH proceeded smoothly to furnish dimeric chalcone **6**, which was obtained as a yellow powder.

The cyclization of **6** into the corresponding biflavone **7** was initially attempted by using a catalytic amount of iodine in



Scheme 1: Synthesis of ochnaflavone (**1**).

DMSO at 130–140 °C, conditions often used for the oxidative cyclization of chalcones to flavones [25]. However, at this temperature, the reaction resulted in decomposition of the starting material. The reaction was repeated under microwave conditions as described by Menezes et al. [26] to decrease the time in which **6** was exposed to a high temperature, but decomposition was still observed. The reaction was repeated under same conditions ($DMSO/I_2$) at various temperatures, and it was observed that at lower temperatures, a longer time was taken for the starting material to be consumed, but it still resulted in a mixture of products. The cyclization reaction was repeated with DDQ in dry dioxane under reflux (101 °C) [27], but the starting material again decomposed, and when the temperature was lowered to 80 °C, a mixture of products was observed. It was clear that the ether-linked dimeric chalcone decomposes at temperatures exceeding 100 °C. Reaction of dimeric chalcone **6** with oxalic acid as a catalyst in absolute ethanol at 80 °C for 24 h as described by Zambare et al. [28] did not yield the desired compound **7** and instead an ether-linked pentamethoxybiflavanone **8** was obtained. After 72 h, the starting material could still be observed on TLC due to the interconvertibility of the two compounds through chalcone–flavanone equilibrium [29,30] (Scheme 2). Biflavanone **8** is the permethyl ether of 2,3,2",3"-tetrahydroochnaflavone, a natural product isolated from the New Zealand tree *Quintinia acutifolia*, which is cytotoxic against P388 murine lymphocytic leukemia cells [31]. The synthesis of this compound has not been reported previously.

The desired biflavone **7** was finally obtained in good yield by treating the dimeric chalcone with a catalytic amount of iodine in pyridine. Ochnaflavone (**1**) was obtained as a yellow solid by the reaction of **7** with boron tribromide in dry CH_2Cl_2 and had the same spectroscopic properties as the product isolated in our laboratory from the leaves of *Ochna serrulata*.

Conclusion

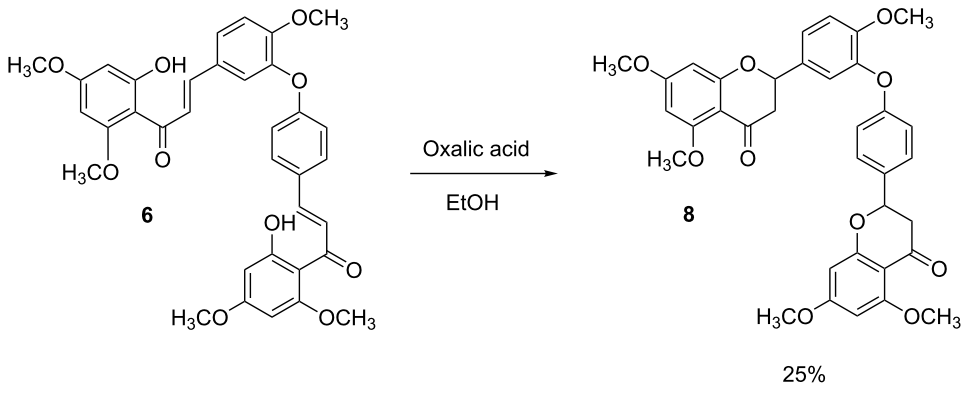
In conclusion, we have managed to optimize conditions for the preparation of ochnaflavone (**1**) in a synthetic sequence that is amenable to the synthesis of derivatives of **1**. The synthesis of the pentamethyl ether of a natural-occurring cytotoxic 2,3,2",3"-tetrahydroochnaflavone was also achieved, albeit in a low yield.

Experimental

3-(4-Formylphenyloxy)-4-methoxybenzaldehyde (4) [32]**:** To a mixture of isovanillin (**3**) (500 mg, 3.29 mmol) and anhydrous potassium carbonate (681 mg, 4.93 mmol) in 15 mL dry DMF under nitrogen, 4-fluorobenzaldehyde (**2**) (448 mg, 3.61 mmol) was added. The mixture was heated at 80 °C under stirring until all the starting material had been consumed (monitored by TLC). The reaction was then left to cool to room temperature, 20 mL cold water was added, and the mixture was extracted with 3 × 20 mL $CHCl_3$. The organic layer was dried over anhydrous magnesium sulfate, and the solvent was removed in vacuo. The residue obtained was purified by silica-gel column chromatography (EtOAc/hexanes, 3:7) as eluent to yield 748 mg (89%) of **4** as a light yellow solid.

^{1}H NMR (400 MHz, $CDCl_3$) δ_H 9.94 (s, 1H), 9.93 (s, 1H), 7.89 (d, J = 8.8 Hz, 2H), 7.89 (dd, J = 8.5, 2.0 Hz, 1H), 7.69 (d, J = 2.0 Hz, 1H), 7.38 (d, J = 8.5 Hz, 1H), 7.06 (d, J = 8.8 Hz, 2H), 3.91 (s, 3H); ^{13}C NMR (100 MHz, $CDCl_3$) δ_C 190.6, 190.0, 162.6 (2C), 156.9, 143.4, 131.9 (2C), 130.9, 129.5, 122.3, 116.3 (2C), 113.4, 55.9; HRMS–ESI (positive-ionization mode): m/z 279.0625 $[M + Na]^+$ (calculated for $C_{15}H_{12}O_4Na$, 279.0633).

2'-Hydroxy-4',6'-dimethoxyacetophenone (5) [33]**:** To a well-stirred mixture of 2',4',6'-trihydroxyacetophenone (500 mg, 2.97 mmol) and methyl iodide (1.06 g, 7.47 mmol) in 20 mL acetone, 1.02 g (7.38 mmol) of anhydrous potassium carbonate



Scheme 2: Oxalic acid-induced ring closure of bichalcone **6**.

was added. The reaction mixture was heated under reflux for 5 h while being monitored by TLC until all the starting material had been consumed. The reaction mixture was left to cool and 40 mL of cold acidified distilled water was added, followed by extraction with 3 × 20 mL $CHCl_3$. The obtained organic layer was dried over anhydrous magnesium sulfate, and the solvent was removed in vacuo. The residue was purified by silica gel column chromatography (EtOAc/hexanes, 1:9) to afford **5** (291 mg, 50%) as a white solid.

^{1}H NMR (400 MHz, $CDCl_3$) δ_H 13.99 (s, 1H), 6.02 (d, J = 2.1 Hz, 1H), 5.89 (d, J = 2.1 Hz, 1H), 3.83 (s, 3H), 3.79 (s, 3H), 2.58 (s, 3H); ^{13}C NMR (100 MHz, $CDCl_3$) δ_C 203.1, 167.5, 166.1, 162.9, 105.9, 93.5, 90.6, 55.5 (2C), 32.9; HRMS–ESI (negative-ionization mode): m/z 195.0662 (calculated for $C_{10}H_{11}O_4$, 195.0657).

Synthesis of ether-linked dimeric chalcone 6: To a solution of 404 mg (1.58 mmol) of diaryl ether **4** in EtOH (50 mL), 620 mg (3.16 mmol) of 2'-hydroxy-4',6'-dimethoxyacetophenone (**5**) was added. The solution was cooled in an ice bath followed by the addition of powdered KOH (353 mg, 6.29 mmol). After overnight stirring, the reaction mixture was diluted with ice-cold water (50 mL) and acidified with 6 M HCl. The formed **6** precipitated out as a yellow solid and was filtered off under reduced pressure and washed with water. Product **6** (772 mg, 80%) was obtained as a yellow solid.

^{1}H NMR (400 MHz, $CDCl_3$) δ_H 14.34 (s, 1H), 14.31 (s, 1H), 7.85 (d, J = 15.7 Hz, 1H), 7.79 (d, J = 15.7 Hz, 1H), 7.73 (s, 2H), 7.59 (d, J = 8.5 Hz, 2H), 7.42 (dd, J = 8.2, 2.0 Hz, 1H), 7.33 (d, J = 2.0 Hz, 1H), 7.05 (d, J = 8.2 Hz, 1H), 7.0 (d, J = 8.5 Hz, 2H), 6.12 (d, J = 2.2 Hz, 1H), 6.10 (J = 2.2 Hz, 1H), 5.97 (d, J = 2.2 Hz, 1H), 5.94 (d, J = 2.2 Hz, 1H), 3.9 (s, 3H), 3.89 (s, 3H), 3.85 (s, 3H), 3.83 (s, 6H); ^{13}C NMR (100 MHz, $CDCl_3$) δ_C 192.5, 192.3, 168.4 (2C), 166.2 (2C), 162.5 (2C), 159.4, 153.1, 144.6, 141.8, 141.4, 130.3, 130.0 (2C), 129.2, 126.9, 126.2 (2C), 120.2, 117.4 (2C), 112.9, 106.4, 106.3, 93.9 (2C), 91.3, 91.2, 56.1, 55.8, 55.6 (2C); HRMS–ESI (positive-ionization mode), m/z 635.1888 $[M + Na]^+$ (calculated for $C_{35}H_{32}O_{10}Na$, 635.1893).

Pentamethoxybiflavanone 8: To a mixture of oxalic acid (10 mol %) and **6** (400 mg, 0.65 mmol), 20 mL of absolute ethanol was added. The stirred reaction mixture was heated at 80 °C for 72 h while the reaction was monitored by TLC. The reaction mixture was then cooled to room temperature, and the solvent was evaporated under reduced pressure. This was followed by extraction with 50 mL of water and 3 × 30 mL CH_2Cl_2, and the organic layer thus collected was dried over anhydrous magnesium sulfate. CH_2Cl_2 was removed in vacuo and the resulting residue was purified by silica-gel column chromatography with EtOAc/hexanes (1:1) to afford 100 mg (25%) of the ether-linked biflavanone **8** as a light-yellow solid.

^{1}H NMR (400 MHz, $CDCl_3$) δ_H 7.40 (d, J = 8.5 Hz, 2H), 7.26 (dd, J = 8.5, 2.0 Hz, 1H), 7.16 (d, J = 2.0 Hz, 1H), 7.06 (d, J = 8.5 Hz, 1H), 6.99 (d, J = 8.5 Hz, 2H), 6.16 (d, J = 2.2 Hz, 1H), 6.14 (d, J = 2.0 Hz, 1H), 6.10 (d, J = 2.0 Hz, 2H), 5.37 (m, 2H), 3.9 (s, 6H), 3.87 (s, 3H), 3.83 (s, 6H), 3.02 (m, 2H), 2.8 (m, 2H); HRMS–ESI (positive-ionization mode), m/z 635.1887 $[M + Na]^+$ (calculated for $C_{35}H_{32}O_{10}Na$, 635.1893).

5,5'',7,7'',4'-Penta-*O*-methylochnaflavone (7) [12]**:** To a stirred solution of dimeric chalcone **6** (600 mg, 0.98 mmol) in 15 mL pyridine, 498 mg (1.93 mmol) of iodine was added and the mixture was heated to 80 °C while being stirred for 24 h. The reaction was left to cool to room temperature, and a cold solution of sodium thiosulfate was added to the reaction mixture until all excess iodine had been consumed. This was followed by extraction with 3 × 30 mL CH_2Cl_2, the obtained organic layer was washed with 30 mL of water and dried over anhydrous magnesium sulfate. The solvent was removed in vacuo and the crude reaction mixture was purified by silica-gel column chromatography with EtOAc/hexanes (8:2) to obtain **7** (417 mg, 70%) as a yellow solid.

^{1}H NMR (400 MHz, $CDCl_3$) δ_H 7.82 (d, J = 8.8 Hz, 2H), 7.73 (dd, J = 8.7, 2.3 Hz, 1H), 7.61 (d, J = 2.3 Hz, 1H), 7.12 (d, J = 8.7 Hz, 1H), 7.02 (d, J = 8.8 Hz, 2H), 6.54 (d, J = 2.2 Hz, 1H), 6.51 (d, J = 2.4 Hz, 1H), 6.36 (d, J = 2.2 Hz, 1H), 6.35 (d, J = 2.4 Hz, 1H), 6.59 (s, 1H), 6.55 (s, 1H), 3.94 (s, 3H), 3.93 (s, 3H), 3.89 (s, 3H), 3.88 (s, 3H), 3.87 (s, 3H); ^{13}C NMR (100 MHz, $CDCl_3$) δ_C 177.5, 177.4, 164.0, 164.0, 160.9, 160.3, 160.3, 159.8, 159.7, 159.6, 154.0, 143.8, 127.7, 125.8, 124.7, 124.0, 119.8, 116.6, 113.0, 109.2, 109.1, 108.2, 96.2, 96.1, 92.8, 56.4, 56.1, 55.7; HRMS–ESI (positive-ionization mode), m/z 631.1573 $[M + Na]^+$ (calculated for $C_{35}H_{28}O_{10}Na$, 631.1580).

Ochnaflavone (1) [12]**:** A solution of boron tribromide (206 mg, 0.82 mmol) in 5 mL dry CH_2Cl_2 was slowly added with a syringe to a stirred solution of 40 mg (0.07 mmol) **7** in 10 mL CH_2Cl_2 under nitrogen. After complete addition of BBr_3, the reaction mixture was stirred at room temperature for 72 h, and then poured into 30 mL ice water. The mixture was then shaken to hydrolyse the excess BBr_3 and boron complexes; a phenolic product was obtained by extraction with 3 × 20 mL EtOAc. The combined organic layers was dried over anhydrous magnesium sulfate and the solvent was removed in vacuo to obtain a dry crude reaction mixture. Purification of the reaction mixture by silica-gel column chromatography with

MeOH/$CHCl_3$ (1:9) afforded 21.2 mg (60%) of **1** as a yellow solid.

^{1}H NMR (400 MHz, $(CD_3)_2CO$) δ_H 12.95 (s, 1H), 12.94 (s, 1H), 8.08 (d, J = 8.9 Hz, 2H), 7.90 (dd, J = 8.5, 2.1 Hz, 1H), 7.89 (d, J = 2.1 Hz, 1H), 7.29 (d, J = 8.5 Hz, 1H), 7.16 (d, J = 8.9 Hz, 2H), 6.73 (s, 2H), 6.56 (d, J = 2.0 Hz, 1H), 6.55 (d, J = 2.4 Hz, 1H), 6.28 (d, J = 2.0 Hz, 1H), 6.27 (d, J = 2.0 Hz, 1H); ^{13}C NMR (100 MHz, $(CD_3)_2CO$) δ_C 182.2, 182.2, 164.2, 164.18, 163.5, 163.1, 162.5, 161.1, 157.9 (2C), 154.1, 142.4, 128.3 (2C), 125.4, 123.6, 120.7, 118.1, 116.6 (2C), 104.3, 104.52, 104.5, 104.0, 98.9 (2C), 93.9 (2C); HRMS–ESI (negative ionization mode): m/z 537.0826 (calculated for $C_{30}H_{17}O_{10}$, 537.0822).

Acknowledgements

Financial support from the University of Dar es Salaam (CoNAS)-World Bank project, University of KwaZulu-Natal and National Research Foundation (South Africa) is acknowledged.

References

1. Lee, E.-J.; Shin, S.-Y.; Kim, J.-K.; Woo, E.-R.; Kim, Y.-M. *Bull. Korean Chem. Soc.* **2012,** *33,* 2878–2882. doi:10.5012/bkcs.2012.33.9.2878
2. Che, H.; Park, B. K.; Lim, H.; Kim, H. P.; Chang, H. W.; Jeong, J.-H.; Park, H. *Bioorg. Med. Chem. Lett.* **2009,** *19,* 74–76. doi:10.1016/j.bmcl.2008.11.017
3. Ye, Y.; Guo, Y.; Luo, Y.-T. *Int. J. Mol. Sci.* **2012,** *13,* 12401–12411. doi:10.3390/ijms131012401
4. Wong, I. L. K.; Chan, K.-F.; Chan, T. H.; Chow, L. M. C. *J. Med. Chem.* **2012,** *55,* 8891–8902. doi:10.1021/jm301172v
5. Gontijo, V. S.; Judice, W. A. S.; Codonho, B.; Pereira, I. O.; Assis, D. M.; Januário, J. P.; Caroselli, E. E.; Juliano, M. A.; Dosatti, A. d. C.; Marques, M. J.; Viegas Junior, C.; dos Santos, M. H. *Eur. J. Med. Chem.* **2012,** *58,* 613–623. doi:10.1016/j.ejmech.2012.06.021
6. Dhooghe, L.; Maregesi, S.; Mincheva, I.; Ferreira, D.; Marais, J. P. J.; Lemière, F.; Matheeussen, A.; Cos, P.; Maes, L.; Vlietinck, A.; Apers, S.; Pieters, L. *Phytochemistry* **2010,** *71,* 785–791. doi:10.1016/j.phytochem.2010.02.005
7. Chukwujekwu, J. C.; de Kock, C. A.; Smith, P. J.; van Heerden, F. R.; van Staden, J. *Planta Med.* **2012,** *78,* 1857–1860. doi:10.1055/s-0032-1315386
8. Kunert, O.; Swamy, R. C.; Kaiser, M.; Presser, A.; Buzzi, S.; Appa Rao, A. V. N.; Schühly, W. *Phytochem. Lett.* **2008,** *1,* 171–174. doi:10.1016/j.phytol.2008.09.003
9. Reutrakul, V.; Ningnuek, N.; Pohmakotr, M.; Yoosook, C.; Napaswad, C.; Kasisit, J.; Santisuk, T.; Tuchinda, P. *Planta Med.* **2007,** *73,* 683–688. doi:10.1055/s-2007-981538
10. Sasaki, H.; Kitoh, Y.; Miki, K.; Kinoshita, K.; Koyama, K.; Kaneda, M.; Takahashi, K. *Heterocycles* **2012,** *85,* 2749–2756. doi:10.3987/COM-12-12561
11. Thapa, A.; Woo, E.-R.; Chi, E. Y.; Sharoar, Md. G.; Jin, H.-G.; Shin, S. Y.; Park, I.-S. *Biochemistry* **2011,** *50,* 2445–2455. doi:10.1021/bi101731d
12. Okigawa, M.; Kawano, N.; Aqil, M.; Rahman, W. *Tetrahedron Lett.* **1973,** *14,* 2003–2006. doi:10.1016/S0040-4039(01)96104-0
13. Bandi, A. K. R.; Lee, D.-U.; Tih, R. G.; Gunasekar, D.; Bodo, B. *Chem. Biodiversity* **2012,** *9,* 251–271. doi:10.1002/cbdv.201100164
14. Lee, S. J.; Choi, J. H.; Son, K. H.; Chang, H. W.; Kang, S. S.; Kim, H. P. *Life Sci.* **1995,** *57,* 551–558. doi:10.1016/0024-3205(95)00305-P
15. Kang, Y.-J.; Min, H.-Y.; Hong, J.-Y.; Kim, Y.-S.; Kang, S.-S.; Lee, S.-K. *Biomol. Ther.* **2009,** *17,* 282–287. doi:10.4062/biomolther.2009.17.3.282
16. Son, M. J.; Moon, T. C.; Lee, E. K.; Son, K. H.; Kim, H. P.; Kang, S. S.; Son, J. K.; Lee, S. H.; Chang, H. W. *Arch. Pharmacal Res.* **2006,** *29,* 282–286. doi:10.1007/BF02968571
17. Lee, J.-H. *Arch. Pharmacal Res.* **2011,** *34,* 1209–1217. doi:10.1007/s12272-011-0720-0
18. Okigawa, M.; Kawano, N.; Aqil, M.; Rahman, W. *J. Chem. Soc., Perkin Trans. 1* **1976,** 580–583. doi:10.1039/P19760000580
19. Bedos-Belval, F.; Rouch, A.; Vanucci-Bacqué, C.; Baltas, M. *MedChemComm* **2012,** *3,* 1356–1372. doi:10.1039/c2md20199b
20. Pitsinos, E. N.; Vidali, V. P.; Couladouros, E. A. *Eur. J. Org. Chem.* **2011,** 1207–1222. doi:10.1002/ejoc.201001520
21. Frlan, R.; Kikelj, D. *Synthesis* **2006,** 2271–2285. doi:10.1055/s-2006-942440
22. Zhu, J.; Price, B. A.; Zhao, S. X.; Skonezny, P. M. *Tetrahedron Lett.* **2000,** *41,* 4011–4014. doi:10.1016/S0040-4039(00)00548-7
23. Peeters, L. D.; Jacobs, S. G.; Eevers, W.; Geise, H. J. *Tetrahedron Lett.* **1994,** *50,* 11533–11540. doi:10.1016/S0040-4020(01)89290-5
24. Capdevielle, P.; Maumy, M. *Tetrahedron Lett.* **1993,** *34,* 1007–1010. doi:10.1016/S0040-4039(00)77477-6
25. Chavan, H. V.; Bandgar, B. P.; Adsul, L. K.; Dhakane, V. D.; Bhale, P. S.; Thakare, V. N.; Masand, V. *Bioorg. Med. Chem. Lett.* **2013,** *23,* 1315–1321. doi:10.1016/j.bmcl.2012.12.094
26. Menezes, M. J.; Manjrekar, S.; Pai, V.; Patre, R. E.; Tilve, S. G. *Indian J. Chem.* **2009,** *48B,* 1311–1314.
27. Lmafuku, K.; Honda, M.; Mcomie, J. F. w. *Synthesis* **1987,** *2,* 199–201. doi:10.1055/s-1987-27891
28. Zambare, A. S.; Sangshetti, J. N.; Kokare, N. D.; Shinde, D. B. *Chin. Chem. Lett.* **2009,** *20,* 171–174. doi:10.1016/j.cclet.2008.10.042
29. González, E. A.; Nazareno, M. A.; Borsarelli, C. D. *J. Chem. Soc., Perkin Trans. 2* **2002,** 2052–2056. doi:10.1039/B207663B
30. Cisak, A.; Mielczarek, C. *J. Chem. Soc., Perkin Trans. 2* **1992,** 1603–1607. doi:10.1039/p29920001603
31. Ariyasena, J.; Baek, S.-H.; Perry, N. B.; Weavers, R. T. *J. Nat. Prod.* **2004,** *67,* 693–696. doi:10.1021/np0340394
32. Kametani, T.; Fukumoto, K. *J. Chem. Soc.* **1964,** 6141–6146. doi:10.1039/JR9640006141
33. Cunningham, B. D. M.; Lowe, P. R.; Threadgill, M. D. *J. Chem. Soc., Perkin Trans. 2* **1989,** 1275–1283. doi:10.1039/p29890001275

License and Terms

This is an Open Access article under the terms of the Creative Commons Attribution License (http://creativecommons.org/licenses/by/2.0), which permits unrestricted use, distribution, and reproduction in any medium, provided the original work is properly cited.

The license is subject to the *Beilstein Journal of Organic Chemistry* terms and conditions: (http://www.beilstein-journals.org/bjoc)

The definitive version of this article is the electronic one which can be found at: doi:10.3762/bjoc.9.152

Beilstein Journal of Organic Chemistry

Synthesis and biological activities of the respiratory chain inhibitor aurachin D and new ring versus chain analogues

Xu-Wen Li[1], Jennifer Herrmann[2], Yi Zang[1], Philippe Grellier[1], Soizic Prado[1], Rolf Müller[*2] and Bastien Nay[*1]

Full Research Paper

Open Access

Address:
[1]Muséum National d'Histoire Naturelle, Unité Molécules de Communication et Adaptation des Micro-organismes (UMR 7245 CNRS-MNHN), 57 rue Cuvier (CP 54), 75005 Paris, France and [2]Department of Microbial Natural Products, Helmholtz-Institute for Pharmaceutical Research Saarland (HIPS), Helmholtz Centre for Infection Research (HZI) and Pharmaceutical Biotechnology, Saarland University, Campus C2 3, 66123 Saarbrücken, Germany

Email:
Rolf Müller[*] - rom@helmholtz-hzi.de; Bastien Nay[*] - bnay@mnhn.fr

* Corresponding author

Keywords:
antiplasmodial activities; Conrad–Limpach reaction; mitochondrial membrane potential; natural products; quinolones; total synthesis

Beilstein J. Org. Chem. **2013,** *9,* 1551–1558.
doi:10.3762/bjoc.9.176

Received: 10 May 2013
Accepted: 10 July 2013
Published: 31 July 2013

This article is part of the Thematic Series "Natural products in synthesis and biosynthesis".

Guest Editor: J. S. Dickschat

© 2013 Li et al; licensee Beilstein-Institut.
License and terms: see end of document.

Abstract

Aurachins are myxobacterial 3-farnesyl-4(1*H*)-quinolone derived compounds initially described as respiratory chain inhibitors, more specifically as inhibitors of various cytochrome complexes. They are also known as potent antibiotic compounds. We describe herein the first synthesis of aurachin D through a key Conrad–Limpach reaction. The same strategy was used to reach some ring as opposed to chain analogues, allowing for the description of structure–activity relationships. Biological screening of the analogues showed antiparasitic, cytotoxic, antibacterial and antifungal activities, and depletion of the mitochondrial membrane potential. The strongest activity was found on *Plasmodium falciparum* with a selectivity index of 345, compared to Vero cells, for the natural product and its geranyl analogue. The loss of mitochondrial membrane potential induced by aurachins in human U-2 OS osteosarcoma cells was studied, showing the best activity for aurachin D and a naphthalene analogue, yet without totally explaining the observed cytotoxic activity of the compounds. Finally, a synthetic entry is given to the complete carboheterocyclic core of aurachin H through the N-oxidation/epoxidation of aurachin D and a shorter chain analogue, followed by subsequent biomimetic cyclization.

Introduction

The four aurachins A–D (**1**–**4**) were first isolated from the myxobacterium *Stigmatella aurantiaca* strain Sg a15 in 1987 (Figure 1) [1]. This class of compounds is characterized by a quinolone or quinoline nucleus substituted in position 3 or 4 by a farnesyl chain. In addition, aurachins can further be functionalized by biosynthetic oxidative processes [2-5]. Since then,

additional members of this natural product family were discovered, namely aurachins E–R, from the same strain [3,6], from *Stigmatella erecta* [7] or from *Rhodococcus* sp. Acta 2259 [8].

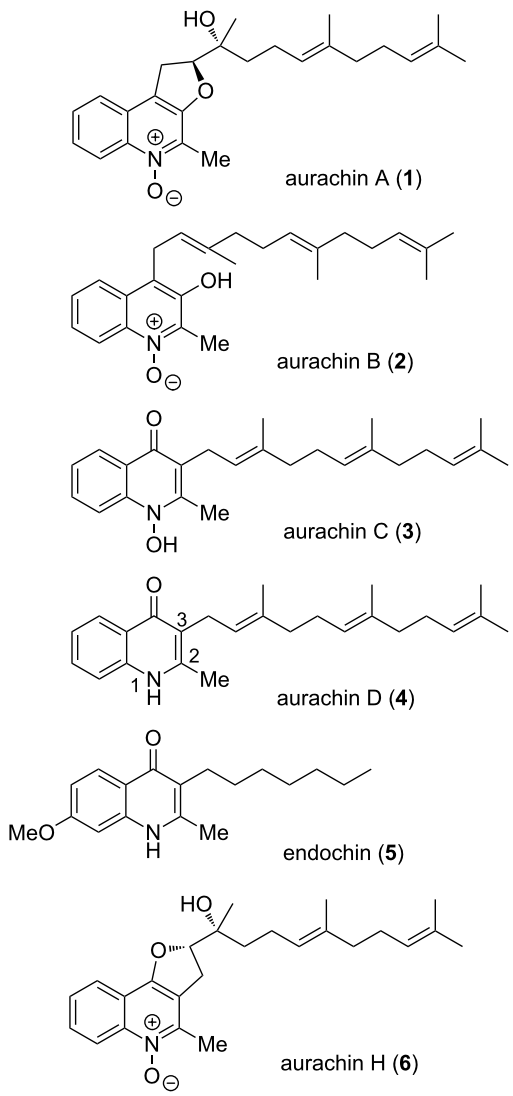


Figure 1: The 2-methyl-4(1*H*)-quinolone compounds: aurachins and endochin.

Initially, aurachins were found to block NADH oxidation in mammalian submitochondrial particles (aurachins C and D being the most active) [1] by the inhibition of complexes I and III of the mitochondrial respiratory chain [9,10]. They are indeed analogues of the physiological ubiquinol and vitamins K. They also affect the photosystem II and the cytochrome *bf* complex of thylakoids in photosynthetic microorganisms [11]. Deeper studies led to the conclusion that these compounds are powerful inhibitors of the quinol oxidation sites of bacterial cytochromes *bo* and *bd*, with dissociation constants in the range of 10 nM. Aurachin D (**4**) was shown to selectively inhibit the cytochrome *bd* complex [12].

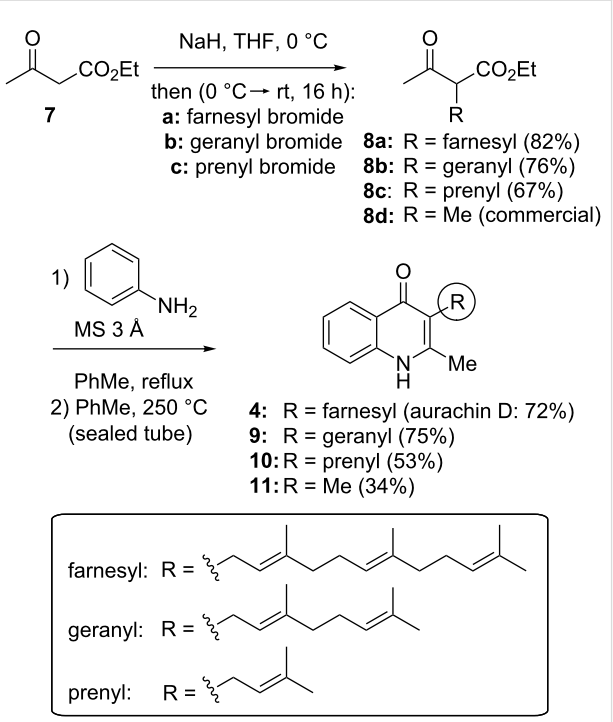
With such biological properties, aurachins and their analogues are also strong antimicrobial agents. Aurachins C and D (**3** and **4**) have been described as better inhibitors against Gram-positive bacteria compared to aurachins A and B (**1** and **2**) [1]. All were cytotoxic on L929 mouse fibroblasts with IC_{50} values in the range of 1–3 μg/mL and some of them strongly inhibited *Plasmodium falciparum* at an IC_{50} around 20 ng/mL (i.e., aurachins B, C and E, whereas aurachin D was 100- to 200-fold less active) [6]. This antimalarial activity was comparable to that of endochin (**5**) [13,14] and 2-methyl-4(1*H*)-quinolone analogues as determined in the course of important structure–activity optimization work [15]. In addition, many *N*-hydroxyquinolone derivatives with variable side chains displayed strong antiplasmodial activity at IC_{50} of ca. 1 nM [16].

In fact, owing to their occurrence in many natural products [17,18] and to the high frequency of their biological activities, compounds containing the 4(1*H*)-quinolone nucleus may be considered as important privileged structures [19-21] for medicinal purposes. This motivated the work therein, dealing with the first synthesis of aurachin D (**4**). On this occasion, the preliminary synthesis of ring versus chain analogues was undertaken, focusing on variations of the chain length or on the modulation of electron density of the aromatic ring including surface extension. Oxidative conditions were finally considered en route to *N*-oxide analogues, eventually leading to the heterocyclic core of aurachin H (**6**) (Figure 1).

Results and Discussion

Synthesis of aurachin D (**4**) and analogues with chain-length variations

Aurachin D (**4**) was synthesized in a three-step sequence from ethyl acetoacetate (**7**) (Scheme 1). Alkylation of the sodium salt of **7** in the presence of farnesyl bromide furnished the ethyl 2-farnesyl(acetoacetate) **8a** in 82% yield. Upon treatment with aniline, a Conrad–Limpach process [22-25] gave aurachin D (**4**) in 72% yield. This transformation was performed in toluene under reflux over 3 Å molecular sieves by formation of an imine intermediate, which was cyclized at 250 °C by Claisen condensation. Precipitation of the product by addition of pentane and subsequent filtration gave the pure synthetic aurachin D (**4**) which shared the same spectral properties as the natural product [3]. Analogous compounds bearing a shorter side chain (geranyl: **9** [26], prenyl: **10**, or methyl: **11**) were obtained by the same reaction sequence through the respective 2-alkyl(acetoacetate) **8b–8d**, yet with unexpectedly lower yields for the shorter-chain analogues **10** and **11**.



Scheme 1: Synthesis of aurachin D (**4**) and geranyl (**9**), prenyl (**10**) and methyl (**11**) analogues.

This method allowed for the rapid gram-scale synthesis of aurachin D (max. 1.1 g made in this work) with good yields and in a minimum of steps, which has to be compared to the extraction yield of the natural product. Indeed from a culture batch of 60 L, the production of compound **4** by *Stigmatella aurantiaca* Sg a15 under basal conditions was described as less than 1 mg/L after about 6 days [1]. This production was improved by the addition of anthranilic acid (i.e., the aurachin biosynthetic precursor) to the culture medium, furnishing 40 mg of **4** from 120 L [3].

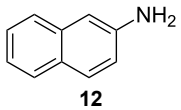
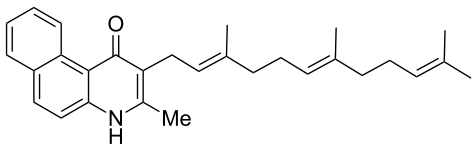
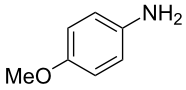
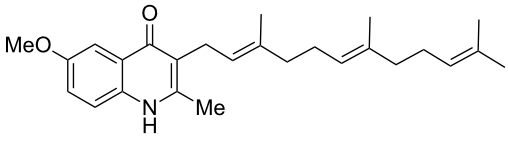
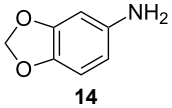
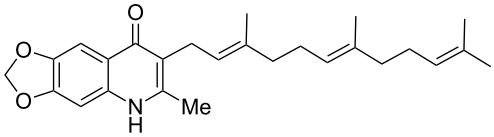
Aurachin D analogues with variations of the aromatic cycles

The same methodology was tentatively applied to other anilines such as 2-naphthylamine (**12**), *p*-anisidine (**13**), 3,4-(methylenedioxy)aniline (**14**), 3,4-difluoroaniline (**15**) and methyl 3-aminobenzoate (**16**), using the 2-farnesyl(acetoacetate) **8a**. Not surprisingly, only the electron-rich anilines **12**–**14** were reactive enough to furnish the expected 3-farnesyl-4(1*H*)-quinolones **17**–**19** in moderate to good yields (Table 1). The electron-poor anilines **15** and **16** were unreactive under these experimental conditions, although the intermediate imine was supposedly formed during the reaction but not isolated.

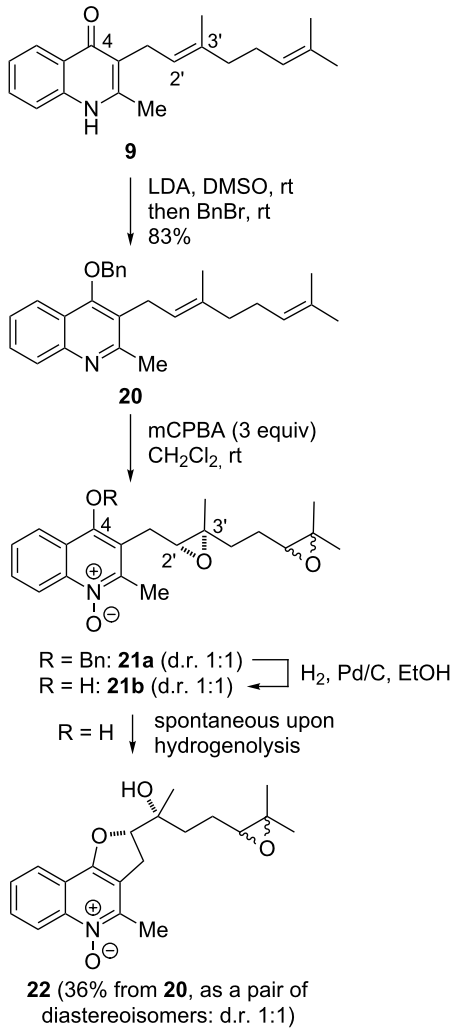
The carbocyclic core of aurachin H

Aurachin H (**6**) was isolated from *Stigmatella aurantiaca* at the same time as the aurachin series A–L [3]. Biosynthetically, it may arise from the double oxidation of the quinolone nitrogen and the olefin epoxidation (2',3'-position) of the farnesyl chain, with the epoxide being ring-opened with 5-*exo* selectivity by the 4-hydroxy group of the resulting 4-hydroxyquinoline *N*-oxide. Taking the geranyl analogue **9** as a model compound (Scheme 2), after benzylic protection of the 4-hydroxyquinoline form into **20**, oxidative conditions were applied to perform both N-oxidation and olefin epoxidations, in the presence of

Table 1: Synthesis of aurachin D analogues with aromatic variations.

Starting aniline	Product	Yield
 **12**	 **17**	45%
 **13**	 **18**	65%
 **14**	 **19**	70%

three equivalents of *m*-chloroperbenzoic acid (mCPBA). The use of smaller quantities of the oxidant only led to complex mixtures of nonselectively oxidized products. The crude product **21a** was then submitted to benzyl group hydrogenolysis. As expected upon completion of the reaction, the 4,5-dihydrofuro[3,2-*c*]quinoline *N*-oxide ring system **22** was obtained as a racemic pair of diastereoisomers in a 1:1 ratio, supposedly formed through the spontaneous cyclization of intermediate **21b**, which was not isolated. We also performed the same reaction sequence from aurachin D (**4**), giving the aurachin-H diepoxide with comparable yields [27]. After optimizing the selectivity of the epoxidation, this reaction may furnish a rapid strategy toward aurachin H (**6**) and related compounds in a bio-inspired manner.



Scheme 2: Strategy toward the heterocyclic core of aurachin H.

Biological activities

The cytotoxic activity of aurachin D (**4**) and analogues **9**–**11** and **17**–**19** was evaluated in growth inhibition experiments on mammalian cell lines (Table 2). After 5 days treatment, half inhibitory concentrations (IC_{50}) were determined for human HCT-116 colon carcinoma and human K562 myelogenous leukemia cells. The synthesized natural product **4** and its geranyl and methoxy analogues (**9** and **18**) were the most active amongst the tested derivatives with IC_{50} values in the low µg/mL range, whereas analogues **10**, **11**, **17**, and **19** displayed no significant toxicity up to concentrations of 10 µg/mL.

Since aurachins are described as electron-transport inhibitors of the mitochondrial respiratory chain (complex I and III) [28], we analyzed the synthetic analogues in high-content screening experiments with respect to a decrease of the mitochondrial membrane potential (MMP). Human U-2 OS osteosarcoma cells were treated for 16 hours with aurachins **4**, **9**–**11**, and **17**–**19** at concentrations between 1 and 10 µg/mL, and mitochondria were labeled with tetramethylrhodamine methyl ester (TMRM) in order to assess changes in MMP (Figure 2). Most prominent concentration-dependent effects were determined for aurachin D (**4**) and one of its analogues (**17**). At concentrations as low as 5 µg/mL, **4** and **17** significantly reduced the MMP, which was further diminished at higher concentrations (Figure 2A). Other analogues with aromatic variations (**18** and **19**) were essentially inactive in the tested concentration range, although aurachin analogue **18** was determined to have a cytotoxic activity (IC_{50}) at ca. 1 µg/mL. This might be due to differential effects on different cell lines, a different time course of electron-transport inhibition, or a different mode of inducing apoptosis (e.g., via

Table 2: Cytotoxicity tests on HCT-116 human colon carcinoma and K562 myelogenous leukemia cells (showing IC_{50}: half inhibitory concentrations, µg/mL)[a,b].

Compounds:	**4**	**9**	**10**	**11**	**17**	**18**	**19**
HCT-116	2.23 ± 0.76	2.52 ± 0.48	>10	>10	>10	1.64 ± 0.47	>10
K562	0.65 ± 0.16	1.50 ± 0.31	ca. 10	>10	ca. 10	1.15 ± 0.22	>10

[a]Activities on Vero cells (nontumor cells) were all at IC_{50} >10 µg/mL, with aurachin D (**4**) being cytotoxic at 13.8 µg/mL, except compound **19** at 4.4 µg/mL (the aurachin H analogue **22** was also not active at any concentration up to 50 µg/mL); [b]All tests performed in triplicate; values were calculated by sigmoidal curve fitting and are displayed as mean ±SD.

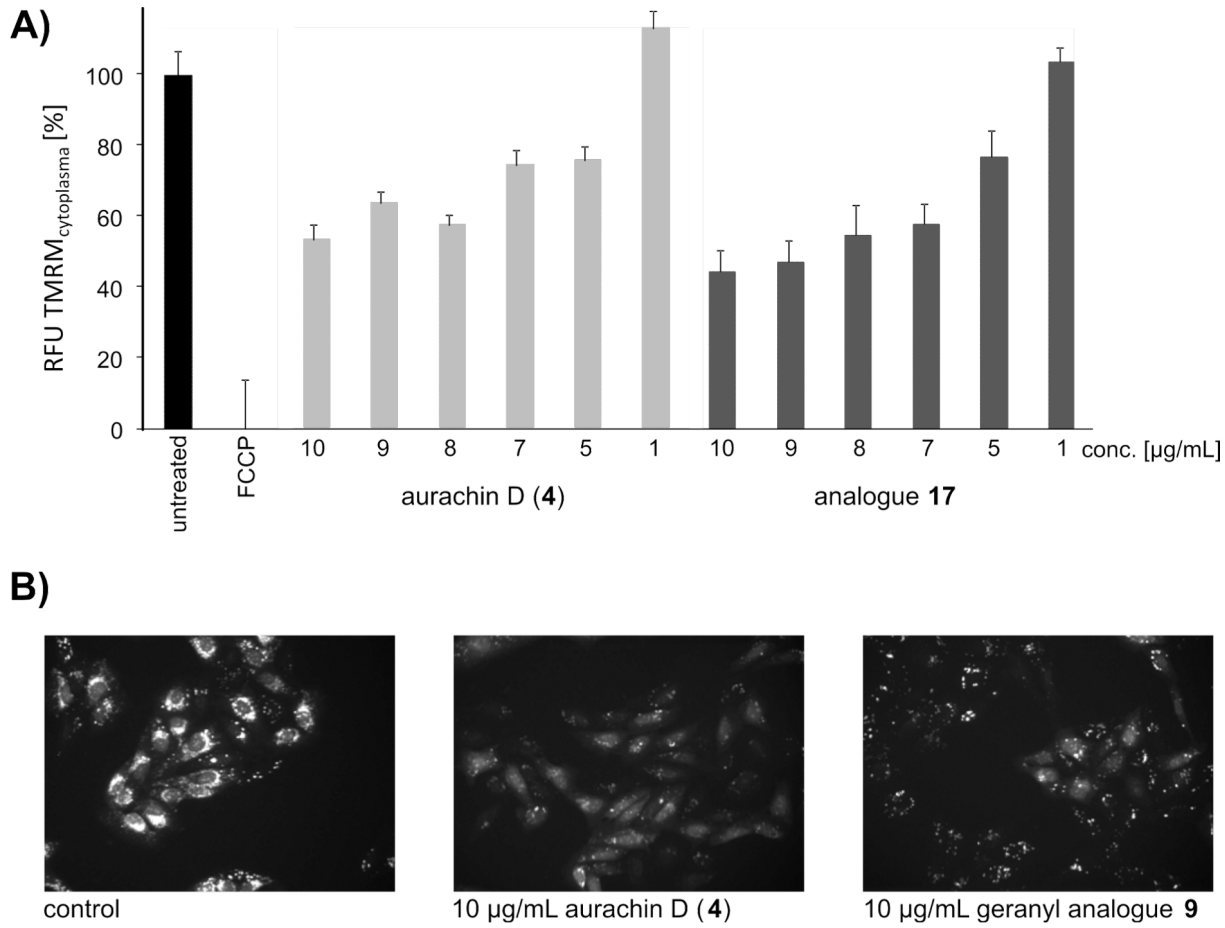


Figure 2: (A) Loss of mitochondrial membrane potential in human U-2 OS osteosarcoma cells that were treated with aurachin D (**4**) and analogue **17**. Images were acquired on a BD Pathway855 automated microscope and subsequently processed in AttoVision v1.6.2. The relative MMP was calculated based on TMRM fluorescence intensity in the cytoplasmic segments. The value of the negative control (untreated cells) was set to 100% and the value of FCCP-treated cells (positive control) was set to 0%. Bars represent the mean ±SEM of all cellular segments within a well. (B) Representative HCS images of U-2 OS cells that were treated with aurachin D (**4**) or the geranyl analogue **9**. Cells were labeled with TMRM and imaged in the rhodamine channel at 200× magnification.

enhanced ROS formation) [29]. However, at the highest assay concentration also shorter chain analogues **9**–**11** reduced the MMP to approximately 60–80% of the control value as exemplarily shown for geranyl analogue **9** (Figure 2B).

Antiparasitic activities were evaluated on the chloroquine-resistant *Plasmodium falciparum* FcB1 and on *Trypanosoma brucei gambiense*. Aurachin D (**4**) and its geranyl analogue **9** showed a strong antiplasmodial activity at 0.04 and 0.07 µg/mL, respectively, while analogues **10**, **11** and **17**–**19** were 10- to 100-fold less active (Table 3). Based on the simplest but less active 3-methyl analogue **11**, we compared the activity with the commercial 2-methyl-4(1*H*)-quinolone (**23**), the 3-bromo-2-methyl-4(1*H*)-quinolone (**24**) and *N*-hydroxy-2,3-dimethyl-

Table 3: Antiparasitic activities on *Plasmodium falciparum* FcB1 and *Trypanosoma brucei gambiense* (IC_{50}, µg/mL).[a]

Compounds:	**4**	**9**	**10**	**11**	**17**	**18**	**19**	**23**	**24**	**25**
P. falciparum FcB1	0.04 ± 0.02	0.07 ± 0.02	0.55 ± 0.16	2.30 ± 1.40	0.51 ± 0.18	0.20 ± 0.04	0.42 ± 0.09	7.70 ± 2.50	1.10	2.70 ± 1.30
T. brucei gambiense	0.4	1.5	5.8	>10	0.8	1.6	>10	>10	1.7	>10

[a]For *P. falciparum* FcB1, all tests performed in triplicate (except compound **24**); values were calculated by sigmoidal curve fitting and are displayed as mean ±SD.

4(1*H*)-quinolone (**25**), showing the importance of a substituent in position 3. The *N*-hydroxy substitution of **25** had no effect on the activity of the 2,3-dimethylquinolone core (compared to **11**). Due to the lack of the farnesyl chain, this comparison of the quinolone substitution effect yet diverges from previous observations showing an approximately 200-fold higher activity of aurachin C (**3**) compared to aurachin D (**4**) (which however displayed strong activity on our FcB1 strain) [6]. Comparatively, it is known from the literature that farnesol alone is poorly antiplasmodial with an IC_{50} of 64 µM [30], showing the crucial importance of the quinolone core for this strong activity.

The antitrypanosomal activity was found much lower than the antiplasmodial activity, with the most active compounds being the natural product **4** and the aromatic analogue **17** at IC_{50} = 0.4 and 0.8 µg/mL, respectively (Table 3). The geranyl (**9**) and prenyl (**10**) analogues still retained some activity at 1.5 and 5.8 µg/mL, respectively. Overall, we found interesting antiparasitic activities for these compounds relative to the cytotoxicity on human Vero cells, with antiplasmodial and antitrypanosomal selectivity indexes of 345 and 35, respectively, for aurachin D (**4**), which still make it medicinally relevant for antiparasitic purposes [31].

In accordance with previous reports [1], antibacterial activities (Table 4) were mainly observed on Gram-positive bacteria while Gram-negative bacteria were not affected, except *Escherichia coli* TolC which is deficient in the corresponding multidrug efflux transporter. The tested compounds were neither active on yeast (*Candida albicans*) nor on molds (*Mucor hiemalis*, *Fusarium oxysporum*, *Alternaria alternata*). The natural compound **4** was one of the most active compounds, but also shorter chain analogues **9** and **10** inhibited, for instance, the growth of *Staphylococcus aureus* at concentrations in the low µg/mL range, whereas analogue **9** was approximately twice as active as **10**. As the 3-methyl analogue **11**, aurachin D analogues with variations of the aromatic cycle (**17**–**19**) were essentially inactive. Solely analogues **18** and **19** displayed a significant growth inhibitory effect on *Bacillus subtilis*.

Conclusion

During this work, not only the total synthesis of aurachin D (**4**) was accomplished, but also that of analogues with variations in chain length or aromatic cycle. The general strategy involved a key Conrad–Limpach synthesis of quinolones. Additionally, we were able to build the carboheterocyclic core of aurachin H (**6**) under epoxidation conditions, i.e., the 4,5-dihydrofuro[2,3-*c*]quinoline *N*-oxide, and thus to synthesize chain analogues of **6**. Biological investigations demonstrated the superiority of the natural product **4** regarding its inhibitory effect on Gram-positive bacteria, human cancer cell lines, and above all on the parasites *Plasmodium falciparum* FcB1 (with an excellent selectivity index of 345) and *Trypanosoma brucei gambiense*. We found that the biological activities were mostly conserved with the geranyl analogue **9**. Also other shorter chain analogues (**10** and **11**) retained some activities. Inhibitory concentrations were, however, by one or two orders of magnitude higher than those determined for aurachin D (**4**) and its geranyl analogue **9**. Variants with modifications of the aromatic cycle (**17**, **18**) were generally less potent although it was found that the methoxy variant **18** is cytotoxic on human cancer cell lines. Indeed, this cytotoxic effect might be rather unspecific or only in part linked to

Table 4: Antibacterial activities of 4(1*H*)-quinolone derivatives (MIC_{50}, µg/mL).[a]

Compounds:	**4**	**9**	**10**	**11**	**17**	**18**	**19**
Gram-positive							
Bacillus subtilis DSM10	<0.1	<0.1	0.22 ± 0.06	49.04 ± 6.26	>64	6.75 ± 0.60	4.66 ± 0.50
Micrococcus luteus	1.47 ± 0.12	2.59 ± 0.34	14.31 ± 1.29	>64	>64	49.17 ± 3.94	>64
Staphylococcus aureus Newman (MSSA)	5.46 ± 1.05	3.96 ± 0.49	9.66 ± 2.39	>64	>64	>64	34.56 ± 5.13
Staphylococcus aureus DSM11822 (MRSA)	2.10 ± 0.19	4.50 ± 0.74	11.3 ± 1.44	>64	>64	>64	>64
Gram-negative							
Escherichia coli DH5α (wt)	>64	>64	>64	>64	>64	>64	>64
Escherichia coli (TolC)	8.36 ± 1.00	1.41 ± 0.45	6.55 ± 1.36	>64	>64	>64	>64
Klebsiella pneumoniae DSM30104	>64	>64	>64	>64	>64	>64	>64

[a]All tests performed in duplicate; values were calculated by sigmoidal curve fitting and are displayed as mean ±SD.

inhibition of the electron transport chain. Finally, the biological activity of the compounds was assessed in a high-content screen on mitochondrial dysfunction. For aurachin D (**4**) and its shorter-chain analogues (**9**–**11**) we found that the mitochondrial membrane potential was reduced to approximately 50% and 60–80% of the control, respectively. Analogues **18** and **19** with variations of the aromatic cycle were inactive up to concentrations of 10 µg/mL. However, analogue **17** strongly diminished the MMP, whereas it remains to be elucidated whether this effect is induced by selectively blocking the electron transport chain or by other apoptotic processes, which, in turn, induce a loss of MMP.

Supporting Information

Supporting information is available, featuring the synthetic procedures and spectral data for compounds **9**, **10**, **17**–**22**.

Supporting Information File 1

Experimental part.
[http://www.beilstein-journals.org/bjoc/content/supplementary/1860-5397-9-176-S1.pdf]

Acknowledgements

We acknowledge receipt of a scholarship from the China Scholarship Council for XWL and YZ. We thank Alexandre Deville, Lionel Dubost and Caroline Bance for performing NMR, MS and antifungal tests, respectively. The CNRS and the MNHN are acknowledged for daily financial support.

References

1. Kunze, B.; Höfle, G.; Reichenbach, H. *J. Antibiot.* **1987,** *40,* 258–265. doi:10.7164/antibiotics.40.258
2. Sandmann, A.; Dickschat, J.; Jenke-Kodama, H.; Kunze, B.; Dittmann, E.; Müller, R. *Angew. Chem., Int. Ed.* **2007,** *46,* 2712–2716. doi:10.1002/anie.200603513
3. Höfle, G.; Kunze, B. *J. Nat. Prod.* **2008,** *71,* 1843–1849. doi:10.1021/np8003084
4. Pistorius, D.; Li, Y.; Sandmann, A.; Müller, R. *Mol. BioSyst.* **2011,** *7,* 3308–3315. doi:10.1039/c1mb05328k
5. Katsuyama, Y.; Harmrolfs, K.; Pistorius, D.; Li, Y.; Müller, R. *Angew. Chem., Int. Ed.* **2012,** *51,* 9437–9440. doi:10.1002/anie.201204138
6. Höfle, G.; Böhlendorf, B.; Fecker, T.; Sasse, F.; Kunze, B. *J. Nat. Prod.* **2008,** *71,* 1967–1969. doi:10.1021/np8004612
7. Höfle, G.; Irschik, H. *J. Nat. Prod.* **2008,** *71,* 1946–1948. doi:10.1021/np800325z
8. Nachtigall, J.; Schneider, K.; Nicholson, G.; Goodfellow, M.; Zinecker, H.; Imhoff, J. F.; Süssmuth, R. D.; Fiedler, H.-P. *J. Antibiot.* **2010,** *63,* 567–569. doi:10.1038/ja.2010.79
9. Oettmeier, W.; Masson, K.; Soll, M.; Reil, E. *Biochem. Soc. Trans.* **1994,** *22,* 213–216.
10. Friedrich, T.; Ohnishi, T.; Forche, E.; Kunze, B.; Jansen, R.; Trowitzsch, W.; Höfle, G.; Reichenbach, H.; Weiss, H. *Biochem. Soc. Trans.* **1994,** *22,* 226–230.
11. Oettmeier, W.; Dostatni, R.; Majewski, C.; Höfle, G.; Fecker, T.; Kunze, B.; Reichenbach, H. *Z. Naturforsch.* **1990,** *45,* 322–328.
12. Meunier, B.; Madgwick, S. A.; Reil, E.; Oettmeier, W.; Rich, P. R. *Biochemistry* **1995,** *34,* 1076–1083. doi:10.1021/bi00003a044
13. Salzer, W.; Timmler, H.; Andersag, H. *Chem. Ber.* **1948,** *81,* 12–19. doi:10.1002/cber.19480810103
14. Cross, R. M.; Manetsch, R. *J. Org. Chem.* **2010,** *75,* 8654–8657. doi:10.1021/jo1014504
15. Cross, R. M.; Monastyrskyi, A.; Mutka, T. S.; Burrows, J. N.; Kyle, D. E.; Manetsch, R. *J. Med. Chem.* **2010,** *53,* 7076–7094. doi:10.1021/jm1007903
16. Tietze, L. F.; Ma, L. *Heterocycles* **2010,** *82,* 377–396. doi:10.3987/COM-10-S(E)9
17. Michael, J. P. *Nat. Prod. Rep.* **1997,** *14,* 605–618. doi:10.1039/np9971400605
18. Michael, J. P. *Nat. Prod. Rep.* **2008,** *25,* 166–187. doi:10.1039/b612168n
19. DeSimone, R. W.; Currie, K. S.; Mitchell, S. A.; Darrow, J. W.; Pippin, D. A. *Comb. Chem. High Throughput Screening* **2004,** *7,* 473–494. doi:10.2174/1386207043328544
20. Duarte, C. D.; Barreiro, E. J.; Fraga, C. A. M. *Mini-Rev. Med. Chem.* **2007,** *7,* 1108–1119. doi:10.2174/138955707782331722
21. Welsch, M. E.; Snyder, S. A.; Stockwell, B. R. *Curr. Opin. Chem. Biol.* **2010,** *14,* 347–361. doi:10.1016/j.cbpa.2010.02.018
22. Conrad, M.; Limpach, L. *Ber. Dtsch. Chem. Ges.* **1887,** *20,* 944–948. doi:10.1002/cber.188702001215
23. Conrad, M.; Limpach, L. *Ber. Dtsch. Chem. Ges.* **1887,** *20,* 948–959. doi:10.1002/cber.188702001216
24. Manske, R. H. *Chem. Rev.* **1942,** *30,* 113–144. doi:10.1021/cr60095a006
25. For more recent examples involving the Conrad–Limpach reaction, the reader can refer to references [14-16].
26. Abe, H.; Kawada, M.; Inoue, H.; Ohba, S.-i.; Nomoto, A.; Watanabe, T.; Shibasaki, M. *Org. Lett.* **2013,** *15,* 2124–2127. doi:10.1021/ol400587a Intervenolin, a 2-geranyl analogous compound with antitumor activity, was very recently synthesized through a key Suzuki–Miyaura coupling.
27. However, since the epoxidation was not stereoselective, a complex mixture of four racemic stereoisomers was obtained from aurachin D (**4**).
28. Friedrich, T.; van Heek, P.; Leif, H.; Ohnishi, T.; Forche, E.; Kunze, B.; Jansen, R.; Trowitzsch-Kienast, W.; Höfle, G.; Reichenbach, H.; Weiss, H. *Eur. J. Biochem.* **1994,** *219,* 691–698. doi:10.1111/j.1432-1033.1994.tb19985.x
29. Li, N.; Ragheb, K.; Lawler, G.; Sturgis, J.; Rajwa, B.; Melendez, J. A.; Robinson, J. P. *J. Biol. Chem.* **2003,** *278,* 8516–8525. doi:10.1074/jbc.M210432200
30. Rodrigues Goulart, H. R.; Kimura, E. A.; Peres, V. J.; Couto, A. S.; Aquino Duarte, F. A.; Katzin, A. M. *Antimicrob. Agents Chemother.* **2004,** *48,* 2502–2509. doi:10.1128/AAC.48.7.2502-2509.2004
31. The selectivity index (SI) is defined as the ratio between the cytotoxic concentration (Vero cells in this work) and the concentration active on the target. Compounds are medicinally relevant when the SI is high.

License and Terms

This is an Open Access article under the terms of the Creative Commons Attribution License (http://creativecommons.org/licenses/by/2.0), which permits unrestricted use, distribution, and reproduction in any medium, provided the original work is properly cited.

The license is subject to the *Beilstein Journal of Organic Chemistry* terms and conditions: (http://www.beilstein-journals.org/bjoc)

The definitive version of this article is the electronic one which can be found at: doi:10.3762/bjoc.9.176

Beilstein Journal of Organic Chemistry

New tridecapeptides of the theonellapeptolide family from the Indonesian sponge *Theonella swinhoei*

Annamaria Sinisi[1], Barbara Calcinai[2], Carlo Cerrano[2], Henny A. Dien[3], Angela Zampella[1], Claudio D'Amore[4], Barbara Renga[4], Stefano Fiorucci[4] and Orazio Taglialatela-Scafati[*1,§]

Full Research Paper

Open Access

Address:
[1]Dipartimento di Farmacia, Università di Napoli "Federico II", via D. Montesano 49, 80131 Napoli, Italy, [2]Dipartimento di Scienze della Vita e dell'Ambiente, Università Politecnica delle Marche, Via Brecce Bianche, 60131 Ancona, Italy, [3]Faculty of Fishery and Marine Science, Sam Ratulangi University, Manado, Indonesia and [4]Dipartimento di Medicina Clinica e Sperimentale, Università di Perugia, Via Gambuli 1, 06132 Perugia, Italy

Email:
Orazio Taglialatela-Scafati[*] - scatagli@unina.it

* Corresponding author
§ Tel.: (0039) 081-678509, Fax (0039) 081-678552

Keywords:
antiproliferative activity; cyclic peptides; marine metabolites; theonellapeptolides; 2D NMR

Beilstein J. Org. Chem. **2013,** *9,* 1643–1651.
doi:10.3762/bjoc.9.188

Received: 05 June 2013
Accepted: 23 July 2013
Published: 13 August 2013

This article is part of the Thematic Series "Natural products in synthesis and biosynthesis".

Guest Editor: J. S. Dickschat

© 2013 Sinisi et al; licensee Beilstein-Institut.
License and terms: see end of document.

Abstract

Chemical analysis of the organic extract of *Theonella swinhoei* yielded two new tridecadepsipeptides of the theonellapeptolide family, namely sulfinyltheonellapeptolide, characterized by a methylsulfinylacetyl group at the *N*-terminus, and theonellapeptolide If, the first member of this class of compounds to show four valine residues. The structures of the compounds, isolated along with the known theonellapeptolide Id, were determined by extensive 2D NMR and MS/MS analyses followed by application of Marfey's method. The isolated peptides exhibited moderate antiproliferative activity against HepG2 cells, a hepatic carcinoma cell line.

Introduction

Three decades of extensive chemical investigation [1] have clearly evidenced that marine sponges of the genus *Theonella* (Lithistida, Theonellidae) are treasure troves of secondary metabolites. The chemical diversity of the isolated compounds ranges from unusual steroids (exemplified by the 4-methylene sterol theonellasterol [2,3] and truncated side-chain sulfated steroids [4]), to complex macrocyclic polyketides (as the well-known swinholide A, now a reference compound in the class of actin interacting cell growth inhibitors [5]), polyene derivatives (as aurantosides [6]), and polypeptides/depsipeptides. The biosynthesis of several secondary metabolites of *Theonella* has been ascribed to symbiotic microorganisms, as in the case of the polyketide onnamide [7] and the polypeptide polytheonamide [8]. It is, however, not unreasonable to presume that a symbiotic role in the production of secondary metabolites could be crucial in many other cases.

Probably the most distinctive class of secondary metabolites of *Theonella* is given by complex polypeptides whose uncommon amino acids have been postulated to have either nonribosomal (NR) or post-translationally modified ribosomal (PMR) origin [8]. Several classes of *Theonella* polypeptides have been isolated to date, and they often show peculiar features such as largely rearranged amino acidic units, either D- or L-configurations at the α-carbons, and the formation of macrocycles through amide or ester bonds. To categorize the plethora of *Theonella* polypeptides we could identify at least eight structural types: theonellamides (glycosylated imidazole-containing macrocycles) [9], keramamides (including oxazole or thiazole rings) [10], papuamides (HIV inhibitory macrocyclic depsipeptides) [11], polytheonamides (cytotoxic linear polypeptides) [12], cyclotheonamides (thrombin and serine protease inhibitors) [13], perthamides (anti-inflammatory cyclopeptides) [14,15], solomonamides [16] and theonellapeptolides (cyclic tridecapeptides including several *N*-methylated and D-amino acids) [17].

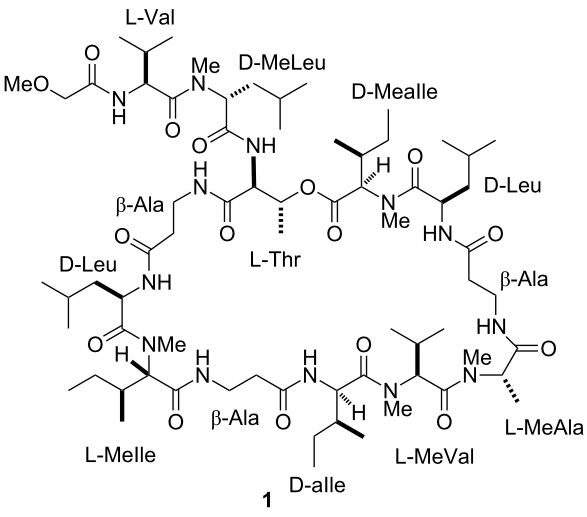


Figure 1: Structure of the known compound theonellapeptolide Id (**1**).

In the context of our long-standing interest for bioactive secondary metabolites from marine invertebrates, we have recently investigated a specimen of *T. swinhoei* collected off the coasts of Manado (North Sulawesi, Indonesia), which proved to be rich in aurantosides [6] and 4-methylene steroids [18], while polyketide macrolides and peptide-based derivatives were extremely rare if not absent. Remarkably, the chemical analysis of a different specimen of *T. swinhoei*, collected in the same area as the previous one, exhibited an extremely different secondary metabolite composition. In particular, this second specimen has been found to be rich in polypeptides and, from the $CHCl_3$ phase of the organic extract, we have identified the major member of this class as theonellapeptolide Id (**1**) (Figure 1). In this paper we report the results of the chemical analysis of the polypeptide-containing fraction, which resulted in the isolation of two new theonellapeptolides, namely sulfinyltheonellapeptolide (**2**) and theonellapeptolide If (**3**) (Figure 2). We describe the structural elucidation of these new metabolites and the results of the preliminary pharmacological evaluation of the isolated compounds on HepG2 cells (hepatocarcinoma cell line).

Results and Discussion

Theonella swinhoei was collected in the Bunaken Marine Park of Manado (North Sualwesi, Indonesia) in January 2010 and frozen immediately after collection. The frozen material was repeatedly extracted with methanol, and the crude extract was subjected to a modified Kupchan's partitioning procedure [19] to obtain *n*-hexane, $CHCl_3$ and *n*-BuOH extracts. The $CHCl_3$

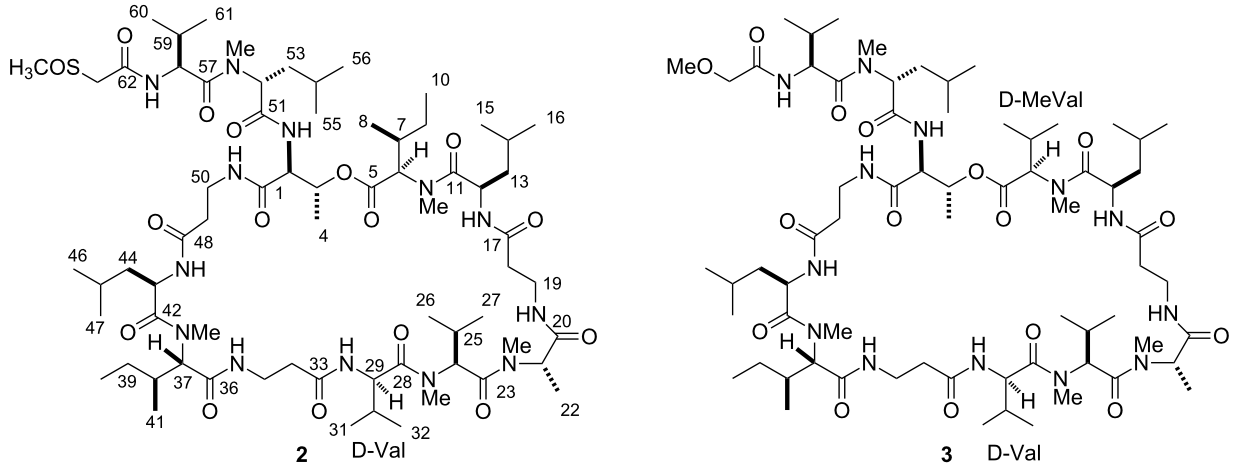


Figure 2: Structures of sulfinyltheonellapeptolide (**2**) and theonellapeptolide If (**3**).

extract was chromatographed by silica gel MPLC, and fractions eluted with CH_2Cl_2/MeOH 97:3 were further purified by HPLC on Nucleodur or Ascentis reversed-phase columns (eluent MeOH/H_2O 87:13) to obtain the known theonellapeptolide Id (**1**, 68.5 mg), and the new analogues sulfinyltheonellapeptolide (**2**, 4.6 mg) and theonellapeptolide If (**3**, 2.1 mg) (Figure 2). The known compound was identified on the basis of the comparison of its spectroscopic data with those published in the literature [17].

Theonellapeptolides are tridecapeptide lactones characterized by the presence of aliphatic and non-polar amino acids including high ratio of D-amino acids, *N*-methyl amino acids, and β-amino acids. In particular, the structure of theonellapeptolide Id (**1**) includes three β-Ala, three D-Leu (one *N*-methylated), two L-Val (one *N*-methylated), one L-MeAla, one L-Thr, one L-MeIle, and two D-alloIle (one *N*-methylated) units.

Sulfinyltheonellapeptolide (**2**, $[\alpha]_D$ −38.1, *c* 0.1, MeOH) was isolated as a colorless amorphous solid with pseudomolecular ion peaks at *m*/*z* 1423 $[M + H]^+$ and 1445 $[M + Na]^+$ in the ESIMS, and high-resolution analysis established the molecular formula $C_{69}H_{123}N_{13}O_{16}S$. Inspection of its ^1H NMR spectrum (CD_3OD, Table 1) clearly suggested the peptide nature of **2** and

Table 1: ^1H (500 MHz) and ^{13}C (125 MHz) NMR data of sulfinyltheonellapeptolide in CD_3OD (**2**).

AA	Position	δ_H, m, *J* in Hz	δ_C	AA	Position	δ_H, m, *J* in Hz	δ_C
L-Thr	1	–	171.2	β-Ala	33	–	173.2
	2	4.36, m	58.5		34/34’	2.29, m; 2.59, m	36.5
	3	5.19, m	70.6		35/35’	3.10, m; 4.23, m	36.8
	4	1.11, d, 6.5	19.1	L-Me-Ile	36	–	172.5
D-Me-Ile	5	–	173.4		37	3.14, m	71.2
	6	5.06, m	62.5		38	2.48, m	36.5
	7	2.14[a]	34.2		39/39’	1.04, m; 1.92[a]	30.2
	8	0.78, d, 7.2	11.5		40	1.00[a]	13.2
	9/9’	1.10, m; 1.38, m	26.5		41	0.81, d, 6.4	15.3
	10	0.98, t, 7.6	17.0		37-NMe	3.35, s	39.9
	6-NMe	3.22, s	32.0	D-Leu	42	–	176.2
D-Leu	11	–	177.0		43	5.06, m	50.6
	12	5.03, m	50.5		44	1.72[a]; 1.25[a]	41.2
	13/13’	1.74[a], 1.25[a]	40.4		45	1.80[a]	26.6
	14	1.81[a]	26.3		46	1.03[a]	21.0
	15	0.89[a]	11.1		47	1.04[a]	25.0
	16	0.94 d, 7.3	17.2	β-Ala	48	–	175.0
β-Ala	17	–	174.3		49/49’	2.28, m; 2.36, m	39.1
	18/18’	2.23, m 2.29 m	39.5		50/50’	3.14, m; 3.81, m	37.7
	19/19’	3.24, m 3.69, m	38.2	D-Me-Leu	51	–	175.2
L-Me-Ala	20	–	172.5		52	5.24, m	57.5
	21	5.17[a]	58.5		53/53’	1.41[a]; 2.03 m	39.5
	22	1.45, d, 7.1	16.0		54	1.52[a]	27.1
	21-NMe	2.77 s	30.5		55	0.83, d, 6.7	22.1
L-Me-Val	23	–	173.0		56	0.95[a]	24.3
	24	5.02[a]	59.4		52-NMe	3.30 s	33.0
	25	2.40, m	30.2	L-Val	57	–	176.0
	26	0.86[a]	20.6		58	4.76, m	57.7
	27	0.92, d, 6.1	20.8		59	2.12, m	32.5
	24-NMe	3.31 s	31.9		60	0.96[a]	20.4
D-Val	28	–	173.2		61	1.01[a]	19.2
	29	4.76, m	68.9	Me-SAc	62		166.5
	30	2.68, m	27.6		63/63’	3.67, d, 11.2;	58.9
	31	0.86[a]	18.1			3.86, d, 11.2	
	32	1.17, d, 6.5	23.3		63-SOMe	2.79, s	39.2

[a]Overlapped with other signals.

placed it into the theonellapeptolide class. Given this characterization of **2** the presence of the sulfur atom in the molecular formula appeared especially remarkable. In particular, the ^{1}H and ^{13}C NMR data of **2** indicated the presence of six methyl singlets (δ_H 2.77, 2.79, 3.22, 3.30, 3.31, and 3.35) and fourteen carbonyl groups (resonating from δ_C 166.5 to 177.0). Extensive analysis of homonuclear and heteronuclear 2D NMR spectra including $^{1}H/^{1}H$ COSY, $^{1}H/^{1}H$ TOCSY, $^{1}H/^{13}C$ HSQC and $^{1}H/^{13}C$ HMBC allowed us to overcome the difficulty posed by the severe signal overlap in the ^{1}H NMR spectrum and to establish the presence of three β-Ala, three Leu (one *N*-methylated), two Ile (both *N*-methylated), three Val (one *N*-methylated), one Thr, and one *N*-methylAla, the same amino acid composition as in theonellapeptolide Id (**1**) except for one residue. The above analysis left unassigned a methyl singlet at δ_H 2.79 (δ_C 39.2) and a pair of mutually coupled doublets at δ_H 3.67 and 3.86, with these latter signals showing HMBC correlations both with the methyl carbon at δ_C 39.2 and an amide carbonyl resonating at δ_C 166.5. The ^{1}H and ^{13}C NMR chemical shift values of both the methyl and the methylene groups strongly suggested their linkage to a sulfoxide group, and the presence of a methylsulfinylacetyl (MeS(O)Ac) subunit was also in full agreement with the molecular formula. The amino acid sequence of **2** was then disclosed by careful analysis of the pattern of HMBC correlations, whose key cross-peaks are shown in Figure 3. The cross-peak of the Thr low-field shifted β-CH (δ_H 5.19) with the Me-Ile carbonyl group revealed the presence of an ester linkage.

HMBC analysis also revealed that the amide carbonyl at δ_C 166.5 assigned to the methylsulfinylacetyl subunit was correlated to the Hα of Val-1 residue, thus establishing the acetylation of the *N*-terminus in **2**. Methanolysis of **2**, followed by ESI (positive ion mode) MS/MS analysis of the obtained acyclic methyl ester derivative provided key fragment peaks, shown in Figure 3, giving definitive confirmation of the sulfinyltheonellapeptolide gross structure. In addition to the pseudomolecular ion at *m*/*z* 1454 $[M + H]^+$, corresponding to the introduction of 32 mass units (MeOH) in the molecule, the ESIMS/MS spectrum provided several fragment ion peaks corresponding to *N*-terminus fragments due to the cleavage of the amide bond, and referred to as the b series in Roepstorff and Fohlman nomenclature [20]. In particular, the presence of the b2 fragmentation peak at *m*/*z* 331 supported, once again, the presence of the MeS(O)Ac unit.

Complete acid hydrolysis of **2** and Marfey's analysis [21] on the hydrolysate (derivatization with L-FDAA, 1-fluoro-2,4-dinitrophenyl-5-L-alanine amide, followed by LC–MS comparison with the FDAA derivatives of appropriate standards) enabled us to determine the configuration of the chiral amino acid residues as L-MeAla, D-Leu (×2), D-MeLeu, L-Thr, L-Me-Val, L-Me-Ile, D-Me-*allo*-Ile, D-Val and L-Val. This result left the ambiguity on the localization of the two methylisoleucine residues and of the two enantiomeric valine residues. Since the ^{1}H and ^{13}C NMR resonances for the amino acids at positions 5–10 and 36–41 of **2** were almost superimposable with the corresponding values reported for theonellapeptolide Id (**1**) [22], we assumed that the two peptides share the configurations at those positions, thus inferring the configurations of the two isoleucine residues. Similarly, it appeared reasonable to assume that, as in the co-occurring theonellapeptolide Id (and in all the theonellapeptolide found to date), the L-Val could be the *N*-terminal amino acid and thus, the D-Val should be the amino acid at positions 28–32. A D-Val residue at these positions has been found previ-

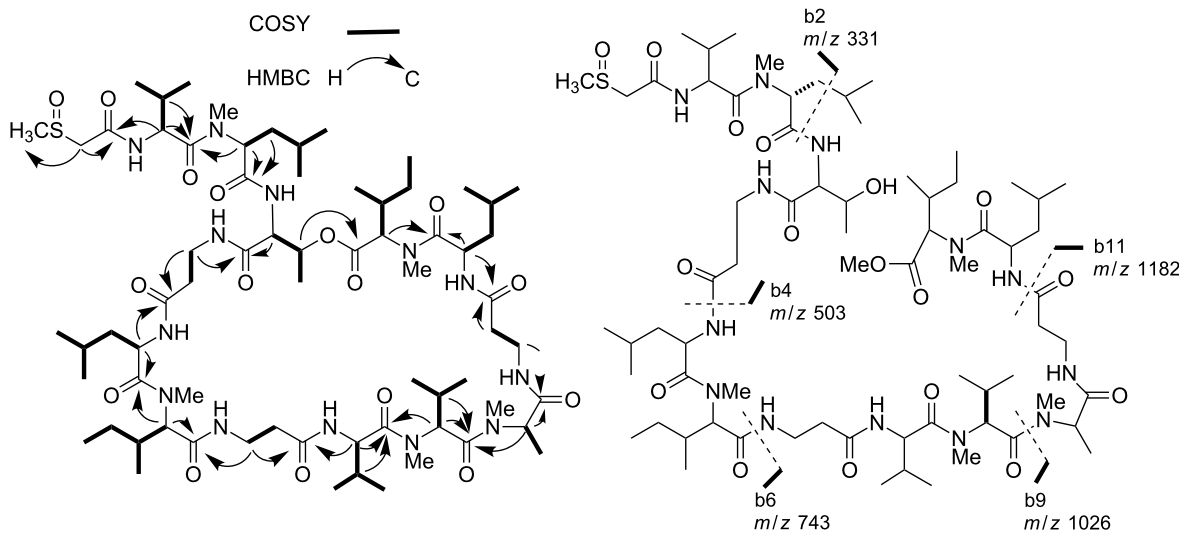


Figure 3: COSY and key HMBC correlations (left) and MS/MS fragmentations of **2** and its ring-opened methanolysis product, respectively.

ously in the structure of theonellapeptolide Ia [23]. The configuration at the stereogenic sulfur atom of **2** has been left undetermined.

Theonellapeptolide If (**3**, $[\alpha]_D$ −26.7, *c* 1.0, MeOH) was isolated as a colorless amorphous solid and its molecular formula was established to be $C_{68}H_{121}N_{13}O_{16}$ by means of high resolution ESIMS. Inspection of ^1H and ^{13}C NMR spectra of **3** (CD_3OD, Table 2) revealed extensive similarities with parallel data detected for **2**. The most important differences could be recognized in the downfield shift of one methyl singlet (from δ_H 2.79, δ_C 39.2 in **2** to δ_H 3.38, δ_C 59.1 in **3**) and of a pair of mutually coupled doublets (from δ_H 3.67 and 3.86, δ_C 58.9 in **2** to δ_H 3.88 and 3.97, δ_C 71.8 in **3**). These data were easily rationalized with the replacement of the terminal methylsulfinylacetyl group with a methoxyacetyl group, a typical *N*-terminus acylating unit, already found in the theonellapeptolide family.

Careful inspection of COSY and TOCSY spectra revealed also that, in agreement with the molecular formula, one isoleucine residue of **2** is replaced by a valine residue in **3**. A subsequent combined analysis of homonuclear and heteronuclear 2D NMR

Table 2: ^1H (500 MHz) and ^{13}C (125 MHz) NMR data of theonellapeptolide If (**3**) in CD_3OD [24].

AA	Position	δ_H, m, *J* in Hz	δ_C	AA	Position	δ_H, m, *J* in Hz	δ_C
L-Thr	1	–	169.2	β-Ala	33	–	173.2
	2	4.38, m	57.5		34/34’	2.29, m; 2.59, m	36.5
	3	5.15, m	69.3		35/35’	3.10, m; 4.17, m	36.8
	4	1.13, d, 6.5	17.5	L-Me-Ile	36	–	172.5
D-Me-Val	5	–	171.5		37	3.14, m	71.2
	6	4.95, m	62.2		38	2.48, m	36.5
	7	2.27[a]	26.7		39/39’	1.04, m; 1.92[a]	30.2
	8	0.76, d, 7.2	11.5		40	1.00[a]	13.2
	9	0.99, d, 7.2	23.5		41	0.81, d, 6.4	15.3
	6-NMe	3.17, s	31.3		37-NMe	3.35, s	39.9
				D-Leu	42		176.2
D-Leu	11	–	177.0		43	5.09, m	50.6
	12	5.01, m	48.5		44	1.72[a]; 1.25[a]	41.2
	13/13’	1.65[a], 1.25[a]	40.3		45	1.78[a]	26.6
	14	1.74[a]	24.9		46	1.03[a]	21.0
	15	0.96[a]	11.1		47	1.04[a]	25.0
	16	0.98 d, 7.3	17.2	β- Ala	48	–	175.0
β-Ala	17	–	174.3		49/49’	2.28, m; 2.36, m	39.1
	18/18’	2.23, m 2.31 m	39.5		50/50’	3.14, m; 3.81, m	37.7
	19/19’	3.15, m 3.85, m	38.2	D-Me-Leu	51	–	175.2
L-Me-Ala	20	–	172.5		52	5.18, m	56.4
	21	5.17[a]	58.5		53/53’	1.41[a]; 2.03 m	39.5
	22	1.45, d, 7.1	16.0		54	1.52[a]	27.1
	21-NMe	2.77 s	30.5		55	0.83, d, 6.7	22.1
L-Me-Val	23	–	173.0		56	0.95[a]	24.3
	24	5.02[a]	59.4		52-NMe	3.30 s	33.0
	25	2.40, m	30.2	L-Val	57	–	176.0
	26	0.86[a]	20.6		58	4.98, m	54.6
	27	0.92, d, 6.1	20.8		59	2.08, m	31.6
	24-NMe	3.31 s	31.9		60	0.98[a]	20.4
D-Val	28	–	173.2		61	1.01[a]	19.2
	29	4.76, m	68.9	MeO-Ac	62		169.2
	30	2.68, m	27.6		63/63’	3.88, d, 11.2;	71.8
	31	0.86[a]	18.1			3.97, d, 11.2	
	32	1.17, d, 6.5	23.3		63-OMe	3.38	59.1

[a]Overlapped with other signals.

spectra disclosed the presence of the following residues: three β-Ala, three Leu (one *N*-methylated), one *N*-methyl-Ile, four Val (two *N*-methylated), one Thr, and one *N*-methylAla. As detailed for **2**, the amino acid sequence of **3** was deduced by careful analysis of HMBC correlations and supported by the MS/MS spectrum of the methanolysis product mixture (see Supporting Information File 1). Thus, theonellapeptolide If (**3**) has been identified as a new member of the theonellapeptolide family differing from theonellapeptolide Id (**1**) by the replacement of two isoleucine residues (positions 5–10 and 28–32) with valine residues. Complete acid hydrolysis of **3** and Marfey's analysis [21] on the hydrolysate mixture provided the configuration of the chiral amino acid residues as L-MeAla, D-Leu (×2), D-MeLeu, L-Thr, L-Me-Ile, D-Me-Val, D-Val, L-Me-Val and L-Val. With these data in hands, it was not possible to unambiguously define the exact localization of the valine residues. However, if we assume that the L-Val and L-Me-Val residues are localized at the same positions as in theonellapeptolide Id, then the positions of their enantiomeric counterparts are consequently deduced. In summary, compound **3** is a valine-rich theonellapeptolide, being the first member of this class to possess four valine residues.

Theonellapeptolides are structurally similar to the widely used immunosuppressant drug cyclosporin A, sharing at least three important features: i) the exclusive presence of hydrophobic aliphatic amino acids; ii) the abundance of *N*-methylated residues and iii) the presence of a macrocycle made up by more than ten amino acids. Only a few theonellapeptolides have been tested for immunosuppressive activity and they revealed a moderate potency [25]. In general, the potential bioactivity of this class of unique cyclopeptides has not been investigated in great detail, and an inhibition of the development of fertilized eggs of sea urchin [26], an activity on the transport of Na^+ and K^+ ions [23], and a moderate cytotoxicity [23] have been reported.

The three theonellapeptolides isolated during the present investigation (**1**–**3**) have been evaluated for their antiproliferative activity against HepG2 cells, a hepatic carcinoma cell line. As reported in Figure 4, all tested compounds showed antiproliferative activity at low micromolar doses, with a similar pattern of potency. At the dose 10 μM, the proliferation rate of HepG2 cells was significantly reduced by theonallapeptolide Id (**1**), sulfinyltheonellapeptolide (**2**) and theonellapeptolide If (**3**) to about 50%, 30% and 50%, respectively (Figure 4, panels A, B and C; * $p<0.05$ compared to untreated cells; $n = 4$). Only theonellapeptolide Id was able to significantly reduce the proliferation at 1 μM. At this dose, the proliferation reduction was equal to 20% (Figure 4, panel A; * $p < 0.05$ compared to untreated cells; $n = 4$). Computation of 50% inhibitory drug concentration (IC_{50}) revealed that compounds **1**, **2** and **3** were characterized by very similar IC_{50} values of about 1.5 μM for theonellapeptolide Id and 3 μM for sulfinyltheonellapeptolide and theonellapeptolide If.

Conclusion

In conclusion, the chemical analysis of the organic extract of an Indonesian *Theonella swinhoei* allowed the isolation of two new members of the theonellapeptolide family, namely sulfinyltheonellapeptolide, characterized by a methylsulfinylacetyl group at the *N*-terminus, and theonellapeptolide If, the first member of this class to show four valine residues. The structures of the compounds have been determined by extensive 2D NMR and MS/MS analyses followed by the application of Marfey's method. The position of D- and L-residues was also assigned on the basis of a comparison with known compounds.

A moderate antiproliferative activity on a hepatic carcinoma cell line has been disclosed for the isolated compounds. A more detailed evaluation of the pharmacological profile of this class of marine peptides is underway in our groups.

Experimental

General experimental procedures: Optical rotations were measured on a Perkin–Elmer 243 B polarimeter. Low and high-resolution ESIMS and MS/MS experiments were carried out on a LTQ OrbitrapXL (Thermo Scientific) mass spectrometer. NMR spectra were obtained on Varian Inova 500 MHz spectrometer (^1H at 500 MHz, ^{13}C at 125 MHz); δ (ppm), *J* in Hz, spectra referred to CD_3OD (δ_H 3.32, δ_C 55.0) as an internal standard. Homonuclear ^1H connectivities were determined by COSY experiments. Single-bond heteronuclear $^1H/^{13}C$ connectivities were determined with the HSQC experiment. Two and three bond $^1H/^{13}C$ connectivities were determined by gradient 2D HMBC experiments optimized for a $^{2,3}J = 9$ Hz. Medium-pressure liquid chromatography was performed on a Büchi apparatus by using a silica gel (230–400 mesh) column. HPLC was achieved on a Knauer apparatus equipped with a refractive index detector and analytical LUNA (Phenomenex) columns. The purities of compounds were determined to be greater than 95% by HPLC.

Animal material, extraction and isolation: *Theonella swinhoei* (order Lithistida, family Theonellidae) was collected in the Bunaken Marine Park of Manado (North Sualwesi, Indonesia) in January 2010 and frozen immediately after collection. A reference sample of the sponge has been deposited at the Department of Pharmacy, University of Naples Federico II, with the code Man-10-06. The frozen material (16.5 g) was extracted with methanol (3 × 1.5 L) at room temperature, and the crude methanolic extract was subjected to a modified

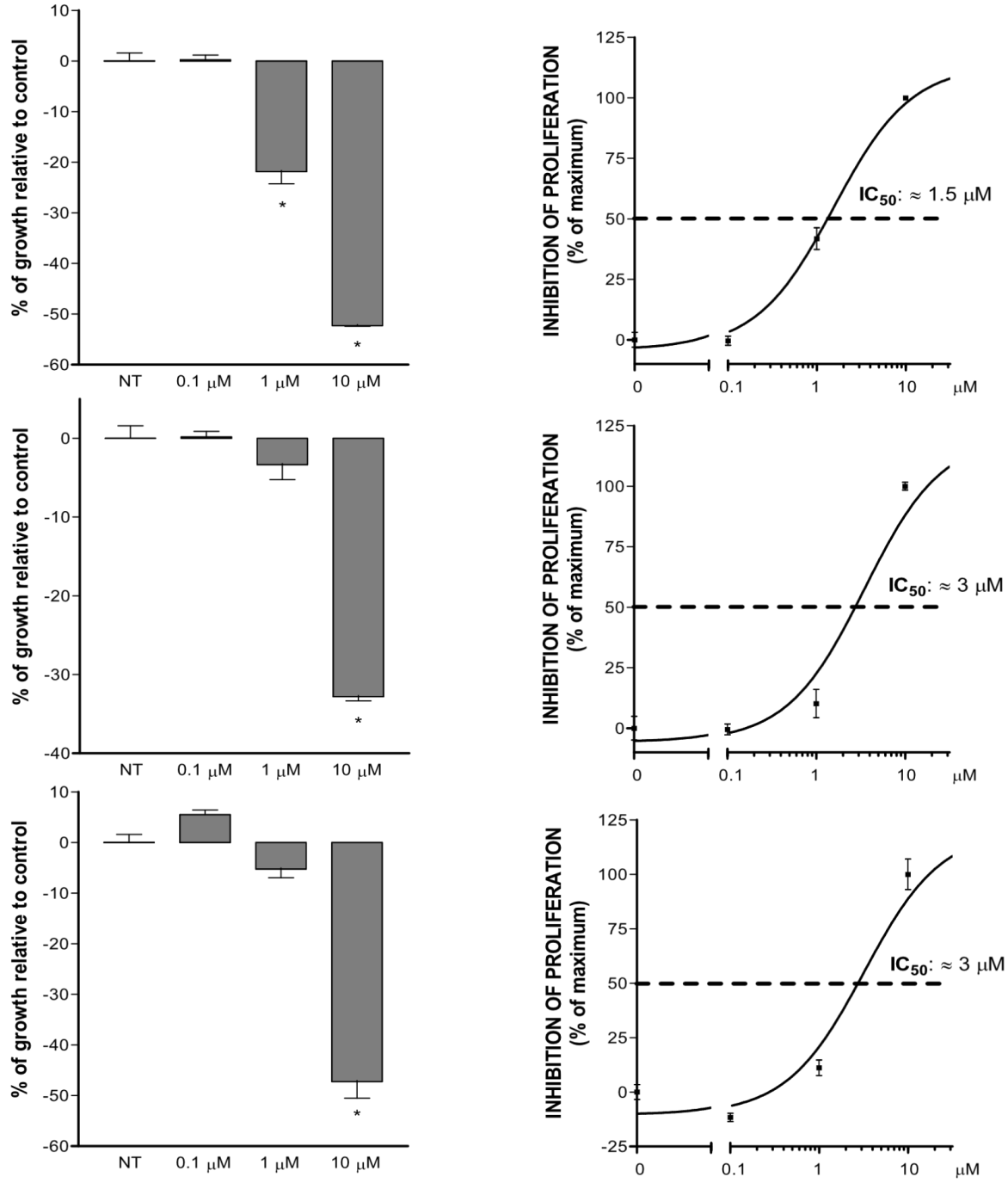


Figure 4: Antiproliferative activity of theonellapeptolides **1**–**3** on hepatic carcinoma cell line. The MTT assay was performed on HepG2 cells treated with increasing doses for 48 hours. Left panel: Proliferation rate expressed as Δ% of absorbance compared to untreated cells. The values are expressed as the mean ± standard error. Right panel: Computation of IC_{50} values. From top to bottom: Theonellapeptolide Id, sulfinyltheonellapeptolide and theonellapeptolide If (* $p < 0.05$ compared to untreated cells; $n = 4$).

Kupchan's partitioning procedure as described in [26]. The $CHCl_3$ extract (4.76 g) was chromatographed with a silica gel MPLC by using a solvent gradient system from CH_2Cl_2 to CH_2Cl_2/MeOH 8:2. The fractions eluted with CH_2Cl_2/MeOH 97:3 (853.3 mg) were further purified by silica gel column chromatography followed by HPLC on a Nucleodur 100-5 C_{18} (Phenomenex) (5 μm; 7.8 mm i.d. × 250 mm) with MeOH/H_2O (9:1) as an eluent (flow rate 0.9 mL/min) to give theonellapeptolide Id (**1**) (68.5 mg), sulfinyltheonellapeptolide (**2**, 4.6 mg) and theonellapeptolide If (**3**, 2.1 mg).

Sulfinyltheonellapeptolide (2): Colorless amorphous solid; $[\alpha]_D^{25}$ −38.0 (*c* 0.1, CH_3OH); ^1H and ^{13}C NMR data in CD_3OD are given in Table 1; ESIMS: *m*/*z* 1423 $[M + H]^+$ and 1445 $[M + Na]^+$. HRMS–ESI (*m*/*z*): $[M + Na]^+$ calcd for $C_{69}H_{123}N_{13}NaO_{16}S$, 1444.8829; found, 1444.8834.

Theonellapeptolide If (3): Colorless amorphous solid; $[\alpha]_D^{25}$ −26.7 (*c* 0.1, CH_3OH); ^1H and ^{13}C NMR data in CD_3OD are given in Table 2; ESIMS (*m*/*z*): 1377 $[M + H]^+$ and 1399 $[M + Na]^+$. HRMS–ESI (*m*/*z*): $[M + Na]^+$ calcd for $C_{69}H_{121}N_{13}NaO_{16}$, 1398.8952; found, 1398.8949.

Acid hydrolysis and Marfey's analysis: Peptide samples (600 μg) were subjected to acid hydrolysis and subsequent Marfey's analysis in a similar manner as described in [27]. LC–MS analysis (ESIMS, positive ion mode): individual FDAA-amino acid peak was identified by co-injection with standard amino acid derivatives. The retention times (min) of the FDAA standards were 18.15 for L-Thr, 21.50 for L-MeAla, 29.91 for l-Val, 34.04 for L-MeVal, 34.23 for D-Val, 38.25 for L-MeIle, 34.42 for D-MeVal, 41.35 for D-*allo*-MeIle, 43.20 for D-Leu, 45.08 for D-MeLeu. Observed amino acids and their retention times (min) for FDAA derivatives of acid hydrolysate of **2** and **3**: **2** 18.12 for L-Thr, 21.39 for L-MeAla, 29.98 for l-Val, 34.01 for L-MeVal, 34.31 for D-Val, 38.18 for L-MeIle, 41.32 for D-*allo*-MeIle, 43.19 for D-Leu, 45.01 for D-MeLeu. **3** 18.12 for L-Thr, 21.36 for L-MeAla, 29.99 for l-Val, 34.02 for L-MeVal, 34.29 for D-Val, 38.19 for L-MeIle, 34.40 for D-MeVal, 43.17 for D-Leu, 45.02 for D-MeLeu.

Evaluation of antiproliferative activity: HepG2 cells were plated in a 24-wells plate at 3×10^4 cells/well, in Minimum Essential Medium with Earl's salts containing 10% fetal bovine serum (FBS), 1% L-glutamine and 1% penicillin/streptomycin. On day 2, cells were treated with increasing doses of theonellapeptolide Id (0.1, 1 and 10 μM), sulfinyltheonellapeptolide (0.1, 1 and 10 μM) and theonellapeptolide If (0.1, 1 and 10 μM) for 48 hours. On day 4, a MTT assay was assessed: 100 μL of MTT solution (5mg/mL) were added to each well and the cells were incubated at 37 °C for 4 hours. After the incubation, the culture medium was removed and 1 mL of DMSO was added to each well. The absorbance was read by using a spectrophotometer at 590 nM. The proliferation rate was reported as the delta of absorbance compared to untreated cells, and values are expressed as mean ± standard error. Experiments were performed in quadruplicate. For each compound the IC_{50} value was evaluated as follows: The inhibition of proliferation was expressed as percentage compared to the inhibition of proliferation observed at the highest dose of any experimental setting (which was arbitrarily assigned a value of 100%).

Supporting Information

Supporting Information File 1

COSY, key HMBC correlations and MS/MS fragmentations of **3**, and ^1H and COSY spectra for sulfinyltheonellapeptolide (**2**) and theonellapeptolide If (**3**).
[http://www.beilstein-journals.org/bjoc/content/supplementary/1860-5397-9-188-S1.pdf]

Acknowledgements

This work was supported by the EU project Bluegenics (Grant 311848) and by the University of Naples Federico II (MOU with Universitas Sam Ratulangi, Manado). NMR spectra were recorded at the CSIAS, Centro Interdipartimentale di Analisi Strumentale, Department of Pharmacy, University of Naples Federico II. This research was partially conduced during the Master Course "Tropical Marine Biodiversity and Natural Products" of the Università Politecnica delle Marche.

References

1. Kho, E.; Imagawa, D. K.; Rohmer, M.; Kashman, Y.; Djerassi, C. *J. Org. Chem.* **1981,** *46,* 1836–1839. doi:10.1021/jo00322a019 The first paper reporting a chemical investigation on a Theonella sponge dates back to 1981.
2. De Marino, S.; Ummarino, R.; D'Auria, M. V.; Chini, M. G.; Bifulco, G.; Renga, B.; D'Amore, C.; Fiorucci, S.; Debitus, C.; Zampella, A. *J. Med. Chem.* **2011,** *54,* 3065–3075. doi:10.1021/jm200169t
3. Renga, B.; Mencarelli, A.; D'Amore, C.; Cipriani, S.; D'Auria, M. V.; Sepe, V.; Chini, M. G.; Monti, M. C.; Bifulco, G.; Zampella, A.; Fiorucci, S. *PLoS One* **2012,** *7,* e30443. doi:10.1371/journal.pone.0030443
4. Festa, C.; De Marino, S.; D'Auria, M. V.; Bifulco, G.; Renga, B.; Fiorucci, S.; Petek, S.; Zampella, A. *J. Med. Chem.* **2011,** *54,* 401–405. doi:10.1021/jm100968b
5. Bubb, M. R.; Spector, I.; Bershadsky, A. D.; Korn, E. D. *J. Biol. Chem.* **1995,** *270,* 3463–3466.
6. Angawi, R. F.; Bavestrello, G.; Calcinai, B.; Dien, H. A.; Donnarumma, G.; Tufano, M. A.; Paoletti, I.; Grimaldi, E.; Chianese, G.; Fattorusso, E.; Taglialatela-Scafati, O. *Mar. Drugs* **2011,** *9,* 2809–2817. doi:10.3390/md9122809
7. Piel, J.; Hui, D.; Wen, G.; Butzke, D.; Platzer, M.; Fusetani, N.; Matsunaga, S. *Proc. Natl. Acad. Sci. U. S. A.* **2004,** *101,* 16222–16227. doi:10.1073/pnas.0405976101
8. Freeman, M. F.; Gurgui, C.; Helf, M. J.; Morinaka, B. I.; Uria, A. R.; Oldham, N. J.; Sahl, H.-G.; Matsunaga, S.; Piel, J. *Science* **2012,** *338,* 387–390. doi:10.1126/science.1226121
9. Matsunaga, S.; Fusetani, N. *J. Org. Chem.* **1995,** *60,* 1177–1181. doi:10.1021/jo00110a020
10. Kobayashi, J.; Itagaki, F.; Shigemori, H.; Takao, T.; Shimonishi, Y. *Tetrahedron* **1995,** *51,* 2525–2532. doi:10.1016/0040-4020(95)00017-3
11. Ford, P. W.; Gustafson, K. R.; McKee, T. C.; Shigematsu, N.; Maurizi, L. K.; Pannell, L. K.; Williams, D. E.; Dilip de Silva, E.; Lassota, P.; Allen, T. M.; Van Soest, R.; Andersen, R. J.; Boyd, M. R. *J. Am. Chem. Soc.* **1999,** *121,* 5899–5909. doi:10.1021/JA990582O

12. Hamada, T.; Matsunaga, S.; Yano, G.; Fusetani, N. *J. Am. Chem. Soc.* **2005,** *127,* 110–118. doi:10.1021/ja045749e
13. Fusetani, N.; Matsunaga, S.; Matsumoto, H.; Takebayashi, Y. *J. Am. Chem. Soc.* **1990,** *112,* 7053–7054. doi:10.1021/ja00175a045
14. Festa, C.; De Marino, S.; D'Auria, M. V.; Monti, M. C.; Bucci, M.; Vellecco, V.; Debitus, C.; Zampella, A. *Tetrahedron* **2012,** *68,* 2851–2857. doi:10.1016/j.tet.2012.01.097
15. Festa, C.; De Marino, S.; Sepe, V.; D'Auria, M. V.; Bifulco, G.; Andrés, R.; Terencio, M. C.; Payá, M.; Debitus, C.; Zampella, A. *Tetrahedron* **2011,** *67,* 7780–7786. doi:10.1016/j.tet.2011.07.077
16. Festa, C.; De Marino, S.; Sepe, V.; D'Auria, M. V.; Bifulco, G.; Débitus, C.; Bucci, M.; Vellecco, V.; Zampella, A. *Org. Lett.* **2011,** *13,* 1532–1535. doi:10.1021/ol200221n
17. Kitagawa, I.; Kobayashi, M.; Lee, N. K.; Shibuya, H.; Kawata, Y.; Sakiyama, F. *Chem. Pharm. Bull.* **1986,** *34,* 2664–2667. doi:10.1248/cpb.34.2664
18. Angawi, R. F.; Calcinai, B.; Cerrano, C.; Dien, H. A.; Fattorusso, E.; Scala, F.; Taglialatela-Scafati, O. *J. Nat. Prod.* **2009,** *72,* 2195–2198. doi:10.1021/np900669d
19. Kupchan, S. M.; Britton, R. W.; Ziegler, M. F.; Sigel, C. W. *J. Org. Chem.* **1973,** *38,* 178–179. doi:10.1021/jo00941a049
20. Roepstorff, P.; Fohlman, J. *Biomed. Mass Spectrom.* **1984,** *11,* 601. doi:10.1002/bms.1200111109
21. Marfey, P. *Carlsberg Res. Commun.* **1984,** *49,* 591–596. doi:10.1007/BF02908688
22. Kitagawa, I.; Lee, N. K.; Kobayashi, M.; Shibuya, H. *Tetrahedron* **1991,** *47,* 2169–2180. doi:10.1016/S0040-4020(01)96128-9
23. Kobayashi, M.; Lee, N. K.; Shibuya, H.; Momose, T.; Kitagawa, I. *Chem. Pharm. Bull.* **1991,** *39,* 1177–1184. doi:10.1248/cpb.39.1177
24. In the numbering system of theonellapeptolide If (**3**) we have skipped position 10 to allow for a better comparison between the NMR data of theonellapeptolide If (**3**) and sulfinyltheonellapeptolide (**2**).
25. Kobayashi, M.; Kanzaki, K.; Katayama, S.; Ohashi, K.; Okada, H.; Ikegami, S.; Kitagawa, I. *Chem. Pharm. Bull.* **1994,** *42,* 1410–1415. doi:10.1248/cpb.42.1410
26. Gala, F.; D'Auria, M. V.; De Marino, S.; Zollo, F.; Smith, C. D.; Copper, J. E.; Zampella, A. *Tetrahedron* **2007,** *63,* 5212–5219. doi:10.1016/j.tet.2007.03.162
27. Sepe, V.; D'Orsi, R.; Borbone, N.; D'Auria, M. V.; Bifulco, G.; Monti, M. C.; Catania, A.; Zampella, A. *Tetrahedron* **2006,** *62,* 833–840. doi:10.1016/j.tet.2005.10.058

License and Terms

This is an Open Access article under the terms of the Creative Commons Attribution License (http://creativecommons.org/licenses/by/2.0), which permits unrestricted use, distribution, and reproduction in any medium, provided the original work is properly cited.

The license is subject to the *Beilstein Journal of Organic Chemistry* terms and conditions: (http://www.beilstein-journals.org/bjoc)

The definitive version of this article is the electronic one which can be found at: doi:10.3762/bjoc.9.188

Beilstein Journal of Organic Chemistry

Synthesis of the reported structure of piperazirum using a nitro-Mannich reaction as the key stereochemical determining step

James C. Anderson*[1], Andreas S. Kalogirou[1], Michael J. Porter[1] and Graham J. Tizzard[2,§]

Letter

Open Access

Address:
[1]Department of Chemistry, University College London, 20 Gordon Street, London, WC1H 0AJ, UK and [2]National Crystallography Service, School of Chemistry, University of Southampton, Southampton, SO17 1BJ, UK

Email:
James C. Anderson* - j.c.anderson@ucl.ac.uk; Graham J. Tizzard - gjt1@soton.ac.uk

* Corresponding author
§ Corresponding author for crystallographic results

Keywords:
alkaloid; aza-Henry; natural products; nitro-Mannich; piperazinone; stereoselective synthesis

Beilstein J. Org. Chem. **2013,** *9,* 1737–1744.
doi:10.3762/bjoc.9.200

Received: 10 July 2013
Accepted: 01 August 2013
Published: 23 August 2013

This article is part of the Thematic Series "Natural products in synthesis and biosynthesis".

Guest Editor: J. S. Dickschat

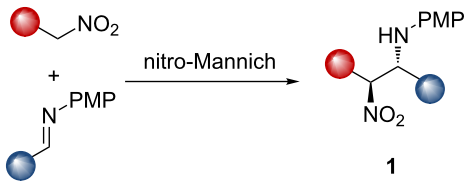
© 2013 Anderson et al; licensee Beilstein-Institut.
License and terms: see end of document.

Abstract

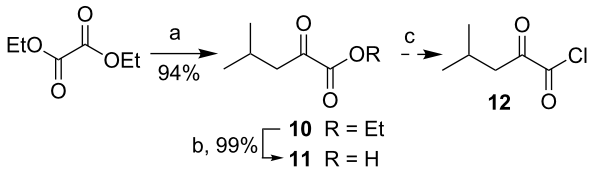
Piperazirum, isolated from *Arum palaestinum* Boiss, was originally assigned as *r*-3,*c*-5-diisobutyl-*c*-6-isopropylpiperazin-2-one. The reported structure was synthesised diastereoselectively using a key nitro-Mannich reaction to set up the C5/C6 relative stereochemistry. The structure was unambiguously assigned by single crystal X-ray diffraction but the spectroscopic data did not match those reported for the natural product. The structure of the natural product must therefore be revised.

Introduction

The nitro-Mannich reaction (or aza-Henry reaction) has been developed to a standard where the product β-nitroamines **1** are now privileged building blocks. In part this is due to the complementary synthetic flexibility available from the two different nitrogen atom oxidation states (Scheme 1) [1]. They have been used to synthesise many nitrogen-containing functional groups including α-amino carbonyls [2,3], peptidomimetics [4], natural products [5-10] and many heterocyclic small molecules [11-24] of importance to drug discovery. Enantioselective reactions have been controlled by asymmetric metal-centred Lewis acids; chiral hydrogen bond donors, in particular by the use of asymmetric thiourea organocatalysts, chiral Brønsted acids, phase-transfer catalysts and Brønsted base catalysts [3,15,25-39]. A large part of our own work in developing the nitro-Mannich reaction was to demonstrate the preparation of stereodefined 1,2-diamines [40-45].



Scheme 1: Schematic nitro-Mannich reaction.



Scheme 3: (a) iBuMgCl, Et_2O, −78 °C; (b) KOH, EtOH/H_2O, 100 °C; (c) $(COCl)_2$.

As part of a programme aimed at using these 1,2-diamines as building blocks in target synthesis we focused on the synthesis of a novel bioactive alkaloid, piperazirum (**2**, Scheme 2), which to our knowledge had not been previously synthesised. Piperazirum was isolated from the leaf extract of *Arum palaestinum* Boiss and was shown to possess significant cytotoxicity against cultured tumor cell lines in vitro [46]. Its chemical structure and relative stereochemistry were elucidated by high resolution mass spectrometry, infrared, 1D and 2D NMR spectroscopy [46]. Retrosynthetically we envisaged that the C-3 stereocentre could be set up by hydrogenation from the less hindered face of α-iminolactam **3** or α,β-unsaturated lactam **4** (Scheme 2). These heterocycles could be derived from a common α-keto acid derivative **5** and either diamine **6** or **7**, that could in turn be prepared from β-nitroamine **8** or **9**. Each of the β-nitroamines could be prepared enantioselectively by using our previously reported methodology [28,43,45] and would allow elucidation of the absolute stereochemistry of piperazirum (**2**).

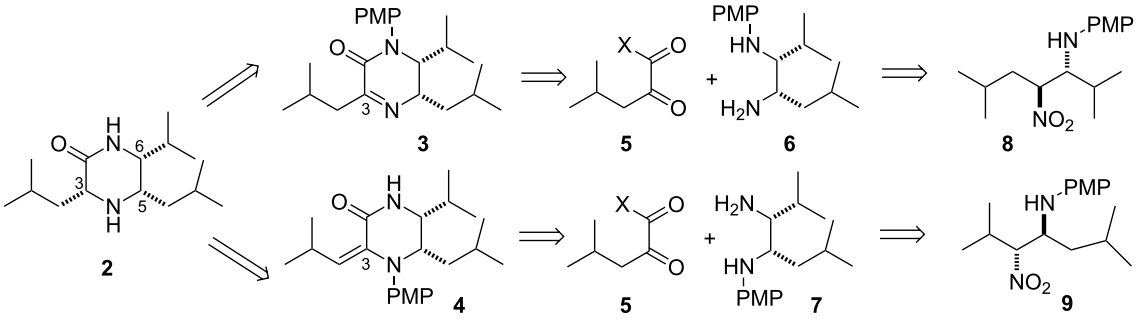
Results and Discussion

The common α-keto acid derivative **5** was easily prepared from a Grignard reaction of isobutylmagnesium chloride with diethyl oxalate to give α-keto ester **10** in 94% yield (Scheme 3) [47]. Saponification of **10** with KOH provided α-keto acid **11** in excellent yield [48], and the corresponding acid chloride **12** was prepared in situ by treatment with oxalyl chloride [49].

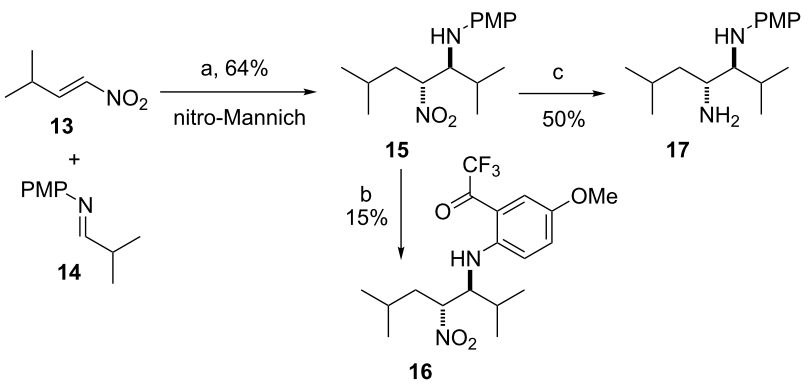
For the synthesis of β-nitroamine **8** we decided to make use of the reductive nitro-Mannich reaction as the starting nitroalkene **13** is readily available from a Henry reaction [50], imine **14** from the condensation of *p*-anisidine and isobutyraldehyde, and the process can easily be made asymmetric [45]. Conjugate addition of hydride to **13** and subsequent trapping of the nitronate anion with freshly prepared imine **14** in THF gave β-nitroamine **15** in 64% conversion and a dr of 70:30 (Scheme 4). Quite frequently β-nitroamines are unstable and susceptible to retroaddition [43,44]. Formation of the corresponding trifluoroacetamide derivative confers stability and allows them to be purified. Using previously developed conditions to protect the amine in situ using $(CF_3CO)_2O$ gave only β-nitroamine **16** as a single diastereoisomer in a low 15% yield. These results are consistent with the poor conversions and dr, as well as resistance to trifluoroacetamide protection, we have observed before from imines derived from α-branched aldehydes such as cyclohexanecarbaldehyde [44].

In cases where trifluoroacetylation fails, it is quite common to purify the β-nitroamine by rapid column chromatography, quickly followed by reduction to give the corresponding 1,2-diamine. In this case rapid purification of **15** followed by reduction with Zn/HCl gave the 1,2-diamine **17** as a single diastereoisomer in 50% yield (Scheme 4).

With diamine **17** in hand, the reaction with a suitable keto acid derivative was investigated. We presumed that the nitrogen of the primary amine would be the more nucleophilic and hence should react with the more electrophilic carbonyl group – i.e.



Scheme 2: Retrosynthetic analysis of piperazirum.



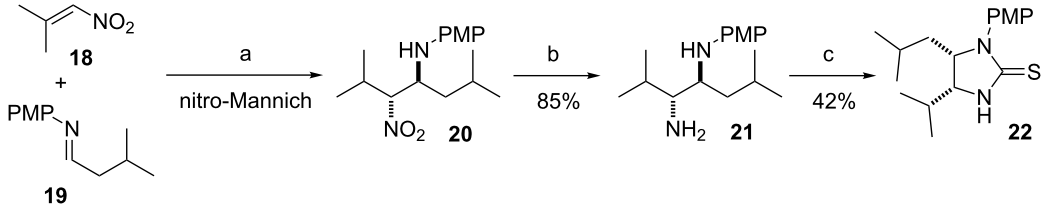
Scheme 4: (a) Li(Et_3BH), THF, rt then **14**, CF_3CO_2H, −78 °C, dr 70:30; (b) $(CF_3CO)_2O$, Py, CH_2Cl_2, 0 °C to rt; (c) Zn, 6 M HCl, EtOAc/EtOH, rt.

the ketone – in **10** [51,52]. Attempted formation of **4** by heating a mixture of **10** and **17** in H_2O at 50 °C gave a complicated mixture of products and attempts under Dean–Stark conditions in toluene with TsOH gave only recovered starting materials [53].

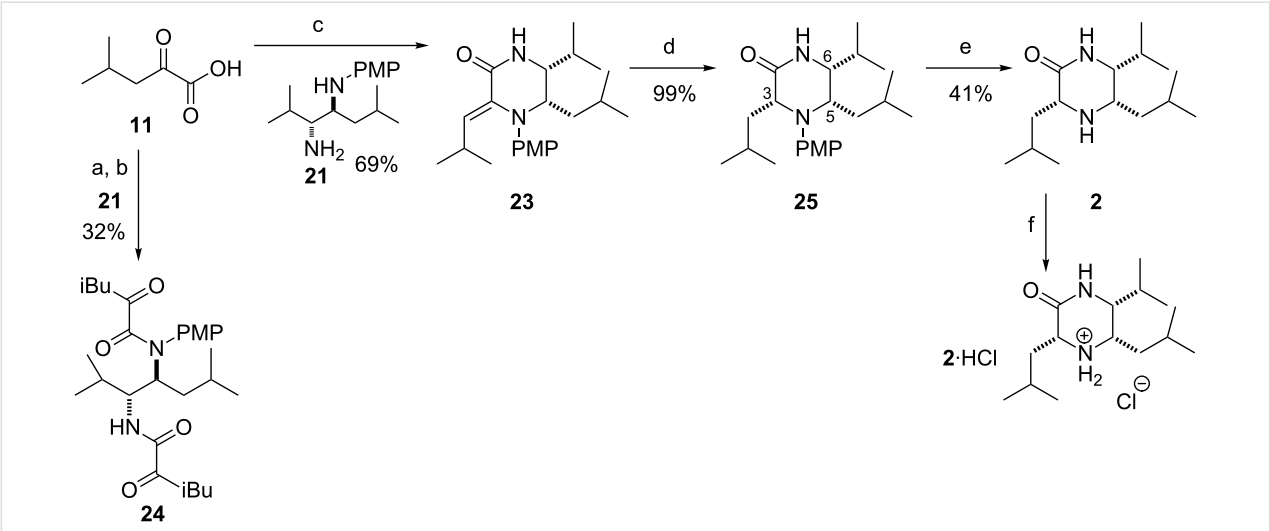
In light of this poor result, the alternative route to **2** via β-nitroamine **9** was investigated. A reductive nitro-Mannich reaction between nitroalkene **18** [54] and freshly prepared imine **19** in CH_2Cl_2 followed by rapid flash chromatography gave β-nitroamine **20** with complete conversion and dr >95:5 [55]. As before immediate reduction with Zn/HCl gave the PMP-protected diamine **21** in 85% yield as a single diastereoisomer determined by ^{1}H NMR (Scheme 5).

From a comprehensive series of examples of the reductive nitro-Mannich reaction, the vast majority of substrates demonstrate *anti*-relative stereochemistry [23,44,45]. More direct proof for **21** was gleaned from the corresponding imidazolidine-2-thione formed by treatment with thiophosgene to give **22** (Scheme 5). In one dimensional nOe studies irradiation of the C*H*NH peak (δ 3.70, 1H, dd, J = 8.4, 5.4 Hz) caused a 3.65% enhancement of the C*H*N peak (δ 4.31, 1H, dt, J = 7.9, 5.9 Hz), indicating a *cis*-relative stereochemistry between the two protons, which confirmed the *anti*-relative stereochemistry of **21**. The observed coupling constant between the same two protons was 8.2 Hz (averaged) and was similar to other imidazolidine-2-thiones we have prepared that have been corroborated by single crystal X-ray crystallography [56]. Further stereochemical proof was provided by a single crystal X-ray structure determination of **2**·HCl (vide infra).

We presumed again that the primary amine of **21** would be more nucleophilic towards a keto acid derivative **5**. In order to obtain a piperazinone of the desired connectivity (**23**) a keto acid derivative would be required where the carboxylate carbonyl is more reactive than the ketone carbonyl. Two possible such compounds were considered, acid chloride **12** and carboxylic acid **11** treated with a suitable coupling agent. Acid chloride **12** was prepared in situ by treatment of acid **11** with oxalyl chloride (2.00 equiv) and catalytic DMF. Subsequent reaction with diamine **21** in the presence of pyridine (1.20 equiv) and catalytic DMAP over 24 h, according to previously reported reactions for similar keto acids [49], gave only the bis-adduct **24** and none of the desired piperazinone **23**. By contrast, the reaction of carboxylic acid **11** with diamine **21**, in the presence of EDC (1.50 equiv) and 1-hydroxybenzotriazole (1.50 equiv) at rt, gave the desired product **23** in good yield (Scheme 6) [57]. The double bond geometry was assigned as *Z* by NOESY ^{1}H NMR and probably results from steric inhibi-



Scheme 5: (a) Li(Et_3BH), CH_2Cl_2, rt then **19**, CF_3CO_2H, −78 °C, dr >95:5; (b) Zn, 6 M HCl, EtOAc/EtOH, rt, single diastereoisomer; (c) $CSCl_2$, aq $NaHCO_3$ CH_2Cl_2/ MeOH, rt.



Scheme 6: (a) $(COCl)_2$, DMF, CH_2Cl_2, rt; (b) **21**, Py, DMAP, CH_2Cl_2, rt; (c) EDC, HOBt, THF/CH_2Cl_2, rt; (d) H_2 (1 atm), Pd/C, MeOH, rt; (e) CAN, MeCN/H_2O, 0 °C; (f) 4 M HCl in dioxane, MeCN/Et_2O.

tion of resonance which would result in the formation of the *E* iPr group and the planar amide group during formation of **23**.

Reduction of the double bond with hydrogen over palladium on charcoal gave a single diastereoisomer **25** in quantitative yield. In one dimensional nOe studies irradiation of H-3 (δ 4.09, 1H, dd, J = 9.9, 4.5 Hz) caused a 0.17% enhancement of the H-6 signal (δ 3.18, 1H, dd, J = 10.0, 3.5 Hz) with negligible enhancement of the H-5 signal (δ 3.37, 1H, dt, J = 12.4, 3.1 Hz). Irradiation of H-5 caused a 2.90% enhancement of the H-6 signal and a 0.07% enhancement of the H-3 signal. The nOe data tentatively suggested that protons H-3, H-5 and H-6 were all on the same face of the molecule. Deprotection of the PMP group with CAN gave compound **2**. Extensive NMR (COSY, HMBC and NOESY) and analytical data were consistent with the structure drawn (**2**), but the ^1H and ^{13}C NMR did not match that published for piperazirum (Table 1) [46]. The original authors recorded their NMR data for piperazirum in D_2O [58], but our sample **2** was insoluble. Compound **2** was readily soluble in DMSO-d_6 and $CDCl_3$, but neither gave a satisfactory match to the reported NMR data. Preparation of **2**·HCl allowed the recording of NMR spectra in D_2O, but again the chemical shifts were inconsistent with those reported. Single crystal X-ray structure determination of **2** proved unambiguously the assigned structure obtained from spectroscopic data (Figure 1) [59].

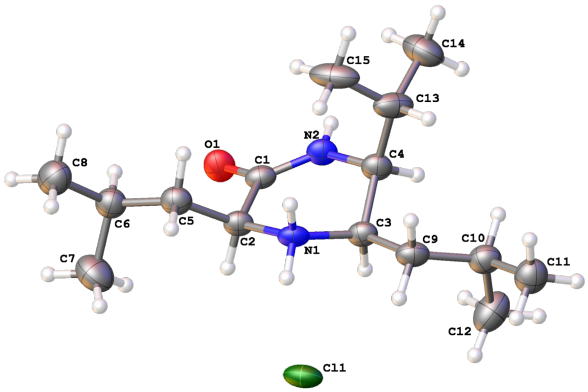


Figure 1: X-ray crystal structure of **2**·HCl.

Table 1: Comparison of selected ^{13}C NMR chemical shifts of piperazirum, **2** and **2**·HCl.

Carbon atom	piperazirum δc (ppm) D_2O [49]	**2** δc (ppm) DMSO-d_6	**2** δc (ppm) $CDCl_3$	**2**·HCl δc (ppm) D_2O
C-2	175.7	172.5	174.3	169.9
C-3	53.6	56.4	56.9	54.9
C-5	59.7	53.2	53.3	53.9
C-6	60.6	58.1	59.4	56.3
CH_2C-3	40.0	41.5	41.1	38.8
CH_2C-5	24.6	40.2	40.5	36.3

Conclusion

The rapid synthesis of *r*-3,*c*-5-diisobutyl-*c*-6-isopropyl-piperazin-2-one has been achieved using an efficient nitro-Mannich reaction to establish the C-5/C-6 relative stereochemistry which in turn controls the formation of the stereocentre at C-3. Spectrosocpic and single crystal X-ray data have shown that the reported structure for piperazirum is erroneous and that the structure of the natural product needs to be revised. While the reported data point strongly towards piperazirum having the same connectivity as **2**, it is not clear which of the three alternative diastereomers corresponds to the natural product. In view of the lack of natural material, further chemical synthesis, guided by GIAO chemical shift prediction, is currently underway in an effort to elucidate the correct structure for piperazirum. In addition the determination of further biological activity of **2** and its diastereoisomers will be investigated.

Experimental

Unless otherwise stated, all reactions were carried out under an atmosphere of nitrogen. All glassware was flame dried and allowed to cool under a stream of nitrogen before use. Cooling to 0 °C was effected using an ice–water bath. Cooling to temperatures below 0 °C was effected using dry ice–acetone mixtures. Reactions were monitored by thin layer chromatography (TLC) using 0.25 mm silica precoated plastic plates with fluorescent indicator. Sheets were visualised using ultraviolet light (254 nm) and/or anisaldehyde or $KMnO_4$ solutions, as appropriate. Removal of solvents (in vacuo) was achieved using a water aspirator and rotary evaporators. Flash column chromatography was performed using silica gel 60, 40–63 μm. Commercial solvents and reagents were used as supplied or purified in accordance with standard procedures [60]. Diethyl ether (Et_2O), tetrahydrofuran (THF), dichloromethane (CH_2Cl_2) and toluene (PhMe) were obtained from a solvent tower, where degassed solvent was passed through two columns of activated alumina and a 7 micron filter under 4 bar pressure. All NMR samples were made as dilute solutions of $CDCl_3$ unless otherwise stated. All chemical shifts (δ) are reported in parts per million (ppm) relative to residual solvent peaks except in D_2O where they are relative to dioxane (D_2O) ^{1}H 3.75 ppm and ^{13}C 67.2 ppm. Multiplicities for ^{1}H coupled signals are denoted as s = singlet, d = doublet, t = triplet, q = quartet, quint = quintet, m = multiplet. Coupling constants (*J*) are reported in Hertz. ^{13}C multiplicities were assigned using a DEPT sequence. Where appropriate, HMQC, COSY, HMBC and NOE experiments were carried out to aid assignment. Melting points are uncorrected.

(*E*)-4-Methoxy-*N*-(3-methylbutylidene)aniline (19): To a mixture of *p*-anisidine (123 mg, 1.00 mmol) and basic alumina (1.00 g) in CH_2Cl_2 (5 mL) at −78 °C was added isovaleraldehyde (107 μL, 1.00 mmol) and the mixture stirred for 1 h, then warmed to rt, filtered and evaporated in vacuo to give crude imine **19** (182 mg, 95%) as a colourless oil that was used immediately without further purification; ^{1}H NMR (600 MHz) δ 1.02 (d, *J* = 6.7, 6H, C*H*$_3$), 2.04 (sept, *J* = 6.7, 1H, C*H*(CH$_3$)$_2$), 2.34 (dd, *J* = 7.0, 5.4, 2H, C*H*$_2$), 3.80 (s, 1H, OC*H*$_3$), 6.87 (app. d, *J* = 8.9, 2H, Ar*H*), 7.02 (app. d, *J* = 8.9, 2H, Ar*H*), 7.86 (t, *J* = 5.4, 1H, N=C*H*); ^{13}C NMR (150 MHz) data were in agreement to that reported [61].

(3*R,4*S**)-N^4-(4-Methoxyphenyl)-2,6-dimethylheptane-3,4-diamine (21):** To a solution of nitroalkene **18** (202 mg, 2.00 mmol), in CH_2Cl_2 (12.0 mL) was added Superhydride® (2.20 mL, 1 M in THF, 2.20 mmol) and the mixture stirred for 15 min at rt. The mixture was cooled to −78 °C before the dropwise addition of a solution of freshly prepared imine **19** (564 mg, 4.00 mmol) in CH_2Cl_2 (12.0 mL). The reaction was stirred for 10 min before the dropwise addition of a solution of CF_3CO_2H (460 μL, 6.00 mmol) in CH_2Cl_2 (4.0 mL). The reaction was stirred for 1 h and then quenched with brine (20 mL) at −78 °C, warmed to rt and extracted with Et_2O (3 × 20 mL). The combined organics were dried ($MgSO_4$) and evaporated in vacuo to give crude β-nitroamine **20**, that was purified by column chromatography (petrol ether/Et_2O 4:1). Subsequent reaction with 6 M HCl (6.60 mL, 40.0 mmol) and Zn dust (1.30 g, 20.0 mmol) and purification by flash column chromatography (CH_2Cl_2/MeOH 10:1) gave diamine **21** (452 mg, 85%) as a brown oil; R_f 0.50 (CH_2Cl_2/MeOH 10:1); IR ν_{max} (thin film): 3374 (br, N-H), 2955 (w, C-H), 1618 (w), 1508 (s, C=C), 1465 (m), 1441 (w), 1385 (w), 1366 (w), 1292 (w), 1238 (s), 1179 (w), 1154 (w), 1038 (m), 816 (m), 752 (s) cm^{-1}; ^{1}H NMR (600 MHz) δ 0.90 (d, *J* = 6.5, 3H, C*H*$_3$), 0.92 (d, *J* = 6.7, 3H, C*H*$_3$), 0.99 (d, *J* = 6.6, 6H, C*H*$_3$), 1.21 (m, 1H, C*H*$_2$), 1.35 (m, 1H, C*H*$_2$), 1.59 (m, 1H, C*H*(CH$_3$)$_2$), 1.80 (m, 1H, C*H*(CH$_3$)$_2$), 2.53 (dd, *J* = 9.1, 2.7, 1H, C*H*NH$_2$), 3.52 (m, 1H, C*H*NH), 3.73 (s, 3H, OC*H*$_3$), 6.57 (app. d, *J* = 8.9, 2H, Ar*H*), 6.76 (app. d, *J* = 8.9, 2H, Ar*H*); ^{13}C NMR (150 MHz) δ 19.6 (*C*H$_3$), 20.6 (*C*H$_3$), 21.7 (*C*H$_3$), 24.1 (*C*H$_3$), 24.7 (*C*H(CH$_3$)$_2$), 31.4 (*C*H(CH$_3$)$_2$), 37.2 (*C*H$_2$), 52.9 (*C*HNH), 55.8 (O*C*H$_3$), 59.1 (*C*HNH$_2$), 114.4 (*C*H arom.), 115.0 (*C*H arom.), 142.3 (*C*q arom.), 151.6 (*C*q arom.); MS (EI$^+$) *m/z*: 264 (M$^+$, 5%), 192 (M$^+$ − (CH$_3$)$_2$CHCHNH$_2$, 100%); HRMS *m/z*: calcd for $C_{16}H_{28}N_2O$, 264.2196; found, 264.2201.

(5*S,6*R**,*Z*)-5-Isobutyl-6-isopropyl-4-(4-methoxyphenyl)-3-(2-methylpropylidene)piperazin-2-one (23):** To a solution of diamine **21** (61 mg, 0.23 mmol) in THF (5 mL) was added *N*-(3-dimethylaminopropyl)-*N*′-ethylcarbodiimide hydrochloride (EDC, 67 mg, 0.35 mmol) and 1-hydroxybenzotriazole hydrate (47 mg, 0.35 mmol) followed by a solution of keto acid **11** (30 mg, 0.23 mmol) in CH_2Cl_2 (5 mL) at rt. The

mixture was stirred for 24 h, then diluted with CH_2Cl_2 (20 mL) and washed with brine (10 mL). The combined organic phases were dried ($MgSO_4$), evaporated in vacuo and purified by flash column chromatography (petrol ether/EtOAc 7:3) to give piperazinone **23** (57 mg, 69%) as a brown solid; mp 152–153 °C; R_f 0.30 (petrol ether/EtOAc 7:3); IR ν_{max} (thin film): 3209 (br, N-H), 2956 (w, C-H), 1671 (s, C=C), 1622 (s), 1499 (s), 1464 (m), 1442 (m), 1409 (m), 1384 (m), 1366 (m), 1331 (m), 1283 (m), 1241 (s), 1180 (m), 1153 (m), 1037 (m), 826 (s), 767 (m) cm^{-1}; ^1H NMR (600 MHz) δ 0.68 (d, *J* = 6.6, 3H, CH_3), 0.79 (d, *J* = 6.6, 3H, CH_3), 0.88 (d, *J* = 6.6, 3H, CH_3), 0.93 (d, *J* = 6.5, 3H, CH_3), 0.95 (d, *J* = 6.7, 3H, CH_3), 1.07 (d, *J* = 6.5, 3H, CH_3), 1.07 (m, 1H, CH_2), 1.55 (m, 1H, CH_2), 1.55 (m, 1H, CH(CH$_3$)$_2$), 1.94 (m, 1H, CH(CH$_3$)$_2$), 2.43 (m, 1H, CH(CH$_3$)$_2$), 3.18 (dd, *J* = 10.3, 3.6, 1H, CHNH), 3.53 (br. d, *J* = 12.2, 1H, NCHCH$_2$), 3.76 (s, 3H, OCH_3), 5.89 (br. s, 1H, NH), 6.48 (d, *J* = 10.6, 1H, =CH), 6.78 (app. d, *J* = 8.8, 2H, ArH), 6.89 (app. d, *J* = 8.8, 2H, ArH); ^{13}C NMR (150 MHz) δ 17.9 (*C*H$_3$), 19.4 (*C*H$_3$), 20.3 (*C*H$_3$), 21.5 (*C*H$_3$), 22.2 (*C*H$_3$), 23.7 (*C*H$_3$), 24.1 (*C*H(CH$_3$)$_2$), 26.4 (*C*H(CH$_3$)$_2$), 29.0 (*C*H(CH$_3$)$_2$), 34.4 (*C*H$_2$), 55.4 (O*C*H$_3$), 58.0 (*C*HNH), 58.8 (N*C*HCH$_2$), 114.3 (*C*H arom.), 122.0 (*C*H arom.), 129.7 (CH=*C*q), 140.0 (Cq=*C*H), 143.4 (*C*q arom.), 154.3 (*C*q arom.), 164.3 (*C*=O); MS (EI$^+$) *m/z*: 359 (MH$^+$, 100%), 343 (12%), 192 (13%); HRMS *m/z*: calcd for $C_{22}H_{35}N_2O_2$, 359.2693; found, 359.2678.

(3*R,5*S**,6*R**)-3,5-diisobutyl-6-isopropyl-4-(4-methoxyphenyl)piperazin-2-one (25):** To a solution of piperazinone **23** (170 mg, 0.470 mmol) in MeOH (10 mL) was added palladium on carbon (50 mg, 10% by weight, 0.047 mmol) and the mixture was flushed with hydrogen, then stirred under a hydrogen atmosphere (balloon) at rt. After the piperazinone starting material was consumed (TLC, 4 h) the mixture was filtered through celite®, washed with CH_2Cl_2 (20 mL) and evaporated in vacuo to give crude piperazinone that was purified by flash column chromatography (petrol ether/Me_2CO 4:1) to give piperazinone **25** (170 mg, 99%) as a colourless oil; R_f 0.50 (petrol ether/Me_2CO 4:1); IR ν_{max} (thin film): 3207 (br, N-H), 2954 (m, C-H), 1658 (s, C=O), 1505 (C=C), 1465 (m), 1367 (m), 1242 (s), 1180 (m), 1039 (m), 827 (m), 788 (m), 733 (m) cm^{-1}; ^1H NMR (600 MHz) δ 0.70 (d, *J* = 6.5, 3H, CH_3), 0.77 (d, *J* = 6.7, 3H, CH_3), 0.90 (d, *J* = 6.7, 3H, CH_3), 0.97 (d, *J* = 6.5, 3H, CH_3), 0.98 (d, *J* = 6.8, 3H, CH_3), 1.03 (d, *J* = 6.5, 3H, CH_3), 1.03 (m, 1H, CHCHCH_2), 1.55 (m, 1H, CHCHCH_2), 1.55 (m, 1H, O=CCHCH_2), 1.55 (m, 1H, CHCH(CH$_3$)$_2$), 1.84 (m, 1H, O=CCHCH_2), 1.92 (m, 1H, O=CCHCH$_2$CH(CH$_3$)$_2$), 2.06 (m, 1H, CHCHCH$_2$CH(CH$_3$)$_2$), 3.18 (dd, *J* = 10.0, 3.5, 1H, NHCH), 3.37 (dt, *J* = 12.4, 3.1, 1H, NHCHCHN), 3.77 (s, 3H, OCH_3), 4.09 (dd, *J* = 9.9, 4.5, 1H, O=CCH), 6.02 (br. s, 1H, NH), 6.80 (app. d, *J* = 8.9, 2H, ArH), 6.91 (app. d, *J* = 8.9, 2H, ArH); ^{13}C NMR (150 MHz) δ 18.0 (*C*H$_3$), 19.5 (*C*H$_3$), 21.5 (*C*H$_3$), 21.6 (*C*H$_3$), 23.3 (*C*H$_3$), 23.4 (CHCHCH$_2$*C*H(CH$_3$)$_2$), 23.7 (*C*H$_3$), 24.7 (O=CCHCH$_2$*C*H(CH$_3$)$_2$), 29.2 (NHCH*C*H(CH$_3$)$_2$), 34.7 (*C*H$_2$CHCH), 44.0 (*C*H$_2$CHC=O), 55.4 (O*C*H$_3$), 57.2 (N*C*HC=O), 58.4 (N*C*HCH), 58.5 (NH*C*H), 114.5 (*C*H arom.), 122.6 (*C*H arom.), 146.2 (*C*H arom.), 154.3 (*C*H arom.), 173.9 (*C*=O); MS (EI$^+$) *m/z*: 360 (M$^+$, 15%), 303 (18%), 192 (100%); HRMS *m/z*: calcd for $C_{22}H_{36}N_2O_2$, 360.2771; found, 360.2774.

(3*R,5*S**,6*R**)-3,5-diisobutyl-6-isopropylpiperazin-2-one (2):** To a solution of piperazinone **25** (320 mg, 0.880 mmol) in MeCN (10 mL) at 0 °C was added a solution of CAN (2.08 g, 3.52 mmol) in H_2O (10 mL) dropwise over 3 min. The solution turned from pale yellow to dark orange. The mixture was stirred at 0 °C for 2 h, over which time the solution became light orange. Water (30 mL) was then added and the mixture extracted with EtOAc (3 × 20 mL), washed with saturated aqueous $NaHCO_3$ (40 mL), dried ($MgSO_4$) and evaporated in vacuo to give crude piperazinone that was purified by flash column chromatography (petrol ether/Me_2CO 3:2) to give piperazinone **2** (91 mg, 41%) as a brown oil; R_f 0.53 (petrol ether/Me_2CO 3:2); IR ν_{max} (thin film): 3209 (w, N-H), 2955 (C-H), 1658 (s, C=O), 1467 (m), 1367 (m), 1165 (w), 918 (w), 722 (w) cm^{-1}; ^1H NMR (600 MHz, $CDCl_3$) δ 0.89 (d, *J* = 6.6, 3H, C-3CH$_2$CHCH_3), 0.90 (d, *J* = 6.2, 3H, C-5CH$_2$CHCH_3), 0.91 (d, *J* = 5.6, 3H, C-6CHCH_3), 0.93 (d, *J* = 6.9, 3H, C-3CH$_2$CHCH_3), 0.94 (d, *J* = 6.8, 3H, C-5CH$_2$CHCH_3), 0.98 (d, *J* = 6.7, 3H, C-6CHCH_3), 1.30 (ddd, *J* = 13.9, 7.1, 6.5, 1H, C-5CH_2), 1.33 (ddd, *J* = 13.9, 8.2, 5.6, 1H, C-5CH_2), 1.40 (ddd, *J* = 14.2, 10.0, 4.1, 1H, C-3CH_2), 1.65 (nonet, *J* = 6.7, 1H, C-5CH$_2$CH), 1.74 (m, 1H, C-3CH$_2$CH), 1.88 (ddd, *J* = 13.7, 10.3, 3.3, 1H, C-3CH_2), 1.91 (hepd, *J* = 6.8, 2.5, 1H, C-6CH), 3.06 (dd, *J* = 6.7, 3.6, 1H, C-6*H*), 3.15 (dt, *J* = 7.8, 5.3, 1H, C-5*H*), 3.40 (dd, *J* = 10.2, 3.4, 1H, C-3*H*), 6.22 (brs, 1H, N^1H), N^4H peak is missing; ^{13}C NMR (125 MHz, $CDCl_3$) δ 17.7 (C-6CH*C*H$_3$), 21.0 (C-3CH$_2$CH*C*H$_3$), 21.5 (C-5CH$_2$CH*C*H$_3$), 22.4 (C-6CH*C*H$_3$), 23.1 and 23.7 (C-3CH$_2$CH*C*H$_3$/C-5CH$_2$CH*C*H$_3$), 24.4 (C-3CH$_2$*C*H), 24.8 (C-5CH$_2$*C*H), 27.9 (C-6*C*H), 40.5 (C-5*C*H$_2$), 41.1 (C-3*C*H$_2$), 53.3 (C-5), 57.0 (C-3), 59.4 (C-6), 174.2 (C=O); MS (EI$^+$) *m/z*: 254 (M$^+$, 30%), 197 (22%), 169 (43%), 154 (31%); HRMS *m/z*: calcd for $C_{15}H_{30}N_2O$, 254.2353; found, 254.2355.

^1H NMR (600 MHz, DMSO-d_6) δ 0.83–0.89 (m, 18H, 6xMe), 1.25 (m, 3H, C-3CH_2 + 2xC-5CH_2), 1.65 (m, 2H, C-3CH$_2$CH + C-5CH$_2$CH), 1.79 (m, 2H, C-3CH_2 + C-6CH), 2.90 (brd, *J* = 3.2, 1H, C-6*H*), 3.01 (td, *J* = 7.1, 3.7, 1H, C-5*H*), 3.21 (dd, *J* = 9.3, 3.2, 1H, C-3*H*), 7.63 (brs, 1H, N*H*). Assignments based on above; ^{13}C NMR (125 MHz, DMSO-d_6) δ 18.4, 21.5, 22.0, 22.8, 23.0, 23.8, 23.9, 24.2, 27.4, 40.2, 41.5, 53.2, 56.4, 58.1, 172.5.

In a clean vial HCl in dioxane (~1 equiv) was added to a small sample of **2** in MeCN, the mixture layered with Et_2O and then left in the fridge until colourless blades of **2**·HCl had formed at the interface. mp 121–123 °C. ^{1}H NMR (600 MHz, D_2O) δ 0.89–0.99 (6xMe), 1.52–1.68 (m, 4H), 1.72–1.79 (m, 1H), 1.94–1.99 (m, 2H), 3.50 (dd, *J* = 6.2, 4.3, 1H, C-6*H*), 3.79 (m, 1H, C-5*H*), 4.01 (dd, *J* = 8.3, 5.3, 1H, C-3*H*); ^{13}C NMR (150 MHz, D_2O) δ 18.8, 20.6, 21.3, 22.0, 22.5, 24.2, 24.7, 25.7, 27.4, 36.3, 38.8, 53.9, 54.9, 56.3, 169.9 (C=O).

Supporting Information

Supporting Information File 1

Further experimental and characterisation data.
[http://www.beilstein-journals.org/bjoc/content/supplementary/1860-5397-9-200-S1.pdf]

Acknowledgements

We thank the Cyprus State Scholarship Foundation for funding, Dr. L. Haigh and Mr. J. Hill for providing mass spectra and Ms. J. Maxwell for microanalytical data.

References

1. Noble, A.; Anderson, J. C. *Chem. Rev.* **2013,** *113,* 2887. doi:10.1021/cr300272t
   See for a comprehensive review of the nitro-Mannich reaction.
2. Ballini, R.; Petrini, M. *Tetrahedron* **2004,** *60,* 1017. doi:10.1016/j.tet.2003.11.016
3. Palomo, C.; Oiarbide, M.; Halder, R.; Laso, A.; López, R. *Angew. Chem., Int. Ed.* **2006,** *45,* 117. doi:10.1002/anie.200502674
4. Bursavich, M. G.; Rich, D. H. *J. Med. Chem.* **2002,** *45,* 541. doi:10.1021/jm010425b
5. Shen, B.; Johnston, J. N. *Org. Lett.* **2008,** *10,* 4397. doi:10.1021/ol801797h
6. Jakubec, P.; Cockfield, D. M.; Dixon, D. J. *J. Am. Chem. Soc.* **2009,** *131,* 16632. doi:10.1021/ja908399s
7. Jakubec, P.; Kyle, A. F.; Calleja, J.; Dixon, D. J. *Tetrahedron Lett.* **2011,** *52,* 6094. doi:10.1016/j.tetlet.2011.09.016
8. Kyle, A. F.; Jakubec, P.; Cockfield, D. M.; Cleator, E.; Skidmore, J.; Dixon, D. J. *Chem. Commun.* **2011,** *47,* 10037. doi:10.1039/c1cc13665h
9. Kumaraswamy, G.; Pitchaiah, A. *Helv. Chim. Acta* **2011,** *94,* 1543. doi:10.1002/hlca.201100013
10. Jakubec, P.; Hawkins, A.; Felzmann, W.; Dixon, D. J. *J. Am. Chem. Soc.* **2012,** *134,* 17482. doi:10.1021/ja308826x
11. Tsuritani, N.; Yamada, K.-I.; Yoshikawa, N.; Shibasaki, M. *Chem. Lett.* **2002,** *31,* 276. doi:10.1246/cl.2002.276
12. Xu, X.; Furukawa, T.; Okino, T.; Miyabe, H.; Takemoto, Y. *Chem.–Eur. J.* **2006,** *12,* 466. doi:10.1002/chem.200500735
13. Anderson, J. C.; Chapman, H. A. *Org. Biomol. Chem.* **2007,** *5,* 2413–2422. doi:10.1039/b705081j
14. Hynes, P. S.; Stupple, P. A.; Dixon, D. J. *Org. Lett.* **2008,** *10,* 1389. doi:10.1021/ol800108u
15. Handa, S.; Gnanadesikan, V.; Matsunaga, S.; Shibasaki, M. J. *J. Am. Chem. Soc.* **2010,** *132,* 4925. doi:10.1021/ja100514y
16. Weng, J.; Li, Y.-B.; Wang, R.-B.; Li, F.-Q.; Liu, C.; Chan, A. S. C.; Lu, G. *J. Org. Chem.* **2010,** *75,* 3125. doi:10.1021/jo100187m
17. Kumaraswamy, G.; Pitchaiah, A. *Tetrahedron* **2011,** *67,* 2536. doi:10.1016/j.tet.2011.02.031
18. Davis, T. A.; Johnston, J. N. *Chem. Sci.* **2011,** *2,* 1076. doi:10.1039/c1sc00061f
19. Xie, H.; Zhang, Y.; Zhang, S.; Chen, X.; Wang, W. *Angew. Chem., Int. Ed.* **2011,** *50,* 11773. doi:10.1002/anie.201105970
20. Jensen, K. L.; Poulsen, P. H.; Donslund, B. S.; Morana, F.; Jørgensen, K. A. *Org. Lett.* **2012,** *14,* 1516. doi:10.1021/ol3002514
21. Anderson, J. C.; Horsfall, L. R.; Kalogirou, A. S.; Mills, M. R.; Stepney, G. J.; Tizzard, G. J. *J. Org. Chem.* **2012,** *77,* 6186–6198. doi:10.1021/jo301000r
22. Davis, T. A.; Danneman, M. W.; Johnston, J. N. *Chem. Commun.* **2012,** *48,* 5578. doi:10.1039/c2cc32225k
23. Anderson, J. C.; Noble, A.; Tocher, D. A. *J. Org. Chem.* **2012,** *77,* 6703. doi:10.1021/jo3010827
24. Anderson, J. C.; Noble, A.; Ribelles Torres, P. *Tetrahedron Lett.* **2012,** *53,* 5707. doi:10.1016/j.tetlet.2012.08.062
25. Marquéz-López, E.; Merino, P.; Tejero, T.; Herrera, R. P. *Eur. J. Org. Chem.* **2009,** 2401. doi:10.1002/ejoc.200801097
    See for a review specific to asymmetric methods.
26. Yamada, K.-I.; Moll, G.; Shibasaki, M. *Synlett* **2001,** 980. doi:10.1055/s-2001-14639
27. Knudsen, K. R.; Risgaard, T.; Nishiwaki, N.; Gothelf, K. V.; Jørgensen, K. A. *J. Am. Chem. Soc.* **2001,** *123,* 5843. doi:10.1021/ja010588p
28. Anderson, J. C.; Howell, G. P.; Lawrence, R. M.; Wilson, C. S. *J. Org. Chem.* **2005,** *70,* 5665. doi:10.1021/jo050762i
29. Trost, B. M.; Lupton, D. W. *Org. Lett.* **2007,** *9,* 2023. doi:10.1021/ol070618e
30. Chen, Z.; Morimoto, H.; Matsunaga, S.; Shibasaki, M. *J. Am. Chem. Soc.* **2008,** *130,* 2170. doi:10.1021/ja710398q
31. Yamada, K.-I.; Harwood, S. J.; Gröger, H.; Shibasaki, M. *Angew. Chem., Int. Ed.* **1999,** *38,* 3504. doi:10.1002/(SICI)1521-3773(19991203)38:23<3504::AID-ANIE3504>3.0.CO;2-E
32. Handa, S.; Gnanadesikan, V.; Matsunaga, S.; Shibasaki, M. *J. Am. Chem. Soc.* **2007,** *129,* 4900. doi:10.1021/ja0701560
33. Okino, T.; Nakamura, S.; Furukawa, T.; Takemoto, Y. *Org. Lett.* **2004,** *6,* 625. doi:10.1021/ol0364531
34. Nugent, B. M.; Yoder, R. A.; Johnston, J. N. *J. Am. Chem. Soc.* **2004,** *126,* 3418. doi:10.1021/ja031906i
35. Yoon, T. P.; Jacobsen, E. N. *Angew. Chem., Int. Ed.* **2005,** *44,* 466. doi:10.1002/anie.200461814
36. Fini, F.; Sgarzani, V.; Petterson, D.; Herrera, R. P.; Bernardi, L.; Ricci, A. *Angew. Chem., Int. Ed.* **2005,** *44,* 7975. doi:10.1002/anie.200502646
37. Palomo, C.; Oiarbide, M.; Laso, A.; López, R. *J. Am. Chem. Soc.* **2005,** *127,* 17622. doi:10.1021/ja056594t
38. Robak, M. T.; Trincado, M.; Ellman, J. A. *J. Am. Chem. Soc.* **2007,** *129,* 15110. doi:10.1021/ja075653v
39. Wang, C.-J.; Dong, X.-Q.; Zhang, Z.-H.; Xue, Z.-Y.; Teng, H.-L. *J. Am. Chem. Soc.* **2008,** *130,* 8606. doi:10.1021/ja803538x
40. Adams, H.; Anderson, J. C.; Peace, S.; Pennell, A. M. K. *J. Org. Chem.* **1998,** *63,* 9932. doi:10.1021/jo981700d
41. Anderson, J. C.; Peace, S.; Pih, S. *Synlett* **2000,** 850. doi:10.1055/s-2000-6710

42. Anderson, J. C.; Blake, A. J.; Howell, G. P.; Wilson, C. *J. Org. Chem.* **2005,** *70,* 549. doi:10.1021/jo048304h
43. Anderson, J. C.; Stepney, G. J.; Mills, M. R.; Horsfall, L. R.; Blake, A. J.; Lewis, W. *J. Org. Chem.* **2011,** *76,* 1961. doi:10.1021/jo102408u
44. Anderson, J. C.; Blake, A. J.; Koovits, P. J.; Stepney, G. J. *J. Org. Chem.* **2012,** *77,* 4711. doi:10.1021/jo300535h
45. Anderson, J. C.; Koovits, P. *J. Chem. Sci.* **2013,** *4,* 2897. doi:10.1039/c3sc50613d
46. El-Desouky, S.-K.; Ryu, S. Y.; Kim, Y.-K. *Tetrahedron Lett.* **2007,** *48,* 4015. doi:10.1016/j.tetlet.2007.04.032
47. Rambaud, M.; Bakasse, M.; Duguay, G.; Villieras, J. *Synthesis* **1988,** 564. doi:10.1055/s-1988-27642
48. Ramage, R.; Griffiths, G. J.; Shutt, F. E.; Sweeney, J. N. A. *J. Chem. Soc., Perkin Trans. 1* **1984,** 1531. doi:10.1039/P19840001531
49. Fuse, S.; Masui, H.; Tannna, A.; Shimizu, F.; Takahashi, T. *ACS Comb. Sci.* **2012,** *14,* 17. doi:10.1021/co200081j
50. Kumaran, G.; Kulkarni, G. H. *Synthesis* **1995,** 1545. doi:10.1055/s-1995-4137
51. Boeykens, M.; De Kimpe, N.; Tehrani, K. A. *J. Org. Chem.* **1994,** *59,* 6973. doi:10.1021/jo00102a022
52. Li, L.-S.; Zhou, Y.; Zhao, J.; Dragovich, P. S.; Stankovic, N.; Bertolini, T. M.; Murphy, D. E.; Sun, Z.; Tran, C. V.; Ayida, B. K.; Ruebsam, F.; Webber, S. E. *Synthesis* **2007,** 3301. doi:10.1055/s-2007-990823
53. Murthy, S. N.; Madhav, B.; Nageswar, Y. V. D. *Helv. Chim. Acta* **2010,** *93,* 1216. doi:10.1002/hlca.200900358
54. Lambert, A.; Lowe, A. *J. Chem. Soc.* **1947,** 1517. doi:10.1039/jr9470001517
55. Reaction in THF gave a lower stereoselectivity of dr 85:15. The use of CH_2Cl_2 as solvent in reductive nitro-Mannich reactions can give enhanced diastereoselectivities. See [24].
56. Kaliogirou, A. S. Ph.D. Thesis, University College London, London, 2013.
57. Grijalvo, S.; Bedia, C.; Triola, G.; Casas, J.; Llebaria, A.; Teixidó, J.; Rabal, O.; Levade, T.; Delgado, A.; Fabriàs, G. *Chem. Phys. Lipids* **2006,** *144,* 69. doi:10.1016/j.chemphyslip.2006.07.001
58. The publication [49] states in the discussion that the NMR were recorded in DMSO-d_6, but is then tabulated in D_2O. The author confirmed the data was recorded in D_2O and that there were no suitable samples of the material left for re-analysis and the original spectra were unobtainable. Private communication from Prof Young-Kyoon Kim.
59. Crystallographic data (excluding structure factors) for the structure of **2**·HCl has been deposited with the Cambridge Crystallographic Data Centre under supplementary publication numbers CCDC 949530. Copies of the data can be obtained, free of charge, upon request from the CCDC, 12 Union Road, Cambridge CB2 1EZ, UK [fax: +44(0)-1223-336033 or email: deposit@ccdc.cam.ac.uk].
60. Perrin, D. D.; Armarego, W. L. F.; Perrin, D. R. *Purification of Laboratory Chemicals,* 2nd ed.; Pergamon Press Ltd., 1980.
61. Oiima, I.; Habus, H.; Zhao, M.; Zucco, M.; Park, Y. H.; Sun, C. M.; Brigaud, T. *Tetrahedron* **1992,** *48,* 6985. doi:10.1016/S0040-4020(01)91210-4

License and Terms

This is an Open Access article under the terms of the Creative Commons Attribution License (http://creativecommons.org/licenses/by/2.0), which permits unrestricted use, distribution, and reproduction in any medium, provided the original work is properly cited.

The license is subject to the *Beilstein Journal of Organic Chemistry* terms and conditions: (http://www.beilstein-journals.org/bjoc)

The definitive version of this article is the electronic one which can be found at: doi:10.3762/bjoc.9.200

Beilstein Journal of Organic Chemistry

Activation of cryptic metabolite production through gene disruption: Dimethyl furan-2,4-dicarboxylate produced by *Streptomyces sahachiroi*

Dinesh Simkhada, Huitu Zhang, Shogo Mori, Howard Williams and Coran M. H. Watanabe*

Letter

Open Access

Address:
Texas A&M University, Department of Chemistry, College Station, TX 77843, USA

Email:
Coran M. H. Watanabe* - watanabe@chem.tamu.edu

* Corresponding author

Keywords:
cryptic metabolite; dimethyl furan-2,4-dicarboxylate; genetic knockout; natural products; non-ribosomal peptide synthetase module; *Streptomyces*

Beilstein J. Org. Chem. **2013,** *9,* 1768–1773.
doi:10.3762/bjoc.9.205

Received: 16 June 2013
Accepted: 09 August 2013
Published: 29 August 2013

This article is part of the Thematic Series "Natural products in synthesis and biosynthesis".

Guest Editor: J. S. Dickschat

© 2013 Simkhada et al; licensee Beilstein-Institut.
License and terms: see end of document.

Abstract

At least 65% of all small molecule drugs on the market today are natural products, however, re-isolation of previously identified and characterized compounds has become a serious impediment to the discovery of new bioactive natural products. Here, genetic knockout of an unusual non-ribosomal peptide synthetase (NRPS) C-PCP-C module, *aziA2*, is performed resulting in the accumulation of the secondary metabolite, dimethyl furan-2,4-dicarboxylate. The cryptic metabolite represents the first non-azinomycin related compound to be isolated and characterized from the soil bacterium, *S. sahachiroi*. The results from this study suggest that abolishing production of otherwise predominant natural products through genetic knockout may constitute a means to "activate" the production of novel secondary metabolites that would otherwise lay dormant within microbial genome sequences.

Findings

It has become increasingly apparent that microbial diversity in nature far exceeds that reflected in laboratory strain collections. The advent of microbial genomics and the availability of published genome sequences suggest, that as much as 90% of the chemical potential of these organisms remain "silent" within the genome [1,2]. While the biosynthetic machinery appears functional, the genetic loci are frequently (but not always) unexpressed. The activation of such pathways has garnered interest from the scientific community. Quorum sensing refers to the process by which microorganisms communicate (within a single bacterial species or between diverse species) and alter their gene expression through production of certain signaling molecules [3]. In this regard, the culturing of microbial communities or the co-culture of two specific microbial organisms has been

successfully implemented to "activate" secondary metabolite production [4,5]. In some instances, shot-gun cloning and expression of soil samples and bacterial symbiont genomes have led to the discovery of a representative set of natural products and enzymes, albeit typically of small biosynthetic pathways (less than 10 kb) [6,7]. Direct manipulation, "induced" biosynthetic activation, of a sequenced cluster has also met with some success. The *Aspergillus nidulans* genome was mined for cryptic orphan gene clusters from which a single, unexpressed PKS-NRPS hybrid was identified. The expression of the gene cluster was activated by the ectopic expression of a specific regulatory gene, *apdR*, resulting in the production of the aspyridones [8]. Sometimes, a cryptic pathway is fully expressed and has simply gone unnoticed. In this regard, a genome-isotopic approach has proven useful where stable isotope-labeled putative precursors of the orphan pathway are fed to the organism and used to screen extracts of the fermentation broth, to identify metabolites containing the labeled precursors [9,10].

Here, we have carried out a functional knockout of *aziA2* within the azinomycin gene cluster of *Streptomyces sahachiroi* [11,12]. The gene encodes a NRPS (non-ribosomal peptide synthetase, an enzyme involved in the biosynthesis of various peptide containing secondary metabolites) module of unusual domain architecture consisting of condensation, peptidyl carrier protein, and condensation domains (C-PCP-C), respectively. Gene inactivation led to the abolishment of azinomycin production, confirming the involvement of *aziA2* in the biosynthesis of the antitumor agent [11,13] and also led to overproduction of a compound, dimethyl furan-2,4-dicarboxylate. The metabolite represents one of many cryptic pathway metabolites from the *S. sahachiroi* genome and is the first non-azinomycin related compound to be isolated from the *S. sahachiroi* strain (Figure 1). Previously isolated metabolites consisted of azinomycin intermediates lacking the 1-azabicyclo[3.1.0] ring system, including naphthoate and naphthoate epoxide derivatives [11].

The *aziA2* disruption construct (pKC-AziA2) was generated by replacing the mid-portion (1500 bp) of the gene with a thiostrepton resistance marker within the vector pKC1139. The plasmid was introduced into *S. sahachiroi* by conjugal transformation. Single crossover mutants were initially selected by culturing the strain on both apramycin and thiostrepton MS-agar plates. The double crossover mutants were subsequently generated from the single crossover mutants by growing the colonies on MS-agar plates in the presence of only thiostrepton antibiotic, resulting in the occurrence of double crossover events. The *S. sahachiroi*/Δ*aziA2* disruptants were confirmed by PCR and Southern hybridization of thiostrepton resistant and apramycin sensitive colonies. Direct comparison of HPLC profiles of the wild-type and *ΔaziA2* crude organic extracts were striking (Figure 2). The *ΔaziA2* mutant gave a single major peak. 3-Methoxy-5-methyl-1-naphthoic acid was detected in trace amounts (suggesting that the metabolite is released in solution from the PKS and not directly transferred to that of a subsequent NRPS module) and complete abolishment of the azinomycins was observed. The production of the naphthoic acid derivative and lack of azinomycin production confirms the involvement of *aziA2* (C-PCP-C NRPS module) in azinomycin biosynthesis; given the unique domain architecture of this module, this is a significant finding as non-functional NRPS modules have been found imbedded in certain gene clusters [14].

Structural characterization of the major metabolite was carried out using LC–MS analysis and 1D and 2D cryoprobe NMR spectroscopy (data provided in Supporting Information File 1).

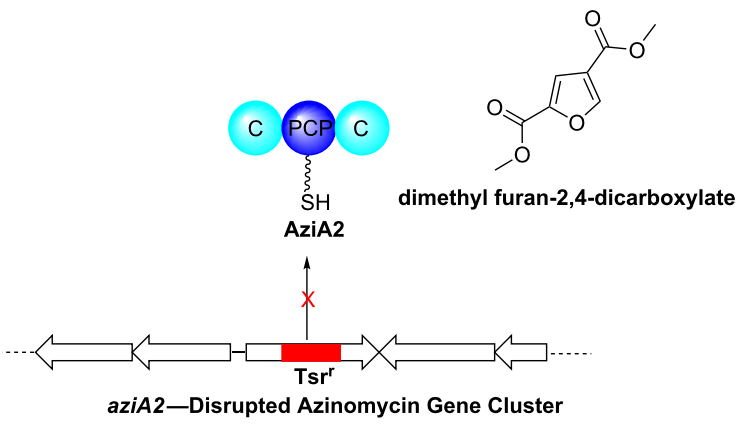


Figure 1: Schematic diagram illustrating the phenotypic effects arising through deletion of the *aziA2* gene.

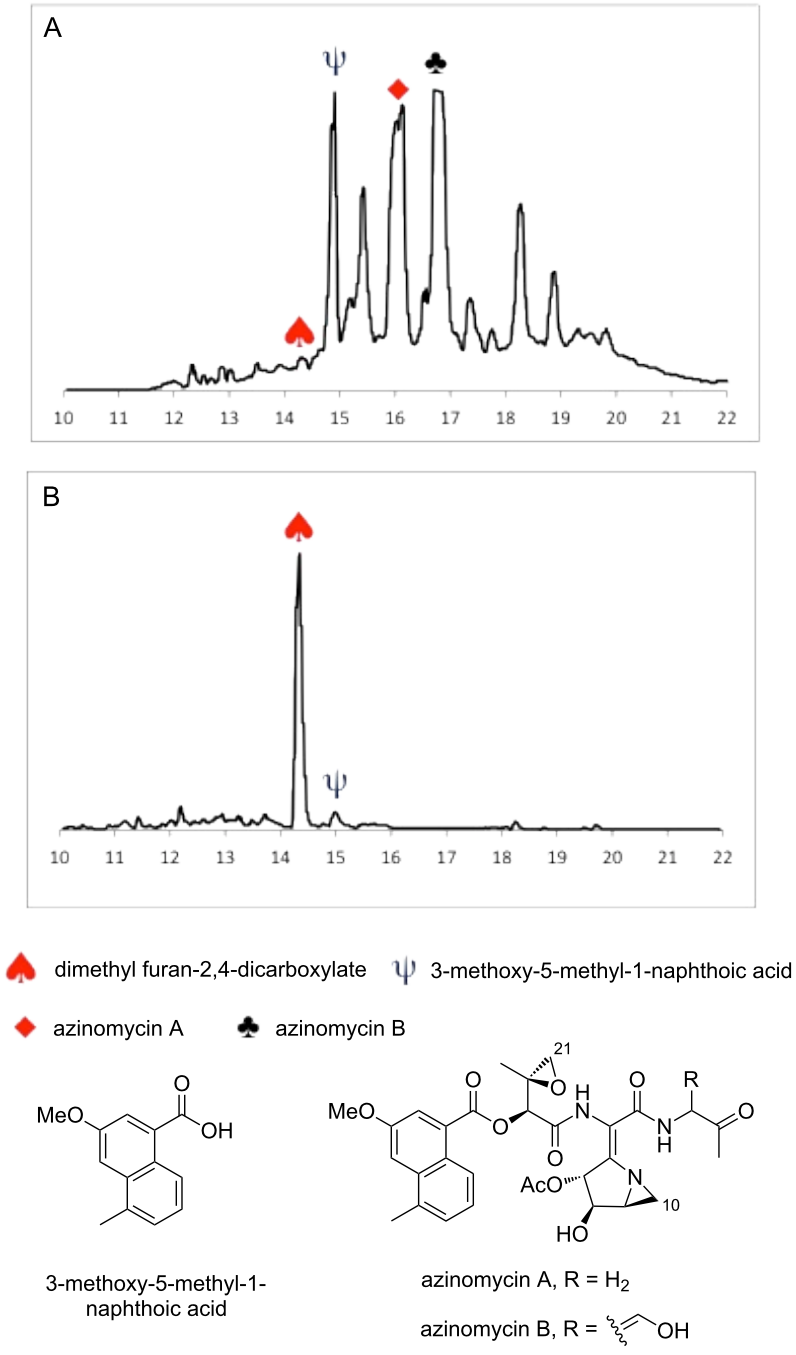
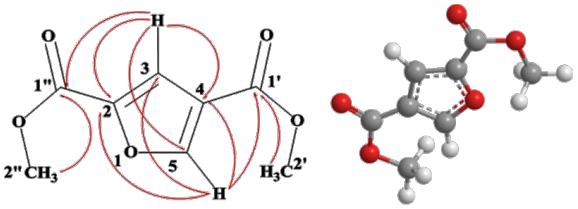


Figure 2: HPLC profiles of (A) *S. sahachiroi* wild-type and (B) *ΔaziA2* crude organic extracts.

The molecular formula was established as $C_8H_8O_5$ based upon a molecular ion peak observed by LC–APCIMS at *m*/*z* 185.0453 $[M + H]^+$ and GC–MS. The GC–MS fragmentation of the compound matched that provided in the Ultra GC–DSQ (ThermoElectron, Waltham, MA) GC–MS database. The structure of the compound was determined by NMR analysis in $CDCl_3$ (Table 1). The presence of two O-CH_3 groups at C-2' (δ_c 51.99, δ_H 3.94) and C-2" (δ_c 52.31, δ_H 3.88) and double bonds in the aromatic ring at C-3 (δ_c 117.07, δ_H 7.49, d, J = 0.811) and C5 (δ_c 150.14 δ_H 8.14, d, J = 0.845) were observed by ^{1}H NMR, DEPT, HMQC and HMBC. C-1" (δ_c 158.53), C-2 (δ_c 145.44), C-5 (δ_c 150.14) and C-1' (δ_c 162.34) signals were detected by ^{13}C NMR (Table 1). The data identified the compound as dimethyl furan-2,4-dicarboxylate, which

has been previously observed in microbial head-space or vapor phase extracts and its structure determined through chemical synthesis [15]. The biosynthetic origin of dimethyl furan-2,4-dicarboxylate could be polyketide derived where the furan ring system could be envisioned to form through nucleophilic attack of an epoxide as in the case with monensin and other similar natural products [16]. Alternatively, the biosynthesis might involve the dimerization of pyruvate [17-19]. Examination of a draft genome sequence of the *S. sahachiroi* strain has implicated a pyruvate aldolase and methyltransferase containing gene cluster as well as potential polyketide gene clusters containing methyltransferase genes, which will be evaluated in due course through genetic knockout experiments of the *ΔaziA2* mutant strain.

Table 1: ^{13}C NMR (δ_C) and ^{1}H NMR (δ_H, *J* in Hz) 500 MHz spectroscopic data in $CDCl_3$.



Position	δ_C	δ_H (*J* in Hz)	HMBC (H→C)
1			
2	145.44, CO		
3	117.07, CH	7.49, (0.811) d	2,4,5,1”
4	120.96, C		
5	150.14, CH	8.14, (0.845) d	2,3,4,1’
1’	162.34, C		
1”	158.53, C		
2’	51.99, CH_3	3.94, s	1”
2”	52.32, CH_3	3.88, s	1’

Disruption of the *aziA2* gene gave overproduction of the cryptic metabolite dimethyl furan-2,4-dicarboxylate and led to complete abolishment of azinomycin production. It is the first non-azinomycin related metabolite to be reported from the *S. sahachiroi* strain, a microorganism that has been mined for its natural product constituents since 1954 [20]. These results demonstrate that while some disruption strains will certainly be more easily characterized than others, the act of simply inactivating genes from highly expressed or represented biosynthetic gene clusters can be a useful strategy toward revealing or unmasking novel natural products or cryptic metabolites for subsequent isolation and characterization. Secondary metabolite production by microorganisms is often viewed as a line of defense against competing microbes for nutrients. Natural products like azinomycin, a DNA crosslinking agent, can offer a means of protection to the producing organism. It is tempting to speculate that when biosynthetic pathways of these metabolites are inactivated, the microorganism begins to adapt and evolve in an effort to develop new self defense mechanisms. Such adaptations (which may or may not be immediately useful to the host) can lead to the production of new metabolites such as dimethyl furan-2,4-dicarboxylate.

Experimental

DNA manipulation and methods

Conventional recombinant DNA techniques were utilized for plasmid and genomic DNA isolation, restriction enzyme digestion, agarose gel electrophoresis, and DNA ligations [21]. DNA sequencing was performed using ABI BigDye chemistry at the Gene Technologies Lab, Texas A&M University. The computer-based analysis and comparisons of nucleotide and protein sequences were performed with BLAST, FASTA, CLUSTALW and GENEDOC programs. See Supporting Information File 1 for details on bacterial strains, plasmids, PCR primer sequences, and bacterial culture conditions.

Construction of disruption plasmid pKCAziA2

Disruption of *aziA2* was performed using a homologous recombination approach with pKC1139. PCR with primer pairs aziA2UF/aziA2UR and aziA2DF/aziA2DR was utilized to generate a 930 bp upstream fragment and 923 bp downstream fragment relative to *aziA2*. Amplification was carried out as follows: initial denaturation at 98 °C for 30 s; 30 total cycles of denaturation for 10 s; annealing at 66.4 °C for aziA2UF/aziA2UR and 62 °C for aziA2DF/aziA2DR for 40 s; polymerization at 72 °C for 60 s and finally gap filing at 72 °C for 10 min. The amplified DNA fragment of azia2-U was digested with *Hind*III/*Xba*I (azia2-U) and *Xba*I/*Eco*RI (azia2-D) and cloned into the corresponding sites of pKC1139, resulting in pKCA2UD. pKCA2UD was digested with *Xba*I and ligated with the thiostrepton-resistance gene (1056 bp), which was amplified with TsrF/TsrR primers using the same amplification condition as detailed for aziA2DF/aziA2DR, to give the final disruption recombinant plasmid pKC-AziA2, where *aziA2* is replaced by tsr^r in-frame.

Conjugal transformation with plasmid pKCAziA2

pKC-AziA2 was transformed into *E. coli* S-17, a donor host and subsequently transferred into wild type, *S. sahachiroi* by conjugal transformation, as described by Kieser et al. (with some modification) [22] for deletion with a replicative plasmid as mediated by homologous recombination. From an overnight 5 mL culture of *E. coli* donor strain, 100 µL was transferred into 100 mL fresh LB medium and cultured for 4 h. The cells at

OD600 0.6 were harvested, washed twice and solubilized in 500 µL of 2xYT medium. Spores of *S. sahachiroi* were prepared in MS agar plates and collected after one week. Spores were washed, heat shocked at 70 °C for 10 min and incubated at 37 °C for 4 h. Following incubation, they were washed and resuspended in 500 µL of 2xYT medium. These recipient cells were mixed with an equal volume of *E. coli* donor cells and 200 µL of the mixture were plated on MS-agar plates. The plates were incubated at 30 °C for 18 h, and overlayed with 1 mL water containing nalidixic acid (500 µg), to inhibit the growth of *E. coli*, and apramycin (25 µg) to select *S. sahachiroi* exconjugants. Incubation at 30 °C was continued for 6–8 days to allow growth of the exconjugants. Apramycin exconjugants were screened for several generations until the exconjugants were found to be apramycin sensitive and thiostrepton resistant to detect the double crossover allelic exchange. For further confirmation of deletion of *aziA2* from *S. sahachiroi*, genomic DNA was isolated from both *S. sahachiroi* wild-type and *aziA2* knockout strains (*S. sahachiroi*/*ΔaziA2*) and PCR performed. The AziA2UF/TsrR and TsrF/AziA2DR primer set was utilized: initial denaturation at 98 °C for 30 s; 30 total cycles of denaturation for 10 s; annealing at 64.5 °C for 40 s; polymerization at 72 °C for 60 s and finally gap filing at 72 °C for 10 min. Southern hybridization was carried out following standard procedures [21] with a radioactive ^{32}P-ATP labeled probe. The probe was generated through PCR amplification using the *aziA2* probe-F/aziA2 Probe R set of primers and following the same PCR condition as detailed above.

Fermentation and analysis of secondary metabolites

Fermentation was carried out in 10 L following established procedures [23]. After 72 h of incubation, the culture broth was centrifuged and the supernatant extracted with dichloromethane (2× the volume of the medium). The organics were concentrated in vacuo and analyzed by reversed-phase HPLC. The column, Phenomenex, Columbus 5µ C8 100A (250 × 3.20 mm 5 µ) was equilibrated with 10% of A (75% MeOH/25% isopropanol) and 90% of B (water) and run with the following program: Time 0 min A-10%; 1 min A-10%; 5 min A-35%; 14 min A-95%; 15 min A-95%; 20 min A-10%; 25 min A-10%; 60 min A-100%. This was carried out at a flow rate of 0.75 mL/min in 254 nm UV. The same program was used for LC–APCI analysis. For GC–MS analysis, the sample was diluted 1:10 in DCM and was performed on an Ultra GC/DSQ (ThermoElectron, Waltham, MA). A Rxi-5ms gas chromatographic column was utilized with dimensions of 60 m length, 0.25 mm i.d., and 0.25 µm film thickness (Restek; Bellefonte, PA). Helium was implemented as a carrier gas at a constant flow rate of 1.5 mL/min. The transfer line and ion source were held at 250 °C. The column temperature was maintained at 50 °C for 5 min then raised to 320 °C for 20 °C/min. Mass spectra were acquired in full scan mode in the range of 30–500 m/z.

Cryoprobe NMR analysis

NMR spectra were acquired on a Bruker Avance III 500 MHz instrument at 25 °C, equipped with a 5 mm H–C–N cryoprobe. The sample was dissolved in 125 µL $CDCl_3$ and contained in a 3 mm wilmad 335 pp NMR tube. Proton, carbon, Dept 90, Dept 135, HMQC and HMBC spectra were recorded. A 30° observe pulse was used to acquire the ^{1}H NMR spectrum, while a 45° pulse was used to obtain the ^{13}C NMR spectrum.

Supporting Information

Supporting Information File 1

Details on genetic knockout, Southern blot analysis, LC–MS analysis and NMR data.
[http://www.beilstein-journals.org/bjoc/content/supplementary/1860-5397-9-205-S1.pdf]

Acknowledgements

The authors are indebted to the American Cancer Society and the Welch Foundation (Grant #A-1828) for financial support of this work.

References

1. Bentley, S. D.; Chater, K. F.; Cerdeño-Tárraga, A.-M.; Challis, G. L.; Thomson, N. R.; James, K. D.; Harris, D. E.; Quail, M. A.; Kieser, H.; Harper, D.; Bateman, A.; Brown, S.; Chandra, G.; Chen, C. W.; Collins, M.; Cronin, A.; Fraser, A.; Goble, A.; Hidalgo, J.; Hornsby, T.; Howarth, S.; Huang, C.-H.; Kieser, T.; Larke, L.; Murphy, L.; Oliver, K.; O'Neil, S.; Rabbinowitsch, E.; Rajandream, M.-A.; Rutherford, K.; Rutter, S.; Seeger, K.; Saunders, D.; Sharp, S.; Squares, R.; Squares, S.; Taylor, K.; Warren, T.; Wietzorrek, A.; Woodward, J.; Barrell, B. G.; Parkhill, J.; Hopwood, D. A. *Nature* **2002,** *417,* 141–147. doi:10.1038/417141a
2. Oliynyk, M.; Samborskyy, M.; Lester, J. B.; Mironenko, T.; Scott, N.; Dickens, S.; Haydock, S. F.; Leadlay, P. F. *Nat. Biotechnol.* **2007,** *25,* 447–453. doi:10.1038/nbt1297
3. Reading, N. C.; Sperandio, V. *FEMS Microbiol. Lett.* **2006,** *254,* 1–11. doi:10.1111/j.1574-6968.2005.00001.x
4. Angell, S.; Bench, B. J.; Williams, H.; Watanabe, C. M. H. *Chem. Biol.* **2006,** *13,* 1349–1359. doi:10.1016/j.chembiol.2006.10.012
5. Oh, D.-C.; Kauffman, C. A.; Jensen, P. R.; Fenical, W. *J. Nat. Prod.* **2007,** *70,* 515–520. doi:10.1021/np060381f
6. Brady, S. F.; Chao, C. J.; Clardy, J. *J. Am. Chem. Soc.* **2002,** *124,* 9968–9969. doi:10.1021/ja0268985
7. Courtois, S.; Cappellano, C. M.; Ball, M.; Francou, F.-X.; Normand, P.; Helynck, G.; Martinez, A.; Kolvek, S. J.; Hopke, J.; Osburne, M. S.; August, P. R.; Nalin, R.; Guérineau, M.; Jeannin, P.; Simonet, P.; Pernodet, J.-L. *Appl. Environ. Microbiol.* **2003,** *69,* 49–55. doi:10.1128/AEM.69.1.49-55.2003

8. Bergmann, S.; Schümann, J.; Scherlach, K.; Lange, C.; Brakhage, A. A.; Hertweck, C. *Nat. Chem. Biol.* **2007,** *3,* 213–217. doi:10.1038/nchembio869
9. Challis, G. L. *Microbiology* **2008,** *154,* 1555–1569. doi:10.1099/mic.0.2008/018523-0
10. Gross, H. *Appl. Microbiol. Biotechnol.* **2007,** *75,* 267–277. doi:10.1007/s00253-007-0900-5
11. Foulke-Abel, J.; Agbo, H.; Zhang, H.; Mori, S.; Watanabe, C. M. H. *Nat. Prod. Rep.* **2011,** *28,* 693–704. doi:10.1039/c0np00049c
12. Zhao, Q.; He, Q.; Ding, W.; Tang, M.; Kang, Q.; Yu, Y.; Deng, W.; Zhang, Q.; Fang, J.; Tang, G.; Liu, W. *Chem. Biol.* **2008,** *15,* 693–705. doi:10.1016/j.chembiol.2008.05.021
13. Kelly, G. T.; Liu, C.; Smith, R., III; Coleman, R. S.; Watanabe, C. M. H. *Chem. Biol.* **2006,** *13,* 485–492. doi:10.1016/j.chembiol.2006.02.015
14. Finking, R.; Marahiel, M. A. *Annu. Rev. Microbiol.* **2004,** *58,* 453–488. doi:10.1146/annurev.micro.58.030603.123615
15. Citron, C. A.; Rabe, P.; Dickschat, J. S. *J. Nat. Prod.* **2012,** *75,* 1765–1776. doi:10.1021/np300468h
16. Oliynyk, M.; Stark, C. B. W.; Bhatt, A.; Jones, M. A.; Hughes-Thomas, Z. A.; Wilkinson, C.; Oliynyk, Z.; Demydchuk, Y.; Staunton, J.; Leadlay, P. F. *Mol. Microbiol.* **2003,** *49,* 1179–1190. doi:10.1046/j.1365-2958.2003.03571.x
17. Wang, W.; Mazurkewich, S.; Kimber, M. S.; Seah, S. Y. K. *J. Biol. Chem.* **2010,** *285,* 36608–36615. doi:10.1074/jbc.M110.159509
18. Hara, H.; Masai, E.; Miyauchi, K.; Katayama, Y.; Fukuda, M. *J. Bacteriol.* **2003,** *185,* 41–50. doi:10.1128/JB.185.1.41-50.2003
19. Maruyama, K.; Miwa, M.; Tsujii, N.; Nagai, T.; Tomita, N.; Harada, T.; Sobajima, H.; Sugisaka, H. *Biosci., Biotechnol., Biochem.* **2001,** *65,* 2701–2709. doi:10.1271/bbb.65.2701
20. Hata, T.; Koga, F.; Sano, Y.; Kanamori, K.; Matsumae, A.; Sugawara, R.; Hoshi, T.; Shima, T.; Ito, S.; Tomizawa, S. *J. Antibiot., Ser. A* **1954,** *7,* 107–112.
21. Sambrook, J. R.; Russell, D. W. *Molecular Cloning a Laboratory Manual;* Cold Spring Harbour Laboratory Press: Cold Spring Harbour, 2001; 6.33–6.38.
22. Kieser, T.; Bibb, M. J.; Buttner, M. J.; Chater, K. F.; Hopwood, D. A. *Practical Streptomyces Genetics;* The John Innes Foundation: Norwich, UK, 2000.
23. Kelly, G. T.; Sharma, V.; Watanabe, C. M. H. *Bioorg. Chem.* **2008,** *36,* 4–15. doi:10.1016/j.bioorg.2007.08.002

License and Terms

This is an Open Access article under the terms of the Creative Commons Attribution License (http://creativecommons.org/licenses/by/2.0), which permits unrestricted use, distribution, and reproduction in any medium, provided the original work is properly cited.

The license is subject to the *Beilstein Journal of Organic Chemistry* terms and conditions: (http://www.beilstein-journals.org/bjoc)

The definitive version of this article is the electronic one which can be found at: doi:10.3762/bjoc.9.205

Beilstein Journal of Organic Chemistry

Synthesis and antibacterial activity of monocyclic 3-carboxamide tetramic acids

Yong-Chul Jeong and Mark G. Moloney*

Full Research Paper

Open Access

Address:
Chemistry Research Laboratory, University of Oxford, Mansfield Rd, University of Oxford, OX1 3TA, UK

Email:
Mark G. Moloney* - mark.moloney@chem.ox.ac.uk

* Corresponding author

Keywords:
acylation; antibacterial; drug discovery; natural products; tetramate

Beilstein J. Org. Chem. **2013,** *9,* 1899–1906.
doi:10.3762/bjoc.9.224

Received: 25 June 2013
Accepted: 23 August 2013
Published: 19 September 2013

This article is part of the Thematic Series "Natural products in synthesis and biosynthesis".

Guest Editor: J. S. Dickschat

© 2013 Jeong and Moloney; licensee Beilstein-Institut.
License and terms: see end of document.

Abstract

A chemical library of carboxamide-substituted tetramates designed by analogy with antibacterial natural products, a method for their rapid construction, and the evaluation of their antibacterial activity is reported.

Introduction

The discovery of new antibiotic families with novel modes of action is a promising way to overcome resistant or virulent bacteria, since novel modes of action might be expected to slow target-based endogenous resistance [1]. In this regard, natural products play a major role by providing a biologically validated starting point [2]. Recently discovered antibiotic lead compounds of major interest include platensimycin (a FabF inhibitor) [3], R207910 (an ATP synthase inhibitor) [4] and moiramide B (a bacterial acetyl-CoA carboxylase inhibitor) [5]. Both natural 3-acyltetramic acids, for example streptolydigin **1a** (bacterial RNA polymerase (RNAP) inhibitory activity) [6] and kibdelomycin **1b** (bacterial type II topoisomerase inhibitory activity) [7] and unnatural systems, such as 3-carboxamide tetramic acid **1c** and 3-carboxamide piperidine-2,4-dione **1d** (undecaprenyl pyrophosphate synthase (UPPS) inhibitory activity) [8] exhibit high levels of antibacterial activity (Figure 1). All these systems share a β-dicarbonyl core. A drug discovery programme inspired by these natural products, as promoted by Waldmann [9], was of interest to us. We have recently focused on the construction and evaluation of libraries derived from tetramic acid scaffolds and discovered that bicyclic 3-carboxamide **1e**, bicyclic 3-acyl **1f** and monocyclic 3-acyl **1g** exhibit a dual targeting ability at RNAP and UPPS, while 3-acyl piperidine-2,4-dione **1h** only targets UPPS [10]. Although tetramates are well-known as a core component in many natural products that continue to excite interest [11-14], we carried out a more detailed study of the synthesis, tautomeric behaviour and antibiotic activity of related monocyclic 3-carboxamide tetramic acid systems **2** and **3** (Schemes 1–3), the results of which are outlined below. In

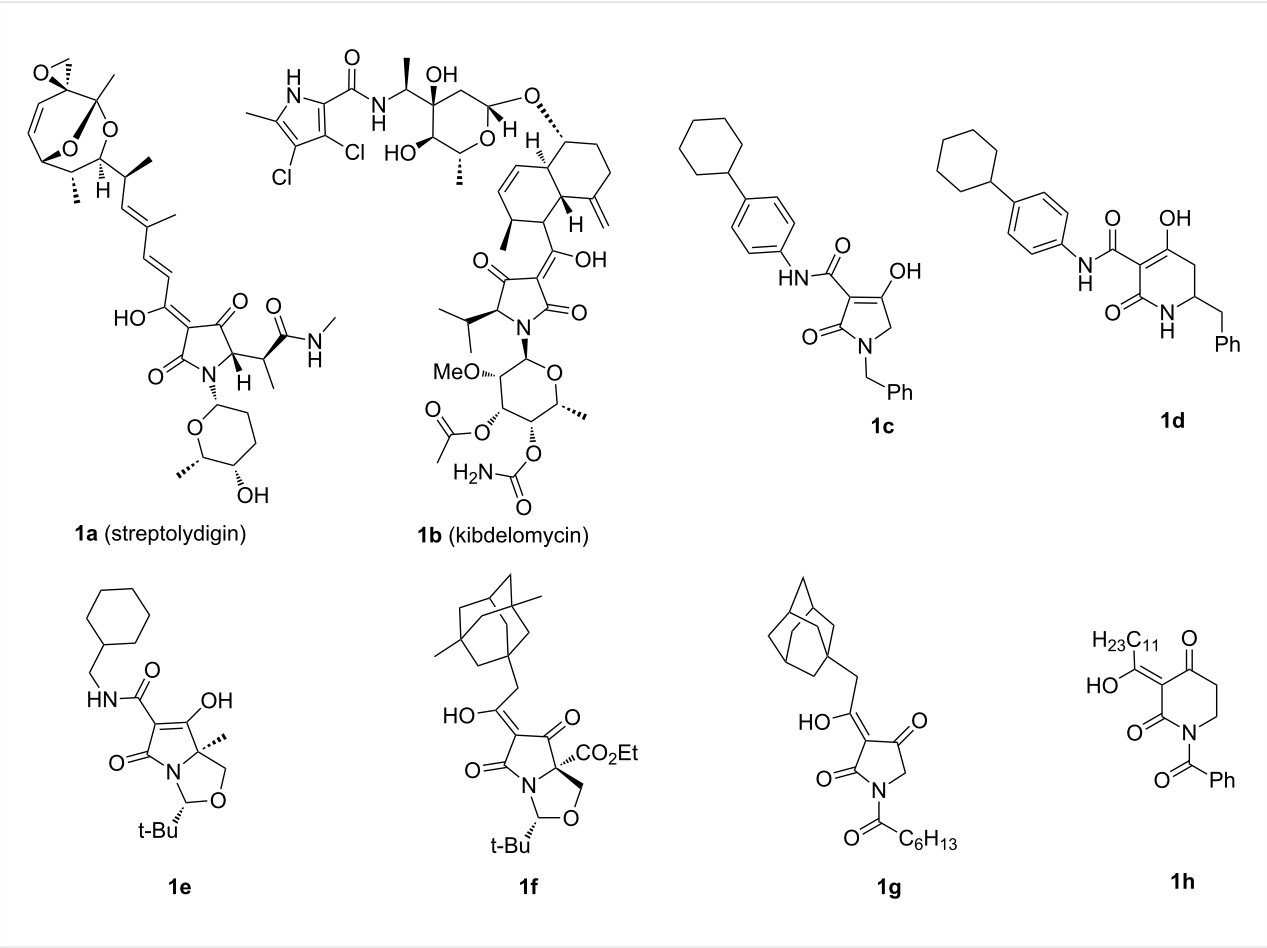
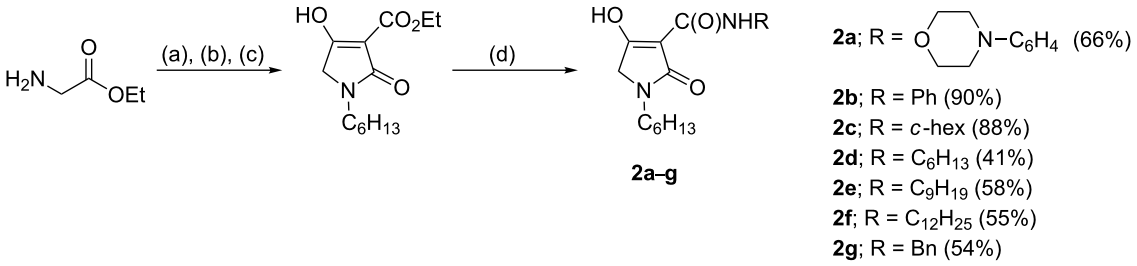


Figure 1: Some antibiotic natural and unnatural tetramic acids.



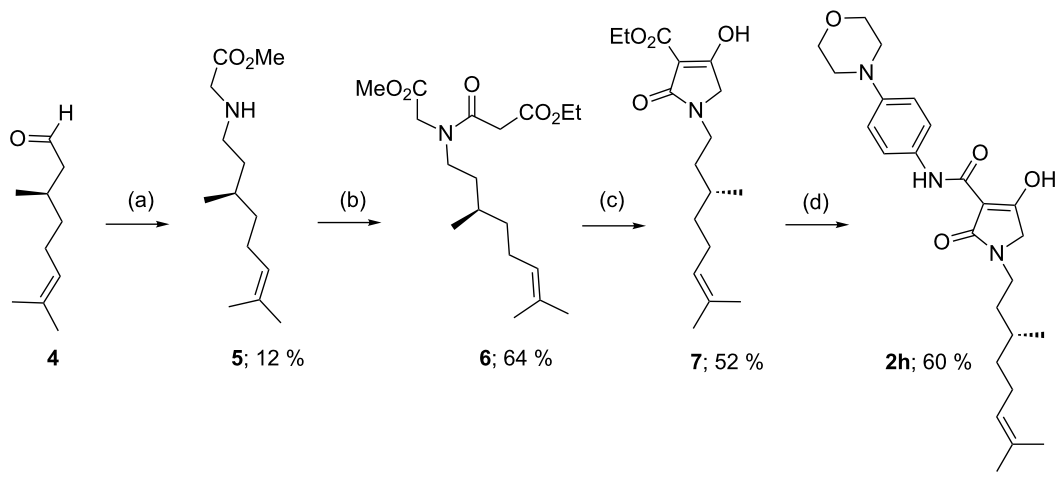
Scheme 1: Synthesis of simple 3-carboxamide tetramic acids. Reaction conditions: (a) triethylamine (2.0 equiv), 1-bromohexane (0.5 equiv), EtOH, reflux; (b) monoethyl malonate (1.1 equiv), DCC (1.1 equiv), CH_2Cl_2, rt; (c) NaOMe (1.1 equiv), benzene, EtOH, reflux; (d) RNH_2 (1.0 equiv), toluene, reflux.

system **2**, the N(1) and C(5) substituents were chosen in order to probe the effect of the length of the *N*-alkyl chain on antibiotic activity. The substituents of system **3** were chosen in order to probe the effect of a C(3) substituent containing a sulfur heteroatom, which we had earlier seen results in enhanced antibacterial activity compared with the oxygen counterpart [10], for two types of amide substituent and a range of C(3) carboxamides.

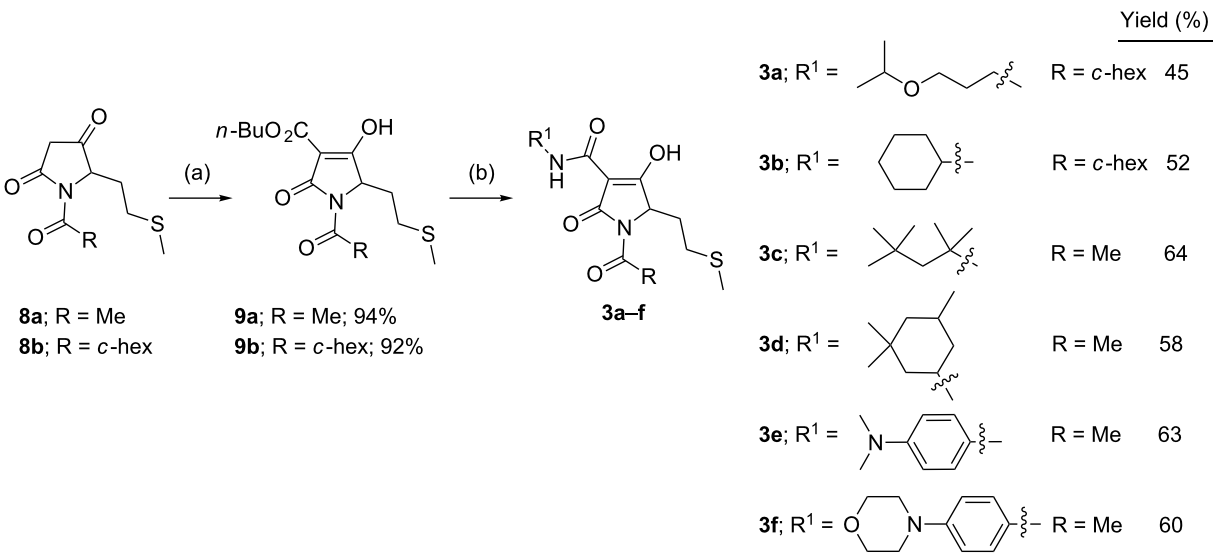
Results and Discussion

Synthesis

The synthesis of the required tetramic acid systems **2a**–**g** (Scheme 1), **2h** (Scheme 2) and **3a**–**f** (Scheme 3) was achieved by Dieckmann cyclisation of the required *N*-alkyl-*N*-malonyl glycine (readily prepared from glycine). A similar strategy for the base-mediated cyclisation of *N*-acetoacetylamino acid esters leading to 3-acetyltetramates has been reported, which give



Scheme 2: Synthesis of *N*-alkyl 3-carboxamide tetramic acid. Reaction conditions: (a) 1. glycine methyl ester·HCl (1.0 equiv), Et_3N (1.2 equiv), $MgSO_4$ (2.0 equiv), THF, rt. 2. $NaBH_4$ (2.0 equiv), MeOH, rt; (b) ethyl malonyl chloride (1.05 equiv), Et_3N (1.2 equiv), CH_2Cl_2, rt; (c) KO*t*-Bu (1.1 equiv), THF, reflux; (d) amine (1.0 equiv), toluene, reflux; (e) butyl chloroformate (1.2 equiv), DMAP (2.2 equiv), CH_2Cl_2, rt.



Scheme 3: Synthesis of C(5)-alkyl 3-carboxamide tetramic acids. Reaction conditions: (a) butyl chloroformate (1.2 equiv), DMAP (2.2 equiv), CH_2Cl_2, rt; (b) RNH_2 (1.0 equiv), toluene, reflux.

N–H rather than *N*-alkyl systems [15-17]. Tetramate **7** was obtained from amino acid **6**, except that the key intermediate **5** was obtained by reductive amination (Scheme 2) of (*R*)-citronellal (**4**), which although proceeding in poor yield gave enough material with which to proceed [18]. By contrast, *N*-acyl derivatives could not be easily prepared by an equivalent approach because of the difficulty of a controlled double acylation on N(1). Although the synthesis of *N*-acetyl 3-alkoxycarbonyls from *N*-hydroxysuccinimide esters of *N*-acetylamino acids has been reported [19], we wished to exploit an alternative approach based upon C-acyloxylation of enolates followed by amine exchange, which had been shown to be very effective in a pyroglutamate series, since it offered synthetic simplicity and the potential for generality [20,21]. We found that an approach based upon direct acylation of methyl thioethers **8a**,**b** (these were readily obtained from the required *N*-acylmethionine by DCC/DMAP coupling with Meldrum's acid and cyclisation under reflux) was possible, which made use of the high acidity of the tetramate system. Thus, conversion to the *n*-butyloxycarbonyl derivatives *N*-acyl **9a**,**b** by using 1.2 equivalents of butyl chloroformate along with 2.2 equivalents of 4-(dimethylamino)pyridine (DMAP) proceeded in good

yields (over 90%) (Scheme 3) [10]. With the 3-alkoxycarbonyl tetramic acid core systems **7** and **9** in hand, conversion to 3-carboxamides **2a**–**g** and **3a**–**f** by direct ester–amide exchange under reflux in toluene was readily achieved, providing access to a range of amides in good to excellent yield (Schemes 1–3). This process neatly complements a strategy we had earlier used for the introduction of amine substituents in pyroglutamates by a conjugate addition of amines [22].

Tautomerism

Tautomerism in tricarbonyl 3-acyltetramate systems is known to be complex and strongly dependent on the identity of the side chain acyl group [23]. 3-Acyl (X = CH_2) [10,24,25], 3-carboxamide (X = NH) [8,10] and 3-alkoxycarbonyl (X = O) tetramic acids (Figure 2) have been found to exist as a pair of external conformers (AB and CD) in slow equilibrium (AB ⇌ CD), each consisting of a pair of internal tautomers in rapid equilibrium (A ⇌ B and C ⇌ D). The tautomerisation of 3-acyltetramic acids has been shown to be mainly affected by substitution on N(1) rather than the functionalities on the 3-acyl and C(5) positions. Thus, the dominant tautomer of N-unsubstituted and *N*-alkyltetramates is D, while *N*-acyltetramates exist as a mixture of external tautomers AB and D in approximately equal ratio [23]. By contrast, it was found that the tautomerisation of 3-carboxamides and 3-alkoxycarbonyls was not affected by substitution on N(1). Therefore, the dominant tautomer of 3-carboxamide tetramates is tautomer A (over 80%) with a minor contribution of tautomer D, while 3-alkoxycarbonyltetramates exist as only tautomer A (>99%). In order to understand this phenomenon, the ground state energy of simplified 3-carboxamides **11a**,**b** and 3-alkoxycarbonyls **12a**,**b** was calculated and compared with that of 3-acyl derivatives **10a**,**b** (Table 1). To the best of our knowledge, such a detailed analysis has not been previously reported. In the calculation for *N*-alkyl 3-acyltetramate **10a**, the ground-state energies of tautomers B and D, which shows preference for tautomer D, is considerably lower than those of tautomers A and C. This outcome supports experimental NMR observations (>80% of tautomer D and <20% of tautomer B, Table 1, entry 1). On the other hand, the ground state energy of tautomer C of *N*-acyl **10b** is considerably higher than that of tautomers A, B and D, also supporting the NMR observations (tautomer AB:D = about 50:50, Table 1, entry 2). However, tautomer A of 3-carboxamides was the most stable for both of *N*-alkyl tetramate **11a** and *N*-acyl tetramate **11b** (>80% of tautomer A and <20% of tautomer D, Table 1, entry 3 and entry 4), while for 3-alkoxycarbonyltetramates **12a**,**b**, tautomer A was the most stable, and significantly more stable than tautomers B–D. These finding support the conclusion that 3-alkoxycarbonyls exist only as tautomer A (Table 1, entry 5 and entry 6).

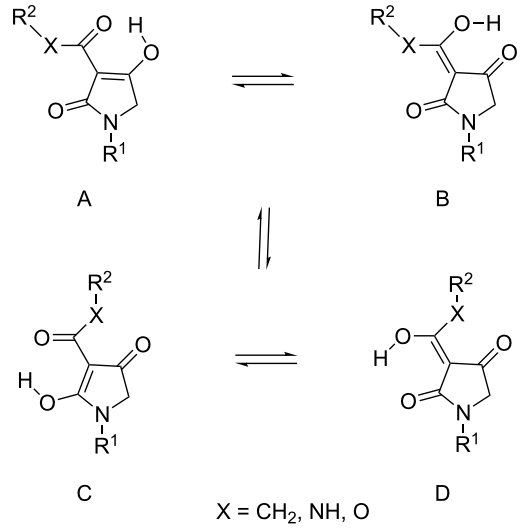
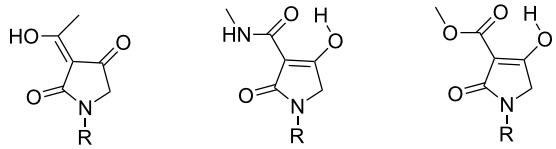


Figure 2: Tautomerism of tetramates.

Table 1: Calculated energy of the ground state of 3-acyltetramic acids **10a**,**b**, 3-carboxamide tetramic acids **11a**,**b** and 3-alkoxycarbonyl tetramic acids **12a**,**b**.



10a; R = Me
10b; R = Acetyl

11a; R = Me
11b; R = Acetyl

12a; R = Me
12b; R = Acetyl

Entry	Compound	Calcd relative energy (kcal/mol)[a,b]			
		Form A	Form B	Form C	Form D
1	**10a**	+4.16	+1.61	+4.30	0
2	**10b**[c]	+1.59	+0.17	+5.62	0
3	**11a**	−0.51	+0.42	+1.74	0
4	**11b**	−0.91	−0.15	+3.82	0
5	**12a**	−3.58	+1.75	−1.41	0
6	**12b**	−6.24	−0.64	+3.20	0

[a]The energy difference between each tautomer related to tautomer D. [b]Calculated by using DFT B3LYP (6-31G*) in Spartan 02. [c]Reported in our previous paper [10].

Antibacterial activity

The antibiotic activities of tetramates **2a**–**h** and **3a**–**f** along with analogues **1c** and **1d** (reported by Novartis [8]) were determined against 4 species of Gram-positive bacteria, consisting of 4 strains of *Staphylococcus aureus*, including a methicillin-resistant strain (MRSA, S2), vancomycin susceptible *Enterococcus faecalis* (VSE, E1), vancomycin resistant *E. faecium* (VanA VRE, E2)), and 2 strains of *Streptococcus pneumoniae*,

including multi-drug resistant strain (MDRSP, P9), as well as 3 species of Gram-negative bacteria, consisting of *Pseudomonas aeruginosa* and 2 strains of *Haemophilus influenzae*, including an efflux-negative strain, and 2 strains of *Escherichia coli*, including an efflux-negative strain (Table 2). Relevant physicochemical properties of the analogues are also shown in Table 3. These were used to elaborate structure–activity relationships (SAR) [26]. In the assay against Gram-negative bacteria, no activity against *E. coli* and *P. aeruginosa* was found (MIC > 64 μg/mL, data not shown), consistent with the inactivity of 3-acyl and 3-carboxamide tetramic acids against these strains seen earlier [7,8,10]. This result is most likely explained by their poor cell permeability as a result of their hydrophobic character [14,27]. However, activities against another Gram-negative bacterium, *H. influenzae*, were found, the magnitude of which depended on the substituent. An SAR consistent with transportation by the efflux pump was found [28]. Analogues **2e**,**h** and **1c**,**d**, for which activity differences between efflux-positive (H3) and negative (H4) *H. influenza* strains are large, are more lipophilic compared with other active analogues (rel-PSA < 13.5, c log P > 2.79 and c log D (7.4) > 1.41). On the other hand, analogues **2** and **3** show a broad-spectrum activity against Gram-positive bacteria, although the activity depends on the substituent identities. Importantly, the variation of antibacterial activity for analogues **2** and **3** was less pronounced in the resistant strains MRSA, VRE and MDRSP (normally less than 8 times variation, with the exception of analogues **2e** and **3b**), while the activities of Novartis analogue **1c** against MRSA [8], amoxicillin against MDRSP and ciprofloxacin against MRSA and VRE were significantly lower (more than 250 times compared with the activity against the most sensitive strain). Among the various substituent groups, *N*-alkyl phenyl derivatives **2a**,**b**,**h** were active, while *N*-acetyl phenyl derivatives **3e**,**f** were inactive or only very weakly active. This SAR might be accounted for by their physicochemical properties: the less lipophilic character of *N*-acetyl **3e**,**f** (rel-PSA > 17.0%, c log P < 0.80 and c log D (7.4) < −1.20) compared with those of *N*-alkyl **2a**,**b**,**h** (rel-PSA < 15.0%, c log P > 1.77 and c log D (7.4) > 0.41) might make penetration of the bacterial cell membrane more difficult. However, 3-carboxamides **2c**–**g** and **3a**–**d**, all possessing alkyl substituents, including a benzyl group on the

Table 2: In vitro antibiotic activity (MIC, μg/mL) of tetramic acids.[a,b]

	S1	S26	S4	S2	E1	E2	P1	P9	P9B	H3	H4
2a[c]	4	8	8	8	8	8	16	8	32	16	4
2b[c]	1	1	1	2	2	4	4	4	–[d]	2	0.5
2c[c]	8	8	8	8	8	8	16	8	8	4	0.25
2d[c]	2	2	2	2	2	2	4	1	4	1	0.12
2e[c]	2	16	16	16	8	0.5	4	1	4	>64	≤0.1
2f	>64	>64	>64	>64	>64	>64	16	8	16	>64	>64
2g	8	8	8	8	16	8	64	16	8	4	0.25
2h	2	2	2	2	2	2	8	4	>64	>64	8
3a	>64	>64	32	>64	16	16	8	8	8	>64	>64
3b	4	8	2	8	1	2	0.5	0.5	0.5	8	1
3c	8	32	32	16	8	16	8	8	8	32	4
3d	8	64	32	32	8	16	8	8	4	64	4
3e	>64	>64	>64	>64	>64	>64	64	64	64	>64	64
3f	>64	>64	>64	>64	>64	>64	>64	>64	>64	>64	>64
1c[c]	0.1	0.12	1	**64**	≤0.1	≤0.1	2	2	2	>64	0.5
1d	8	64	32	64	32	4	64	64	>64	>64	16
Line[c]	2	2	2	2	2	2	1	0.5	0.5	16	4
Cip	0.1	0.5	0.12	**16**	1	**32**	1	1	1	0.5	≤0.1
Amox	–[d]	–[d]	–[d]	–[d]	–[d]	–[d]	>0.03	**8**	–[d]	–[d]	–[d]
Caz	8	16	16	–[d]	–[d]	–[d]	–[d]	–[d]	–[d]	–[d]	–[d]

[a]Abbreviation; **S1**; *S. aureus* 1, ATCC13709 in vivo (methicillin sensitive), **S26**; *S. aureus* 26, ATCC25923 (vancomycin susceptible), **S4**; *S. aureus* 4, Oxford, **S2**; *S. aureus* 2, (MRSA in vivo), **E1**; *E. faecalis* 1, ATCC29212 VanS (vancomycin susceptible), **E2**; *E. faecium* 1, VanA (vancomycin resistant), **P1**; *S. pneumonia* 1, ATCC49619 (erythromycin susceptible), **P9**; *S. pneumonia* 9, (multi-drug resistant), **P9B**; *S. pneumonia* 9 in presence of 2.5% horse blood, **H3**; *H. influenzae* 3, ATCC31517 MMSA, **H4**; *H. influenzae* 4, LS2 Efflux knock out, **Line**; linezolid, **Cip**; ciprofloxacin, **Amox**; amoxicillin, **Caz**; ceftazidime. [b]All analogues are inactive (MIC > 64 μg/mL) against *E. coli* 1, ATCC25922 (non pathogenic strain), *E. coli* 50, Ec49 No efflux and *P. aeruginosa* 1, ATCC27853. [c]The activity was reported in our previous publication [10]. [d]Not determined.

Table 3: Physicochemical properties of 3-carboxamide tetramic acids.[a,b]

	MW	MSA	PSA	rel-PSA	c log P	c log D (7.4)	HD/HA	RB
2a[c]	387	599	82.1	13.7	1.77	0.41	2/5	8
2b[c]	302	462	69.6	15.1	1.85	0.64	2/3	7
2c[c]	308	509	69.6	13.7	1.28	−0.15	2/3	7
2d[c]	310	540	69.6	12.9	1.69	0.23	2/3	11
2e[c]	353	632	69.6	11.0	2.88	1.42	2/3	14
2f	395	725	69.6	9.6	4.07	2.61	2/3	17
2g	316	492	69.6	14.1	1.47	−0.04	2/3	8
2h	442	691	82.1	11.9	2.79	1.41	2/5	9
3a	427	662	95.9	14.5	0.90	−1.32	2/5	10
3b	409	613	86.7	14.1	1.84	−0.19	2/4	6
3c	371	590	86.7	14.7	0.84	−1.13	2/4	7
3d	383	586	86.7	14.8	1.06	−0.96	2/4	5
3e	377	530	90.0	17.0	0.80	−1.20	2/5	6
3f	419	577	99.2	17.2	0.46	−1.54	2/6	6
1c	390	568	69.6	12.3	3.51	2.03	2/3	5
1d	405	591	78.4	13.3	3.63	2.96	3/3	5

[a]MW; molecular weight, MSA; molecular surface area, PSA; polar surface area, %PAS; relative polar surface area = (PSA/MSA) × 100, c log P; calculated partition coefficient, c log D (7.4); calculated distribution coefficient at pH 7.4, HD; hydrogen-bond donor count, HA; hydrogen-bond acceptor count, RB; rotatable bond count. [b]Tautomer A was selected for the calculation. [c]Reported in our previous publication [10].

amide function, are also active to Gram-positive strains. Furthermore, the activities of *n*-alkyl **2d**–**f** depended on the chain length, with a marked drop-off in activity for the longer chain **2f**. In addition, the activity of the more lipophilic analogues **2a**,**d**–**f**,**h** (PSA ≤ 13.7%, c log P ≥ 1.69 and c log D (7.4) ≥ 0.23) in the presence of 2.5% horse blood was shifted to high MICs even though that of less lipophilic analogues **2c**,**g** and **3a**–**e** (PSA ≥ 13.7%, c log P ≤ 1.84 and c log D (7.4) ≤ −0.04) was maintained. This serum-protein binding significantly affected the activity against *S. aureus* S26, since almost all analogues showed inactivity (MIC > 64 μg/mL) in the presence of 10% human serum with the exception of **2a** (32 μg/mL) and **2b** (64 μg/mL) (data not shown).

After screening to find the most active compound, tetramate **2b** was selected for a detailed investigation and its antibiotic activity against various drug-resistant strains was further evaluated with reference antibiotics (Table 4). Tetramate **2b** was

Table 4: Antibiotic activity of tetramic acid **2b**.[a]

Strains	Phenotype	MIC (μg/mL)					
		2b	Moxi	Amox	Ery	Vanco	Caz
S. pneumoniae Pn7	EryR	2	0.125	**4**	**16**	0.25	–[c]
S. pneumoniae Pn10	PenR, EryR	2	0.125	**4**	**>32**	0.5	–[c]
S. pneumoniae Pn11	PenR	2	0.125	**4**	<0.03	0.25	–[c]
S. pneumoniae Pn19	EryR	2	0.06	0.06	**>32**	0.5	–[c]
S. pneumoniae Pn21	EryR	2	0.06	0.125	**4**	0.25	–[c]
S. pneumoniae Pn31	EryR	0.13	<0.03	<0.03	**16**	0.5	–[c]
S. aureus Sa5	ermR PK2[b]	1	≤0.03	–[c]	–[c]	–[c]	**32**
S. aureus Sa18	FQR	1	**32**	–[c]	–[c]	–[c]	**16**
S. aureus Sa40	mecA[b]	1	≤0.03	–[c]	–[c]	–[c]	**32**

[a]Abbreviation: EryR; erythromycin resistant, PenR; penicillin resistant, FQR; fluoroquinolone resistant, Moxi; moxifloxacin, Amox; amoxicillin, Ery; erythromycin, Caz; ceftazidime. [b]Methicillin-resistant strain. [c]Not determined.

found to be active against virulent and resistant strains, such as methicillin and fluoroquinolone-resistant *S. aureus* and penicillin and/or erythromycin-resistant *S. pneumoniae*. Remarkably, tetramate **2b** maintained the activities against all the strains and was highly effective against erythromycin resistant *S. pneumoniae* Pn31 (MIC = 0.125 μg/mL). By way of comparison, the activities of moxifloxacin (a fourth generation fluoroquinolone) to *S. aureus* Sa18 (MIC = 32 μg/mL), amoxicillin (β-lactam) to *S. pneumoniae* Pn7, Pn10 and Pn11 (MIC = 4 μg/mL), erythromycin to *S. pneumoniae* Pn7, Pn10, Pn19, Pn21 and Pn31 (MIC ≥ 4 μg/mL) and ceftazidime (a third generation cephalosporin) to *S. aureus* Sa5, Sa18 and Sa40 (MIC ≥ 16 μg/mL) were substantially decreased.

Lipophilic efficiency (LipE) has been used to assess the suitability of drug candidates as CB agonists [29], and the usage of a similar calculation for the data presented in this work (with LipE = pMIC(nM) − c Log P) (see Table S1 and Figure S1 in Supporting Information File 1; pMIC values were calculated according to a literature protocol [30]), facilitated the identification of compounds with potential for optimisation. According to Figure S1, strongly active compounds can be found at c log P values of 1–2, 3 or 4, and for the highly susceptible strain H4, for example, compounds of interest would be **2b**–**e** and **2g**.

Conclusion

We have prepared monocyclic 3-carboxamide tetramic acids from 3-alkoxycarbonyl tetramic acids based on a direct ester–amide exchange by using butyl chloroformate with DMAP, thereby providing a general access to this type of system. The tautomerization of 3-alkoxycarbonyl and 3-carboxamide tetramic acids compared to 3-acyltetramic acids has been investigated. It has been found that 3-alkoxycarbonyl and 3-carboxamide tetramic acids prefer tautomer A, while the preference of 3-acyltetramic acids depends on the N(1)-functionality. Of particular interest is that 3-carboxamide analogues, especially **2b**, have shown bioactivity against various Gram-positive bacteria including clinically resistant strains such as MRSA, fluoroquinolone-resistant *S. aureus*, MDRSP, penicillin and erythromycin-resistant *S. pneumonia* and VRE as well as Gram-negative *H. influenzae*. Further optimisation, especially for overcoming high plasma-protein binding, is warranted but these compounds may be suitable for an evaluation for topical use [31,32]. Significantly, these results suggest that a drug discovery approach based upon deconstruction–reconstruction inspired by suitable natural products with demonstrable biological activity provides a route for the rapid assembly of compound libraries, which, even if not fully optimized, provide a useful starting point for further elaboration.

Experimental

General. Melting points were determined with a Stuart Scientific SMP1 melting point device and are uncorrected. The ^{1}H and ^{13}C NMR spectra were obtained by using a Bruker Avance AV400 (400 MHz and 100 MHz, respectively) with residual solvent peaks as the internal reference. Mass spectra (MS) and high-resolution mass spectra (HRMS) were obtained with Micro Mass LCT and GCT spectrometers under the conditions of electrospray ionization (ESI) and chemical ionization (CI) respectively, and values were reported as a ratio of mass to charge in Daltons.

Synthesis. The synthesis of monocyclic precursor tetramate compounds from glycine has been reported in our previous publication [33].

Calculations. Density Functional B3LYP (6-31G*) in Spartan 02 was used for the calculation of the energy in equilibrium geometry at ground state. MarvinSketch Version 5.3.8. (http://www.chemaxon.org) was used for the calculation of the van der Waals molecular surface area (MSA), the polar surface area (PSA), the calculated partition coefficient (c log P) under VG method, the calculated distribution coefficient at pH 7.4 [c log D (7.4)] under VG method, the hydrogen-bond donor count, the hydrogen-bond acceptor count, and the rotatable bond count.

Antibacterial activity. Antibiotic activity was measured by using standard methodology (Clinical and Laboratory Standards Institute. Methods for antimicrobial susceptibility test for bacteria that grow aerobically, approved standard M7-A7, 7th ed., CLSI, Wayne, PA, 2006): compounds were diluted in DMSO to obtain 2.56 mg/mL, then 100 μL were diluted in Mueller-Hinton broth to 0.256 mg/mL and assayed against the bacterial panel by incubation in 96-well microplates at 37 °C for 24 h. The MIC was determined by visually reading the first concentration where no growth (no turbidity) appeared.

Supporting Information

Supporting Information File 1

Experimental details, calculated energies (Spartan) for selected compounds and NMR spectra.
[http://www.beilstein-journals.org/bjoc/content/supplementary/1860-5397-9-224-S1.pdf]

Acknowledgements

We are particularly grateful for valuable input by Drs Phil Dudfield and John Lowther, and for funding by Galapagos SASU (France).

References

1. Donadio, S.; Maffioli, S.; Monciardini, P.; Sosio, M.; Jabes, D. *J. Antibiot.* **2010,** *63,* 423–430. doi:10.1038/ja.2010.62
2. von Nussbaum, F.; Brands, M.; Hinzen, B.; Weigand, S.; Häbich, D. *Angew. Chem., Int. Ed.* **2006,** *45,* 5072–5129. doi:10.1002/anie.200600350
3. Wang, J.; Soisson, S. M.; Young, K.; Shoop, W.; Kodali, S.; Galgoci, A.; Painter, R.; Parthasarathy, G.; Tang, Y. S.; Cummings, R.; Ha, S.; Dorso, K.; Motyl, M.; Jayasuriya, H.; Ondeyka, J.; Herath, K.; Zhang, C.; Hernandez, L.; Allocco, J.; Basillo, A.; Tormo, J. R.; Genilloud, O.; Vicente, F.; Pelaez, F.; Colwell, L.; Lee, S. H.; Michael, B.; Felcetto, T.; Gill, C.; Silver, L. L.; Hermes, J. D.; Bartizal, K.; Barrett, J.; Schmatz, D.; Becker, J. W.; Cully, D.; Singh, S. B. *Nature* **2006,** *441,* 358–361. doi:10.1038/nature04784
4. Andries, K.; Verhasselt, P.; Guillemont, J.; Göhlmann, H. W. H.; Neefs, J.-M.; Winkler, H.; Gestel, J. V.; Timmerman, P.; Zhu, M.; Lee, E.; Williams, P.; de Chaffoy, D.; Huitric, E.; Hoffner, S.; Cambau, E.; Truffot-Pernot, C.; Lounis, N.; Jarlier, V. *Science* **2005,** *307,* 223–227. doi:10.1126/science.1106753
5. Freiberg, C.; Brunner, N. A.; Schiffer, G.; Lampe, T.; Pohlmann, J.; Brands, M.; Raabe, M.; Häbich, D.; Ziegelbauer, K. *J. Biol. Chem.* **2004,** *279,* 26066–26073. doi:10.1074/jbc.M402989200
6. Tuske, S.; Sarafianos, S. G.; Wang, X.; Hudson, B.; Sineva, E.; Mukhopadhyay, J.; Birktoft, J. J.; Leroy, O.; Ismail, S.; Clark, A. D.; Dharia, C.; Napoli, A.; Laptenko, O.; Lee, J.; Borukhov, S.; Ebright, R. H.; Arnold, E. *Cell* **2005,** *122,* 541–552. doi:10.1016/j.cell.2005.07.017
7. Phillips, J. W.; Goetz, M. A.; Smith, S. K.; Zink, D. L.; Polishook, J.; Onishi, R.; Salowe, S.; Wiltsie, J.; Allocco, J.; Sigmund, J.; Dorso, K.; Lee, S.; Skwish, S.; de la Cruz, M.; Martin, J.; Vicente, F.; Genilloud, O.; Lu, J.; Painter, R. E.; Young, K.; Overbye, K.; Donald, R. G. K.; Singh, S. B. *Chem. Biol.* **2011,** *18,* 955–965. doi:10.1016/j.chembiol.2011.06.011
8. Peukert, S.; Sun, Y.; Zhang, R.; Hurley, B.; Sabio, M.; Shen, X.; Gray, C.; Dzink-Fox, J.; Tao, J.; Cebula, R.; Wattanasin, S. *Bioorg. Med. Chem. Lett.* **2008,** *18,* 1840–1844. doi:10.1016/j.bmcl.2008.02.009
9. Kumar, K.; Waldmann, H. *Angew. Chem., Int. Ed.* **2009,** *48,* 3224–3242. doi:10.1002/anie.200803437
10. Jeong, Y.-C.; Anwar, M.; Bikadi, Z.; Hazai, E.; Moloney, M. G. *Chem. Sci.* **2013,** *4,* 1008–1015. doi:10.1039/c2sc21713a
11. Royles, B. J. L. *Chem. Rev.* **1995,** *95,* 1981–2001. doi:10.1021/cr00038a009
12. Schobert, R.; Schlenk, A. *Bioorg. Med. Chem.* **2008,** *16,* 4203–4221. doi:10.1016/j.bmc.2008.02.069
13. Barnickel, B.; Bayliffe, F.; Diestel, R.; Kempf, K.; Laschat, S.; Pachali, S.; Sasse, F.; Schlenk, A.; Schobert, R. *Chem. Biodiversity* **2010,** *7,* 2830–2845. doi:10.1002/cbdv.201000179
14. Athanasellis, G.; Igglessi-Markopoulou, O.; Markopoulos, J. *Bioinorg. Chem. Appl.* **2010,** 315056. doi:10.1155/2010/315056
15. Yuki, H.; Tohira, Y.; Aoki, B.; Kano, T.; Takama, S.; Yamazaki, T. *Chem. Pharm. Bull.* **1967,** *15,* 1107–1111. doi:10.1248/cpb.15.1107
16. Suzuki, S.; Sano, F.; Yuki, H. *Chem. Pharm. Bull.* **1967,** *15,* 1120–1122. doi:10.1248/cpb.15.1120
17. Toda, S.; Nakagawa, S.; Naito, T.; Kawaguchi, H. *J. Antibiot.* **1980,** *33,* 173–181. doi:10.7164/antibiotics.33.173
18. Yendapally, R.; Hurdle, J. G.; Carson, E. I.; Lee, R. B.; Lee, R. E. *J. Med. Chem.* **2008,** *51,* 1487–1491. doi:10.1021/jm701356q
19. Petroliagi, M.; Igglessi-Markopoulou, O. *Tetrahedron: Asymmetry* **1999,** *10,* 1873–1875. doi:10.1016/S0957-4166(99)00192-5
20. Bailey, J. H.; Cherry, D. T.; Dyer, J.; Moloney, M. G.; Bamford, M. J.; Keeling, S.; Lamont, R. B. *J. Chem. Soc., Perkin Trans. 1* **2000,** 2783–2792. doi:10.1039/B001999M
21. Hill, T. J.; Kocis, P.; Moloney, M. G. *Tetrahedron Lett.* **2006,** *47,* 1461–1463. doi:10.1016/j.tetlet.2005.12.068
22. Chan, P. W. H.; Cottrell, I. F.; Moloney, M. G. *Tetrahedron Lett.* **1997,** *38,* 5891–5894. doi:10.1016/S0040-4039(97)01312-9
23. Yamaguchi, T.; Saito, K.; Tsujimoto, T.; Yuki, H. *J. Heterocycl. Chem.* **1976,** *13,* 533–537. doi:10.1002/jhet.5570130323
24. Jeong, Y.-C.; Moloney, M. G. *J. Org. Chem.* **2011,** *76,* 1342–1354. doi:10.1021/jo102304y
25. Detsi, A.; Micha-Screttas, M.; Igglessi-Markopoulou, O. *J. Chem. Soc., Perkin Trans. 1* **1998,** 2443–2449. doi:10.1039/A801896K
26. O'Shea, R.; Moser, H. E. *J. Med. Chem.* **2008,** *51,* 2871–2878. doi:10.1021/jm700967e
27. Gänzle, M. G. *Appl. Microbiol. Biotechnol.* **2004,** *64,* 326–332. doi:10.1007/s00253-003-1536-8
28. Fernandes, J.; Gattass, C. R. *J. Med. Chem.* **2009,** *52,* 1214–1218. doi:10.1021/jm801389m
29. Ryckmans, T.; Edwards, M. P.; Horne, V. A.; Correia, A. M.; Owen, D. R.; Thompson, L. R.; Tran, I.; Tutt, M. F.; Young, T. *Bioorg. Med. Chem. Lett.* **2009,** *19,* 4406–4409. doi:10.1016/j.bmcl.2009.05.062
30. Selvaraj, C.; Tripathi, S. K.; Reddy, K. K.; Singh, S. K. *Curr. Trends Biotechnol. Pharm.* **2011,** *5,* 1104–1109.
31. Mc Chlery, S.; Ramage, G.; Bagg, J. *Periodontology 2000* **2009,** *49,* 151–165. doi:10.1111/j.1600-0757.2008.00278.x
32. Fogo, A.; Kemp, N.; Morris-Jones, R. *BMJ [Br. Med. J.]* **2011,** *343,* d5343. doi:10.1136/bmj.d5343
33. Jeong, Y.-C.; Moloney, M. G. *Synlett* **2009,** 2487–2491. doi:10.1055/s-0029-1217745

License and Terms

This is an Open Access article under the terms of the Creative Commons Attribution License (http://creativecommons.org/licenses/by/2.0), which permits unrestricted use, distribution, and reproduction in any medium, provided the original work is properly cited.

The license is subject to the *Beilstein Journal of Organic Chemistry* terms and conditions: (http://www.beilstein-journals.org/bjoc)

The definitive version of this article is the electronic one which can be found at: doi:10.3762/bjoc.9.224

Beilstein Journal of Organic Chemistry

Stereoselective synthesis of the C79–C97 fragment of symbiodinolide

Hiroyoshi Takamura*[1], Takayuki Fujiwara[1], Isao Kadota*[1] and Daisuke Uemura[2]

Letter

Open Access

Address:
[1]Department of Chemistry, Graduate School of Natural Science and Technology, Okayama University, 3-1-1 Tsushimanaka, Kita-ku, Okayama 700-8530, Japan and [2]Department of Chemistry, Faculty of Science, Kanagawa University, 2946 Tsuchiya, Hiratsuka 259-1293, Japan

Email:
Hiroyoshi Takamura* - takamura@cc.okayama-u.ac.jp; Isao Kadota* - kadota-i@cc.okayama-u.ac.jp

* Corresponding author

Keywords:
Julia–Kocienski olefination; polyol marine natural product; Sharpless asymmetric dihydroxylation; spiroacetalization; symbiodinolide

Beilstein J. Org. Chem. **2013,** *9,* 1931–1935.
doi:10.3762/bjoc.9.228

Received: 18 July 2013
Accepted: 03 September 2013
Published: 25 September 2013

This article is part of the Thematic Series "Natural products in synthesis and biosynthesis".

Guest Editor: J. S. Dickschat

© 2013 Takamura et al; licensee Beilstein-Institut.
License and terms: see end of document.

Abstract

Symbiodinolide is a polyol marine natural product with a molecular weight of 2860. Herein, a streamlined synthesis of the C79–C97 fragment of symbiodinolide is described. In the synthetic route, a spiroacetalization, a Julia–Kocienski olefination, and a Sharpless asymmetric dihydroxylation were utilized as the key transformations.

Findings

A 62-membered polyol marine natural product, symbiodinolide (**1**, Figure 1), was isolated from the 80% aqueous ethanol extract of the cultured symbiotic dinoflagellate *Symbiodinium* sp. in 2007 [1]. Symbiodinolide shows voltage-dependent N-type Ca^{2+} channel-opening activity at 7 nmol/L and COX-1 inhibitory effect at 2 μmol/L (65% inhibition). Furthermore, **1** ruptures the tissue surface of the acoel flatworm *Amphiscolops* sp. at 2.5 μmol/L. The entire planar structure of **1** was established by the detailed 2D NMR spectroscopic analysis. However, the complete stereostructural determination of **1** with its 61 chirality centres and a molar mass of 2860 has been an unsolved issue. Therefore, in order to complete the configurational elucidation of **1**, we are now investigating its chemical degradation [1-3] and chemical synthesis of the fragments [4-11].

Previously, we reported the stereoselective synthesis of the spiroacetal C79–C96 fragment [4], which is summarized in Scheme 1. Triflate **2** was reacted with the lithium acetylide prepared from alkyne **3** to give the desired coupling product **4**. The TBDPS ether **4** was transformed to TIPS ether **5** because of the lability of the TBDPS protecting group under the following Birch conditions. The alkyne **5** was subjected to the Birch reduction to afford the *trans*-alkene **6**, wherein the benzyl

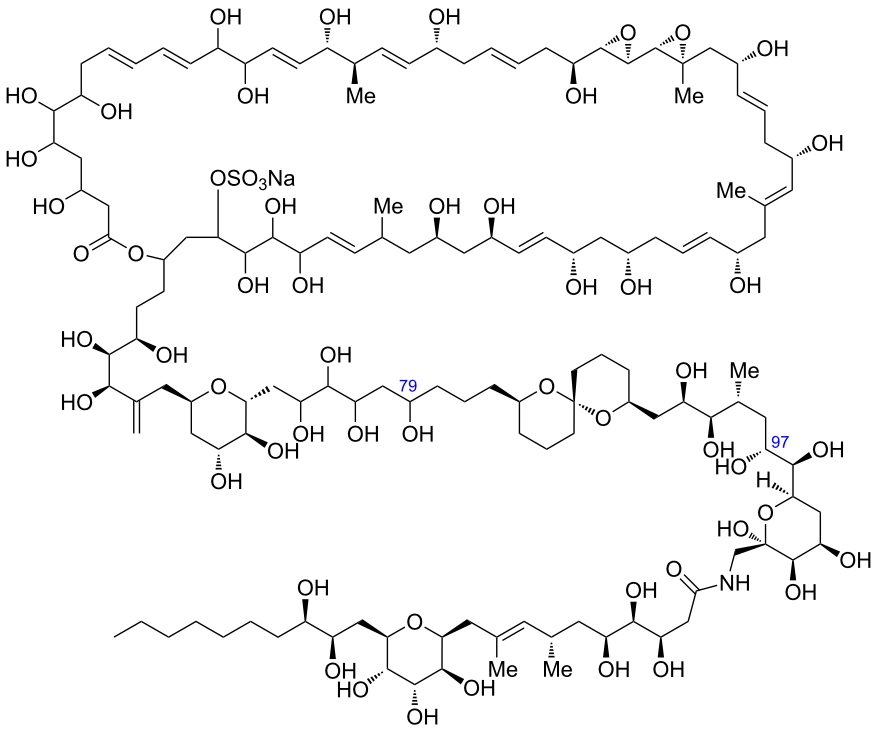
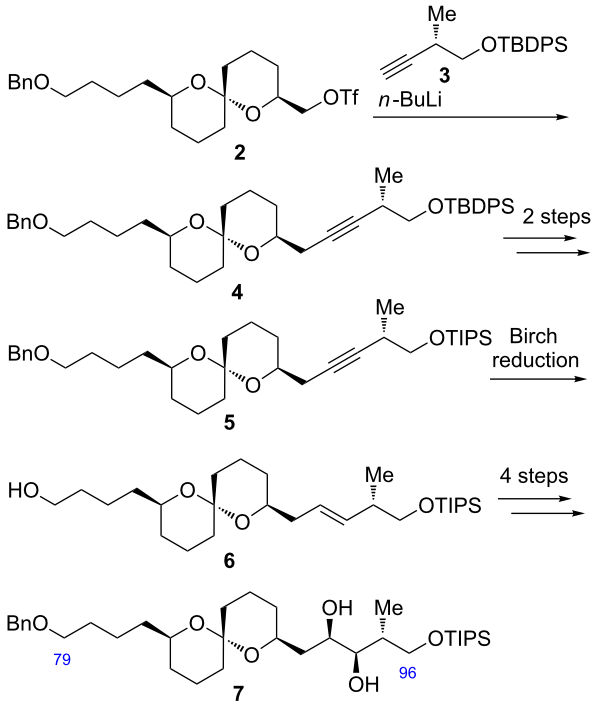


Figure 1: Structure of symbiodinolide (**1**).

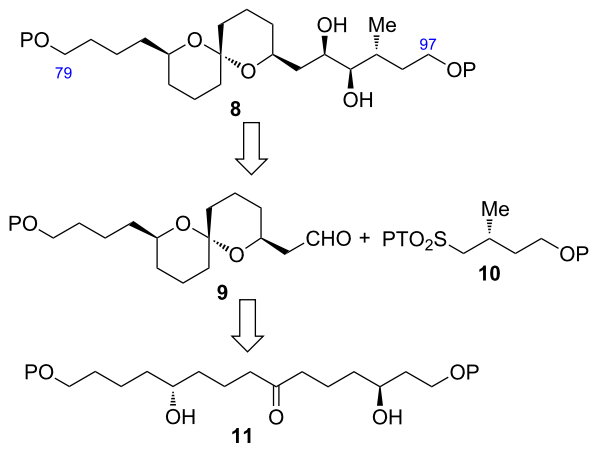


Scheme 1: Our previous synthesis of the C79–C96 fragment **7**.

moiety was deprotected. The alkene **6** was derivatized to the spiroacetal C79–C96 fragment **7** in four steps including the benzyl protection and Sharpless asymmetric dihydroxylation (AD). Although the desired spiroacetal fragment **7** was synthesized stereoselectively, the transformation starting with the coupling between **2** and **3** to the final product **7** needed eight steps. Therefore, we decided to examine the more efficient synthesis of the spiroacetal fragment. Herein, we report the improved synthesis of the spiroacetal fragment by utilizing Julia–Kocienski olefination as the coupling reaction.

The new retrosynthetic analysis of the C79–C97 fragment **8** is described in Scheme 2. We envisaged that the diol **8** could be synthesized by the Julia–Kocienski olefination [12-14] between aldehyde **9** and 1-phenyl-1*H*-tetrazol-5-yl (PT)-sulfone **10** and subsequent Sharpless AD [15], wherein the target molecule **8** could be prepared in two steps from the coupling. The carbon framework of **9** could be constructed through the stereoselective spiroacetalization of dihydroxyketone **11**.

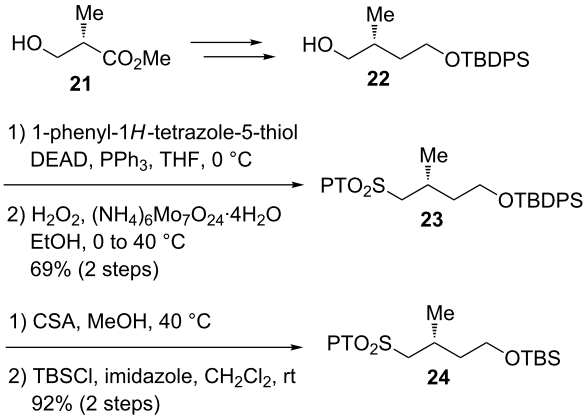
First, we commenced the stereocontrolled synthesis of aldehyde **20** (Scheme 3). Treatment of epoxide **13**, which was prepared from L-aspartic acid (**12**) by the known procedure [8], with 3-butenylmagnesium bromide/CuI [16] provided the corresponding secondary alcohol. Protection of the alcohol with



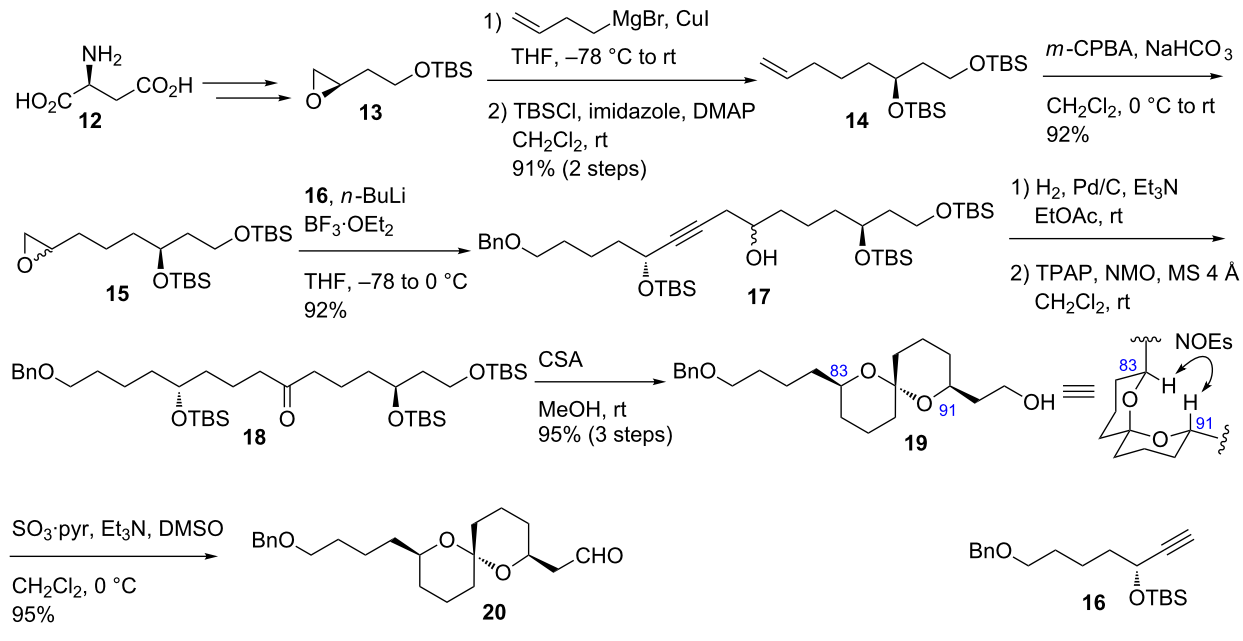
Scheme 2: Retrosynthetic analysis of the C79–C97 fragment **8**.

TBSCl afforded TBS ether **14** in 91% yield in two steps. Alkene **14** was reacted with *m*-CPBA to produce epoxide **15** as a 1:1 diastereomeric mixture. Epoxide **15** was coupled with alkyne **16** [4] in the presence of *n*-BuLi/BF_3·OEt_2 [17] to give the desired product **17** in 92% yield from **15**. Hydrogenation of the alkyne moiety of **17** followed by TPAP oxidation [18] yielded ketone **18**. Removal of the three TBS protecting groups and subsequent stereoselective spiroacetalization were performed in one-pot with CSA in MeOH to provide spiroacetal **19** as a single stereoisomer [19,20]. The stereochemistry of **19** was elucidated by the observed NOE correlations between H-83 and H-91 as indicated by an arrow. The plausible rationale for the stereoselective formation of **19** is the thermodynamic stability due to the double anomeric effect. Oxidation of the alcohol **19** with SO_3·pyr/Et_3N/DMSO [21] afforded aldehyde **20**.

Next, we carried out the synthesis of PT-sulfones **23** and **24** which were the coupling partners of the aldehyde **20** (Scheme 4). The synthesis started from commercially available methyl (*S*)-3-hydroxy-2-methylpropanoate (**21**), which was converted to alcohol **22** by the known method [22]. Alcohol **22** was treated with 1-phenyl-1*H*-tetrazole-5-thiol/DEAD/PPh_3 to furnish the corresponding PT-sulfide, which was oxidized with



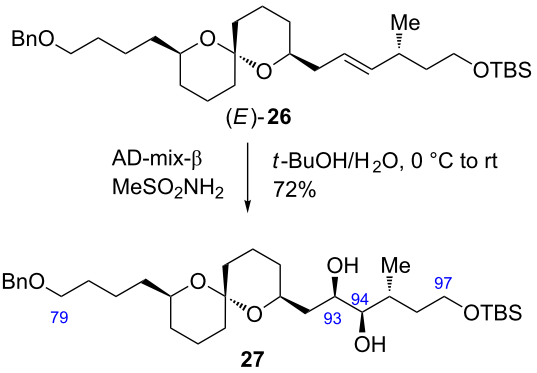
Scheme 4: Synthesis of PT-sulfones **23** and **24**.



Scheme 3: Synthesis of aldehyde **20**.

H_2O_2/Mo(VI) [23] to yield PT-sulfone **23**. The TBDPS protecting group of **23** was transformed to the TBS group in two steps to provide PT-sulfone **24**.

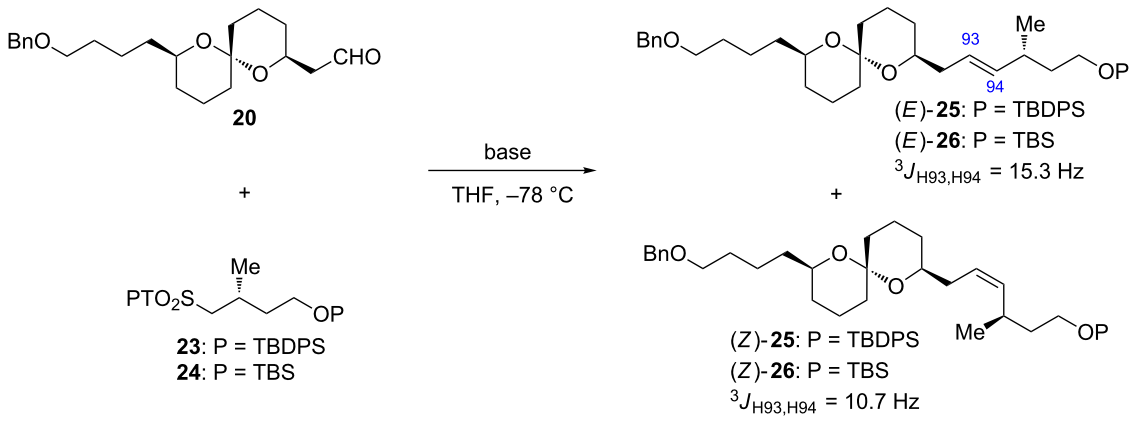
With the coupling precursors aldehyde **20** and PT-sulfones **23** and **24** in hand, we next examined the Julia–Kocienski olefination [12-14] of these compounds (Table 1). Deprotonation of the PT-sulfone **23** with KHMDS, followed by addition of the aldehyde **20**, gave rise to the desired coupling product (*E*)-**25** along with (*Z*)-**25** in 27% combined yield at a 3.5:1 diastereomeric ratio (Table 1, entry 1). When NaHMDS was used as the base, the chemical yield was improved to 77%, however, the *E*/*Z* ratio was decreased to 1.3:1 (Table 1, entry 2). When LDA was used as the base, the chemical yield and diastereomeric ratio were increased to 98% and 2.6:1, respectively (Table 1, entry 3). Reaction of PT-sulfone **24** using LDA gave the coupling products (*E*)- and (*Z*)-**26** in 86% yield, wherein the diastereomeric ratio was increased to 5.0:1 (Table 1, entry 4). The configurations of the coupling products were elucidated by their coupling constants between H-93 and H-94 (15.3 Hz in (*E*)-**25** and (*E*)-**26**, 10.7 Hz in (*Z*)-**25** and (*Z*)-**26**). Finally, the desired alkene (*E*)-**26** was subjected to the Sharpless AD [15] with AD-mix-β to furnish the C79–C97 fragment **27** in 72% yield as a single diastereomer (Scheme 5). The configuration of the resulting two vicinal hydroxy groups at C93 and C94 of **27** were unambiguously confirmed by the modified Mosher method, respectively (see Supporting Information File 1).



Scheme 5: Synthesis of the C79–C97 fragment **27**.

In conclusion, we have achieved the stereoselective synthesis of the C79–C97 fragment. The synthetic route has featured a stereoselective spiroacetalization, a Julia–Kocienski olefination, and a Sharpless asymmetric dihydroxylation. This synthesis of the spiroacetal fragment, wherein the two-step sequence was conducted and the overall yield was 52% from the coupling, has been improved over the previous synthesis wherein the eight-step transformation was needed and the overall yield was 31% from the coupling. Further synthetic effort of symbiodinolide toward the complete structural elucidation is currently underway and will be reported in due course.

Table 1: Julia–Kocienski olefination between aldehyde **20** and PT-sulfones **23** and **24**.



Entry	PT-Sulfone	Base	Yield (%)[a]	Ratio (*E*:*Z*)[b]
1	**23**	KHMDS	27	3.5:1
2	**23**	NaHMDS	77	1.3:1
3	**23**	LDA	98	2.6:1
4	**24**	LDA	86	5.0:1

[a]Isolated yield from **20**. [b]Determined by ^{1}H NMR spectroscopy.

Supporting Information

Supporting Information File 1

Experimental procedures, spectroscopic data, and NMR spectra of all new compounds.
[http://www.beilstein-journals.org/bjoc/content/supplementary/1860-5397-9-228-S1.pdf]

Acknowledgements

We are grateful to Mr. Yohei Kawakubo (Okayama University) for valuable discussions. We acknowledge The Kurata Memorial Hitachi Science and Technology Foundation, The Research Foundation for Pharmaceutical Sciences, and The Society of Synthetic Organic Chemistry, Japan (Shionogi Award in Synthetic Organic Chemistry, Japan) for financial supports. This research was supported by a Grant-in-Aid for Scientific Research (No. 24710250) from the Japan Society for the Promotion of Science (JSPS).

References

1. Kita, M.; Ohishi, N.; Konishi, K.; Kondo, M.; Koyama, T.; Kitamura, M.; Yamada, K.; Uemura, D. *Tetrahedron* **2007,** *63,* 6241–6251. doi:10.1016/j.tet.2007.02.093
2. Han, C.; Uemura, D. *Tetrahedron Lett.* **2008,** *49,* 6988–6990. doi:10.1016/j.tetlet.2008.09.118
3. Han, C.; Yamano, Y.; Kita, M.; Takamura, H.; Uemura, D. *Tetrahedron Lett.* **2009,** *50,* 5280–5282. doi:10.1016/j.tetlet.2009.07.014
4. Takamura, H.; Ando, J.; Abe, T.; Murata, T.; Kadota, I.; Uemura, D. *Tetrahedron Lett.* **2008,** *49,* 4626–4629. doi:10.1016/j.tetlet.2008.05.078
5. Murata, T.; Sano, M.; Takamura, H.; Kadota, I.; Uemura, D. *J. Org. Chem.* **2009,** *74,* 4797–4803. doi:10.1021/jo900546k
6. Takamura, H.; Murata, T.; Asai, T.; Kadota, I.; Uemura, D. *J. Org. Chem.* **2009,** *74,* 6658–6666. doi:10.1021/jo901162v
7. Takamura, H.; Kadonaga, Y.; Yamano, Y.; Han, C.; Aoyama, Y.; Kadota, I.; Uemura, D. *Tetrahedron Lett.* **2009,** *50,* 863–866. doi:10.1016/j.tetlet.2008.11.056
8. Takamura, H.; Kadonaga, Y.; Yamano, Y.; Han, C.; Kadota, I.; Uemura, D. *Tetrahedron* **2009,** *65,* 7449–7456. doi:10.1016/j.tet.2009.07.019
9. Takamura, H.; Kadonaga, Y.; Kadota, I.; Uemura, D. *Tetrahedron Lett.* **2010,** *51,* 2603–2605. doi:10.1016/j.tetlet.2010.03.014
10. Takamura, H.; Kadonaga, Y.; Kadota, I.; Uemura, D. *Tetrahedron* **2010,** *66,* 7569–7576. doi:10.1016/j.tet.2010.07.045
11. Takamura, H.; Tsuda, K.; Kawakubo, Y.; Kadota, I.; Uemura, D. *Tetrahedron Lett.* **2012,** *53,* 4317–4319. doi:10.1016/j.tetlet.2012.06.005
12. Blakemore, P. R.; Cole, W. J.; Kocieński, P. J.; Morley, A. *Synlett* **1998,** 26–28. doi:10.1055/s-1998-1570
13. Aïssa, C. *Eur. J. Org. Chem.* **2009,** 1831–1844. doi:10.1002/ejoc.200801117
14. Blakemore, P. R. *J. Chem. Soc., Perkin Trans. 1* **2002,** 2563–2585. doi:10.1039/B208078H
15. Kolb, H. C.; VanNieuwenhze, M. S.; Sharpless, K. B. *Chem. Rev.* **1994,** *94,* 2483–2547. doi:10.1021/cr00032a009
16. Paterson, I.; Anderson, E. A.; Dalby, S. M.; Lim, J. H.; Maltas, P.; Loiseleur, O.; Genovino, J.; Moessner, C. *Org. Biomol. Chem.* **2012,** *10,* 5861–5872. doi:10.1039/c2ob25100k
17. Yamaguchi, M.; Hirao, I. *Tetrahedron Lett.* **1983,** *24,* 391–394. doi:10.1016/S0040-4039(00)81416-1
18. Ley, S. V.; Norman, J.; Griffith, W. P.; Marsden, S. P. *Synthesis* **1994,** 639–666. doi:10.1055/s-1994-25538
19. Perron, F.; Albizati, K. F. *Chem. Rev.* **1989,** *89,* 1617–1661. doi:10.1021/cr00097a015
20. Aho, J. E.; Pihko, P. M.; Rissa, T. K. *Chem. Rev.* **2005,** *105,* 4406–4440. doi:10.1021/cr050559n
21. Parikh, J. R.; Doering, W. v. E. *J. Am. Chem. Soc.* **1967,** *89,* 5505–5507. doi:10.1021/ja00997a067
22. Kurosawa, S.; Mori, K. *Eur. J. Org. Chem.* **2000,** 955–962. doi:10.1002/(SICI)1099-0690(200003)2000:6<955::AID-EJOC955>3.0.CO;2-Y
23. Schultz, H. S.; Freyermuth, H. B.; Buc, S. R. *J. Org. Chem.* **1963,** *28,* 1140–1142. doi:10.1021/jo01039a512

License and Terms

This is an Open Access article under the terms of the Creative Commons Attribution License (http://creativecommons.org/licenses/by/2.0), which permits unrestricted use, distribution, and reproduction in any medium, provided the original work is properly cited.

The license is subject to the *Beilstein Journal of Organic Chemistry* terms and conditions: (http://www.beilstein-journals.org/bjoc)

The definitive version of this article is the electronic one which can be found at:
doi:10.3762/bjoc.9.228

Beilstein Journal of Organic Chemistry

A concise enantioselective synthesis of the guaiane sesquiterpene (−)-oxyphyllol

Martin Zahel and Peter Metz*

Full Research Paper

Open Access

Address:
Fachrichtung Chemie und Lebensmittelchemie, Organische Chemie I, Technische Universität Dresden, Bergstrasse 66, 01069 Dresden, Germany

Email:
Peter Metz* - peter.metz@chemie.tu-dresden.de

* Corresponding author

Keywords:
asymmetric synthesis; hydration; natural products; terpenes; transannular epoxide opening

Beilstein J. Org. Chem. **2013,** *9,* 2028–2032.
doi:10.3762/bjoc.9.239

Received: 05 August 2013
Accepted: 20 September 2013
Published: 08 October 2013

This article is part of the Thematic Series "Natural products in synthesis and biosynthesis".

Guest Editor: J. S. Dickschat

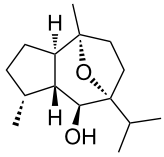
© 2013 Zahel and Metz; licensee Beilstein-Institut.
License and terms: see end of document.

Abstract

(−)-Oxyphyllol was prepared in only 4 steps from an epoxy enone that already served as an intermediate for the total synthesis of the anticancer guaiane (−)-englerin A. A regio- and diastereoselective Co(II)-catalyzed hydration of the olefin and a transannular epoxide opening were used as the key reactions.

Introduction

The hydroazulene framework is present in many natural products that are often associated with interesting biological properties [1,2]. The guaiane sesquiterpene (−)-oxyphyllol (**1**) has been isolated from the roots of the Thai medicinal plant *Phyllanthus oxyphyllus* [3]. A recent enantioselective synthesis of the unnatural enantiomer of **1** enabled a structural revision of this compound and established its relative and absolute configuration as depicted in Figure 1 [4]. During the total synthesis of (−)-9-deoxyenglerin A, compound **1** had already been prepared enantiomerically pure in 14 steps starting from (−)-isopulegol [5]. Remarkably, its cinnamate [(−)-9-deoxyenglerin A] displayed a cytotoxic activity in the µM range against several cancer cell lines [5]. Herein we report a concise enantioselective access to (−)-oxyphyllol (**1**) in a few preparatively simple operations.



(–)-oxyphyllol (**1**)

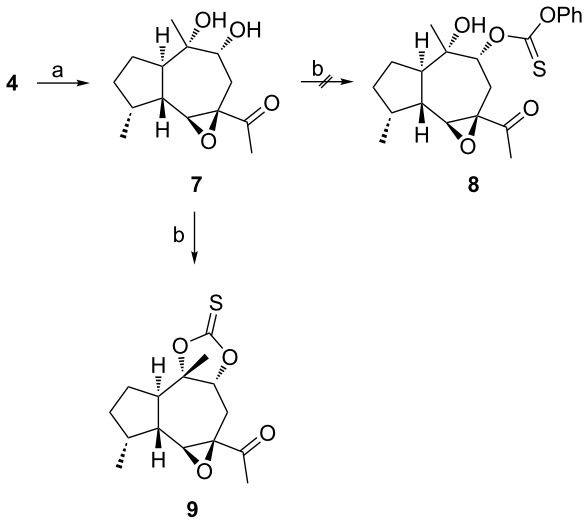
Figure 1: Structure of the guaiane (−)-oxyphyllol (**1**).

Results and Discussion

Recently, we developed an efficient access to the anticancer guaiane (−)-englerin A (**5**) starting from (−)-photocitral A (**6**), which in turn can be prepared in only 2 steps from commercially available (−)-isopulegol through dual catalysis [6]. Due to

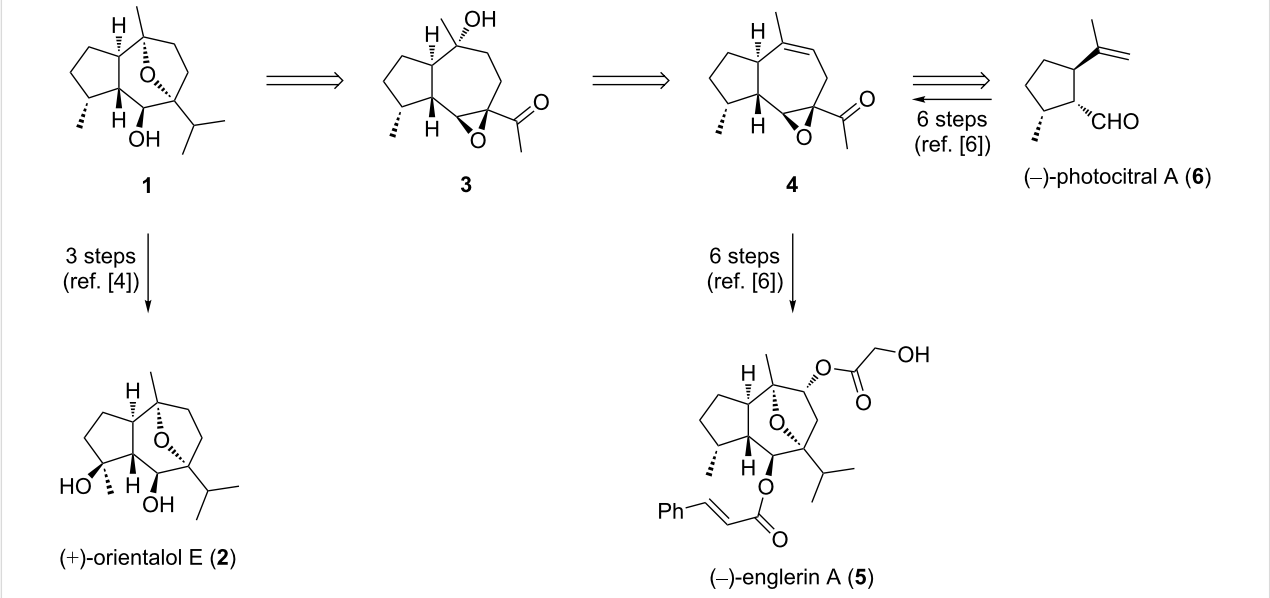
the structural similarity of the hydroazulene core in (−)-oxyphyllol (**1**) and **5**, we decided to use a modification of our route to **5** for the synthesis of **1** that would also constitute a formal synthesis of the related guaiane (+)-orientalol E (**2**) [4,7]. As illustrated in Scheme 1, we selected tertiary alcohol **3** as a retrosynthetic precursor for **1**. The acetyl group of **3** can be utilized to generate the isopropyl group, and a regioselective transannular epoxide opening would construct the oxygen-bridged bicyclic hydroazulene framework. Alcohol **3** was traced back to the known epoxy enone **4** that already served as an intermediate for the total synthesis of **5** [6].

As shown in Scheme 2, we first planned to use the known diol **7**, which is available by diastereoselective dihydroxylation of **4** [6]. Since a chemoselective deoxygenation of the secondary alcohol of **7** would give rise to the desired intermediate **3**, we investigated a radical defunctionalization strategy [8]. To this end, we tried to prepare the thionocarbonate **8** from **7** with phenyl chlorothionoformate [9,10]. However, all attempts at selective activation of the secondary hydroxy group led to the cyclic product **9** instead. A similar problem was already encountered earlier [11].

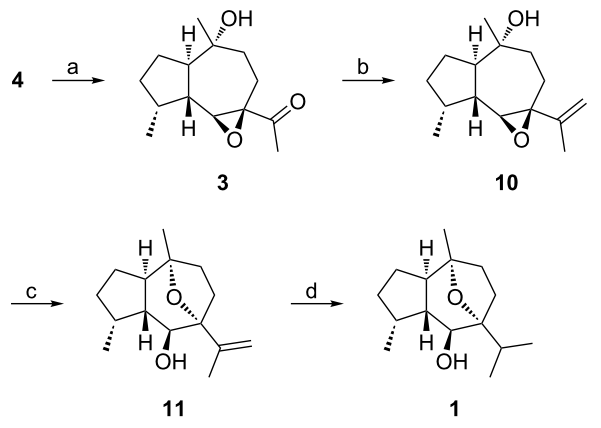


Scheme 2: Attempted selective deoxygenation of diol **7**. a) 1 mol % K_2OsO_4, NMO, acetone, water, THF, rt, 97%, diastereomeric ratio = 2:1 (ref. [6]); b) PhOC(S)Cl, pyridine, CH_2Cl_2, 0 °C to rt, 42% **9**. NMO = *N*-methylmorpholine *N*-oxide.

Scheme 3 depicts the efficacious completion of the synthesis of (−)-oxyphyllol (**1**) from **4**. To our delight, a direct regio- and diastereoselective Co(II)-catalyzed hydration [12] of the olefin in **4** succeeded to give the required α-stereoisomer **3** in 58% isolated yield after chromatographic separation of the minor β-alcohol. Compared to the envisaged deoxygenation route (Scheme 2), this key transformation saved 2 steps and paved the way for a final reaction sequence that was based on our synthesis of (−)-englerin A (**5**) [6]. Thus, Wittig olefination of the acetyl group in **3** afforded the sensitive vinyl epoxide **10** along with some cyclized product **11**. In contrast to the smooth transannular epoxide opening [13,14] encountered during the synthesis of **5**, an attempted complete cyclization of **10** to give **11** during acidic work-up of the methylenation reaction led to considerable decomposition. Fortunately, catalytic amounts of ytterbium triflate accomplished a high yielding formation of the



Scheme 1: Retrosynthetic analysis for (−)-oxyphyllol (**1**) and structures of the guaiane sesquiterpenes (+)-orientalol E (**2**) and (−)-englerin A (**5**).



Scheme 3: Conversion of **4** to **1**. a) 20 mol % $Co(acac)_2$, $PhSiH_3$, 1 atm O_2, THF, 0°C, 82%, diastereomeric ratio = 2.4:1; b) $Ph_3P{=}CH_2$, THF, rt; c) 2 mol % $Yb(OTf)_3$, CH_2Cl_2, rt, 80% (2 steps); d) 1 atm H_2, 10% Pd/C, MeOH, rt, 98%. acac = acetylacetonate, Tf = trifluoromethanesulfonyl.

oxygen-bridged bicyclic hydroazulene **11**. Finally, hydrogenation of **11** proceeded uneventfully to deliver the target molecule **1** nearly quantitatively.

Conclusion

In summary, we have accomplished a short enantioselective total synthesis of (−)-oxyphyllol (**1**) and thus, a formal synthesis of (+)-orientalol E (**2**) as well by a modification of our previously developed route for setting up the oxygen-bridged framework present in (−)-englerin A (**5**). The reaction sequence presented herein allows the preparation of the guaiane **1** in only 10 steps with an overall yield of 22% starting from (−)-photocitral A (**6**).

Experimental

General information: Tetrahydrofuran and dichloromethane were dried and purified by passage through a MB-SPS-800 device using molecular sieves. All commercially available reagents were used as received. Reactions were performed under argon atmosphere. Thin layer chromatography (TLC) was performed on Merck silica gel 60 F_{254} 0.2 mm precoated plates. Product spots were visualized by UV light at 254 nm and subsequently developed using anisaldehyde solution as appropriate. Flash column chromatography was carried out using silica gel (Merck, particle size 40–63 microns). Melting points were measured on a Wagner & Munz PolyTherm A and are uncorrected. Infrared spectra were recorded on a THERMO-NICOLET Avatar 360 instrument using ATR. NMR spectra were recorded on a Bruker DRX500P (500.13 MHz ^{1}H, 125.77 MHz ^{13}C) or else on an Avance-III-600 (600.16 MHz ^{1}H, 150.92 MHz ^{13}C) spectrometer. Chemical shifts (δ) are quoted in parts per million (ppm) downfield of tetramethylsilane, using residual proton-containing solvent as internal standard ($CDCl_3$ at 7.27). Abbreviations used in the description of resonances are: s (singlet), d (doublet), t (triplet), q quartet), br (broad). Coupling constants (*J*) are quoted to the nearest 0.1 Hz. Mass spectra were recorded with an Agilent 5973N detector coupled with an Agilent 6890N GC (GC–MS, 70 eV). HRMS spectra were recorded on a Finnigan MAT 95 (EI, 70 eV). Optical rotations were measured on a Perkin Elmer 341 LC polarimeter. Elemental analysis was performed on a Hekatech EA 3000.

Thionocarbonate 9: Diol **7** (10.0 mg, 39 µmol) and pyridine (6.2 mg, 78 µmol) were dissolved in dichloromethane (0.5 mL). The solution was cooled to 0 °C, and phenyl chlorothionoformate (10.3 mg, 60 µmol) was added. The solution was warmed to room temperature and stirred for 72 h. Then silica gel was added, and the solvents were removed in vacuo. Purification by flash chromatography (isohexane/ethyl acetate 2:1) afforded thionocarbonate **9** (4.9 mg, 17 µmol, 42%) as a colorless solid.

9: $[\alpha]_D^{20} = -58$ (*c* 0.50, $CHCl_3$); Mp = 203 °C; ^{1}H NMR (600 MHz, $CDCl_3$) δ 4.62 (dd, *J* = 11.7, 3.8 Hz, 1H), 3.20 (s, 1H), 2.82 (dd, *J* = 15.8, 11.7 Hz, 1H), 2.63 (dd, *J* = 15.6, 3.6 Hz, 1H), 2.54 (dt, *J* = 12.1, 8.8 Hz, 1H), 2.48–2.43 (m, 1H), 2.19 (dd, *J* = 12.4, 7.2 Hz, 1H), 2.04 (s, 3H), 2.03–1.88 (m, 2H), 1.65–1.58 (m, 1H), 1.46 (s, 3H), 1.43–1.37 (m, 1H), 0.93 (d, *J* = 7.2 Hz, 3H) ppm; ^{13}C NMR (150 MHz, $CDCl_3$) δ 205.9 (C), 190.4 (C), 91.6 (C), 85.5 (CH), 64.3 (C), 58.4 (CH), 44.5 (CH), 41.1 (CH), 35.8 (CH), 31.2 (CH_2), 27.4 (CH_2), 24.9 (CH_2), 23.0 (CH_3), 19.4 (CH_3), 16.9 (CH_3) ppm; IR (ATR) ν: 2962, 2869, 1789, 1701, 1291, 1253, 1152, 977 cm^{-1}; GC–MS: *m*/*z* = 296 $[M]^+$; anal. calcd for $C_{15}H_{20}O_4S$: C 60.79, H 6.80; found: C 60.88, H 6.92.

Alcohol 3: Epoxide **4** (100.0 mg, 454 µmol) and cobalt(II) acetylacetonate (23.3 mg, 91 µmol) were dissolved in THF (5 mL), and the solution was cooled to 0 °C. Oxygen was bubbled through the solution for 1 h, and phenylsilane (196.5 mg, 1.816 mmol) was added afterwards. After a reaction time of 22 h, ethyl acetate was added, and the mixture was filtered through silica gel. The filtrate was concentrated under reduced pressure, and the residue was purified by flash chromatography (isohexane/ethyl acetate 2:1) to yield alcohol **3** (63.2 mg, 265 µmol, 58%) as a colorless solid.

3: $[\alpha]_D^{20} = +3$ (*c* 0.54, $CHCl_3$); Mp = 84 °C; ^{1}H NMR (600 MHz, $CDCl_3$) δ 3.23 (d, *J* = 7.2 Hz, 1H), 2.55 (ddd, *J* = 14.8, 7.4, 1.5 Hz, 1H), 2.40–2.32 (m, 1H), 2.03 (s, 3H), 1.96–1.89 (m, 1H), 1.85–1.80 (m, 2H), 1.76–1.68 (m, 2H), 1.64–1.51 (m, 2H), 1.38–1.31 (m, 1H), 1.24–1.19 (m, 1H), 1.13 (s, 3H), 1.11 (d, *J* = 7.2 Hz, 3H) ppm; ^{13}C NMR (150 MHz, $CDCl_3$) δ 208.2 (C), 74.8 (C), 64.0 (C), 60.0 (CH), 52.1 (CH), 44.8 (CH), 40.8

(CH_2), 35.9 (CH), 34.6 (CH_2), 25.4 (CH_2), 24.4 (CH_2), 23.3 (CH_3), 19.9 (CH_3), 15.5 (CH_3) ppm; IR (ATR) ν: 3446, 2957, 2930, 2874, 1708, 1130, 852 cm^{-1}; GC–MS: *m*/*z* = 238 $[M]^+$; HRMS (EI) *m*/*z*: $[M]^+$ calcd for $C_{14}H_{22}O_3$, 238.1569; found, 238.1564.

Allyl ether 11: Methyltriphenylphosphonium bromide (131.5 mg, 368 µmol) was suspended in THF (1.5 mL), and a solution of sodium hexamethyldisilazide in THF (2.0 M, 172 µL, 344 µmol) was added. The mixture was stirred for 5 min at room temperature, and then a solution of alcohol **3** (29.0 mg, 122 µmol) in THF (1.5 mL) was added dropwise. After stirring for 5 min at room temperature, ethyl acetate was added, and the mixture was filtered through a plug of silica gel. Purification of the residue by flash chromatography (isohexane/ethyl acetate 2:1) afforded a mixture of olefin **10** and the cyclized product **11** as a colorless oil.

The mixture above and ytterbium(III) triflate (1.5 mg, 2.4 µmol) were dissolved in dichloromethane (1.5 mL) and stirred for 1 h at room temperature. Afterwards the reaction mixture was filtered through silica gel, and the filtrate was evaporated in vacuo. Flash chromatography (isohexane/ethyl acetate 10:1) of the residue afforded the oxygen-bridged bicyclic hydroazulene **11** (22.9 mg, 97 µmol, 80% over 2 steps) as a colorless oil.

11: $[\alpha]_D^{20}$ = –36 (*c* 0.61, MeOH); ^{1}H NMR (500 MHz, $CDCl_3$) δ 5.02 (t, *J* = 1.6 Hz, 1H), 4.80 (s, 1H), 3.38 (d, *J* = 10.4 Hz, 1H), 2.30–1.38 (m, 1H), 2.20–2.07 (m, 1H), 2.06–1.92 (m, 1H), 1.86 (s, 3H), 1.82–1.72 (m, 2H), 1.71–1.60 (m, 2H), 1.54–1.45 (m, 1H), 1.41–1.36 (m, 1H), 1.28 (s, 3H), 1.22–1.13 (m, 1H), 1.10–1.00 (m, 1H), 0.89 (d, *J* = 7.3 Hz, 3H) ppm; ^{13}C NMR (125 MHz, $CDCl_3$) δ 147.2 (C), 113.2 (CH_2), 88.0 (C), 82.9 (C), 69.8 (CH), 48.9 (CH), 46.7 (CH), 31.4 (CH_2), 31.4 (CH_2), 31.1 (CH), 30.7 (CH_2), 26.0 (CH_2), 24.3 (CH_3), 19.3 (CH_3), 17.1 (CH_3) ppm; IR (ATR) ν: 3467, 3082, 1073, 2952, 2869, 890 cm^{-1}; GC–MS: *m*/*z* = 236 $[M]^+$. HRMS (EI) *m*/*z*: $[M]^+$ calcd for $C_{15}H_{24}O_2$, 236.1776; found, 236.1766.

(−)-Oxyphyllol (1): Olefin **11** (22.9 mg, 97 µmol) and palladium on charcoal (10 wt %, 5.1 mg) were placed in a flask, and methanol (2 mL) was added. The resulting mixture was stirred under hydrogen (1 atm) for 4 h at room temperature. Then the mixture was filtered through silica gel, and the solvents were removed in vacuo. Flash chromatography of the residue (isohexane/ethyl acetate 10:1) afforded **1** as a colorless oil (22.7 mg, 95 µmol, 98%).

1: $[\alpha]_D^{20}$ = −51 (*c* 0.82, $CHCl_3$); (Lit. [3]: $[\alpha]_D^{26}$ = −40.25 (*c* 0.225, $CHCl_3$)); ^{1}H NMR (500 MHz, $CDCl_3$) δ 3.69 (d, *J* = 10.1 Hz, 1H), 2.37–2.21 (m, 1H), 2.05–1.87 (m, 2H), 1.85–1.76 (m, 1H), 1.75–1.54 (m, 4H), 1.44–1.32 (m, 2H), 1.23 (s, 3H), 1.21–1.13 (m, 1H), 1.05–0.99 (m, 1H), 1.03 (d, *J* = 6.9 Hz, 3H), 1.02 (d, *J* = 6.6 Hz, 3H), 0.88 (d, *J* = 7.3 Hz, 3H) ppm; ^{13}C NMR (125 MHz, $CDCl_3$) δ 86.4 (C), 83.0 (C), 71.8 (CH), 49.3 (CH), 48.6 (CH), 32.4 (CH), 31.7 (CH_2), 31.5 (CH_2), 30.5 (CH), 29.2 (CH_2), 25.9 (CH_2), 24.3 (CH_3), 18.4 (CH_3), 17.5 (CH_2), 17.1 (CH_3) ppm; IR (ATR) ν: 3408, 2953, 2870, 1473, 1378, 1064, 1004 cm^{-1}; GC–MS: *m*/*z* = 238 $[M]^+$.

Supporting Information

The Supporting Information contains ^{1}H and ^{13}C NMR spectra for compounds **1**, **3**, **9** and **11**.

Supporting Information File 1

^{1}H NMR and ^{13}C NMR spectra.
[http://www.beilstein-journals.org/bjoc/content/supplementary/1860-5397-9-239-S1.pdf]

References

1. Fraga, B. M. *Nat. Prod. Rep.* **2012,** *29,* 1334–1366. doi:10.1039/c2np20074k
2. Foley, D. A.; Maguire, A. R. *Tetrahedron* **2010,** *66,* 1131–1175. doi:10.1016/j.tet.2009.11.045
3. Sutthivaiyakit, S.; Nakorn, N. N.; Kraus, W.; Sutthivaiyakit, P. *Tetrahedron* **2003,** *59,* 9991–9995. doi:10.1016/j.tet.2003.10.023
4. Wang, J.; Chen, S.-G.; Sun, B.-F.; Lin, G.-Q.; Shang, Y.-J. *Chem.–Eur. J.* **2013,** *19,* 2539–2547. doi:10.1002/chem.201203467
5. Ushakov, D. B.; Navickas, V.; Ströbele, M.; Maichle-Mössmer, C.; Sasse, F.; Maier, M. E. *Org. Lett.* **2011,** *13,* 2090–2093. doi:10.1021/ol200499t
6. Zahel, M.; Keßberg, A.; Metz, P. *Angew. Chem.* **2013,** *125,* 5500–5502. doi:10.1002/ange.201301247
   Angew. Chem., Int. Ed. **2013**, *52,* 5390–5392. doi:10.1002/anie.201301247
7. Peng, G.-P.; Tian, G.; Huang, X.-F.; Lou, F.-C. *Phytochemistry* **2003,** *63,* 877–881. doi:10.1016/S0031-9422(03)00222-X
8. Hartwig, W. *Tetrahedron* **1983,** *39,* 2609–2645. doi:10.1016/S0040-4020(01)91972-6
9. Robins, M. J.; Wilson, J. S. *J. Am. Chem. Soc.* **1981,** *103,* 932–933. doi:10.1021/ja00394a033
10. Wang, Y.; Metz, P. *Chem.–Eur. J.* **2011,** *17,* 3335–3337. doi:10.1002/chem.201003399
11. Jung, P. M. J.; Burger, A.; Biellmann, J.-F. *J. Org. Chem.* **1997,** *62,* 8309–8314. doi:10.1021/jo9704568
12. Isayama, S.; Mukaiyama, T. *Chem. Lett.* **1989,** *18,* 1071–1074. doi:10.1246/cl.1989.1071
13. Willot, M.; Radtke, L.; Könning, D.; Fröhlich, R.; Gessner, V. H.; Strohmann, C.; Christmann, M. *Angew. Chem.* **2009,** *121,* 9269–9272. doi:10.1002/ange.200905032
    Angew. Chem., Int. Ed. **2009,** *48,* 9105–9108. doi:10.1002/anie.200905032
14. Yoshikawa, M.; Fukuda, Y.; Hatakeyama, S.; Tanaka, N.; Matsuda, H.; Yamahara, J.; Murakami, N. *Chem. Pharm. Bull.* **1993,** *41,* 1194–1196. doi:10.1248/cpb.41.1194

License and Terms

This is an Open Access article under the terms of the Creative Commons Attribution License (http://creativecommons.org/licenses/by/2.0), which permits unrestricted use, distribution, and reproduction in any medium, provided the original work is properly cited.

The license is subject to the *Beilstein Journal of Organic Chemistry* terms and conditions: (http://www.beilstein-journals.org/bjoc)

The definitive version of this article is the electronic one which can be found at: doi:10.3762/bjoc.9.239

Beilstein Journal of Organic Chemistry

The chemistry of isoindole natural products

Klaus Speck and Thomas Magauer*

Review

Open Access

Address:
Department of Chemistry, Ludwig-Maximilians-Universität München, Butenandtstraße 5–13, 81377 München, Germany

Email:
Thomas Magauer* - thomas.magauer@lmu.de

* Corresponding author

Keywords:
isoindole; isoindoline; isoindolinone; isoindolone; natural products

Beilstein J. Org. Chem. **2013,** *9,* 2048–2078.
doi:10.3762/bjoc.9.243

Received: 12 July 2013
Accepted: 18 September 2013
Published: 10 October 2013

This article is part of the Thematic Series "Natural products in synthesis and biosynthesis" and is dedicated to Prof. Dr. Wolfgang Steglich on the occasion of his 80th birthday.

Guest Editor: J. S. Dickschat

© 2013 Speck and Magauer; licensee Beilstein-Institut.
License and terms: see end of document.

Abstract

This review highlights the chemical and biological aspects of natural products containing an oxidized or reduced isoindole skeleton. This motif is found in its intact or modified form in indolocarbazoles, macrocyclic polyketides (cytochalasan alkaloids), the aporhoeadane alkaloids, meroterpenoids from *Stachybotrys species* and anthraquinone-type alkaloids. Concerning their biological activity, molecular structure and synthesis, we have limited this review to the most inspiring examples. Within different congeners, we have selected a few members and discussed the synthetic routes in more detail. The putative biosynthetic pathways of the presented isoindole alkaloids are described as well.

Introduction

Isoindole (2*H*-isoindole, **1**), known since more than a century, consists of a fused benzopyrrole ring system and constitutes the regioisomer of the abundant 1*H*-indole heterocycle. The fully reduced member of the isoindole family is termed isoindoline (2,3-dihydro-1*H*-isoindole, **2**). Formal oxidation to the 10π-system leads to isoindole (**1**), which is usually only stable when the labile *ortho*-quinoid structure is embedded in a π-system [1]. Incorporation of additional oxygen gives the isoindolinone (1,3-dihydro-2*H*-isoindole-1-one, **3**) and phthalimide (1,3-dihydro-2*H*-isoindole-1,3-dione, **4**) substitution pattern.

The isoindole structure has attracted scientists for decades and can be found in several natural and pharmaceutical compounds [2,3]. A number of structures were explored over the years and promising drug conjugates such as **5**–**11** could be developed (Figure 1).

Compared to the synthesis of indoles, where a number of named-reactions have been reported, only conventional methods are used for the related isoindole motif. For the construction of this rare skeleton inter- and intramolecular Diels–Alder reactions are one of the most powerful methods. This was also exemplified by medicinal chemists from AstraZeneca in the manufacturing route to an mGluR2 positive allosteric modulator [4]. In 2012, a programmable enantioselective one-pot synthesis of isoindolines was reported by

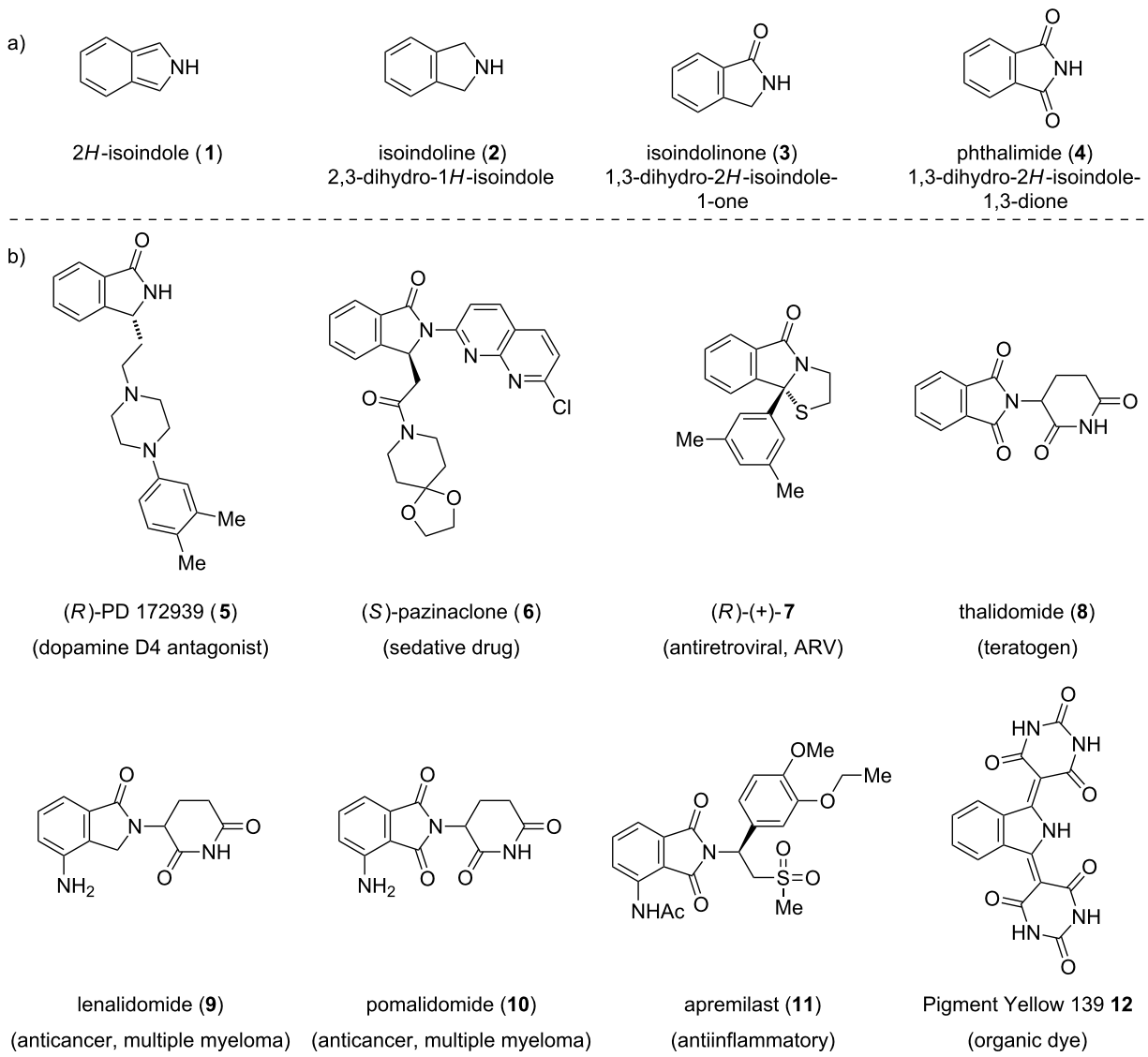


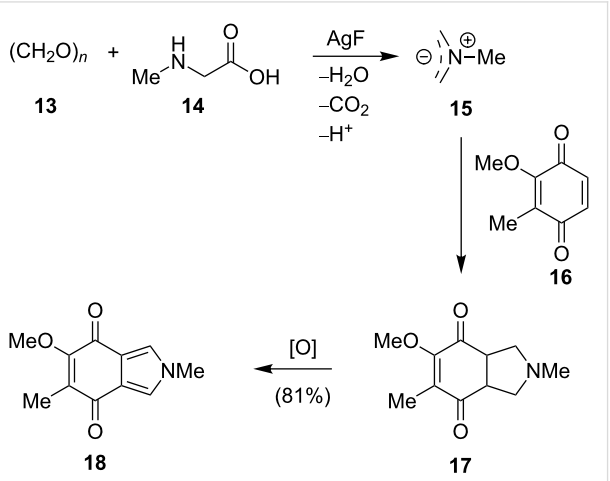
Figure 1: a) Structural features and b) selected examples of non-natural congeners.

Waldmann [5]. Several other strategies were pursued for the synthesis of isoindoline-type structures and the synthesis, chemical and spectroscopic properties of this substance class were reviewed elsewhere [6-8].

In the late 1950s, thalidomide (**8**), a phthalimide-based drug used by pregnant women against morning sickness, became the most infamous drug in history and caused thousands of fatal casualties as well as numerous severe birth defects. Modification of the phthalimide core led to the approval of lenalidomide (**9**) [9] in 2004 and pomalidomide (**10**) in 2013 by the Food and Drug Administration (FDA) as drugs against multiple myeloma. The phosphodiesterase 4 (PDE4) inhibitor apremilast (**11**), which lacks the glutarimide is currently in phase III clinical trials.

The first naturally occurring isoindole, 6-methoxy-2,5-dimethyl-2*H*-isoindole-4,7-dione (**18**), was isolated from the sponge *Reniera* sp. in 1982 [10]. The postulated structure was elucidated through extensive NMR studies and unambiguously confirmed by a four-step synthesis. In 1991, a more concise and elegant route to this antimicrobial metabolite was established by Schubert-Zsilavecz [11]. The reaction was initiated by heating paraformaldehyde (**13**) and sarcosine (**14**) in the presence of benzoquinone **16**. This transformation proceeds via a 1,3-dipolar cycloaddition between the in situ formed azome-

thinylide **15** and the benzoquinone **16** to directly give **17** (Scheme 1). Spontaneous oxidation of the so-obtained cyclization adduct generates isoindole **18**.



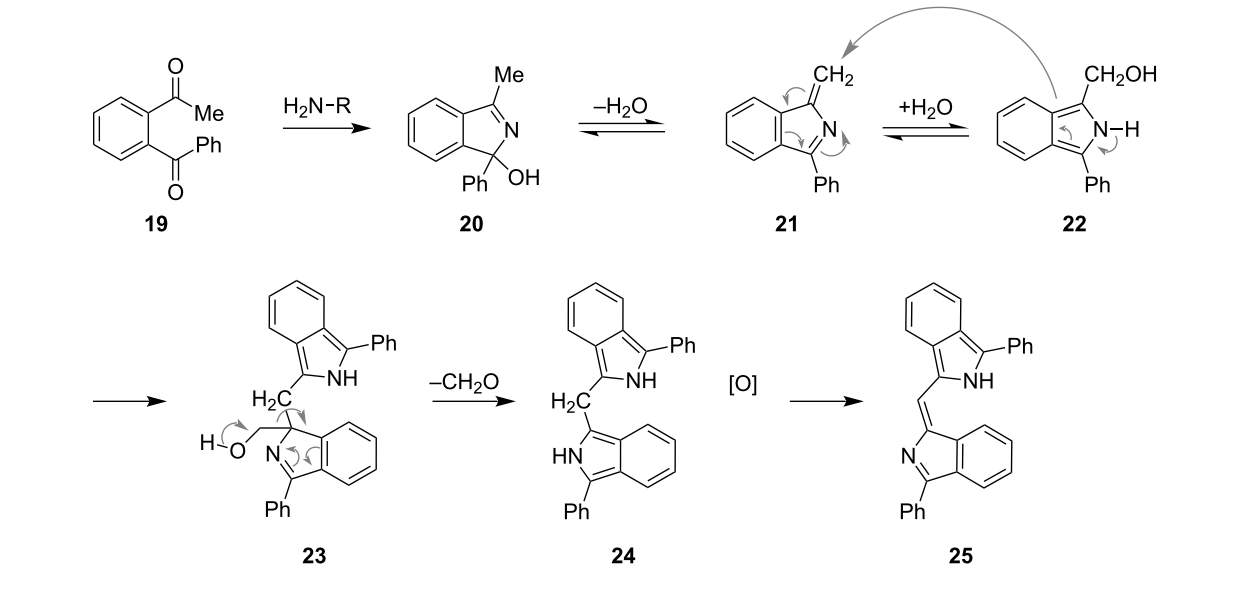
Scheme 1: Synthesis of isoindole **18**.

Isoindoles have also found application as dyes. Pigment yellow 139 (**12**), which is sold by BASF as Paliotol® Yellow K 1841 belongs to the class of highly resistant and effective 1,3-disubstituted isoindoline dyes. Recently, the use of isoindoles as red to near-infrared fluorophores was reported [12]. Another interesting isoindole-based dye, **25**, arises from the condensation of primary amines with *o*-diacylbenzene **19** (Scheme 2) [13]. After initial formation of **20**, isomerization to **21** and **22** can occur through a sequential dehydration–hydration process. Dimerization of **21** and **22** generates **23**, the substrate for a formal retro-Aldol reaction. Loss of formaldehyde gives **24**, which is spontaneously oxidized to the intensive blue-violet pigment **25**. This reaction sequence is characterized by its high sensitivity and has found application as a marker in analytical chemistry (e.g. staining of primary amines) [14,15].

The following review section highlights synthetic and biochemical aspects of selected isoindole-type natural products. The presented results are not meant to be exhaustive but should give a better understanding about the structurally and biologically most attracting structures. We intend to inspire today´s chemists and are convinced that these natural products have a huge potential for the development of new chemistry.

Review

Indolocarbazoles. Staurosporine (**26**) was the first member of the indolocarbazole alkaloid family to be discovered by Ōmura from *Streptomyces staurosporeus* at the Kitasato Institute in 1977 [16]. Over the past 35 years, more than 60 natural indolocarbazole compounds have been isolated from several bacteria and marine invertebrates either as their glycosides (**26**–**29**) or aglycones (**30**–**33**) [17]. Based on the number of glycosidic bonds linking the carbohydrate moiety to the isoindole framework, the latter can be divided into two subclasses. The first comprises two linkages, exemplified by (+)-staurosporine (**26**) and (+)-K252a (**27**), whereas the second class contains only one glycosidic bond as found in rebeccamycin (**28**) and holyrine A (**29**). Selected members of the indolocarbazole alkaloid family are depicted in Figure 2.



Scheme 2: Staining amines with 1,4-diketone **19** (R = H).

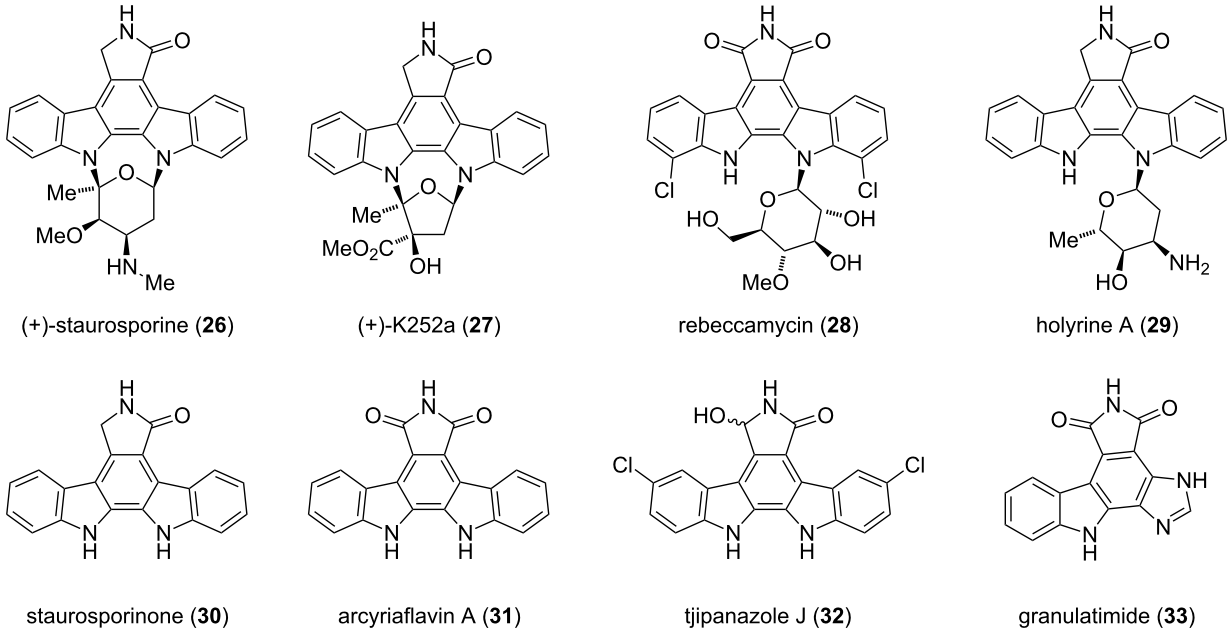


Figure 2: Representative members of the indolocarbazole alkaloid family.

The strong antimicrobial activity against fungi and yeast of **26** was simultaneously reported with its isolation [16]. Moreover, with IC_{50} values in the low nanomolar range (1–20 nM), staurosporine (**26**) is one of the most potent protein kinase inhibitors to date [18]. It took nine years to identify the crucial protein kinase inhibitory effects of **26** [18]. Solving the crystal structure of the catalytic subunit Cα of cAMP-dependent protein kinase bound to **26** gave pivotal insights in the binding mode [19]. Staurosporine (**26**) targets the active site of the adenosine-binding pocket of most protein kinases. This is achieved mimicking several aspects of the adenosine moiety, by induced-fit structural changes and the conformational flexibility of the enzyme residues (Figure 3). Together with several related analogues, **26** displays significant cytotoxic and antiproliferative effects [19].

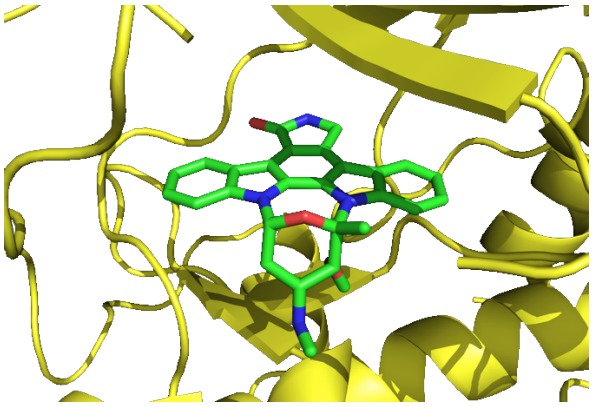


Figure 3: Staurosporine (**26**) bound to the adenosine-binding pocket [19] (from pdb1stc).

Due to the key role of protein kinases in cellular signaling and their association with cancer, a tremendous effort in the development of selective protein kinase inhibitors was undertaken. This resulted in the discovery of the anticancer agent imatinib (Gleevec, **34**) by rational drug design (Figure 4). Midostaurin (**35**), a semisynthetic derivative of staurosporine (**26**), is currently in clinical trials for the treatment of acute myeloid leukemia [20].

Although rebeccamycin (**28**) and its congeners only differ in the lack of the second glycosidic linkage, a completely different mode of action is effective. By stabilizing the topoisomerase I DNA-cleavable complex they prevent the replication of DNA and act as efficient antitumor compounds [21].

The extraordinary bioactivity of indolocarbazoles has drawn a lot of attention from chemists and biologists. The biosynthesis of staurosporine (**26**) and rebeccamycin (**28**), both being the most prominent representatives of this distinct class of natural products, has been studied extensively and reviewed by Knölker and Ōmura [17,22]. The biogenesis of staurosporine (**26**) is outlined in Scheme 3. Biosynthetically, the indolocarbazole scaffold is derived from two fused tryptophan molecules, whereas the sugar moiety originates from glucose and methio-

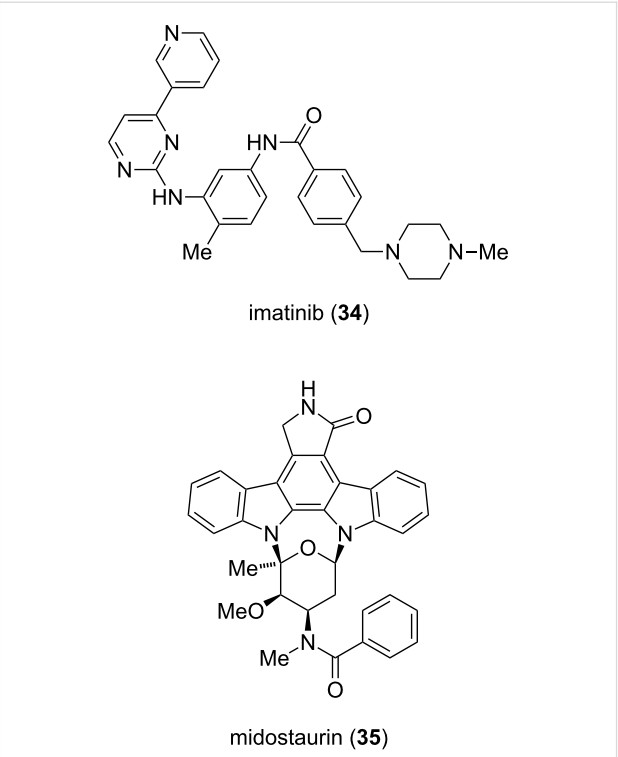
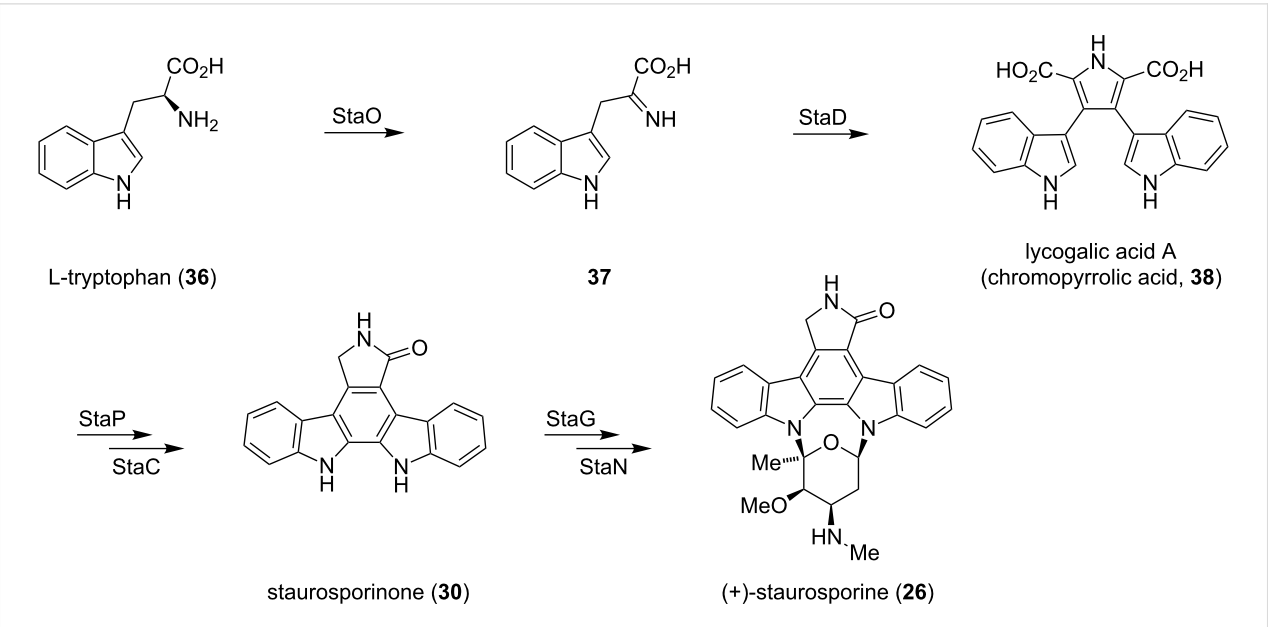


Figure 4: Structure of imatinib (**34**) and midostaurin (**35**).

nine [23]. In 1996, Steglich isolated lycogalic acid A (**38**), also known as chromopyrolic acid, along with staurosporinone (**30**) and traces of arcyriaflavin A (**31**) from the extracts of *Lycogala epidendrum* [24]. This finding and results from Hoshino, which demonstrated that **38** is derived from L-tryptophan (**36**) [25], indicate a close biosynthetic relationship between these alkaloids. After additional experiments, the authors concluded that lycogalic acid A (**38**) is the biosynthetic key intermediate for the biogenesis of indolocarbazoles. This hypothesis was verified through gene disruption studies and the isolation of putative intermediates [26-28]. The formation of the isoindole framework is initiated by the oxidation of L-tryptophan (**36**) to imino indolepyruvic acid **37**, a process, which is catalyzed through the enzyme StaO. The subsequent condensation of two molecules of imine **37** is catalyzed by the oxidase StaD and gives lycogalic acid A (**38**) [26-28]. StaP and StaC convert **38** into staurosporinone (**30**) via an intramolecular aryl–aryl coupling and an oxidative decarboxylation [29,30]. Formation of the *N*-glycosidic bonds is carried out by StaG/StaN and after methylation, **26** is obtained [27].

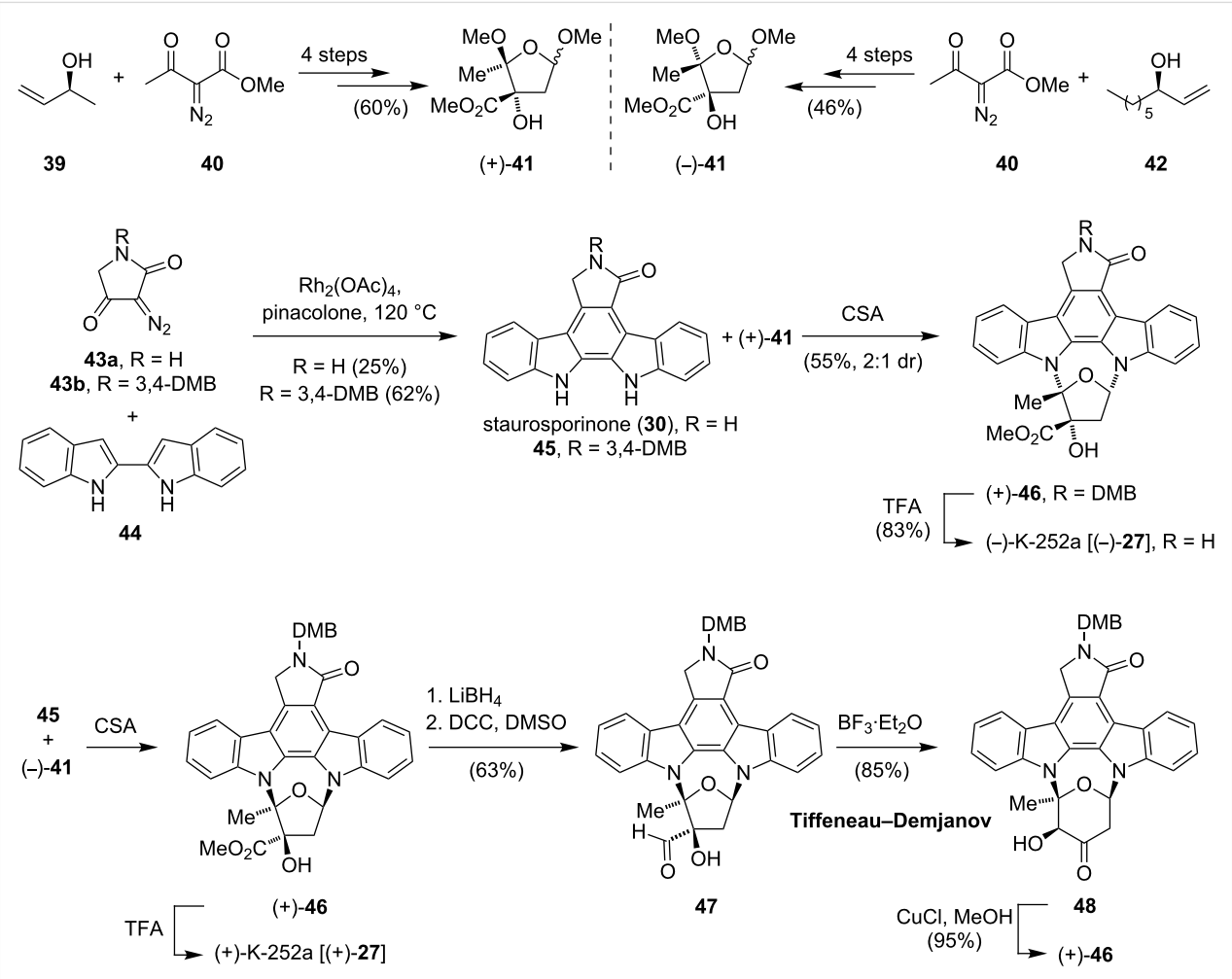
As already mentioned before, indolocarbazoles are characterized by their excellent biological activities and unusual architecture and hence drawing an enormous interest from the synthetic organic chemistry community. This led to several syntheses of the natural occurring aglycone staurosporinone (**30**) [31-35] and culminated in the first total synthesis of staurosporine (**26**) by Danishefsky in 1995 [36]. The elegant syntheses of a series of closely related indolocarbazoles, staurosporine (**26**), K252a (**27**), RK-286c (**49**), MLR-52 (**20**) and staurosporinone (**30**), which were elaborated by Wood in 1996 and reviewed by Knölker in more detail [37], will be discussed below. Based on their previous results [38], the common intermediate **48** was recognized as an ideal branching point. The synthetic route to this component is characterized by the beautiful application of



Scheme 3: Biosynthesis of staurosporine (**26**).

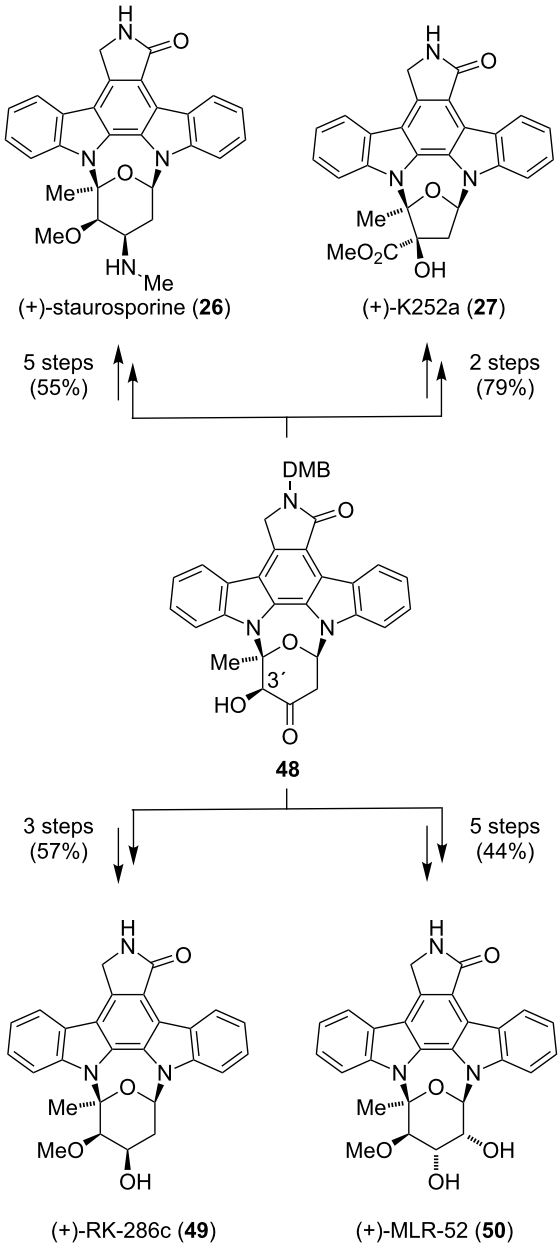
Rh(II)-catalyzed C–H and OH insertion reactions (Scheme 4). The preparation of both enantiomeric furanose building blocks commenced with the $Rh_2(OAc)_4$-catalyzed OH insertion of **39**, respectively **40** into the α-diazo-β-ketoester **40**. A tandem [3,3]/[1,2]-rearrangement cascade, followed by reductive ozonolysis and acid-promoted cyclization afforded (+)-**41** and (−)-**41** in an overall yield of 60% and 46%, respectively. For the synthesis of staurosporinone (**30**) and its 3,4-dimethoxybenzyl (DMB)-protected derivative **45**, a ruthenium-catalyzed C–H insertion/electrocyclization cascade using 2,2'-bisindole **44** and diazolactams **43a**/**b** was developed. The necessary cycloglycosidative coupling of **45** and (+)-**41** was promoted by camphorsulfonic acid to give the DMB-protected K252a [(−)-**46**] as a 2:1 mixture, slightly favoring the desired diastereomer. Cleavage of the N-protecting group gave (−)-K252a [(−)-**27**] as its unnatural enantiomer. With eleven synthetic operations and a longest linear sequence of only seven steps, this route is highly convergent and employs a novel Rh-carbenoid-mediated formation of **30** as its key step. The synthesis of the natural enantiomer of (+)-K252a [(+)-**27**] was carried out in an analogous fashion using (*R*)-(−)-1-nonen-3-ol (**42**) instead of (*S*)-but-3-en-2-ol (**39**) to give the enantiomeric coupling partner of **45**. Although no yields for the following coupling were reported, multigram quantities of optically pure (+)-**46** could be obtained [37]. Further reduction and Moffat oxidation gave **47**, which was believed to be the direct precursor for the common intermediate **48**. Lewis acid catalyzed Tiffenau–Demjanov-type ring expansion of **47** gave **48** as a single product.

With α-hydroxy ketone **48** in hand, the stage was set for further modifications to access **26**, **27**, **49** and **50** (Scheme 5). During their attempts to methylate **48**, an unprecedented benzilic acid-type rearrangement (ring contraction) was discovered. Exposure of **48** to copper(I) chloride in methanol furnished (+)-**46** in 95% yield, which after removal of the protecting group gave (+)-K252a (**27**). Staurosporine (**26**) could be synthesized in five steps from **48** and in a longest linear sequence of 19 steps. For the preparation of (+)-RK-286c (**49**) and (+)-MLR-52 (**50**),



Scheme 4: Wood's synthesis of K-252a via the common intermediate **48**.

ketone **48** was reduced and regioselectively methylated at the C3' position. Cleavage of the protecting group gave **49**, whereas **50** was obtained after dehydration using Martin's sulfurane, dihydroxylation and a final deprotection step.



Scheme 5: Synthesis of **26**, **27**, **49** and **50** diverging from the common intermediate **48**.

Macrocyclic polyketides: The first cytochalasan alkaloids, cytochalasin A (**51**) and B (**52**), originally named phomins [39], were isolated in 1966 [39-42]. Since then, the number of natural products belonging to this family has increased to over 80. Some representative members are depicted in Figure 5 [43]. Cyctochalasan alkaloids display a wide range of biological properties, such as cytotoxic, antimicrobial, antiviral and phytotoxic activities and were reviewed in detail by Hertweck in 2010 [44]. Structurally, they consist of one amino acid and a highly substituted hydroisoindolone moiety fused to a macrocyclic ring (ring size 9–14). In certain cases, the ring system can be oxidized to an unusual cyclic carbonate as observed for cytochalasin E (**53**). Depending on the amino acid incorporated in the isoindolone moiety, the cytochalasans can be further subdivided into cytochalasins [41] (phenylalanine), chaetoglobosins [45,46] (tryptophan), aspochalasins [47] (leucine), pyrichalasins [48] (tyrosine) or alachalasins [49,50] (alanine).

The biosynthesis of cytochalasans was established on the basis of various isotope labeling experiments using cytochalasin B (**52**) as a model system [51-55]. It was hypothesized that the carbon backbone, which is connected to an amino acid, most likely originates from a polyketide synthase (PKS)/nonribosomal peptide synthetase (NRPS) hybrid machinery [56]. The discovery of a gene locus for a PKS-NRPS synthetase of the chaetoglobosin producing fungus *Penicillium expansum* led to a more sophisticated biosynthetic insight of chaetoglobosin A (**57**) (Scheme 6). The stepwise assembly of the nonaketide **61** is realized from activated tryptophan (**36**), one acetyl-CoA (**59**) starter and eight malonyl-CoA extender (**60**) units. The remaining methyl groups are believed to be installed by *S*-adenosyl methionine (SAM). An intramolecular Aldol condensation generates the pyrrolinone **62**, which reacts via an [4 + 2]-cycloaddition to prochaetoglobosin I (**63**) [56]. Recently, gene disruption studies of *Chaetomium globosum* revealed the enzymes involved in the final oxidative transformations leading to chaetoglobosin A (**57**) [57].

The diverse biological activities and unique molecular architecture of the cytochalasan alkaloids have made them a famous synthetic target. Total syntheses of several members of the cytochalasans were reported, which were reviewed by Hertweck and Bräse [44,58]. In line with the focus on the construction of the isoindole component, one can identify the Diels–Alder reaction as the most popular strategy. A linear, biomimetic synthesis using a late stage intramolecular Diels–Alder reaction was implemented in the Stork synthesis of cytochalasin B (**52**) [59] and the Thomas synthesis of cytochalasin H, D, G and O [60-63]. An intermolecular reaction was reported for the synthesis of aspochalasin B (**58**) by Trost and Vedejs [64-67]. The synthesis of cytochalasin D (**70**) by Thomas is outlined in Scheme 7. The intermediate **67**, which contains all of the carbon atoms of the natural product, was synthesized in eight steps starting from the advanced building blocks **64**, **65** and **66**. Selective deprotonation and trapping the so-formed enolate with phenylselenyl chloride gave an intermediate selenide. Oxi-

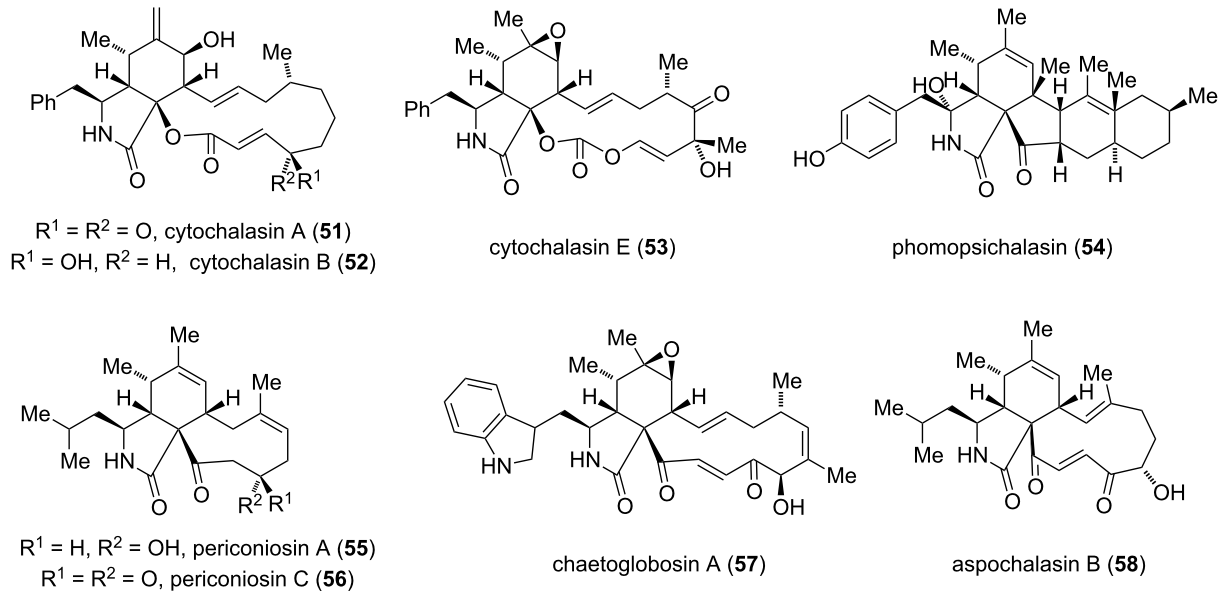
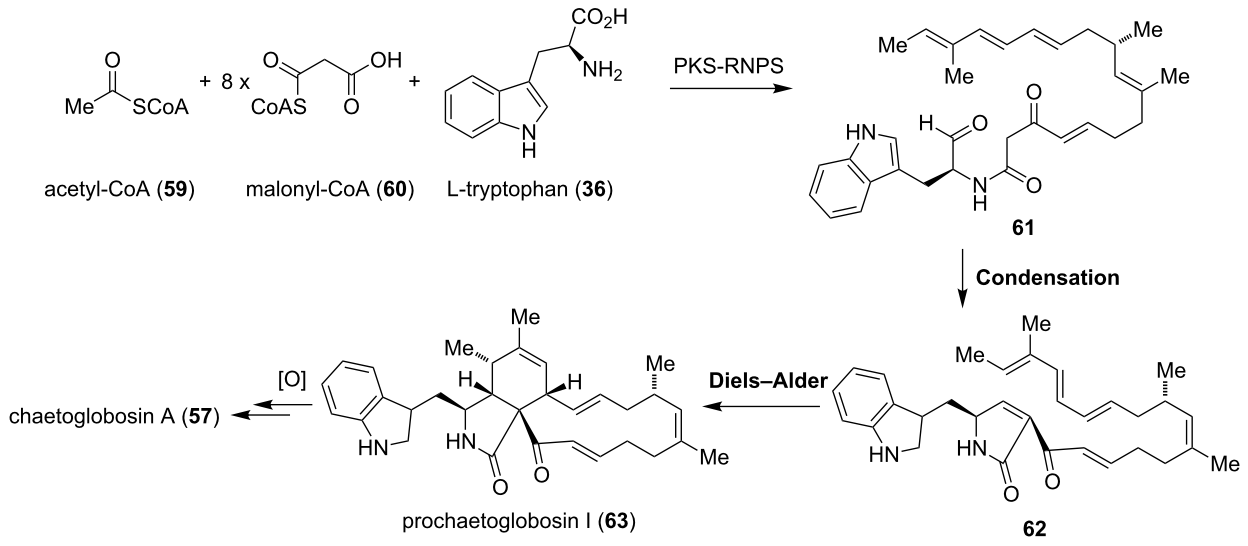


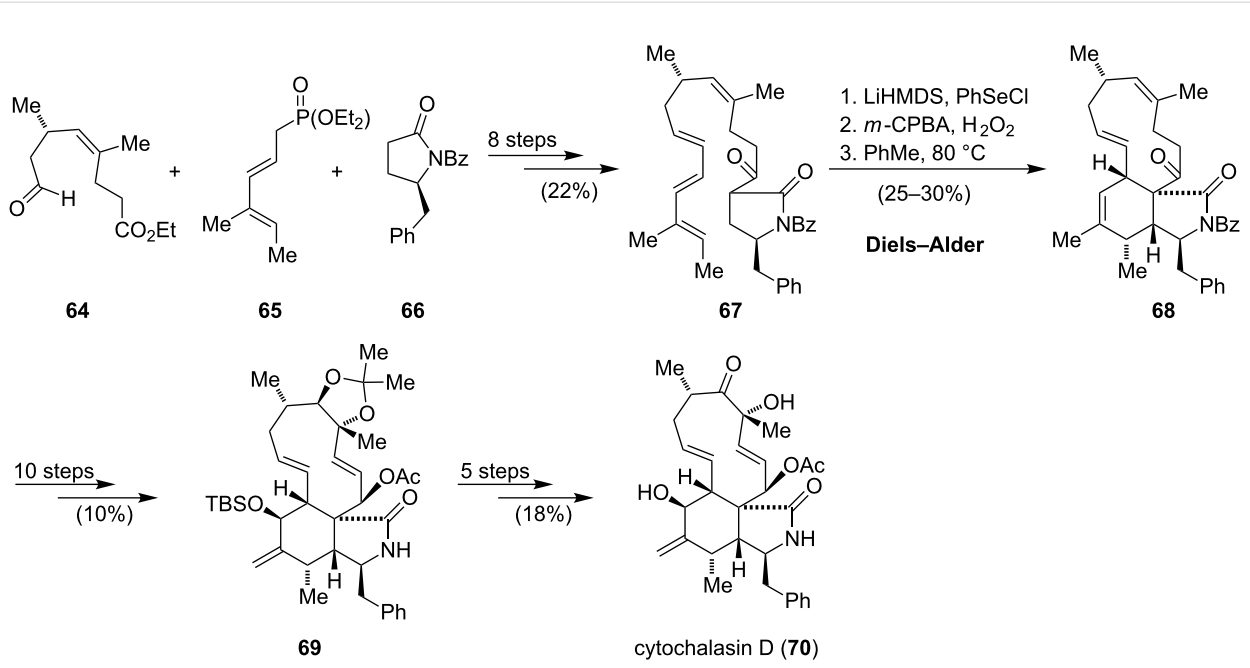
Figure 5: Selected members of the cytochalasan alkaloid family.



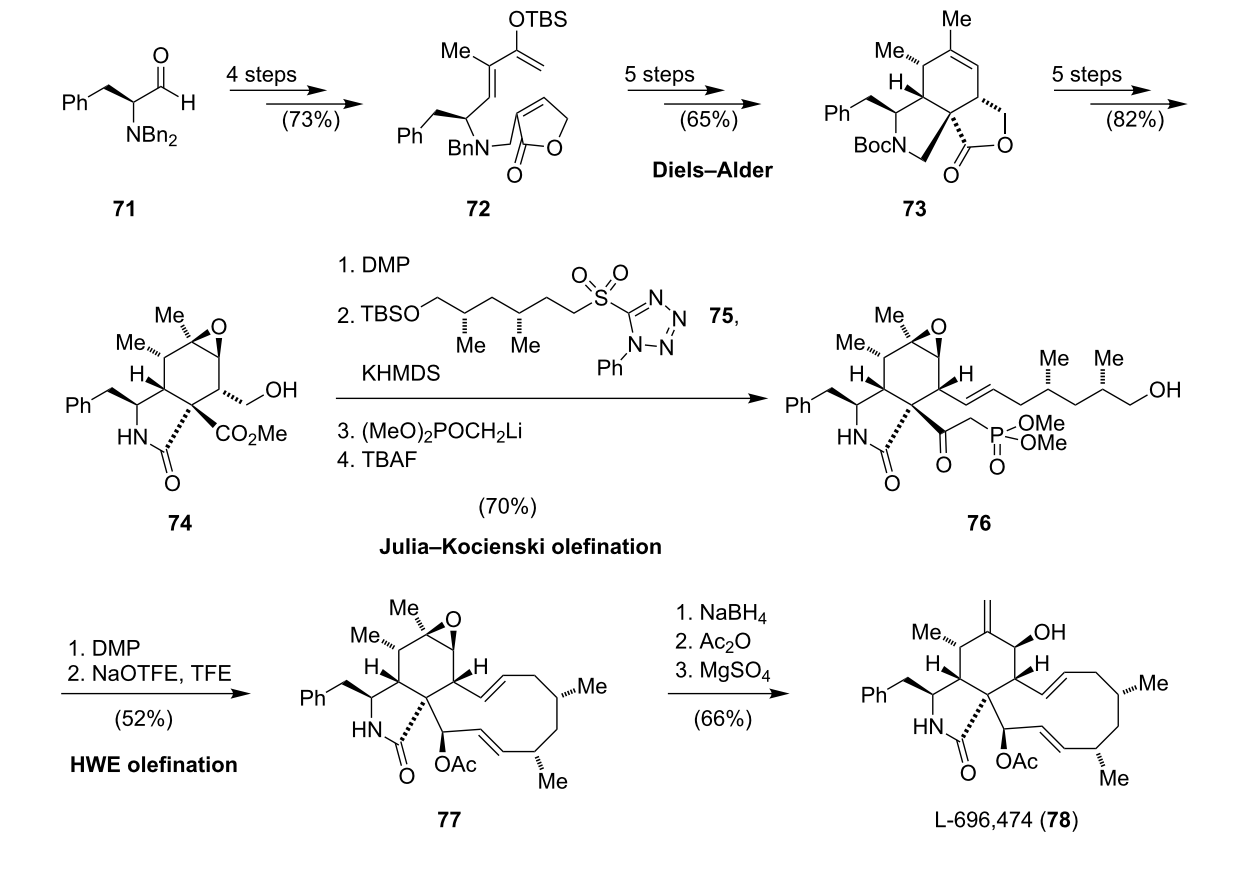
Scheme 6: Biosynthesis of chaetoglobosin A (**57**) [56].

dation and elimination of the corresponding selenoxide at elevated temperature generated the necessary dienophile, which directly underwent an intramolecular *endo*-Diels–Alder reaction to give the isoindolinone **68**. For the synthesis of **69** another ten steps were necessary to discriminate between the three remaining double bonds, functionalize the full carbon skeleton and set the remaining stereocenters. Five steps, including the exchange of protecting groups and one oxidation, completed the synthesis of cytochalasin D (**70**).

In comparison to the syntheses mentioned before (Stork, Thomas, Trost, Vedejs), the convergent approach reported by Myers allows a modular entry to diverse members of the cytochalasin alkaloid family [68]. As proof of concept, the macrolactone cytochalasin B (**52**) and the carbocyclic cytochalasin L-696,474 (**78**), a potent HIV-1 protease inhibitor [69-72], were synthesized (Scheme 8). Strategic bond disconnections revealed the common isoindolinone precursor **73**. The synthesis of the latter commenced from *N*,*N*-dibenzylphenylala-



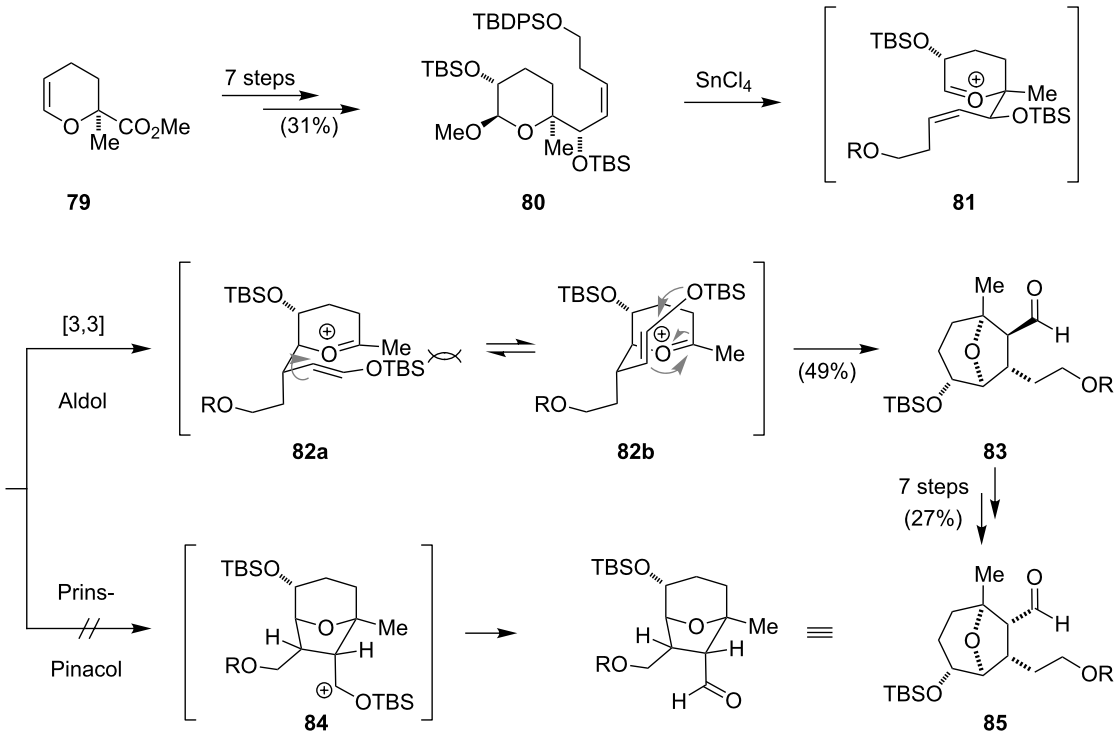
Scheme 7: Synthesis of cytochalasin D (**70**) by Thomas [63].



Scheme 8: Synthesis of L-696,474 (**78**).

nine (**71**) to afford the Diels–Alder substrate **72** in four steps. The envisioned intramolecular Diels–Alder cyclization of the silyl enol ether **72** provided the depicted *endo*-diastereomer in good yield. Exchange of the *N*-benzyl for a Boc-protecting group and cleavage of the silyl enol ether gave the corresponding ketone, which was first converted to an enol-triflate and then to the tricyclic alkene **73**. At this stage, the syntheses of cytochalasin B (**52**) and cytochalasin L-696,474 (**78**) diverged. For **78**, another five steps were necessary to form the isoindolinone **74**. After oxidation of the primary alcohol with Dess–Martin periodinane, the obtained aldehyde was coupled with the readily available *N*-phenyltetrazole sulfone **75** via a Julia–Kocienski olefination. Installation of the phosphonate and desilylation gave **76**, which, after oxidation, reacted in the presence of sodium 2,2,2-trifluoroethanol (NaOTFE) in 2,2,2-trifluoroethanol (TFE) via an intramolecular Horner–Wadsworth–Emmons reaction to **77**. Cytochalasin L-696,474 (**78**) was obtained from **77** via reduction, acetylation and a magnesium sulfate induced rearrangement of the epoxide to the allylic alcohol. The synthesis of cytochalasin B **52** (15 steps from **73**) proceeded in a similar fashion and was highlighted in detail by Hertweck [44]. The authors state that this approach is highly diversifiable and allows for a rapid access to a variety of members of the cytochalasin alkaloid family.

The power of the intramolecular Diels–Alder strategy for the synthesis of the isoindolinone moiety was also recognized during the synthesis of aspergillin PZ (**91**) [73]. This secondary metabolite has a remarkable architecture and was first isolated from the fungus *Aspergillus awamori* in 2002 [74]. The highly functionalized pentacyclic skeleton comprises a unique 12-oxatricyclo[6.3.1.$0^{2,7}$]dodecane ring system and ten stereogenic centers. Its carbon framework is closely related to other members of the aspochalasin/cytochalasin alkaloids such as cytochalasin D (**70**), which lacks the unusual oxatricyclo ring system. The novel structure and cytotoxic activities of natural analogues of aspergillin PZ (**91**) against the HL-60 cancer cell line (IC_{50} = 50–80 nM) initiated Tanis' synthetic program to further evaluate the therapeutic potential of **91** and derivatives thereof (Scheme 9) [73]. The synthesis could be accomplished in 26 steps and includes two key steps: the 8-oxabicyclo[3.2.1]octane unit was synthesized via an unprecedented 2-oxonia-[3,3]-sigmatropic aldol reaction cascade and the isoindolinone moiety was assembled using an intramolecular Diels–Alder reaction. The synthetic endeavor began with the conversion of dihydropyran **79** to the acetal **80** (Scheme 9). Activation of the anomeric position with tin(IV) chloride presumably led to the formation of the oxonium ion **81**. This intermediate was envisioned to undergo a Prins–Pinacol rearrangement



Scheme 9: Synthesis of aldehyde **85** (R = TBDPS).

via intermediate **84** to give the *cis*-aldehyde **85**. However, only the diastereomeric *trans*-aldehyde **83** was isolated in moderate yields from the reaction mixture. The authors concluded that a competing 2-oxonia-[3,3]-sigmatropic aldol pathway via **82a** and **82b** might be operative for this system. The stereochemical outcome could be attributed to the sterically less demanding transition state **82b**. The epimerization of **83** to **85** proceeded via an intermediate lactone and extended the route by seven steps.

After having secured the *cis*-epimer **85**, the diene moiety was introduced in four steps to give aldehyde **86**, which was reacted with the lithium enolate of lactam **87** to furnish the aldol adduct **88** (Scheme 10). Oxidation of the secondary alcohol to the corresponding ketone and selective selenation with phenylselenyl chloride gave **89**. Following the reported sequence for the synthesis of cytochalasin D (**70**), namely oxidation of the selenide to the selenoxide, elimination and intramolecular Diels–Alder reaction, isoindolinone **90** could be obtained in moderate yield. Removal of the protecting groups then yielded aspergillin PZ (**91**).

Though having established a rather long and low yielding synthesis, ample quantities could be obtained for a preliminary evaluation of the biological activity of **79**. In a first screen against A2058 melanoma and DU145 prostate cancer cell lines, **79** showed to be inactive [73].

Isoindolinones derived from isoquinoline alkaloids: The aporhoeadane alkaloids, a term designated by Shamma [75], are abundantly found in South American members of the botanical family of *Berberis* (*Berberidaceae*). Along with the ever present isoquinoline berberine (**92**), the isoindole-containing benzazepines chilenine (**93**) [76], lennoxamine (**94**) [77] and chilenamine (**95**) [78], the isoquinoline nuevamine (**96**) [77] and the benzazocine magallanesine (**97**) [79] were isolated from different *Berberidaceae* species (Figure 6).

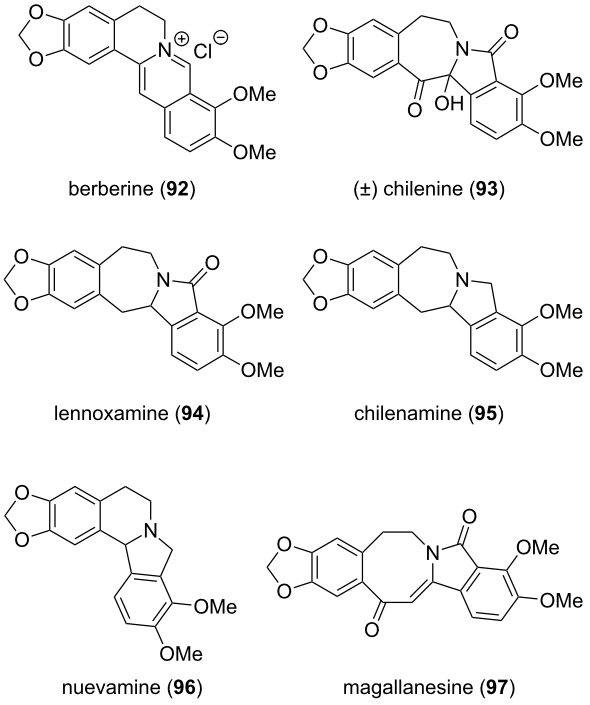
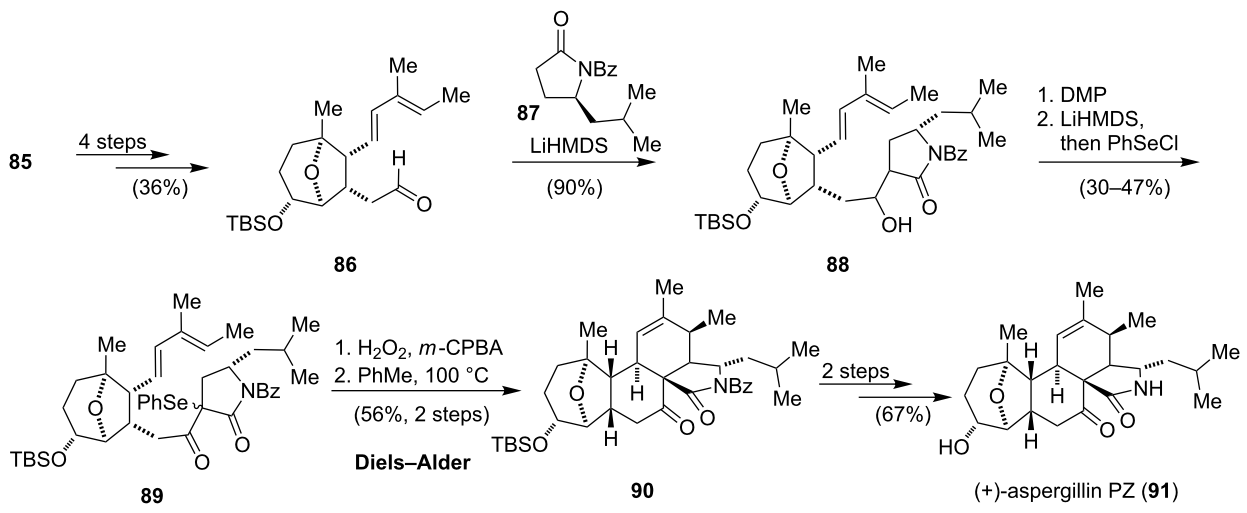


Figure 6: Representative *Berberis* alkaloids.

Chilenine (**93**) was the first isoindolobenzazepine alkaloid isolated from *Berberis empetrifolia* in 1982. The biogenesis proceeds most likely via a Pictet–Spengler reaction of dopamine (**99**) with 4-hydroxyphenylacetaldehyde (**100**), both derived

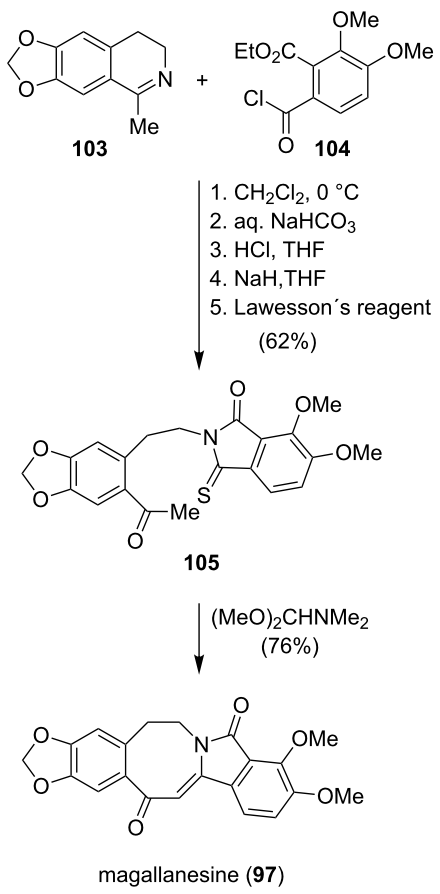


Scheme 10: Synthesis of (+)-aspergillin PZ (**79**) by Tanis.

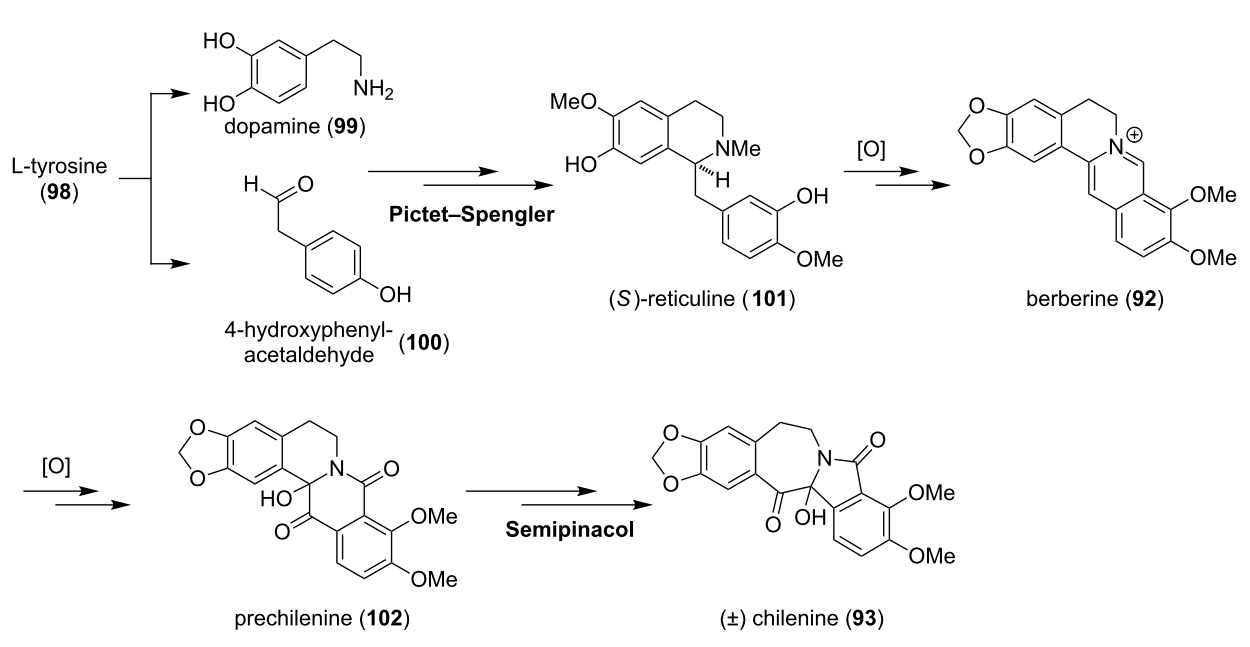
from L-tyrosine (**98**) (Scheme 11). After oxidation and *O*-methylation, which is carried out by *S*-adenosylmethionine (SAM), (*S*)-reticuline (**101**) is obtained. Oxidation of the *N*-methyl group to the iminium ion and cyclization gives the tetracyclic carbon skeleton, which upon further methylation and oxidation furnishes berberine (**92**) [80]. Prechilenine (**102**), itself isolated as its *O*-methyl ether is formed via oxidation [78]. A base-catalyzed semipinacol-type rearrangement yields **93** [76]. Chilenine (**93**) can be further transformed to the [4.4.0]-tricycle lennoxamine (**94**) and the [5.3.0]-ring system chilenamine (**95**) [77-79]. Other members such as nuevamine (**96**) and magallanesine (**97**) contain the corresponding [4.3.0] and [6.3.0]-scaffold.

Since their first isolation in the 80's of the last century, a myriad of syntheses of these small, sometimes highly functionalized and mainly biological inactive alkaloids have been described in the literature. Most of this work is summarized in an excellent review by Leonard [81]. We confine this section to the syntheses of magallanesine (**97**) by Danishefsky and Kurihara, which were also mentioned by Evans and Bentley [82,83].

Magallanesine (**97**), which was isolated in 1985 from *Berberis darwinii*, a plant native to southern Chile and Argentina, is the first known isoindolobenzazocine alkaloid. The seminal total synthesis of **97** was achieved in the group of Danishefsky (Scheme 12) using a dimethylformamide acetal-mediated cyclodehydration of **105**. The isoindole unit of **105** was prepared from the condensation of **103** and **104**. Oxygen–sulfur



Scheme 12: Synthesis of magallanesine (**97**) by Danishefsky [84].



Scheme 11: Proposed biosynthetic pathway to chilenine (**93**).

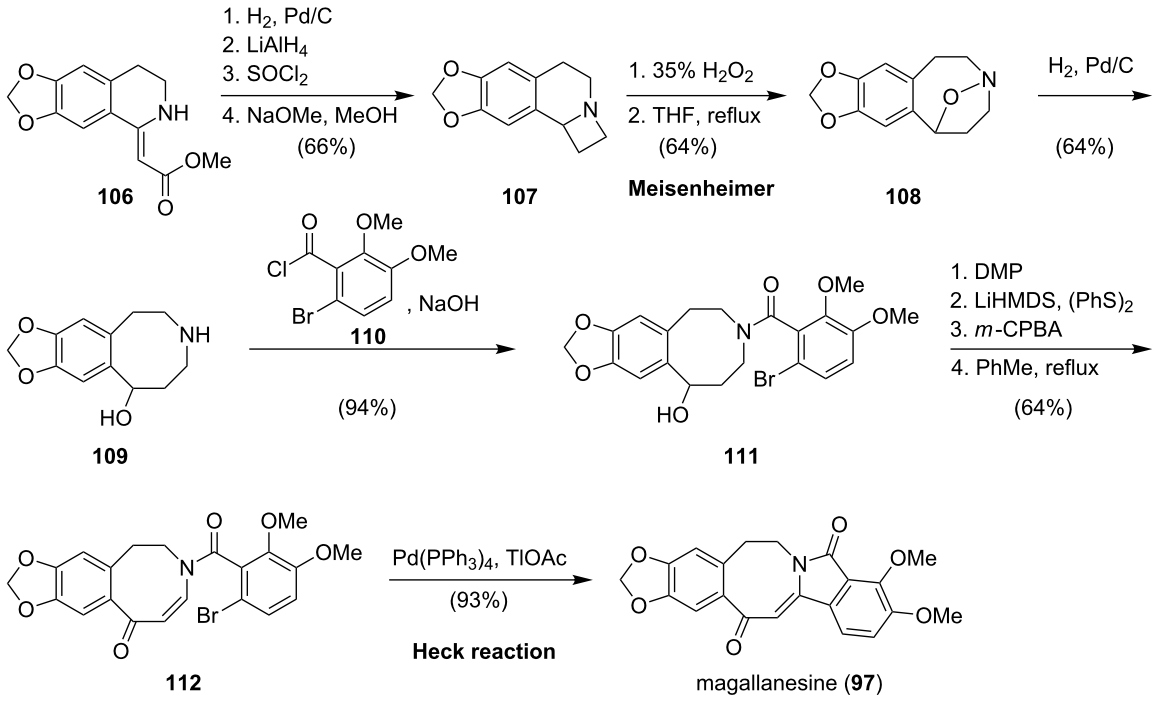
exchange provided the thiophthalimide **105**, which could be converted to magallanesine (**97**) via an intramolecular aldol condensation in one step [84].

In 1996, Kurihara (Scheme 13) reported a [1,2]-Meisenheimer rearrangement followed by an intramolecular Heck cyclization to elaborate the isoindolobenzazocine moiety [85]. The synthesis commenced with the preparation of ester **106** from piperonal according to a known procedure [86]. A four-step sequence yielded azetidine **107**. After oxidation with hydrogen peroxide, the resulting *N*-oxide cleanly underwent a [1,2]-Meisenheimer rearrangement upon heating in tetrahydrofuran. The so-formed azocine **108** was converted to amine **109** by hydrogenolysis of the N–O bond. Amide formation with acid chloride **110** gave **111**, which upon sequential oxidation yielded enaminone **112**. Finally, the isoindolinone moiety was generated via an intramolecular Heck reaction using tetrakis(triphenylphosphine)palladium(0) and thallium acetate, to give magallanesine (**97**) in excellent yield [85].

Aporphine alkaloids: The aristolactam alkaloids are classified as members of the aporphine alkaloid family and contain a characteristic phenanthrene lactam core. Aristolactams (**113**–**116**) along with aristolochic acids (**117**,**118**) and 4,5-dioxoaporphines (**119**,**120**) were mainly isolated from *Aristolochiaceae* but can also be found in several other plant species (Table 1) [87-92]. Several comprehensive overviews of various aristolactams were published by Shamma, Parmar and Bentley [87,92-95].

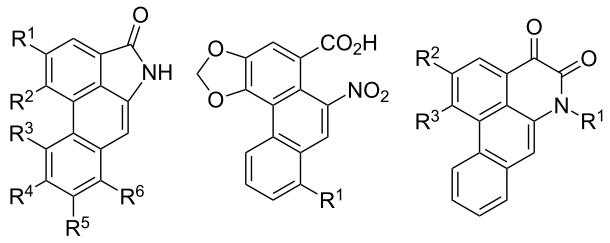
The co-occurrence of aristolactams, aristolochic acids and 4,5-dioxoaporphines led to the assumption of a close biogenetic relationship between these three classes [87,96]. The biosynthesis of aristolochic acid I (**117**) was elucidated via labeling experiments and is depicted in Scheme 14 [97-100]. First, two molecules of the amino acid L-tyrosine (**98**) are transformed to (*R*)-orientaline (**121**) in a similar fashion as described for the biogenesis of (*S*)-reticuline (**101**) (compare Scheme 11). A de-aromatizing spirocyclization of **121** leads to (*R*)-orientalinone (**122**), which, after reduction of the ketone to the secondary alcohol **123**, undergoes a [1,2]-alkyl migration with concomitant loss of water. Re-aromatization and dioxolane formation gives stephanine (**124**). It is hypothesized that direct oxidation of **124** forms 4,5-dioxoaporphine **125**, which upon benzilic acid rearrangement, *N*-methyl cleavage and decarboxylation provides aristolactam I (**113**) [96]. Additional oxidation of the amide function furnishes aristolochic acid I (**117**).

The aristolactams and aristolochic acids have a broad spectrum of biologically interesting properties. Although both can be isolated from the same plants, their biological activity is highly variable. Herbal drugs containing aristolochic acids display

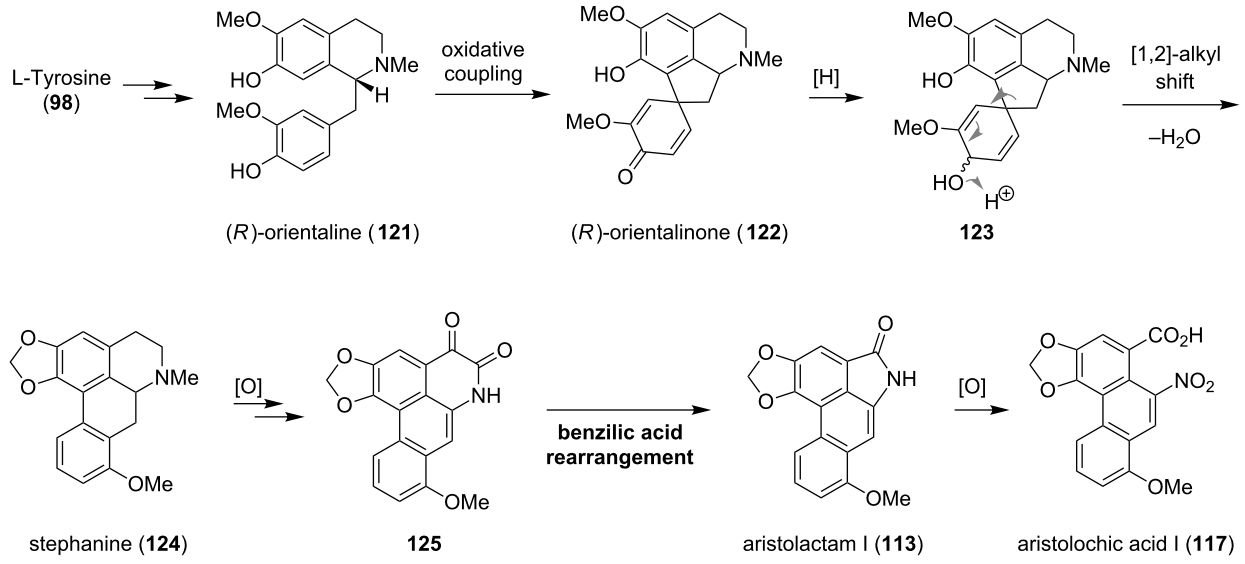


Scheme 13: Kurihara's synthesis of magallanesine (**85**).

Table 1: Selected members of the aporphine alkaloid family.

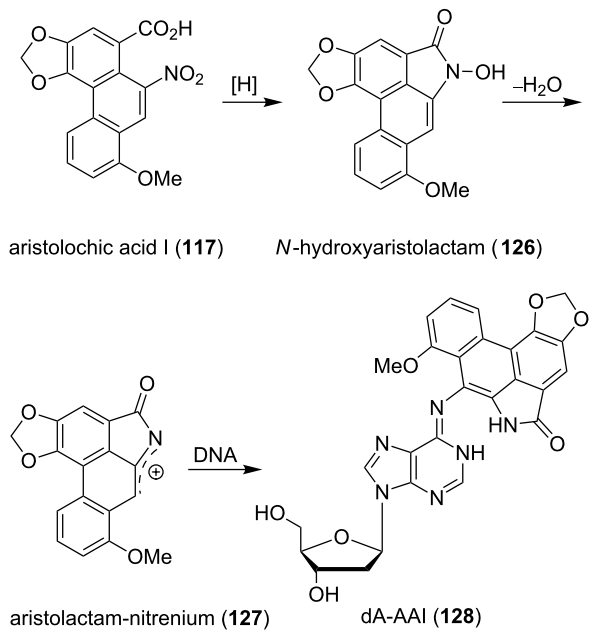


	R^1	R^2	R^3	R^4	R^5	R^6
aristolactams						
aristolactam I (**113**)	O–CH_2–O		H	H	H	OMe
aristolactam AII (**114**)	OH	OMe	H	H	H	H
aristolactam BII (**115**)	OMe	OMe	H	H	H	H
enterocarpam II (**116**)	OH	OMe	H	H	H	OMe
aristolochic acids						
aristolochic acid I (**117**)	OMe					
aristolochic acid II (**118**)	H					
4,5-dioxoaporphines						
aristolodione (**119**)	Me	OH	OMe			
cepharadione A (**120**)	Me	O–CH_2–O				



Scheme 14: Proposed biosynthesis of **113**, **117** and **125**.

cytotoxic activities and inhibitory effects on platelet aggregation and were traditionally used in folk medicine [101]. However, since the early 1980's aristolochic acids are associated with the development of several cancer types and nephropathy (Chinese herbs nephropathy). The mechanism for the formation of covalent DNA adducts is shown in Scheme 15 [102,103]. The DNA damage is initiated by metabolic reduction and cyclization of **117** to *N*-hydroxyaristolactam **126**. After loss of water, the aristolactam nitrenium ion **127**, which is believed to be the main carcinogen, reacts with DNA bases such as adenosine, to give the corresponding 7-(deoxyadenosin-N^6-yl)aristolactam I (dA–AAI, **128**).

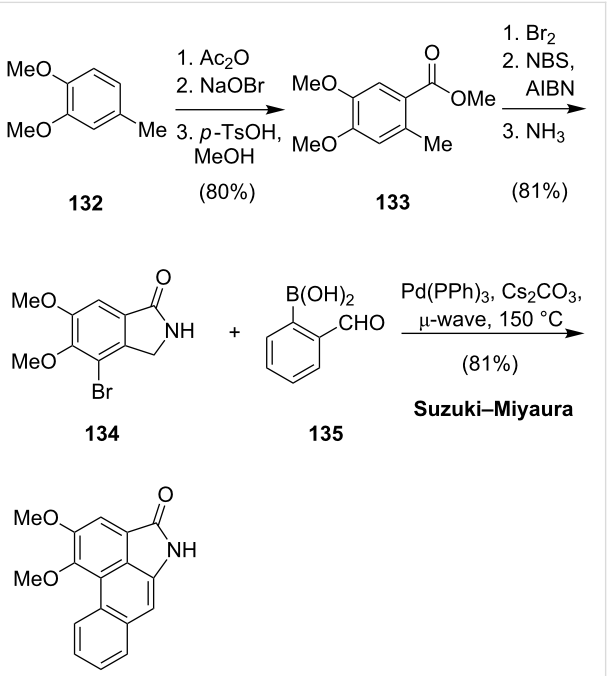


Scheme 15: DNA lesion caused by aristolochic acid I (**117**) [102].

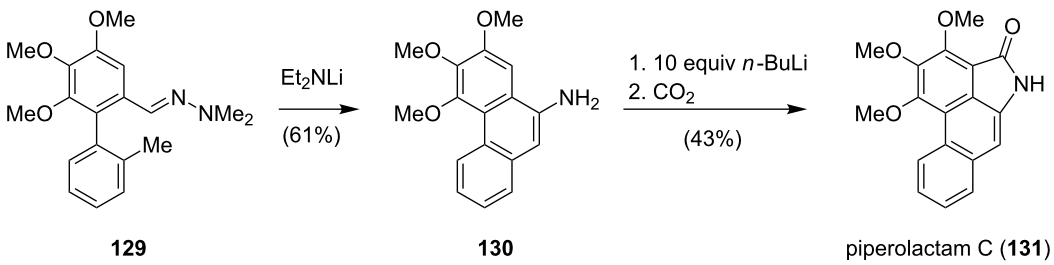
Interestingly, aristolactams are not mutagenic themselves but show immunosuppressant [104], antiplatelet [105], antimycobacterial [106], neuroprotective [107] activities and are excellent inhibitors of cyclin-dependent kinases (CDKs) with IC_{50} values in the nanomolar range [108,109]. CDKs are regulatory proteins, which play an important role in the cell cycle and are considered to be a potential target for anticancer treatment. This makes the aristolactams promising lead components for further drug discovery [108]. The similarity of the aromatic moiety of aristolactams and staurosporines, which are also known to be potent kinase inhibitors could explain the observed inhibition of cyclin-dependent kinases [109]. Over the past years, considerable synthetic efforts have been dedicated to the aristolactams and the development of non-natural analogues.

Pioneering work was carried out in the groups of Castedo [110] and Couture [111,112]. A beautiful application of a directed *ortho*-metalation (DoM) strategy was reported in the synthesis of piperolactam C (**131**) by Snieckus (Scheme 16) [113]. Treatment of **129** with base afforded aminophenanthrene **130** via a remote lateral metalation–cyclization sequence. Metalation of **130** with excess *n*-butyllithium followed by carbonation then yielded piperolactam C (**131**).

In 2008, Heo and coworkers reported the synthesis of several aristolactams employing a one-pot cross-coupling/aldol condensation cascade reaction (Scheme 17) [91]. The synthesis commenced with the preparation of the isoindolinone building block **134**. Friedel–Crafts acetylation of **132**, followed by a Lieben haloform degradation gave the corresponding acid, which after methylation yielded **133**. Bromination and lactam formation afforded isoindolinone **134**. The following one-pot Suzuki–Miyaura/aldol condensation of **134** with boronic acid **135** was carried out at 150 °C in a microwave reactor and gave



Scheme 17: Synthesis of aristolactam BII (**104**).



Scheme 16: Snieckus' synthesis of piperolactam C (**131**).

aristolactam BII (**115**) in good yield. By variation of the coupling partners, Heo was able to efficiently synthesize a library of natural and non-natural analogues.

Cularine alkaloids: Another prominent class of isoquinoline alkaloids, typically found in the botanical family of *Fumariaceae* and in particular in *Sarcocapnos enneaphylla*, are the cularines (**136**–**142**) (Figure 7) [114-116]. In comparison to the related aporphine alkaloids, the cularine skeleton contains a benzoxepine ring system. The parent alkaloid (+)-cularine (**138**) was first isolated by Manske in 1938 [117], and its molecular skeleton was assigned on the basis of NMR and X-ray crystallographic studies. The structure elucidation revealed a twist-boat conformation of the dihydrooxepine ring [118-120]. Within this family, aristoyagonine (**136**), which was first isolated by Castedo in 1984, is the only known naturally occurring member of the cularine alkaloids bearing an isoindolinone moiety [121]. Aristocularine (**137**), a synthetic derivative of aristoyagonine (**136**), is known to display cytotoxic activities in the micromolar range [122].

Biosynthetically, the cularines can be traced back to L-tyrosine (**98**) (Scheme 18) [123,124]. Incorporation of radioactively labeled L-tyrosine into crassifoline (**144**), which is an established cularine precursor, most likely occurs via alkaloid **143**. Hydroxylation and sequential methylation of **143** leads to **144**. Oxidative phenol coupling then forms the cularine alkaloid skeleton. The generated cularine enneaphylline (**145**) and the

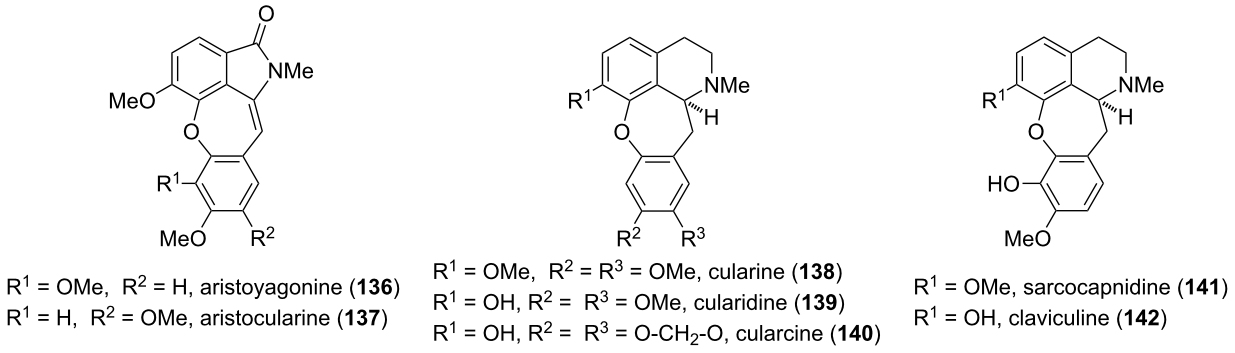
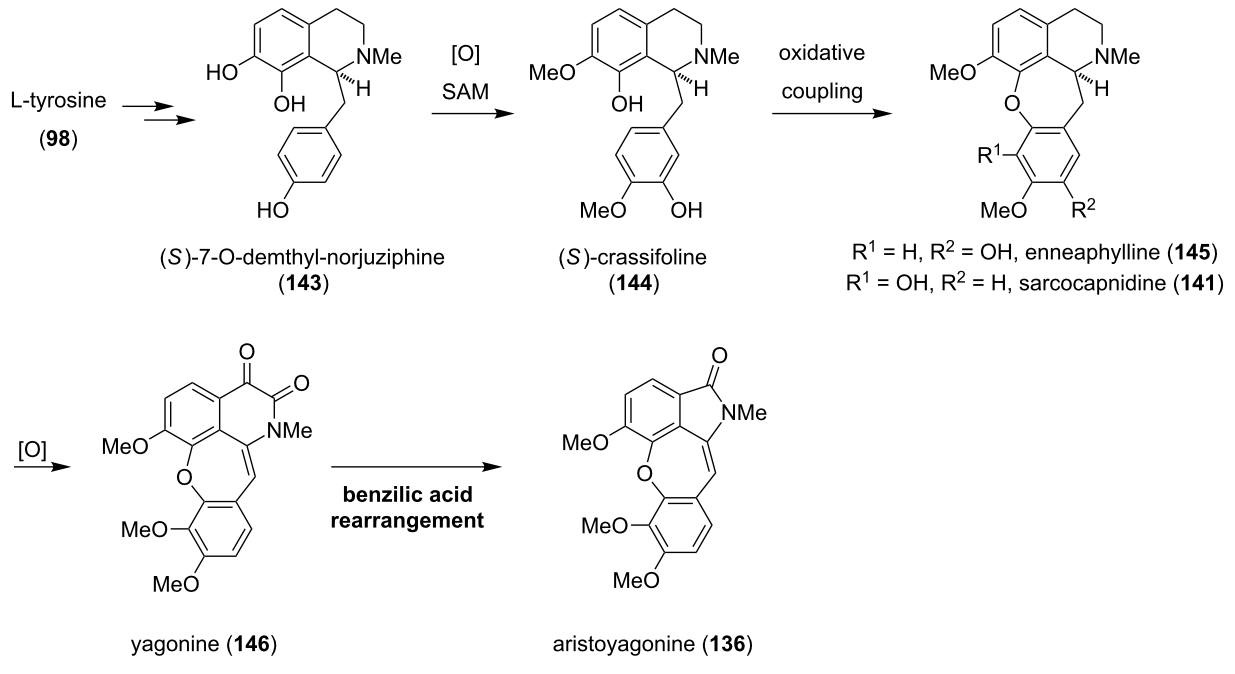


Figure 7: Representative cularine alkaloids.



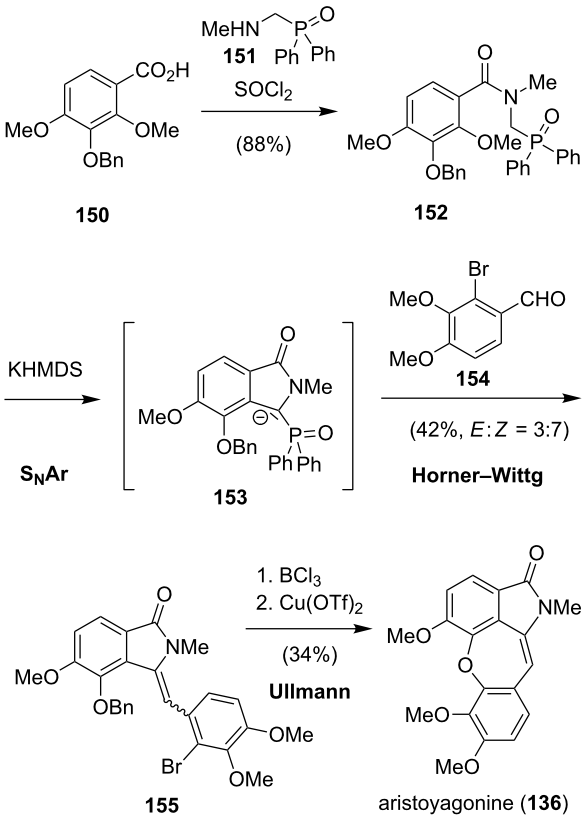
Scheme 18: Proposed biosynthesis of **136**.

regioisomeric *iso*-cularine sarcocapnidine (**141**) could serve as branching points for the synthesis of further cularine derivatives. Sequential oxidations of **141**, similar to the biosynthesis of the aristolactams (Scheme 14), yields yagonine (**146**), which could be converted to aristoyagonine (**136**) via a benzilic acid-type rearrangement [121].

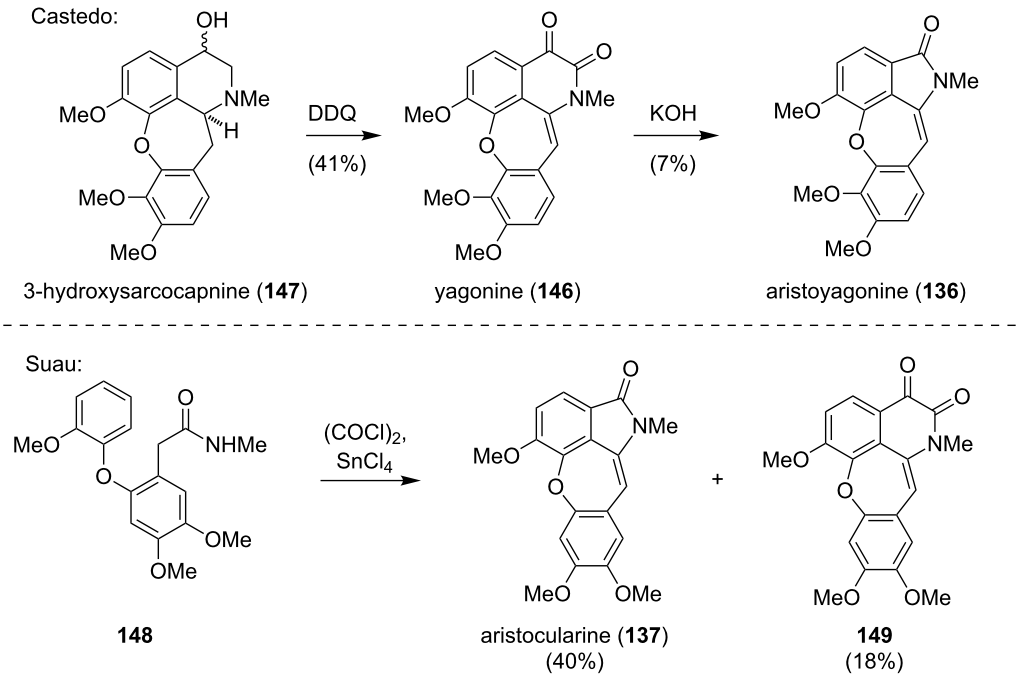
The first syntheses of aristoyagonine (**136**) were reported by Castedo and Suau (Scheme 19) [121,122,125-127]. The approach carried out by Castedo relied on 3-hydroxysarcocapnine (**147**), which could either be isolated from natural sources or prepared via an Ullmann coupling of a 1-(2-bromobenzyl)-8-hydroxyisoquinoline derivative [121,125]. Oxidation of **147** with 2,3-dichloro-5,6-dicyano-1,4-benzoquinone (DDQ) gave the dioxocularine yagonine (**146**). The bioinspired, base-mediated transformation of **146** to **136** obviously proceeds via a benzilic acid rearrangement–oxidation sequence.

In 1996, the group of Suau accessed aristocularine **137** along with **149** in one step from acetamide **148**. In the presence of oxalyl chloride and the Lewis acid tin(IV) chloride, a tandem cyclization (Bischler–Napieralski/Friedel–Crafts acylation reaction) was triggered to directly give **137** and **149** [122,127].

In 2006, another approach to aristoyagonine (**136**) was reported by the group of Couture (Scheme 20) [128]. For the preparation of **136**, their previously developed procedures for the syntheses



Scheme 20: Synthesis of **136** by Couture.



Scheme 19: The syntheses of **136** and **137** reported by Castedo and Suau.

of aristolactams were adopted [111,112]. The synthesis commenced with the generation of the amide **152** from the coupling of **150** with **151**. Exposure of **152** to potassium bis(trimethylsilyl)amide gave the isoindolinone **153** via an intramolecular addition–elimination reaction. In the presence of the aldehyde **154**, **153** underwent a Horner–Wittig reaction to generate **155** as a 1:2.3 mixture of *E*- and *Z*-isomers. Treatment of **155** with boron trichloride not only liberated the phenol but also isomerized the *E*-double bond to the *Z*-isomer. Finally, a copper(II) triflate-catalyzed Ullmann coupling furnished **136**.

Meroterpenoids: The term meroterpenoids describes a family of natural products with a mixed biosynthetic origin, partially derived from terpenoids and polyketides [129]. Several members of this class containing an isoindolinone motif, for instance compounds **156**, **157** and **159**–**161**, can be extracted from *Stachybotrys* fungi (Figure 8) [130-135]. Memnobotrin A (**158**) is found in the closely related *Memnoniella echinata* fungus [136], and hericenone B (**162**) and erinacerin A (**163**) were isolated from the mushroom *Hericium erinaceum* [137,138]. Another member of this family, aspernidine A (**164**), was recently isolated form the fungus *Aspergillus nidulans* by Hertweck [139]. A comprehensive review about meroterpenoids produced by fungi was published by Simpson in 2009 [140]. The isolated molecules display a broad spectrum of interesting biological properties, such as high antiviral activity (**156**) [141], inhibition of the HIV-1 protease (**157**) [132], antibacterial and antifungal activities (**159**–**160**) [133] or neuri-

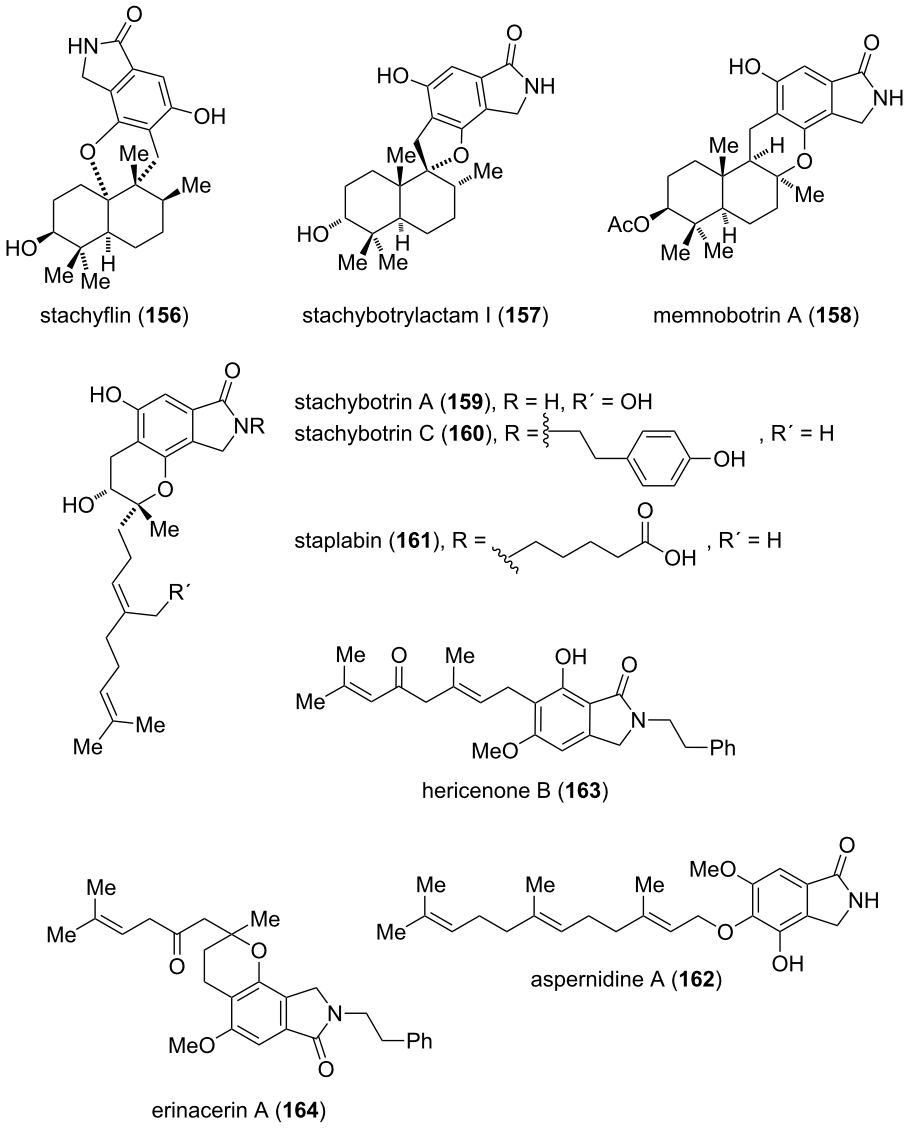


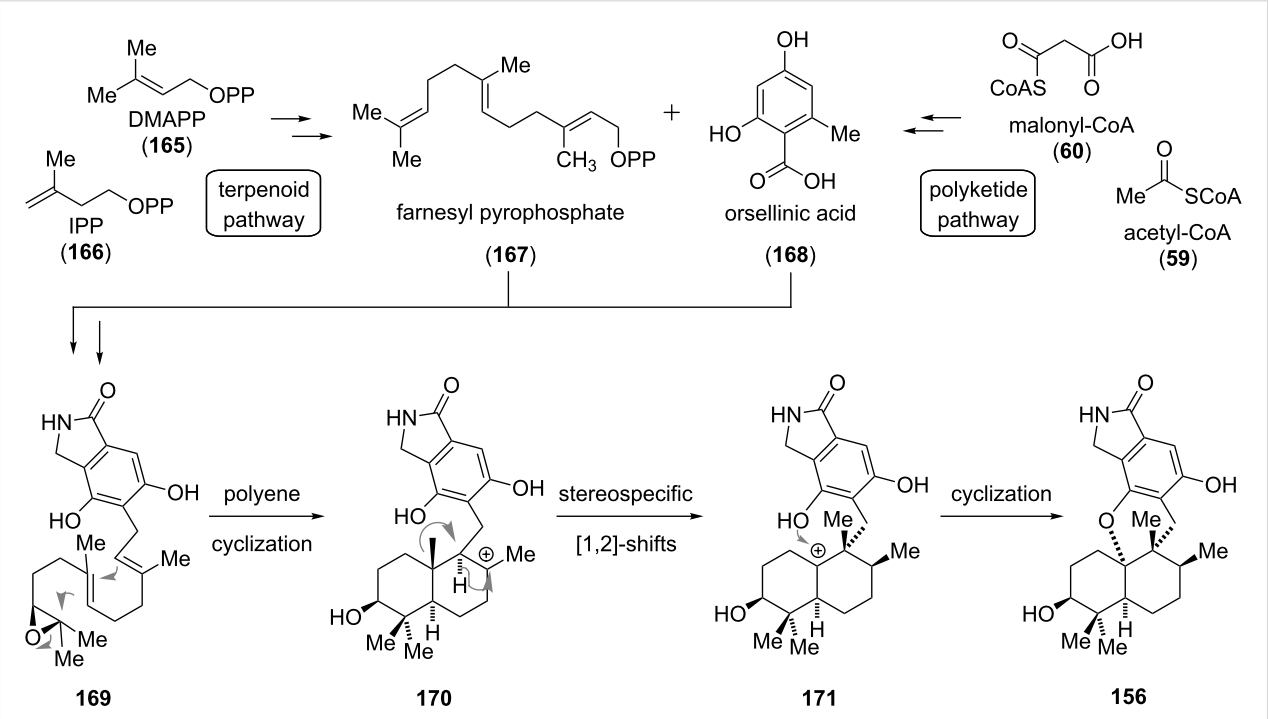
Figure 8: Representative isoindolinone meroterpenoids.

togenic properties (**161**) [134]. So far, only a few total syntheses were accomplished and the exact biosynthetic pathways are unknown.

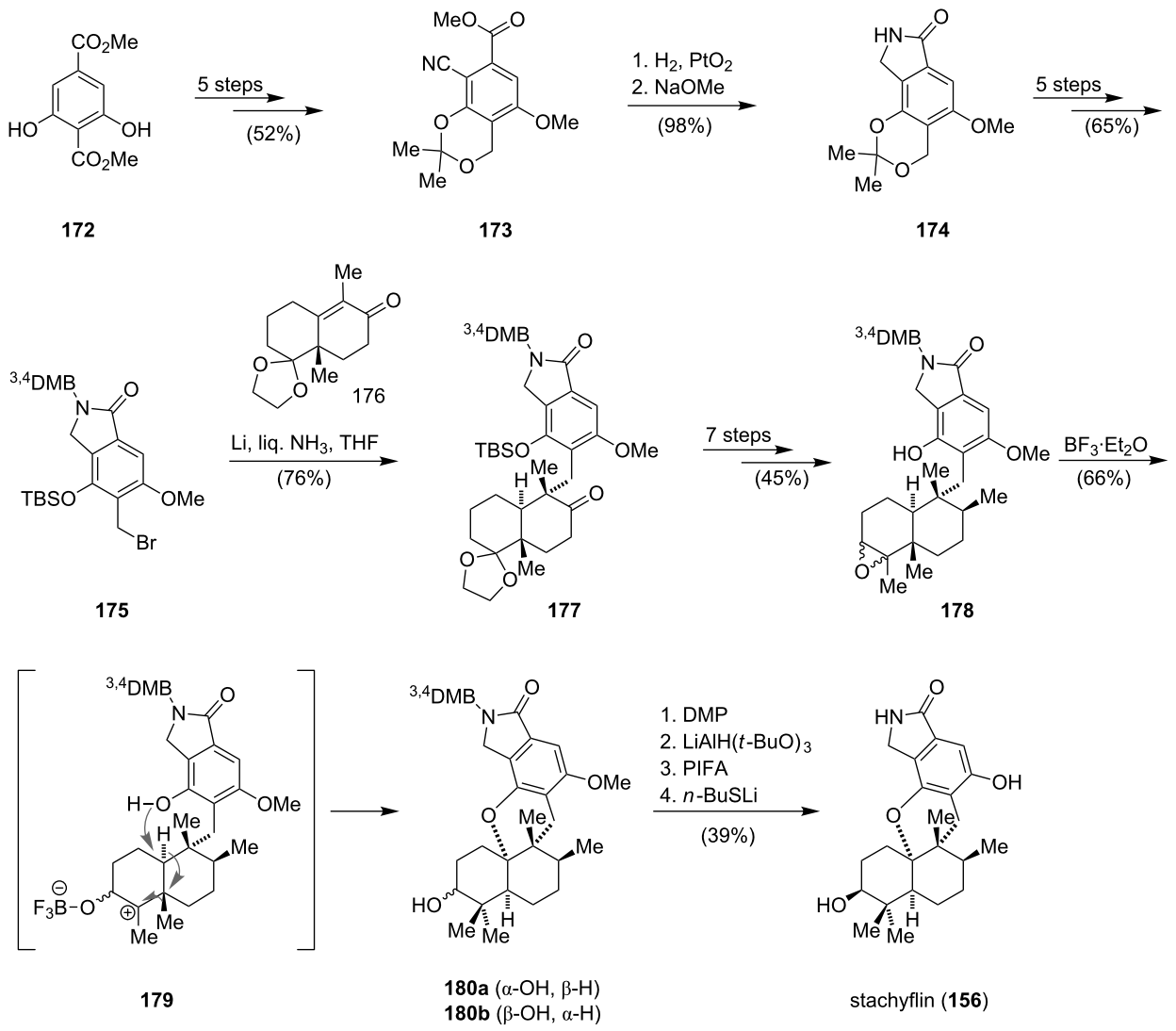
The sesquiterpenoid stachyflin (**156**) was first isolated from the fungus *Stachybotrys* sp. RF-7260 by Shionogi & Co., Ltd., Japan, in 1997 [130] and shows outstanding antiviral activity against the influenza A subtype H1N1 (IC_{50} = 3 nM), outperforming current drugs such as amantadine and zanamivir [141]. The putative biosynthesis of **156**, which contains a pentacyclic ring system with a *cis*-fused decalin is depicted in Scheme 21. Farnesyl pyrophosphate (**167**), which originates from the terpenoid pathway through the condensation of dimethylallyl pyrophosphate (DMAPP, **165**) with two units of isopentyl pyrophosphate (IPP, **166**), and orsellinic acid (**168**), which is derived from a fungal iterative type I polyketide pathway [142], are connected to give **169**. This substrate is already poised for a polyene cyclization cascade, which only has to be triggered via activation of the epoxide. After the decalin moiety has formed, two sigmatropic, stereospecific [1,2]-shifts of intermediate **170** provide the tertiary carbocation **171**, which could be trapped by the phenolic alcohol to give stachyflin (**156**) [143].

In 2011, the first enantioselective total synthesis of (+)-stachyflin (**156**) via a Lewis acid induced domino epoxide-opening/rearrangement/cyclization cascade was accomplished by the group of Katoh (Scheme 22) [144]. The synthesis commenced with the conversion of dimethyl 2,6-dihydroxyterephthalate (**172**) to nitrile **173** within five consecutive steps. Hydrogenation and lactam formation of **173** gave isoindolinone **174**, which was converted to bromide **175**. Reductive alkylation of the protected Wieland–Miescher ketone **176** with bromide **175** using Birch conditions gave **177** as a single diastereoisomer. Epoxide **178** could be prepared in seven steps from **177**, but was obtained as a mixture of inseparable diastereoisomers. The Lewis acid induced key step, a domino epoxide-opening/rearrangement/cyclization cascade, most likely proceeded in a stepwise manner via intermediate **179**. Activation of the epoxide with boron trifluoride etherate induces the planned sigmatropic [1,2]-methyl and [1,2]-hydride shifts to generate the tertiary carbocation at the ring junction. This is then trapped by the phenol to give the pentacyclic compounds **180a** and **180b**. The former diastereoisomer could be converted to **180b** via inversion of the secondary alcohol. Cleavage of the methyl ether and the 3,4-dimethoxybenzyl (^{3,4}DMB) group of **180b** led to (+)-stachyflin (**156**). The synthesis proceeded in 25 steps with an overall yield of 2.6%.

Another novel class of isoindolinone-containing natural products, categorized as spirodihydrobenzofuranlactams or stachybotrylactams (**157**, **181**, **182**), was isolated from different *Stachybotrys* species by Jarvis and Roggo between 1995 and 1996 (Figure 9) [131,132]. These compounds are antagonists of endothelin and display strong immunosuppressant activities.



Scheme 21: Postulated biosynthetic pathway for the formation of **156** (adopted from George) [143].



Scheme 22: Synthesis of stachyflin (**156**) by Katoh [144].

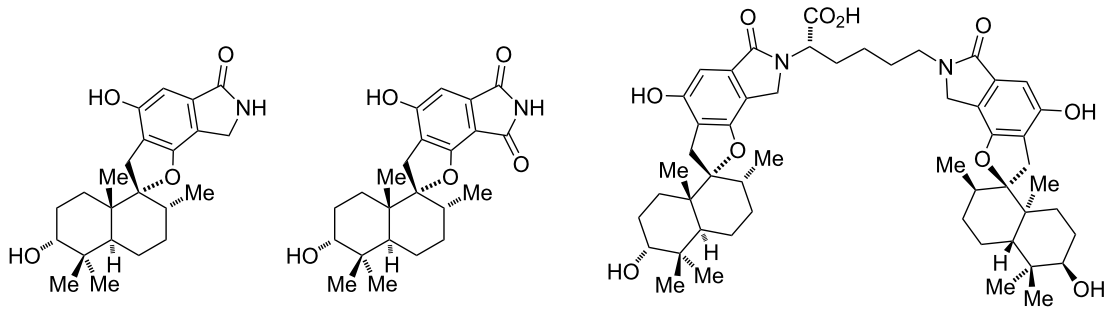
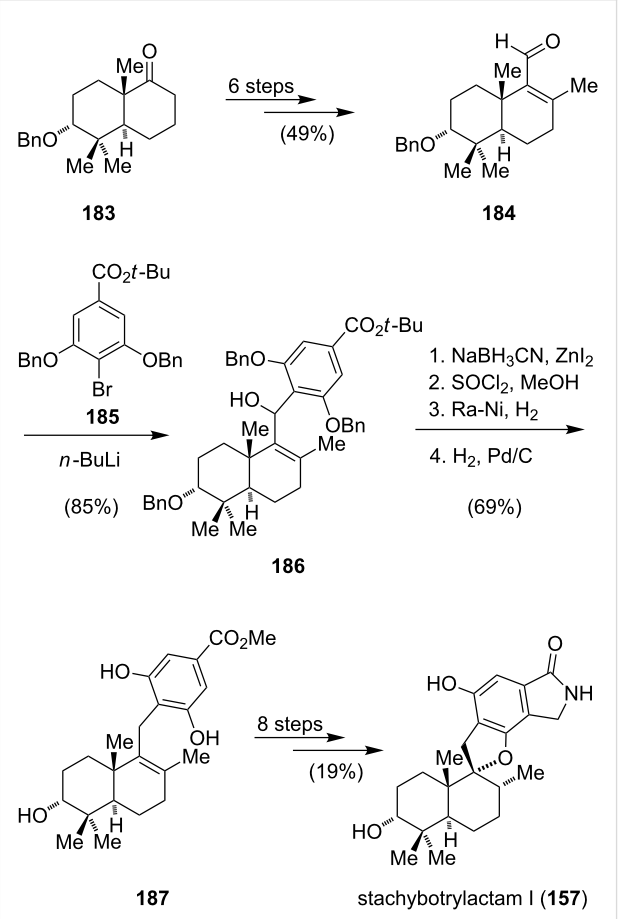


Figure 9: Selected examples of spirodihydrobenzofuranlactams.

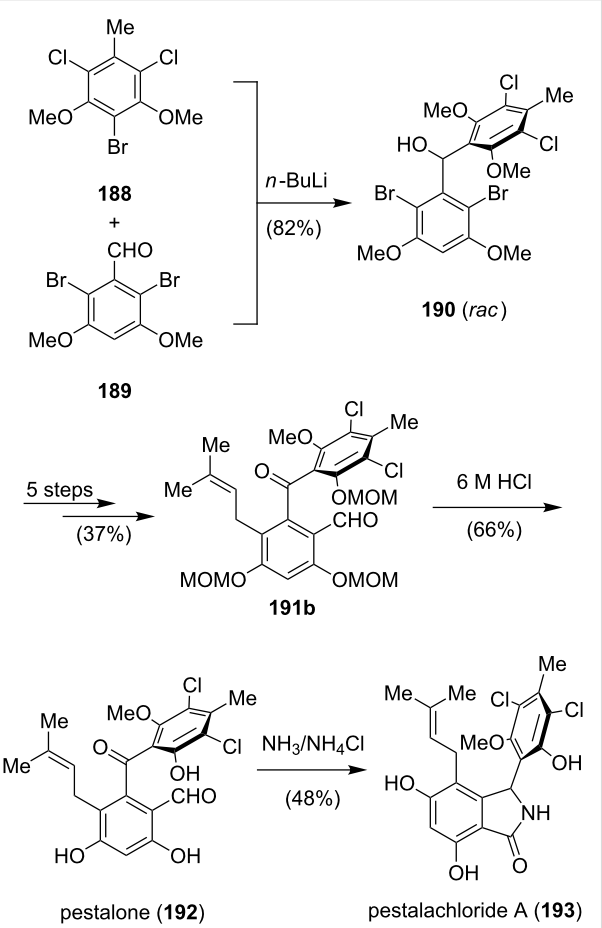
The pseudosymmetric dimer stachybocin A (**182**), which was isolated by Ogawa in 1995 [145], constitutes the most potent representative [132]. Oxidation of the isoindolinone unit of **157** gives the relatively scarce phthalimide motif, which is present in stachybotrylactam V (**181**).

To date, only one enantioselective total synthesis of spirodihydrobenzofuranlactam I **157** has been published (Scheme 23) [146]. The synthesis carried out by the group of Guo commenced with *trans*-decalone **183**, which was derived from the Wieland–Miescher ketone. For the conversion of **183** to the α,β-unsaturated aldehyde **184** six steps were necessary. Halogen–metal exchange of **185** with *n*-butyllithium followed by the addition of **184** gave the carbinol **186** in good yield. Removal of the benzyl groups, cleavage of the *tert*-butyl group with concomitant formation of the methoxy ester (COO*t*-Bu → COOMe), and global deprotection gave **187**. Acid-catalyzed (Amberlyst 15) spiroannulation afforded a 1.7:1 mixture of the benzofuran and the benzopyran (90% overall conversion). For the installation of the isoindolinone, a seven-step sequence similar to the one described for stachyflin (**156**) was used (Scheme 23). The arene appendage was desymmetrized via monobromination and cross coupling with copper cyanide provided a nitrile. Hydrogenation and lactam formation under basic conditions completed the synthesis of stachybotrylactam I (**157**).

Chlorinated isoindolinone alkaloids: Pestalachloride A (**193**) was isolated from the plant endophytic fungus *Pestalotiopsis adusta* as a racemate and displays potent antifungal activities against *Fusarium culmorum* (IC_{50} = 0.89 μM) [147]. Pestalone (**192**), a natural product and synthetic precursor of **193** shows strong antibiotic activity against methicillin-resistant *Staphylococcus aureus* (MRSA, MIC = 84 nM) and vancomycin-resistant *Enterococcus* (VRE, MIC = 178 nM) [148]. The structural similarity between pestalachloride A (**193**) and pestalone (**192**), which both contain the same prenylated polyketide core imply a direct biosynthetic relationship [147]. The reaction of **192** with an equivalent of ammonia gives a cyclic iminohemiaminal, which first tautomerizes to the hydroxy isoindole and then to the isoindolinone **193**. This biosynthetic transformation was also used in the total synthesis of **193** by Schmalz (Scheme 24)



Scheme 23: Synthesis of stachybotrylactam I (**157**).



Scheme 24: Synthesis of pestalachloride A (**193**) by Schmalz.

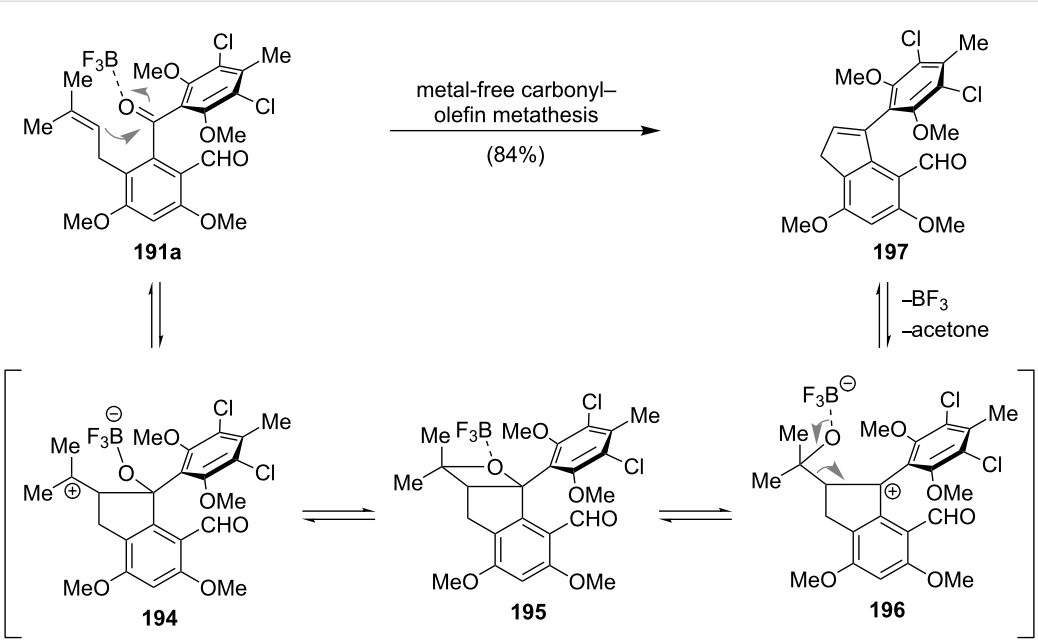
[149]. Reaction of lithiated **188** (three steps from commercially available 5-methylresorcinol) with the aldehyde **189** (double bromination of 3,5-dimethoxybenzaldehyde) gave the racemic alcohol **190**.

Oxidation to the benzophenone, installation of the prenyl side chain and introduction of the formyl group was accomplished within five steps to give **191a** (Scheme 25). The envisioned deprotection of **191a** using Lewis acidic conditions led to an unexpected and unprecedented metal-free carbonyl–olefin metathesis. Coordination of boron trifluoride etherate to **191a** promotes the formation of the tertiary carbenium ion **194**, which isomerizes via the oxetane intermediate **195** to the benzylic cation **196**. Expulsion of acetone then yields indene **197** in excellent yield. Avoiding this side reaction could only be achieved by exchanging the methyl ether protecting group for a more labile methoxymethyl ether at the benzophenone stage. The following prenylation and formylation proceeded smoothly under the same conditions to give **191b** (Scheme 24). Cleavage of the MOM ethers afforded pestalone (**192**), which could be converted into **193** in a single step by treatment of **192** with ammonia in aqueous ammonium chloride solution (pH 8).

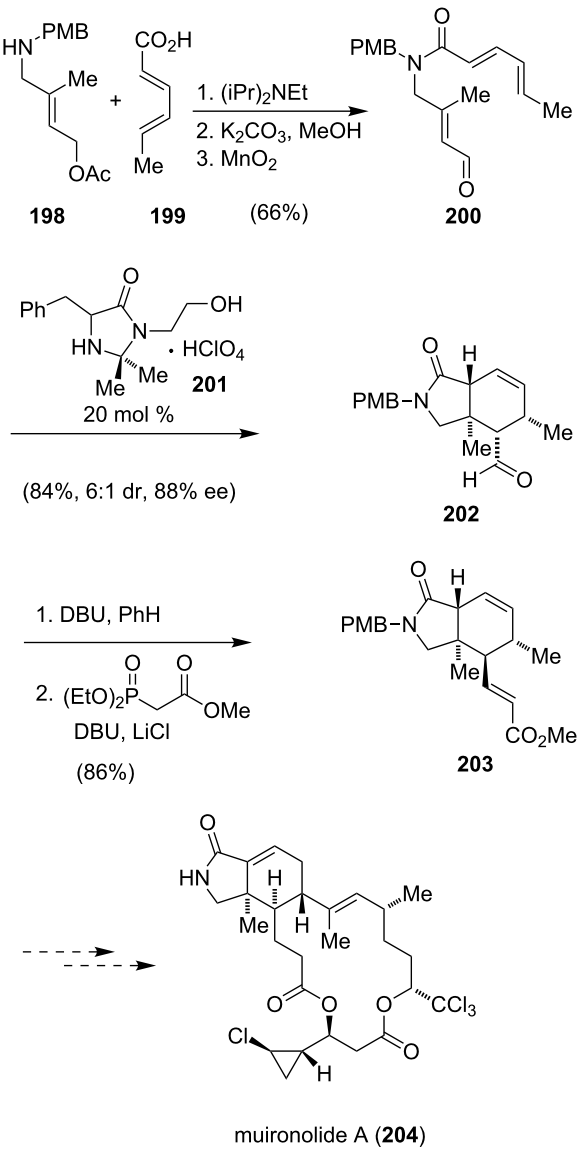
Muironolide A (**204**) was isolated by Molinski from the marine sponge *Phorbas* sp. in 2009 [150]. The molecular framework of this unique natural product has a hexahydro-1*H*-isoindolinone-triketide, a *trans*-2-chlorocyclopropane and a trichlorocarbinol ester. A first biological evaluation showed that **204** displays antifungal activity. However, only 90 µg could be isolated and further biological screening was not possible [151]. Several sponge-derived macrolides have proven to be effective cytotoxic agents [152,153] and one could speculate that muironolide A (**204**) shares this potential. A first attempt to access **204** in the laboratory was reported by Molinski shortly after the isolation (Scheme 26) [151]. Coupling of the dienophile precursor **198** with sorbic acid (**199**) gave a tertiary amide, which was converted to **200** via a reduction–oxidation sequence. The asymmetric intramolecular Diels–Alder reaction was then catalyzed by Kristensens' catalyst (**201**) to give **202**. A base-promoted epimerization of the aldehyde and a Horner–Wadsworth–Emmons reaction furnished **203**, the most advanced intermediate reported so far.

Just recently, the group of Zakarian reported another approach to the fully elaborated isoindolinone core of **204** [154].

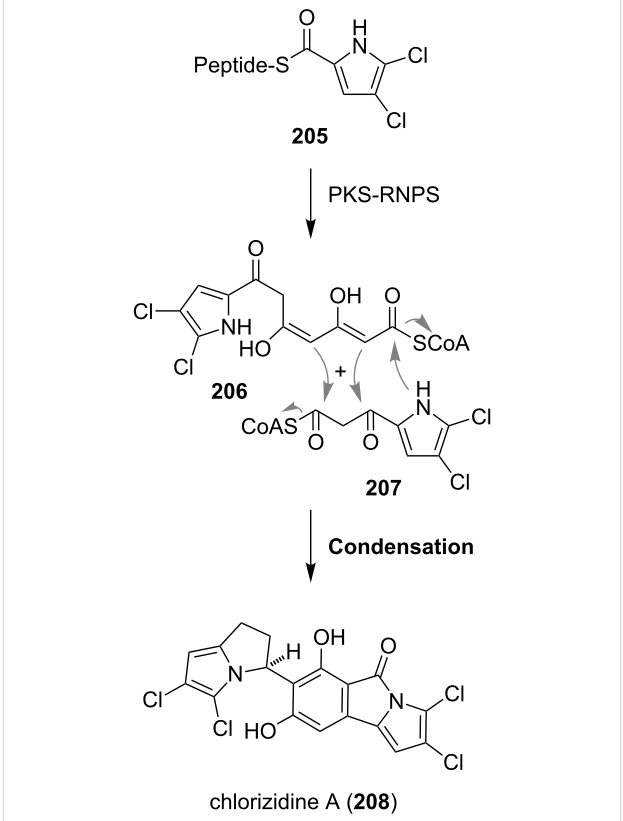
Chlorizidine A (**208**) (Scheme 27), a cytotoxic metabolite from a marine *Streptomyces* species shows an unprecedented 5*H*-pyrrolo[2,1-*a*]isoindolinone ring system, which is connected to a dichlorinated pyrrolizine [155]. Chlorizidine A (**208**) and its semisynthetic derivatives display significant cytotoxic activities against various human cancer cell lines. The IC_{50} value of **208** against the colon cancer cell line HCT-116 was determined to be in the micromolar range (3.2–4.9 µM) [155]. A first biosynthesis was postulated on the basis of the structural similarity between **208** and marinopyrrole A, another secondary metabolite derived from a marine *Streptomyces* species [156]. The common biosynthetic precursor **206** stems from a mixed



Scheme 25: Proposed mechanism for the BF_3-catalyzed metal-free carbonyl–olefin metathesis [149].



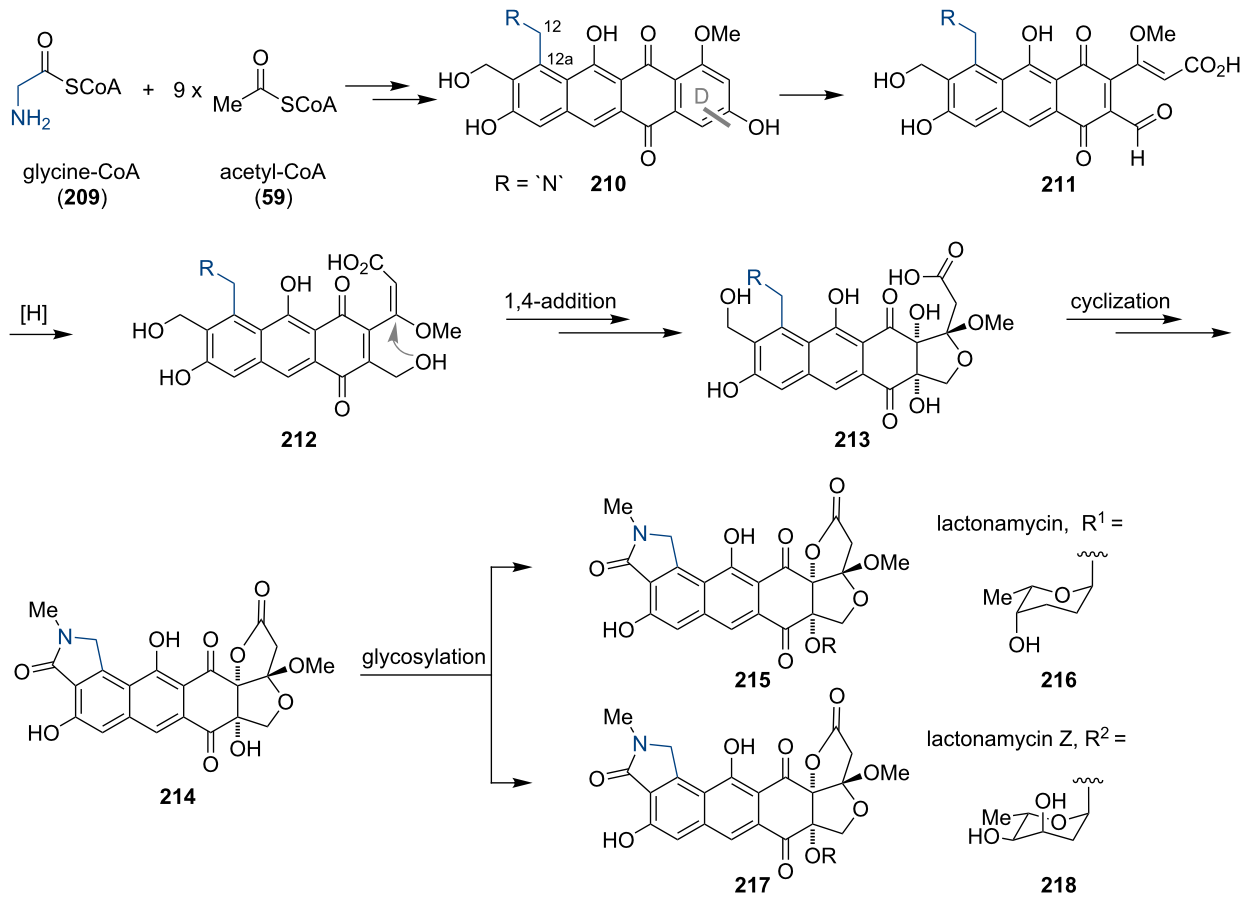
Scheme 26: Preparation of the isoindoline core of muironolide A (**204**).



Scheme 27: Proposed biosynthesis of **208**.

nonribosomal peptide synthetase (NRPS)/polyketide synthase (PKS) pathway. The amino acid proline is first oxidized and chlorinated by an $FADH_2$-dependent halogenase to give **205**, which after extension by the polyketide synthase gives the polyketides **206** and **207**, respectively. The intermolecular condensation of these two components yields chlorizidine A (**208**) [155].

Anthraquinone-type alkaloids: Lactonamycin (**215**) and lactonamycin Z (**217**) were isolated from *Streptomyces rishiriensis* and *Streptomyces anglieri* in 1996 and 2003 [157,158]. Both compounds are potent antibacterial agents against Gram-positive bacteria, including methicillin-resistant *Staphylococcus aureus* (MRSA) and vancomycin-resistant *Enterococcus* (VRE) [159]. Beyond that, the modest cytotoxic activity of **215** and **217** against human cancer cell lines makes them interesting lead components for drug discovery. The IC_{50} values of **215** for different leukemia cell lines range from 0.11–0.22 μM. For **217**, an IC_{50} value of 0.32 μM against gastric adenocarcinoma was observed [157,158]. The hexacyclic aglycone of **215** and **217**, lactonamycinone (**214**), consists of a densely oxygenated fused hydrofuran–hydrofuranone and a naphta[*e*]isoindole ring system. The core of lactonamycin (**215**) is decorated with the 2-deoxysugar α-L-rhodinopyranose (**216**), whereas α-L-2,6-dideoxyribopyranose (**218**) is found in **217**. The structure of the aglycone **214** is related to tetracenomycins, a family of tetracyclic aromatic polyketides, which are produced by several *Streptomyces* species [159]. Biosynthetic investigations revealed a striking similarity of the gene cluster responsible for the biogenesis of lactonamycinone (**214**) to those clusters found in tetracenomycin-producing bacteria. Cloning experiments and incorporation of various labeled precursors resulted in a first hypothesis for the biogenesis of **215** and **217** (Scheme 28) [159]. This led to the assumption that the aglycone **214** is assembled from nine acetate units and glycine, respectively *N*-methylglycine derivative, which contributes both carbon atoms and the nitrogen to the skeleton of **210** (position 12 and 12a). The latter are uncommon starter

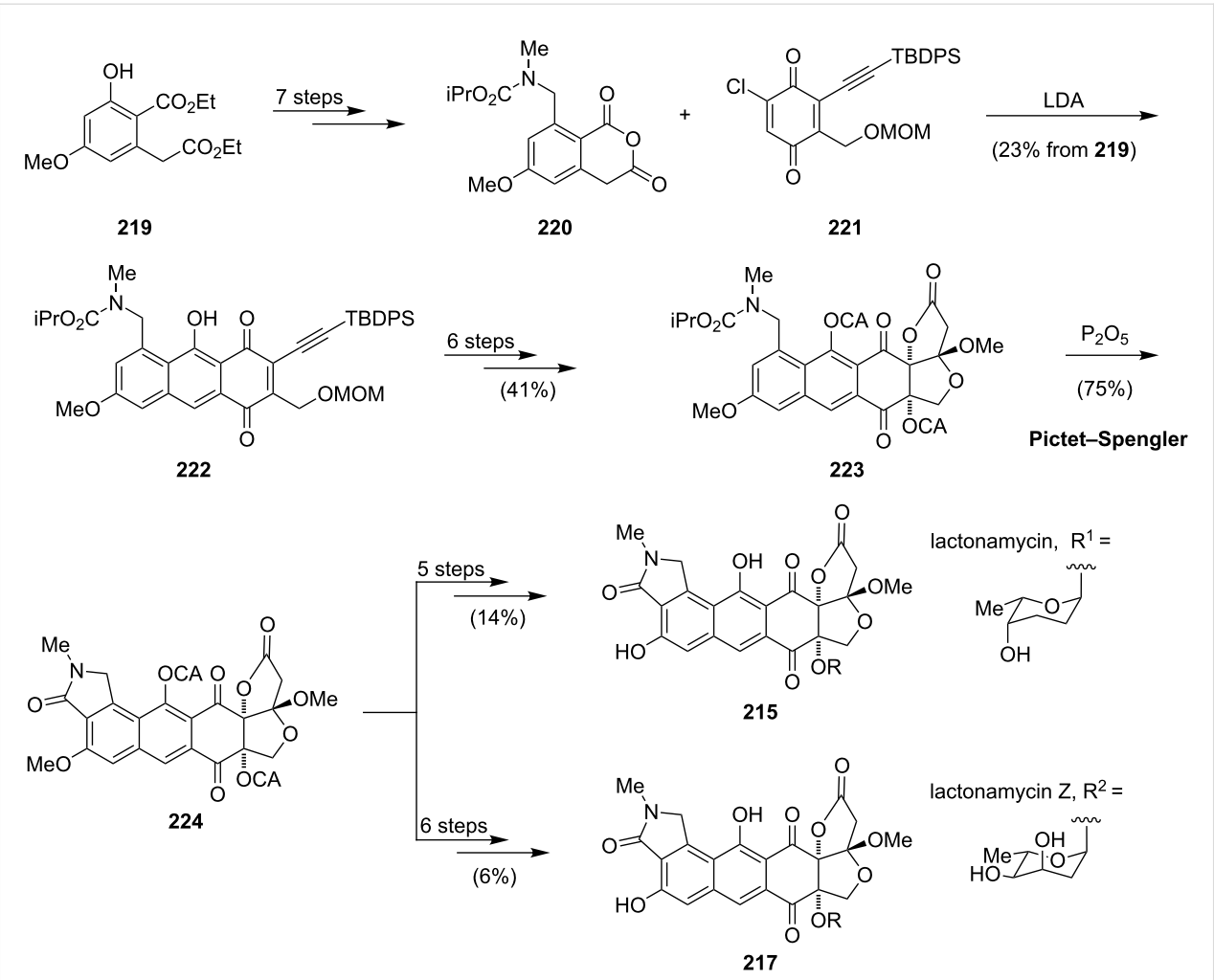


Scheme 28: Model for the biosynthesis of **215** and **217**.

units in a type II polyketide assembly line [160]. Upon oxidative cleavage of the D-ring of the putative tetracenomycin-like intermediate **210**, the aldehyde **211** is reduced to the corresponding alcohol **212**. Acetalization and introduction of the 1,2-*cis*-diol moiety furnishes **213**. Sequential formation of the lactone and the isoindolinone generates **214**. A final glycosylation step leads to lactonamycin (**215**) and lactonamycin Z (**217**).

The remarkable structure and the promising biological activities have attracted many synthetic groups. Several total syntheses of **215** and **217** were reported in recent years [161] (and references therein). The group of Danishefsky was the first to report a diastereoselective synthesis of lactonamycinone (**214**) employing a Diels–Alder reaction [162,163]. In 2010, Tastuta completed the first total synthesis of lactonamycin (**215**) by using a sequential conjugate addition, a stereoselective glycosylation reaction and a Michael–Dieckmann-type cyclization [164]. The recently published total synthesis of lactonamycin (**215**) and lactonamycin Z (**217**) by Saikawa and Nakata is based on a late-stage glycosylation strategy (Scheme 29). This enables the specific variation of the sugar components and gives access to various lactonamycin derivatives [161].

Starting from alcohol **219**, the diene precursor **220** could be prepared in seven steps. The following Diels–Alder reaction with chloroethynylquinone **221**, which was synthesized according to a known procedure [165] proceeded in a highly regioselective manner to give antharaquinone **222**. Introduction of the fused hydrofuran–hydrofuranone moiety was accomplished via deprotection, palladium-catalyzed cyclization–methoxycarbonylation [166] and an acid-catalyzed lactone formation to afford **223**. For the generation of the isoindolinone via a Bischler–Napieralski reaction, a chloroacetyl (CA)-protected phenol was essential to avoid competing carbamate formation of the starting material. Upon exposure of **223** to phosphorus pentoxide, the desired isoindolinone **224** was formed in 75% yield. Deprotection led to lactonamycinone (**214**), which was the substrate for a ytterbium triflate-catalyzed glycosylation to give **215** and **217**, respectively.



Scheme 29: Synthesis of lactonamycin (**215**) and lactonamycin Z (**217**).

Miscellaneous: At first glance, the hetisine alkaloids do not show any structural similarities with the compound classes described before. However, though lacking an "intact" isoindole core, one can spot the corresponding perhydro motif. Since their first discovery more than 70 years ago, more than 100 different hetisine alkaloids have been isolated from different species of the plants *Aconitum* and *Delphinium*, and to a lesser extend from *Rumex*, *Consolida* and *Spiraea* [167,168]. These plants have been widely used in traditional herbal medicine and further pharmacological studies revealed that hetisine alkaloids are highly bioactive compounds [167,168]. The diverse spectrum includes vasodilatoring, anti-arrhythmic, immunomodulating and analgesic activities. Hetisines can be classified, according to Wang and Liang, as C_{20}-diterpenoid alkaloids, which belong to the family of atisane alkaloids [167]. The hetisines comprise a heptacyclic core and are structurally the most complex members derived from the atisine skeleton. The most prominent representatives, nominine (**225**) [169,170], kobusine (**226**) [171,172], pseudokobusine (**227**) [173,174] and hetisine (**228**) [174-176] are depicted in Figure 10.

The putative biosynthetic pathway for the formation of the hetisine alkaloids is derived from phytochemical data and basic biochemical transformations (Scheme 30) [167]. Cyclization of geranylgeranyl pyrophosphate (**229**), involving the *ent*-copalyl diphosphate synthase, could give *ent*-copalyl diphosphate (**230**). After loss of the pyrophosphate group and double cyclization, a 1,3-hydride shift and Wagner–Meerwein rearrangement leads to the naturally occurring *ent*-atisir-16-ene (**231**). Oxidative incorporation of nitrogen, which might be derived from β-aminoethanol, generates the atisine-type skeleton **232**. Oxidative C–C-bond formation gives the hetidine core (**233**) and C–N-bond formation the hetisine skeleton (**234**).

The first total synthesis of a hetisine-type alkaloid was accomplished by Muratake and Natsume in 2004 [177]. In their

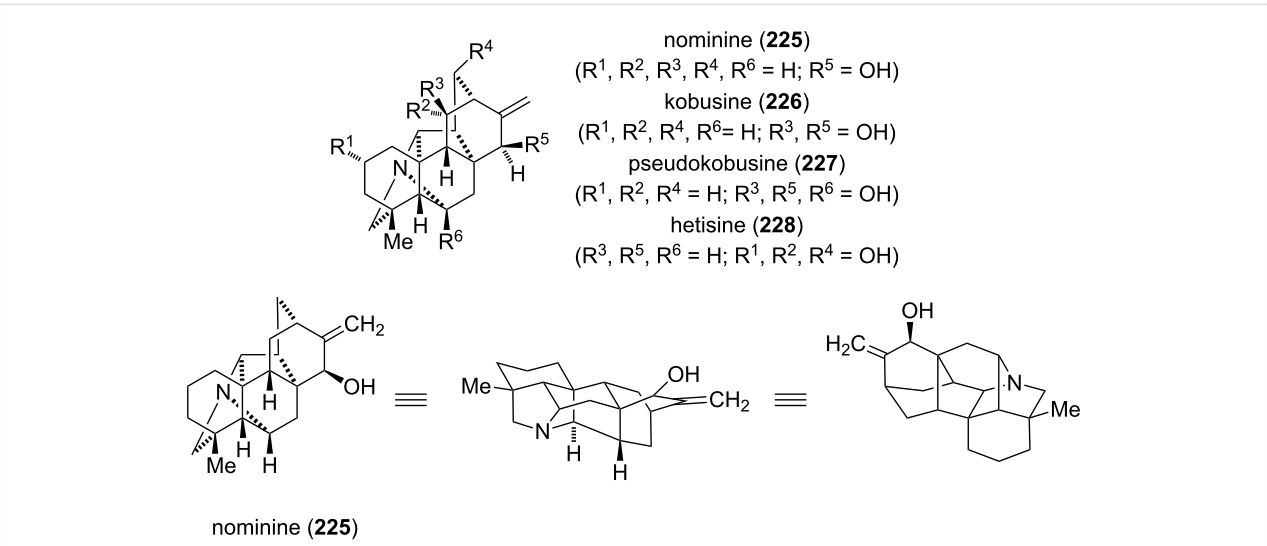
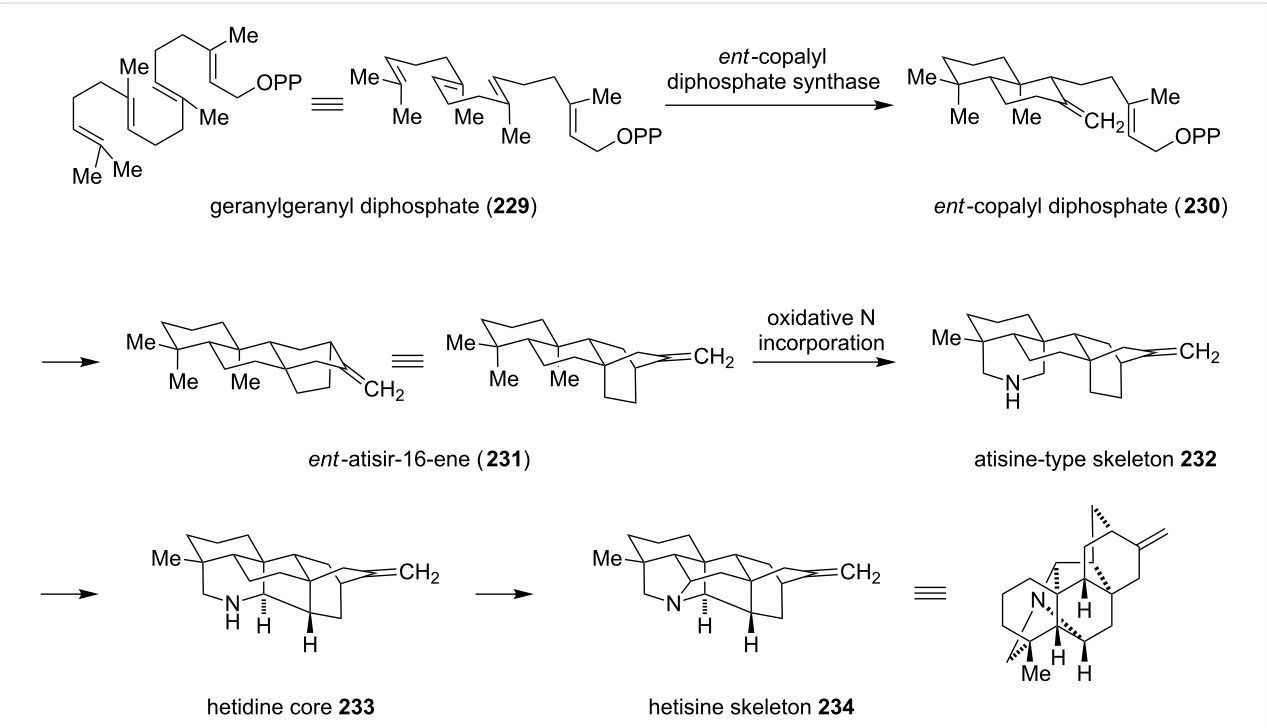
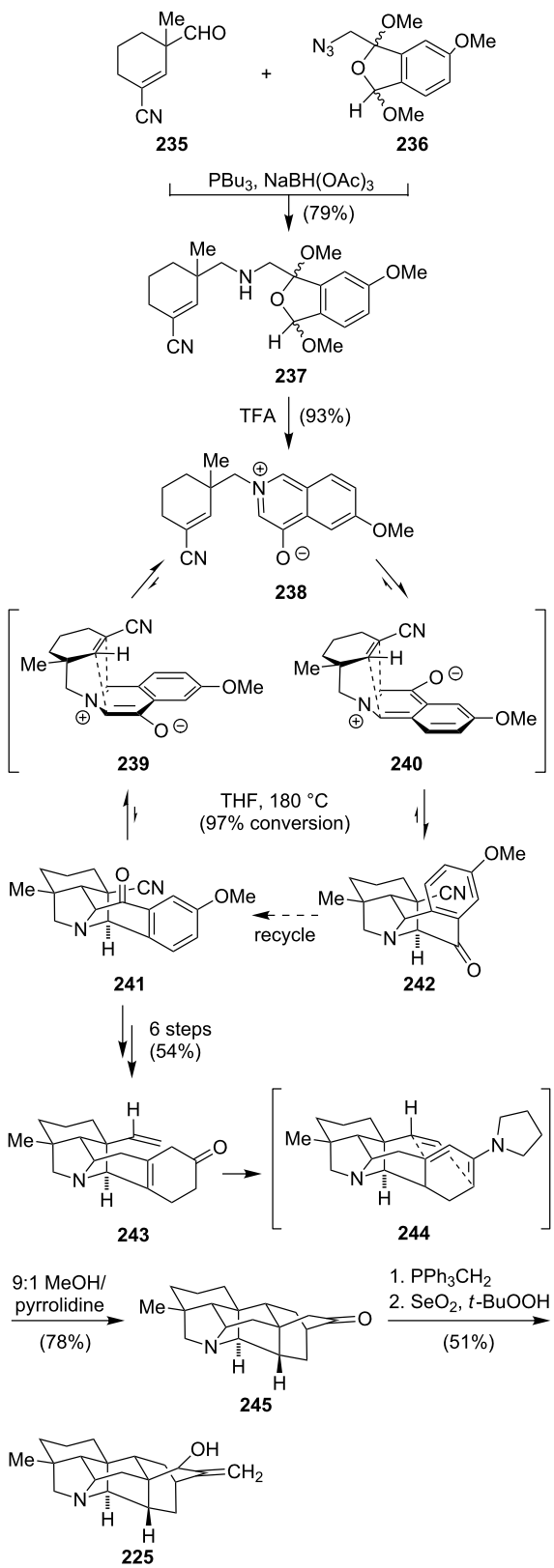


Figure 10: Hetisine alkaloids **225**–**228**.



Scheme 30: Biosynthetic proposal for the formation of the hetisine core [167].

seminal work, (±)-nominine (**225**) was synthesized within 40 steps and 0.15% overall yield. Two years later, a more concise and efficient access to (±)-nominine (**225**), featuring a oxidoisoquinolinium-1,3-dipolar cycloaddition and a dienamine-Diels–Alder reaction, was accomplished by Gin (Scheme 31) [178]. Coupling of **235** and **236**, both synthesized within three steps from simple starting materials, via a Staudinger–aza-Wittig reaction gave amine **237** as a mixture of four diastereoisomers. Conversion into 4-oxido-isoquinolinium betaine **238** could be achieved by an acid-catalyzed methanol extrusion and isomerization. Betaine **238** served as the substrate for the following 1,3-aza-dipolar cycloaddition. Carrying out the reaction at 180 °C in tetrahydrofuran provided a separable mixture of pyrrolidine isomers **241** and **242** (1:3.6). The undesired cycloadduct **242** could be equilibrated to **241** due to the reversibility of the reaction. Conversion to the β,γ-cyclohexenone **243**



Scheme 31: Synthesis of nominine (**225**).

was accomplished within 6 consecutive steps. Generation of the dienamine **244** with pyrrolidine in methanol at 60 °C triggered an intramolecular Diels–Alder reaction to provide the full carbon skeleton **245**. The final transformations of the synthesis involved a Wittig olefination of the ketone and a diastereoselective allylic oxidation to provide (±)-nominine (**225**). In 2008, the same group reported the first total synthesis of (+)-nominine by introducing the desired stereochemical information to the nitrile **235** [179].

Conclusion

The outlined syntheses of natural products containing the uncommon isoindole skeleton are still far away from being ideal. Low yielding multistep strategies dominate for more complex molecules and often cannot provide the amounts necessary for further investigations. Several biologically active members are still precluded from extensive biological studies due to their low abundance in nature. This and the fact, that many compounds are underexplored offers plenty opportunities for the development of innovative chemical transformations. The biosynthesis of many isoindole natural products is still uncertain and has yet to be unraveled. The presented examples could serve as an inspiration for the development of novel synthetic methods, new biosynthetic insights and drug development. Considerably more discoveries remain to be uncovered through exciting projects.

Acknowledgements

Support from the Fonds der Chemischen Industrie (Liebig-Stipendium to T.M.) and Prof. Dirk Trauner is gratefully acknowledged. We thank Prof. Wolfgang Steglich and Dr. David Woodmansee for helpful discussions. We acknowledge the many scientists whose important discoveries could not be included or referenced in this article.

References

1. Heugebaert, T. S. A.; Roman, B. I.; Stevens, C. V. *Chem. Soc. Rev.* **2012,** *41,* 5626–5640. doi:10.1039/c2cs35093a
2. Subbarayappa, A.; Patoliya, P. U. *Indian J. Chem., Sect. B: Org. Chem. Incl. Med. Chem.* **2009,** *48,* 545–552.
3. Belliotti, T. R.; Brink, W. A.; Kesten, S. R.; Rubin, J. R.; Wustrow, D. J.; Zoski, K. T.; Whetzel, S. Z.; Corbin, A. E.; Pugsley, T. A.; Heffner, T. G.; Wise, L. D. *Bioorg. Med. Chem. Lett.* **1998,** *8,* 1499–1502. doi:10.1016/S0960-894X(98)00252-2
4. Ball, M.; Boyd, A.; Churchill, G.; Cuthbert, M.; Drew, M.; Fielding, M.; Ford, G.; Frodsham, L.; Golden, M.; Leslie, K.; Lyons, S.; McKeever-Abbas, B.; Stark, A.; Tomlin, P.; Gottschling, S.; Hajar, A.; Jiang, J.-l.; Lo, J.; Suchozak, B. *Org. Process Res. Dev.* **2012,** *16,* 741–747. doi:10.1021/op300002f
5. Potowski, M.; Schürmann, M.; Preut, H.; Antonchick, A. P.; Waldmann, H. *Nat. Chem. Biol.* **2012,** *8,* 428–430. doi:10.1038/nchembio.901

6. Babichev, F. S.; Kovtunenko, V. A.; Tyltin, A. K. *Russ. Chem. Rev.* **1981,** *50,* 1087–1103. doi:10.1070/RC1981v050n11ABEH002738
7. Kovtunenko, V. A.; Voitenko, Z. V. *Russ. Chem. Rev.* **1994,** *63,* 997–1018. doi:10.1070/RC1994v063n12ABEH000131
8. Couture, A.; Grandclaudon, P. *Stud. Cercet. Stiint.: Chim. Ing. Chim., Biotehnol., Ind. Aliment. (Univ. Bacau)* **2010,** *11,* 11–44.
9. Armoiry, X.; Aulagner, G.; Facon, T. *J. Clin. Pharm. Ther.* **2008,** *33,* 219–226. doi:10.1111/j.1365-2710.2008.00920.x
10. Frincke, J. M.; Faulkner, D. J. *J. Am. Chem. Soc.* **1982,** *104,* 265–269. doi:10.1021/ja00365a048
11. Schubert-Zsilavecz, M.; Schramm, H. W. *Liebigs Ann. Chem.* **1991,** 973. doi:10.1002/jlac.1991199101168
12. Yu, C.; Xu, Y.; Jiao, L.; Zhou, J.; Wang, Z.; Hao, E. *Chem.–Eur. J.* **2012,** *18,* 6437–6442. doi:10.1002/chem.201200398
13. Maekawa, E.; Suzuki, Y.; Sugiyama, S. *Chem. Ber.* **1968,** *101,* 847–854. doi:10.1002/cber.19681010314
14. Riemschneider, R.; Hennig, K.; Wons, T. *Monatsh. Chem.* **1987,** *118,* 831–835. doi:10.1007/BF00809233
15. Médici, R.; de María, P. D.; Otten, L. G.; Straathof, A. J. J. *Adv. Synth. Catal.* **2011,** *353,* 2369–2376. doi:10.1002/adsc.201100386
16. Omura, S.; Iwai, Y.; Hirano, A.; Nakagawa, A.; Awaya, J.; Tsuchiya, H.; Takahashi, Y.; Asuma, R. *J. Antibiot.* **1977,** *30,* 275–282. doi:10.7164/antibiotics.30.275
17. Schmidt, A. W.; Reddy, K. R.; Knölker, H.-J. *Chem. Rev.* **2012,** *112,* 3193–3328. doi:10.1021/cr200447s
18. Tamaoki, T.; Nomoto, H.; Takahashi, I.; Kato, Y.; Morimoto, M.; Tomita, F. *Biochem. Biophys. Res. Commun.* **1986,** *135,* 397–402. doi:10.1016/0006-291X(86)90008-2
19. Prade, L.; Engh, R. A.; Girod, A.; Kinzel, V.; Huber, R.; Bossemeyer, D. *Structure* **1997,** *5,* 1627–1637. doi:10.1016/S0969-2126(97)00310-9
20. Hatzimichael, E.; Georgiou, G.; Benetatos, L.; Briasoulis, E. *Am. J. Blood Res.* **2013,** *3,* 29–51.
21. Yamashita, Y.; Fujii, N.; Murakata, C.; Ashizawa, T.; Okabe, M.; Nakano, H. *Biochemistry* **1992,** *31,* 12069–12075. doi:10.1021/bi00163a015
22. Nakano, H.; Omura, S. *J. Antibiot.* **2009,** *62,* 17–26. doi:10.1038/ja.2008.4
23. Pearce, C. J.; Doyle, T. W.; Forenza, S.; Lam, K. S.; Schroeder, D. R. *J. Nat. Prod.* **1988,** *51,* 937–940. doi:10.1021/np50059a020
24. Fröde, R.; Hinze, C.; Josten, I.; Schmidt, B.; Steffan, B.; Steglich, W. *Tetrahedron Lett.* **1994,** *35,* 1689–1690. doi:10.1016/0040-4039(94)88320-3
25. Hoshino, T.; Kojima, Y.; Hayashi, T.; Uchiyama, T.; Kaneko, K. *Biosci., Biotechnol., Biochem.* **1993,** *57,* 775–781. doi:10.1271/bbb.57.775
26. Sánchez, C.; Butovich, I. A.; Braña, A. F.; Rohr, J.; Méndez, C.; Salas, J. A. *Chem. Biol.* **2002,** *9,* 519–531. doi:10.1016/S1074-5521(02)00126-6
27. Onaka, H.; Taniguchi, S.; Igarashi, Y.; Furumai, T. *J. Antibiot.* **2002,** *55,* 1063–1071. doi:10.7164/antibiotics.55.1063
28. Onaka, H.; Taniguchi, S.; Igarashi, Y.; Furumai, T. *Biosci., Biotechnol., Biochem.* **2003,** *67,* 127–138. doi:10.1271/bbb.67.127
29. Howard-Jones, A. R.; Walsh, C. T. *J. Am. Chem. Soc.* **2006,** *128,* 12289–12298. doi:10.1021/ja063898m
30. Howard-Jones, A. R.; Walsh, C. T. *J. Am. Chem. Soc.* **2007,** *129,* 11016–11017. doi:10.1021/ja0743801
31. Sarstedt, B.; Winterfeldt, E. *Heterocycles* **1983,** *20,* 469–476. doi:10.3987/R-1983-03-0469
32. Hughes, I.; Nolan, W. P.; Raphael, R. A. *J. Chem. Soc., Perkin Trans. 1* **1990,** 2475–2480. doi:10.1039/P19900002475
33. Moody, C. J.; Rahimtoola, K. F. *J. Chem. Soc., Chem. Commun.* **1990,** 1667–1668. doi:10.1039/C39900001667
34. Moody, C. J.; Rahimtoola, K. F.; Porter, B.; Ross, B. C. *J. Org. Chem.* **1992,** *57,* 2105–2114. doi:10.1021/jo00033a036
35. Harris, W.; Hill, C. H.; Keech, E.; Malsher, P. *Tetrahedron Lett.* **1993,** *34,* 8361–8364. doi:10.1016/S0040-4039(00)61431-4
36. Link, J. T.; Raghavan, S.; Danishefsky, S. J. *J. Am. Chem. Soc.* **1995,** *117,* 552–553. doi:10.1021/ja00106a072
37. Wood, J. L.; Stoltz, B. M.; Goodman, S. N. *J. Am. Chem. Soc.* **1996,** *118,* 10656–10657. doi:10.1021/ja9626143
38. Wood, J. L.; Stoltz, B. M.; Dietrich, H.-J. *J. Am. Chem. Soc.* **1995,** *117,* 10413–10414. doi:10.1021/ja00146a039
39. Rothweiler, W.; Tamm, C. *Experientia* **1966,** *22,* 750–752. doi:10.1007/BF01901360
40. Rothweiler, W.; Tamm, C. *Helv. Chim. Acta* **1970,** *53,* 696–724. doi:10.1002/hlca.19700530404
41. Aldridge, D. C.; Armstrong, J. J.; Speake, R. N.; Turner, W. B. *Chem. Commun.* **1967,** 26–27. doi:10.1039/c19670000026
42. Aldridge, D. C.; Armstrong, J. J.; Speake, R. N.; Turner, W. B. *J. Chem. Soc. C* **1967,** 1667–1676. doi:10.1039/J39670001667
43. Zhang, D.; Ge, H.; Xie, D.; Chen, R.; Zou, J.-h.; Tao, X.; Dai, J. *Org. Lett.* **2013,** *15,* 1674–1677. doi:10.1021/ol400458n
44. Scherlach, K.; Boettger, D.; Remme, N.; Hertweck, C. *Nat. Prod. Rep.* **2010,** *27,* 869–886. doi:10.1039/b903913a
45. Sekita, S.; Yoshihira, K.; Natori, S.; Kuwano, H. *Chem. Pharm. Bull.* **1982,** *30,* 1618–1628. doi:10.1248/cpb.30.1618
46. Sekita, S.; Yoshihira, K.; Natori, S.; Kuwano, H. *Chem. Pharm. Bull.* **1982,** *30,* 1629–1638. doi:10.1248/cpb.30.1629
47. Zhou, G. X.; Wijeratne, E. M. K.; Bigelow, D.; Pierson, L. S.; VanEtten, H. D.; Gunatilaka, A. A. L. *J. Nat. Prod.* **2004,** *67,* 328–332. doi:10.1021/np030353m
48. Nukina, M. *Agric. Biol. Chem.* **1987,** *51,* 2625–2628. doi:10.1271/bbb1961.51.2625
49. Zhang, Y.; Tian, R.; Liu, S.; Chen, X.; Liu, X.; Che, Y. *Bioorg. Med. Chem.* **2008,** *16,* 2627–2634. doi:10.1016/j.bmc.2007.11.042
50. Zhang, Y.; Tian, R.; Liu, S.; Chen, X.; Liu, X.; Che, Y. *Bioorg. Med. Chem.* **2009,** *17,* 428. doi:10.1016/j.bmc.2007.11.084
51. Vederas, J. C.; Graf, W.; David, L.; Tamm, C. *Helv. Chim. Acta* **1975,** *58,* 1886–1898. doi:10.1002/hlca.19750580704
52. Vederas, J. C.; Tamm, C. *Helv. Chim. Acta* **1976,** *59,* 558–566. doi:10.1002/hlca.19760590221
53. Robert, J.-L.; Tamm, C. *Helv. Chim. Acta* **1975,** *58,* 2501–2504. doi:10.1002/hlca.19750580830
54. Probst, A.; Tamm, C. *Helv. Chim. Acta* **1981,** *64,* 2056–2064. doi:10.1002/hlca.19810640710
55. Hadener, A.; Roth, P.; Tamm, C. *Z. Naturforsch., C* **1989,** *44,* 19–32.
56. Schümann, J.; Hertweck, C. *J. Am. Chem. Soc.* **2007,** *129,* 9564–9565. doi:10.1021/ja072884t
57. Ishiuchi, K.; Nakazawa, T.; Yagishita, F.; Mino, T.; Noguchi, H.; Hotta, K.; Watanabe, K. *J. Am. Chem. Soc.* **2013,** *135,* 7371–7377. doi:10.1021/ja402828w
58. Bräse, S.; Encinas, A.; Keck, J.; Nising, C. F. *Chem. Rev.* **2009,** *109,* 3903–3990. doi:10.1021/cr050001f

59. Stork, G.; Nakamura, E. *J. Am. Chem. Soc.* **1983,** *105,* 5510–5512. doi:10.1021/ja00354a072
60. Dyke, H.; Sauter, R.; Steel, P.; Thomas, E. J. *J. Chem. Soc., Chem. Commun.* **1986,** 1447–1449. doi:10.1039/C39860001447
61. Thomas, E. J.; Whitehead, J. W. F. *J. Chem. Soc., Chem. Commun.* **1986,** 727–728. doi:10.1039/C39860000727
62. Merifield, E.; Thomas, E. J. *J. Chem. Soc., Chem. Commun.* **1990,** 464–466. doi:10.1039/C39900000464
63. Merifield, E.; Thomas, E. J. *J. Chem. Soc., Perkin Trans. 1* **1999,** 3269–3283. doi:10.1039/A906412E
64. Trost, B. M.; Ohmori, M.; Boyd, S. A.; Okawara, H.; Brickner, S. J. *J. Am. Chem. Soc.* **1989,** *111,* 8281–8284. doi:10.1021/ja00203a042
65. Vedejs, E.; Rodgers, J. D.; Wittenberger, S. J. *J. Am. Chem. Soc.* **1988,** *110,* 4822–4823. doi:10.1021/ja00222a047
66. Vedejs, E.; Wittenberger, S. J. *J. Am. Chem. Soc.* **1990,** *112,* 4357–4364. doi:10.1021/ja00167a037
67. Vedejs, E.; Reid, J. G.; Rodgers, J. D.; Wittenberger, S. J. *J. Am. Chem. Soc.* **1990,** *112,* 4351–4357. doi:10.1021/ja00167a036
68. Haidle, A. M.; Myers, A. G. *Proc. Natl. Acad. Sci. U. S. A.* **2004,** *101,* 12048–12053. doi:10.1073/pnas.0402111101
69. Dombrowski, A. W.; Bills, G. F.; Sabnis, G.; Koupal, L. R.; Meyer, R.; Ondeyka, J. G.; Giacobbe, R. A.; Monaghan, R. L.; Lingham, R. B. *J. Antibiot.* **1992,** *45,* 671–678. doi:10.7164/antibiotics.45.671
70. Ondeyka, J.; Hensens, O. D.; Zink, D.; Ball, R.; Lingham, R. B.; Bills, G.; Dombrowski, A.; Goetz, M. *J. Antibiot.* **1992,** *45,* 679–685. doi:10.7164/antibiotics.45.679
71. Lingham, R. B.; Hsu, A.; Silverman, K. C.; Bills, G. F.; Dombrowski, A.; Goldman, M. E.; Darke, P. L.; Huang, L.; Koch, G.; Ondeyka, J. G.; Goetz, M. A. *J. Antibiot.* **1992,** *45,* 686–691. doi:10.7164/antibiotics.45.686
72. Hungate, R. W.; Chen, J. L.; Starbuck, K. E.; Macaluso, S. A.; Rubino, R. S. *Tetrahedron Lett.* **1996,** *37,* 4113–4116. doi:10.1016/0040-4039(96)00778-2
73. Canham, S. M.; Overman, L. E.; Tanis, P. S. *Tetrahedron* **2011,** *67,* 9837–9843. doi:10.1016/j.tet.2011.09.079
74. Zhang, Y.; Wang, T.; Pei, Y.; Hua, H.; Feng, B. *J. Antibiot.* **2002,** *55,* 693–695. doi:10.7164/antibiotics.55.693
75. Moniot, J. L.; Hindenlang, D. M.; Shamma, M. *J. Org. Chem.* **1979,** *44,* 4347–4351. doi:10.1021/jo01338a022
76. Fajardo, V.; Elango, V.; Cassels, B. K.; Shamma, M. *Tetrahedron Lett.* **1982,** *23,* 39–42. doi:10.1016/S0040-4039(00)97526-9
77. Valencia, E.; Freyer, A. J.; Shamma, M.; Fajardo, V. *Tetrahedron Lett.* **1984,** *25,* 599–602. doi:10.1016/S0040-4039(00)99948-9
78. Valencia, E.; Weiss, I.; Firdous, S.; Freyer, A. J.; Shamma, M.; Urzús, A.; Fajardo, V. *Tetrahedron* **1984,** *40,* 3957–3962. doi:10.1016/0040-4020(84)85073-5
79. Valencia, E.; Fajardo, V.; Freyer, A. J.; Shamma, M. *Tetrahedron Lett.* **1985,** *26,* 993–996. doi:10.1016/S0040-4039(00)98494-6
80. Dewick, P. M. *Medicinal natural products: a biosynthetic approach,* 2nd ed.; Wiley: Chichester, 2002.
81. Leonard, M. S. *ARKIVOC* **2013,** *1,* 1–65.
82. Evans, P. A.; Holmes, A. B. *Tetrahedron* **1991,** *47,* 9131–9166. doi:10.1016/S0040-4020(01)96203-9
83. Bentley, K. W. *Nat. Prod. Rep.* **1997,** *14,* 387–411. doi:10.1039/np9971400387
84. Fang, F. G.; Feigelson, G. B.; Danishefsky, S. J. *Tetrahedron Lett.* **1989,** *30,* 2743–2746. doi:10.1016/S0040-4039(00)99114-7
85. Yoneda, R.; Sakamoto, Y.; Oketo, Y.; Harusawa, S.; Kurihara, T. *Tetrahedron* **1996,** *52,* 14563–14576. doi:10.1016/0040-4020(96)00900-3
86. Sano, T.; Toda, J.; Kashiwaba, N.; Ohshima, T.; Tsuda, Y. *Chem. Pharm. Bull.* **1987,** *35,* 479–500. doi:10.1248/cpb.35.479
87. Shamma, M.; Moniot, J. L. *Isoquinoline alkaloids research, 1972-1977;* Plenum Press: New York, 1978. doi:10.1007/978-1-4615-8819-1
88. Achari, B.; Chakrabarty, S.; Bandyopadyay, S.; Pakrashi, S. *Heterocycles* **1982,** *19,* 1203–1206. doi:10.3987/R-1982-07-1203
89. Mix, D. B.; Guinaudeau, H.; Shamma, M. *J. Nat. Prod.* **1982,** *45,* 657–666. doi:10.1021/np50024a001
90. Chia, Y.-C.; Chang, F.-R.; Teng, C.-M.; Wu, Y.-C. *J. Nat. Prod.* **2000,** *63,* 1160–1163. doi:10.1021/np000063v
91. Kim, J. K.; Kim, Y. H.; Nam, H. T.; Kim, B. T.; Heo, J.-N. *Org. Lett.* **2008,** *10,* 3543–3546. doi:10.1021/ol801291k
92. Kumar, V.; Poonam; Prasad, A. K.; Parmar, V. S. *Nat. Prod. Rep.* **2003,** *20,* 565–583. doi:10.1039/b303648k
93. Bentley, K. W. *Nat. Prod. Rep.* **2000,** *17,* 247–268. doi:10.1039/a900251k
94. Bentley, K. W. *Nat. Prod. Rep.* **2001,** *18,* 148–170. doi:10.1039/a909672h
95. Bentley, K. W. *Nat. Prod. Rep.* **2002,** *19,* 332–356. doi:10.1039/b009713f
96. Bentley, K. W. *The isoquinoline alkaloids;* Harwood Academic Pub.: Amsterdam, 1998.
97. Spenser, I. D.; Tiwari, H. P. *Chem. Commun.* **1966,** 55–56. doi:10.1039/c19660000055
98. Schütte, H. R.; Orban, U.; Mothes, K. *Eur. J. Biochem.* **1967,** *1,* 70–72. doi:10.1111/j.1432-1033.1967.tb00045.x
99. Comer, F.; Tiwari, H. P.; Spenser, I. D. *Can. J. Chem.* **1969,** *47,* 481–487. doi:10.1139/v69-070
100. Sharma, V.; Jain, S.; Bhakuni, D. S.; Kapil, R. S. *J. Chem. Soc., Perkin Trans. 1* **1982,** 1153–1155. doi:10.1039/P19820001153
101. Fugmann, B.; Steglich, W.; Lang-Fugmann, S.; Adam, G. *Roempp Encyclopedia Natural Products;* Thieme Medical Publishers: Stuttgart, 2000.
102. Arlt, V. M.; Stiborova, M.; Schmeiser, H. H. *Mutagenesis* **2002,** *17,* 265–277. doi:10.1093/mutage/17.4.265
103. Mei, N.; Arlt, V. M.; Phillips, D. H.; Heflich, R. H.; Chen, T. *Mutat. Res.* **2006,** *602,* 83–91. doi:10.1016/j.mrfmmm.2006.08.004
104. Zhang, Y.-N.; Zhong, X.-G.; Zheng, Z.-P.; Hu, X.-D.; Zuo, J.-P.; Hu, L.-H. *Bioorg. Med. Chem.* **2007,** *15,* 988–996. doi:10.1016/j.bmc.2006.10.034
105. Chen, Y.-C.; Chen, J.-J.; Chang, Y.-L.; Teng, C.-M.; Lin, W.-Y.; Wu, C.-C.; Chen, I.-S. *Planta Med.* **2004,** *70,* 174–177. doi:10.1055/s-2004-815497
106. Mata, R.; Morales, I.; Pérez, O.; Rivero-Cruz, I.; Acevedo, L.; Enriquez-Mendoza, I.; Bye, R.; Franzblau, S.; Timmermann, B. *J. Nat. Prod.* **2004,** *67,* 1961–1968. doi:10.1021/np0401260
107. Kim, S. R.; Sung, S. H.; Kang, S. Y.; Koo, K. A.; Kim, S. H.; Ma, C. J.; Lee, H.-S.; Park, M. J.; Kim, Y. C. *Planta Med.* **2004,** *70,* 391–396. doi:10.1055/s-2004-818964
108. Marti, G.; Eparvier, V.; Morleo, B.; Le Ven, J.; Apel, C.; Bodo, B.; Amand, S.; Dumontet, V.; Lozach, O.; Meijer, L.; Guéritte, F.; Litaudon, M. *Molecules* **2013,** *18,* 3018–3027. doi:10.3390/molecules18033018

109. Hegde, V. R.; Borges, S.; Pu, H.; Patel, M.; Gullo, V. P.; Wu, B.; Kirschmeier, P.; Williams, M. J.; Madison, V.; Fischmann, T.; Chan, T.-M. *Bioorg. Med. Chem. Lett.* **2010,** *20,* 1384–1387. doi:10.1016/j.bmcl.2010.01.007
110. Estévez, J. C.; Estévez, R. J.; Castedo, L. *Tetrahedron* **1995,** *51,* 10801–10810. doi:10.1016/0040-4020(95)00644-N
111. Couture, A.; Deniau, E.; Grandclaudon, P.; Hoarau, C. *J. Org. Chem.* **1998,** *63,* 3128–3132. doi:10.1021/jo972247t
112. Couture, A.; Deniau, E.; Grandclaudon, P.; Rybalko-Rosen, H.; Léonce, S.; Pfeiffer, B.; Renard, P. *Bioorg. Med. Chem. Lett.* **2002,** *12,* 3557–3559. doi:10.1016/S0960-894X(02)00794-1
113. Benesch, L.; Bury, P.; Guillaneux, D.; Houldsworth, S.; Wang, X.; Snieckus, V. *Tetrahedron Lett.* **1998,** *39,* 961–964. doi:10.1016/S0040-4039(97)10670-0
114. Boente, J. M.; Castedo, L.; Domínguez, D.; Fariña, A.; De Lera, A. R.; Villaverde, M. C. *Tetrahedron Lett.* **1984,** *25,* 889–892. doi:10.1016/S0040-4039(01)80054-X
115. Boente, J. M.; Castedo, L.; De Lera, A. R.; Saá, J. M.; Suau, R.; Vidal, M. C. *Tetrahedron Lett.* **1984,** *25,* 1829–1830. doi:10.1016/S0040-4039(01)90052-8
116. Tojo, E.; Dominguez, D.; Castedo, L. *Phytochemistry* **1991,** *30,* 1005–1010. doi:10.1016/0031-9422(91)85296-C
117. Manske, R. H. F. *Can. J. Res., Sect. B* **1938,** *16,* 81–90.
118. Manske, R. H. F. *J. Am. Chem. Soc.* **1950,** *72,* 55–59. doi:10.1021/ja01157a017
119. Bhacca, N. S.; Craig, J. C.; Manske, R. H. F.; Roy, S. K.; Shamma, M.; Slusarchyk, W. A. *Tetrahedron* **1966,** *22,* 1467–1475. doi:10.1016/S0040-4020(01)99444-X
120. Kametani, T.; Shibuya, S. *J. Chem. Soc.* **1965,** 5565–5566. doi:10.1039/jr9650005565
121. Campello, M. J.; Castedo, L.; Dominguez, D.; De Lera, A. R.; Saá, J. M.; Suau, R.; Tojo, E.; Vidal, M. C. *Tetrahedron Lett.* **1984,** *25,* 5933–5936. doi:10.1016/S0040-4039(01)81724-X
122. Suau, R.; Rico, R.; López-Romero, J. M.; Nájera, F.; Ruiz, A.; López, F. J. O. *ARKIVOC* **2002,** No. 5, 62–72. doi:10.3998/ark.5550190.0003.508
123. Blaschke, G.; Scriba, G. *Phytochemistry* **1985,** *25,* 111–113. doi:10.1016/S0031-9422(00)94512-6
124. Mueller, M. J.; Zenk, M. H. *Liebigs Ann. Chem.* **1993,** 557–563. doi:10.1002/jlac.199319930191
125. De Lera, A. R.; Suau, R.; Castedo, L. *J. Heterocycl. Chem.* **1987,** *24,* 313–319. doi:10.1002/jhet.5570240204
126. Lamas, C.; Castedo, L.; Dominguez, D. *Tetrahedron Lett.* **1990,** *31,* 6247–6248. doi:10.1016/S0040-4039(00)97036-9
127. Suau, R.; LópezRomero, J. M.; Rico, R. *Tetrahedron Lett.* **1996,** *37,* 9357–9360. doi:10.1016/S0040-4039(97)82963-2
128. Moreau, A.; Couture, A.; Deniau, E.; Grandclaudon, P. *J. Org. Chem.* **2004,** *69,* 4527–4530. doi:10.1021/jo049869g
129. Cornforth, J. W. *Chem. Br.* **1968,** *4,* 102–106.
130. Kamigauchi, T.; Fujiwara, T.; Tani, H.; Kawamura, Y.; Horibe, I. Sesquiterpene derivatives having antiviral activity. W.O. Patent 9711947 A1, April 3, 1997.
131. Jarvis, B. B.; Salemme, J.; Morals, A. *Nat. Toxins* **1995,** *3,* 10–16. doi:10.1002/nt.2620030104
132. Roggo, B. E.; Petersen, F.; Sills, M.; Roesel, J. L.; Moerker, T.; Peter, H. H. *J. Antibiot.* **1996,** *49,* 13–19. doi:10.7164/antibiotics.49.13
133. Xu, X.; De Guzman, F. S.; Gloer, J. B.; Shearer, C. A. *J. Org. Chem.* **1992,** *57,* 6700–6703. doi:10.1021/jo00051a006
134. Nozawa, Y.; Ito, M.; Sugawara, K.; Hanada, K.; Mizoue, K. *J. Antibiot.* **1997,** *50,* 641–645. doi:10.7164/antibiotics.50.641
135. Shinohara, C.; Hasumi, K.; Hatsumi, W.; Endo, A. *J. Antibiot.* **1996,** *49,* 961–966. doi:10.7164/antibiotics.49.961
136. Hinkley, S. F.; Fettinger, J. C.; Dudley, K.; Jarvis, B. B. *J. Antibiot.* **1999,** *52,* 988–997. doi:10.7164/antibiotics.52.988
137. Kawagishi, H.; Ando, M.; Mizuno, T. *Tetrahedron Lett.* **1990,** *31,* 373–376. doi:10.1016/S0040-4039(00)94558-1
138. Yaoita, Y.; Danbara, K.; Kikuchi, M. *Chem. Pharm. Bull.* **2005,** *53,* 1202–1203. doi:10.1248/cpb.53.1202
139. Scherlach, K.; Schuemann, J.; Dahse, H.-M.; Hertweck, C. *J. Antibiot.* **2010,** *63,* 375–377. doi:10.1038/ja.2010.46
140. Geris, R.; Simpson, T. J. *Nat. Prod. Rep.* **2009,** *26,* 1063–1094. doi:10.1039/b820413f
141. Minagawa, K.; Kouzuki, S.; Yoshimoto, J.; Kawamura, Y.; Tani, H.; Iwata, T.; Terui, Y.; Nakai, H.; Yagi, S.; Hattori, N.; Fujiwara, T.; Kamigauchi, T. *J. Antibiot.* **2002,** *55,* 155–164. doi:10.7164/antibiotics.55.155
142. Schroeckh, V.; Scherlach, K.; Nützmann, H. W.; Shelest, E.; Schmidt-Heck, W.; Schuemann, J.; Martin, K.; Hertweck, C.; Brakhage, A. A. *Proc. Natl. Acad. Sci. U. S. A.* **2009,** *106,* 14558–14563. doi:10.1073/pnas.0901870106
143. Kuan, K. K. W.; Pepper, H. P.; Bloch, W. M.; George, J. H. *Org. Lett.* **2012,** *14,* 4710–4713. doi:10.1021/ol301715u
144. Sakurai, J.; Kikuchi, T.; Takahashi, O.; Watanabe, K.; Katoh, T. *Eur. J. Org. Chem.* **2011,** 2948–2957. doi:10.1002/ejoc.201100173
145. Nakamura, M.; Ito, Y.; Ogawa, K.; Michisuji, Y.; Sato, S.; Takada, M.; Hayashi, M.; Yaginuma, S.; Yamamoto, S. *J. Antibiot.* **1995,** *48,* 1389–1395. doi:10.7164/antibiotics.48.1389
146. Kende, A. S.; Deng, W.-P.; Zhong, M.; Guo, X.-C. *Org. Lett.* **2003,** *5,* 1785–1788. doi:10.1021/ol030039j
147. Li, E.; Jiang, L.; Guo, L.; Zhang, H.; Che, Y. *Bioorg. Med. Chem.* **2008,** *16,* 7894–7899. doi:10.1016/j.bmc.2008.07.075
148. Cueto, M.; Jensen, P. R.; Kauffman, C.; Fenical, W.; Lobkovsky, E.; Clardy, J. *J. Nat. Prod.* **2001,** *64,* 1444–1446. doi:10.1021/np0102713
149. Slavov, N.; Cvengroš, J.; Neudörfl, J. M.; Schmalz, H.-G. *Angew. Chem., Int. Ed.* **2010,** *49,* 7588–7591. doi:10.1002/anie.201003755
150. Dalisay, D. S.; Morinaka, B. I.; Skepper, C. K.; Molinski, T. F. *J. Am. Chem. Soc.* **2009,** *131,* 7552–7553. doi:10.1021/ja9024929
151. Flores, B.; Molinski, T. F. *Org. Lett.* **2011,** *13,* 3932–3935. doi:10.1021/ol201461n
152. West, L. M.; Northcote, P. T.; Battershill, C. N. *J. Org. Chem.* **2000,** *65,* 445–449. doi:10.1021/jo991296y
153. Bai, R. L.; Paull, K. D.; Herald, C. L.; Malspeis, L.; Pettit, G. R.; Hamel, E. *J. Biol. Chem.* **1991,** *266,* 15882–15889.
154. Xiao, Q.; Young, K.; Zakarian, A. *Org. Lett.* **2013,** *15,* 3314–3317. doi:10.1021/ol401354a
155. Alvarez-Mico, X.; Jensen, P. R.; Fenical, W.; Hughes, C. C. *Org. Lett.* **2013,** *15,* 988–991. doi:10.1021/ol303374e
156. Hughes, C. C.; Prieto-Davo, A.; Jensen, P. R.; Fenical, W. *Org. Lett.* **2008,** *10,* 629–631. doi:10.1021/ol702952n
157. Matsumoto, N.; Tsuchida, T.; Maruyama, M.; Sawa, R.; Kinoshita, N.; Homma, Y.; Takahashi, Y.; Iinuma, H.; Naganawa, H.; Sawa, T.; Hamada, M.; Takeuchi, T. *J. Antibiot.* **1996,** *49,* 953–954. doi:10.7164/antibiotics.49.953
158. Höltzel, A.; Dieter, A.; Schmid, D. G.; Brown, R.; Goodfellow, M.; Beil, W.; Jung, G.; Fiedler, H.-P. *J. Antibiot.* **2003,** *56,* 1058–1061. doi:10.7164/antibiotics.56.1058
159. Zhang, X.; Alemany, L. B.; Fiedler, H.-P.; Goodfellow, M.; Parry, R. J. *Antimicrob. Agents Chemother.* **2008,** *52,* 574–585. doi:10.1128/AAC.00717-07

160. Moore, B. S.; Hertweck, C. *Nat. Prod. Rep.* **2002,** *19,* 70–99. doi:10.1039/b003939j
161. Adachi, S.; Watanabe, K.; Iwata, Y.; Kameda, S.; Miyaoka, Y.; Onozuka, M.; Mitsui, R.; Saikawa, Y.; Nakata, M. *Angew. Chem., Int. Ed.* **2013,** *52,* 2087–2091. doi:10.1002/anie.201209205
162. Cox, C. D.; Siu, T.; Danishefsky, S. J. *Angew. Chem., Int. Ed.* **2003,** *42,* 5625–5629. doi:10.1002/anie.200352591
163. Siu, T.; Cox, C. D.; Danishefsky, S. J. *Angew. Chem., Int. Ed.* **2003,** *42,* 5629–5634. doi:10.1002/anie.200352592
164. Tatsuta, K.; Tanaka, H.; Tsukagoshi, H.; Kashima, T.; Hosokawa, S. *Tetrahedron Lett.* **2010,** *51,* 5546–5549. doi:10.1016/j.tetlet.2010.08.035
165. Watanabe, K.; Iwata, Y.; Adachi, S.; Nishikawa, T.; Yoshida, Y.; Kameda, S.; Ide, M.; Saikawa, Y.; Nakata, M. *J. Org. Chem.* **2010,** *75,* 5573–5579. doi:10.1021/jo100913s
166. Kato, K.; Sasaki, T.; Takayama, H.; Akita, H. *Tetrahedron* **2003,** *59,* 2679–2685. doi:10.1016/S0040-4020(03)00300-4
167. Wang, F.-P.; Liang, X.-T. C20-diterpenoid alkaloids. *The Alkaloids. Chemistry and Biology;* Academic Press, 2002; Vol. 59, pp 1–280. doi:10.1016/S0099-9598(02)59008-8
168. Wang, F.-P.; Chen, Q.-H.; Liu, X.-Y. *Nat. Prod. Rep.* **2010,** *27,* 529–570. doi:10.1039/b916679c
169. Ochiai, E.; Okamoto, T.; Sakai, S.-i.; Saito, A. *Yakugaku Zasshi* **1956,** *76,* 1414–1418.
170. Sakai, S.; Yamamoto, I.; Yamaguchi, K.; Takayama, H.; Ito, M.; Okamoto, T. *Chem. Pharm. Bull.* **1982,** *30,* 4579–4582. doi:10.1248/cpb.30.4579
171. Jacobs, W. A.; Craig, L. C. *J. Biol. Chem.* **1942,** *143,* 605–609.
172. Przybylska, M. *Can. J. Chem.* **1962,** *40,* 566–568. doi:10.1139/v62-087
173. Suginome, H.; Kakimoto, S.; Sonoda, J.; Noguchi, S. *Proc. Jpn. Acad.* **1946,** *22,* 122.
174. Pelletier, S. W.; Wright, L. H.; Newton, M. G.; Wright, H. *J. Chem. Soc. D* **1970,** 98–99. doi:10.1039/c29700000098
175. Suginome, H.; Shimanouti, F. *Justus Liebigs Ann. Chem.* **1940,** *545,* 220–228. doi:10.1002/jlac.19405450121
176. Okamoto, T. *Chem. Pharm. Bull.* **1959,** *7,* 44–49. doi:10.1248/cpb.7.44
177. Muratake, H.; Natsume, M. *Angew. Chem., Int. Ed.* **2004,** *43,* 4646–4649. doi:10.1002/anie.200460332
178. Peese, K. M.; Gin, D. Y. *J. Am. Chem. Soc.* **2006,** *128,* 8734–8735. doi:10.1021/ja0625430
179. Peese, K. M.; Gin, D. Y. *Chem.–Eur. J.* **2008,** *14,* 1654–1665. doi:10.1002/chem.200701290

License and Terms

This is an Open Access article under the terms of the Creative Commons Attribution License (http://creativecommons.org/licenses/by/2.0), which permits unrestricted use, distribution, and reproduction in any medium, provided the original work is properly cited.

The license is subject to the *Beilstein Journal of Organic Chemistry* terms and conditions: (http://www.beilstein-journals.org/bjoc)

The definitive version of this article is the electronic one which can be found at: doi:10.3762/bjoc.9.243

Beilstein Journal of Organic Chemistry

Flexible synthesis of anthracycline aglycone mimics via domino carbopalladation reactions

Markus Leibeling and Daniel B. Werz*

Full Research Paper

Open Access

Address:
Institut für Organische Chemie, Technische Universität Braunschweig, Hagenring 30, 38106 Braunschweig, Germany

Email:
Daniel B. Werz* - d.werz@tu-braunschweig.de

* Corresponding author

Keywords:
anthracyclines; carbohydrates; carbopalladation; catalysis; domino reaction; natural products

Beilstein J. Org. Chem. **2013,** *9,* 2194–2201.
doi:10.3762/bjoc.9.258

Received: 28 August 2013
Accepted: 08 October 2013
Published: 24 October 2013

This article is part of the Thematic Series "Natural products in synthesis and biosynthesis".

Guest Editor: J. S. Dickschat

© 2013 Leibeling and Werz; licensee Beilstein-Institut.
License and terms: see end of document.

Abstract

A synthesis of anthracycline aglycone derivatives is described. The key step utilizes a powerful domino carbopalladation approach and subsequent ring closure. During this process two of the four rings of the anthracycline scaffold are formed. Differently substituted carbohydrates and dialkyne chains serve as versatile and simple starting materials for the reaction sequence. Diverse building blocks lead to a variety of different products and a broad range of structural diversity.

Introduction

Anthracyclines are a widespread class of natural products which belong to the group of aromatic polyketides [1]. Most of them have been isolated from bacteria of the order *Streptomycetales*. The group of Brockmann, who first found anthracyclines in 1963, described them as red to orange dyes [2]. Their structure elucidation revealed a linear fourfold annulated ring system including two benzene units (A-ring and C-ring). The substitution pattern of the D-ring bares most of the functionalities, i.e., a secondary and a tertiary alcohol, the former of which is commonly glycosylated with 2,6-dideoxy sugars (Figure 1) [3]. These carbohydrates are of highest importance for the biological activity of anthracyclines and bind to the minor groove of double-stranded DNA [4,5]. While the mode of action of anthracyclines is still not fully understood, it is widely accepted that these chemotherapeutic agents form a ternary complex with double-stranded DNA and topoisomerase II thereby leading to DNA damage and cell death [6,7]. They are used to treat different types of diseases such as leukemias, lymphomas, breast, uterine, ovarian and lung cancers [8].

Thus, many research groups faced the challenge of investigating suitable pathways for the synthesis of diverse anthracycline natural products and mimics thereof. Because of the inherent lack of efficient synthetic approaches to anthracyclines

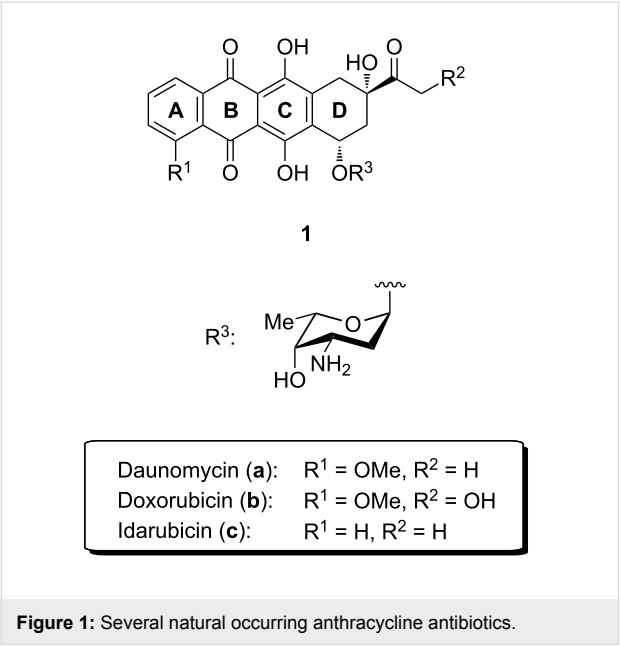
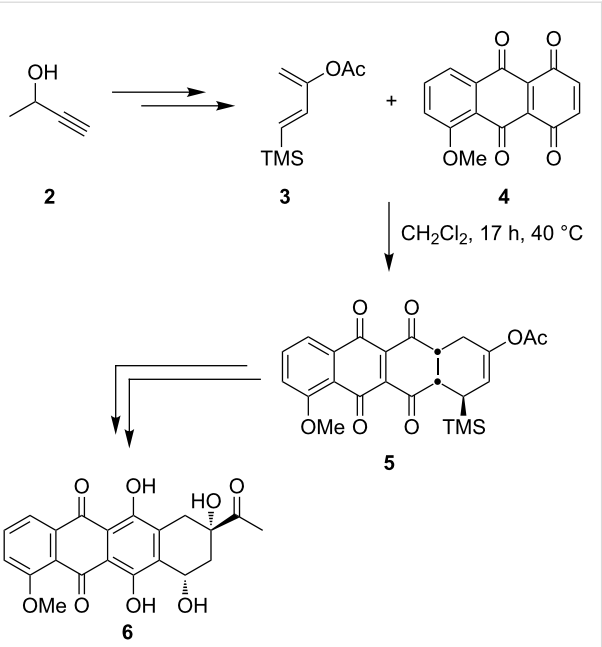


Figure 1: Several natural occurring anthracycline antibiotics.

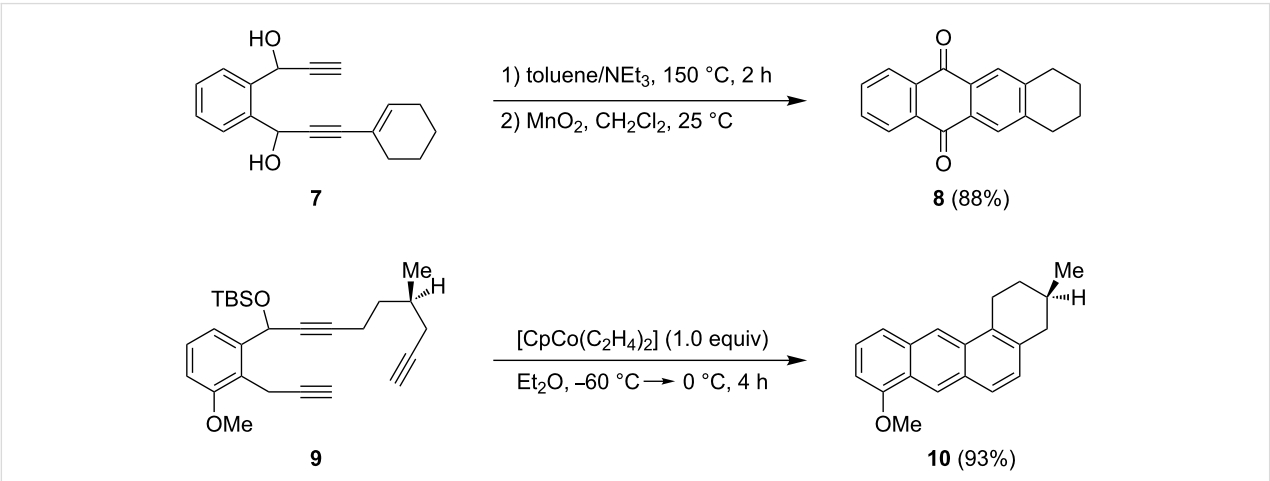


Scheme 1: Total synthesis of daunomycinone **6** according to Hansen.

many industrial approaches still rely on the use of recombinant microorganisms with a mutated gene of the anthracycline metabolism [9].

Different convenient synthetic transformations involve the application of a Diels–Alder reaction as key step for the aspired synthesis [10-13]. A classical synthesis was published in 1988 by Hansen where a silyl-substituted diene **3** was used for the [4 + 2]-cycloaddition (Scheme 1) [14]. Starting from bisquinone **4** the annulated ring system **5** is obtained in a 1:1 mixture of *cis-endo* regioisomers. Subsequent aromatization of the C-ring and several additional steps generated the daunomycin aglycon **6** and the corresponding isodaunomycin aglycone (dependent on the regioisomers) in a total of 16 steps.

In 2003, Saá published a concise route to anthraquinone derivatives by using an intramolecular dehydro-Diels–Alder reaction of an aryldiacetylene system (Scheme 2) [15]. Compound **7** reacts at high temperature in a mixture consisting of toluene and triethylamine to an inseparable mixture of cyclized diol (52%) and quinone **8** (36%). Quantitative oxidation of the diol by MnO_2 provided the desired tetracycle **8** in 88% overall yield (over two steps). Another approach to non-linear systems utilizes a cobalt-mediated intramolecular [2 + 2 + 2]-cycloaddition of a triyne system **9** leading to the fourfold annulated ring system **10** in only one step [16]. Late stage functionalization led to the anticipated structural motif in a few additional steps.



Scheme 2: Synthesis of simplified anthracycline derivatives.

Results and Discussion

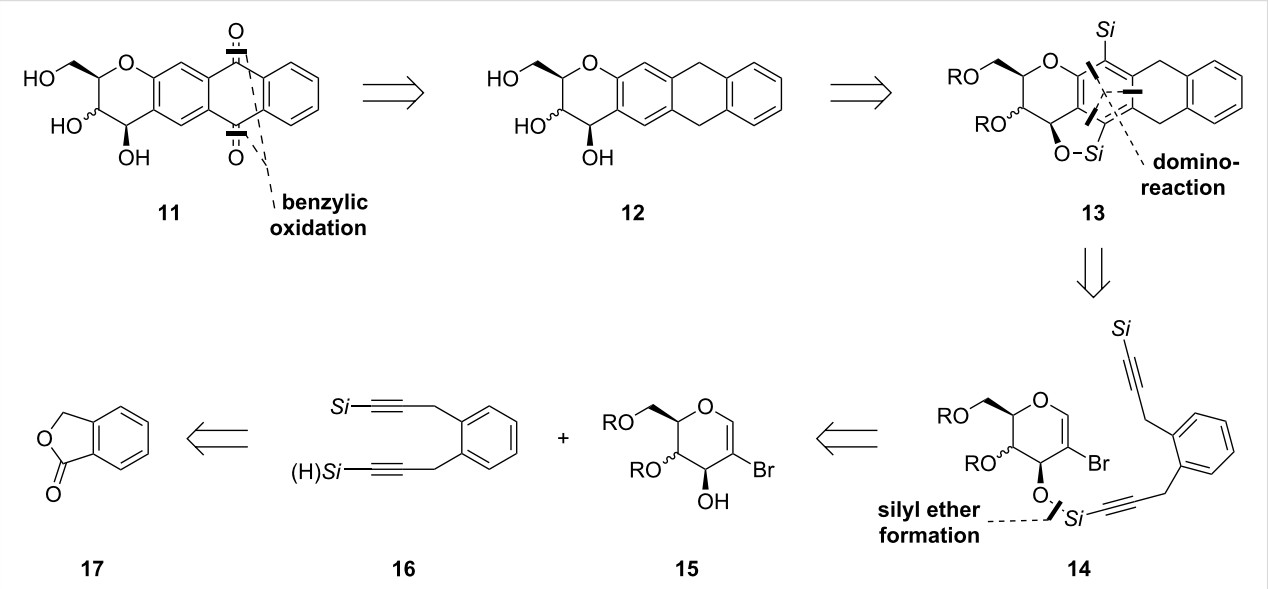
Retrosynthetic strategy

After having established several methods of domino carbopalladation reactions which employ dialkynyl-substituted bromoglycals [17-20] or bromoarenes [21], we envisioned to apply a similar procedure for the preparation of anthracycline derivatives. Therefore, the D-ring was exchanged for a pyranose, as described in our previous synthetic approaches for the syntheses of chromans, isochromans and biphenyls, respectively. These 2-bromoglycals **15** are well-known compounds and their synthesis was accomplished according to literature-known procedures [17,18]. The dialkyne unit provides both the A-ring and the information for the formation of the B and C-ring within the palladium-catalyzed domino transformation [22-27]. Such an approach should allow an easy differentiation between all four annulated cycles and their possible modification, whereupon the main focus was the preparation of several D-ring derivatives.

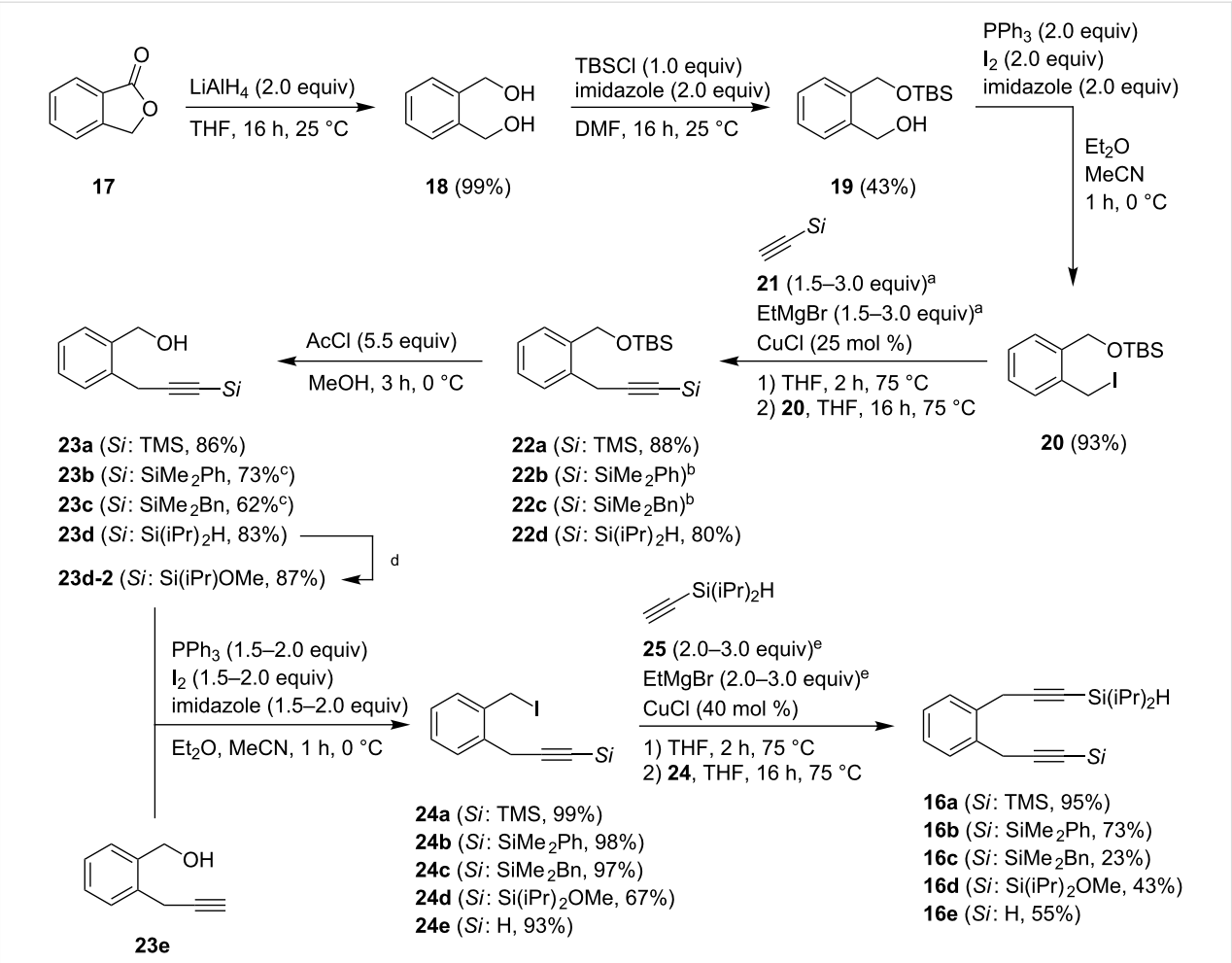
The anthraquinone moiety **11** should be formed within the last steps of the synthetic approach by benzylic oxidation of compound **12** (Scheme 3). The terminal silyl group and the silyl ether should be removed by using hydrolysis and fluoride-mediated desilylation, respectively. It was assumed that the multiple carbopalladation/cyclization sequence should give access to the fourfold-annulated ring system **13** in a single step. However, we knew that the domino process works much better in an intra- than in an intermolecular fashion [19]. Thus, we decided to employ a silyl ether moiety to connect both subunits **15** and **16**. As the terminus of the other alkyne unit we also chose a silyl group. Depending on the kind of the silyl group a variety of further functionalization might be envisioned. Respective silyl-substituted diynes **16** can be traced back to phthalide (**17**). To differentiate between the insertion of two differently substituted silylacetylenes, the lactone **17** had to be first converted into a monoprotected diol for further transformations.

Synthesis of dialkyne building blocks

The choice of the right diyne is crucial for a successful synthesis of the target compound. Preliminary investigations had shown that both dialkynes with benzylic hydroxy functionalities and 1,2-bis(2-propynyl)benzene did not yield viable results in the domino reaction. The selective installation of only one silyl group at a dialkyne with two terminal acetylene moieties presented difficulties. Thus, we sought for a consecutive introduction of the corresponding silylacetylene functionalities. An appropriate starting material was selected to achieve a highly convergent and convenient synthetic strategy. We started our investigation with the reduction of commercially available phthalide (**17**) by $LiAlH_4$ into dialcohol **18** in quantitative yield [28] (Scheme 4). The polar compound was easily converted into the mono-TBS-protected substrate by utilization of 1 equivalent of TBSCl [29]. Column chromatography afforded three fractions consisting of the starting material, the monoprotected and the diprotected product. The remaining alcohol moiety of compound **19** was converted into the respective iodide **20** by a Mukaiyama redox-condensation using elemental iodine, triphenylphosphine and imidazole [30]. The installation of a suitable leaving group sets the stage for the introduction of the first silylacetylene. Four different terminal alkynes **21** (**a**: *Si* = TMS; **b**: *Si* = $SiMe_2Ph$; **c**: *Si* = $SiMe_2Bn$; **d**: *Si* = $Si(iPr)_2H$) were employed. Best results with yields of over 80% were obtained by the use of acetylene **21a**, ethylmagnesium bromide, and



Scheme 3: Retrosynthetic analysis of anthracycline aglycone mimics. *Si*: any silyl group.



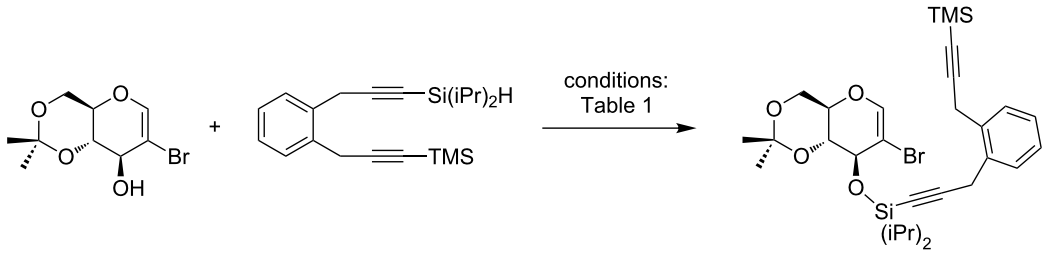
Scheme 4: Synthetic route for the synthesis of various dialkynes **16**. [a]*Si*: TMS, $SiMe_2Bn$ (2.0 equiv); *Si*: $SiMe_2Ph$ (1.5 eq equiv); $Si(iPr)_2H$ (3.0 equiv). [b]Products for *Si*: $SiMe_2Ph$ and $SiMe_2Bn$ could not be isolated. [c]Yield: over two steps. [d]Conditions: Br_2 (1.0 equiv), MeOH, 0.5 h, 0 °C, NEt_3 (2.0 equiv), CCl_4, MeOH, 1 h, 0 °C. [e]*Si*: TMS, Si(iPr)OMe, H (3.0 equiv of **25**); *Si*: $SiMe_2Ph$, $SiMe_2Bn$ (2.0 equiv of **25**).

copper chloride in tetrahydrofuran for one hour at 75 °C, successive addition of iodide **20** in THF at room temperature and additional 16 h under reflux [31]. Products **22b** and **22c** could not be isolated in pure form due to small impurities. The deprotection of the silyl ethers proceeded smoothly with high yields ranging from 62% to 86% over two steps [32]. Silane **23d** was converted into the corresponding silyl bromide and trapped with methanol to install an electron-deficient substituent at the silane moiety **23d-2**. The synthesis of **23e** was accomplished according to a literature-known procedure starting from isochromanone and trimethylsilyl-diazomethane [33]. The initially formed alcohols **23** were again converted into the respective iodides **24** as described before and subsequently substituted with diisopropylsilylacetylene **25** [34] providing five different dialkynes **16**, each of them with a terminal silyl substituent (or terminal hydrogen) at one side and a silane moiety at the other (Scheme 4). It is possible to access differently substituted dialkynes **16** by the silylation of **16e**. This approach was not considered because of the low tolerance of **16e** against base and the expensive starting materials for the synthesis of **23e**.

Silyl ether formation and domino reaction

The union between both building blocks proved to be more difficult than originally envisioned. During our previous studies of chromans and isochromans the implementation of ether linkages afforded good results. The synthesis of anthracycline derivatives requires a more labile connection to circumvent the formation of an additional cycle at the annulated ring system. Previous investigations revealed that silyl ether formations could be accomplished by the transformation of the silane into the corresponding silyl bromide by using NBS [35]. This highly reactive species should be easily trapped by the hydroxy functionality of the respective 2-bromoglycal. Therefore, we chose **15a** and **16a** as model substrates to explore suitable reaction conditions for the silyl ether formation. Table 1 reveals that of

Table 1: Optimization study for the silyl ether formation.



15a **16a** **14a**

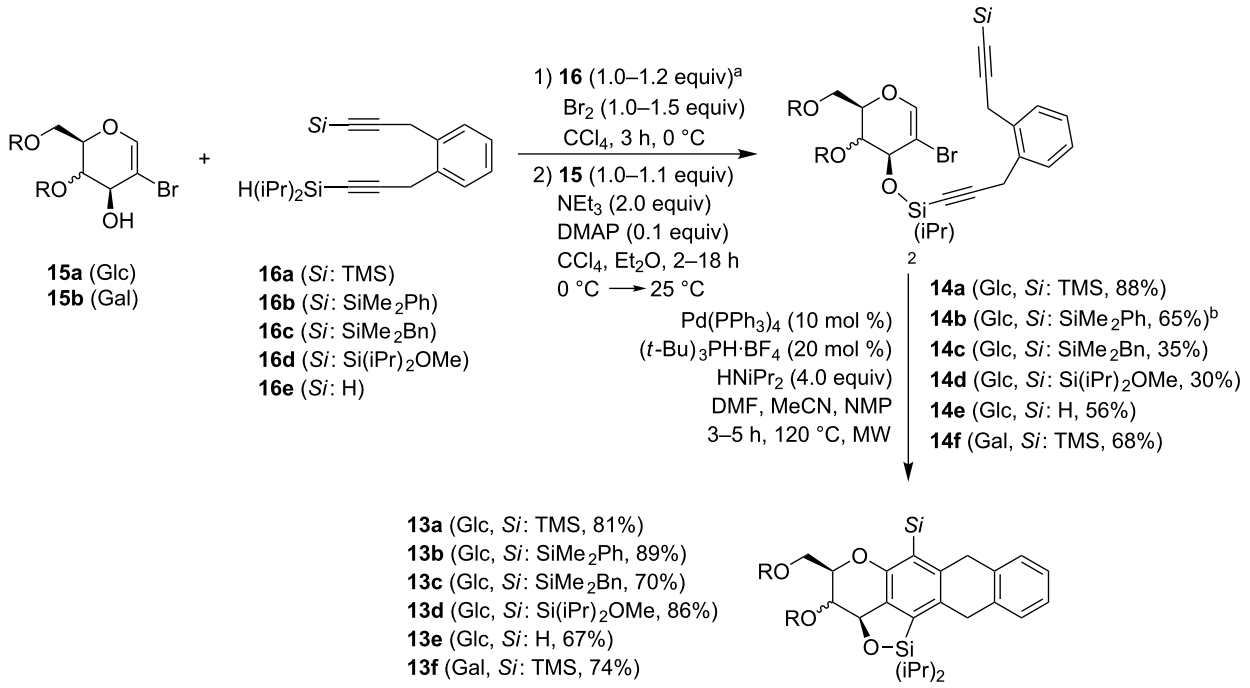
entry	conditions[a]	yield [%]
1	1) **15a** (1.1 equiv), NBS (1.1 equiv). 2) **16a** (1.0 equiv), NEt_3 (2.0 equiv), CH_2Cl_2	23
2	1) **15a** (1.1 equiv), NCS (1.1 equiv). 2) **16a** (1.0 equiv), NEt_3 (2.0 equiv), CH_2Cl_2	12
3	1) **15a** (1.1 equiv), NIS (1.1 equiv). 2) **16a** (1.0 equiv), NEt_3 (2.0 equiv), CH_2Cl_2	–
4	1) **15a** (1.1 equiv), Br_2 (1.1 equiv). 2) **16a** (1.0 equiv), NEt_3 (2.0 equiv), CH_2Cl_2	27
5	1) **15a** (1.0 equiv), Br_2 (1.1 equiv). 2) **16a** (1.0 equiv), NEt_3 (1.3 equiv), Et_2O	42[b]
6	1) **15a** (1.1 equiv), Br_2 (1.1 equiv). 2) **16a** (1.0 equiv), NEt_3 (1.1 equiv), THF	–
7	1) **15a** (1.3 equiv), Br_2 (1.4 equiv). 2) **16a** (1.0 equiv), NEt_3 (1.3 equiv), Et_2O	36
8	1) **15a** (1.0 equiv), Br_2 (1.0 equiv). 2) **16a** (1.0 equiv), NEt_3 (2.0 equiv), Et_2O	25
9	1) **15a** (1.0 equiv), Br_2 (1.0 equiv). 2) **16a** (1.0 equiv), NEt_3 (2.0 equiv), CCl_4	75
10	1) **15a** (1.2 equiv), Br_2 (1.2 equiv), CCl_4. 2) **16a** (1.0 equiv), NEt_3 (2.0 equiv), CCl_4/Et_2O (4:1)	88

[a]First reaction: Br_2 (1 M in CCl_4), 1 h, 0 °C. Second reaction: DMAP (0.1 equiv), 2 h, 0 °C → 25 °C. [b]65% were obtained once for a small scale reaction.

the halogenated succinimides only NCS and NBS are able to convert the silane into a reactive species. However, the yields were low in all cases. Changing the bromination reagent to elemental bromine significantly improved the yields (Table 1, entries 4 and 5) [36]. Diethyl ether proved to be important as a solvent, the change to THF led to a total decomposition – most probably due to ring-opening reactions with bromosilanes [37]. Further, we investigated the influence of the amount of bromine on the reaction and concluded that stoichiometric quantities entirely fulfill the demands of the bromination (Table 1, entries 7 and 8). Finally, we found that the silyl bromide formation proceeded better in tetrachloromethane. However, to assure solubility of the glycals, small amounts of diethyl ether were added for the coupling step (Table 1, entries 8–10). In all cases, a very slow addition of bromine and bromosilane proved to be necessary to ensure optimal yields.

With optimized conditions in hand we explored the scope of the silyl ether coupling. Therefore, two different glycals and five different dialkynes were employed. In summary, seven different coupling products **14** were prepared baring alkynes with terminal H, TMS, $SiMe_2Ph$, $SiMe_2Bn$ and $Si(iPr)_2OMe$ groups (Scheme 5). The best results were obtained with TMS-substituents. Although the $SiMe_2Ph$-substituted product was not synthesized under optimal reaction conditions the desired product was formed in high yield. In addition, terminal alkynes were tolerated in the reaction. Contrary, benzyl and methoxide-substituted silanes **14c** and **14d** provided inferior yields.

With several domino precursors in hand we started the investigation of the domino-carbopalladation sequence. To our delight, it was possible to adjust the catalytic system that we developed for the synthesis of chromans and isochromans. Optimal reaction conditions comprise the use of $Pd(PPh_3)_4$ as a palladium source, $(t\text{-}Bu)_3PH{\cdot}BF_4$ (Fu's salt) [38] as an additional electron-rich and sterically encumbered ligand and $HN(iPr)_2$ as a base. As solvent a mixture consisting of *N*,*N*-dimethylformamide, acetonitrile and *N*-methylpyrrolidone (8:8:1) was used. The reaction was performed in a sealed vial at 120 °C under microwave irradiation for 3–5 h. The unusual combination of $Pd(PPh_3)_4$ and $(t\text{-}Bu)_3PH{\cdot}BF_4$ as an additional ligand proved beneficial for the transformation of long-chained dialkynes. The domino reaction proceeded smoothly and delivered the desired compounds as major products. Scheme 5 illustrates that all attached substituents at the terminal triple bond were tolerated. Even unsubstituted alkyne **14e** and electron-deficient silane **14d** furnished the product in high yields. TMS, $SiMe_2Ph$ and $Si(iPr)_2OMe$-substituted silanes delivered the best results with yields of up to 89%. For the reaction mechanism we assume that the palladium(0) inserts into the $C(sp^2)$–Br bond to form a



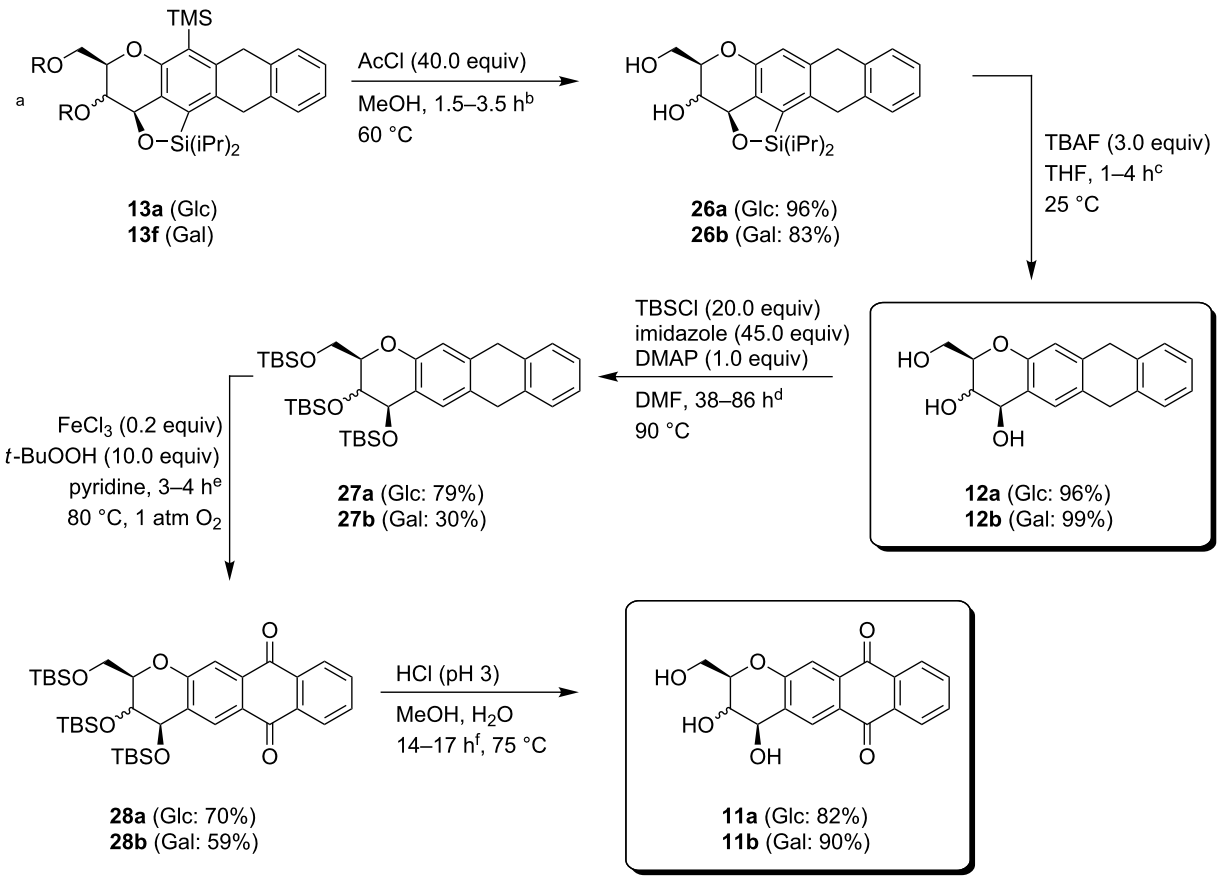
Scheme 5: Silyl ether synthesis and domino carbopalladation reaction. *R*,*R* (Glc): isopropylidene. *R*,*R* (Gal): benzylidene. [a]The respective equivalents of alkynes **16**, glycals **15** and bromine as well as reaction times are given in the Experimental. [b]The reaction was performed according to entry 5 of Table 1.

Pd(II) species. A sequence of two carbopalladation reactions form a triene system which is able to cyclize by a Heck-type reaction, a 6π-electrocyclization [39] or a direct CH-activation to the respective anthracycline precursor **13**. The design of the dialkyne provides a simultaneous formation of the linear ring system. All four cycles were annulated in a single step, in which the B and C-ring were formed as a consequence of the reaction cascade.

Derivatization to anthracycline derivatives

The derivatization of the domino products turned out to be challenging. Utilization of a fluoride source (e.g. tetrabutylammonium fluoride or tetramethylammonium fluoride) and **13a** lead to total decomposition of the starting materials. Application of Tamao–Fleming-like oxidative procedures provided only the mono-oxidized products in trace amounts [40-42]. The oxidation of phenyl-substituted silanes to respective phenols is difficult [43,44]. However, literature precedence revealed that benzyl-substituted silane **13c** or electron-deficient silane **13d** [43,45] should be more promising candidates. But none of these domino products **13b**–**13f** provided better results in a Tamao–Fleming reaction. When oxidizing reaction conditions were applied to silane **13b,** only desilylation of the cyclic silyl ether occurred. Interestingly, benzylsilane **13c** afforded the globally desilylated product in 90% yield under oxidative reaction conditions ($KHCO_3$, H_2O_2, KF in THF and MeOH), i.e., both silyl ether and terminal silane were cleaved. However, it was not possible to utilize this procedure for compound **13a**. Under these conditions, the silyl ether was cleaved without touching the trimethylsilyl moiety. Another approach of selective silyl ether cleavage was employed by utilization of Cs_2CO_3 (5.0 equiv) in methanol at 100 °C.

Hydrolysis of the respective domino products **13a** and **13f** with in situ formed HCl in methanol furnished the diols **26a** and **26b** under loss of the terminal TMS group [46]. Opening of the silyl ether moiety was accomplished by treatment with TBAF in quantitative yield and gained access to the natural substitution pattern of the carbohydrate backbone. It was not possible to open the silyl ether moiety of **26** by the utilization of Cs_2CO_3 in methanol starting from **13** as described before. To install the anthraquinone moiety it was necessary to reprotect the alcohol functionalities. It has proven challenging to install the TBS protecting group at the substrates, particular for the galactose-derived derivatives **12b** which could be obtained in only poor yield [47-49]. For **27a** the $FeCl_3$-catalyzed benzylic oxidation proceeded smoothly with yields of up to 70% [50]. A final hydrolysis with hydrochloric acid afforded the desired carbohydrate-based anthracycline derivatives **11** in good yield (Scheme 6).



Scheme 6: Derivatisation of anthracycline derivatives. [a]*R*,*R* (Glc): isopropylidene. *R*,*R* (Gal): benzylidene. Reactions times: [b]1.5 h (Glc), 3.5 h (Gal). [c]1.0 h (Glc), 4.0 h (Gal). [d]38 h (Glc), 86 h (Gal). [e]4.0 h (Glc), 3.0 h (Gal). [f]14 h (Glc), 17 h (Gal).

Conclusion

In conclusion, we have developed a concise and robust approach to anthracycline aglycone derivatives. Starting materials were bromoglycals and benzene moieties with two propynyl residues. The first key step is the union of these moieties by a silyl ether linkage. In a second key step the tetracyclic anthracycline scaffold is formed by a domino carbopalladation sequence generating both, the B and the C-ring of the system in a single step. Further derivatisation included the cleavage of the silyl ether and two-fold benzylic oxidation to the quinone moiety. We believe that these natural product mimics might be of interest as useful candidates for drug discovery research.

Supporting Information

Supporting Information File 1

Experimental details and analytical data of all new compounds as well as their ^{1}H and ^{13}C NMR spectra.
[http://www.beilstein-journals.org/bjoc/content/supplementary/1860-5397-9-258-S1.pdf]

Acknowledgements

We are grateful to the Deutsche Forschungsgemeinschaft (DFG) and the Fonds der Chemischen Industrie (FCI) for financial support (Emmy Noether and Heisenberg Fellowships as well as Dozentenstipendium to D.B.W.). M.L. thanks the State of Lower Saxony for his Ph.D. Lichtenberg Fellowship within the CaSuS (Catalysis for Sustainable Synthesis) program. We thank Prof. Dr. Lutz F. Tietze (University of Göttingen) for helpful discussions and generous support of our work.

References

1. Laatsch, H.; Fotso, S. *Top. Curr. Chem.* **2008,** *282,* 3–74. doi:10.1007/128_2008_5
2. Brockmann, H. *Fortschr. Chem. Org. Naturst.* **1963,** *21,* 121–182.
3. Grynkiewicz, G.; Wieslaw, S. *Top. Curr. Chem.* **2008,** *282,* 249–284. doi:10.1007/128_2007_7
4. Leng, F.; Savkur, R.; Fokt, I.; Przewloka, T.; Priebe, W.; Chaires, J. B. *J. Am. Chem. Soc.* **1996,** *118,* 4731–4738. doi:10.1021/ja9542606
5. Chaires, J. B.; Satyanarayana, S.; Suh, D.; Fokt, I.; Przewloka, T.; Priebe, W. *Biochemistry* **1996,** *35,* 2047–2053. doi:10.1021/bi952812r
6. Menna, P.; Salvatorelli, E.; Gianni, L.; Minotti, G. *Top. Curr. Chem.* **2008,** *283,* 21–44. doi:10.1007/128_2007_11

7. Minotti, G.; Menna, P.; Salvatorelli, E.; Cairo, G.; Gianni, L. *Pharmacol. Rev.* **2004,** *56,* 185–229. doi:10.1124/pr.56.2.6
8. Cortés-Funes, H.; Coronado, C. *Cardiovasc. Toxicol.* **2007,** *7,* 56–60. doi:10.1007/s12012-007-0015-3
9. Filippini, S.; Lomovskaya, N.; Fonstein, L.; Colombo, A. L.; Hutchinson, C. R.; Otten, S. L.; Breme, U. Process for preparing doxorubicin. U.S. Patent 6,210,930 B1, April 3, 2001.
10. Vogel, P. *Top. Curr. Chem.* **2008,** *282,* 187–214. doi:10.1007/128_2007_148
11. Gupta, R. C.; Harland, P. A.; Stoodley, R. J. *J. Chem. Soc., Chem. Commun.* **1983,** 754–756. doi:10.1039/C39830000754
12. Tamariz, J.; Vogel, P. *Tetrahedron* **1984,** *40,* 4549–4560. doi:10.1016/S0040-4020(01)91514-5
13. Carrupt, P.-A.; Vogel, P. *Tetrahedron Lett.* **1979,** *20,* 4533–4536. doi:10.1016/S0040-4039(01)86642-9
14. Hansen, D. W., Jr.; Pappo, R.; Garland, R. B. *J. Org. Chem.* **1988,** *53,* 4244–4253. doi:10.1021/jo00253a016
15. Rodríguez, D.; Castedo, L.; Domínguez, D.; Saá, C. *Org. Lett.* **2003,** *5,* 3119–3121. doi:10.1021/ol035168e
16. Kesenheimer, C.; Kalogerakis, A.; Meißner, A.; Groth, U. *Chem.–Eur. J.* **2010,** *16,* 8805–8821. doi:10.1002/chem.201000804
17. Leibeling, M.; Koester, D. C.; Pawliczek, M.; Schild, S. C.; Werz, D. B. *Nat. Chem. Biol.* **2010,** *6,* 199–201. doi:10.1038/nchembio.302
18. Leibeling, M.; Koester, D. C.; Pawliczek, M.; Kratzert, D.; Dittrich, B.; Werz, D. B. *Bioorg. Med. Chem.* **2010,** *18,* 3656–3667. doi:10.1016/j.bmc.2010.03.004
19. Leibeling, M.; Milde, B.; Kratzert, D.; Stalke, D.; Werz, D. B. *Chem.–Eur. J.* **2011,** *17,* 9888–9892. doi:10.1002/chem.201101917
20. Leibeling, M.; Werz, D. B. *Chem.–Eur. J.* **2012,** *18,* 6138–6141. doi:10.1002/chem.201200175
21. Leibeling, M.; Pawliczek, M.; Kratzert, D.; Stalke, D.; Werz, D. B. *Org. Lett.* **2012,** *14,* 346–349. doi:10.1021/ol2030923
22. Tietze, L.-F.; Brasche, G.; Gericke, K. M. *Domino Reactions in Organic Synthesis;* Wiley-VCH: Weinheim, Germany, 2006. doi:10.1002/9783527609925
23. Tietze, L. F. *Chem. Rev.* **1996,** *96,* 115–136. doi:10.1021/cr950027e
24. Nicolaou, K. C.; Edmonds, D. J.; Bulger, P. G. *Angew. Chem., Int. Ed.* **2006,** *45,* 7134–7186. doi:10.1002/anie.200601872
25. Sugihara, T.; Copéret, C.; Owczarczyk, Z.; Harring, L. S.; Negishi, E.-i. *J. Am. Chem. Soc.* **1994,** *116,* 7923–7924. doi:10.1021/ja00096a070
26. Negishi, E.-i.; Copéret, C.; Ma, S.; Liou, S.-Y.; Liu, F. *Chem. Rev.* **1996,** *96,* 365–394. doi:10.1021/cr950020x
27. Tietze, L. F.; Sommer, K. M.; Zinngrebe, J.; Stecker, F. *Angew. Chem., Int. Ed.* **2005,** *44,* 257–259. doi:10.1002/anie.200461629
28. Jay-Smith, M.; Furkert, D. P.; Sperry, J.; Brimble, M. A. *Synlett* **2011,** 1395–1398. doi:10.1055/s-0030-1260564
29. Aïssa, C.; Fürstner, A. *J. Am. Chem. Soc.* **2007,** *129,* 14836–14837. doi:10.1021/ja0746316
30. Chan, J.; Jamison, T. F. *J. Am. Chem. Soc.* **2003,** *125,* 11514–11515. doi:10.1021/ja0373925
31. Takahashi, T.; Li, S.; Huang, W.; Kong, F.; Nakajima, K.; Shen, B.; Ohe, T.; Kanno, K.-i. *J. Org. Chem.* **2006,** *71,* 7967–7977. doi:10.1021/jo060923y
32. Krohn, K.; Micheel, J. *Tetrahedron* **1998,** *54,* 4827–4838. doi:10.1016/S0040-4020(98)00188-4
33. Imahori, T.; Ojima, H.; Yoshimura, Y.; Takahata, H. *Chem.–Eur. J.* **2008,** *14,* 10762–10771. doi:10.1002/chem.200801439
34. Sharma, P.; Moses, J. E. *Org. Lett.* **2010,** *12,* 2860–2863. doi:10.1021/ol100968t
35. Petit, M.; Chouraqui, G.; Aubert, C.; Malacria, M. *Org. Lett.* **2003,** *5,* 2037–2040. doi:10.1021/ol034207j
36. Pichaandi, K. R.; Mague, J. T.; Fink, M. J. *J. Organomet. Chem.* **2011,** *696,* 1957–1963. doi:10.1016/j.jorganchem.2010.10.043
37. Voronkov, M. G.; Puzanova, V. E.; Pavlov, S. F.; Dubinskaya, É. I. *Russ. Chem. Bull.* **1975,** *24,* 377–378. doi:10.1007/BF00925793
38. Netherton, M. N.; Fu, G. C. *Org. Lett.* **2001,** *3,* 4295–4298. doi:10.1021/ol016971g
39. Beaudry, C. M.; Trauner, D. *Org. Lett.* **2002,** *4,* 2221–2224. doi:10.1021/ol026069o
40. Tamao, K.; Akita, M.; Kumada, M. *J. Organomet. Chem.* **1983,** *254,* 13–22. doi:10.1016/0022-328X(83)85112-2
41. Tamao, K.; Ishida, N.; Kumada, M. *J. Org. Chem.* **1983,** *48,* 2120–2122. doi:10.1021/jo00160a046
42. Fleming, I.; Henning, R.; Plaut, H. *J. Chem. Soc., Chem. Commun.* **1984,** 29–31. doi:10.1039/C39840000029
43. Ihara, H.; Suginome, M. *J. Am. Chem. Soc.* **2009,** *131,* 7502–7503. doi:10.1021/ja902314v
44. Sunderhaus, J. D.; Lam, H.; Dudley, G. B. *Org. Lett.* **2003,** *5,* 4571–4573. doi:10.1021/ol035695y
45. Goh, S. S.; Baars, H.; Gockel, B.; Anderson, E. A. *Org. Lett.* **2012,** *14,* 6278–6281. doi:10.1021/ol303041j
46. Li, S.; Zhou, L.; Song, Z.; Bao, F.; Kanno, K.-i.; Takahashi, T. *Heterocycles* **2007,** *73,* 519–536. doi:10.3987/COM-07-S(U)28
47. Koester, D. C.; Leibeling, M.; Neufeld, R.; Werz, D. B. *Org. Lett.* **2010,** *12,* 3934–3937. doi:10.1021/ol101625p
48. Koester, D. C.; Werz, D. B. *Beilstein J. Org. Chem.* **2012,** *8,* 675–682. doi:10.3762/bjoc.8.75
49. Koester, D. C.; Kriemen, E.; Werz, D. B. *Angew. Chem., Int. Ed.* **2013,** *52,* 2985–2989. doi:10.1002/anie.201209697
50. Nakanishi, M.; Bolm, C. *Adv. Synth. Catal.* **2007,** *349,* 861–864. doi:10.1002/adsc.200600553

License and Terms

This is an Open Access article under the terms of the Creative Commons Attribution License (http://creativecommons.org/licenses/by/2.0), which permits unrestricted use, distribution, and reproduction in any medium, provided the original work is properly cited.

The license is subject to the *Beilstein Journal of Organic Chemistry* terms and conditions: (http://www.beilstein-journals.org/bjoc)

The definitive version of this article is the electronic one which can be found at: doi:10.3762/bjoc.9.258

Beilstein Journal of Organic Chemistry

Synthesis and characterization of novel bioactive 1,2,4-oxadiazole natural product analogs bearing the *N*-phenylmaleimide and *N*-phenylsuccinimide moieties

Catalin V. Maftei[1], Elena Fodor[1], Peter G. Jones[1], M. Heiko Franz[2], Gerhard Kelter[3], Heiner Fiebig[3] and Ion Neda[*4,§]

Full Research Paper

Open Access

Address:
[1]Institut für Anorganische und Analytische Chemie, Technische Universität Carola Wilhelmina, Hagenring 30, D-38106 Braunschweig, Germany, [2]InnoChemTech GmbH, Hagenring 30, D-38106 Braunschweig, Germany, [3]Oncotest GmbH, Am Flughafen 12–14, 79108 Freiburg, Germany and [4]Institutul National de Cercetare Dezvoltare pentru Electrochimie si Materie Condensata, Str. Dr. A. Paunescu Podeanu Nr. 144, Ro-300569 Timisoara, Romania

Email:
Ion Neda[*] - neda@innochemtech.de

* Corresponding author
§ Fax: (+) 49 531 391 5387

Keywords:
antitumor activity; bioisosteres; maleimide; natural product analogs; 1,2,4-oxadiazoles

Beilstein J. Org. Chem. **2013,** *9,* 2202–2215.
doi:10.3762/bjoc.9.259

Received: 01 August 2013
Accepted: 26 September 2013
Published: 25 October 2013

This article is part of the Thematic Series "Natural products in synthesis and biosynthesis".

Guest Editor: J. S. Dickschat

© 2013 Maftei et al; licensee Beilstein-Institut.
License and terms: see end of document.

Abstract

Taking into consideration the biological activity of the only natural products containing a 1,2,4-oxadiazole ring in their structure (quisqualic acid and phidianidines A and B), the natural product analogs 1-(4-(3-*tert*-butyl-1,2,4-oxadiazol-5-yl)phenyl)pyrrolidine-2,5-dione (**4**) and 1-(4-(3-*tert*-butyl-1,2,4-oxadiazol-5-yl)phenyl)-1*H*-pyrrole-2,5-dione (**7**) were synthesized starting from 4-(3-*tert*-butyl-1,2,4-oxadiazol-5-yl)aniline (**1**) in two steps by isolating the intermediates 4-(4-(3-*tert*-butyl-1,2,4-oxadiazol-5-yl)phenylamino)-4-oxobutanoic acid (**3**) and (*Z*)-4-(4-(3-*tert*-butyl-1,2,4-oxadiazol-5-yl)phenylamino)-4-oxobut-2-enoic acid (**6**). The two natural product analogs **4** and **7** were then tested for antitumor activity toward a panel of 11 cell lines in vitro by using a monolayer cell-survival and proliferation assay. Compound **7** was the most potent and exhibited a mean IC_{50} value of approximately 9.4 μM. Aniline **1** was synthesized by two routes in one-pot reactions starting from *tert*-butylamidoxime and 4-aminobenzoic acid or 4-nitrobenzonitrile. The structures of compounds **1**, **2**, **4**, **5** and **6** were confirmed by X-ray crystallography.

Introduction

The five-membered heterocyclic 1,2,4-oxadiazole motif is of synthetic and pharmacological interest. It also forms an important constituent of biologically active compounds including natural products [1]. Sawyer et al. have described such compounds as bioisosteres for amides and esters [2], with the 1,2,4-oxadiazoles showing higher hydrolytic and metabolic stability.

To the best of our knowledge, there are only a few examples of natural products with a 1,2,4-oxadiazole core or a structure based on it. The 3-substituted indole alkaloids, phidianidines A and B (Figure 1), have been isolated by Carbone et al. from the aeolid opisthobranch *Phidiana militaris* [3]. They are selective inhibitors of the dopamine transporter DAT and partial agonists of the μ opioid receptor [4]. Moreover, these selective molecules are attractive as CNS targets because neither phidianidine A nor B is cytotoxic. Another example of a natural product with a oxadiazole core is quisqualic acid (Figure 1). This metabolite was obtained from the seeds of *Quisqualis indica* and *Q. fructus* [5,6] and is a strong agonist for AMPA (α-amino-3-hydroxy-5-methyl-4-isoxazolepropionic acid) receptors and group I metabotropic glutamate receptors [7].

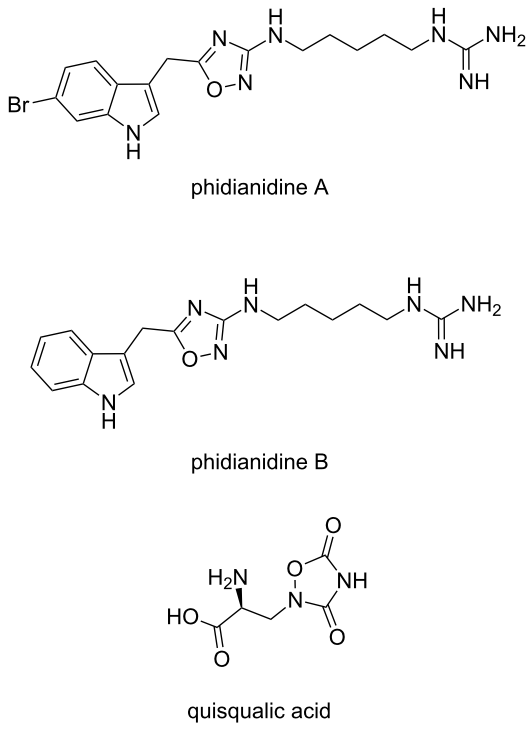


Figure 1: Natural products having a 1,2,4-oxadiazole core.

Furthermore, 1,2,4-oxadiazoles are widely used in synthetic chemistry, e.g., in the search for antitumor agents. Cancer consists of more than one hundred different diseases, all of which are characterized by the uncontrolled growth and spread of abnormal cells. In this context, the identification of drugs acting as apoptosis inducers represents an attractive approach for the discovery of new anticancer agents. 1,2,4-oxadiazole **A** (Figure 2) was found to act as an apoptosis agent by a high-throughput screening (HTS) assay [8]. A series of 1,2,4-oxadiazole-5-carboxamides **B** have been synthesized and tested as inhibitors of the glycogen synthase kinase 3 (GSK-3), a key regulator of both differentiation and cellular proliferation [9].

An alternative antitumor strategy involves the inhibition of processes involved in tumor growth, e.g., angiogenesis. Integrin $\alpha_v\beta_3$ is a receptor that has been found on the surface of many tumor cells and recognizes the arginine–glycine–aspartic acid (RGD) sequence. Antagonists of this receptor are able to inhibit angiogenesis. 1,2,4-Oxadiazolebutanoic acids such as **C** were tested as non-peptidic analogs of $\alpha_v\beta_3$ antagonists [10]. Furthermore, substituted 1,2,4-oxadiazoles have been described as antirhinovirals [11], benzodiazepine receptor partial agonists [12], anti-inflammatory [13], muscarinic agonists [14], serotoninergic (5-HT_3) antagonists [15], and growth hormone secretagogues [16].

The maleimide motif is also a useful five-membered heterocycle in pharmacological chemistry. Kratz et al. synthesized maleimide derivatives of doxorubicin and camptothecin. After intravenous administration these designed anticancer drugs bind

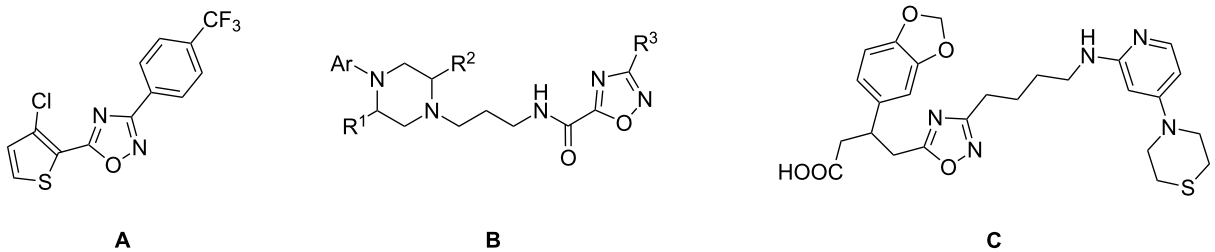


Figure 2: Examples of 1,2,4-oxadiazole antitumorals.

rapidly to circulating albumin [17-19]. Endogenous albumin could be seen as a drug carrier, as it accumulates in solid tumors according to the pathophysiology of tumor tissue [20,21]. Therefore, designed prodrugs have a higher antitumor efficacy in vivo than drugs. Furthermore, maleimides possess strong antifungal activities against important human opportunistic pathogenic fungi. These antifungal drugs appear to be excellent candidates for further development [22-27]. Barrett et al. point out that the possibility of performing chemical modifications is a requirement for developing novel drugs, a strong activity is just the starting point [28].

Another moiety worth investigation is succinimide, because *N*-phenylsuccinimides are regarded as some of the most efficacious agricultural fungicides [29,30]. They have also been shown to be selective nephrotoxic compounds [31,32].

Considering natural products with the 1,2,4-oxadiazol moiety, such as phidianidines A and B (selective inhibitors of DAT), we decided to synthesize, isolate and characterize novel natural product analogs of 1,2,4-oxadiazole derivatives bearing *N*-phenylmaleimide or *N*-phenylsuccinimide functionalities in order to improve their biological activity. The new derivatives have been tested for in vitro antitumor activity toward a panel of 11 cell lines.

Results and Discussion

Clapp reviewed the synthesis of 1,2,4-oxadiazoles [33]. He pointed out that two general methods dominate the practical preparation (≈95%):

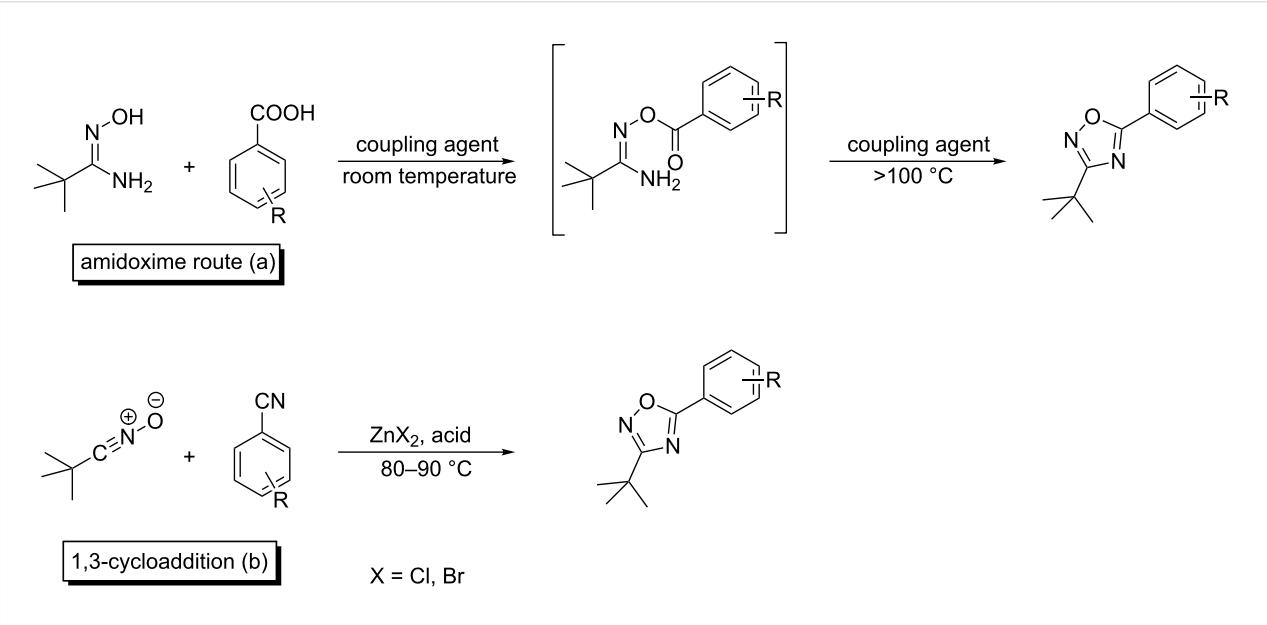
(a) The condensation of amidoximes with carboxylic acid derivatives.

(b) The dipolar cycloaddition of nitrile oxides to nitriles.

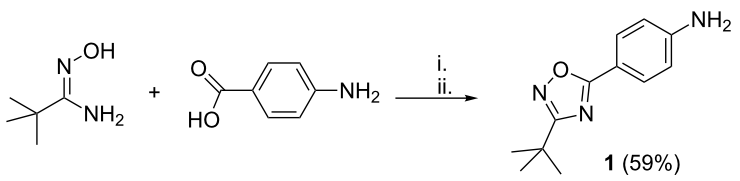
The general approach for the synthesis of 1,2,4-oxadiazoles is illustrated in Scheme 1.

Using route (a), the amidoxime route, the carboxylic acid has to be employed in an activated form. The activated carboxylic acid can be prepared beforehand or in situ by several methods [34], e.g., as an acyl chloride or by the use of *N*,*N*′-carbonyldiimidazole (CDI). In the first step the amidoxime is *O*-acylated with the activated derivative in a condensation reaction. The *O*-acylated amidoxime can be isolated or it can immediately undergo the cyclisation to the heterocyclic oxadiazole ring. This cyclodehydration reaction takes place by heating to temperatures above 100 °C [35,36]. Microwave techniques have also been employed in the synthesis of such heterocycles. The advantage of CDI is that it activates the carboxylic acid in situ and can be used for step 1 and step 2 in DMF.

Scheme 2 presents the one-pot synthesis of 4-(3-*tert*-butyl-1,2,4-oxadiazol-5-yl)aniline (**1**) starting from *tert*-butylamidoxime and 4-aminobenzoic acid. Activation of the 4-aminobenzoic acid with CDI and further acylation of the *tert*-butylamidoxime with DMF as a solvent furnished the *O*-acylamidoxime, which was not isolated. After heating to 120 °C for four hours, it underwent a cyclodehydration reaction, delivering aniline **1** with 59% yield after purification.



Scheme 1: Common synthetic strategies toward 1,2,4-oxadiazoles; (a) amidoxime route; (b) 1,3 dipolar cycloaddition route.



Scheme 2: One-pot synthesis of 4-(3-*tert*-butyl-1,2,4-oxadiazol-5-yl)aniline (**1**) by using the amidoxime route. i. 1.1 equiv CDI in DMF, 30 minutes; ii. 1.1 equiv CDI in DMF, 120 °C, 4 h.

The structure of compound **1** was confirmed by X-ray structure determination (Figure 3 and Figure 4). It crystallizes with two molecules in the asymmetric unit, which differ in the relative orientation of the rings (interplanar angles 22° and 9°). Three of the four NH hydrogens are involved in hydrogen bonds, leading to ribbons of H-bonded rings parallel to the *a* axis.

Following the second route, the 1,3-dipolar cycloaddition, with the purpose of increasing the yield of compound **1**, we used *p*-toluenesulfonic acid (PTSA)–$ZnCl_2$ as a catalyst for the synthesis of aniline **1** from amidoximes and organic nitriles [37]. *tert*-Butylamidoxime and 4-aminobenzonitrile were mixed in DMF with catalytic amounts of PTSA–$ZnCl_2$. First, *tert*-butyl-

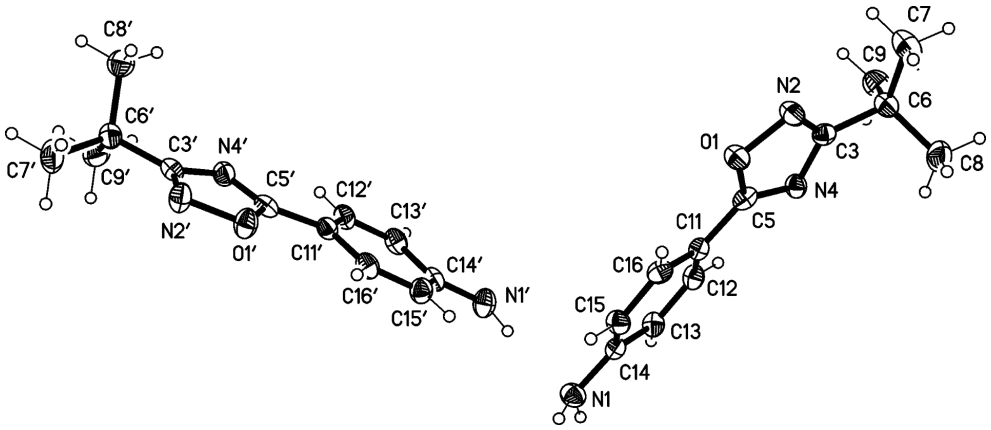


Figure 3: Molecular structure of 4-(3-*tert*-butyl-1,2,4-oxadiazol-5-yl)aniline (**1**). Atoms are drawn as 50% thermal ellipsoids. One hydrogen at N1' is eclipsed.

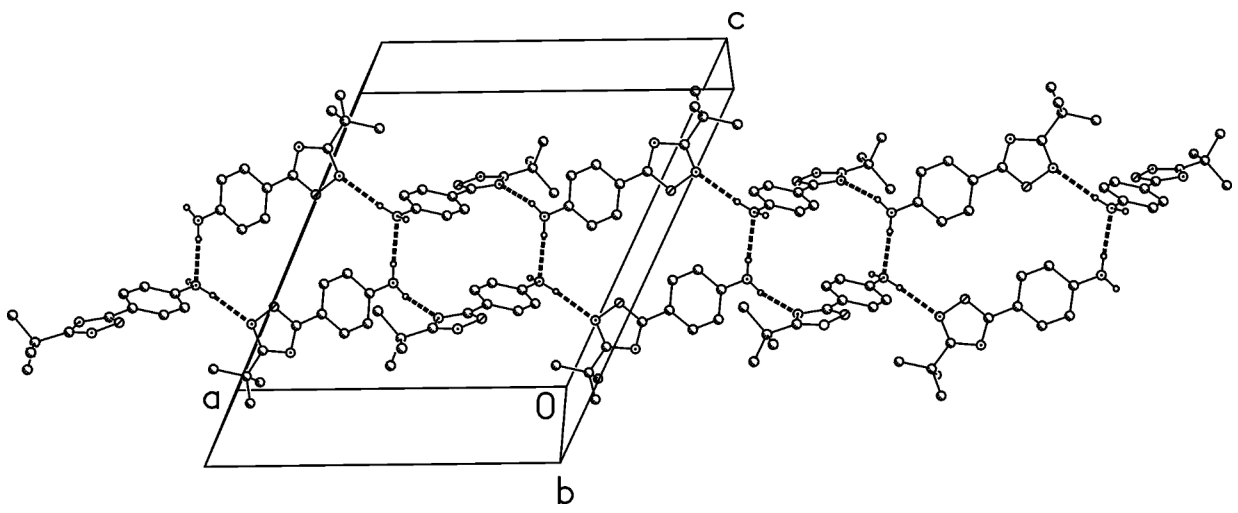


Figure 4: Packing diagram of compound **1**. Hydrogen bonds are indicated as dashed lines.

amidoxime is activated by PTSA–$ZnCl_2$; resulting in the formation of a Lewis acid–ammonia complex as a leaving group, giving rise to the formation of the nitrile oxide. The 1,2,4-oxadiazole moiety is established by the 1,3-dipolar cycloaddition of nitrile oxide to the 4-aminobenzonitrile. However, the Lewis acid might also be involved in the formation of the heterocycle via a Lewis acid catalyzed [3 + 2] cycloaddition reaction. Unfortunately, the yield for this reaction was very low (<20%).

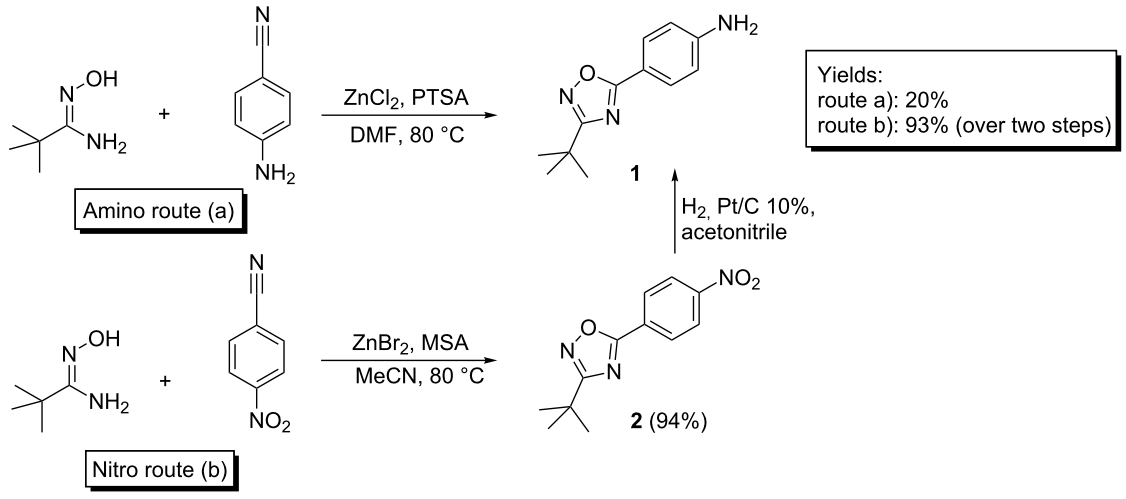
In order to obtain compound **1** by the 1,3 dipolar cycloaddition route we changed the protocol. We synthesized the nitro derivative **2** (3-*tert*-butyl-5-(4-nitrophenyl)-1,2,4-oxadiazole) in situ by using the same catalyst pair as in the first synthesis route. Then, we attempted to hydrogenate nitro compound **2** to the corresponding amine **1** in the same reaction pot without having to isolate the intermediate. The overall yield in this case was 64%. The intermediate **2** was isolated to be fully charazterized. After a series of tests by using various acids as catalyst (*p*-toluensulfonic acid (PTSA), 2-mesitylenesulfonic acid (MSA) and methanesulfonic acid (MeSA) in combination with $ZnCl_2$ and $ZnBr_2$), MSA–$ZnBr_2$ in acetonitrile proved to be the best combination for the preparation of compound **2** from *tert*-butylamidoxime and 4-nitrobenzonitrile under mild conditions. The results are summarized in Table 1. The optimized yield was 93% (Scheme 3) which makes this route more practical than the amidoxime route presented in Scheme 2 with a yield of only 59%.

The structure of compound **2** was confirmed by X-ray structure determination (Figure 5 and Figure 6). The interplanar angle in compound **2** is only 3° and the molecules are

Table 1: Optimal conditions for the 1,3-dipolar cycloaddition route.[a]

Entry	Catalyst 1	Catalyst 2	Solvent	Time (h)	Yield (%)
1	PTSA	$ZnCl_2$	DMF	5	64
2	MSA	$ZnCl_2$	DMF	3	76
3	MeSA	$ZnCl_2$	DMF	12	56
4	PTSA	$ZnBr_2$	DMF	5	70
5	MSA	$ZnBr_2$	DMF	3	79
6	MeSA	$ZnBr_2$	DMF	12	58
7	PTSA	$ZnCl_2$	MeCN	2	82
8	MSA	$ZnCl_2$	MeCN	2	92
9	MeSA	$ZnCl_2$	MeCN	12	63
10	PTSA	$ZnBr_2$	MeCN	2	86
11	MSA	$ZnBr_2$	MeCN	2	93
12	MeSA	$ZnBr_2$	MeCN	12	65

[a]General conditions: *tert*-butylamidoxime (1 equiv), 4-nitrobenzonitrile (1 equiv), catalyst 1 (0.3 equiv), catalyst 2 (0.3 equiv), 80 °C.



Scheme 3: One-pot synthesis of 4-(3-*tert*-butyl-1,2,4-oxadiazol-5-yl)aniline (**1**) by using the 1,3-dipolar cycloaddition route.

linked to ribbons parallel to the *b* axis by two C–H···O interactions.

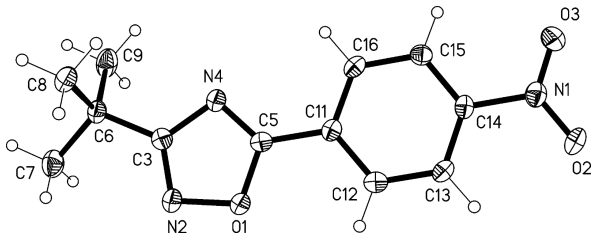


Figure 5: Molecular structure of 3-*tert*-butyl-5-(4-nitrophenyl)-1,2,4-oxadiazole (**2**). Atoms are drawn as 50% thermal ellipsoids.

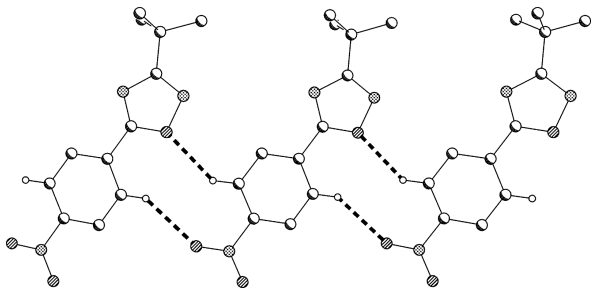


Figure 6: Packing diagram of compound (**2**) showing C–H···O interactions.

Imide derivatives have been found to possess a broad spectrum of biological activities. A variety of methods have been reported for the preparation of this class of compounds. The synthesis follows a two-step protocol. First, it is necessary to synthesize the amide derivative.

The synthesis of amide **3** was performed under inert conditions by mixing an equimolar amount of aniline **1** and succinic anhydride in a minimum volume of dichloromethane (Scheme 4). Compound **3** was obtained with a short reaction time and a high yield (91%). The ester derivative methyl 4-(4-(3-*tert*-butyl-1,2,4-oxadiazol-5-yl)phenylamino)-4-oxobutanoate (**5**) was prepared by the addition of a diethyl ether solution of diazomethane to a suspension of amide **3**. The ester **5** was afforded in a quantitative amount.

For the synthesis of imide **4** the starting material, amide **3**, was mixed with an equimolar amount of sodium acetate in acetic anhydride and the mixture was heated for 4 h at 80–85 °C; resulting in the corresponding *N*-arylsuccinimide **4** (87%).

The structures of compounds **4** and **5** were also confirmed by X-ray structure analysis (Figure 7, Figure 8 and Figure 9). In compound **4** the oxazoline and phenyl rings are approximately coplanar (6°), but the pyrrolidine ring is rotated by 52° with respect to the phenyl ring. The main packing interaction is an

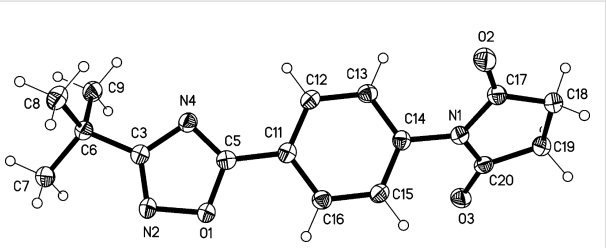
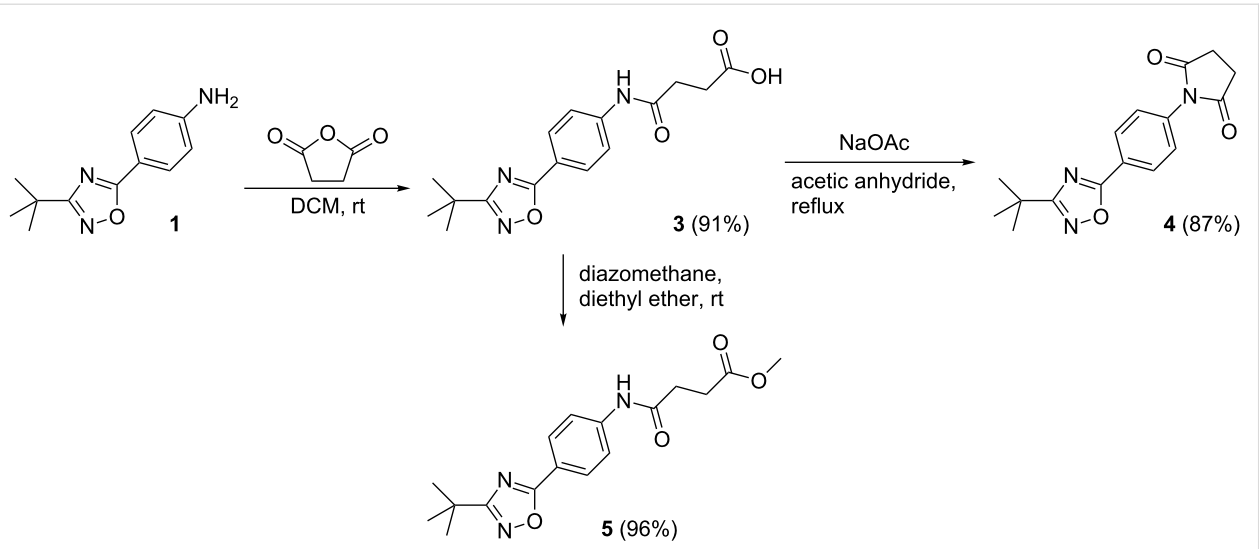


Figure 7: Molecular structure of 1-(4-(3-*tert*-butyl-1,2,4-oxadiazol-5-yl)phenyl)pyrrolidine-2,5-dione (**4**). Atoms are drawn as 50% thermal ellipsoids.



Scheme 4: Synthesis of 1-(4-(3-*tert*-butyl-1,2,4-oxadiazol-5-yl)phenyl)pyrrolidine-2,5-dione (**4**).

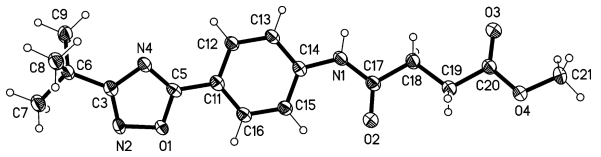


Figure 8: Molecular structure of 4-(4-(3-*tert*-butyl-1,2,4-oxadiazol-5-yl)phenylamino)-4 oxobutanoate (**5**). Atoms are drawn as 50% thermal ellipsoids.

offset stacking parallel to the *c* axis (not shown). Compound **5** has an interplanar angle of 14°. The molecules are associated into ribbons parallel to [110] by one long N–H···N and two shorter C–H···O interactions.

The synthesis of amide **6** was performed by mixing an equimolar amount of aniline **1** and maleic anhydride in dichloromethane (Scheme 5). The amide **6** was obtained with a good yield (84%). For the synthesis of imide **7** the amide **6** was mixed with an equimolar amount of sodium acetate in acetic anhydride and the mixture was heated for 4 h at 80–85 °C resulting in the corresponding *N*-arylmaleimide **7** (75%).

The structure of compound **6** was also confirmed by X-ray structure analysis (Figure 10 and Figure 11). In compound **6** the

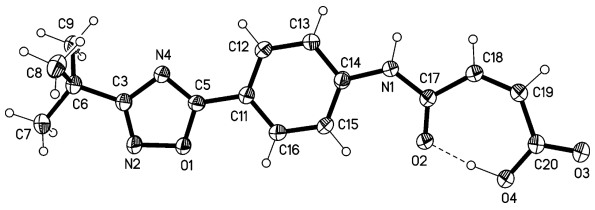


Figure 10: Molecular structure of (*Z*)-4-(4-(3-*tert*-butyl-1,2,4-oxadiazol-5-yl)phenylamino)-4-oxobut-2-enoic acid (**6**). Atoms are drawn as 50% thermal ellipsoids.

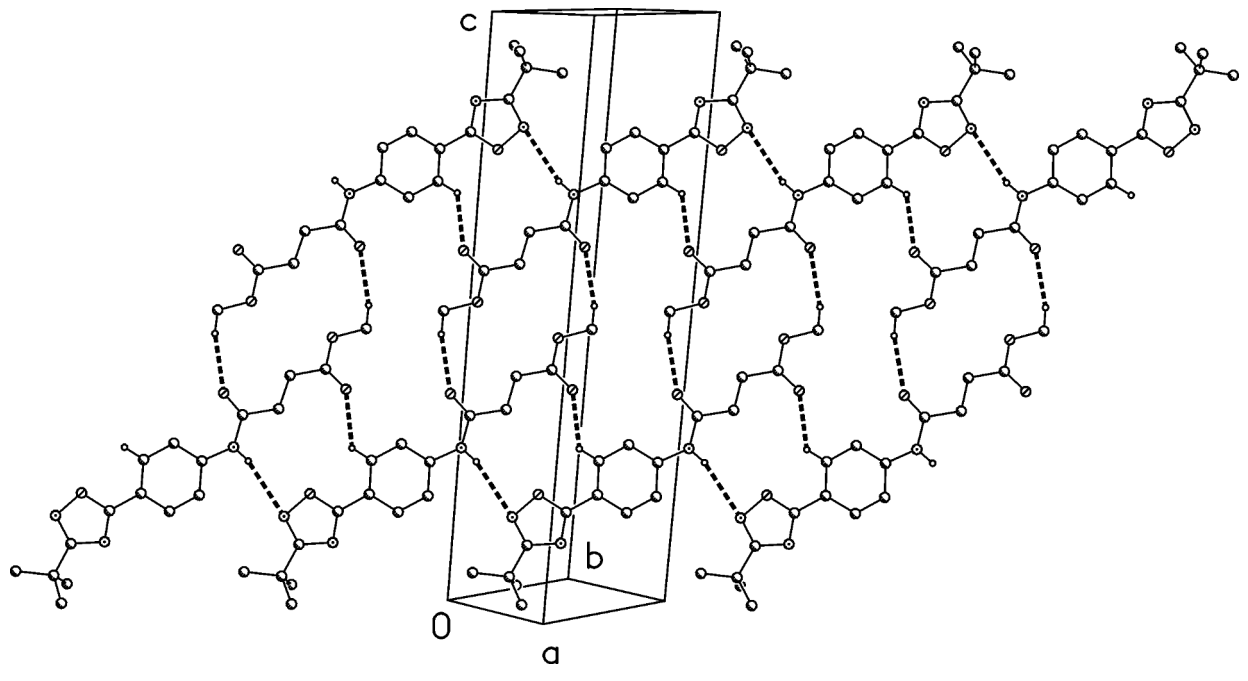
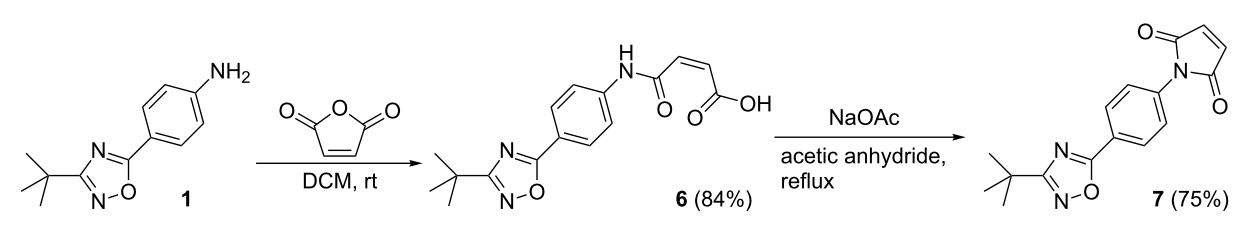


Figure 9: Packing diagram of compound (**5**). Dashed lines indicate hydrogen bonds.



Scheme 5: Synthesis of 1-(4-(3-*tert*-butyl-1,2,4-oxadiazol-5-yl)phenyl)-1*H*-pyrrole-2,5-dione (**7**).

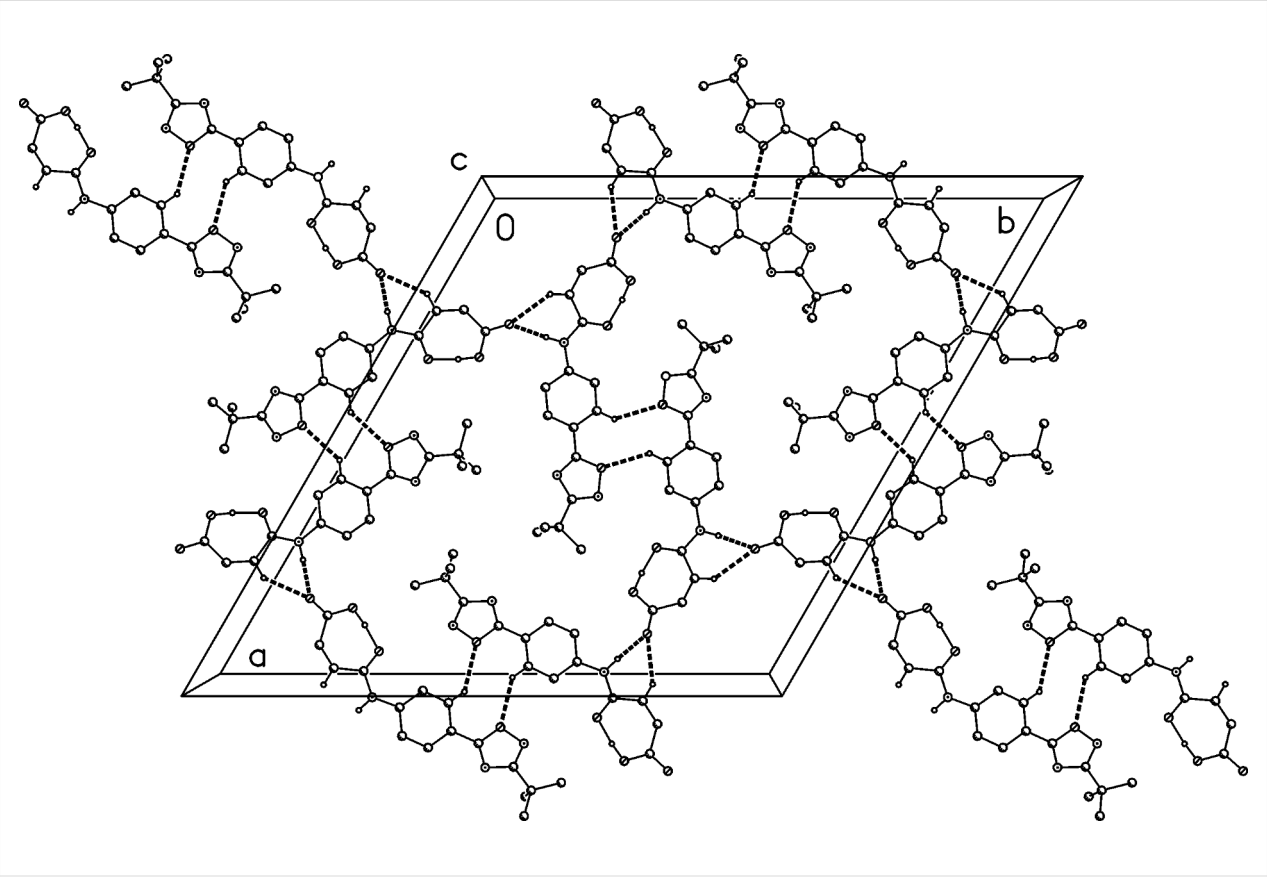


Figure 11: Packing diagram of compound **6**. Dashed lines indicate hydrogen bonds.

interplanar angle is 11°; the intramolecular hydrogen bond is almost symmetrical (O4–H04 1.03(3), H04···O2 1.47(3)) Å. The molecules are linked to form layers perpendicular to the hexagonal *c* axis by one C–H···O and one three-centre (N–H, C–H)···O interaction. The double bond has a *Z*-configuration.

Antitumor activity

The in vitro antitumor activity of six synthesized compounds toward a panel of 11 cell lines was assessed by using a monolayer cell survival and proliferation assay. By exhibiting a mean IC_{50} value of 9.4 µM **7** was the most potent compound. Compounds **1**, **5**, **4**, **6** and **3** have only marginal antitumor activity toward the 11 tested cell lines (Figure 12).

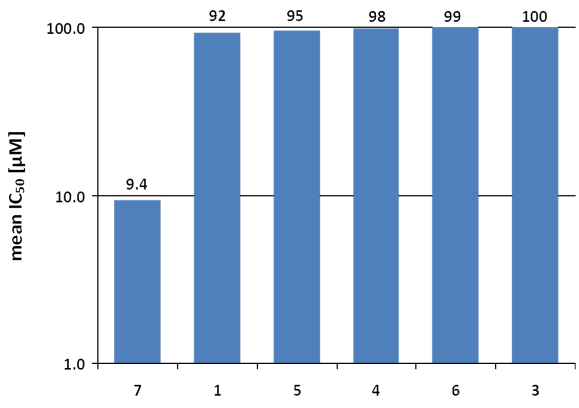


Figure 12: In vitro antitumor activity of compounds **1**, **3**–**7** toward 11 human tumor cell lines.

An investigation of the activity of compounds in a cell line panel representing various tumor histo-types, as performed in this study, allows the analysis of potency and tumor selectivity and the identification of active compounds which qualify for further preclinical development. Tumor selectivity of the compounds is illustrated in Figure 13 by a heat-map presentation of the individual IC_{50} values. Good tumor selectivity is reflected by cell lines exhibiting above-average sensitivity (i.e., an individual IC_{50} value smaller than 0.5 of the mean IC_{50} value; marked in green) and the range of activity among the cell lines (i.e., the IC_{50} value of the most resistant cell line divided by the IC_{50} value of the most sensitive cell line). Overall, a good antitumor potency (i.e., a mean IC_{50} < 30 µM) combined with a good selectivity (i.e., a range of activity > 8 or at least 2 cell lines exhibiting above-average sensitivity) was obvious for compound **7**.

#	compound	CXF HT-29	GXF 251	LXFA 629	LXFL 529	MAXF 401	MEXF 462	OVXF 899	PAXF 1657	PXF 1752	RXF 486	UXF 1138	geomean IC50 [µM]	range of activity[a]
1	7	15.00	28.12	22.01	6.92	9.26	7.76	10.93	3.94	11.10	4.49	5.05	9.39	7.1
2	1	100.00	55.33	100.00	76.78	98.08	100.00	100.00	100.00	100.00	100.00	100.00	92.4	1.8
3	5	100.00	100.00	100.00	57.28	100.00	100.00	100.00	100.00	100.00	100.00	100.00	95.1	1.7
4	4	100.00	100.00	100.00	82.92	100.00	100.00	100.00	100.00	100.00	100.00	100.00	98.3	1.2
5	6	100.00	92.39	100.00	100.00	100.00	100.00	100.00	100.00	100.00	100.00	100.00	99.3	1.1
6	3	100.00	100.00	100.00	100.00	100.00	100.00	100.00	100.00	100.00	100.00	100.00	100.0	1.0

[a]IC50 value of the most resistant cell line divided by the IC50 value of the most senstive cell line

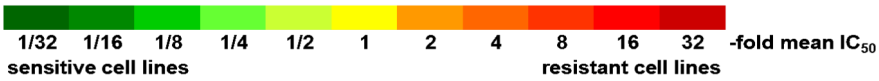


Figure 13: Individual IC_{50} values [µM] of compounds **1**, **3**–**7** in a panel of 11 human tumor cell lines.

Conclusion

Two novel 1,2,4-oxadiazol natural product-inspired derivatives bearing *N*-phenylmaleimide or *N*-phenylsuccinimide moieties were synthesized in two steps starting from 1,2,4-oxadiazole amine **1**. All intermediate derivatives were isolated, characterized and tested in vitro for antitumor activity toward a panel of 11 cell lines by using a monolayer cell survival and proliferation assay. With an IC_{50} value of 9.4 µM, compound **7** was the most active, probably because maleimide is able to rapidly bind to the cysteine-34 position of circulating albumin, transported as an albumin conjugate (macromolecular drug), and then released in the target tissue by acid related cleavage or enzymatic cleavage. Compounds **1**, **3**, **4**, **5** and **6** have no or only marginal activity toward the 11 cell lines tested. Considering the bioactive natural products (quisqualic acid and phidianidines A and B), it is of great pharmacologic interest to synthesize new derivates of 1,2,4-oxadiazole with an efficient biological transport in cells by using natural transporters such as amino acids, peptides or sugars. Moreover, it is desirable to reduce, or even remove completely, the secondary effects to minimize the toxicity and increase the selectivity. All derivatives were obtained with a high purity (at least 97% based on ^{1}H NMR) and good to high yields (75–96%). The structural assignments were corroborated by X-ray structure analysis.

Experimental

General

All reagents were purchased from commercial sources (Sigma-Aldrich or Acros) and used without further purification. Solvents were of analytical grade. ^{1}H and ^{13}C NMR spectra were recorded at room temperature on a Bruker Avance 200 operating at 200 MHz for ^{1}H and 50 MHz for ^{13}C. Chemical shifts (δ) are reported relative to the tetramethylsilane peak set at 0.00 ppm. In the case of multiplets, the signals are reported as intervals. Signals were abbreviated as s, singlet; d, doublet; t, triplet; q, quadruplet; m, multiplet. IR spectra were recorded with a Bruker Vertex 70 ATR. Mass spectra (electronic ionisation, 70 eV) were recorded on a Finnigan MAT 8400-MSS and Finnigan MAT 4515. High resolution mass spectra were recorded on a Finnigan MAT 95 XP. Melting points were measured with a Schropp Gerätetechnik MPM-HV2. The melting points are uncorrected. Column chromatography was carried out by using Merck silica gel 60 (70–200 mesh).

Procedures

Synthesis of 4-(3-*tert*-butyl-1,2,4-oxadiazol-5-yl)aniline (**1**)

a. 1.0 g (7.2 mmol) of 4-aminobenzoic acid was dissolved under an inert atmosphere in 20 mL of DMF, and 1.28 g (7.9 mmol) of CDI solved in 30 mL of DMF was added. After 30 minutes of stirring at room temperature 0.91 g (7.9 mmol) of *tert*-butylamidoxime was added. A second portion of CDI (1.28 g, 7.9 mmol) was added, and the reaction mixture was heated under reflux until the reaction was complete. The mixture was cooled to room temperature and poured into 500 mL of water–ice mixture. The formed solid was filtered off, washed with water, dried and flash chromatographed (silica, ethyl acetate/hexane 2:1), yielding after purification 0.92 g (4.2 mmol, 59%) of **1** as a yellow solid.

b. To a mixture of 0.116 g (1 mmol) of *tert*-butylamidoxime in 5 mL of solvent (acetonitrile or DMF) under an inert atmosphere was added 0.15 g (1 mmol) of 4-nitrobenzonitrile. To this reaction mixture was added 0.3 mmol of acid catalyst 1 (57.0 mg PTSA, 70.8 mg MSA or 28.8 mg MeSA) and 0.3 mmol of catalyst 2 (40.9 mg $ZnCl_2$ or 67.5 mg $ZnBr_2$), and

the mixture was heated to 80 °C until no further change was observed (2–12 hours). Then the reaction mixture was cooled to room temperature, 10 mg of Pt/C 10% catalyst was added, and hydrogen was bubbled through the solution until intermediate **2** was no longer detected. The reaction mixture was filtered through a layer of Celite, and then the solvent was removed under reduced pressure. The solid that remained was dried and flash chromatographed (silica, ethyl acetate/hexane 2:1), yielding after purification **1** as a yellow solid. Yield: PTSA/$ZnCl_2$/DMF 139.0 mg, 0.64 mmol, 64%; MSA/$ZnCl_2$/DMF 165.0 mg, 0.76 mmol, 76%; MeSA/$ZnCl_2$/DMF 121.6 mg, 0.56 mmol, 56%; PTSA/$ZnBr_2$/DMF 152.0 mg, 0.7 mmol, 70%; MSA/$ZnBr_2$/DMF 171.5 mg, 0.79 mmol, 79%; MeSA/$ZnBr_2$/DMF 125.9 mg, 0.58 mmol, 58%; PTSA/$ZnCl_2$/CH_3CN 178.1 mg, 0.82 mmol, 82%; MSA/$ZnCl_2$/CH_3CN 199.8 mg, 0.92 mmol, 92%; MeSA/$ZnCl_2$/CH_3CN 136.8 mg, 0.63 mmol, 63%; PTSA/$ZnBr_2$/CH_3CN 186.7 mg, 0.86 mmol, 86%; MSA/$ZnBr_2$/CH_3CN 201.9 mg, 0.93 mmol, 93%; MeSA/$ZnBr_2$/CH_3CN 141.1 mg, 0.65 mmol, 65%. MS *m*/*z*: 217 (M^+, 60), 202 (5), 120 (100); HRMS: calcd. for $C_{12}H_{15}N_3O^+$, 217.12096; found, 217.12159; ^{1}H NMR (200 MHz, $CDCl_3$) δ 7.87–7.78 (m, 2H), 6.68–6.56 (m, 2H), 4.08 (bs, 2H), 1.32 (s, 9H); ^{13}C NMR (50 MHz, $CDCl_3$) δ 27.8 (-CH_3), 31.7, 113.5, 113.7, 129.1, 149.7, 174.7, 177.3; mp 120–122 °C; IR (ATR): 1/λ 3437 (w), 3326 (w), 3218 (w), 2966 (w), 2360 (w), 2162 (w), 1699 (w), 1652 (w), 1603 (s), 1581 (m), 1522 (w), 1510 (m), 1491 (m), 1463 (m), 1442 (m), 1415 (w) 1394 (w), 1351 (s), 1329 (w), 1291 (w), 1197 (m), 1186 (s), 1172 (s), 1096 (w), 1028 (w), 962 (w), 845 (m), 835 (m), 777 (s), 700 (w), 645 (s) cm^{-1}.

Representative procedure for the synthesis of 3-*tert*-butyl-5-(4-nitrophenyl)-1,2,4-oxadiazole (**2**)

To a mixture of 0.116 g (1 mmol) of *tert*-butylamidoxime in acetonitrile under an inert atmosphere was added 0.150 g (1 mmol) of 4-nitrobenzonitrile in molar ratio 1:1. To this reaction mixture was added 0.3 mmol (0.07 g) of 2-mesitylenesulfonic acid and 0.3 mmol (0.067 g) of $ZnBr_2$, and the mixture was heated to 80 °C for 2 hours. After the reaction was finished the heating was removed, and the mixture was cooled to room temperature. The solvent was concentrated under reduced pressure, and ethyl acetate was added. The mixture was washed with sodium hydrogen carbonate solution, water and brine. The organic phase was dried over anhydrous sodium sulfate, filtered, and the solvent was removed. The resulting residue was dried in vacuum and flash chromatographed (silica, ethyl acetate/hexane 2:1), yielding after purification 0.232 g (0.94 mmol, 94%) of **2** as a white solid. MS *m*/*z*: 247 (M^+, 25), 232 (45), 150 (100); ^{1}H NMR (200 MHz, $CDCl_3$) δ 8.43–8.28 (m, 4H), 1.45 (s, 9H); ^{13}C NMR (50 MHz, $CDCl_3$) δ 28.4, 32.6, 124.2, 129.9, 144.6, 148.9, 174.2, 178.4.

Synthesis of 4-(4-(3-*tert*-butyl-1,2,4-oxadiazol-5-yl)phenylamino)-4-oxobutanoic acid (**3**)

0.3 g (1.38 mmol) of 4-(3-*tert*-butyl-1,2,4-oxadiazol-5-yl)aniline (**1**) was mixed under inert conditions with an equimolar amount (0.138 g, 1.38 mmol) of succinic anhydride in 20 mL of DCM. This mixture was vigorously stirred at room temperature for 5 hours. The remaining residue was freed from solvent, suspended in 50 mL of water, and the pH value adjusted to 2–3 with a 1 N solution of HCl. The resulting suspension was filtered, and the product was dried in vacuum. It was purified by flash chromatography (silica gel, ethyl acetate/hexane 1:1), yielding 0.398 g (1.25 mmol, 91%) of **3** as a white solid after purification. MS *m*/*z*: 317 (M^+, 15), 299 (55), 217 (50), 202 (100), 120 (55); HRMS: calcd. for $C_{16}H_{19}N_3O_4^+$, 317.13701; found, 317.13717; ^{1}H NMR (200 MHz, DMSO-d_6) δ 12.24 (bs, 1H), 10.42 (s, 1H, -NH), 8.07–8.02 (m, 2H), 7.96–7.92 (m, 2H), 2.67–2.59 (m, 4H), 1.38 (s, 9H); ^{13}C NMR (50 MHz, DMSO-d_6) δ 28.1 (-CH_3), 28.5, 31.1, 31.9, 117.6, 118.8, 128.6, 143.3, 170.7, 173.6, 174.3, 177.5; mp 201–203 °C; IR (ATR): 1/λ 3385 (w), 2964 (w), 1696 (s), 1608 (m), 1594 (w), 1506 (s), 1492 (m), 1464 (w), 1410 (m), 1394 (w), 1351 (m), 1337 (m), 1313 (m), 1281 (w), 1249 (w), 1200 (m), 1177 (m), 1159 (s), 994 (w), 859 (m), 830 (w), 802 (w), 773 (m), 681 (m), 612 (m) cm^{-1}.

Synthesis of 1-(4-(3-*tert*-butyl-1,2,4-oxadiazol-5-yl)phenyl)pyrrolidine-2,5-dione (**4**)

0.3 g (0.94 mmol) of 4-(4-(3-*tert*-butyl-1,2,4-oxadiazol-5-yl)phenylamino)-4-oxobutanoic acid (**3**) was mixed with an equimolar amount of sodium acetate (0.077 g, 0.94 mmol) in 15 mL of acetic anhydride, and the mixture was then heated for 4 h at 80–85 °C. After cooling, the product was washed with 100 mL H_2O at pH ≈ 2–3. The solid was dried in vacuum and flash chromatographed (silica, ethyl acetate/hexane 2:1), yielding after purification 0.244 g (0.81 mmol, 87%) of **4** as a white solid. MS *m*/*z*: 299 (M^+, 55), 284 (15), 202 (100); HRMS: calcd. for $C_{16}H_{17}N_3O_3^+$, 299.12644; found, 299.12695; ^{1}H NMR (200 MHz, $CDCl_3$) δ 8.18–8.09 (m, 2H), 7.48–7.39 (m, 2H), 2.80 (s, 4H), 1.34 (s, 9H); ^{13}C NMR (50 MHz, $CDCl_3$) δ 28.3 (-CH_3), 32.3, 124.2, 126.6, 128.6, 135.3, 174.0, 175.5, 178.3; mp 136–138 °C; IR (ATR): 1/λ 2970 (w), 2875 (w), 1776 (w), 1709 (s), 1613 (w), 1520 (w), 1500 (w), 1465 (w), 1419 (w), 1382 (m), 1351 (w), 1275 (w), 1197 (m), 1171 (s), 923 (w), 904 (w), 841 (m), 810 (w), 771 (w), 737 (w), 697 (m), 659 (w) cm^{-1}.

Synthesis of methyl 4-(4-(3-*tert*-butyl-1,2,4-oxadiazol-5-yl)phenylamino)-4-oxobutanoate (**5**)

A suspension of 0.3 g (0.94 mmol) of 4-(4-(3-*tert*-butyl-1,2,4-oxadiazol-5-yl)phenylamino)-4-oxobutanoic acid (**3**) in 10 mL of diethyl ether was cooled in an ice bath, and a solution of

diazomethane in diethyl ether 2.5 N was added dropwise until the white solid disappeared, and the gas evolution stopped. The solvent was removed under high vacuum to afford 0.298 g (0.9 mmol, 96%) of **5** as a white solid. No further purification was necessary. MS *m*/*z*: 331 (M^+, 10), 299 (50), 284 (15), 202 (100); HRMS: calcd. for $C_{17}H_{21}N_3O_4^+$, 331.15266; found, 331.15275; ^{1}H NMR (200 MHz, $CDCl_3$) δ 8.34 (s, 1H-NH), 8.11–8.02 (m, 2H), 7.70–7.66 (m, 2H), 3.72 (s, 3H), 2.82–2.67 (m, 4H), 1.42 (s, 9H); ^{13}C NMR (50 MHz, $CDCl_3$) δ 27.8 (-CH_3), 28.3, 31.3, 31.7, 51.4, 118.7, 119.3, 128.4, 141.0, 169.5, 173.0, 173.9, 177.6; mp 144–146 °C; IR (ATR): 1/λ 3391 (w), 2966 (w), 1738 (m), 1702 (m), 1607 (m), 1595 (w), 1507 (s), 1492 (m), 1524 (w), 1392 (w), 1351 (m), 1327 (s), 1274 (w), 1251 (w), 1197 (m), 1172 (s), 1156 (s), 1097 (w), 991 (w), 988 (w), 863 (m), 836 (w), 797 (w), 773 (m), 699 (w), 690 (w), 617 (s) cm^{-1}.

Synthesis of (*Z*)-4-(4-(3-*tert*-butyl-1,2,4-oxadiazol-5-yl)phenylamino)-4-oxobut-2-enoic acid (**6**)

0.3 g (1.38 mmol) of 4-(3-*tert*-butyl-1,2,4-oxadiazol-5-yl)aniline (**1**) was mixed under inert conditions with an equimolar amount of 0.135 g (1.38 mmol) of maleic anhydride in 20 mL of DCM. This mixture was vigorously stirred at room temperature for 3 hours. The remaining residue was freed from solvent and suspended in 50 mL of water, and the pH value was adjusted to 2–3 with a 1 N solution of HCl. The resulting suspension was filtered, the product dried in vacuum and flash chromatographed (silica, ethyl acetate/hexane 2:1), yielding after purification 0.365 g (1.15 mmol, 84%) of **6** as a white solid. MS *m*/*z*: 315 (M^+, 15), 297 (50), 217 (55), 200 (100), 120 (75); HRMS: calcd. for $C_{16}H_{17}N_3O_4^+$, 315.12136; found, 315.12144; ^{1}H NMR (200 MHz, DMSO-d_6) δ 12.94 (bs, 1H), 10.73 (s, 1H, -NH), 8.14–8.03 (m, 2H), 7.96–7.85 (m, 2H), 6.61–6.32 (m, 2H), 1.38 (s, 9H); ^{13}C NMR (50 MHz, DMSO-d_6) δ 28.0 (-CH_3), 31.9, 118.3, 119.4, 128.7, 130.1, 131.4, 142.7, 163.6, 166.8, 174.2, 177.5; mp 214–216 °C; IR (ATR): 1/λ 3288 (w), 3104 (w), 2974 (w), 1707 (m), 1633 (w), 1616 (w), 1586 (m), 1566 (w), 1532 (s), 1520 (s), 1496 (s), 1467 (m), 1409 (w), 1396 (w), 1348 (w), 1325 (m), 1281 (w), 1267 (w), 1188 (m), 1101 (w), 976 (m), 899 (w), 849 (s), 776 (m), 737 (w), 738 (w), 632 (w), 615 (m) cm^{-1}.

Synthesis of 1-(4-(3-*tert*-butyl-1,2,4-oxadiazol-5-yl)phenyl)-1*H*-pyrrole-2,5-dione (**7**)

0.25 g (0.79 mmol) of (*Z*)-4-(4-(3-*tert*-butyl-1,2,4-oxadiazol-5-yl)phenylamino)-4-oxobut-2-enoic acid (**6**) was mixed with an equimolar amount of sodium acetate (0.065 g, 0.79 mmol) in 15 mL of acetic anhydride, and the mixture was then heated for 4 h at 80–85 °C. After cooling, the product was washed with 100 mL of water at pH ≈ 2–3. The solid was dried in vacuum and flash chromatographed (silica, ethyl acetate/hexane 2:1), yielding after purification 0.176 g (0.59 mmol, 75%) of **7** as a white solid. MS *m*/*z*: 297 (M^+, 60), 282 (15), 200 (100); HRMS: calcd. for $C_{16}H_{15}N_3O_3^+$, 297.11079; found, 297.11127; ^{1}H NMR (200 MHz, $CDCl_3$) δ 8.26–8.14 (m, 2H), 7.62–7.54 (m, 2H), 6.88 (s, 2H), 1.44 (s, 9H); ^{13}C NMR (50 MHz, $CDCl_3$) δ 28.2 (-CH_3), 32.3, 123.2, 125.5, 128.5, 134.2, 134.8, 168.6, 174.0, 178.3; mp 123–125 °C; IR (ATR): 1/λ 3474 (w), 3096 (w), 2975 (w), 2927 (w), 1713 (s), 1614 (w), 1567 (w), 1521 (m), 1502 (m), 1466 (w), 1395 (m), 1385 (m), 1351 (w), 1306 (w), 1238 (w), 1195 (m), 1149 (s), 1064 (w), 1022 (w), 988 (w), 949 (w), 905 (w), 842 (m), 827 (s), 771 (m), 737 (w), 700 (s), 686 (m), 652 (w), 624 (w) cm^{-1}.

X-ray structure determinations

Data are summarized in Table 2. Intensities were determined at 100 K on Oxford Diffraction diffractometers by using monochromated Mo Kα or mirror-focussed Cu Kα radiation. Structures were refined on F^2 using the program SHELXL-97 [38]. Hydrogen atoms were refined either freely (NH), by using rigid methyl groups allowed to rotate but not tip or by using a riding model starting from calculated positions. Structure **5** was treated as a non-merohedral twin.

CCDC–924911 (**1**), CCDC–951265 (**2**), CCDC–924912 (**4**), CCDC–924913 (**5**), CCDC–924914 (**6**) contain the supplementary crystallographic data for this paper. These data can be obtained free of charge from the Cambridge Crystallographic Data Centre via http://www.ccdc.cam.ac.uk/.

In vitro antitumor activity toward human tumor cell lines

Antitumor activity of the compounds was tested in a monolayer cell survival and proliferation assay with human tumor cell lines. Studies carried out with panels of human tumor cell lines of different origin and histotype allow for the analysis of potency and tumor selectivity of test compounds.

Ten out of the eleven tested cell lines were established at Oncotest from patient-derived human tumor xenografts passaged subcutaneously in nude mice [39]. The origin of the donor xenografts was described [40,41]. The cell line HT-29 was kindly provided by the National Cancer Institute (Bethesda, MA, USA). Cells were cultured in RPMI 1640 medium, supplemented with 10% fetal calf serum and 0.1 mg/mL gentamicin under standard conditions (37 °C, 5% CO_2). Authenticity of all cell lines was proven by STR analysis at the DSMZ (Braunschweig, Germany).

A modified propidium iodide assay was used to assess the compounds' activity toward human tumor cell lines [42]. Briefly, cells were harvested from exponential phase cultures by

Table 2: Crystallographic data for compounds **1**, **2**, **4**–**6**.

Compound	**1**	**2**	**4**	**5**	**6**
Formula	$C_{12}H_{15}N_3O$	$C_{12}H_{137}N_3O_3$	$C_{16}H_{17}N_3O_3$	$C_{17}H_{21}N_3O_4$	$C_{17}H_{21}N_3O_4$
M_r	217.27	247.25299.33	299.33	331.37	331.37
Habit	colourless tablet	colourless tablet	colourless needle	colourless plate	colourless prism
Cryst. size (mm)	0.15 × 0.15 × 0.1	0.24 × 0.12 × 0.07	0.11 × 0.05 × 0.02	0.18 × 0.09 × 0.02	0.07 × 0.05 × 0.03
Crystal system	monoclinic	orthorhombic	monoclinic	monoclinic	trigonal
Space group	$P2_1/c$	Pbca	$P2_1/c$	$P\bar{1}$	$R\bar{3}$
Cell constants:					
a (Å)	15.6514(10)	6.7175(4)	13.8569(4)	5.4494(5)	28.0192(6)
b (Å)	9.0961(6)	13.8116(6)	15.3562(4)	6.1403(6)	28.0192(6)
c (Å)	18.4999(12)	26.1018(9)	6.8926(2)	25.283(2)	10.0740(8)
α (°)	90	90	90	86.906(8)	90
β (°)	114.371(8)	90	94.918(2)	85.277(8)	90
γ (°)	90	90	90	72.926(8)	120
V (Å^3)	2399.1	2421.7	1461.27	805.57	6849.3
Z	8	8	4	2	18
D_x (Mg m^{-3})	1.203	1.356	1.361	1.366	1.376
μ (mm^{-1})	0.08	0.10	0.80	0.81	0.84
F(000)	928	1040	632	352	2988
T (°C)	−173	−173	−173	−173	−173
Wavelength (Å)	0.71073	0.71073	1.54184	1.54184	1.54184
$2\theta_{max}$	52.8	56.6	152	152	152
Refl. measured	41755	55696	16680		28530
Refl. indep.	4908	2483	3034	3747	3156
R_{int}	0.064	0.074	0.027		0.067
Parameters	311	166	202	226	219
wR(F^2, all refl.)	0.057	0.061	0.086	0.179	0.098
R(*F*, >4σ(*F*))	0.035	0.031	0.032	0.062	0.039
S	0.73	0.81	1.06	1.07	1.04
max. Δ/ρ (e Å^{-3})	0.17	0.18	0.21	0.38	0.17

trypsinization, counted and plated in 96-well flat-bottom microtiter plates at a cell density dependent on the cell line (4.000–20.000 cells/well). After 24 h recovery period to allow the cells to adhere and resume exponential growth, compounds were added at 10 concentrations in half-log increments and incubated for 4 days. The inhibition of proliferation was determined by measuring the DNA content with an aqueous propidium iodide solution (7 μg/mL). Fluorescence was measured by using a Cytofluor micro-plate reader (excitation λ = 530 nm, emission λ = 620 nm) and thus establishing a direct relationship to the total viable cell number. In each experiment, all measurements were carried out twice.

Acknowledgements

We like to thank Dr. Constantin Daniliuc for the measurement and analysis of the X-ray data. This work was supported by the Romanian National Authority for Scientific Research (EXPLORATORY RESEARCH PROGRAM IDEI-PCE-PROJECT NR. 341-/05.10.2011 – Immunomodulatory Fluoroglycopeptide Molecular Architectures, Ion Neda).

References

1. Jochims, J. C. 1,2,4-Oxadiazoles. In *Five-membered rings with more than two heteroatoms and fused carbocyclic derivatives;* Katritzky, A. R.; Rees, C. W.; Scriven, E. V. F., Eds.; Comprehen-sive Heterocyclic Chemistry II, Vol. 4; Pergamon Press: London, 1996; pp 179–228.
2. Vu, C. B.; Corpuz, E. G.; Merry, T. J.; Pradeepan, S. G.; Bartlett, C.; Bohacek, R. S.; Botfield, M. C.; Eyermann, C. J.; Lynch, B. A.; MacNeil, I. A.; Ram, M. K.; van Schravendijk, M. R.; Violette, S.; Sawyer, T. K. *J. Med. Chem.* **1999,** *42,* 4088–4098. doi:10.1021/jm990229t
3. Carbone, M.; Li, Y.; Irace, C.; Mollo, E.; Castelluccio, F.; Di Pascale, A.; Cimino, G.; Santamaria, R.; Guo, Y.-W.; Gavagnin, M. *Org. Lett.* **2011,** *13,* 2516–2519. doi:10.1021/ol200234r
4. Brogan, J. T.; Stoops, S. L.; Lindsley, C. W. *ACS Chem. Neurosci.* **2012,** *3,* 658–664. doi:10.1021/cn300064r

5. Takemoto, T.; Takagi, N.; Nakajima, T.; Koike, K. *Yakugaku Zasshi* **1975,** *95,* 176–179.
6. Flippen, J. L.; Gilardi, R. D. *Acta Crystallogr., Sect. B* **1976,** *32,* 951–953. doi:10.1107/S0567740876004299
7. Jin, R.; Horning, M.; Mayer, M. L.; Gouaux, E. *Biochemistry* **2002,** *41,* 15635–15643. doi:10.1021/bi020583k
8. Zhang, H.-Z.; Kasibhatla, S.; Kuemmerle, J.; Kemnitzer, W.; Ollis-Mason, K.; Qiu, L.; Crogan-Grundy, C.; Tseng, B.; Drewe, J.; Cai, S. X. *J. Med. Chem.* **2005,** *48,* 5215–5223. doi:10.1021/jm050292k
9. Fujii, S.; Ohta, K.; Goto, T.; Kagechika, H.; Endo, Y. *Bioorg. Med. Chem.* **2009,** *17,* 344–350. doi:10.1016/j.bmc.2008.10.060
10. Boys, M. L.; Schretzman, L. A.; Chandrakumar, N. S.; Tollefson, M. B.; Mohler, S. B.; Downs, V. L.; Penning, T. D.; Russell, M. A.; Wendt, J. A.; Chen, B. B.; Stenmark, H. G.; Wu, H.; Spangler, D. P.; Clare, M.; Desai, B. N.; Khanna, I. K.; Nguyen, M. N.; Duffin, T.; Engleman, V. Q.; Finn, M. B.; Freeman, S. K.; Hanneke, M. L.; Keene, J. L.; Klover, J. A.; Nickols, G. A.; Nickols, M. A.; Steininger, C. N.; Westlin, M.; Westlin, W.; Yu, Y. X.; Wang, Y.; Dalton, C. R.; Norring, S. A. *Bioorg. Med. Chem. Lett.* **2006,** *16,* 839–844. doi:10.1016/j.bmcl.2005.11.008
11. Diana, G. D.; Volkots, D. L.; Nitz, T. J.; Bailey, T. R.; Long, M. A.; Vescio, N.; Aldous, S.; Pevear, D. C.; Dutko, F. J. *J. Med. Chem.* **1994,** *37,* 2421–2436. doi:10.1021/jm00041a022
12. Watjen, F.; Baker, R.; Engelstoff, M.; Herbert, R.; MacLeod, A.; Knight, A.; Merchant, K.; Moseley, J.; Saunders, J.; Swain, C. J.; Wong, E.; Springer, J. P. *J. Med. Chem.* **1989,** *32,* 2282–2291. doi:10.1021/jm00130a010
13. Bezerra, N. M. M.; De Oliveira, S. P.; Srivastava, R. M.; Da Silva, J. R. *Farmaco* **2005,** *60,* 955–960. doi:10.1016/j.farmac.2005.08.003
14. Orlek, B. S.; Blaney, F. E.; Brown, F.; Clark, M. S. G.; Hadley, M. S.; Hatcher, J.; Riley, G. J.; Rosenberg, H. E.; Wadsworth, H. J.; Wyman, P. J. *J. Med. Chem.* **1991,** *34,* 2726–2735. doi:10.1021/jm00113a009
15. Swain, C. J.; Baker, R.; Kneen, C.; Moseley, J.; Saunders, J.; Seward, E. M.; Stevenson, G.; Beer, M.; Stanton, J.; Watling, K. *J. Med. Chem.* **1991,** *34,* 140–151. doi:10.1021/jm00105a021
16. Ankersen, M.; Peschke, B.; Hansen, B. S.; Hansen, T. K. *Bioorg. Med. Chem. Lett.* **1997,** *7,* 1293–1298. doi:10.1016/S0960-894X(97)00216-3
17. Kratz, F.; Müller-Driver, R.; Hofmann, I.; Drevs, J.; Unger, C. *J. Med. Chem.* **2000,** *43,* 1253–1256. doi:10.1021/jm9905864
18. Kratz, F.; Warnecke, A.; Scheuermann, K.; Stockmar, C.; Schwab, J.; Lazar, P.; Drückes, P.; Esser, N.; Drevs, J.; Rognan, D.; Bissantz, C.; Hinderling, C.; Folkers, G.; Fichtner, I.; Unger, C. *J. Med. Chem.* **2002,** *45,* 5523–5533. doi:10.1021/jm020276c
19. Warnecke, A.; Kratz, F. *Bioconjugate Chem.* **2003,** *14,* 377–387. doi:10.1021/bc0256289
20. Kratz, F.; Beyer, U. *Drug Delivery* **1998,** *5,* 281–299. doi:10.3109/10717549809065759
21. Maeda, H.; Wu, J.; Sawa, T.; Matsumura, Y.; Hori, K. *J. Controlled Release* **2000,** *65,* 271–284. doi:10.1016/S0168-3659(99)00248-5
22. Lopez, S.; Castelli, M.; de Campos, F.; Correa, R.; Cechinel Filho, V.; Yunes, R.; Zamora, M.; Enriz, R.; Ribas, J.; Furlan, R.; Zacchino, S. *Arzneim. Forsch.* **2005,** *55,* 123–132.
23. Derita, M.; Castelli, M.; Sortino, M. In *Manual de Técnicas in vitro para la Detección de Compuestos Antifúngicos;* Zacchino, S.; Gupta, M., Eds.; Corpus: Rosario: Argentina, 2007; pp 75–84.
24. Cos, P.; Vlietinck, A.; Vanden Berghe, D.; Maes, L. *J. Ethnopharmacol.* **2006,** *106,* 290–320. doi:10.1016/j.jep.2006.04.003
25. CLSI, *Clinical and Laboratory Standards Institute Document M27-A3*, 3rd ed.; Wayne Ed.; NCCLS: Pennsylvania, 2008; Vol. 28, pp 1–25.
26. CLSI, *Clinical and Laboratory Standards Institute Document M38-A2*, 2nd ed.; Wayne Ed.; NCCLS: Pennsylvania, 2008; Vol. 28, pp 1–35.
27. Sortino, M.; Cechinel Filho, V.; Corrêa, R.; Zacchino, S. *Bioorg. Med. Chem.* **2008,** *16,* 560–568. doi:10.1016/j.bmc.2007.08.030
28. Barret, D. *Biochim. Biophys. Acta* **2002,** *1587,* 224–233. doi:10.1016/S0925-4439(02)00085-6
29. Fujinami, A.; Ozaki, T.; Yamamoto, S. *Agric. Biol. Chem.* **1971,** *35,* 1707–1719. doi:10.1271/bbb1961.35.1707
30. Fujinami, A.; Ozaki, T.; Nodera, K.; Tanaka, K. *Agric. Biol. Chem.* **1972,** *36,* 318–323. doi:10.1271/bbb1961.36.318
31. Rankin, G. O. *Toxicology* **1982,** *23,* 21–31. doi:10.1016/0300-483X(82)90038-5
32. Sugihara, S.; Shinohara, Y.; Miyata, Y.; Inoue, K.; Ito, N. *Lab. Invest.* **1975,** *33,* 219–230.
33. Clapp, L. B. *Adv. Heterocycl. Chem.* **1976,** *20,* 65–116. doi:10.1016/S0065-2725(08)60852-1
34. Maftei, C. V.; Fodor, E.; Mangalgaiu, I.; Jones, P. G.; Daniliuc, C. G.; Franz, M. H.; Neda, I. *Rev. Roum. Chim.* **2010,** *55,* 989–994.
35. Maurer, F.; Fuchs, R.; Erdelen, C.; Turberg, A. Substituierte Pyrazoline als Schädlingsbekämpfungsmittel. WO2003059887 A1, July 24, 2003.
36. Maurer, F.; Erdelen, C.; Reckmann, U. Oxadiazolyl- und Thiadiazolyl-benzoylharnstoffe. Ger. Patent Appl. DE10139721 A1, Feb 27, 2003.
37. Augustine, J. K.; Akabote, V.; Hegde, S. G.; Alagarsamy, P. *J. Org. Chem.* **2009,** *74,* 5640–5643. doi:10.1021/jo900818h
38. Sheldrick, G. M. *Acta Crystallogr., Sect. A* **2008,** *65,* 112–122. doi:10.1107/S0108767307043930
39. Roth, T.; Burger, A. M.; Dengler, W.; Willmann, H.; Fiebig, H. H. Human tumor cell lines demonstrating the characteristics of the patient tumors as useful models for anticancer drug screening. In *Relevance of Tumor Models for Anticancer Drug Development;* Fiebig, H. H.; Burger, A. M., Eds.; Contribution to Oncology, Vol. 54; Karger: Basel, Switzerland, 1999; pp 145–156.
40. Fiebig, H. H.; Dengler, W. A.; Roth, T. Human Tumor Xenografts: Predictivity, Characterization, and Discovery of New Anticancer Agents. In *Relevance of Tumor Models for Anticancer Drug Development;* Fiebig, H. H.; Burger, A. M., Eds.; Contribution to Oncology, Vol. 54; Karger: Basel, Switzerland, 1999; pp 29–50.
41. Fiebig, H. H.; Berger, D. P.; Dengler, W. A.; Wallbrecher, E.; Winterhalter, B. R. *Strahlenther. Onkol.* **1992,** *42,* 321–351.
42. Dengler, W. A.; Schulte, J.; Berger, D. P.; Mertelsmann, R.; Fiebig, H. H. *Anti-Cancer Drugs* **1995,** *6,* 522–532. doi:10.1097/00001813-199508000-00005

License and Terms

This is an Open Access article under the terms of the Creative Commons Attribution License (http://creativecommons.org/licenses/by/2.0), which permits unrestricted use, distribution, and reproduction in any medium, provided the original work is properly cited.

The license is subject to the *Beilstein Journal of Organic Chemistry* terms and conditions: (http://www.beilstein-journals.org/bjoc)

The definitive version of this article is the electronic one which can be found at: doi:10.3762/bjoc.9.259

Beilstein Journal of Organic Chemistry

Elucidation of the regio- and chemoselectivity of enzymatic allylic oxidations with *Pleurotus sapidus* – conversion of selected spirocyclic terpenoids and computational analysis

Verena Weidmann[1], Mathias Schaffrath[2], Holger Zorn[3], Julia Rehbein[*4] and Wolfgang Maison[*1]

Full Research Paper

Open Access

Address:
[1]Department of Chemistry, University of Hamburg, Bundesstr. 45, 20146 Hamburg, Germany, [2]LGCR Chemistry, Sanofi-Aventis Deutschland GmbH, 65926 Frankfurt am Main, Germany, [3]Justus-Liebig-University Giessen, Institute of Food Chemistry and Food Biotechnology, Heinrich-Buff-Ring 58, 35392 Gießen and [4]Department of Chemistry, University of Hamburg, Martin-Luther-King-Platz 6, 20146 Hamburg, Germany

Email:
Julia Rehbein[*] - rehbein@chemie.uni-hamburg.de;
Wolfgang Maison[*] - maison@chemie.uni-hamburg.de

* Corresponding author

Keywords:
allylic oxidation; CH-activation; chiral separation; enones; flavors; natural products; terpenes

Beilstein J. Org. Chem. **2013,** *9,* 2233–2241.
doi:10.3762/bjoc.9.262

Received: 08 August 2013
Accepted: 10 October 2013
Published: 29 October 2013

This article is part of the Thematic Series "Natural products in synthesis and biosynthesis".

Guest Editor: J. S. Dickschat

© 2013 Weidmann et al; licensee Beilstein-Institut.
License and terms: see end of document.

Abstract

Allylic oxidations of olefins to enones allow the efficient synthesis of value-added products from simple olefinic precursors like terpenes or terpenoids. Biocatalytic variants have a large potential for industrial applications, particularly in the pharmaceutical and food industry. Herein we report efficient biocatalytic allylic oxidations of spirocyclic terpenoids by a lyophilisate of the edible fungus *Pleurotus sapidus*. This ''mushroom catalysis'' is operationally simple and allows the conversion of various unsaturated spirocyclic terpenoids. A number of new spirocyclic enones have thus been obtained with good regio- and chemoselectivity and chiral separation protocols for enantiomeric mixtures have been developed. The oxidations follow a radical mechanism and the regioselectivity of the reaction is mainly determined by bond-dissociation energies of the available allylic CH-bonds and steric accessibility of the oxidation site.

Introduction

Selective oxidations of CH-bonds are attractive synthetic transformations with a broad spectrum of applications in academia and a high impact on the industrial chemical value chain as they convert relatively cheap precursors into value-added products [1,2]. Among these transformations, allylic oxidations are of high interest because the olefinic starting materials are readily

available as cheap bulk chemicals and many interesting derivatives such as terpenes are available from renewable sources [3-5]. In addition, the resulting allyl alcohols [6-10] or α,β-unsaturated carbonyl compounds are attractive synthetic targets of high economic and scientific interest [11-17]. Allylic oxidations of olefins to enones have classically been performed with strong oxidants such as chromium or other metal-based reagents [18,19]. In addition, metal-free and biocatalytic methods have been reported [5]. Several of these biocatalytic protocols have been applied to the synthesis of fine chemicals [20-22], drugs [23], and food ingredients [24-26]. A particularly interesting biocatalytic system for allylic oxidation is the edible fungus *Pleurotus sapidus* (PSA), which is able to oxidize selected terpenes and fatty acids [27-31]. We have recently shown that the lyophilisate of PSA is able to affect allylic and benzylic oxidations in a broad range of olefinic substrates including simple cyclohexene derivatives and several functionalized terpenoids (Figure 1) [32].

Biocatalytic allylic oxidations with PSA may be performed with the lyophilisate from submerged cultures. Cyclic alkenes and particularly cyclohexene derivatives are the preferred substrates of PSA. A PSA-derived dioxygenase has been shown to be responsible for the allylic oxidation of valencene to nootkatone, and the same enzyme oxidizes unsaturated fatty acids [29,31]. It is thus likely that this dioxygenase is the major oxidant in other allylic oxidations with PSA-lyophilisate, too. However, since the lyophilisate is a mixture of enzymes, alternative oxidation pathways cannot be ruled out for other substrates. Reviewing the available examples for PSA-mediated conversions in the literature, the regio- and chemoselectivity of these oxidations seems to be determined by the radical mechanism of the reactions and would thus follow well-established rules for other radical-type allylic oxidations [33-36].

A notable example of an allylic oxidation with PSA is the conversion of theaspirane (**1**), a spirocyclic flavor compound of tea, vanilla and different fruits [37] to the corresponding theaspirone (**2**) (Scheme 1) [32].

The reaction is quite clean and gives the enone **2** in good yield along with minor amounts of the corresponding allyl alcohol **3** and the epoxide **4a**. This successful conversion of theaspirane (**1**) encouraged us to investigate the oxidation of other spirocyclic terpenoids. Many oxidized spiroethers are valuable flavor compounds or have other interesting biological properties such as phytotoxic activity. A few selected examples are depicted in Figure 2.

In this paper, we report biocatalytic allylic oxidations of spirocyclic model compounds and of the natural product vitispirane with the lyophilisate of PSA. A rationalization of the observed selectivity is provided by means of computational determination of bond-dissociation enthalpies and correlation with structural and electronic features. In addition, a short synthesis of vitispirane is presented.

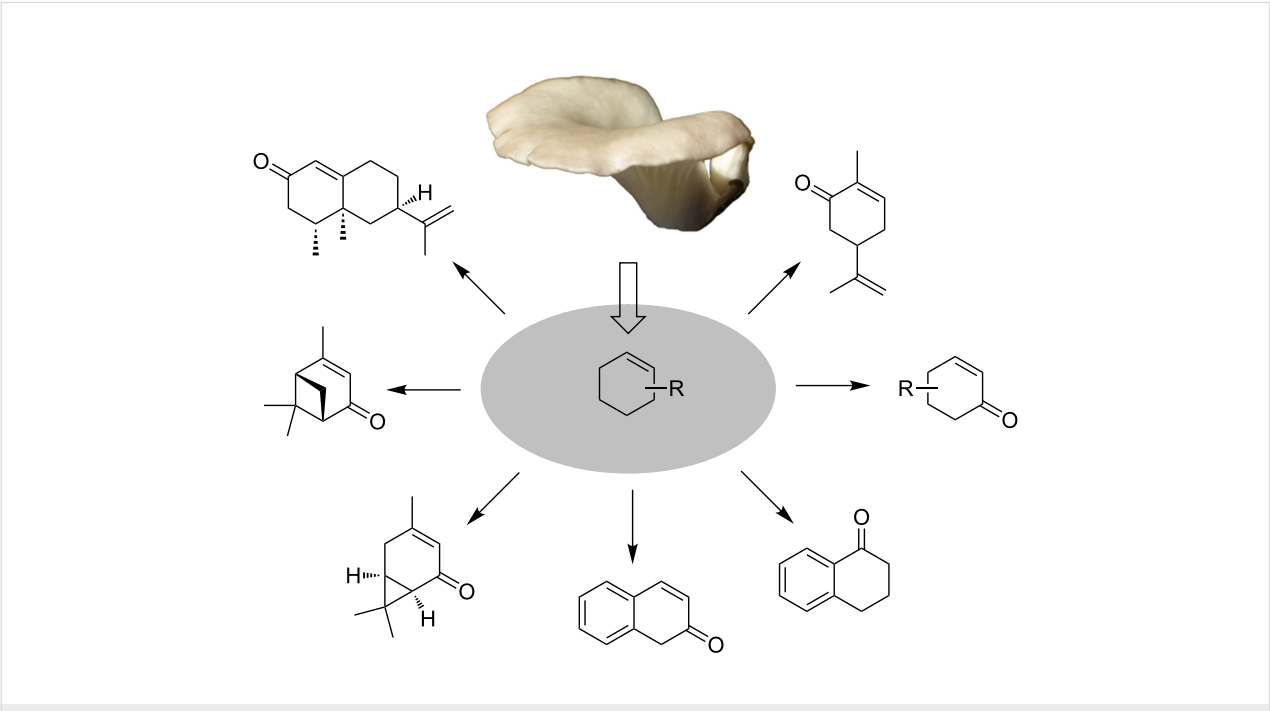
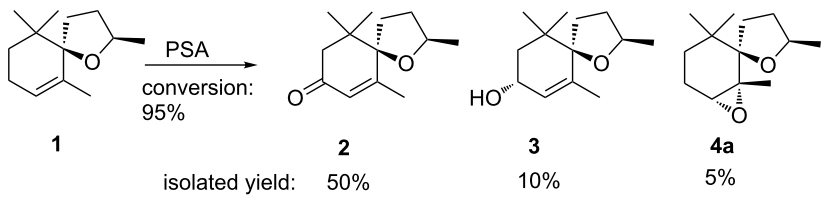


Figure 1: Selected biocatalytic allylic and benzylic oxidations with the lyophilisate of *Pleurotus sapidus* (PSA).



Scheme 1: Biocatalytic allylic oxidation of theaspirane (**1**) with lyophilisates of PSA. Only one enantiomer of racemic compounds is shown.

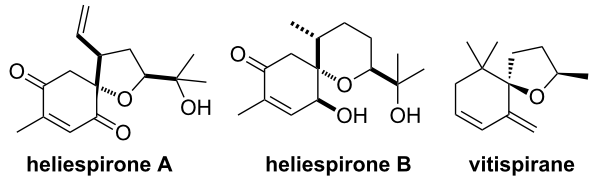


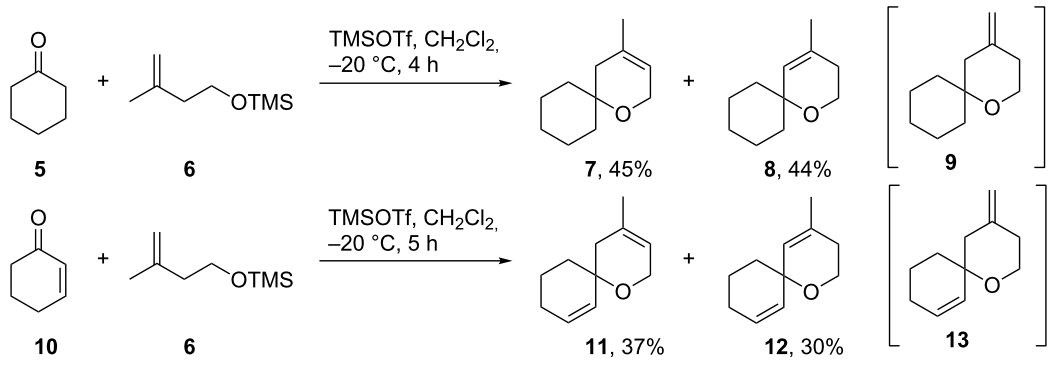
Figure 2: Selected bioactive terpenoids based on spiroether backbones [38,39].

Results and Discussion

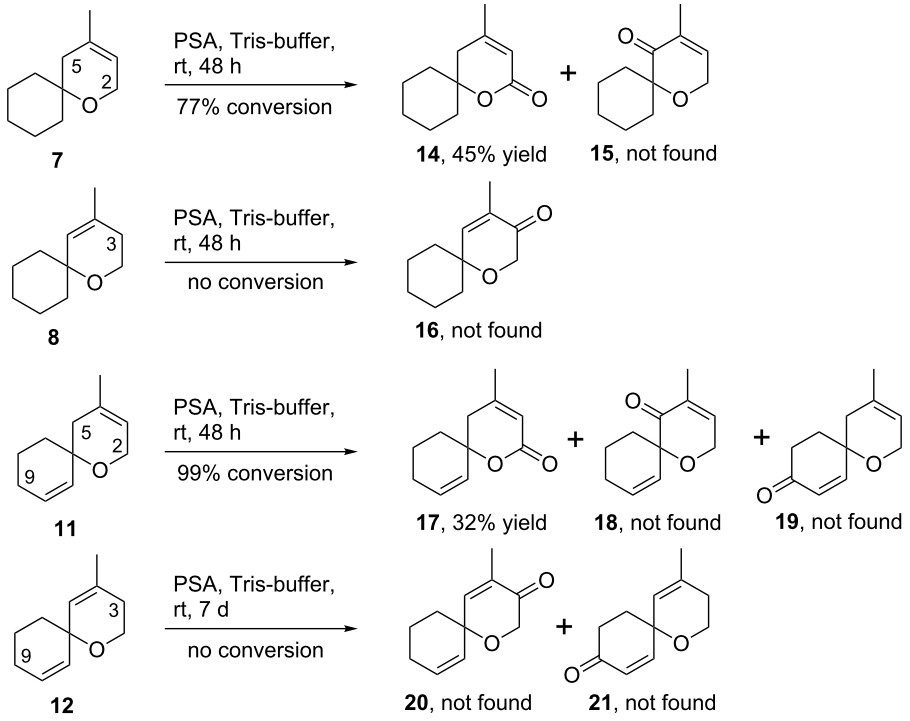
Allylic spiroethers, such as theaspirane (**1**) (Scheme 1) are suitable substrates for allylic oxidations with PSA. Due to their interesting properties as flavor compounds, we focused our attention to the oxidation of terpenoid spiroethers. As model compounds, unsaturated spiroethers **7**, **8**, **11** and **12** were synthesized by the intramolecular silyl-modified Sakurai reaction of precursors **5** and **10** and alkene **6** (Scheme 2). Two pairs of regioisomeric endocyclic derivatives **7**, **8** and **11**, **12** were obtained as the major products of cyclization in a 1:1 mixture. The third regioisomer **9** and **13** respectively, with an exocyclic double bond was observed in minor amounts only. Separation of the regioisomeric spiroethers by column chromatography proved to be difficult, and in both cases only the two major isomers with endocyclic double bonds were isolated in pure form. The regioisomeric spiroethers **7**, **8**, **11** and **12** are interesting model compounds for the allylic oxidation with PSA because they contain allylic positions with different stereoelectronic properties.

All four spiroethers **7**, **8**, **11** and **12** were submitted to identical conditions and were treated with PSA lyophilisate in Tris-buffer at room temperature (Scheme 3). The reactions were monitored by GC. The oxidation of allyl ether **7** may follow two alternative pathways either to the α,β-unsaturated lactone **14** or to the enone **15** (allylic oxidations at exocyclic positions are generally less favorable if radical mechanisms are operating) [35]. Due to sterical hindrance at position 5 and the strong activation for hydrogen abstraction in position 2, spiroether **7** was selectively converted to the spirolactone **14**. The alternative oxidation product **15** was not found by GC–MS. The regioisomeric spiroether **8** offers only one plausible path for allylic oxidation in position 3. However, this spiroether was not converted at all and the starting material **8** was recovered almost quantitatively from the reaction mixture. This finding may reflect the increased sterical hindrance of the allylic position in **8** compared to the site of oxidation in regioisomer **7** and a less stable radical intermediate.

Similar results were obtained for oxidation of spiroethers **11** and **12** which contain two separated double bonds. The allyl ether **11** allows three plausible oxidation products **17**–**19**. However, due to our experiences with oxidations of **7**, **8** and



Scheme 2: Intramolecular silyl modified Sakurai reaction to spiroethers **7**–**9** and **11**–**13**.



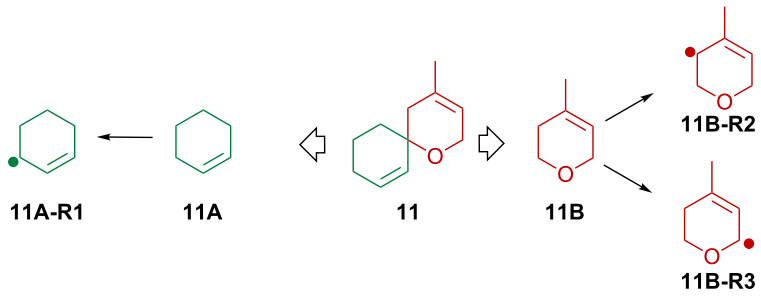
Scheme 3: Biocatalytic allylic oxidation of spiroethers **7**, **8**, **11** and **12** with the lyophilisate of PSA. Conversion was measured by GC and yields are given after isolation of the oxidation products and purification by chromatography.

theaspirane (**1**), position 2 should be activated most strongly for hydrogen abstraction and should thus be privileged for oxidation. As a consequence, the α,β-unsaturated lactone **17** is indeed the major product along with some unidentified more complex oxidation products. Again, oxidation in 5-position of **11** to the enone **18** was not observed. In addition, the allylic hydrogens in 9-position are obviously also of low reactivity and the corresponding oxidation product **19** was also not detectable. In agreement with the oxidation of **8**, substrate **12** was not oxidized by PSA at all and the starting material was reisolated almost quantitatively.

Computational analysis (for full computational details see Supporting Information File 1) of relative radical stabilities and bond-dissociation enthalpies (BDH_{298}) based on DFT (B3LYP/6-31+G** and B3LYP/6-31G* + PCM) and composite method (CBS-QB3) calculations enable a quantification and visual rationalization of the observed experimental results. Since PCM and gas phase results do not differ significantly neither in terms of geometry nor energy, we will restrict the discussion to gas phase values only unless otherwise stated (for details of the PCM results see Supporting Information File 1). The CBS-QB3 method has been used to obtain accurate energies and to evaluate the DFT-energies in terms of relative and absolute values. For this comparison CBS-QB3 has been applied to model structures **11A** and **11B** that contain key structural features of **11** and **12** (Table 1). According to the data summarized in Table 1 and Table 2 B3LYP/6-31+G** gives reasonable results and is a suitable method to predict at least relative BDH-values of C–H bonds of the spiro compounds at hand. In absolute terms, B3LYP underestimates the BDH systematically by 2.9–4.6 kcal/mol.

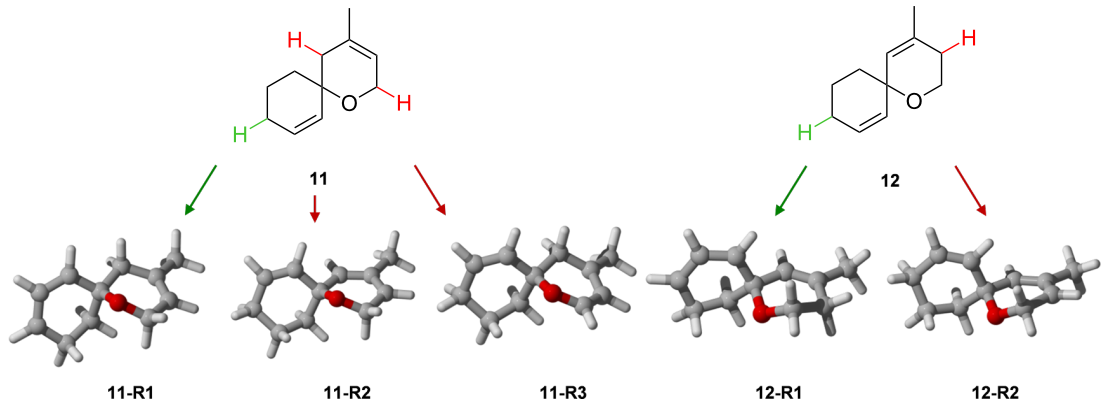
The experimental observation as summarized in Scheme 3, e.g., the selective oxidation in 2-position of an allyl ether subunit may be rationalized by the particularly low BDH_{298} for the corresponding C–H bond compared to the other allylic C–H bonds (Table 2). Carbon-centered radicals adjacent to an oxygen atom are commonly known to be stabilized as they benefit from inductive effects as well as from orbital interactions of the p-type lone pair of the oxygen atom with the half-filled p-orbital of the mainly sp^2 hybridized radical [40]. The picture of the SOMO and the mapped out spin density of **11-R3** illustrate the latter effect (Figure 3). In addition, the methyl group in 3-position of the allylic system in **11-R3** as well as in the model system **11B-R3** helps to stabilize the radical further, mainly by hyperconjugation. In total, both substituent effects result in a rather low C–H bond-dissociation enthalpy of 79.5 kcal/mol at CBS-QB3 level of theory (74.9 kcal/mol B3LYP/6-31+G**, Table 2).

Table 1: Model substrates **11A** and **11B** that allowed a determination of accurate BDH_{298} values with the CBS-QB3 method.



entry	compd	CBS-QB3	
		BDH_{298} [kcal/mol]	ΔG [kcal/mol]
1	**11A-R1**	83.5	75.0
2	**11B-R2**	86.9	77.4
3	**11B-R3**	79.5	70.8

Table 2: Optimized geometries and BDH_{298} values of radicals derived from **11** and **12** for gas phase and PCM calculations.



entry	compd	B3LYP/6-31+G**			B3LYP/6-31G* + PCM		
		ΔH^a [kcal/mol]	ΔG^a [kcal/mol]	BDH_{298} [kcal/mol]	ΔH^a [kcal/mol]	ΔG^a [kcal/mol]	BDH_{298} [kcal/mol]
1	**11**	1.2	1.3	—	1.0	1.2	—
2	**11-R1**	−1.5	−0.2	80.9	−1.9	−0.3	81.6
3	**11-R2**	0.5	0.7	82.9	0.3	0.7	83.7
4	**11-R3**	−7.5	−6.4	74.9	−7.8	0.0	74.6
5	**12**	0.0	0.0	—	0.0	0.0	—
6	**12-R1**	−3.3	−2.1	80.3	3.4	2.0	80.1
7	**12-R2**	0.0	0.0	83.6	0.0	0.0	83.4

[a]Referring to **12** for closed-shell species and **12-R2** for radicals.

Compared to the other potential allylic radicals like **11-R1** and **11-R2**, **11-R3** is up to 8 kcal/mol more stable. Within the subset of allylic radicals that differ only by their alkyl substitution pattern (**11-R1**, **11-R2**, **12-R1** and **12-R2**) the energetic differences are less pronounced. Equally, the reasons for the small variations in BDH_{298} values are more subtle and might be referred to additional steric strain imposed by a change in hybridization of the carbon atom from sp^3 to sp^2 upon radical

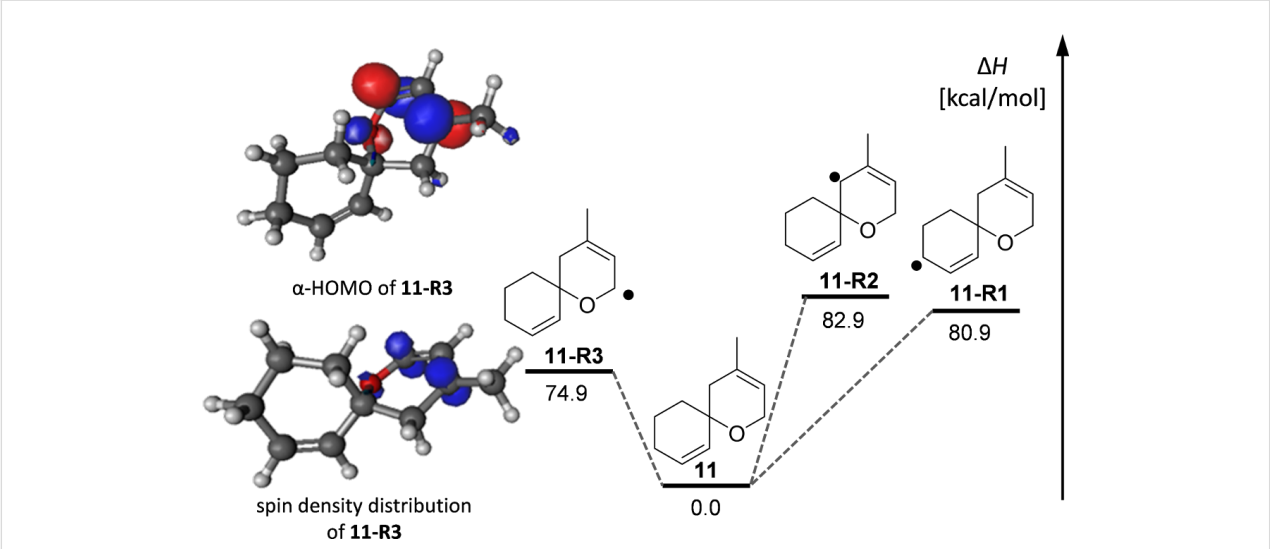


Figure 3: Bond-dissociation enthalpies for three allylic C–H bonds in **11**. Double stabilization of the radical in **11-R3** by the adjacent oxygen and hyperconjugation lead to a rather low BDH of 74.9 kcal/mol (B3LYP/6-31+G**).

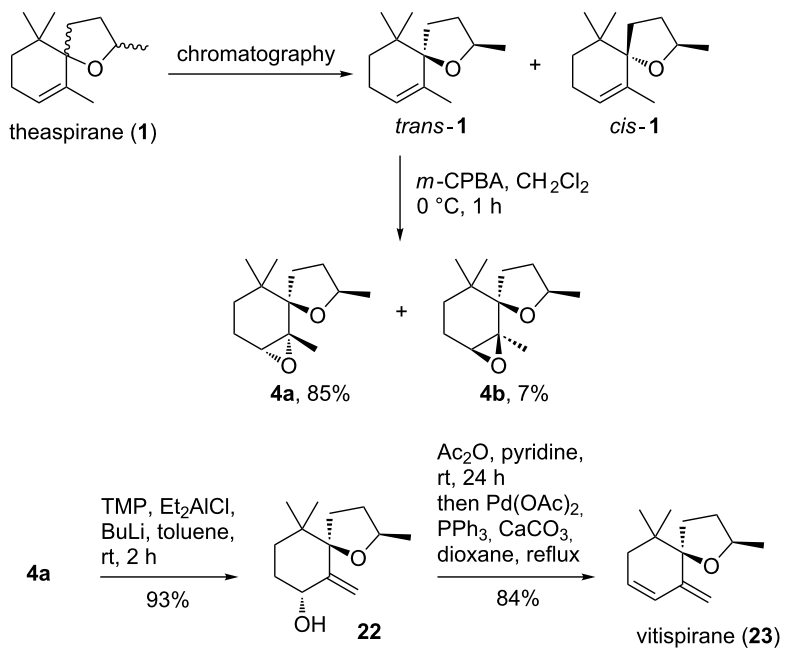
formation and hyperconjugation effects (Table 2). Correlating the experimental observations with the computational results, one can deduce that a BHD_{298} of around 80 kcal/mol (CBS-QB3) seems to be a threshold that might be used as a guideline to decide whether an allylic oxidation of spiro compounds related to **11** and **12** with PSA takes places or not.

As a further test on the substrate scope of the reaction, we were interested in the biocatalytic oxidation of vitispirane as a terpenoid with a conjugated double bond and a sterically hindered allylic position (Figure 2). Vitispirane is a flavor compound of vanilla and quince fruit and was identified in grape juice and wine [41,42]. Various syntheses of vitispirane have been reported in the literature [43-45]. To get sufficient quantity of the oxidation precursor, we focused on a strategy reported by Ohloff starting from commercially available theaspirane (**1**) [46]. As described by Ohloff and coworkers, the separation of vitispirane diastereoisomers is quite difficult. Therefore we decided to start with diastereomerically pure theaspirane (*trans*-**1**) that was obtained by chromatographic separation of the commercial diastereomeric mixture of *cis*- and *trans*-theaspirane (**1**). As depicted in Scheme 4, *trans*-theaspirane (*trans*-**1**) was converted to the corresponding epoxides **4a** and **4b** following the literature protocol using *m*-chloroperbenzoic acid. The major epoxide **4a** was obtained in good yield and a diastereoselectivity of 11:1.

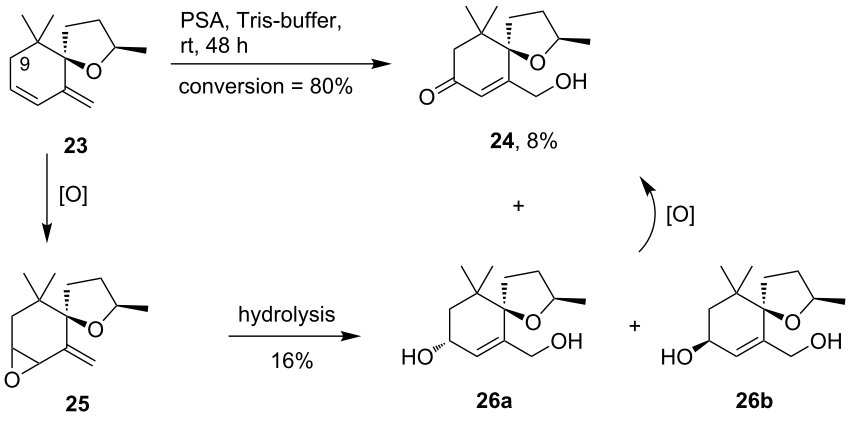
Isomerisation of epoxide **4a** to allyl alcohol **22** was reported with aluminium triisopropoxide at 140 °C [46]. However, in our hands this procedure gave only complex reaction mixtures containing minor amounts of the target allyl alcohol **22**. In an alternative protocol, we used Yamamoto´s conditions [47] for the isomerization of epoxides (TMP, *n*-BuLi, Et_2AlCl) and obtained allyl alcohol **22** in excellent 93% yield. The conversion of allyl alcohol **22** to vitispirane (**23**) has been reported with $POCl_3$ in pyridine. Again, this known protocol did not work satisfactory for us resulting in only minor amounts of the desired vitispirane (**23**). As a consequence, we decided to use an alternative method via acetylation and Pd-catalyzed elimination. This conversion gave vitispirane (**23**) in good yield [48]. Overall, this improved protocol gave racemic vitispirane (**23**) in three steps from theaspirane (*trans*-**1**) in excellent 72% overall yield. It should be noted that the gas chromatographic separation of racemic vitispirane (**23**) has been reported by Schreier [45]. In addition, we have been able to separate racemic vitispirane by HPLC on a chiral stationary phase (see Supporting Information File 1).

Vitispirane (**23**) is a challenging substrate for allylic oxidation with PSA. As outlined above, the oxidation with PSA is quite sensitive to steric and electronic factors and the allylic position 9 in vitispirane (**23**) is sterically hindered (Scheme 5).

Treatment of vitispirane (**23**) with PSA was indeed not a clean conversion giving a number of different oxidation products. From this mixture, however, three main products **24**, **26a** and **26b** were identified unambiguously. So far, we have never detected similar oxidation products with PSA and rationalize their formation by an initial epoxidation of the endocyclic double bond to give the allyl epoxide **25**, which might then be hydrolyzed to two diastereomeric alcohols **26a** and **26b**. The latter reaction is known for similar allyl epoxides under slightly



Scheme 4: Improved 3-step synthesis of vitispirane (**23**) from theaspirane (**1**). Only one enantiomer of racemic compounds is shown.



Scheme 5: Oxidation of vitispirane (**23**) with PSA gave enone **24** and two diastereomeric allyl alcohols **26a** and **26b**. A putative intermediate is epoxide **25**, which upon hydrolysis would give allyl alcohols **26a** and **26b**. Oxidation of the latter might provide enone **24**. Only one enantiomer of racemic compounds is shown.

acidic conditions [49]. However, participation of hydrolases from the PSA lyophilisate is also possible. A fraction of the resulting alcohols **26** would then finally be oxidized to give enone **24**. Support for an epoxide intermediate comes from oxidations of substrates containing similarly hindered allylic CH-bonds. For β-ionone, for example, we have previously observed epoxidation to be the major oxidation pathway.

It should be noted, that all three compounds **24**, **26a** and **26b** are new derivatives of vitispirane **24** with potentially interesting properties as flavors. The relative stereochemistry of **26a** and **26b** was evaluated after HPLC separation of the two diastereoisomers by 2D-NOESY NMR.

The compounds **24**, **26a** and **26b** were obtained as racemic mixtures. However, we found HPLC protocols for the sep-

aration of these terpenoids with commercial chiral stationary phases (see Supporting Information File 1). This allows the isolation of large quantities of the enantiomerically pure derivatives and their detailed olfactory analysis.

Conclusion

The edible fungus PSA allows efficient allylic oxidations of terpenoid olefins. The oxidation protocols are quite simple, because the lyophilisate of PSA can be used as a catalyst. In this paper we have investigated the substrate scope of these biocatalytic oxidations with a special focus on spiroether derivatives due to their high relevance as flavor compounds. Several new spirocyclic model compounds and the natural product vitispirane (**23**) were synthesized and submitted to oxidation with PSA. The outcome of these oxidations was found to be dependent on steric and electronic factors of the substrate. The reactivity of most terpenoids towards allylic oxidation with PSA can thus be estimated using the same rules established for conventional radical oxidations: The reactivity is determined by bond-dissociation energies of the allylic CH-bonds. Correlating the experimental observations of this study with computational results we deduced a threshold BHD_{298} of around 80 kcal/mol as a guideline to decide whether an allylic oxidation with PSA takes places or not.

Allyl spiroethers **7** and **11** were oxidized to the corresponding α,β-unsaturated lactone derivatives **14** and **17**, whereas the close derivatives **8** and **12** containing slightly less reactive allylic C–H bonds were not converted by PSA at all. The natural product vitispirane (**23**) was oxidized by PSA, and three new vitispirane derivatives **24**, **26a** and **26b** were isolated. In this case, the oxidation pathway is not favoring products of allylic oxidation but most likely those of epoxidation with subsequent hydrolysis of the epoxide. HPLC protocols with chiral stationary phases allow the separation of racemic mixtures of oxidized vitispirane derivatives.

Supporting Information

Supporting Information File 1

Computational details, experimental procedures, analytical data, NMR spectra and chromatograms of new compounds.
[http://www.beilstein-journals.org/bjoc/content/supplementary/1860-5397-9-262-S1.pdf]

Acknowledgements

H. Zorn would like to thank the DFG and the State of Hesse for funding the GC system (INST 162/381-1 FUGG) and the excellence initiative of the Hessian Ministry of Science and Art for the generous grant for the LOEWE research focus “integrative fungal research”. M. Schaffrath would like to thank Peter Hamley and Martin Will from Sanofi for their support.

References

1. Roduner, E.; Kaim, W.; Sarkar, B.; Urlacher, V. B.; Pleiss, J.; Gläser, R.; Einicke, W.-D.; Sprenger, G. A.; Beifuß, U.; Klemm, E.; Liebner, C.; Hieronymus, H.; Hsu, S.-F.; Plietker, B.; Laschat, S. *ChemCatChem* **2013,** *5,* 82–112. doi:10.1002/cctc.201200266
2. Newhouse, T.; Baran, P. S. *Angew. Chem., Int. Ed.* **2011,** *50,* 3362–3374. doi:10.1002/anie.201006368
3. Page, P. C. B.; McCarthy, T. J. 2.1 - Oxidation Adjacent to C=C Bonds. In *Comprehensive Organic Synthesis;* Trost, B. M.; Fleming, I., Eds.; Pergamon: Oxford, 1991; Vol. 7, pp 83–117. doi:10.1016/B978-0-08-052349-1.00184-0
4. Nakamura, A.; Nakada, M. *Synthesis* **2013,** *45,* 1421–1451. doi:10.1055/s-0033-1338426
5. Weidmann, V.; Maison, W. *Synthesis* **2013,** *45,* 2201–2221. doi:10.1055/s-0033-1338491
6. Kharasch, M. S.; Sosnovsky, G. *J. Am. Chem. Soc.* **1958,** *80,* 756. doi:10.1021/ja01536a062
7. Andrus, M. B.; Lashley, J. C. *Tetrahedron* **2002,** *58,* 845–866. doi:10.1016/S0040-4020(01)01172-3
8. Rispens, M. T.; Zondervan, C.; Feringa, B. L. *Tetrahedron: Asymmetry* **1995,** *6,* 661–664. doi:10.1016/0957-4166(95)00054-S
9. Moiseev, I. I.; Vargaftik, M. N. *Coord. Chem. Rev.* **2004,** *248,* 2381–2391. doi:10.1016/j.ccr.2004.05.020
10. Christie, S. D. R.; Warrington, A. D. *Synthesis* **2008,** 1325–1341. doi:10.1055/s-2008-1067031
11. Joseph, T.; Sawant, D. P.; Gopinath, C. S.; Halligudi, S. B. *J. Mol. Catal. A: Chem.* **2002,** *184,* 289–299. doi:10.1016/S1381-1169(02)00010-9
12. Smith, A. B., III; Konopelski, J. P. *J. Org. Chem.* **1984,** *49,* 4094–4095. doi:10.1021/jo00195a055
13. Berger, R. G. *Biotechnol. Lett.* **2009,** *31,* 1651–1659. doi:10.1007/s10529-009-0083-5
14. Hanson, J. R. *Nat. Prod. Rep.* **2007,** *24,* 1342–1349. doi:10.1039/b705948p
15. Fraatz, M. A.; Berger, R. G.; Zorn, H. *Appl. Microbiol. Biotechnol.* **2009,** *83,* 35–41. doi:10.1007/s00253-009-1968-x
16. Salvador, J. A. R.; Silvestre, S. M.; Moreira, V. M. *Curr. Org. Chem.* **2012,** *16,* 1243–1276. doi:10.2174/138527212800564204
17. Salvador, J. A. R.; Silvestre, S. M.; Moreira, V. M. *Curr. Org. Chem.* **2006,** *10,* 2227–2257. doi:10.2174/138527206778742641
18. Muzart, J. *Chem. Rev.* **1992,** *92,* 113–140. doi:10.1021/cr00009a005
19. Muzart, J. *Mini-Rev. Org. Chem.* **2009,** *6,* 9–20. doi:10.2174/157019309787316120
20. Çelik, A.; Flitsch, S. L.; Turner, N. J. *Org. Biomol. Chem.* **2005,** *3,* 2930–2934. doi:10.1039/b506159h
21. Bellucci, G.; Chiappe, C.; Pucci, L.; Gervasi, P. G. *Chem. Res. Toxicol.* **1996,** *9,* 871–874. doi:10.1021/tx9600053
22. Straathof, A. J. J.; Panke, S.; Schmid, A. *Curr. Opin. Biotechnol.* **2002,** *13,* 548–556. doi:10.1016/S0958-1669(02)00360-9
23. Tao, J.; Xu, J.-H. *Curr. Opin. Chem. Biol.* **2009,** *13,* 43–50. doi:10.1016/j.cbpa.2009.01.018
24. Fraatz, M. A.; Riemer, S. J. L.; Stöber, R.; Kaspera, R.; Nimtz, M.; Berger, R. G.; Zorn, H. *J. Mol. Catal. B: Enzym.* **2009,** *61,* 202–207. doi:10.1016/j.molcatb.2009.07.001

25. Janssens, L.; De Pooter, H. L.; Schamp, N. M.; Vandamme, E. J. *Process Biochem.* **1992,** *27,* 195–215. doi:10.1016/0032-9592(92)80020-4
26. Kirk, O.; Borchert, T. V.; Fuglsang, C. C. *Curr. Opin. Biotechnol.* **2002,** *13,* 345–351. doi:10.1016/S0958-1669(02)00328-2
27. Onken, J.; Berger, R. G. *J. Biotechnol.* **1999,** *69,* 163–168. doi:10.1016/S0168-1656(99)00040-1
28. Krings, U.; Lehnert, N.; Fraatz, M. A.; Hardebusch, B.; Zorn, H.; Berger, R. G. *J. Agric. Food Chem.* **2009,** *57,* 9944–9950. doi:10.1021/jf901442q
29. Krügener, S.; Krings, U.; Zorn, H.; Berger, R. G. *Bioresour. Technol.* **2010,** *101,* 457–462. doi:10.1016/j.biortech.2009.08.087
30. Zelena, K.; Krings, U.; Berger, R. G. *Bioresour. Technol.* **2012,** *108,* 231–239. doi:10.1016/j.biortech.2011.12.097
31. Plagemann, I.; Zelena, K.; Arendt, P.; Ringel, P. D.; Krings, U.; Berger, R. G. *J. Mol. Catal. B: Enzym.* **2013,** *87,* 99–104. doi:10.1016/j.molcatb.2012.11.004
32. Rickert, A.; Krombach, V.; Hamers, O.; Zorn, H.; Maison, W. *Green Chem.* **2012,** *14,* 639–644. doi:10.1039/c2gc16317a
33. Wiberg, K. B.; Nielsen, S. D. *J. Org. Chem.* **1964,** *29,* 3353–3361. doi:10.1021/jo01034a055
34. Dauben, W. G.; Lorber, M. E.; Fullerton, D. S. *J. Org. Chem.* **1969,** *34,* 3587–3592. doi:10.1021/jo01263a079
35. Rothenberg, G.; Sasson, Y. *Tetrahedron* **1998,** *54,* 5417–5422. doi:10.1016/S0040-4020(98)00215-4
36. Howard, J. A.; Ingold, K. U. *Can. J. Chem.* **1967,** *45,* 793–802. doi:10.1139/v67-132
37. Kaiser, R.; Kappeler, A.; Lamparsky, D. *Helv. Chim. Acta* **1978,** *61,* 387–400. doi:10.1002/hlca.19780610136
38. Macías, F. A.; Galindo, J. L. G.; Varela, R. M.; Torres, A.; Molinillo, J. M. G.; Fronczek, F. R. *Org. Lett.* **2006,** *8,* 4513–4516. doi:10.1021/ol061673a
39. Huang, C.; Liu, B. *Chem. Commun.* **2010,** *46,* 5280–5282. doi:10.1039/c0cc00481b
40. Laarhoven, L. J. J.; Mulder, P.; Wayner, D. D. M. *Acc. Chem. Res.* **1999,** *32,* 342–349. doi:10.1021/ar9703443
41. Humpf, H. U.; Wintoch, H.; Schreier, P. *J. Agric. Food Chem.* **1992,** *40,* 2060–2062. doi:10.1021/jf00023a006
42. Kato, T.; Kondo, H. *Bull. Chem. Soc. Jpn.* **1981,** *54,* 1573–1574. doi:10.1246/bcsj.54.1573
43. Marschall, H.; Penninger, J.; Weyerstahl, P. *Liebigs Ann. Chem.* **1982,** 68–72. doi:10.1002/jlac.198219820107
44. Nilsson, Y. I. M.; Aranyos, A.; Andersson, P. G.; Bäckvall, J.-E.; Parrain, J.-L.; Ploteau, C.; Quintard, J.-P. *J. Org. Chem.* **1996,** *61,* 1825–1829. doi:10.1021/jo9505031
45. Herion, P.; Full, G.; Winterhalter, P.; Schreier, P.; Bicchi, C. *Phytochem. Anal.* **1993,** *4,* 235–239. doi:10.1002/pca.2800040509
46. Schulte-Elte, K. H.; Gautschi, F.; Renold, W.; Hauser, A.; Frankhauser, P.; Limacher, J.; Ohloff, G. *Helv. Chim. Acta* **1978,** *61,* 1125–1133. doi:10.1002/hlca.19780610326
47. Yasuda, A.; Yamamoto, H.; Nozaki, H. *Bull. Chem. Soc. Jpn.* **1979,** *52,* 1705–1708. doi:10.1246/bcsj.52.1705
48. Hauser, F. M.; Tommasi, R.; Hewawasam, P.; Rho, Y. S. *J. Org. Chem.* **1988,** *53,* 4886–4887. doi:10.1021/jo00255a047
49. Valverde, S.; Lopez, J. C.; Rabanal, R. M.; Escudero, J. *Tetrahedron* **1986,** *42,* 573–582. doi:10.1016/S0040-4020(01)87456-1

License and Terms

This is an Open Access article under the terms of the Creative Commons Attribution License (http://creativecommons.org/licenses/by/2.0), which permits unrestricted use, distribution, and reproduction in any medium, provided the original work is properly cited.

The license is subject to the *Beilstein Journal of Organic Chemistry* terms and conditions: (http://www.beilstein-journals.org/bjoc)

The definitive version of this article is the electronic one which can be found at: doi:10.3762/bjoc.9.262

Beilstein Journal of Organic Chemistry

Cyclopamine analogs bearing exocyclic methylenes are highly potent and acid-stable inhibitors of hedgehog signaling

Johann Moschner[1], Anna Chentsova[1], Nicole Eilert[1], Irene Rovardi[1], Philipp Heretsch[*2] and Athanassios Giannis[*1]

Full Research Paper

Open Access

Address:
[1]Universität Leipzig, Institut für Organische Chemie, Johannisallee 29, D-04103 Leipzig, Germany and [2]Rice University, Department of Chemistry, BioScience Research Collaborative, 6500 Main St., Houston, Texas 77030, USA

Email:
Philipp Heretsch[*] - heretsch@rice.edu; Athanassios Giannis[*] - giannis@uni-leipzig.de

* Corresponding author

Keywords:
cyclopamine; hedgehog signaling pathway; natural products; steroidal alkaloids; structure–activity relationship

Beilstein J. Org. Chem. **2013,** *9,* 2328–2335.
doi:10.3762/bjoc.9.267

Received: 16 August 2013
Accepted: 15 October 2013
Published: 31 October 2013

This article is part of the Thematic Series "Natural products in synthesis and biosynthesis".

Guest Editor: J. S. Dickschat

© 2013 Moschner et al; licensee Beilstein-Institut.
License and terms: see end of document.

Abstract

The chemical synthesis and biological evaluation of new cyclopamine analogs bearing exocyclic methylenes in different positions is described. Bis-*exo*-cyclopamine **6** was identified as a potent inhibitor of the Gli1-dependent luciferase expression in Shh-LIGHTII cells. An extension of this study to F-ring-modified structures shows the necessity of a rigidly positioned nitrogen atom for bioactivity as well as the presence of the C21 methyl group for acid stability and bioactivity.

Introduction

Hedgehog signaling is involved in embryonic development and plays an important role in the maintenance of stem cells, tissue repair and regeneration in adult organisms [1-4]. The erroneous activation of hedgehog signaling is tightly associated with the occurrence of basal cell carcinoma and medulloblastoma [5]. In addition, several other tumors are co-dependent on hedgehog signaling, examples for this type are cancers of the skin [6,7], brain [8,9], lung [10], pancreas [11], breast [12], prostate [13,14], colon [15], rhabdomyosarcoma [16], lymphoma [17-19], multiple myeloma [17,20], and chronic myeloic leukemia [21-23]. More recently, other diseases like diabetes [24,25], neurodegenerative disorders [26], and trisomy [27,28], have been linked with hedgehog signaling.

Cyclopamine (**1**, see Figure 1) was the first inhibitor of the hedgehog signaling pathway to be identified. As a highly selec-

tive inhibitor of the transmembrane protein Smoothened (Smo), an integral component of hedgehog signaling, it presents an attractive target for medicinal and pharmaceutical research [29,30]. Unfortunately, its direct development into a drug is hampered by its low metabolic stability (decomposition at pH < 3) [31] and rather moderate potency (IC_{50} ~ 5 μM).

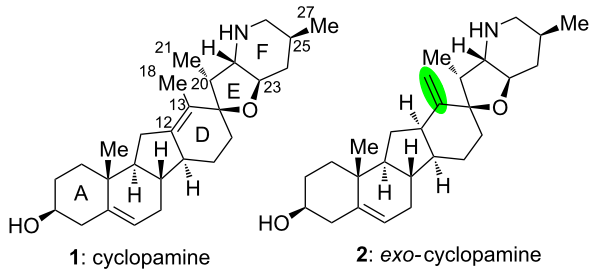


Figure 1: Structures of cyclopamine and *exo*-cyclopamine.

We previously reported the first chemical synthesis of cyclopamine (**1**) starting from dehydroepiandrosterone and utilizing the C–H-functionalization logic and a biomimetic skeleton rearrangement [32,33]. Furthermore, quantum mechanical calculations guided our design and synthesis of *exo*-cyclopamine (**2**, see Figure 1), a ten-fold more potent and acid-stable analog with an *exo*-methylene unit at C13–C18 [34]. Herein, we describe a comprehensive study of cyclopamine analogs bearing *exo*-methylene units in different positions and extent this rational to F-ring-modified structures.

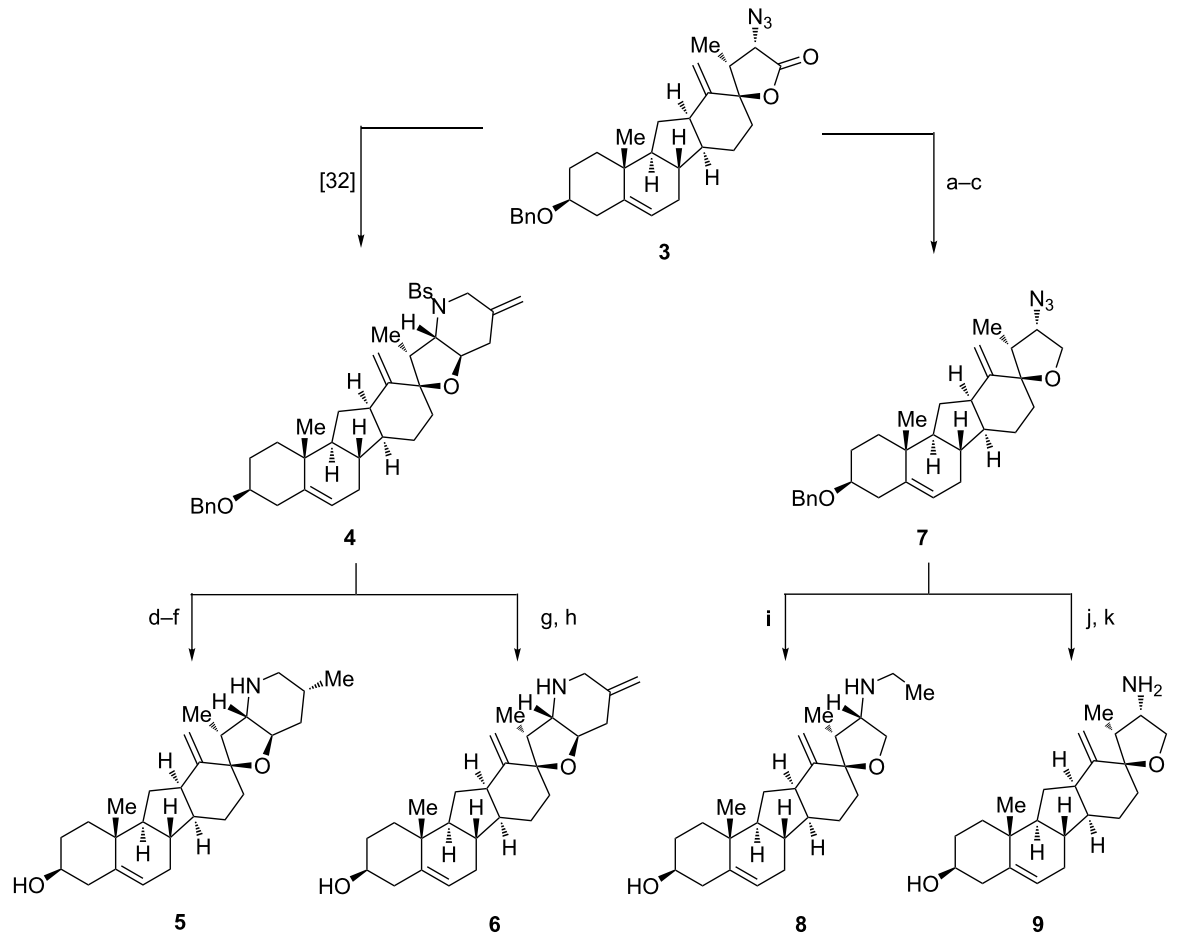
Results and Discussion

Our synthetic approach to the analogs described here started from previously reported azide **3** which was converted in six steps [32] to the protected bis-*exo*-methylene compound **4**. Carefully chosen conditions for the deprotection of the benzyl ether (DDQ, DCE/pH 7 phosphate buffer, 40 °C, 86%) and the benzenesulfonylamine (sodium naphthalenide, DME, −78 °C, 79%) allowed for the isolation of bis-*exo*-cyclopamine **6** in 18% overall yield from **3**. The hydrogenation of intermediate **4** by using Wilkinson's catalyst in benzene yielded previously described *exo*-cyclopamine **2** and its C25 epimer **5**. Deprotection with Raney-nickel (EtOH, 78 °C) and then sodium naphthalenide (DME, −78 °C, 41% over two steps) furnished 25-epi-*exo*-cyclopamine **5** in 3% overall yield from **3**.

A first set of *exo*-cyclopamine analogs with a modified F-ring was obtained starting again from azide **3** (see Scheme 1). Reduction of the lactone moiety to give a tetrahydrofuran was accomplished in three steps including (1) partial reduction to the lactol (DIBAl-H, THF, −78 °C to −60 °C, 95%), (2) acetylation (Ac_2O, pyridine, cat. DMAP, quant.) and (3) reductive removal of the so-obtained acetate (Et_3SiH, $BF_3{\cdot}Et_2O$, −78 °C to −20 °C, 79%). Removal of the benzyl ether, reduction of the azide moiety and concomitant alkylation was then all effected in one pot by using Raney-nickel in EtOH to give analog **8**, an F-ring-opened *exo*-cyclopamine derivative in 27% overall yield from **3**. Alternatively, the use of previously devised conditions for benzyl deprotection (DDQ, DCE/pH 7 phosphate buffer, 45 °C, 78%) and then sodium borohydride-mediated reduction of the azide (EtOH, 65 °C, 62%) cleanly furnished primary amine **9**, an *exo*-cyclopamine derivative with no F-ring (35% overall yield from **3**).

A second set of F-ring-modified *exo*-cyclopamine derivatives was obtained starting from previously described 12-ß-triethylsilyloxy compound **10** (see Scheme 2) [32]. To construct the spirolactone **12**, a three-step process consisting of (1) allylation (allylcerium chloride, THF, 0 °C, 93%), (2) hydroboration/oxidation (9-BBN, THF, 70 °C; then $NaBO_3$, H_2O, 50 °C, 91%) and finally, (3) oxidative cyclization (BAIB, cat. TEMPO, CH_2Cl_2, 25 °C, 73%) was employed. Deprotection of the silyl ether (HF, MeCN, 25 °C, 87%) and base-induced rearrangement of the steroid skeleton via the corresponding triflate (Tf_2O, pyridine, 0 °C→50 °C, 46%) gave C-*nor*-D-*homo*-derivative **13** which, in turn, was transformed into lactone azide **14** by using Evans' conditions (LDA, THF, −78 °C to −30 °C, 10 min; then trisylazide, THF, −78 °C, 1.5 h, 43%) [35]. From **14** two additional *exo*-cyclopamine derivatives became accessible. Partial reduction to the lactol (DIBAl-H, THF, −78 °C to −65 °C, 88%) and Horner–Wadsworth–Emmons reaction by using previously reported dimethyl {3-[(4-methoxybenzyl)oxy]-2-oxopropyl}phosphonate [32], ($Ba(OH)_2$, THF/H_2O, 80 °C, 50%) led to **15** which, in turn, was methylenated by employing the Peterson protocol ($TMSCH_2CeCl_2$, THF, −78 °C; then TMEDA; then HF, MeCN, 25 °C, 64%) [36]. Towards this end the azide moiety was reduced and monoprotection of the so-obtained amine as a sulfonamide ($LiAlH_4$, THF, 0 °C→25 °C; then benzenesulfonyl chloride, Et_3N, DMF, 0 °C, 69%) gave **17**. Deprotetion of the 4-methoxybenzyl ether (DDQ, DCE/pH 7 phosphate buffer, 25 °C, 59%) and cyclization under Mitsunobu conditions (*n*-Bu_3P, DEAD, toluene, 0 °C→25 °C, 93%) yielded piperidine **18**. Deprotection of the benzyl ether by using previously devised conditions (DDQ, DCE/pH 7 phosphate buffer, 44 °C, 70%) and the benzenesulfonylamine (sodium naphthalenide, DME, −78 °C, 95%) gave 20-demethyl-bis-*exo*-cyclopamine **19** in 7% overall yield starting from **14**.

Starting from azido lactone **14** (see Scheme 2) a partial reduction to the lactol (DIBAl-H, THF, −78 °C to −65 °C, 88%) and the Horner–Wadsworth–Emmons reaction by using triethyl phosphonoacetate ($Ba(OH)_2$, THF/H_2O, 80 °C, 55%) led to

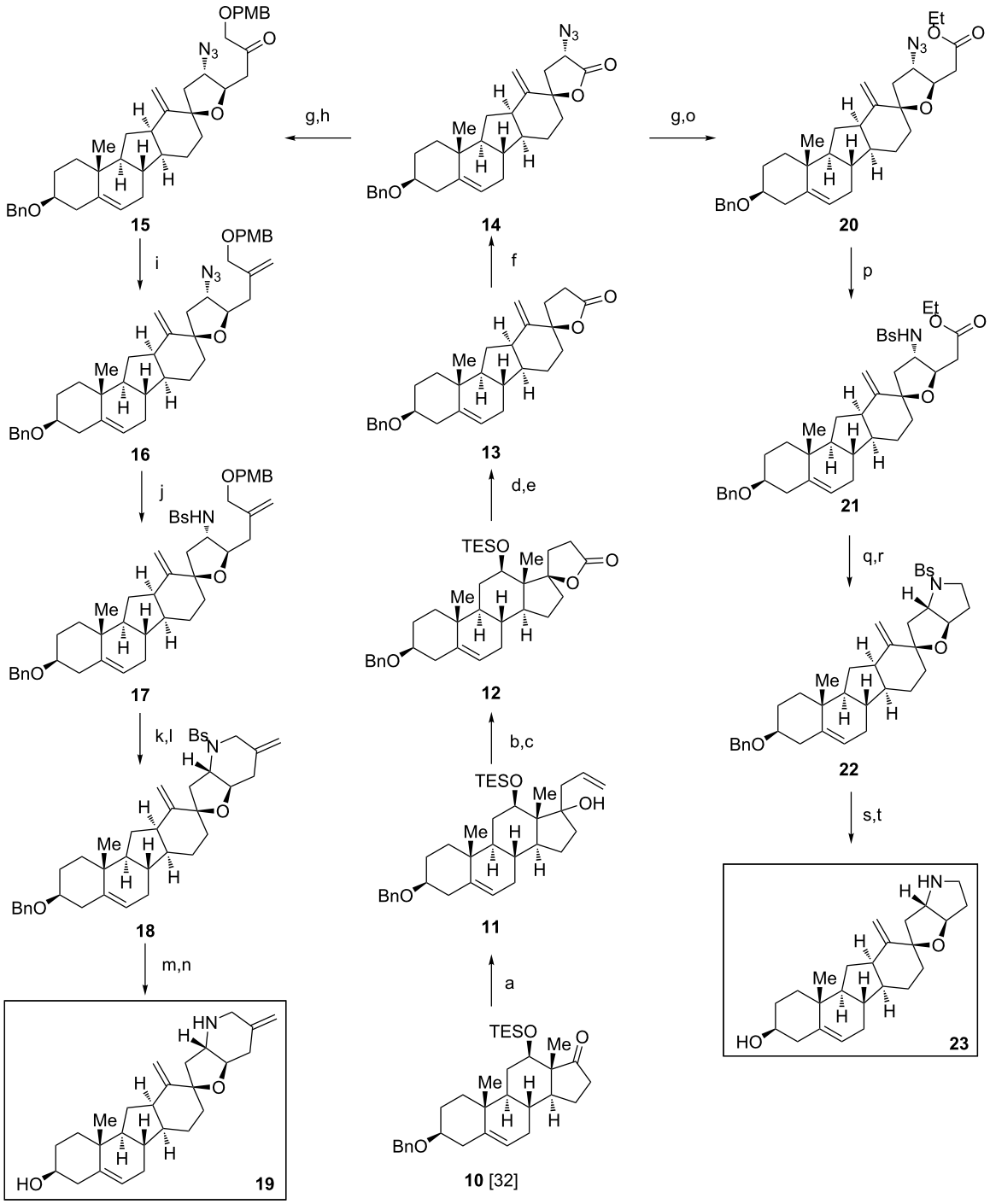


Scheme 1: Synthesis of 25-epi-*exo*-cyclopamine **5**, bis-*exo*-cyclopamine **6**, and derivatives **8** and **9**. Reaction conditions: (a) DIBAl-H, THF, −78 °C to −65 °C, 4 h, 95%; (b) Ac_2O, pyridine, DMAP (cat.), 25 °C, 20 h, quant; (c) $BF_3{\cdot}Et_2O$, Et_3SiH, CH_2Cl_2, −78 °C to −20 °C, 7 h, 79%; (d) $Rh(PPh_3)_3Cl$, benzene, H_2, 25 °C, 24 h, quant. (3:1 dr); (e) Raney-nickel (W2), EtOH, 78 °C, 5 min; (f) sodium naphthalenide, DME, −78 °C, 30 min, 41% over two steps; (g) DDQ, DCE/phosphate buffer (pH 7), 40 °C, 95 min, 86%; (h) sodium naphthalenide, DME, −78 °C, 1 h, 79%; (i) Raney-nickel (W2), EtOH, 37%; (j) DDQ, DCE/phosphate buffer (pH 7), 45 °C, 1.5 h, 78%, (k) $NaBH_4$, EtOH, 65 °C, 5 d, 62%.

ethyl ester **20**. Reduction of the azide moiety in **20** was carried out by using Staudinger's protocol (Ph_3P, THF/H_2O, 50 °C). Immediate protection of the obtained amine (benzenesulfonyl chloride, Et_3N, CH_2Cl_2, 40 °C, 97% over 2 steps) gave sulfonylamide **21**. Reduction of the ester in **21** to the primary alcohol (DIBAl-H, THF, −78 °C to −40 °C, 97%) and cyclization by employing Mitsunobu conditions (*n*-Bu_3P, DEAD, toluene, 0 °C→25 °C, 81%) yielded pyrrolidine **22**. Previously devised conditions for the deprotection (1. DDQ, DCE/pH 7 phosphate buffer, 40 °C; 2. sodium naphthalenide, DME, −78 °C, 46%) finally afforded F-*nor*-20,25-bis-demethyl-*exo*-cyclopamine **23** in 9% overall yield starting from **14**.

Next, we examined all synthesized compounds for their ability to inhibit the Gli1-dependent luciferase expression in Shh-LIGHTII cells, a clonal mouse fibroblast cell line which stably incorporates a Gli-dependent firefly luciferase reporter and a constitutive *Renilla* luciferase reporter [37]. The compounds were tested in a concentration range from 0.01 μM to 10 μM. While analogs **8**, **9**, and **19** showed no activity (data not shown) in this concentration range, **5**, **6**, and **23** were active with 25-epi-*exo*-cyclopamine **5** having an IC_{50} of 3.29 ± 0.31 μM, F-*nor*-20,25-bis-demethyl-*exo*-cyclopamine **23** of 6.4 ± 0.9 μM, and bis-*exo*-cyclopamine **6** being the most active with an IC_{50} of 0.20 ± 0.01 μM (see Figure 2).

Given the negative test results of compounds **8** and **9** it becomes evident that the F-ring is necessary for bioactivity. The piperidine moiety provides a rather rigidly placed nitrogen atom. Nevertheless, a pyrrolidine as in compound **23** still provides the correct orientation of the nitrogen atom. Despite compounds **8** and **9** being inactive in the assay, both derivatives induced cytotoxicity in the concentration range tested. Very subtle changes of the conformation of the piperidine ring significantly change



Scheme 2: Synthesis of 20-demethyl-bis-*exo*-cyclopamine **19** and F-*nor*-20,25-bis-demethyl-*exo*-cyclopamine **23**. Reaction conditions: (a) allylcerium chloride, THF, 0 °C, 30 min, 93%; (b) 9-BBN, THF, 70 °C, 6 h; then $NaBO_3$, 50 °C, 12 h, 91%; (c) BAIB, TEMPO, CH_2Cl_2, 25 °C, 3 h, 73%; (d) HF 50 wt % in H_2O, MeCN, 20 min, 25 °C, 87%; (e) Tf_2O, pyridine, 0 °C→50 °C, 1.5 h; then additional Tf_2O, 0 °C→50 °C, 2 h, 46%; (f) LDA, THF, −78 °C to −30 °C, 10 min; then trisylazide, THF, −78 °C, 1.5 h, 43%; g) DIBAl-H, THF, −78 °C to −65 °C, 2 h, 88%; (h) dimethyl (3-((4-methoxybenzyl)oxy)-2-oxopropyl)phosphonate, $Ba(OH)_2$, THF/H_2O, 80 °C, 13 h, 50%; (i) (trimethylsilyl)methylcerium chloride, THF, −78 °C, 30 min; then TMEDA, −78 °C, 15 min; then HF 50 wt % in H_2O, MeCN, 25 °C, 10 min, 64%; (j) $LiAlH_4$, THF, 0 °C→25 °C, 13 h; then benzenesulfonyl chloride, Et_3N, DMF, 0 °C, 25 min, 69%; (k) DDQ, CH_2Cl_2/phosphate buffer (pH 7), 25 °C, 2 h, 59%; (l) *n*-Bu_3P, DEAD, toluene, 0 °C→25 °C, 12 h, 93%; (m) DDQ, DCE/phosphate buffer (pH 7), 44 °C, 50 min, 70%; (n) sodium naphthalenide, DME, −78 °C, 30 min, 95%; (o) triethyl phosphonoacetate, $Ba(OH)_2$, THF, 80 °C, 12 h, 55%; (p) PPh_3, THF/H_2O, 50 °C, 24 h; then benzenesulfonyl chloride, Et_3N, CH_2Cl_2, 40 °C, 5 h, 97%; (q) DIBAl-H, THF, −78 °C to −40 °C, 3 h, 97%; (r) *n*-Bu_3P, DEAD, toluene, 0 °C→25 °C, 24 h, 81%; (s) DDQ, DCE/phosphate buffer (pH 7), 40 °C, 30 min, 62%; (t) sodium naphthalenide, DME, −78 °C, 40 min, 74%.

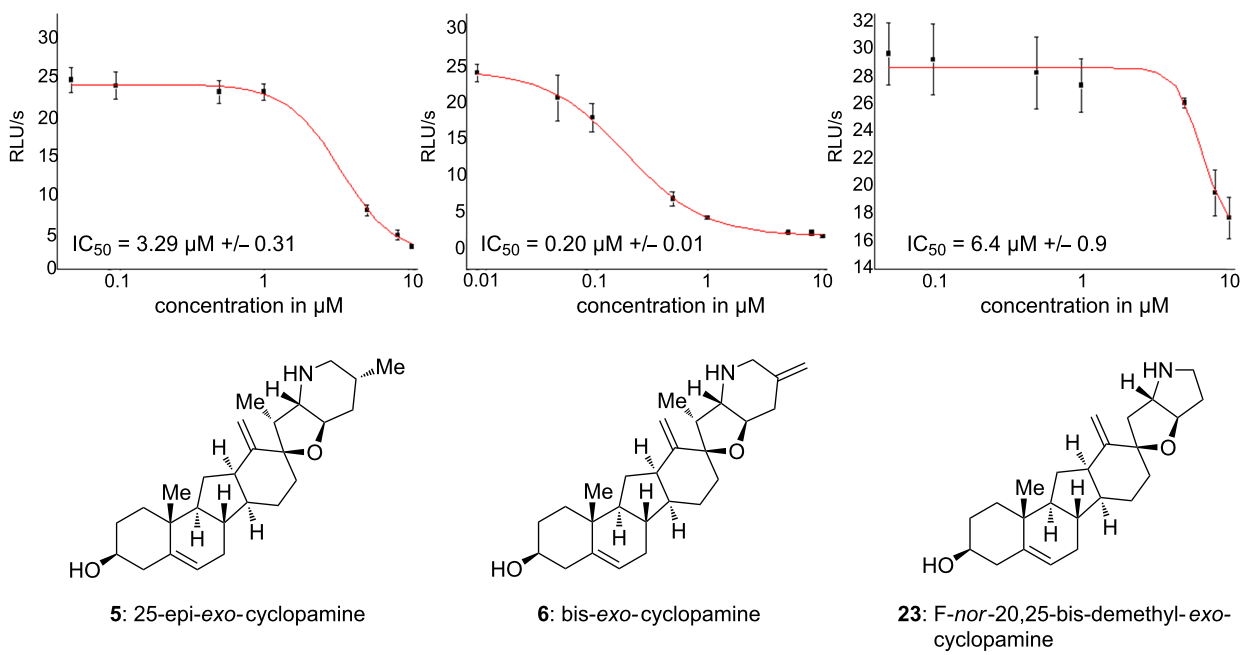


Figure 2: IC_{50} values of Shh inhibition by compounds **5**, **6** and **23** in a Gli1-reporter gene assay. Data were obtained from three independent experiments and represent the mean ± standard deviation.

bioactivity: While 25-epi-*exo*-cyclopamine **5** shows reduced activity in comparison to *exo*-cyclopamine **2**, bis-*exo*-cyclopamine **6** is the most active compound tested in this study. Furthermore, the methyl group at C-20 seems to have a pronounced effect on the bioactivity, with 20-demethyl-bis-*exo*-cyclopamine **19** being completely inactive in the tested concentration range.

Finally, we studied the stability of all newly synthesized compounds towards acidic conditions. Therefore, they were exposed to a pH of approximately 1 (MeOH, 1 M HCl) for 24 h. After evaporation of all volatiles, ^{1}H NMR spectra were acquired and compared to the initially obtained spectra of the pure compounds. While compounds **5**, **6**, **8**, and **9** remained unchanged, compounds **19** and **23** showed decomposition. This experiment emphasizes the importance of the C-21 methyl group for the stability of *exo*-cyclopamine derivatives. All synthesized compounds, the number of steps required, and the respective overall yield starting from **3** or **14**, as well as their biological activity and stability under acidic conditions are summarized in Table 1.

Conclusion

In conclusion, we succeeded in identifying the new cyclopamine derivative bis-*exo*-cyclopamine **6** which surpasses the biological potency of the parent compound by the 25-fold and is stable at pH 1. Further insights were gained into the structure–activity relationship of F-ring-modified analogs of cyclopamine and the necessity of the C-21 methyl group for

Table 1: Synthesized *exo*-cyclopamine derivatives, number of steps, yields, results of their biological testing, and stability towards acid.

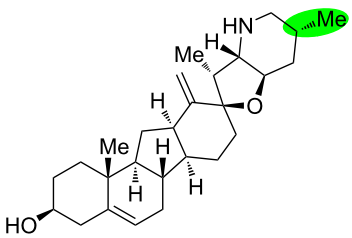
Compound	Number of steps from **3** or **14**	Overall yield	Potency in Gli-assay	Stability towards acid (pH ~1, 24 h)
 **5**: 25-epi-*exo*-cyclopamine	9 steps from **3**	3%	3.29 ± 0.31 μM	stable

Table 1: Synthesized *exo*-cyclopamine derivatives, number of steps, yields, results of their biological testing, and stability towards acid. (continued)

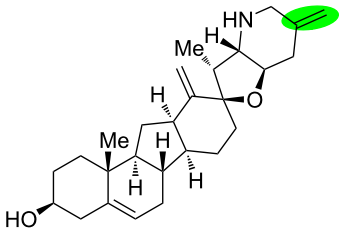
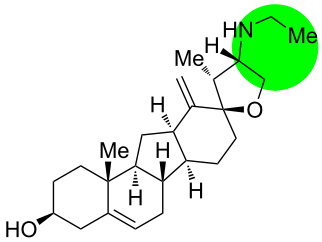
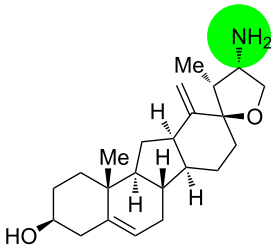
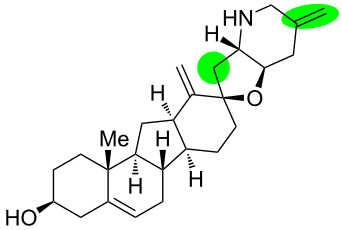
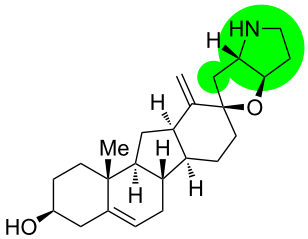
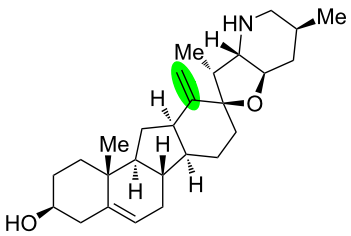
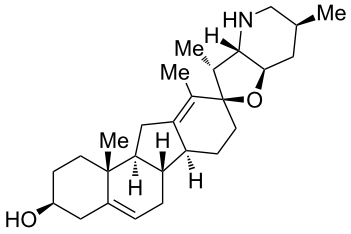
 **6**: bis-*exo*-cyclopamine	8 steps from **3**	18%	0.2 ± 0.01 μM	stable
 **8**	4 steps from **3**	27%	> 10 μM	stable
 **9**	5 steps from **3**	35%	> 10 μM	stable
 **19**: 20-demethyl-bis-*exo*-cyclopamine	8 steps from **14**	7%	> 10 μM	decomp.
 **23**: F-*nor*-20,25-bis-demethyl-*exo*-cyclopamine	7 steps from **14**	9%	6.40 ± 0.90 μM	decomp.
Previously synthesized and biologically evaluated:				
 **2**: *exo*-cyclopamine	9 steps from **3**	7%	0.5 μM [34]	stable

Table 1: Synthesized *exo*-cyclopamine derivatives, number of steps, yields, results of their biological testing, and stability towards acid. (continued)

 **1**: cyclopamine	10 steps from **3**	5%	5 μM [34]	decomp.

bioactivity and acid stability was revealed. Our designed analogs of cyclopamine are accessible in noticeably shorter and higher yielding synthetic routes than the parent compound, a fact that will further contribute to their usefulness in biological and medicinal studies.

Supporting Information

Supporting Information File 1

Experimental details and analytical data of all synthesized compounds are provided.
[http://www.beilstein-journals.org/bjoc/content/supplementary/1860-5397-9-267-S1.pdf]

Acknowledgements

We thank Dr Lothar Hennig for recording NMR spectra and for his help in interpreting the 2D NMR spectra.

References

1. Keeler, R. F. *Phytochemistry* **1968,** *7,* 303. doi:10.1016/S0031-9422(00)86328-1
2. Keeler, R. F. *Teratology* **1970,** *3,* 169. doi:10.1002/tera.1420030209
3. Beachy, P. A.; Karhadkar, S. S.; Berman, D. M. *Nature* **2004,** *432,* 324. doi:10.1038/nature03100
4. Taipale, J.; Beachy, P. A. *Nature* **2001,** *411,* 349. doi:10.1038/35077219
5. Hidalgo, M.; Maitra, A. *N. Engl. J. Med.* **2009,** *361,* 2094. doi:10.1056/NEJMcibr0905857
6. Gailani, M. R.; Ståhle-Bäckdahl, M.; Leffell, D. J.; Glyn, M.; Zaphiropoulos, G.; Undén, A. B.; Dean, M.; Brash, D. E.; Bale, A. E.; Toftgård, R. *Nat. Genet.* **1996,** *14,* 78. doi:10.1038/ng0996-78
7. Hahn, H.; Wicking, C.; Zaphiropoulos, P. G.; Gailani, M. R.; Shanley, S.; Chidambaram, A.; Vorechovsky, I.; Holmberg, E.; Undén, A. B.; Gillies, S.; Negus, K.; Smyth, I.; Pressman, C.; Leffell, D. J.; Gerrard, B.; Goldstein, A. M.; Dean, D.; Toftgård, R.; Chenevix-Trench, G.; Wainwright, B.; Bale, A. E. *Cell* **1996,** *85,* 841. doi:10.1016/S0092-8674(00)81268-4
8. Zurawel, R. H.; Allen, C.; Chiappa, S.; Cato, W.; Biegel, J.; Cogen, P.; de Sauvage, F.; Raffel, C. *Genes, Chromosomes Cancer* **2000,** *27,* 44. doi:10.1002/(SICI)1098-2264(200001)27:1<44::AID-GCC6>3.0.CO;2-V
9. Bar, E. E.; Chaudhry, A.; Lin, A.; Fan, X.; Schreck, K.; Matsui, W.; Piccirillo, S.; Vescovi, A. L.; DiMeco, F.; Olivi, A.; Eberhart, C. G. *Stem Cells* **2007,** *25,* 2524. doi:10.1634/stemcells.2007-0166
10. Watkins, D. N.; Berman, D. M.; Baylin, S. B. *Cell Cycle* **2003,** *2,* 195. doi:10.4161/cc.2.3.378
11. Dosch, J. S.; di Magliano, M. P.; Simeone, D. M. *Pancreatology* **2010,** *10,* 151. doi:10.1159/000225923
12. Vořechovský, I.; Benediktsson, K. P.; Toftgård, R. *Eur. J. Cancer* **1999,** *35,* 711. doi:10.1016/S0959-8049(99)00017-9
13. Fan, L.; Pepicelli, C. V.; Dibble, C. C.; Catbagan, W.; Zarycki, J. L.; Laciak, R.; Gipp, J.; Shaw, A.; Lamm, M. L. G.; Munoz, A.; Lipinski, R.; Thrasher, J. B.; Bushman, W. *Endocrinology* **2004,** *145,* 3961. doi:10.1210/en.2004-0079
14. Karhadkar, S. S.; Bova, G. S.; Abdallah, N.; Dhara, S.; Gardner, D.; Maitra, A.; Isaacs, J. T.; Berman, D. M.; Beachy, P. A. *Nature* **2004,** *431,* 707. doi:10.1038/nature02962
15. Berman, D. M.; Karhadkar, S. S.; Maitra, A.; Montes de Oca, R.; Gerstenblith, M. R.; Briggs, K.; Parker, A. R.; Shimada, Y.; Eshleman, J. R.; Watkins, D. N.; Beachy, P. A. *Nature* **2003,** *425,* 846. doi:10.1038/nature01972
16. Teglund, S.; Toftgård, R. *Biochim. Biophys. Acta, Rev. Cancer* **2010,** *1805,* 181. doi:10.1016/j.bbcan.2010.01.003
17. Dierks, C.; Grbic, J.; Zirlik, K.; Beigi, R.; Englund, N. P.; Guo, G.-R.; Veelken, H.; Engelhardt, M.; Mertelsmann, R.; Kelleher, J. F.; Schultz, P.; Warmuth, M. *Nat. Med.* **2007,** *13,* 944. doi:10.1038/nm1614
18. Hegde, G. V.; Munger, C. M.; Emanuel, K.; Joshi, A. D.; Greiner, T. C.; Weisenburger, D. D.; Vose, J. M.; Joshi, S. S. *Mol. Cancer Ther.* **2008,** *7,* 1450. doi:10.1158/1535-7163.MCT-07-2118
19. Kawahara, T.; Kawaguchi-Ihara, N.; Okuhashi, Y.; Itoh, M.; Nara, N.; Tohda, S. *Anticancer Res.* **2009,** *29,* 4629.
20. Peacock, C. D.; Wang, Q.; Gesell, G. S.; Corcoran-Schwartz, I. M.; Jones, E.; Kim, J.; Devereux, W. L.; Rhodes, J. T.; Huff, C. A.; Beachy, P. A.; Watkins, D. N.; Matsui, W. *Proc. Natl. Acad. Sci. U. S. A.* **2007,** *104,* 4048. doi:10.1073/pnas.0611682104
21. Zhao, C.; Chen, A.; Jamieson, C. H.; Fereshteh, M.; Abrahamsson, A.; Blum, J.; Kwon, H. Y.; Kim, J.; Chute, J. P.; Rizzieri, D.; Munchhof, M.; VanArsdale, T.; Beachy, P. A.; Reya, T. *Nature* **2009,** *458,* 776. doi:10.1038/nature07737
22. Bai, L.-Y.; Chiu, C.-F.; Lin, C.-W.; Hsu, N.-Y.; Lin, C.-L.; Lo, W.-J.; Kao, M.-C. *Leukemia* **2008,** *22,* 226. doi:10.1038/sj.leu.2404978
23. Dierks, C.; Beigi, R.; Guo, G.-R.; Zirlik, K.; Stegert, M. R.; Manley, P.; Trussel, C.; Schmitt-Graeff, A.; Landwerlin, K.; Veelken, H.; Warmuth, M. *Cancer Cell* **2008,** *14,* 238. doi:10.1016/j.ccr.2008.08.003
24. Suh, J. M.; Gao, X.; McKay, J.; McKay, R.; Salo, Z.; Graff, J. M. *Cell Metab.* **2006,** *3,* 25. doi:10.1016/j.cmet.2005.11.012

25. Teperino, R.; Amann, S.; Bayer, M.; McGee, S. L.; Loipetzberger, A.; Connor, T.; Jaeger, C.; Kammerer, B.; Winter, L.; Wiche, G.; Dalgaard, K.; Selvaraj, M.; Gaster, M.; Lee-Young, R. S.; Febbraio, M. A.; Knauf, C.; Cani, P. D.; Aberger, F.; Penninger, J. M.; Pospilik, J. A.; Esterbauer, H. *Cell* **2012,** *151,* 414. doi:10.1016/j.cell.2012.09.021
26. Gonzalez-Reyes, L. E.; Verbitsky, M.; Blesa, J.; Jackson-Lewis, V.; Paredes, D.; Tillack, K.; Phani, S.; Kramer, E. R.; Przedborski, S.; Kottmann, A. H. *Neuron* **2012,** *75,* 306. doi:10.1016/j.neuron.2012.05.018
27. Nowaczyk, M. J.; Huggins, M. J.; Tomkins, D. J.; Rossi, E.; Ramsay, J. A.; Woulfe, J.; Scherer, S. W.; Belloni, E. *Clin. Genet.* **2000,** *57,* 388. doi:10.1034/j.1399-0004.2000.570510.x
28. Decker, S.; Zirlik, K.; Djebatchie, L.; Hartmann, D.; Ihorst, G.; Schmitt-Graeff, A.; Herchenbach, D.; Jumaa, H.; Warmuth, M.; Veelken, H.; Dierks, C. *Blood* **2012,** *119,* 997. doi:10.1182/blood-2011-06-359075
29. Heretsch, P.; Tzagkaroulaki, L.; Giannis, A. *Bioorg. Med. Chem.* **2010,** *18,* 6613. doi:10.1016/j.bmc.2010.07.038
30. Heretsch, P.; Tzagkaroulaki, L.; Giannis, A. *Angew. Chem.* **2010,** *122,* 3492. doi:10.1002/ange.200906967
31. Wilson, S. R.; Strand, M. F.; Krapp, A.; Rise, F.; Petersen, D.; Krauss, S. *J. Pharm. Biomed. Anal.* **2010,** *52,* 707. doi:10.1016/j.jpba.2010.02.017
32. Giannis, A.; Heretsch, P.; Sarli, V.; Stößel, A. *Angew. Chem.* **2009,** *121,* 8052. doi:10.1002/ange.200902520
33. Heretsch, P.; Rabe, S.; Giannis, A. *J. Am. Chem. Soc.* **2010,** *132,* 9968. doi:10.1021/ja103152k
34. Heretsch, P.; Büttner, A.; Tzagkaroulaki, L.; Zahn, S.; Kirchner, B.; Giannis, A. *Chem. Commun.* **2011,** *47,* 7362. doi:10.1039/C1CC11782C
35. Evans, D. A.; Britton, T. C. *J. Am. Chem. Soc.* **1987,** *109,* 6881. doi:10.1021/ja00256a069
36. Johnson, C. R.; Tait, B. D. *J. Org. Chem.* **1987,** *52,* 281. doi:10.1021/jo00378a024
37. Taipale, J.; Chen, J. K.; Cooper, M. K.; Wang, B.; Mann, R. K.; Milenkovic, L.; Scott, M. P.; Beachy, P. A. *Nature* **2000,** *406,* 1005. doi:10.1038/35023008

License and Terms

This is an Open Access article under the terms of the Creative Commons Attribution License (http://creativecommons.org/licenses/by/2.0), which permits unrestricted use, distribution, and reproduction in any medium, provided the original work is properly cited.

The license is subject to the *Beilstein Journal of Organic Chemistry* terms and conditions: (http://www.beilstein-journals.org/bjoc)

The definitive version of this article is the electronic one which can be found at: doi:10.3762/bjoc.9.267

Beilstein Journal of Organic Chemistry

Towards stereochemical control: A short formal enantioselective total synthesis of pumiliotoxins 251D and 237A

Jie Zhang[1], Hong-Kui Zhang[*1] and Pei-Qiang Huang[*1,2]

Full Research Paper

Open Access

Address:
[1]Department of Chemistry and Fujian Provincial Key Laboratory of Chemical Biology, College of Chemistry and Chemical Engineering, Xiamen University, Xiamen, Fujian 361005, P. R. China and [2]State Key Laboratory of Applied Organic Chemistry Lanzhou University, Lanzhou 730000, P. R. China

Email:
Jie Zhang - 394261694@qq.com; Hong-Kui Zhang[*] - hkzhang@xmu.edu.cn; Pei-Qiang Huang[*] - pqhuang@xmu.edu.cn

* Corresponding author

Keywords:
enantioselective synthesis; Grignard reagent; pumiliotoxin 237A; pumiliotoxin 251D; reductive dehydroxylation; ring closure; *trans*-methylation

Beilstein J. Org. Chem. **2013,** *9,* 2358–2366.
doi:10.3762/bjoc.9.271

Received: 26 August 2013
Accepted: 10 October 2013
Published: 05 November 2013

This article is part of the Thematic Series "Natural products in synthesis and biosynthesis".

Guest Editor: J. S. Dickschat

© 2013 Zhang et al; licensee Beilstein-Institut.
License and terms: see end of document.

Abstract

A concise enantioselective synthesis of the advanced intermediate **5** for the synthesis of pumiliotoxins (Gallagher's intermediate) is described. The synthesis started from the regio- and *trans*-diastereoselective (dr = 98:2) reductive 3-butenylation of (*R*)-3-(*tert*-butyldimethylsilyloxy)glutarimide **14**. After *O*-desilylation and Dess–Martin oxidation, the resulting keto-lactam **10** was subjected to a highly *trans*-stereoselective addition of the methylmagnesium iodide to give carbinol **11** as sole diastereomer. An efficient ring closure procedure consisting of ozonolysis and reductive dehydroxylation provided the indolizidine derivative **5**, which completed the formal enantioselective total synthesis of pumiliotoxins 251D and 237A.

Introduction

Pumiliotoxins (PTXs, **1**, Figure 1) such as pumiliotoxin 251D (**2**) are a subclass of indolizidine alkaloids isolated from the skin secretion of neotropical frogs. A total of 19 members have been isolated and partially characterized [1]. Pumiliotoxins are structurally characterized by a (*Z*)-6-alkylidene-8-hydroxy-8-methylindolizidine ring system, which distinguishes from one to another by the 6-alkylidene side chain [1]. Interestingly, it is known that poison frogs don't produce the alkaloids themselves, instead, they accumulate alkaloids from dietary alkaloid-containing arthropods serving as a chemical defense against predators. It is not surprising that the alkaloids found in poison frogs can also be detected from ants, and most of them show remarkable bioactivities [2,3]. For example, formicine ants have been shown to be an arthropod source of the pumiliotoxin alka-

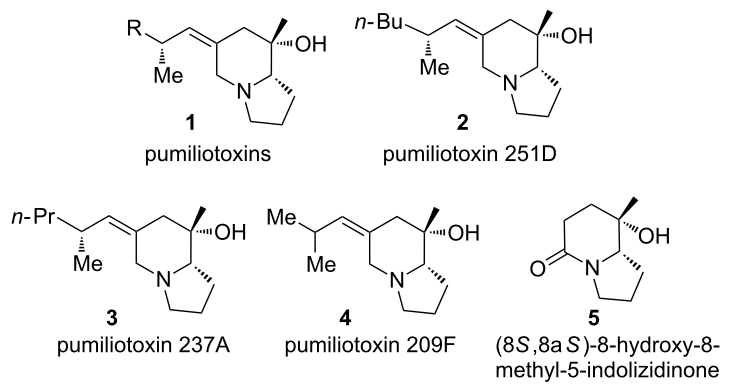


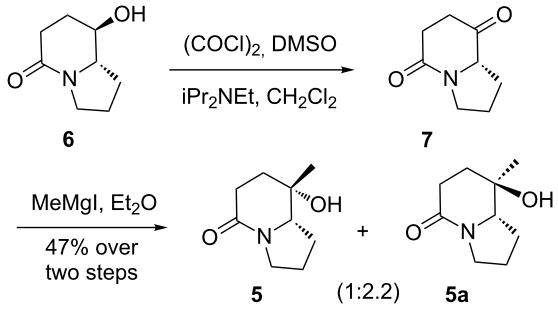
Figure 1: Structures of some pumiliotoxins and an advanced intermediate.

loids of dendrobatid poison frogs [4,5]. Forthermore, from the extracts of an unidentified *Scheloribates sp*. of mites, pumiliotoxin 237A (**3**) was detected as a minor component [6].

That the wide range of biological activities possessed by these molecules have attracted much attention of synthetic organic chemists, and numerous approaches have been reported [7-9]. Pumiliotoxin 251D (PTX 251D) (**2**) is the first structurally defined member of pumiliotoxins, a class of dendrobatid alkaloids isolated from Ecuadorean poisonous frog, *Dendrobares tricolor* in 1980 [10]. Since the pioneering work of Overman [11], a number of approaches have been developed for the synthesis of PTX 251D [12-26]. Among them, that of Gallagher [12] has attracted much attention. They demonstrated that (8*S*,8a*S*)-8-hydroxy-8-methyl-5-indolizidinone (**5**, Figure 1) can serve as an advanced intermediate for the synthesis of pumiliotoxin 251D [12]. Later on, Nubbemeyer and co-workers used the Horner olefination to convert **5** and its diastereomer into (+)-PTX 251D (**2**) and the 8-epimer of PTX 209F (**4**), respectively [17]. Recently, (8*S*,8a*S*)-**5** has been used for the synthesis of PTX 237A (**3**) [6]. Thus, it is logic to envision that an efficient synthesis of this key intermediate would allow access to other member of pumiliotoxins and their analogues. To date more than ten synthetic approaches to (8*S*,8a*S*)-**5** have been published [12-15,18-22,27-31], among them L-proline and its derivative were used as popular precursors from the pool of chiral compounds [13-15,18-22]. Herein, we report a concise diastereoselective synthesis of (8*S*,8a*S*)-**5** starting from (*R*)-3-(*tert*-butyldimethylsilyloxy)glutarimide **14**, a versatile building block developed from our laboratory [32].

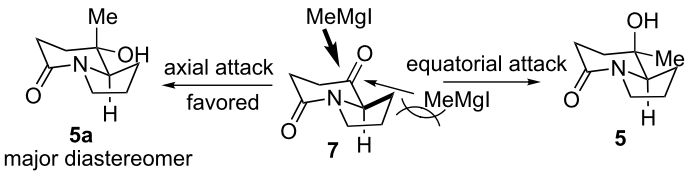
Results and Discussion

In recent years, we have been engaged in the development of efficient methodologies for the synthesis of nitrogen-containing bioactive heterocycles [33-37], and recently reported an approach for the synthesis of (8*R*,8a*S*)-8-hydroxy-5-indolizidinone (**6**) [38]. As a continuation of that study, the synthesis of (8*S*,8a*S*)-**5** starting from compound **6** was envisioned. For this purpose, alcohol **6** was subjected to Swern oxidation (DMSO, $(COCl)_2$, iPr_2NEt, −78 to 0 °C, 3 h), and the resulting keto-lactam **7** treated with MeMgI in diethyl ether (−78 to 0 °C, 1 h), which gave alcohols **5**/**5a** as an inseparable mixture of diastereomers in a ratio of 1:2.2 (combined yield: 47% over 2 steps) (Scheme 1). A comparison of spectral data (^1H and ^{13}C NMR) of our products **5**/**5a** with those reported [12,22,28] showed that the desired (8*S*,8a*S*)-**5** was the minor diastereomer. Similar results have been reported by Nubbemeyer [27] and Li [8]. In view of the fruitless efforts of Nubbemeyer [27] and Li [8] in inversing the diastereoselectivity of the methylation reaction of keto-lactam **7**, an alternative approach was envisaged.



Scheme 1: Synthesis of **5** from **6** via oxidation–addition sequence.

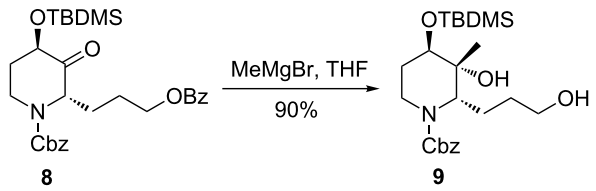
To develop a diastereoselective approach to (8*S*,8a*S*)-**5**, it would be helpful to analyze the plausible stereochemical course of the methylation of keto-lactam **7**. The observed unusual stereoselective *cis*-methylation implicates a preferential axial attack of the methylmagnesium iodide to the bicyclic keto-lactam **7** (Scheme 2). Although the preferential axial attack of "small" nucleophiles to cyclohexanone is well known [39-41], the "small" nucleophiles are limited to some metallo-hydrides,



Scheme 2: Plausible stereochemical course of the preferential axial addition of methylmagnesium iodide to bicyclic keto-lactam **7**.

metallo-acetylenide [42] and (cyanomethyl)lithium [43]. In the case of bicyclic keto-lactam **7**, presumably, the equatorial attack of methylmagnesium iodide to give **5**, suffers from unfavorable eclipsing interactions between the incoming methylmagnesium iodide and the vicinal methylene group. As a consequence, the axial attack to give **5a** is more favorable.

It was envisioned that if a monocyclic keto-lactam was used, the situation would be changed and an equatorial attack of the nucleophile giving the *cis*-product would be preferable. Indeed, Holmes and co-workers have reported that methylmagnesium bromide addition to *N*-Cbz-protected piperidin-3-one **8** produced exclusively the *trans*-methylation product **9** [44] (Scheme 3). In that case, the *N*-benzyloxycarbonyl group imposed $A^{1,3}$-strain on piperidine derivatives founded the basis for the observed stereocontrol.

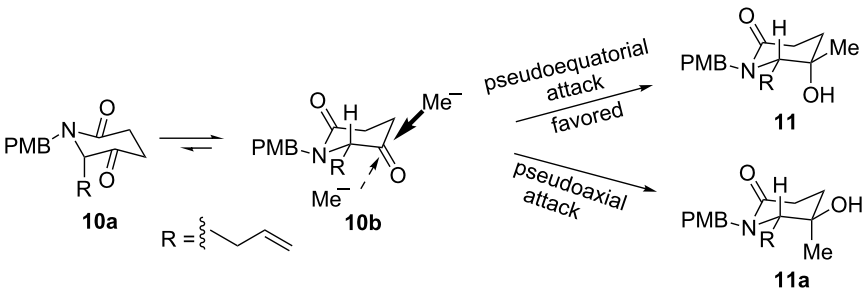


Scheme 3: Holmes' exclusive *trans*-diastereoselective methylation of *N*-Cbz-protected piperidin-3-one **8**.

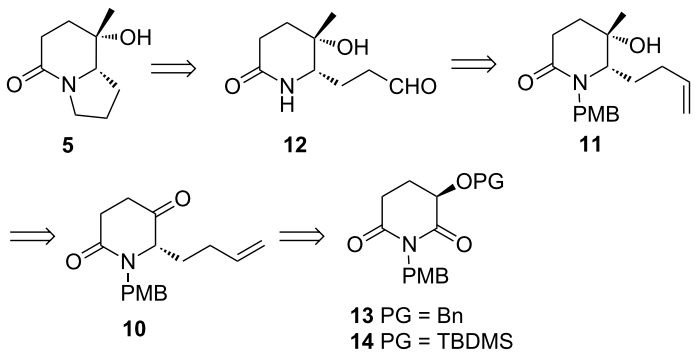
Thus, we chose keto-lactam **10** as our substrate. Although compound **10** is not a urethane, and a $A^{1,3}$-strain not longer exists, a simple chair conformational-controlled preferential equatorial attack could be expected (Scheme 4). Substrate **10** may adopt two plausible chair conformations **10a** and **10b**, in which conformation **10b** with a pseudoequatorially positioned *N*-α-substitutent is more stable. Thus, the pseudoequatorial attack of MeMgI would be preferential, which gives the product **11** as the major product.

On the basis of the abovementioned analysis, a retrosynthetic analysis of (8*S*,8a*S*)-**5** is displayed in Scheme 5, which features the formation of the fused pyrrolidine ring from the but-3-ene-1-yl group, the expected *trans*-diastereoselective methylation as the key step, and protected (*R*)-3-hydroxyglutarimide-based regio- and *trans*-diastereoselective reductive alkylation, a synthetic methodology developed from our laboratory [32,38,45,46], as the starting point.

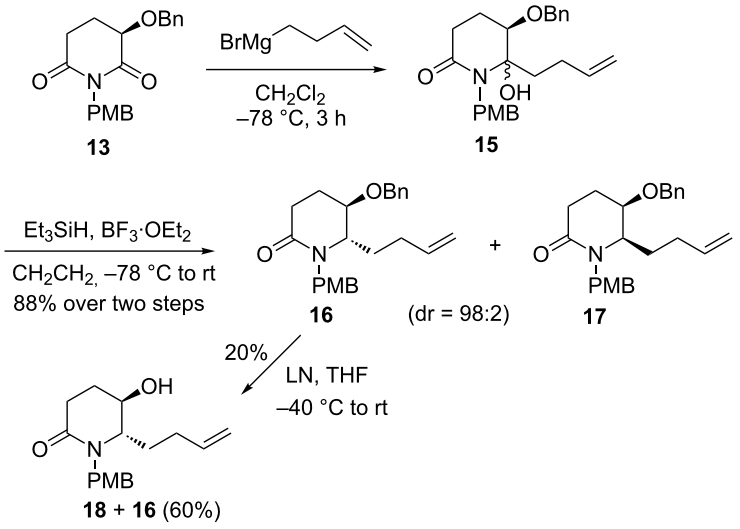
Our synthesis started from the addition of a freshly prepared 3-butenylmagnesium bromide to imide **13** [47] in dichloromethane at −78 °C for 3 h, which gave regioselective carbinol **15** as a mixture of two diastereomers. Without separation, the mixture was treated with $Et_3SiH/BF_3{\cdot}Et_2O$ (−78 °C to rt, 2 h) [32] to yield the reductive dehydroxylation products **16** and **17** in a ratio of 98:2 (determined by ^1H NMR) [32] (combined yield: 88% over 2 steps), from which only the major product **16** was isolated (Scheme 6). For the chemoselective debenzylation, lithium naphthalenide (LN) was used [48]. To our disappointment, attempted cleavage of the benzyl group by LN (THF, −40 °C to rt, 2 h) gave the desired **18** in only 20% yield along with 60% of the recovered starting material **16**.



Scheme 4: Our plan for the *trans*-diastereoselective methylation of keto-lactam **10**.



Scheme 5: Retrosynthetic analysis of (8*S*,8a*S*)-8-hydroxy-8-methylindolizidin-5-one (**5**).

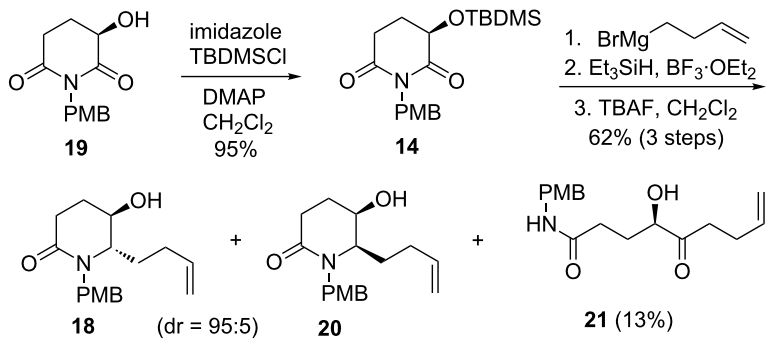


Scheme 6: Synthesis of compound **18**.

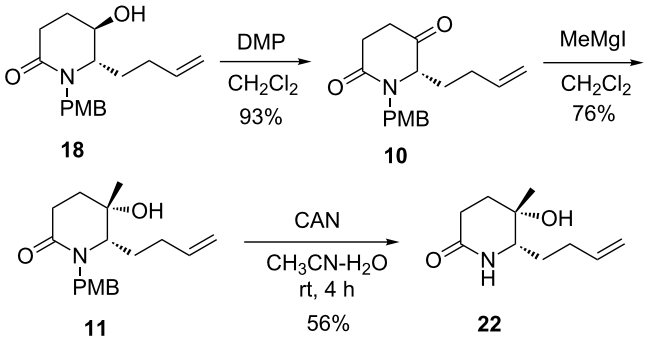
Due to the low yield in the debenzylation process, we decided to change the *O*-protecting group from benzyl to TBDMS, namely, use of TBDMS ether **14** as the starting material. Thus, (*R*)-3-(*tert*-butyldimethylsilyloxy)glutarimide **14** [49] was prepared from the known (*R*)-3-hydroxyglutarimide **19** (prepared from (*R*)-glutamic acid in 69% overall yield over 4 steps [47]) in a yield of 95%. Successive treatment of imide **14** with 3-butenylmagnesium bromide (CH_2Cl_2, −20 °C, 3 h) and the resulting hemi-aminal with $Et_3SiH/BF_3{\cdot}Et_2O$ (CH_2Cl_2, −78 °C, 2 h, then −20 °C, 2 h) gave a diastereomeric mixture of lactams. Without separation, the mixture was treated with TBAF in dichloromethane to produce alcohols **18** and **20** (combined yield: 62% over 3 steps) in a ratio of 95:5 (determined by ^{1}H NMR), along with the keto-amide **21** in 13% yield (Scheme 7). Separation of the mixture by column chromatography gave pure diastereomer **18** in 59% overall yield from **14**. The *trans*-stereochemistry was tentatively assigned to compound **18** on the basis of our previous results, which was confirmed by the conversion of **18** into the known compound **5** (vide infra).

With lactam **18** in hand, its conversion to novel tertiary alcohol **22** was investigated. Oxidation of alcohol **18** with an excess of Dess–Martin periodinane (DMP) in dichloromethane at room temperature for 2 h proceeded smoothly to give ketone **10** in 93% yield. It is noteworthy that keto-lactam **10** is configurational labile, and should be used immediately in the next reaction. Treatment of keto-lactam **10** with MeMgI (3 equiv) in dichloromethane (0 °C to rt, 12 h) gave a 76% yield of the desired methylation product **11** as the sole observable diastereomer (Scheme 8), whose stereochemistry was determined after converting into the known (8*S*,8a*S*)-**5**. This result verifies the previous assumption outlined in Scheme 4.

To remove the PMB protecting group, compound **11** was treated with ammonium cerium nitrate (CAN) in CH_3CN/H_2O



Scheme 7: Synthesis of hydroxylactam **18**.

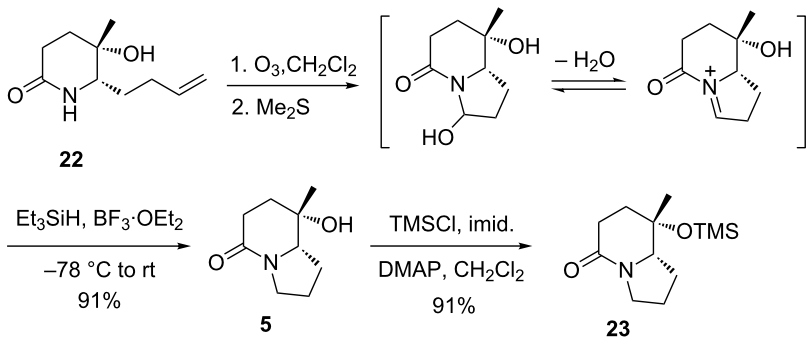


Scheme 8: Synthesis of tertiary alcohol **22**.

(v/v 3:1) [50] at room temperature for 4 h to afford the deprotected lactam **22** in 56% yield.

Our next task was the oxidative cyclization of the olefin **22** to form the indolizidinone ring. Thus, ozonolysis of olefin **22** in dichloromethane [51], followed by quenching with Me_2S furnished the hemiaminal tautomer via intermediacy of lactam-aldehyde. Without isolation, the crude was subjected to the reductive dehydroxylation with $Et_3SiH/BF_3{\cdot}Et_2O$ (CH_2Cl_2, −78 °C) to give the desired indolizidinone **5** in an overall yield of 91% from **22** (Scheme 9).

The spectral data of the our synthetic (8*S*,8a*S*)-**5** are in agreement with those reported [12,22,27-29]. Due to the differences between the reported optical rotation values $\{[\alpha]_D^{20}$ −42.7 (*c* 1.0, $CHCl_3$); lit. [12] $[\alpha]_D^{21}$ −47.0 (*c* 0.97, $CHCl_3$); lit. [22]



Scheme 9: Synthesis of (8*S*,8a*S*)-**5** and its silyl ether **23**.

$[\alpha]_D^{22}$ −55 (*c* 0.79, $CHCl_3$); lit. [28] $[\alpha]_D^{25}$ −41.3 (*c* 0.48, $CHCl_3$); lit. [29] $[\alpha]_D^{25}$ −32.1 (*c* 1.0, $CHCl_3$)}, compound **5** was converted into the known silyl ether **23** (TMSCl, imidazole, DMAP, CH_2Cl_2, 0 °C to rt, 24 h, 91% yield), which is identical in all aspects with that reported by Nubbemeyer {$[\alpha]_D^{20}$ −35.3 (*c* 0.89, $CHCl_3$); lit. [27] $[\alpha]_D^{20}$ −35.1 (*c* 1.08, $CHCl_3$)}. Silyl ether **23** may serve as an advanced intermediate in the synthesis of pumiliotoxin 209F [17].

Conclusion

In summary, an eight-step synthesis of the advanced intermediate (8*S*,8a*S*)-**5** for the syntheis of pumiliotoxins has been achieved in 21% overall yield starting from (*R*)-3-silyloxyglutarimide derivative **14**. The method is based on the versatile building block **14** and relied on a highly diastereoselective *trans*-addition of methylmagnesium iodide to keto-lactam **10**. Since compound (8*S*,8a*S*)-**5** has been converted into pumiliotoxins 251D (**2**) and 237A (**3**), by Gallagher, Nubbemeyer, and Mori, respectively, its synthesis constitutes a formal enantioselective total synthesis of pumiliotoxins 251D and 237A. Compound (8*S*,8a*S*)-**5** would be of value for the synthesis of other pumiliotoxins as well. The highly diastereoselective *trans*-addition of a methylmagnesium iodide to keto-lactam **10** provides a new example of achieving the desired diastereoselection simply by the chair-conformation control [52,53].

Experimental

Optical rotations were recorded on a Perkin-Elmer 341 automatic polarimeter. ^{1}H NMR and ^{13}C NMR spectra were recorded on bruker 400 spectrometer. ^{1}H NMR spectra were measured in $CDCl_3$, and chemical shifts are expressed in parts per million (ppm) relative to internal Me_4Si. IR spectra were recorded on a Nicolet Avatar 330 RT-IR spectrophotometer. Mass spectra were recorded by Bruker Dalton Esquire 3000 plus and Finnigan Mat-LCQ (ESI direct injection). HRFABMS spectra were recorded on a Bruker APEX-FTMS apparatus. Elemental analyses were performed using a Vario RL analyzer. Melting points were determined on a Yanaco MP-500 melting point apparatus and are uncorrected.

Tetrahydrofuran (THF) was distilled prior to use from sodium benzophenone ketyl. Dichloromethane was distilled from phosphorus pentoxide. Silica gel (zhifu, 300–400 mesh) from Yantai silica gel factory (China) was used for column chromatography, eluting (unless otherwise stated) with ethyl acetate/petroleum ether (PE) (60–90 °C) mixture.

(*R*)-3-(*tert*-Butyldimethylsilyloxy)-1-(4-methoxybenzyl)piperidine-2,6-dione (14): To a solution of (*R*)-3-hydroxy-1-(4-methoxybenzyl)piperidine-2,6-dione **19** [47] (125 mg, 0.5 mmol), DMAP (10 mg) and imidazole (67 mg, 1 mmol) in CH_2Cl_2 (15 mL) was added TBDMSCl (52 µL, 0.6 mmol). The mixture was stirred at room temperature for 24 h before quenching with H_2O (5 mL). The organic layer was separated and the aqueous phase extracted with CH_2Cl_2 (10 mL × 5). The combined organic layers were washed with brine, dried over anhydrous Na_2SO_4, filtered and concentrated under reduced pressure. The residue was purified by column chromatography on silica gel (EtOAc/hexane 1:2) to give silyl ether **14** (517 mg, yield: 95%) as a colorless oil. $[\alpha]_D^{20}$ +19.2 (*c* 1.1, $CHCl_3$); IR (film) ν_{max}: 3062, 2936, 1728, 1658, 1494, 1451, 1367 cm^{-1}; ^{1}H NMR (400 MHz, $CDCl_3$) δ 0.11 (s, 3H), 0.12 (s, 3H), 0.87 (s, 9H), 1.92–2.07 (m, 2H), 2.59 (ddd, *J* = 17.7, 7.5, 5.4 Hz, 1H), 2.91 (ddd, *J* = 17.7, 8.1, 5.4 Hz, 1H), 3.76 (s, 3H), 4.30 (dd, *J* = 7.4, 4.0 Hz, 1H), 4.83 (d, *J* = 14.0 Hz, 1H), 4.86 (d, *J* = 14.0 Hz, 1H), 6.79 (d, *J* = 8.7 Hz, 2H), 7.30 (d, *J* = 8.7 Hz, 2H); ^{13}C NMR (100 MHz, $CDCl_3$) δ −5.4, −4.7, 18.2, 25.6 (3C), 26.4, 29.1, 42.4, 55.2, 69.3, 113.7 (2C), 129.4, 130.3 (2C), 158.9, 171.8, 172.2; HRMS ESI (*m*/*z*): [M + Na]$^+$ calcd for $C_{19}H_{29}NO_4SiNa$, 386.1758; found, 386.1757.

(5*R*,6*S*)-6-(But-3-enyl)-5-hydroxy-1-(4-methoxybenzyl)piperidin-2-one (18): To a solution of compound **14** (2.8 g, 7.71 mmol) in anhydrous CH_2Cl_2 (100 mL) at −20 °C was added dropwise a freshly prepared 3-butenylmagnesium bromide (1 M in THF, 15 mL, 15 mmol). After being stirred at −20 °C for 3 h, the reaction was quenched with a saturated aqueous solution of NH_4Cl (15 mL). The organic layer was separated and the aqueous phase was extracted with CH_2Cl_2 (25 mL × 5). The combined organic layers were washed with brine (10 mL × 5), dried over anhydrous Na_2SO_4, filtered and concentrated under reduced pressure. Without further separation, the crude product (2.4 g, 5.7 mmol) was treated with Et_3SiH (9 mL, 57 mmol) and $BF_3{\cdot}Et_2O$ (2.12 mL, 17.2 mmol) in CH_2Cl_2 (100 mL) at −78 °C. The mixture was stirred at −78 °C for 2 h, and then allowed to warm to −20 °C. After being stirred for another 2 h, saturated aqueous solution of $NaHCO_3$ (25 mL) was added and aqueous layer was extracted with CH_2Cl_2 (15 mL × 5). The combined organic layers were washed with brine, dried over anhydrous Na_2SO_4, filtered and concentrated under reduced pressure to give a crude product, which was used in the next step without further purification. To a solution of the crude product in THF (50 mL) was added a 1 M solution of TBAF in THF (17.1 mL, 17.1 mmol) at 0 °C. The mixture was allowed to warm to room temperature. After being stirred for 4 h at room temperature, the reaction was quenched with water, and extracted with CH_2Cl_2 (15 mL × 5). The combined organic phases were washed with brine, dried over anhydrous Na_2SO_4, filtered and concentrated under reduced pressure. The residue was purified by column chromatography on silica gel (EtOAc/hexane 2:1) to give diastereomers **18** (969 mg, yield: 59%) and **20** (51 mg, yield: 3%). Com-

pound **18**: white solid, mp 102–105 °C (EtOAc/hexane); $[\alpha]_D^{20}$ −65.0 (*c* 1.0, $CHCl_3$); IR (film) ν_{max}: 3375, 2934, 1612, 1512, 1193, 1056, 784, 560 cm^{-1}; ^1H NMR (400 MHz, $CDCl_3$) δ 1.37–1.49 (m, 1H), 1.67–1.64 (m, 2H), 1.91–2.00 (m, 2H), 2.28 (ddd, *J* = 18.1, 7.2, 2.8 Hz, 1H), 2.58 (ddd, *J* = 18.1, 10.5, 7.6 Hz, 2H), 3.20 (dt, *J* = 9.4, 2.6 Hz, 1H), 3.72 (s, 3H), 3.81 (d, *J* = 14.9 Hz, 1H), 3.93 (dt, *J* = 4.6, 2.6 Hz, 1H), 4.91–5.01 (m, 2H), 5.14 (d, *J* = 14.9 Hz, 1H), 5.69 (ddt, *J* = 16.9, 10.3, 6.6 Hz, 1H), 6.78 (d, *J* = 8.6 Hz, 2H), 7.15 (d, *J* = 8.6 Hz, 2H); ^{13}C NMR (100 MHz, $CDCl_3$) δ 23.9, 26.7, 30.0, 31.3, 47.3, 55.1, 61.8, 65.0, 113.8 (2C), 115.5, 129.0, 129.1 (2C), 136.9, 158.7, 169.8; HRMS ESI (*m*/*z*): $[M + Na]^+$ calcd for $C_{17}H_{23}NO_3Na$, 312.1570; found, 312.1570.

(*S*)-6-(But-3-en-1-yl)-1-(4-methoxybenzyl)piperidine-2,5-dione (10): To a stirred solution of compound **18** (100 mg, 0.34 mmol) in CH_2Cl_2 (5 mL) was added Dess–Martin periodinane (220 mg, 0.52 mmol) at room temperature. After being stirred for 2 h, the reaction was quenched with a 10% aqueous solution of $Na_2S_2O_3$. The aqueous phase was extracted with EtOAc (15 mL × 3). The combined organic layers were washed successively with a saturated aqueous solution of $NaHCO_3$ (5 mL × 3) and brine (5 mL × 2). The combined organic phases were dried over Na_2SO_4, filtered and concentrated under reduced pressure. The residue was purified by column chromatography on silica gel (EtOAc/hexane 1:2) to give compound **10** (98 mg, yield: 93%) as a colorless oil. $[\alpha]_D^{20}$ +37.5 (*c* 1.0, $CHCl_3$); IR (film) ν_{max}: 2955, 2926, 2834, 1725, 1625, 1512, 1246, 1173, 1032 cm^{-1}; ^1H NMR (400 MHz, $CDCl_3$) δ 1.79–2.11 (m, 4H), 2.57–2.69 (m, 2H), 2.73–2.80 (m, 2H), 3.68 (dd, *J* = 7.5, 4.6 Hz, 1H), 3.79 (s, 3H), 3.85 (d, *J* = 14.7 Hz, 1H), 4.97–5.08 (m, 2H), 5.28 (d, *J* = 14.7 Hz, 1H), 5.70 (ddt, *J* = 16.7, 10.2, 6.4 Hz, 1H), 6.84 (d, *J* = 8.7 Hz, 2H), 7.15 (d, *J* = 8.7 Hz, 2H); ^{13}C NMR (100 MHz, $CDCl_3$) δ 29.0, 29.2, 30.6, 35.3, 47.2, 55.2, 63.9, 114.2 (2C), 116.3, 128.3, 129.5 (2C), 136.4, 159.3, 169.6, 206.2; HRMS ESI (*m*/*z*): $[M + Na]^+$ calcd for $C_{17}H_{21}NO_3Na$, 310.1414; found, 310.1419.

(5*S*,6*S*)-6-(But-3-enyl)-5-hydroxy-1-(4-methoxybenzyl)-5-methylpiperidin-2-one (11): To a solution of compound **10** (92 mg, 0.32 mmol) in anhydrous CH_2Cl_2 (100 mL) was added dropwise a freshly prepared 1 M diethyl ether solution of CH_3MgI (1.0 mL, 1.0 mmol) at 0 °C. After being stirred at room temperature overnight, the reaction was quenched with a saturated aqueous solution of NH_4Cl (5 mL). The organic layer was separated and the aqueous phase was extracted with CH_2Cl_2 (15 mL × 5). The combined organic layers were washed with brine, dried over anhydrous Na_2SO_4, filtered and concentrated under reduced pressure. The residue was purified by column chromatography on silica gel (EtOAc/hexane 1:1) to give compound **11** (75 mg, yield: 76%) as a colorless oil. $[\alpha]_D^{20}$ −73.5 (*c* 1.0, $CHCl_3$); IR (film) ν_{max}: 3378, 2928, 2925, 2874, 1612, 1512, 1247, 1150, 1034, 914, 847 cm^{-1}; ^1H NMR (400 MHz, $CDCl_3$) δ 0.99 (s, 3H), 1.57–1.65 (m, 2H), 1.73 (d, *J* = 16.5 Hz, 1H), 2.04–2.12 (m, 2H), 2.20–2.27 (m, 2H), 2.41 (ddd, *J* = 18.6, 9.5, 8.8 Hz, 1H), 2.55 (ddd, *J* = 18.6, 8.8, 2.2 Hz, 1H), 3.00 (td, *J* = 5.4, 1.6 Hz, 1H), 3.59 (d, *J* = 14.3 Hz, 1H), 3.78 (s, 3H), 5.00–5.10 (m, 2H), 5.45 (d, *J* = 14.3 Hz, 1H), 5.81 (ddt, *J* = 16.8, 10.2, 6.7 Hz, 1H), 6.83 (d, *J* = 8.6 Hz, 2H), 7.20 (d, *J* = 8.6 Hz, 2H); ^{13}C NMR (100 MHz, $CDCl_3$) δ 26.9, 29.0, 30.5, 30.8, 32.5, 48.6, 55.2, 63.1, 70.1, 113.8 (2C), 115.5, 129.0, 130.4 (2C), 138.0, 159.1, 168.7; HRMS ESI (*m*/*z*): $[M + Na]^+$ calcd for $C_{18}H_{25}NO_3Na$, 326.1727; found, 326.1728.

(5*S*,6*S*)-6-(But-3-enyl)-5-hydroxy-5-methylpiperidin-2-one (22): To a solution of compound **11** (463 mg, 1.52 mmol) in a mixture of CH_3CN (32 mL) and H_2O (11 mL) was added ammonium cerium nitrate (2.5 g, 4.56 mmol) in one portion. The mixture was stirred for 4 h at room temperature. To the resulting mixture was added H_2O (5 mL), and the mixture was extracted with EtOAc (30 mL × 5). The combined organic layers were washed successively with a saturated solution aqueous of $NaHCO_3$ and brine. The organic phases were dried over anhydrous Na_2SO_4, filtered and concentrated under reduced pressure. The residue was purified by column chromatography on silica gel (MeOH/CH_2Cl_2 1:40) to give compound **22** (153 mg, yield: 56%) as a pale yellow oil. $[\alpha]_D^{20}$ −43.0 (*c* 1.18, $CHCl_3$); IR (film) ν_{max}: 3366, 2932, 1612, 1475, 1406, 1312, 919 cm^{-1}; ^1H NMR (400 MHz, $CDCl_3$) δ 1.31 (s, 3H), 1.52–1.61 (m, 1H), 1.76–1.93 (m, 3H), 2.10 (m, 1H), 2.22–2.35 (m, 2H), 2.57 (ddd, *J* = 18.2, 11.1, 7.0 Hz, 1H), 2.80 (s, 1H, OH, D_2O exchangeable), 3.17 (dd, *J* = 10.2, 1.8 Hz, 1H), 5.03–5.12 (m, 2H), 5.79 (ddt, *J* = 17.0, 10.2, 6.6 Hz, 1H), 6.03 (s, 1H, NH); ^{13}C NMR (100 MHz, $CDCl_3$) δ 26.3, 27.5, 28.7, 30.0, 34.1, 60.1, 67.9, 115.9, 137.1, 172.4; HRMS ESI (*m*/*z*): $[M + Na]^+$ calcd for $C_{10}H_{17}NO_2Na$, 206.1151; found, 206.1160.

(8*S*,8a*S*)-8-Hydroxy-8-methyloctahydroindolizidin-5-one (5): To a stirred solution of compound **22** (90 mg, 0.49 mmol) in a mixture of CH_2Cl_2 (8 mL) and MeOH (2 mL) was bubbled O_3 at −78 °C for 10 min. The reaction was quenched with Me_2S (0.2 mL). The mixture was allowed to warm to room temperature. The organic layer was separated, and the aqueous phase was extracted with CH_2Cl_2 (15 mL × 5). The combined organic layers were washed with brine, dried over anhydrous Na_2SO_4, filtered and concentrated under reduced pressure. Without further purification, to a solution of the crude mixture in CH_2Cl_2 (5 mL) was added Et_3SiH (0.77 mL, 4.9 mmol) and $BF_3{\cdot}Et_2O$ (0.18 mL, 1.47 mmol) at −78 °C. The mixture was allowed to warm slowly to the room temperature. A saturated aqueous solution of $NaHCO_3$ (2 mL) was added and aqueous

phase was extracted with CH_2Cl_2 (15 mL × 5). The combined organic layers were washed with brine, dried over anhydrous Na_2SO_4, filtered and concentrated under reduced pressure. The residue was purified by column chromatography on silica gel (MeOH/CH_2Cl_2 1:20) to give compound **5** (75 mg, yield: 91%) as a colorless waxy solid. $[\alpha]_D^{20}$ −42.7 (*c* 1.0, $CHCl_3$) {lit. [12] $[\alpha]_D^{20}$ −47.0 (*c* 0.8, $CHCl_3$) lit. [28] $[\alpha]_D^{25}$ −41.3 (*c* 0.48, $CHCl_3$); lit. [29] $[\alpha]_D^{25}$ −32.1 (*c* 1.0, $CHCl_3$)}; IR (film) ν_{max}: 3364, 2926, 2877, 1612, 1469, 1265, 740, 703 cm^{-1}; ^1H NMR (400 MHz, $CDCl_3$) δ 1.29 (s, 3H), 1.74–1.97 (m, 6H), 2.20 (br s, 1H, OH, D_2O exchangeable), 2.38 (dd, *J* = 18.4, 7.4 Hz, 1H), 2.53 (ddd, *J* = 18.4, 11.7, 7.4 Hz, 1H), 3.35 (dd, *J* = 10.3, 5.3 Hz, 1H), 3.48–3.53 (m, 2H); ^{13}C NMR (100 MHz, $CDCl_3$) δ 22.0, 26.3, 26.4, 28.0, 35.1, 45.7, 66.1, 67.7, 169.0; HRMS ESI (*m*/*z*): $[M + Na]^+$ calcd for $C_9H_{15}NO_2Na$, 192.0995; found, 192.0999.

(8*S*,8a*S*)-8-Methyl-8-trimethylsilyloxyoctahydroindolizidin-5-one (23): TMSCl (25 μL, 0.28 mmol) was added a solution of compound **5** (40 mg, 0.24 mmol), DMAP (5 mg) and imidazole (32 mg, 0.48 mmol) in CH_2Cl_2 (8 mL) at 0 °C. The mixture was stirred at room temperature for 24 h, and then diluted with H_2O (2 mL). The organic layer was separated and the aqueous phase was extracted with CH_2Cl_2 (5 mL × 5). The combined organic layers were washed with brine, dried over anhydrous Na_2SO_4, filtered and concentrated under reduced pressure. The residue was purified by column chromatography on silica gel (EtOAc/hexane 1:2) to give compound **23** (53 mg, yield: 91%) as a pale yellow oil. $[\alpha]_D^{20}$ −35.3 (*c* 0.89, $CHCl_3$) {lit. [27] $[\alpha]_D^{20}$ −35.1 (*c* 1.08, $CHCl_3$)}; IR (film) ν_{max}: 2955, 2880, 1621, 1470, 1413, 1378, 1316, 1273, 1265, 1253, 1224, 1134, 1068, 1021 cm^{-1}; ^1H NMR (400 MHz, $CDCl_3$) δ 0.05 (s, 9H), 1.26 (s, 3H), 1.60–1.90 (m, 6H), 2.25–2.33 (m, 1H), 2.33–2.45 (m, 1H), 3.15–3.20 (dd, *J* = 10.0, 5.5 Hz, 1H), 3.38–3.48 (m, 2H); ^{13}C NMR (100 MHz, $CDCl_3$) δ 2.1, 21.9, 26.2, 26.3 , 28.2, 35.2, 45.7, 67.3, 70.4, 168.9; HRMS ESI (*m*/*z*): $[M + Na]^+$ calcd for $C_{12}H_{23}NO_2SiNa$, 264.1390; found, 264.1392.

Supporting Information

Supporting Information File 1

^1H and ^{13}C NMR of key compounds.
[http://www.beilstein-journals.org/bjoc/content/supplementary/1860-5397-9-271-S1.pdf]

Acknowledgments

The authors are grateful to National Basic Research Program (973 Program) of China (Grant No. 2010CB833200), the NSF of China (21072160; 21332007), and the Program for Changjiang Scholars and Innovative Research Team in University (PCSIRT) of Ministry of Education, China for financial support. We thank Mr. Xin Li for the initial work displayed in Scheme 1.

References

1. Daly, J. W.; Spande, T. F.; Garraffo, H. M. *J. Nat. Prod.* **2005,** *68,* 1556–1575. doi:10.1021/np0580560
2. Vandendriessche, T.; Abdel-Mottaleb, Y.; Maertens, C.; Cuypers, E.; Sudau, A.; Nubbemeyer, U.; Mebs, D.; Tytgat, J. *Toxicon* **2008,** *51,* 334–344. doi:10.1016/j.toxicon.2007.10.011
3. Daly, J. W.; Gusovsky, F.; McNeal, E. T.; Secunda, S.; Bell, M.; Creveling, C. R.; Nichizawa, Y.; Overman, L. E.; Sharp, M. J.; Rossignol, D. P. *Biochem. Pharmacol.* **1990,** *40,* 315–326. doi:10.1016/0006-2952(90)90694-G
4. Smith, S. Q.; Jones, T. H. *Proc. Natl. Acad. Sci. U. S. A.* **2004,** *101,* 7841–7842. doi:10.1073/pnas.0402599101
5. Saporito, R. A.; Garraffo, H. M.; Donnelly, M. A.; Edwards, A. L.; Longino, J. T.; Daly, J. W. *Proc. Natl. Acad. Sci. U. S. A.* **2004,** *101,* 8045–8050. doi:10.1073/pnas.0402365101
6. Takada, W.; Sakata, T.; Shimano, S.; Enami, Y.; Mori, N.; Nishida, R.; Kuwahara, Y. *J. Chem. Ecol.* **2005,** *31,* 2403–2415. doi:10.1007/s10886-005-7109-9
7. Kibayashi, C. *Chem. Pharm. Bull.* **2005,** *53,* 1375–1386. doi:10.1248/cpb.53.1375
8. Tang, B. C.; Li, W. D. *Chin. J. Org. Chem.* **2004,** *24,* 1151–1158.
9. Franklin, A. S.; Overman, L. E. *Chem. Rev.* **1996,** *96,* 505–522. doi:10.1021/CR950021P
10. Daly, J. W.; Tokuyama, T.; Fujiwara, T.; Higher, R. J.; Karlet, I. L. *J. Am. Chem. Soc.* **1980,** *102,* 830–836. doi:10.1021/ja00522a064
11. Overman, L. E.; Bell, K. L. *J. Am. Chem. Soc.* **1981,** *103,* 1851–1853. doi:10.1021/ja00397a052
12. Fox, D. N. A.; Lathbury, D.; Mahon, M. F.; Molloy, K. C.; Gallagher, T. *J. Am. Chem. Soc.* **1991,** *113,* 2652–2656. doi:10.1021/ja00007a044
13. Pinho, V. D.; Procter, D. J.; Burtoloso, A. C. B. *Org. Lett.* **2013,** *15,* 2434–2437. doi:10.1021/ol400903n
14. Bernardim, B.; Pinho, V. D.; Burtoloso, A. C. B. *J. Org. Chem.* **2012,** *77,* 9926–9931. doi:10.1021/jo301967w
15. Sultane, P. R.; Mohite, A. R.; Bhat, R. G. *Tetrahedron Lett.* **2012,** *53,* 5856–5858. doi:10.1016/j.tetlet.2012.08.061
16. Woodin, K. S.; Jamison, T. F. *J. Org. Chem.* **2007,** *72,* 7451–7454. doi:10.1021/jo071132e
17. Sudau, A.; Münch, W.; Bats, J. W.; Nubbemeyer, U. *Eur. J. Org. Chem.* **2002,** 3315–3325. doi:10.1002/1099-0690(200210)2002:19<3315::AID-EJOC3315>3.0.CO;2-2
18. Ni, Y.; Zhao, G.; Ding, Y. *J. Chem. Soc., Perkin Trans. 1* **2000,** 3264–3266. doi:10.1039/b004450o
19. Barrett, A. G. M.; Damiani, F. *J. Org. Chem.* **1999,** *64,* 1410–1411. doi:10.1021/jo9820972
20. Cossy, J.; Cases, M.; Gomez Pardo, D. *Bull. Soc. Chim. Fr.* **1997,** *134,* 141–144.
21. Cossy, J.; Cases, M.; Gomez Pardo, D. *Synlett* **1996,** 909–910. doi:10.1055/s-1996-5590
22. Martin, S. F.; Bur, S. K. *Tetrahedron* **1999,** *55,* 8905–8914. doi:10.1016/S0040-4020(99)00452-4
23. Bargar, T. M.; Lett, R. M.; Johnson, P. L.; Hunter, J. E.; Chang, C. P.; Pernich, D. J.; Sabol, M. R.; Dick, M. R. *J. Agric. Food Chem.* **1995,** *43,* 1044–1051. doi:10.1021/jf00052a037

24. Honda, T.; Hoshi, M.; Kanai, K.; Tsubuki, M. *J. Chem. Soc., Perkin Trans. 1* **1994,** 2091–2101. doi:10.1039/p19940002091
25. Honda, T.; Hoshi, M.; Tsubuki, M. *Heterocycles* **1992,** *34,* 1515–1518. doi:10.3987/COM-92-6098
26. Overman, L. E.; Bell, K. L.; Ito, F. *J. Am. Chem. Soc.* **1984,** *106,* 4192–4201. doi:10.1021/ja00327a022
27. Sudau, A.; Münch, W.; Bats, J. W.; Nubbemeyer, U. *Eur. J. Org. Chem.* **2002,** 3304–3314. doi:10.1002/1099-0690(200210)2002:19<3304::AID-EJOC3304>3.0.CO;2-A
28. Wu, H.; Yu, M.; Zhang, Y.; Zhao, G. *Chin. J. Chem.* **2009,** *27,* 183–188. doi:10.1002/cjoc.200990015
29. O'Mahony, G.; Nieuwenhuyzen, M.; Armstrong, P.; Stevenson, P. J. *J. Org. Chem.* **2004,** *69,* 3968–3971. doi:10.1021/jo0497205
30. Chen, B.-F.; Tasi, M.-R.; Yang, C.-Y.; Chang, J.-K.; Chang, N.-C. *Tetrahedron* **2004,** *60,* 10223–10231. doi:10.1016/j.tet.2004.09.001
31. Wang, B.; Fang, F.; Lin, G.-Q. *Tetrahedron Lett.* **2003,** *44,* 7981–7984. doi:10.1016/j.tetlet.2003.08.113
32. Huang, P.-Q. *Synlett* **2006,** 1133–1149. doi:10.1055/s-2006-941565 See for an account on the methodology of the regio-and *trans*-diastereoselective reductive addition of glutarimide.
33. Liu, X.-K.; Ye, J.-L.; Ruan, Y.-P.; Li, Y.-X.; Huang, P.-Q. *J. Org. Chem.* **2013,** *78,* 35–41. doi:10.1021/jo3014484
34. Huo, H.-H.; Xia, X.-E.; Zhang, H.-K.; Huang, P.-Q. *J. Org. Chem.* **2013,** *78,* 455–465. doi:10.1021/jo302362b
35. Liu, X.-K.; Zheng, X.; Ruan, Y.-P.; Ma, J.; Huang, P.-Q. *Org. Biomol. Chem.* **2012,** *10,* 1275–1284. doi:10.1039/c1ob06697h
36. Zhuang, J.-J.; Ye, J.-L.; Zhang, H.-K.; Huang, P.-Q. *Tetrahedron* **2012,** *68,* 1750–1755. doi:10.1016/j.tet.2011.12.063
37. Liu, X.-K.; Qiu, S.; Xiang, Y.-G.; Ruan, Y.-P.; Zheng, X.; Huang, P.-Q. *J. Org. Chem.* **2011,** *76,* 4952–4963. doi:10.1021/jo200600n
38. Zhang, H.-K.; Li, X.; Huang, H.; Huang, P.-Q. *Sci. China: Chem.* **2011,** *54,* 737–744. doi:10.1007/s11426-011-4256-4
39. Wu, Y. D.; Houk, K. N.; Florez, J.; Trost, B. M. *J. Org. Chem.* **1991,** *56,* 3656–3664. doi:10.1021/jo00011a039
40. Ashby, E. C.; Laemmle, J. T. *Chem. Rev.* **1975,** *75,* 521–546. doi:10.1021/cr60296a005
41. Trost, B. M.; Florez, J.; Jebaratnam, D. J. *J. Am. Chem. Soc.* **1987,** *109,* 613–615. doi:10.1021/ja00236a067
42. Huang, P. Q.; Zhou, W. S. *Tetrahedron: Asymmetry* **1991,** *2,* 875–878. doi:10.1016/S0957-4166(00)82199-0
43. Dimitrov, V.; Panev, S. *Tetrahedron: Asymmetry* **2000,** *11,* 1513–1516. doi:10.1016/S0957-4166(00)00099-9
44. Tan, C.-H.; Holmes, A. B. *Chem.–Eur. J.* **2001,** *7,* 1845–1854. doi:10.1002/1521-3765(20010504)7:9<1845::AID-CHEM1845>3.0.CO;2-2
45. Liu, L.-X.; Xiao, K.-J.; Huang, P.-Q. *Tetrahedron* **2009,** *65,* 3834–3841. doi:10.1016/j.tet.2009.03.021
46. Liu, L.-X.; Ruan, Y.-P.; Guo, Z.-Q.; Huang, P.-Q. *J. Org. Chem.* **2004,** *69,* 6001–6009. doi:10.1021/jo049166z
47. Yu, D.-S.; Xu, W.-X.; Liu, L.-X.; Huang, P.-Q. *Synlett* **2008,** 1189–1192. doi:10.1055/s-2008-1072737
48. Liu, H.-J.; Yip, J.; Shia, K.-S. *Tetrahedron Lett.* **1997,** *38,* 2253–2256. doi:10.1016/s0040-4039(97)00345-6
49. Huang, P.-Q.; Wei, B.-G.; Ruan, Y.-P. *Synlett* **2003,** 1663–1667. doi:10.1055/s-2003-40988
50. Fukuyama, T.; Frank, R. K.; Jewell, C. F., Jr. *J. Am. Chem. Soc.* **1980,** *102,* 2122–2123. doi:10.1021/ja00526a076
51. Smith, A. B., III; Wang, Z. *J. Org. Chem.* **2000,** *65,* 3738–3753. doi:10.1021/jo991958j
52. Tuo, S.; Liu, X.; Huang, P. *Chin. J. Chem.* **2013,** *31,* 55–62. doi:10.1002/cjoc.201200904
53. Wang, Y.-H.; Ou, W.; Xie, L.-F.; Ye, J.-L.; Huang, P.-Q. *Asian J. Org. Chem.* **2012,** *1,* 359–365. doi:10.1002/ajoc.201200113 See for part I of this series.

License and Terms

This is an Open Access article under the terms of the Creative Commons Attribution License (http://creativecommons.org/licenses/by/2.0), which permits unrestricted use, distribution, and reproduction in any medium, provided the original work is properly cited.

The license is subject to the *Beilstein Journal of Organic Chemistry* terms and conditions: (http://www.beilstein-journals.org/bjoc)

The definitive version of this article is the electronic one which can be found at: doi:10.3762/bjoc.9.271

Beilstein Journal of Organic Chemistry

A protecting group-free synthesis of the Colorado potato beetle pheromone

Zhongtao Wu, Manuel Jäger, Jeffrey Buter and Adriaan J. Minnaard*

Letter

Open Access

Address:
Stratingh Institute for Chemistry, University of Groningen, Nijenborgh 7, 9747 AG, Groningen, The Netherlands

Email:
Adriaan J. Minnaard* - a.j.minnaard@rug.nl

* Corresponding author

Keywords:
aggregation pheromone; catalysis; Colorado potato beetle; *Leptinotarsa decemlineata*; oxidation; natural product

Beilstein J. Org. Chem. **2013,** *9,* 2374–2377.
doi:10.3762/bjoc.9.273

Received: 20 August 2013
Accepted: 18 October 2013
Published: 06 November 2013

This article is part of the Thematic Series "Natural products in synthesis and biosynthesis".

Guest Editor: J. S. Dickschat

© 2013 Wu et al; licensee Beilstein-Institut.
License and terms: see end of document.

Abstract

A novel synthesis of the aggregation pheromone of the Colorado potato beetle, *Leptinotarsa decemlineata,* has been developed based on a Sharpless asymmetric epoxidation in combination with a chemoselective alcohol oxidation using catalytic $[(\text{neocuproine})\text{PdOAc}]_2\text{OTf}_2$. Employing this approach, the pheromone was synthesized in 3 steps, 80% yield and 86% ee from geraniol.

Introduction

The Colorado potato beetle *Leptinotarsa decemlineata*, a worldwide pest causing considerable damage in the US annually, has developed resistance to more than 25 insecticides [1-4]. For crop protection, currently several insecticides are used such as the neonicotinoids imidacloprid, thiamethoxam and thiachloprid [1,5], albeit these are expensive and moreover resistance lies in wait [6]. From the standpoint of environmental protection and economics, it is important to reduce the use of insecticides controlling the Colorado potato beetle, and an attractive alternative is to use a pheromone management strategy.

An important finding in this connection was the isolation of the male produced aggregation pheromone by Dickens and Oliver et al. in 2002 [7], which was subsequently identified as (*S*)-1,3-dihydroxy-3,7-dimethyl-6-octen-2-one (**1**, Figure 1) [8]. (*S*)-**1** is attractive for both male and female *Leptinotarsa decemlineata* while (*R*)-**1** is inactive or inhibitory, as was demonstrated by the inactivity of the racemate [7]. Since then, (*S*)-**1** has been synthesized by the groups of Oliver [8], Mori [9], Chauhan [10] and

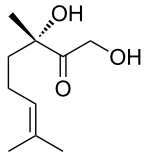
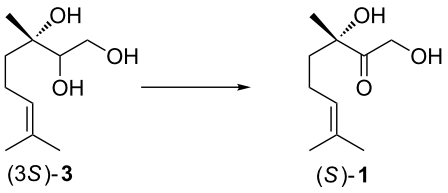


Figure 1: (*S*)-1,3-dihydroxy-3,7-dimethyl-6-octen-2-one (**1**).

very recently by Faraldos [11] respectively, and the first field evaluation of synthetic (*S*)-**1** in a trap crop pest management strategy showed its practical utility [1].

The commercial enantioselective production of chiral pheromones of many pest insects is hampered by prohibitively high costs. The selective introduction of stereocenters and the number of steps are the main reasons. In 2002, Oliver described the first synthesis of both enantiomers of **1** from (*R*)- and (*S*)-linalool, and also the synthesis of its racemate from geraniol, to establish the absolute configuration. Although the approach is elegant, (*S*)-linalool required for natural (*S*)-**1** is not commercially available. In 2005, Mori employing lipase-catalyzed kinetic resolution of (±)-2,3-epoxynerol as the key step, synthesized both (*S*)- and (*R*)-**1** in gram quantities with high ee. In Chauhan's work, Grignard reaction, oxidation and stereoselective methylation using organometallic reagents are the key steps, affording (*S*)-**1** in high enantiomeric purity and in gram quantities. In all these approaches, however, protection of the primary hydroxy group of the 1,2,3-triol substructure is required for the selective oxidation of the secondary alcohol at C-2. The synthesis by Faraldos runs via epoxidation of fluoronerol, subsequent acetylation of the alcohol and solvolysis.

In 2010, Waymouth reported the chemoselective, catalytic oxidation of glycerol to dihydroxyacetone (Scheme 1) using catalytic $[(\text{neocuproine})\text{PdOAc}]_2\text{OTf}_2$ (**2**) in the presence of either benzoquinone or air as the terminal oxidant [12]. More recently, the transformation of unprotected vicinal polyols to α-hydroxy ketones was achieved by regio- and chemoselective oxidation using catalyst **2** [13]. We used this method for the catalytic regioselective oxidation of glycosides (Scheme 1) [14] and expected that the approach might also be applicable in the synthesis of (*S*)-**1**. Triol **3**, with vicinal primary, secondary, and tertiary hydroxy groups should be a suitable substrate for chemoselective oxidation with catalyst **2**, enabling a protecting group-free synthesis of the Colorado potato beetle pheromone (Scheme 2). An additional challenge was the presence of an alkene in the substrate, as the orthogonality of **2**-catalyzed alcohol oxidations with alkenes had not been studied.

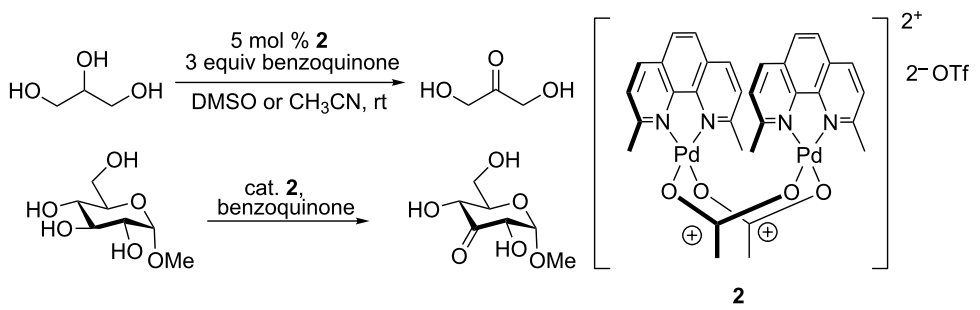


Scheme 2: Approach of synthesis of (*S*)-**1**.

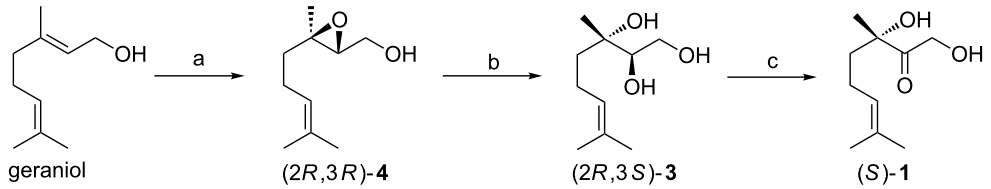
In our approach, Sharpless asymmetric epoxidation of readily available geraniol or nerol [16-18] followed by stereoselective ring-opening with water would lead to the desired triol **3**. Subsequently regioselective oxidation of **3** would provide (*S*)-**1** in a concise 3 step route. The resulting synthesis would be interesting also for commercial application, moreover because the oxidation pattern in **1** occurs more widespread in natural products and pharmaceuticals such as in cortisol (hydrocortisone).

Results and Discussion

The synthesis of (*S*)-**1** is summarized in Scheme 3. The choice for either geraniol or nerol should have been based on the stereoselectivity of the Sharpless epoxidation. For both reactions, however, varying enantioselectivities had been reported, so both substrates were studied. According to the published procedure, upon treatment of freshly distilled geraniol (Scheme 3) with *tert*-butyl hydroperoxide in the presence of D-(−)-diisopropyl tartrate (DIPT) and Ti(OiPr)_4 in dry CH_2Cl_2 at –10 to –23 °C for 2 h, the desired epoxide (2*R*,3*R*)-**4** was obtained in 93% yield and 88% ee. The ee was determined by HPLC analysis of its corresponding TBDPS ether. This result compares well with the ones reported in the literature: 77–95% yield and 81–95% ee [17-21]. According to Sharpless et al. [18], 5 mol % of Ti(OiPr)_4 and 7.5 mol % of DIPT were used, so at least 20% excess of tartrate ester in order to obtain the



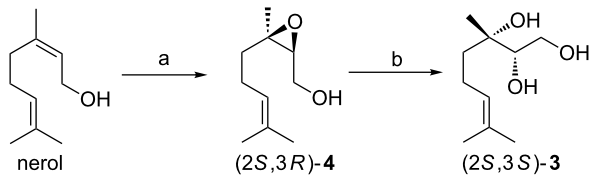
Scheme 1: Selective oxidation of glycerol [15] and methyl α-D-glucopyranoside.



Scheme 3: Synthesis of (*S*)-**1** from geraniol. Reagents and conditions: a) D-(−)-diisopropyl tartrate, $Ti(OiPr)_4$, *tert*-butyl hydroperoxide, CH_2Cl_2, 4 Å MS, –10 to –23 °C, 2 h, 93%, 94:6 er; b) $HClO_4$ (70%), THF/water, rt, 30 min, 94%; c) 0.5 mol % **2**, *p*-benzoquinone, CH_3CN/water, rt, overnight, 91%.

maximum enantiomeric excess. The use of freshly distilled DIPT and $Ti(OiPr)_4$ was important to obtain consistently 88% ee. With epoxide (2*R*,3*R*)-**4** at hand, an acid-catalyzed ring-opening reaction was carried out using $HClO_4$ in THF/water at room temperature [22]. In the process of ring-opening, close to quantitative inversion of configuration at C-3 takes place [23,24], a result which was confirmed in our research as determination of the ee of both substrate and product shows a slight drop in ee from 88% to 86% (see Supporting Information File 1). Triol (2*R*,3*S*)-**3** was obtained from (2*R*,3*R*)-**4** in high yield by this regio- and stereoselective ring-opening reaction. Subsequently (2*R*,3*S*)-**3** was converted into (*S*)-**1** by treatment with 0.5 mol % of catalyst **2** and benzoquinone in CH_3CN/water at room temperature. The reaction turned out to be very selective for the secondary alcohol and neither oxidation of the primary alcohol nor of the alkene was observed. (*S*)-**1** was obtained in 91% yield and both ^1H NMR and ^{13}C NMR spectra coincided with those reported in the literature [8,9].

Starting from nerol, Sharpless asymmetric epoxidation afforded the epoxide (2*S*,3*R*)-**4** in a disappointing 74% ee, a result which is nevertheless in accordance with the reported values: 70–94% [25-30] (Scheme 4). Applying the same ring-opening reaction to epoxide (2*S*,3*R*)-**4**, triol (2*S*,3*S*)-**3** was obtained in high yield but a 6% loss in enantiomeric excess was observed (see Supporting Information File 1). Considering these disappointing results using nerol as the starting material, oxidation to (*S*)-**1** was not performed.



Scheme 4: Synthesis starting from nerol. Reagents and conditions: a) L-(+)-diisopropyl tartrate, $Ti(OiPr)_4$, *tert*-butyl hydroperoxide, CH_2Cl_2, 4 Å MS, −10 to −23 °C, 2 h, 89%, 87:13 er; b) $HClO_4$ (70%), THF/H_2O, rt, 30 min, 92%.

Conclusion

In summary, we have developed an efficient synthesis of the aggregation pheromone of the Colorado potato beetle (*S*)-1,3-dihydroxy-3,7-dimethyl-6-octen-2-one (**1**). Combining Sharpless asymmetric epoxidation, stereoselective epoxide ring-opening and catalytic chemoselective alcohol oxidation with $[(neocuproine)PdOAc]_2OTf_2$ (**2**), (*S*)-**1** was synthesized in 80% overall yield and 86% ee over 3 steps from geraniol. Nerol turned out to be less suitable as starting material as its asymmetric epoxidation provided a lower ee. It has been shown that (*S*)-**1** with an ee of 92% is as active as enantiopure (*S*)-**1** (99% ee), therefore it is probably safe to conclude that the currently obtained 86% ee suffices.

Supporting Information

Supporting Information File 1

Experimental and spectroscopic details for **1**, **3** and **4**, and determination of the ee of **3** and **4**.
[http://www.beilstein-journals.org/bjoc/content/supplementary/1860-5397-9-273-S1.pdf]

Acknowledgements

This work was supported by the NRSC-Catalysis program. J. G. Edens is kindly acknowledged for support in literature studies.

References

1. Kuhar, T. P.; Mori, K.; Dickens, J. C. *Agr. Forest Entomol.* **2006,** *8,* 77–81. doi:10.1111/j.1461-9555.2006.00286.x
2. Roush, R. T.; Hoy, C. W.; Ferro, D. N.; Tingey, W. M. *J. Econ. Entomol.* **1990,** *83,* 315–319.
3. Ioannidis, P. M.; Grafius, E.; Whalon, M. E. *J. Econ. Entomol.* **1991,** *84,* 1417–1423.
4. Grafius, E. *J. Econ. Entomol.* **1997,** *90,* 1144–1151.
5. Połeć, I. *Pestycydy/Pesticides* **2010,** *1–4,* 33–41.
6. Olson, E. R.; Dively, G. P.; Nelson, J. O. *J. Econ. Entomol.* **2000,** *93,* 447–458. doi:10.1603/0022-0493-93.2.447
7. Dickens, J. C.; Oliver, J. E.; Hollister, B.; Davis, J. C.; Klun, J. A. *J. Exp. Biol.* **2002,** *205,* 1925–1933.
8. Oliver, J. E.; Dickens, J. C.; Glass, T. E. *Tetrahedron Lett.* **2002,** *43,* 2641–2643. doi:10.1016/S0040-4039(02)00349-0

9. Tashiro, T.; Mori, K. *Tetrahedron: Asymmetry* **2005,** *16,* 1801–1806. doi:10.1016/j.tetasy.2005.03.030
10. Babu, B. N.; Chauhan, K. R. *Tetrahedron Lett.* **2009,** *50,* 66–67. doi:10.1016/j.tetlet.2008.10.092
11. Faraldos, J. A.; Coates, R. M.; Giner, J.-L. *J. Org. Chem.* **2013,** *78,* 10548–10554. doi:10.1021/jo4017056
12. Painter, R. M.; Pearson, D. M.; Waymouth, R. M. *Angew. Chem., Int. Ed.* **2010,** *49,* 9456–9459. doi:10.1002/anie.201004063
13. Chung, K.; Banik, S. M.; De Crisci, A. G.; Pearson, D. M.; Blake, T. R.; Olsson, J. V.; Ingram, A. J.; Zare, R. N.; Waymouth, R. M. *J. Am. Chem. Soc.* **2013,** *135,* 7593–7602. doi:10.1021/ja4008694
14. Jäger, M.; Hartmann, M.; de Vries, J. G.; Minnaard, A. J. *Angew. Chem., Int. Ed.* **2013,** *52,* 7809–7812. doi:10.1002/anie.201301662
15. Conley, N. R.; Labios, L. A.; Pearson, D. M.; McCrory, C. C. L.; Waymouth, R. M. *Organometallics* **2007,** *26,* 5447–5453. doi:10.1021/om700492n
16. Hashimoto, M.; Harigaya, H.; Yanagiya, M.; Shirahama, H. *J. Org. Chem.* **1991,** *56,* 2299–2311. doi:10.1021/jo00007a013
17. Katsuki, T.; Sharpless, K. B. *J. Am. Chem. Soc.* **1980,** *102,* 5974–5976. doi:10.1021/ja00538a077
18. Gao, Y.; Hanson, R. M.; Klunder, J. M.; Ko, S. Y.; Masamune, H.; Sharpless, K. B. *J. Am. Chem. Soc.* **1987,** *109,* 5765–5780. doi:10.1021/ja00253a032
19. Nacro, K.; Baltas, M.; Escudier, J.-M.; Gorrichon, L. *Tetrahedron* **1996,** *52,* 9047–9056. doi:10.1016/0040-4020(96)00453-X
20. Molawi, K.; Delpont, N.; Echavarren, A. M. *Angew. Chem., Int. Ed.* **2010,** *49,* 3517–3519. doi:10.1002/anie.201000890
21. Mohapatra, D. K.; Pramanik, C.; Chorghade, M. S.; Gurjar, M. K. *Eur. J. Org. Chem.* **2007,** 5059–5063. doi:10.1002/ejoc.200700401
22. González, I. C.; Forsyth, C. J. *J. Am. Chem. Soc.* **2000,** *122,* 9099–9108. doi:10.1021/ja000001r
23. Hanson, R. M. *Tetrahedron Lett.* **1984,** *25,* 3783–3786. doi:10.1016/S0040-4039(01)91166-9
24. Corey, E. J.; Ha, D.-C. *Tetrahedron Lett.* **1988,** *29,* 3171–3174. doi:10.1016/0040-4039(88)85113-X
25. Kolb, M.; Van Hijfte, L.; Ireland, R. E. *Tetrahedron Lett.* **1988,** *29,* 6769–6772. doi:10.1016/S0040-4039(00)82450-8
26. Marshall, J. A.; Trometer, J. D.; Cleary, D. G. *Tetrahedron* **1989,** *45,* 391–402. doi:10.1016/0040-4020(89)80067-5
27. Van Hijfte, L.; Kolb, M. *Tetrahedron* **1992,** *48,* 6393–6402. doi:10.1016/S0040-4020(01)88229-6
28. Ray, N. C.; Raveendranath, P. C.; Spencer, T. A. *Tetrahedron* **1992,** *48,* 9427–9432. doi:10.1016/S0040-4020(01)88311-3
29. Mori, N.; Kuwahara, Y.; Kurosa, K. *Bioorg. Med. Chem.* **1996,** *4,* 289–295. doi:10.1016/0968-0896(96)00005-3
30. Underwood, B. S.; Tanuwidjaja, J.; Ng, S.-S.; Jamison, T. F. *Tetrahedron* **2013,** *69,* 5205–5220. doi:10.1016/j.tet.2013.04.041

License and Terms

This is an Open Access article under the terms of the Creative Commons Attribution License (http://creativecommons.org/licenses/by/2.0), which permits unrestricted use, distribution, and reproduction in any medium, provided the original work is properly cited.

The license is subject to the *Beilstein Journal of Organic Chemistry* terms and conditions: (http://www.beilstein-journals.org/bjoc)

The definitive version of this article is the electronic one which can be found at: doi:10.3762/bjoc.9.273

Beilstein Journal of Organic Chemistry

Biosynthesis of rare hexoses using microorganisms and related enzymes

Zijie Li[1], Yahui Gao[2], Hideki Nakanishi[1], Xiaodong Gao[*1] and Li Cai[*3]

Review

Open Access

Address:
[1]The Key Laboratory of Carbohydrate Chemistry and Biotechnology, Ministry of Education, School of Biotechnology, Jiangnan University, Wuxi, 214122, China, [2]School of Food Science and Technology, Jiangnan University, Wuxi, 214122, China and [3]Division of Mathematics and Science, University of South Carolina Salkehatchie, Walterboro, South Carolina, 29488, USA

Email:
Xiaodong Gao[*] - xdgao@jiangnan.edu.cn; Li Cai[*] - caili@mailbox.sc.edu

* Corresponding author

Keywords:
biosynthesis; enzyme; hexose; microorganism; rare sugars

Beilstein J. Org. Chem. **2013,** *9,* 2434–2445.
doi:10.3762/bjoc.9.281

Received: 25 July 2013
Accepted: 15 October 2013
Published: 12 November 2013

This article is part of the Thematic Series "Natural products in synthesis and biosynthesis".

Guest Editor: J. S. Dickschat

© 2013 Li et al; licensee Beilstein-Institut.
License and terms: see end of document.

Abstract

Rare sugars, referred to as monosaccharides and their derivatives that rarely exist in nature, can be applied in many areas ranging from foodstuffs to pharmaceutical and nutrition industry, or as starting materials for various natural products and drug candidates. Unfortunately, an important factor restricting the utilization of rare sugars is their limited availability, resulting from limited synthetic methods. Nowadays, microbial and enzymatic transformations have become a very powerful tool in this field. This article reviews the biosynthesis and enzymatic production of rare ketohexoses, aldohexoses and sugar alcohols (hexitols), including D-tagatose, D-psicose, D-sorbose, L-tagatose, L-fructose, 1-deoxy-L-fructose, D-allose, L-glucose, L-talose, D-gulose, L-galactose, L-fucose, allitol, D-talitol, and L-sorbitol. New systems and robust catalysts resulting from advancements in genomics and bioengineering are also discussed.

Introduction

Rare sugars are referred to as monosaccharides and their derivatives that rarely exist in nature (http://isrs.kagawa-u.ac.jp/activities.html) [1]. Seeberger et al. did some interesting statistical research on bacterial and mammalian glycomes, with one emphasis placed on the abundance of monosaccharide units (most abundant monosaccharides are listed therein) [2,3]. Rare sugars are thus classified by their low natural abundance, compared to those common sugars such as D-glucose, D-galactose, *N*-acetylglucosamine, etc that exist in significant amounts. Nonetheless, rare sugars can be applied in many areas ranging from foodstuffs to pharmaceutical and nutrition industry [4]. In recent years, the interest in rare carbohydrates and the nucleosides (e.g. L-nucleoside analogues) derived from them has substantially increased in medicine because these molecules are

potential candidates of anticancer and antiviral drugs [4-6]. Unfortunately, the limited availability of these compounds restricts their potential applications and the chemical synthesis does not satisfy the increasing demand. Izumori et al. created beautiful "Izumoring" schemes displaying all rare sugars in tree form to illustrate possible strategies for the production of these monosaccharides [7]. Recently, inspired by the "Izumoring" tree, microbial and enzymatic transformations have become a very powerful tool for the synthesis of rare sugars owing to the advancements in genomics and an increasing availability of new and robust biocatalysts. Microbial transformation has the advantages of using cheaper catalysts without purification and the avoidance of cofactor recycling in vitro, while enzymatic conversion is more controllable and scalable. In addition, immobilized enzymes offer advantages over free and soluble enzymes in many aspects: 1) immobilized enzymes can be used repeatedly and the enzymatic processes can be operated continuously and readily controlled; 2) products can be easily harvested and purified; 3) enzyme properties (such as activity and stability) could be potentially improved through immobilization. In this review, we mainly focus on the biosynthesis and enzymatic production of rare hexoses, including ketohexoses, aldohexoses, and sugar alcohols (hexitols). To improve the production of these rare sugars, strategies for enhancing the catalytic efficiency and/or substrate selectivity of related enzymes are also discussed.

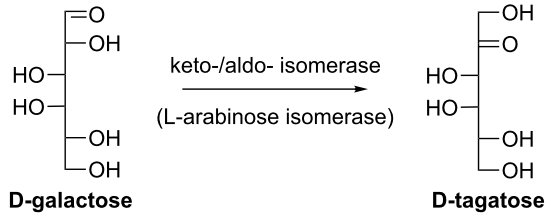
Review

I. Biosynthesis of rare ketohexoses

The most common ketohexoses (ketone-containing hexoses), each of which represents a pair of enantiomers (D- and L-isomers), include tagatose, psicose, sorbose, and fructose. Among the eight sugars, D-tagatose, D-psicose, D-sorbose, L-tagatose and L-fructose are generally regarded as rare sugars due to their low abundance in nature. In addition, 1-deoxy-L-fructose is also a very rare but important monosaccharide [8]. The biosynthesis of these rare ketohexoses using microorganisms and related enzymes is summarized below.

D-Tagatose

D-Tagatose is a keto-/aldo-isomer of D-galactose. It has been approved by the FDA as a food additive and gained much attention owing to its properties and health benefits, including low calorie [9], no glycemic effect [10], promotion of weight loss [11], tooth care [12], and prebiotic [13]. D-Tagatose production through bioconversion has been extensively studied, particularly from D-galactose by L-arabinose isomerase (AI, EC 5.3.1.4) (Scheme 1) [14-20]. As the interconversion equilibrium between D-galactose and D-tagatose shifts toward D-tagatose at higher temperatures, biocatalysts with greater thermal stability are preferred. Thus AIs from thermophilic or hyperthermophilic bacteria are of special interest. It was reported that the highest level of D-tagatose production was 230 g/L from 500 g/L D-galactose catalyzed by an immobilized AI from *Geobacillus stearothermophilus* [21] and the highest yield was 68% at 80 °C by AI from *Thermotoga neapolitana* [22]. However, two main problems still exist for the AI-catalyzed D-tagatose synthesis. The catalytic efficiency of AI for D-galactose is relatively low compared to its natural substrate L-arabinose. Enzyme engineering has thus been reported to improve the efficiency of AI towards D-galactose [23]. Another challenge lies in the product purification due to very similar properties of D-galactose and D-tagatose. Liang et al. elegantly employed *Saccharomyces cerevisiae* to selectively consume D-galactose and thus D-tagatose could be obtained at above 95% purity [24].

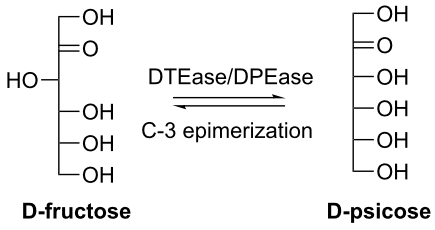


Scheme 1: Synthesis of D-tagatose from D-galactose using L-arabinose isomerase.

D-Psicose

D-Psicose is a C-3 epimer of D-fructose and a potential sucrose substitute sweetening agent. The suppression of hepatic lipogenic enzymes activity of D-psicose has been noticed for its use as a non-caloric sweetener [25,26]. In addition, antioxidant properties have been observed for foods containing this rare sugar [25]. More interestingly, D-psicose has also been used to prepare several D-psicose containing disaccharides, aiming to learn the function of the rare sugar containing oligosaccharides and glycosides [27]. D-Psicose can be prepared through the epimerization of D-fructose at C-3 catalyzed by an ezyme of the D-tagatose 3-epimerase family (DTEase, EC 5.1.3.-), which is a commercially attractive enzymatic reaction for D-psicose production (Scheme 2). To date, five DTEases from different organisms have been characterized and employed for the D-psicose synthesis. Izumori et al. firstly characterized the DTEase from *Pseudomonas sp.* ST-24 [28] and utilized this enzyme in the mass production of D-psicose with a final concentration of 150 g/L [29]. They further packed the immobilized DTEase from *Pseudomonas sp.* ST-24 (on Chitopearl beads) into a column that could be continuously used for 10 days and 90 g of D-psicose were produced from 500 g of D-fructose as the starting material [30]. Kim et al. also characterized a putative DTEase from *Agrobacterium tumefaciens*

[31] and due to its high substrate specificity towards D-psicose, this enzyme was renamed as D-psicose 3-epimerase (DPEase, EC 5.1.3.-).



Scheme 2: Synthesis of D-psicose from D-fructose using D-tagatose 3-epimerase/D-psicose 3-epimerase.

It was discovered that borate could promote the conversion of D-fructose to D-psicose through the formation of a psicose–borate complex [32]. The maximum conversion yield of D-psicose in the presence of borate was about two-fold compared to the reaction without borate. Lim et al. established a stable immobilized *A. tumefaciens* DPEase system containing borate [33]. It could generate 441 g/L D-psicose from 700 g/L D-fructose for one batch, and the reaction performed in a packed-bed bioreactor could continuously produce 325 g/L D-psicose from 500 g/L D-fructose over a long time period. Zhang et al. characterized the third DTEase from *Rhodobacter sphaeroides* SK011 [34] and the specificity of this enzyme towards D-fructose was the highest under optimized conditions. Recently, Mu et al. characterized the fourth and fifth DTEase from *Clostridium cellulolyticum* H10 and *Clostridium scindens* 35704 respectively. As these two enzymes showed high preference towards D-psicose, they were both renamed as DPEase as well. The activity of these two enzymes is strictly metal-dependent and requires Mn^{2+} as the optimum cofactor. Under optimal conditions, the epimerization yields were 32% and 28%, respectively [35,36].

The enzymes described above are all generally named as DTEase family enzymes, despite the fact that all enzymes do not demonstrate strict specificity towards D-tagatose and low to moderate homology (20–60%) was found among them [37]. However, high similarities are observed for key amino acid residues in the active site, the metal coordinating site and the substrate-binding site of these enzymes (Figure 1) [37,38]. After all, the interconversion between D-fructose and D-psicose catalyzed by DTEase enzymes is an equilibrium process, thus large scale and high yield production of D-psicose as well as product purification remain problematic. Our lab mainly focuses on the in vitro production of rare sugars using dihydroxyacetone phosphate (DHAP)-dependent aldolases. In our previous work, we utilized L-fuculose-1-phosphate aldolase (EC 4.1.2.17) from *Thermus thermophilus* HB8 ($FucA_{T.HB8}$) to stereoselectively synthesize D-psicose. The donor molecule DHAP, a highly expensive starting material ($970.00/250 mg, Sigma-Aldrich), was generated in situ from less expensive L-glycerol-3-phosphate or DL-glycerol-3-phosphate (Scheme 3) [39]. Such a one-pot multi-enzyme approach represents a cost-effective non-equilibrium pathway for the large-scale preparation of D-psicose (Scheme 3) [40].

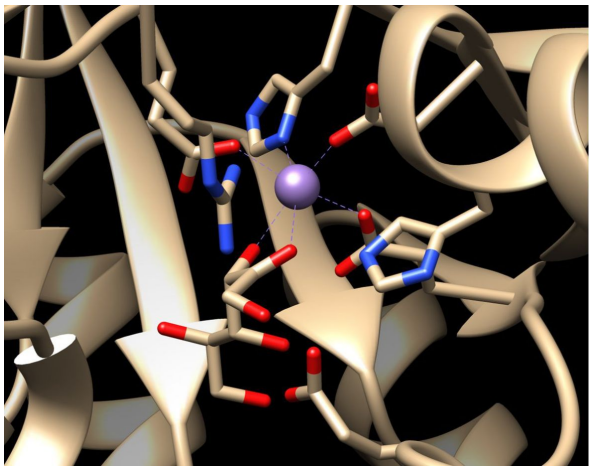
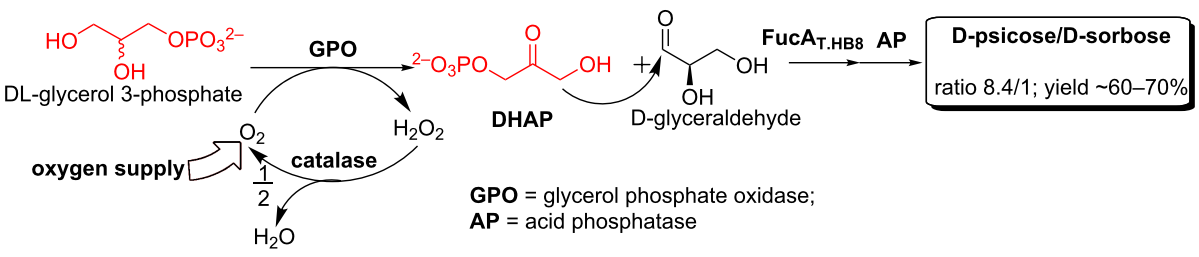


Figure 1: The active site in D-psicose 3-epimerase (DPEase) in the presence of D-fructose, showing the metal coordinating site and the substrate-binding site. The purple ball indicates the manganese(II) ion coordinating with key amino acid residues (Glu150, Asp183, His209, and Glu244) and the O-2 and O-3 of fructose. This figure was created using PDB File 2HK1 [38].



Scheme 3: Enzymatic synthesis of D-psicose using aldolase FucA.

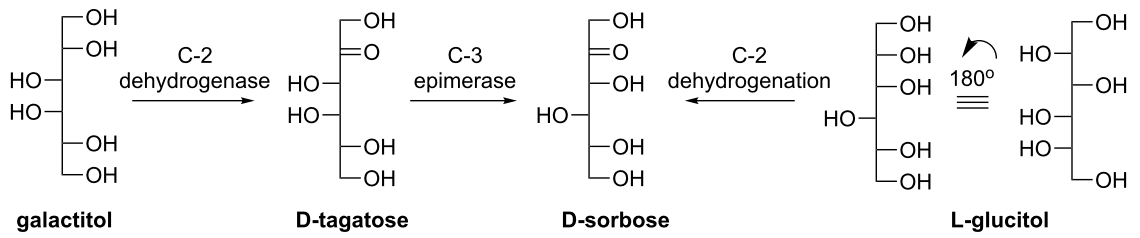
D-Sorbose

D-Sorbose can be potentially utilized as a low-caloric sweetener [41], an insect control agent, and a starting material for producing industrially significant compounds [42]. D-Sorbose was reported to be prepared from galactitol catalyzed by *Pseudomonas sp.* ST 24 and the production yield was as high as 70%. The possible transformation route from galactitol to D-sorbose in this strain was deduced as follows (Scheme 4): the substrate galactitol is dehydrogenated at C-2 to afford D-tagatose followed by C-3 epimerization [43].

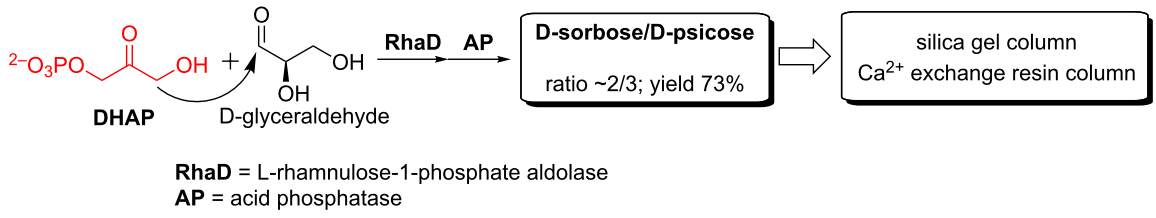
Izumori et al. established a method for the preparation of D-sorbose directly from D-tagatose with immobilized DTEase from *Pseudomonas sp*. ST-24 and 2 g of D-sorbose could be obtained from 3 g of D-tagatose. The conversion yield maintained at about 70% each time even if the batch was repeated five times [44]. Alternatively, D-sorbose could be prepared from L-glucitol via C-2 dehydrogenation through microbial conversion within a reasonable period of time (>95% yield and multigram scale, Scheme 4) [45,46]. The starting material L-glucitol could be obtained from the chemical reduction of a significantly cheaper starting material D-gulono-1,4-lactone instead of expensive L-glucose. In our previous work, we discovered that two rare sugars, D-sorbose and D-psicose, were simultaneously generated when L-rhamnulose-1-phosphate aldolase (RhaD, EC 4.1.2.19) [47] catalyzed the aldol addition between DHAP and D-glyceraldehyde (Scheme 5) [48]. Fortunately, the resulting diastereomers were easily separated with cation exchange resin (Ca^{2+} form) under elevated temperature to realize the preparative-scale production of both sugars [48-51].

L-Tagatose

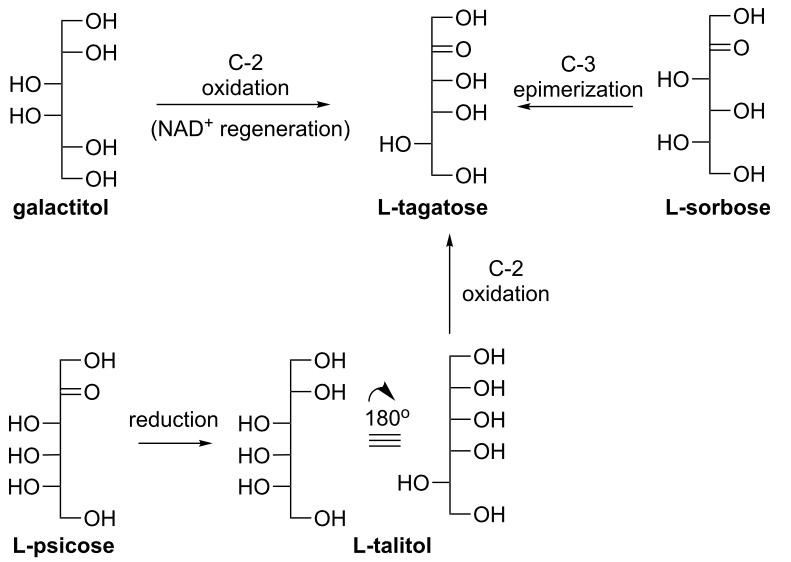
Unlike its enantiomer D-tagatose which is a widely used rare sugar and produced in bulk quantity, L-tagatose has not yet been well studied or broadly utilized due to limited production pathway and high cost involved [52,53]. L-Tagatose can be synthesized via oxidation of galactitol (Scheme 6) by *Klebsiella pneumoniae* 40b (70% yield) [54]. Huwig et al. also reported an efficient oxidation of galactitol to L-tagatose through the use of galactitol dehydrogenase (GDH, EC 1.1.1.16) from *Rhodobacter sphaeroides* D and the overall yield was 78% [55]. This oxidation only requires catalytic amounts of NAD^+, which is regenerated in situ through the reduction of pyruvate by L-lactate dehydrogenase (EC 1.1.1.27) [55]. Alternatively, Itoh et al. discovered that DTEase from *Pseudomonas sp.* ST-24 was a promising enzyme, which was active not only on D-ketohexoses but also on L-ketohexoses [56]. Therefore, L-tagatose was successfully prepared by immobilized DTEase using L-sorbose as the substrate although the production yield was only 20% (Scheme 6) [56]. Moreover, L-tagatose could be directly produced from L-psicose through microbial reduction followed by oxidation by *Enterobacter aerogenes* 230S (Scheme 6) and cells grown on xylitol have the best conversion potential [52]. The production yield could reach above 60% in the presence of glycerol [52] which may be responsible for NAD^+/NADH regeneration. Large-scale preparation of L-tagatose has not been extensively studied yet due to elaborate



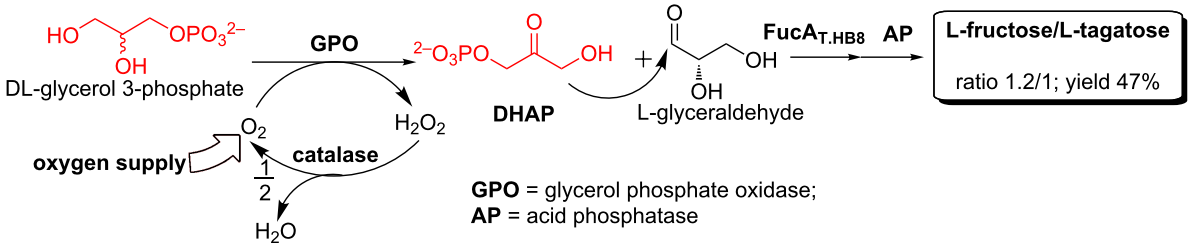
Scheme 4: Proposed pathway of the D-sorbose synthesis from galactitol or L-glucitol.



Scheme 5: Simultaneous enzymatic synthesis of D-sorbose and D-psicose.



Scheme 6: Biosynthesis of L-tagatose.

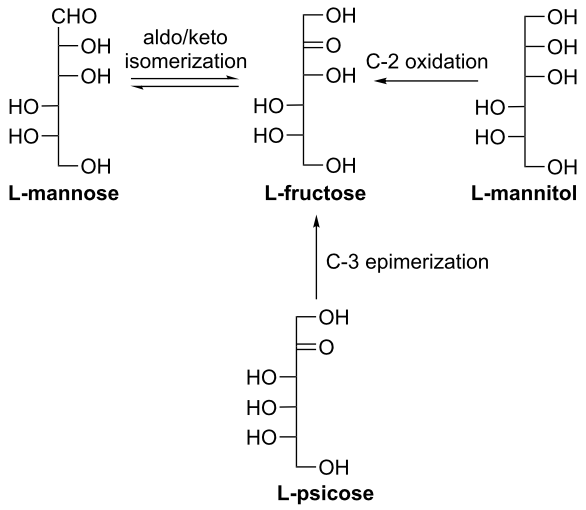


Scheme 7: Preparative-scale synthesis of L-tagatose and L-fructose using aldolase.

routes or expensive starting materials. In our lab, the synthesis of L-tagatose was easily achieved by employing the previous discussed cost-effective one-pot four-enzyme system containing L-fuculose-1-phosphate aldolase (FucA, EC 4.1.2.17) (Scheme 7). In this case, L-glyceraldehyde was used as the aldol acceptor and L-tagatose and L-fructose were obtained simultaneously that can be easily separated and purified with cation exchange resin chromatography [39,57].

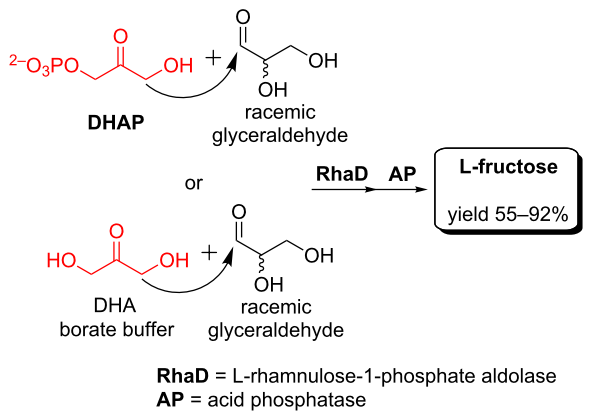
L-Fructose

L-Fructose is a well known nonnutritive sweetener [9] and can be used as a potential inhibitor of several glycosidases [58]. Mayo et al. firstly established an enzymatic approach for the synthesis of L-fructose using L-mannose as a substrate through aldo–keto isomerization (Scheme 8) [59]. Dhawale et al. demonstrated another route via bacterial oxidation of L-mannitol (Scheme 8) [42]. Interestingly, the previously mentioned versatile DTEase from *Pseudomonas sp.* ST-24 could also catalyze the epimerization of L-psicose to produce



Scheme 8: Biosynthesis of L-fructose.

L-fructose in a yield of 65% (Scheme 8) [56]. In addition, Franke et al. reported that the dihydroxyacetone phosphate (DHAP)-dependent aldolase L-rhamnulose-1-phosphate aldolase (RhaD) could selectively use L-glyceraldehyde out of racemic glyceraldehyde to produce L-fructose exclusively (55% yield) using expensive DHAP as the other substrate (Scheme 9) [60]. Sugiyama et al. further discovered that this aldolase RhaD could even tolerate dihydroxyacetone (DHA), instead of DHAP, as a donor substrate in the presence of borate buffer, which could function as a phosphate ester mimic in the aldolase-catalyzed reactions [61]. Based on this discovery, a practical one-step synthesis of L-fructose was established using DHA and racemic glyceraldehyde as substrates (Scheme 9) and the production yield was as high as 92% on a gram scale [61]. Our lab optimized their synthesis as well aiming to reduce the cost by employing the one-pot four-enzyme system as described before (also see Scheme 3 and Scheme 7) and obtained an overall isolated yield of 66% on a preparative scale [48,57].



Scheme 9: Preparative-scale synthesis of L-fructose using aldolase RhaD.

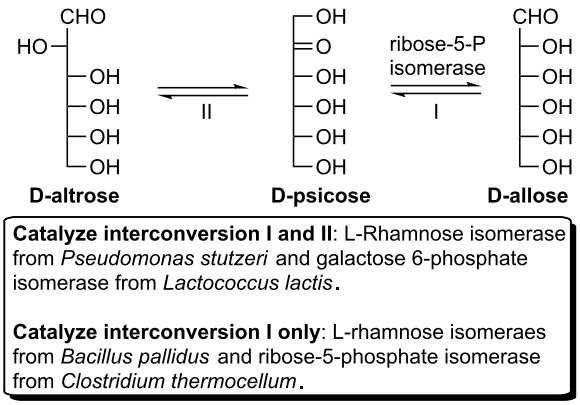
1-Deoxy-L-fructose

Deoxy sugars play significant roles in central metabolism [62], cell signaling, immunological recognition and host–pathogen interactions [63,64]. Gullapalli et al. demonstrated an effective way of obtaining deoxy L-fructose by combining chemical and biotechnological approaches (Scheme 10) [8]. Hydrogenation of 6-deoxy-L-mannose (L-rhamnose) produced 6-deoxy-L-mannitol (L-rhamnitol) which was subsequently oxidized by *Enterobacter aerogenes* IK7 to afford the rare sugar 1-deoxy-L-fructose. The whole process was performed in an environmentally friendly fashion.

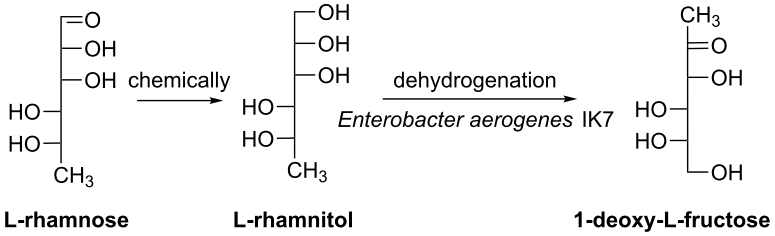
II. Biosynthesis of rare aldohexoses

D-Allose

D-Allose is the C-3 epimer of D-glucose or the aldo/keto-isomer of D-psicose (Scheme 11). Recently, increasing attention has been paid to this rare sugar due to its beneficial activities and potential pharmaceutical effects, such as antitumor [65], anticancer [66], anti-inflammatory [67], anti-oxidative [68], antihypertensive [69], cytoprotective [70], and immunosuppressant [71]. L-Rhamnose isomerase (EC 5.3.1.14), ribose-5-phosphate isomerase (EC 5.3.1.6), and galactose-6-phosphate isomerase (EC 5.3.1.26) were reported as potential enzymes for the bioconversion of D-psicose to D-allose [72]. L-Rhamnose isomerase from *Pseudomonas stutzeri* [73] and galactose 6-phosphate isomerase from *Lactococcus lactis* [74] catalyze two reversible isomerization reactions (interconversion between D-psicose and D-allose vs interconversion between D-psicose



Scheme 11: Potential enzymes (isomerases) for the bioconversion of D-psicose to D-allose.



Scheme 10: Chemoenzymatically synthesis of 1-deoxy-L-fructose [8].

and D-altrose) with D-altrose as a byproduct. In contrast, L-rhamnose isomerase from *Bacillus pallidus* [75] and ribose-5-phosphate isomerase from *Clostridium thermocellum* [76] produce D-allose without D-altrose formation via only one type of isomerization. In addition, due to its thermostability and high conversion yield reported, ribose-5-phosphate isomerase from *Clostridium thermocellum* is the most suitable enzyme for the D-allose production.

D-Allose can also be synthesized from inexpensive D-glucose as a starting material via a three-step bioconversion, sequentially catalyzed by D-xylose isomerase (EC 5.3.1.5), D-psicose 3-epimerase, and ribose-5-phosphate isomerase (Scheme 12). The overall conversion yield for the reaction sequence is expected to be higher compared to each step due to the promotion effect of the second and third step [72]. It remains a challenge to discover a D-allose epimerase which can directly epimerize D-glucose C-3 to afford D-allose because microorganisms do not generally consume such a rare monosaccharide for their growth.

L-Glucose

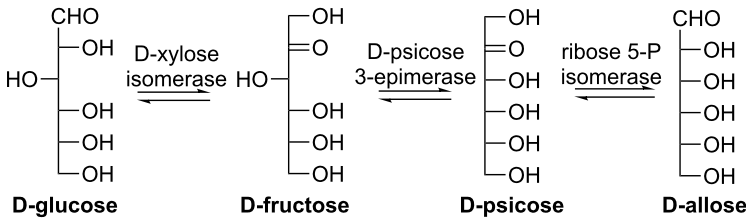
L-Glucose does not occur naturally in higher living organisms, although it has many potential applications, such as a low calorie sweetener [77], a bulking agent [78], an inhibitor for bacterial growth [79] and various glucosidases. L-Glucose can also be used as an ideal starting material for glycoconjugate vaccines against the enteropathogenic bacterium *Shigella sonne* [80]. Enzymatically, L-glucose can be synthesized by isomerizing L-fructose (Scheme 13) catalyzed by D-xylose isomerase from *Candida utilis* [81] or whole cells of a mutant *Klebsiella pneumoniae* strain, which constitutively express D-arabinose isomerase (EC 5.3.1.3) [82]. An overall yield of 35% on a gram-scale was reported using this mutant strain [82]. Moreover, Yadav et al. immobilized galactose oxidase (EC 1.1.3.9) and catalase (EC 1.11.1.6) on a solid support (crab-shell particles or *Ocimum sanctum* seeds) and investigated their synthetic application for L-glucose production from D-sorbitol (Scheme 13) [83,84]. Catalase could degrade the hydrogen peroxide byproduct and increase the conversion by removing the inhibition effect of hydrogen peroxide toward galactose oxidase and regenerating oxygen.

L-Talose and D-gulose

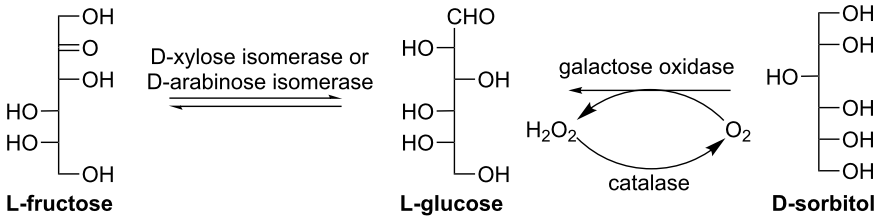
The aldohexoses L-talose and D-gulose (C-3 epimer of D-galactose) are both very expensive owing to their scarcity in nature. L-Talofuranosyladenine, an adenine nucleoside derivative of L-talose, was found to be a slow-reacting substrate for calf intestinal adenosine deaminase and thus to inhibit the growth of leukaemia L1210 cells in vitro [85]. Crystalline D-gulose can be used as a drug-formulation agent and food additive. Bhuiyan et al. reported a simple enzymatic method for L-talose and D-gulose using immobilized L-rhamnose isomerase (EC 5.3.1.14) from *Pseudomonas sp.* strain LL172 (Scheme 14). Starting from rare sugars L-tagatose and D-sorbose (which were obtained from D-galactose via several steps of bioconversions), the production yields for L-talose and D-gulose were 12% and 10% respectively at equilibrium [86].

L-Galactose

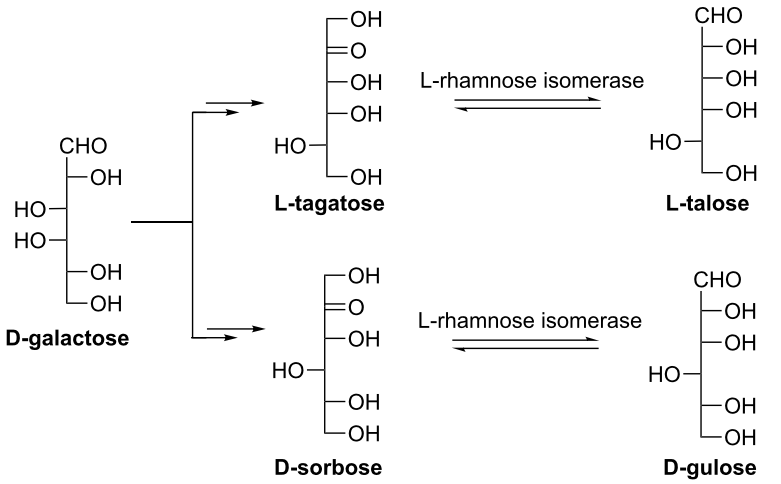
L-Galactose was reported to be an effective precursor of the L-ascorbate synthesis [87]. Leang et al. established an efficient



Scheme 12: Three-step bioconversion of D-glucose to D-allose.



Scheme 13: Biosynthesis of L-glucose.

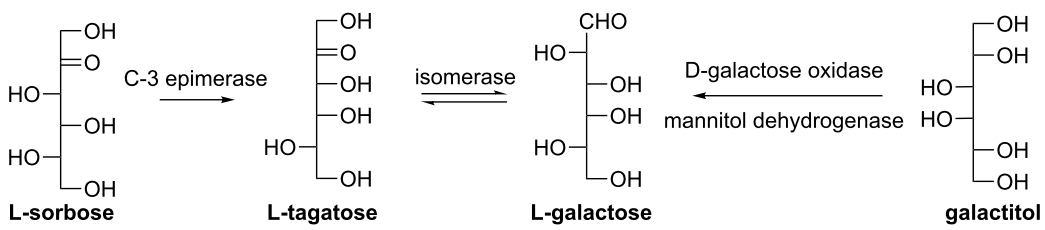


Scheme 14: Enzymatic synthesis of L-talose and D-gulose.

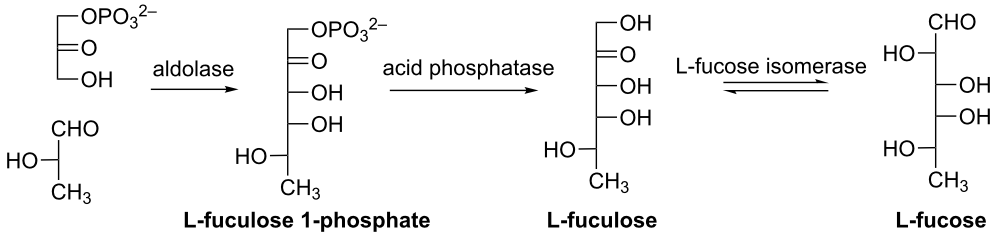
two-step method for synthesizing L-galactose on a large scale from a common sugar L-sorbose, catalyzed by immobilized DTEase from a mutant *Pseudomonas sp.* ST-24 and recombinant L-rhamnose isomerase from *Escherichia coli* JM109 [88]. L-Sorbose was first epimerized by DTEase at C-3 to give L-tagatose (28% yield), which reached an equilibrium with L-galactose (~30%) catalyzed by the L-rhamnose isomerase (Scheme 15). L-Galactose was also directly synthesized by oxidizing galactitol using D-galactose oxidase [89], including the previously mentioned immobilized galactose oxidase [83,84], but the yields were generally low. In contrast, whole cells of recombinant *Escherichia coli* carrying a unique mannitol dehydrogenase (EC 1.1.1.255) represent a more scalable system [90] for oxidizing galactitol (Scheme 15). Alternatively, it was reported that L-galactose could be biosynthesized by epimerizing D-glucose through a novel but rare metabolic pathway during the biosynthesis of a sulfated L-galactan in the ascidian tunic, requiring a triple epimerization which brings about inversion of the configuration of carbon 2, 3, and 5 [91].

L-Fucose (6-deoxy-L-galactose)

L-Fucose is a rare sugar belonging to the deoxy sugar family, which is a naturally occurring sugar widely found in biomass, especially in plant, but in minor amounts. It is also found on the mammalian cell surface and a fundamental core moiety of various carbohydrate antigens [92,93]. Microbiological synthesis of L-fucose is based on the fermentation by microorganisms, which generate L-fucose-containing exopolysaccharides (EPS). Then, L-fucose can be released by enzymatic hydrolysis and recovered from the hydrolysate [94]. Interestingly, metabolically engineered *Corynebacterium glutamicum* was used to produce guanosine-5'-diphosphate (GDP)-L-fucose, the precursor of fucosyl-oligosaccharides, from glucose and mannose [95]. L-Fucose (or its analogs) can also be prepared in vitro enzymatically in a three-step procedure (Scheme 16) [96]. Firstly, L-fuculose-1-phosphate (or the analogues) is synthesized by aldol addition catalyzed by L-fuculose-1-phosphate aldolase (FucA). Then, L-fuculose is produced after dephosphorylation by acid phosphatase (EC 3.1.3.2). Finally, L-fuculose is converted to L-fucose by L-fucose isomerase (EC 5.3.1.25).



Scheme 15: Enzymatic synthesis of L-galactose.



Scheme 16: Enzymatic synthesis of L-fucose.

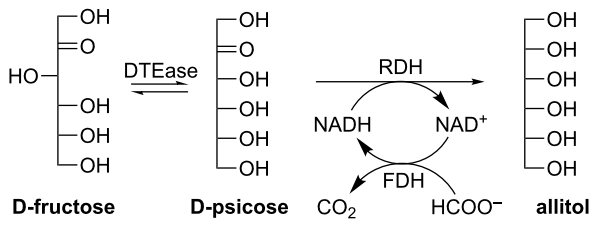
The procedure may be performed in a one-pot fashion or with purification after each step.

III. Biosynthesis of rare sugar alcohols (hexitols)

Sugar alcohols are mainly derived from pentoses and hexoses. They are hydrogenated form of carbohydrates, in which the carbonyl group is reduced. Their flavor is like sucrose but they have less energy. Xylitol is very popularly used in the food industry while some other sugar alcohols such as allitol, D-talitol and L-sorbitol, are very expensive and unexploited. Here we summarize the biosynthesis of some hexitols derived from rare sugars.

Allitol

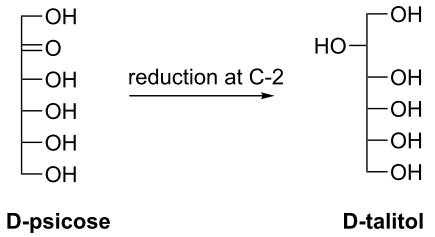
Allitol can be prepared by reducing/hydrogenating the rare sugar D-psicose [97,98], which is derived from D-fructose via DTEase catalyzed conversion (Scheme 17). However, two problems exist in this pathway: low conversion rate for D-psicose and low D-psicose concentration available for bacterial reduction. These drawbacks could be overcome by a multi-enzyme system containing DTEase, ribitol dehydrogenase (RDH, EC 1.1.1.56) and formate dehydrogenase (FDH, EC 1.2.1.2) [99]. In this system, NADH is regenerated by an irreversible formate dehydrogenation reaction, promoting the conversion of D-psicose to allitol. As a result, the D-fructose and D-psicose equilibrium was shifted towards the formation of D-psicose and a complete conversion could be reached (Scheme 17).



Scheme 17: Synthesis of allitol from D-fructose using a multi-enzyme system.

D-Talitol

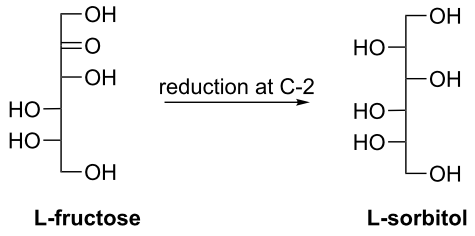
D-Talitol is the other C-2 reduction product of D-psicose with a different stereospecificity to that of the allitol (Scheme 18). The conversion rate from D-psicose to D-talitol catalyzed by a halotolerant yeast strain *Candida famata* R28 could be significantly increased in the presence of various carbohydrates such as erythritol, D-sorbitol, ribitol and glycerol in the reaction mixture [100]. The faster consumption of the substrate could be explained by the in situ NADH regeneration while those supplementary carbohydrates are oxidized by a dehydrogenase. At 10% substrate concentration, the conversion rate could reach as high as 95% catalyzed by whole cells supplemented with 5% of D-sorbitol [100]. In addition, this bioconversion/reduction could also be carried out by various strains of *Mucoraceae* fungi [101]. However, D-talitol has not yet been well investigated for its applications due to the lack of a practical preparation method.



Scheme 18: Biosynthesis of D-talitol via C-2 reduction of rare sugars.

L-Sorbitol

L-Sorbitol was prepared from L-fructose (Scheme 19) catalyzed by whole cells of *Aureobasidium pullulans* strain LP23 and the conversion activity could be induced by L-arabinose [102].



Scheme 19: Biosynthesis of L-sorbitol via C-2 reduction of rare sugars.

Moreover, supplement of erythritol to the reaction mixture enhanced the conversion to L-sorbitol and one possible reason also lies in NADH regeneration resulting from erythritol dehydrogenation/oxidation.

Conclusion

The preparation and functional study of rare sugars has become a hot topic because of their potential applications in different fields. An important factor restricting the utilization of rare sugars is their limited availabilities, resulting from limited synthetic methods. Biocatalysis often offers advantages over chemical synthesis, because enzyme-catalyzed reactions are often highly enantioselective and regioselective. In addition, enzymatic reactions are usually performed under mild conditions and are environmentally friendly. However, two major challenges remain in this endeavor: 1) microorganisms and related enzymes presently applied in rare sugar synthesis are from non-generally regarded as safe (GRAS) sources, which may stimulate an increasing demand for introducing related enzymes into GRAS microorganisms; 2) many biosynthetic methods involve a chemical equilibrium (isomerization or epimerization) between two or more sugars that may lead to low to moderate yields and difficulties in product purification. Advancements in genomics and bioengineering can potentially solve this problem by improving the properties (activity, thermostability, or substrate-binding affinity) of existing enzymes or discovering new systems and robust biocatalysts for industrial-scale applications.

Acknowledgements

This work was partially supported by the Natural Science Foundation of China Project (21302069), the Key Grant Project of Chinese Ministry of Education (313027), the Self-Determined Research Program of Jiangnan University (JUSRP1003) and the Open Project Program of the Key Laboratory of Industrial Biotechnology (Ministry of Education, China, KLIB-KF201206). L.C. acknowledges the support from the RISE (Research Initiative for Summer Engagement) Program and the ASPIRE (Advanced Support for Innovative Research Excellence) Program of University of South Carolina.

References

1. Definition of rare sugars in 2011. http://isrs.kagawa-u.ac.jp/activities.html. And http://sites.google.com/site/raresugars/activity
2. Werz, D. B.; Ranzinger, R.; Herget, S.; Adibekian, A.; von der Lieth, C.-W.; Seeberger, P. H. *ACS Chem. Biol.* **2007,** *2,* 685–691. doi:10.1021/cb700178s
3. Adibekian, A.; Stallforth, P.; Hecht, M.-L.; Werz, D. B.; Gagneux, P.; Seeberger, P. H. *Chem. Sci.* **2011,** *2,* 337–344. doi:10.1039/c0sc00322k
4. Poonperm, W.; Takata, G.; Ando, Y.; Sahachaisaree, V.; Lumyong, P.; Lumyong, S.; Izumori, K. *J. Biosci. Bioeng.* **2007,** *103,* 282–285. doi:10.1263/jbb.103.282
5. Beerens, K.; Desmet, T.; Soetaert, W. *J. Ind. Microbiol. Biotechnol.* **2012,** *39,* 823–834. doi:10.1007/s10295-012-1089-x
6. Alajarin, R.; Garcia-Junceda, E.; Wong, C.-H. *J. Org. Chem.* **1995,** *60,* 4294–4295. doi:10.1021/jo00118a058
7. Granström, T. B.; Takata, G.; Tokuda, M.; Izumori, K. *J. Biosci. Bioeng.* **2004,** *97,* 89–94. doi:10.1016/S1389-1723(04)70173-5
8. Gullapalli, P.; Shiji, T.; Rao, D.; Yoshihara, A.; Morimoto, K.; Takata, G.; Fleet, G. W. J.; Izumori, K. *Tetrahedron: Asymmetry* **2007,** *18,* 1995–2000. doi:10.1016/j.tetasy.2007.08.009
9. Levin, G. V.; Zehner, L. R.; Saunders, J. P.; Beadle, J. R. *Am. J. Clin. Nutr.* **1995,** *62,* 1161S–1168S.
10. Donner, T. W.; Wilber, J. F.; Ostrowski, D. *Diabetes Obes. Metab.* **1999,** *1,* 285–291. doi:10.1046/j.1463-1326.1999.00039.x
11. Buemann, B.; Toubro, S.; Raben, A.; Blundell, J.; Astrup, A. *Br. J. Nutr.* **2000,** *84,* 227–231.
12. Wong, D. *Dent. Today* **2000,** *19,* 34–35.
13. Bertelsen, H.; Jensen, B. B.; Buemann, B. *World Rev. Nutr. Diet.* **1999,** *85,* 98–109. doi:10.1159/000059685
14. Cheng, L.; Mu, W.; Jiang, B. *J. Food Biochem.* **2011,** *35,* 1298–1310. doi:10.1111/j.1745-4514.2010.00452.x
15. Salonen, N.; Salonen, K.; Leisola, M.; Nyyssölä, A. *Bioprocess Biosyst. Eng.* **2013,** *36,* 489–497. doi:10.1007/s00449-012-0805-2
16. Seo, M. J. *Biosci., Biotechnol., Biochem.* **2013,** *77,* 385–388.
17. Wanarska, M.; Kur, J. *Microb. Cell Fact.* **2012,** *11,* No. 113. doi:10.1186/1475-2859-11-113
18. Rhimi, M.; Chouayekh, H.; Gouillouard, I.; Maguin, E.; Bejar, S. *Bioresour. Technol.* **2011,** *102,* 3309–3315. doi:10.1016/j.biortech.2010.10.078
19. Li, Y.; Zhu, Y.; Liu, A.; Sun, Y. *Extremophiles* **2011,** *15,* 441–450. doi:10.1007/s00792-011-0375-2
20. Jebors, S.; Tauran, Y.; Aghajari, N.; Boudebbouze, S.; Maguin, E.; Haser, R.; Coleman, A. W.; Rhimi, M. *Chem. Commun.* **2011,** *47,* 12307–12309. doi:10.1039/c1cc14930j
21. Kim, H.-J.; Ryu, S.-A.; Kim, P.; Oh, D.-K. *Biotechnol. Prog.* **2003,** *19,* 400–404. doi:10.1021/bp025675f
22. Kim, B. C.; Lee, Y. H.; Lee, H. S.; Lee, D. W.; Choe, E. A.; Pyun, Y. R. *FEMS Microbiol. Lett.* **2002,** *212,* 121–126.
23. Kim, P.; Yoon, S. H.; Seo, M. J.; Oh, D. K.; Choi, J. H. *Biotechnol. Appl. Biochem.* **2001,** *34,* 99–102.
24. Liang, M.; Chen, M.; Liu, X.; Zhai, Y.; Liu, X.-W.; Zhang, H.; Xiao, M.; Wang, P. *Appl. Microbiol. Biotechnol.* **2012,** *93,* 1469–1474. doi:10.1007/s00253-011-3638-z
25. Sun, Y.; Hayakawa, S.; Ogawa, M.; Fukada, K.; Izumori, K. *J. Agric. Food Chem.* **2008,** *56,* 4789–4796. doi:10.1021/jf800050d

26. Matsuo, T.; Suzuki, H.; Hashiguchi, M.; Izumori, K. *J. Nutr. Sci. Vitaminol.* **2002,** *48,* 77–80. doi:10.3177/jnsv.48.77
27. Oshima, H.; Kimura, I.; Izumori, K. *J. Biosci. Bioeng.* **2006,** *101,* 280–283. doi:10.1263/jbb.101.280
28. Itoh, H.; Okaya, H.; Khan, A. R.; Tajima, S.; Hayakawa, S.; Izumori, K. *Biosci., Biotechnol., Biochem.* **1994,** *58,* 2168–2171. doi:10.1271/bbb.58.2168
29. Takeshita, K.; Suga, A.; Takada, G.; Izumori, K. *J. Biosci. Bioeng.* **2000,** *90,* 453–455. doi:10.1016/S1389-1723(01)80018-9
30. Itoh, H.; Sato, T.; Izumori, K. *J. Ferment. Bioeng.* **1995,** *80,* 101–103. doi:10.1016/0922-338X(95)98186-O
31. Kim, H.-J.; Hyun, E.-K.; Kim, Y.-S.; Lee, Y.-J.; Oh, D.-K. *Appl. Environ. Microbiol.* **2006,** *72,* 981–985. doi:10.1128/AEM.72.2.981-985.2006
32. Kim, N.-H.; Kim, H.-J.; Kang, D.-I.; Jeong, K.-W.; Lee, J.-K.; Kim, Y.; Oh, D.-K. *Appl. Environ. Microbiol.* **2008,** *74,* 3008–3013. doi:10.1128/AEM.00249-08
33. Lim, B.-C.; Kim, H.-J.; Oh, D.-K. *Process Biochem.* **2009,** *44,* 822–828. doi:10.1016/j.procbio.2009.03.017
34. Zhang, L.; Mu, W.; Jiang, B.; Zhang, T. *Biotechnol. Lett.* **2009,** *31,* 857–862. doi:10.1007/s10529-009-9942-3
35. Mu, W.; Chu, F.; Xing, Q.; Yu, S.; Zhou, L.; Jiang, B. *J. Agric. Food Chem.* **2011,** *59,* 7785–7792. doi:10.1021/jf201356q
36. Zhang, W.; Fang, D.; Xing, Q.; Zhou, L.; Jiang, B.; Mu, W. *PLoS One* **2013,** *8,* e62987. doi:10.1371/journal.pone.0062987
37. Mu, W.; Zhang, W.; Feng, Y.; Jiang, B.; Zhou, L. *Appl. Microbiol. Biotechnol.* **2012,** *94,* 1461–1467. doi:10.1007/s00253-012-4093-1
38. Kim, K.; Kim, H.-J.; Oh, D.-K.; Cha, S.-S.; Rhee, S. *J. Mol. Biol.* **2006,** *361,* 920–931. doi:10.1016/j.jmb.2006.06.069
39. Li, Z.; Cai, L.; Qi, Q.; Styslinger, T. J.; Zhao, G.; Wang, P. G. *Bioorg. Med. Chem. Lett.* **2011,** *21,* 5084–5087. doi:10.1016/j.bmcl.2011.03.072
40. Samland, A. K.; Sprenger, G. A. *Appl. Microbiol. Biotechnol.* **2006,** *71,* 253–264. doi:10.1007/s00253-006-0422-6
41. Noma, A.; Sato, M.; Tsuzuki, Y. *Comp. Biochem. Physiol., Part A: Mol. Integr. Physiol.* **1974,** *48,* 249–262.
42. Dhawale, M. R.; Szarek, W. A.; Hay, G. W.; Kropinski, A. B. *Carbohydr. Res.* **1986,** *155,* 262–265. doi:10.1016/S0008-6215(00)90156-3
43. Khan, A. R.; Takahata, S.; Okaya, H.; Tsumura, T.; Izumori, K. *J. Ferment. Bioeng.* **1992,** *74,* 149–152. doi:10.1016/0922-338X(92)90074-5
44. Itoh, H.; Sato, T.; Takeuchi, T.; Khan, A. R.; Izumori, K. *J. Ferment. Bioeng.* **1995,** *79,* 184–185. doi:10.1016/0922-338X(95)94091-5
45. Huwig, A.; Emmel, S.; Giffhorn, F. *Carbohydr. Res.* **1996,** *281,* 183–186. doi:10.1016/0008-6215(95)00332-0
46. Mayerskuntzer, H.; Reichert, A.; Schneider, K. H.; Giffhorn, F. *J. Biotechnol.* **1994,** *36,* 157–164.
47. Fessner, W.-D.; Badia, J.; Eyrisch, O.; Schneider, A.; Sinerius, G. *Tetrahedron Lett.* **1992,** *33,* 5231–5234. doi:10.1016/S0040-4039(00)79140-4
48. Li, Z.; Cai, L.; Qi, Q.; Wang, P. G. *Bioorg. Med. Chem. Lett.* **2011,** *21,* 7081–7084. doi:10.1016/j.bmcl.2011.09.087
49. Doten, R. C.; Mortlock, R. P. *Appl. Environ. Microbiol.* **1985,** *49,* 158–162.
50. Woodyer, R. D.; Wymer, N. J.; Racine, F. M.; Khan, S. N.; Saha, B. C. *Appl. Environ. Microbiol.* **2008,** *74,* 2967–2975. doi:10.1128/AEM.02768-07
51. Huang, W.; Mu, W.; Jiang, B. *Food and Fermentation Industries (Shipin Yu Fajiao Gongye)* **2008,** 168–171.
52. Rao, D.; Gullapalli, P.; Yoshihara, A.; Jenkinson, S. F.; Morimoto, K.; Takata, G.; Akimitsu, K.; Tajima, S.; Fleet, G. W. J.; Izumori, K. *J. Biosci. Bioeng.* **2008,** *106,* 473–480. doi:10.1263/jbb.106.473
53. Yoshihara, A.; Haraguchi, S.; Gullapalli, P.; Rao, D.; Morimoto, K.; Takata, G.; Jones, N.; Jenkinson, S. F.; Wormald, M. R.; Dwek, R. A.; Fleet, G. W. J.; Izumori, K. *Tetrahedron: Asymmetry* **2008,** *19,* 739–745. doi:10.1016/j.tetasy.2008.02.013
54. Shimonishi, T.; Okumura, Y.; Izumori, K. *J. Ferment. Bioeng.* **1995,** *79,* 620–622. doi:10.1016/0922-338X(95)94759-K
55. Huwig, A.; Emmel, S.; Jäkel, G.; Giffhorn, F. *Carbohydr. Res.* **1997,** *305,* 337–339. doi:10.1016/S0008-6215(97)00265-6
56. Itoh, H.; Izumori, K. *J. Ferment. Bioeng.* **1996,** *81,* 351–353. doi:10.1016/0922-338X(96)80590-3
57. Fessner, W.-D.; Sinerius, G. *Angew. Chem.* **1994,** *106,* 217–220. doi:10.1002/ange.19941060220
Angew. Chem., Int. Ed. Engl. **1994,** *33,* 209–212. doi:10.1002/anie.199402091
58. Muniruzzaman, S.; Pan, Y. T.; Zeng, Y.; Atkins, B.; Izumori, K.; Elbein, A. D. *Glycobiology* **1996,** *6,* 795–803. doi:10.1093/glycob/6.8.795
59. Mayo, J. W.; Anderson, R. L. *Carbohydr. Res.* **1968,** *8,* 344–347. doi:10.1016/S0008-6215(00)82241-7
60. Franke, D.; Machajewski, T.; Hsu, C.-C.; Wong, C.-H. *J. Org. Chem.* **2003,** *68,* 6828–6831. doi:10.1021/jo030021m
61. Sugiyama, M.; Hong, Z.; Whalen, L. J.; Greenberg, W. A.; Wong, C.-H. *Adv. Synth. Catal.* **2006,** *348,* 2555–2559. doi:10.1002/adsc.200600356
62. Zhang, X.; Deslandes, E.; Villedieu, M.; Poulain, L.; Duval, M.; Gauduchon, P.; Schwartz, L.; Icard, P. *Anticancer Res.* **2006,** *26,* 3561–3566.
63. Hallis, T. M.; Liu, H.-w. *Acc. Chem. Res.* **1999,** *32,* 579–588. doi:10.1021/ar9602056
64. Weymouth-Wilson, A. C. *Nat. Prod. Rep.* **1997,** *14,* 99–110. doi:10.1039/NP9971400099
65. Mitani, T.; Hoshikawa, H.; Mori, T.; Hosokawa, T.; Tsukamoto, I.; Yamaguchi, F.; Kamitori, K.; Tokuda, M.; Mori, N. *Head Neck* **2009,** *31,* 1049–1055. doi:10.1002/hed.21070
66. Sui, L.; Dong, Y.; Watanabe, Y.; Yamaguchi, F.; Hatano, N.; Tsukamoto, I.; Izumori, K.; Tokuda, M. *Int. J. Oncol.* **2005,** *27,* 907–912.
67. Gao, D.; Kawai, N.; Tamiya, T. *Med. Hypotheses* **2011,** *76,* 911–913. doi:10.1016/j.mehy.2011.03.007
68. Ishihara, Y.; Katayama, K.; Sakabe, M.; Kitamura, M.; Aizawa, M.; Takara, M.; Itoh, K. *J. Biosci. Bioeng.* **2011,** *112,* 638–642. doi:10.1016/j.jbiosc.2011.08.005
69. Kimura, S.; Zhang, G.-X.; Nishiyama, A.; Nagai, Y.; Nakagawa, T.; Miyanaka, H.; Fujisawa, Y.; Miyatake, A.; Nagai, T.; Tokuda, M.; Abe, Y. *J. Hypertens.* **2005,** *23,* 1887–1894. doi:10.1097/01.hjh.0000182523.29193.e3
70. Sui, L.; Nomura, R.; Dong, Y.; Yamaguchi, F.; Izumori, K.; Tokuda, M. *Cryobiology* **2007,** *55,* 87–92. doi:10.1016/j.cryobiol.2007.05.003
71. Hossain, M. A.; Wakabayashi, H.; Goda, F.; Kobayashi, S.; Maeba, T.; Maeta, H. *Transplant. Proc.* **2000,** *32,* 2021–2023. doi:10.1016/S0041-1345(00)01540-2

72. Lim, Y.-R.; Oh, D.-K. *Appl. Microbiol. Biotechnol.* **2011,** *91,* 229–235. doi:10.1007/s00253-011-3370-8
73. Menavuvu, B. T.; Poonperm, W.; Leang, K.; Noguchi, N.; Okada, H.; Morimoto, K.; Granstrom, T. B.; Takada, G.; Izumori, K. *J. Biosci. Bioeng.* **2006,** *101,* 340–345. doi:10.1263/jbb.101.340
74. Park, H.-Y.; Park, C.-S.; Kim, H.-J.; Oh, D.-K. *J. Biotechnol.* **2007,** *132,* 88–95. doi:10.1016/j.jbiotec.2007.08.022
75. Poonperm, W.; Takata, G.; Okada, H.; Morimoto, K.; Granstrom, T. B.; Izumori, K. *Appl. Microbiol. Biotechnol.* **2007,** *76,* 1297–1307. doi:10.1007/s00253-007-1109-3
76. Yoon, R.-Y.; Yeom, S.-J.; Kim, H.-J.; Oh, D.-K. *J. Biotechnol.* **2009,** *139,* 26–32. doi:10.1016/j.jbiotec.2008.09.012
77. Livesey, G.; Brown, J. C. *J. Nutr.* **1995,** *125,* 3020–3029.
78. Levin, G. V.; Zehner, L. R.; Sanders, J. P.; Beadle, J. R. *Am. J. Clin. Nutr.* **1995,** *62,* 1161S–1168S.
79. Bautista, D. A.; Pegg, R. B.; Shand, P. J. J. *Food Prot.* **2000,** *63,* 71–77.
80. Medgyes, A.; Farkas, E.; Lipták, A.; Pozsgay, V. *Tetrahedron* **1997,** *53,* 4159–4178. doi:10.1016/S0040-4020(97)00145-2
81. Horwath, R. O.; Colonna, W. J. Process for isomerizing L-glucose to L-fructose. U.S. Patent 4,463,093, June 30, 1982.
82. Leang, K.; Sultana, I.; Takada, G.; Izumori, K. *J. Biosci. Bioeng.* **2003,** *95,* 310–312. doi:10.1016/S1389-1723(03)80036-1
83. Yadav, K. K.; Vernwal, S. K.; Afaq, Z.; Yadav, K. D. S. *J. Sci. Ind. Res.* **2002,** *61,* 361–365.
84. Yadav, K. K.; Vernwal, S. K.; Afaq, Z.; Yadav, K. D. S. *Indian J. Chem. Technol.* **2002,** *9,* 218–222.
85. Lerner, L.; Mennitt, G. *Carbohydr. Res.* **1994,** *259,* 191–200.
86. Bhuiyan, S. H.; Itami, Y.; Takada, G.; Izumori, K. *J. Biosci. Bioeng.* **1999,** *88,* 567–570. doi:10.1016/S1389-1723(00)87677-X
87. Wheeler, G. L.; Jones, M. A.; Smirnoff, N. *Nature* **1998,** *393,* 365–369. doi:10.1038/30728
88. Leang, K.; Maekawa, K.; Menavuvu, B. T.; Morimoto, K.; Granstöm, T. B.; Takada, G.; Izumori, K. *J. Biosci. Bioeng.* **2004,** *97,* 383–388. doi:10.1016/S1389-1723(04)70223-6
89. Root, R. L.; Durrwachter, J. R.; Wong, C. H. *J. Am. Chem. Soc.* **1985,** *107,* 2997–2999. doi:10.1021/ja00296a041
90. Woodyer, R. D.; Christ, T. N.; Deweese, K. A. *Carbohydr. Res.* **2010,** *345,* 363–368. doi:10.1016/j.carres.2009.11.023
91. Mourao, P. A. S. *Biochemistry* **1991,** *30,* 3458–3464. doi:10.1021/bi00228a016
92. Yin, Z.; Huang, X. *J. Carbohydr. Chem.* **2012,** *31,* 143–186. doi:10.1080/07328303.2012.659364
93. Guo, Z.; Wang, Q. *Curr. Opin. Chem. Biol.* **2009,** *13,* 608–617. doi:10.1016/j.cbpa.2009.08.010
94. Saari, P.; Häkkä, K.; Heikkilä, H.; Jumppanen, J.; Hurme, M. *J. Liq. Chromatogr. Relat. Technol.* **2009,** *32,* 2050–2064. doi:10.1080/10826070903126922
95. Chin, Y.-W.; Park, J.-B.; Park, Y.-C.; Kim, K. H.; Seo, J.-H. *Bioprocess Biosyst. Eng.* **2013,** *36,* 749–756. doi:10.1007/s00449-013-0900-z
96. Wong, C.-H. Enzymatic synthesis of L-fucose and L-fucose analogs. U.S. Patent 6,713,287, Oct 24, 1995.
97. Muniruzzaman, S.; Kunihisa, Y.; Ichiraku, K.; Izumori, K. *J. Ferment. Bioeng.* **1995,** *79,* 496–498. doi:10.1016/0922-338X(95)91269-B
98. Muniruzzaman, S.; Tokunaga, H.; Izumori, K. *J. Ferment. Bioeng.* **1995,** *79,* 323–327. doi:10.1016/0922-338X(95)93989-W
99. Takeshita, K.; Ishida, Y.; Takada, G.; Izumori, K. *J. Biosci. Bioeng.* **2000,** *90,* 545–548. doi:10.1016/S1389-1723(01)80038-4
100. Sasahara, H.; Mine, M.; Izumori, K. *J. Ferment. Bioeng.* **1998,** *85,* 84–88. doi:10.1016/S0922-338X(97)80359-5
101. Yoshihara, K.; Shinohara, Y.; Hirotsu, T.; Izumori, K. *J. Biosci. Bioeng.* **2006,** *101,* 219–222. doi:10.1263/jbb.101.219
102. Sasahara, H.; Izumori, K. *J. Biosci. Bioeng.* **2005,** *100,* 223–226. doi:10.1263/jbb.100.223

License and Terms

This is an Open Access article under the terms of the Creative Commons Attribution License (http://creativecommons.org/licenses/by/2.0), which permits unrestricted use, distribution, and reproduction in any medium, provided the original work is properly cited.

The license is subject to the *Beilstein Journal of Organic Chemistry* terms and conditions: (http://www.beilstein-journals.org/bjoc)

The definitive version of this article is the electronic one which can be found at: doi:10.3762/bjoc.9.281

Beilstein Journal of Organic Chemistry

Synthesis of the spiroketal core of integramycin

Evgeny. V. Prusov

Letter

Open Access

Address:
Department of Medicinal Chemistry, Helmholtz Centre for Infection Research, Inhoffenstr. 7, 38124 Braunschweig, Germany

Email:
Evgeny. V. Prusov - evgeny.prusov@helmholtz-hzi.de

Keywords:
anti-infectives; hydrozirconation; natural products; spiroketals; total synthesis

Beilstein J. Org. Chem. **2013,** *9,* 2446–2450.
doi:10.3762/bjoc.9.282

Received: 14 August 2013
Accepted: 23 October 2013
Published: 12 November 2013

This article is part of the Thematic Series "Natural products in synthesis and biosynthesis".

Guest Editor: J. S. Dickschat

© 2013 Prusov; licensee Beilstein-Institut.
License and terms: see end of document.

Abstract

A concise synthetic strategy towards the spiroketal core of the HIV-integrase inhibitor integramycin (**1**) was developed. The required ketone precursor was efficiently constructed from two simple and easily accessible subunits by means of a hydrozirconation/copper catalyzed acylation reaction. The effects of different protecting groups on the spiroketalization step were also investigated.

Findings

Integramycin is a polyketide natural product isolated from *Actinoplanes sp*. by the Singh group at Merck [1] (Figure 1). The compound was found to inhibit HIV-1 integrase coupled strand transfer reactions with IC_{50} values of 3 and 4 μM, respectively. Structurally, the molecule architecture of integramycin features four distinct elements: a 3,5-dihydroxy-substituted aromatic ring, a spiroketal core, a highly functionalized octalin moiety and a 5-hydroxylated 3-acyltetramic acid. Studies on the syntheses of the spiroketal core [2,3] and the octalin fragment [4] of integramycin were recently reported by Roush and Floreancig, however, a total synthesis of this rather complex natural product has yet to be accomplished. Intrigued by its biological properties and capitalizing on our previous experience [5] in the total synthesis of natural products with tetramic acid fragments we embarked on the development of a concise and modular approach towards integramycin and related natural products.

According to the retrosynthetic analysis, which is outlined in Figure 2, the target molecule may be assembled from an appropriate spiroketal advanced intermediate **4.** This spiroketal compound is logically traced back to ketone **5**, which can be further divided in the vicinity of the C22 carbonyl group into two readily accessible building blocks **6** and **7**. For the construction of the octalin fragment we planned to use two sequential olefination reactions followed by an intramolecular Diels–Alder cycloaddition. The installation of the tetramic acid moiety would proceed via Lassey–Dickmann condensation with subsequent introduction of the 5-hydroxy group by oxidation of the corresponding vinylogous enolate. Herein a straightforward

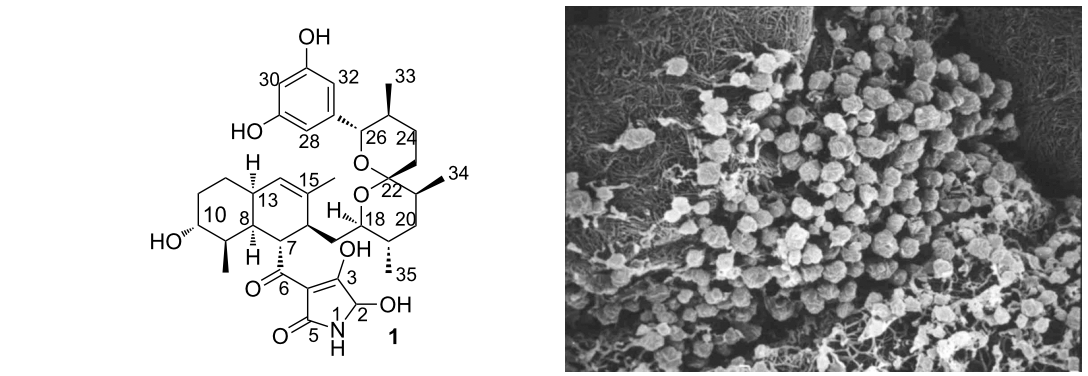


Figure 1: Structure of integramycin (**1**) and its producing organism, *Actinoplanes sp.* (*Photo: J. Wink, HZI, Microbial drugs*).

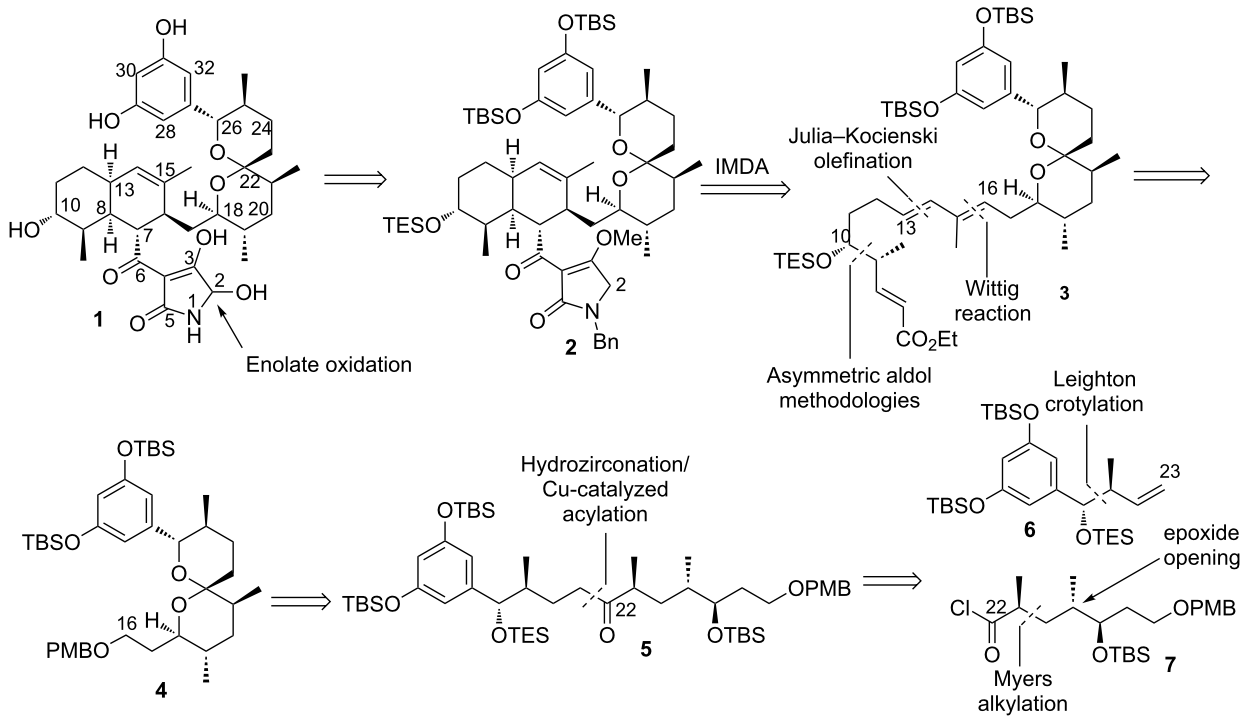
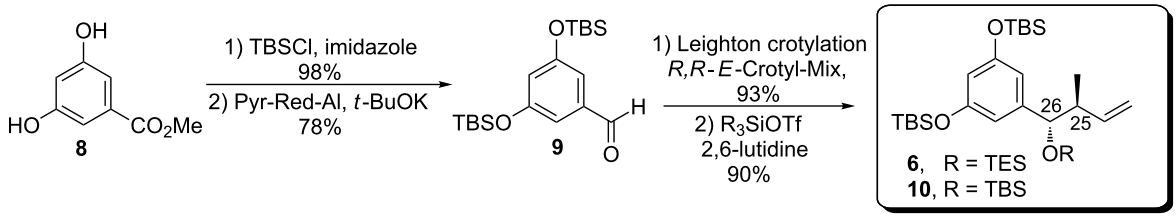


Figure 2: Retrosynthetic analysis of integramycin.

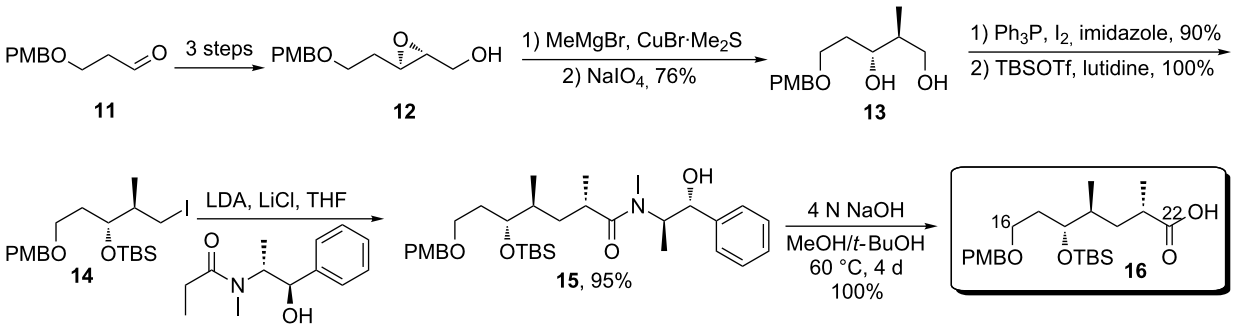
synthesis of the C16–C35 spiroketal core of integramycin based on a hydrozirconation/acylation reaction sequence is reported.

The synthesis of the aryl-substituted part of the spiroketal fragment was started from 3,5-dihydroxybenzoate **8** which was converted into aldehyde **9** via protection and partial reduction [6] (Scheme 1). Subsequent Leighton crotylation [7] using commercially available (*R*,*R*)-*E*-Crotyl-Mix was employed to introduce the two stereocenters at C25/C26 with *anti*-relationship in excellent yield and enatioselectivity. The enantiomeric excess of the crotylation product was estimated by esterification with (*R*)-α-methoxyphenylacetic acid with subsequent NMR analysis and found to be close to 90%. The resulting alcohol was protected as TBS and TES ethers to investigate the cleavage regime of different protecting groups during the acid catalyzed ketalization step.

The second part of the spiroketal core was constructed from the PMB-protected 3-hydroxypropanal via Horner–Wadsworth-Emmons olefination, reduction to the allylic alcohol and Sharples epoxidation [8] (Scheme 2). Subsequent Cu-catalyzed epoxide-opening using methylmagnesium bromide [9] produced



Scheme 1: Synthesis of the aromatic subunit.



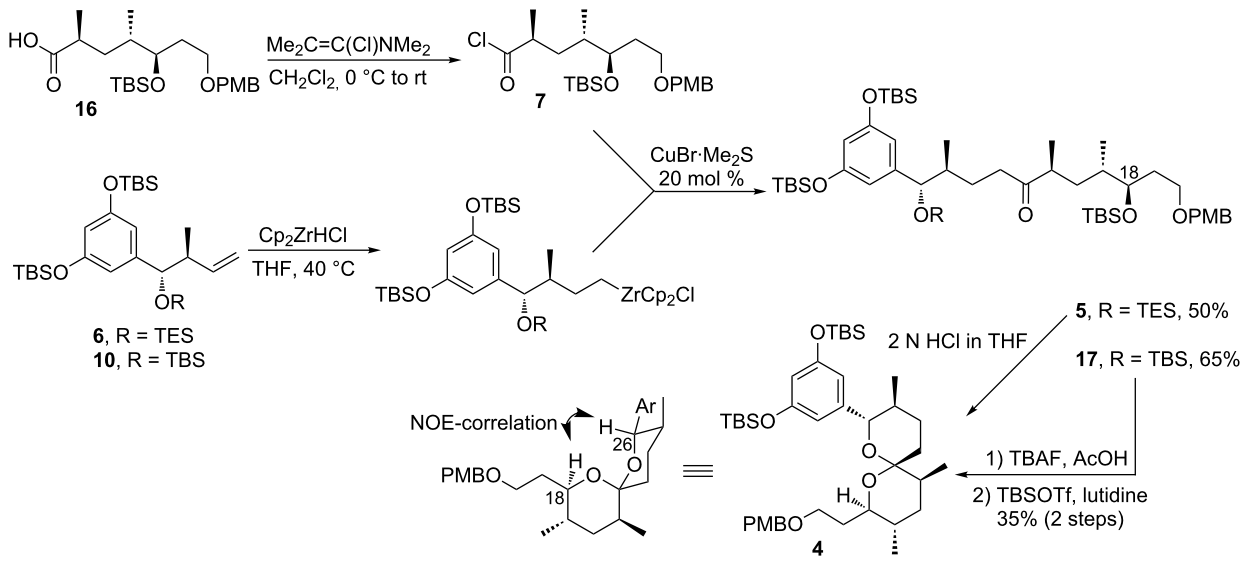
Scheme 2: Sharpless epoxidation/Myers alkylation approach to the C16–C22 carboxylic acid fragment.

an inseparable mixture of 1,2- and 1,3-diol products, which upon treatment with sodium periodate furnished pure **13**. The primary hydroxy group was selectively converted to alkyl iodide by using Ph_3P/I_2/imidazole conditions [10]. Then the protected iodide **14** was subjected to Myers alkylation [11] reaction with an excess of enolate to install the last required stereocenter. Hydrolytic cleavage of the pseudoephedrine auxiliary by prolonged exposure to sodium hydroxide at elevated temperature afforded the carboxylic acid **16**.

With both fragments in hand, the key coupling was attempted. Initially, the conditions recently reported by Vasse [12] were investigated (Scheme 3). In the event, treatment of the carboxylic acid **16** with Ghosez reagent [13] provided the corresponding acid chloride **7**, which was allowed to react with the hydrozirconation products of alkenes **6** and **10** in dichloromethane in the presence of a stoichiometric amount of $CuBr{\cdot}Me_2S$. The reaction was rather capricious and produced only modest amounts of the target compound. However, application of the original Wipf protocol [14] resulted in a much more favourable outcome and, upon some further optimization of the catalyst load, provided the desired ketone in 65% yield for the TBS protected alkene. The yield for the TES-protected alkene was somewhat lower, probably due to a partial cleavage of the protecting group during the acylation or hydrozirconation step.

Finally, several conditions were studied for the spiroacetalization step. Exposure of the *all*-TBS protected ketone **17** to moderately strong acids, e.g. the HF–pyridine complex in THF or CSA in THF/H_2O mixture, resulted in the predominant cleavage of the TBS group at C18, whereas the benzylic TBS ether remained mostly untouched. Application of more acidic conditions (3 N HCl in THF) led to a messy reaction. However, treatment of the same ketone with an excess of TBAF buffered with acetic acid caused removal of all protecting groups with concomitant spiroketalization and upon reinstallation of the phenolic protecting groups the desired compound **4** was obtained in 35% yield. The stereochemistry of the spiroketal was confirmed by observation of the strong NOE-correlation for H-18 and H-22 protons in the NOESY spectrum of **4** (see Supporting Information File 2). In the case of the ketone with the TES-protected benzylic alcohol, exposure to 2 N HCl in THF resulted in formation of numerous products, including the spiroketal **4**, thus demanding further optimization of this reaction.

In summary, an efficient route to the C16–C35 spiroketal fragment of integramycin was developed. The key step of the synthesis is a Cu-catalysed coupling of an acid chloride with an alkyl zirconium species. The stereocenters were introduced using Leighton crotylation, Sharpless epoxidation and Myers alkylation. Although the presented route achieves approxi-



Scheme 3: Coupling of the fragments and spiroketalization.

mately the same overall yield of target compound as that of Floreancig [2] (11.2 vs 11.5%, respectively), it features utilization of easily scalable transformation and upon further optimization of the spiroketalization step would be advantageous for the preparation of intermediate **4**. Efforts towards the completion of the total synthesis of integramycin are currently underway in our laboratory and will be reported in due course.

Supporting Information

Supporting Information File 1

Experimental procedures.
[http://www.beilstein-journals.org/bjoc/content/supplementary/1860-5397-9-282-S1.pdf]

Supporting Information File 2

Copies of NMR spectra.
[http://www.beilstein-journals.org/bjoc/content/supplementary/1860-5397-9-282-S2.pdf]

References

1. Singh, S. B.; Zink, D. L.; Heimbach, B.; Genilloud, O.; Teran, A.; Silverman, K. C.; Lingham, R. B.; Felock, P.; Hazuda, D. J. *Org. Lett.* **2002,** *4,* 1123–1126. doi:10.1021/ol025539b
2. Wang, L.; Floreancig, P. E. *Org. Lett.* **2004,** *6,* 569–572. doi:10.1021/ol036339i
3. Sun, H.; Abbott, J. R.; Roush, W. R. *Org. Lett.* **2011,** *13,* 2734–2737. doi:10.1021/ol200834p
4. Dineen, T. A.; Roush, W. R. *Org. Lett.* **2005,** *7,* 1355–1358. doi:10.1021/ol050191g
5. Höfle, G.; Gerth, K.; Reichenbach, H.; Kunze, B.; Sasse, F.; Forche, E.; Prusov, E. V. *Chem.–Eur. J.* **2012,** *18,* 11362–11370. doi:10.1002/chem.201201879
6. Abe, T.; Haga, T.; Negi, S.; Morita, Y.; Takayanagi, K.; Hamamura, K. *Tetrahedron* **2001,** *57,* 2701–2710. doi:10.1016/S0040-4020(01)00143-0
7. Kim, H.; Ho, S.; Leighton, J. L. *J. Am. Chem. Soc.* **2011,** *133,* 6517–6520. doi:10.1021/ja200712f
8. Katsuki, T.; Sharpless, K. B. *J. Am. Chem. Soc.* **1980,** *102,* 5974–5976. doi:10.1021/ja00538a077
9. Hodgson, D. M.; Arif, T. *Org. Lett.* **2010,** *12,* 4204–4207. doi:10.1021/ol101843q
10. Paterson, I.; Britton, R.; Delgado, O.; Gardner, N. M.; Meyer, A.; Naylor, G. J.; Poullennec, K. G. *Tetrahedron* **2010,** *66,* 6534–6545. doi:10.1016/j.tet.2010.01.083
11. Myers, A. G.; Yang, B. H.; Chen, H.; McKinstry, L.; Kopecky, D. J.; Gleason, J. L. *J. Am. Chem. Soc.* **1997,** *119,* 6496–6511. doi:10.1021/ja970402f
12. Coia, N.; Mokhtari, N.; Vasse, J.-L.; Szymoniak, J. *Org. Lett.* **2011,** *13,* 6292–6295. doi:10.1021/ol202796w
13. Devos, A.; Remion, J.; Frisque-Hesbain, A.-M.; Colens, A.; Ghosez, L. *J. Chem. Soc., Chem. Commun.* **1979,** 1180–1181. doi:10.1039/C39790001180
14. Wipf, P.; Xu, W. *Synlett* **1992,** 718–720. doi:10.1055/s-1992-21466

License and Terms

This is an Open Access article under the terms of the Creative Commons Attribution License (http://creativecommons.org/licenses/by/2.0), which permits unrestricted use, distribution, and reproduction in any medium, provided the original work is properly cited.

The license is subject to the *Beilstein Journal of Organic Chemistry* terms and conditions: (http://www.beilstein-journals.org/bjoc)

The definitive version of this article is the electronic one which can be found at: doi:10.3762/bjoc.9.282

Beilstein Journal of Organic Chemistry

Bidirectional cross metathesis and ring-closing metathesis/ring opening of a C_2-symmetric building block: a strategy for the synthesis of decanolide natural products

Bernd Schmidt* and Oliver Kunz

Full Research Paper

Open Access

Address:
Institut für Chemie, Organische Synthesechemie, Universität Potsdam, Karl-Liebknecht-Straße 24-25, 14476 Potsdam-Golm, Germany

Email:
Bernd Schmidt* - bernd.schmidt@uni-potsdam.de

* Corresponding author

Keywords:
dienes; enzyme catalysis; lactones; metathesis; natural products; ruthenium

Beilstein J. Org. Chem. **2013,** *9,* 2544–2555.
doi:10.3762/bjoc.9.289

Received: 14 August 2013
Accepted: 29 October 2013
Published: 18 November 2013

This article is part of the Thematic Series "Natural products in synthesis and biosynthesis".

Guest Editor: J. S. Dickschat

© 2013 Schmidt and Kunz; licensee Beilstein-Institut.
License and terms: see end of document.

Abstract

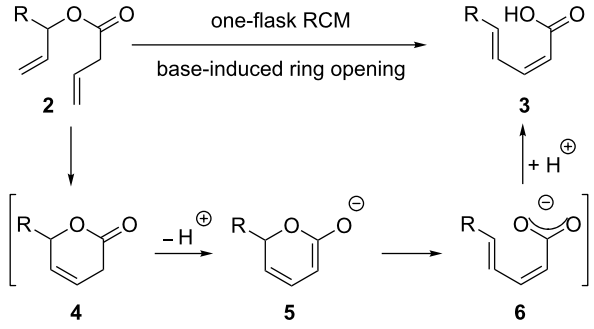
Starting from the conveniently available ex-chiral pool building block (*R*,*R*)-hexa-1,5-diene-3,4-diol, the ten-membered ring lactones stagonolide E and curvulide A were synthesized using a bidirectional olefin-metathesis functionalization of the terminal double bonds. Key steps are (i) a site-selective cross metathesis, (ii) a highly diastereoselective extended tethered RCM to furnish a (*Z*,*E*)-configured dienyl carboxylic acid and (iii) a Ru–lipase-catalyzed dynamic kinetic resolution to establish the desired configuration at C9. Ring closure was accomplished by macrolactonization. Curvulide A was synthesized from stagonolide E through Sharpless epoxidation.

Introduction

Bidirectional synthesis through termini differentiation of *meso*, C_2-symmetric or unsymmetric building blocks has emerged as an important strategy in natural product synthesis over the past two decades [1]. Early on, enantiomerically pure C_2-symmetric compounds were identified as particularly useful starting materials, because their termini are homotopic. Therefore, desymmetrization can be accomplished by monofunctionalization, making elaborate reagent or catalyst-controlled transformations unnecessary [2]. In this regard, (*R*,*R*)-hexa-1,5-diene-3,4-diol (**1**) [3-6] and its enantiomer *ent*-**1** [7] have emerged as highly valuable starting points for target molecule syntheses which rely on dual olefin metathesis reactions. The two metathesis transformations may either be two identical CM [8,9] or RCM steps [10], yielding C_2-symmetric products in which the newly formed double bonds remain homotopic, or two different CM or RCM steps, or a combination of one CM and one RCM trans-

formation. The latter cases lead to C_1-symmetric products and hence a differentiation of the C–C double bonds generated through metathesis. Examples for the utilization of these approaches in the synthesis of target molecules from **1** or *ent*-**1** include sialic acids [11], cladospolide C [12], iriomoteolide 3a [13,14], thromboxane B2 [15], didemniserinolipid B [16], squamostolide [17], muricatacine [18], rollicosin [19], phomopsolide C [7] and both enantiomers of seimatopolide A [20].

Over the past few years the development and application of one-flask sequences comprising at least one metathesis step has attracted increasing attention [21-23]. Such sequences provide rapid access to constitutional isomers or functionalized derivatives of the actual metathesis products in just one step. An example recently published by us combines RCM of butenoates **2** with a base-induced highly stereoselective ring opening of the transient metathesis products **4**, furnishing exclusively *Z*,*E*-dienes **3** [24]. We assume that the reaction proceeds via formation of an enolate **5**, followed by electrocyclic ring opening to carboxylates **6** [25], although a non-concerted pathway can not be excluded (Scheme 1).



Scheme 1: RCM/base-induced ring-opening sequence.

To the best of our knowledge, metathesis/non-metathesis one flask sequences have not been used before for the two directional elaboration or desymmetrization of C_2-symmetric building blocks. In this contribution, we demonstrate that this combination can be advantageously used for the synthesis of decanolides. These natural products share a ten-membered lactone structure and are normally isolated from fungi. Diverse bioactivities have been reported, such as phytotoxicity, cytotoxicity, antimalarial and antibacterial activity, which are a strong motivation for total synthesis [26,27]. In addition, several ambiguities in the structural assignment of some of these natural products still exist, and chemical synthesis has been proven to be a powerful and reliable tool for completing the structure elucidation and for correcting erroneous assignments. In particular if ex-chiral pool starting materials with well established absolute configurations are used, such as D-mannitol-derived **1** or L-tartrate-derived *ent*-**1**, highly reliable structural assignments become possible. Two decanolides, for which the absolute configuration was only assigned based on analogy to related natural products are stagonolide E [28,29] and curvulide A [30]. Stagonolide E is a secondary metabolite of *Stagonospora cirsii*, which is a fungal pathogen of the weed *Cirsium arvense* [28]. It has also been isolated from the fungus *Curvularia* sp. PSU-F22 [29]. Curvulide A was identified as a metabolite of a different strain of *Curvularia* sp. [30]. In this case, the absolute configuration at C9 was assigned as 9*R* based on a comparison of its CD spectrum with that of a structurally related compound, whereas the configuration at C6 could not be clarified. For the epoxide moiety of curvulide A, only the relative configurations at C4 and C5 were elucidated based on H,H-coupling constants (Figure 1) [30].

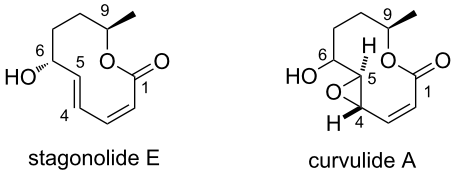


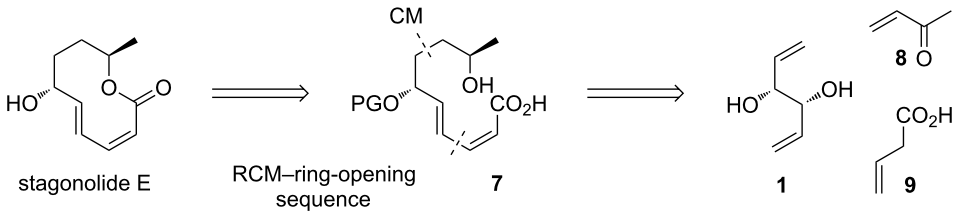
Figure 1: Structures and numbering scheme for stagonolide E and curvulide A.

So far, two syntheses of stagonolide E have been published, which both rely on asymmetric synthesis for establishing both stereocenters. The crucial (2*Z*,4*E*)-configuration of the diene moiety was constructed via Still–Gennari olefination [31] or via RCM of an acrylate with an *E*-configured diene at the opposite terminus [32]. Curvulide A has, to the best of our knowledge, not been synthesized previously.

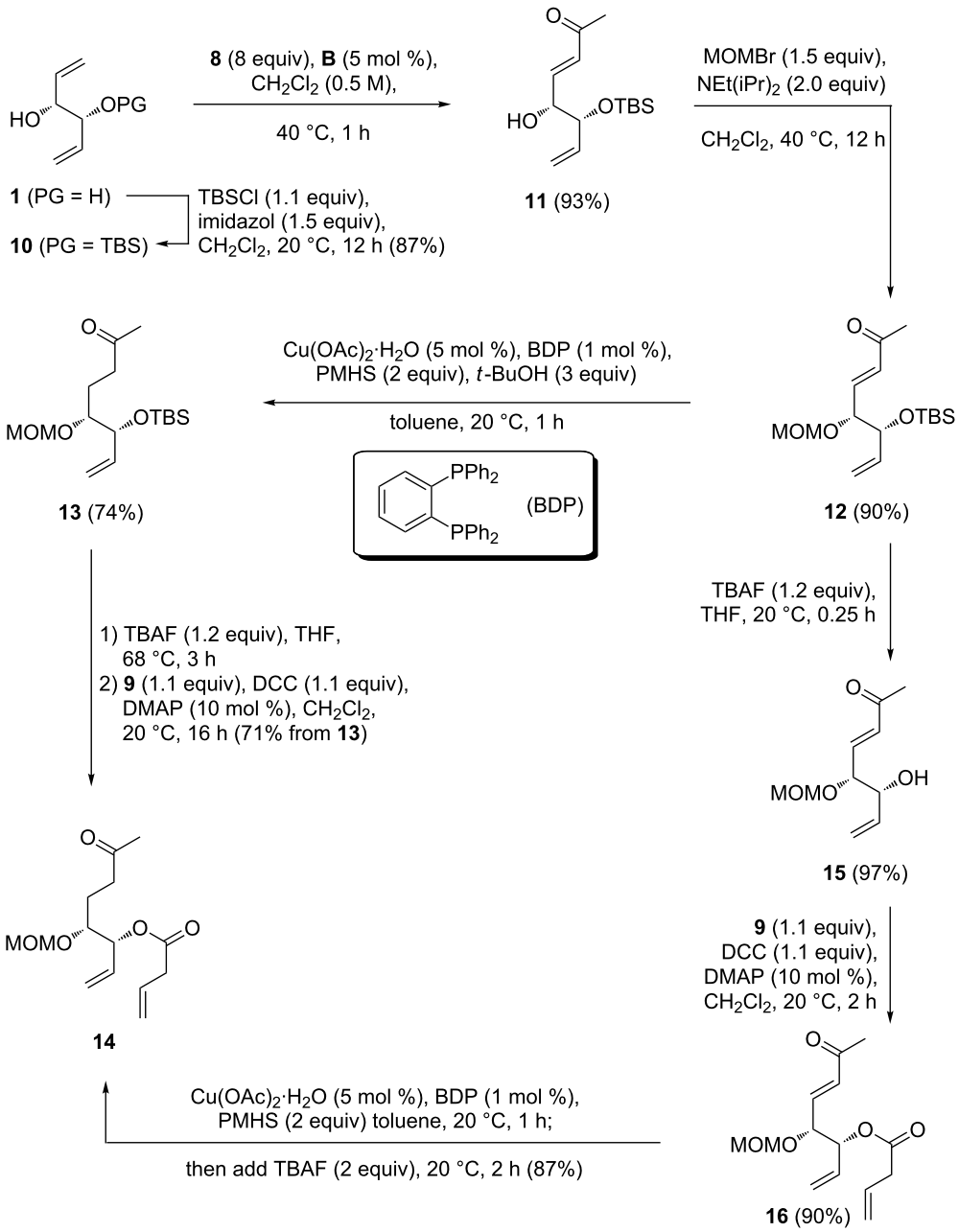
Results and Discussion

We planned to use a macrolactonization of precursor **7** as the cyclization step. For the synthesis of **7**, a cross metathesis of **1** (or a protected derivative) with methyl vinyl ketone (**8**) was envisaged as the first step, followed by an esterification of the more distant OH group with vinylacetic acid (**9**). This would provide a precursor **2** (Scheme 1) for the RCM-ring opening sequence (Scheme 2).

Our synthesis of stagonolide E started with a selective protection of one hydroxy group of diol **1** to furnish the known TBS-ether **10** [6,19], because we knew from previous experience that a desymmetrization based solely on cross metathesis would most likely be inefficient and yield substantial amounts of double functionalized product (Scheme 3) [9]. We tested methyl vinyl ketone (**8**) as a cross-metathesis partner, and the recently described Umicore $M5_1$ initiator (**A**) [20,33,34], as well as



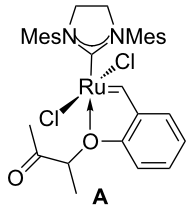
Scheme 2: Synthetic plan for stagonolide E.



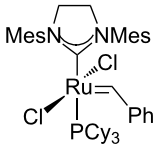
Scheme 3: Synthesis of RCM/ring opening precursor **14**.

Grubbs' second generation carbene complex **B** [35] as precatalysts (Table 1). Phosphine-free precatalysts with a hemilabile alkoxy ligand are supposed to be well-suited for cross metathesis reactions [36,37]. With a moderate catalyst loading of 2.0 mol % of **A**, we isolated the expected cross metathesis product **11** in an acceptable yield of 76% (Table 1, entry 1). Surprisingly, the yield decreased considerably to 51% with an increased catalyst loading of 5.0 mol %, and formation of a byproduct with an R_f value very similar to that of the cross metathesis product **11** was observed by TLC (Table 1, entry 2). Inspection of the ^{1}H NMR spectrum of the crude reaction mixture revealed that two singlets at 2.35 ppm and 6.75 ppm in a 1:3 ratio were present, which matches the NMR data previously reported for (*E*)-hex-3-ene-2,5-dione [38]. Obviously, catalyst **A** is sufficiently active to initiate the self metathesis of methyl vinyl ketone (**8**) to a considerable extent at a catalyst loading of 5.0 mol %, and consequently lower amounts of catalyst were tested in the following experiments. With 0.5 mol %, the isolated yield was 67% under otherwise identical conditions (Table 1, entry 3), and 85% of **11** were obtained with 1.0 mol % of **A** (Table 1, entry 4). With these catalyst loadings self metathesis of **8** is largely suppressed and the chromatographic isolation of **11** is facilitated, which might explain the improved yields under these conditions. With second generation Grubbs' catalyst **B**, the self metathesis of the supposedly less reactive CM partner occurs only to a minor extent, even at elevated temperatures and catalyst loadings. When we used 2 mol % of **B** (Table 1, entry 5) the yield was 61%, but could be improved to 78% by adding phenol (Table 1, entry 6). The beneficial effect of phenol in cross metathesis reactions is known and has been attributed to a stabilization of the reactive 14-electron species [39]. A very high yield of 93% was eventually obtained by using 5 mol % of **B** in refluxing dichloromethane (Table 1, entry 7).

Table 1: Optimization of conditions for CM of **10** and methyl vinyl ketone (**8**).[a]



A



B

entry	catalyst (mol %)	solvent	*T*	yield of **11**
1	**A** (2.0)	CH_2Cl_2	40 °C	76%
2[b]	**A** (5.0)	CH_2Cl_2	40 °C	51%
3	**A** (0.5)	CH_2Cl_2	40 °C	67%
4	**A** (1.0)	CH_2Cl_2	40 °C	85%
5	**B** (2.0)	toluene	80 °C	61%
6[c]	**B** (2.0)	toluene	80 °C	78%
7	**B** (5.0)	CH_2Cl_2	40 °C	93%

[a]General conditions: 8.0 equiv of **8**, initial substrate concentration: *c* = 0.5 M; [b]formation of (*E*)-hex-3-ene-2,5-dione observed in the ^{1}H NMR spectrum of the crude reaction mixture. [c]With phenol (0.5 equiv) as additive.

In the next step, the remaining hydroxy group was protected as a MOM ether **12**, which was then selectively reduced at the electron-deficient double bond, using polymethylhydrosiloxane (PMHS) [40] as a reducing agent and a BDP–Cu hydride catalyst. This variant of Stryker's reagent [41] has more recently been described by Lipshutz et al. [42] and was found to furnish ketone **13** in 74% yield. Desilylation of **13** could be accomplished quantitatively using TBAF at elevated temperature. However, an unidentified byproduct presumably a six-membered lacol was formed, which could not be separated by chromatography. Therefore the mixture was subjected to the second step, a Steglich esterification [43] with vinylacetic acid, to give the desired precursor **14** in pure form in 71% yield. To avoid the formation of the inseparable byproduct, we investigated a reversed order of steps. To this end, **12** was first desilylated to allyl alcohol **15**, which was then converted to butenoate **16**, again via Steglich esterification. For the selective reduction of the enoate **16**, the Stryker–Lipshutz protocol was again the method of choice and optimized conditions eventually furnished **14** in 87% yield (Scheme 3).

For the Stryker–Lipshutz reduction of **16** slightly different conditions were used than for the reduction of **12**. In particular, *tert*-butanol was omitted as a co-solvent, and TBAF was added to the reaction mixture after completed reduction. This modification was the result of an optimization study based on mechanistic considerations (Table 2) [44].

The conditions previously used for the reduction of enoate **12** involved the use of *tert*-butanol as a co-solvent, together with toluene. Under these conditions, reproducible yields in the range between 67% and 78% were obtained (Table 2, entries 1–3). The alcohol is believed to protonate the Cu-enolate formed upon conjugate addition, resulting in the ketone and a Cu-alkoxide, which is then reduced with silane to regenerate the Cu-hydride. Alternatively, the Cu-enolate might enter a competing catalytic cycle by reacting with silane, furnishing a silyl enol ether and the catalytically active Cu-hydride species. The silyl enol ether is inert to protonation by *tert*-butanol, and therefore the competing secondary cycle will result in a decreased yield of reduction product. This reasoning prompted us to run the reaction in toluene without any protic co-solvent, which should exclusively lead to the silyl enol ether, and add TBAF as a desilylating agent after complete consumption of the

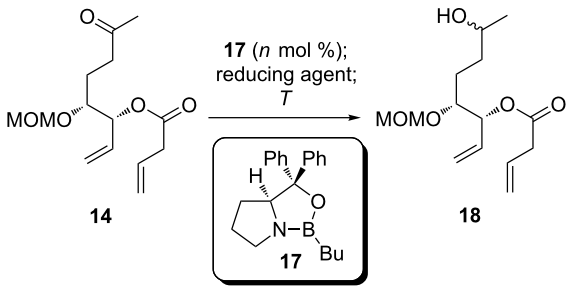
Table 2: Optimization of Cu–H-catalysed reduction of **16**.

entry	$Cu(OAc)_2 \cdot H_2O$ (mol %)	BDP (mol %)	PMHS (equiv)	solvent	yield of **14**
1	5	1	2	toluene/*t*-BuOH (5:1)	72%
2	5	1	2	toluene/*t*-BuOH (2:1)	78%
3	1	0.5	1.2	toluene/*t*-BuOH (2:1)	67%
4[a]	5	1	2	toluene	87%

[a]TBAF (2 equiv) added after complete consumption of starting material.

starting material. The reduced product **14** was isolated under these conditions in 87% yield (Table 2, entry 4). With ketone **14** in hands, we decided to establish the required configuration at C9 in the next step. To this end, a CBS reduction [45,46] catalysed by the oxazaborolidine **17** was tested first (Table 3).

Table 3: Investigation of CBS reduction of ketone **14**.



entry	catalyst (mol %)	reducing agent	*T*	dr[a]
1	**17** (10)	$H_3B \cdot SMe_2$	−78 °C	no conversion
2	**17** (20)	$H_3B \cdot THF$	20 °C	complex mixture
3	**17** (20)	$H_3B \cdot THF$	−50 °C	1:1
4	**17** (20)	catechol borane	−78 °C	3:2

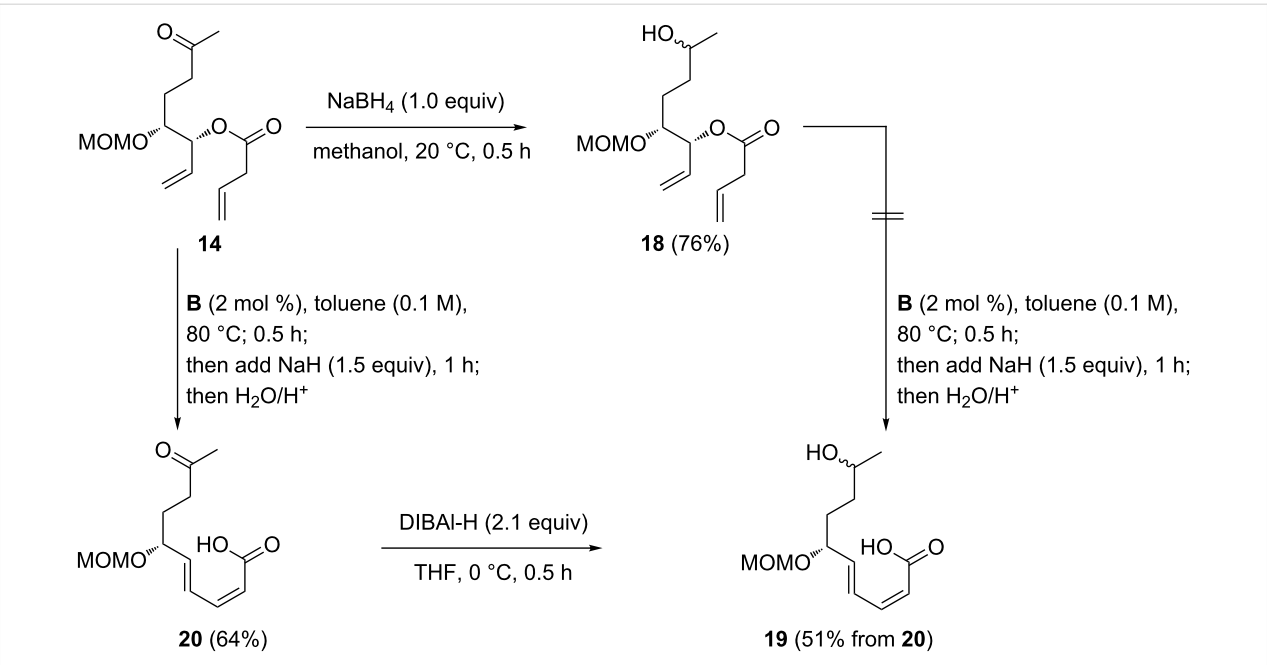
[a]Determined from ^1H NMR spectra of the crude reaction mixtures.

With borane–dimethylsulfide complex as the reductant and 10 mol % of catalyst, no conversion was observed at −78 °C (Table 3, entry 1), whereas attempted reduction at ambient temperature (Table 3, entry 2) resulted in the formation of a complex mixture, presumably due to competing hydroboration of the alkenes. With borane–THF at −50 °C the reduction proceeded to completion, but gave a 1:1 mixture of diastereomers (Table 3, entry 3). With catechol borane at −78 °C conversion was again complete, but the diastereoselectivity was far from being synthetically useful (Table 3, entry 4). Due to these rather discouraging results we did not pursue enantioselective reduction methods further to establish the required 9*R*-configuration, but considered a resolution approach. Ketone **14** was first reduced with $NaBH_4$ to the expected diastereomeric mixture of alcohols **18**, which were then subjected to the conditions of the RCM/base-induced ring-opening sequence. Unfortunately, the expected macrolactonization precursor **19** was not obtained, but an inseparable mixture of products. To access the intended substrate for the resolution, secondary alcohol **19**, we investigated an inverted sequence of steps: ketone **14** was first converted to the 9-oxodienoic acid **20** under RCM/ring-opening conditions, followed by a reduction of the ketone with DIBAl-H to furnish **19**. Unfortunately, the yields obtained via this two-step sequence were only moderate and most likely to low to provide sufficient amounts of material for an efficient resolution (Scheme 4).

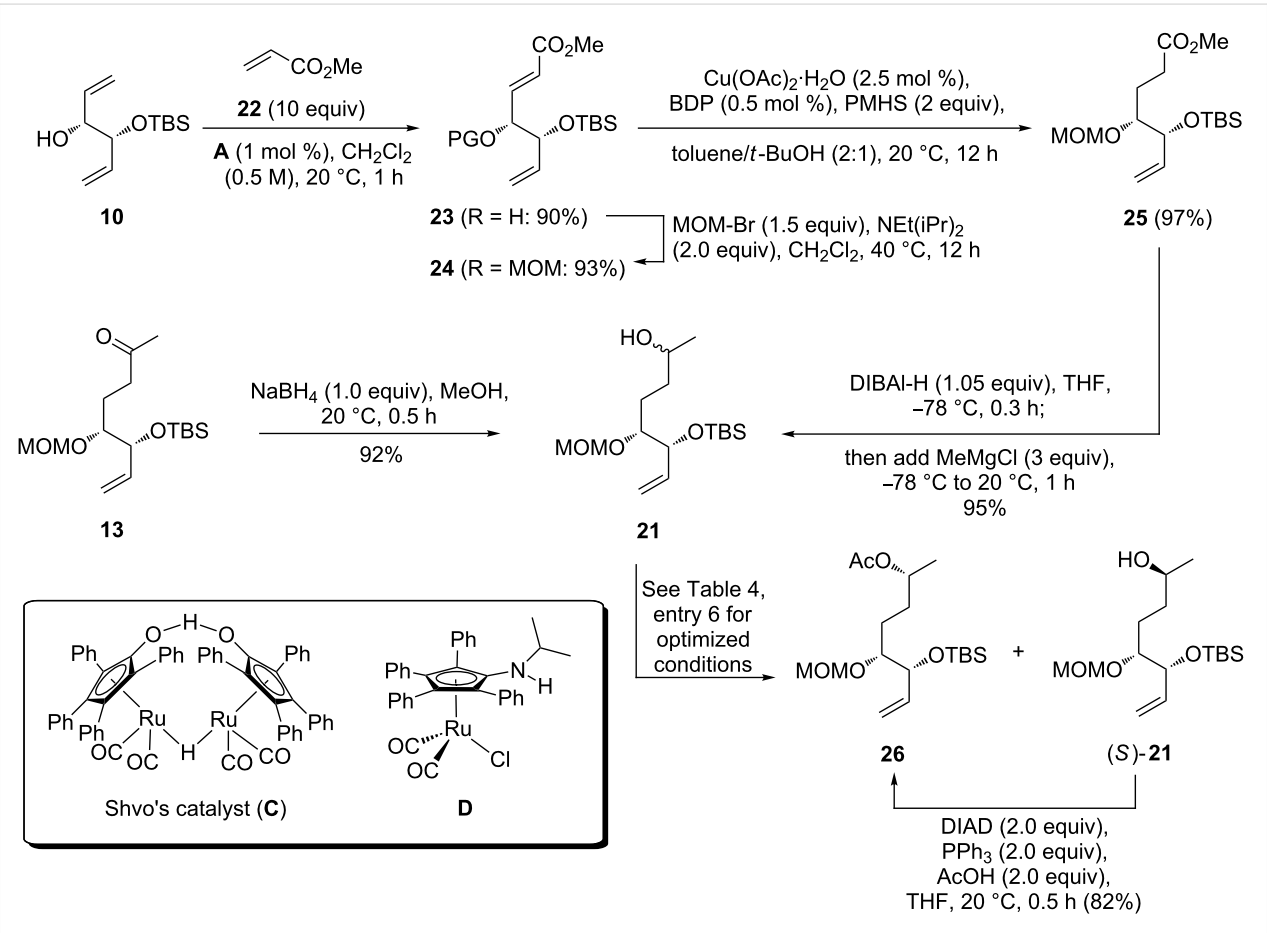
These unsuccessful attempts to establish the correct configuration at C9 led to a revision of the synthetic strategy. We decided to investigate a dynamic kinetic resolution (DKR) approach at an earlier stage of the synthesis and identified the secondary alcohol **21** as a promising starting point for this approach (Scheme 5).

Compound **21** was obtained via two alternate routes, either by reduction of ketone **13** (Scheme 3) with $NaBH_4$ or from ester **25** via one-flask reduction to the corresponding aldehyde and addition of methylmagnesium chloride. Ester **25** was in turn synthesized in three steps from monoprotected dienediol **10** via cross metathesis with methyl acrylate (**22**) [47] using a comparatively low loading of phosphine-free catalyst **A**, followed by MOM protection and Stryker–Lipshutz reduction of **24**. Notably the latter step proceeds significantly more efficient in a toluene/*tert*-butanol solvent mixture than the analogous enone reductions outlined in Scheme 3 and Table 2. Compared to these reactions, the saturated ester **25** was obtained in a nearly quantitative yield using half the amount of Cu precatalyst and BDP ligand.

In order to obtain enantiomerically pure **21**, an enzyme/transition metal-catalysed approach was investigated [48,49]. In this regard, the combination of Ru complexes such as Shvo's catalyst (**C**) [50], the amino-Cp catalyst **D** [51], or $[Ru(CO)_2Cl(\eta^5C_5Ph_5)]$ [52], and the lipase novozym 435 has emerged as particularly useful [53,54]. We tested Ru catalysts **C** and **D** under a variety of conditions (Table 4). In the absence of a Ru catalyst, a kinetic resolution occurs and **26** and



Scheme 4: Synthesis of a substrate **19** for "late stage" resolution.



Scheme 5: Synthesis of substrate **21** for "early stage" resolution.

Table 4: Optimization of conditions for Ru–lipase-catalysed DKR of **21**.

entry	conditions[a]	**26**	(2*S*)-**21**[b,c]	**13**[c]
1[d]	Novozym 435, iPPA (1.0 equiv), toluene, 20 °C, 24 h	49%	44%	n. d.
2[d]	**C** (2 mol %), Novozym 435, iPPA (10.0 equiv), toluene, 70 °C, 72 h	17%	n. d.	65%
3[d]	**C** (1 mol %), Novozym 435, iPPA (10.0 equiv), Na_2CO_3 (1.0 equiv), toluene, 70 °C, 24 h	30%	n. d.	30%
4[d]	**D** (2 mol %), Novozym 435, iPPA (1.5 equiv), Na_2CO_3 (1.0 equiv); *t*-BuOK (5 mol %), toluene, 20 °C, 7 d	50%	38%	n. d.
5[d]	**D** (2 mol %); Novozym 435, iPPA (1.5 equiv), *t*-BuOK (5 mol %), toluene, 20 °C, 7 d	50%	n. i.	n. d.
6[d]	**D** (2 mol %), Novozym 435, iPPA (3.0 equiv), Na_2CO_3 (1.0 equiv), *t*-BuOK (3 mol %), toluene, 30 °C, 7 d	67%	31%	n. d.
7[e]	**D** (5 mol %), Novozym 435, iPPA (1.5 equiv), Na_2CO_3 (1.0 equiv), *t*-BuOK (6 mol %), toluene, 30 °C, 5 d	76%	20%	n. d.
8[f]	**D** (5 mol %), Novozym 435, iPPA (3.0 equiv), Na_2CO_3 (1.0 equiv), *t*-BuOK (6 mol %), toluene, 30 °C, 14 d	80%	n. i.	n. d.

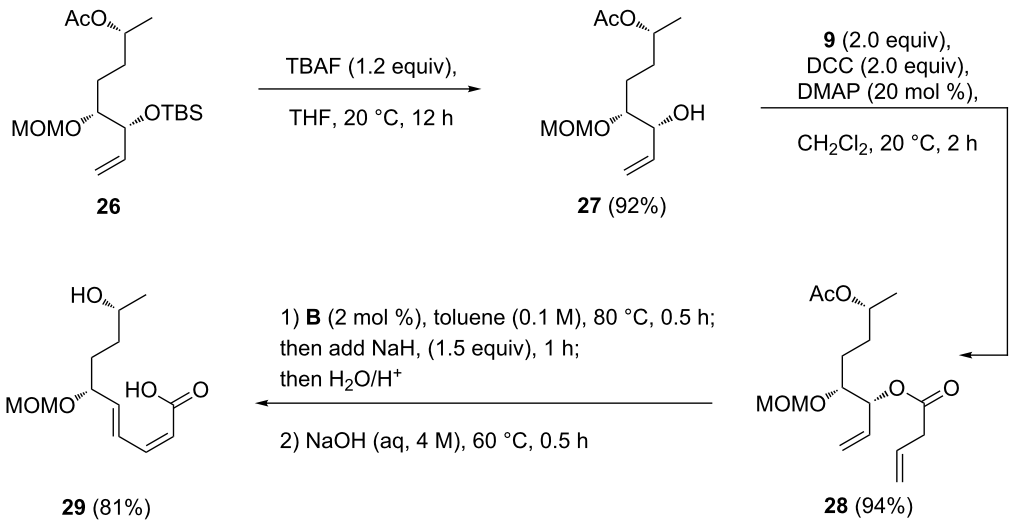
[a]iPPA: isopropenyl acetate; [b]n. d.: not determined; [c]n. i.: not isolated; [d]dr's of **26** and (2*S*)-**21** >19:1; [e]dr of **26** = 6:1; [f]dr of **26** = 3:1.

the resolved alcohol (2*S*)-**21** were isolated in similar yields (Table 4, entry 1). Upon addition of Shvo's catalyst **C**, only minor amounts of the desired acetate **26** and no resolved alcohol were obtained. Instead, the dehydrogenation product **13** was the predominant product (Table 4, entry 2). Addition of the base Na_2CO_3 led only to a small improvement (Table 4, entry 3). Ketone formation has previously been described in attempted DKR's of secondary alcohols when catalyst **C** was used in combination with isopropenyl or vinyl acetate as acylating agents [54]. For this reason, the aminocyclopentadienyl–Ru complex **D** was evaluated next. Very similar results were obtained with a catalytic amount of KO*t*-Bu in the presence or absence of a stoichiometric amount of Na_2CO_3 as a base, at ambient temperature and a reaction time of one week (Table 4, entries 4 and 5). A slightly elevated temperature led to a significantly improved yield of 67% of **26** and 31% of (2*S*)-**21**. Both compounds were obtained in a diastereomeric ratio higher than 19:1, as judged from the ^{1}H NMR spectrum (Table 4, entry 6). In an attempt to further improve the yield of **26**, the amount of catalyst **D** was increased to 5 mol %. This resulted indeed in an increased amount of **26**, but at the expense of diastereoselectivity, which dropped to 6:1 (Table 4, entry 7). A prolonged reaction time of 14 d led, under otherwise identical conditions, to a slightly improved yield, but at the same time to an even more dramatic erosion of diastereoselectivity (dr = 3:1, Table 4, entry 8). Thus, the conditions listed in Table 4, entry 6 were identified as the optimum. As the alcohol (2*S*)-**21** could also be isolated in a diastereomeric ratio higher than 19:1, it was converted to **26** via Mitsunobu inversion [55] with acetic acid as the nucleophile.

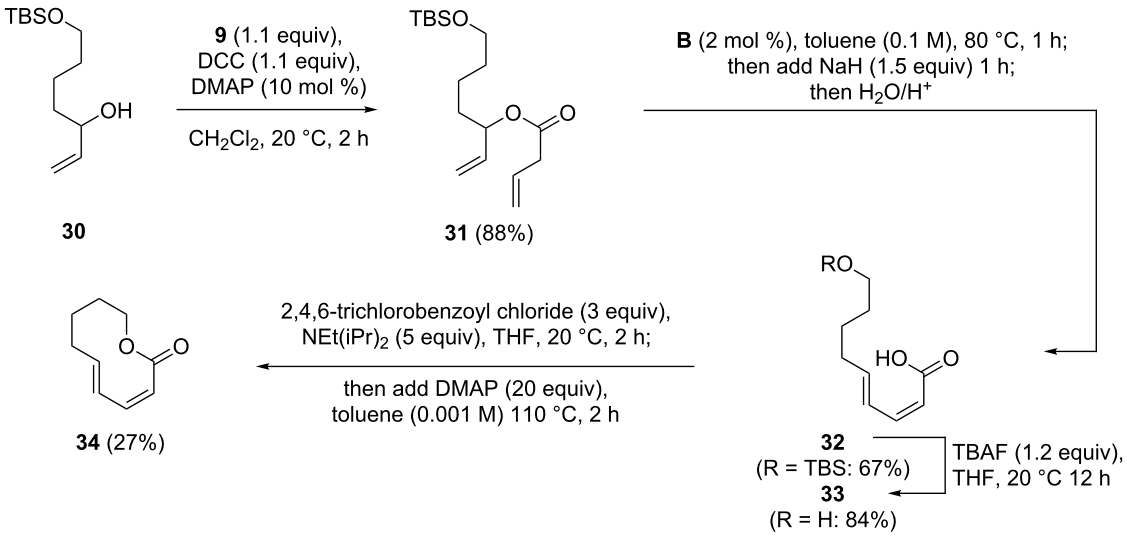
The synthesis of stagonolide E commenced with the desilylation of **26** and Steglich esterification of the resulting allyl alcohol **27**. One-flask reaction of **28** with catalyst **B**, followed by treatment with NaH, resulted in the expected RCM/ring-opening sequence, but also in a partial deacetylation. For this reason, the crude reaction mixture was subsequently treated with aqueous NaOH to complete the ester cleavage, giving the macrolactonization precursor **29** [31] in 81% yield (Scheme 6).

In a previous study [24], we had investigated the macrolactonization of the 6-deoxygenated derivative of **29**, which is itself a natural product named curvulalic acid (**35**) [29], and experienced enormous difficulties. No conversion to the expected cyclization product, another naturally occurring decanolide named fusanolide A (**36**) [56], was observed using the Steglich [43], Mukaiyama [57], Yamaguchi [58] or Shiina method [59] under their published standard conditions. For these reasons, we decided to investigate whether the macrolactonization of (2*Z*,4*E*)-9-hydroxy-2,4-dienoic acids is generally hampered, which might be caused by the build-up of ring strain. We started this investigation with the simple derivative **33**, which was synthesized from **30** [60] via a sequence of three steps. For the macrolactonization of **33** we chose Yamaguchi's method, but applied significantly more forcing conditions by using increased amounts of reagents and in particular a large excess of DMAP, in combination with higher dilution and elevated reaction temperatures. This led indeed to the formation of the desired lactone **34**, which could be isolated in a moderate yield of 27% (Scheme 7).

With this result in hand, we reinvestigated the cyclization of **35** [24] to fusanolide A (**36**) under the conditions outlined above. Gratifyingly, **36** was obtained in a yield of 53%, which allowed us to compare its analytical data with those reported for natural fusanolide A [56]. This comparison confirmed our previously suggested revision of the ten-membered lactone structure originally assigned to fusanolide A, as the spectroscopic data obtained for synthetic **36** differ significantly from those reported for the natural product. As we mentioned in our



Scheme 6: Synthesis of macrolactonization precursor **29**.

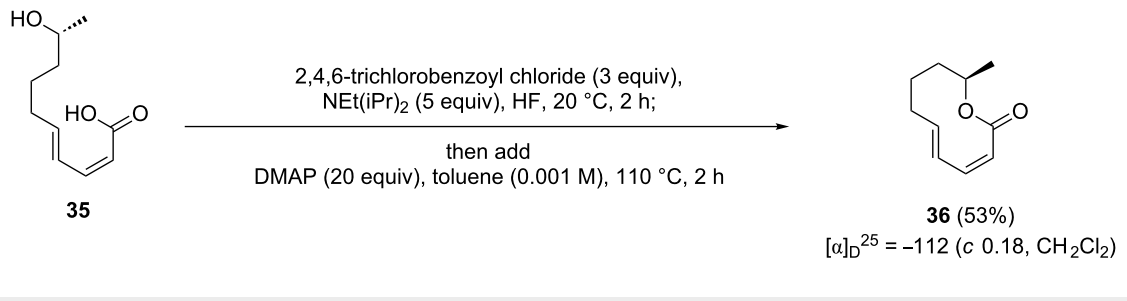


Scheme 7: Synthesis of (2*Z*,4*E*)-9-hydroxy-2,4-dienoic acid (**33**) and its macrolactonization.

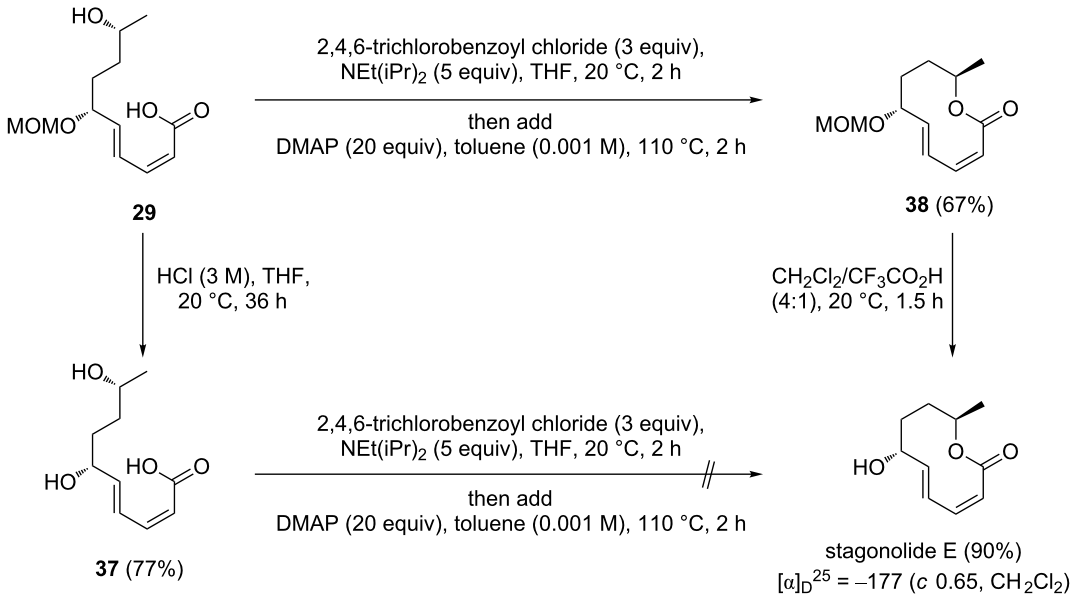
previous publication describing the synthesis of curvulalic acid (**35**) [24], all spectroscopic data obtained for this compound match those reported for fusanolide A [56] perfectly, suggesting that curvulalic acid and fusanolide A are probably identical. It should, however, be noted that **36** might well be a natural product which has not yet been isolated from a natural source (Scheme 8).

To complete the synthesis of stagonolide E, the MOM-protected precursor **29** and the deprotected derivative **37** were subjected to the Yamaguchi conditions that were found to be successful for the synthesis of **34** and **36** (Scheme 9). While the attempted Yamaguchi lactonization of **37** failed completely and resulted only in the quantitative recovery of unreacted starting material, the 6-MOM-protected precursor **29** underwent cyclization to the protected decanolide **38** [31] in 67% yield. Deprotection of **38** was accomplished with TFA in dichloromethane at ambient temperature without noticeable epimerization or elimination of water. Stagonolide E was isolated in 90% yield and its analytical data were identical to those reported for the natural product [28].

Only few examples for the macrolactonization of ω-hydroxy-2*Z*,4*E*-dienoic acids such as **29**, **33** and **34** have been described



Scheme 8: Synthesis of published structure of fusanolide A (**36**).

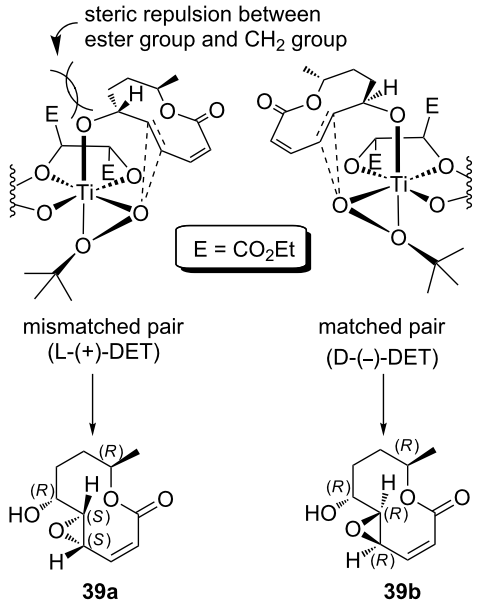


Scheme 9: Completion of stagonolide E synthesis.

in the literature, and we are not aware of another study which describes the cyclization of differently substituted derivatives under identical conditions. Notably, the yield of macrolactones is significantly affected by the substitution pattern and increases from 27% for the unsubstituted lactone **34** (Scheme 7) to 53% for the 9-methyl-substituted derivative **36** (Scheme 8) and to 67% for the 6,9-disubstituted compound **38** (Scheme 9). The presence of substituents and their relative configuration may have severe conformational effects on transition states, activation barriers and product stability [61,62]. An example for which a dramatically increased yield was reported upon incorporation of substituents has been reported in the course of an octalactin synthesis [61].

Having established a reliable route to stagonolide E, we investigated its epoxidation under Sharpless conditions [63]. We expected that this transformation would give either curvulide A [30] or one of its diastereomers, and help to resolve the remaining structural ambiguities, i.e. the absolute configurations at C4, C5 and C6. Based on the transition-state model for the Sharpless epoxidation of allylic alcohols bearing a stereogenic centre in the allylic position [64], we expected that levorotatory stagonolide E and L-(+)-diethyl tartrate (DET) should form the mismatched pair, while the matched pair would result with D-(−)-DET (Scheme 10).

We subjected (−)-stagonolide E to the conditions of a Sharpless epoxidation, using both L-(+)-DET and D-(−)-DET. As expected on the basis of the transition-state model, no reaction occurred after 2 d with L-(+)-DET, and the starting material could be recovered nearly quantitatively. In contrast, the use of D-(−)-DET led to the formation of an epoxide **39b** in 58% yield. A comparison of the analytical data of **39b** with those reported for curvulide A revealed that the NMR spectroscopic data are identical, and the value for the specific rotation of **39b** is reasonably close to the value reported for the natural product



Scheme 10: Transition-state models for the Sharpless epoxidation of stagonolide E with L-(+)-DET (left) and D-(−)-DET (right).

([α]$_D^{23}$ +133) [30]. Therefore, we conclude that the Sharpless-epoxidation product of stagonolide E is identical with curvulide A and suggest the (4*R*,5*R*,6*R*,9*R*)-configuration shown for **39b** (Scheme 11).

While the *R*-configuration assigned to C6 and C9 is unequivocally established, because these stereocenters originate from stagonolide E, there still remains an uncertainty for the absolute configurations at C4 and C5. While the relative *trans*-configuration at these stereocenters is evident from a small ^3J(H4–H5) value of 2.2 Hz and from the *E*-configuration of the precursor, the relative configuration of C6 and C5, and hence the absolute configurations at C4 and C5, can not be assigned with absolute reliability. However, a comparatively large coupling constant ^3J(H5–H6) of 8.2 Hz is pointing towards a *trans*-orientation of these protons with a large dihedral angle. Unfortunately, we could not obtain the (4*S*,5*S*,6*R*,9*R*)-configured **39a** and compare the crucial ^3J(H5–H6) coupling constants of the two diastereoisomers. However, the calculated energy-minimized structures of **39a** and **39b** suggest that the H5–H6 dihedral angles should differ substantially (Figure 2). For **39a**, this angle should be close to 90°, which is not in agreement with a coupling constant of 8.2 Hz. In contrast, the same dihedral angle can be expected to be approximately 170° in the case of the diastereomeric epoxide **39b**, and this value fits well to the observed ^3J(H5–H6) value (Figure 2) [65].

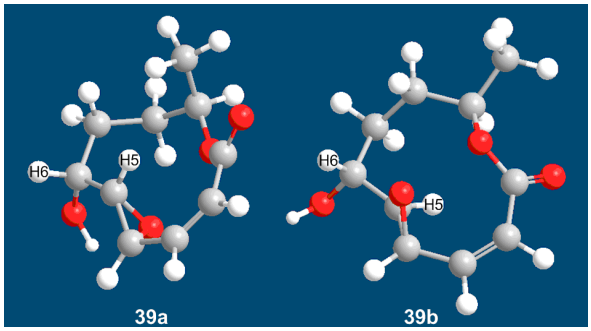
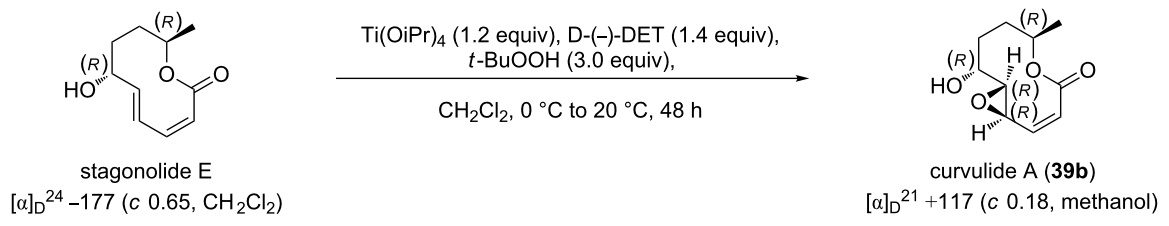


Figure 2: MM2 energy-minimized structures of **39a** and **39b**.

Conclusion

In summary, we synthesized the naturally occurring ten-membered lactones stagonolide E and curvulide A, starting from the ex-chiral pool building block (*R*,*R*)-hexa-1,5-diene-3,4-diol. Key elements of the stagonolide E synthesis are the two-directional functionalization of the enantiopure, C_2-symmetrical starting material through cross metathesis and a one-flask ring-closing metathesis/base-induced ring-opening sequence, a Ru–lipase-catalyzed dynamic kinetic resolution to establish the stereochemistry at C6, and a Yamaguchi macrolactonization. The first synthesis of curvulide A was accomplished by Sharpless epoxidation of stagonolide E. While the previously assigned absolute and relative configurations of stagonolide E could be confirmed by the synthesis described herein, we were able to provide additional information concerning missing structural assignments for curvulide A, which is most likely (4*R*,5*R*,6*R*,9*R*)-configured.



Scheme 11: Synthesis of **39b** (curvulide A) from stagonolide E.

Supporting Information

Supporting Information File 1

Experimental procedures, characterization data and copies of ^{1}H and ^{13}C NMR spectra.
[http://www.beilstein-journals.org/bjoc/content/supplementary/1860-5397-9-289-S1.pdf]

Acknowledgements

Generous financial support by the Deutsche Forschungsgemeinschaft (DFG grant Schm 1095/6-2) is gratefully acknowledged. We thank Evonik Oxeno for generous donations of solvents, and Umicore for generous donations of metathesis catalysts.

References

1. Poss, C. S.; Schreiber, S. L. *Acc. Chem. Res.* **1994,** *27,* 9–17. doi:10.1021/ar00037a002
2. Magnuson, S. R. *Tetrahedron* **1995,** *51,* 2167–2213. doi:10.1016/0040-4020(94)01070-G
3. Rama Rao, A. V.; Mysorekar, S. V.; Gurjar, M. K.; Yadav, J. S. *Tetrahedron Lett.* **1987,** *28,* 2183–2186. doi:10.1016/S0040-4039(00)96076-3
4. Crombez-Robert, C.; Benazza, M.; Fréchou, C.; Demailly, G. *Carbohydr. Res.* **1997,** *303,* 359–365. doi:10.1016/S0008-6215(97)00151-1
5. Burke, S. D.; Sametz, G. M. *Org. Lett.* **1999,** *1,* 71–74. doi:10.1021/ol9905506
6. Schmidt, B.; Nave, S. *Adv. Synth. Catal.* **2007,** *349,* 215–230. doi:10.1002/adsc.200600473
7. Michaelis, S.; Blechert, S. *Org. Lett.* **2005,** *7,* 5513–5516. doi:10.1021/ol052332k
8. Purser, S.; Claridge, T. D. W.; Odell, B.; Moore, P. R.; Gouverneur, V. *Org. Lett.* **2008,** *10,* 4263–4266. doi:10.1021/ol8017402
9. Schmidt, B.; Staude, L.; Kelling, A.; Schilde, U. *Eur. J. Org. Chem.* **2011,** 1721–1727. doi:10.1002/ejoc.201001528
10. Schmidt, B.; Nave, S. *Chem. Commun.* **2006,** 2489–2491. doi:10.1039/b604359c
11. Voight, E. A.; Rein, C.; Burke, S. D. *J. Org. Chem.* **2002,** *67,* 8489–8499. doi:10.1021/jo0263014
12. Chou, C.-Y.; Hou, D.-R. *J. Org. Chem.* **2006,** *71,* 9887–9890. doi:10.1021/jo061767y
13. Cribiú, R.; Jäger, C.; Nevado, C. *Angew. Chem., Int. Ed.* **2009,** *48,* 8780–8783. doi:10.1002/anie.200903379
14. Reddy, C. R.; Dharmapuri, G.; Rao, N. N. *Org. Lett.* **2009,** *11,* 5730–5733. doi:10.1021/ol9025183
15. Marvin, C. C.; Clemens, A. J. L.; Burke, S. D. *Org. Lett.* **2007,** *9,* 5353–5356. doi:10.1021/ol7021214
16. Marvin, C. C.; Voight, E. A.; Burke, S. D. *Org. Lett.* **2007,** *9,* 5357–5359. doi:10.1021/ol702454m
17. Quinn, K. J.; Smith, A. G.; Cammarano, C. M. *Tetrahedron* **2007,** *63,* 4881–4886. doi:10.1016/j.tet.2007.03.151
18. Quinn, K. J.; Isaacs, A. K.; Arvary, R. A. *Org. Lett.* **2004,** *6,* 4143–4145. doi:10.1021/ol040047f
19. Quinn, K. J.; Isaacs, A. K.; DeChristopher, B. A.; Szklarz, S. C.; Arvary, R. A. *Org. Lett.* **2005,** *7,* 1243–1245. doi:10.1021/ol047352l
20. Schmidt, B.; Kunz, O.; Petersen, M. H. *J. Org. Chem.* **2012,** *77,* 10897–10906. doi:10.1021/jo302359h
21. Schmidt, B. *Pure Appl. Chem.* **2006,** *78,* 469–476. doi:10.1351/pac200678020469
22. Alcaide, B.; Almendros, P.; Luna, A. *Chem. Rev.* **2009,** *109,* 3817–3858. doi:10.1021/cr9001512
23. Arisawa, M.; Terada, Y.; Takahashi, K.; Nakagawa, M.; Nishida, A. *Chem. Rec.* **2007,** *7,* 238–253. doi:10.1002/tcr.20121
24. Schmidt, B.; Kunz, O. *Eur. J. Org. Chem.* **2012,** 1008–1018. doi:10.1002/ejoc.201101497
25. Roush, W. R.; Spada, A. P. *Tetrahedron Lett.* **1982,** *23,* 3773–3776. doi:10.1016/S0040-4039(00)87703-5
26. Dräger, G.; Kirschning, A.; Thiericke, R.; Zerlin, M. *Nat. Prod. Rep.* **1996,** *13,* 365–375. doi:10.1039/np9961300365
27. Sun, P.; Lu, S.; Ree, T. V.; Krohn, K.; Li, L.; Zhang, W. *Curr. Med. Chem.* **2012,** *19,* 3417–3455. doi:10.2174/092986712801215874
28. Evidente, A.; Cimmino, A.; Berestetskiy, A.; Mitina, G.; Andolfi, A.; Motta, A. *J. Nat. Prod.* **2008,** *71,* 31–34. doi:10.1021/np0703038
29. Trisuwan, K.; Rukachaisirikul, V.; Phongpaichit, S.; Preedanon, S.; Sakayaroj, J. *Arch. Pharmacal Res.* **2011,** *34,* 709–714. doi:10.1007/s12272-011-0502-8
30. Greve, H.; Schupp, P. J.; Eguereva, E.; Kehraus, S.; König, G. M. *J. Nat. Prod.* **2008,** *71,* 1651–1653. doi:10.1021/np8003326
31. Sabitha, G.; Padmaja, P.; Reddy, P. N.; Jadav, S. S.; Yadav, J. S. *Tetrahedron Lett.* **2010,** *51,* 6166–6168. doi:10.1016/j.tetlet.2010.09.072
32. Das, T.; Nanda, S. *Tetrahedron Lett.* **2012,** *53,* 256–258. doi:10.1016/j.tetlet.2011.11.059
33. Arlt, D.; Bieniek, M.; Karch, R. Novel Metathesis Catalysts. WO 2008/034552 A1, March 27, 2008.
34. Mutlu, H.; Montero de Espinosa, L.; Türünç, O.; Meier, M. A. R. *Beilstein J. Org. Chem.* **2010,** *6,* 1149–1158. doi:10.3762/bjoc.6.131
35. Scholl, M.; Ding, S.; Lee, C. W.; Grubbs, R. H. *Org. Lett.* **1999,** *1,* 953–956. doi:10.1021/ol990909q
36. Connon, S. J.; Blechert, S. *Angew. Chem., Int. Ed.* **2003,** *42,* 1900–1923. doi:10.1002/anie.200200556
37. Connon, S. J.; Blechert, S. *Top. Organomet. Chem.* **2004,** *11,* 93–124. doi:10.1007/b94650
38. Bach, J.; Berenguer, R.; Garcia, J.; López, M.; Manzanal, J.; Vilarrasa, J. *Tetrahedron* **1998,** *54,* 14947–14962. doi:10.1016/S0040-4020(98)00936-3
39. Forman, G. S.; McConnell, A. E.; Tooze, R. P.; van Rensburg, W. J.; Meyer, W. H.; Kirk, M. M.; Dwyer, C. L.; Serfontein, D. W. *Organometallics* **2005,** *24,* 4528–4542. doi:10.1021/om0503848
40. Lawrence, N. J.; Drew, M. D.; Bushell, S. M. *J. Chem. Soc., Perkin Trans. 1* **1999,** 3381–3391. doi:10.1039/A903662H
41. Mahoney, W. S.; Brestensky, D. M.; Stryker, J. M. *J. Am. Chem. Soc.* **1988,** *110,* 291–293. doi:10.1021/ja00209a048
42. Baker, B. A.; Bošković, Ž. V.; Lipshutz, B. H. *Org. Lett.* **2008,** *10,* 289–292. doi:10.1021/ol702689v
43. Neises, B.; Steglich, W. *Angew. Chem., Int. Ed. Engl.* **1978,** *17,* 522–524. doi:10.1002/anie.197805221
44. Deutsch, C.; Krause, N.; Lipshutz, B. H. *Chem. Rev.* **2008,** *108,* 2916–2927. doi:10.1021/cr0684321
45. Corey, E. J.; Bakshi, R. K.; Shibata, S. *J. Am. Chem. Soc.* **1987,** *109,* 5551–5553. doi:10.1021/ja00252a056

46. Corey, E. J.; Helal, C. J. *Angew. Chem., Int. Ed.* **1998,** *37,* 1986–2012. doi:10.1002/(SICI)1521-3773(19980817)37:15<1986::AID-ANIE1986>3.0.CO;2-Z
47. Lu, K.-J.; Chen, C.-H.; Hou, D.-R. *Tetrahedron* **2009,** *65,* 225–231. doi:10.1016/j.tet.2008.10.059
48. Stürmer, R. *Angew. Chem., Int. Ed. Engl.* **1997,** *36,* 1173–1174. doi:10.1002/anie.199711731
49. Pàmies, O.; Bäckvall, J.-E. *Chem. Rev.* **2003,** *103,* 3247–3262. doi:10.1021/cr020029g
50. Shvo, Y.; Czarkie, D.; Rahamim, Y.; Chodosh, D. F. *J. Am. Chem. Soc.* **1986,** *108,* 7400–7402. doi:10.1021/ja00283a041
51. Choi, J. H.; Choi, Y. K.; Kim, Y. H.; Park, E. S.; Kim, E. J.; Kim, M.-J.; Park, J. *J. Org. Chem.* **2004,** *69,* 1972–1977. doi:10.1021/jo0355799
52. Martín-Matute, B.; Edin, M.; Bogár, K.; Kaynak, F. B.; Bäckvall, J.-E. *J. Am. Chem. Soc.* **2005,** *127,* 8817–8825. doi:10.1021/ja051576x
53. Larsson, A. L. E.; Persson, B. A.; Bäckvall, J.-E. *Angew. Chem., Int. Ed. Engl.* **1997,** *36,* 1211–1212. doi:10.1002/anie.199712111
54. Persson, B. A.; Larsson, A. L. E.; Le Ray, M.; Bäckvall, J.-E. *J. Am. Chem. Soc.* **1999,** *121,* 1645–1650. doi:10.1021/ja983819+
55. Mitsunobu, O. *Synthesis* **1981,** 1–28. doi:10.1055/s-1981-29317
56. Shimada, A.; Kusano, M.; Matsumoto, K.; Nishibe, M.; Kawano, T.; Kimura, Y. *Z. Naturforsch., B* **2002,** *57b,* 239–242.
57. Mukaiyama, T.; Usui, M.; Saigo, K. *Chem. Lett.* **1976,** *5,* 49–50. doi:10.1246/cl.1976.49
58. Inanaga, J.; Hirata, K.; Saeki, H.; Katsuki, T.; Yamaguchi, M. *Bull. Chem. Soc. Jpn.* **1979,** *52,* 1989–1993. doi:10.1246/bcsj.52.1989
59. Shiina, I.; Kubota, M.; Oshiumi, H.; Hashizume, M. *J. Org. Chem.* **2004,** *69,* 1822–1830. doi:10.1021/jo030367x
60. Enders, D.; Nguyen, D. *Synthesis* **2000,** 2092–2098. doi:10.1055/s-2000-8732
61. Andrus, M. B.; Argade, A. B. *Tetrahedron Lett.* **1996,** *37,* 5049–5052. doi:10.1016/0040-4039(96)01014-3
62. Parenty, A.; Moreau, X.; Niel, G.; Campagne, J. M. *Chem. Rev.* **2013,** *113,* PR1–PR40. doi:10.1021/cr300129n
63. Katsuki, T.; Martin, V. S. *Org. React.* **1995,** *48,* 1–299. doi:10.1002/0471264180.or048.01
64. Johnson, R. B.; Sharpless, K. B. Catalytic Asymmetric Epoxidation of Allylic Alcohols. In *Catalytic Asymmetric Synthesis;* Ojima, I., Ed.; Wiley-VCH: Weinheim, Germany, 1993; pp 103–158.
65. Karplus, M. *J. Chem. Phys.* **1959,** *30,* 11–15. doi:10.1063/1.1729860

License and Terms

This is an Open Access article under the terms of the Creative Commons Attribution License (http://creativecommons.org/licenses/by/2.0), which permits unrestricted use, distribution, and reproduction in any medium, provided the original work is properly cited.

The license is subject to the *Beilstein Journal of Organic Chemistry* terms and conditions: (http://www.beilstein-journals.org/bjoc)

The definitive version of this article is the electronic one which can be found at: doi:10.3762/bjoc.9.289

Beilstein Journal of Organic Chemistry

The regulation and biosynthesis of antimycins

Ryan F. Seipke*[1,2] and Matthew I. Hutchings*[1]

Review

Open Access

Address:
[1]School of Biological Sciences, University of East Anglia, Norwich Research Park, Norwich, NR4 7TJ, United Kingdom and [2]School of Molecular and Cellular Biology, Garstang Buildling, Faculty of Biological Sciences, University of Leeds, Leeds, LS2 9JT, United Kingdom

Email:
Ryan F. Seipke* - r.seipke@leeds.ac.uk; Matthew I. Hutchings* - m.hutchings@uea.ac.uk

* Corresponding author

Keywords:
antimycins; gene regulation; genome mining; natural products; Streptomyces

Beilstein J. Org. Chem. **2013,** *9,* 2556–2563.
doi:10.3762/bjoc.9.290

Received: 12 August 2013
Accepted: 01 November 2013
Published: 19 November 2013

This article is part of the Thematic Series "Natural products in synthesis and biosynthesis".

Guest Editor: J. S. Dickschat

© 2013 Seipke and Hutchings; licensee Beilstein-Institut.
License and terms: see end of document.

Abstract

Antimycins (>40 members) were discovered nearly 65 years ago but the discovery of the gene cluster encoding antimycin biosynthesis in 2011 has facilitated rapid progress in understanding the unusual biosynthetic pathway. Antimycin A is widely used as a piscicide in the catfish farming industry and also has potent killing activity against insects, nematodes and fungi. The mode of action of antimycins is to inhibit cytochrome c reductase in the electron transport chain and halt respiration. However, more recently, antimycin A has attracted attention as a potent and selective inhibitor of the mitochondrial anti-apoptotic proteins Bcl-2 and Bcl-x_L. Remarkably, this inhibition is independent of the main mode of action of antimycins such that an artificial derivative named 2-methoxyantimycin A inhibits Bcl-x_L but does not inhibit respiration. The Bcl-2/Bcl-x_L family of proteins are overproduced in cancer cells that are resistant to apoptosis-inducing chemotherapy agents, so antimycins have great potential as anticancer drugs used in combination with existing chemotherapeutics. Here we review what is known about antimycins, the regulation of the *ant* gene cluster and the unusual biosynthetic pathway.

Review

It is estimated that around 60% of all known antibiotics are derived from secondary metabolites made by filamentous actinomycete bacteria, most notably *Streptomyces* species [1]. *Streptomyces* species are predominantly known as saprophytic soil bacteria that have a complex differentiating life cycle. The life cycle begins with spore germination and outgrowth of a substrate mycelium and ends with the production of reproductive aerial hyphae, which undergo cell division to form chains of unigenomic spores [2]. Aerial hyphae production and sporulation is triggered by nutritional stress and is accompanied by the production of secondary metabolites. These specialised metabolites likely function both as chemical weapons against competing organisms in the soil and as signaling molecules to neighbouring microbes [3]. In recent years genome sequencing

has revealed that each *Streptomyces* species encodes many more specialised metabolites than it makes in laboratory culture, leading to new efforts to activate these so-called "silent pathways." The number of known antibiotics made by *Streptomyces* species is likely to grow rapidly with the advent of genome mining approaches, which start by identifying promising specialised metabolite gene clusters in whole genome sequences and then inducing their expression through chemical or genetic manipulation of the gene cluster in the native or a heterologous host. This approach has already been used to identify novel chemical scaffolds of antibiotics produced by well-studied *Streptomyces* species [4-6] and to identify the biosynthetic gene clusters for commercially important antibiotics [7-11]. The latter allows cloning, optimisation and engineering of such pathways to generate new derivatives with improved pharmacological properties.

We recently sequenced the genome of *Streptomyces albus* S4, which we isolated from the cuticle of the leaf-cutter ant *Acromyrmex octospinosus* [12,13]. Using genome-mining strategies, we identified the biosynthetic gene cluster for a group of compounds called antimycins that were discovered more than 60 years ago [7,14]. Antimycins, including structurally related uranchimycins, kitamycins and splenocins have unique structures comprising a nine-membered dilactone core conjugated to a rare 3-formamidosalicylic acid moiety and they comprise more than 40 known members (Figure 1) [15-22]. Antimycins can undergo base-catalysed decomposition resulting in the production of volatile blastmycinones and butenolides [23]. The main mode of action of antimycins is to inhibit cytochrome c reductase, an enzyme in the electron transport chain in mitochondria and bacteria and as such they are bioactive against a wide range of oragnisms including fish, fungi, insects and nematodes [24].

Antimycins are widely used as a piscicide (brandname Fintrol) in the catfish farming industry. Catfish are easy to farm and they provide an inexpensive source of food in large parts of Asia and in the Southern USA. Catfish are relatively insensitive to antimycins and Fintrol is used to selectively kill other unwanted scaled fish species during aquaculture [26]. Antimycins are also used as research tools to study the structure and function of cytochromes [27]. More recently antimycins have been shown to be potent and selective inhibitors of the mitochondrial Bcl-2/Bcl-x_L-related anti-apoptotic proteins [28]. Over-production of Bcl-2/Bcl-x_L-related proteins in cancer cells confers resistance to multiple chemotherapeutic agents whose mode of action is to trigger apoptosis. A small molecule screen identified antimycins as potent inhibitors of Bcl-2-related proteins where they were shown to bind to the hydrophobic groove [28]. A synthetic derivative of antimycin A_3, 2-methoxyantimycin A_3 (Figure 1), no longer inhibits the respiratory chain, but still promotes apoptosis in cells overproducing Bcl-2-related proteins [29]. This suggests antimycin derivatives could be used alongside traditional apoptosis-inducing chemotherapeutics to block drug resistance and kill cancer cells [30]. Therefore, there is significant interest in better understanding the biosynthesis and regulation of antimycins, with a view toward bioengineering improved pharmacological properties for the treatment of drug-resistant cancers in the future.

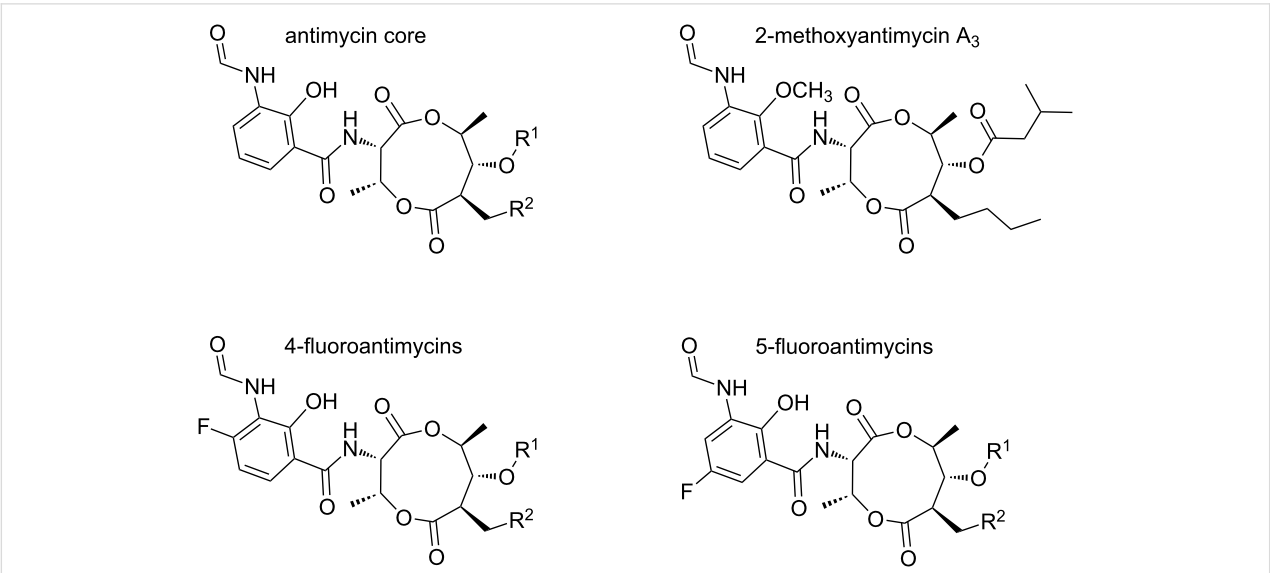


Figure 1: Antimycins: Antimycins A_1, A_2, A_3, and A_4 and non-natural antimycins referenced in the text. Antimycin A_1, $R^1 = COCH(CH_3)CH_2CH_3$, $R^2 = (CH_2)_4CH_3$; Antimycin A_2, $R^1 = COCH(CH_3)_2$, $R^2 = (CH_2)_4CH_3$; Antimycin A_3, $R^1 = COCH_2CH(CH_3)_2$, $R^2 = (CH_2)_2CH_3$; Antimycin A_4, $R^1 = COCH(CH_3)_2$, $R^2 = (CH_2)_2CH_3$. For a recent summary of the chemical diversity in the antimycin family see [25].

The *ant* gene cluster

Since our discovery of the *ant* gene cluster in *S. albus* S4, we and others have identified *ant* gene clusters in 14 out of 117 fully or partially sequenced genomes available in Genbank for the genus *Streptomyces* (Figure 2). The 14 *ant* gene clusters can be classified as long-form (L-form, 17 genes), intermediate-form (I-form, 16 genes) or short-form (S-form, 15 genes). L-form *ant* gene clusters contain two genes, *antP* and *antQ*, which are not encoded by S-form gene clusters [25], and I-form gene clusters contain either *antP* or *antQ*, but not both.

L-form *ant* gene clusters are encoded by six taxa, *S. ambofaciens* ATCC 23877 [7,33], *S. blastmyceticus* NBRC 12747 [25], *S. gancidicus* BKS 13–15 and *S. griseoflavus* Tü4000 [23]. Interestingly, *S. hygroscopicus* subsp. *jinggangensis* 5008 and *S. hygroscopicus* subsp. *jinggangensis* TL01 encode L-form *ant*

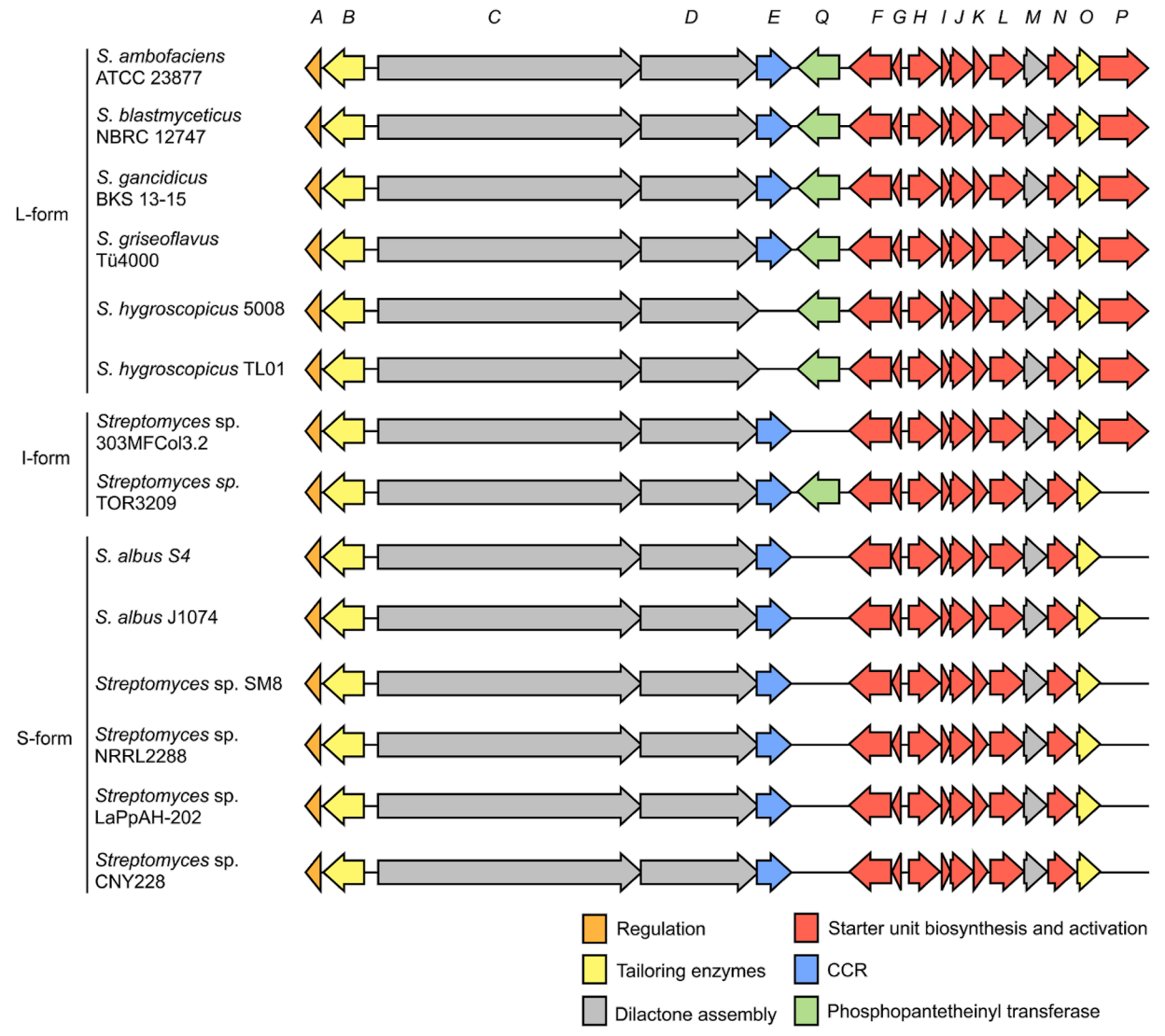


Figure 2: Schematic representation of *ant* biosynthetic gene clusters. L-form *ant* gene clusters are encoded by: *S. ambofaciens* ATCC 23877 (AM238663), *S. blastmyceticus* NBRC 12747 (AB727666), *S. gancidicus* BKS 13-15 (AOHP01000135, AOHP01000134, AOHP01000056, [31]), *S. griseoflavus* Tü4000 (ACFA01000901, ACFA01000902, ACFA01000903, ACFA01000904, ACFA01000905, ACFA01000906, ACFA01000907); *S. hygroscopicus* subsp. *jinggangensis* 5008 (NC_017765); *S. hygroscopicus* subsp. *jinggangensis* TL01 (NC_020895). I-form *ant* gene clusters are encoded by: *Streptomyces* sp. 303MFCol5.2 (ARTR01000061), *Streptomyces* sp. TOR3209 (AGNH01000419, AGNH01000420, AGNH01000421, [32]). S-form *ant* gene clusters are encoded by: *S. albus* S4 (CADY01000091); *S. albus* J1074 (NC_020990); *Streptomyces sp.* SM8 (AMPN01000393, AMPN01000430, AMPN01000050); *Streptomyces* sp. NRRL2288 [25]; *Streptomyces* sp. LaPpAH-202 (ARDM01000016); *Streptomyces* sp. CNY228 (ARIN01000033). The Genbank accession numbers provided correspond to either the complete genome sequence or the contig(s) of draft genome sequences encoding the *ant* gene cluster. It is worth noting that there is a probable sequencing error in the *S. gancidicus* BKS 13–15 cluster which causes the AntD orthologue not to have a stop codon. There is also a probable sequencing error in *S. griseoflavus* Tü4000, which truncates the truncates C1 of AntC into a discrete protein. CCR, crotonyl-CoA reductase.

gene clusters, but do not encode AntE (Figure 2). I-form *ant* gene clusters are encoded by two species, *Streptomyces* sp. 303MFCol5.2 and *Streptomyces* sp. TOR3209, which lack *antQ* and *antP*, respectively (Figure 2). There are six taxa, all highly related to *S. albus* S4, that encode S-form *ant* gene clusters: *S. albus* S4 [7], *S. albus* J1074 [7], *Streptomyces sp.* SM8, *Streptomyces* sp. NRRL2288 [25], *Streptomyces* sp. LaPpAH-202 and *Streptomyces* sp. CNY228.

Based on our analysis of *S. albus* S4, the S-form gene cluster is organised into four transcriptional units; *antAB*, *antCDE*, *antFG* and *antHIJKLMNO* (Seipke and Hutchings, unpublished results; Figure 2). The *antFGHIJKLN* genes encode the biosynthesis pathway for the unusual starter unit, 3-aminosalicylate, *antCD* encode the hybrid NRPS/PKS machinery and *antE* and *antM* encode a crotonyl-CoA reductase and a discrete ketoreductase, respectively. The *antB* and *antO* genes encode tailoring enzymes and *antA* encodes an extracytoplasmic function (ECF) RNA polymerase σ factor named σ^{AntA}. The additional genes found in the 17 gene L-form and I-form *ant* gene clusters are *antP* and *antQ*, which encode a kynureninase and phosphopantetheinyl transferase, respectively [25] (Figure 2).

The availability of 14 *ant* gene clusters will facilitate a better understanding of how the different forms of the *ant* gene cluster evolved. More work in this area is required, however it is tempting to speculate that the L-form *ant* gene cluster is the ancestral gene cluster and *antP* and *antQ* were lost, giving rise to the S-form gene cluster. The I-form *ant* gene clusters encoded by *Streptomyces* 303MFCol5.2 and *Streptomyces* sp. TOR3209, which lack *antP* and *antQ,* respectively could be midway points toward evolving into S-form clusters, which presumably use the kynureninase involved in tryptophan catabolism and a phosphopantetheinyl transferase encoded elsewhere in the genome to compensate for the loss of *antP* and *antQ*, respectively.

Biosynthesis of the antimycin dilactone core

Antimycins are produced by a hybrid non-ribosomal peptide synthetase (NRPS)/polyketide synthase (PKS) assembly line for which the complete biosynthetic pathway has been proposed [25,34] (Figure 3). The biosynthesis of antimycins involves the activities of fourteen proteins, AntBCDEFGHIJKLMNO. The biosynthesis begins with the opening of the indole ring of tryptophan by a pathway-specific tryptophan-2,3-dioxygenase, AntN, to produce *N*-formyl-L-kynurenine. For L-form *ant* gene clusters, *N*-formyl-L-kynurenine is likely converted to anthranilate by the pathway-specific kynureninase, AntP, whereas S-form gene clusters lack AntP and likely use the kynureninase involved in primary tryptophan metabolism. Anthranilate and not *N*-formylanthranilate is activated by the acyl-CoA ligase protein, AntF and loaded onto its cognate carrier protein, AntG [34]. Once loaded onto AntG, anthranilate is converted to 3-aminosalicylate by a multicomponent oxygenase, AntHIJKL [33,34]. The anthraniloyl-S-AntG carboxylic acid-CoA thioester undergoes a never before seen 1,2-shift. Spiteller and colleagues suggested that AntHIJKL promotes this reaction via an epoxide intermediate similar to a reaction in phenylacetate catabolism [35] resulting in hydryoxylation of C-2 [33]. 3-Aminosalicylate serves as the starter unit and is presented to the NRPS, AntC. The AntC protein possesses two modules organised as follows: C1-A1-T1-C2-A2-KR-T2. The A1 domain activates and loads threonine onto T1, followed by condensation of 3-aminosalicylate and threonine promoted by C1. The A2 domain activates and loads pyruvate onto T2. Pyruvate is subsequently stereospecifically reduced by the KR domain and condensed with threonine by C2. The PKS, AntD posseses one module composed of the domains KS-AT-ACP-TE. The AT domain promotes the transfer of a 2-carboxylated acyl-CoA to ACP. The acyl-CoAs that are utilised by $AntD^{AT}$ are the product of AntE, a crotonyl-CoA reductase homologue, which biosynthesises 'unusual' acylmalonyl-CoAs utilised as PKS extender units [34,36,37]. The AntD AT domain is promiscuous and accepts multiple acylmalonyl-CoAs. In combination with AntE, $AntD^{AT}$ is the source of the large chemical diversity observed at position R^2 within the antimycin family. Interestingly, *S. hygroscopicus* subsp. *jinggangensis* 5008 and *S. hygroscopicus* subsp. *jinggangensis* TL01 do not encode AntE, suggesting that these strains produce antimycins with less chemical diversity at the R^2 position (Figure 2 and Figure 3). The KS domain catalyses the decarboxylative condensation between the aminoacyl thioester attached to $AntC^{T2}$ and the 2-carboxy-acyl moiety attached to $AntD^{ACP}$. Next, a discrete ketoreductase, AntM catalyses the stereoselective reduction of the β-keto group, which precedes $AntD^{TE}$ – promoted regiospecific macrolactonisation and release of the nine-membered dilactone. Sandy et al. heterologously produced and purified AntCDEFGM and used building monomers anthranilate, L-threonine, pyruvate, and 2*E*-hexenoyl-CoA to conclusively demonstrate the minimum set of enzymes required for biosynthesis of the antimycin dilactone scaffold in vitro [34].

Antimycin tailoring genes

All known antimycin gene clusters contain two tailoring enzymes, AntB and AntO (Figure 2). AntB is a discrete acyltransferase, which catalyses a transesterification reaction resulting in the formation of a C-8 acyloxyl moiety and is responsible for generating the chemical diversity at R^1 (Figure 1). AntB likely performs this reaction after assembly of the dilactone core, as wild-type levels of biosynthetic intermediates possessing a C-8 hydroxyl and not a C-8 acyloxyl were detected in a Δ*antB* mutant [38]. In vitro enzymatic synthesis showed

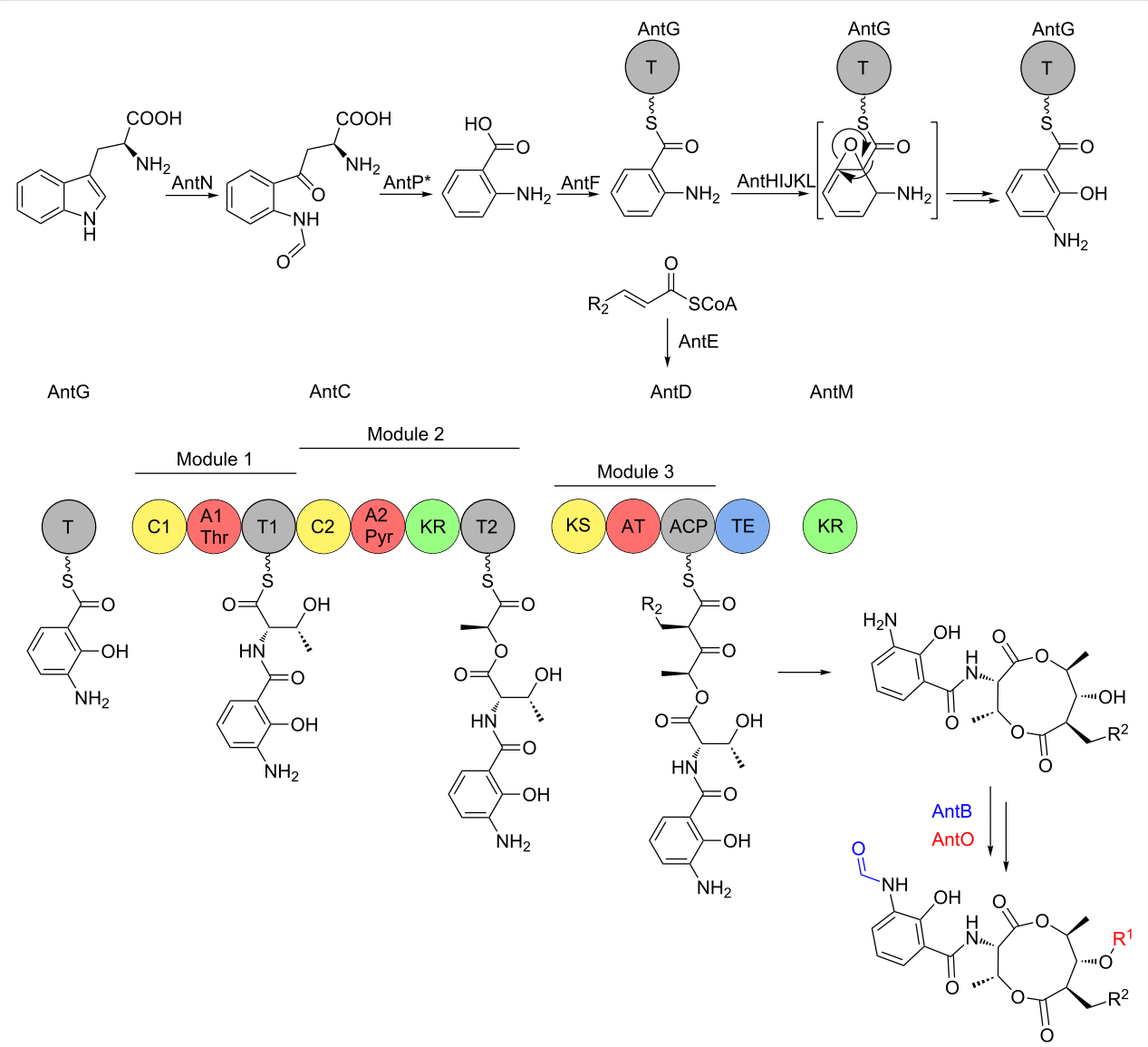


Figure 3: Proposed biosynthetic pathway for antimycins. The antimycin biosynthetic pathway is described in detail in the text. C = condensation; A, adenylation; T, thiolation; KR, ketoreduction; KS, ketosynthase; AT, acyltransferase; ACP, acyl carrier protein; TE, thioesterase; *AntP is a pathway-specific kynureninase that is encoded by L- and l-form *ant* gene clusters.

that AntB is incredibly promiscuous and is capable of accepting a wide variety of substrates, including an alkyne-containing moiety, which has not been observed previously in the antimycin family [38]. AntB is also able to accept substrates presented by an alternate acyl carrier, *N*-acetylcysteamine (SNAC), though the turnover rate of acyl-SNACs is 100-fold lower than acyl-CoAs [38]. Despite the lower turnover rate, acyl-SNAC substrates are cell-permeable and thus AntB's ability to utilise acyl-SNACs provides the possibility to employ feeding studies to introduce new chemistry at C-8. AntO is a lipase homologue and is predicted to install the *N*-formyl group resulting in the 3-formamidosalicylate moiety. AntO is required for bioactivity against the human pathogenic fungus, *Candida albicans* (Seipke and Hutchings, unpublished results), but the exact time in which AntO installs the *N*-formyl group is unclear and requires investigation.

Regulation of the *ant* gene cluster

Antimycin biosynthesis is linked to development, as is the case for many *Streptomyces* secondary metabolites. However, antimycin biosynthesis is unusual because all four *ant* operons are highly expressed in substrate mycelium (after 24 hours growth on solid medium) whereas antimycins are not detected until after the production of aerial mycelium when *ant* gene expression is switched off (after 48 hours growth) (Seipke and Hutchings, unpublished results). This lag between gene expres-

sion and antimycin production may be due to the complex biosynthetic machinery that needs to be assembled to first make the unusual starter unit 3-aminosalicylate and then finally assemble the antimycin scaffold. The down-regulation of all the *ant* genes in stationary phase also suggests that specific regulatory mechanisms must exist to switch off the expression of all four *ant* operons. Despite this, the 14 *ant* gene clusters contain only a single conserved regulatory gene, *antA*, which encodes an orphan ECF RNA polymerase σ factor named σ^{AntA} (Figure 2). This sigma factor appears to be unique to the 14 known *ant* clusters in the database and they form a new subfamily of ECF sigma factors (Figure 4). Expression of the *antFG* and *antHIJKLMNO* genes is completely dependent on σ^{AntA} and over-expression of *antA* results in *antFGHIJKLMNO* expression in differentiated cultures, suggesting it regulates production of the starter unit, 3-aminosalicylate (Seipke and Hutchings, unpublished results). An unknown regulator, which is not encoded within the *ant* cluster, controls expression of the *antAB* and *antCDE* operons. Despite an earlier report that the S-form *ant* cluster (from *Streptomyces* sp. NRRL 2288) can be heterologously expressed in *S. lividans and S. coelicolor*, we have been unable to replicate this with the cloned S-form *ant* clusters from *S. albus* S4 or *Streptomyces* sp. NRRL 2288 (a kind gift from Professor Wen Liu). This suggests that the regulator of *antAB* and *antCDE* is a transcriptional activator that is encoded outside of the *ant* gene cluster and is absent from the heterologous host strains (Seipke and Hutchings, unpublished results).

Regulation of antibiotic gene clusters by ECF σ factors has only been reported in two rare actinomycete strains and in both cases there is a co-encoded anti-σ factor, which regulates σ factor activity, along with a pathway specific transcriptional activator. In *Microbispora corallina* production of the lantibiotic microbisporicin is regulated by the pathway-specific transcription factor MibR and the ECF σ^{MibX}, whose activity is modulated by its cognate anti-σ factor, MibW [8]. Biosynthesis of the lantibiotic planosporicin by *Planomonospora alba* is also regulated by a σ and anti-σ factor pair (PspX and PspW) whose closest homologues are MibX and MibW, respectively, and by the pathway-specific LuxR-family regulator, PspR [42]. There are no anti-σ factors encoded in any of the 14 *ant* gene clusters and no transcriptional regulators other than σ^{AntA} (Figure 2). Production of σ^{AntA} is regulated at the transcriptional level, by

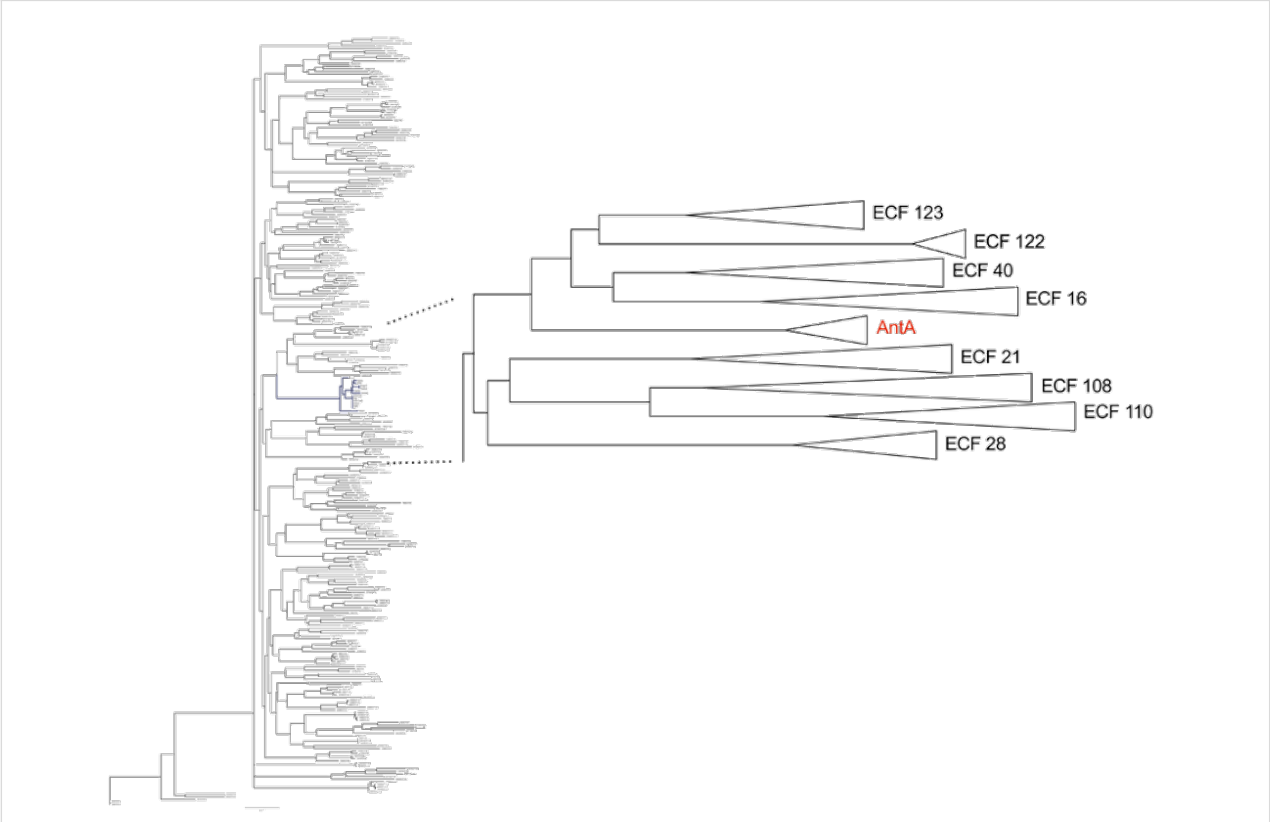


Figure 4: σ^{AntA} comprises a new subfamily of ECF RNA polymerase σ factors. σ^{AntA} amino acid sequences were aligned to amino acid sequences of random representative of each ECF RNA polymerase σ factor subfamily reported by [39] using ClustalΩ [40]. The phylogenetic tree was created using PhyML 3.0 [41] and visualised using FigTree v1.4. The relevant region of the phylogenetic tree is enhanced for visualisation and reveals that all σ^{AntA} protein sequences cluster together and have a distinct phylogenetic lineage and represents a new ECF RNA polymerase σ factor subfamily.

an unknown transcription factor, and it appears that σ^{AntA} is rapidly cleared from the cell once transcription of *antA* is switched off (Seipke and Hutchings, unpublished results). One striking feature of the 14 known σ^{AntA} proteins is that they all terminate in Ala–Ala, a well-known signal for the ClpXP protease. Attempts to N-terminally 6xHis-tag σ^{AntA} so that we could detect it using monoclonal anti-His antibodies were unsuccessful because His_6-σ^{AntA} does not complement the *antA* mutant strain of *S. albus* S4, suggesting the protein is inactive. Furthermore, polyclonal antibodies raised against purified σ^{AntA} reacted with the purified σ^{AntA} protein in immunoblotting experiments, but could not detect σ^{AntA} in whole cell extracts, even from strains over-expressing *antA*, perhaps suggesting the protein is very unstable. Intriguingly, a variant of the *S. albus* S4 σ^{AntA} protein in which the C-terminal Ala–Ala was changed to Asp–Asp resulted in higher levels of expression for the *antFG* and *antHIJKLMNO* operons suggesting this may increase the stability or activity of σ^{AntA} (Seipke and Hutchings, unpublished results). A role for ClpXP in regulating σ^{AntA} activity remains to be proven however.

Future perspectives: toward bioengineering antimycins with improved pharmacological properties

There is significant interest in bioengineering new antimycin analogues with improved pharmacological properties for use as antifungal therapeutics and to be used to treat cancers, alongside traditional chemotherapy agents. Substantial progress has been made in a relatively short time and has mostly been driven by studies rooted in better understanding the biosynthesis of these unusual molecules.

Initial success toward bioengineering new antimycins was achieved by feeding modified monomer building blocks to batch bacterial fermentations. Spiteller and colleagues showed that by feeding fluoroanthranilates to *S. ambofaciens* ATCC 23877 and *S. odorifer* DSM 40347 cultures they could produce 5-fluoroantimycins and 4-fluoroantimycins [33] (Figure 1). Similarly, feeding 6-fluoro-L-tryptophan to cultures of *Streptomyces* sp. NRRL 2288 resulted in the production of 5-fluoroantimycins [25]. Liu and coworkers analysed the bioactivity of 5-fluoroantimycins and reported they retained potent antifungal activity against *Candida albicans*, but were significantly reduced in cytotoxity in a leukemia P388 mouse cell line compared to the parent compounds [25]. Sandy et al. recently showed AntB can accept both acyl-CoAs and acyl-SNACs to form the C-8 acyloxy group and generate diversity at R^1 in vitro [38]. Acyl-SNACs are cell permeable, and the ability of AntB to utilise these substrates provides the opportunity to perform feeding studies using synthesised acyl-SNACs to introduce new chemistry at R^1 [38].

The gene clusters for JBIR-06 (12-membered ring), neoantimycin (15-membered ring), and 18-membered ringed respirantin were recently identified [43,44]. JBIR-06 and neoantimycin inhibit GRB78 chaperone involved in the unfolded protein response [45,46]. Although the DNA sequence for the gene clusters for these ring-expanded antimycins has not yet been made publically available, they all encode the machinery necessary to assemble the 9-membered antimycin core suggesting a common evolutionary past [44]. The vast chemical diversity in the antimycin family together with the recent characterisations of the promiscuous biosynthetic machinery suggest it is possible to use synthetic biology to bioengineer non-natural analogues in large enough quantity to test their efficacies in the clinic. In line with that view, generating a chemistry-dereplicated culture collection of antimycin-type depsipeptide producers to build a library of swappable biosynthetic gene cassettes to introduce new chemical diversity should result in rapid generation of new analogues in the antimycin family.

Acknowledgements

This work was funded by a Medical Research Council Milstein Award (G0801721) and a Natural Environment Research Council responsive mode grant (NE/J01074X/1) to MIH. We thank all Hutchings' Lab members past and present and Mark Buttner, Mervyn Bibb and Barrie Wilkinson (John Innes Centre, Norwich) for useful discussions as well as Jeroen Dickschat for inviting our contribution to this Thematic Series.

References

1. Challis, G. L.; Hopwood, D. A. *Proc. Natl. Acad. Sci. U. S. A.* **2003,** *100,* 14555–14561.
2. Flärdh, K.; Buttner, M. J. *Nat. Rev. Microbiol.* **2009,** *7,* 36–49. doi:10.1038/nrmicro1968
3. Davies, J.; Spiegelman, G. B.; Yim, G. *Curr. Opin. Microbiol.* **2006,** *9,* 445–453. doi:10.1016/j.mib.2006.08.006
4. Gottelt, M.; Kol, S.; Gomez-Escribano, J. P.; Bibb, M.; Takano, E. *Microbiology* **2010,** *156,* 2343–2353. doi:10.1099/mic.0.038281-0
5. Laureti, L.; Song, L.; Huang, S.; Corre, C.; Leblond, P.; Challis, G. L.; Aigle, B. *Proc. Natl. Acad. Sci. U. S. A.* **2011,** *108,* 6258–6263. doi:10.1073/pnas.1019077108
6. Bunet, R.; Song, L.; Mendes, M. V.; Corre, C.; Hotel, L.; Rouhier, N.; Framboisier, X.; Leblond, P.; Challis, G. L.; Aigle, B. *J. Bacteriol.* **2011,** *193,* 1142–1153. doi:10.1128/JB.01269-10
7. Seipke, R. F.; Barke, J.; Brearley, C.; Hill, L.; Yu, D. W.; Goss, R. J. M.; Hutchings, M. I. *PLoS One* **2011,** *6,* e22028. doi:10.1371/journal.pone.0022028
8. Foulston, L. C.; Bibb, M. J. *Proc. Natl. Acad. Sci. U. S. A.* **2010,** *107,* 13461–13466. doi:10.1073/pnas.1008285107
9. Sherwood, E. J.; Hesketh, A. R.; Bibb, M. J. *J. Bacteriol.* **2013,** *195,* 2309–2321. doi:10.1128/JB.02291-12
10. Claesen, J.; Bibb, M. *Proc. Natl. Acad. Sci. U. S. A.* **2010,** *107,* 16297–16302. doi:10.1073/pnas.1008608107

11. Rackham, E. J.; Grüschow, S.; Ragab, A. E.; Dickens, S.; Goss, R. J. M. *ChemBioChem* **2010,** *11,* 1700–1709. doi:10.1002/cbic.201000200
12. Barke, J.; Seipke, R. F.; Grüschow, S.; Heavens, D.; Drou, N.; Bibb, M. J.; Goss, R. J. M.; Yu, D. W.; Hutchings, M. I. *BMC Biol.* **2010,** *8,* No. 109. doi:10.1186/1741-7007-8-109
13. Seipke, R. F.; Crossman, L.; Drou, N.; Heavens, D.; Bibb, M. J.; Caccamo, M.; Hutchings, M. I. *J. Bacteriol.* **2011,** *193,* 4270–4271. doi:10.1128/JB.05275-11
14. Dunshee, B. R.; Leben, C.; Keitt, G. W.; Strong, F. M. *J. Am. Chem. Soc.* **1949,** *71,* 2436–2437. doi:10.1021/ja01175a057
15. van Tamelen, E. E.; Dickie, J. P.; Loomans, M. E.; Dewey, R. S.; Strong, F. M. *J. Am. Chem. Soc.* **1961,** *83,* 1639–1646. doi:10.1021/ja01468a023
16. Imamura, N.; Nishijima, M.; Adachi, K.; Sano, H. *J. Antibiot.* **1993,** *46,* 241–246. doi:10.7164/antibiotics.46.241
17. Hayashi, K.; Nozaki, H. *J. Antibiot.* **1999,** *52,* 325–328. doi:10.7164/antibiotics.52.325
18. Shiomi, K.; Hatae, K.; Hatano, H.; Matsumoto, A.; Takahashi, Y.; Jiang, C.-L.; Tomoda, H.; Kobayashi, S.; Tanaka, H.; Omura, S. *J. Antibiot.* **2005,** *58,* 74–78. doi:10.1038/ja.2005.10
19. Hosotani, N.; Kumagai, K.; Nakagawa, H.; Shimatani, T.; Saji, I. *J. Antibiot.* **2005,** *58,* 460–467. doi:10.1038/ja.2005.61
20. Chen, G.; Lin, B.; Lin, Y.; Xie, F.; Lu, W.; Fong, W.-F. *J. Antibiot.* **2005,** *58,* 519–522. doi:10.1038/ja.2005.70
21. Yan, L.-L.; Han, N.-N.; Zhang, Y.-Q.; Yu, L.-Y.; Chen, J.; Wei, Y.-Z.; Li, Q.-P.; Tao, L.; Zheng, G.-H.; Yang, S.-E.; Jiang, C.-X.; Zhang, X.-D.; Huang, Q.; Habdin, X.; Hu, Q.-B.; Li, Z.; Liu, S.-W.; Zhang, Z.-Z.; He, Q.-Y.; Si, S.-Y.; Sun, C.-H. *J. Antibiot.* **2010,** *63,* 259–261. doi:10.1038/ja.2010.21
22. Strangman, W. K.; Kwon, H. C.; Broide, D.; Jensen, P. R.; Fenical, W. *J. Med. Chem.* **2009,** *52,* 2317–2327. doi:10.1021/jm801110j
23. Riclea, R.; Aigle, B.; Leblond, P.; Schoenian, I.; Spiteller, D.; Dickschat, J. S. *ChemBioChem* **2012,** *13,* 1635–1644. doi:10.1002/cbic.201200260
24. Tappel, A. L. *Biochem. Pharmacol.* **1960,** *3,* 289–296. doi:10.1016/0006-2952(60)90094-0
25. Yan, Y.; Zhang, L.; Ito, T.; Qu, X.; Asakawa, Y.; Awakawa, T.; Abe, I.; Liu, W. *Org. Lett.* **2012,** *14,* 4142–4145. doi:10.1021/ol301785x
26. Finlayson, B. J.; Schnick, R. A.; Cailteux, R. L.; DeMong, L.; Horton, W. D.; McClay, W.; Thompson, C. W. *Fisheries* **2002,** *27,* 10–18. doi:10.1577/1548-8446(2002)027<0010:AOAAUI>2.0.CO;2
27. Cramer, W. A.; Hasan, S. S.; Yamashita, E. *Biochim. Biophys. Acta, Bioenerg.* **2011,** *1807,* 788–802. doi:10.1016/j.bbabio.2011.02.006
28. Tzung, S.-P.; Kim, K. M.; Basañez, G.; Giedt, C. D.; Simon, J.; Zimmerberg, J.; Zhang, K. Y.; Hockenbery, D. M. *Nat. Cell Biol.* **2001,** *3,* 183–191. doi:10.1038/35055095
29. Schwartz, P. S.; Manion, M. K.; Emerson, C. B.; Fry, J. S.; Schulz, C. M.; Sweet, I. R.; Hockenbery, D. M. *Mol. Cancer Ther.* **2007,** *6,* 2073–2080. doi:10.1158/1535-7163.MCT-06-0767
30. Thomas, S.; Quinn, B. A.; Das, S. K.; Dash, R.; Emdad, L.; Dasgupta, S.; Wang, X.-Y.; Dent, P.; Reed, J. C.; Pellecchia, M.; Sarkar, D.; Fisher, P. B. *Expert Opin. Ther. Targets* **2013,** *17,* 61–75. doi:10.1517/14728222.2013.733001
31. Kumar, S.; Kaur, N.; Singh, N. K.; Raghava, G. P. S.; Mayilraj, S. *Genome Announc.* **2013,** *1,* e00150–13. doi:10.1128/genomeA.00150-13
32. Hu, D.; Li, X.; Chang, Y.; He, H.; Zhang, C.; Jia, N.; Li, H.; Wang, Z. *J. Bacteriol.* **2012,** *194,* 1627. doi:10.1128/JB.06684-11
33. Schoenian, I.; Paetz, C.; Dickschat, J. S.; Aigle, B.; Leblond, P.; Spiteller, D. *ChemBioChem* **2012,** *13,* 769–773. doi:10.1002/cbic.201200033
34. Sandy, M.; Rui, Z.; Gallagher, J.; Zhang, W. *ACS Chem. Biol.* **2012,** *7,* 1956–1961. doi:10.1021/cb300416w
35. Teufel, R.; Mascaraque, V.; Ismail, W.; Voss, M.; Perera, J.; Eisenreich, W.; Haehnel, W.; Fuchs, G. *Proc. Natl. Acad. Sci. U. S. A.* **2010,** *107,* 14390–14395. doi:10.1073/pnas.1005399107
36. Quade, N.; Huo, L.; Rachid, S.; Heinz, D. W.; Müller, R. *Nat. Chem. Biol.* **2012,** *8,* 117–124. doi:10.1038/nchembio.734
37. Wilson, M. C.; Moore, B. S. *Nat. Prod. Rep.* **2012,** *29,* 72–86. doi:10.1039/c1np00082a
38. Sandy, M.; Zhu, X.; Rui, Z.; Zhang, W. *Org. Lett.* **2013,** *15,* 3396–3399. doi:10.1021/ol4014365
39. Staro, A.; Sofia, H. J.; Dietrich, S.; Ulrich, L. E.; Liesegang, H.; Mascher, T. *Mol. Microbiol.* **2009,** *74,* 557–581. doi:10.1111/j.1365-2958.2009.06870.x
40. Sievers, F.; Wilm, A.; Dineen, D.; Gibson, T. J.; Karplus, K.; Li, W.; Lopez, R.; McWilliam, H.; Remmert, M.; Söding, J.; Thompson, J. D.; Higgins, D. G. *Mol. Syst. Biol.* **2011,** *7,* No. 539. doi:10.1038/msb.2011.75
41. Guindon, S.; Dufayard, J.-F.; Lefort, V.; Anisimova, M.; Hordijk, W.; Gascuel, O. *Syst. Biol.* **2010,** *59,* 307–321. doi:10.1093/sysbio/syq010
42. Sherwood, E. J.; Bibb, M. J. *Proc. Natl. Acad. Sci. U. S. A.* **2013,** *110,* E2500–E2509. doi:10.1073/pnas.1305392110
43. Li, X.; Zvanych, R.; Vanner, S. A.; Wang, W.; Magarvey, N. A. *Bioorg. Med. Chem. Lett.* **2013,** *23,* 5123–5127. doi:10.1016/j.bmcl.2013.07.031
44. Vanner, S. A.; Li, X.; Zvanych, R.; Torchia, J.; Sang, J.; Andrews, D. W.; Magarvey, N. A. *Mol. BioSyst.* **2013,** *9,* 2712–2719. doi:10.1039/c3mb70219g
45. Ueda, J.; Nagai, A.; Izumikawa, M.; Chijiwa, S.; Takagi, M.; Shin-ya, K. *J. Antibiot.* **2008,** *61,* 241–244. doi:10.1038/ja.2008.35
46. Umeda, Y.; Chijiwa, S.; Furihata, K.; Furihata, K.; Sakuda, S.; Nagasawa, H.; Watanabe, H.; Shin-ya, K. *J. Antibiot.* **2005,** *58,* 206–209. doi:10.1038/ja.2005.25

License and Terms

This is an Open Access article under the terms of the Creative Commons Attribution License (http://creativecommons.org/licenses/by/2.0), which permits unrestricted use, distribution, and reproduction in any medium, provided the original work is properly cited.

The license is subject to the *Beilstein Journal of Organic Chemistry* terms and conditions: (http://www.beilstein-journals.org/bjoc)

The definitive version of this article is the electronic one which can be found at: doi:10.3762/bjoc.9.290

Beilstein Journal of Organic Chemistry

Stereodivergent synthesis of jaspine B and its isomers using a carbohydrate-derived alkoxyallene as C_3-building block

Volker M. Schmiedel, Stefano Stefani and Hans-Ulrich Reissig*

Full Research Paper

Open Access

Address:
Institut für Chemie und Biochemie, Freie Universität Berlin, Takustr. 3, D-14195 Berlin, Germany

Email:
Hans-Ulrich Reissig* - hreissig@chemie.fu-berlin.de

* Corresponding author

Keywords:
chiral auxiliaries; gold catalysis; jaspine B; lithiated alkoxyallenes; natural product synthesis; pachastrissamine; tetrahydrofurans

Beilstein J. Org. Chem. **2013,** *9,* 2564–2569.
doi:10.3762/bjoc.9.291

Received: 27 August 2013
Accepted: 28 October 2013
Published: 19 November 2013

This article is part of the Thematic Series "Natural products in synthesis and biosynthesis".

Guest Editor: J. S. Dickschat

© 2013 Schmiedel et al; licensee Beilstein-Institut.
License and terms: see end of document.

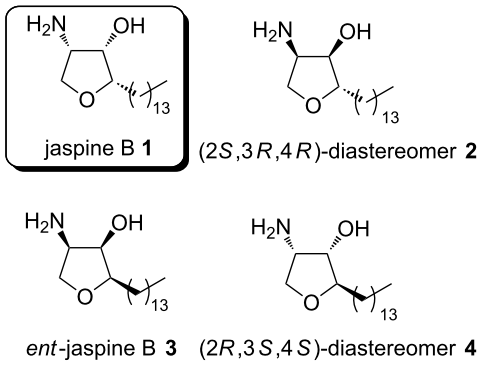
Abstract

Herein we present the synthesis of the anhydrophytosphingosine jaspine B and three of its stereoisomers using a carbohydrate-derived alkoxyallene in order to obtain the products in enantiopure form. Key step of the reaction sequence is the addition of the lithiated alkoxyallene to pentadecanal, setting the configuration at the later C-2 of the ring system. This reaction step proceeds with moderate selectivity and therefore leads to a stereodivergent approach to the natural product and its enantiomer. The gold-catalyzed 5-*endo*-cyclization affords the corresponding dihydrofurans, which after separation, azidation of the enol ether moiety and two subsequent reduction steps give the natural product and its stereoisomers.

Introduction

Jaspine B, also known as pachastrissamine (**1**, Scheme 1), is an anhydrophytosphingosine derivative, isolated 2002 from the marine sponge *Pachastrissa sp.* by Higa et al. [1]. In 2003 Debitus et al. were able to extract this natural product from the marine sponge *Jaspis sp.* [2]. Jaspine B (**1**) comprises a densely functionalized tetrahydrofuran ring, bearing three contiguous (2*S*,3*S*,4*S*)-configured stereogenic centers with a long alkyl chain at C-2 and a 1,2-amino alcohol moiety at C-3 and C-4. Due to its interesting structure and biological activities, for instance cytotoxicity and apoptosis promotion of several cancer cell lines [3-6] the synthesis of this natural product attracted the attention of many research groups resulting in more than 30 published syntheses up to now. Most frequently they are based on transformations of starting materials available from the "chiral pool", e.g. L-serine [7-18], or by asymmetric catalysis [19-25]. Several publications also focused on the synthesis of stereoisomers of the natural product [4,12,16,17,19,26-28] because these compounds also showed comparable biological activities [4,5].

During our current studies on the synthesis of highly functionalized heterocycles utilizing alkoxyallenes as versatile C_3-build-



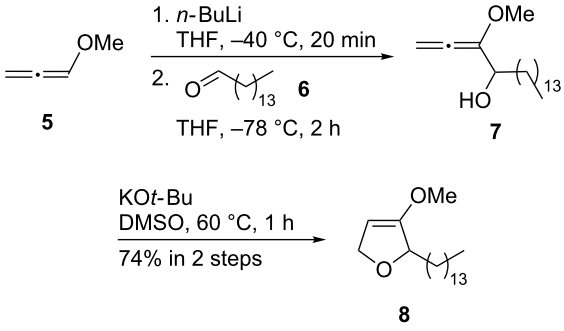
Scheme 1: Structure of jaspine B **1** and its stereoisomers **2**–**4**.

ing blocks we chose jaspine B (**1**) as an attractive target [29-33]. Our approach to **1** is based on the addition of a lithiated alkoxyallene with a chiral auxiliary to pentadecanal as electrophile. This step will generate the first stereogenic center and install the C_{14}-alkyl chain at the later C-2 position of the natural product (Scheme 2). A subsequent 5-*endo*-cyclization of the resulting allenyl alcohols leads to a mixture of diastereomeric dihydrofurans, which can be separated by HPLC (only the (*S*)-enantiomer is depicted). This allows the synthesis of the natural product and its enantiomer by functionalization of both diastereomers. The *cis*-configured amino alcohol moiety at C-3 and C-4 is installed by azidation and subsequent reduction steps leading to the final products. The presented strategy allows the preparation of jaspine B, its enantiomer and two diastereomers, all of which are known for their biological activities (Scheme 2).

Results and Discussion

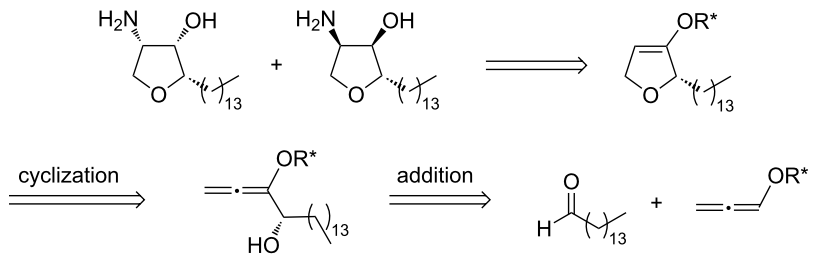
Synthesis of racemic jaspine B and its C-2-epimer

Initial studies examined the feasibility of this planned approach for the generation of the functionalized tetrahydrofuran system. They were based on methoxyallene (**5**) and led to the preparation of the racemic natural product. Methoxyallene (**5**), which is easily prepared in two steps from propargyl alcohol in large scale [34], was deprotonated with *n*-BuLi and the generated lithiated methoxyallene was subsequently treated with pentadecanal (**6**). The resulting allenyl alcohol **7** was not sufficiently stable for purification and hence was directly used for the next cyclization step (Scheme 3). After a 5-*endo*-cyclization of **7** employing KO*t*-Bu in DMSO dihydrofuran derivative **8** was obtained in 74% overall yield from **5**. The strongly basic conditions as first described by Brandsma and Arens [35] used for the cyclization of **7** gave a higher yield than the attempted gold(I) catalysis (39% overall yield), which might be due to the deactivation of the gold catalyst by impurities still present in the crude allenyl alcohol **7**.

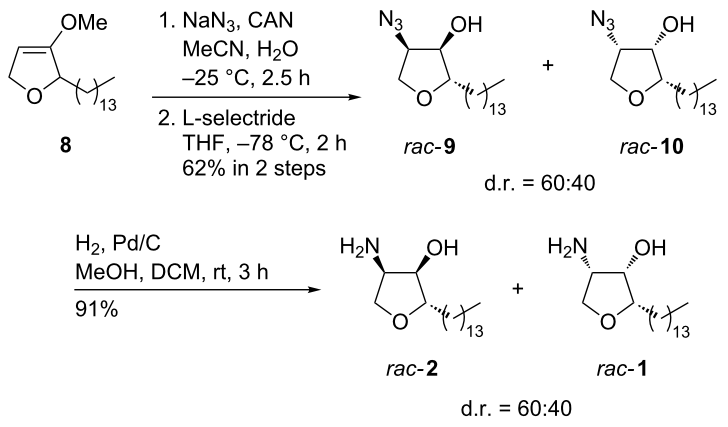


Scheme 3: Synthesis of racemic dihydrofuran **8**.

Next, several methods for the introduction of the amino group were examined. We were very pleased to discover that the oxidative azidation [36] allowed a direct access to the corresponding α-azidofuranones in one step. The two diastereomers of the azides were obtained in a 60:40 ratio. The subsequent reduction of the carbonyl group with L-selectride in THF furnished the α-azidotetrahydrofuranols *rac*-**9** and *rac*-**10** in a satisfying yield of 62% over two steps (Scheme 4). Only the two diastereomers shown in Scheme 4 were isolated, whereas the two other possible isomers could not be detected. The obtained diastereoselectivity of the reduction is likely due to stereoelectronic effects of the α-azido group overcoming the steric hindrance of the slim alkyl chain. We assume that in both diastereomers the azido group occupies a pseudoaxial position shielding this face of the furanone ring and therefore steers the



Scheme 2: Retrosynthetic analysis of jaspine B leading to pentadecanal and an alkoxyallene.



Scheme 4: Synthesis of racemic jaspine B *rac*-**1** and its diastereomer *rac*-**2**.

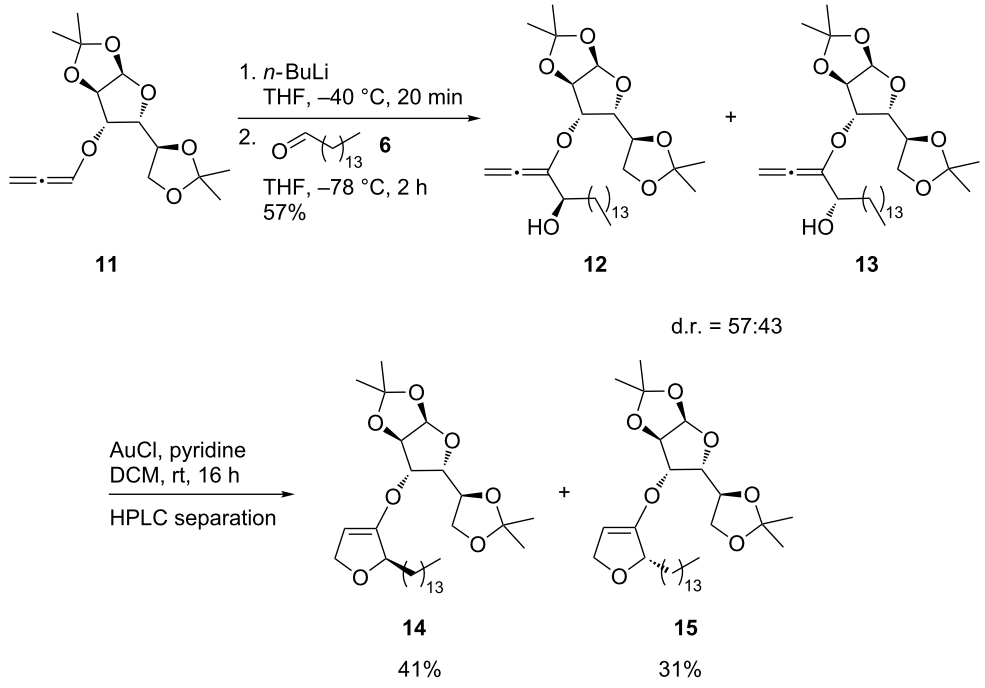
hydride attack to the other side. Similar observations have been reported for the reduction of carbonyl compounds bearing an electronegative group in α-position [37]. After palladium-catalyzed hydrogenolysis of α-azidotetrahydrofuranols *rac*-**9** and *rac*-**10** an inseparable mixture of racemic jaspine B (*rac*-**1**) and its C-2-epimer *rac*-**2** was obtained. Hence the natural product and its diastereomer were obtained in five steps with a good overall yield of 42% with respect to aldehyde **6**. This result was very encouraging and we therefore started the preparation of the enantiopure natural product and its stereoisomers.

Synthesis of enantiopure jaspine B using a carbohydrate-derived alkoxyallene

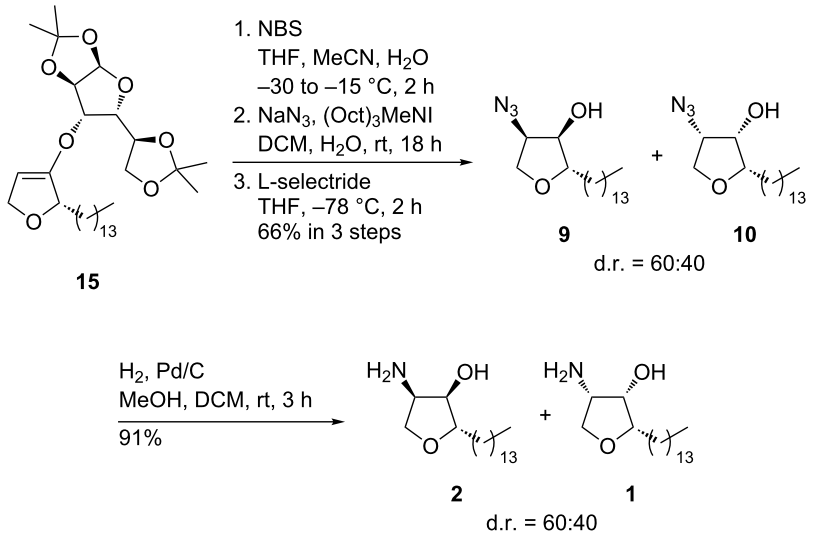
Having established suitable conditions for the construction of the functionalized tetrahydrofuran core we focused our attention on the synthesis of enantiopure jaspine B (**1**). Earlier investigations by Goré [38] and our group already showed the feasibility of alkoxyallenes with carbohydrate-derived chiral auxiliaries for the synthesis of enantiopure natural products such as preussin [39] and anisomycin [40] or in hetero Diels–Alder reactions [41,42]. For the stereodivergent synthesis of both enantiomers of jaspine B (**1**), we chose diacetone-glucose-derived alkoxyallene **11**, which is easily accessible on gram scale in two steps, starting from propargyl bromide (Scheme 5) [43]. Lithiation of **11** with *n*-BuLi and subsequent addition to pentadecanal (**6**) in analogous fashion to the synthesis of allenyl alcohol **7** led after column chromatography to a 57:43 mixture of the diastereomeric allenyl alcohols **12** and **13** in 57% yield. Base catalysis at higher temperatures, which was successfully used for the cyclization of **7**, apparently induced partial decomposition of the auxiliary and led to only moderate yields (46%) of dihydrofurans **14** and **15**. Better yields of **14** and **15** were achieved under mild reaction conditions employing gold(I) catalysis [44], which after purification and separation afforded the expected products in 41% and 31% yields, respectively. The dihydrofurans **14** and **15** are more stable than the allenyl alcohols **12** and **13** and therefore allowed smooth separation by HPLC. At this point, the assignment of the absolute configuration at C-2 of **14** and **15** was only based on the comparison of reactions earlier studied in our group [45]. They could later be confirmed by comparison of the optical rotation of the final products with values reported in the literature.

Unfortunately, the attempted functionalization of dihydrofurans **14** and **15** by oxidative azidation (see above) only led to very low yields of the desired α-azidotetrahydrofuranones (6%). The conditions obviously cause decomposition of the auxiliary. As an alternative, the electrophilic bromination of **15** with NBS and the subsequent substitution with sodium azide furnished the desired diastereomeric α-azidotetrahydrofuranones in a ratio comparable to that of the direct oxidative azidation of **8** (Scheme 6). Slightly higher selectivities in favor of the *trans*-configured α-azidofuranone could be observed when the substitution reaction was run for a shorter period. This indicates that a (partial) epimerization at C-4 occurs under the reaction conditions employed. The diastereoselective reduction of the carbonyl group with L-selectride afforded the α-azidotetrahydrofuranones **9** and **10** in 66% yield over three steps. Subsequent hydrogenolysis of **9** and **10** afforded a mixture of jaspine B (**1**) and its (2*S*,3*R*,4*R*)-diastereomer **2** in 91% yield.

Unfortunately, none of the diastereomeric mixtures obtained in all steps depicted in Scheme 6 were easily separable by HPLC, either due to the instability of the obtained compounds or the similar R_f values of the tetrahydrofuranol pairs **9**/**10** and **1**/**2**. In order to solve this problem and to obtain pure stereoisomers, the α-azidotetrahydrofuranols **9**/**10** were treated with benzyl chloroformate and converted into carbonates **16** and **17**. This protection allowed the smooth separation of the diastereomers by simple flash chromatography, probably due to an enhanced



Scheme 5: Synthesis of dihydrofurans **14** and **15**.



Scheme 6: Synthesis of jaspine B (**1**) and its (2*S*,3*R*,4*R*)-diastereomer **2**.

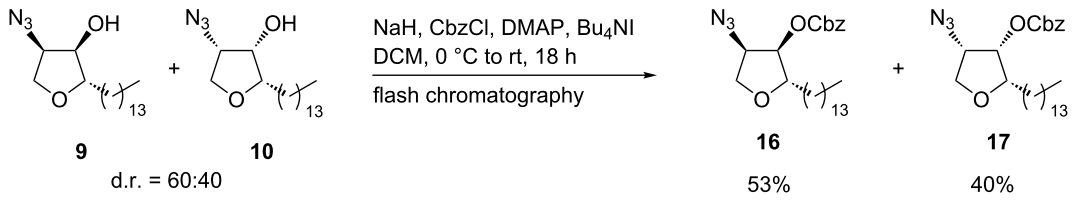
difference of dipole moments and hence R_f values of the two isomers (Scheme 7).

Final hydrogenolysis of the separated diastereomers **16** and **17** led to deprotection of the hydroxy group and simultaneous reduction of the azido group. Jaspine B (**1**) and its (2*S*,3*R*,4*R*)-diastereomer **2** were each obtained in quantitative yield showing the expected optical rotations (Scheme 8).

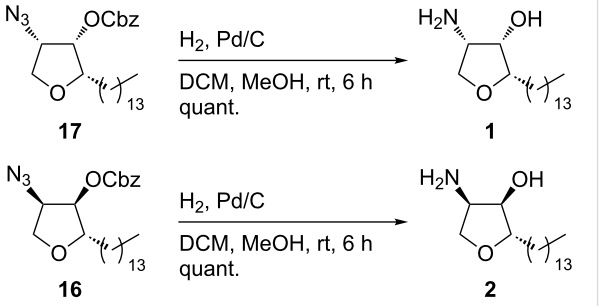
Analogously to the reaction sequence leading to **1** and **2**, the synthesis of *ent*-jaspine B (**3**) and the (2*R*,3*S*,4*S*)-diastereomer **4** was also achieved in similar yields employing (2*R*)-configured dihydrofuran **14** as starting material (Scheme 9).

Conclusion

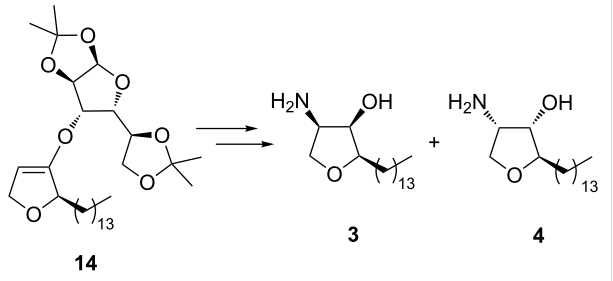
We developed a stereodivergent synthesis of enantiopure jaspine B and three of its stereoisomers. Important knowledge



Scheme 7: Protection and separation of the diastereomers.



Scheme 8: Reduction of the separated diastereomers leading to jaspine B (**1**) and its diastereomer **2**.



Scheme 9: Route to *ent*-jaspine B (**3**) and the (2*R*,3*S*,4*S*)-diastereomer **4**.

could also be gained during the preparation of the racemic compounds. The carbohydrate-derived alkoxyallene **11** proved to be useful as a chiral C_3-building block and allowed the synthesis of both enantiomers of the natural product in a fairly short manner (seven steps starting from the allene). The 5-*endo*-cyclization of allenyl alcohols **12** and **13** by gold catalysis afforded a separable mixture of diastereomeric dihydrofurans **14** and **15** in good yield. Subsequent functionalization using oxidative azidation, as shown for methoxy-substituted dihydrofuran **8**, did not give the expected α-azidotetrahydrofuranones in acceptable yields, but electrophilic bromination and subsequent substitution with sodium azide turned out to be a good alternative for the synthesis of the desired intermediates. Difficulties of the separation of the diastereomeric tetrahydrofuranols were successfully overcome by protection of the C-3 hydroxy group as carbonate, which enabled an easy chromatographic separation of the diastereomers and a global deprotection/reduction leading to pure stereoisomers **1** and **2**. Although the crucial steps of our approach to jaspine B are not stereoselective we found a simple access to the natural product and three of its stereoisomers, demonstrating again the usefulness of intermediates obtained from alkoxyallenes as C_3-building block [46-50]. Employing other aldehydes instead of pentadecanal our straightforward route should also allow the synthesis of analogues of jaspine B.

Supporting Information

Experimental details and NMR spectra of all new products and the final compounds are available in the Supporting information.

Supporting Information File 1

Experimental procedures and analytical data and NMR spectra.
[http://www.beilstein-journals.org/bjoc/content/supplementary/1860-5397-9-291-S1.pdf]

Acknowledgements

This work was generously supported by Bayer HealthCare. We also thank C. Groneberg for the HPLC separations, Dr. R. Zimmer for valuable discussions and help during the preparation of the manuscript as well as Prof. Dr. M. Christmann for useful suggestions.

References

1. Kuroda, I.; Musman, M.; Ohtani, I. I.; Ichiba, T.; Tanaka, J.; Gravalos, D. G.; Higa, T. *J. Nat. Prod.* **2002,** *65,* 1505–1506. doi:10.1021/np010659y
2. Ledroit, V.; Debitus, C.; Lavaud, C.; Massiot, G. *Tetrahedron Lett.* **2003,** *44,* 225–228. doi:10.1016/S0040-4039(02)02541-8
3. Salma, Y.; Lafont, E.; Therville, N.; Carpentier, S.; Bonnafé, M.-J.; Levade, T.; Génisson, Y.; Andrieu-Abadie, N. *Biochem. Pharmacol.* **2009,** *78,* 477–485. doi:10.1016/j.bcp.2009.05.002
4. Canals, D.; Mormeneo, D.; Fabriàs, G.; Llebaria, A.; Casas, J.; Delgado, A. *Bioorg. Med. Chem.* **2009,** *17,* 235–241. doi:10.1016/j.bmc.2008.11.026
5. Yoshimitsu, Y.; Oishi, S.; Miyagaki, J.; Inuki, S.; Ohno, H.; Fujii, N. *Bioorg. Med. Chem.* **2011,** *19,* 5402–5408. doi:10.1016/j.bmc.2011.07.061

6. Yoo, H.; Lee, Y. S.; Lee, S.; Kim, S.; Kim, T.-Y. *Phytother. Res.* **2012,** *26,* 1927–1933. doi:10.1002/ptr.4673
7. Abraham, E.; Davies, S. G.; Roberts, P. M.; Russell, A. J.; Thomson, J. E. *Tetrahedron: Asymmetry* **2008,** *19,* 1027–1047. doi:10.1016/j.tetasy.2008.04.017
8. Ichikawa, Y.; Matsunaga, K.; Masuda, T.; Kotsuki, H.; Nakano, K. *Tetrahedron* **2008,** *64,* 11313–11318. doi:10.1016/j.tet.2008.09.036
9. Inuki, S.; Yoshimitsu, Y.; Oishi, S.; Fujii, N.; Ohno, H. *Org. Lett.* **2009,** *11,* 4478–4481. doi:10.1021/ol901904w
10. Inuki, S.; Yoshimitsu, Y.; Oishi, S.; Fujii, N.; Ohno, H. *J. Org. Chem.* **2010,** *75,* 3831–3842. doi:10.1021/jo100544v
11. Yoshimitsu, Y.; Inuki, S.; Oishi, S.; Fujii, N.; Ohno, H. *J. Org. Chem.* **2010,** *75,* 3843–3846. doi:10.1021/jo1005284
12. Vichare, P.; Chattopadhyay, A. *Tetrahedron: Asymmetry* **2010,** *21,* 1983–1987. doi:10.1016/j.tetasy.2010.06.024
13. Prasad, K. R.; Penchalaiah, K. *Tetrahedron: Asymmetry* **2011,** *22,* 1400–1403. doi:10.1016/j.tetasy.2011.07.010
14. Passiniemi, M.; Koskinen, A. M. P. *Org. Biomol. Chem.* **2011,** *9,* 1774–1783. doi:10.1039/c0ob00643b
15. Srinivas Rao, G.; Venkateswara Rao, B. *Tetrahedron Lett.* **2011,** *52,* 6076–6079. doi:10.1016/j.tetlet.2011.08.170
16. Zhao, M.-L.; Zhang, E.; Gao, J.; Zhang, Z.; Zhao, Y.-T.; Qu, W.; Liu, H.-M. *Carbohydr. Res.* **2012,** *351,* 126–129. doi:10.1016/j.carres.2012.01.013
17. Srinivas Rao, G.; Chandrasekhar, B.; Venkateswara Rao, B. *Tetrahedron: Asymmetry* **2012,** *23,* 564–569. doi:10.1016/j.tetasy.2012.04.009
18. Yoshimitsu, Y.; Miyagaki, J.; Oishi, S.; Fujii, N.; Ohno, H. *Tetrahedron* **2013,** *69,* 4211–4220. doi:10.1016/j.tet.2013.03.091
19. Enders, D.; Terteryan, V.; Palecek, J. *Synthesis* **2008,** 2278–2282. doi:10.1055/s-2008-1067142
20. Urano, H.; Enomoto, M.; Kuwahara, S. *Biosci., Biotechnol., Biochem.* **2010,** *74,* 152–157. doi:10.1271/bbb.90670
21. Salma, Y.; Ballereau, S.; Maaliki, C.; Ladeira, S.; Andrieu-Abadie, N.; Génisson, Y. *Org. Biomol. Chem.* **2010,** *8,* 3227–3243. doi:10.1039/c004218h
22. Llaveria, J.; Díaz, Y.; Matheu, M. I.; Castillón, S. *Eur. J. Org. Chem.* **2011,** 1514–1519. doi:10.1002/ejoc.201001477
23. Dhand, V.; Chang, S.; Britton, R. *J. Org. Chem.* **2013,** *78,* 8208–8213. doi:10.1021/jo4013223
24. Santos, C.; Fabing, I.; Saffon, N.; Ballereau, S.; Génisson, Y. *Tetrahedron* **2013,** *69,* 7227–7233. doi:10.1016/j.tet.2013.06.091
25. Lin, C.-W.; Liu, S.-W.; Hou, D.-R. *Org. Biomol. Chem.* **2013,** *11,* 5292–5299. doi:10.1039/c3ob40797g
26. Reddipalli, G.; Venkataiah, M.; Mishra, M. K.; Fadnavis, N. W. *Tetrahedron: Asymmetry* **2009,** *20,* 1802–1805. doi:10.1016/j.tetasy.2009.07.004
27. Sánchez-Eleuterio, A.; Quintero, L.; Sartillo-Piscil, F. *J. Org. Chem.* **2011,** *76,* 5466–5471. doi:10.1021/jo200639t
28. Martinková, M.; Pomikalová, K.; Gonda, J.; Vilková, M. *Tetrahedron* **2013,** *69,* 8228–8244. doi:10.1016/j.tet.2013.07.028
29. Hormuth, S.; Reissig, H. U. *J. Org. Chem.* **1994,** *59,* 67–73. doi:10.1021/jo00080a013
30. Hormuth, S.; Schade, W.; Reissig, H.-U. *Liebigs Ann.* **1996,** 2001–2006. doi:10.1002/jlac.199619961209
31. Brasholz, M.; Reissig, H.-U. *Angew. Chem.* **2007,** *119,* 1659–1662. doi:10.1002/ange.200604078
Angew. Chem. Int. Ed. **2007**, *46*, 1634-1637. doi:10.1002/anie.200604078
32. Brasholz, M.; Reissig, H.-U. *Eur. J. Org. Chem.* **2009,** 3595–3604. doi:10.1002/ejoc.200900450
33. Brasholz, M.; Dugovič, B.; Reissig, H.-U. *Synthesis* **2010,** 3855–3864. doi:10.1055/s-0030-1258265
34. Hoff, S.; Brandsma, L.; Arens, J. F. *Recl. Trav. Chim. Pays-Bas* **1968,** *87,* 916–924. doi:10.1002/recl.19680870807
35. Hoff, S.; Brandsma, L.; Arens, J. F. *Recl. Trav. Chim. Pays-Bas* **1969,** *88,* 609–619. doi:10.1002/recl.19690880513
36. Magnus, P.; Barth, L. *Tetrahedron* **1995,** *51,* 11075–11086. doi:10.1016/0040-4020(95)00681-W
37. Rosenberg, R. E.; Abel, R. L.; Drake, M. D.; Fox, D. J.; Ignatz, K.; Kwiat, D. M.; Schaal, K. M.; Virkler, P. R. *J. Org. Chem.* **2001,** *66,* 1694–1700. doi:10.1021/jo0011787
38. Rochet, P.; Vatèle, J.-M.; Goré, J. *Synthesis* **1994,** 795–799. doi:10.1055/s-1994-25577
39. Hausherr, A. Ph.D. Thesis, Freie Universität, Berlin, Germany, 2001.
40. Kaden, S.; Brockmann, M.; Reissig, H.-U. *Helv. Chim. Acta* **2005,** *88,* 1826–1838. doi:10.1002/hlca.200590143
41. Arnold, T.; Orschel, B.; Reissig, H.-U. *Angew. Chem.* **1992,** *104,* 1084–1086. doi:10.1002/ange.19921040833
Angew. Chem. Int. Ed. Engl. **1992**, *31*, 1033-1035. doi:10.1002/anie.199210331
42. Zimmer, R.; Orschel, B.; Scherer, S.; Reissig, H.-U. *Synthesis* **2002,** 1553–1563. doi:10.1055/s-2002-33328
43. Hausherr, A.; Orschel, B.; Scherer, S.; Reissig, H.-U. *Synthesis* **2001,** 1377–1385. doi:10.1055/s-2001-15225
44. Gockel, B.; Krause, N. *Org. Lett.* **2006,** *8,* 4485–4488. doi:10.1021/ol061669z
45. Sörgel, S. Ph.D. Thesis, Freie Universität, Berlin, Germany, 2006.
46. Brasholz, M.; Reissig, H.-U.; Zimmer, R. *Acc. Chem. Res.* **2009,** *42,* 45–56. doi:10.1021/ar800011h
47. Lechel, T.; Reissig, H.-U. *Pure Appl. Chem.* **2010,** *82,* 1835–1844. doi:10.1351/PAC-CON-09-09-06
48. Pfrengle, F.; Reissig, H.-U. *Chem. Soc. Rev.* **2010,** *39,* 549–557. doi:10.1039/b914356d
49. Bouché, L.; Reissig, H.-U. *Pure Appl. Chem.* **2012,** *84,* 23–36. doi:10.1351/PAC-CON-11-09-20
50. Zimmer, R. *Synthesis* **1993,** 165–178. doi:10.1055/s-1993-25823

License and Terms

This is an Open Access article under the terms of the Creative Commons Attribution License (http://creativecommons.org/licenses/by/2.0), which permits unrestricted use, distribution, and reproduction in any medium, provided the original work is properly cited.

The license is subject to the *Beilstein Journal of Organic Chemistry* terms and conditions: (http://www.beilstein-journals.org/bjoc)

The definitive version of this article is the electronic one which can be found at: doi:10.3762/bjoc.9.291

Beilstein Journal of Organic Chemistry

The myxocoumarins A and B from *Stigmatella aurantiaca* strain MYX-030

Tobias A. M. Gulder*[1], Snežana Neff[2], Traugott Schüz[2], Tammo Winkler[2], René Gees[2] and Bettina Böhlendorf*[2]

Full Research Paper

Open Access

Address:
[1]Kekulé Institute of Organic Chemistry and Biochemistry, University of Bonn, Gerhard-Domagk-Straße 1, 53121 Bonn, Germany and
[2]Syngenta Crop Protection AG, CH-4002 Basel, Switzerland

Email:
Tobias A. M. Gulder* - tgulder@uni-bonn.de; Bettina Böhlendorf* - bettina.boehlendorf@dsm.com

* Corresponding author

Keywords:
antifungal activity; myxobacteria; natural products; *Stigmatella aurantiaca*; structure elucidation

Beilstein J. Org. Chem. **2013,** *9,* 2579–2585.
doi:10.3762/bjoc.9.293

Received: 21 August 2013
Accepted: 01 November 2013
Published: 20 November 2013

This article is part of the Thematic Series "Natural products in synthesis and biosynthesis" and is dedicated to Prof. Dr. Gerhard Höfle on the occasion of his 74th birthday.

Guest Editor: J. S. Dickschat

© 2013 Gulder et al; licensee Beilstein-Institut.
License and terms: see end of document.

Abstract

The myxobacterial strain *Stigmatella aurantiaca* MYX-030 was selected as promising source for the discovery of new biologically active natural products by our screening methodology. The isolation, structure elucidation and initial biological evaluation of the myxocoumarins derived from this strain are described in this work. These compounds comprise an unusual structural framework and exhibit remarkable antifungal properties.

Introduction

Despite declining interest of most big R&D-driven chemical companies in recent years, natural products continue to serve as one of the most important sources of new bioactive chemical entities, both in the pharmaceutical [1-4] as well as in the agrochemical industry [5-8]. A particularly rich source of intriguing secondary metabolites with interesting biological properties are the myxobacteria [9-12]. These organisms are especially talented in assembling PKS-, NRPS- and PKS/NRPS-hybrid products, often incorporating unusual biochemistry in the respective biosynthetic pathways [13-15]. The most well-known myxobacterial natural products are the epothilones (e.g. epothilones A (**1**), Figure 1), microtubule-stabilizing macrolactones that are clinically used in cancer therapy [16-20].

But also from an agrochemical point of view, myxobacteria have already furnished a large set of promising lead structures, in particular in the context of antifungal compounds with around 50% of myxobacteria-derived natural products exhibiting such properties [10]. This activity of myxobacterial metabolites results from diverse modes of action, such as inhibition of DNA replication, transcription and translation, as well as interference with cell membrane stability [21]. Inhibition of acetyl-

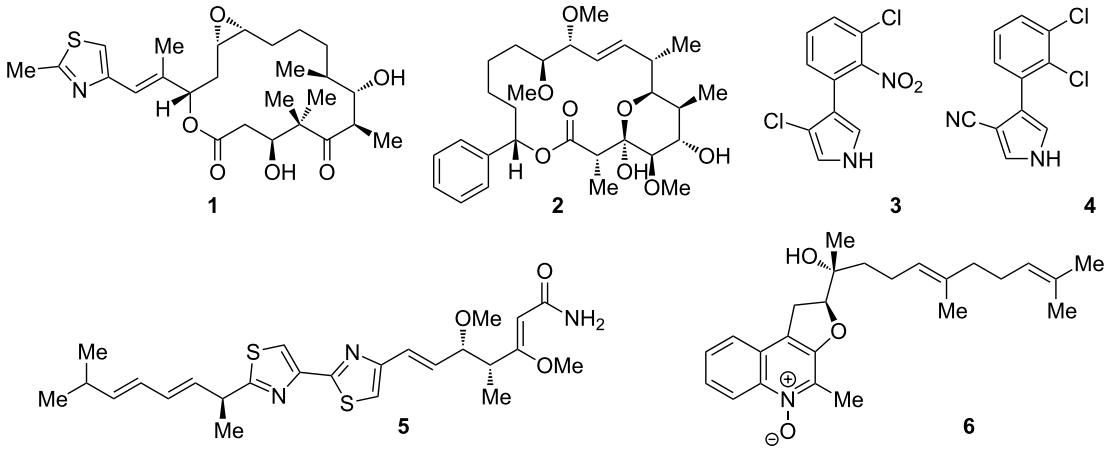


Figure 1: Structures of epothilone A (**1**), soraphen $A_{1\alpha}$ (**2**), pyrrolnitrin (**3**), fenpiclonil (**4**), myxothiazol A (**5**), and aurachin A (**6**).

CoA carboxylase is exerted by soraphen $A_{1\alpha}$ (**2**), which has been shown to be a potent and broad spectrum fungicide [22,23]. The most dominant target of myxobacterial antifungal agents, however, is the mitochondrial respiratory chain [21]. The compounds thereby either target complex I (NADH dehydrogenase) of the electron transport chain, as for example pyrrolnitrin (**3**) [24,25], which is in use for the treatment of fungal skin infections [26] and served as a lead structure for the development of the agrochemical agents fenpiclonil (**4**) and fludioxonil [27], or complex III (cytochrome bc_1), as for example myxothiazol A (**5**) [28,29]. Compounds of the same structural family can also target different target complexes simultaneously, as for example in the case of aurachins (e.g. aurachin A (**6**), Figure 1) [30-32]. Due to the remarkably high percentage of antifungal myxobacterial natural products, we investigated the potential of new myxobacterial isolates towards the production of novel, agrochemically relevant antifungal lead structures. The results obtained with strain *Stigmatella aurantiaca* MYX-030 are described herein.

Results and Discussion

The myxobacterial strain *Stigmatella aurantiaca* MYX-030 has been selected as interesting producer of bioactive natural products by our standardized hit follow-up process. Initial dereplication of known compounds was performed by using HPLC–UV–MS [33] combined with Peak–Activity–Correlation (PAC) data. Taken together these results indicated the presence of the known antifungal myxobacterial compound myxothiazole A (**5**), as well as the aurachins A (**6**) and C in the extract. In addition to these metabolites, a series of non-polar compounds exhibiting strong antifungal activity was detected. Comparison of UV and molecular mass data of these secondary metabolites with an in-house compound library resulted in no hits, thus prompting us to their isolation and structural elucidation.

The UV spectrum of **7** revealed maxima at 218 and 286 nm, strongly suggesting the presence of an aromatic system within the structure. Negative mode ESIMS analysis of the most abundant congener **7** of this set of natural products showed strong signals at 378.2 ($[M - H]^-$) and 757.4 ($[2M - H]^-$) as well as a positive ESIMS signal at 362.2 ($[M - H_2O + H]^+$). High resolution positive mode ESI–TOF mass analysis resulted in a molecular mass of 380.2097 u, which best fits a calculated molecular formula of $C_{20}H_{30}NO_6$ for the $[M + H]^+$ ion of **7**, thus indicating 7 degrees of unsaturation. The calculated number of carbon atoms was further substantiated by the 20 resolved signals observed in the compound's ^{13}C NMR spectrum (Table 1). These signals were assigned to three methyl groups (14.0, 16.5, and 21.2 ppm), eight methylene units (22.6, 23.4, 29.2, 29.3, 29.4, 29.8, 31.8, and 38.3 ppm), a quaternary carbon at 46.5 ppm, a heteroatom-substituted quaternary carbon – most likely a tertiary alcohol – at 79.1 ppm, an ester-type functionality at 172.5 ppm, and six sp^2-hybridized carbon atoms as part of an highly heteroatom-substituted aromatic system (103.2, 108.0, 118.6, 148.3, 149.2, and 157.8 ppm). The presence of the latter moiety was further corroborated by the ^1H NMR spectral data: two doublets with chemical shifts at 7.43 and 7.35 ppm and a coupling constant of 2 Hz clearly evidenced a highly substituted aromatic ring system bearing two protons in meta-position to each other.

The proton signals at 7.43 and 7.35 ppm correlated in an HSQC experiment with the ^{13}C NMR signals at 108.0 and 103.2 ppm, respectively. The structural organization of the aromatic system was further investigated by HMBC spectroscopy. The proton at

Table 1: NMR data of compound **7** at 500 (^{1}H) and 150 (^{13}C) MHz.

Position	δ_C, type[a]	δ_H (*J* in Hz)[b]	HMBC[b]
1			
2	172.5, C		
3	46.5, C		
4	79.1, C		
4’	118.6, C		
5	157.8, C		
6	108.0, CH	7.43, d (2)	4’, 5, 7, 8
7	148.3, C		
8	103.2, CH	7.35, d (2)	4’, 7, 8’
8’	149.2, C		
9	38.3, CH_2	1.56, td 1.99, td	3, 4, 4’, 10, 11 3, 4, 4’, 10, 11
10	23.4, CH_2	1.49, m 1.08, m	
11	29.2*, CH_2	1.14-1.30, m	
12	29.3*, CH_2	1.14-1.30, m	
13	29.4*, CH_2	1.14-1.30, m	
14	29.8*, CH_2	1.14-1.30, m	
15	31.8, CH_2	1.14-1.30, m	
16	22.6, CH_2	1.14-1.30, m	
17	14.0, CH_3	0.86, t (7)	15, 16
18	16.5, CH_3	1.33, s	2, 3, 4, 19
19	21.2, CH_3	1.18, s	2, 3, 4, 18

[a]Recorded in $CDCl_3$ containing a drop of CD_3OD; [b]^{1}H, HSQC and HMBC data recorded in CD_3OD. *Signal assignment interchangeable.

7.43 ppm showed strong correlations with two of the heteroatom-substituted carbons at 157.8 and 148.3 ppm, the putatively alkyl substituted position at 118.6 ppm, as well as the C atom at 103.2 ppm. The proton at 7.35 ppm, in turn, correlated with the C atoms at 149.2, 148.3, and 118.6 ppm, leading to overall structural fragment I (F-I) shown in Figure 2. In addition to the aromatic protons, three methyl signals were observed in the ^{1}H NMR spectra: a triplet at 0.86 ppm (^3J = 7 Hz), suggesting a methyl group directly attached to a CH_2-unit, as well as two singlets at 1.18 and 1.33 ppm. Furthermore, a pair of diastereomeric protons at 1.56 and 1.99 (higher order multiplets with a triplet of doublets structure) and a set of diastereomeric protons at 1.08 and 1.49 ppm (m) were observed. The signals of the other six methylene units formed a multiplet at 1.14–1.30 ppm, indicating the presence of a linear alkyl chain in the molecule. This is corroborated by the HSQC correlations to the C atoms at 29 ppm, as well as 22.6 and 31.8 ppm. In the HMBC data, strong correlations of the isolated methyl groups to each other, to the putative ester functionality, the quaternary carbon at 46.5 ppm, and the tertiary alcohol carbon at 79.1 ppm led to the assembly of structural fragment II (F-II, Figure 2). Further substitution of the latter was obvious from HMBC cross peaks of the diastereotopic CH_2 group (1.56 and 1.99 ppm) to the latter position (79.1 ppm) and to the carbon bearing the two methyl groups (46.5 ppm), as well as to the aromatic carbon at 118.6 ppm. In addition, this methylene unit exhibited correlations with two further CH_2 groups of the linear alkyl chain. This side chain turned out to consist of 8 neighboring CH_2 units with the methyl functionality at 0.86 ppm as the end group, as evident from HMBC correlations of the latter to the final two methylene units of this chain (F-III, Figure 2). Taken together, this information allowed the assembly of all aforementioned structural fragments to give a draft structure **8**. Given the chemical shifts of the carbonyl C-2 (172.5 ppm) and of carbon C-8’ (149.2 ppm), the presence of a lactone moiety can be deduced. The resulting overall structure still lacks three oxygens, a hydrogen, and a nitrogen atom combined with one degree of unsaturation when compared to the calculated molecular formula of **7**. Consequently, the substituents at C-5 and C-7 can be identified as an OH and a nitro function, respectively, as also indicated by the chemical shifts of C-5 (157.8 ppm) and C-7 (148.3 ppm). This results in the final overall structure **7** of this

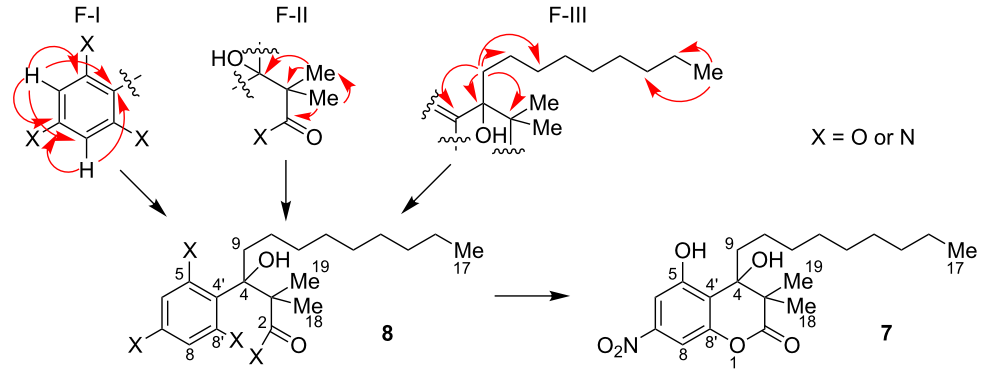


Figure 2: HMBC interactions used for the structure elucidation of myxocoumarin A (**7**).

natural product. To unambiguously prove the substitution pattern at the aromatic ring system, the phenolic OH-group was selectively methylated using diazomethane. The resulting methyl ether was irradiated in a 1D NOE experiment, which resulted in the expected strong increase of the proton bound to C-6. This observation thus firmly validated that the methyl ether had to be situated at C-5, as its alternative location at C-7 would have led to a strong increase in signal intensity of the protons bound to both, C-6 and C-7.

Owing to its coumarin core structure and its biological origin, compound **7** was named myxocoumarin A (**7**). Besides **7**, a second metabolite **9** with a highly similar NMR spectrum was isolated. ESIMS analysis of **9** showed a molecular ion peak at 346.2 ($[M - H]^-$, negative mode) and 348.2 ($[M + H]^+$, positive mode), consistent with a formal loss of MeOH when compared to the molecular mass of myxocoumarin A (**7**). In addition, no loss of water was observable in the MS data, suggesting the hydroxy function at C-4 in **7** not to be present in **9**. Comparison of the ^{1}H NMR spectra of **7** and **9** furthermore revealed the missing signals of the methyl groups 18 and 19 of **7** in the spectrum of **9**, along with a new singlet at 2.20 ppm integrating for three protons. In conclusion, this lead to the proposed structure of myxocoumarin B (**9**) as shown in Figure 3, which was unambiguously verified by in-depth analysis of chemical shifts in comparison with literature data (see Supporting Information File 1).

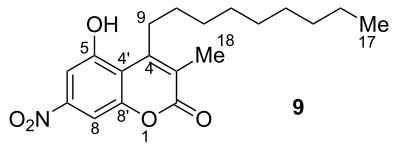


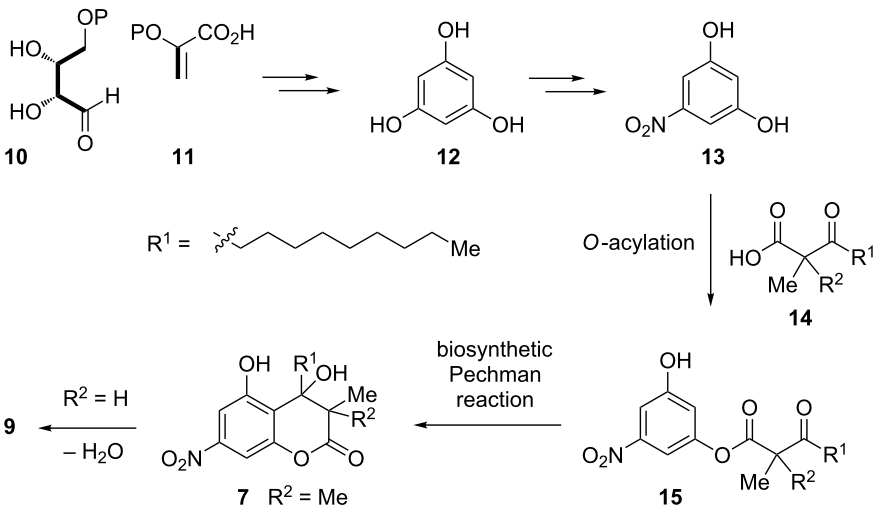
Figure 3: Chemical structure of myxocoumarin B (**9**).

Unfortunately, the amount of **7** isolated from the initial fermentation broth was not sufficient for stereochemical investigations, nor did the obtained amount of **9** suffice to obtain high quality ^{13}C NMR data. Attempts to produce more crude material were not successful, as cryo cultures of the producing strain failed to be transformed into actively growing cultures again.

Coumarins in general constitute a large group of bioactive natural products, mostly isolated from plants. Most of these plant-derived compounds are polyphenols that are often further modified by most diverse functionalization reactions, such as *O*-methylation, glycosylation, prenylation, oxygenation and subsequent cyclization or dimerization events [34]. Nitrogen-bearing congeners are rather scarce, with the bacterial aminocoumarins, such as the gyrase inhibitor novobiocin, being the most well-known examples [35]. Despite the larger number of existing coumarin structures in literature, the 5-hydroxy-7-nitro substitution pattern combined with the unusual long-chain, fully saturated alkyl substituent at C-4 are unique to the myxcoumarins **7** and **9**.

With the production of myxothiazol A (**5**) and aurachin A (**6**), the investigated strain *Stigmatella aurantiaca* MYX-030 resembles the secondary metabolite profile of previously chemically investigted *S. aurantiaca* and *S. erecta* strains. Interestingly, both, *S. aurantiaca* Sg a15 and *S. erecta* Pd e21, were reported to produce 5-nitroresorcinol (**13**) [36]. The biosynthesis of **13** was investigated in *S. erecta* Pd e21 using isotope-labeling experiments that revealed its precursor molecules to be glucose-derived erythrose-4-phosphate (**10**) and phosphoenol-pyruvate (**11**, Scheme 1). Due to the observed scrambling of the expected labeling pattern in **13**, its biosynthesis has to proceed via a symmetrical intermediate, putatively phloroglucinol (**12**) [36]. Nitrophenol **13** likely constitutes a direct biosynthetic precursor of the myxocoumarins. Upon *O*-acetylation of **13** with the long-chain β-keto acid building block **14**, putatively recruited from fatty-acid biosynthesis, the intermediate ester **15** could undergo C–C bond formation by nucleophilic attack of the aromatic system to the side-chain keto functionality, comparable to the first step of a Pechman condensation reaction. This would already furnish mycoxoumarin A (**7**, R^2 = Me), with myxocoumarin B (**9**, for R^2 = H) being formed after additional loss of H_2O. In order to identify further myxocoumarin producing strains, chemical screenings of the secondary metabolite profiles of *S. aurantiaca* Sg a15 and *S. erecta* Pd e21 using the fermentation conditions identified for *S. aurantiaca* MYX-030 might thus be worthwhile.

To verify the initially measured antifungal activity from the PAC, myxocoumarin A (**7**) was subjected to leaf disk assays against a series of agriculturally relevant pathogenic fungi. The compound revealed interesting antifungal activities with complete inhibition of agronomically important pathogens such as *Botrytis cinerea* at 200 mg/L as well as *Magnaporthe grisea* and *Phaeosphaeria nodorum* at 67 mg/L. Partial effects were found against *Blumeria graminis* (67 mg/L). The compound was, however, inactive against *Drechslera teres* and *Phytophthora infestans*. These findings indicate a broad range antifungal activity of **7**, comparable to commercial standard fungicides, although on a somewhat lower activity level. To further substantiate these results, liquid culture assays against a set of fungal pathogens were performed, showing strong intrinsic antifungal activities against *M. grisea* (100% inhibition at 0.7 mg/L) as well as *B. cinerea*, *Fusarium culmorum*, and *P. nodorum* (all at 2 mg/L), with no activity against *Pythium*



Scheme 1: Postulated biosynthetic pathway to myxocoumarins A (**7**) and B (**9**).

ultimum and *Rhizoctonia solani*. So far, no insecticidal and herbicidal activities have been observed. Due to the problems arising from the lacking culturability of the producing strain *S. aurantiaca*, further tests with **7** were so far not possible. Structure–activity relationship (SAR) studies on synthetic myxocoumarin derivatives as well as in-depth investigation of their antibacterial potential are currently performed in our laboratory and will be reported in due course.

Experimental

Cultivation and extraction. The preculture of *S. aurantiaca* MYX-030, inoculated directly from a single culture of an agar plate, was incubated by shaking (150 rpm) at 30 °C for 7 days in a 500 mL shake flask without baffle containing 80 mL of medium MIX-5 (composition: 2 g glucose, 5 g potato starch, 2 g peptone, 0.5 g $MgSO_4$, 0.5 g $CaCl_2$, 10 g HEPES for 1 L H_2O, pH 7.4). For production of myxocoumarins, 3 × 200 mL production cultures in 500 mL flasks without baffle were inoculated with 20 mL of the preculture. Production was carried out by shaking (150 rpm) at 30 °C for 10 days in MIX-1 media (composition: 5 g casitone, 2 g starch, 2 g $MgSO_4$, 0.5 g $CaCl_2$, 1 mL mineral solution (consisting of 0.1 g H_3BO_3, 5 g $FeSO_4{\cdot}7H_2O$, 0.05 g KI, 2 g $CoCl_2{\cdot}6H_2O$, 0.2 g $CuSO_4{\cdot}5H_2O$, 2 g $MnCl_2{\cdot}4H_2O$, 4 g $ZnSO_4{\cdot}7H_2O$, 1 g 95% H_2SO_4 for 1 L solution), 10 mL vitamin solution (consisting of 10 mg folic acid, 6 mg biotin, 0.2 g *p*-aminobenzoic acid, 1 g thiamin·HCl, 1.2 g panthothenic acid, 1 g riboflavin, 2.3 g nicotinic acid, 1.2 g pyridoxine·HCl, 0.1 g vitamin B12 for 1 L solution) for 1 L H_2O, pH 7.4) supplemented with 10% XAD-16 for continued product absorption during fermentation. Cells and XAD-16 were separated from the culture broth by filtration and subsequently extracted using methanol and acetone.

Isolation of mycoxoumarins A (7) and B (9). The crude material obtained by extraction of bacterial cells and XAD (341 mg) was subjected to chromatography on Sephadex LH-20 (3 × 69 cm column, flow: 1.6 mL/min) using methanol as the eluent. The myxocoumarin containing fraction (12.1 mg) was purified by reversed-phase preparative HPLC (Bischoff Kromasil 100 C-18, 10 µm, 2 cm diameter, 20 cm length) using H_2O + 0.1% TFA (solvent A) and acetonitrile (ACN) + 0.1% TFA (solvent B) as the eluents at a flow rate of 10 mL/min using the following linear gradient: 0 min 80% A, 2 min 80% A, 20 min 50% A, 25 min 20% A. Myxocoumarin A (**7**) was collected at a retention time of 12.5 min and myxocoumarin B (**9**) at 14.7 min to give 1.9 mg and 0.5 mg pure material, respectively.

Myxocoumarin A (**7**): pale yellow solid, $[\alpha]_D^{20}$ −6.3 (*c* 0.2, methanol); ^1H and ^{13}C NMR data, see Table 1; UV (H_2O (64%)/ACN (36%) + 0.1% TFA, online) λ_{max}, nm: 218, 286, 340 (sh); ESIMS(−) *m*/*z*: 57.4 $[2M - H]^-$, 378.2 $[M - H]^-$; ESIMS(+) *m*/*z* 362.2 $[M - H_2O + H]^+$; HRMS–ESI(+) *m*/*z*: $[M + H]^+$ calcd. for $C_{20}H_{30}NO_6$, 380.207; found, 380.2097 (calculated for).

Myxocoumarin B (**9**): pale yellow solid, ^1H NMR (500 MHz, CD_3OD) δ_H 7.55 (d, *J* = 2 Hz, 1H, H-6), 7.51 (d, *J* = 2 Hz, 1H, H-8), 3.18 (m, 2H, H-9), 2.20 (s, 3H, H-18), 1.62 (m, 2H, H-10), 1.49 (m, 2H, H-11), 1.42–1.26 (m, 10H, H-12, H-13,

H-14, H-15, H-16), 0.90 (t, J = 7 Hz, 3H, H-17); UV (H_2O (61%)/ACN (39%) + 0.1% TFA, online) λ_{max}, nm: 233, 260, 332 (sh); ESIMS(−) m/z: 693.3 $[2M - H]^-$, 346.2 $[M - H]^-$; ESIMS(+) m/z: 348.2 $[M + H]^+$.

Biological testing. Cut leaf disks (15 mm^2) of the respective host plants (see below) were placed on water agar in multi-well plates (24-well format) and sprayed with 12 µL aqueous test solution of varying concentrations (dose range 22–200 mg/L) using automated microspray technology. After drying, the leaf disks were inoculated with a spore suspension of the respective pathogenic fungus (see below). The activity of myxocoumarin A (**7**) was assessed 4–6 days after inoculation as percent preventive antifungal activity as compared to the non-treated controls. The following host/pathogen combinations were used: *Phytophthora infestans* (Mont) de Bary (late blight) on tomato; *Botrytis cinerea* Pers.: Fr. (gray mould) on bean; *Blumeria graminis* f.sp. *hordei* (DC.) Speer (powdery mildew) on barley; *Drechslera teres* (Sacc.) Shoemaker (net blotch) on barley; *Phaeosphaeria nodorum* (E. Müll.) Hedjar. (glume blotch) on wheat; *Magnaporthe grisea* (T.T. Hebert) M.E. Barr(rice blast) on rice.

The intrinsic antifungal activity of the compounds was tested in liquid culture assays. Mycelial fragments prepared from a fresh liquid culture (*Pythium ultimum* Trow; *Rhizoctonia solani* Kühn) or conidia of the fungus from cryogenic storage (*B. cinerea*; *P. nodorum*; *P. grisea*; *Fusarium culmorum* (Wm. G. Sm.) Sacc.) were directly mixed into PDB potato dextrose broth. 10 µL test solution in DMSO (2%) of different concentration of **7** was placed into microtiter plates (96-well format) and the nutrient broth (90 µL) containing the fungal cells was added. The test plates were incubated at 24 °C and percent inhibition of fungal growth was determined photometrically after 48 h (*P. ultimum*; *F. culmorum*; *R. solani*) or 72 h (*B. cinerea*; *P. nodorum*; *P. grisea*) in relation to the non-treated control.

Supporting Information

Supporting Information File 1

NMR and MS spectra of myxocoumarin A (**7**) and B (**9**). In-depth discussion and analysis of chemical shifts for the verification of the structure of **9**.
[http://www.beilstein-journals.org/bjoc/content/supplementary/1860-5397-9-293-S1.pdf]

Acknowledgements

We thank Florence Pfyffer (fermentations), Riet Luck (PAC), and Marie-Madeleine Stempien (NMR spectra) for skillful technical assistance. We are grateful to Andreas Fredenhagen for early recognition and MS and to Hülya Aldemir for her efforts to re-cultivate the producing strain from a cryo stock culture. Funding of the work in the T.A.M.G. laboratory by the Fonds of the Chemical Industry, the North Rhine-Westphalian Academy of Sciences, Humanities and the Arts (Junges Kolleg), and the Emmy Noether Program of the DFG (GU 1233/1-1) are gratefully acknowledged.

References

1. Cragg, G. M.; Newman, D. J.; Snader, K. M. *J. Nat. Prod.* **1997,** *60,* 52–60. doi:10.1021/np9604893
2. Newmann, D. J.; Cragg, G. M.; Snader, K. M. *J. Nat. Prod.* **2003,** *66,* 1022–1037. doi:10.1021/np030096l
3. Newmann, D. J.; Cragg, G. M. *J. Nat. Prod.* **2007,** *70,* 461–477. doi:10.1021/np068054v
4. Newmann, D. J.; Cragg, G. M. *J. Nat. Prod.* **2012,** *75,* 311–335. doi:10.1021/np200906s
5. Copping, L. G.; Duke, S. O. *Pest Manage. Sci.* **2007,** *63,* 524–554. doi:10.1002/ps.1378
6. Duke, S. O.; Rimando, A. M.; Schrader, K. K.; Cantrell, C. L.; Meepagala, K. M.; Wedge, D. E.; Tabanca, N.; Dayan, F. E. In *Selected Topics in the Chemistry of Natural Products;* Ikan, R., Ed.; World Scientific: Singapore, 2008; pp 209–251.
7. Dayan, F. E.; Owens, D. K.; Duke, S. O. *Pest Manage. Sci.* **2012,** *68,* 519–528. doi:10.1002/ps.2332
8. Cantrell, C. L.; Dayan, F. E.; Duke, S. O. *J. Nat. Prod.* **2012,** *75,* 1231–1242. doi:10.1021/np300024u
9. Reichenbach, H. *J. Ind. Microbiol. Biotechnol.* **2001,** *27,* 149–156. doi:10.1038/sj.jim.7000025
10. Gerth, K.; Pradella, S.; Perlova, O.; Beyer, S.; Müller, R. *J. Biotechnol.* **2003,** *106,* 233–253. doi:10.1016/j.jbiotec.2003.07.015
11. Nett, M.; König, G. M. *Nat. Prod. Rep.* **2007,** *24,* 1245–1261. doi:10.1039/b612668p
12. Wenzel, S. C.; Müller, R. *Mol. BioSyst.* **2009,** *5,* 567–574. doi:10.1039/b901287g
13. Wenzel, S. C.; Müller, R. *Nat. Prod. Rep.* **2007,** *24,* 1211–1224. doi:10.1039/b706416k
14. Wenzel, S. C.; Müller, R. *Curr. Opin. Drug Discovery Dev.* **2009,** *12,* 220–230.
15. Wenzel, S. C.; Müller, R. *Nat. Prod. Rep.* **2009,** *26,* 1385–1407. doi:10.1039/b817073h
16. Gerth, K.; Bedorf, N.; Höfle, G.; Irschik, H.; Reichenbach, H. *J. Antibiot.* **1996,** *49,* 560–563. doi:10.7164/antibiotics.49.560
17. Reichenbach, H.; Höfle, G. *Drugs R&D* **2008,** *9,* 1–10. doi:10.2165/00126839-200809010-00001
18. Altmann, K. H.; Memmert, K. *Prog. Drug Res.* **2008,** *66,* 275–334.
19. Trivedi, M.; Budihardjo, I.; Loureiro, K.; Reid, T. R.; Ma, J. D. *Future Oncol.* **2008,** *4,* 483–500. doi:10.2217/14796694.4.4.483
20. Altmann, K.-H.; Höfle, G.; Müller, R.; Mulzer, J.; Prantz, K. In *The Epothilones – An Outstanding Family of Anti-Tumour Agents: From Soil to the Clinic;* Kinghorn, A. D.; Falk, H.; Kobayashi, J., Eds.; Springer: Wien, 2009. doi:10.1007/978-3-211-78207-1
21. Weissman, K. J.; Müller, R. *Nat. Prod. Rep.* **2010,** *27,* 1276–1295. doi:10.1039/c001260m
22. Gerth, K.; Bedorf, N.; Irschik, H.; Höfle, G.; Reichenbach, H. *J. Antibiot.* **1994,** *47,* 23–31. doi:10.7164/antibiotics.47.23

23. Böhlendorf, B.; Höfle, G.; Kiffe, M.; O'Sullivan, A. C.; Schummer, D.; Sutter, M. Chemistry and fungicidal activity of soraphen A_{1a} derivatives. In *Phytochemicals for Pest Control;* Hedin, P. A.; Hollingworth, R. M.; Masler, E. P., Eds.; American Chemical Society: Washington, DC, 1997; pp 249–266. doi:10.1021/bk-1997-0658.ch019
24. Arima, K.; Imanaka, H.; Kousaka, M.; Fukuda, A.; Tamura, G. *Agric. Biol. Chem.* **1964,** *28,* 575–576. doi:10.1271/bbb1961.28.575
25. Tripathi, R. K.; Gottlieb, D. *J. Bacteriol.* **1969,** *100,* 310–318.
26. van Pee, K.-H.; Ligon, J. M. *Nat. Prod. Rep.* **2000,** *17,* 157–164. doi:10.1039/a902138h
27. Knauf-Beiter, G.; Zeun, R. In *Modern Crop Protection Compounds;* Krämer, W.; Schirmer, U.; Jeschke, P.; Witschel, M., Eds.; Wiley-VCH: Weinheim, 2012; Vol. 1, pp 721–730.
28. Thierbach, G.; Reichenbach, H. *Biochim. Biophys. Acta, Bioenerg.* **1981,** *638,* 282–289. doi:10.1016/0005-2728(81)90238-3
29. Gerth, K.; Irschik, H.; Reichenbach, H.; Trowitzsch, W. *J. Antibiot.* **1980,** *33,* 1474–1479. doi:10.7164/antibiotics.33.1474
30. Kunze, B.; Höfle, G.; Reichenbach, H. *J. Antibiot.* **1987,** *40,* 258–265. doi:10.7164/antibiotics.40.258
31. Höfle, G.; Kunze, B. *J. Nat. Prod.* **2008,** *71,* 1843–1849. doi:10.1021/np8003084
32. Friedrich, T.; van Heek, P.; Leif, H.; Ohnishi, T.; Forche, E.; Kunze, B.; Jansen, R.; Trowitsch-Kienast, W.; Höfle, G.; Reichenbach, H.; Weiss, H. *Eur. J. Biochem.* **1994,** *219,* 691–698. doi:10.1111/j.1432-1033.1994.tb19985.x
33. Fredenhagen, A.; Derrien, C.; Gassmann, E. *J. Nat. Prod.* **2005,** *68,* 385–391. doi:10.1021/np049657e
34. Murray, R. D. H. *Nat. Prod. Rep.* **1989,** *6,* 591–624. doi:10.1039/np9890600591
35. Heide, L. *Nat. Prod. Rep.* **2009,** *26,* 1241–1250. doi:10.1039/b808333a See for comprehensive information on the aminocoumarins; and references cited therein.
36. Höfle, G.; Irschik, H. *J. Nat. Prod.* **2008,** *71,* 1946–1948. doi:10.1021/np800325z

License and Terms

This is an Open Access article under the terms of the Creative Commons Attribution License (http://creativecommons.org/licenses/by/2.0), which permits unrestricted use, distribution, and reproduction in any medium, provided the original work is properly cited.

The license is subject to the *Beilstein Journal of Organic Chemistry* terms and conditions: (http://www.beilstein-journals.org/bjoc)

The definitive version of this article is the electronic one which can be found at: doi:10.3762/bjoc.9.293

Beilstein Journal of Organic Chemistry

Garner's aldehyde as a versatile intermediate in the synthesis of enantiopure natural products

Mikko Passiniemi and Ari M.P. Koskinen*

Review

Open Access

Address:
Aalto-University, School of Chemical Technology, Department of Chemistry P.O. Box 16100 (Kemistintie 1), FI-00076 Aalto, Finland

Email:
Ari M.P. Koskinen* - ari.koskinen@aalto.fi

* Corresponding author

Keywords:
asymmetric synthesis; Garner's aldehyde; natural product synthesis; L-serine

Beilstein J. Org. Chem. **2013,** *9,* 2641–2659.
doi:10.3762/bjoc.9.300

Received: 14 August 2013
Accepted: 29 October 2013
Published: 26 November 2013

This article is part of the Thematic Series "Natural products in synthesis and biosynthesis".

Guest Editor: J. S. Dickschat

© 2013 Passiniemi and Koskinen; licensee Beilstein-Institut.
License and terms: see end of document.

Abstract

Since its introduction to the synthetic community in 1984, Garner's aldehyde has gained substantial attention as a chiral intermediate for the synthesis of numerous amino alcohol derivatives. This review presents some of the most successful carbon chain elongation reactions, namely carbonyl alkylations and olefinations. The literature is reviewed with particular attention on understanding how to avoid the deleterious epimerization of the existing stereocenter in Garner's aldehyde.

Introduction

"*The universe is a dissymmetrical whole. I am inclined to think that life, as manifested to us, must be a function of the dissymmetry of the universe and of the consequences it produces. The universe is dissymmetrical; for, if the whole of the bodies which compose the solar system were placed before a glass moving with their individual movements, the image in the glass could not be superimposed on reality. Even the movement of solar life is dissymmetrical. A luminous ray never strikes in a straight line the leaf where vegetable life creates organic matter [...] Life is dominated by dissymmetrical actions. I can even foresee that all living species are primordially, in their structure, in their external forms, functions of cosmic dissymmetry.*" [1]

- Louis Pasteur

These visionary words were written over 100 years ago by Louis Pasteur. Little did he know how great of a challenge underlies these words. Natural products, secondary metabolites produced by living organisms, have their own distinct structures. Some of them have the same chemical structure, but

differ from each other only by being mirror images (e.g., (*R*)(+)/(*S*)(−)-limonene and (*S*)(+)/(*R*)(−)-carvone, Figure 1). This sounds like an insignificant difference, but in reality enantiomers can have a totally different, even contradictory, effect on living organisms. As an example, (*R*)-limonene smells of oranges, whereas the (*S*)-enantiomer has a turpentine-like (with a lemon note) odor. The difference in physiological effects of enantiomers is of utmost importance especially for the pharmaceutical industry, but increasingly also in agrochemicals [2,3] and even in materials sciences, as evidenced by the introduction of chiral organic light emitting diodes [4,5]. In certain cases, one enantiomer may be harmful. This was the case, for example, with the drug thalidomide (Figure 1), the (*R*)-enantiomer of which was sold to pregnant women as a sedative and antiemetic in the 1960s. The (*S*)-enantiomer turned out to be teratogenic.

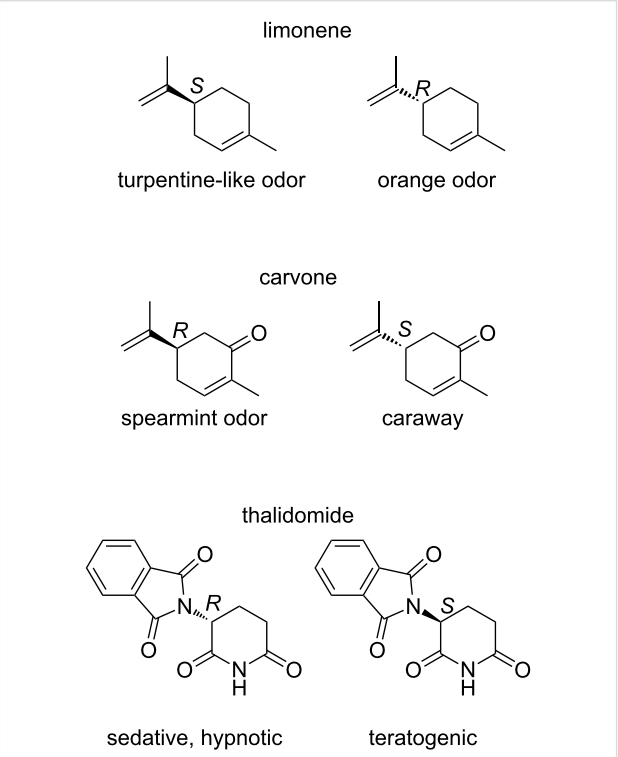


Figure 1: Structures of limonene, carvone and thalidomide.

The crucial role of chirality presents a great challenge for synthetic chemists. Asymmetric synthetic methods have emerged and after the development of ample analytical methods over the last few decades, asymmetric synthesis has seen an exponential growth. This has allowed us to tackle even more challenging targets like palytoxin [6-8], vinblastine [9-14], and paclitaxel [15-23]. The field is still far from being mature, and there remains a huge demand for more advanced methods for the introduction of chirality to substrates.

This review presents a general overview of the synthesis and use of Garner's aldehyde in natural product synthesis. Particular attention will be paid on the preservation of chiral information in the addition reaction of nucleophiles to the aldehyde. Models are presented for understanding the factors affecting the stability of the stereocenters, as well as those affecting diastereoselectivity in the generation of the new stereocenter.

Review

Philip Garner was the first to report a synthesis for 1,1-dimethylethyl 4-formyl-2,2-dimethyloxazolidine-3-carboxylate (**1**, Figure 2), today better known as Garner's aldehyde [24,25]. This configurationally stable aldehyde has shown its power as a chiral building block in the synthesis of various natural products as well as their synthetic intermediates. It is one of the most cited chiral building blocks in recent times and has been used in over 600 publications.

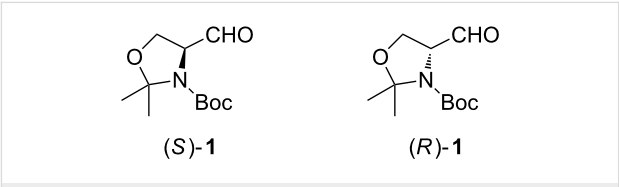


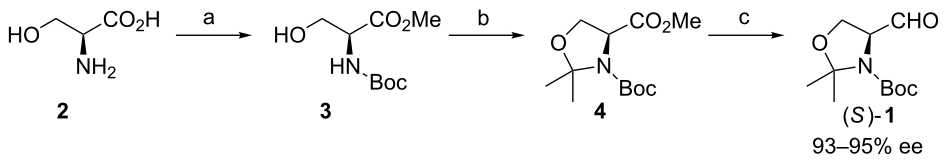
Figure 2: Structure of Garner's aldehyde.

Synthesis of Garner's aldehyde

Garner's aldehyde (**1**) has been widely used as an intermediate in multistep synthesis. Thus the synthesis of **1** has to meet some essential requirements: 1) easy and large scale preparation and 2) configurational and chemical stability of all intermediates.

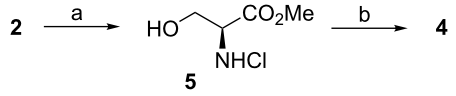
In his original paper, Garner first protected the amino group with Boc anhydride in dioxane, then esterified the carboxylic acid with iodomethane under basic conditions in dimethylformamide (DMF) and finally formed the dimethyloxazolidine ring of **4** with catalytic *p*-toluenesulfonic acid and 2,2-dimethoxypropane (DMP) in refluxing benzene (Scheme 1) [24,25]. Reduction of the methyl ester **4** to aldehyde **1** was performed with DIBAL-H (175 mol %) at −78 °C. Garner later reported that they had detected some epimerization of the chiral center (5–7% loss of ee down to 93–95% ee) [26]. Another drawback of this route is the use of the toxic and carcinogenic iodomethane in the esterification reaction.

Since the first synthesis of aldehyde (*S*)-**1** by Garner there have been many modifications and improvements to the synthesis of the enantiomers ((*R*)-**1** and (*S*)-**1**). Modifications to the original synthesis have focused either on the reaction sequence (esterification first and then Boc protection) or on the reduction to aldehyde. Other groups have tried to improve the synthesis of the



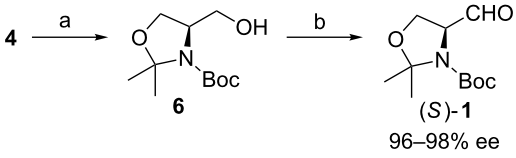
Scheme 1: (a) i) Boc_2O, 1.0 N NaOH (pH >10), dioxane, +5 °C → rt; ii) MeI, K_2CO_3, DMF, 0 °C → rt (86% over two steps); (b) $Me_2C(OMe)_2$, cat. *p*-TsOH, benzene, reflux (70–89%); (c) 1.5 M DIBAL-H, toluene, −78 °C (76%).

aldehyde. McKillop et al. found that the esterification reaction is performed best first with 235 mol % of HCl (formed in situ from the reaction of AcCl with MeOH) in MeOH [27]. The serine methyl ester hydrochloride salt was then protected with Boc anhydride. The *N*,*O*-acetal was formed using $BF_3{\cdot}Et_2O$ and DMP in acetone (Scheme 2). For the reduction they followed Garner's procedure. This method allows an easy access to the fully protected methyl ester **4**, but the problem of chiral degradation could not be solved (reported rotation −89 vs −91.7 in [26]).



Scheme 2: (a) AcCl, MeOH, 0 °C → reflux (99%); (b) i) $(Boc)_2O$, Et_3N, THF, 0 °C → rt → 50 °C (89%); ii) $Me_2C(OMe)_2$, $BF_3{\cdot}Et_2O$, acetone, rt (91%).

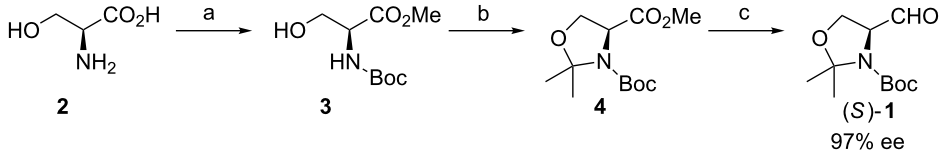
Dondoni adopted McKillop's procedure for the preparation of **4** [28]. In order to reduce the loss of enantiopurity, they decided to follow Roush's protocol [29] for the preparation of the aldehyde, i.e. reduction of **4** to alcohol **6** and oxidation of this alcohol to (*S*)-**1**. Moffatt–Swern oxidation provided the final aldehyde (*S*)-**1** from the primary alcohol **6**. In the standard Swern procedure the transformation of the activated alcohol intermediate to the final carbonyl compound (i.e. cleaving off the proton) is done by the addition of Et_3N at cold temperatures (–78 to –60 °C). According to Roush, the use of triethylamine for this transformation led to partial racemization of **1** (85% ee). Dondoni noticed that changing the base to the bulkier base *N*,*N*-diisopropylethylamine (Hünig's base, DIPEA) inhibits the epimerization (Scheme 3) [28]. With DIPEA as the base they could isolate the aldehyde (*S*)-**1** with an enantiopurity of 96–98% ee. The drawback of this route is an additional reaction step, the "overreduction" of the ester **4** to alcohol **6** and the necessary re-oxidation to aldehyde **1**.



Scheme 3: (a) $LiAlH_4$, THF, rt (93–96%); (b) $(COCl)_2$, DMSO, iPr_2NEt, CH_2Cl_2, −78 °C → −55 °C (99%).

As a conclusion of the above results we see that reversing the order of the two first reaction steps has a significant effect on the overall yield (from Garner's 86% to Dondoni's 94–98%). Less racemization can be observed with the reduction–oxidation sequence. Of course, other methods for the reduction can be used. The ester can be reduced to alcohol **6** (e.g., with $NaBH_4$/LiCl) and then oxidized to **1** with non-basic methods (e.g., IBX/DMP [30] or TEMPO/NaOCl [31] to name a few), which will not epimerize the α-center.

For our synthesis of **1**, we adopted a slightly modified sequence [32]. L-Serine (**2**) is first esterified under traditional Fischer conditions (Scheme 4). The hydrochloride **5** is *N*-protected using $(Boc)_2O$. The acetonide is then introduced under mild Lewis acidic conditions to give the desired fully protected serine ester **4**. This is reduced to the aldehyde **1** with DIBAL-H, while keeping the reaction temperature below −75 °C. This



Scheme 4: The Koskinen procedure for the preparation of Garner's aldehyde. (a) i) AcCl, MeOH, 0 °C → 50 °C (99%); ii) $(Boc)_2O$, Et_3N, CH_2Cl_2, 0 °C → rt (95–99%); (b) $Me_2C(OMe)_2$, $BF_3{\cdot}Et_2O$, CH_2Cl_2, rt (86%, after high vacuum distillation); (c) DIBAL-H, toluene, −84 °C (EtOAc/N_2 bath) (82–84%, after high vacuum distillation).

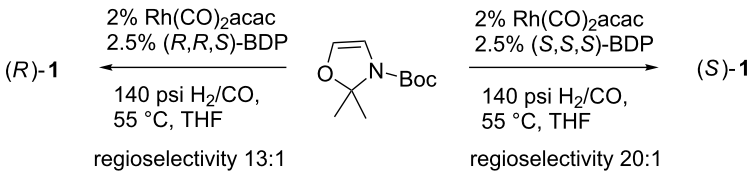
allowed us to isolate the aldehyde (*S*)-**1** in 97% ee. This reaction sequence was performed in more than 1.0 mol scale starting from L-serine and the reduction to Garner's aldehyde was performed on a 0.5 mol scale. DIBAL-H is an efficient reducing agent, but at times causes problems during work-up, especially in larger scale reactions. We, among others, have observed the gelatinous aluminium salts after the addition of an aqueous solution. Due to the formation of insoluble gel-like aluminium salts, the extraction procedure gets more challenging and sometimes a small portion of the substrate remains with the aluminium salts. Another drawback of DIBAL-H is the overreduction to alcohol **6**. When only small amounts of the overreduced alcohol are present, one high vacuum distillation is enough to purify the crude aldehyde. When present in amounts greater than 10%, two high vacuum distillations are required. Pure aldehyde **1** crystallizes in the freezer and forms semi-transparent white crystals.

Our procedure provides Garner's aldehyde (*S*)-**1** in a 66–71% overall yield. The original Garner procedure provides (*S*)-**1** in 46–58% and Dondoni's in 75–85% yield. Dondoni did neither purify his intermediates (from **2** to (*S*)-**1**) nor the final product. They just reported that all of the products are >95% pure based on NMR analysis.

A very recent approach to the synthesis of Garner's aldehyde was published by Burke and Clemens [33]. They reported that **1** could be synthesized by asymmetric formylation reaction from Funk's achiral alkene (Scheme 5) [34]. The formylation reaction provided (*R*)-**1** and (*S*)-**1** in acceptable yields (71% and 70%, respectively) and excellent enantioselectivities (94% ee and 97% ee, respectively). However, this synthesis suffers from many drawbacks. Firstly, the synthesis of the Funk's alkene commences from DL-serine and is a multistep sequence requiring $Pb(OAc)_4$. DL-Serine costs 524 €/kg (Aldrich, June 2013 price) compared to L-serine's 818 €/kg (Aldrich, June 2013). Secondly, both the formylation catalyst and bis(diazaphospholane) ligand are expensive and have to be used in large amounts. Thirdly, the formylation reaction was performed only in a 5 mmol scale and was not optimized for large scale synthesis.

Asymmetric induction with Garner's aldehyde

Nucleophilic addition to Garner's aldehyde gives an easy access to 2-amino-1,3-dihydroxypropyl substructures. This structural motif can be found in many natural products, such as iminosugars (**7** and **9**), peptide antibiotics (**8**), sphingosines and their derivatives (**10** and **11**, Figure 3). These naturally occurring polyhydroxylated compounds have attracted increasing



Scheme 5: Burke's synthesis of Garner's aldehyde. BDP - bis(diazaphospholane).

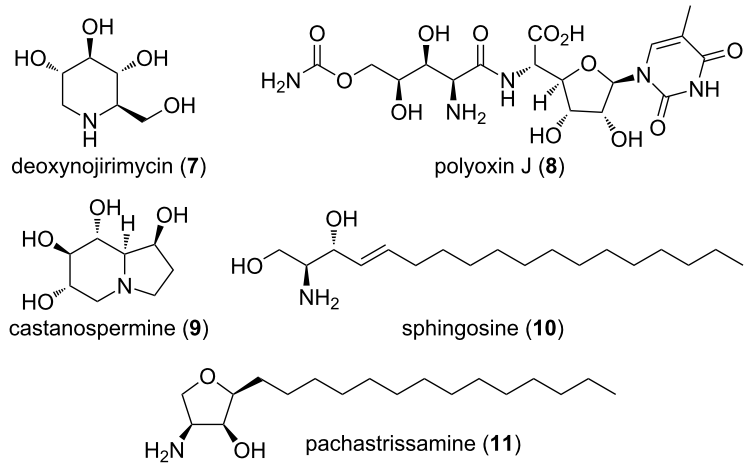


Figure 3: Structures of some iminosugars (**7**, **9**), peptide antibiotics (**8**) and sphingosine (**10**) and pachastrissamine (**11**).

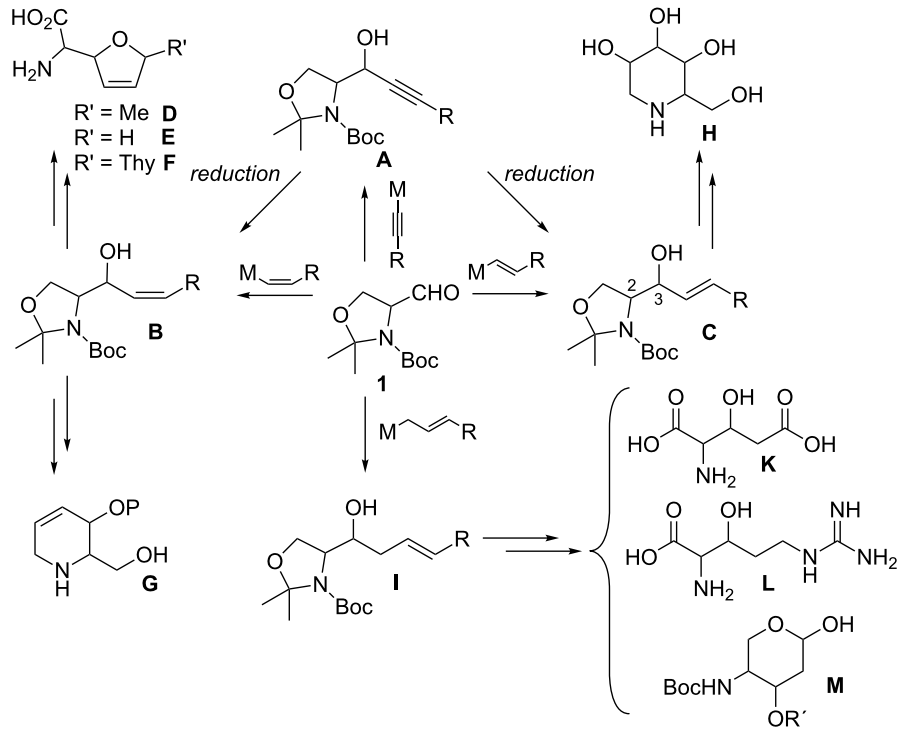
interest from synthetic chemists, because they are frequently found to be potent inhibitors of many carbohydrate-processing enzymes involved in important biological systems. These unique molecules have tremendous potential as therapeutic agents in a wide range of diseases such as metabolic diseases (lysosomal storage disorders, diabetes), viral infections, tumour metastasis, and neurodegenerative disorders.

Through the addition of a nucleophile to the aldehyde (*S*)/(*R*)-**1**, a new C–C bond is formed, hence allowing carbon chain elongation and further functionalization. Nucleophilic addition of an alkyne to **1** gives access to propargylic alcohols of the structure **A** (Scheme 6). This alcohol can be selectively reduced either to *cis*- (**B**) or *trans*-allylic alcohol **C**. *cis*-Selective reduction of **A** can be achieved with Lindlar's catalyst with H_2 under atmospheric pressure. The thermodynamic *trans*-allylic alcohol **C** arises from the reaction of **A** with Red-Al. Both isomers **B** and **C** can also be directly accessed from **1** with the corresponding *cis*- and *trans*-vinyl nucleophiles. Allylic alcohol **B** can be used as an intermediate in the synthesis of various natural products or intermediates thereof. The *cis*-double bond allows cyclizations to five- or six-membered rings. Five-membered dihydrofuran rings lead to the synthesis of furanomycin **D** [35,36], norfuranomycin **E** [37], and the polyoxin family **F** [38]. The six-membered tetrahydropyridine **G** synthesized via this route can be used as an intermediate in the synthesis of iminosugars, e.g., of the deoxynojirimycin family **H** [39-43]. The *trans*-allylic alcohol **C** contains already the functional groups of sphingosines and depending on the stereochemistry at C_2 and C_3, the synthesis of all four isomers can be achieved [44-47]. Isomer **C** leads also to the synthesis of deoxynojirimycin family **H** [48]. Addition of an allylic nucleophile provides access to homoallylic alcohols **I**. These can be derivatized to unnatural amino acids, such as **K** [49] and **L** [50] or to aminosugar derivatives like **M** [29,51].

Additions of various nucleophiles to **1** have been summarized by Bols and co-workers in 2001 [52]. We have recently reviewed the literature on the synthesis of 1,2-vicinal amino alcohols [53]. Use of Garner's aldehyde for the synthesis of non-natural amino acids through ethynylglycine has been reviewed [54]. In the following section, significant findings in the use of **1** as an electrophile and chiral intermediate will be discussed.

Addition of organometallic reagents to Garner's aldehyde

The addition of a nucleophile to Garner's aldehyde provides a facile access to 2-amino-1,3-dihydroxypropyl substructures. Through the addition of a carbon nucleophile also a new stereocenter is formed. Depending on the stereofacial selectivity, one can access either the *anti*-isomer **12** or *syn*-isomer **13** as the

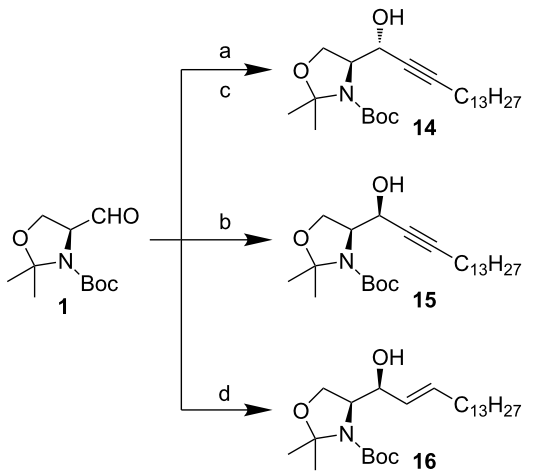


Scheme 6: Use of Garner's aldehyde **1** in multistep synthesis.

major product (Scheme 7). The high *anti*-selectivity can be rationalized with the attack of the nucleophile from the sterically least hindered side (*re*-side attack). The Felkin–Anh non-chelation transition state model explains this selectivity [55]. The nucleophile attacks not only from the least hindered side (substituent effects), but also from the side where the low-lying σ*C–N orbital is aligned parallel with the π- and π*-orbital of the carbonyl group, allowing delocalization of electron density from the reaction center toward nitrogen. In cases where *syn*-selectivity is observed, the Cram's chelation control model provides an explanation [56,57]. Chelating metal coordinates between the two carbonyls (the aldehyde and the carbamate), thus forcing the nucleophile to attack from the *si*-side and affecting the selectivity with opposite stereocontrol [58].

In 1988, in pioneering work independently done by Herold [59] and Garner [44] investigated the use of chiral aminoaldehydes as intermediates for the synthesis of nitrogen containing natural products. Both groups realized that the nucleophilic addition of a lithiated alkynyl group to **1** in THF was selective, favouring the *anti*-adduct **14** (Scheme 8). Herold also noticed that the addition of hexamethylphosphorous triamide (HMPT) increased the selectivity from 8:1 (Garner) to >20:1 (*anti*/*syn*). HMPT co-ordinates to the Li-cation, thus breaking the lithium clusters. This increases the nucleophilicity of the alkyne and favours the kinetic *anti*-adduct **14**. Through the use of chelating metals ($ZnBr_2$ in Et_2O [59]) Herold noticed a reversal in selectivity favouring the *syn*-adduct **15** (1:20 *anti*/*syn*). Garner used a slightly different method. He formed the nucleophile reductively from pentadecyne with iBu_2AlH in THF [44]. This vinylalane provided the *syn*-adduct **16** in modest stereoselectivity (1:2 *anti*/*syn*).

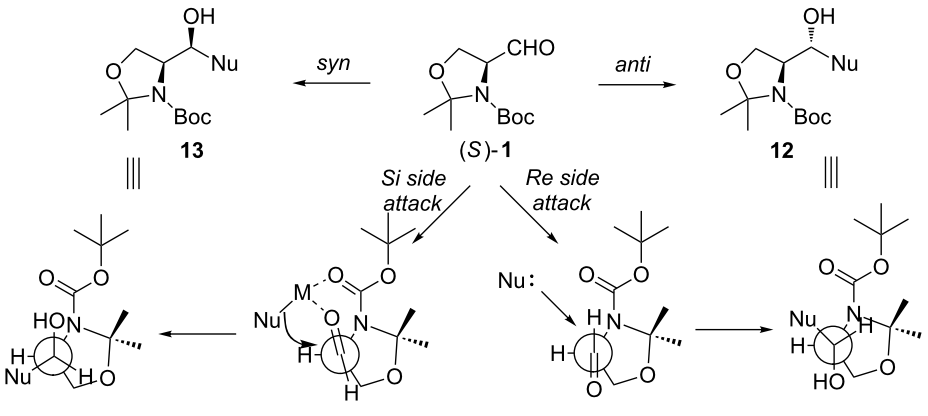
For the addition reaction to be feasible for asymmetric synthesis, the configurational integrity during this step is important.



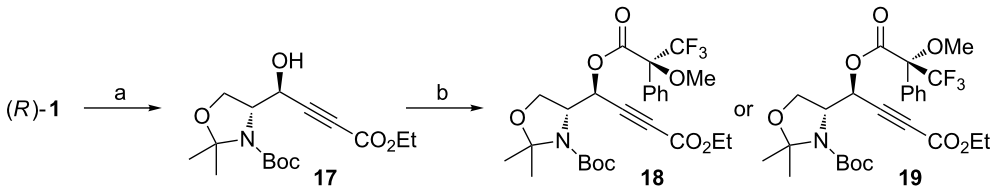
Scheme 8: Herold's method: (a) Lithium 1-pentadecyne, HMPT, THF, −78 °C (71%); (b) Lithium 1-pentadecyne, $ZnBr_2$, Et_2O, −78 °C → rt (87%). Garner's method: (c) Lithium 1-pentadecyne, THF, −23 °C (83%); (d) 1-Pentadecyne, DIBAL-H, hexanes/toluene, −78 °C (>80%).

Garner and many others have demonstrated that there is practically no epimerization of the α-carbon center of **1** during the addition reaction [38]. While working on the synthesis of thymine polyoxin C, Garner coupled the lithium salt of ethyl propiolate with (*R*)-**1** (Scheme 9) in HMPT/THF at −78 °C. The reaction was highly *anti*-selective (13:1 *anti*/*syn*) giving adduct **17** in a good yield (75%). The propargylic alcohol **17** was converted to the corresponding Mosher esters [60] **18** and **19**. A careful NMR analysis indicated that there was less than 2% cross-contamination.

Since the first results of stereoselective additions by Herold and Garner, much attention has been paid on the factors influencing the stereoselectivity. Coleman and Carpenter studied the nucleophilic addition of vinyl organometallic reagents to (*S*)-**1**



Scheme 7: Explanation of the *anti*- and *syn*-selectivity in the nucleophilic addition reaction.

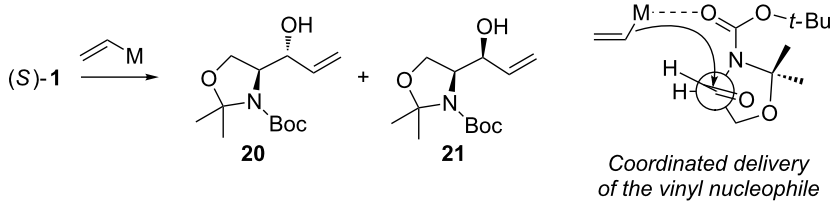


Scheme 9: (a) Ethyl lithiumpropiolate, HMPT, THF, −78 °C; (b) (*S*)- or (*R*)-MTPA, DCC, DMAP, THF, rt (**18**, 81%) or (**19**, 87%).

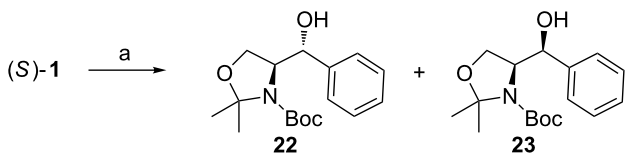
(Scheme 10) [61]. They noticed that the addition of vinyllithium in THF provided the *anti*-adduct **20** in a moderate 5:1 *anti*/*syn*-selectivity. By changing the metal to magnesium (vinylMgBr) the selectivity slightly dropped to 3:1 (*anti*/*syn*) still favouring adduct **20**. Addition of a Lewis acid ($TiCl_4$) did not affect the diastereoselectivity with vinyllithium species. The addition of vinyllithium to (*S*)-**1** in the presence of 100 mol % of $TiCl_4$ in THF gave a 5:1 (*anti*/*syn*) mixture of adducts **20** and **21**. Tetrahydrofuran coordinates quite strongly to Lewis acids, which increases the electron density at the metal atom. This lowers the metal atom's ability to coordinate to other Lewis bases, such as the carbonyl group. By changing the solvent to a poorer donor (≈ less Lewis basic), one can alter the electron density brought about by the solvent molecules to the metal atom. With vinyllithium species in the presence of $TiCl_4$ in Et_2O or toluene, the *anti*-selectivity dropped to 3:1 and 2:1, respectively. Best *syn*-selectivities were achieved with vinylZnCl in Et_2O (1:6 *anti*/*syn*). Coleman also noticed that the addition of excess $ZnCl_2$ did not increase the *syn*-selectivity at all. They attributed this to the mono-coordination of the metal to the carbamate instead of the usual "bidentate" chelation control model (as shown in Scheme 10).

Joullié observed that the more reactive Grignard reagents (e.g., PhMgBr or MeMgBr) give rise to kinetic *anti*-products via the non-chelation pathway [62]. Since these reagents are highly reactive, the reaction takes place before the metal has coordinated to any of the carbonyl groups, thus causing the Felkin–Anh control. When the steric bulk of the nucleophile was increased from PhMgBr to iPrMgBr the selectivity reversed from 5:1 *anti*/*syn* to 1:6 with iPrMgBr. A distinct solvent effect was also observed (Scheme 11). The selectivity obtained by Joullie for the reaction of **1** with PhMgBr was reversed for our system [63]. Joullié obtained a 5:1 (*anti*/*syn*) selectivity of alcohols **22** and **23** in THF compared to the 2:3 ratio observed in Et_2O. This change in selectivity can be explained by diethyl ether being a less coordinating solvent [64].

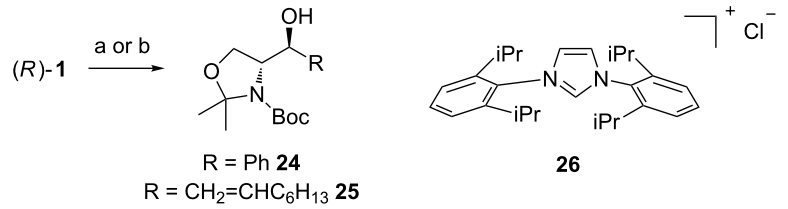
Fürstner investigated the use of organorhodium nucleophiles with aldehydes (Scheme 12) [65]. They screened catalysts, ligands and bases in order to find the best conditions for the alkylation reaction. They found $RhCl_3{\cdot}3H_2O$ together with imidazolium chloride **26** as the ligand precursor and the base NaOMe to be the catalyst system of choice. NaOMe reacts with the ligand precursor **26** and forms an *N*-heterocyclic carbene.



Scheme 10: Coleman's selectivity studies and their transition state model for the co-ordinated delivery of the vinyl nucleophile.



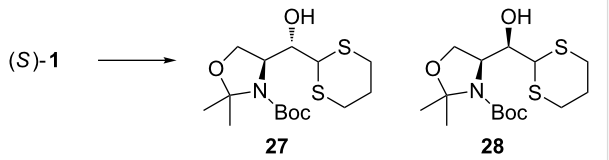
Scheme 11: (a) PhMgBr, THF, −78 °C → 0 °C [62] or (a) PhMgBr, Et_2O, 0 °C [63].



Scheme 12: (a) cat. $RhCl_3·3H_2O$, cat. **26**, NaOMe, Ph-$B(OH)_2$, aq DME, 80 °C (**24**, 71%); (b) cat. $RhCl_3·3H_2O$, cat. **26**, NaOMe, $C_6H_{13}CH=CH_2$-$B(OH)_2$, aq DME, 55 °C (**25**, 78%).

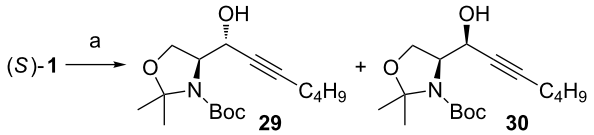
The method was tested also with Garner's aldehyde and two different boronic acid derived nucleophiles (R = Ph or 1-octenyl). High *anti*-selectivity was observed. With the in situ formed phenyl nucleophile the selectivity was excellent >30:1 (*anti*/*syn*) giving **24** in a good yield (71%), but with the open chain alkene the selectivity eroded to 4.6:1 (*anti*/*syn*) giving **25** in 78% yield. The (*E*)-octenylboronic acid undergoes protodeborylation at elevated temperatures, so the reaction had to be performed at 55 °C and with slightly higher catalyst loading (5% instead of the usual 3%).

Fujisawa studied the addition of lithiated dithiane to (*S*)-**1** (Scheme 13) [66]. Without additives the reaction in THF provided alcohols **27** and **28** in a 7:3 ratio (*anti*/*syn*). Addition of aggregation braking HMPT slightly improved the selectivity (10:3). Almost complete selectivity was achieved when $BF_3·Et_2O$ (6 equiv) and CuI (0.3 equiv) were used (>99:1 *anti*/*syn*). They reasoned that the high selectivity arose from the use of a monodentate Lewis acid and the highly dissociated anion derived from the organocopper species.



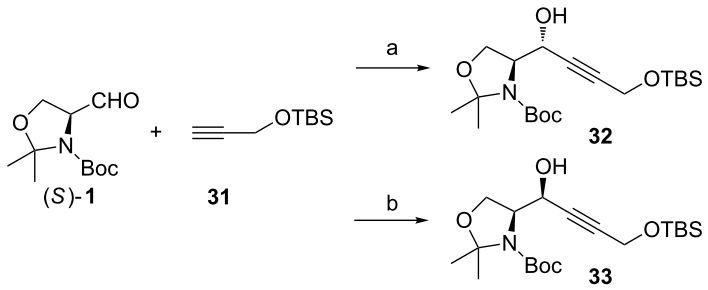
Scheme 13: Lithiated dithiane (3 equiv), CuI (0.3 equiv), $BF_3·Et_2O$ (6 equiv), THF, −50 °C, 12 h (70%).

Recently Lam reported interesting results on the stereoselective addition of a lithiated alkynyl species to (*S*)-**1** (Scheme 14) [67]. According to their results, temperature plays a crucial role on the outcome of the reaction. When the reaction was performed at −15 °C (1.36 equiv of alkyne and 1.16 equiv of *n*-BuLi), no *anti*-adduct **29** was detected, instead the *syn*-adduct **30** was obtained as the sole stereoisomer. By lowering the temperature to −40 °C and keeping the amount of reagents the same, the selectivity was inverted! Only the *anti*-adduct **29** was isolated. This change in selectivity was explained with two different transition states. At lower temperatures (−40 °C) under kinetic control the Felkin–Anh product is predominant. At higher temperatures (−15 °C) the nucleophilic addition occurs via a thermodynamically more stable transition state that resembles the chelation control TS. These results are interesting as this is the first time anyone reports a complete inversion of selectivity just by raising the reaction temperature. Decrease in *anti*-selectivity has been evidenced by others, when the reaction temperature has been raised by 40 to 100 °C (e.g., from −78 °C to rt), but never a total reverse. If these results are reliable, there has to be a total change in the transition state towards total chelation control and most likely also in the aggregation level of lithiated reagents.



Scheme 14: Addition reaction reported by Lam et al. (a) 1-Hexyne, *n*-BuLi, THF, −15 °C or −40 °C.

Jurczak has investigated the effect of additives on the selectivity of the nucleophilic addition reaction in toluene [58]. When lithiated **31** was used as the nucleophile, their results were similar to Herold's [59]. With HMPT as an additive they obtained a selectivity of 20:1 favouring the *anti*-allylic alcohol **32** (Scheme 15). Without additives the selectivity decreased to mere 3:1 (*anti*/*syn*). Under the same conditions but by raising the reaction temperature to rt the selectivity dropped further down to 3:2 (*anti*/*syn*). With chelating metals, such as Mg, Zn and Sn, the stereofacial preference changed from the *re* to the *si* side attack. The use of tin(IV) chloride as the chelating agent gave the highest *syn*-selectivities (>1:20 *anti*:*syn*), but poor yields. Slightly higher yields were achieved with $ZnCl_2$ giving the *syn*-adduct **33** in 65% yield, but with lower selectivities (1:10).



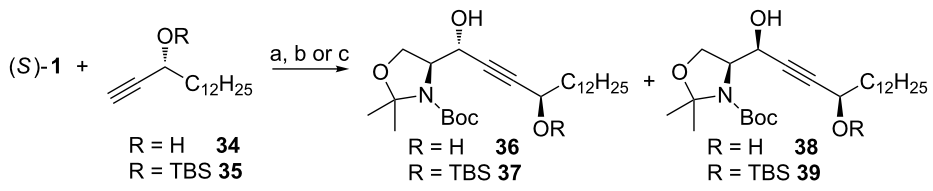
Scheme 15: (a) *n*-BuLi, HMPT, toluene, −78 °C → rt (85%); (b) *n*-BuLi, $ZnCl_2$, toluene/Et_2O, −78 °C → rt (65%).

The additions of propargylic alcohols **34** and **35** were also selective (Scheme 16). Mori performed the addition using unprotected alcohol **34** as nucleophile [68]. The selectivity at −40 °C was 4.2:1 favouring the *anti*-adduct **36**. Bittman performed similar addition with **32** as the nucleophile at −78 °C [69]. The selectivity was 7.9:1 favouring the *anti*-adduct **37**. In the same year Yadav did the same addition reaction with HMPT which raised the *anti*-selectivity to >20:1 (*anti*/*syn*) [70].

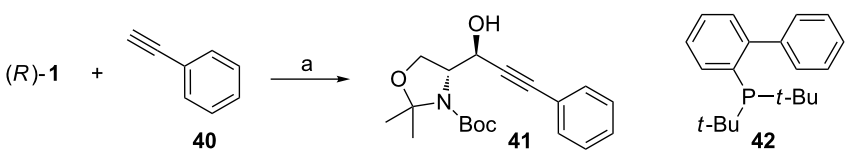
Chisholm has been looking for milder catalytic metal-alkyne nucleophiles for carbonyl 1,2-addition reactions, which wouldn't enolize the labile *α*-protons next to a carbonyl group (Scheme 17) [71]. They found that a Rh(I)-catalyst with a monodentate electron rich phosphine ligand **42** formed a nucleophilic metal-acetylide with terminal alkynes, such as **40**. The phosphine ligand had to be monodentate; bidentate ligands gave a lot lower yields. Their catalyst system worked very efficiently with many carbonyl electrophiles, also with Garner's aldehyde (*R*)-**1**. The reaction of **1** with **40** gave **41** with high selectivity (>20:1 *anti*/*syn*) in good yield (74%). Unfortunately they do not discuss whether the substrate racemizes under these conditions.

Van der Donk has been interested in the synthesis of dehydro amino acids (Scheme 18) [72]. In two of their examples they used copper-acetylide nucleophiles, which led to high *syn*-selectivities. With propyneCuI the selectivity was 1:16 (*anti*/*syn*) providing the propargylic alcohol **43** in 95% yield. By changing the nucleophile to TMS-ethyneCuI the *syn*-selectivity increased to over 1:20, but providing the *syn*-adduct **44** in lower yield (82%). HPLC analysis showed that no epimerization had occurred. These results support Herold's seminal work published 20 years earlier [59]. Reginato et al. coupled ethyne to Garner's aldehyde (*S*)-**1** under chelation control [73]. Surprisingly, a 1:1 (*anti*/*syn*) mixture of adducts **45** and **46** was obtained. Hanessian et al. have shown that also electron deficient acetylide nucleophiles can be used in the reaction [74]. After carefully studying the reaction conditions and various additives, they found $ZnBr_2$ to be the best coordinating agent. The diastereoselectivity was good, favouring the *syn*-adduct **47** (1:12 *anti*/*syn*). The *anti*-selective addition of a lithiopropiolate to (*R*)-**1** was presented by Garner already in 1990 [38].

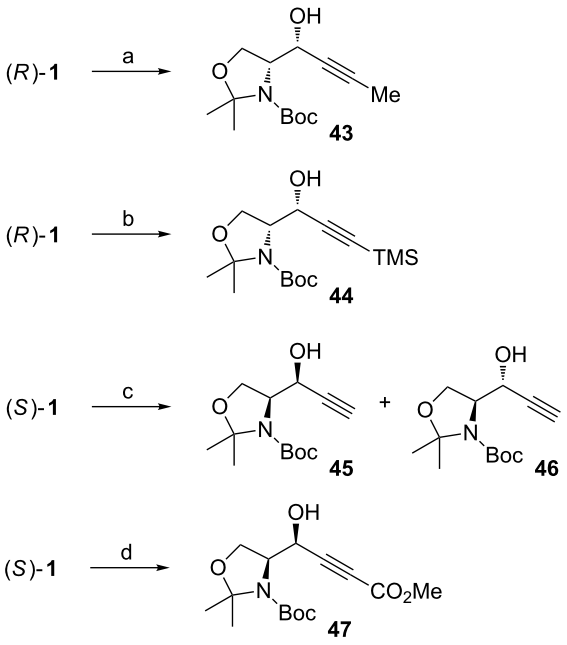
Soai et al. have examined the use of vinylzinc nucleophiles as alkenylating agents in the synthesis of D-*erythro*-sphingosine



Scheme 16: (a) *n*-BuLi, **34**, THF, −40 °C [69]; (b) *n*-BuLi, **35**, THF, −78 °C → rt (80%) [70]; (c) *n*-BuLi, **35**, HMPT, THF, −78 °C (87%) [71].



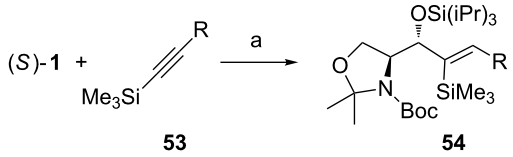
Scheme 17: (a) cat. $Rh(acac)(CO)_2$, **42**, THF, 40 °C (74%).



Scheme 18: (a) 1-PropynylMgBr, CuI, THF, Me_2S, −78 °C (95%); (b) Ethynyltrimethylsilane, EtMgBr, CuI, THF, Me_2S, −78 °C (82%) [72]; (c) EthynylMgCl, $ZnBr_2$, toluene, −78 °C [73]; (d) *n*-BuLi, methyl propiolate, Et_2O, −78 °C → 0 °C, then **(*S*)-1** at −20 °C (62%) [74].

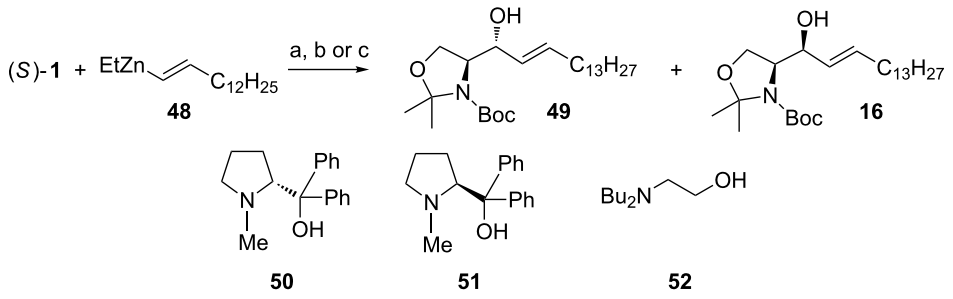
(Scheme 19) [45]. Treatment of (*S*)-**1** with pentadecenyl(ethyl)-zinc (**48**) in the presence of catalytic (*R*)-diphenyl(1-methylpyrrolidin-2-yl)methanol (**50**, (*R*)-DPMPM) [75] in toluene at 0 °C gave adducts **49** and **16** in a 4:1 ratio (*anti*/*syn*). By changing the chiral ligand to (*S*)-DPMPM **51** the selectivity dropped to 2:1 (*anti*/*syn*). When the addition reaction was performed in the presence of achiral *N*,*N*-dibutylaminoethanol **52** they obtained the highest selectivities (7.3:1 *anti*/*syn*). Despite performing the reaction seemingly under chelation control, the selectivity follows the Felkin–Anh transition state model. This selectivity arises from the use of metal coordinating *N*,*O*-ligands. These ligands affect both the reactivity of the metalated nucleophiles and also the metal's capability of coordination.

Montgomery studied the nickel-catalyzed reductive additions of α-aminoaldehydes with silylalkynes (Scheme 20) [76]. The reduction of TMS-alkyne **53** was performed with a trialkylsilane and a $Ni(COD)_2$ catalyst ligated with an in situ formed N-heterocyclic carbene. In all cases studied, they found both the *anti*/*syn*- and the *Z*/*E*-selectivity to be high (>20:1), but the chemical yield was varying. Highest yields (78–80%) were achieved with short alkyl chains (R = Me) or when R = phenyl. When the alkyl chain was lengthened (R = $C_{13}H_{27}$), while aiming for the synthesis of D-*erythro*-sphingosine, the yield drastically dropped to 18%. By changing the reaction conditions (2 equiv of (*S*)-**1** with 1% water in THF) the yield increased to acceptable levels (65%) while the selectivity remained practically the same. They also tested the reaction with other serinal derivatives, but the best results were achieved with (*S*)-**1**.

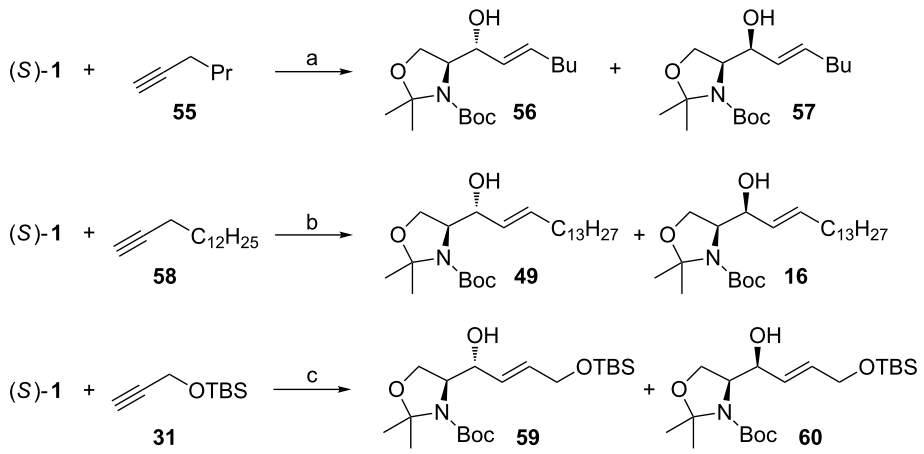


Scheme 20: (a) $(iPr)_3SiH$, cat. $Ni(COD)_2$, dimesitylene-imidazolium·HCl, *t*-BuOK, THF, rt.

Alkynes can be converted to (*E*)-vinyl nucleophiles through hydrozirconation. In view of the relatively low electronegativity (1.2–1.4) of Zr, which is roughly comparable with that of Mg and somewhat lower than that of Al, the low reactivity of organylzirconocene chlorides towards carbonyl compounds is puzzling. It is likely that the presence of two sterically demanding cyclopentadienyl (Cp) groups is at least partially responsible for their low reactivity. Suzuki noticed that Lewis acids promote C–C-bond forming reactions of organylzirconocene nucleophiles (Scheme 21) [77]. They used $AgAsF_6$ as the Lewis acid promoter and found that also Garner's aldehyde reacts under these conditions with 1-hexenylzirconocene. The



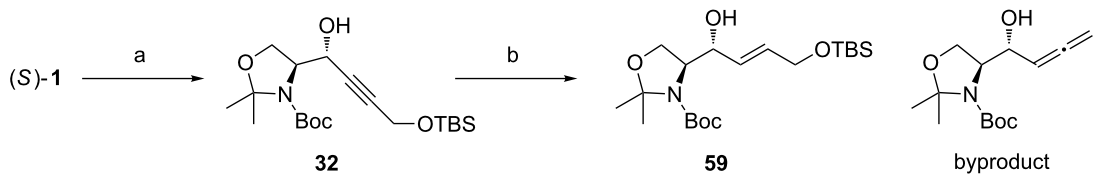
Scheme 19: (a) cat. **50**, toluene, 0 °C (52%); (b) cat. **51**, toluene, 0 °C (51%); (c) cat. **52**, toluene, 0 °C (50%).



Scheme 21: (a) $Cp_2Zr(H)Cl$, cat. $AgAsF_6$, CH_2Cl_2, rt; (b) $Cp_2Zr(H)Cl$, 1-pentadecyne, cat. $ZnBr_2$ in THF for *anti*-selective or $ZnEt_2$ in CH_2Cl_2 for *syn*-selective reaction. (c) $Cp_2Zr(H)Cl$, Et_2Zn, in CH_2Cl_2, for *syn*-selective reaction or in THF for *anti*-selective reaction.

reaction gave a good yield of the addition products **56** and **57** (70% combined yield), but no diastereoselectivity was observed. Peter Wipf has done pioneering work on the hydrozirconation–transmetallation sequence [78,79]. Murakami used this information when investigating the reaction of transmetallated 1-(*E*)-pentadecenylzirconocene chloride with (*S*)-**1** [46,47]. When the reaction was performed in THF at 0 °C and 50 mol % of $ZnBr_2$ was added, the reaction gave the *anti*-adduct **49** as the major diastereomer (12:1 *anti*/*syn*). When the amount of $ZnBr_2$ was lowered to half (25 mol %) the selectivity rose to 20:1 (*anti*/*syn*). The selectivity was reversed to 1:15 (*anti*/*syn*) favouring the *syn*-adduct **16**, when the solvent was changed to less coordinating CH_2Cl_2 and the 1-(*E*)-pentadecenylzirconocene chloride was transmetallated with Et_2Zn prior to the addition of (*S*)-**1**. Interestingly, when the addition was performed in THF in the presence of the transmetallated 1-(*E*)-pentadecenyl(ethyl)zinc, the selectivity was inverted, and the *anti*-adduct **49** was favoured (12:1 *anti*/*syn*).

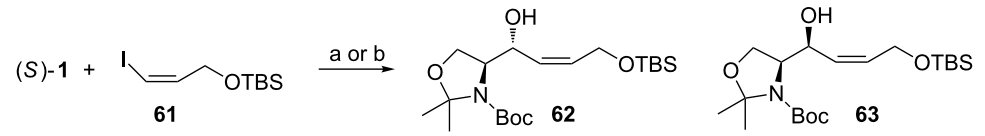
We have also been interested in the use of hydrozirconation–transmetallation process while working on the synthesis of galactonojirimycin (Scheme 21) [48]. We used the TBS-protected propargyl alcohol **31** as the nucleophile, which had been investigated by Negishi for the hydrozirconation–transmetallation process [80]. Our findings were in agreement with the results of Murakami. High *syn*-selectivity (>1:20 *anti*/*syn*) was achieved in CH_2Cl_2 with Et_2Zn as the transmetallating agent. The reaction could also be performed in toluene, but the hydrozirconation had to be done in CH_2Cl_2 due to the low solubility of the Schwartz's reagent in toluene. After formation of the hydrozirconated species, the solvent could be changed to toluene. This reaction gave a slightly lower yield in toluene, but identical selectivity favouring adduct **60**. By changing the solvent to THF the stereochemical outcome was reversed. The *anti*-adduct **59** could be isolated in a >20:1 *anti*/*syn* ratio. Unfortunately, the chemical yield was substantially lower (20%) and many byproducts were observed. Most importantly, these reaction conditions did not affect the chiral integrity of (*S*)-**1**. In a recent synthesis of (−)-1-deoxyaltronojirimycin we tried to synthesize the *anti*-adduct **59** [43]. Poor yield for vinylic addition forced us to look for alternative methods (Scheme 22). Despite the literature precedence of *anti*-selective reactions, we were unable to selectively synthesize this adduct in a good yield. We then turned to the lithiated nucleophile **31**. In THF at −78 °C high diastereoselectivity (15:1 *anti*/*syn*) was obtained. Unfortunately, direct reduction of **32** to **59** produced allene as a byproduct, which forced us to modify the synthetic route.



Scheme 22: (a) i) **31**, *n*-BuLi, THF, −78 °C; ii) (*S*)-**1**, THF, −78 °C; (b) Red-Al, THF, 0 °C.

We have also successfully used (*Z*)-vinyl nucleophiles created from the vinyl iodide **61** in the stereoselective synthesis of pachastrissamine (**11**) [81,82] and norfuranomycin [37] (Scheme 23). After halogen–metal exchange with *n*-BuLi, the newly formed nucleophile reacts with (*S*)-**1**. When HMPT or dimethylpropyleneurea (DMPU) were used, high *anti*-selectivities were achieved (up to 17:1 *anti*/*syn*). Without additives the reaction gave a 4:1 *anti*/*syn* mixture of allylic alcohols **62** and **63**. Chelating metals gave rise to the *syn*-adduct **63**. When we used $ZnCl_2$ dissolved in Et_2O as the chelating agent, the *syn*-selectivity rose to about 1:6 favouring adduct **63**. These results are in agreement with the findings of Jurczak [68].

The alkylation results are summarized in Table 1, and overall one can conclude that Garner's aldehyde **1** is a highly versatile intermediate for organic synthesis. The selectivity of the 1,2-



Scheme 23: (a) **61**, *n*-BuLi, DMPU, toluene, −78 °C, then (*S*)-**1**, toluene, −95 °C (57%); (b) **61**, *n*-BuLi, $ZnCl_2$, toluene, −78 °C, then (*S*)-**1**, toluene, −95 °C (72%).

Table 1: Selectivities and yield for additions of various nucleophiles to Garner's aldehyde **1**.

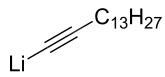
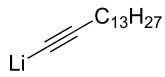
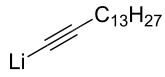
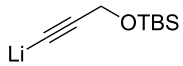
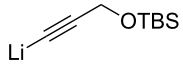
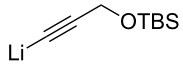
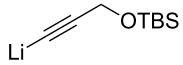
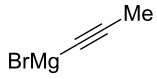
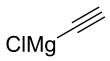
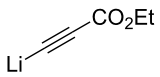
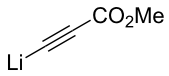
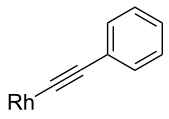
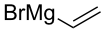
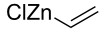
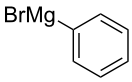
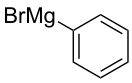
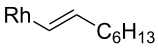
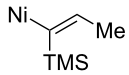
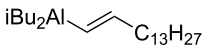
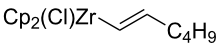
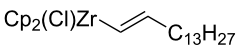
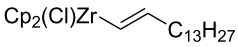
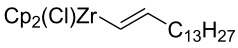
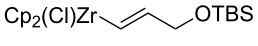
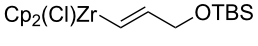
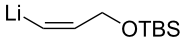
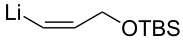
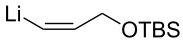
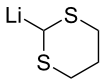
Entry	Nucleophile	Additive	Solvent	*T* (°C)	*anti*/*syn*	Yield (%)	Ref.
1		HMPT	THF	−78	>20:1	71	[59]
2		–	THF	−23	8:1	83	[50]
3		$ZnBr_2$	Et_2O	−78 → rt	1:15	87	[59]
4		HMPT	toluene	−78 → 0	20:1	85	[58]
5		–	THF	−78	15:1	80	[43]
6		–	toluene	−78 → rt	3:1	80	[58]
7		$ZnCl_2$	toluene/Et_2O	−78 → rt	1:10	65	[58]
8		CuI	THF/Me_2S	−78	1:16	95	[72]
9		$ZnBr_2$	THF/toluene	−78	1:1	–	[73]
10		HMPT	THF	−78	13:1	75	[38]
11		–	Et_2O	−78 → 0	1:12	62	[74]
12		–	THF	40	20:1	74	[71]

Table 1: Selectivities and yield for additions of various nucleophiles to Garner's aldehyde **1**. (continued)

13		–	THF	−78	5:1	–	[61]
14		–	THF	−78	3:1	–	[61]
15		–	Et_2O	−78 → rt	1:6	85	[61]
16		–	THF	−78 → 0	5:1	–	[62]
17		–	Et_2O	0	2:3	–	[63]
18		–	aq DME	55	4.6:1	78	[65]
19		–	THF	rt	>20:1	78	[76]
20		–	THF	−78	1:2	>80	[50]
21		$AgAsF_6$	CH_2Cl_2	rt	1:1	70	[78]
22		$ZnBr_2$	THF	0 → rt	20:1	70	[46]
23		Et_2Zn	CH_2Cl_2	−30 → 0	1:15	84	[46]
24		Et_2Zn	THF	−20 → rt	12:1	67	[46]
25		Et_2Zn	CH_2Cl_2	−40 → 0	>1:20	78	[48]
26		Et_2Zn	THF	−40 → 0	>20:1	20	[48]
27		DMPU	toluene	−95	17:1	57	[81,82]
28		–	toluene	−95	4:1	63	[81,82]
29		$ZnCl_2$	toluene/Et_2O	−95	1:6	72	[81,82]
30		CuI (cat.) $BF_3{\cdot}Et_2O$	THF	−50	>99:1	70	[66]

asymmetric induction can be controlled, either by choice of the nucleophilic reagent, chelating or aggregates breaking additives, solvent and sometimes also by the reaction temperature. Less coordinating metals and more reactive nucleophiles tend to give Felkin–Anh products (Table 1, entries 2, 5, 6, 12–14, 16, 18, 19 and 28). Smaller alkyne nucleophiles seem to give a roughly 8:1 *anti*/*syn*-selectivity. The larger organovinyl reagents give slightly lower *anti*-selectivities of about 3:1 to 5:1. Highest selectivities are reached with transition metals, such as Rh and Ni (Table 1, entries 12, 18 and 19). The *anti*-selectivity can be enhanced either by the addition of aggregation breaking additives, such as HMPT and DMPU (Table 1, entries 1, 4, 10 and 27) or by the use of strongly Lewis basic solvents, like THF (Table 1, entries 2, 5, 13, 14, 16 and 24). Using aggregate breaking additives increases the *anti*-selectivities from 4–5:1 to >20:1. The increase of nucleophilicity diminishes the metal cations capability or chances to coordinate to the carbonyl groups. This promotes the attack of the nucleophile from the least hindered *re* side.

Chelation control can also be achieved by the proper choice of solvents. Even changing from THF to Et_2O is often enough to inverse the selectivity (Table 1, entries 10, 11, 16 and 17). Less coordinating solvents, such as toluene or CH_2Cl_2 can also affect the selectivity. A greater effect on the selectivity can be reached by the addition of Lewis acids. Usually Zn(II)-salts give fair to good *syn*-selectivities (Table 1, entries 3, 7, 23, 25 and 29), if the solvent is non-coordinating (Et_2O, toluene or CH_2Cl_2). Zn(II)-salts do not necessarily give *syn*-selectivities, especially if they are too reactive to chelate to the substrate (Table 1,

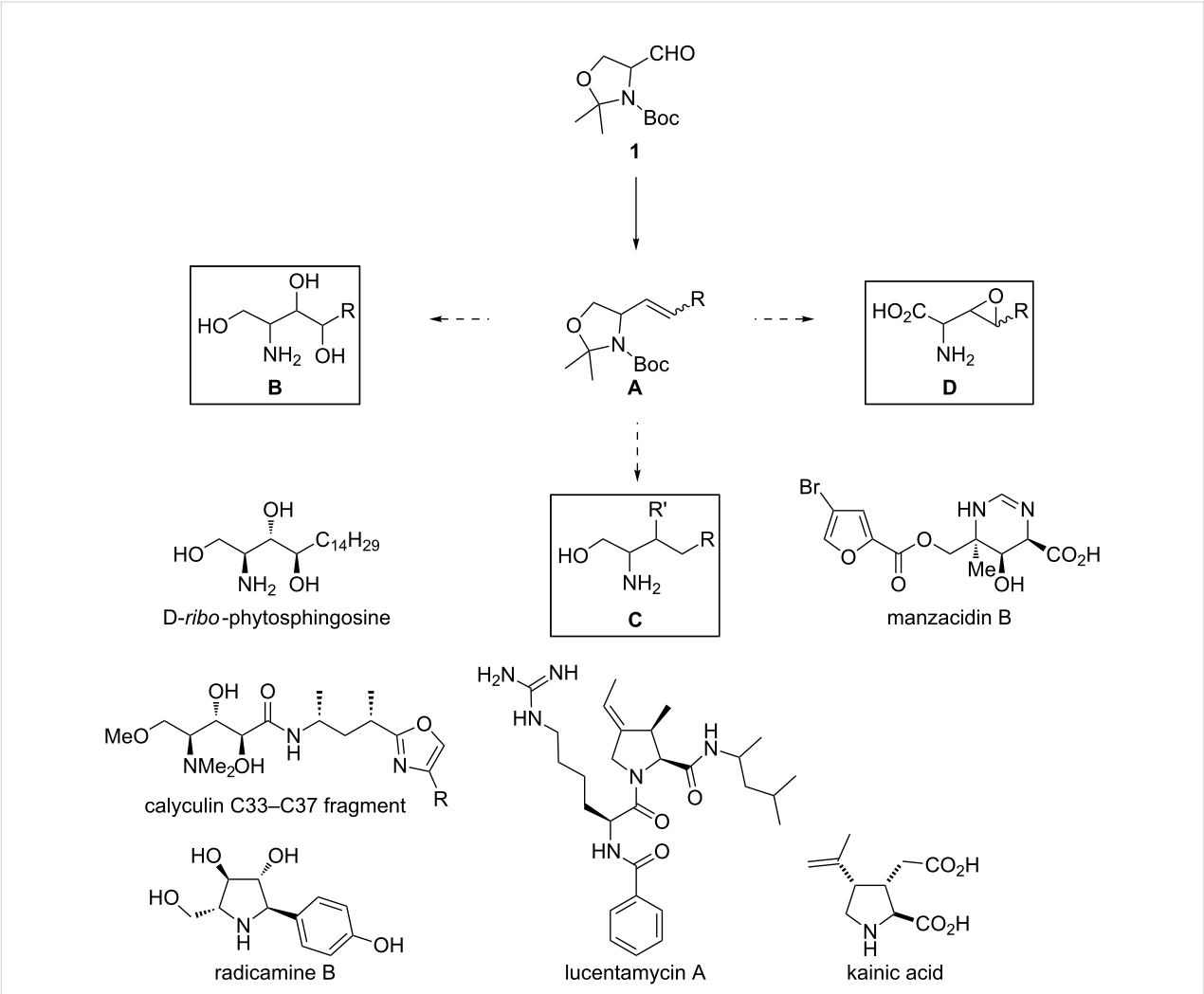
entry 9). Vinylalanes give varying results, preferring either *anti*- or *syn*-selectivity (Table 1, entry 20).

Olefination of Garner's aldehyde

Olefination of **1** provides an easy access to chiral 2-aminohomoallylic alcohols **A** (Scheme 24). The intermediate can be derivatized further, thus providing a route for greater molecular diversity. Diastereoselective dihydroxylation of **A** with OsO_4 leads to triols **B**, which have been utilized in the syntheses of calyculins family [83,84], D-*ribo*-phytosphingosine [85], and radicamine [86,87]. If the R-group in **A** is an ester, diastereoselective Michael addition leads to structures **C** [88-92]. Kainic acid was synthesized using such conjugate addition [93], and a recent synthesis of lucentamycin A was achieved using this strategy [94]. Epoxidation of **A** leads to a highly functional intermediate **C**, which has been used in the synthesis of manzacidin B [95].

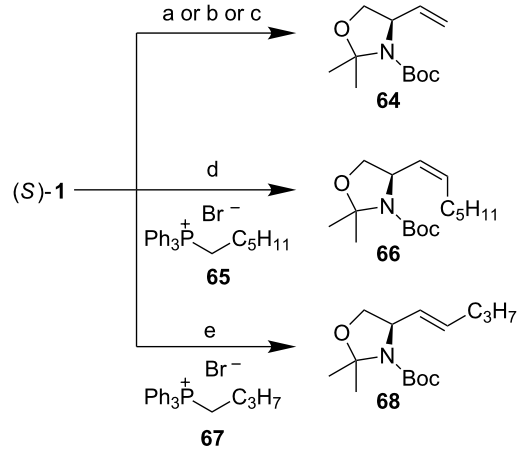
Among the plethora of olefination reactions, the Wittig [96,97] and Horner–Wadsworth–Emmons [98-100] reactions are most commonly used for the introduction of a double bond to Garner's aldehyde **1**. Two things need to be considered before performing the olefination reactions: 1) epimerization of the stereocenter in the aldehyde (i.e. basicity vs nucleophilicity of the olefinating reagents) and 2) *E*/*Z*-selectivity of the reaction.

Moriwake et al. noticed in their synthesis of vinylglycinol **64** that the reaction of methyltriphenylphosphonium bromide with KH as the base provided **62** in fairly good yield, but with complete racemization of the product (Scheme 25) [101]. This racemization could be overcome by performing the olefination with $AlMe_3$–Zn–CH_2I_2 in benzene under non-basic conditions. While looking for non-racemizing conditions for the same reaction, Beaulieu et al. found that the ylide formed from methyltriphenylphosphonium bromide and *n*-BuLi in THF gave **62** in



Scheme 24: Olefin **A** as an intermediate in natural product synthesis.

69% ee, but in low yield (27%) [102]. With a different unstabilized ylide **65**, the enantiopurity of the Wittig product increased to >95% ee. The erosion of enantiopurity was attributed to the ylide ($Ph_3P{=}CH_2$) being too basic. It is well known that phosphonium ylides form stable complexes with alkali metals during the dehydrohalogenation of the phosphonium salt [103]. These complexes react with carbonyl compounds differently. Addition reactions of other ylides to **1**, proceeded with little or no racemization of **1**. The *E*/*Z*-ratio of the reaction was 1:13 favouring the *Z*-adduct **66**. In comparison to Beaulieu's results, McKillop [27] noticed that with KHMDS as the base, there was no epimerization at all! To prepare "salt-free" ylides, it is necessary to remove lithium halide from the reaction solution. On the other hand KHMDS is a convenient base for the preparation of "salt-free" ylides.

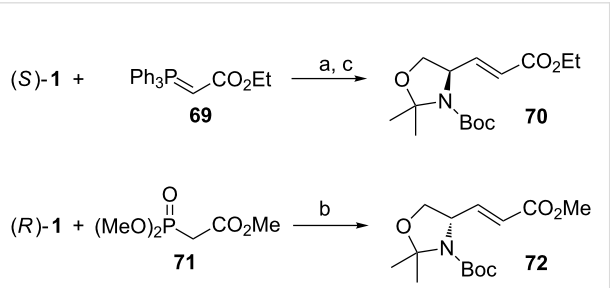


Scheme 25: (a) $Ph_3(Me)PBr$, KH, benzene (66%, *rac*-**64**) or (b) $AlMe_3$, Zn, CH_2I_2, THF (76%) [101]; (c) $Ph_3(Me)PBr$, *n*-BuLi, THF, −75 °C, then (*S*)-**1** (27%, 69% ee) [102]; (d) **65**, *n*-BuLi, THF, −75 °C, then (*S*)-**1** (78%, 1:13 *E*/*Z*, >95% ee); (e) **67**, KHMDS, THF, −78 °C, then (*S*)-**1**, quenching with MeOH (70%, >10:1 *E*/*Z*) [104].

High *Z*-selectivity is a typical outcome with unstabilized ylides. Kim has investigated means of reversing the *E*/*Z*-selectivity to favour the *E*-isomer [104]. They noticed that olefination under the usual Wittig conditions provided high *Z*-selectivity (1:15 *E*/*Z*). When the reaction was quenched with MeOH at −78 °C, the *E*/*Z*-ratio was reversed to >10:1 favouring adduct **68** [105].

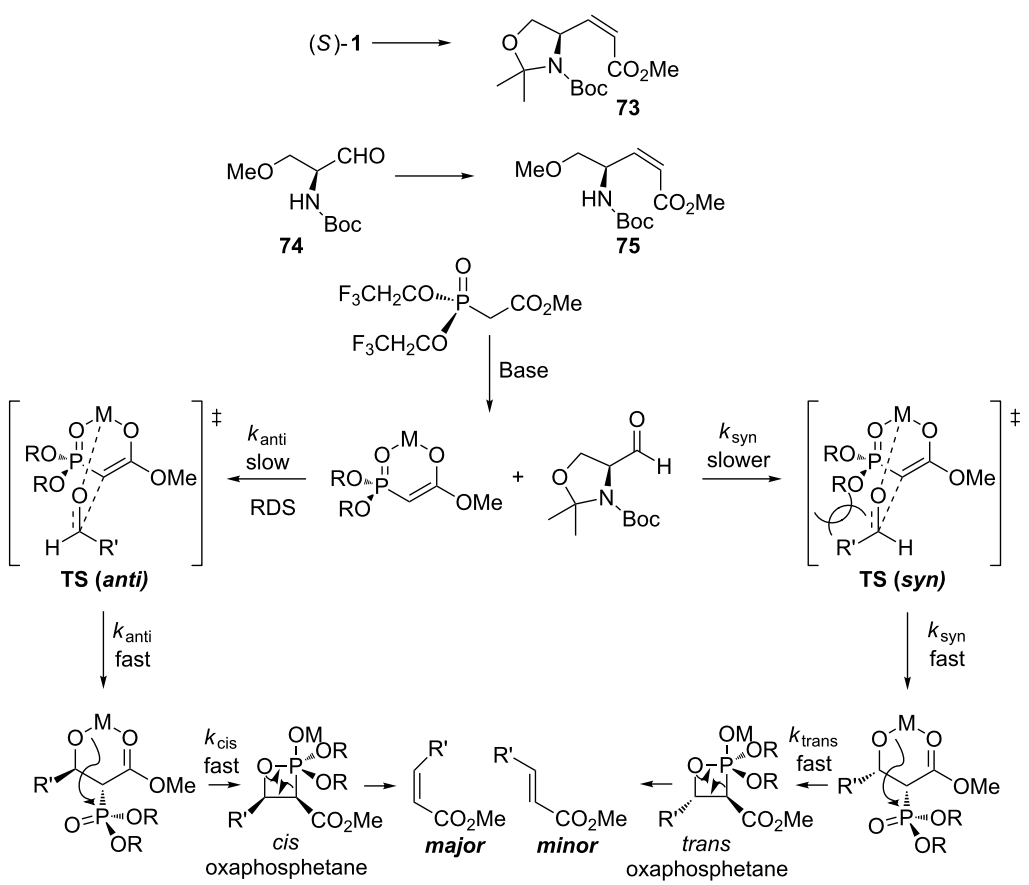
α,β-Unsaturated esters can be synthesized from stabilized ylides. Reaction of **1** with ylide **69** is *E*-selective. Depending on the solvent, the *E*/*Z*-ratio can vary from 3:1 (in MeOH) [106] to 100:0 (THF [107] or benzene [108]). Since stabilized ylides are less reactive compared to their non-stabilized counterparts, they tend to epimerize the existing chiral center of **1** a lot less, if at all (pK_{aH} value of **69** in DMSO is 8.5 compared to the pK_a value of $Ph_3(Me)PBr$, which is 22.5) [109].

Another method to prepare α,β-unsaturated esters is the Horner–Wadsworth–Emmons reaction (HWE). The HWE reaction has many advantages over the Wittig olefination. The phosphonate anions tend to be more nucleophilic (less basic) than the corresponding phosphorous ylides. The byproducts, dialkyl phosphates are water soluble and hence easier to remove from the product compared to, e.g., triphenylphospine oxide. As with the Wittig reaction, the HWE reaction can also promote the epimerization of the α-proton (pK_a of triethoxyphosphonoacetate in DMSO is 18.6) [109]. We have experienced this tendency especially with α-amino ketophosphonates [110], but there is also evidence that aldehyde **1** can lose some of its chiral integrity in the HWE reaction. For base sensitive substrates the use of metal salts (LiCl or NaI) and an amine base (DBU or DIPEA) has proven to be effective in avoiding epimerization [111]. The use of $Ba(OH)_2$ in aq THF has also been advocated to prevent epimerization [112], and recently Myers has reported the superiority of lithium hexafluoroisopropoxide as a mild base for HWE olefinations of epimerizable aldehydes [113]. Jako et al. showed that *E*-enoate **72** can be synthesized from Garner's aldehyde (*R*)-**1** in 95:5 *E*/*Z*-selectivity and practically with no degradation of chiral integrity (Scheme 26) [89]. As an alternative, Lebel and Ladjel used a catalytic amount of $[Ir(COD)Cl]_2$ for the in situ preparation of ylide **69** [114]. They obtained a 81% yield in the reaction.



Scheme 26: (a) Benzene, rt (82%) [108]; (b) K_2CO_3, MeOH (85%) [89]; (c) iPrOH, $[Ir(COD)Cl]_2$, PPh_3, THF, rt (81%) [114].

We have been interested in the synthesis of *Z*-enoate **73** [84]. The Still–Gennari modification to the phosphonate makes the synthesis of *Z*-enoates possible [115]. The two electron-withdrawing CF_3CH_2O-groups destabilize the *cis*-oxaphosphetane intermediate (Scheme 27) and make the elimination reaction to the kinetic product *Z*-alkene a lot faster. As the elimination step becomes fast, the rate difference in the initial addition step between k_{anti} and k_{syn} determines the overall *Z*-selectivity. When the reaction was performed with K_2CO_3/18-crown-6 as the base in toluene at −15 °C, we could isolate only the *Z*-enoate **73** in good yield (90%). HPLC analysis showed that there was no epimerization.



Scheme 27: Mechanism of the Still–Gennari modification of the HWE reaction leading to both olefin isomers.

We have recently shown that the open-chain aldehyde **74** reacts with the Still–Gennari phosphonate and provides the *Z*-enoate **75** in good *E*/*Z*-selectivity (1:12) [84]. The slight decrease in the *E*/*Z*-selectivity can be reasoned with the smaller size of the aldehyde **74**. When the aldehyde is coordinating to the phosphonate, the steric hindrance caused by the interaction of the trifluoroethoxy group with the aldehyde R' in **TS (*syn*)** is smaller compared with aldehyde **1**. This allows some of the aldehyde to react via the *trans*-oxaphosphetane intermediate. Using these reaction conditions no epimerization was observed.

Conclusion

Garner's aldehyde has developed into a useful and reliable synthetic intermediate for the synthesis of enantiopure complex natural products, their analogues and other pharmacologically active compounds. Several reaction types have been studied sufficiently so that one has reliable tools to plan a synthesis. Simple addition reactions to the carbonyl group give access to vicinal amino alcohols, important building blocks for many natural products. Another possibility for carbon chain elongation are olefination reactions, which often lead to epimerization of the α-stereocenter. As with the alkylations, strategies to avoid this undesired reaction have been developed. However, despite these important achievements, much more research needs to be done to increase the scopes of these reactions, the overall efficiency, and environmental sustainability.

References

1. Vallery-Radot, R.; Devonshire, R. L. *Life of Pasteur (transl.);* Dover Publications: New York, 1960; p 484.
2. Ramos Tombo, G. M.; Belluš, D. *Angew. Chem., Int. Ed. Engl.* **1991,** *30,* 1193–1215. doi:10.1002/anie.199111933
3. Lamberth, C. *Tetrahedron* **2010,** *66,* 7239–7256. doi:10.1016/j.tet.2010.06.008
4. Vaenkatesan, V.; Wegh, R. T.; Teunissen, J.-P.; Lub, J.; Bastiaansen, C. W. M.; Broer, D. J. *Adv. Funct. Mater.* **2005,** *15,* 138–142. doi:10.1002/adfm.200400122
5. Zhuang, X. X.; Sun, X. X.; Li, L.; Li, Y. C. *Adv. Mat. Res.* **2011,** *337,* 151–154. doi:10.4028/www.scientific.net/AMR.337.151
6. Armstrong, R. W.; Beau, J. M.; Cheon, S. H.; Christ, W. J.; Fujioka, H.; Ham, W. H.; Hawkins, L. D.; Jin, H.; Kang, S. H.; Kishi, Y.; Martinelli, M. J.; McWhorter, W. W., Jr.; Mizuno, M.; Nakata, M.; Stutz, A. E.; Talamas, F. X.; Taniguchi, M.; Tino, J. A.; Ueda, K.; Uenishi, J.; White, J. B.; Yonaga, M. *J. Am. Chem. Soc.* **1989,** *111,* 7525–7530. doi:10.1021/ja00201a037

7. Armstrong, R. W.; Beau, J. M.; Cheon, S. H.; Christ, W. J.; Fujioka, H.; Ham, W. H.; Hawkins, L. D.; Jin, H.; Kang, S. H.; Kishi, Y.; Martinelli, M. J.; McWhorter, W. W., Jr.; Mizuno, M.; Nakata, M.; Stutz, A. E.; Talamas, F. X.; Taniguchi, M.; Tino, J. A.; Ueda, K.; Uenishi, J.; White, J. B.; Yonaga, M. *J. Am. Chem. Soc.* **1989,** *111,* 7530–7533. doi:10.1021/ja00201a038
8. Suh, E. M.; Kishi, Y. *J. Am. Chem. Soc.* **1994,** *116,* 11205–11206. doi:10.1021/ja00103a065
9. Mangeney, P.; Andriamialisoa, R. Z.; Langlois, N.; Langlois, Y.; Potier, P. *J. Am. Chem. Soc.* **1979,** *101,* 2243–2245. doi:10.1021/ja00502a072
10. Kutney, J. P.; Choi, L. S. L.; Nakano, J.; Tsukamoto, H.; McHugh, M.; Boulet, C. A. *Heterocycles* **1988,** *27,* 1845–1853. doi:10.3987/COM-88-4611
11. Kuehne, M. E.; Matson, P. A.; Bornmann, W. G. *J. Org. Chem.* **1991,** *56,* 513–528. doi:10.1021/jo00002a008
12. Magnus, P.; Mendoza, J. S.; Stamford, A.; Ladlow, M.; Willis, P. *J. Am. Chem. Soc.* **1992,** *114,* 10232–10245. doi:10.1021/ja00052a020
13. Yokoshima, S.; Ueda, T.; Kobayashi, S.; Sato, A.; Kuboyama, T.; Tokuyama, H.; Fukuyama, T. *J. Am. Chem. Soc.* **2002,** *124,* 2137–2139. doi:10.1021/ja0177049
14. Ishikawa, H.; Colby, D. A.; Seto, S.; Va, P.; Tam, A.; Kakei, H.; Rayl, T. J.; Hwang, I.; Boger, D. L. *J. Am. Chem. Soc.* **2009,** *131,* 4904–4916. doi:10.1021/ja809842b
15. Nicolaou, K. C.; Yang, Z.; Liu, J. J.; Ueno, H.; Nantermet, P. G.; Guy, R. K.; Claiborne, C. F.; Renaud, J.; Couladouros, E. A.; Paulvannan, K.; Sorensen, E. J. *Nature* **1994,** *367,* 630–634. doi:10.1038/367630a0
16. Holton, R. A.; Somoza, C.; Kim, H. B.; Liang, F.; Biediger, R. J.; Boatman, P. D.; Shindo, M.; Smith, C. C.; Kim, S.; Nadizadeh, H.; Suzuki, Y.; Tao, C.; Vu, P.; Tang, S.; Zhang, P.; Murthi, K. K.; Gentile, L. N.; Liu, J. H. *J. Am. Chem. Soc.* **1994,** *116,* 1597–1598. doi:10.1021/ja00083a066
17. Holton, R. A.; Somoza, C.; Kim, H. B.; Liang, F.; Biediger, R. J.; Boatman, P. D.; Shindo, M.; Smith, C. C.; Kim, S.; Nadizadeh, H.; Suzuki, Y.; Tao, C.; Vu, P.; Tang, S.; Zhang, P.; Murthi, K. K.; Gentile, L. N.; Liu, J. H. *J. Am. Chem. Soc.* **1994,** *116,* 1599–1600. doi:10.1021/ja00083a067
18. Danishefsky, S. J.; Masters, J. J.; Young, W. B.; Link, J. T.; Snyder, L. B.; Magee, T. V.; Jung, D. K.; Isaacs, R. C. A.; Bornmann, W. G.; Alaimo, C. A.; Coburn, C. A.; Di Grandi, M. J. *J. Am. Chem. Soc.* **1996,** *118,* 2843–2859. doi:10.1021/ja952692a
19. Wender, P. A.; Badham, N. F.; Conway, S. P.; Floreancig, P. E.; Glass, T. E.; Gränicher, C.; Houze, J. B.; Jaenichen, J.; Lee, D.; Marquess, D. G.; McGrane, P. L.; Meng, W.; Mucciaro, T. P.; Mühlebach, M.; Natchus, M. G.; Paulsen, H.; Rawlins, D. B.; Satkofsky, J.; Shuker, A. J.; Sutton, J. C.; Taylor, R. E.; Tomooka, K. *J. Am. Chem. Soc.* **1997,** *119,* 2755–2756. doi:10.1021/ja9635387
20. Wender, P. A.; Badham, N. F.; Conway, S. P.; Floreancig, P. E.; Glass, T. E.; Houze, J. B.; Krauss, N. E.; Lee, D.; Marquess, D. G.; McGrane, P. L.; Meng, W.; Natchus, M. G.; Shuker, A. J.; Sutton, J. C.; Taylor, R. E. *J. Am. Chem. Soc.* **1997,** *119,* 2757–2758. doi:10.1021/ja963539z
21. Morihira, K.; Hara, R.; Kawahara, S.; Nishimori, T.; Nakamura, N.; Kusama, H.; Kuwajima, I. *J. Am. Chem. Soc.* **1998,** *120,* 12980–12981. doi:10.1021/ja9824932
22. Mukaiyama, T.; Shiina, I.; Iwadare, H.; Saitoh, M.; Nishimura, T.; Ohkawa, N.; Sakoh, H.; Nishimura, K.; Tani, Y.-I.; Hasegawa, M.; Yamada, K.; Saitoh, K. *Chem.–Eur. J.* **1999,** *5,* 121–161. doi:10.1002/(SICI)1521-3765(19990104)5:1<121::AID-CHEM121>3.3.CO;2-F
23. Doi, T.; Fuse, S.; Miyamoto, S.; Nakai, K.; Sasuga, D.; Takahashi, T. *Chem.–Asian J.* **2006,** *1,* 370–383. doi:10.1002/asia.200600156
24. Garner, P. *Tetrahedron Lett.* **1984,** *25,* 5855–5858. doi:10.1016/S0040-4039(01)81703-2
25. Garner, P.; Park, J. M. *Org. Synth.* **1990,** *70,* 18–28.
26. Garner, P.; Park, J. M. *J. Org. Chem.* **1987,** *52,* 2361–2364. doi:10.1021/jo00388a004
27. McKillop, A.; Taylor, R. J. K.; Watson, R. J.; Lewis, N. *Synthesis* **1994,** 31–33. doi:10.1055/s-1994-25398
28. Dondoni, A.; Perroni, D. *Org. Synth.* **2000,** *77,* 64–77.
29. Roush, W. R.; Hunt, J. A. *J. Org. Chem.* **1995,** *60,* 798–806. doi:10.1021/jo00109a008
30. Ocejo, M.; Vicario, J. L.; Badía, D.; Carrillo, L.; Reyes, E. *Synlett* **2005,** 2110–2112. doi:10.1055/s-2005-871947
31. Jurczak, J.; Gryko, D.; Kobrzycka, E.; Gruza, H.; Prokopowicz, P. *Tetrahedron* **1998,** *54,* 6051–6064. doi:10.1016/S0040-4020(98)00299-3
32. Rauhala, V. Master's thesis, Department of Chemistry, University of Oulu, **1998**, p. 87.
33. Clemens, A. J. L.; Burke, S. D. *J. Org. Chem.* **2012,** *77,* 2983–2985. doi:10.1021/jo300025t
34. Huntley, R. J.; Funk, R. L. *Org. Lett.* **2006,** *8,* 4775–4778. doi:10.1021/ol0617547
35. Chattopadhyay, S. K.; Sarkar, K.; Karmakar, S. *Synlett* **2005,** 2083–2085. doi:10.1055/s-2005-871944
36. Bandyopadhyay, A.; Pal, B. K.; Chattopadhyay, S. K. *Tetrahedron: Asymmetry* **2008,** *19,* 1875–1877. doi:10.1016/j.tetasy.2008.07.032
37. Passiniemi, M.; Koskinen, A. M. P. *Tetrahedron Lett.* **2011,** *52,* 6736–6738. doi:10.1016/j.tetlet.2011.10.007
38. Garner, P.; Park, J. M. *J. Org. Chem.* **1990,** *55,* 3772–3787. doi:10.1021/jo00299a017
39. Takahata, H.; Banba, Y.; Ouchi, H.; Nemoto, H. *Org. Lett.* **2003,** *5,* 2527–2529. doi:10.1021/ol034886y
40. Takahata, H.; Banba, Y.; Sasatani, M.; Nemoto, H.; Kato, A.; Adachi, I. *Tetrahedron* **2004,** *60,* 8199–8205. doi:10.1016/j.tet.2004.06.112
41. Guaragna, A.; D'Errico, S.; D'Alonzo, D.; Pedatella, S.; Palumbo, G. *Org. Lett.* **2007,** *9,* 3473–3476. doi:10.1021/ol7014847
42. Guaragna, A.; D'Alonzo, D.; Paolella, C.; Palumbo, G. *Tetrahedron Lett.* **2009,** *50,* 2045–2047. doi:10.1016/j.tetlet.2009.02.111
43. Karjalainen, O. K.; Koskinen, A. M. P. *Org. Biomol. Chem.* **2011,** *9,* 1231–1236. doi:10.1039/c0ob00747a
44. Garner, P.; Park, J. M.; Malecki, E. *J. Org. Chem.* **1988,** *53,* 4395–4398. doi:10.1021/jo00253a039
45. Soai, K.; Takahashi, K. *J. Chem. Soc., Perkin Trans. 1* **1994,** 1257–1258. doi:10.1039/P19940001257
46. Murakami, T.; Furusawa, K. *Tetrahedron* **2002,** *58,* 9257–9263. doi:10.1016/S0040-4020(02)01190-0
47. Murakami, T.; Furusawa, K.; Tamai, T.; Yoshikai, K.; Nishikawa, M. *Bioorg. Med. Chem. Lett.* **2005,** *15,* 1115–1119. doi:10.1016/j.bmcl.2004.12.010
48. Karjalainen, O. K.; Passiniemi, M.; Koskinen, A. M. P. *Org. Lett.* **2010,** *12,* 1145–1147. doi:10.1021/ol100037c

49. Tamborini, L.; Conti, P.; Pinto, A.; Colleoni, S.; Gobbi, M.; De Micheli, C. *Tetrahedron* **2009,** *65,* 6083–6089. doi:10.1016/j.tet.2009.05.054
50. Lemke, A.; Büschleb, M.; Ducho, C. *Tetrahedron* **2010,** *66,* 208–214. doi:10.1016/j.tet.2009.10.102
51. Chisholm, J. D.; Van Vranken, D. L. *J. Org. Chem.* **2000,** *65,* 7541–7553. doi:10.1021/jo000911r
52. Liang, X.; Andersch, J.; Bols, M. *J. Chem. Soc., Perkin Trans. 1* **2001,** 2136–2157. doi:10.1039/B101054I
53. Karjalainen, O. K.; Koskinen, A. M. P. *Org. Biomol. Chem.* **2012,** *10,* 4311–4326. doi:10.1039/c2ob25357g
54. Reginato, G.; Meffre, P.; Gaggini, F. *Amino Acids* **2005,** *29,* 81–87. doi:10.1007/s00726-005-0184-y
55. Ahn, N. T. *Top. Curr. Chem.* **1980,** *88,* 146–162.
56. Cram, D. J.; Abd Elhafez, F. A. *J. Am. Chem. Soc.* **1952,** *74,* 5828–5835. doi:10.1021/ja01143a007
57. Reetz, M. T.; Hüllmann, M.; Seitz, T. *Angew. Chem., Int. Ed. Engl.* **1987,** *26,* 477–480. doi:10.1002/anie.198704771
58. Gruza, H.; Kiciak, K.; Krasiński, A.; Jurczak, J. *Tetrahedron: Asymmetry* **1997,** *8,* 2627–2631. doi:10.1016/S0957-4166(97)00306-6
59. Herold, P. *Helv. Chim. Acta* **1988,** *71,* 354–362. doi:10.1002/hlca.19880710208
60. Dale, J. A.; Dull, D. L.; Mosher, H. S. *J. Org. Chem.* **1969,** *34,* 2543–2549. doi:10.1021/jo01261a013
61. Coleman, R. S.; Carpenter, A. J. *Tetrahedron Lett.* **1992,** *33,* 1697–1700. doi:10.1016/S0040-4039(00)91709-X
62. Williams, L.; Zhang, Z.; Shao, F.; Carroll, P. J.; Joullié, M. M. *Tetrahedron* **1995,** *52,* 11673–11694. doi:10.1016/0040-4020(96)00672-2
63. Koskinen, A. M. P.; Hassila, H.; Myllymäki, V. T.; Rissanen, K. *Tetrahedron Lett.* **1995,** *36,* 5619–5622. doi:10.1016/0040-4039(95)01029-H
64. Marcus, Y. *The Properties of Solvents;* John Wiley & Sons: Chichester, 1998; pp 142–160.
65. Fürstner, A.; Krause, H. *Adv. Synth. Catal.* **2001,** *343,* 343–350. doi:10.1002/1615-4169(20010430)343:4<343::AID-ADSC343>3.3.CO;2-Q
66. Shimizu, M.; Wakioka, I.; Fujisawa, T. *Tetrahedron Lett.* **1997,** *38,* 6027–6030. doi:10.1016/S0040-4039(97)01340-3
67. Wong, L.; Tan, S. S. L.; Lam, Y.; Melendez, A. J. *J. Med. Chem.* **2009,** *52,* 3618–3626. doi:10.1021/jm900121d
68. Mori, K.; Masuda, Y. *Tetrahedron Lett.* **2003,** *44,* 9197–9200. doi:10.1016/j.tetlet.2003.10.025
69. Chun, J.; Byun, H.-S.; Bittman, R. *J. Org. Chem.* **2003,** *68,* 348–354. doi:10.1021/jo026240+
70. Yadav, J. S.; Geetha, V.; Krishnam Raju, A.; Gnaneshwar, D.; Chandrasekhar, S. *Tetrahedron Lett.* **2003,** *44,* 2983–2985. doi:10.1016/S0040-4039(03)00390-3
71. Dhondi, P. K.; Carberry, P.; Choi, L. B.; Chisholm, J. D. *J. Org. Chem.* **2007,** *72,* 9590–9596. doi:10.1021/jo701643h
72. Zhang, X.; van der Donk, W. A. *J. Am. Chem. Soc.* **2007,** *129,* 2212–2213. doi:10.1021/ja067672v
73. Reginato, G.; Mordini, A.; Tenti, A.; Valacchi, M.; Broguiere, J. *Tetrahedron: Asymmetry* **2008,** *19,* 2882–2886. doi:10.1016/j.tetasy.2008.12.025
74. Hanessian, S.; Yang, G.; Rondeau, J.-M.; Neumann, U.; Betschart, C.; Tinelnot-Blomley, M. *J. Med. Chem.* **2006,** *49,* 4544–4567. doi:10.1021/jm060154a
75. Soai, K.; Ookawa, A.; Kaba, T.; Ogawa, K. *J. Am. Chem. Soc.* **1987,** *109,* 7111–7115. doi:10.1021/ja00257a034
76. Sa-ei, K.; Montgomery, J. *Tetrahedron* **2009,** *65,* 6707–6711. doi:10.1016/j.tet.2009.05.029
77. Suzuki, K.; Hasegawa, T.; Imai, T.; Maeta, H.; Ohba, S. *Tetrahedron* **1995,** *51,* 4483–4494. doi:10.1016/0040-4020(94)01135-M
78. Wipf, P.; Xu, W. *Tetrahedron Lett.* **1994,** *35,* 5197–5200. doi:10.1016/S0040-4039(00)77062-6
79. Wipf, P.; Jahn, H. *Tetrahedron* **1996,** *52,* 12853–12910. doi:10.1016/0040-4020(96)00754-5
80. Xu, C.; Negishi, E. *Tetrahedron Lett.* **1999,** *40,* 431–434. doi:10.1016/S0040-4039(98)02394-6
81. Passiniemi, M.; Koskinen, A. M. P. *Tetrahedron Lett.* **2008,** *49,* 980–983. doi:10.1016/j.tetlet.2007.12.014
82. Passiniemi, M.; Koskinen, A. M. P. *Org. Biomol. Chem.* **2011,** *9,* 1774–1783. doi:10.1039/c0ob00643b
83. Koskinen, A. M. P.; Chen, Y. *Tetrahedron Lett.* **1991,** *32,* 6977–6980. doi:10.1016/0040-4039(91)80459-J
84. Passiniemi, M.; Koskinen, A. M. P. *Synthesis* **2010,** 2816–2822. doi:10.1055/s-0029-1218843
85. Jeon, J.; Shin, M.; Yoo, J. W.; Oh, J. S.; Bae, J. G.; Jung, S. H.; Kim, Y. G. *Tetrahedron Lett.* **2007,** *48,* 1105–1108. doi:10.1016/j.tetlet.2006.12.084
86. Ribes, C.; Falomir, E.; Carda, M.; Marco, J. A. *J. Org. Chem.* **2008,** *73,* 7779–7782. doi:10.1021/jo8012989
87. Mallesham, P.; Vijaykumar, B. V. D.; Shin, D.-S.; Chandrasekhar, S. *Tetrahedron Lett.* **2011,** *52,* 6145–6147. doi:10.1016/j.tetlet.2011.09.034
88. Jako, I.; Uiber, P.; Mann, A.; Taddei, M.; Wermuth, C. G. *Tetrahedron Lett.* **1990,** *31,* 1011–1014. doi:10.1016/S0040-4039(00)94416-2
89. Yoda, H.; Shirai, T.; Katagiri, T.; Takabe, K.; Kimata, K.; Hosoya, K. *Chem. Lett.* **1990,** 2037–2038. doi:10.1246/cl.1990.2037
90. Hanessian, S.; Sumi, K. *Synthesis* **1991,** 1083–1089. doi:10.1055/s-1991-28396
91. Hanessian, S.; Demont, E.; van Otterlo, W. A. L. *Tetrahedron Lett.* **2000,** *41,* 4999–5003. doi:10.1016/S0040-4039(00)00765-6
92. Rastogi, S. K.; Kornienko, A. *Tetrahedron: Asymmetry* **2006,** *17,* 3170–3178. doi:10.1016/j.tetasy.2006.11.029
93. Jako, I.; Uiber, P.; Mann, A.; Wermuth, C.-G. *J. Org. Chem.* **1991,** *56,* 5729–5733. doi:10.1021/jo00019a055
94. Ranatunga, S.; Tang, C.-H. A.; Hu, C.-C. A.; Del Valle, J. R. *J. Org. Chem.* **2012,** *77,* 9859–9864. doi:10.1021/jo301723y
95. Sankar, K.; Rahman, H.; Das, P. P.; Bhimireddy, E.; Sridhar, B.; Mohapatra, D. K. *Org. Lett.* **2012,** *14,* 1082–1085. doi:10.1021/ol203466m
96. Wittig, G.; Schöllkopf, U. *Chem. Ber.* **1954,** *87,* 1318–1330. doi:10.1002/cber.19540870919
97. Wittig, G.; Haag, W. *Chem. Ber.* **1955,** *88,* 1654–1666. doi:10.1002/cber.19550881110
98. Horner, L.; Hoffmann, H.; Wippel, H. G. *Chem. Ber.* **1958,** *91,* 61–63. doi:10.1002/cber.19580910113
99. Horner, L.; Hoffmann, H.; Wippel, H. G.; Klahre, G. *Chem. Ber.* **1959,** *92,* 2499–2505. doi:10.1002/cber.19590921017
100. Wadsworth, W. S., Jr.; Emmons, W. D. *J. Am. Chem. Soc.* **1961,** *83,* 1733–1738. doi:10.1021/ja01468a042
101. Moriwake, T.; Hamano, S.; Saito, S.; Torii, S. *Chem. Lett.* **1987,** 2085–2088. doi:10.1246/cl.1987.2085
102. Beaulieu, P. L.; Duceppe, J.-S.; Johnson, C. *J. Org. Chem.* **1991,** *56,* 4196–4204. doi:10.1021/jo00013a023

103. Kolodiazhnyi, O. I. *Phosphorus ylides – Chemistry and Application in Organic Synthesis;* Wiley-VCH: Weinheim, Germany, 1999; pp 9–156. doi:10.1002/9783527613908.ch02
104. Oh, J. S.; Kim, B. H.; Kim, Y. G. *Tetrahedron Lett.* **2004,** *45,* 3925–3928. doi:10.1016/j.tetlet.2004.03.101
105. Schlosser, M.; Christmann, K. F. *Angew. Chem., Int. Ed. Engl.* **1966,** *5,* 126. doi:10.1002/anie.196601261
106. Drew, M. G. B.; Harrison, R. J.; Mann, J.; Tench, A. J.; Young, R. J. *Tetrahedron* **1999,** *55,* 1163–1172. doi:10.1016/S0040-4020(98)01094-1
107. Upadhyay, P. K.; Kumar, P. *Synthesis* **2010,** 3063–3066. doi:10.1055/s-0030-1258185
108. Dondoni, A.; Merino, P.; Perrone, D. *Tetrahedron* **1993,** *49,* 2939–2956. doi:10.1016/S0040-4020(01)80389-6
109. Bordwell, F. G. *Acc. Chem. Res.* **1988,** *21,* 456–463. doi:10.1021/ar00156a004
110. Pelšs, A.; Kumpulainen, E. T. T.; Koskinen, A. M. P. *J. Org. Chem.* **2009,** *74,* 7598–7601. doi:10.1021/jo9017588
111. Blanchette, M. A.; Choy, W.; Davis, J. T.; Essenfeld, A. P.; Masamune, S.; Roush, W. R.; Sakai, T. *Tetrahedron Lett.* **1984,** *25,* 2183–2186. doi:10.1016/S0040-4039(01)80205-7
112. Paterson, I.; Yeung, K.-S.; Smaill, J. B. *Synlett* **1993,** 774–776. doi:10.1055/s-1993-22605
113. Blasdel, L. K.; Myers, A. G. *Org. Lett.* **2005,** *7,* 4281–4283. doi:10.1021/ol051785m
114. Lebel, H.; Ladjel, C. *Organometallics* **2008,** *27,* 2676–2678. doi:10.1021/om800255c
115. Still, W. C.; Gennari, C. *Tetrahedron Lett.* **1983,** *24,* 4405–4408. doi:10.1016/S0040-4039(00)85909-2

License and Terms

This is an Open Access article under the terms of the Creative Commons Attribution License (http://creativecommons.org/licenses/by/2.0), which permits unrestricted use, distribution, and reproduction in any medium, provided the original work is properly cited.

The license is subject to the *Beilstein Journal of Organic Chemistry* terms and conditions: (http://www.beilstein-journals.org/bjoc)

The definitive version of this article is the electronic one which can be found at: doi:10.3762/bjoc.9.300

Beilstein Journal of Organic Chemistry

Halogenated volatiles from the fungus *Geniculosporium* and the actinomycete *Streptomyces chartreusis*

Tao Wang, Patrick Rabe, Christian A. Citron and Jeroen S. Dickschat*

Full Research Paper

Open Access

Address:
Institut für Organische Chemie, TU Braunschweig, Hagenring 30, 38106 Braunschweig, Germany

Email:
Jeroen S. Dickschat* - j.dickschat@tu-bs.de

* Corresponding author

Keywords:
constitutional isomerism; GC-MS; natural products; organohalogen compounds; volatiles

Beilstein J. Org. Chem. **2013,** *9,* 2767–2777.
doi:10.3762/bjoc.9.311

Received: 29 August 2013
Accepted: 07 November 2013
Published: 03 December 2013

This article is part of the Thematic Series "Natural products in synthesis and biosynthesis".

Associate Editor: S. Bräse

© 2013 Wang et al; licensee Beilstein-Institut.
License and terms: see end of document.

Abstract

Two unidentified chlorinated volatiles **X** and **Y** were detected in headspace extracts of the fungus *Geniculosporium*. Their mass spectra pointed to the structures of a chlorodimethoxybenzene for **X** and a dichlorodimethoxybenzene for **Y**. The mass spectra of some constitutional isomers for **X** and **Y** were included in our databases and proved to be very similar, thus preventing a full structural assignment. For unambiguous structure elucidation all possible constitutional isomers for **X** and **Y** were obtained by synthesis or from commercial suppliers. Comparison of mass spectra and GC retention times rigorously established the structures of the two chlorinated volatiles. Chlorinated volatiles are not very widespread, but brominated or even iodinated volatiles are even more rare. Surprisingly, headspace extracts from *Streptomyces chartreusis* contained methyl 2-iodobenzoate, a new natural product that adds to the small family of iodinated natural products.

Introduction

Today several thousands of halogenated natural products are known, most of them being produced by marine organisms [1]. The majority of halogenated natural products are chlorinated or brominated, while iodinated and particularly fluorinated compounds are significantly less abundant (Table 1) [2]. Reasons for this distribution are (I) the different concentrations of the halogenides in sea water and (II) the differences in their redox potentials [3]. In terrestrial habitats local halogenide concentrations can strongly differ from those found in marine ecosystems, but the overall trend is similar, and therefore chlorine and bromine are also the most widespread halogens in natural products from terrestrial organisms.

Many biologically active halogenated secondary metabolites are known from actinomycetes including vancomycin [4], chloramphenicol [5], rebeccamycin [6], marinopyrrols [7,8], armeni-

Table 1: Approximate number of known halogenated natural products and redox potential and natural abundance of the halogenides in sea water.

Halogenide	Natural products[a]	Redox potential [V][b]	Sea water [mg L^{-1}][b]
F^-	30	+2.87	1.4
Cl^-	2200	+1.36	18100
Br^-	1900	+1.07	68
I^-	100	+0.54	0.06

[a]Estimated number of known natural products in 2002 according to reference [2]. [b]Redox potentials and concentrations in sea water as given in reference [3].

aspirols [9], and salinosporamide [10]. Also a few volatile halogenated compounds are known, e.g., from algae as summarised in a recent review [11]. Particularly interesting is the production of chloroform by termites that was estimated to account for 15% of the global chloroform emissions [12].

The introduction of halogens into natural products is catalysed by various known types of enzymes [13,14], including the $FADH_2$-dependent halogenases [15], α-ketoglutarate/Fe^{2+}-dependent halogenases [16], SAM-dependent halogenases [17,18], and vanadium-dependent haloperoxidases [19].

Here we report on the identification of two chlorinated volatile compounds from the fungus *Geniculosporium* and a iodinated volatile from *Streptomyces chartreusis*.

Results and Discussion

Chlorinated volatiles from *Geniculosporium*

The volatiles emitted by agar plate cultures of the fungus *Geniculosporium* sp. 9910 were trapped on charcoal filters by using a closed-loop stripping apparatus (CLSA) [20]. After one day of collection a solvent extract of the trapped material was analysed by GC–MS. The analytical process was performed three times to demonstrate reproducibility of the results, and a representative chromatogram is shown in Figure 1. Besides the main compound **1** and some structurally related volatiles **2** and **3** that were identified by delinating a structural proposal from the mass spectra followed by synthesis of reference compounds [21], two additional volatiles **X** and **Y** were observed in all investigated samples. Their mass spectra are shown in Figure 2.

Both volatiles were suggested to be chlorinated compounds due to their characteristic isotope patterns of the molecular ions with compound **X** containing one chlorine and volatile **Y** containing two chlorine atoms. Furthermore, a comparison of the mass spectrum of **X** to data base spectra revealed strong similarities to mass spectra of chlorodimethoxybenzenes, but the data base mass spectra of various constitutional isomers showed only marginal differences. Similarly, the mass spectrum of **Y** was very similar to data base spectra of dichlorodimethoxybenzenes, but also in this case the mass spectra of several constitutional isomers were highly similar. Therefore, the comparison of mass spectra was not a sufficient criterion for unambiguous compound identification, and thus the additional comparison of GC

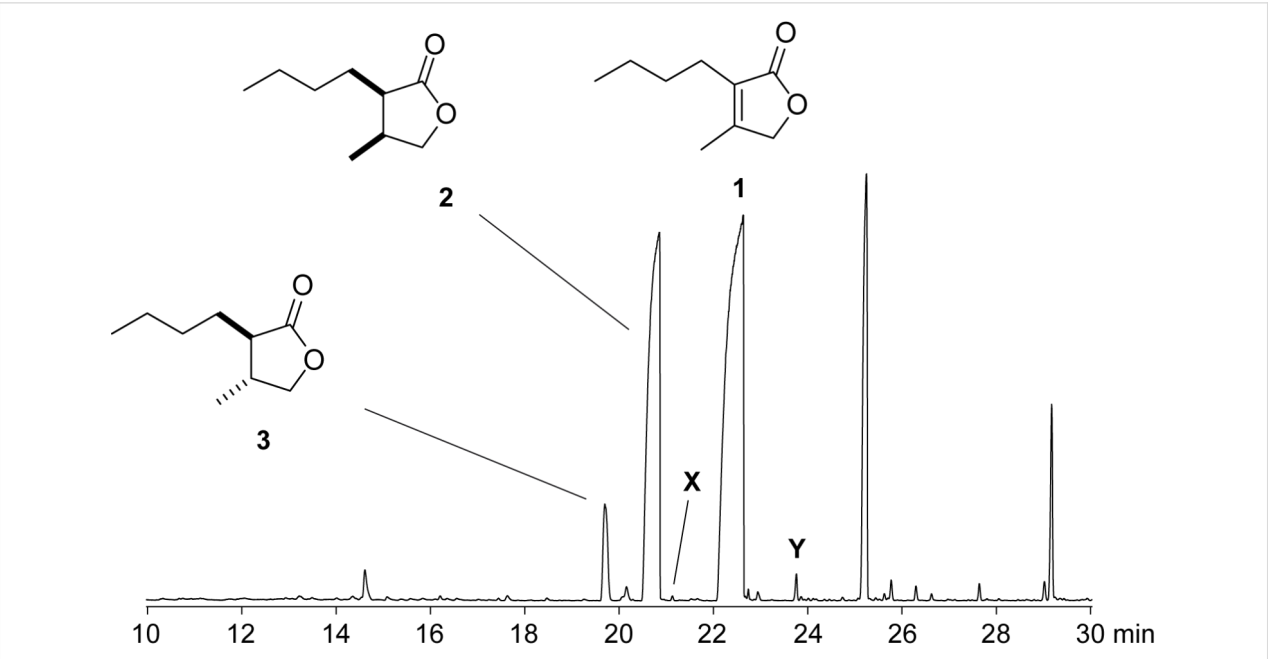


Figure 1: Total ion chromatogram of a CLSA headspace extract from *Geniculosporium*.

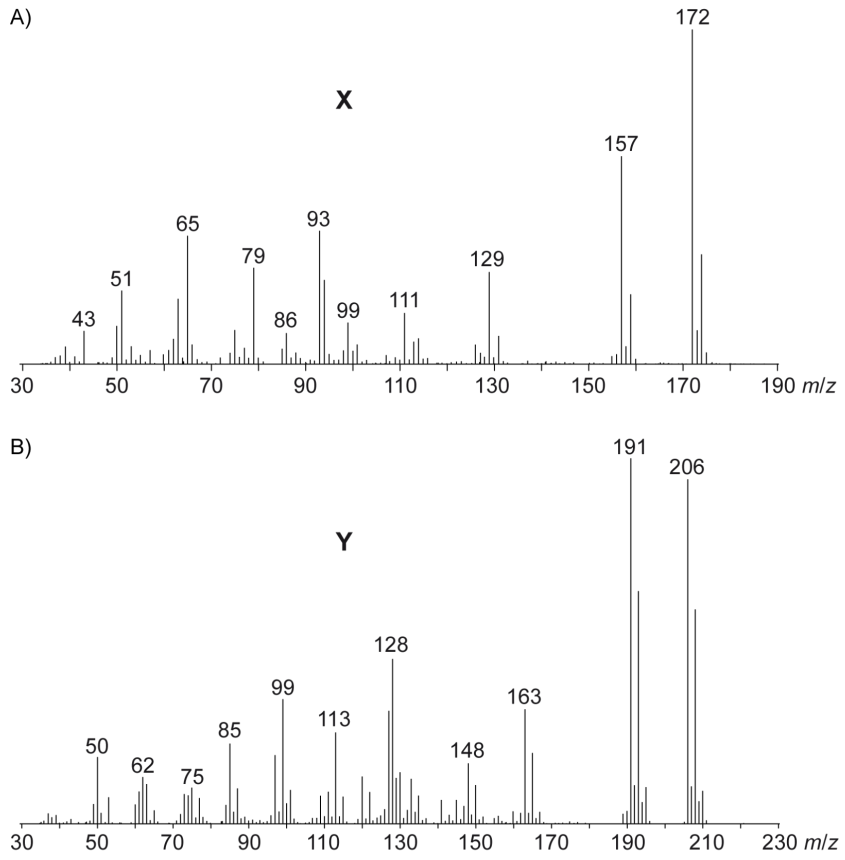


Figure 2: Mass spectra of A) the chlorinated volatile **X** and B) the chlorinated volatile **Y**.

retention indices of both natural products to authentic standards of all possible structural isomers was pursued.

The six constitutional isomers of a chlorodimethoxybenzene **4a**–**4f** as candidate structures for **X** are summarised in Figure 3. Compounds **4d** and **4e** were commercially available, while the remaining isomers were obtained by synthesis according to Scheme 1. Surprisingly, no satisfying synthetic procedure for compound **4a** was available from literature, but *ortho*-lithiation of veratrole (**5**) followed by treatment with trifluorosulfonyl chloride and triethylamine gave acceptable yields (47%). Conversion of 4-aminoveratrole (**6**) into the corresponding diazonium salt followed by a Sandmeyer reaction resulted in **4b** (61% over two steps). The isomer **4c** was efficiently prepared by double methylation of 2-chlororesorcinol (**8**) with potassium carbonate and methyl iodide in acetone (88%), while **4f** was obtained by chlorination of dimethoxybenzene **9** with benzyltrimethylammonium tetrachloroiodate in moderate yield (34%) [22]. All six compounds were subjected to GC–MS analysis using the same type of GC column as for the headspace extract from *Geniculosporium* (HP5-MS) and their retention indices together with the NMR spectroscopic data are summarised in Table 2. Mass spectra, ^{1}H and ^{13}C NMR spectra of all six compounds are given in Supporting Information File 1. The structure of **4b** was unambiguously assigned to the natural product **X** by comparison of mass spectra and retention indices (Table 2).

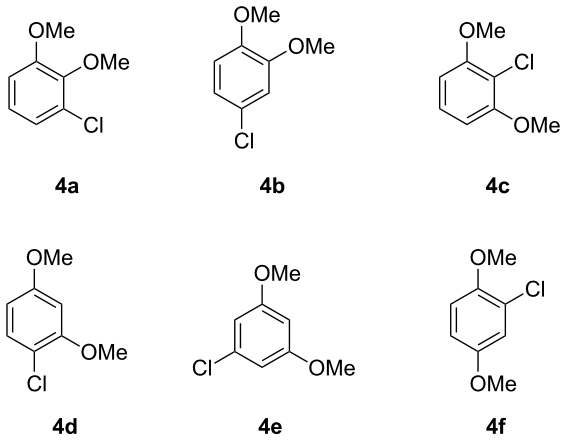
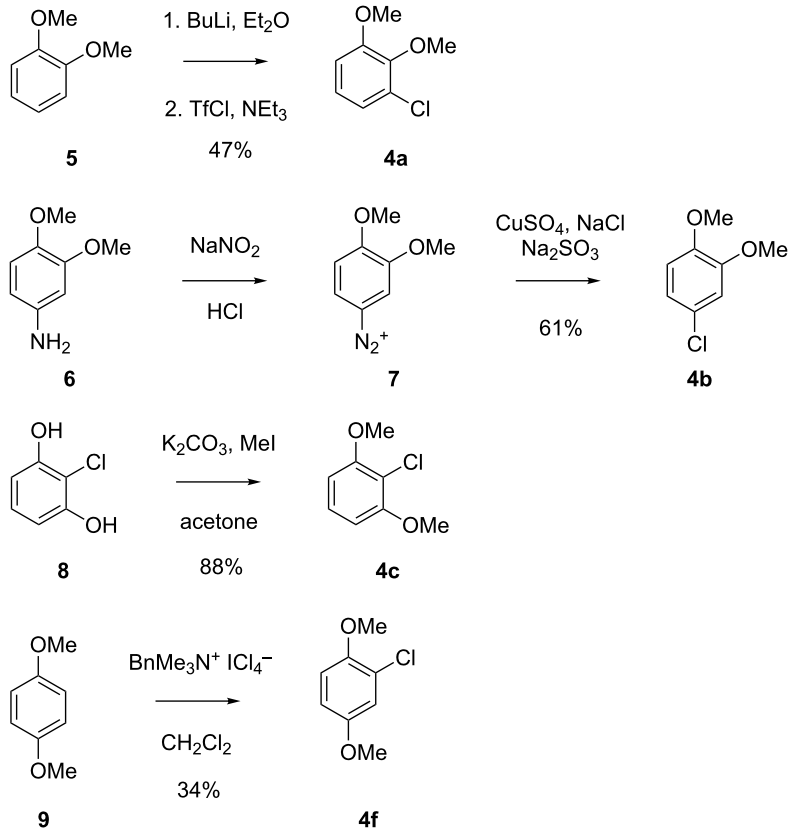


Figure 3: Constitutional isomers of chlorodimethoxybenzene as candidate structures for **X**.



Scheme 1: Synthesis of chlorodimethoxybenzenes as reference compounds for **X**.

Table 2: NMR spectroscopic data and GC retention indices of all constitutional isomers of chlorodimethoxybenzene in comparison to natural **X**.

Compound	^{1}H NMR	^{13}C NMR	*I*
4a	6.96 (m, 2H, 2 × CH) 6.81 (m, 1H, CH) 3.87 (s, 3H, OCH_3) 3.86 (s, 3H, OCH_3)	154.0 (C_q) 145.5 (C_q) 128.4 (C_q) 124.3 (CH) 122.0 (CH) 110.9 (CH) 60.6 (OCH_3) 56.1 (OCH_3)	1278
4f	6.95 (d, 1H, $^4J_{H,H}$ = 3.0 Hz, CH) 6.86 (d, 1H, $^4J_{H,H}$ = 3.0 Hz, $^3J_{H,H}$ = 9.0 Hz) 6.76 (dd, 1H, $^3J_{H,H}$ = 3.0 Hz, $^4J_{H,H}$ = 9.0 Hz, CH) 3.84 (s, 3H, OCH_3) 3.75 (s, 3H, OCH_3)	153.8 (C_q) 149.4 (C_q) 123.0 (C_q) 116.1 (CH) 113.2 (CH) 112.8 (CH) 56.7 (OCH_3) 55.8 (OCH_3)	1292
4b	6.87 (dd, 1H, $^3J_{H,H}$ = 8.5 Hz, $^4J_{H,H}$ = 2.4 Hz, CH) 6.84 (d, 1H, $^4J_{H,H}$ = 2.4 Hz, CH) 6.76 (d, 1H, $^3J_{H,H}$ = 8.5 Hz, CH) 3.85 (s, 3H, OCH_3) 3.84 (s, 3H, OCH_3)	149.5 (C_q) 147.8 (C_q) 125.6 (C_q) 120.2 (CH) 112.0 (CH) 111.9 (CH) 56.02 (OCH_3) 55.98 (OCH_3)	1322

Table 2: NMR spectroscopic data and GC retention indices of all constitutional isomers of chlorodimethoxybenzene in comparison to natural **X**. (continued)

4e	6.51 (d, 2H, $^4J_{H,H}$ = 2.2 Hz, 2 × CH) 6.34 (t, 1H, $^4J_{H,H}$ = 2.2 Hz, CH) 3.77 (s, 6H, 2 × OCH_3)	161.1 (2 × C_q) 135.2 (C_q) 106.9 (2 × CH) 99.2 (CH) 55.5 (2 × OCH_3)	1340
4d	7.24 (d, 1H, $^3J_{H,H}$ = 8.7 Hz, CH) 6.50 (d, 1H, $^4J_{H,H}$ = 2.7 Hz, CH) 6.42 (dd, 1H, $^3J_{H,H}$ = 8.7 Hz, $^4J_{H,H}$ = 2.7 Hz, CH) 3.87 (s, 3H, OCH_3) 3.79 (s, 3H, OCH_3)	159.5 (C_q) 155.6 (C_q) 130.1 (CH) 114.1 (C_q) 105.2 (CH) 100.0 (CH) 56.0 (OCH_3) 55.5 (OCH_3)	1374
4c	7.17 (t, 1H, $^3J_{H,H}$ = 8.4 Hz, CH) 6.60 (d, 2H, $^3J_{H,H}$ = 8.4 Hz, 2 × CH) 3.90 (s, 6H, 2 × OCH_3)	156.2 (2 × C_q) 127.1 (CH) 110.6 (C_q) 104.7 (2 × CH) 56.3 (2 × OCH_3)	1404
X			1322

For compound **Y** a series of eleven constitutional isomers as shown in Figure 4 were possible. All eleven compounds were obtained by synthesis as summarised in Scheme 2. The compounds **10a**, **10c**, and **10e** were obtained by treatment of 1,2,3,4-tetrachlorobenzene (**11**) with sodium methoxide in hot HMPA. This reaction is reported to yield mainly 1,2,3-trichloro-4-methoxybenzene and 1,2,4-trichloro-3-methoxybenzene by monosubstitution [23], but small amounts of disubstitution products were also formed that were rigorously purified from the mixture by repeated column chromatography. Starting from 1,2,3,5-tetrachlorobenzene (**12**) the same reaction conditions also provided a mixture of mono- and disubstitution products, but the target compounds **10f** and **10g** were obtained in better yields (29% and 17%). Derivative **10b** was prepared from 3,5-dichlorocatechol (**13**) by methylation with potassium carbonate and methyl iodide in high yield (80%). Accordingly, methylation of 4,6-dichlororesorcinol (**14**) provided **10h** in 80% yield, and methylation of 2,3-dichlorohydroquinone (**16**), prepared from benzoquinone (**15**) by treatment with SO_2Cl_2 under acidic conditions, generated **10i** (13% via two steps). Reduction of 2,6-dichlorobenzoquinone with ascorbic acid to the corresponding hydroquinone **18** followed by methylation yielded 48% of **10k**. Chlorination of veratrole (**5**) with two equivalents of benzyltrimethylammonium tetrachloroiodate resulted in **10d** (45%), while the same procedure starting from 1,4-dimethoxybenzene gave access to **10j** (38%). The NMR spectroscopic data and results of GC–MS analyses for all eleven dichlorodimethoxybenzenes in comparison to the volatile **Y** are summarised in Table 3. All mass spectra, ^1H and ^{13}C NMR spectra are shown in Supporting Information File 1. Comparison of mass spectra and retention indices unequivocally established the identity of **Y** and **10b** (Table 3).

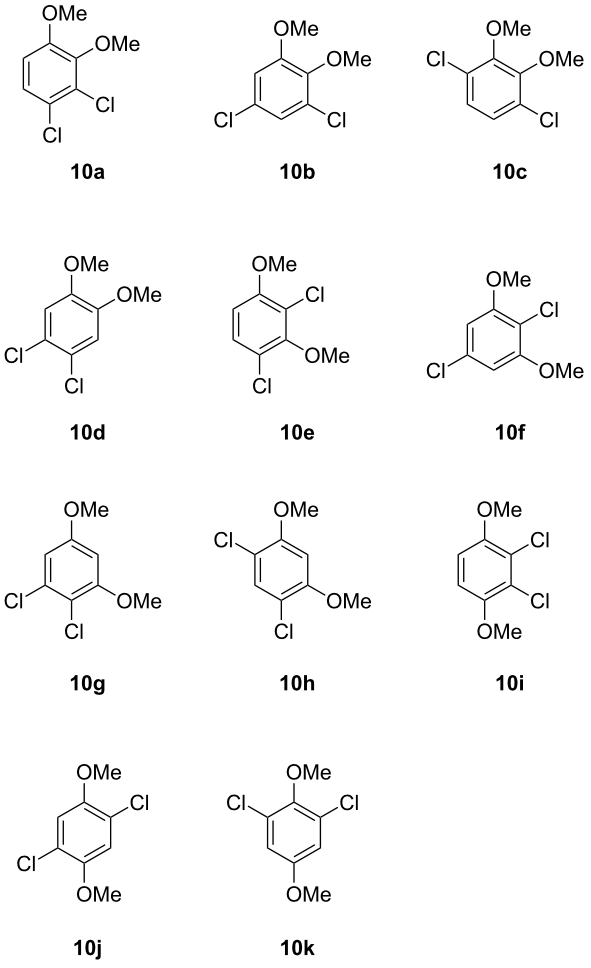
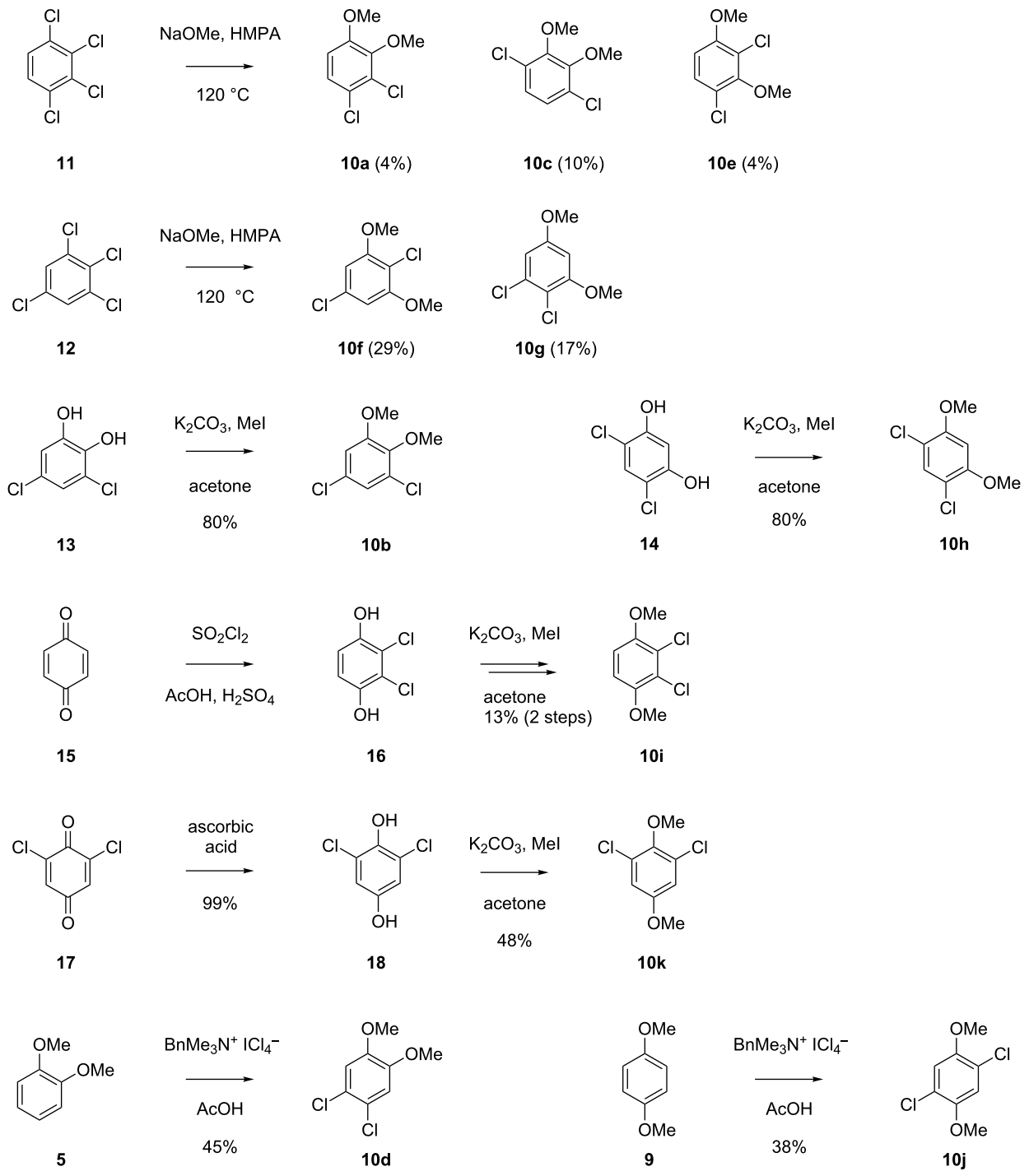


Figure 4: Constitutional isomers of dichlorodimethoxybenzene as candidate structures for **Y**.



Scheme 2: Synthesis of chlorodimethoxybenzenes as reference compounds for **Y**.

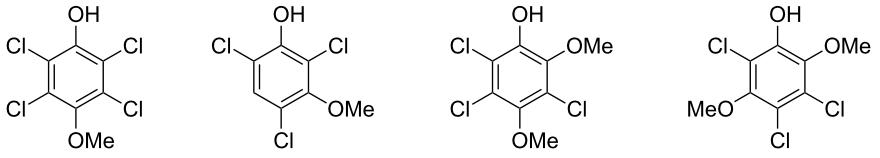
Both compounds **4b** and **10b** that were identified in this study as volatiles emitted by *Geniculosporium* have not been reported as natural products before. However, the structurally related compounds **4f** and **10k** are known from the fungus *Bjerkandera adusta* [24]. It is interesting to note that in both cases the dichlorodimethoxybenzene (**10b** or **10k**) can arise by a second chlorination from the monochlorodimethoxybenzene (**4b** or **4f**, respectively), suggesting that in both organisms the sets of chlorinated compounds arise via one and the same biosynthetic pathway. Known structurally related compounds from fungi are drosophilin A (**19**) [25] or the trichlorinated phenols **20**–**22** (Figure 5) [26]. The biological function of **4b** and **10b** in

Table 3: NMR spectroscopic data and GC retention indices of all constitutional isomers of dichlorodimethoxybenzene in comparison to natural **Y**.

Compound	^{1}H NMR	^{13}C NMR	*I* (HP5-MS)
10c	7.07 (s, 2H, 2 × CH) 3.92 (s, 6H, 2 × OCH_3)	150.7 (2 × C_q) 127.1 (2 × C_q) 125.1 (2 × CH) 61.1 (2 × OCH_3)	1339
10b	6.98 (d, 1H, $^4J_{H,H}$ = 2.5 Hz, CH) 6.80 (d, 1H, $^4J_{H,H}$ = 2.5 Hz, CH) 3.86 (s, 3H, OCH_3) 3.84 (s, 3H, OCH_3)	154.1 (C_q) 144.4 (C_q) 129.1 (C_q) 128.9 (C_q) 121.6 (CH) 111.7 (CH) 60.8 (OCH_3) 56.3 (OCH_3)	1426
10k	6.84 (s, 2H, 2 × CH) 3.84 (s, 3H, OCH_3) 3.76 (s, 3H, OCH_3)	155.7 (C_q) 146.2 (C_q) 129.5 (2 × C_q) 114.5 (2 × CH) 60.8 (OCH_3) 55.9 (OCH_3)	1443
10j	6.97 (s, 2H, 2 × CH) 3.85 (s, 6H, 2 × OCH_3)	149.2 (2 × C_q) 120.9 (2 × C_q) 114.5 (2 × CH) 56.8 (2 × OCH_3)	1448
10a	7.15 (d, 1H, $^3J_{H,H}$ = 9.0 Hz, CH) 6.76 (d, 1H, $^3J_{H,H}$ = 9.0 Hz, CH) 3.86 (s, 3H, OCH_3) 3.85 (s, 3H, OCH_3)	152.4 (Cq) 146.7 (Cq) 127.5 (Cq) 124.7 (CH) 124.5 (Cq) 111.0 (CH) 60.6 (OCH_3) 56.2 (OCH_3)	1466
10e	7.23 (d, 1H, $^3J_{H,H}$ = 9.0 Hz, CH) 6.66 (d, 1H, $^3J_{H,H}$ = 9.0 Hz, CH) 3.90 (s, 3H, OCH_3) 3.89 (s, 3H, OCH_3)	155.1 (C_q) 153.2 (C_q) 127.7 (CH) 120.7 (C_q) 118.2 (C_q) 107.9 (CH) 60.6 (OCH_3) 56.5 (OCH_3)	1487
10d	6.90 (s, 2H, 2 × CH) 3.86 (s, 6H, 2 × OCH_3)	148.3 (2 × C_q) 123.4 (2 × C_q) 112.9 (2 × CH) 56.2 (2 × OCH_3)	1505
10h	7.34 (s, 1H, CH) 6.53 (s, 1H, CH) 3.90 (s, 6H, 2 × CH_3)	154.5 (2 × C_q) 130.5 (CH) 114.0 (2 × C_q) 97.8 (CH) 56.5 (2 × OCH_3)	1545
10f	6.60 (s, 2H, 2 × CH) 3.89 (s, 6H, 2 × CH_3)	156.4 (2 × C_q) 133.0 (C_q) 109.3 (C_q) 105.5 (2 × CH) 56.5 (2 × OCH_3)	1556
10g	6.62 (d, 1H, $^4J_{H,H}$ = 2.7 Hz, CH) 6.42 (d, 1H, $^4J_{H,H}$ = 2.7 Hz, CH) 3.87 (s, 3H, OCH_3) 3.79 (s, 3H, OCH_3)	158.7 (C_q) 156.7 (C_q) 133.8 (C_q) 113.5 (C_q) 106.4 (CH) 98.6 (CH) 56.4 (OCH_3) 55.7 (OCH_3)	1565

Table 3: NMR spectroscopic data and GC retention indices of all constitutional isomers of dichlorodimethoxybenzene in comparison to natural **Y**. (continued)

10i	6.81 (s, 2H, 2 × CH) 3.86 (s, 6H, 2 × OCH_3)	150.3 (2 × C_q) 123.1 (2 × C_q) 110.0 (2 × CH) 56.8 (2 × OCH_3)	1574
Y			1426



19 **20** **21** **22**

Figure 5: Known natural products that are structurally related to **4b** and **10b** from *Geniculosporium*.

Geniculosporium is unknown, but the antibiotic activity of the related compound drosophilin A towards bacteria is well known [27].

A iodinated volatile from *Streptomyces chartreusis*

During the course of our work on volatiles from various bacteria and fungi we rarely encountered chlorinated volatiles. Brominated and iodinated volatiles are even more rare. Investigations on the volatiles released by the actinomycete *Streptomyces chartreusis* during growth on 84 GYM medium, also collected by use of a CLSA followed by GC–MS analysis of the obtained headspace extracts, led to a surprising result. The extracts contained a trace compound that was readily identified from its mass spectrum and comparison to an authentic standard as methyl 2-iodobenzoate (**23**, Figure 6A). This compound was observed as the principal compound in headspace extracts during growth of *S. chartreusis* on 84 GYM supplemented with 2-iodobenzoic acid suggesting that **23** arises by efficient methylation of the carboxylic acid (Figure 6B). 2-Iodobenzoic acid is frequently used in many chemical laboratories including ours, e.g., as a starting material for the preparation of the oxidising agents IBX and DMP. A contamination of a bacterial agar plate with traces of 2-iodobenzoic acid was assumed as a possible, albeit unlikely explanation for the formation of **23** in the bacterial cultures. In our laboratories all analytical work is strictly spatially separated from the other chemical (synthetic) work. Furthermore, a contamination with 2-iodobenzoic acid as the reason for the emission of **23** by *S. chartreusis* was excluded by the sixfold repetition of the headspace analyses during a time period of almost two years (January 2012–August 2013), using new batches of medium in all cases. Compound **23** was repeatedly detected in all six analyses which clearly supports the natural origin of this volatile.

The iodinated compound **23** has never been reported as a natural product. One of the few reported iodinated compounds is the structurally highly complex calicheamicin **24** (Figure 7) from *Micromonospora echinospora* [28] that also contains an iodinated aromatic subunit.

Conclusion

In summary, we have presented the identification of 4-chloro-1,2-dimethoxybenzene (**4b**) and 1,5-dichloro-2,3-dimethoxybenzene (**10b**) as volatile natural products released by the fungus *Geniculosporium*. Furthermore, *Streptomyces chartreusis* was shown to emit methyl 2-iodobenzoate (**23**). All three compounds are new natural products. Future work on the biological function of these metabolites and the biosynthetic pathways is now possible.

Experimental

Strains and culture conditions: *Geniculosporium* sp. 9910 was obtained from Barbara Schulz (Braunschweig) and grown on potato–carrot medium [29] on petri dishes and incubated for 21 d at 28 °C prior to analysis. *Streptomyces chartreusis* NRRL 3882 (= DSM 41447) was obtained from DSMZ (Braunschweig, Germany) and grown on 84 GYM (20.0 g rolled oats, boiled in 1 L of distilled water for 20 min, then oats were filtered off, trace element solution (1 mL) containing 1 g L^{-1}

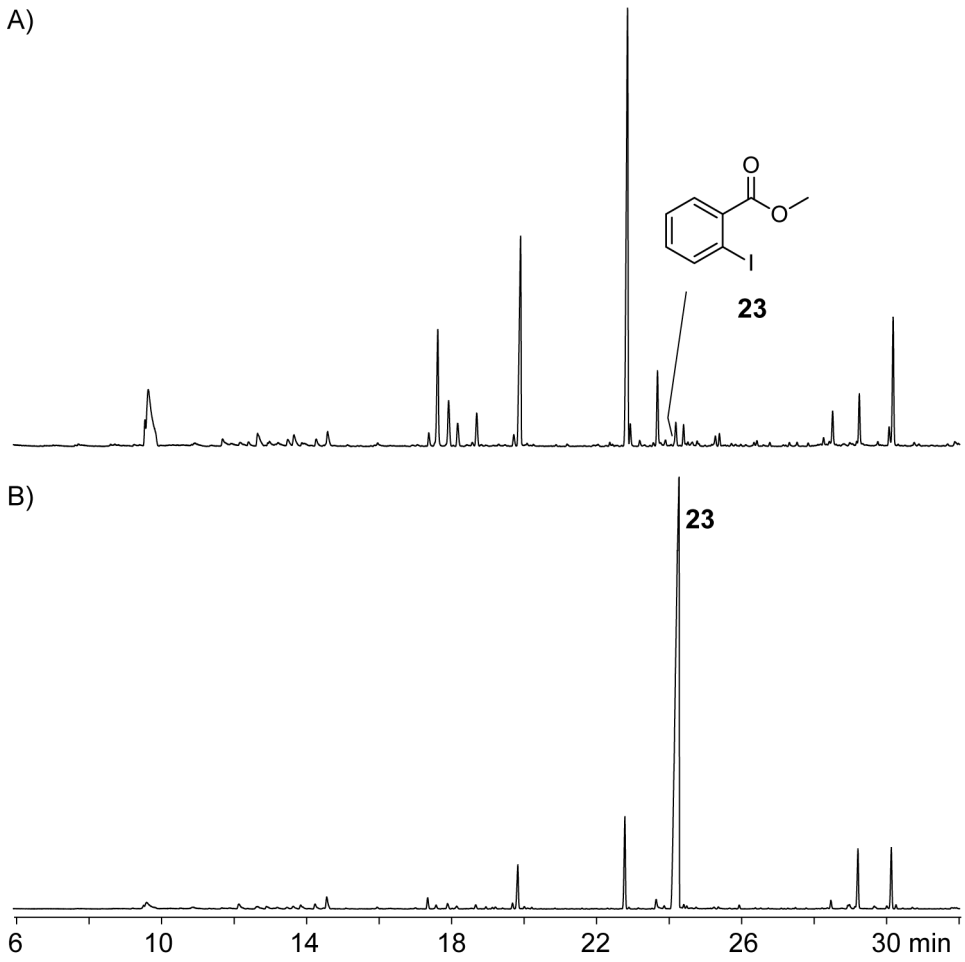


Figure 6: Total ion chromatograms of headspace extracts from *S. chartreusis*. A) Growth on 84 GYM showing production of **23** as a trace compound. B) Growth on 84 GYM amended with 2-iodobenzoic acid (1 mM) results in the emission of **23** as the principal volatile compound.

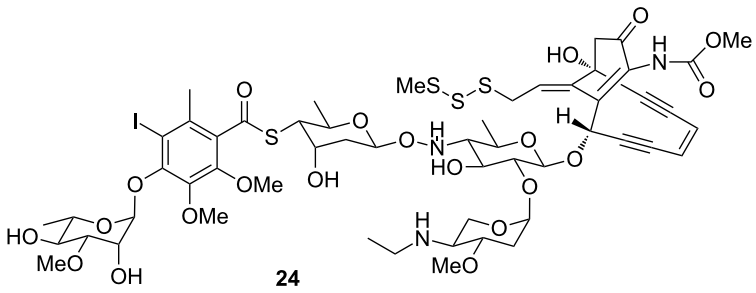


Figure 7: Calicheamicin, a known iodinated compound from the actinomycete *Micromonspora echinospora*.

$FeSO_4 \cdot 7H_2O$, 1 g L^{-1} $MnCl_4 \cdot 4H_2O$, and 1 g L^{-1} $ZnSO_4 \cdot 7H_2O$ was added, followed by sterilisation at 121 °C for 20 min).

Headspace analyses: The volatiles released by *Geniculosporium* or *Streptomyces chartreusis* were trapped by use of the CLSA (closed-loop stripping analysis) technique as described previously [30]. GC–MS analyses of the obtained headspace extracts were carried out on an Agilent 7890A connected with an Agilent 5975C inert mass detector fitted with a HP5-MS fused silica capillary column (30 m, 0.25 mm i. d., 0.25 µm film, Agilent). GC conditions were as follows: inlet pressure 77.1 kPa, He 23.3 mL min^{-1}, injection volume 1.5 µL, transfer line 300 °C, electron energy 70 eV. The operation mode was splitless (60 s valve time) and the carrier gas was He at

1.2 mL min^{-1}. The GC was programmed as follows: 5 min at 50 °C increasing with 5 °C min^{-1} to 320 °C. Retention indices (*I*) were determined from a homologous series of *n*-alkanes (C_8–C_{38}). The mass spectra of the natural compounds **X** and **Y** are shown in Figure 2. For comparison the mass spectra of all commercially available and synthetic chlorodimethoxybenzenes **4a**–**4f** and dichlorodimethoxybenzenes **10a**–**10k** are shown in Figures S1 and S2 of Supporting Information File 1. Retention indices of natural **X** and **Y** and of all chlorodimethoxybenzenes **4a**–**4f** and dichlorodimethoxybenzenes **10a**–**10k** are listed in Table 1 and Table 2.

Supporting Information

Supporting Information File 1

Synthetic procedures, characterization data, mass spectra of all isomers of chlorodimethoxybenzene and dichlorodimethoxybenzene and ^1H, ^{13}C, and DEPT spectra of all synthetic compounds.
[http://www.beilstein-journals.org/bjoc/content/supplementary/1860-5397-9-311-S1.pdf]

Acknowledgements

This work was funded by the Deutsche Forschungsgemeinschaft with an Emmy Noether fellowship (DI1536/1-3) and a Heisenberg fellowship (DI1536/4-1) (to JSD), by the State of Lower Saxony with a Ph. D scholarship (to TW), and by the Beilstein Institut zur Förderung der chemischen Wissenschaften with a Ph. D scholarship (to PR). We thank Stefan Schulz (Braunschweig) for his support.

References

1. Gribble, G. W. *Acc. Chem. Res.* **1998,** *31,* 141–152. doi:10.1021/ar9701777
2. Gribble, G. W. The Diversity of Naturally Produced Organohalogens. In *Natural Production of Organohalogen Compounds;* Gribble, G. W., Ed.; Springer-Verlag: Berlin, 2003; pp 1–15. doi:10.1007/b10445
3. Wiberg, N. *Lehrbuch der Anorganischen Chemie,* 102nd ed.; Walter de Gruyter: Berlin, 2007.
4. Sheldrick, G. M.; Jones, P. G.; Kennard, O.; Williams, D. H.; Smith, G. A. *Nature* **1978,** *271,* 223–225. doi:10.1038/271223a0
5. Ehrlich, J.; Bartz, Q. R.; Smith, R. M.; Joslyn, D. A. *Science* **1947,** *106,* 417. doi:10.1126/science.106.2757.417
6. Nettleton, D. E.; Doyle, T. W.; Krishnan, B.; Matsumoto, G. K.; Clardy, J. *Tetrahedron Lett.* **1985,** *26,* 4011–4014. doi:10.1016/S0040-4039(00)89280-1
7. Hughes, C. C.; Prieto-Davo, A.; Jensen, P. R.; Fenical, W. *Org. Lett.* **2008,** *10,* 629–631. doi:10.1021/ol702952n
8. Hughes, C. C.; Kauffman, C. A.; Jensen, P. R.; Fenical, W. *J. Org. Chem.* **2010,** *75,* 3240–3250. doi:10.1021/jo1002054
9. Couturier, C.; Bauer, A.; Rey, A.; Schroif-Dufour, C.; Broenstrup, M. *Bioorg. Med. Chem. Lett.* **2012,** *22,* 6292–6296. doi:10.1016/j.bmcl.2012.06.107
10. Fenical, W.; Jensen, P. R.; Palladino, M. A.; Lam, K. S.; Lloyd, G. K.; Potts, B. C. *Bioorg. Med. Chem.* **2009,** *17,* 2175–2180. doi:10.1016/j.bmc.2008.10.075
11. Paul, C.; Pohnert, G. *Nat. Prod. Rep.* **2011,** *28,* 186–195. doi:10.1039/c0np00043d
12. Khalil, M. A. K.; Rasmussen, R. A.; French, J. R. J.; Holt, J. A. *J. Geophys. Res.: Atmos.* **1990,** *95,* 3619–3634. doi:10.1029/JD095iD04p03619
13. Wagner, C.; El Omari, M.; König, G. M. *J. Nat. Prod.* **2009,** *72,* 540–553. doi:10.1021/np800651m
14. Blasiak, L. C.; Drennan, C. L. *Acc. Chem. Res.* **2009,** *42,* 147–155. doi:10.1021/ar800088r
15. Hammer, P. E.; Hill, D. S.; Lam, S. T.; van Pée, K. H.; Ligon, J. M. *Appl. Environ. Microbiol.* **1997,** *63,* 2147–2154.
16. Galonic, D. P.; Barr, E. W.; Walsh, C. T.; Bollinger, J. M., Jr.; Krebs, C. *Nat. Chem. Biol.* **2007,** *3,* 113–116. doi:10.1038/nchembio856
17. Eustáquio, A. S.; Pojer, F.; Noel, J. P.; Moore, B. S. *Nat. Chem. Biol.* **2008,** *4,* 69–74. doi:10.1038/nchembio.2007.56
18. Dong, C.; Huang, F.; Deng, H.; Schaffrath, C.; Spencer, J. B.; O'Hagan, D.; Naismith, J. H. *Nature* **2004,** *427,* 561–565. doi:10.1038/nature02280
19. Bernhardt, P.; Okino, T.; Winter, J. M.; Miyanaga, A.; Moore, B. S. *J. Am. Chem. Soc.* **2011,** *133,* 4268–4270. doi:10.1021/ja201088k
20. Grob, K.; Zürcher, F. *J. Chromatogr.* **1976,** *117,* 285–294. doi:10.1016/0021-9673(76)80005-2
21. Citron, C. A.; Wickel, S. M.; Schulz, B.; Draeger, S.; Dickschat, J. S. *Eur. J. Org. Chem.* **2012,** 6636–6646. doi:10.1002/ejoc.201200991
22. Kajigaeshi, S.; Shinmasu, Y.; Fujisaki, S.; Kakinami, T. *Chem. Lett.* **1989,** *18,* 415–418. doi:10.1246/cl.1989.415
23. Testaferri, L.; Tiecco, M.; Tingoli, M.; Chianelli, D.; Montanucci, M. *Tetrahedron* **1983,** *39,* 193–197. doi:10.1016/S0040-4020(01)97647-1
24. Silk, P. J.; Aubry, C.; Lonergan, G. C.; Macaulay, J. B. *Chemosphere* **2001,** *44,* 1603–1616. doi:10.1016/S0045-6535(00)00537-3
25. Anchel, M. *J. Am. Chem. Soc.* **1952,** *74,* 2943. doi:10.1021/ja01131a520
26. Swarts, H. J.; Verhagen, F. J. M.; Field, J. A.; Wijnberg, J. B. P. A. *Phytochemistry* **1998,** *49,* 203–206. doi:10.1016/S0031-9422(97)01067-4
27. Kavanagh, F.; Hervey, A.; Robbins, W. J. *Proc. Natl. Acad. Sci. U. S. A.* **1952,** *38,* 555–560. doi:10.1073/pnas.38.7.555
28. Maiese, W. M.; Lechevalier, M. P.; Lechevalier, H. A.; Korshalla, J.; Kuck, N.; Fantini, A.; Wildey, M. J.; Thomas, J.; Greenstein, M. *J. Antibiot.* **1989,** *42,* 558–563. doi:10.7164/antibiotics.42.558
29. Höller, U.; Wright, A. D.; Matthée, G. F.; König, G. M.; Draeger, S.; Aust, H.-J.; Schulz, B. *Mycol. Res.* **2000,** *104,* 1354–1365. doi:10.1017/S0953756200003117
30. Dickschat, J. S.; Wenzel, S. C.; Bode, H. B.; Müller, R.; Schulz, S. *ChemBioChem* **2004,** *5,* 778–787. doi:10.1002/cbic.200300813

License and Terms

This is an Open Access article under the terms of the Creative Commons Attribution License (http://creativecommons.org/licenses/by/2.0), which permits unrestricted use, distribution, and reproduction in any medium, provided the original work is properly cited.

The license is subject to the *Beilstein Journal of Organic Chemistry* terms and conditions: (http://www.beilstein-journals.org/bjoc)

The definitive version of this article is the electronic one which can be found at: doi:10.3762/bjoc.9.311

Beilstein Journal of Organic Chemistry

[$^2H_{26}$]-1-*epi*-Cubenol, a completely deuterated natural product from *Streptomyces griseus*

Christian A. Citron and Jeroen S. Dickschat*

Full Research Paper

Open Access

Address:
Institut für Organische Chemie, Technische Universität Braunschweig, Hagenring 30, 38106 Braunschweig, Germany

Email:
Jeroen S. Dickschat* - j.dickschat@tu-bs.de

* Corresponding author

Keywords:
biosynthesis; deuterium; labelling; natural products; *Streptomyces*; terpenes

Beilstein J. Org. Chem. **2013,** *9,* 2841–2845.
doi:10.3762/bjoc.9.319

Received: 12 September 2013
Accepted: 05 November 2013
Published: 10 December 2013

This article is part of the Thematic Series "Natural products in synthesis and biosynthesis".

Associate Editor: K. N. Ganesh

© 2013 Citron and Dickschat; licensee Beilstein-Institut.
License and terms: see end of document.

Abstract

During growth on fully deuterated medium the volatile terpene [$^2H_{26}$]-1-*epi*-cubenol was released by the actinomycete *Streptomyces griseus*. This compound represents the first completely deuterated terpene obtained by fermentation. Despite a few previous reports in the literature the operability of this approach to fully deuterated compounds is still surprising, because the strong kinetic isotope effect of deuterium is known to slow down all metabolic processes in living organisms. Potential applications of completely labelled compounds from natural sources in structure elucidation, biosynthetic or pharmacokinetic investigations are discussed.

Introduction

The actinomycete *Streptomyces griseus* is a producer of three terpenes, 2-methylisoborneol (2-MIB, **1**), (+)-caryolan-1-ol (**2**), and (+)-1-*epi*-cubenol (**3**, Figure 1). The biosynthesis of **2** and **3** requires the action of well characterized terpene cyclases [1,2], while the biosynthesis of the homomonoterpene **1** proceeds by *S*-adenosylmethionine-dependent methylation of GPP followed by a cyclisation reaction [3-5]. For biosynthetic studies on secondary metabolites isotopically labelled precursors are frequently used. Historically, the usage of radiolabelled compounds was most important, because incorporation can be detected with high sensitivity by scintillation counting or autoradiography. However, the site of incorporation was in most cases difficult to deduce, requiring a complex and laborious chemical degradation that was sometimes even performed without knowledge of the full structure of the natural product [6]. A drawback is the health risk emanating from radioactively labelled compounds, thus requiring high safety standards in their handling. Feeding experiments are today in most cases performed with stable isotopes [7]. For ^{13}C-labelled compounds the locus of incorporation can be detected by ^{13}C NMR spectroscopy. As we have recently shown the sensitivity of modern ^{13}C NMR spectrometers is even good enough for analysis of microgram amounts of isotopically enriched material in complex headspace extracts [8,9]. Deuterium is very

powerful, particularly when hydrogen shifts [10], stereospecific conversions along multistep biosynthetic pathways [11], hydride abstractions in oxidation steps [12], or deprotonations [13] are to be followed. Its incorporation is best observed by GC–MS, and if fragmentation mechanisms are known [14], the site of incorporation can be deduced from the mass spectrum. Due to the significantly shorter C–D bond compared to a C–H bond resulting in a lower polarisability and weaker interaction of the deuterated analyte with the stationary phase deuterated compounds can be gas chromatographically separated from their non-labelled counterparts [15], allowing for a detailed interpretation of the mass spectrum of a deuterated analyte. A drawback is that high incorporation rates are required to investigate the site of incorporation by ^{1}H NMR spectroscopy, but ^{2}H NMR spectroscopy offers a suitable alternative [16,17]. Furthermore, deuterium kinetic isotope effects [18] may alter product distributions in branching biosynthetic pathways, which can be useful for their mechanistic interpretation [19]. At high deuterium concentrations such kinetic isotope effects slow down all metabolic processes, and consequently only very few reports on the cultivation of microorganisms in highly deuterated media are available from the literature [20-23]. For eukaryotes high deuterium oxide concentrations are even toxic, e.g., in mice intoxication with deuterium oxide resulted in degenerative defects on multiple organs [24]. Our current research on terpene biosynthesis using stable isotope labellings prompted us to investigate whether it is possible to obtain a fully deuterated terpene by culturing a bacterium in a 100% deuterated medium. Here we report the successful production of the first completely deuterated terpene by fermentation and discuss potential applications.

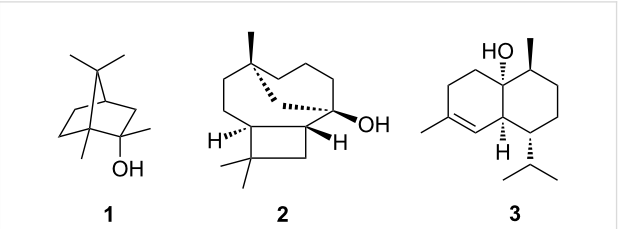


Figure 1: Terpenoids from *Streptomyces griseus*.

Results and Discussion

Streptomyces griseus was grown on agar plates containing completely deuterated minimal medium (DMM, ca. 99% deuterium) or normal 65.GYM. While the agar plate cultures on normal 65.GYM were fully grown within two days, the cultures grown on DMM agar required eight to ten days of incubation until fully grown, reflecting the significantly slowed metabolism due to a strong deuterium kinetic isotope effect. After full growth of the culture the volatiles emitted by *S. griseus* were collected on charcoal traps by use of a closed-loop stripping apparatus (CLSA) [25], followed by extraction with dichloromethane and GC–MS analysis of headspace extracts. While 2-MIB (**1**), caryolan-1-ol (**2**) and 1-*epi*-cubenol (**3**) were all produced during growth on full medium (65.GYM), consistent with previous results using other full media [26], only for **3** similar levels of production were observed on DMM (Figure 2). This demonstrated that all relevant terpene biosynthetic pathways including the deoxyxylulose phosphate pathway for the biosynthesis of the terpene monomers dimethylallyl diphosphate (DMAPP) and isopentenyl diphosphate (IPP) as well as polyisoprenoid biosynthesis for the linear precursors geranyl diphosphate (GPP) and farnesyl diphosphate (FPP) were active. However, the volatile **2** was found only in traces, while the production of **1** was completely abolished. Reasons for these findings may be that the production of **2** is under positive control of the bacterial hormone A-factor [1], and A-factor biosynthesis may be significantly delayed on DMM. It is unknown whether the biosynthesis of **1** is also A-factor controlled in *S. griseus*, but an alternative explanation for its abolished production is that the biosynthesis of **1** requires additional chemistry, i.e., a methylation step [3-5]. It is a well described phenomenon that biosynthetic pathways may be differentially expressed under variant culture conditions [27], and the respective pathway to **1** may be downregulated on DMM either due to the different carbon source in this medium or due to a generally slowed down metabolism because of the high deuterium content.

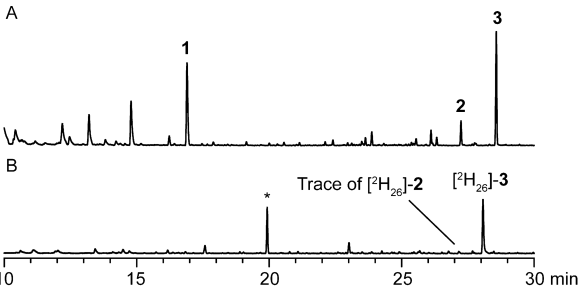


Figure 2: Total ion chromatograms of CLSA headspace extracts from *S. griseus* obtained after (A) incubation on 65.GYM agar and (B) incubation on DMM agar. The peak labelled "[$^{2}H_{26}$]-**3**" is composed of [$^{2}H_{26}$]-**3** (17%), [$^{2}H_{25}$]-**3** (50%), and [$^{2}H_{24}$]-**3** (33%), as discussed in detail below. The peak labelled with an asterisk represents a contamination with *exo*-bornyl acetate (non-deuterated) of unknown origin. Deuterated **1** could not be detected.

Deuterated **3** eluted almost 1 min earlier than unlabeled *epi*-cubenol. Its mass spectrum obtained after growth on DMM in comparison to the natural compound revealed a shifted molecular ion from m/z = 222 for the sesquiterpene alcohol **3** ($C_{15}H_{26}0$) to m/z = 248 for deuterated **3** (Figure 3), clearly indicating the uptake of up to 26 deuterium atoms. A detailed

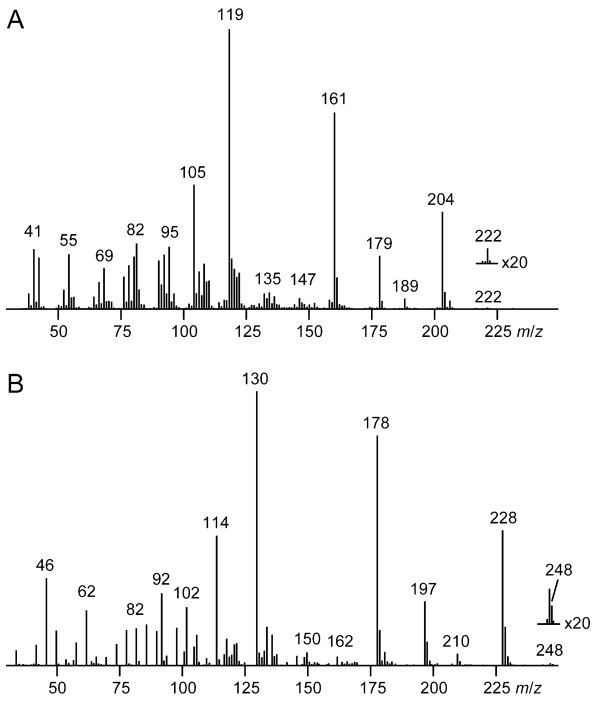


Figure 3: Mass spectra of 1-*epi*-cubenol. (A) Mass spectrum of natural **3** obtained after growth on 65.GYM; (B) mass spectrum of [$^2H_{26}$]-**3** obtained after growth on DMM.

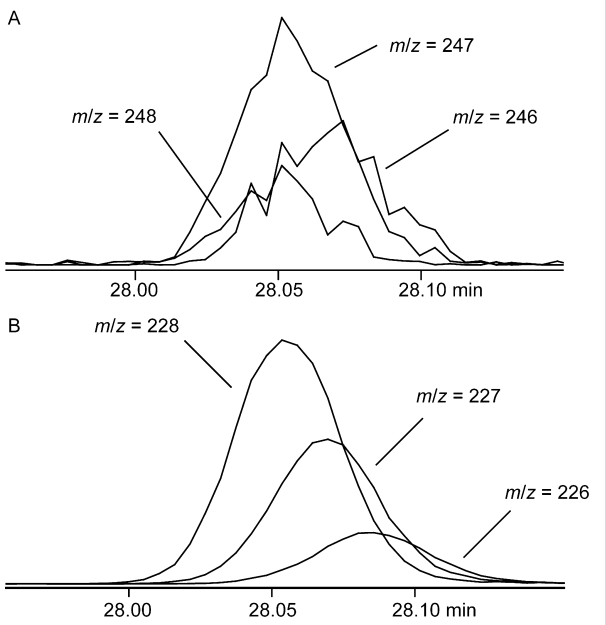


Figure 4: Ion chromatograms of fully deuterated **3** for (A) the molecular ion (*m*/*z* = 248, 247, and 246), and (B) the fragment ion arising by neutral loss of water (*m*/*z* = 228, 227, and 226).

analysis of the ion chromatograms of the ions *m*/*z* = 248, 247, and 246 (Figure 4A) demonstrated that 17% of the material were completely deuterated, while 50% of the material represented [$^2H_{25}$]-**3** and 33% were [$^2H_{24}$]-**3**. Analysis of the corresponding ion traces of the fragment ions formed by neutral loss of water (*m*/*z* = 228, 227, and 226, Figure 4B) showed that formation of these ions is mainly due to loss of HOD from [$^2H_{25}$]-**3** and, secondly, of D_2O from [$^2H_{26}$]-**3**, resulting in an abundance of the maximum deuterated fragment ion at *m*/*z* = 228 of 55%. Conclusively, the main content of ^1H resides in the alcohol function of deuterated **3** that is explained by a D–H exchange during CLSA sampling, workup of the sample, or during chromatography that can result from any contact with traces of moisture. At the same time this detailed analysis of ion chromatograms revealed that the carbon backbone of **3** is completely deuterated (only ca. 2% of the whole hydrogen content in **3** were ^1H). The major fragment ions of **3** at *m*/*z* = 204, 179, 161, 119, and 105 gave clear shifts to *m*/*z* = 228, 197, 178, 130, and 114, much clearer as in only partially deuterated compounds where H,D-scrambling along the carbon backbone is usually observed in mass spectrometric analyses. The advantage of these clear mass shifts is that the deuterium content of each fragment ion can immediately be deduced, e.g., the shift of the base peak ion from *m*/*z* = 119 to 130 points to eleven deuterium atoms. This in turn directly reveals the number of hydrogens in each of the fragment ions also for the unlabelled analyte, without the need for high resolution mass spectrometry (HRMS), similar to a recent report using ^{13}C and ^{15}N labellings for the determination of the numbers of carbons and nitrogens in a natural product [28]. Therefore, such labelling experiments using a growth medium with a deuterium content of nearly 100% offer a suitable alternative to determine the number of hydrogens in an analyte, if no HRMS instrument is available. As pointed out in Bode's study a labelling approach may even be more accurate for determination of the sum formula of a natural product, because a measured accurate mass may be in agreement with more than one molecular composition [28].

Completely deuterated compounds as exemplified by [$^2H_{26}$]-*epi*-cubenol in this work are not only a curiosity, but are also of interest to natural product chemists for the elucidation of biosynthetic pathways. Interesting options for their applications in biosynthetic studies include the use of non-labelled compounds in an inverse feeding experiment [29-31]. Such inverse feedings have a much broader scope, because many more non-labelled compounds than labelled precursors are commercially available. Deuterated compounds can also be applied in pharmacokinetic investigations by tracing the isotopic label in the catabolites of a pharmacological agent [32]. Another potential application of uniformly deuterated compounds is in neutron crystallography that takes advantage of the enhanced visibility of deuterium as compared to hydrogen [33]. Generally, deuterated compounds can synthetically be obtained by hydrogen

isotope exchange reactions using Lewis acid, transition metal or enzyme catalysis [34], but such approaches may not be suitable for terpenes that are in many cases unstable under acidic conditions or may tend to thermal rearrangements [35]. The successful formation of a completely deuterated natural product (up to 90% ^{2}H) by fermentation has recently been reported for rhamnolipids in *Pseudomonas* and sophorolipids in *Candida apicola* [36], but no examples for completely deuterated terpenes with a deuterium content of >98% as presented here are known. In conclusion, fermentation in fully deuterated medium as performed in this work may offer a good and practicable approach to many other structurally complex and completely deuterated natural products that are difficult to access by synthetic methods.

Conclusion

In summary, we have observed the first nearly 100% deuterated terpene in bacterial headspace extracts, and discussed the various potential applications of completely deuterated compounds for structure elucidations, biosynthetic or pharmacokinetic investigations that reach far beyond the initially curiosity-driven starting point of this work.

Experimental

Strain and culture conditions. The actinomycete *Streptomyces griseus* NBRC102592 was obtained from the National Biological Research Center, Chiba, Japan. Medium ingredients and dichloromethane (GC grade) were purchased from Carl Roth GmbH (Karlsruhe, Germany). Incubation was performed on regular (non-labelled) 65.GYM agar (glucose: 4.0 g, yeast extract: 4.0 g, malt extract: 10.0 g, $CaCO_3$: 2.0 g, agar: 12.0 g, H_2O: 1000 mL) for a control of terpene production under normal growth conditions, or fully deuterated minimal medium (DMM, [$^2H_8$]glycerol: 5 mL, (N^2H_4)SO_4: 1.0 g, K_2[^{2}H]PO_4: 0.5 g, $MgSO_4 \cdot 7$[$^2H_2$]O: 0.2 g, $FeSO_4 \cdot 7$[$^2H_2$]O: 0.01 g, agar: 12.0 g, [$^2H_2$]O: 1000 mL) to obtain [$^2H_{26}$]-**3**. DMM liquid culture medium was devoid of agar and $CaCO_3$. Deuterated [$^2H_8$]glycerol (99% ^{2}H) was obtained from Eurisotop (Saarbrücken, Germany), deuterium oxide (99.9% ^{2}H) was obtained from Deutero GmbH (Kastellaun, Germany), and all deuterated hydrated salts were obtained by dissolving the non-deuterated analogs in a large excess of deuterium oxide (100 equiv) followed by lyophilization. Agar that is composed of ca. 1 wt % of hydrogen atoms that are exchangable with water was added as the only unlabelled compound. The added agar (12 g L^{-1}) is equal to ca. 1 mL of water (0.1% of the medium).

Headspace analysis. For analysis of the volatiles liquid cultures were inoculated and incubated at 28 °C for 2 d (65.GYM) or 8–10 d (DMM). From these cultures 1 mL was transferred onto agar plates containing the same medium, and incubation was continued for 2 d (65.GYM) or 7–10 d (DMM). The volatile products emitted by the agar plate cultures were collected by use of a closed-loop stripping apparatus (CLSA) [25]. Briefly, in a closed apparatus containing the agar plate a circulating air stream was passed over the agar plate cultures and then through a charcoal filter (Chromtech GmbH, Idstein, Germany, Precision Char Coal Filter 5 mg) for 18–24 h. The absorbed volatiles were eluted with analytically pure dichloromethane (40–50 µL) and the extract (1 µL) was immediately analyzed by GC–MS. The rest was stored at −80 °C for future reference.

GC–MS. GC–MS analyses were carried out on an Agilent 7890A connected with an Agilent 5975C inert mass detector fitted with a HP5-MS fused silica capillary column (30 m, 0.25 mm i. d., 0.25 µm film, Agilent). Instrumental parameters were (1) inlet pressure 77.1 kPa, He 23.3 mL min^{-1}, (2) injection volume 1.5 µL, (3) transfer line 300 °C, and (4) electron energy 70 eV. The operation mode was splitless (60 s valve time) and the carrier gas was He at 1.2 mL min^{-1}. The GC was programmed as follows: 5 min at 50 °C increasing with 5 °C min^{-1} to 320 °C. Retention indices (*I*) were determined from a homologous series of *n*-alkanes (C_8–C_{38}).

Acknowledgements

We thank Stefan Schulz (Braunschweig) for support. This work was funded by the Deutsche Forschungsgemeinschaft (DFG) with an Emmy-Noether fellowship and a Heisenberg fellowship (to J.S.D., DI1536/1-3 and DI1536/4-1) and by a grant ("Duftstoffe aus Actinomyceten", DI1536/2-1).

References

1. Nakano, C.; Horinouchi, S.; Ohnishi, Y. *J. Biol. Chem.* **2011,** *286,* 27980–27987. doi:10.1074/jbc.M111.265652
2. Nakano, C.; Tezuka, T.; Horinouchi, S.; Ohnishi, Y. *J. Antibiot.* **2012,** *65,* 551–558. doi:10.1038/ja.2012.68
3. Dickschat, J. S.; Nawrath, T.; Thiel, V.; Kunze, B.; Müller, R.; Schulz, S. *Angew. Chem., Int. Ed.* **2007,** *46,* 8287–8290. doi:10.1002/anie.200702496
4. Wang, C.-M.; Cane, D. E. *J. Am. Chem. Soc.* **2008,** *130,* 8908–8909. doi:10.1021/ja803639g
5. Komatsu, M.; Tsuda, M.; Omura, S.; Oikawa, H.; Ikeda, H. *Proc. Natl. Acad. Sci. U. S. A.* **2008,** *105,* 7422–7427. doi:10.1073/pnas.0802312105
6. Birch, A. J.; Richards, R. W.; Smith, H. *Tetrahedron* **1959,** *7,* 241–251. doi:10.1016/S0040-4020(01)93192-8
7. Vederas, J. C. *Nat. Prod. Rep.* **1987,** *4,* 277–337. doi:10.1039/np9870400277
8. Brock, N. L.; Ravella, S. R.; Schulz, S.; Dickschat, J. S. *Angew. Chem., Int. Ed.* **2013,** *52,* 2100–2104. doi:10.1002/anie.201209173
9. Brock, N. L.; Dickschat, J. S. *ChemBioChem* **2013,** *14,* 1189–1193. doi:10.1002/cbic.201300254

10. Citron, C. A.; Riclea, R.; Brock, N. L.; Dickschat, J. S. *RSC Adv.* **2011,** *1,* 290–297. doi:10.1039/c1ra00212k
11. Citron, C. A.; Brock, N. L.; Rabe, P.; Dickschat, J. S. *Angew. Chem., Int. Ed.* **2012,** *51,* 4053–4057. doi:10.1002/anie.201201110
12. Brock, N. L.; Tudzynski, B.; Dickschat, J. S. *ChemBioChem* **2011,** *12,* 2667–2676. doi:10.1002/cbic.201100516
13. Chou, W. K. W.; Fanizza, I.; Uchiyama, T.; Komatsu, M.; Ikeda, H.; Cane, D. E. *J. Am. Chem. Soc.* **2010,** *132,* 8850–8851. doi:10.1021/ja103087w
14. McLafferty, F. W.; Turecek, F. *Interpretation of Mass Spectra,* 4th ed.; University Science Books: Sausalito, 1993.
15. Dickschat, J. S.; Citron, C. A.; Brock, N. L.; Riclea, R.; Kuhz, H. *Eur. J. Org. Chem.* **2011,** 3339–3346. doi:10.1002/ejoc.201100188
16. Cane, D. E.; Buchwald, S. L. *J. Am. Chem. Soc.* **1977,** *99,* 6132–6134. doi:10.1021/ja00460a065
17. Scott, F. E.; Simpson, T. J.; Trimble, L. A.; Vederas, J. C. *J. Chem. Soc., Chem. Commun.* **1984,** 756–758. doi:10.1039/C39840000756
18. Bell, R. P. *Chem. Soc. Rev.* **1974,** *3,* 513–544. doi:10.1039/cs9740300513
19. Zu, L.; Xu, M.; Lodewyk, M. W.; Cane, D. E.; Peters, R. J.; Tantillo, D. J. *J. Am. Chem. Soc.* **2012,** *134,* 11369–11371. doi:10.1021/ja3043245
20. Lovett, S. *Nature* **1964,** *203,* 429–430. doi:10.1038/203429a0
21. de Giovanni, R.; Zamenhof, S. *Biochem. J.* **1963,** *87,* 79–82.
22. de Giovanni, R. *Z. Vererbungsl.* **1961,** *92,* 389–402. doi:10.1007/BF00890060
23. Hirai, K.; Tomida, M.; Kikuchi, Y.; Ueda, O.; Ando, H.; Asanuma, N. *Bull. Tokyo Dent. Coll.* **2010,** *51,* 175–183. doi:10.2209/tdcpublication.51.175
24. Dybing, O.; Guldberg, G.; Hansen, K. *Klin. Wochenschr.* **1938,** *17,* 1585. doi:10.1007/BF01777243
25. Grob, K.; Zürcher, F. *J. Chromatogr.* **1976,** *117,* 285–294. doi:10.1016/0021-9673(76)80005-2
26. Citron, C. A.; Gleitzmann, J.; Laurenzano, G.; Pukall, R.; Dickschat, J. S. *ChemBioChem* **2012,** *13,* 202–214. doi:10.1002/cbic.201100641
27. Bode, H. B.; Bethe, B.; Höfs, R.; Zeeck, A. *ChemBioChem* **2002,** *3,* 619–627. doi:10.1002/1439-7633(20020703)3:7<619::AID-CBIC619>3.0.CO;2-9
28. Bode, H. B.; Reimer, D.; Fuchs, S. W.; Kirchner, F.; Dauth, C.; Kegler, C.; Lorenzen, W.; Brachmann, A. O.; Grün, P. *Chem.–Eur. J.* **2012,** *18,* 2342–2348. doi:10.1002/chem.201103479
29. Barber, J.; Staunton, J. *J. Chem. Soc., Perkin Trans. 1* **1980,** 2244–2248. doi:10.1039/P19800002244
30. Joyce, S. A.; Brachmann, A. O.; Glazer, I.; Lango, L.; Schwär, G.; Clarke, D. J.; Bode, H. B. *Angew. Chem., Int. Ed.* **2008,** *47,* 1942–1945. doi:10.1002/anie.200705148
31. Brachmann, A. O.; Forst, S.; Furgani, G. M.; Fodor, A.; Bode, H. B. *J. Nat. Prod.* **2006,** *69,* 1830–1832. doi:10.1021/np060409n
32. Gelijkens, C. F.; van Peer, A.; Lenoir, H.; Knaeps, A.; Woestenborghs, R.; Heykants, J. *Biomed. Mass Spectrom.* **1985,** *12,* 38–42. doi:10.1002/bms.1200120108
33. Blakeley, M. P.; Langan, P.; Niimura, N.; Podjarny, A. *Curr. Opin. Struct. Biol.* **2008,** *18,* 593–600. doi:10.1016/j.sbi.2008.06.009
34. Junk, T.; Catallo, W. J. *Chem. Soc. Rev.* **1997,** *26,* 401–406. doi:10.1039/cs9972600401
35. Adio, A. M. *Tetrahedron* **2009,** *65,* 1533–1552. doi:10.1016/j.tet.2008.11.050
36. Smyth, T. J.; Perfumo, A.; Marchant, R.; Banat, I. M.; Chen, M.; Thomas, R. K.; Penfold, J.; Stevenson, P. S.; Parry, N. J. *Appl. Microbiol. Biotechnol.* **2010,** *87,* 1347–1354. doi:10.1007/s00253-010-2592-5

License and Terms

This is an Open Access article under the terms of the Creative Commons Attribution License (http://creativecommons.org/licenses/by/2.0), which permits unrestricted use, distribution, and reproduction in any medium, provided the original work is properly cited.

The license is subject to the *Beilstein Journal of Organic Chemistry* terms and conditions: (http://www.beilstein-journals.org/bjoc)

The definitive version of this article is the electronic one which can be found at: doi:10.3762/bjoc.9.319

Beilstein Journal of Organic Chemistry

SF002-96-1, a new drimane sesquiterpene lactone from an *Aspergillus* species, inhibits survivin expression

Silke Felix[1], Louis P. Sandjo[2], Till Opatz[*2] and Gerhard Erkel[*3]

Full Research Paper

Open Access

Address:
[1]Institute of Biotechnology and Drug Research (IBWF), Erwin-Schrödinger-Straße 56, D-67663 Kaiserslautern, Germany, [2]Institute of Organic Chemistry, University of Mainz, Duesbergweg 10–14, D-55128 Mainz, Germany, and [3]Department of Molecular Biotechnology and Systems Biology, University of Kaiserslautern, Paul-Ehrlich-Straße 23, D-67663 Kaiserslautern, Germany

Email:
Till Opatz[*] - opatz@uni-mainz.de; Gerhard Erkel[*] - erkel@bio.uni-kl.de

* Corresponding author

Keywords:
apoptosis; inhibitor; natural products; secondary metabolite; structure elucidation; survivin

Beilstein J. Org. Chem. **2013,** *9,* 2866–2876.
doi:10.3762/bjoc.9.323

Received: 11 September 2013
Accepted: 13 November 2013
Published: 13 December 2013

This article is part of the Thematic Series "Natural products in synthesis and biosynthesis".

Guest Editor: J. S. Dickschat

© 2013 Felix et al; licensee Beilstein-Institut.
License and terms: see end of document.

Abstract

Survivin, a member of the IAP (inhibitor of apoptosis) gene family, is overexpressed in virtually all human cancers and is functionally involved in the inhibition of apoptosis, regulation of cell proliferation, metastasis and resistance to therapy. Because of its upregulation in malignancy, survivin has currently attracting considerable interest as a new target for anticancer therapy. In a screening of approximately 200 strains of imperfect fungi for the production of inhibitors of survivin promoter activity, a new drimane sesquiterpene lactone, SF002-96-1, was isolated from fermentations of an *Aspergillus* species. The compound inhibited survivin promoter activity in transiently transfected Colo 320 cells in a dose dependent manner with IC_{50} values of 3.42 µM (1.3 µg/mL). Moreover, it also reduced mRNA levels and protein synthesis of survivin and triggered apoptosis.

Introduction

Survivin, a member of the inhibitor of apoptosis (IAP) protein family is one of the most prominent cancer-associated proteins identified to date, being upregulated in almost all human cancer types while usually undetectable in normal terminally differentiated adult tissues [1,2]. It plays a key role in both apoptosis and control of cell cycle progression and high expression of survivin in tumors correlates with increased drug resistance, an accelerated rate of recurrence and poor patient survival [3,4]. Survivin blocks apoptosis by protein–protein interactions via its characteristic baculovirus IAP repeat domain (BIR) resulting in the formation of a complex with hepatitis B X-interacting protein bound to caspase 9 that prevents recruitment of apop-

totic protease activating factor 1 (Apaf-1) to the apoptosome and enhancement of X-linked inhibitor of apoptosis (XIAP)-mediated caspase 3 and 9 inhibition [5,6]. In addition, survivin plays an important role in controlling cell division. In normal differentiated tissues the expression of survivin is cell cycle-regulated with an expression maximum in G2/M phase [7]. During mitosis, survivin is associated in the chromosomal passenger complex (CPC), a multi-protein complex, including the proteins Aurora B kinase, inner centromere protein (INCENP) and Borealin/Dasra-B. In this complex, survivin promotes mitosis by mediating the segregation of sister chromatids, stabilization of microtubules in late mitosis and acting as an interphase between the centromere/central spindle and the CPC [8,9]. Furthermore, survivin shuttles between the nucleus and the cytoplasm where the dynamic intracellular localization is regulated by active nuclear export. Nuclear survivin has been described to control cell division whereas cytoplasmic survivin plays a role in cytoprotection. Several studies have shown a correlation between overexpression of cytoplasmic survivin and a poor outcome in various types of cancer although nuclear survivin has also been associated with a poor prognosis in cancer patients [10-12]. Given the critical role of survivin in cancer progression and treatment resistance, survivin has been emerged as an attractive target for new anticancer therapeutics [13]. In a search for new inhibitors of survivin expression from natural sources, we found that cultures of *Aspergillus* sp. strain IBWF002-96 produced a new drimane sesquiterpene lactone, SF002-96-1, with inhibitory activity on survivin promoter activity in transiently transfected Colo 320 cells. In the current study, the fermentation, structure elucidation, and some biological properties of the compound are described.

Results and Discussion

Identification and structure elucidation

SF002-96-1 was obtained by a bio-guided isolation procedure as a colourless oil. It gave a pseudo-molecular ion of *m*/*z* 403.2090 (calcd for $[C_{21}H_{32}O_6 + Na]^+$, 403.2097) in its HR-ESI mass spectrum. The composition accounted for six double bond equivalents and a characteristic absorption band for α,β-unsaturated γ-lactones was revealed in the UV spectrum at 207 nm. This was supported by IR absorption bands at 1757 and 1632 cm^{-1}. Apart from that, absorption bands of an OH-group (3411 cm^{-1}) and ester function (1737 cm^{-1}) were revealed in the IR spectrum of the compound. The NMR spectra disclosed four CH_3 groups (δ 0.97/32.6, 1.15/24.9, 1.04/12.8, and 0.87/14.2), seven CH_2 groups (δ 1.28/31.9, 1.30/23.0, 1.59/25.1, 2.32/35.1, (1.34, 1.37)/42.7, (1.57, 1.66)/28.2, and (4.23, 4.48)/77.4), four CH groups (δ 1.94/45.7, 4.02/70.7, 5.72/67.0, and 6.57/133.5) and six quaternary carbons (δ 34.0, 44.7, 77.0, 133.8, 169.8, and 173.5, Table 1).

Table 1: ^1H (600 MHz) and ^{13}C NMR (150 MHz) data of SF002-96-1 in CD_3CN.

Position	δ_H (multiplicity, coupling constant)	δ_C
1	4.02 (dd, 4.4, 11.9 Hz, 1H)	70.7
2	1.57 (m, 1H), 1.66 (m, 1H)	28.2
3	1.34 (m, 1H), 1.37(m, 1H)	42.7
4	–	34.0
5	1.94 (overlapped with the solvent peak)	45.7
6	5.72 (dd, 4.0, 4.7 Hz, 1H)	67.0
7	6.57 (d, 4.0 Hz, 1H)	133.5
8	–	133.8
9	–	77.0
10	–	44.7
11	4.23 (d, 10.5 Hz, 1H), 4.48 (d, 10.5 Hz, 1H)	77.4
12	–	169.8
13	1.15 (s, 3H)	24.9
14	0.97 (s, 3H)	32.6
15	1.04 (s, 3H)	12.8
1′	–	173.5
2′	2.32 (m, 2H)	35.1
3′	1.59 (m, 2H)	25.1
4′	1.30 (m, 2H)	23.0
5′	1.28 (m, 2H)	31.9
6′	0.87 (t, 7.0 Hz, 3H)	14.2
OH-1	2.96 (br s, 1H)	–
OH-9	3.76 (br s, 1H)	–

The proton signal at δ 4.02 showed a COSY contact with methylene protons at δ 1.57 and 1.66 while the latter presented the same correlation with methylene protons at δ 1.34 and 1.37. The protons of two geminal methyl groups (δ 0.97, 1.15) displayed HBMC correlations with the methine carbon at δ 45.7, a quaternary carbon at δ 34.0 and the methylene carbon at δ 42.7 bearing protons at δ 1.34 and 1.37. Furthermore, a methyl group at δ 1.04 correlated with the oxymethine at δ 70.7, a methine at δ 45.7, and two quaternary carbons at δ 44.6 and 77.0. The correlations from the COSY spectrum between the proton signals at δ 1.94 and 5.72, as well as between those at δ 5.72 and 6.57 in conjunction with HMBC correlations observed between the proton signal at δ 6.57 and quaternary carbons at δ 77.0 and 133.8 suggested a decalin core for SF002-96-1. Further HMBC correlations disclosed between the signals at δ 6.57 and 169.8 as well as between the methylene protons at δ 4.23 and 4.48 and the carbons at δ 44.6, 77.0, 133.8, and 169.8 suggested SF002-96-1 to be a drimane sesquiterpene (Figure 1).

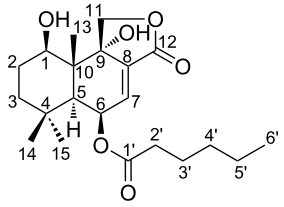


Figure 1: Structure of SF002-96-1.

The proton signals of the methyl group (δ 0.87), four methylene groups (δ 1.28, 1.30, 1.59 and 2.32) and a carbonyl group (δ 173.5) constituted an *n*-hexanoyl chain. This conclusion was supported by correlations found in the COSY and HMBC spectra (Figure 2).

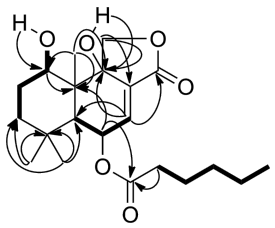


Figure 2: COSY (bold) and HMBC (arrow) correlations of SF002-96-1.

The latter NMR data indicated that the side chain was attached to the allylic oxymethine in the drimane scaffold based on a HMBC contact between the proton signal at δ 5.72 and the carbonyl of the side chain (δ 173.5). The relative configuration was deduced from NOESY data. Thus, protons of a methyl group at δ 1.04 showed NOE correlations with those of one of the geminal methyl groups (δ 1.15) and one of the oxymethylene protons (δ 4.48) of the lactone ring (Figure 3).

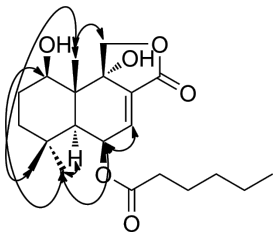


Figure 3: NOESY correlations of SF002-96-1.

Besides, the protons of the second geminal methyl group (δ 0.97) showed spatial correlations with a methine proton at δ 1.94 and two downfield protons at δ 4.02 and 5.72. Based on the absolute configuration reported for drimane sesquiterpenes [14,15], the *trans*-decalin core of SF002-96-1 was tentatively assigned the configurations *R*, *S*, *R*, *S*, and *R*, at C-1, C-5, C-6, C-9, and C-10, respectively. The foregoing data led to identify SF002-96-1 as (5*R*,5a*S*,9*R*,9aR,9bS)-9,9b-dihydroxy-6,6,9a-trimethyl-3-oxo-1,3,5,5a,6,7,8,9,9a,9b-decahydronaphtho[1,2-*c*]furan-5-yl hexanoate.

Biological activity

For the identification of active secondary metabolites and the characterization of their influence on survivin expression, we employed a human survivin-promoter dependent transcriptional reporter in the transiently transfected human colorectal carcinoma cell line Colo 320. Due to the overexpression of survivin in many human cancers, including colon cancer, a strong constitutive luciferase activity could be observed 24 h after transfection caused by the binding of transcription factors to the regulatory sites of the survivin gene [16]. As shown in Figure 4A, SF002-96-1 inhibited survivin promoter activity in a dose dependent manner with an IC_{50} value of 3.42 μM (1.3 μg/mL), whereas the constitutive activity of the CMV promoter was not affected at concentrations up to 10.5 μM (4 μg/mL) indicating that the compound does not interfere with transcription in a general manner.

The expression of the survivin gene is regulated by a number of transcription factors including Stat3, NF-κB and the β-catenin activated T-cell factor (TCF) [17]. Constitutive activation of Stat3 by paracrine and autocrine mechanisms has been detected in diverse human cancer cell lines and tissues which contribute to oncogenesis by promoting cell proliferation and inhibiting apoptosis by increasing the expression of anti-apoptotic genes such as survivin [18]. We therefore investigated the effect of SF002-96-1 on Stat3-driven expression of the reporter gene luciferase in IL-6 stimulated Colo 320 cells. The compound

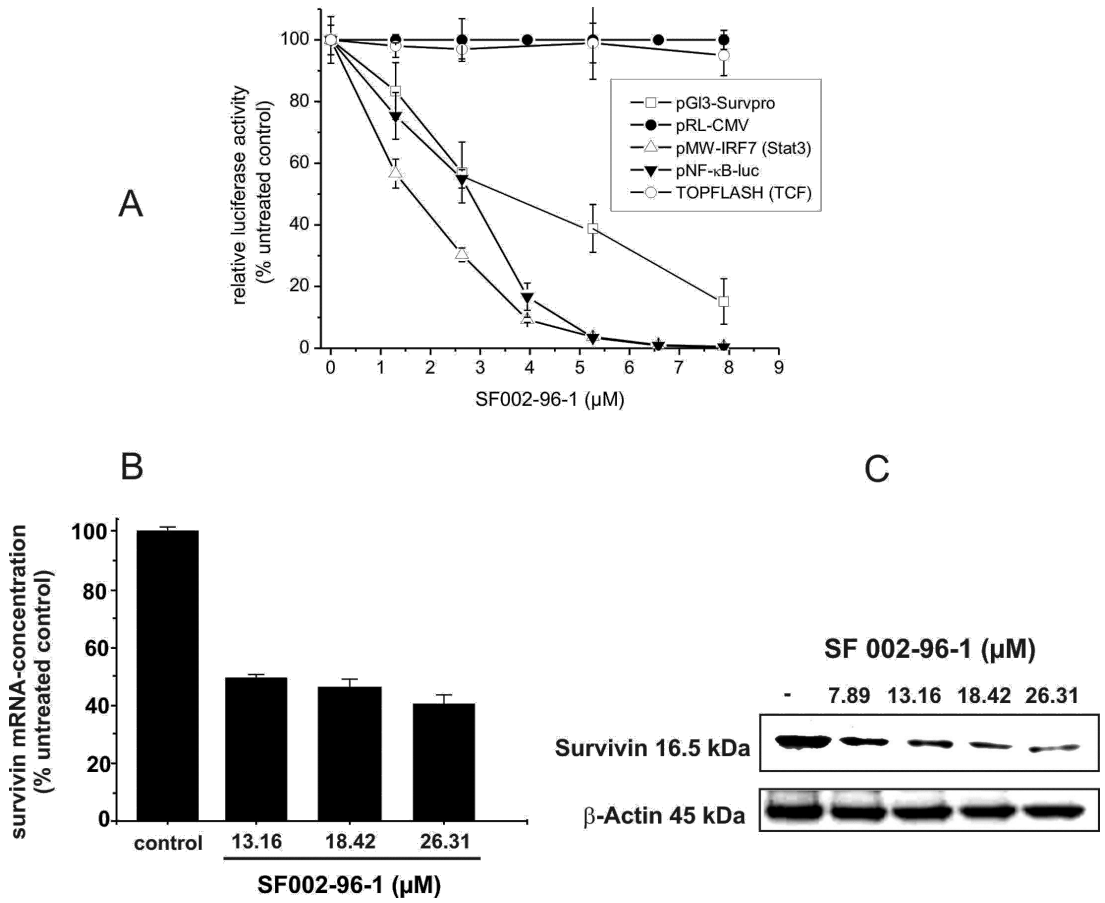


Figure 4: Effect of SF002-96-1 on survivin promoter activity, survivin mRNA levels and expression. (A) Colo 320 cells were transiently transfected with a human survivin-, CMV-, or β-catenin/TCF-dependent reporter construct for 24 h with or without test compound. Control (100%): untreated cells only. For NF-κB- and Stat3-driven reporter gene expression, cells were transfected with the indicated reporter gene construct and stimulated with 10 ng/mL TNF-α, 5 ng/mL IL-1β (for pNF-κB-luc) or 10 ng/mL IL-6 (for Stat3 dependent pMW-IRF7) with or without test compound for 24 h. Control: (100%): stimulation only. Results represent the mean ± SD of at least three independent experiments. The expression of the reporter gene was determined as described in the experimental section. (B) Effect on survivin mRNA levels. Colo 320 cells were treated with different concentrations of SF002-96-1 for 8 h. mRNA levels of survivin were measured by real-time PCR as described in the experimental section. Control (100%): untreated cells. Results represent the mean ± SD of at least three independent experiments. (C) Western blot analysis for survivin. Colo 320 cells were treated with different concentrations of SF002-96-1 for 8 h. Subsequently total cell extracts were prepared and analyzed by Western blot analyses. β-Actin was used as internal control.

strongly inhibited the Stat3-dependent luciferase expression with an IC_{50} value of 1.6 µM (0.6 µg/mL). In addition to Stat3, the response of the survivin promoter construct also depends on the transcription factor NF-κB [19] and as shown in Figure 4A, SF002-96-1 inhibited the inducible NF-κB-dependent reporter gene expression in Colo 320 cells with an IC_{50} value of 2.63 µM (1 µg/mL). Previous studies in colon cancer cells have shown that regulation of survivin expression is, in addition, TCF/β-catenin dependent mediated by three TCF/β-catenin consensus sequences within the survivin promoter [20]. Dysregulation of TCF/β-catenin dependent gene regulation originating from aberrantly stabilized β-catenin or mutations in the associated protein adenomatous polyposis coli (APC) results in the activation of target genes implicated in cell proliferation and transformation [21]. We therefore investigated the effect of SF002-96-1 on canonical Wnt signaling using a synthetic TCF-responsive reporter (TOPFLASH) in Colo 320 cells which contain a truncated APC protein [22] and therefore display high constitutive TCF/β-catenin transcription. Interestingly, SF002-96-1 showed no significant inhibition of the TCF/β-catenin dependent luciferase expression up to the highest concentration tested (8 µM).

To investigate the effect of the compound on the transcription of the survivin gene, quantitative real-time PCR experiments were performed with total RNA isolated from Colo 320 cells treated with different concentrations of the test compound for 8 h as described in the experimental section. As illustrated in Figure 4B, application of 18.42 µM (7 µg/mL) SF002-96-1 reduced the survivin mRNA level in Colo 320 cells by around

50%. To confirm the data obtained from the qRT-PCR experiments, Western blot experiments were performed for survivin protein expression. As shown in Figure 4C, SF002-96-1 significantly reduced endogenous survivin protein level starting at 13.16 µM (5 µg/mL) after 8 h treatment which suggests that the suppression of survivin by SF002-96-1 is through the transcriptional inhibition of the survivin gene promoter.

To further investigate whether the fungal compound could affect the binding of Stat3 and NF-κB to the survivin promoter in living cells, we performed ChIP assays with primers covering suggested Stat3 and NF-κB (p65) binding sites [23,24]. Q-PCR of the −1231/−1009 (primers Sat3_1), −131/+46 (primers Stat3_2) and −920/−773 (primers Stat3_3) regions of the survivin promoter with Stat3-immunoprecipitated and IL-6 treated samples resulted in a strong induction of Stat3 binding to the two distal as well as to the proximal binding sites of the survivin promoter (Figure 5).

Pretreatment of the cells with 18.42 µM SF002-96-1 resulted in a strong reduction of Stat3 binding to all binding sites in the survivin promoter. ChIP experiments with primers comprising the suggested proximal NF-κB p65 binding site surrounding the transcriptional start site revealed a reduction of p65 binding after stimulation of NF-κB activity with 10 ng/mL TNF-α, 5 ng/mL IL-1β and treatment of the cells with the fungal compound (Figure 5), corroborating the results obtained in the reporter gene assays. As a control, we investigated the influence of the compound on the binding of lysine9 acetylated histone H3 (H3K9Ac) to the constitutive *gapdh* promoter as a marker for accessible chromatin that is transcriptionally active. SF002-96-1 did not significantly affect the levels of H3K9Ac in the constitutive *gpdh* promoter (Figure 5). These results indicate that the compound inhibits survivin expression by preventing the DNA binding of Stat3 and NF-κB transcription factors.

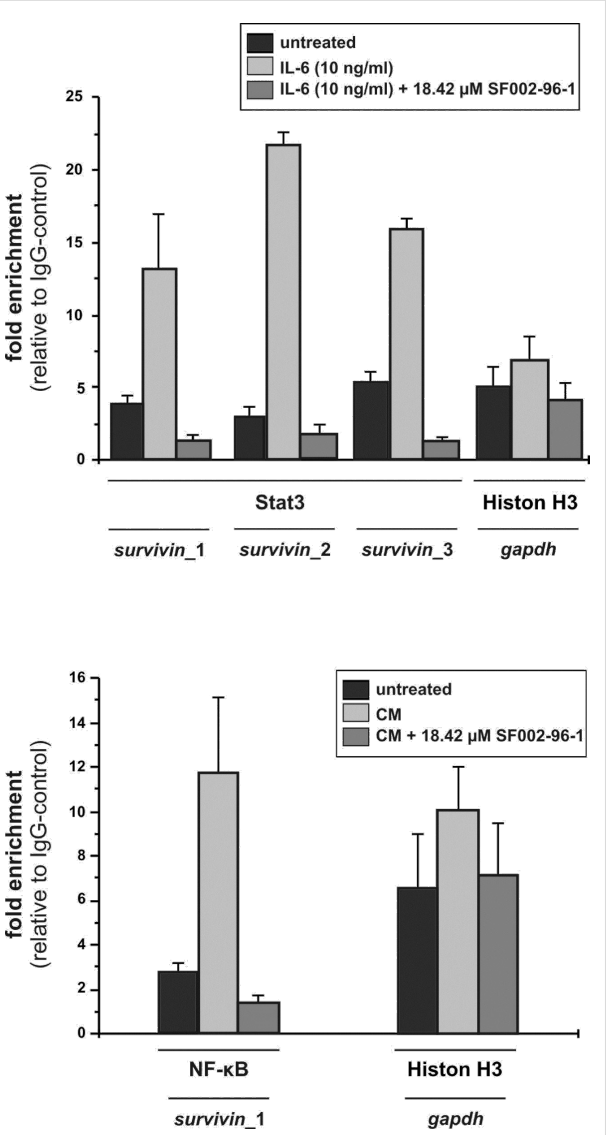


Figure 5: Effect of SF002-96-1 on Sat3 and NF-κB binding to the survivin promoter in Colo 320 cells analyzed by ChIP assay. Colo 320 cells were pretreated with 18.42 µM (5 µg/mL) SF002-96-1 for 1 h before stimulation with 10 ng/mL IL-6 (for Stat3) and 10 ng/mL TNF-α, 5 ng/mL IL-1β (for NF-κB) for 30 min. Chromatin was cross-linked and immunoprecipitated using antibodies against Stat3, NF-κB p65, acetylated histone 3 (H3K9Ac) or rabbit IgG. DNA isolated from immunoprecipitates or from total chromatin preparation before immunoprecipitation (input) was subjected to quantitative real-time PCR using primers specific for Stat3 and p65 binding sites in the survivin promoter or control primers flanking the *gapdh* promoter. Values are expressed as fold enrichment of transcription factor binding relative to IgG as negative control. Data are shown as mean values ± SD of three independent experiments.

To determine the induction of cell death by SF002-96-1 in Colo 320 cells, the cells were treated with the compound for 48 h, after which the cell viability was assessed by measuring the reduction of the tetrazolium compound 2,3-bis-(2-methoxy-4-nitro-5-sulfophenyl)-2*H*-tetrazolium-5-carboxanilide sodium (XTT) into a colored formazan. SF002-96-1, at concentrations from 10.5 µM (4 µg/mL) significantly decreased cell viability of Colo 320 cells in a dose-dependent manner (Figure 6A). In our studies, the compound proved to be a strong inducer of apoptosis in Colo-320 cells showing the typically biochemical characteristic of apoptosis, like cleavage of the chromosomal DNA at internucleosomal sites into fragments of approximately 200 bp and the fragmented morphology of the nuclear bodies (Figure 6B,C) after 5 h of treatment. Exposure of the cells with different concentrations of SF002-96-1 showed a concomitant increase in caspase-3 activity (Figure 6D), indicating that the compound triggers the apoptotic cascade.

Although several agents including natural products (e.g. curcumin, cucurbitacin, resveratrol) have been described to

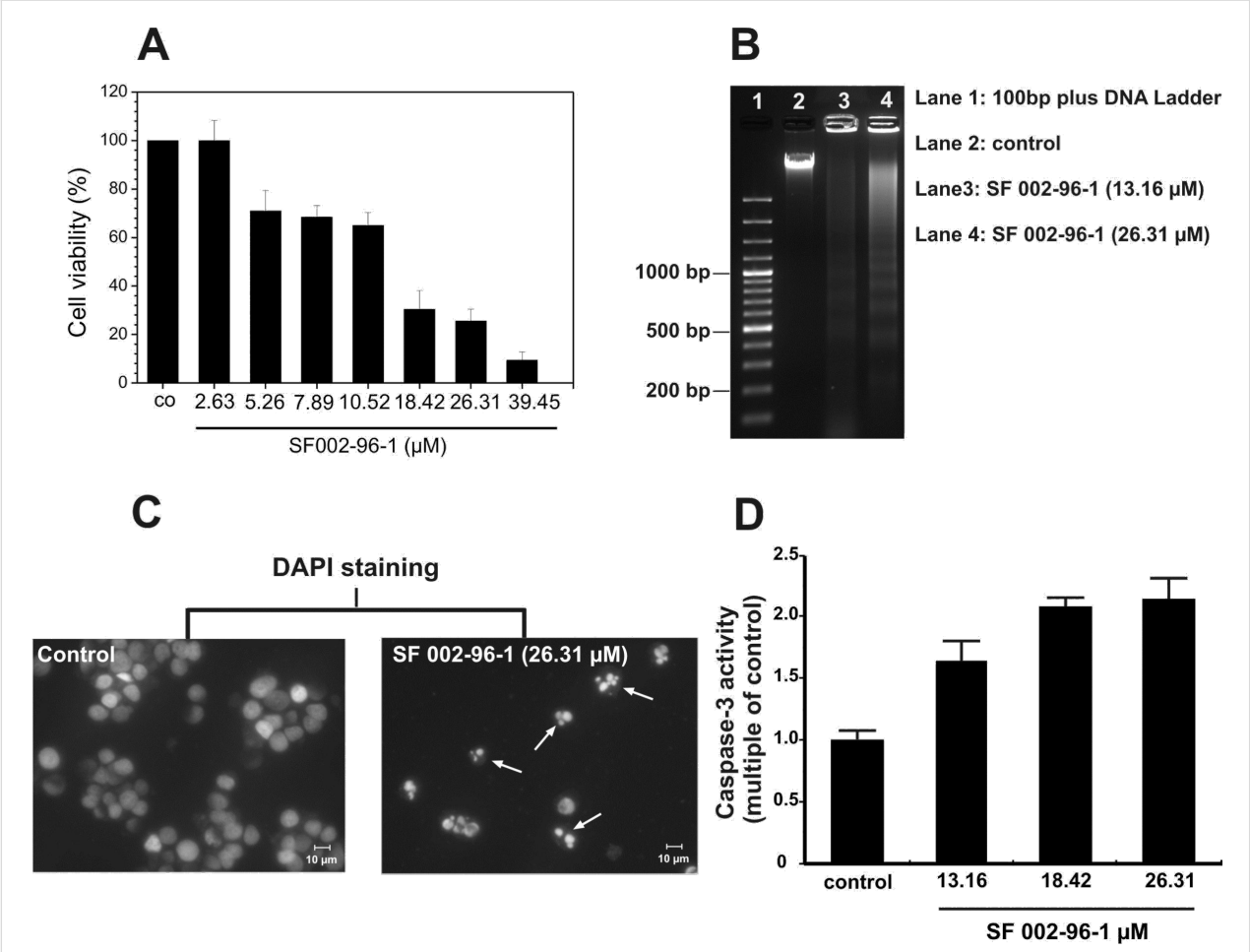


Figure 6: SF002-96-1 induces apoptosis of Colo 320 cells. (A) Colo 320 cells were treated without (control) or with SF002-96-1 at the indicated concentrations for 48 h. Cell viability was determined in triplicate using the XTT colorimetric assay. (B) Detection of DNA fragmentation by agarose gel electrophoresis after treatment of Colo 320 cells for 5 h with different concentrations of the test compound. Control: untreated cells only. (C) Morphology analysis of the cell nuclei by DAPI staining after treatment of Colo 320 cells with 26.31 µM of SF002-96-1 for 5 h. (D) Induction of apoptosis by SF002-96-1 as measured by caspase-3 activity. Colo 320 cells were treated without (control) and with different concentrations of SF002-96-1 for 5 h. After lysis of the cells, 20 µM Ac-DEVD-AMC was added as fluorogenic substrate. AMC released from Ac-DEVD-AMC was measured by a spectrofluorimeter with excitation and emission wavelengths of 335 nm and 460 nm, respectively. Data are shown as mean values ± SD of three independent experiments.

inhibit survivin expression by interfering with oncogenic signaling pathways [25-27], only two survivin transcriptional inhibitors (e. g. YM155, terameprocol) are in development or in clinical trials [28,29].

Recently, FL188, a camptothecin analog, has been described to inhibit survivin promoter activity and inhibits the expression of cancer-associated survival genes (Mcl-1, XIAP, cAP2) in p53 status independent manner at nanomolar concentrations [30]. We have identified a new drimane sesquiterpene lactone, SF002-96-1, which inhibits survivin expression by interfering with critical signaling cascades (JAK/Stat, NF-κB) involved in transcriptional activation of the survivin promoter and subsequently triggering apoptosis in Colo 320 cells. Drimane sesquiterpenes are widespread in plants, fungi and marine organisms such as algae, sponges and corals and have attracted some attention for their potent antibacterial, antifungal, cytotoxic, antifeedant, phytotoxic, piscicidal and molluscicidal activities [31-33].

Conclusion

In summary, we identified a new fungal drimane sesquiterpene lactone, SF002-96-1, which inhibits survivin expression by blocking the binding of critical transcription factors (Stat3, NF-κB) to the promoter of the *survivin* gene and triggers apoptosis in the colon carcinoma cell line Colo 320. Due to the lack of a larger portfolio of survivin antagonists, SF002-96-1 may serve as lead structure for the development of novel cancer therapeutics. Further investigations on the cellular targets and the mode of action of the compound are now under way.

Experimental

General procedures

1D and 2D NMR data were recorded with a Bruker AVANCE III 600 MHz spectrometer equipped with a 5 mm inverse TCI cryoprobe using standard pulse sequences. APCI–MS spectra were measured from a solution of the analyte in MeCN/H_2O with a Hewlett Packard MSD 1100 using an evaporator temperature of 400 °C, a drying gas temperature of 350 °C at a flow of 6 L/h (N_2). In positive ionization mode, the capillary voltage amounted to 3.5 kV, the corona discharge current was 4 µA. In negative ionization mode, the capillary voltage amounted to 2.2 kV, the corona discharge current was 6 µA. HRESI–MS data were measured from a solution of the analyte in acetonitrile with a Waters Q-TOF-Ultima 3 equipped with a LockSpray interface (tri-*n*-octylamine as external reference). IR and UV spectra were measured with a Bruker IFS48 FTIR spectrometer and a Perkin-Elmer Lambda-16 spectrophotometer, respectively. The optical rotation was measured on a Perkin-Elmer 241 polarimeter at 578 nm and 546 nm and extrapolated to 589 nm using Drude's equation [34].

Producing organism, fermentation and isolation of compound SF002-96-1

Aspergillus sp. strain IBWF002-96 was obtained from the culture collection of the Institute of Biotechnology and Drug Research (IBWF e.V.), Kaiserslautern, Germany. The strain IBWF002-96 showed all characteristics of the genus *Aspergillus*, the species however could not be unequivocally determined. ITS sequence analysis of the ITS1-5.8S rDNA-ITS2 region of nuclear DNA [35] showed high similarity to an uncultured soil fungus (100% in 554 bp, Genbank accession no. GQ921753.1) and to *Aspergillus janus* (98% in 575 bp, Genbank accession no. EU021598).

For maintenance, the fungus was grown on HMG agar slants consisting of: 1% malt extract, 1% glucose, 0.4% yeast extract, pH 5.5 and 2% agar for solid media. Fermentation was performed in a Biolafitte C-6 fermenter containing 20 L of KG media (0.4% mashed potato flakes, 2% glucose, pH 5.5) with aeration (3 L air/min) and agitation (120 rpm) at 22 °C. The production of SF002-96-1 was followed by the inhibitory effect of various concentrations of a crude extract of the culture fluid in the survivin promoter dependent reporter gene assay as described below. The compounds were isolated from the culture fluid by bioactivity-guided fractionation using the survivin transcriptional reporter assay in Colo 320 cells. The fermentation was stopped after 18 days, when the glucose in the medium was depleted and the inhibition of the survivin promoter activity reached a maximum. The culture fluid was separated from the mycelium by filtration, extracted twice with an equal volume of ethyl acetate (EtOAc) and dried over Na_2SO_4. The solvent was evaporated in vacuo and the crude extract (3.2 g) was separated by chromatography on silica gel (Merck 60). Elution with cyclohexane/EtOAc (50:50 v/v) resulted in 580 mg of an enriched fraction which was further purified by preparative HPLC (Macherey-Nagel, Düren, Germany; Nucleosil RP18; column 21 × 250 mm, flow 20 mL/min) with MeCN/H_2O (60:40) as eluent to yield 28 mg of SF002-96-1 (t_R: 13 min). During bioactivity-guided fractionation and isolation of compound SF002-96-1, no other compounds have been detected inhibiting survivin promoter activity.

The purity of the isolated compound was analyzed with a Hewlett-Packard Series 1100LC-MSD instrument fitted with a LiChroCART Superspher 100 RP-18 column (125 × 2 mm, 4 mm particle size; Merck). The chromatographic conditions consisted of a gradient from 1% to 100% acetonitrile in 20 min, and an isocratic step at 100% acetonitrile for 1 min at 40 °C and 10 µL injection volume was used. The flow rate was 0.45 mL/min. The fragmentor voltage was set to 140 V in the positive and negative APCI modes. The compound showed the highly characteristic fragmentation pattern in the APCI-positive mass spectrum revealing the pseudo-molecular ion $[M + H]^+$ with *m*/*z* of 281.2. The purity of SF002-96-1 as estimated by HPLC-DAD/MS analysis was greater than 98.5% (Figure 7).

SF002-96-1: colourless oil, UV (CH_3CN) (λ_{max}, log ε): 207 (3.94) nm; $[\alpha]_D^{20}$ –167.0 (*c* 0.4, CD_3CN); IR (ν): 3411, 2934, 1757, 1737, 1632, 1464, 1379, 1249 cm^{-1}; HRESI–MS (*m*/*z*): $[M + Na]^+$ calcd for $C_{21}H_{32}O_6Na$, 403.2097; found, 403.2090; APCI–MS neg. mode *m*/*z*: 380.2 $[M]^+$, 362 $[M - H_2O]^+$, pos. mode *m*/*z*: 363.2 $[M - H_2O + H]^+$, 265.1 $[M - H_3C(CH_2)_4CO_2H + H]^+$, 247.1 $[M - H_3C(CH_2)_4CO_2H - H_2O + H]^+$; ^1H NMR (600 MHz, CD_3CN) δ 6.57 (d, 4.0 Hz, 1H, H-7), 5.72 (dd, 4.0, 4.7 Hz, 1H, H-6), 4.48 (d, 10.5 Hz, 1H, H-11b), 4.23 (d, 10.5 Hz, 1H, H-11a), 4.02 (dd, 4.4, 11.9 Hz, 1H, H-1), 3.76 (br s, 1H, O<u>H</u>-9), 2.96 (br s, 1H, O<u>H</u>-1), 2.32 (m, 2H, H-2'), 1.94 (H-5, overlapped with the solvent peak), 1.66 (m, 1H, H-2b), 1.59 (m, 2H, H-3'), 1.57 (m, 1H, H-2a), 1.37 (m, 1H, H-3b), 1.34 (m, 1H, H-3a), 1.30 (m, 2H, H-4'), 1.28 (m, 2H, H-5'), 1.15 (s, 3H, Me-13), 1.04 (s, 3H, Me-15), 0.97 (s, 3H, Me-14), 0.87 (t, 7.0 Hz, 3H, Me-6); ^{13}C NMR (150 MHz, CD_3CN) δ 173.5 (C-1'), 169.8 (C-12), 133.8 (C-8), 133.5 (C-7), 77.4 (C-11), 77.0 (C-9), 70.7 (C-1), 67.0 (C-6), 45.7 (C-5), 44.7 (C-10), 42.7 (C-3), 35.1 (C-2'), 34.0 (C-4), 32.6 (C-14), 31.9 (C-5'), 28.2 (C-2), 25.1 (C-3'), 24.9 (C-13), 23.0 (C-4'), 14.2 (C-6'), 12.8 (C-15).

Cell culture

Colo 320 (DSMZ ACC 144) cells were maintained in RPMI 1640 medium with 25 mM HEPES buffer and 2 mM L-gluta-

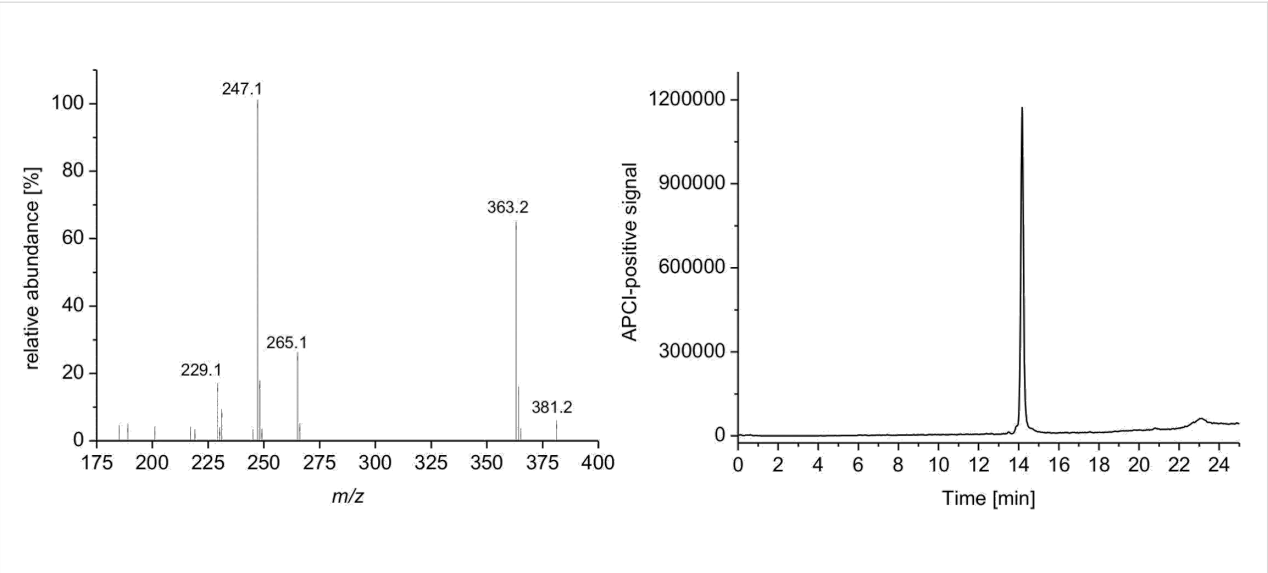


Figure 7: Single-quadrupole mass spectrumof SF002-96-1 obtained using an atmospheric pressure chemical ionization interface showing the pseudo-molecular ion. HPLC–MS analysis of the purified compound (APCI, total ion current).

mine, supplemented with 10% fetal calf serum, 100 U/mL penicillin, 100 µg/mL streptomycin at 37 °C and 5% CO_2.

Reporter gene assays

The 1092 bp human survivin promoter (region between nucleotide 1821 and nucleotide 2912 within the human survivin gene; GenBank™ accession number U75285) was amplified by polymerase chain reaction from genomic DNA isolated from MonoMac6 cells using oligonucleotides derived from published sequences [36]. The PCR product was cloned into the *Xho*I-*Hind*III site of the promoterless luciferase vector pGL3-basic (Promega, Mannheim, Germany) to generate the hSurvivin-promoter-driven luciferase reporter plasmid (pGL3-hsurvpro). The plasmid pRL-CMV for normalizing transfection efficiency was obtained from Promega (Dual-Luciferase-Reporter-Assay). The NF-κB driven reporter plasmid pNF-κB-Luc was obtained from Clontech (Saint-Germain-en-Laye, France). The IL-6 responsive STAT3-dependent reporter vector pMW-IRF7 has been described previously [37]. TOPFLASH and FOPFLASH luciferase reporters were obtained from Upstate Biotechnology, Inc. (Lake Placid, USA).

Transient transfections of Colo 320 cells were performed by electroporation (BioRad, Gene Pulser) of 1×10^7 cells/mL in 0.4 mL RPMI 1640 medium containing 10% FCS together with 50 µg of the indicated plasmids at 290 V and 975 m. After electroporation, the cells were seeded at 1×10^6 cells/mL in RPMI medium containing 10% FCS in a 24 well plate and allowed to recover for 24 h. For induction of reporter gene expression, the cells were treated with 10 ng/mL TNF-α and 5 ng/mL IL-1β for pNF-κB-Luc and 10 ng/mL IL-6 for pMW-IRF7 with or without test compounds. Luciferase activity was measured 24 h after induction using the Dual-Glo luciferase assay system (Promega, Mannheim, Germany) according to the manufacturer´s instructions with a luminometer.

Cell viability testing

The cytotoxicity of the compound was determined after 48 h using a XTT-based cell viability assay as previously described by Roehm et al. [38].

Quantitative real-time polymerase chain reaction analysis (qRT-PCR analysis)

The mRNA expression in human Colo 320 cells was analyzed by two-step real-time RT-PCR as described before [39] with gene-specific primers for human survivin (Genbank Accession NM001168) forward: 5´-ACCAGGTGAGAAGTGAGGGA-3´ and reverse: 5´-AACAGTAGAGGAGCCAGGGA-3´ (size of the PCR product is 309 bp) and *GAPDH* (Genbank Accession M33197) forward: 5'-CCTCCGGGAAACTGTGG-3' and reverse: 5'-AGTGGGGACACGGAAG-3' (size of the PCR product is 140 bp). Relative mRNA amounts were determined using the mathematical model for relative quantification in real-time PCR proposed by Pfaffl [40].

Chromatin immunoprecipitation (ChIP) assay

Colo 320 cells were seeded out in 75 cm^2 tissue culture flasks at a density of 5×10^5 cells per mL. After 24 h of cultivation, cells were starved for additional 16 h in RPMI 1640 medium with 0.5% FCS. After that, cells were pretreated with SF002-96-1 for 1 h. Stimulation of the NF-κB signaling pathway was performed for 30 min with a cytokine mixture consisting of 10 ng/mL

TNF-α and 5 ng/mL IL-1β. Stimulation of the Stat3 signaling pathway was performed for 30 min with 10 ng/mL IL-6. Chromatin immunoprecipitation (ChIP) assays were performed as described by Carey et al. [41], using specific anti-Stat3 (79D7, New England Biolabs, Frankfurt/M), anti-NF-κB p65 (SC-109X, Santa Cruz Biotechnology, Santa Cruz, CA, USA) and anti-lysine9 acetylated histone H3 antibody (9671, New England Biolabs, Frankfurt/M) at dilutions recommended by the manufacturers (1:50). The immunoprecipitates were pelleted and incubated at 65 °C overnight to reverse cross-links. The DNA was extracted by phenol–chloroform extraction and precipitated with ethanol. The precipitated DNA was resuspended in 50 µL TE buffer (10 mM Tris-HCl, 1 mM EDTA, pH 7.4) and used for PCR amplification. Three putative Stat3-binding sites within the survivin promoter were analyzed. The sequences of the PCR primers used are as followed: Stat3_1: forward primer, 5′-CAGTGAGCTGAGATCATGCC-3′; 5′-TATTAGCCCTCCAGCCCCAC-3′ reverse primer (fragment size: 223 bp), Stat3_2: forward primer, 5′-CGCCTCTACTCCCAGAAG-3′; 5′-TGTAGAGATGCGGTGGTC-3′ reverse primer (fragment size: 195 bp), Stat3_3: forward primer, 5′-CCAAAGCAGAGGACACAC-3′; 5′-GGCCACTACCGTGATAAG-3′ reverse primer (fragment size: 165 bp). The primer sequences used for the NF-κB binding site within the survivin promoter were: NF-κB: forward primer, 5′-CTGCACGCGTTCTTTGA-3′; 5′-GCGGTGGTCCTTGAGA-3′ reverse primer (fragment size: 327 bp). The gapdh primer mixture was obtained from New England Biolabs, Frankfurt/M (SimpleChIP® Human GAPDH Exon 1 primers).

Western immunoblotting

Colo 320 cells were seeded into a 6-well plate at cell density of 5×10^5 cells/mL and allowed to grow for 24 h. The cells were then treated for an additional 8 h with and without different concentrations of test compound and total cell extracts were prepared by lysing the cells with Totex buffer (20 mM HEPES, pH 7.4, 350 mM NaCl, 20% glycerol, 1% NP-40, 1 mM $MgCl_2$, 0.5 mM EDTA, 0.1 mM EGTA, 0.5 mM DTT, 10 mM β-glycerophosphate, 10 mM NaF, 1 mM Na_3VO_4, 1:25 complete protease-inhibitor cocktail according to the manufacturer´s recommendation (Roche Diagnostics, Mannheim, Germany)). 25 µg total cell extracts were subjected to 10% SDS-PAGE, transferred onto a nitrocellulose membrane, probed with antibodies specific for human survivin (1:1000, 71G4B7, New England Biolabs Frankfurt/M) or β-actin (1:1000, 13E5, New England Biolabs Frankfurt/M) and then with the appropriate secondary antibody conjugated to horse radish peroxidase (1:2000, Anti-rabbit IgG, HRP-linked New England Biolabs, Germany). Immunoreactive proteins were visualized by the enhanced chemoluminiscent detection system (New England Biolabs, Germany).

Caspase-3 activity assay

Colo 320 cells were seeded at a density of 5×10^5 cells/mL in 96 well plates and treated with test compound for 5 h. After incubation, the cells were centrifuged at 1000*g* for 10 min at 4 °C, washed with PBS and lysed with 50 µL cell lysis buffer (50 mM HEPES, 0.1% CHAPS, 5 mM DTT, 0.1 mM EDTA, pH 7.4). After a freezing step at −80 °C and rethawing, the cell lysate was centrifuged at 1000*g* for 10 min at 4 °C. 25 µL of the supernatants were transferred into a new 96-well plate and incubated with 75 µL assay buffer (50 mM HEPES, 100 mM NaCl, 0.1% CHAPS, 10 mM DTT, 1 mM EDTA, 10% glycerol, pH: 7.4) containing 20 µM Ac-DEVD-amino-4-methylcoumarin (AC-DEVD-AMC; Calbiochem, Bad Soden, Germany) for 2 h at 37 °C. AMC released from the cleavage of AC-DEVD-AMC was measured by a spectrofluorimeter with excitation and emission wavelengths of 355 nm and 460 nm respectively.

Measurement of DNA fragmentation

Colo 320 cells were resuspended at 5×10^6–1×10^7 cells/mL and incubated with the test compound for 5 h. After incubation, the cells were centrifugated (1000*g*, 10 min), washed once with ice cold PBS and lysed with 600 µL lysis buffer (10 mM Tris-HCl, 10 mM EDTA, 0.2% Triton X-100, pH 7.5) on ice for 10 min. The lysate was centrifuged at 14 000 rpm for 10 min at 4 °C and the supernatant was extracted twice with phenol/chloroform/isoamyl alcohol (25:24:1). The aqueous phase was precipitated with two volumes of ethanol (100%) and 0.1 volume of sodium acetate (3 M, pH 5) overnight. The DNA pellet was rinsed with ethanol (70%) and dissolved in TE buffer (10 mM Tris-HCl, 1 mM EDTA, pH: 7.4) and incubated with RNase (0.1 mg/mL) for 30 min at 37 °C. The samples were separated on a 1.5 % agarose gel and stained with ethidium bromide.

DAPI staining

Colo 320 cells were incubated for 5 h with test compound and washed once with ice cold PBS. After centrifugation at 1000*g* for 10 min at 4 °C, the cell pellet was resuspend in 5% PBS buffered paraformaldehyde solution containing 10 µg/mL DAPI (4',6-diamidino-2-phenylindole) and incubated for 10 min on ice. A portion (10 µL) of the cell suspension was then placed on a glass-slide, covered with a coverslip and the morphology of the cell nuclei was observed by using a fluorescence microscope (Zeiss, Axioskop).

Supporting Information

Supporting Information File 1

1D and 2D NMR spectra of compound SF002-96-1.
[http://www.beilstein-journals.org/bjoc/content/supplementary/1860-5397-9-323-S1.pdf]

Acknowledgements

This work was supported by a grant from the Stiftung Rheinland-Pfalz für Innovation (S.F., G.E.) as well as by the Zeiss foundation (L.P.S., T.O.). We thank Prof. Dr. T. Anke and Prof. Dr. H. Anke for providing *Aspergillus spec.*strain IBWF002-96, Dr. J. C. Liermann for NMR spectroscopy, the Naturstoffzentrum Rheinland-Pfalz for helpful discussions, and P. Stark for skillful technical assistance.

References

1. Mita, A. C.; Mita, M. M.; Nawrocki, S. T.; Giles, F. J. *Clin. Cancer Res.* **2008,** *14,* 5000–5005. doi:10.1158/1078-0432.CCR-08-0746
2. Altieri, D. C. *Nat. Rev. Cancer* **2003,** *3,* 46–54. doi:10.1038/nrc968
3. Altieri, D. C. *Nat. Rev. Cancer* **2008,** *8,* 61–70. doi:10.1038/nrc2293
4. Jha, J.; Shukla, M.; Pandey, M. *Surg. Oncol.* **2012,** *21,* 125–131. doi:10.1016/j.suronc.2011.01.001
5. Dallaglio, K.; Marconi, A.; Pincelli, C. *J. Invest. Dermatol.* **2012,** *132,* 18–27. doi:10.1038/jid.2011.279
6. Altieri, D. C. *Biochem. J.* **2010,** *430,* 199–205. doi:10.1042/BJ20100814
7. Vader, G.; Kauw, J. J.; Medema, R. H.; Lens, S. M. A. *EMBO Rep.* **2006,** *7,* 85–92. doi:10.1038/sj.embor.7400562
8. Carmena, M.; Wheelock, M.; Funabiki, H.; Earnshaw, W. C. *Nat. Rev. Mol. Cell Biol.* **2012,** *13,* 789–803. doi:10.1038/nrm3474
9. van der Waal, M. S.; Hengeveld, R. C. C.; van der Horst, A.; Lens, S. M. A. *Exp. Cell Res.* **2012,** *318,* 1407–1420. doi:10.1016/j.yexcr.2012.03.015
10. Stauber, R. H.; Mann, W.; Knauer, S. K. *Cancer Res.* **2007,** *67,* 5999–6002. doi:10.1158/0008-5472.CAN-07-0494
11. Connell, C. M.; Colnaghi, R.; Wheatley, S. P. *J. Biol. Chem.* **2008,** *283,* 3289–3296. doi:10.1074/jbc.M704461200
12. Saito, T.; Arifin, M. T.; Hama, S.; Kajiwara, Y.; Sugiyama, K.; Yamasaki, F.; Hidaka, T.; Arita, K.; Kurisu, K. *J. Neuro-Oncol.* **2007,** *82,* 193–198. doi:10.1007/s11060-006-9267-1
13. Altieri, D. C. *Cancer Lett.* **2013,** *332,* 225–228. doi:10.1016/j.canlet.2012.03.005
14. Sakio, Y.; Hirano, Y. J.; Hayashi, M.; Komiyama, K.; Ishibashi, M. *J. Nat. Prod.* **2001,** *64,* 726–731. doi:10.1021/np000639g
15. Xu, M.; Litaudon, M.; Krief, S.; Martin, M.-T.; Kasenene, J.; Kiremire, B.; Dumontet, V.; Guéritte, F. *Molecules* **2009,** *14,* 3844–3850. doi:10.3390/molecules14103844
16. Li, F.; Altieri, D. C. *Biochem. J.* **1999,** *344,* 305–311. doi:10.1042/0264-6021:3440305
17. Yamamoto, H.; Ngan, C. Y.; Monden, M. *Cancer Sci.* **2008,** *99,* 1709–1714. doi:10.1111/j.1349-7006.2008.00870.x
18. Gritsko, T.; Williams, A.; Turkson, J.; Kaneko, S.; Bowman, T.; Huang, M.; Nam, S.; Eweis, I.; Diaz, N.; Sullivan, D.; Yoder, S.; Enkemann, S.; Eschrich, S.; Lee, J.-H.; Beam, C. A.; Cheng, J.; Minton, S.; Muro-Cacho, C. A.; Jove, R. *Clin. Cancer Res.* **2009,** *12,* 11–19. doi:10.1158/1078-0432.CCR-04-1752
19. Kawakami, H.; Tomita, M.; Matsuda, T.; Ohta, T.; Tanaka, Y.; Fujii, M.; Hatano, M.; Tokuhisa, T.; Mori, N. *Int. J. Cancer* **2005,** *115,* 967–974. doi:10.1002/ijc.20954
20. Kim, P. J.; Plescia, J.; Clevers, H.; Fearon, E. R.; Altieri, D. C. *Lancet* **2003,** *362,* 205–209. doi:10.1016/S0140-6736(03)13910-4
21. Anastas, J. N.; Moon, R. T. *Nat. Rev. Cancer* **2013,** *13,* 11–26. doi:10.1038/nrc3419
22. Ikenoue, T.; Ijichi, H.; Kato, N.; Kanai, F.; Masaki, T.; Rengifo, W.; Okamoto, M.; Matsumura, M.; Kawabe, T.; Shiratori, Y.; Omata, M. *Jpn. J. Cancer Res.* **2002,** *93,* 1213–1220. doi:10.1111/j.1349-7006.2002.tb01226.x
23. Dasgupta, P.; Kinkade, R.; Joshi, B.; DeCook, C.; Haura, E.; Chellappan, S. *Proc. Natl. Acad. Sci. U. S. A.* **2006,** *103,* 6332–6337. doi:10.1073/pnas.0509313103
24. Papanikolaou, V.; Iliopoulos, D.; Dimou, I.; Dubos, S.; Kappas, C.; Kitsiou-Tzeli, S.; Tsezou, A. *J. Cell. Mol. Med.* **2011,** *15,* 1542–1550. doi:10.1111/j.1582-4934.2010.01149.x
25. Glienke, W.; Maute, L.; Bergmann, L. *Cancer Invest.* **2010,** *28,* 166–171. doi:10.3109/07357900903287006
26. Zhang, M.; Sun, C.; Shan, X.; Yang, X.; Li-Ling, J.; Deng, Y. *Pancreas* **2010,** *39,* 923–929. doi:10.1097/MPA.0b013e3181ce719e
27. Trung, L. Q.; Espinoza, J. L.; Takami, A.; Nakao, S. *PLoS One* **2013,** *8,* e55183. doi:10.1371/journal.pone.0055183
28. Doolittle, H.; Morel, A.; Talbot, D. *Eur. Oncol.* **2010,** *6,* 10–14.
29. Kanwar, J. R.; Kamalapuram, S. K.; Kanwar, R. K. *Drug Discovery Today* **2011,** *16,* 485–494. doi:10.1016/j.drudis.2011.04.001
30. Ling, X.; Cao, S.; Cheng, Q.; Keefe, J. T.; Rustum, Y.; Li, F. *PLoS One* **2012,** *7,* e5571. doi:10.1371/journal.pone.0045571
31. Fraga, B. M. *Nat. Prod. Rep.* **2011,** *28,* 1580–1610. doi:10.1039/c1np00046b
32. Ebel, R. *Mar. Drugs* **2010,** *8,* 2340–2368. doi:10.3390/md8082340
33. Gershenzon, J.; Dudareva, N. *Nat. Chem. Biol.* **2007,** *3,* 408–414. doi:10.1038/nchembio.2007.5
34. Lippke, G.; Thaler, H. *Starch/Staerke* **1970,** *22,* 344–351. doi:10.1002/star.19700221005
35. White, T. J.; Bruns, T.; Lee, S.; Taylor, J. Amplification and direct sequencing of fungal ribosomal RNA genes for phylogenetics. In *PCR Protocols: A Guide to Methods and Applications;* Innis, M. A.; Gelfand, D. H.; Sninsky, J. J.; White, T. J., Eds.; Academic Press: San Diego, 1990; pp 315–322.
36. Hoffman, W. H.; Biade, S.; Zilfou, J. T.; Chen, J.; Murphy, M. *J. Biol. Chem.* **2002,** *277,* 3247–3257. doi:10.1074/jbc.M106643200
37. Weidler, M.; Rether, J.; Anke, T.; Erkel, G. *FEBS Lett.* **2000,** *484,* 1–6. doi:10.1016/S0014-5793(00)02115-3
38. Roehm, N. W.; Rodgers, G. H.; Hatfield, S. M.; Glasebrook, A. L. *J. Immunol. Methods* **1991,** *142,* 257–265. doi:10.1016/0022-1759(91)90114-U
39. Schreiber, D.; Jung, M.; Sandjo, L. P.; Liermann, J. C.; Opatz, T.; Erkel, G. *J. Antibiot.* **2012,** *65,* 473–477. doi:10.1038/ja.2012.46
40. Pfaffl, M.-W. *Nucleic Acids Res.* **2001,** *29,* e45. doi:10.1093/nar/29.9.e45
41. Carey, M. F.; Peterson, C. L.; Smale, S. T. *Cold Spring Harb. Protoc.* **2009**. doi:10.1101/pdb.prot5279

License and Terms

This is an Open Access article under the terms of the Creative Commons Attribution License (http://creativecommons.org/licenses/by/2.0), which permits unrestricted use, distribution, and reproduction in any medium, provided the original work is properly cited.

The license is subject to the *Beilstein Journal of Organic Chemistry* terms and conditions: (http://www.beilstein-journals.org/bjoc)

The definitive version of this article is the electronic one which can be found at: doi:10.3762/bjoc.9.323

Beilstein Journal of Organic Chemistry

Studies toward bivalent κ opioids derived from salvinorin A: heteromethylation of the furan ring reduces affinity

Thomas A. Munro*[1,2], Wei Xu[3], Douglas M. Ho[4], Lee-Yuan Liu-Chen[3] and Bruce M. Cohen[1]

Full Research Paper

Open Access

Address:
[1]McLean Hospital, Belmont, MA 02478, USA and Department of Psychiatry, Harvard Medical School, Boston, MA 02215, USA, [2]School of Chemistry and Bio21 Institute, University of Melbourne, Parkville 3010, Australia, [3]Center for Substance Abuse Research and Department of Pharmacology, Temple University School of Medicine, Philadelphia, PA 19140, USA and [4]Department of Chemistry and Chemical Biology, Harvard University, Cambridge MA 02138, USA

Email:
Thomas A. Munro* - thomas@munro.com

* Corresponding author

Keywords:
allotopic; bivalent ligand; designed multiple ligand; JDTic; κ-opioid receptor; natural products; Salvinorin A

Beilstein J. Org. Chem. **2013,** *9,* 2916–2924.
doi:10.3762/bjoc.9.328

Received: 01 September 2013
Accepted: 21 November 2013
Published: 20 December 2013

This article is part of the Thematic Series "Natural products in synthesis and biosynthesis".

Guest Editor: J. S. Dickschat

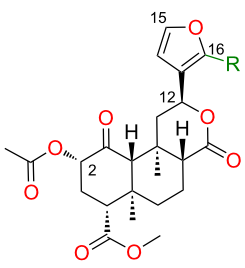
© 2013 Munro et al; licensee Beilstein-Institut.
License and terms: see end of document.

Abstract

The recent crystal structure of the κ-opioid receptor (κ-OR) revealed, unexpectedly, that the antagonist JDTic is a bivalent ligand: in addition to the orthosteric pocket occupied by morphinans, JDTic also occupies a distinct (allotopic) pocket. Mutagenesis data suggest that salvinorin A (**1**) also binds to this allotopic pocket, adjacent to the aspartate residue that anchors the basic nitrogen atom of classical opiates (Asp138). It has been suggested that an H-bond donor appended to **1** might interact with Asp138, increasing affinity. Such a bivalent ligand might also possess altered functional selectivity. Based on modeling and known *N*-furanylmethyl opioid antagonists, we appended H-bond donors to the furan ring of **1**. (Dimethylamino)methyl groups at C-15 or C-16 abolished affinity for κ-OR. Hydroxymethylation at C-16 was tolerated, but 15,16-bis-hydroxymethylation was not. Since allosteric modulators may go undetected in binding assays, we also tested these and other low-affinity derivatives of **1** for allosteric modulation of dynorphin A in the [^{35}S]GTPγS assay. No modulation was detected. As an alternative attachment point for bivalent derivatives, we prepared the 2-(hydroxyethoxy)methyl ether, which retained high affinity for κ-OR. We discuss alternative design strategies for linked, fused or merged bivalent derivatives of **1**.

Introduction

The structure–activity relationships of salvinorin A (**1**), a potent and selective κ (kappa) opioid, have been extensively investigated [1]. Modifications at C-2 have yielded compounds with increased potency and duration of action [2,3], and other compounds with unprecedented functional selectivity at the μ (mu) opioid receptor (μ-OR) [4]. However, modifications at other positions substantially reduce or eliminate affinity for opioid receptors [1]. In particular, most modifications of the furan ring tested to date dramatically reduce affinity for κ-OR [1], although small substituents at C-16 have little effect (Figure 1). Unexpectedly, epimerization at C-12, inverting the configuration of the furan ring, reduces efficacy in G-protein activation [5], but not in arrestin recruitment, resulting in functional selectivity (biased agonism) [6].



	R =	K_i (nM)
1 (salvinorin A)	H	2.5
	Br	2.9
		7.1

Figure 1: Binding affinities of salvinorin A (**1**) and furan derivatives for κ-OR [5].

Extensive receptor mutagenesis data are available on the interactions of κ-OR with **1** and derivatives [1,7-9]. In Figure 2A, the crystal structure of κ-OR in complex with the selective antagonist JDTic is shown. Essential residues for high affinity binding of **1**, where mutation reproducibly reduces affinity ≥10-fold, are shown with thick bonds for emphasis [7-9]. These

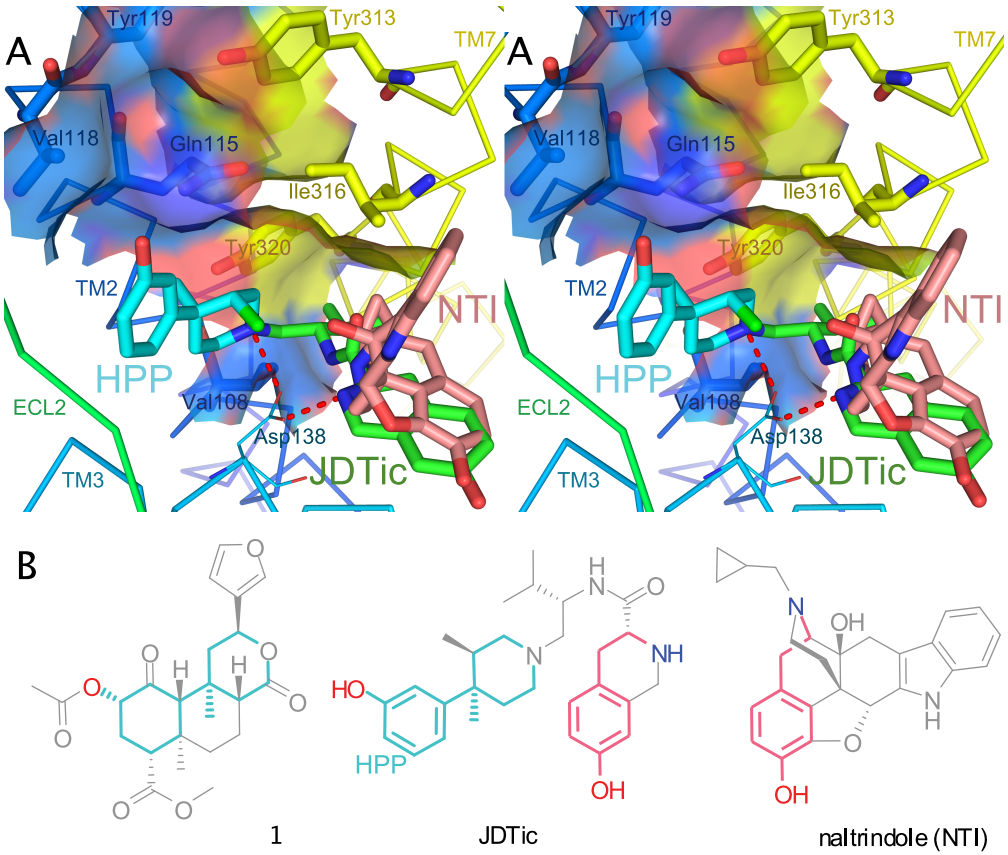


Figure 2: Crystal structure of κ-OR in complex with JDTic compared to naltrindole's binding pose in δ-OR. A: Cross-eyed stereoview of the crystal structure of κ-OR (PDB 4DJH). All residues known to be required for high-affinity binding of **1** (mutation reproducibly reduces affinity ≥10-fold [7-9]) are shown with thick bonds and water-accessible surfaces. JDTic is shown in green with the hydroxyphenylpiperidine substructure (HPP) in light blue. Ionic H-bonds from JDTic to Asp138$^{3.32}$ are shown in red. The binding pose of naltrindole (NTI, pink) to δ-OR is also superimposed (PDB 4EJ4). B: Structural similarities: atoms in **1** common to the HPP substructure of JDTic are shown in light blue; superimposable portions of naltrindole and JDTic are shown in pink.

key residues are all located in transmembrane helices (TMs) 2 and 7. The surfaces of these residues are contiguous, forming one face of a deep pocket between TMs 2, 3, and 7. Mutations of many other residues outside this pocket (TMs 1, 3, 5, 6, 7, and extracellular loop 2) failed to substantially reduce affinity for **1** [1,7-9]. Collectively, these results provide compelling evidence that **1** binds to this face of the binding pocket. The plausibility of this proposal is strengthened by the position of the hydroxyphenylpiperidine moiety of JDTic in the crystal structure (HPP, light blue). The HPP moiety and its *N*-substituent interact with five of the seven key residues for binding of **1**: Val108$^{2.53}$, Gln115$^{2.60}$, Val118$^{2.63}$, Ile316$^{7.39}$, and Tyr320$^{7.43}$ (superscripts refer to Ballesteros–Weinstein numbering) [7]. Intriguingly, **1** contains a substructure very similar to HPP (light blue in Figure 2B). Given that HPP is a near substructure of **1** and binds to these same key residues, it is tempting to speculate that the binding pose of **1** may be similar.

By contrast, the morphinan naltrindole (shown in pink) binds to a different pocket of δ-OR among TMs 3, 6, and 7 [10]; β-funaltrexamine adopts a near-identical pose in complex with μ-OR (not shown) [11]. Interestingly, JDTic occupies this morphinan pocket as well. The tetrahydroisoquinoline moiety of JDTic adopts a pose almost identical to that of naltrindole; the superimposable atoms are shown in pink in Figure 2B [10]. JDTic is thus a bivalent ligand, containing two linked pharmacophores [12], also known as a linked multiple ligand [13]. Bivalent ligands can exhibit greatly increased potency and unusual functional selectivity [12]. Consistent with this, JDTic is extremely potent (K_e < 40 pM) [14]; also, despite acting as an antagonist toward other κ-OR-mediated signaling pathways [7], JDTic reportedly activates JNK1 (MAPK8), causing extremely prolonged desensitization of κ-OR [15].

These two binding pockets are almost entirely separate, but overlap around Tyr320$^{7.43}$. This residue interacts with JDTic [7], and the corresponding residue (Tyr$^{7.43}$) also interacts with naltrindole in δ-OR [10] and β-funaltrexamine in μ-OR [11].

Interestingly, Tyr320$^{7.43}$ and two adjacent residues (Val108$^{2.53}$ and Ile316$^{7.39}$) are also key residues for the binding of **1** [7]. Together, they surround the bottom of the binding pocket, strongly suggesting that an extremity of **1** occupies this space, overlapping with both the morphinan and hydroxyphenylpiperidine binding sites.

Immediately adjacent to these residues is Asp138$^{3.32}$, a critical residue for binding of morphinans and related opioids. Asp$^{3.32}$ forms strong ionic H-bonds ('salt bridges') to the basic nitrogen atoms found in almost all opioids, as in the crystal structures of JDTic (red in Figure 2A), naltrindole [10], β-funaltrexamine [11], and the NOP antagonist C-24 [16]. Beyond opioids, ionic H-bonds to Asp$^{3.32}$ are conserved across biogenic amine receptors; indeed, this residue$^{3.32}$ interacts with the ligand in almost all GPCR crystal structures reported to date [17].

In summary, **1** appears to bind adjacent to Asp138$^{3.32}$, but not to interact with it strongly: mutation of this residue either has little effect or actually increases affinity [7-9]. Based on this proximity, Kane proposed appending a positively-charged moiety to **1**, thereby creating an ionic H bond to Asp138$^{3.32}$ that should increase affinity [18]. Like JDTic, this ligand would be bivalent. Kane also proposed linking to fragments of other κ-opioids such as arylacetamides, creating additional interactions. By this strategy, "designed multiple ligands" of several kinds could be obtained: linked, fused or merged [13].

A suitable attachment point and linker for this second moiety would also be required. Docking **1** to an early rhodopsin-based homology model of κ-OR, Kane proposed a binding pose qualitatively similar to that of the HPP moiety of JDTic, placing the furan ring near Tyr320$^{7.43}$ [8,18]. Indeed, at the time we commenced our work, all published mutagenesis-based models placed the furan ring in contact with Tyr320$^{7.43}$ [1]. This interaction is plausible in light of the structure–activity relationships of opioid antagonists. In JDTic, the *N*-substituent of the HPP moiety interacts with Tyr320$^{7.43}$ [7], and *N*-furanylalkyl substi-

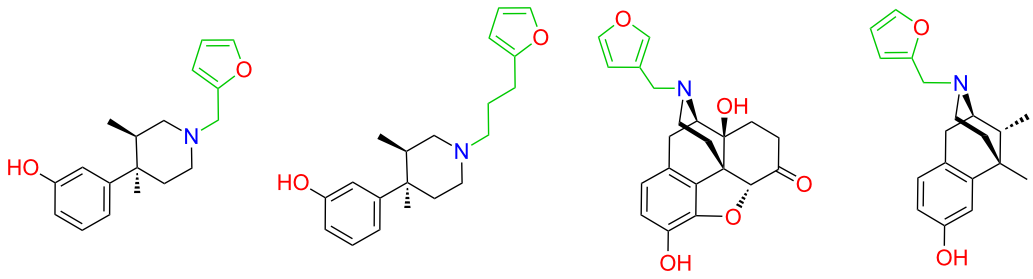


Figure 3: Previously reported *N*-furanylalkyl opioid antagonists [19,20].

tution of this scaffold yields potent opioid antagonists (Figure 3) [19]. Likewise, the *N*-substituents of naltrindole and β-funaltrexamine also interact with $Tyr^{7.43}$ [10,11], and *N*-furanylmethyl substitution of morphinans and related scaffolds consistently yields potent opioid antagonists [20]. These convergent results firmly establish that residues adjacent to $Asp^{3.32}$, including $Tyr^{7.43}$, interact favorably with furan substituents; thus, models placing the furan ring of **1** in this region are plausible. The region appears to be quite tolerant to the position, orientation and substitution of the furan ring [20].

We therefore selected the furan ring as an attachment point for initial explorations of Kane's bivalent ligand concept. Given the tolerance of **1** to modification at C-16 noted above, we chose to append H-bond donors (amino and hydroxy groups) at this position. Based on previous high-affinity ligands with a furanylmethyl substituent (Figure 3), we decided to use a short linker.

As an alternative approach, bivalent ligands with much longer linkers can bind simultaneously to both protomers in a receptor dimer, allowing selective targeting of specific receptor oligomers [21]. We also sought to provide a suitable attachment point for such linkers based on our previous studies of C-2 alkoxymethyl ethers [22,23], which have higher tolerance to alkyl chain extension [24] than other derivatives of **1** [1].

Results

Synthesis

Initial attempts to form the 16-dimethylaminomethyl derivative **2** by treatment of **1** with dimethylamine and paraformaldehyde in acetic acid [25] gave no desired product. However, *N*,*N*-dimethylmethyleneiminium chloride [26] in dimethylformamide gave **2** and the 15-regioisomer **3** in good total yield (Scheme 1). Treatment of **2** with HCl in Et_2O gave the hydrochloride salt, but the same treatment of **3** gave a cloudy suspension, with decomposition products evident in the ^{1}H NMR spectrum.

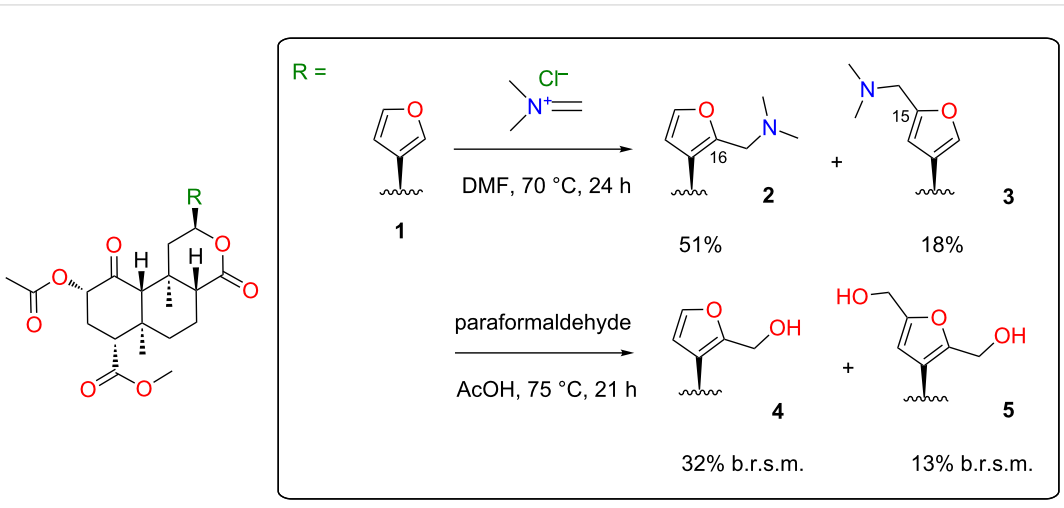
We next targeted hydroxymethyl substituents. Treatment of **1** with aqueous formaldehyde (40% w/v) and Amberlyst-15® resin at room temperature [27] gave complex mixtures of products. However, heating **1** with paraformaldehyde in acetic acid [28] gave **4** and **5**, albeit in low yields based on recovered starting material (b.r.s.m.) (Scheme 1). Prolonging the reaction or raising temperatures did not increase yields. No 15-hydroxymethyl derivative was isolated. Excess paraformaldehyde tended to precipitate during chromatography, blocking the column. This was therefore extracted from the crude product with hot water. Our results conflict with a previous report that heating **1** in acetic acid led to deacetylation and epimerization [29]. In our hands, **1** was freely soluble in glacial acetic acid and was recovered unchanged after heating overnight at reflux.

As an alternative linker attachment point, (2-hydroxyethoxy)methyl ether **6** was prepared from the known methylthiomethyl ether **7** using a slight modification of previous conditions (Scheme 2) [24].

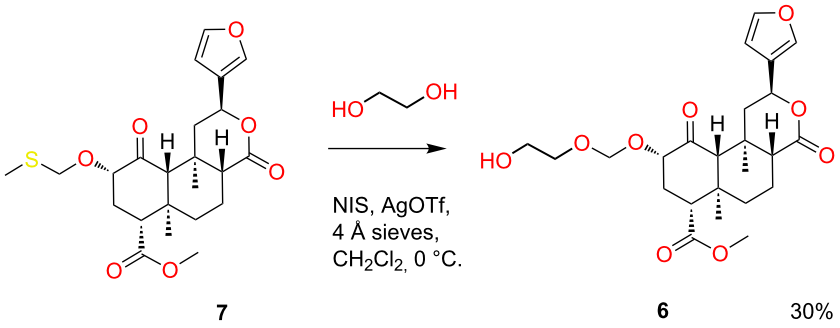
Structure elucidation

The molecular formula of **2** and **3** was established by HRMS, confirming the addition of a dimethylaminomethyl group in each case. The structure of **2** was established by X-ray crystallography (Figure 4) after recrystallization from ethanol/hexanes.

Consistent with the crystal structure, comparison of the ^{1}H NMR spectrum of **2** with the fully assigned spectrum of **1**



Scheme 1: Syntheses of heteromethylated derivatives of **1**. b.r.s.m. = based on recovered starting material.



Scheme 2: Synthesis of (2-hydroxyethoxy)methyl ether **6**.

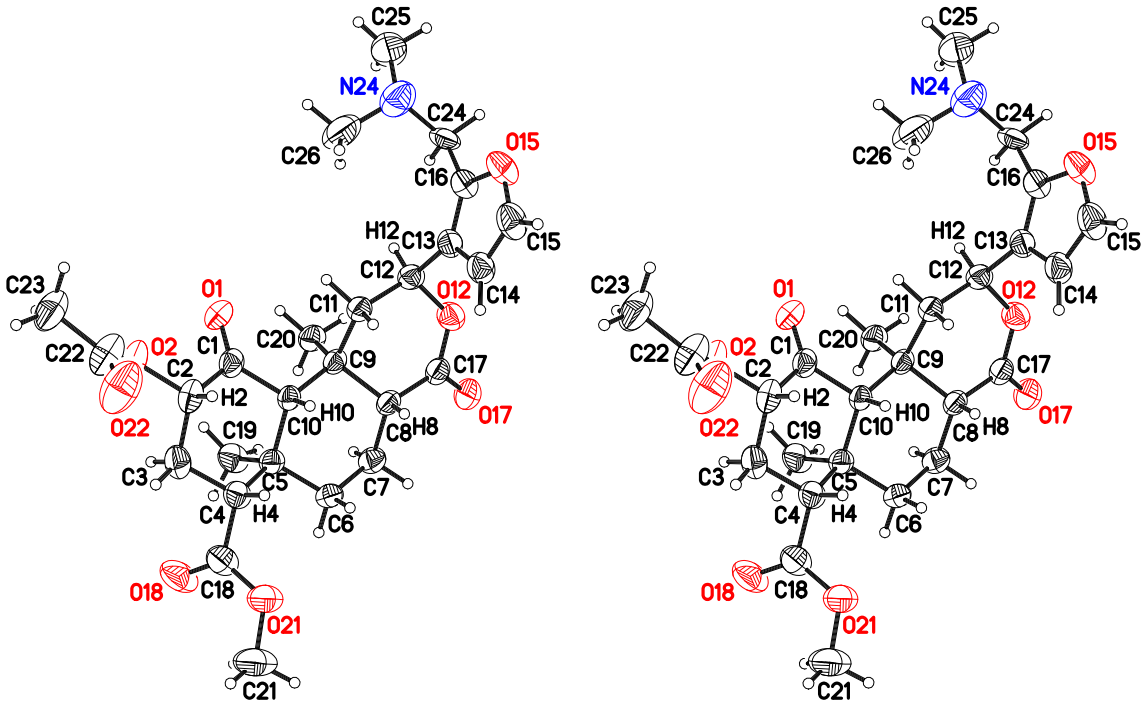


Figure 4: Crystal structure of **2** with 50% probability thermal displacement ellipsoids (cross-eyed stereoview). For clarity, only one of the two observed orientations for the disordered dimethylamino group is shown. For the other orientation and partially-occupied ethanol solvate, see Supporting Information File 1, Figure S1. For coordinates, see Supporting Information File 3 or CCDC 970639.

[30,31] revealed new dimethylamino (δ 2.22, s, 6H) and aminomethylene (δ ~3.4, m, 2H) signals and the loss of one furan oxymethine. The remaining oxymethine signal (δ 7.31) was a doublet with a typical vicinal coupling constant (1.7 Hz) to H-14 (δ 6.28), confirming that they were adjacent. The multiple-bond ^{1}H–^{13}C (HMBC) correlations for **2** shown in Figure 5 confirm substitution at C-16.

The structure of the other regioisomer, **3**, was confirmed using NMR data. The oxymethine signal (δ 7.34) showed only long-range couplings (J = 0.8 Hz), confirming that it was isolated. The HMBC correlations (Figure 5) confirmed substitution at C-15.

The molecular formula of **4**, established by HRMS, confirmed the addition of a hydroxymethyl group. Like the C-16-substituted **4**, the two furan peaks in the ^{1}H NMR spectrum were doublets with a typical vicinal coupling constant (1.9 Hz). The same HMBC correlations were observed as for **2** (Figure 5), confirming substitution at C-16. The molecular formula of **5**,

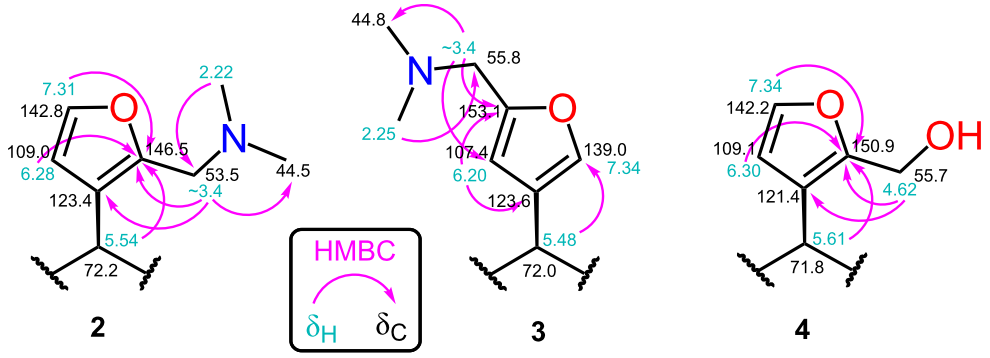


Figure 5: Key ^{1}H–^{13}C HMBC correlations.

established by HRMS, indicated the addition of two hydroxymethyl groups. The remaining furan oxymethine signal seen in the ^{1}H NMR spectrum of **4** was lost, leaving an H-14 singlet (δ 6.21), confirming substitution at C-15 and C-16. An oxymethylene triplet (δ 4.61, t, 2H) and doublet (δ 4.55, d, 2H) collapsed to a doublet and singlet, respectively, after washing with D_2O.

The molecular formula of (2-hydroxyethoxy)methyl ether **6** was confirmed by HRMS. The structure was confirmed by comparison of ^{1}H and ^{13}C NMR spectra with the previously reported (2-methoxyethoxy)methyl ether [24].

Bioassays

We next determined the binding affinities of these compounds in blinded tests for the human κ-OR expressed in Chinese hamster ovary cells (CHO-κ-OR). In an initial screening of the furan derivatives at 3 μM, only **4** caused ≥50% inhibition of [^{3}H]diprenorphine binding. The K_i of **4** was 110 nM (Table 1), a substantial reduction in affinity relative to **1**. None of these compounds showed detectable affinity for μ- or δ-OR (K_i > 1 μM in all cases). Thus, **4** showed modest affinity and selectivity for κ-OR, while **2**, **3** and **5** showed no affinity for any opioid receptor. Follow-up testing in the [^{35}S]GTPγS functional assay demonstrated that **4** was an agonist less potent than **1** at κ-OR, but giving an equal maximal response (Table 1). (2-Hydroxyethoxy)methyl ether **6** showed high affinity for κ-OR, but not for μ- or δ-OR (K_i > 1 μM), similar to other alkoxymethyl ethers [23,24].

Despite the low affinities and potencies of the furan derivatives, we undertook further investigations. As discussed in the Introduction, the key residues for the binding of **1** are almost entirely separate from the morphinan binding pocket. Although it seems likely that the two pockets overlap, it is possible that they are separate, or allotopic [32]. If so, **1** could bind simultaneously with morphinans and act as an allosteric modulator. Indeed, it has been reported that **1** is a low-affinity allosteric modulator of μ-OR [33]. Since it is possible for allosteric ligands to bind, and to modulate signaling, without displacing orthosteric ligands such as diprenorphine [34], binding assays can give false negative results.

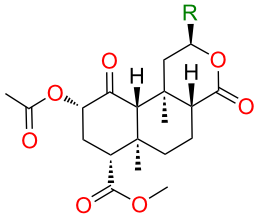
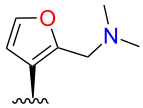
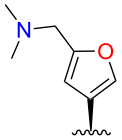
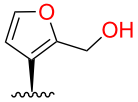
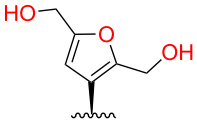
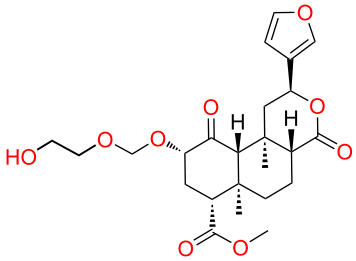
We therefore tested whether the furan derivatives of **1** that failed to displace [^{3}H]diprenorphine from κ-OR nonetheless modulated signaling. Given our interest in the development of κ-opioid antagonists [35], we tested for negative modulation. To maximize the physiological relevance of the assays, we used the endogenous agonist dynorphin A. In addition to **2**–**5**, we retested a number of derivatives of **1** we had previously found to exhibit negligible affinity for κ-OR; these featured modifications at C-12 [5], C-4 [36] and C-1 [31] (Figure 6).

In a primary screen at 3 μM, none of the compounds tested caused detectable antagonism of dynorphin A (10 nM) in the [^{35}S]GTPγS assay (Supporting Information File 1, Table S1). By comparison, the positive control, JDTic, abolished response to dynorphin A. These results reveal no evidence of allosteric modulation, but do not exclude the possibility [34].

Discussion

While the affinities of all these furan derivatives were low, they may nonetheless provide starting points for the development of bivalent derivatives. Installation of a leaving group on hydroxymethyl compound **4**, for instance, would permit coupling with diverse *N*-dealkylated opiate scaffolds. Alternative attachment points would also be worth exploring, such as the C-17 lactone, which tolerates reduction and alkylation [1]. As noted in the Introduction, there is compelling evidence that **1** binds adjacent to Asp138$^{3.32}$, but the involvement of the furan ring is based on modeling rather than direct evidence, and is thus highly speculative. A subsequent model for the binding of **1** derivative

Table 1: Binding affinity, potency and maximal response at κ-OR.

	R		K_i ± SEM[a] nM	EC_{50} ± SEM[b] nM	E_{max}[c] %
		**1**	3.0[d]	7.6 ± 0.3	106
		**2**	>1,000		
		**3**	>1,000		
		**4**	110 ± 10	345 ± 47	103
		**5**	>1,000		
		**6**	12.7 ± 1.3		
		U50,488H	1.2 ± 0.2	6.8 ± 1.1	100

[a]Displacement of [^{3}H]diprenorphine from CHO cell membranes expressing human κ-OR. Results represent mean ± standard error of the mean for three independent experiments (n = 3) performed in duplicate. [b]Potency in enhancement of [^{35}S]GTPγS binding to CHO-κ-OR membranes (n = 3–5). [c]Maximal [^{35}S]GTPγS binding relative to U50,488H. [d]As reported previously [6].

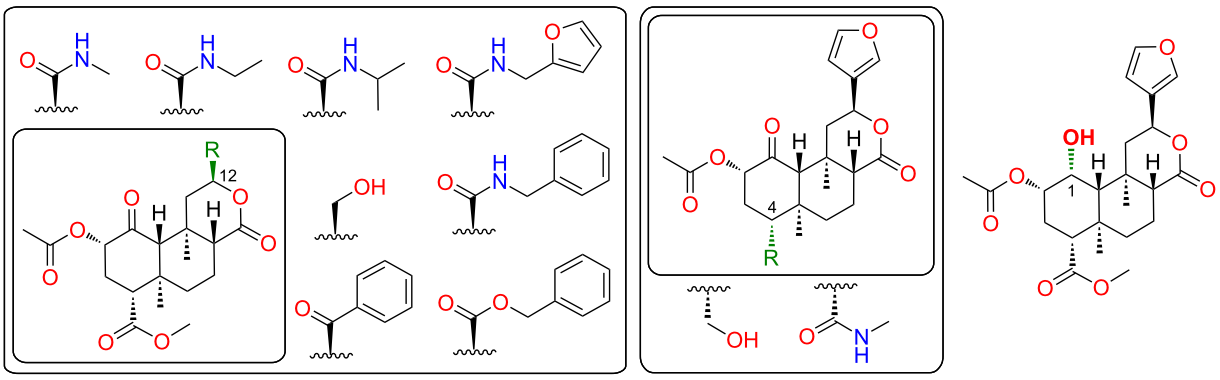


Figure 6: Known low-affinity derivatives of **1** screened in addition to **2**–**5** for negative allosteric modulation of dynorphin A at κ-OR in the [^{35}S]GTPγS assay. No compound caused detectable antagonism at 3 μM.

RB-64 places the C-18 methyl ester rather than the furan ring close to Asp138$^{3.32}$ [7]. In our previous studies, however, substitution of amine groups for the C-18 methyl ester abolished affinity for κ-OR [36]. Indeed, all modifications of this group tested to date greatly reduce affinity, in most cases abolishing binding altogether [1]. C-18 is thus not a promising attachment point. At the opposite extreme, the C-2 alkoxymethyl ether series is highly tolerant to alkyl chain extension. Compound **6** and the synthetic route used may prove useful for the attachment of very long linkers, as used with other scaffolds to bridge receptor dimers [21].

Rather than linking pharmacophores, another approach to bivalent ligands is to design hybrid structures, or merged multiple ligands [13]. As noted above, the HPP moiety of JDTic interacts with many of the key residues for binding of **1**, and shares a very similar substructure, suggesting that the binding pose of **1** may be similar. If so, converting the lactone to a cyclic amine may provide the desired H-bond to Asp138$^{3.32}$ without the need for additional functional groups.

Our results provide no evidence of negative allosteric modulation of κ-OR by low-affinity derivatives of **1**, and the mutagenesis results discussed in the Introduction suggest some overlap with other opioids. However, given the report that **1** is an allosteric modulator of μ-OR [33], high-affinity μ-selective derivatives such as herkinorin [1] also represent potential scaffolds for bivalent and possibly bitopic (orthosteric–allosteric) derivatives [12].

Conclusion

In conclusion, compelling evidence suggests that **1** binds to an allotopic pocket of κ-OR, leaving the classical opiate binding site largely unoccupied. This suggests the possibility of creating bivalent derivatives by linking these scaffolds, with the potential for dramatic increases in potency and altered functional selectivity. A suitable attachment point and linker remain to be determined. Our preliminary modifications at C-2, C-15 and C-16 yielded no potent derivatives, but may prove useful as intermediates in further exploration of this concept.

Author Contributions

T.A.M. designed and prepared the compounds, wrote the manuscript and prepared the figures. W.X. and L.Y.L.C. performed and analyzed the bioassays. D.M.H. obtained the crystal structure. B.M.C. supervised and coordinated the project.

Competing Interests

B.M.C., L.Y.L.C., and T.A.M. hold US patents on the preparation and therapeutic use of salvinorin A derivatives (7,629,475 and 8,492,564).

Supporting Information

Supporting Information File 1

Synthetic procedures and ^{1}H and ^{13}C NMR spectra of all new compounds; HMQC and HMBC spectra from Figure 5; supporting Figure S1 and Table S1.
[http://www.beilstein-journals.org/bjoc/content/supplementary/1860-5397-9-328-S1.pdf]

Supporting Information File 2

^{1}H and ^{13}C NMR spectra of all new compounds in jcamp-dx format.
[http://www.beilstein-journals.org/bjoc/content/supplementary/1860-5397-9-328-S2.zip]

Supporting Information File 3

X-ray crystal structure of **2**.
[http://www.beilstein-journals.org/bjoc/content/supplementary/1860-5397-9-328-S3.cif]

Supporting Information File 4

Structure factors for **2**.
[http://www.beilstein-journals.org/bjoc/content/supplementary/1860-5397-9-328-S4.hkl]

Acknowledgements

Funding for this work was provided by the National Institute of Drug Abuse (P30 DA13429 to LYLC). Cécile Béguin suggested compounds for the negative modulation assay.

References

1. Cunningham, C. W.; Rothman, R. B.; Prisinzano, T. E. *Pharmacol. Rev.* **2011,** *63,* 316–347. doi:10.1124/pr.110.003244
2. Hooker, J. M.; Munro, T. A.; Béguin, C.; Alexoff, D.; Shea, C.; Xu, Y.; Cohen, B. M. *Neuropharmacology* **2009,** *57,* 386–391. doi:10.1016/j.neuropharm.2009.06.044
3. Peet, M. M.; Baker, L. E. *Behav. Pharmacol.* **2011,** *22,* 450–457. doi:10.1097/FBP.0b013e328349fc1b
4. Lamb, K.; Tidgewell, K.; Simpson, D. S.; Bohn, L. M.; Prisinzano, T. E. *Drug Alcohol Depend.* **2012,** *121,* 181–188. doi:10.1016/j.drugalcdep.2011.10.026
5. Béguin, C.; Duncan, K. K.; Munro, T. A.; Ho, D. M.; Xu, W.; Liu-Chen, L.-Y.; Carlezon, W. A., Jr.; Cohen, B. M. *Bioorg. Med. Chem.* **2009,** *17,* 1370–1380. doi:10.1016/j.bmc.2008.12.012
6. Béguin, C.; Potuzak, J.; Xu, W.; Liu-Chen, L.-Y.; Streicher, J. M.; Groer, C. E.; Bohn, L. M.; Carlezon, W. A., Jr.; Cohen, B. M. *Bioorg. Med. Chem. Lett.* **2012,** *22,* 1023–1026. doi:10.1016/j.bmcl.2011.11.128
7. Wu, H.; Wacker, D.; Mileni, M.; Katritch, V.; Han, G. W.; Vardy, E.; Liu, W.; Thompson, A. A.; Huang, X.-P.; Carroll, F. I.; Mascarella, S. W.; Westkaemper, R. B.; Mosier, P. D.; Roth, B. L.; Cherezov, V.; Stevens, R. C. *Nature* **2012,** *485,* 327–332. doi:10.1038/nature10939

8. Kane, B. E.; McCurdy, C. R.; Ferguson, D. M. *J. Med. Chem.* **2008,** *51,* 1824–1830. doi:10.1021/jm701040v
9. Vardy, E.; Mosier, P. D.; Frankowski, K. J.; Wu, H.; Katritch, V.; Westkaemper, R. B.; Aubé, J.; Stevens, R. C.; Roth, B. L. *J. Biol. Chem.* **2013,** *288,* 34470–34483. doi:10.1074/jbc.M113.515668
10. Granier, S.; Manglik, A.; Kruse, A. C.; Kobilka, T. S.; Thian, F. S.; Weis, W. I.; Kobilka, B. K. *Nature* **2012,** *485,* 400–404. doi:10.1038/nature11111
11. Manglik, A.; Kruse, A. C.; Kobilka, T. S.; Thian, F. S.; Mathiesen, J. M.; Sunahara, R. K.; Pardo, L.; Weis, W. I.; Kobilka, B. K.; Granier, S. *Nature* **2012,** *485,* 321–326. doi:10.1038/nature10954
12. Valant, C.; Lane, J. R.; Sexton, P. M.; Christopoulos, A. *Annu. Rev. Pharmacol. Toxicol.* **2012,** *52,* 153–178. doi:10.1146/annurev-pharmtox-010611-134514
13. Morphy, R. J. Historical Strategies for Lead Generation. In *Designing Multi-Target Drugs;* Morphy, R. J.; Harris, C. J., Eds.; RSC: Cambridge, 2012; pp 111–129. doi:10.1039/9781849734912-00111
14. Béguin, C.; Cohen, B. M. Medicinal Chemistry of Kappa Opioid Receptor Antagonists. In *Opiate Receptors and Antagonists: from Bench to Clinic;* Dean, R. L.; Bilsky, E. J.; Negus, S. S., Eds.; Humana Press: New York, 2009; pp 99–118. doi:10.1007/978-1-59745-197-0_6
15. Melief, E. J.; Miyatake, M.; Carroll, F. I.; Béguin, C.; Carlezon, W. A., Jr.; Cohen, B. M.; Grimwood, S.; Mitch, C. H.; Rorick-Kehn, L.; Chavkin, C. *Mol. Pharmacol.* **2011,** *80,* 920–929. doi:10.1124/mol.111.074195
16. Thompson, A. A.; Liu, W.; Chun, E.; Katritch, V.; Wu, H.; Vardy, E.; Huang, X.-P.; Trapella, C.; Guerrini, R.; Calo, G.; Roth, B. L.; Cherezov, V.; Stevens, R. C. *Nature* **2012,** *485,* 395–399. doi:10.1038/nature11085
17. Venkatakrishnan, A. J.; Deupi, X.; Lebon, G.; Tate, C. G.; Schertler, G. F.; Babu, M. M. *Nature* **2013,** *494,* 185–194. doi:10.1038/nature11896
18. Kane, B. E. Molecular recognition of G-protein coupled receptor ligands: Insights into salvinorin A and xanomeline. Ph.D. Thesis, University of Minnesota, 2006. http://gradworks.umi.com/32/38/3238362.html
19. Zimmerman, D. M.; Leander, J. D.; Cantrell, B. E.; Reel, J. K.; Snoddy, J.; Mendelsohn, L. G.; Johnson, B. G.; Mitch, C. H. *J. Med. Chem.* **1993,** *36,* 2833–2841. doi:10.1021/jm00072a001
20. Merz, H.; Langbein, A.; Stockhaus, K.; Walther, G.; Wick, H. *Adv. Biochem. Psychopharmacol.* **1974,** *8,* 91–107.
21. Hiller, C.; Kühhorn, J.; Gmeiner, P. *J. Med. Chem.* **2013,** *56,* 6542–6559. doi:10.1021/jm4004335
22. Munro, T. A.; Ho, D. M.; Cohen, B. M. *Acta Crystallogr., Sect. E: Struct. Rep. Online* **2012,** *68,* o3225–o3226. doi:10.1107/S1600536812043449
23. Wang, Y.; Chen, Y.; Xu, W.; Lee, D. Y. W.; Ma, Z.; Rawls, S. M.; Cowan, A.; Liu-Chen, L. Y. *J. Pharmacol. Exp. Ther.* **2008,** *324,* 1073–1083. doi:10.1124/jpet.107.132142
24. Munro, T. A.; Duncan, K. K.; Xu, W.; Wang, Y.; Liu-Chen, L.-Y.; Carlezon, W. A., Jr.; Cohen, B. M.; Béguin, C. *Bioorg. Med. Chem.* **2008,** *16,* 1279–1286. doi:10.1016/j.bmc.2007.10.067
25. Chernov, S. V.; Shul'ts, E. E.; Shakirov, M. M.; Tolstikov, G. A. *Russ. J. Org. Chem.* **2000,** *36,* 1455–1464.
26. Roman, G. *Mini-Rev. Org. Chem.* **2013,** *10,* 27–39. doi:10.2174/1570193x11310010003
27. Iovel, I.; Goldberg, Yu.; Shymanska, M. *J. Mol. Catal.* **1989,** *57,* 91–103. doi:10.1016/0304-5102(89)80129-4
28. Pevzner, L. M.; Ignat'ev, V. M. *J. Org. Chem. USSR* **1987,** *23,* 1169–1170.
29. Harding, W. W.; Schmidt, M.; Tidgewell, K.; Kannan, P.; Holden, K. G.; Dersch, C. M.; Rothman, R. B.; Prisinzano, T. E. *Bioorg. Med. Chem. Lett.* **2006,** *16,* 3170–3174. doi:10.1016/j.bmcl.2006.03.062
30. Ortega, A.; Blount, J. F.; Manchand, P. S. *J. Chem. Soc., Perkin Trans. 1* **1982,** 2505–2508. doi:10.1039/P19820002505
31. Munro, T. A. The Chemistry of Salvia divinorum. Ph.D. Thesis, University of Melbourne, Australia, 2006. http://pqdtopen.proquest.com/#abstract?dispub=3304556
32. Neubig, R. R.; Spedding, M.; Kenakin, T.; Christopoulos, A. *Pharmacol. Rev.* **2003,** *55,* 597–606. doi:10.1124/pr.55.4.4
33. Rothman, R. B.; Murphy, D. L.; Xu, H.; Godin, J. A.; Dersch, C. M.; Partilla, J. S.; Tidgewell, K.; Schmidt, M.; Prisinzano, T. E. *J. Pharmacol. Exp. Ther.* **2007,** *320,* 801–810. doi:10.1124/jpet.106.113167
34. May, L. T.; Leach, K.; Sexton, P. M.; Christopoulos, A. *Annu. Rev. Pharmacol. Toxicol.* **2007,** *47,* 1–51. doi:10.1146/annurev.pharmtox.47.120505.105159
35. Knoll, A. T.; Carlezon, W. A., Jr. *Brain Res.* **2010,** *1314,* 56–73. doi:10.1016/j.brainres.2009.09.074
36. Béguin, C.; Richards, M. R.; Li, J.-G.; Wang, Y.; Xu, W.; Liu-Chen, L.-Y.; Carlezon, W. A., Jr.; Cohen, B. M. *Bioorg. Med. Chem. Lett.* **2006,** *16,* 4679–4685. doi:10.1016/j.bmcl.2006.05.093

License and Terms

This is an Open Access article under the terms of the Creative Commons Attribution License (http://creativecommons.org/licenses/by/2.0), which permits unrestricted use, distribution, and reproduction in any medium, provided the original work is properly cited.

The license is subject to the *Beilstein Journal of Organic Chemistry* terms and conditions: (http://www.beilstein-journals.org/bjoc)

The definitive version of this article is the electronic one which can be found at: doi:10.3762/bjoc.9.328

Beilstein Journal of Organic Chemistry

Synthesis and determination of the absolute configuration of (−)-(5*R*,6*Z*)-dendrolasin-5-acetate from the nudibranch *Hypselodoris jacksoni*

I. Wayan Mudianta[1], Victoria L. Challinor[1], Anne E. Winters[2], Karen L. Cheney[2], James J. De Voss[1] and Mary J. Garson[*1]

Full Research Paper

Open Access

Address:
[1]School of Chemistry and Molecular Biosciences, The University of Queensland, Brisbane QLD 4072, Australia and [2]School of Biological Sciences, The University of Queensland, Brisbane QLD 4072, Australia

Email:
Mary J. Garson* - m.garson@uq.edu.au

* Corresponding author

Keywords:
enantioselective HPLC; *E*/*Z*-isomers; *Hypselodoris*; natural products; nudibranch; sesquiterpene

Beilstein J. Org. Chem. **2013,** *9,* 2925–2933.
doi:10.3762/bjoc.9.329

Received: 11 September 2013
Accepted: 21 November 2013
Published: 23 December 2013

This article is part of the Thematic Series "Natural products in synthesis and biosynthesis".

Guest Editor: J. S. Dickschat

© 2013 Mudianta et al; licensee Beilstein-Institut.
License and terms: see end of document.

Abstract

A small sample of (−)-(5*R*,6*Z*)-dendrolasin-5-acetate, which was fully characterized by 2D NMR studies, was isolated from the nudibranch *Hypselodoris jacksoni*, along with the sesquiterpenes (+)-agassizin, (−)-furodysinin, (−)-euryfuran, (−)-dehydroherbadysidolide and (+)-pallescensone. A synthetic sample ($[\alpha]_D$ −8.7) of the new metabolite was prepared by [1,2]-Wittig rearrangement of a geranylfuryl ether followed by acetylation of purified alcohol isomers. The absolute configuration at C-5 was established as *R* by the analysis of MPA ester derivatives of (*Z*)-5-hydroxydendrolasin obtained by preparative enantioselective HPLC.

Introduction

Marine organisms have been proven a prolific source of natural products that potentially can be used as lead compounds or which have inspired synthetic chemists as synthetic targets [1]. Similarly, extensive studies of marine chemical ecological interactions have enriched our knowledge of biological and evolutionary patterns, and of the role of small molecules in chemical defensive strategies underwater [2,3]. Nudibranchs (Mollusca: Gastropoda: Opisthobranchia) are a group of marine animals that use small molecules for a variety of purposes, including communication, reproduction, and defense against predation [4,5]. These molecules have been extensively studied and as of 2012, seven out of the 20 natural products of marine origin (either directly or as a derivative) that have been approved for FDA use as a drug or are in clinical trials were first isolated from molluscs. For some of these bioactives, the actual biosynthetic source is a microorganism [6].

Within the Nudibranchia, the genus *Hypselodoris* is generally characterized by sesquiterpene chemistry, as evidenced by a number of studies on European [7-13], Indian [14], South African [15], Brazillian [16], and Indo-Pacific specimens [17-20]. During a comparative biogeographical study on opisthobranch molluscs from South East Queensland, Australia, we encountered the new sesquiterpene (−)-(5*R*,6*Z*)-dendrolasin-5-acetate (**1**) in specimens of *H. jacksoni* along with the other known sesquiterpene metabolites (+)-agassizin, (−)-furodysinin, (−)-euryfuran, (−)-dehydroherbadysidolide, (+)-pallescensone. The new metabolite **1** has never been identified from natural sources, although the 6*E*-isomer **2** was previously reported in racemic form during the synthesis of naturally occurring dendrolasin (**3**) by Tsubuki et al. in 2009 [21] (Figure 1). Dendrolasin (**3**) itself has been isolated from both terrestrial and marine sources, including from the nudibranchs *Chromodoris lochi* [22], from three *Hypselodoris* spp. [18], and from the marine sponge *Dictyodendrilla* sp. [23]. The current study reports the isolation and synthesis of (−)-(5*R*,6*Z*)-dendrolasin-5-acetate (**1**), with the determination of the absolute configuration at C-5 by spectroscopic analysis of the methoxyphenylacetic acid (MPA) derivative.

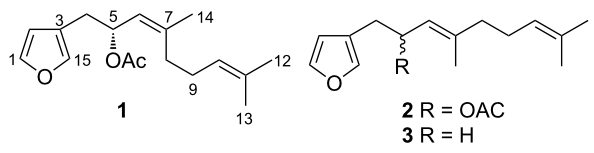


Figure 1: (−)-(5*R*,6*Z*)-Dendrolasin-5-acetate (**1**), its 6*E* derivative and naturally occuring dentrolasin (**3**).

Results and Discussion

Isolation and structure elucidation of natural product 1

Eight individuals of *H. jacksoni* were collected by SCUBA from two locations in SE Queensland. Owing to their small size (21–40 mm), the specimens were not examined individually. Extraction into acetone followed by partitioning into diethyl ether gave an extract which was fractionated first by normal phase (NP) flash chromatography and then by preparative NP HPLC to give (+)-agassizin, (−)-furodysinin, (−)-euryfuran, (−)-dehydroherbadysidolide, (+)-pallescensone, and the new sesquiterpene **1**.

Compound **1**, $[\alpha]_D$ −53 (*c* 0.006, $CHCl_3$), displayed a (+)-HRESIMS ion adduct at *m*/*z* 299.1624 $[M + Na]^+$ consistent with the molecular formula $C_{17}H_{24}O_3$. The ^1H NMR spectrum ($CDCl_3$, 500 MHz) of **1** showed diagnostic signals for a furan [δ_H 7.33 (1H), 7.23 (1H), 6.27 (1H); δ_C 142.7, 140.1, 111.8] along with two alkene signals [δ_H 5.15 (1H), 5.07 (1H); δ_C 123.7, 123.9]. Signals for three methyl groups were observed at δ_H 1.72, 1.67, and 1.59 and were linked to signals at δ_C 23.3, 25.7, and 17.6, respectively, by HSQC. There were also signals characteristic of an acetate group [δ_H 2.01 (s, 3H); δ_C 21.4]. These partial NMR assignments were comparable to those of the known dendrolasin (**3**), a sesquiterpene previously isolated from *Hypselodoris cantabrica* [9] and *H. californiensis* [18]. However, the signal corresponding to H-5 in dendrolasin (**3**) was reported to be a multiplet (2H) resonating at δ_H 2.21 [24] whereas that in **1** was shifted to δ_H 5.64 (brdt, J = 6.4, 9.3 Hz, 1H). The gCOSY spectrum of **1** showed cross peaks from H-5 to H-4/H-6, between the furan signals H-1/H-2 and between H-8/H-9/H-10. The H-5 proton was attached to an oxymethine carbon at δ_C 70.7 based on HSQC data and showed HMBC correlations to neighbouring carbons including C-3 (δ_C 120.2), C-7 (δ_C 141.5), and the OAc carbonyl (δ_C 170.2) (Figure 2). HMBC correlations observed from the alkene proton H-6 (δ_H 5.15) to C-4, C-7, and CH_3-14 secured the position of the double bond between C-6 and C-7. A second double bond was positioned between C-10 and C-11 based on HMBC correlations from the alkene proton H-10 (δ_H 5.07) to CH_3-12 and C-8. The C-6/C-7 configuration was revealed as *Z* rather than the *E*-configuration anticipated, based on 1D nOe experiments in which the signal intensity of H_3-14 increased when the signal attributed to H-6 was irradiated (mixing time 60 ms). 1D nOe irradiation of H-10 provided assignment of the signals corresponding to CH_3-12.

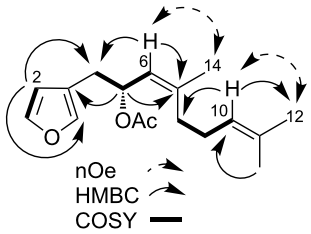
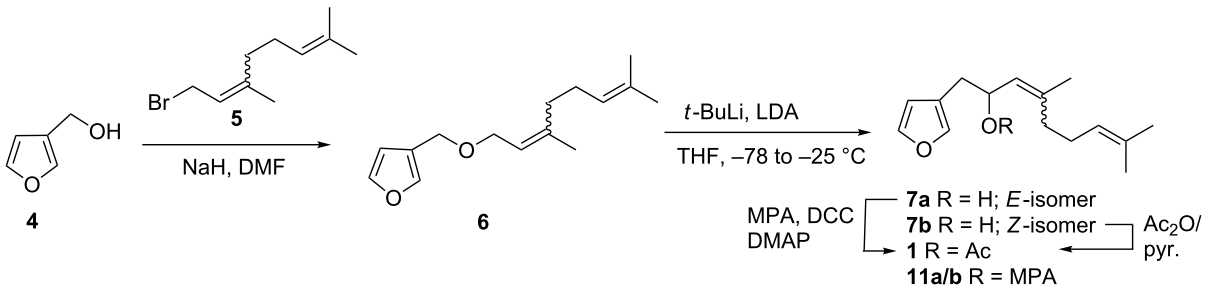


Figure 2: Selected HMBC, COSY, and nOe correlations of **1**.

Total synthesis of (−)-(5*R*,6*Z*)-dendrolasin-5-acetate (1)

In view of the small sample (0.1 mg) of natural material available, a synthetic study was undertaken to provide stereochemical characterization of **1**, in particular the configuration at C-5. The synthesis, which was completed in five steps, involved preparation of 3-furylmethanol (**4**) and of geranyl bromide (**5**), etherification, [1,2]-Wittig rearrangement of geranyl 3-furylmethyl ether (**6**) to produce **7a**/**b**, and acetylation to obtain target **1**. The overall synthesis (Scheme 1) was adapted from Tsubuki et al. [21].

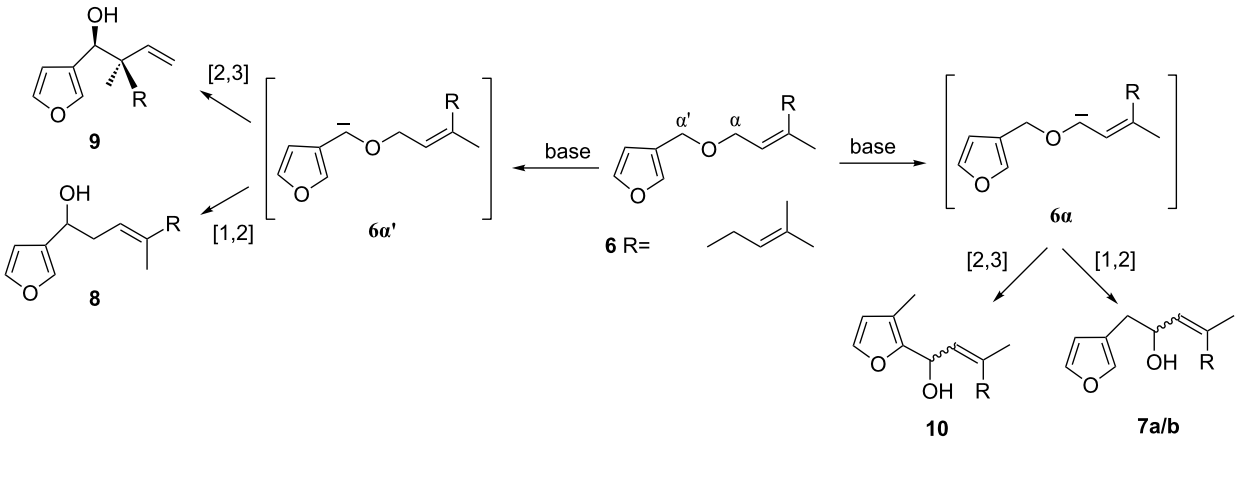


Scheme 1: Synthetic route to sesquiterpene **1**.

Furan-3-ylmethanol (**4**) was prepared in 78% yield by reduction of 2-furoic acid with $LiAlH_4$ in dry diethyl ether, whereas geranyl bromide (**5**) was obtained through bromination of geraniol with carbon tetrabromide and triphenylphosphine in 90% yield. The ^{1}H NMR spectrum of the geraniol sample used indicated the presence of traces of nerol, the *Z*-isomer of geraniol. Etherification of furan-3-ylmethanol (**4**) with the geranyl/neryl bromide mixture (**5**) in the presence of NaH furnished the 3-furylmethyl ether **6** (65% yield) as an *E*/*Z* mixture (3:1). The H-5 signal for the minor *Z*-isomer of **6** resonated at δ_H 3.90 (d, J = 6.8 Hz) compared to that of the *E*-isomer (δ_H 4.00, d, J = 6.8 Hz). Irradiation of the H-5 signal of the *Z*-isomer increased the intensity of the signal associated with the adjacent methyl (CH_3-14), confirming the Z double bond at C6/C7. The isomeric mixture of **6** was immediately subjected to [1,2]-Wittig rearrangement with *t*-BuLi (4 equiv) and LDA at −78 °C to afford racemic 5-hydroxydendrolasin (39% yield), again as an *E*/*Z* mixture (**7a/b**) for which a 3:1 ratio was determined by ^{1}H NMR comparison with data for the individual stereoisomers (see below). The 3:1 ratio of *E*/*Z*-isomers was confirmed via analytical HPLC.

In principle, the rearrangement of **6** could afford either [1,2]-rearranged products (e.g. **7a**/**b** or **8**) or [2,3]-rearranged products such as **9** or **10** depending on which site adjacent to the ether oxygen is preferentially deprotonated (Scheme 2). A thermodynamic optimization study on the Wittig rearrangement of allyl 3-furylmethyl ether by Tsubuki et al. has revealed that deprotonation occurs mainly at the α-position [21]. The results of this theoretical study are fully consistent with our synthetic work since the mixture of **7a**/**b** was the sole [1,2]-Wittig rearrangement product obtained.

Racemic 5-hydroxydendrolasin (**7a**/**b**) was next subjected to HPLC (hexanes/EtOAc, 90:10) to provide the individual *E*- (**7a**) and *Z*-isomers (**7b**) that were each carefully characterised by ^{1}H NMR and 1D nOe experiments. Assignment of the upfield signals corresponding to the three methyl groups attached to the double bonds (Figure 3) was made using HMBC and nOe data. The signal for CH_3-14 in the *Z*-isomer resonated downfield (δ_H 1.74) compared to that in the *E*-isomer (δ_H 1.65) while the signal for H-5 appeared slightly upfield (δ_H 4.48) in the *Z*-isomer compared to that in its *E* counterpart (δ_H 4.51).



Scheme 2: Mechanism of Wittig rearrangement [21].

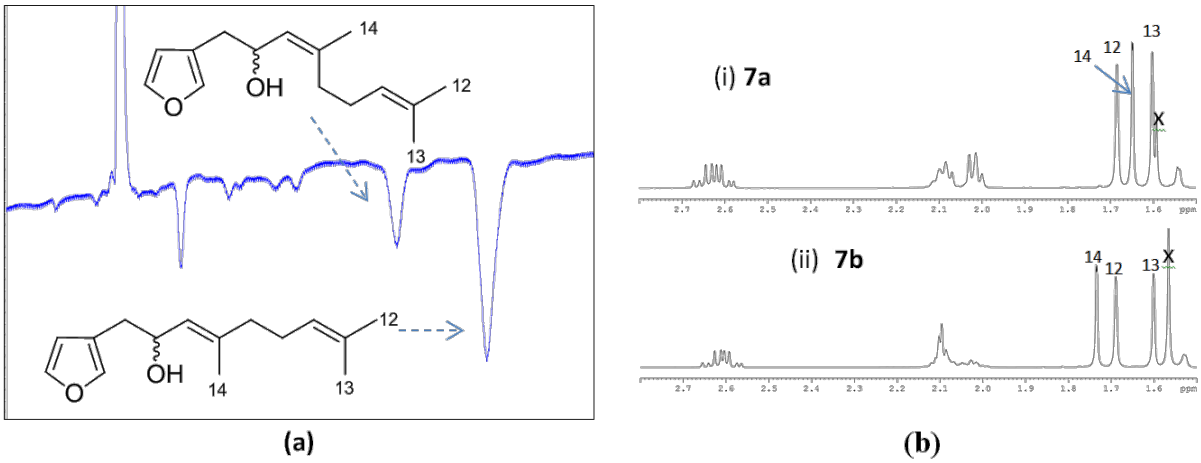


Figure 3: (a) NP HPLC trace showing separation of racemic 5-hydroxydendrolasin (**7a/b**) using hexanes/EtOAc (90:10; flow rate 2 mL/min over 60 minutes (x axis)) and refractive index detection (y axis); (b) ^{1}H NMR spectroscopic comparison of (6*E*)-5-hydroxydendrolasin (**7a**) (i) and (6*Z*)-5-hydroxydendrolasin (**7b**) (ii); × = water signals.

1D NOESY irradiation of the CH_3-14 signal for the *Z*-isomer resulted in enhancement of the alkene signal at δ_H 5.24 (H-6), fully consistent with the *Z* configuration; there was no corresponding nOe between CH_3-14 and H-6 in the *E*-isomer, although such data must be interpreted with care.

With the individual characterization of the *E*/Z-isomers accomplished, preparative enantioselective HPLC separation of racemic (*Z*)-5-hydroxydendrolasin (**7b**) was next undertaken (Figure 4) and provided samples of both of the (+)-**7b** and (−)-**7b** isomers, respectively. Treatment of each enantiomer of **7b** with acetic anhydride and pyridine gave their acetate derivatives. Surprisingly, (+)-**7b** ($[\alpha]_D$ +9.3) gave an acetate derivative with $[\alpha]_D$ −8.7 and vice versa ($[\alpha]_D$ −12 for (−)-**7b** and $[\alpha]_D$ +13 for its acetate derivative). As anticipated, the ^{1}H NMR spectrum ($CDCl_3$, 500 MHz) of the synthetic sample of (−)-(6*Z*)-**1** was fully superimposable with that of the sample of (6*Z*)-dendrolasin-5-acetate isolated from *H. jacksoni* (Figure 5).

Absolute configurational assignment of (6*Z*)-dendrolasin-5-acetate (**1**)

It remained to determine the absolute configuration of C-5 in the natural acetate derivative. A portion of the racemic mixture of **7b** was esterified with (*R*)-MPA acid in the presence of DMAP and DCC at room temperature to give a mixture of diastereomeric (*R,R*)-**11** and (*R,S*)-**11**, which was separated by reversed phase (RP) HPLC (MeCN/H_2O; 63:35) (Figure 6). The H-6 protons in (*R,R*)-**11** and (*R,S*)-**11** resonated at δ_H 5.04 and

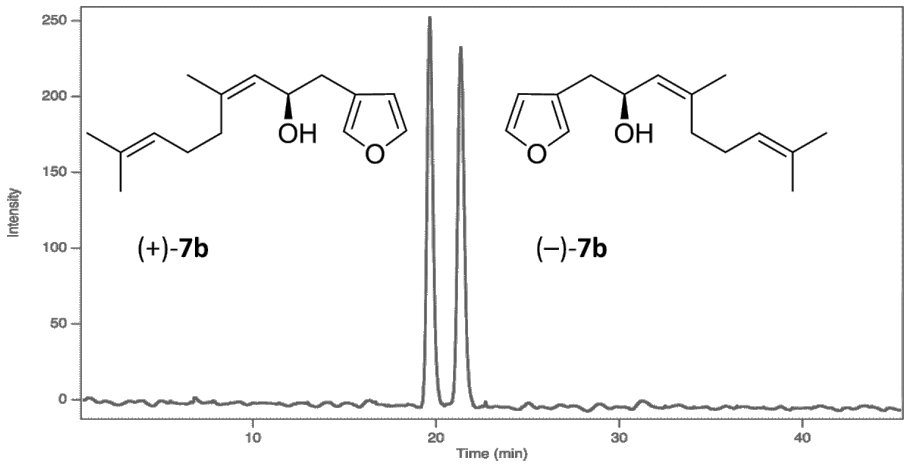


Figure 4: Analytical enantioselective HPLC trace showing separation of individual enantiomers of (6*Z*)-5-hydroxydendrolasin (Chiralpak AD column, 250 × 4.6 mm, 2% IPA in *n*-hexane at 0.5 mL/min, UV detection at 214 nm).

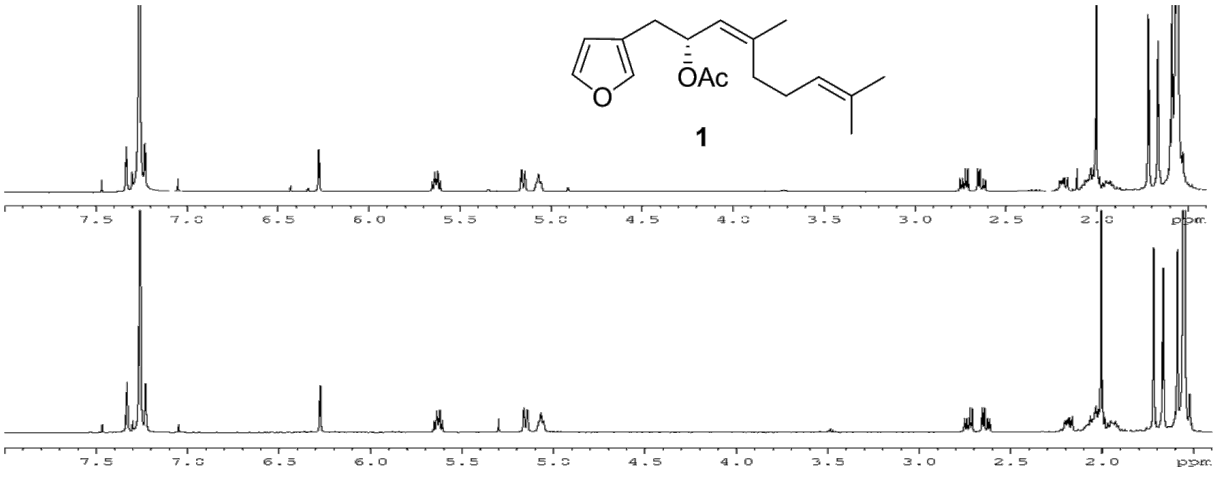


Figure 5: The ^{1}H NMR ($CDCl_3$, 500 MHz) spectroscopic comparison of (6*Z*)-dendrolasin-5-acetate (**1**): (a) sample isolated from *H. jacksoni*; (b) synthetic sample of (−)-(6*Z*)-**1**.

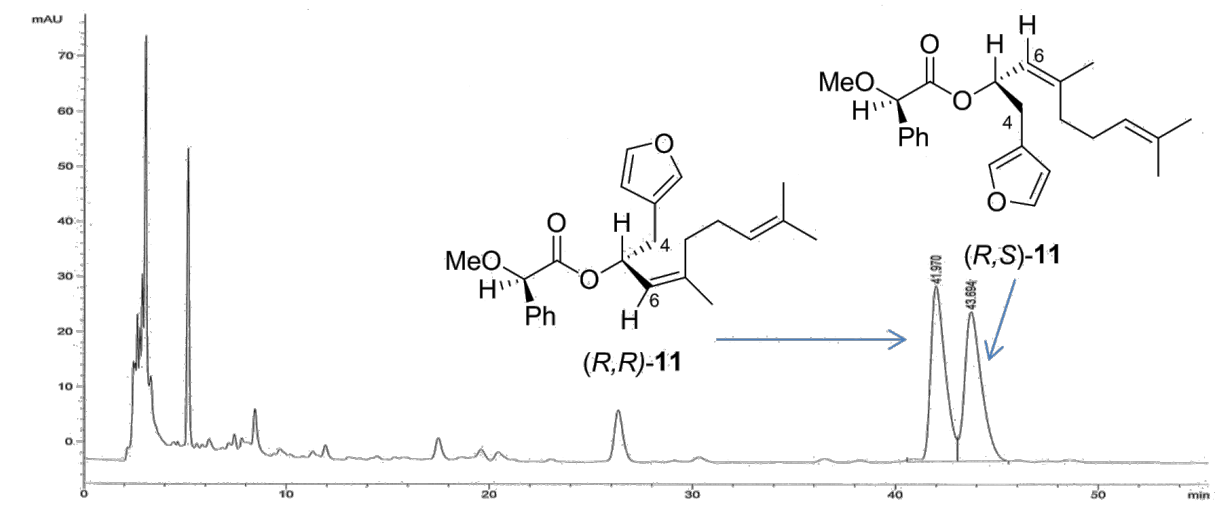


Figure 6: RP HPLC trace showing separation of the MPA esters (*R,R*)-**11** and (*R,S*)-**11** (MeCN/H_2O, 63:35 over 50 minutes, Phenomenex C-18 column, 250 × 4.60 mm, UV detection at 254 nm).

at δ_H 5.13, respectively, in agreement with H-6 of the (*R,R*)-isomer positioned in the shielding cone of the aryl ring of the MPA moiety [25]. The diastereotopic H-4 signals in (*R,S*)-**11** at δ_H 2.51 and 2.58 were shielded compared to those in (*R,R*)-**11** (δ_H 2.64, 2.74). Likewise, the furan proton signals were shifted upfield in the (*R,S*)-isomer compared to the (*R,R*)-isomer. These data were in agreement with the configurations depicted in Figure 6. The MPA ester spectra acted as reference data for determination of the absolute configuration of the natural sample of dendrolasin-5-acetate (**1**). The individually-purified enantiomers of synthetic (6*Z*)-5-hydroxydendrolasin were each treated with (*R*)-MPA to give their respective MPA ester derivatives. The ^{1}H NMR spectra of the MPA ester of (+)-**7b** was identical to that of the synthetic (*R,R*)-**11** and established that (+)-5-hydroxydendrolasin (**7**) has an *R* configuration. Likewise, the ^{1}H NMR spectrum of the MPA ester of (−)-**7b** was identical to that of the synthetic diastereomer (*R,S*)-**11**. Taking into account the change in sign of $[\alpha]_D$ between the alcohol and its acetate derivative, these data verified that the naturally-occurring (−)-acetate **1** had a 5*R* configuration.

Specific rotation values for **1** were measured as $[\alpha]_D$ −53 for the natural sample and −8.7 for the synthetic sample. Despite having the same negative sign of specific optical rotation, the $[\alpha]_D$ values of the natural sample was considerably larger than that of the synthetic sample. Although a partial explanation for

the difference in values was apparent, namely that the natural sample size was small (0.1 mg) compared to the synthetic sample size (0.9 mg), better experimental evidence of their stereochemical uniformity was desirable. Enantioselective HPLC analyses run under identical conditions using 5% isopropanol in *n*-hexane were carried out on the synthetic sample of racemic **1**, the two synthetically prepared *R* and *S* enantiomers of **1**, and the natural sample as shown in Figure 7. The data revealed a clear separation of the individual enantiomers of **1** (shown in trace (a)), and that the (+)-enantiomer elutes before the (−)-enantiomer (traces (b) and (c)). Finally, the natural sample has the same retention time as the (−)-enantiomer (trace (d)). A co-injection experiment performed on a mixture of the synthetic (+)-enantiomer and the natural sample consistently displayed two peaks in which the former compound eluted before the natural sample.

Conclusion

Chemical investigation of *H. jacksoni* collected from Queensland yielded a new sesquiterpene (5*R*,6*Z*)-dendrolasin-5-acetate (**1**) whose structure and stereochemistry were confirmed by means of a five-step synthesis involving [1,2]-Wittig rearrangement of geranyl furyl ether (**6**) followed by acetylation of the purified alcohol products. The absolute configuration in **1** was established as 5*R* by detailed comparison with MPA ester derivatives prepared from individual enantiomers of synthetic (6*Z*)-5-hydroxydendrolasin purified by preparative enantioselective HPLC.

Experimental

Isolation of (−)-(5*R*,6*Z*)-dendrolasin-5-acetate (1) from *Hypselodoris jacksoni*: Eight individuals of *H. jacksoni* (21–40 mm in length) were collected from various dive sites in South East Queensland (specimens #243, 244 Mudjimba Island, Mooloolaba S26°36’54”, E153°06’49”; #75–77 and #125–127 Shag Rock, North Stradbroke Island S27°24'49" E153°31'30”) between March and October of 2012. The whole animals were chopped, macerated in acetone (20 mL), sonicated for 2 min before being filtered through a cotton plug. The resulted filtrate was combined, concentrated under reduced pressure and partitioned between Et_2O (3 × 20 mL) and water. The Et_2O crude fraction (39.2 mg) was resolved by NP flash column chromatography eluted with gradient solvent from 100% hexanes→100% EtOAc to give ten fractions. The first and the second fraction (coded as HJF1–2) (21.3 mg) were combined based on their TLC profile, and yielded the major metabolites (−)-furodysinin (3.8 mg), (+)-agassizin (2.5 mg) and (−)-eurycfuran (0.8 mg) following NP HPLC separation using 100% hexanes. The fourth fraction coded as HJF4 (1.8 mg) was subjected to NP HPLC eluting with 2.5% EtOAc/hexanes to give (−)-dehydroherbadysidolide (0.1 mg), (+)-pallescensone (0.2 mg), and the new sesquiterpene (−)-(5*R*,6*Z*)-dendrolasin-5-

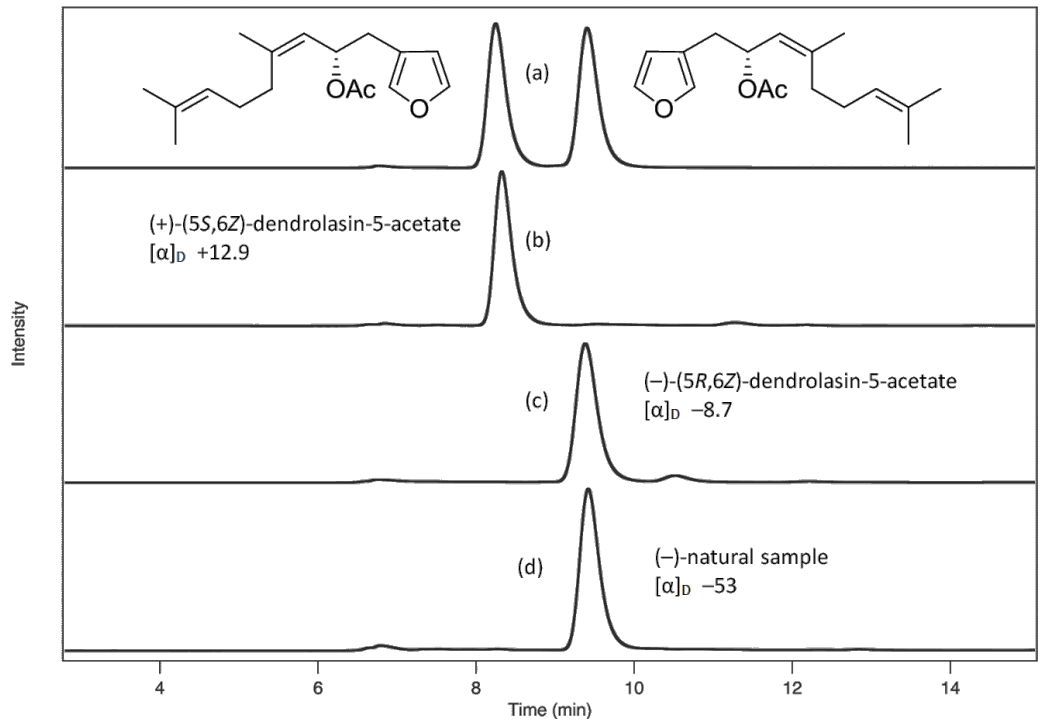


Figure 7: Enantioselective HPLC profiles (5% isopropanol in *n*-hexane) of **1**: (a) synthetic (±) mixture; (b) synthetic (+)-enantiomer; (c) synthetic (−)-enantiomer; (d) natural sample from *H. jacksoni*.

acetate (**1**, 0.1 mg). $[\alpha]_D^{24}$ −53 (*c* 0.006, $CHCl_3$); ^{1}H NMR ($CDCl_3$, 500 MHz) δ_H 7.33 (bs, 1H, H-1), 7.23 (bs, 1H, H-15), 6.27 (s, 1H, H-2), 5.64 (bdt, *J* = 6.4, 9.3 Hz, 1H, H-5), 5.15 (d, *J* = 9.3 Hz, 1H, H-6), 5.07 (brt, *J* = 6.9 Hz, 1H, H-10), 2.73 (dd, *J* = 6.7, 14.5 Hz, 1H, H-4a), 2.63 (dd, *J* = 6.0, 14.5 Hz, 1H, H-4b), 2.15–1.95 (overlapping, m, 4H, H-8, H-9), 1.72 (s, 3H, H-14), 1.67 (s, 3H, H-12), 1.59 (s, 3H, H-13); ^{13}C NMR ($CDCl_3$, 125 MHz) δ_C 142.7 (C-1), 141.5 (C-7), 140.1 (C-15), 132.0 (C-11), 123.9 (C-10), 123.7 (C-6), 120.2 (C-3), 111.8 (C-2), 70.7 (C-5), 32.5 (C-8), 30.7 (C-4), 26.5 (C-9), 25.7 (C-12), 23.3 (C-14), 17.6 (C-13); (+)-HRESIMS *m*/*z*: $[M + Na]^+$ calcd. for $C_{17}H_{24}NaO_3$, 299.1618; found, 299.1624.

Procedure for Wittig rearrangement of 3-furylmethyl ether (6) [21]: To a solution of (*E*/*Z*)-3-furylmethyl ether (**6**, 200 mg) in THF (10 mL) was added dropwise first LDA (3.64 mL, 10 wt % suspension in hexane) followed by *t*-BuLi (2.5 mL, 1.6 M in hexanes;) at −78 °C under Ar. After stirring for 1 h (the reaction mixture was allowed to warm to 0 °C), the reaction mixture was quenched with sat. aq NH_4Cl solution and the solvent was removed under vacuum. The residue was extracted with pentane/Et_2O (1:1, v/v). The extract was washed with brine and dried over Na_2SO_4. Evaporation of the solvent gave a residue, which was chromatographed on silica gel (5.0 g, hexanes/AcOEt 95:5) to afford the desired product (*E*/*Z* ratio ~3:1) as a mixture of enantiomers (83 mg, 39% yield). The *E*- and *Z*-isomers of 5-hydroxydendrolasin were then separated by NP HPLC (hexanes/EtOAc 90:10, flow rate 2 mL/min, refractive index detection, Waters μPorasil™ column 10 μm, 300 × 7.8 mm) to give the individual 6*E* ((**7a**); 25.2 mg; t_R = 50.0 min) and 6*Z* ((**7b**); 8.4 mg; t_R = 40.0 min) isomers. Analytical enantioselective HPLC separation of the *Z*-isomer of 5-hydroxydendrolasin (**7b**) was performed on an Agilent 1200 series liquid chromatography system (isocratic conditions of 2% isopropanol in *n*-hexane, flow rate of 0.5 mL min^{-1}) equipped with UV (214 nm) and ALP (Advanced Laser Polarimeter, PDR-Chiral Inc.) detectors and a Chiralpak AD column (250 × 4.6 mm, Daicel Chemical Industries Ltd.). The preparative enantioselective HPLC purification of **7b** used isocratic conditions (1.5% isopropanol in *n*-hexane, flow rate of 10 mL min^{-1}) with UV detection at 220 nm and a Chiralpak AD column (250 × 20 mm, Daicel Chemical Industries Ltd.) to give the (+)-enantiomer (2.7 mg); (−)-enantiomer (2.6 mg). The retention times were: 29.5 min ((+)-enantiomer); 32.1 min ((−)-enantiomer).

(±)-(*E*)-1-(furan-3-yl)-4,8-dimethylnona-3,7-dien-2-ol (7a) [21]**:** Colorless glass; ^{1}H NMR ($CDCl_3$, 500 MHz) δ_H 7.37 (s, 1H, H-1), 7.29 (s, 1H, H-15), 6.32 (s, 1H, H-2), 5.24 (d, *J* = 8.5 Hz, 1H, H-6), 5.07 (brt, *J* = 7.1 Hz, 1H, H-10), 4.51 (q, *J* = 7.1, 13.6 Hz, 1H, H-5), 2.66 (dd, *J* = 7.1, 14.4 Hz, 1H, H-4a), 2.59 (dd, *J* = 7.1, 14.4 Hz, 1H, H-4b), 2.12–2.01 (m, 4H, H-8 and H-9), 1.65 (d, *J* = 1.1 Hz, 3H, CH_3-14), 1.69 (s, 3H, CH_3-12), 1.60 (s, 3H, CH_3-13); ^{13}C NMR ($CDCl_3$, 125 MHz) δ_C 142.9 (C-1), 140.3 (C-15), 139.5 (C-7), 131.8 (C-11), 127.0 (C-3), 124.0 (C-10), 120.9 (C-6), 111.7 (C-2), 68.5 (C-5), 39.6 (C-8), 33.3 (C-4), 26.4 (C-9), 25.7 (C-12), 17.8 (C-13), 16.7 (C-14); (+)-LRESIMS *m*/*z*: 257 $[M + Na]^+$.

(±)-(*Z*)-1-(furan-3-yl)-4,8-dimethylnona-3,7-dien-2-ol (7b): Colorless glass; ^{1}H NMR ($CDCl_3$, 500 MHz) δ_H 7.37 (s, 1H, H-1), 7.29 (s, 1H, H-15), 6.32 (s, 1H, H-2), 5.24 (d, *J* = 8.8 Hz, 1H, H-6), 5.07 (brt, *J* = 5.4 Hz, 1H, H-10), 4.48 (q, *J* = 6.7, 13.6 Hz, 1H, H-5), 2.65 (dd, *J* = 7.2, 14.4 Hz, 1H, H-4a), 2.58 (dd, *J* = 7.2, 14.4 Hz, 1H, H-4b), 2.12–2.01 (m, 4H, H-8 and H-9), 1.74 (d, *J* = 1.1 Hz, 3H, CH_3-14), 1.69 (s, 3H, CH_3-12), 1.60 (s, 3H, CH_3-13); ^{13}C NMR ($CDCl_3$, 125 MHz) δ_C 142.9 (C-1), 140.3 (C-15), 139.5 (C-7), 132.6 (C-11), 128.0 (C-3), 124.0 (C-10), 121.1 (C-6), 111.7 (C-2), 68.1 (C-5), 33.2 (C-8), 32.5 (C-4), 26.6 (C-9), 25.8 (C-12), 23.5 (C-14), 17.8 (C-13); (+)-HRESIMS *m*/*z*: $[M + Na]^+$ calcd for $C_{15}H_{22}NaO_2$, 257.1512; found, 257.1515.

Procedure for acetylation of (±)-(*Z*)-1-(furan-3-yl)-4,8-dimethylnona-3,7-dien-2-ol (7b): A portion of **7b** (8.4 mg) was dissolved in dry pyridine (0.5 mL) and cooled in an ice bath. After the addition of acetic acid anhydride (1.5 mL) the mixture brought to rt and stirred for 1.5 hours. Toluene (0.5 mL) was added and the resulting azeotrope was evaporated under reduced pressure to give (±)-(6*Z*)-dendrolasin-5-acetate (**1**) (6.4 mg); ^{1}H and ^{13}C NMR data ($CDCl_3$, 500 MHz) are identical to those of **1**. (+)-LRESIMS *m*/*z* 299 $[M + Na]^+$.

Procedure for acetylation of the (+) isomer of 7b: A portion of the (+) isomer of **7b** (1.3 mg) was acetylated using the same procedure as for **7b** to obtain (−)-(6*Z*)-dendrolasin-5-acetate (**1**, 0.9 mg); Colorless glass; $[\alpha]_D$ −8.7 (*c* 0.06, $CHCl_3$); ^{1}H and ^{13}C NMR data ($CDCl_3$, 500 MHz) are the same as those of the **1**. (+)-LRESIMS *m*/*z*: 299 $[M + Na]^+$.

Procedure for acetylation of the (−)-isomer of 7b: A portion of the (−)-isomer of **7b** (1.3 mg) was acetylated using the same procedure as for **7b** to obtain (+)-(6*Z*)-dendrolasin-5-acetate (**1**, 1.1 mg); Colorless glass; $[\alpha]_D$ +12.9 (*c* 0.07, $CHCl_3$); ^{1}H and ^{13}C NMR ($CDCl_3$, 500 MHz) are identical to those of **1**. (+)-LRESIMS *m*/*z*: 299 $[M + Na]^+$.

Procedure for preparation of (*R*)- and (*S*)-MPA esters of racemic (6*Z*)-5-hydroxydendrolasin (7b): (±)-(6*Z*)-5-Hydroxydendrolasin (2.0 mg) was dissolved in dry DCM (0.2 mL) to which (*R*)-methoxyphenylacetic acid (MPA)

(0.83 mg in 0.1 mL of DCM) was added, followed by DCC (2 equiv, 1.03 mg in 0.1 mL of DCM) and DMAP (2 equiv, 0.61 mg in 0.1 mL of DCM). The reaction was stirred at rt for 16 h and then filtered through a cotton wool plug. The solvent was removed by rotary evaporation and the residue passed through a pipette silica column eluted with hexanes/EtOAc (95:5) to give a racemic MPA ester (0.8 mg). The racemic MPA ester was subsequently subjected to RP HPLC ($MeCN/H_2O$, 60:40; flow rate 1 mL/min, UV detection at 254 nm, Phenomenex Gemini 5 µ C18 110 Å, 250 × 4.60 mm) to give the *R,R* (0.2 mg) and *R,S* diastereomers (0.2 mg).

(*R,R*)-(6*Z*)-dendrolasin MPA ester (11a): Colorless glass; $[\alpha]_D$ +10.1 (*c* 0.01, $CHCl_3$); ^1H NMR ($CDCl_3$, 500 MHz) δ_H 7.38–7.30 (m, 5H, MPA phenyl protons), 7.28 (brs, 1H, H-1), 7.14 (s, 1H, H-15), 6.20 (s, 1H, H-2), 5.66 (m, 1H, H-5), 5.04 (d, *J* = 9.8 Hz, 1H, H-6), 5.02 (brt, 1H, H-10), 4.70 (s, 1H, C*H* of MPA), 3.37 (s, 3H, OMe of MPA), 2.73 (dd, *J* = 7.2, 14.7 Hz, 1H, H-4a), 2.63 (dd, *J* = 7.2, 14.7 Hz, 1H, H-4b), 2.16–2.10 (m, 1H, H-8a), 1.98–1.86 (m, 1H, H-8b and 2H, m, H-9), 1.64 (s, 6H, CH_3-14 and CH_3-12), 1.56 (s, 3H, CH_3-13); (+)-HRESIMS *m/z*: $[M + Na]^+$ calcd for $C_{24}H_{30}NaO_4$, 405.2036; found, 405.2038.

(*R,S*)-(6*Z*)-dendrolasin MPA ester (11b): Colorless glass; $[\alpha]_D$ +10.7 (*c* 0.01, $CHCl_3$); ^1H NMR ($CDCl_3$, 500 MHz) δ_H 7.38−7.36 (m, 5H, MPA phenyl protons), 7.17 (bs, 1H, H-1), 6.83 (s, 1H, H-15), 5.95 (s, 1H, H-2), 5.68 (m, 1H, H-5), 5.12 (d, *J* = 9.4 Hz, 1H, H-6), 5.04 (brt, *J* = 7.3 Hz, 1H, H-10), 4.68 (s, 1H, C*H* of MPA), 3.36 (s, 3H, OMe of MPA), 2.58 (dd, *J* = 7.0, 14.7 Hz, 1H, H-4a), 2.51 (dd, *J* = 7.0, 14.7 Hz, 1H, H-4b), 2.24–2.20 (m, 1H, H-8a), 2.06–1.92 (m, 1H, H-8b and m, 2H, H-9), 1.71 (d, *J* = 1.0 Hz, 3H, CH_3-14), 1.67 (s, 3H, CH_3-12), 1.58 (m, 3H, CH_3-13); (+)-HRESIMS *m/z*: $[M + Na]^+$ calcd for $C_{24}H_{30}NaO_4$, 405.2036; found, 405.2043.

Procedure for preparation of MPA ester of the (+)-isomer of 7b: A portion of the (+)-isomer of **7b** (1.3 mg) was treated with (*R*)-MPA (0.83 mg in 0.1 mL of DCM) using the same procedure as for the preparation of MPA ester of the racemic (6*Z*)-5-hydroxydendrolasin (**7b**) to obtain the (+)-MPA ester (1.2 mg). The ^1H NMR data ($CDCl_3$, 500 MHz) were identical to those for the (*R,R*,6*Z*)-dendrolasin MPA ester (**11a**). $[\alpha]_D$ −93 (*c* 0.08, $CHCl_3$); (+)-LRESIMS *m/z*: 405 $[M + Na]^+$.

Procedure for preparation of MPA ester of the (−)-isomer of 7b: A portion of the (−)-isomer of **7b** (1.3 mg) was treated with (*R*)-MPA (0.83 mg in 0.1 mL of DCM) using the same procedure as for the preparation of MPA ester of the racemic (6*Z*)-5-hydroxydendrolasin (**7**) to obtain the (−)-MPA ester (1.0 mg). The ^1H NMR data ($CDCl_3$, 500 MHz) are identical to those of the (*R,S*,6*Z*)-dendrolasin MPA ester (**11b**). $[\alpha]_D$ −22 (*c* 0.07, $CHCl_3$); (+)-LRESIMS *m/z*: 405 $[M + Na]^+$.

Enantioselective HPLC experiments: Enantioselective HPLC analysis of the (±)-(6*Z*)-dendrolasin-5-acetate (**1**) racemic mixture, the individual 5*R*- and 5*S*-enantiomers of (6*Z*)-dendrolasin-5-acetate, and the natural sample of (−)-(5*R*,6Z)-dendrolasin-5-acetate, were performed using an Agilent 1200 series liquid chromatography system (isocratic conditions, 5% isopropanol in *n*-hexane, flow rate of 0.5 mL min^{-1}) equipped with UV (220 nm) and ALP (Advanced Laser Polarimeter, PDR-Chiral Inc.) detectors and a Chiralpak OJ column (4.6 × 250 mm, Daicel Chemical Industries Ltd.). Retention times were: (+)-enantiomer, >97% ee 8.3 min; (−)-enantiomer, >98.5% ee 9.4 min; natural sample 9.4 min.

Supporting Information

Supporting Information File 1 contains experimental details for the preparation of compound **6**, spectroscopic data and other relevant information for compounds **1**, **7b**, **11a**, and **11b**.

Supporting Information File 1

Experimental details and spectroscopic data.
[http://www.beilstein-journals.org/bjoc/content/supplementary/1860-5397-9-329-S1.pdf]

Acknowledgements

We thank the Australian Research Council and The University of Queensland for financial support, and Deb Aston for photography and her assistance with sample collections.

References

1. Blunt, J. W.; Copp, B. R.; Munro, M. H. G.; Northcote, P. T.; Prinsep, M. R. *Nat. Prod. Rep.* **2013,** *20,* 1–48. doi:10.1039/b207130b
2. Paul, V. J.; Ritson-Williams, R.; Sharp, K. *Nat. Prod. Rep.* **2011,** *28,* 345–387. doi:10.1039/c0np00040j
3. Pawlik, J. R. Antipredatory Defensive Roles of Natural Products from Marine Invertebrates. In *Handbook of Marine Natural Products;* Fattorusso, E.; Gerwick, W. H.; Taglialatela-Scafati, O., Eds.; Springer: London, 2012; pp 677–710. doi:10.1007/978-90-481-3834-0_12
4. Cimino, G.; Ghiselin, M. T. *Chemoecology* **1998,** *8,* 51–60. doi:10.1007/PL00001804
5. Cimino, G.; Ghiselin, M. T. *Proc. Calif. Acad. Sci.* **2009,** *60,* 175–422.
6. Gerwick, W. H.; Moore, B. S. *Chem. Biol.* **2012,** *19,* 85–98. doi:10.1016/j.chembiol.2011.12.014
7. Grode, S. H.; Cardellina, J. H., II. *J. Nat. Prod.* **1984,** *47,* 76–83. doi:10.1021/np50031a009
8. Avila, C.; Cimino, G.; Fontana, A.; Gavagnin, M.; Ortea, J.; Trivellone, E. *J. Chem. Ecol.* **1991,** *17,* 625–636. doi:10.1007/BF00982131

9. Fontana, A.; Avila, C.; Martinez, E.; Ortea, J.; Trivellone, E.; Cimino, G. *J. Chem. Ecol.* **1993,** *19,* 339–356. doi:10.1007/BF00993700
10. Cimino, G.; Fontana, A.; Giménez, F.; Marin, A.; Mollo, E.; Trivellone, E.; Zubía, E. *Experientia* **1993,** *49,* 582–586. doi:10.1007/BF01955168
11. Fontana, A.; Giménez, F.; Marin, A.; Mollo, E.; Cimino, G. *Experientia* **1994,** *50,* 510–516. doi:10.1007/BF01920760
12. Fontana, A.; Trivellone, E.; Mollo, E.; Cimino, G.; Avila, C.; Martinez, E.; Ortea, J. *J. Nat. Prod.* **1994,** *57,* 510–513. doi:10.1021/np50106a011
13. da Cruz, J. F.; Gaspar, H.; Calado, G. *Chemoecology* **2012,** *22,* 47–53. doi:10.1007/s00049-011-0097-z
14. Fontana, A.; Ciavatta, M. L.; D'Souza, L.; Mollo, E.; Naik, C. G.; Parameswaran, P. S.; Wahidulla, S.; Cimino, G. *J. Indian Inst. Sci.* **2001,** *81,* 403–415.
15. McPhail, K.; Davies-Coleman, M. T.; Coetzee, P. *J. Nat. Prod.* **1998,** *61,* 961–964. doi:10.1021/np980051y
16. Pereira, F. R.; Berlinck, R. G. S.; Filho, E. R.; Veloso, K.; Ferreira, A. G.; Padula, V. *Quim. Nova* **2012,** *35,* 2194–2201. doi:10.1590/S0100-40422012001100018
17. Schulte, G.; Scheuer, P. J.; McConnell, O. J. *Helv. Chim. Acta* **1980,** *63,* 2159–2167. doi:10.1002/hlca.19800630805
18. Hochlowski, J. E.; Walker, R. P.; Ireland, C.; Faulkner, D. J. *J. Org. Chem.* **1982,** *47,* 88–91. doi:10.1021/jo00340a018
19. Schulte, G. R.; Scheuer, P. J. *Tetrahedron* **1982,** *38,* 1857–1863. doi:10.1016/0040-4020(82)80034-3
20. Karuso, P.; Scheuer, P. J. *Molecules* **2002,** *7,* 1–6. doi:10.3390/70100001-rev
21. Tsubuki, M.; Okita, H.; Kaneko, K.; Shigihara, A.; Honda, T. *Heterocycles* **2009,** *77,* 433–444. doi:10.3987/COM-08-S(F)40
22. Kakou, Y.; Crews, P.; Bakus, G. J. *J. Nat. Prod.* **1987,** *50,* 482–484. doi:10.1021/np50051a023
23. Tran, N. H.; Hooper, J. N. A.; Capon, R. J. *Aust. J. Chem.* **1995,** *48,* 1757–1760. doi:10.1071/CH9951757
24. Chakraborty, A.; Kar, G. K.; Ray, J. K. *Tetrahedron* **1997,** *53,* 8513–8518. doi:10.1016/S0040-4020(97)00509-7
25. Freire, F.; Calderón, F.; Seco, J. M.; Fernandez-Mayoralas, A.; Quinõá, E.; Riguera, R. *J. Org. Chem.* **2007,** *72,* 2297–2301. doi:10.1021/jo061939r

License and Terms

This is an Open Access article under the terms of the Creative Commons Attribution License (http://creativecommons.org/licenses/by/2.0), which permits unrestricted use, distribution, and reproduction in any medium, provided the original work is properly cited.

The license is subject to the *Beilstein Journal of Organic Chemistry* terms and conditions: (http://www.beilstein-journals.org/bjoc)

The definitive version of this article is the electronic one which can be found at: doi:10.3762/bjoc.9.329

Beilstein Journal of Organic Chemistry

Synthesis of novel derivatives of 5-hydroxymethylcytosine and 5-formylcytosine as tools for epigenetics

Anna Chentsova, Era Kapourani and Athanassios Giannis*

Full Research Paper

Open Access

Address:
Institut für Organische Chemie, Fakultät für Chemie und Mineralogie, Universität Leipzig, Johannisallee 29, 04103 Leipzig, Germany

Email:
Athanassios Giannis* - giannis@uni-leipzig.de

* Corresponding author

Keywords:
3,6-dihydrodeoxycytidine derivatives; DNA demethylation; epigenetics; 5-hydroxymethylcytosine (5hmC) derivatives; TET-enzymes

Beilstein J. Org. Chem. **2014,** *10,* 7–11.
doi:10.3762/bjoc.10.2

Received: 17 October 2013
Accepted: 13 December 2013
Published: 03 January 2014

This article is part of the Thematic Series "Natural products in synthesis and biosynthesis".

Guest Editor: J. S. Dickschat

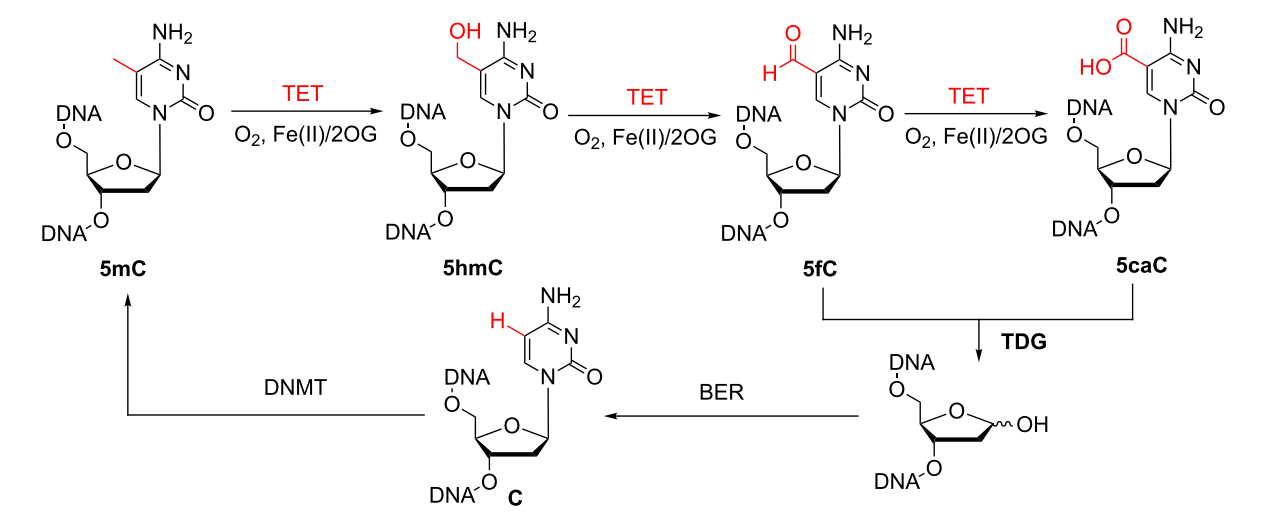
© 2014 Chentsova et al; licensee Beilstein-Institut.
License and terms: see end of document.

Abstract

In this work we present for the first time the synthesis of novel 5-hydroxymethylcytosine (5hmC) and 5-formylcytosine (5fC) derivatives that can be used as tools in the emerging field of epigenetics for deciphering chemical biology of TET-mediated processes.

Introduction

Epigenetic modifications play a crucial role in cell differentiation and cell development [1]. They control gene expression through several mechanisms such as non-coding RNAs, histone modifications (acetylation, methylation, phosphorylation, etc.) [2], and DNA methylation [3-7]. The latter takes place at the C-5 position of the cytosine moiety in CpG islands establishing the so called 5th base: 5-methylcytosine (5mC), a well-known epigenetic mark that correlates with gene silencing [8]. Recently, conversion of the 5mC moiety to 5-hydroxymethylcytosine (5hmC) and to higher oxidation products such as 5-formylcytosine (5fC) and 5-carboxylcytosine (5caC) by the action of ten-eleven-translocation (TET) enzymes was discovered [9-13]. The TET proteins are identified as 2-oxoglutarate (2OG) and Fe(II)-dependent oxygenases [10,14]. Whereas the DNA methylation is a densely studied field, its reverse process has not yet been deciphered. In trying to understand DNA demethylation several mechanisms involving new cytosine-modified bases as intermediates have been proposed (Scheme 1). (1) The most widely accepted pathway includes iterative oxidation of 5mC catalyzed by TET enzymes followed by removal of 5fC and 5caC by thymine DNA glycosylase (TDG). Excision of 5fC and 5caC generates an abasic site, which is further repaired resulting in replacement of 5mC with unmodified cytosine (C) [15-18]. (2) The second alternative scenario still remains controversial [19,20]. It links the oxidative action of TET enzymes, the subsequent deamination of



Scheme 1: Proposed steps for DNA demethylation (for details see text).

5hmC to 5-hydroxymethyluracil (5hmU) by cytidine deaminases AID (activation-induced cytidine deaminase) or APOBEC (apolipoprotein B mRNA editing enzyme, catalytic polypeptide) with the base excision repair (BER) machinery [15-17,21]. (3) Among other putative demethylation mechanisms is the direct dehydroxymethylation of 5hmC to cytosine by action of DNA methyltransferases (DNMT). This enzymatic process was observed in vitro, whether it also works in vivo is yet to be elucidated [15,22]. (4) Lastly, decarboxylation of the 5caC by an unknown decarboxylase excluding action of BER should also be considered [15,23]. This variety of demethylation pathways might indicate that different tissues utilize different demethylation pathways [1,24].

While DNA methylation is usually associated with gene repression [8,25], active demethylation seems to allow cells to unblock silenced genes aiming at epigenetic reprogramming of their genetic material [26]. Current accepted models propose that 5hmC could be involved in epigenetic modulation of gene activity. In fact, 5hmC was discovered also in embryonic stem cells and seems to play a decisive role in their self-renewal process [27]. Interestingly, the levels of 5hmC in several cancer types are strongly reduced relative to the corresponding normal tissue around the tumor [28]. To gain deeper insights into the chemical biology of DNA demethylation pathways further exploration of the TET-mediated processes is necessary. Analogues of 5hmC with substituents preventing formation of 5fC and 5caC species could serve as useful tools for ongoing investigations in this emerging field.

Results and Discussion

Herein, we describe the synthesis of compounds with the general formula **I** which represents modified cytidine analogues bearing a secondary alcohol at position C-5 of cytosine. Additionally, a synthesis of 3,6-dihydrodeoxycytidine derivatives of general formula **II** is presented (Figure 1).

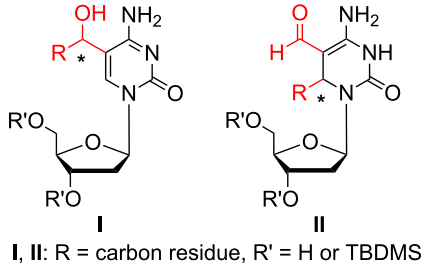
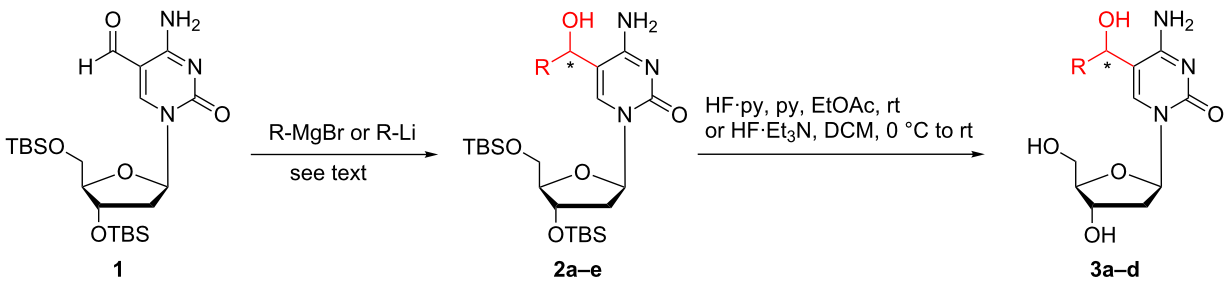


Figure 1: Structures of the synthesized compounds.

We chose the known aldehyde **1** [29] (prepared from commercially available 2'-deoxycytidine) as a starting material for the envisioned transformations (Scheme 2). To the best of our knowledge, the addition of organometallic compounds (organolithium and organomagnesium, etc.) to aldehyde **1** is not described in the literature. Compound **1** was readily converted to 5hmC analogues **2a**–**e** by treatment with various Grignard reagents (methylmagnesium bromide, THF, 0 °C → room temperature, or vinylmagnesium bromide, THF, 0 °C → room temperature) and organolithium reagents (lithium (trimethylsilyl)acetylide, THF, −40 °C → −20 °C or lithium phenylacetylide, THF, −78 °C → −50 °C) (Scheme 2). These alcohols were obtained as a mixture of diastereomers in yields ranging from 43% to 96% (Table 1). Compound **2b** was isolated in moderate yield of 43% due to the cleavage of the TMS-group during the reaction resulting in formation of derivative **2e** with a yield of 26%. The obtained derivatives **2a**–**d** were further



Scheme 2: Synthesis of the 2'-deoxycytidine analogues.

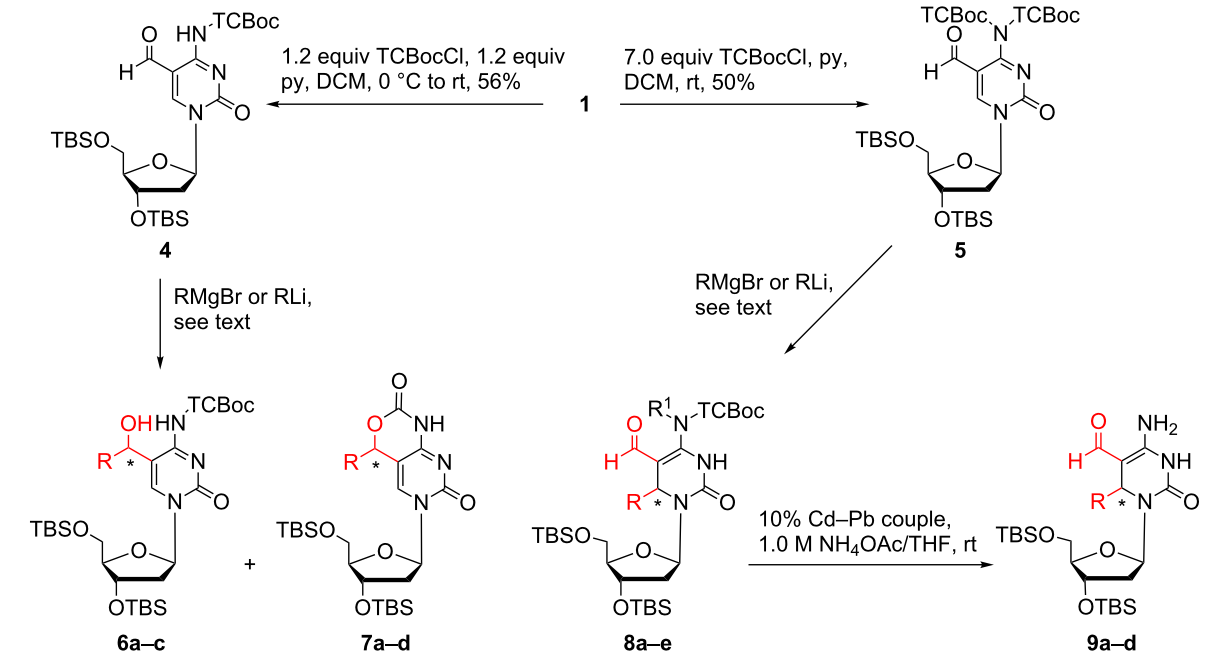
Table 1: Yields and ratios of diastereomeric alcohols **2a–e** and **3a–d**.

Entry	2/3	Yield [%]	Ratio[a]
1	**2a**, R = methyl	96	1.1:1
2	**2b**, R = (TMS)ethynyl	43	1.9:1
3	**2c**, R = phenylethynyl	68	1.2:1
4	**2d**, R = vinyl	77	1.1:1
5	**2e**, R = ethynyl	26	1.2:1
6	**3a**, R = methyl	75	n.d.
7	**3b,** R = ethynyl	60	n.d.
8	**3c**, R = phenylethynyl	72	1.1:1
9	**3d**, R = vinyl	73	n.d.

[a]Determined by ^{1}H NMR; n.d. = not determined.

treated with Olah's reagent and pyridine in EtOAc at room temperature or HF·triethylamine complex [30] in DCM at 0 °C to afford the deprotected 2'-deoxycytidine analogues **3a–d** as mixtures of diastereomers in yields of 60–75%.

Next, we synthesized the *N*-4-protected cytidine derivatives **4** and **5** by treatment of aldehyde **1** with β,β,β-trichloro-*tert*-butoxycarbonyl chloride (TCBocCl) [31] in the presence of pyridine in DCM (Scheme 3). The reaction of **4** with Grignard (methylmagnesium bromide, THF, 0 °C → room temperature, or vinylmagnesium bromide, THF, 0 °C → room temperature) and organolithium reagents (lithium (trimethylsilyl)acetylide, THF, −60 °C → −50 °C or lithium phenylacetylide, THF, −78 °C) afforded derivatives **6a–c** and carbamates **7a–c** as mixtures of diastereomers (Table 2). It should be mentioned that



Scheme 3: Reactions of TCBoc-protected aldehydes **4** and **5** with organometallic reagents.

upon storage at room temperature derivatives **6a**–**c** undergo slow intramolecular cyclization to the corresponding carbamates **7a**–**c**. The reaction of aldehyde **4** and vinylmagnesium bromide yielded directly carbamate **7d**.

Table 2: Yields and ratios of diastereomers **6a–c, 7a–d, 8a–e** and **9a–d**.

Entry	**6/7/8/9**	Yield [%]	Ratio[a]
1	**6a**, R = methyl	28	n.d
2	**6b**, R = (TMS)ethynyl	42	2:1
3	**6c**, R = phenylethynyl	42	1.6:1
4	**7a**, R = methyl	35	1.9:1
5	**7b**, R = (TMS)ethynyl	30	1.1:1
6	**7c**, R = phenylethynyl	30	1.4:1
7	**7d**, R = vinyl	69	2.3:1
8	**8a**, R = methyl, R^1 = H	38	2.4:1
9	**8b**, R = (TMS)ethynyl, R^1 = H	80	3.2:1[b]
10	**8c**, R = phenylethynyl, R^1 = H	71	1.1:1
11	**8d**, R = vinyl, R^1 = H	37	2.6:1
12	**8e**, R = vinyl, R^1 = TCBoc	17	5.7:1
13	**9a**, R = methyl	40	2.4:1
14	**9b**, R = (TMS)ethynyl	77	–
15	**9c**, R = phenylethynyl	44	1:1
16	**9d**, R = vinyl	61	2.6:1

[a]Determined by ^{1}H NMR; [b]pure epimers were isolated by HPLC; n.d. = not determined.

Surprisingly, the reaction of derivative **5** bearing a *N*-(TCBoc)$_2$ group with organometallic compounds (methylmagnesium bromide, THF, 0 °C → room temperature, lithium (trimethylsilyl)acetylide, THF, −50 °C, lithium phenylacetylide, THF, −78 °C → −50 °C, vinylmagnesium bromide, THF, 0 °C) afforded 3,6-dihydrodeoxycytidine derivatives **8a**–**e** as mixtures of diastereomers. In case of **8b** the diastereomers were separated by HPLC. Products arising from addition of the organometallic reagents to the aldehyde group (1,2-addition) were not observed. The formation of compounds **8a**–**d** can be explained assuming a Michael-type reaction of aldehyde **5** with organometallic reagents, subsequent isomerisation of the double bond followed by removal of one TCBoc group during the reaction and work-up as shown in Scheme 4.

Finally, cleavage of the TCBoc group was achieved by the action of the 10% Cd–Pb couple [32] on compounds **8a**–**d** in THF and 1.0 M aq NH_4OAc to provide derivatives **9a**–**d** (Scheme 3).

Conclusion

In summary, the reaction of 5fC derivatives **1**, **4**, and **5** with organometallic reagents (RMgBr, RLi) was investigated and enabled the synthesis of novel derivatives of 5-hydroxymethylcytosine and 5-formylcytosine: whereas aldehydes **1** and **4** afforded cytosine derivatives **2a**–**e**, **6a**–**c** and **7a**–**d**, the reaction of derivative **5** yielded 3,6-dihydrodeoxycytidine derivatives **8a**–**d** which subsequently after removal of the TCBoc group afforded derivatives **9a**–**d**. These new nucleobase modified 2'-deoxycytidine analogues can be used in the synthesis [29,33,34] of modified DNA oligomers for further studies of the TET-mediated processes which are of great importance in the emerging field of epigenetics. In addition they could find application as novel antivirals and/or as antimetabolites [35,36]. The majority of the obtained compounds contain functionalized side chains thus allowing further manipulations.

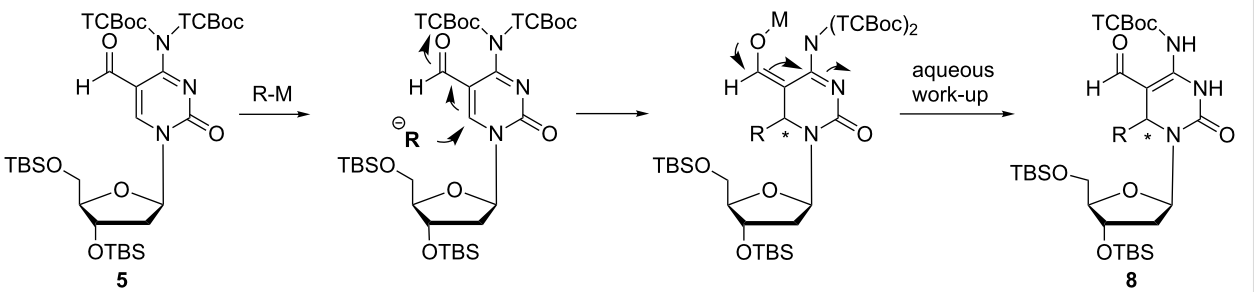
Supporting Information

Supporting Information File 1

Experimental details and analytical data of all synthesized compounds.
[http://www.beilstein-journals.org/bjoc/content/supplementary/1860-5397-10-2-S1.pdf]

Acknowledgements

We thank Dr. Lothar Hennig (Universität Leipzig) for recording NMR spectra and for his help in interpreting the 2D NMR spectra. We also thank Dr. Stephan Rigol (Universität Leipzig) for critical discussion of the manuscript.



Scheme 4: Proposed mechanism for the formation of 3,6-dihydrodeoxycytidine derivatives **8a–d** (M = Li, Mg).

References

1. Branco, M. R.; Ficz, G.; Reik, W. *Nat. Rev. Genet.* **2012,** *13,* 7–13. doi:10.1038/nrg3080
2. Biel, M.; Wascholowski, V.; Giannis, A. *Angew. Chem., Int. Ed.* **2005,** *44,* 3186–3216. doi:10.1002/anie.200461346
3. Esteller, M. *Genes Cancer* **2011,** *2,* 604–606. doi:10.1177/1947601911423096
4. Fuks, F. *Curr. Opin. Genet. Dev.* **2005,** *15,* 490–495. doi:10.1016/j.gde.2005.08.002
5. Dawson, M. A.; Kouzarides, T. *Cell* **2012,** *150,* 12–27. doi:10.1016/j.cell.2012.06.013
6. Dawson, M. A.; Kouzarides, T.; Huntly, B. J. P. *N. Engl. J. Med.* **2012,** *367,* 647–657. doi:10.1056/NEJMra1112635
7. Hamm, C. A.; Costa, F. F. *Drug Discovery Today* **2011,** *16,* 626–635. doi:10.1016/j.drudis.2011.04.007
8. Klose, R. J.; Bird, A. P. *Trends Biochem. Sci.* **2006,** *31,* 89–97. doi:10.1016/j.tibs.2005.12.008
9. Kriaucionis, S.; Heintz, N. *Science* **2009,** *324,* 929–930. doi:10.1126/science.1169786
10. Tahiliani, M.; Koh, K. P.; Shen, Y.; Pastor, W. A.; Bandukwala, H.; Brudno, Y.; Agarwal, S.; Iyer, L. M.; Liu, D. R.; Aravind, L.; Rao, A. *Science* **2009,** *324,* 930–935. doi:10.1126/science.1170116
11. He, Y.-F.; Li, B.-Z.; Li, Z.; Liu, P.; Wang, Y.; Tang, Q.; Ding, J.; Jia, Y.; Chen, Z.; Li, L.; Sun, Y.; Li, X.; Dai, Q.; Song, C.-X.; Zhang, K.; He, C.; Xu, G.-L. *Science* **2011,** *333,* 1303–1307. doi:10.1126/science.1210944
12. Ito, S.; Shen, L.; Dai, Q.; Wu, S. C.; Collins, L. B.; Swenberg, J. A.; He, C.; Zhang, Y. *Science* **2011,** *333,* 1300–1303. doi:10.1126/science.1210597
13. Pfaffeneder, T.; Hackner, B.; Truß, M.; Münzel, M.; Müller, M.; Deiml, C. A.; Hagemeier, C.; Carell, T. *Angew. Chem., Int. Ed.* **2011,** *50,* 7008–7012. doi:10.1002/anie.201103899
14. Rose, N. R.; McDonough, M. A.; King, O. N. F.; Kawamura, A.; Schofield, C. J. *Chem. Soc. Rev.* **2011,** *40,* 4364–4397. doi:10.1039/c0cs00203h
    See for an excellent review on 2-oxoglutarate dependend oxygenases.
15. Pastor, W. A.; Aravind, L.; Rao, A. *Nat. Rev. Mol. Cell Biol.* **2013,** *14,* 341–356. doi:10.1038/nrm3589
16. Fu, Y.; He, C. *Curr. Opin. Chem. Biol.* **2012,** *16,* 516–524. doi:10.1016/j.cbpa.2012.10.002
17. Carell, T.; Brandmayr, C.; Hienzsch, A.; Müller, M.; Pearson, D.; Reiter, V.; Thoma, I.; Thumbs, P.; Wagner, M. *Angew. Chem., Int. Ed.* **2012,** *51,* 7110–7131. doi:10.1002/anie.201201193
18. Pfeifer, G. P.; Kadam, S.; Jin, S. G. *Epigenet. Chromatin* **2013,** *6,* 10. doi:10.1186/1756-8935-6-10
19. Guo, J. U.; Su, Y.; Zhong, C.; Ming, G.-l.; Song, H. *Cell* **2011,** *145,* 423–434. doi:10.1016/j.cell.2011.03.022
20. Nabel, C. S.; Jia, H.; Ye, Y.; Shen, L.; Goldschmidt, H. L.; Stivers, J. T.; Zhang, Y.; Kohli, R. M. *Nat. Chem. Biol.* **2012,** *8,* 751–758. doi:10.1038/nchembio.1042
21. Bhutani, N.; Burns, D. M.; Blau, H. M. *Cell* **2011,** *146,* 866–872. doi:10.1016/j.cell.2011.08.042
22. Chen, C.-C.; Wang, K.-Y.; Shen, C.-K. J. *J. Biol. Chem.* **2012,** *287,* 33116–33121. doi:10.1074/jbc.C112.406975
23. Schiesser, S.; Hackner, B.; Pfaffeneder, T.; Müller, M.; Hagemeier, C.; Truss, M.; Carell, T. *Angew. Chem., Int. Ed.* **2012,** *51,* 6516–6520. doi:10.1002/anie.201202583
24. Auclair, G.; Weber, M. *Biochimie* **2012,** *94,* 2202–2211. doi:10.1016/j.biochi.2012.05.016
25. Brenet, F.; Moh, M.; Funk, P.; Feierstein, E.; Viale, A. J.; Socci, N. D.; Scandura, J. M. *PLoS One* **2011,** *6,* e14524. doi:10.1371/journal.pone.0014524
26. Münzel, M.; Lischke, U.; Stathis, D.; Pfaffeneder, T.; Gnerlich, F. A.; Deiml, C. A.; Koch, S. C.; Karaghiosoff, K.; Carell, T. *Chem.–Eur. J.* **2011,** *17,* 13782–13788. doi:10.1002/chem.201102782
27. Ito, S.; D'Alessio, A. C.; Taranova, O. V.; Hong, K.; Sowers, L. C.; Zhang, Y. *Nature* **2010,** *466,* 1129–1133. doi:10.1038/nature09303
28. Jin, S.-G.; Jiang, Y.; Qiu, R.; Rauch, T. A.; Wang, Y.; Schackert, G.; Krex, D.; Lu, Q.; Pfeifer, G. P. *Cancer Res.* **2011,** *71,* 7360–7365. doi:10.1158/0008-5472.CAN-11-2023
29. Münzel, M.; Globisch, D.; Trindler, C.; Carell, T. *Org. Lett.* **2010,** *12,* 5671–5673. doi:10.1021/ol102408t
30. Münzel, M.; Globisch, D.; Brückl, T.; Wagner, M.; Welzmiller, V.; Michalakis, S.; Müller, M.; Biel, M.; Carell, T. *Angew. Chem., Int. Ed.* **2010,** *49,* 5375–5377. doi:10.1002/anie.201002033
31. Schneiderwind, R. G. K.; Ugi, I. *Tetrahedron* **1983,** *39,* 2207–2210. doi:10.1016/S0040-4020(01)91939-8
32. Dong, Q.; Anderson, C. E.; Ciufolini, M. A. *Tetrahedron Lett.* **1995,** *36,* 5681–5682. doi:10.1016/0040-4039(95)01122-X
33. Steigenberger, B.; Schiesser, S.; Hackner, B.; Brandmayr, C.; Laube, S. K.; Steinbacher, J.; Pfaffeneder, T.; Carell, T. *Org. Lett.* **2013,** *15,* 366–369. doi:10.1021/ol3033219
34. Dai, Q.; He, C. *Org. Lett.* **2011,** *13,* 3446–3449. doi:10.1021/ol201189n
35. Kifli, N.; De Clercq, E.; Balzarini, J.; Simons, C. *Bioorg. Med. Chem.* **2004,** *12,* 4245–4252. doi:10.1016/j.bmc.2004.05.017
36. Matsuda, A.; Sasaki, T. *Cancer Sci.* **2004,** *95,* 105–111. doi:10.1111/j.1349-7006.2004.tb03189.x

License and Terms

This is an Open Access article under the terms of the Creative Commons Attribution License (http://creativecommons.org/licenses/by/2.0), which permits unrestricted use, distribution, and reproduction in any medium, provided the original work is properly cited.

The license is subject to the *Beilstein Journal of Organic Chemistry* terms and conditions: (http://www.beilstein-journals.org/bjoc)

The definitive version of this article is the electronic one which can be found at: doi:10.3762/bjoc.10.2

Beilstein Journal of Organic Chemistry

Total synthesis of (+)-grandiamide D, dasyclamide and gigantamide A from a Baylis–Hillman adduct: A unified biomimetic approach

Andivelu Ilangovan*[1] and Shanmugasundar Saravanakumar[1,2]

Full Research Paper

Open Access

Address:
[1]School of Chemistry, Bharathidasan University, Tiruchirappalli, 620024, India and [2]Syngene International Ltd., Bangalore, 560 099, India

Email:
Andivelu Ilangovan* - ilangovanbdu@yahoo.com

* Corresponding author

Keywords:
Baylis–Hillman reaction; dasyclamide; gigantamide A; (+)-grandiamide D; natural products; putrescine bisamides

Beilstein J. Org. Chem. **2014,** *10,* 127–133.
doi:10.3762/bjoc.10.9

Received: 05 September 2013
Accepted: 26 November 2013
Published: 10 January 2014

This article is part of the Thematic Series "Natural products in synthesis and biosynthesis".

Guest Editor: J. S. Dickschat

© 2014 Ilangovan and Saravanakumar; licensee Beilstein-Institut.
License and terms: see end of document.

Abstract

A unified strategy was followed for the synthesis of three putrescine bisamides, (+)-grandiamide D, dasyclamide and gigantamide A, isolated from leaves of *Aglaia gigantea,* by making use of a common synthetic intermediate prepared by the Baylis–Hillman reaction. Asymmetric synthesis of the natural (+)-grandiamide D was accomplished from camphor sultam.

Introduction

Putrescine bisamides are one of the important naturally occurring polyamine alkaloids found in open chain and cyclic forms. The genera *Aglaia* are the richest source of putrescine bisamides. The cyclic 2-aminopyrrolidine compounds are synthesised in plants from open-chained bisamides by enzymatic cyclization. It is assumed that both forms of bisamides undergo a cycloaddition reaction with a co-occurring flavanol to form highly bioactive flavaglines [1,2]. For example, odorine (**2**) acted as a building block for aglaforbesin A (**1**) and pyramidatin (**4**) for pyramidaglain (**3**) as shown in Figure 1 [3]. The benzopyran and benzoxepine containing flavaglins showed insecticidal, antifungal and antiproliferative activity against various cancer cell lines [4]. Apart from acting as precursors for flavaglins, some of the cyclic bisamides such as odorine, dehydroodorine and odorinol exhibited cytotoxic and antiviral activity [5].

There is only a limited number of putrescine bisamides isolated from natural sources and the amount of synthetic approaches known for these structurally interesting and biologically important molecules is quite low. Except for the elaborate synthetic work carried out by Hesse and Detterbeck [6], who described the synthesis of nine putrescine bisamides isolated from different *Aglaia* species along with the structural revision for

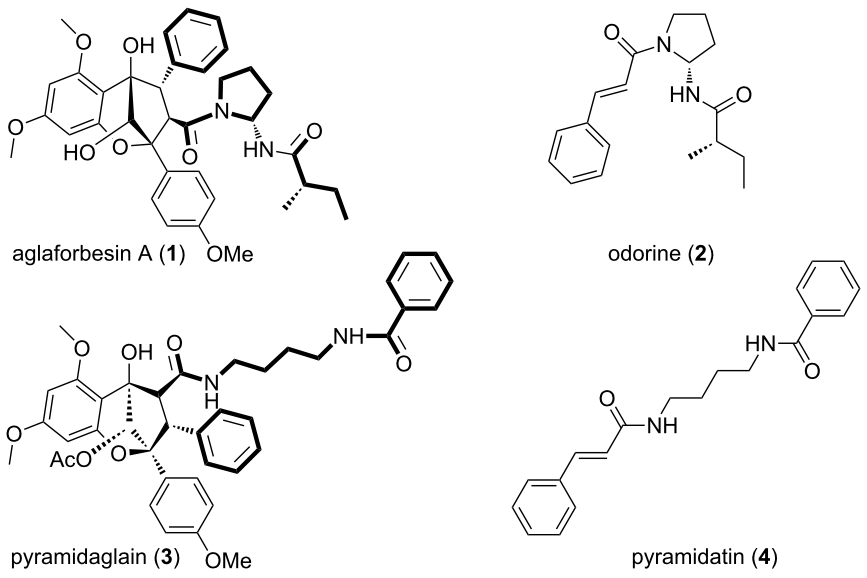


Figure 1: Bisamides as building blocks for flavaglins.

one of the compounds and determination of absolute configuration for another compound, no other literature precedence is available till now.

Duong et al. have isolated three cinnamoyl bisamide derivatives, two new compounds grandiamide D, gigantamide A and the known compound dasyclamide (Figure 2) from the leaves of *Aglaia gigantea* [7]. Even though the structures were determined by spectroscopic means, the total synthesis of these molecules has not been explored so far. As a result of their co-existence, we assumed that these compounds might have been formed from a single precursor with the help of elements present in the plant. Hence we decided to adopt a unified synthetic strategy for the synthesis of all the three compounds **5**–**7** by mimicking the biosynthetic pathway.

Baylis–Hillman adducts are densely functionalized synthons, which mainly consist of three different functional groups such as the ester, olefin and hydroxy group [8]. Recent developments made it possible to introduce additional functional groups on them by replacing the starting materials by activated alkenes and aldehydes. Various multifunctional molecules including natural products have already been successfully synthesized using the Baylis–Hillman adducts [9].

Structural features of grandiamide D, gigantamide A, dasyclamide reveal that the *N*-(4-aminobutyl)cinnamamide segment is common and a remaining part of these molecules could be constructed from this common intermediate. The synthetic versatility of the Baylis–Hillman adducts is a perfect platform for the retrosynthetic plan (Scheme 1). Accordingly, 2-(4-

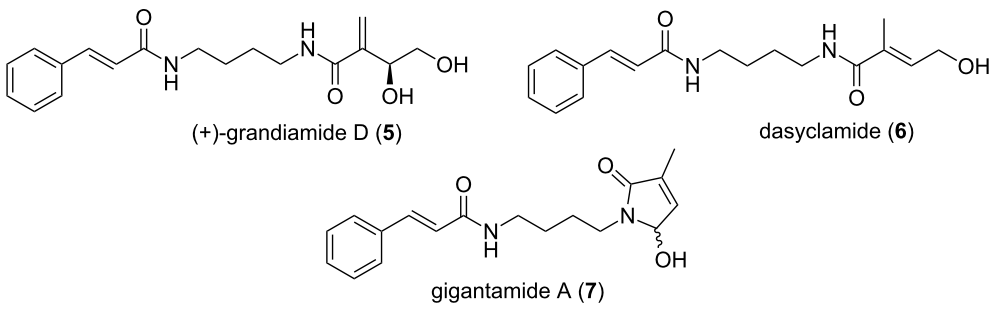
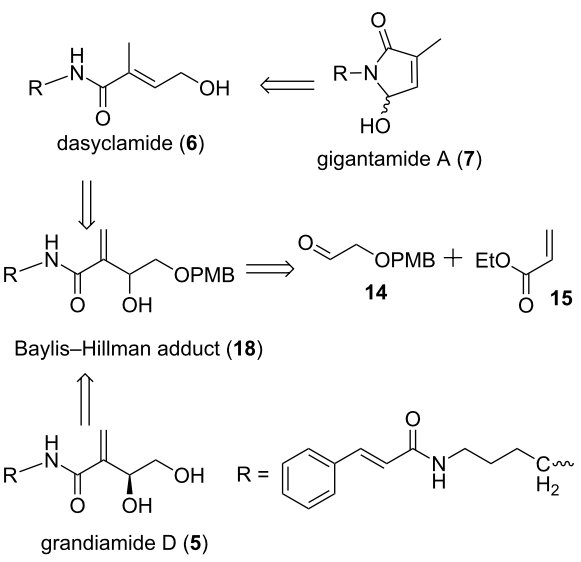


Figure 2: (+)-Grandiamide D, gigantamide A and dasyclamide.



Scheme 1: Retrosynthetic analysis: A unified synthetic approach for the synthesis of grandiamide D, dasyclamide and gigantamide A.

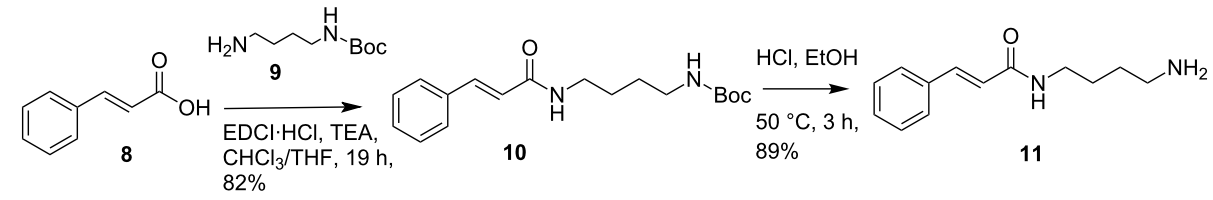
methoxybenzyloxy)acetaldehyde was expected to provide a tetra-functionalized Baylis–Hillman adduct (+)-**16** from which grandiamide D can be obtained. A rearrangement of this common intermediate should be able to provide dasyclamide, which on oxidation, should give gigantamide A.

Results and Discussion

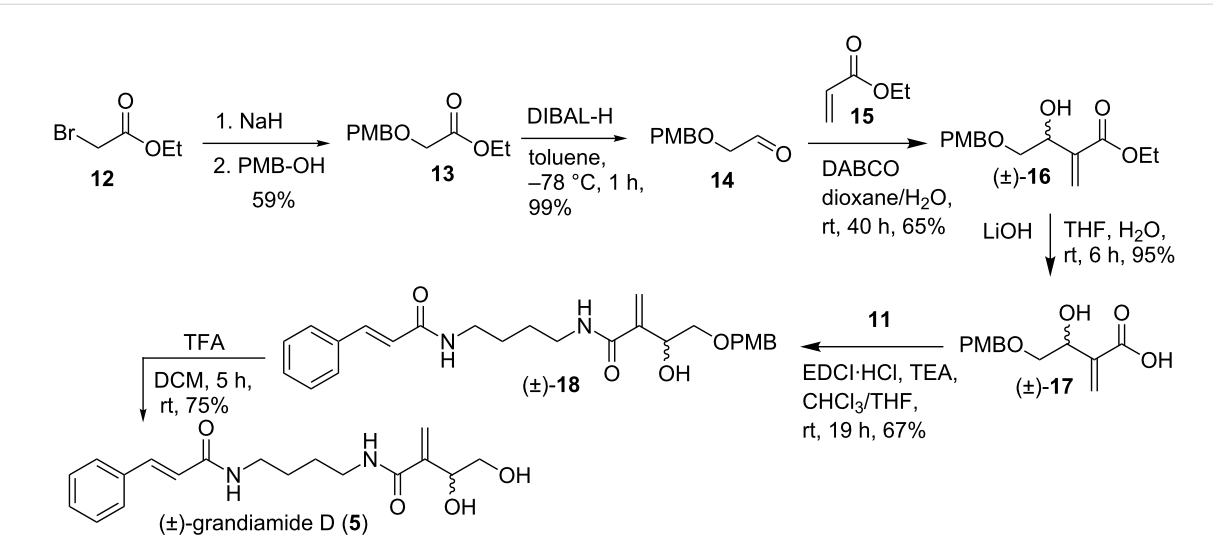
The synthetic plan was started with the preparation of *N*-(4-aminobutyl)cinnamamide (**11**), in two steps from *tert*-butyl 4-aminobutylcarbamate and cinnamic acid by EDCI-mediated coupling followed by removal of the Boc protecting group by refluxing in ethanolic HCl as given in Scheme 2.

Synthesis of (±)-grandiamide D (**5**)

The common and crucial intermediate, β,γ-dihydroxy-α-methyl-enebutyric acid ((±)-**16**) required a selective protection of the hydroxy group at γ position. The PMB (*p*-methoxybenzyl) group was chosen as a result of its robustness and stability towards a wide range of acidic or basic conditions [10]. The entire pathway leading to the synthesis of (±)-grandiamide D is portrayed in Scheme 3.



Scheme 2: Preparation of *N*-(4-aminobutyl)cinnamamide.



Scheme 3: Synthesis of (±)-grandiamide D.

The reaction between ethyl bromoacetate (**12**) and *p*-methoxybenzyl alcohol in the presence of NaH (Scheme 3) furnished the desired ester **13** which on reduction with DIBAL-H provided 2-((4-methoxybenzyl)oxy)acetaldehyde (**14**) [11]. In order to reduce the amount of acrylate and to increase the yield of compound (±)-**16**, the Baylis–Hillman reaction between the aldehyde **14** and ethyl acrylate (**15**) was tried using different catalysts such as DBU, quinuclidine [12] and *n*-Bu_3P. DABCO was found to be a better catalyst and the adduct (±)-**16** was obtained in high yield [13] in dioxane/water (1:1), at room temperature after 40 h [13]. Hydrolysis of the ester (±)-**16** with aqueous LiOH in THF yielded the acid (±)-**17** which on EDCI supported reaction with *N*-(4-aminobutyl)cinnamamide (**11**) gave the PMB protected grandiamide D ((±)-**18**). Among different reagents such as DDQ, CAN, $Yb(OTf)_3$ and $CeCl_3$–NaI used for deprotection of the PMB group, TFA gave the better result. Even though $POCl_3$ [14] was able to effect complete removal of the PMB group in short time, the yield was only moderate. Thus (±)-grandiamide D ((±)-**5**) was obtained in 16.6% overall yield. The spectral data obtained for synthetic compound (±)-**5** matches in all respect with the data reported for the natural product [7].

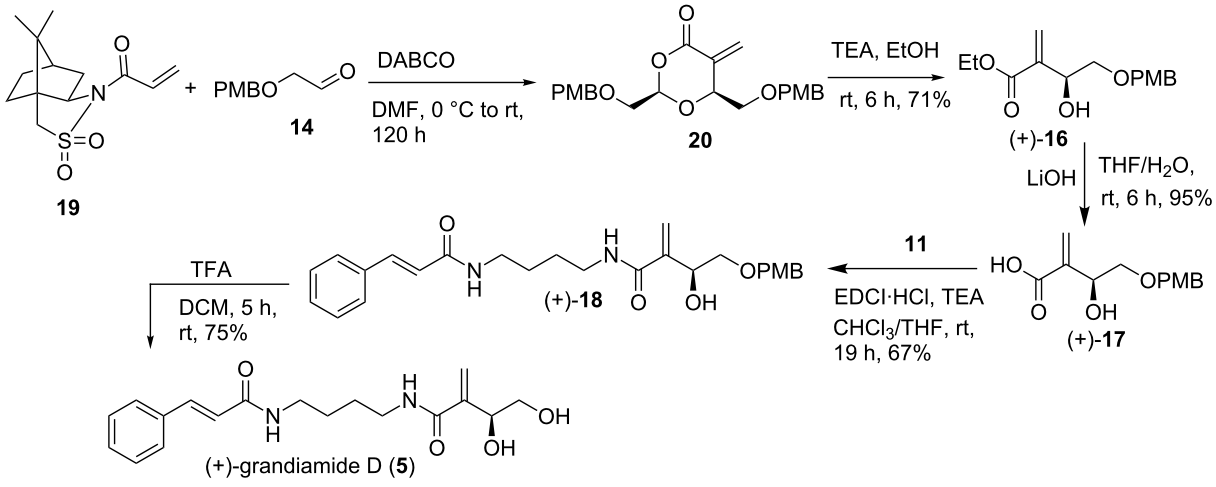
Asymmetric synthesis of (+)-grandiamide D (**5**)

In continuation, we moved on with an asymmetric approach towards the synthesis of natural product (+)-grandiamide D (**5**). We assumed that the asymmetric Baylis–Hillman reaction [15] would be an ideal way to introduce chirality. Reaction between acryloyl sultam **19**, and 2-((4-methoxybenzyl)oxy)acetaldehyde (**14**) in DMF [12], afforded cyclic product **20**, which was then treated as such with TEA in ethanol to afford enantiopure ester (+)-**16** in 71% yield, after purification (Scheme 4). Chiral HPLC analysis of (+)-**16** showed that the enantiomeric ratio is 99.7:0.3 in favour of the (+)-isomer. Further chemistry was carried out as described earlier in Scheme 3, to get (+)-grandiamide D (**5**) in almost the same yield. The enantiomeric purity of (+)-grandiamide D (**5**) was found to be 98.6%, as determined from chiral HPLC analysis. (observed $[\alpha]_D^{25}$ = +4.7 (*c* 0.5, $CHCl_3$); reported [7] $[\alpha]_D^{20}$ = +2.0 (*c* 0.5, $CHCl_3$).

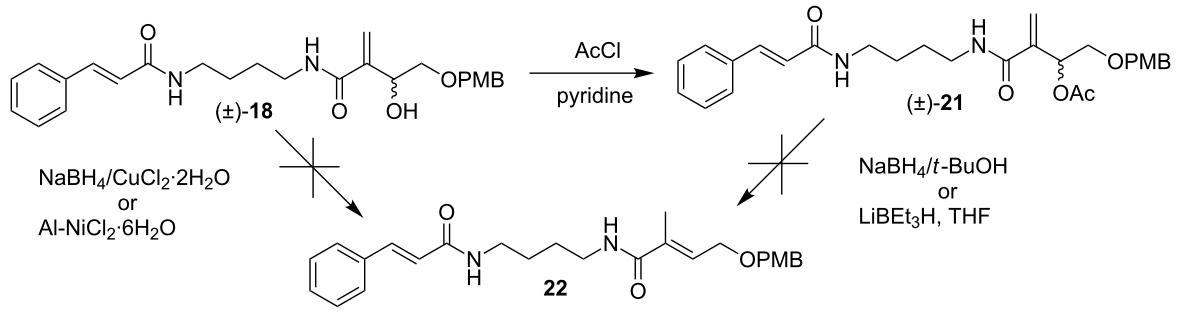
Synthesis of dasyclamide

Since Baylis–Hillman adduct (±)-**18** was considered as the common intermediate, we decided to start with the same for the synthesis of dasyclamide (**6**). As explained in Scheme 5 attempts to get enamide **22** by reductive dehydroxylation of compound (±)-**18** using $NaBH_4/CuCl_2{\cdot}2H_2O$ or Al-$NiCl_2{\cdot}2H_2O$ [16-18] and reductive deacetoxylation of compound (±)-**21** using $NaBH_4$/*t*-BuOH or $LiBEt_3H$, THF [19-21] did not yield fruitful results.

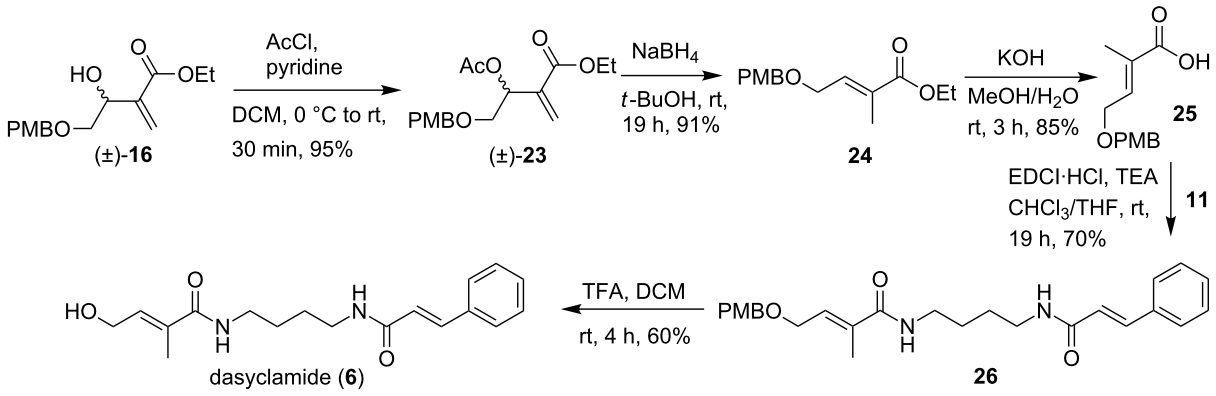
These failures pushed us to explore the dehydroxylation or deacetoxylation reaction using a simpler precursor (±)-**16.** However, attempts to dehydroxylate the Baylis–Hillman adduct (±)-**16** with $NaBH_4/CuCl_2{\cdot}2H_2O$ [17] and Al-$NiCl_2{\cdot}2H_2O$ proved unsuccessful hence, we focused on the deacetoxylation of (±)-**16**. Treatment of (±)-**16** with acetyl chloride in the presence of pyridine afforded the corresponding acetate (±)-**23** in almost quantitative yield, which underwent the desired deacetoxylation with $NaBH_4$/*t*-butanol [20] to provide the ester **24** in good yield (Scheme 6). The ester **24** was hydrolyzed with aqueous KOH in methanol at room temperature to get acid **25** which was then treated with *N*-(4-aminobutyl)cinnamamide (**11**) in the presence of EDCI to get enamide **26**. Further, depro-



Scheme 4: Asymmetric synthesis of natural (+)-grandiamide D.



Scheme 5: Various approaches for the synthesis of (*E*)-*N*-(4-cinnamamidobutyl)-4-((4-methoxybenzyl)oxy)-2-methylbut-2-enamide (**22**).



Scheme 6: Synthesis of dasyclamide.

tection was carried out with TFA to obtain dasyclamide (**6**) in an overall yield of 9.2% (Scheme 6).

The spectral data is in accordance with the published data for natural dasyclamide [7] which further confirms the structure of the natural product.

Synthesis of gigantamide A

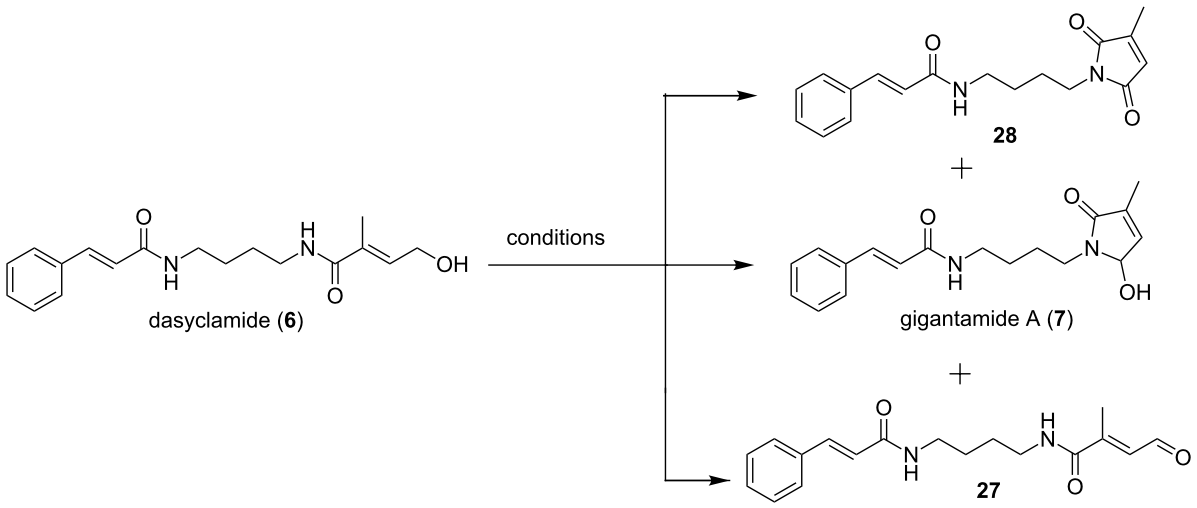
As given in the retrosynthetic analysis and based on the preference in literature for the preparation of jatropham by photocyclization [22], intramolecular cyclization of the aldehyde **27** was considered for the preparation of gigantamide A (**7**). The aldehyde **27** in turn could be prepared from dasyclamide (**6**). Conditions and results for the oxidation of dasyclamide (**6**) to give gigantamide A (**7**) are outlined in Table 1.

The results clearly demonstrated that IBX (Table 1, entry 5) is the best reagent to get the aldehyde **27** in better yield and quality. After analyzing the products obtained from the oxidation with PCC (Table 1, entry 4), we found that the reaction produced gigantamide A (**7**) along with the aldehyde **27**. We have also isolated *N*-(4-(3-methyl-2,5-dioxo-2,5-dihydro-1*H*-pyrrol-1-yl)butyl)cinnamamide (**28**) as one of the products which might have been formed by the oxidation of gigantamide A (**7**) by excess of PCC. Comparison of the NMR data with those reported for the natural gigantamide A (**7**) [7] confirmed the identity of the synthetic product. The overall yield for the synthetic route was found to be 2.3%. Chiral HPLC analysis revealed that it is a racemic compound which was further confirmed by the optical rotation ($[\alpha]_D^{23}$= 0 (*c*, 0.5, $CHCl_3$); reported for the enatio-pure compound: $[\alpha]_D^{20}$= −10 (*c*, 0.3, $CHCl_3$)). Further attempt to get (−)-gigantamide by lipase catalyzed kinetic resolution in line with the reported method for *R*-jatropham [23] was not successful.

Conclusion

In conclusion, a facile synthesis of (±)-grandiamide D (**5**), dasyclamide (**6**) and gigantamide A (**7**) and asymmetric synthesis of natural (+)-grandiamide D (**5**) was achieved with the aid of a Baylis–Hillman adduct. We have also demonstrated a one-step conversion of dasyclamide (**6**) to gigantamide A (**7**) by oxidative intramolecular cyclization by using PCC.

Table 1: Synthesis of gigantamide A (**7**) by oxidation of dasyclamide (**6**).



Entry	Conditions	Results
1	MnO_2, dioxane, reflux	no reaction
2	TPAP, NMO, ACN/DCM, rt	incomplete reaction & close impurities
3	Py·SO_3, TEA, DMSO, rt to 80 °C	no reaction
4	PCC, $CHCl_3$, rt	incomplete reaction & difficulties in isolation
5	IBX, fluorobenzene/DMSO (9:1), 90 °C, 4 h	70% of aldehyde after purification.
6	PCC, $CHCl_3$/DMSO (3:1), rt	30% of aldehyde (**27**) + 25% of gigantamide A + 30% of **28**

Supporting Information

Supporting Information File 1

Detailed experimental procedures, copies of ^1H and ^{13}C NMR spectra for the new compounds and chiral HPLC reports.
[http://www.beilstein-journals.org/bjoc/content/supplementary/1860-5397-10-9-S1.pdf]

Acknowledgements

S.S. thanks Syngene International Ltd for providing research facilities and Dr. G. Manickam for his valuable support.

References

1. Bacher, M.; Hofer, O.; Brader, G.; Vajrodaya, S.; Greger, H. *Phytochemistry* **1999,** *52,* 253–263. doi:10.1016/S0031-9422(99)00185-5
2. Xu, Y.-J.; Wu, X.-H.; Tan, B. K. H.; Lai, Y.-H.; Vittal, J. J.; Imiyabir, Z.; Madani, L.; Khozirah, K. S.; Goh, S. H. *J. Nat. Prod.* **2000,** *63,* 473–476. doi:10.1021/np990454d
3. Dumontet, V.; Thoison, O.; Omobuwajo, O. R.; Martin, M.-T.; Perromat, G.; Chiaroni, A.; Riche, C.; Païs, M.; Sévenet, T. *Tetrahedron* **1996,** *52,* 6931–6942. doi:10.1016/0040-4020(96)00322-5
4. Ebada, S. S.; Lajkiewicz, N.; Porco, J. A., Jr.; Li-Weber, M.; Proksch, P. Chemistry and Biology of Rocaglamides (= Flavaglines) and Related Derivatives from *Aglaia* Species (Meliaceae). *Progress in the Chemistry of Organic Natural Products;* 2011; Vol. 94, pp 1–58.
5. Greger, H.; Hofer, M.; Teichmann, K.; Schinnerl, J.; Pannell, C. M.; Vajrodaya, S.; Hofer, O. *Phytochemistry* **2008,** *69,* 928–938. doi:10.1016/j.phytochem.2007.10.015
6. Detterbeck, R.; Hesse, M. *Tetrahedron* **2002,** *58,* 6887–6893. doi:10.1016/S0040-4020(02)00751-2
7. Duong, T. N.; Edrada, R. A.; Ebel, R.; Wray, V.; Frank, W.; Duong, A. T.; Lin, W. H.; Proksch, P. *J. Nat. Prod.* **2007,** *70,* 1640–1643. doi:10.1021/np070184w
8. Baylis, A. B.; Hillman, M. E. D. German Patent 2155113, 1972. *Chem. Abstr.* **1972,** *77,* 34174q.
9. Basavaiah, D.; Reddy, B. S.; Badsara, S. S. *Chem. Rev.* **2010,** *110,* 5447–5674. doi:10.1021/cr900291g
10. Wuts, P. G. M.; Greene, T. W. *Greene's Protective Groups in Organic Synthesis,* 4th ed.; John Wiley & sons: Hoboken, NJ, 2007.
11. Hatala, P. J.; Kallmerten, J.; Borer, P. N. *Nucleosides Nucleotides* **2001,** *20,* 1961–1973.
12. Shigetomi, K.; Omoto, S.; Kato, Y.; Ubukata, M. *Biosci., Biotechnol., Biochem.* **2011,** *75,* 718–722. doi:10.1271/bbb.100845
13. Yu, C.; Liu, B.; Hu, L. *J. Org. Chem.* **2001,** *66,* 5413–5418. doi:10.1021/jo015628m
14. Ilangovan, A.; Saravanakumar, S.; Malayappasamy, S.; Manickam, G. *RSC Adv.* **2013,** *3,* 14814–14828. doi:10.1039/c3ra42113a

15. Wei, Y.; Shi, M. *Chem. Rev.* **2013,** *113,* 6659–6690. doi:10.1021/cr300192h
16. Shadakshari, U.; Nayak, S. K. *Tetrahedron* **2001,** *57,* 4599–4602. doi:10.1016/S0040-4020(01)00333-7
17. Das, B.; Banerjee, J.; Majhi, A.; Mahender, G. *Tetrahedron Lett.* **2004,** *45,* 9225–9227. doi:10.1016/j.tetlet.2004.10.088
18. Das, B.; Chowdhury, N.; Banerjee, J.; Majhi, A. *Tetrahedron Lett.* **2006,** *47,* 6615–6618. doi:10.1016/j.tetlet.2006.07.014
19. Hoffmann, H. M. R.; Rabe, J. *J. Org. Chem.* **1985,** *50,* 3849–3859. doi:10.1021/jo00220a034
20. Basavaiah, D.; Krishnamacharyulu, M.; Hyma, R. S.; Sarma, P. K. S.; Kumaragurubaran, N. *J. Org. Chem.* **1999,** *64,* 1197–1200. doi:10.1021/jo981761b
21. Li, J.; Xu, H.; Zhang, Y. *Tetrahedron Lett.* **2005,** *46,* 1931–1934. doi:10.1016/j.tetlet.2005.01.136
22. Dittami, J. P.; Xu, F.; Qi, H.; Martin, M. W. *Tetrahedron Lett.* **1995,** *36,* 4201–4204. doi:10.1016/0040-4039(95)00780-G
23. Mase, N.; Nishi, T.; Takamori, Y.; Yoda, H.; Takabe, K. *Tetrahedron: Asymmetry* **1999,** *10,* 4469–4471. doi:10.1016/S0957-4166(99)00513-3

License and Terms

This is an Open Access article under the terms of the Creative Commons Attribution License (http://creativecommons.org/licenses/by/2.0), which permits unrestricted use, distribution, and reproduction in any medium, provided the original work is properly cited.

The license is subject to the *Beilstein Journal of Organic Chemistry* terms and conditions: (http://www.beilstein-journals.org/bjoc)

The definitive version of this article is the electronic one which can be found at: doi:10.3762/bjoc.10.9

Beilstein Journal of Organic Chemistry

Physalin H from *Solanum nigrum* as an Hh signaling inhibitor blocks GLI1–DNA-complex formation

Midori A. Arai*[1], Kyoko Uchida[1], Samir K. Sadhu[2], Firoj Ahmed[3] and Masami Ishibashi*[1]

Full Research Paper

Open Access

Address:
[1]Graduate School of Pharmaceutical Sciences, Chiba University, 1-8-1 Inohana, Chuo-ku, Chiba 260-8675, Japan, [2]Pharmacy Discipline, Life Science School, Khulna University, Khulna-9208, Bangladesh and [3]Department of Pharmaceutical Chemistry, University of Dhaka, Dhaka-1000, Bangladesh

Email:
Midori A. Arai* - midori_arai@chiba-u.jp; Masami Ishibashi* - mish@chiba-u.jp

* Corresponding author

Keywords:
Hedgehog inhibitor; Hedgehog signal; natural products; physalins; *Solanum nigrum*

Beilstein J. Org. Chem. **2014,** *10,* 134–140.
doi:10.3762/bjoc.10.10

Received: 29 August 2013
Accepted: 26 November 2013
Published: 13 January 2014

This article is part of the Thematic Series "Natural products in synthesis and biosynthesis".

Guest Editor: J. S. Dickschat

© 2014 Arai et al; licensee Beilstein-Institut.
License and terms: see end of document.

Abstract

Hedgehog (Hh) signaling plays an important role in embryonic development, cell maintenance and cell proliferation. Moreover, Hh signaling contributes to the growth of cancer cells. Physalins are highly oxidized natural products with a complex structure. Physalins (**1**–**7**) were isolated from *Solanum nigrum* (Solanaceae) collected in Bangladesh by using our cell-based assay. The isolated physalins included the previously reported Hh inhibitors **5** and **6**. Compounds **1** and **4** showed strong inhibition of GLI1 transcriptional activity, and exhibited cytotoxicity against cancer cell lines with an aberrant activation of Hh signaling. Compound **1** inhibited the production of the Hh-related proteins patched (PTCH) and BCL2. Analysis of the structures of different physalins showed that the left part of the physalins was important for Hh inhibitory activity. Interestingly, physalin H (**1**) disrupted GLI1 binding to its DNA binding domain, while the weak inhibitor physalin G (**2**) did not show inhibition of GLI1-DNA complex formation.

Introduction

Hedgehog (Hh) signaling plays an important role in embryonic development and adult tissue maintenance [1,2]. Once the Hh protein binds and inhibits its receptor patched (PTCH), Smoothened (SMO) makes GLIs, which are zinc-finger transcription factors, free to move in the nucleus from the GLIs–SuFu complex. The GLIs then bind to their consensus DNA sequence and turn on the expression of the target gene [3,4]. Although this signal has been identified as one of the key

intercellular signals in many fundamental processes, aberrant activation of this signaling pathway plays a crucial role in the development of tumors such as basal-cell carcinomas and small-cell lung cancer [5-7]. To find a drug for the treatment of cancer, Hh inhibitors have been recently developed. SMO inhibitors are a major category of Hh signaling inhibitors (cyclopamine [8,9], Cur-61414 [10] and SANTs [11]). Robotnikinin interacts with the Shh protein [12], and JK184 induces Hh inhibition through class IV alcohol dehydrogenase [13]. GANT-61 is an inhibitor, which disturbs GLIs binding to their binding site (GACCACCCA) in the promoter region of the target genes [14]. The AAA+ ATPase motor cytoplasmic dynein has been found to be the molecular target for Hh pathway inhibitors (HPIs) [15,16].

Previously, we have constructed a cell-based assay involving a tetracycline-regulated (T-Rex) system for Hh/GLI-mediated transcriptional inhibitors (Figure 1) [17-22]. Naturally occurring Hh inhibitors such as physalin F (**5**; IC_{50}, 0.66 μM) [17], physalin B (**6**; IC_{50}, 0.62 μM) [17], colubrinic acid (IC_{50}, 38 μM) [18], caldenolides (IC_{50}, 0.1–0.45 μM) [19], taepeenin D (IC_{50}, 1.6 μM) [20] and a flavonoid glycoside (IC_{50}, 0.5 μM) [21] were isolated by using this screening assay. Recently, we found that vitetrifolin D (IC_{50}, 20.2 μM) is the first naturally occurring Hh inhibitor that impairs GLI1–DNA binding [22]. Because of the mutation of components of the Hh signal such as SMO, more downstream events such as the binding of GLI1 on DNA would be affected by the inhibition because of the mutation of components in many cancers. In this study, we report the isolation of four physalins (**1**–**4**) along with the previously reported Hh inhibitors **5** and **6**. In addition, we evaluated the Hh inhibitory activity by assessing the cytotoxicity against cancer cells and the expression of Hh-related proteins. Physalin H (**1**) inhibited GLI1 binding to its DNA binding domain as assessed by our previously reported electrophoresis mobility shift assay (EMSA).

Results and Discussion

Isolation of physalins

Among our extract library, *Solanum nigrum* was identified as an active plant with our cell-based assay screening. After the removal of chlorophyll from the MeOH extract of *Solanum nigrum* (leaves) (7.9 g) by Diaion HP-20, each MeOH soluble part of fraction 1A (3.7 g) and fraction 1B (1.2 g) were suspended in H_2O/MeOH 9:1. The suspension thus obtained was successively partitioned between hexane, EtOAc and

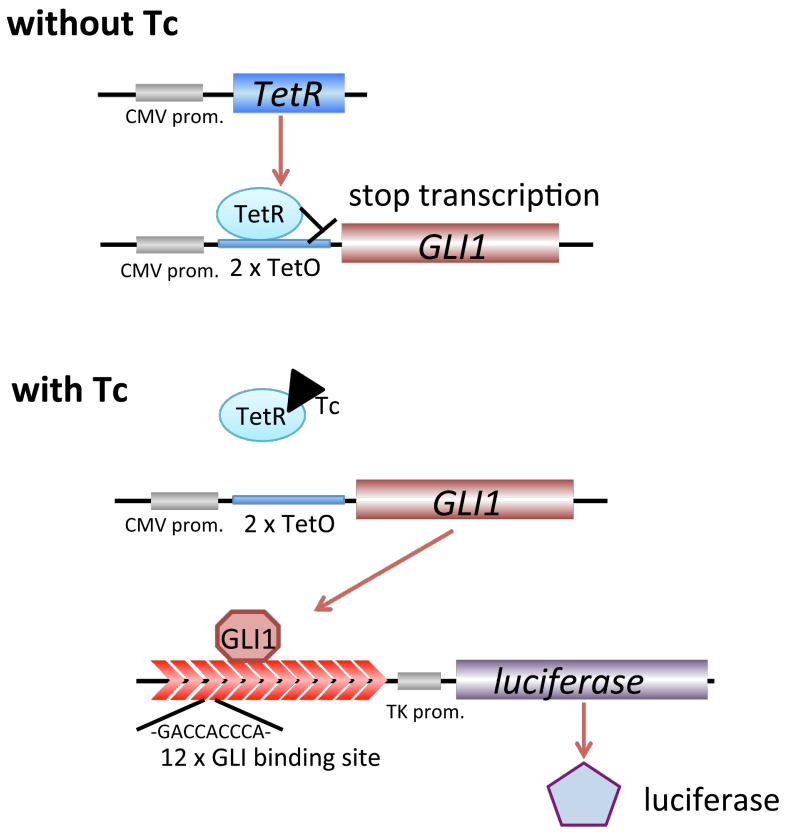


Figure 1: Schematic procedure of the constructed assay system; Tc (tetracycline), TetR (tetracycline repressor), TetO (tetracycline operator).

n-BuOH. Consecutive steps of silica gel column chromatography, and reversed-phase high-performance liquid chromatography (HPLC) of the active EtOAc extracts of fraction 1A and 1B yielded physalin H (**1**) [23], physalin G (**2**) [24], physalin K (**3**) [25], isophysalin B (**4**) [26], physalin F (**5**) [27] and a mixture of physalin B (**6**) [28] and physalin C (**7**) [29]. The structures of these compounds were identified by comparing their spectral data with those reported in the literature (Figure 2).

Evaluation of Hh inhibitory activity of isolated physalins

We evaluated the Hh inhibitory activity of the isolated compounds by using a previously described method [18]. Detection of the Hh inhibitory activity was based on the decrease in the luminescence value due to reduced luciferase expression by GLI1 compared to that of the control (DMSO). In addition we always checked the cytotoxicity of the compounds against the assay cells, because a decrease in the number of living cells also correlates with a reduced luciferase activity. Physalin H (**1**) and isophysalin B (**4**) showed a dose-dependent inhibition of luciferase production (IC_{50} were 0.70 and 4.2 μM, respectively) with a low cytotoxicity against assay cells (Figure 3). Physalin G (**2**) showed a weak Hh inhibition (IC_{50}, 47.1 μM). Physalin K (**3**) did not show Hh inhibition at all, even at a concentration of 17.9 μM. Previously, we reported on the isolation and evaluation of Hh inhibitory activities of physalin F (**5**) (IC_{50}, 0.66 μM) and physalin B (**6**) (IC_{50}, 0.62 μM) [17]. In this study, physalin B (**6**) was isolated as a mixture with physalin C (**7**) at a ratio of 3:2. An equilibrium between **6** and **7** might exist under weakly acidic conditions, because the ratio of the mixture changed from 3:2 to 1:1 in a deuterated chloroform ($CDCl_3$) solution after two months. Further, we examined the cytotoxicity against cancer cells, human pancreatic (PANC1) and prostate (DU145) cancer cell lines, in which Hh signaling is aberrantly activated (Table 1). Physalin H (**1**) (IC_{50}, 0.70 μM) showed cytotoxicity against PANC1 (IC_{50}, 5.7 μM) and DU145 (IC_{50}, 6.8 μM). In addition, isophysalin B (**4**) and previously reported **5** and **6** also exhibited strong cytotoxicity against PANC1 (IC_{50} were 12.0, 2.7 and 5.3 μM, respectively). A moderate selectivity between differentiating cancer cells and normal cells was observed for active compounds **1**, **4**, **5** and **6**, because the survival of C3H10T1/2 cells was not significantly affected by a treatment with these compounds. C3H10T1/2 is a normal cell line in which the Hh signalling pathway is active but does not contribute to abnormal cell survival. Interestingly, the right parts of these isolated physalins, except **7**, were identical. Therefore, the difference in Hh inhibitory activity can be attributed to the left part of their structures. The difference in the Hh inhibitory activity between **4** (IC_{50}, 4.2 μM) and **6** (IC_{50}, 0.62 μM) indicates that an α,β-unsaturated ketone unit present in the physalin structure may be a good nucleophile acceptor and contribute to the Hh inhibition. In addition, a conjugated dienone system in **2** and a peroxy bridge in **3** may be associated with decreased Hh inhibitory activity. Western blot analyses were performed with physalin H (**1**), which was the most active compound, except previously reported compounds **5** and **6**. Physalin H (**1**) showed an inhibition of Hh- related protein expression (Figure 4). The effect of **1** on the expression of a Hh membrane receptor, PTCH, and an anti-apoptosis protein BCL2 in HaCaT cells expressing exogenous GLI1 (reporter assay

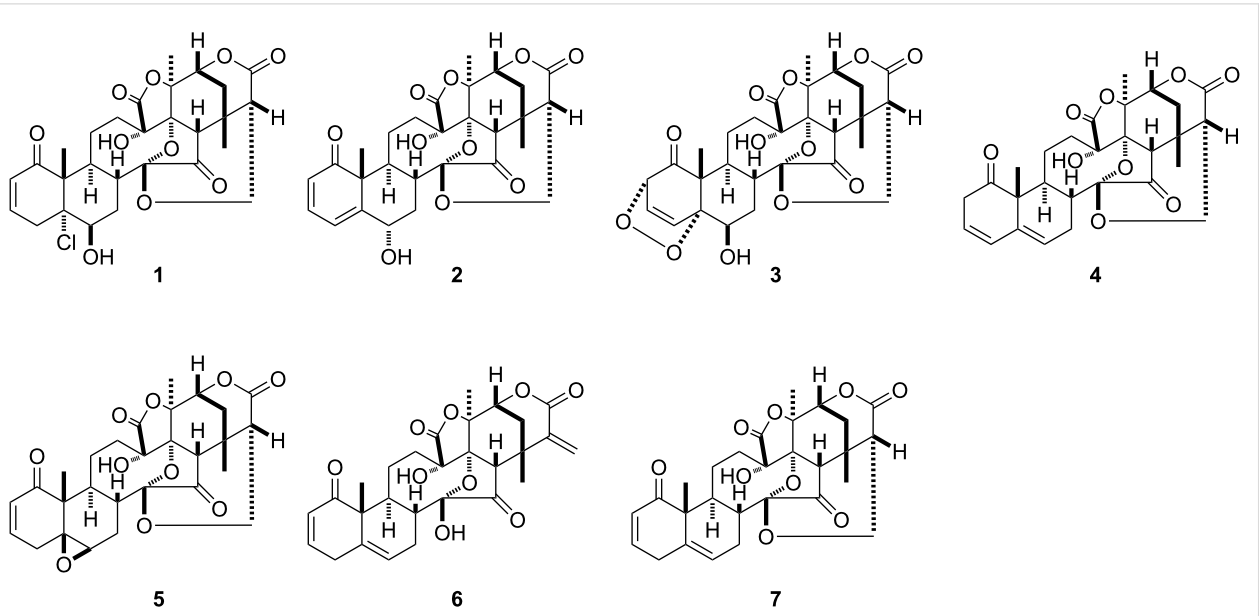


Figure 2: Isolated compounds from *Solanum nigrum*.

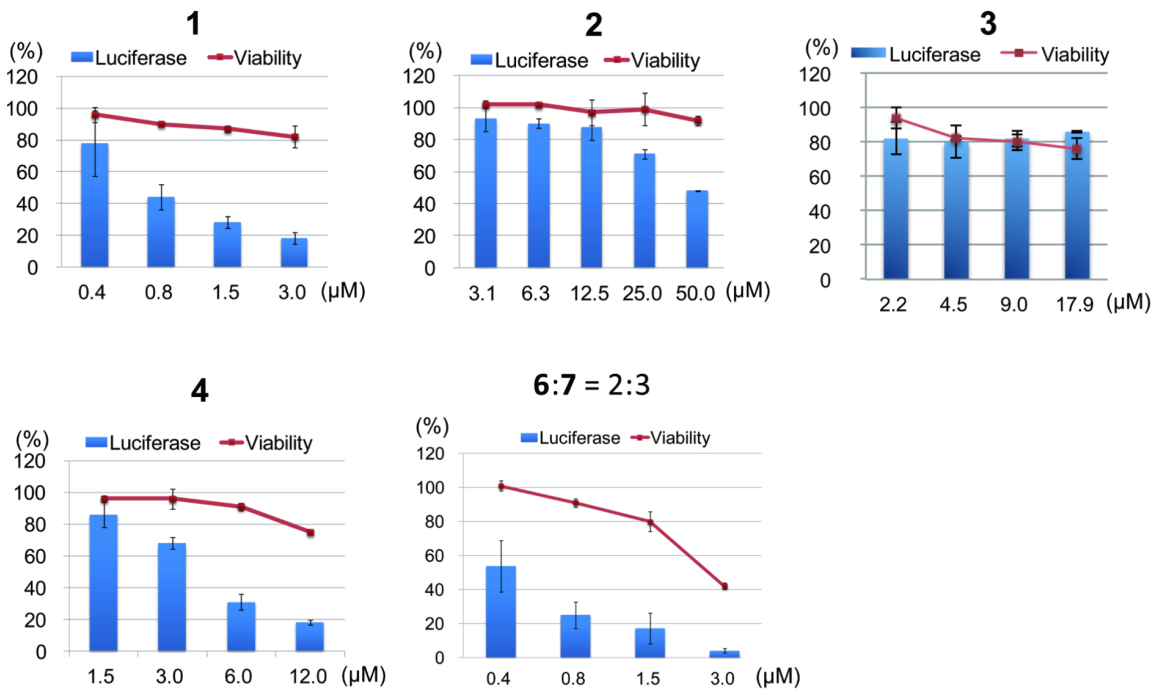


Figure 3: GLI1 transcriptional activity and cytotoxicity. Reporter activity (solid columns) and cell viability (solid curves) of compouds **1**–**4** and mixture of **6** and **7** (2:3). The assays were performed at 0.05% DMSO (n = 3). Error bars represent SD.

Table 1: GLI1 transcriptional activity and cytotoxicity.

Compound	GLI1 transcriptional inhibition, IC_{50} (μM)	Cytotoxicity, IC_{50} (μM)		
		PANC1	DU145	C3H10T1/2
physalin H (**1**)	0.70	5.7	6.8	>6.0
physalin G (**2**)	47.1	–	>12.0	–
physalin K (**3**)	–	–	–	–
isophysalin B (**4**)	4.2	12.0	>12.0	>12.0
physalin F (**5**)[a]	0.66[a]	2.7[a]	–	15.0[a]
physalin B (**6**)[a]	0.62[a]	5.3[a]	–	17.0[a]
6 and **7** mixture (2:3)	0.40	4.0	3.6	>6.0

[a]Data from [17].

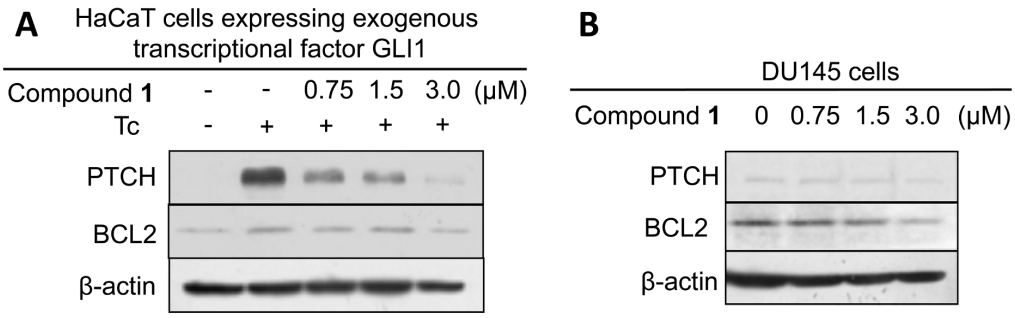


Figure 4: Inhibition of protein expression by compound **1**. (A) Western blot analysis of PTCH, BCL-2 protein levels in GLI1-overexpressing HaCaT cells after treatment with **1**. (B) Western blot analysis of PTCH, BCL-2 protein levels in DU145 cells after treatment with **1**.

cells) is shown in Figure 4A. At a concentration of 3.0 μM, physalin H (**1**) inhibited the expression of both proteins. In addition, at a concentration of 3.0 μM, physalin H (**1**) decreased the expression of BCL2 in DU145 cancer cells, in which Hh signaling was activated (Figure 4B). However, the expression of PTCH was only slightly affected.

Inhibition of GLI1–DNA complex formation by physalin H (**1**)

Disruption of the GLI1–DNA complex in the final stage of this signaling pathway is one of the most attractive molecular mechanisms of Hh inhibitors. Recently, we reported the first small molecule, which directly inhibits the GLI1–DNA complex formation [22].GANT61, a synthetic compound, has been reported to inhibit the GLI1–DNA-complex formation after cells were treated with this compound. The author speculated that GANT61 might affect modifications of the GLI1 protein expression, which causes disruption of the GLI1–DNA complex. In our previous study [22], we constructed an electrophoretic mobility shift assay (EMSA) for the detection of the GLI1–DNA complex. The assay uses a slightly modified biotin-tagged DNA and modified amino acids sequences of GLI1 compared to those reported in literature [30-32]. In a similar manner as described in [22], GLI1 protein was expressed in *Escherichia coli* as a 171–515 amino chain, including the five Zn finger regions. Horseradish peroxidase (HRP)-conjugated streptavidin detected free "biotin-labeled GLI1-BS" (DNA containing GLI1 binding site; biotin-AGCTACCTGGGTGGTCTCTTCGA; the underlined 9 bps are a consensus sequence [30]; Figure 5, lane 1). After mixing with GST–GLI1, GLI1–BS and GST–GLI1 the complex was detected in the upper line, because of an increasing molecular weight (low mobility; lane 2). By using this EMSA, the inhibitory activity of physalin H (**1**, IC_{50}; 0.70 μM) and inactive physalin G (**2**, IC_{50}; 47.1 μM) was examined. Under these experimental conditions, physalin H (**1**) clearly inhibited the formation of GLI1–DNA complex at 200 μM. On the other hand, physalin G (**2**), which is similar in the right part of its structure to physalin H (**1**), did not inhibit the complex formation even at 200 μM. These results suggested that one of the Hh inhibitory mechanisms of physalin H (**1**) involves inhibition of GLI1–DNA-complex formation.

Conclusion

We isolated seven physalins from *S. nigrum* by using Hh inhibitory activity-guided isolation. Among them, four compounds (**1**, **4**, **5** and **6**) showed dose-dependent GLI1-transcriptional inhibitory activity. In addition, these physalins were found to be cytotoxic to cancer cells with an aberrant Hh signaling pathway and inhibited the expression of Hh signaling-related proteins. Structure–activity relationships were observed in the Hh inhibitory activity of physalins and the left part of the structure was found to have an important role in Hh inhibition. Moreover, physalin H (**1**) inhibited the formation of GLI1–DNA complex, but inactive physalin G (**2**) did not. To our knowledge, this is the second study in which the direct inhibition of the formation of the GL1–DNA complex by Hh inhibitors has been reported.

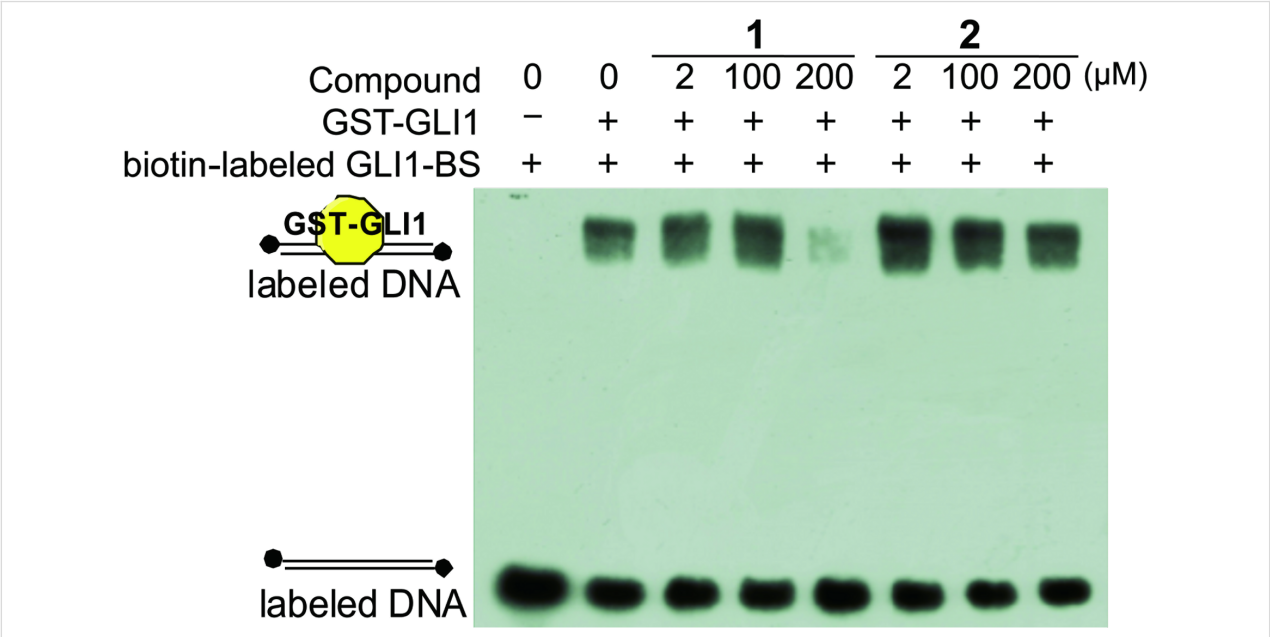


Figure 5: Inhibitory activity of GLI1–DNA-complex formation by electron mobility shift assay (EMSA). GST–GLI1 (171-515aa), DNA containing the GLI1 binding site (GLI1–BS); 5'-AGCTACCTGGGTGGTCTCTTCGA-3'. The reproducibility was checked in five individual experiments.

Experimental

General experimental procedures

The NMR measurements were carried out with JEOL ECP400 and ECP600 spectrometers in deuterated solvents and the residual proton chemical shift was taken as an internal standard. MS data were obtained with a JEOL JMS-T100LP (ESI). IR spectra were measured by using the ATR (attenuated total reflection) method on a Jasco FT-IR 230 spectrophotometer. The DNA concentration was measured by a NanoDrop 2000 (Thermo Fisher Scientific), and the protein concentration was measured by an UVmini 1240 UV–vis Spectrophotometer (SHIMADZU, Kyoto, Japan). The procedures for the GLI1-mediated transcriptional activity assay, Western blot analysis and cytotoxicity test were as previously described [18]. The GST–GLI1 protein was produced as previously described [22].

Plant material

The plant *Solanum nigrum* was collected in Bangladesh in 2011. A voucher specimen (KKB204) was deposited in the Ishibashi laboratory at the Chiba University.

Extraction and isolation

After the removal of chlorophyll from a MeOH extract of *S. nigrum* (leave) (7.9 g) by Diaion HP-20, fraction 1A (3.7 g) was then partitioned between hexane, EtOAc and *n*-BuOH. The active EtOAc extract (623.4 mg) was subjected to silica gel column chromatography (30 × 180 mm; $CHCl_3$/MeOH 1:0 to 0:1, 0:1 + 0.1% TFA) to give 7 fractions (15A–15G). Fraction 15C (68.5 mg) was subjected to ODS HPLC (COSMOSIL Packed Column 5-CN-MS 10 × 250 mm; MeCN/H_2O 68:35, flow rate 2.0 mL/min, UV detection at 254 nm) to give compound **2** (10.1 mg, t_R 10 min), compound **3** (2.4 mg, t_R 17 min) and compound **1** (3.8 mg, t_R 25 min). Fraction 1B (1.2 g) was partitioned between hexane, EtOAc and *n*-BuOH. The active EtOAc extract (294.5 mg) was subjected to silica gel column chromatography (25 × 200 mm; $CHCl_3$/MeOH 40:1 to 0:1, 0:1 + 0.1% TFA) to give 6 fractions (4A–4F). Fraction 4A (179.6 mg) was subjected to silicagel column chromatography (20 × 200 mm; hexane/EtOAc 2:1 to 0:1, MeOH) to give 5 fractions (5A–5E). Fraction 5C (50.7 mg) was subjected to ODS HPLC (COSMOSIL Packed Column 5-CN-MS 10 × 250 mm; MeCN/H_2O 2:3, flow rate 2.0 mL/min, UV detection at 254 nm) to give 8 fractions (6A–6H). Fraction 6E (20.0 mg) was subjected to ODS HPLC (Develosil Packed Column ODS-HG-5, 10 × 250 mm; MeCN/H_2O 2:3, flow rate 2.0 mL/min, UV detection at 254 nm) to give compound **5** (7.0 mg, t_R 31 min). Fraction 5B (91.0 mg) was subjected to ODS HPLC (COSMOSIL Packed Column 5-CN-MS, 10 × 250 mm; MeCN/H_2O 2:3, flow rate 2.0 mL/min, UV detection at 254 nm) to give 6 fractions (7A–7F). Fraction 7E (11.4 mg) was subjected to ODS HPLC (Develosil Packed Column ODS-HG-5, 10 × 250 mm; MeCN/H_2O 1:1, flow rate 2.0 mL/min, UV detection at 254 nm) to give compound **4** (4.0 mg, t_R 32 min). Fraction 7D (34.0 mg) was subjected to ODS HPLC (Develosil Packed Column ODS-HG-5, 10 × 250 mm; MeCN/H_2O 2:3, flow rate 2.0 mL/min, UV detection at 254 nm) to give a 2:3 mixture of compounds **6** and **7** (2.0 mg, t_R 10 min) and compound **4** (1.7 mg, t_R 24 min). Fraction 4B was subjected to ODS HPLC (COSMOSIL Packed Column 5-CN-MS, 10 × 250 mm; MeCN/H_2O 37:63, flow rate 2.0 mL/min, UV detection at 254 nm) to give compound **3** (1.7 mg, t_R 24 min) and compound **1** (3.3 mg, t_R 30 min).

Electrophoretic mobility shift assay (EMSA)

The double-stranded (ds) DNA fragments containing a GLI1 binding site (GLI1–BS) were prepared by annealing of single strand (ss) DNA; for biotin-labeled GLI1–BS, 5'-biotin-AGCTACCTGGGTGGTCTCTTCGA-3' and 5'-biotin-TCGAAGAGACCACCCAGGTAGCT-3'. 10 μL of the ssDNA (100 pmol/μL in TE buffer (NIPPON GENE, Tokyo, Japan)) were mixed and annealed by PCR Thermal Cycler Dice (Takara, Kyoto, Japan) (95 °C, 30 s; 72 °C, 2 min; 37 °C, 2 min; 25 °C, 2 min). For EMSA experiments, dsDNA TE buffer solutions were prepared as follows: biotin-labeled GLI1–BS (50 fmol/μL), unlabeled mutGLI1–BS and unlabeled GLI1–BS (5 pmol/μL). These solutions were stored below −20 °C.

The assays were performed with a Light Shift Chemiluminescent EMSA Kit (Thermo). The binding reaction was set up as follows: 70 ng of GST–GLI1 protein, biotin-labeled GLI1–BS (20 fmol), and compound in DMSO (final DMSO concentration was 0.6%) were combined in 2 μL of 10 × binding buffer (kit), (5 mM $MgCl_2$, 4% glycerol) on ice (total volume 20 μL). After incubation for 20 min on ice, protein–DNA complex, free DNA and free protein were separated on a 6% native polyacrylamide gel containing Tris-Borate-EDTA (TBE; 45 mM tris-borate, 1.0 mM EDTA). After transfer of DNA onto a Biodyne B nylon membrane 0.45 μm (Pall Gelman Laboratory, Ann Arbor, MI) and DNA crosslinking by UV transilluminator (312 nm, 15 min), biotin-labeled DNA was detected by HRP-conjugated streptavidin, following the manufactures' protocols.

Acknowledgements

We are very grateful to Drs. Fritz Aberger and Gerhard Regl (University of Salzburg) for providing us with tetracycline-regulated HaCaT cells, Dr. Rune Toftgård (Karolinska Institute) for the 12GLI-RE-TKO luciferase plasmid, Dr. Bert Vogelstein (Howard Hughes Medical Institute) and Dr. Hiroshi Sasaki (RIKEN) for the human GLI1 plasmid. This study was supported by a Grant-in-Aid for Scientific Research from the Japan Society for the Promotion of Science (JSPS), a Grant-in-Aid for Scientific Research on Innovative Areas 'Chemical

Biology of Natural Products' from The Ministry of Education, Culture, Sports, Science and Technology, Japan (MEXT), Special Funds for Education and Research (Development of SPECT Probes for Pharmaceutical Innovation) from MEXT and the Iodine Research Project in the Chiba University, the Asian Core Program (JSPS), Takeda Science Foundation, Hayashi Memorial Foundation for Female Natural Scientists, the Naito Foundation and the Tokyo Biochemical Research Foundation.

References

1. Jiang, J.; Hui, C.-c. *Dev. Cell* **2008,** *15,* 801–812. doi:10.1016/j.devcel.2008.11.010
2. Riobo, N. A.; Manning, D. R. *Biochem. J.* **2007,** *403,* 369–379. doi:10.1042/BJ20061723
3. Kinzler, K. W.; Vogelstein, B. *Mol. Cell. Biol.* **1990,** *10,* 634–642.
4. Pavletich, N. P.; Pabo, C. O. *Science* **1993,** *261,* 1701–1707. doi:10.1126/science.8378770
   See for the X-ray structure of GLI-DNA complex.
5. di Magliano, M. P.; Hebrok, M. *Nat. Rev. Cancer* **2003,** *3,* 903–911. doi:10.1038/nrc1229
6. Rubin, L. L.; de Sauvage, F. J. *Nat. Rev. Drug Discovery* **2006,** *5,* 1026–1033. doi:10.1038/nrd2086
7. Scales, S. J.; de Sauvage, F. J. *Trends Pharmacol. Sci.* **2009,** *30,* 303–312. doi:10.1016/j.tips.2009.03.007
8. Chen, J. K.; Taipale, J.; Cooper, M. K.; Beachy, P. A. *Genes Dev.* **2002,** *16,* 2743–2748. doi:10.1101/gad.1025302
9. Incardona, J. P.; Gaffield, W.; Kapur, R. P.; Roelink, H. *Development* **1998,** *125,* 3553–3562.
10. Williams, J. A.; Guicherit, O. M.; Zaharian, B. I.; Xu, Y.; Chai, L.; Wichterle, H.; Kon, C.; Gatchalian, C.; Porter, J. A.; Rubin, L. L.; Wang, F. Y. *Proc. Natl. Acad. Sci. U. S. A.* **2003,** *100,* 4616–4621. doi:10.1073/pnas.0732813100
11. Chen, J. K.; Taipale, J.; Young, K. E.; Maiti, T.; Beachy, P. A. *Proc. Natl. Acad. Sci. U. S. A.* **2002,** *99,* 14071–14076. doi:10.1073/pnas.182542899
12. Stanton, B. Z.; Peng, L. F.; Maloof, N.; Nakai, K.; Wang, X.; Duffner, J. L.; Taveras, K. M.; Hyman, J. L.; Lee, S. W.; Koehler, A. N.; Chen, J. K.; Fox, J. L.; Mandinova, A.; Schreiber, S. L. *Nat. Chem. Biol.* **2009,** *5,* 154–156. doi:10.1038/nchembio.142
13. Lee, J.; Wu, X.; Pasca di Magliano, M.; Peters, E. C.; Wang, Y.; Hong, J.; Hebrok, M.; Ding, S.; Cho, C. Y.; Schultz, P. G. *ChemBioChem* **2007,** *8,* 1916–1919. doi:10.1002/cbic.200700403
14. Lauth, M.; Bergström, Å.; Shimokawa, T.; Toftgård, R. *Proc. Natl. Acad. Sci. U. S. A.* **2007,** *104,* 8455–8460. doi:10.1073/pnas.0609699104
15. Hyman, J. M.; Firestone, A. J.; Heine, V. M.; Zhao, Y.; Ocasio, C. A.; Han, K.; Sun, M.; Rack, P. G.; Sinha, S.; Wu, J. J.; Solow-Cordero, D. E.; Jiang, J.; Rowitch, D. H.; Chen, J. K. *Proc. Natl. Acad. Sci. U. S. A.* **2009,** *106,* 14132–14137. doi:10.1073/pnas.0907134106
16. Firestone, A. J.; Weinger, J. S.; Maldonado, M.; Barlan, K.; Langston, L. D.; O'Donnell, M.; Gelfand, V. I.; Kapoor, T. M.; Chen, J. K. *Nature* **2012,** *484,* 125–129. doi:10.1038/nature10936
17. Hosoya, T.; Arai, M. A.; Koyano, T.; Kowithayakorn, T.; Ishibashi, M. *ChemBioChem* **2008,** *9,* 1082–1092. doi:10.1002/cbic.200700511
18. Arai, M. A.; Tateno, C.; Hosoya, T.; Koyano, T.; Kowithayakorn, T.; Ishibashi, M. *Bioorg. Med. Chem.* **2008,** *16,* 9420–9424. doi:10.1016/j.bmc.2008.09.053
19. Arai, M. A.; Tateno, C.; Koyano, T.; Kowithayakorn, T.; Kawabe, S.; Ishibashi, M. *Org. Biomol. Chem.* **2011,** *9,* 1133–1139. doi:10.1039/c0ob00677g
20. Rifai, Y.; Arai, M. A.; Koyano, T.; Kowithayakorn, T.; Ishibashi, M. *J. Nat. Prod.* **2010,** *73,* 995–997. doi:10.1021/np1000818
21. Rifai, Y.; Arai, M. A.; Sadhu, S. K.; Ahmed, F.; Ishibashi, M. *Bioorg. Med. Chem. Lett.* **2011,** *21,* 718–722. doi:10.1016/j.bmcl.2010.11.126
22. Arai, M. A.; Fujimatsu, T.; Uchida, K.; Sadhu, S. K.; Ahmed, F.; Ishibashi, M. *Mol. BioSyst.* **2013,** *9,* 1012–1018. doi:10.1039/c3mb25567k
23. Makino, B.; Kawai, M.; Ogura, T.; Nakanishi, M.; Yamamura, H.; Butsugan, Y. *J. Nat. Prod.* **1995,** *58,* 1668–1674. doi:10.1021/np50125a004
24. Row, L. R.; Reddy, K. S.; Sarma, N. S.; Matsuura, T.; Nakashima, R. *Phytochemistry* **1980,** *19,* 1175–1181. doi:10.1016/0031-9422(80)83078-0
25. Makino, B.; Kawai, M.; Iwata, Y.; Yamaura, H.; Butsugan, Y.; Ogawa, K.; Hayashi, M. *Bull. Chem. Soc. Jpn.* **1995,** *68,* 219–226. doi:10.1246/bcsj.68.219
26. Sunayama, R.; Kuroyanagi, M.; Umehara, K.; Ueno, A. *Phytochemistry* **1992,** *34,* 529–533. doi:10.1016/0031-9422(93)80040-Y
27. Row, L. R.; Sarma, N. S.; Reddy, K. S.; Matsuura, T.; Nakashima, R. *Phytochemistry* **1978,** *17,* 1647–1650. doi:10.1016/S0031-9422(00)94660-0
28. Kawai, M.; Makino, B.; Taga, T.; Miwa, Y.; Yamamoto, T.; Furuta, T.; Yamamura, H.; Butsugan, Y.; Ogawa, K.; Hayashi, M. *Bull. Chem. Soc. Jpn.* **1994,** *67,* 222–226. doi:10.1246/bcsj.67.222
29. Kawai, M.; Matsuura, T. *Tetrahedron* **1970,** *26,* 1743–1745. doi:10.1016/S0040-4020(01)93024-8
30. De Smaele, E.; Fragomeli, C.; Ferretti, E.; Pelloni, M.; Po, A.; Canettieri, G.; Coni, S.; Di Marcotullio, L.; Greco, A.; Moretti, M.; Di Rocco, C.; Pazzaglia, S.; Maroder, M.; Screpanti, I.; Giannini, G.; Gulino, A. *Neoplasia* **2008,** *10,* 89–98. doi:10.1593/neo.07891
31. Ågren, M.; Kogerman, P.; Kleman, M. I.; Wessling, M.; Toftgård, R. *Gene* **2004,** *330,* 101–114. doi:10.1016/j.gene.2004.01.010
32. Sasaki, H.; Hui, C.; Nakafuku, M.; Kondoh, H. *Development* **1997,** *124,* 1313–1322.

License and Terms

This is an Open Access article under the terms of the Creative Commons Attribution License (http://creativecommons.org/licenses/by/2.0), which permits unrestricted use, distribution, and reproduction in any medium, provided the original work is properly cited.

The license is subject to the *Beilstein Journal of Organic Chemistry* terms and conditions: (http://www.beilstein-journals.org/bjoc)

The definitive version of this article is the electronic one which can be found at: doi:10.3762/bjoc.10.10

Beilstein Journal of Organic Chemistry

Recent applications of the divinylcyclopropane–cycloheptadiene rearrangement in organic synthesis

Sebastian Krüger and Tanja Gaich*

Review

Open Access

Address:
Institut für Organische Chemie, Leibniz Universität Hannover, Schneiderberg 1B, 30167 Hannover, Germany

Email:
Tanja Gaich* - tanja.gaich@oci.uni-hannover.de

* Corresponding author

Keywords:
cycloheptadiene; divinylcyclopropane rearrangement; domino reactions; natural products; total synthesis; vinylcyclopropane–carbaldehyde rearrangement

Beilstein J. Org. Chem. **2014,** *10,* 163–193.
doi:10.3762/bjoc.10.14

Received: 20 August 2013
Accepted: 11 November 2013
Published: 16 January 2014

This article is part of the Thematic Series "Natural products in synthesis and biosynthesis".

Guest Editor: J. S. Dickschat

© 2014 Krüger and Gaich; licensee Beilstein-Institut.
License and terms: see end of document.

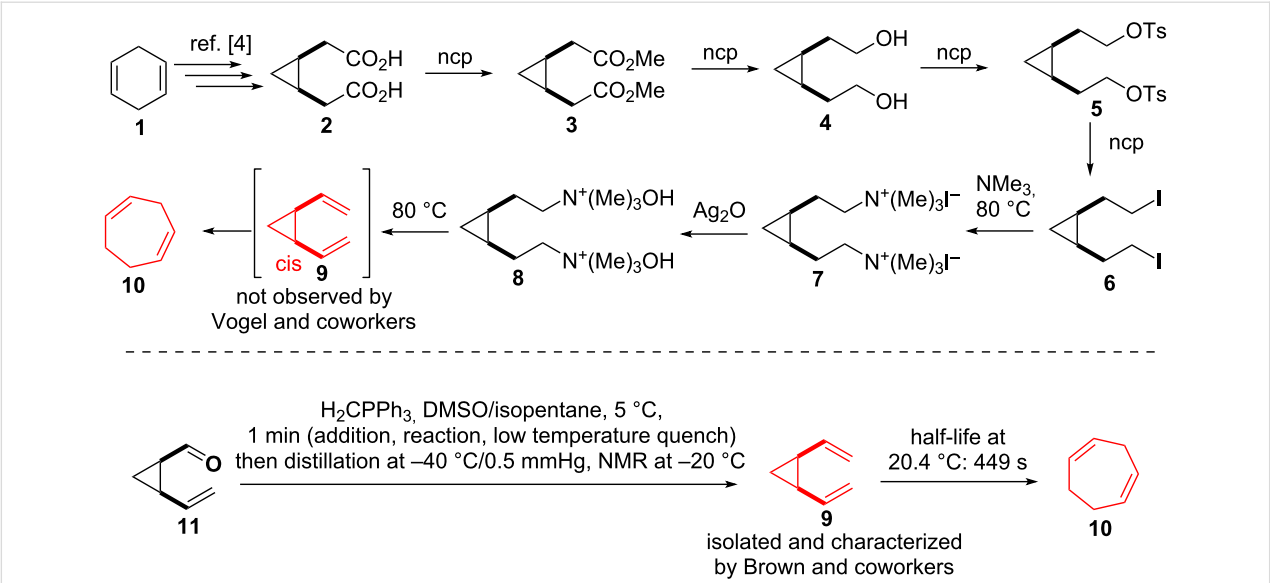
Abstract

This review summarizes the application of the divinylcyclopropane–cycloheptadiene rearrangement in synthetic organic chemistry. A brief overview of the new mechanistic insights concerning the title reaction is provided as well as a condensed account on the biological relevance of the topic. Heteroatom variants of this rearrangement are covered briefly.

Introduction

The first documented divinylcyclopropane–cycloheptadiene rearrangement dates back to 1960 occuring during studies of Vogel and coworkers [1,2] on the thermal rearrangement of small carbocycles. Although the desired *cis*-divinylcyclopropane (**9**) (see Scheme 1) could not be isolated using the depicted synthetic route (see **1** to **10**), as **9** readily rearranged under the final Hofmann elimination conditions, the resulting cycloheptadiene **10** was described as well as the rearrangement of *trans*-divinylcyclopropane taking place at 200 °C. The elusive *cis*-divinylcyclopropane (**9**) was characterized ten years later by Brown and coworkers [3] using a low temperature and very short-timed Wittig reaction between *cis*-vinylcarbaldehyde **11** and methylenetriphenylphoshorane.

This review summarizes the recent synthetic applications of the divinylcyclopropane–cycloheptadiene rearrangement starting in 1991. Earlier classic syntheses of sesquiterpenes are described to underline the synthetic power in the total synthesis of sesquiterpenoid natural products. The title reaction has been subject to previous reviews [5,6], partial overlap with the



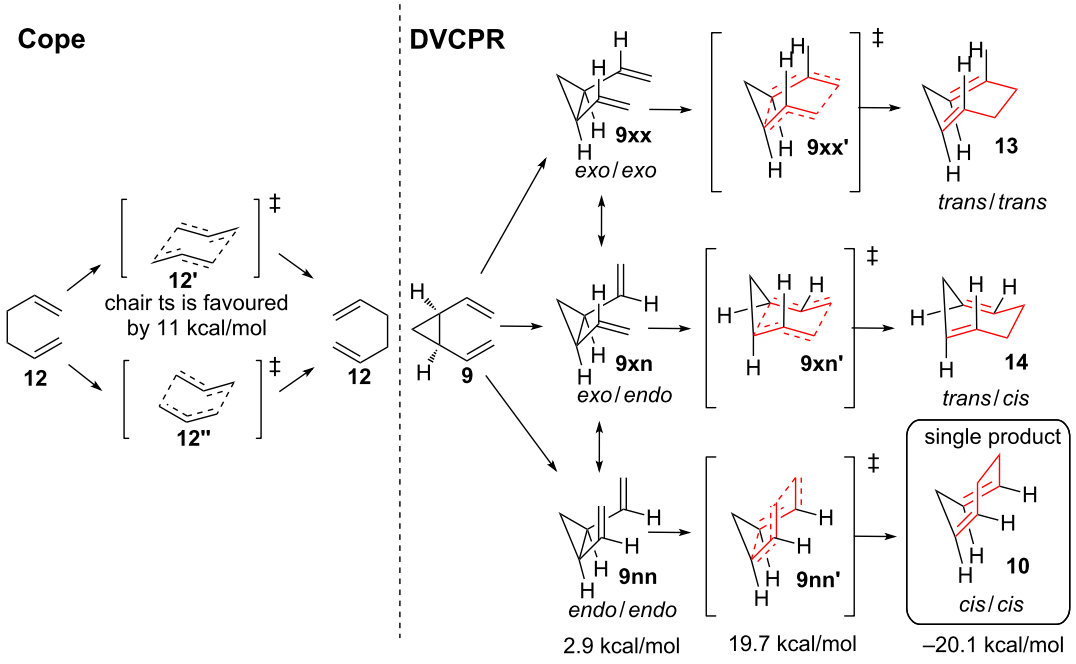
Scheme 1: Vogel's first approach towards the divinylcyclopropane rearrangement [4] and characterization of *cis*-divinylcyclopropane by Brown.

content of this review to other reviews concerning different topics exist [7-10]. The divinylcyclopropane–cycloheptadiene rearrangement will be abbreviated as DVCPR in the following. The divinylcycloproane moiety and the resulting cycloheptadiene will be highlighted in red throughout. The Buchner ring expansion [11,12] as a special case of the DVCPR is not part of this review. The related vinylcylopropane–cyclopentene rearrangement has been reviewed elsewhere [13,14].

Review

Mechanistic considerations

Transition state. Although the *cis*-divinylcyclopropane rearrangement is in fact a tethered version of the Cope rearrangement, it has to be noted that the preference of transition states (chair/boat) is opposite. Whereas the Cope rearrangement of hexa-1,5-diene **12** usually proceeds through chair-like transition state **12'** (see Scheme 2) and not through



Scheme 2: Transition states for the Cope rearrangement and the related DVCPR. Ts = transition state.

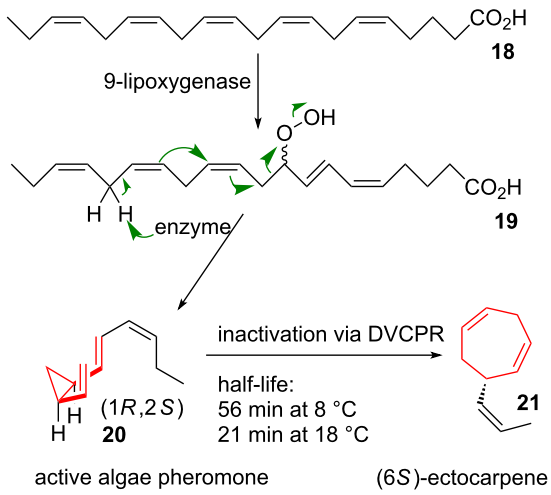
the energetically disfavoured boat-transition state **12''** [15], the DVCPR only proceeds via boat-like transition state **9nn'** where both vinyl-moieties are in the *endo*-orientation reagarding the cyclopropane [16]. The other transition states (**9xx'**/**9xn'**) would result in a cycloheptadiene with at least one *E*-configured double bond (**13**/**14**) after a hypothetical DVCPR, which can be regarded as inaccessible. Calculations revealed that the preferred orientation for *cis*-divinylcyclopropane is *exo*/*exo* **9xx**. The first rotation of a vinyl-moiety into the *endo*-orientation requires 0.8 kcal/mol giving **9xn**, the *endo*-orientation of both vinyl-moities requires 2.9 kcal/mol represented as **9nn** [17-19]. The necessary energy for the only possible transition state **9nn'** results in 19.7 kcal/mol, which is in good agreement with the experimental values of von Doering [20,21]. The rearranged cycloheptadiene **10** is favoured by −20.1 kcal/mol compared to the corresponding *cis*-divinylcyclopropane (**9**). Calculations have been carried out for *cis*-divinylheterocyclopropanes including nitrogen, oxygen, sulfur and phosphorus substitution [22], as well as *cis*-1,2-cyclobutanes [19,23]. Earlier calculations have been carried out for mono-heteroatom substitution in the vinyl moiety [24,25].

Transition state **9nn'** concludes that only *cis*-divinylcyclopropane undergoes the desired rearrangement, whereas *trans*-divinylcyclopropane should not react.

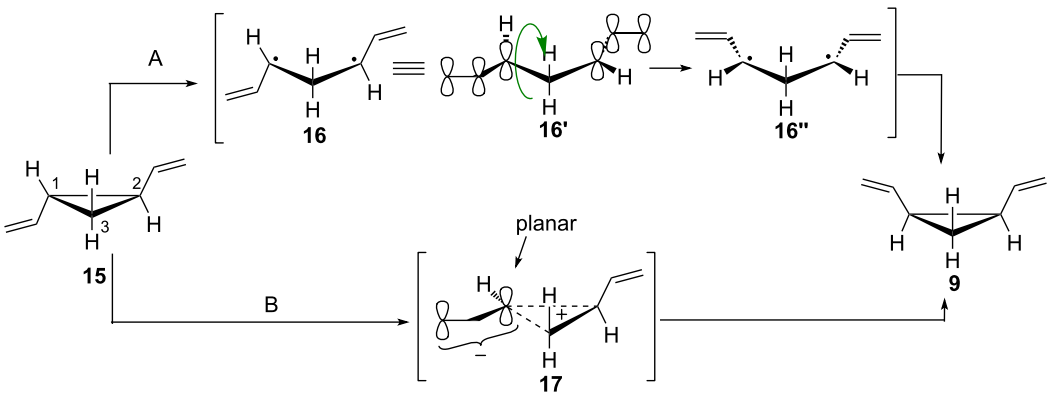
***Trans-cis* isomerization.** Nevertheless, *trans*-divinylcyclopropane **15** (see Scheme 3) can be used in the DVCPR, as it undergoes isomerization to the desired *cis*-isomer **9** at elevated temperature (≈200 °C [1,2], lowered for more conjugated systems). The isomerization pathways have been suggested to proceed either via the formation of intermediate diradical-species (pathway A, Scheme 3) [16,20,26,27] or through one-center epimerization (pathway B) [28,29]. Following pathway A, the C1–C2 bond of **15** is cleaved homolytically to give diradical **16.** The two radicals are stabilized as allylic radicals (depicted as **16'**), rotation around the C1–C3 bond takes place (**16'** to **16''**) followed by radical recombination to give *cis*-divinylcyclopropane (**9**). Pathway B proceeds through the formation of planar allylic anion **17**, which undergoes inversion to give *cis*-divinylcyclopropane (**9**). An alternative reaction pathway of the *trans*-divinylcyclopropane (**15**) to yield the cycloheptadiene product is the direct formation of the seven membered ring from diradical **16**.

Biosynthetic applications

The DVCPR has been shown to be part of the biosynthesis of ectocarpene (**21**, see Scheme 4) [29], an inactivated algae pheromone [30,31]. Starting from all-*cis*-pentaenic acid (**18**) peroxidation is supposed to take place to give **19**, followed by formation of the active algae pheromone **20** upon enzyme



Scheme 4: Proposed biosynthesic pathway to ectocarpene (**21**), an inactive degradation product of a sexual pheromone of brown algae (**20**).

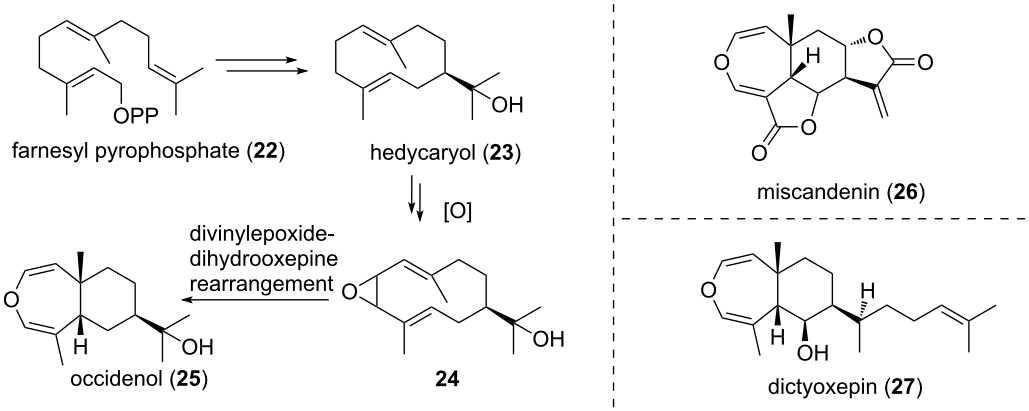


Scheme 3: Two possible mechanisms of *trans-cis* isomerizations of divinylcyclopropanes.

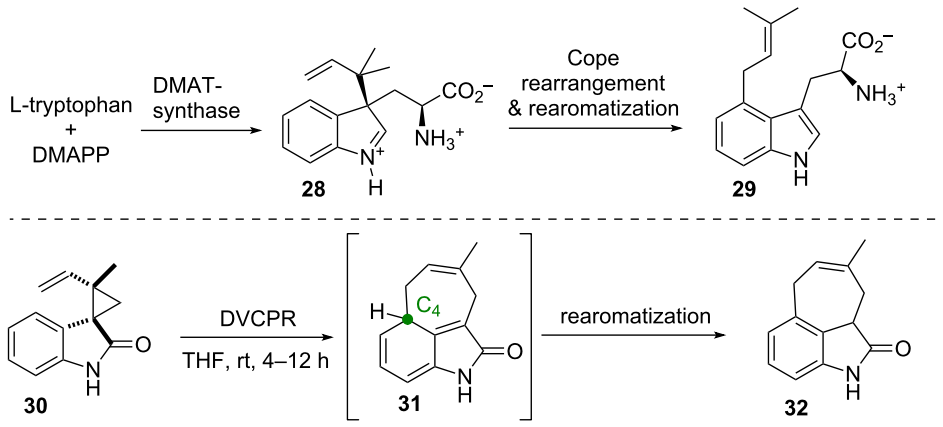
catalyzed fragmentation. Uncatalyzed DVCPR takes places to give **21** within short periods of time. The corresponding activation energies have been determined as well as the half-lifes at different temperatures. Bioassays proved that **20** was far more bioactive than **21**, and since the measured half-life for the conversion from **20** to **21** was longer than the necessary time for sexual encounter of the algae cycloheptadiene **21** was ruled out as a time-dependent sexual pheromone [32].

A divinyloxirane rearrangement has been proposed as the key step in the biosynthesis of several natural products containing a dihydrooxepine moiety. In the case of occidenol (**25**, see Scheme 5), which has been isolated from the wood of *Thuja koraiensis,* farnesyl pyrophosphate (**22**) is supposed to undergo ring closure and the intermediate carbocation is trapped by hydroxide to give hedycaryol (**23**) [33]. Oxidation leads to divinyloxirane **24**, which rearranges to the corresponding dihydrooxepine, yielding occidenol (**25**) [34,35]. Miscandenin (**26,** isolated from *Mikania* species) [36] and dictyoxepin (**27**, isolated from brown algaes) [37] are supposed to originate from the same *cis*-divinyloxirane rearrangement.

Gaich et al. [38,39] used the DVCPR in a biosynthetic investigation targeting the dimethylallyltryptophan synthase. In order to test the biosynthetic hypothesis of the mode of action of the 4-prenylation of indoles by Arigoni and Wenkert (starting from L-tryptophan and dimethylallyl pyrophosphate (DMAPP) through **28** to yield **29**, (Scheme 6) [40-42] the spiro-oxindole **30** was synthesized. The system underwent a *cis*-aryl-vinyl-cyclopropane rearrangement [43] to give **31** followed by rearomatization in 4–12 hours at room temperature yielding tricycle **32**. The formation of the obtained tricyclic cyclohepta[*cd*]oxindole core **32** proved the synthetic versatility of a [3,3]-sigmatropic rearrangement for direct C–C-bond formation at the C4 position of the indole nucleus, and thus provides experimental evidence for the biosynthetic proposal.



Scheme 5: Proposed biosynthesis of occidenol (**25**) and related natural compounds.



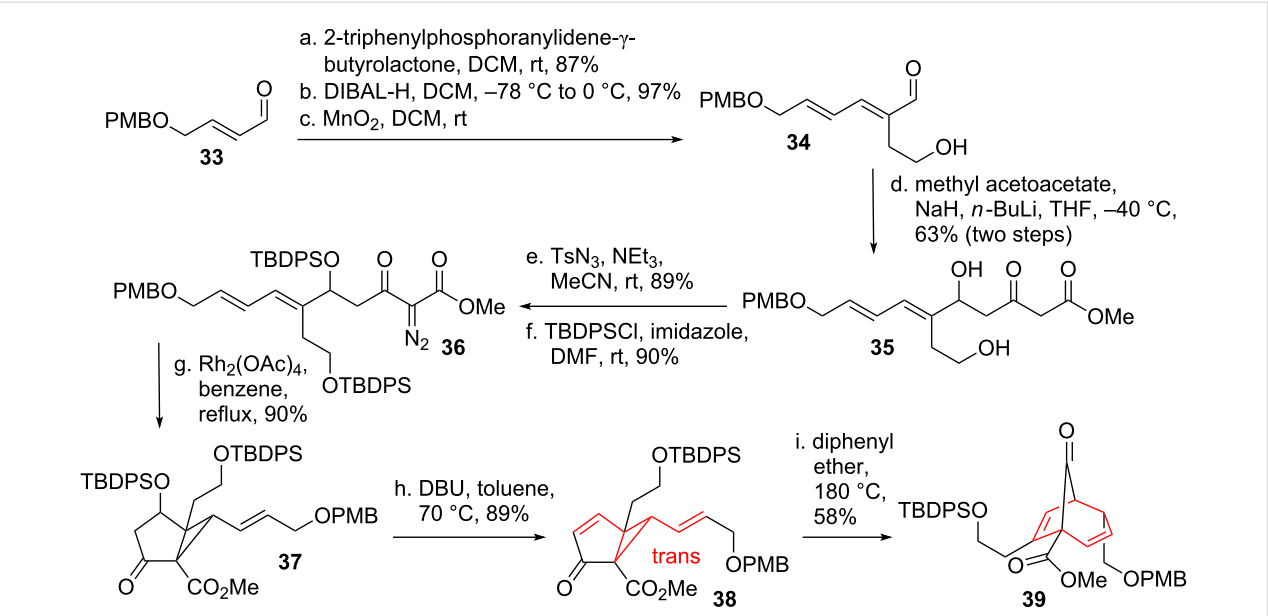
Scheme 6: Gaich's bioinspired system using the DVCPR to mimick the dimethylallyltryptophan synthase. DMAPP = dimethylallyl pyrophosphate.

Applications to natural product synthesis

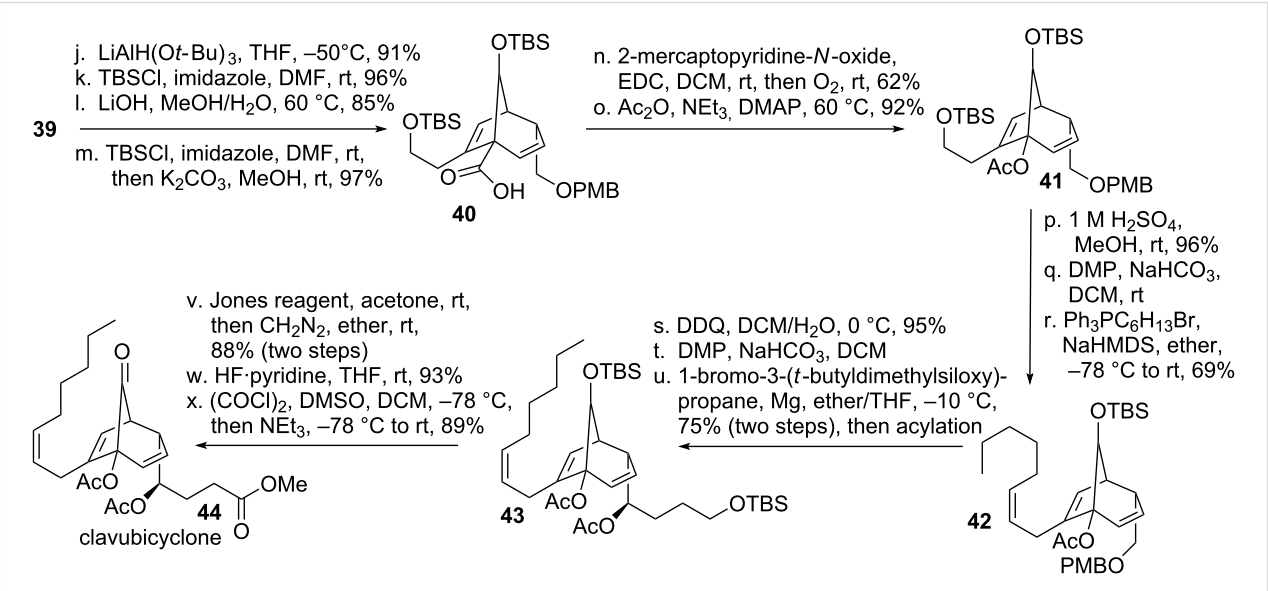
Fatty acid metabolites

Iguchi and co-workers [44] applied the DVCPR to the total synthesis of the marine prostanoid clavubicyclone [45]. Known aldehyde **33** (see Scheme 7) [46] was subjected to Wittig conditions to furnish an intermediate lactone, which was then opened reductively followed by selective oxidation of the allylic alcohol to yield aldehyde **34**. Addition of double deprotonated methyl acetoacetate gave β-ketoester **35**. Diazotransfer followed by double protection resulted in the formation of compound **36**. Rh-catalyzed intramolecular cyclopropanation of this compound gave bicycle **37**. Selective removal of the secondary protected alcohol through β-elimination yielded *trans*-divinylcyclopropane **38**, which underwent DVCPR under forcing conditions after *trans*-*cis*-isomerization to obtain the desired bridged bicycle **39**.

Reduction of ketone **39** (see Scheme 8) introduced a new stereocenter (10:1 selectivity), which was not assigned. The resulting major alcohol was protected, followed by saponifica-



Scheme 7: Iguchi's total synthesis of clavubicyclone, part 1.



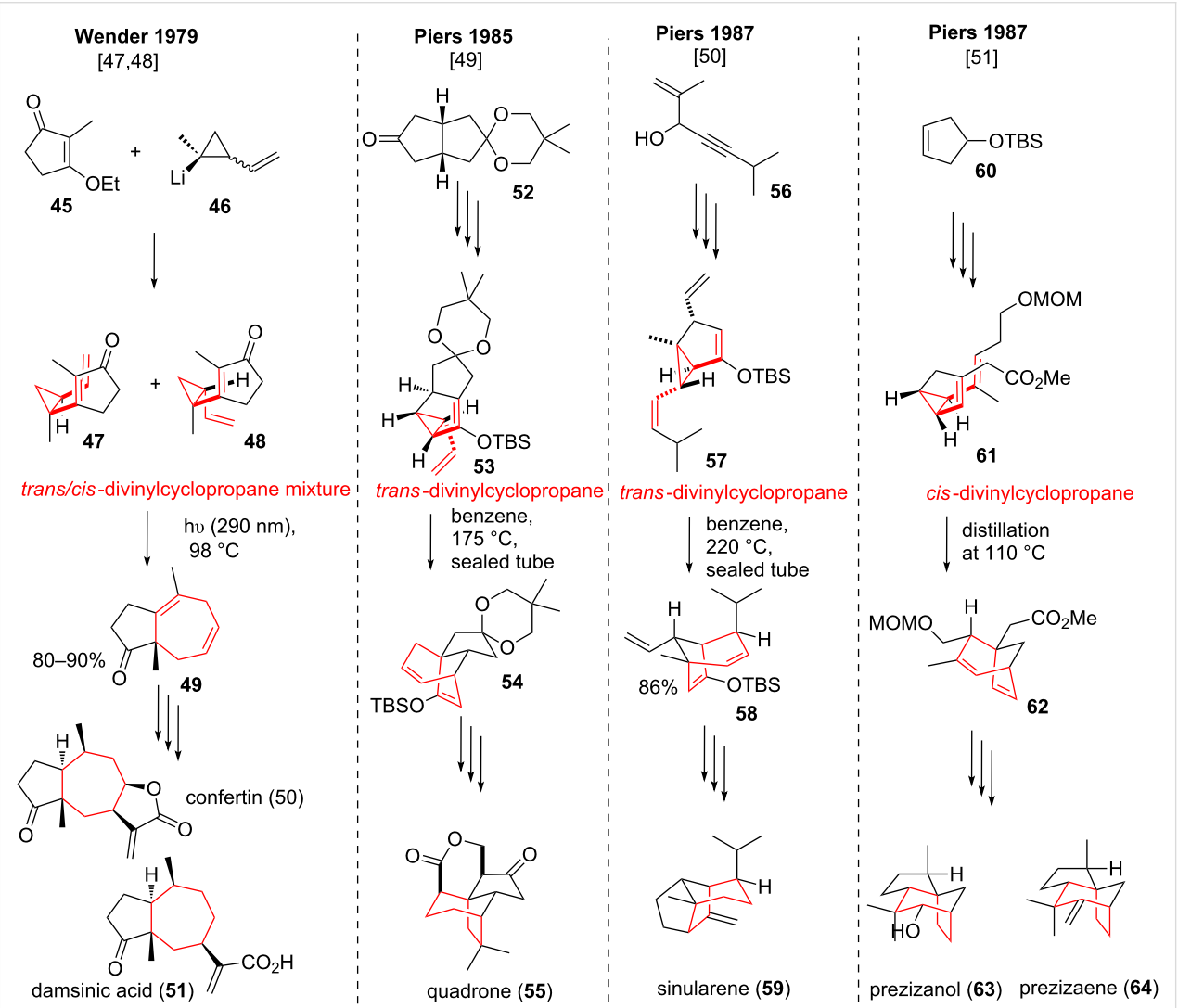
Scheme 8: Iguchi's total synthesis of clavubicyclone, part 2.

tion of the ester with concomitant removal of the TBDPS-protecting group. The resulting free alcohol was then re-protected to give bicycle **40**. Barton decarboxylation was then achieved using standard conditions, followed by trapping of the resulting carbon-centered radical with oxygen. The resulting tertiary alcohol was then protected to give acetate **41**. Standard functional group interconversions led to the formation of the remaining side chain using Wittig-conditions to afford olefin **42**. Another series of standard functional group interconversions furnished diacetate **43**, which could be converted to the desired natural product **44** using a three step sequence.

Terpenoid targets

The group of Wender applied the DVCPR in their total syntheses of (±)-confertin (**50**) and (±)-damsinic acid (**51**) [47]. A mixture a *trans*/*cis*-vinylcyclopropyllithium **46** (see Scheme 9) [48] was added to ketone **45** followed by elimination to give a mixture of *trans*/*cis*-divinylcyclopropanes **47**/**48**. Photoepimerization at the temperature required for *cis*-DVCPR (98 °C, *trans*-DVCPR occurred above 140 °C) gave bicyclic **49** in good yields. (±)-Confertin (**50**) and (±)-damsinic acid (**51**) could be accessed after 10 or 7 steps respectively.

Piers and co-workers were the first to examine the DVCPR as a key step in the formal synthesis of (±)-quadrone (**55**, see Scheme 9) [49], and the total syntheses of sinularene (**59**) [50], prezizanol (**63**) and prezizaene (**64**) [51]. The synthesis of the cytotoxic sesquiterpenoid quadrone (**55**) from *Aspergillus terreus* [52,53] started from tricyclic ketone **52** [54], which was converted into tricycle **53** in 12 steps. *Trans*-divinylcyclo-



Scheme 9: Wender's syntheses of the two pseudoguainanes confertin (**50**) and damsinic acid (**51**) and Pier's approaches towards four sesquiterpenoid natural products using the DVCPR with both *trans*- and *cis*-divinylcyclopropanes. The yields for **53** to **54** and **61** to **62** are stated as yield over several steps (77% over three steps and 98% over two steps, respectively).

propane **53** underwent the desired DVCPR after *trans-cis*-isomerization of the vinyl moiety at 175 °C, forming bridged tetracycle **54**, which already contained the crucial seven-membered ring present in the target molecule **55**. Intermediate **54** was advanced in ten steps to provide an intermediate aldehyde, which had been previously converted to the natural product in seven steps [55-57].

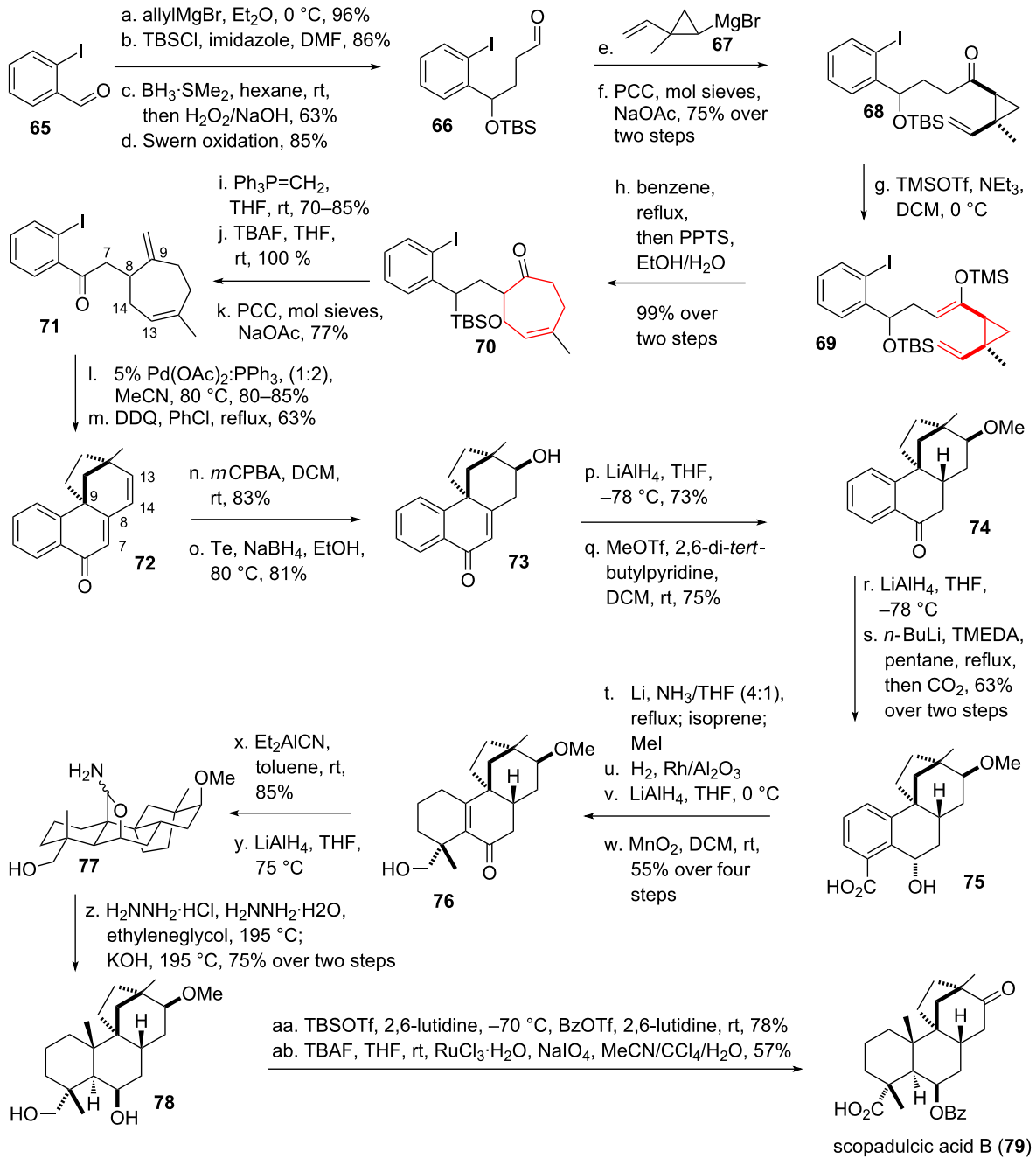
The total synthesis of the sesquiterpenoid sinularene (**59**) from the coral *Sinularia mayi* [58] started from alcohol **56**, which was converted to bicyclic **57** in nine steps. *Trans*-divinylcyclopropane **57** was then subjected to high temperature DVCPR conditions furnishing bridged bicycle **58**. *Trans-cis* isomerization of the vinyl moiety had to take place prior to the rearrangement to access the required boat transition state of the rearrangement. Intermediate **58** was converted to the natural product **59** in four additional steps.

Two other sesquiterpenoids, prezizaene (**63**) [59,60] and prezizanol (**64**) [60], isolated from *Eremophilia georgei* or vetiver oil were synthesized starting from cyclopentene derivative **60** [61]. This rather simple starting material was elaborated to advanced bicyclic **61** in only seven steps. This time the group of Piers used a *cis*-divinylcyclopropane, which underwent smooth DVCPR during distillation at 110 °C to yield bridged bicycle **62**. The desired natural products **63**/**64** were obtained after another ten or eleven steps respectively. For more "classic" applications of the DVCPR in total synthesis see reference [5].

Overman and coworkers [62-65] successfully applied the DVCPR as the key step in their total synthesis of the diterpene scopadulcic acid B (**79**, see Scheme 10), isolated from the Paraguayan plant *Scoparia dulcis* [66]. Starting from 2-iodobenzaldehyde (**65**) allyl-Grignard addition took place followed by TBS-protection of the resulting alcohol. The installed double bond was subjected to hydroboration/oxidation, followed by Swern oxidation of the resulting alcohol to yield aldehyde **66**. Addition of cyclopropyl-Grignard reagent **67** [67,68], followed by oxidation to the corresponding ketone yielded vinylcyclopropane **68**. Deprotonation and TMS-protection furnished silyl-enolether **69**, which underwent the desired DVCPR in almost quantitative yield at elevated temperature, followed by removal of the silyl-protecting group under acidic conditions to furnish cycloheptenone **70**. Standard functional group interconversion furnished diolefin **71**. Subjection of this compound to Heck coupling conditions resulted in in the formation of a bridged tetracycle after initial Heck coupling followed by carbo-palladation and subsequent β-hydride elimination [69-71]. Double bond regioisomers (between C7 & C8 or C13 & C14) were obtained. Oxidation with DDQ yielded the 1,6-unsaturated ketone **72**. Selective epoxidation followed by reductive epoxide opening furnished the desired alcohol **73** [72]. Alcohol-directed 1,4-reduction using $LiAlH_4$ [73] followed by ether formation gave methyl ether **74**. Reduction of the remaining ketone moiety gave the equatorial alcohol exclusively. Ortho-lithiation followed by the addition of carbon dioxide [74,75] resulted in the formation of carboxylic acid **75**. Birch reduction with concomitant methylation [76,77] followed by selective hydrogenation and reduction of the carboxylic acid resulted in the formation of alcohol **76**. Installation of the remaining quaternary carbon center was achieved by the conjugate addition of cyanide [78]. Reduction of the newly introduced nitrile yielded the unexpected stable pentacycle **77**. Formation of the missing methyl group (compound **78**) could be achieved using forcing Wolff–Kishner-conditions. Benzoate formation and global oxidation [79,80] finally furnished scopadulcic acid B (**79**). A similar approach was used by the same group in their total synthesis of scopadulcic acid A [81].

Davies and coworkers [82] utilized the DVCPR embedded in a formal [4 + 3]-cycloaddition [83] in the total syntheses of the related sesquiterpene metabolites tremulenolide A (**88**, see Scheme 11) and tremulenediol A (**89**), isolated from a fungal pathogen [84]. Horner–Wadsworth–Emmons olefination of the starting ketone **80** [85] provided an *E*/*Z*-mixture of α,β-unsaturated ester **81**. Deprotonation followed by an acidic quench resulted in deconjugation to give β,γ-unsaturated ester **82**. Diazotransfer using *p*-ABSA [86] yielded diazoester **83**. Selective rhodium-catalyzed cyclopropanation of the *cis*-double bond [87,88] of diene **84** [89] furnished *cis*-divinylcyclopropane **85**, which underwent DVCPR upon Kugelrohr distillation at 140 °C to give bicyclic **86**. Selective hydrogenation of the less substituted double bond using Wilkinson's catalyst [90] gave α,β-unsaturated ester **87**. Removal of the acetate protecting group with concomitant lactonization concluded the total synthesis of tremulenolide A (**88**), whereas global reduction resulted in the formation of tremulenediol A (**89**).

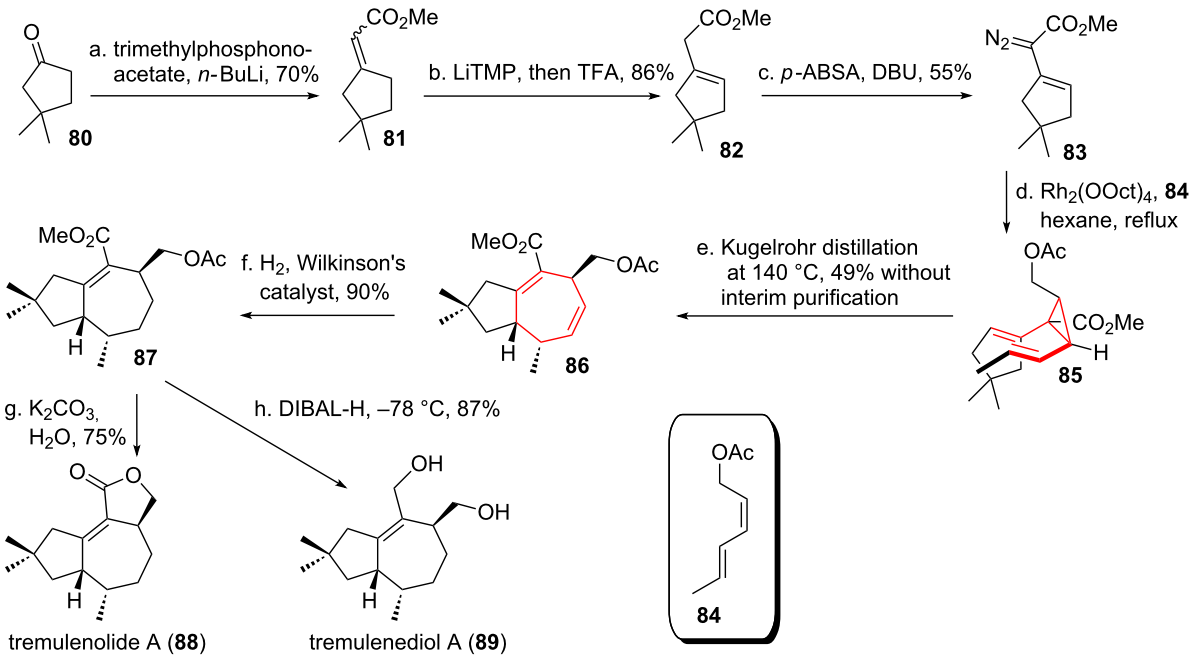
Davies and co-worker [91,92] investigated the formal synthesis of the sequiterpene-hydroquinone derivative frondosin B (**99**, see Scheme 12) [93] via an enantioselective cyclopropanation of *trans*-piperylene and subsequent divinylcyclopropane rearrangement, to further demonstrate the versatility of their formal [4 + 3] cycloaddition [82]. Starting from 4-methoxyphenol (**90**) Friedel–Crafts acylation and cyclization provided bicycle **91**. Wittig olefination furnished benzofuran **92**. Diazotransfer using *p*-ABSA yielded the crucial diazo compound **93**, which was used in the following enantioselective cyclopropanation with the lesser substituted double bond of piperylene under Rh_2(*R*-DOSP)$_4$ catalysis. *Cis*-divinylcyclopropane intermediate **94** underwent in situ DVCPR under the reaction conditions, and rearomatization of the benzofuran moiety provided **95**. Reduc-



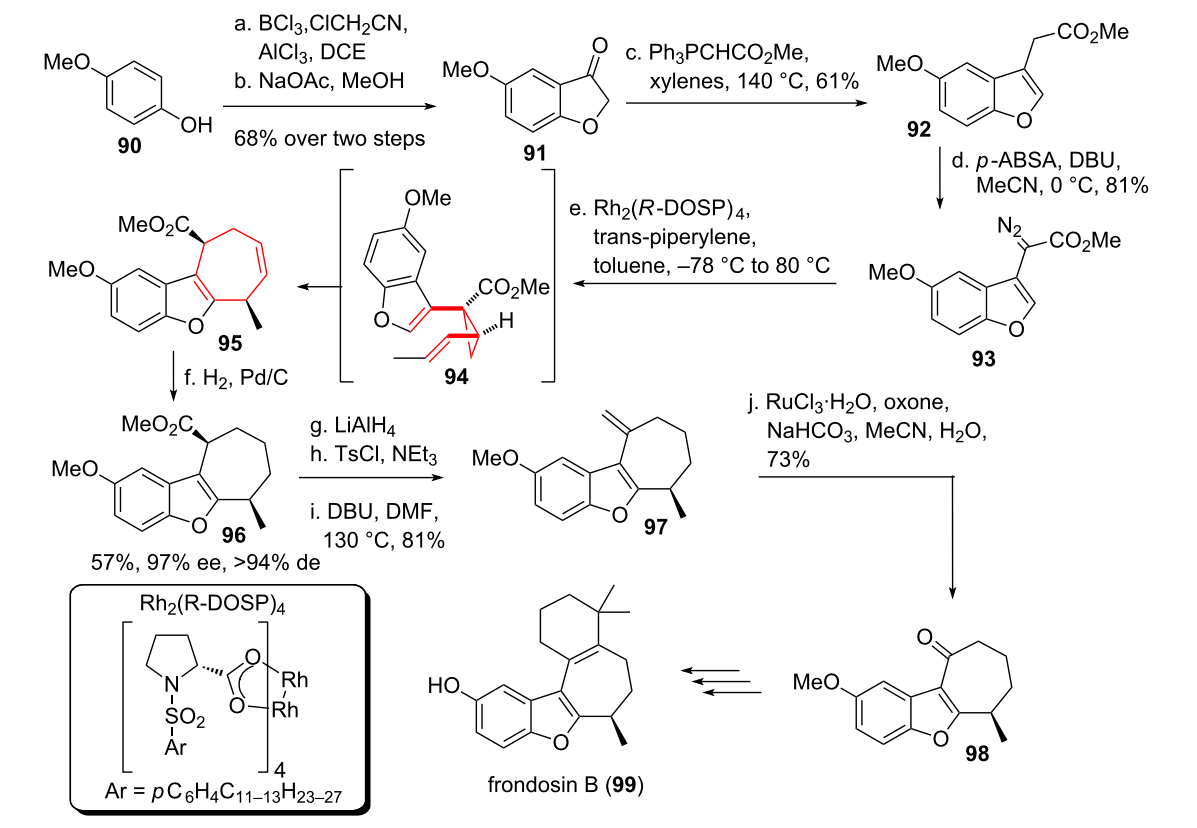
Scheme 10: Overman's total synthesis of scopadulcic acid B.

tion of the less hindered double bond yielded tricycle **96**, for which the yield and enantioselectivity was determined starting from **93**. Standard functional group interconversion first provided *exo*-methylene **97**, followed by ruthenium-catalyzed oxidative cleavage of the installed *exo*-methylene moiety [94] to give tricyclic ketone **98**, which can be converted to frondosin B (**99**) in three steps according to Danishefsky and co-workers [95,96].

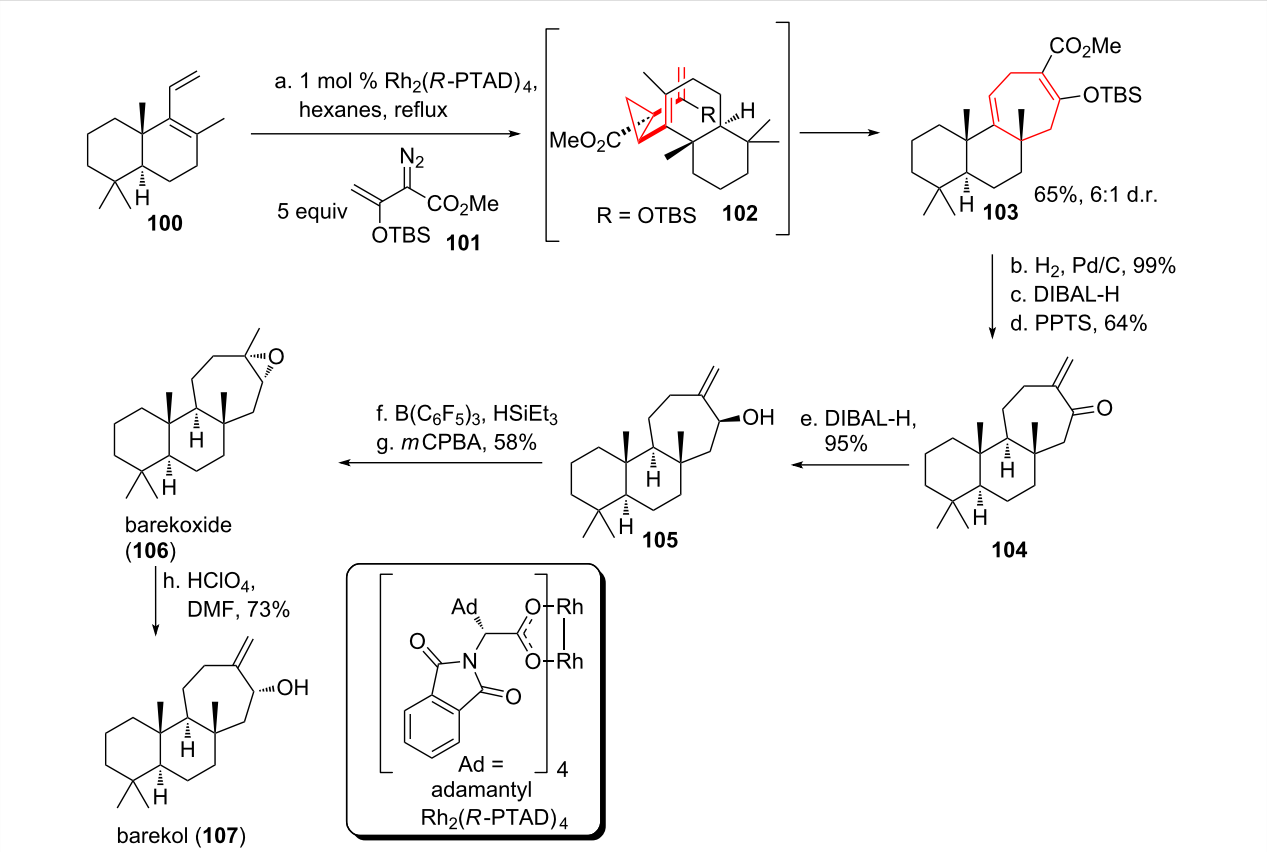
The groups of Davies and Sarpong [97] teamed up for the total syntheses of the diterpenoids barekoxide (**106**, see Scheme 13) [98] and barekol (**107**) [99], isolated from the sponges *Chelonaplysilla erecta* and *Raspailia sp.* They envisioned a formal [4 + 3]-cycloaddition with an intermediate DVCPR [82]. Starting from diene **100,** enantioselective cyclopropanation catalyzed by Rh_2(*R*-PTAD)$_4$ took place using vinyldiazo compound **101** to form *cis*-dinvinylcyclopropane intermediate **102**.



Scheme 11: Davies' total syntheses of tremulenolide A and tremulenediol A.



Scheme 12: Davies formal [4 + 3] cycloaddition approach towards the formal synthesis of frondosin B.

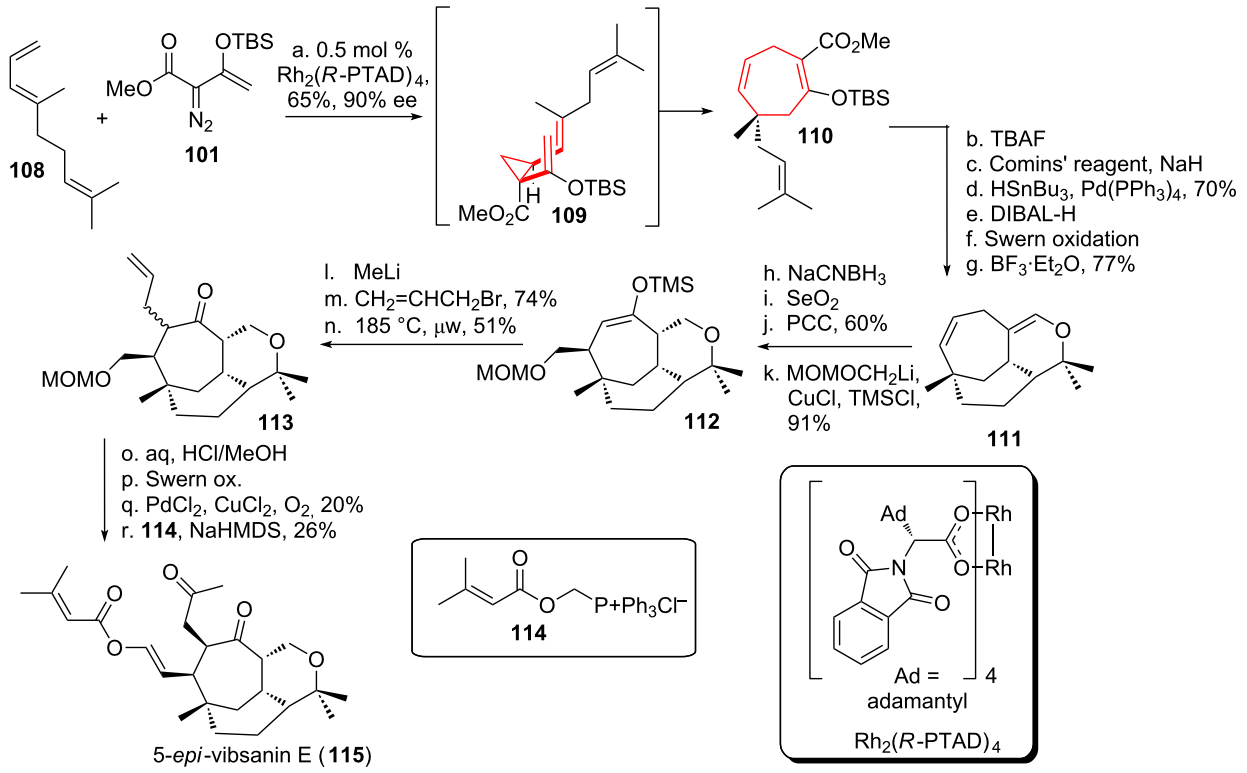


Scheme 13: Davies and Sarpongs formal [4 + 3]-cycloaddition approach towards barekoxide (**106**) and barekol (**107**), involving a DVCPR.

Rearrangement yielded tricycle **103** in both good yield and good diastereomeric ratio. Selective hydrogenation of the more electron rich double bond followed by reduction of the ester furnished α,β-unsaturated ketone **104** after PPTS-catalyzed elimination of water. Subsequent DIBAL-H reduction yielded the alcohol epimer **105** of barekol (**107**). Deoxygenation with concomitant isomerization of the double bond according to Gevorgyan [100] was followed by epoxidation to provide barekoxide (**106**). Acid-catalyzed isomerization finally yielded barekol (**107**).

Davies and coworkers [101-103] used the formal [4 + 3]-cycloaddition approach to access the diterpene 5-*epi*-vibsanin E (**115**), from the plant *Viburnum awabuki* (see Scheme 14) [104]. Starting from triene **108** cyclopropanation was achieved using vinyldiazo compound **101**. The fomal [4 + 3]-cycloaddition proceeded through *cis*-divinylcyclopropane **109** to yield rearranged cycloheptadiene **110**. Desilylation was achieved using TBAF, followed by formation of a vinyl triflate and Stille coupling with tributyltin hydride. The oxidation state of the remaining ester was adjusted to the corresponding aldehyde, followed by a Lewis acid-catalyzed intramolecular inverse-electron-demand hetero-Diels–Alder reaction to give tricycle **111**. The enol ether moiety was reduced using $NaCNBH_3$, followed by allylic Riley oxidation and PCC-mediated enone formation. Copper-catalyzed conjugate addition in the presence of TMSCl [105] yielded silyl enol ether **112**. Subsequent introduction of the side chain in **113** via a Claisen rearrangement was followed by MOM-cleavage. Oxidation furnished an intermediate aldehyde, followed by Wacker oxidation and the Anders–Gaßner variant [106-109] of the Wittig reaction to furnish 5-*epi*-vibsanin E (**115**).

Echavarren and coworkers [110] used a DVCPR to target the sesquiterpenoid schisanwilsonene A (**126**, see Scheme 15), isolated from *Schisandra wilsoniana* [111], a plant used in traditional chinese medicine. Submission of 1,6-enyne **116** to cationic gold-catalyst **117** led to 5-*exo-dig* cyclization and intermediate formation of bridged bicycle **119**. Subsequent 1,5-acyl-shift afforded vinylcarbenoid **120**, which underwent cyclopropanation with the added olefin **118** to give bicycle **121** in decent yield. Double deprotection followed by selective acetal-protection of the less hindered alcohol and oxidation of the remaining unprotected alcohol moiety led to aldehyde **122**. Wittig olefination resulted in the formation of non-isolated *cis*-divinylcyclopropane **123**, which immediately underwent DVCPR to give



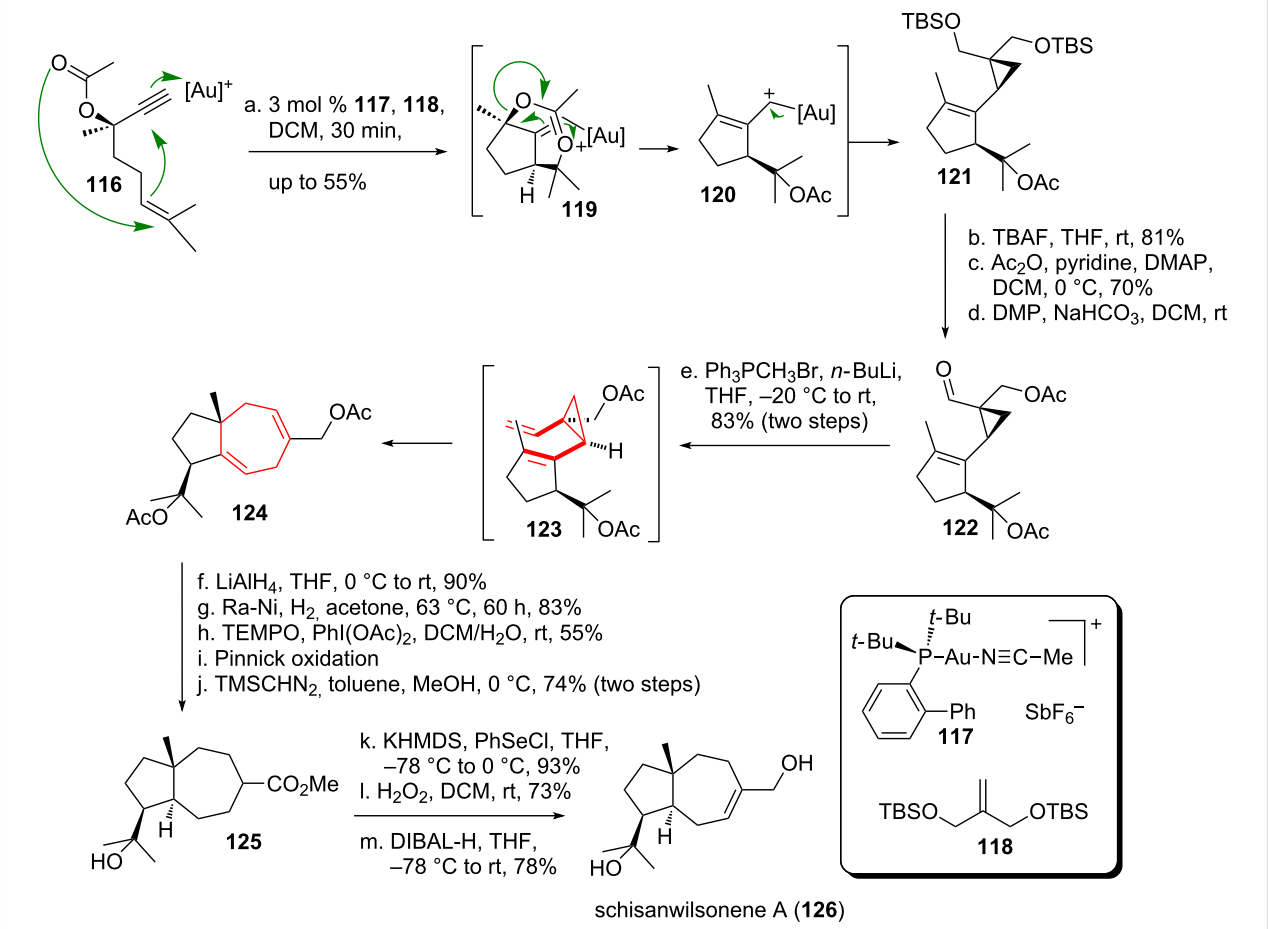
Scheme 14: Davies formal [4 + 3]-cycloaddition approach to 5-*epi*-vibsanin E (**115**) containing an intermediate *cis*-divinylcyclopropane and the corresponding DVCPR.

124 at ambient temperature. Ester **125** was obtained using standard functional group interconversions. The desired natural product schisanwilsonene A (**126**) was obtained after selective formation of the less hindered α,β-unsaturated ester and subsequent reduction.

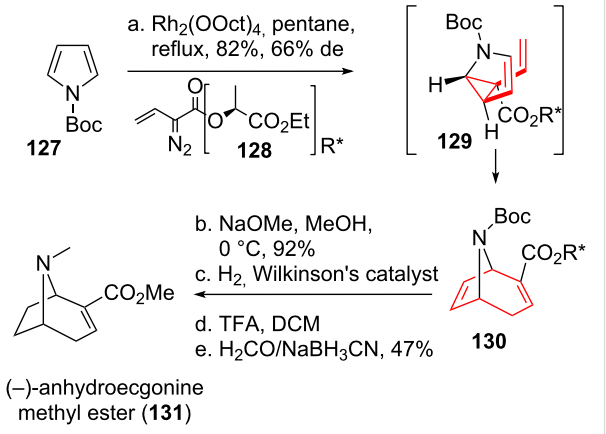
Alkaloid targets

Davies and co-worker [112] were the first to apply the DVCPR to the total synthesis of alkaloids. Anhydroecgonine methyl ester (**131**, see Scheme 16) is a tropane alkaloid structurally related to cocaine, which can be detected in the human body after cocaine consumption. It can be degradatively accessed from cocaine through pyrolysis, cocaine congeners can be prepared via conjugate addition afterwards [113,114]. Boc-protected pyrrole **127** was subjected to rhodium-catalyzed cyclopropanation with vinyldiazo compound **128** [115,116], bearing a chiral auxiliary [117]. The intermediate *cis*-divinylcyclopropane **129** rearranged to the corresponding bridged cycloheptadiene **130** in a DVCPR. The chiral auxiliary was removed in the following using methanolysis conditions, followed by reduction of the more electron rich double bond and reductive amination after Boc-deprotection to yield the desired natural product **131** in only five steps.

Perhaps one of the most prominent alkaloid syntheses using a DVCPR was carried out by Fukuyama and coworker [118-120] and targeted gelsemine (**146**, see Scheme 17 and Scheme 18), an alkaloid with a unique hexacyclic cage structure isolated from *Gelsemium Sempervirens* [121,122]. Starting from methyl acetoacetate (**132**), double deprotonation and addition of the more reactive anion to sorbal aldehyde furnished the corresponding alcohol, which was immediately protected as its acetal **133** using ethyl vinyl ether. The necessary diazo moiety was installed using tosylazide as a diazo-transfer reagent to yield **134**. Copper catalyzed intramolecular cyclopropanation furnished bicycle **135**. Reduction of the carbonyl moiety and protection of the resulting alcohol was followed by ether cleavage and ozonolysis to give aldehyde **136** [123]. Knoevenagel condensation with 4-iodooxindole was achieved in the next step. Pfitzner–Moffatt oxidation [124] followed by elimination furnished *trans*-divinylcycloproane **137**. Submission of this compound to elevated temperature initiated a very smooth DVCPR yielding bicycle **138**. The temperature for the predecessing *trans-cis* divinylcyclopropane isomerization was unusually low. This can be rationalized by the substitution of the divinylcyclopropane with two electron withdrawing groups and the resulting stabilization of the intermediate(s).



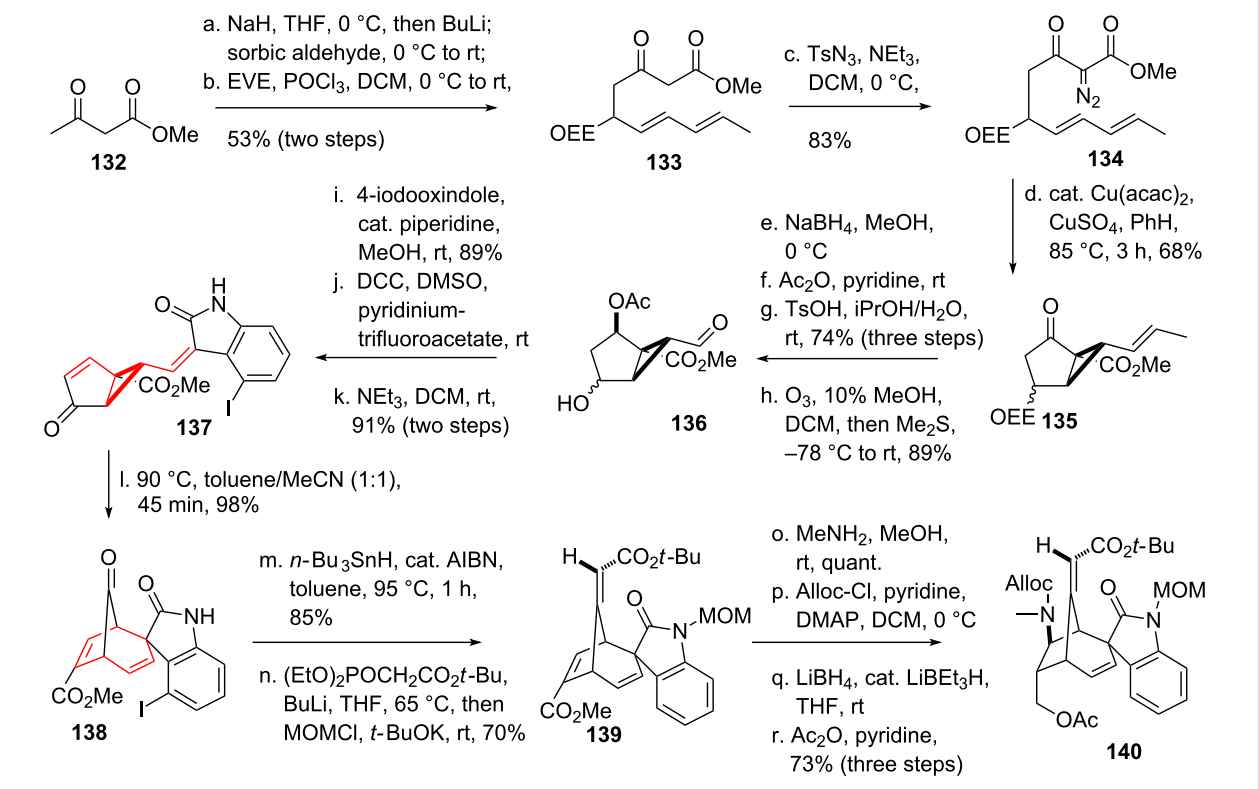
Scheme 15: Echavarren's total synthesis of schisanwilsonene A (**126**) featuring an impressive gold-catalzed cascade reaction and a DVCPR.



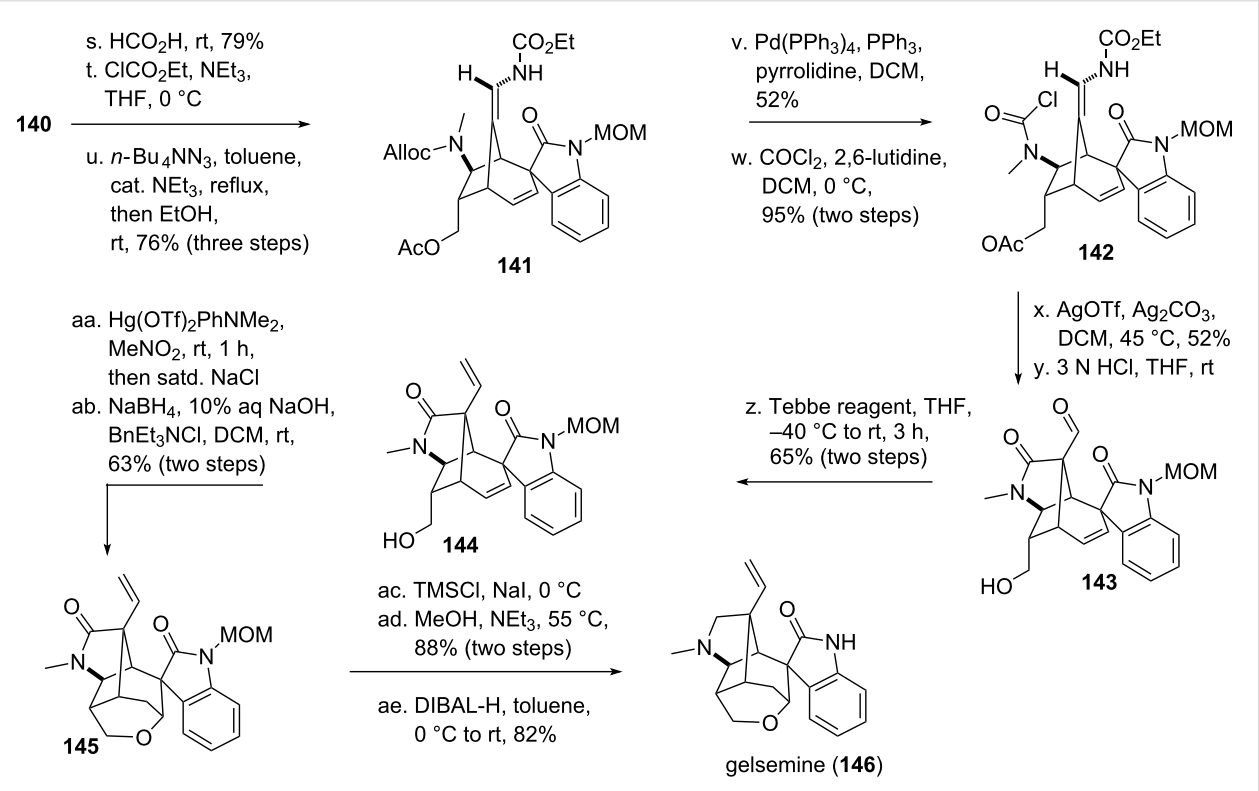
Scheme 16: Davies early example of a formal [4 + 3]-cycloaddition in alkaloids synthesis.

The surplus iodine at the oxindole was crucial for the stereochemical control of the spiro-indolinone system in **138**, it was removed in the next step using radical conditions. Horner–Wadsworth–Emmons olefination on the carbonyl moiety followed by protection of the oxindole gave intermediate **139**. Conjugate addition of methylamine and protection of the amine was followed by selective reduction of the methyl ester [125]. Protection of the resulting alcohol gave tetracycle **140**.

The remaining ester **140** (see Scheme 18) was then converted to the corresponding acid, followed by anhydride formation. Introduction of an acyl azide resulted in a Curtius rearrangement, upon heating the intermediate isocyanate was trapped with EtOH to yield ethyl carbamate protected amine **141**. Deprotection of the Alloc-group [126] and chloro carbamate formation furnished **142**. Exposure of this compound to a silver source led to the formation of the five-membered lactam, together with an acylimine. This was removed under acidic conditions to furnish aldehyde **143**. Tebbe olefination [127] installed the missing double bond in **144**. Oxymercuration [128] followed by reductive biphasic demercurization [129] furnished the remaining tetrahydropyran ring, yielding **145**. Removal of the MOM-protecting group followed by reduction of the amide concluded Fukuyama's total synthesis of gelsemine (**146**).



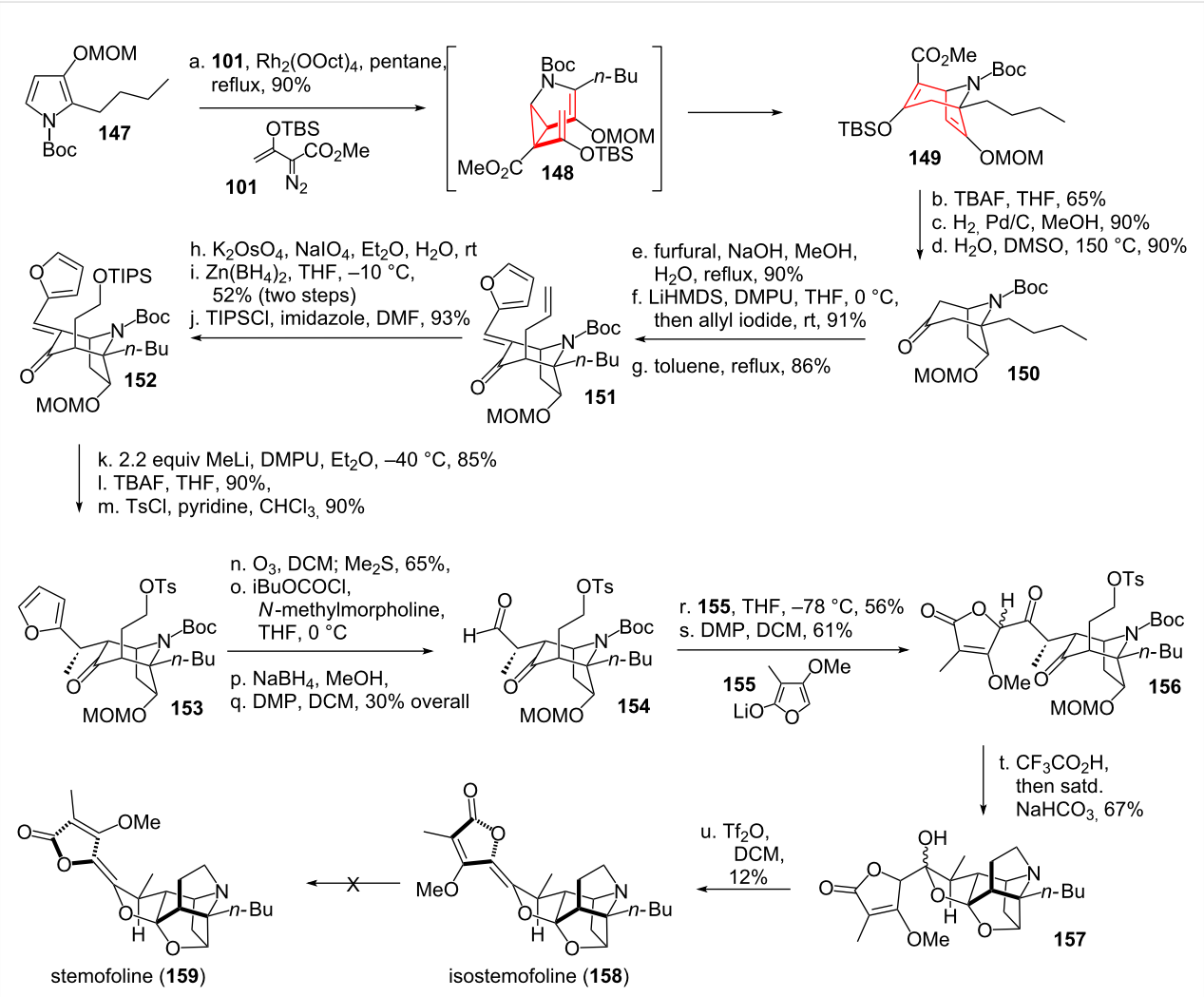
Scheme 17: Fukuyama's total synthesis of gelsemine, part 1.



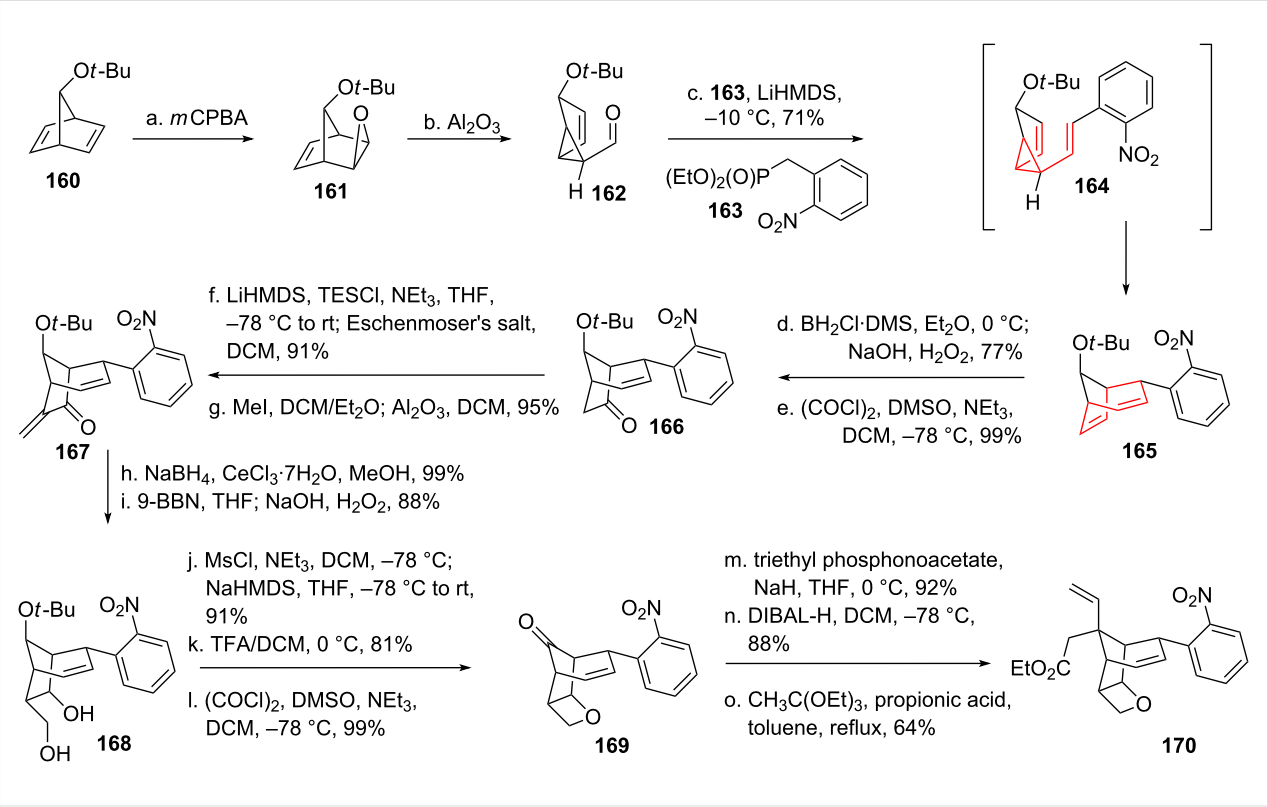
Scheme 18: Fukuyama's total synthesis of gelsemine, featuring a divinylcyclopropane rearrangement, part 2.

An approach similar to Davies formal [4 + 3]-cycloaddition [81] was used by the group of Kende [130] to access the alkaloid isostemofoline (**158**, see Scheme 19) [131]. Rhodium-catalyzed cyclopropanation of silyl-enol-diazo compound **101** and Boc-protected pyrrole **147** resulted in the formation of intermediate *cis*-divinylcyclopropane **148**, that rearranged under the reaction conditions to give the corresponding highly substituted bridged cycloheptadiene **149**. Deprotection of the enolate, reduction of the remaining double bond and subsequent Krapcho decarboxylation [132] resulted in less functionalized ketone **150**. Aldol condensation with furfural followed by *O*-allylation and Claisen rearrangement furnished enone **151**. Standard functional group interconversiones were used to access TIPS-protected alcohol **152**. Addition of methyllithium at low temperature [133] resulted in stereoselective conjugate attachment of the required methyl group. Deprotection of the alcohol and transformation into a suitable leaving group yielded tosylate **153**. Next, the furan was cleaved oxidatively, the resulting acid was converted to the corresponding anhydride, which could be reduced to the alcohol using $NaBH_4$, followed by reoxidation with DMP to yield aldehyde **154**. Attachment of furanone enolate **155** [134,135], followed by reoxidation yielded tricycle **156**. Deprotection of the amine and the MOM-protected alcohol led to a rearrangement cascade, which smoothly yielded hexacycle **157**. This compound could be converted into isostemofoline (**158**), albeit in low yield. Isostemofoline could not be interconverted into stemofoline (**159**) using trifluoroacetic acid [136].

Danishefsky and coworkers [137-139] applied the DVCPR in their total synthesis of gelsemine (**146**, see Scheme 20 and Scheme 21). Starting from bicycle **160** [140] epoxidation using *m*CPBA furnished epoxide **161** [141,142], which could be converted into vinylcyclopropanecarbaldehyde **162** upon



Scheme 19: Kende's total synthesis of isostemofoline, using a formal [4 + 3]-cycloaddition, including an intermediate DVCPR.

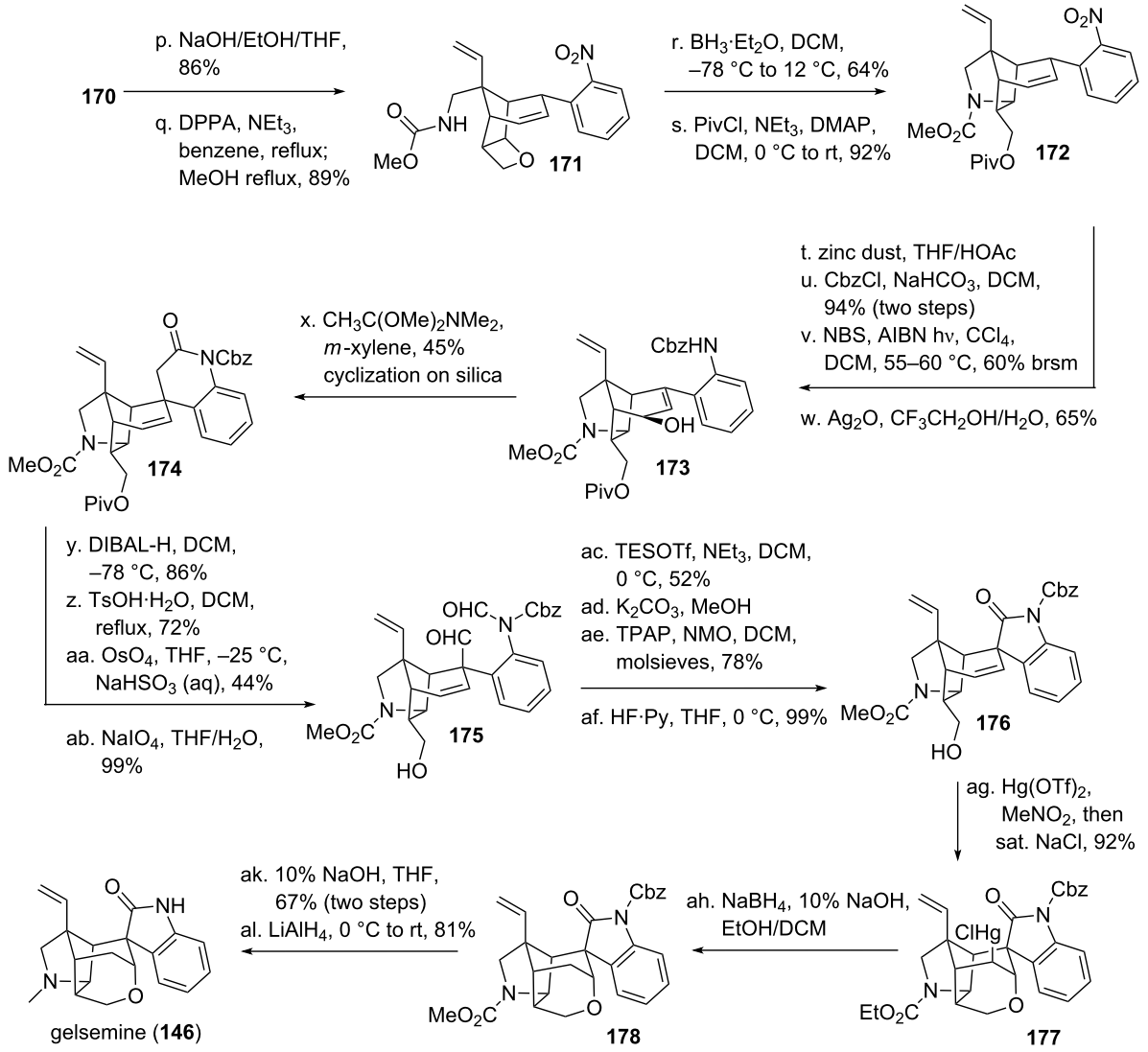


Scheme 20: Danishefsky's total synthesis of gelsemine, part 1.

rearrangement. Olefination using HWE-reagent **163** yielded intermediate *cis*-divinylcyclopropane **164**, which underwent the desired rearrangement at remarkably low temperature to yield bicycle **165**. Selective hydroboration/oxidation (directed through participation of the untouched double bond) followed by Swern oxidation gave ketone **166**. The enone system **167** was prepared through addition of Eschenmoser's salt, followed by Hoffman elimination of the resulting amine. Luche reduction [143] from the less hindered side followed by hydroboration/oxidation gave diol **168**. Mono-mesylation of the primary alcohol followed by the addition of base furnished the signature oxetane moiety. Ether cleavage [144] and Swern oxidation resulted in the formation of ketone **169**. HWE-olefination followed by reduction to the allyl alcohol led to allylic ester **170** after a Johnson–Claisen rearrangement [145] upon treatment with triethyl orthoacetate.

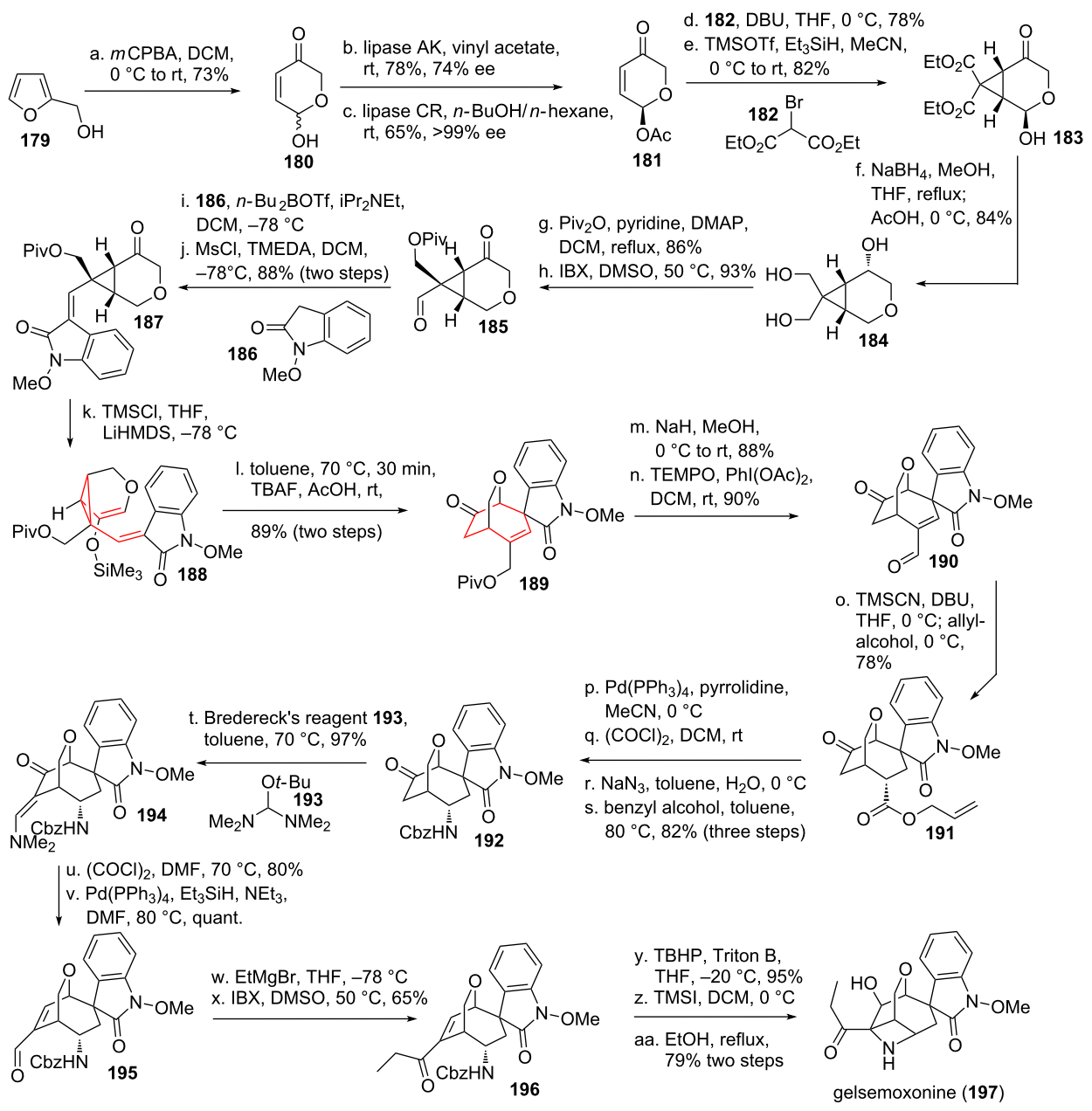
Ester **170** was saponificated (see Scheme 21), followed by the formation of an acid-azide. Shiori version [146,147] of the Curtius rearrangement with concomitant addition of MeOH to the intermediate isocyanate afforded carbamate **171**. Oxetane **171** was then opened under Lewis-acidic conditions. The deprotected alcohol was protected to give pentacycle **172**. Reduction of the nitro group was followed by Cbz-protection. Allylic alcohol **173** resulted from radical allylic bromination followed by displacement of bromine through water under silver-catalysis. Eschenmoser–Claisen rearrangement [148] led to the formation of the remaining quarternary carbon center, the resulting amide cyclized during the purification on silica to give amide **174**. Reduction of this amide to the aminal was followed by dehydration and Lemieux–Johnson [149] oxidative cleavage to give dialdehyde **175**. The liberated alcohol moiety was reprotected, followed by cleavage of the amide under basic conditions. Cyclization and Ley–Griffith oxidation [150] took place, followed by deprotection of the alcohol to give spiro-oxindole **176**. The formation of the remaining tetrahydropyran was much in line with Fukuyama's synthesis, utilizing the same oxymercuration/reductive demercurization [128,129] sequence (through intermediate **177**) yielding **178**. The oxindole protecting group was then removed, followed by reduction of the carbamate to the remaining missing methyl group [151] to finish gelsemine (**146**).

The total synthesis of the monoterpenoid-indole alkaloid gelsemoxonine (**197**, see Scheme 22) [152], isolated from the leaves of *Gelsemium elegans* was accomplished by Fukuyama and coworkers [153,154]. Starting from furfuryl alcohol (**179**) an epoxide initiated Achmatowicz reaction [155] took place to give α,β-unsaturated pyrane **180**. Next in line was an enzyme catalyzed dynamic kinetic resolution [156], albeit with unsatis-



Scheme 21: Danishefsky's total synthesis of gelsemine, part 2.

factory enantiomeric excess. The undesired enantiomer was then selectively cleaved using another enzyme with reversed selectivity to give enantiopure pyranone **181**. Cyclopropanation was achieved using a Michael addition initiated ring closure yielding diester **183**. Complete reduction furnished triol **184**, followed by mono-protection of the least hindered alcohol. The remaining alcohol moieties were then oxidized to the corresponding keto-aldehyde **185**. A two-step procedure was employed to generate α,β-unsaturated oxindole-*N*-methoxide **187** [157,158]. Formation of silyl enol ether **188** furnished the desired *cis*-divinylcyclopropane, which underwent smooth DVCPR under mild conditions to give bridged bicycle **189**. The alcohol was deprotected and oxidized to aldehyde **190**. The aldehyde was transferred into the corresponding cyanohydrin trimethylsilyl ether using TMSCN [159-161], followed by protonation of the TMS-enolate and esterification of the intermediate acyl cyanide yielding allyl ester **191**. This ester was transferred into the corresponding carboxylic acid, followed by formation of the acid chloride. The chloride was displaced with an azide, which underwent Curtius rearrangement upon heating. The intermediate isocyanate was intercepted by benzyl alcohol to provide secondary Cbz-protected amine **192**. Bredereck's reagent (**193**) [162] was used to generate enamine **194**. The enol-form of the remaining carbonyl moiety was transformed into the corresponding vinyl chloride using Vielsmeier's reagent [163,164]. Dechlorination [165,166] was then achieved and yielded α,β-unsaturated aldehyde **195** upon hydrolysis. Grignard addition to the newly formed aldehyde followed by reoxidation furnished the side chain of compound **196**. Treatment of unsaturated ketone **196** with Triton B and TBHP



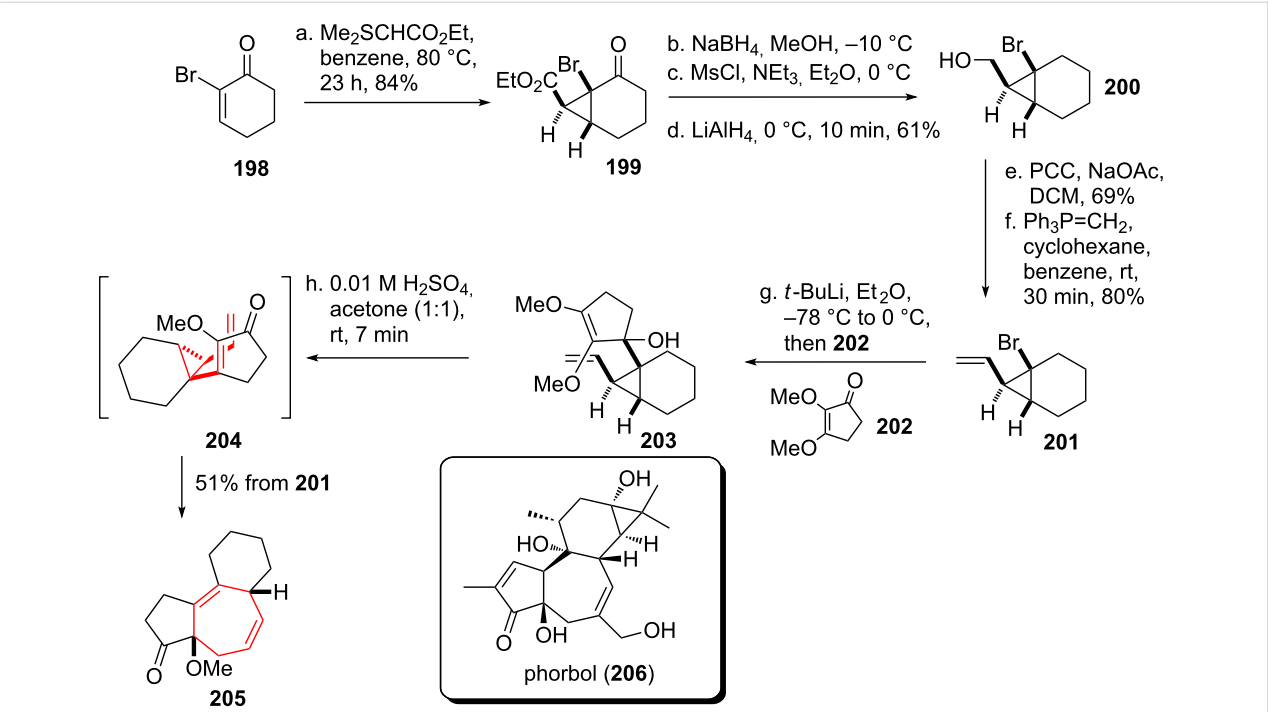
Scheme 22: Fukuyama's total synthesis of gelsemoxonine.

yielded the epoxide resulting from top-face attack. The surplus Cbz-group was then deprotected using TMSI [167,168]. The final azetidine formation took place upon refluxing in ethanol to give gelsemoxonine (**197**).

Further synthetic applications

The group of Wender applied the DVCPR in an approach towards the core skeleton of tiglianes (like phorbol **206**, see Scheme 23), daphnanes and ingenanes [169] in 1980 [170]. Starting from α-bromoenone **198** a Corey–Chaykovsky cyclopropanation reaction was achieved to yield cyclopropane **199**. The keto-group was removed using a three step sequence, with concomitant reduction of the ester to give alcohol **200**. Oxidation and Wittig olefination gave olefin **201**. Lithium bromide exchange followed by 1,2-addition to ketone **202** yielded tricyclic **203**, which was immediately subjected to acidic hydrolysis to give the desired tricyclic core skeleton **205** in 51% yield through transition state **204**.

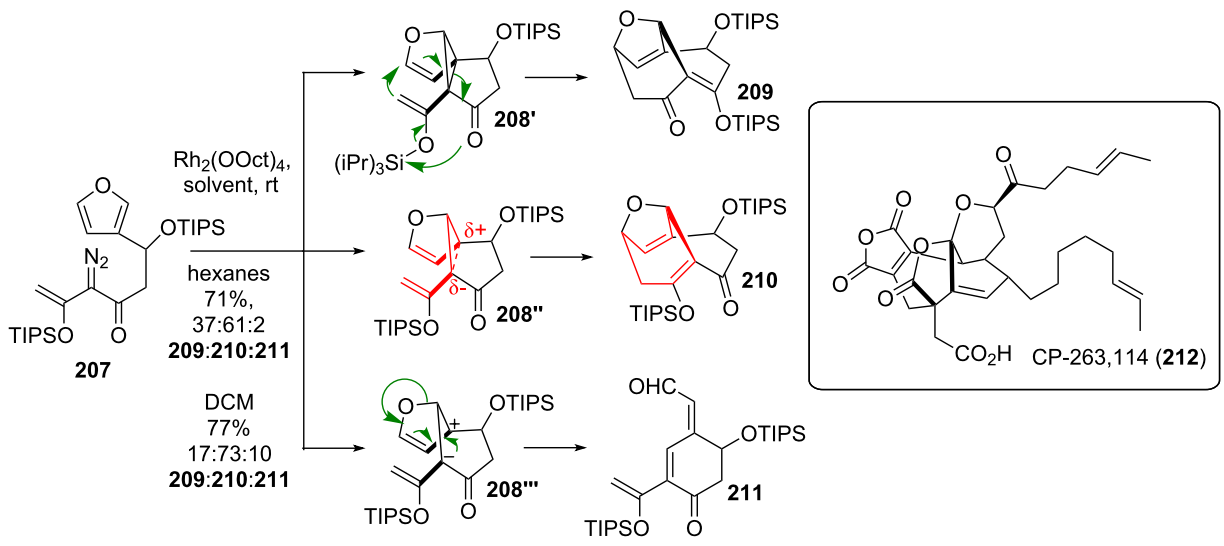
The group of Davies [171] demonstrated the impressive synthetic power of the DVCPR in their core structure synthesis of CP-263,114 (**212**, see Scheme 24) [172,173]. Subjection of



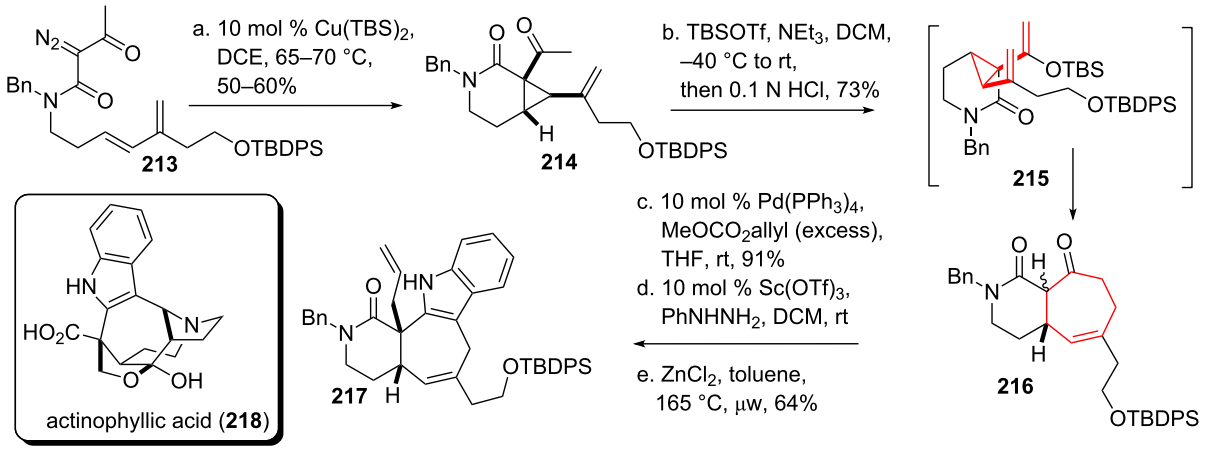
Scheme 23: Wender's synthetic access to the core skeleton of tiglianes, daphnanes and ingenanes.

diazofuran **207** to rhodium catalysis resulted in the formation of **209**, **210** and **211** in solvent-dependent ratios. The sole product arising from the desired DVCPR via **208''** is the major product **210**. The two remaining products arise from *trans*-silylation and fragmentation (**208'** to **209**) or via ionic intermediate **208'''** and fragmentation to give **211**. The different product distribution can be controlled by the choice of the solvent. Notably cycloheptadiene **210** arising from the DVCPR contains two as well as the related *trans*-silylated compound **209**. This demonstrates the huge driving force of the DVCPR, as two highly strained olefins are favoured over a cyclopropane-moiety.

Wood and coworkers [174] applied the DVCPR in the core structure synthesis of actinophyllic acid (**218**, see Scheme 25) [175]. Subjection of diazo compound **213** to copper catalysis yielded vinylcyclopropane **214**. Deprotonation and silyl ether



Scheme 24: Davies' approach towards the core skeleton of CP-263,114 (**212**).

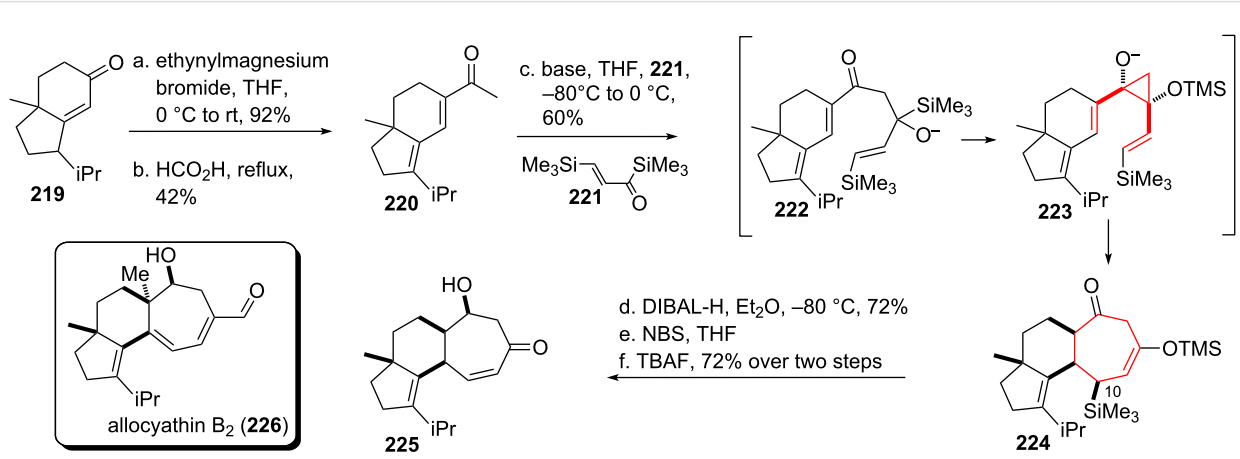


Scheme 25: Wood's approach towards actinophyllic acid.

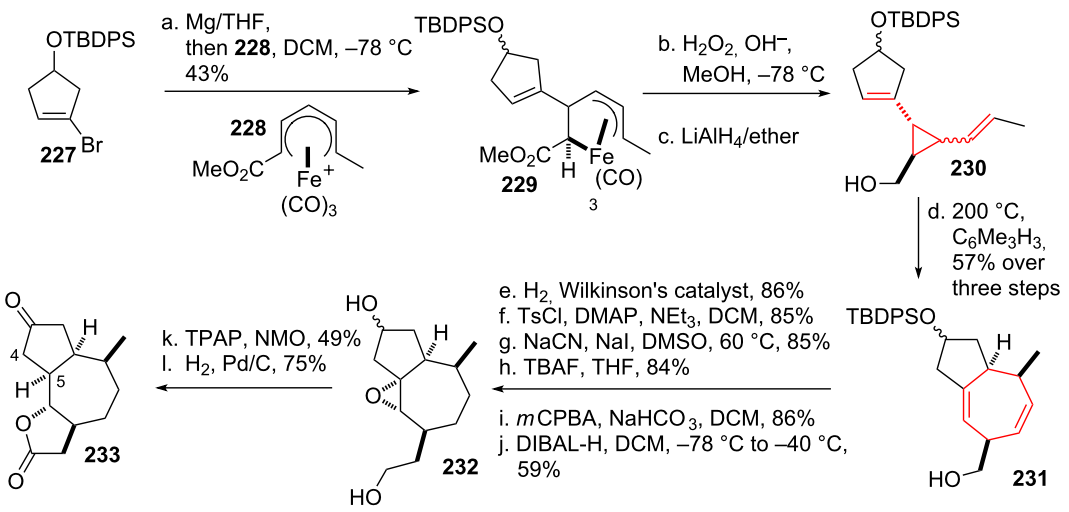
formation resulted in intermediate *cis*-divinylcyclopropane **215**, which smoothly underwent DVCPR to give cyclohexane **216**. Tsuji–Trost allylation [176,177] furnished the quartenary carbon center. A two-step Fischer-indole strategy [178,179] finished tetracycle **217** under forcing conditions.

Takeda and coworkers [180] set out to investigate the use of an anionic oxy-*cis*-divinylcyclopropane rearrangement to build up the diterpenoid cyanthin skeleton [181-183] like that of allocyathin B_2 (**226**, see Scheme 26), which was isolated from bird's nest fungi [184-189]. Starting from α,β-unsaturated ketone **219** addition of ethynylmagnesium bromide took place, followed by a Rupe rearrangement [190] using refluxing acetic acid as solvent to give ketone **220**. Addition of deprotonated ketone **220** onto acryloylsilane **221** [191] gave alkoxy intermediate **222**, which underwent a Brook rearrangement followed by cyclopropane formation to yield anionic **223** in situ [192]. The aforementioned anionic oxy-*cis*-divinylcyclopropane rearrangement took place, yielding tricycle **224**. DIBAL-H reduction gave the corresponding alcohol stereoselectivly, followed by removal of the TMS-group at C10 with NBS and further enone formation upon treatment with TBAF to give tricyclic core skeleton **225** [192]. This reaction sequence constitutes a very nice example of a formal [4 + 3]-cycloaddition, without the use of a transition metal catalyst.

Donaldson and coworkers [193] used the DVCPR en route towards the core skeleton of the sesquiterpenoid guianolide family [194,195]. Starting from readily prepared vinyl bromide **227** (see Scheme 27) formation of the corresponding Grignard species was acomplished, followed by addition to organoiron complex **228** to give (pentenediyl)iron complex **229**. Oxidation led to the formation of the desired divinylcyclopropane, followed by reduction of the ester to the desired alcohol to give



Scheme 26: Takeda's approach towards the skeleton of the cyanthins, utilitizing the divinylcyclopropane rearrangement in a [4 + 3] cycloaddition.



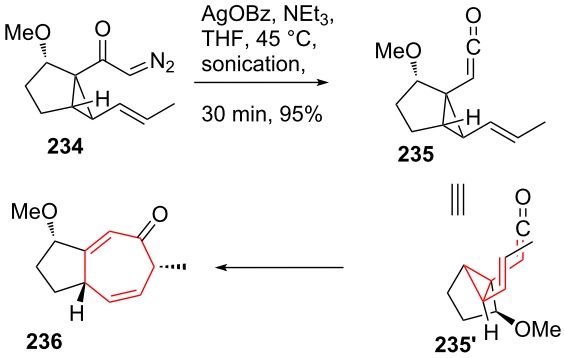
Scheme 27: Donaldson's organoiron route towards the guianolide skeleton.

compound **230**. Subjection of the *trans-cis*-divinylcyclopropane mixture to elevated temperature smoothly formed the desired bicycle **231**. The less hindered double bond was removed using Wilkinson's catalyst, followed by standard functional group interconversions to yield epoxide **232**. When this compound was subjected to oxidative conditions both alcohols were oxidized to the corresponding aldehyde/ketone. Base-induced epoxide opening led to the formation of a double bond (C4/C5) and concomitant lactol-formation. The lactol was oxidized to the corresponding lactone under the same reaction condition. Final reduction gave core skeleton **233**.

DVCPR in tandem reactions

The group of Stoltz [196,197] succeeded in establishing a tandem Wolff rearrangement/divinylcyclopropane rearrangement strategy [198]. Readily accessible α-diazo ketone **234** (see Scheme 28) was shown to undergo Wolff rearrangement [199] upon treatment with silver benzoate. The intermediate ketene **235** underwent stereospecific DVCPR through transition state **235'** under the reaction conditions to give enone **236** in excellent yield. This constituted the first example of the direct formation of an enone through a DVCPR.

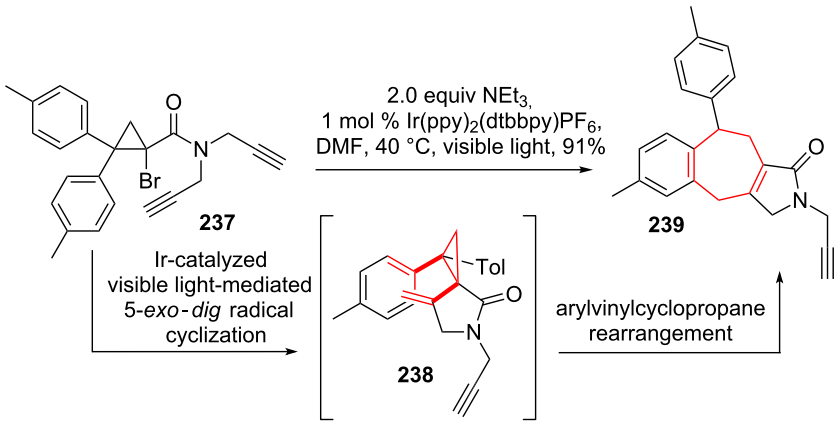
Stephenson and coworker [200] found an intriguing example of a light mediated radical cyclization/arylvinylcyclopropane rearrangement. Subjecting cyclopropyl bromide **237** to an Ir-polypyridyl catalyst and visible light initiated the desired photoredox cascade forming a cyclopropylradical, which readily cyclized in an 5-*exo*-*dig* fashion. Radical quenching gave *cis*-arylvinylcyclopropane **238**. Arylvinylcyclopropane rearrangement was followed by rearomatization to give tetracycle **239** (see Scheme 29).



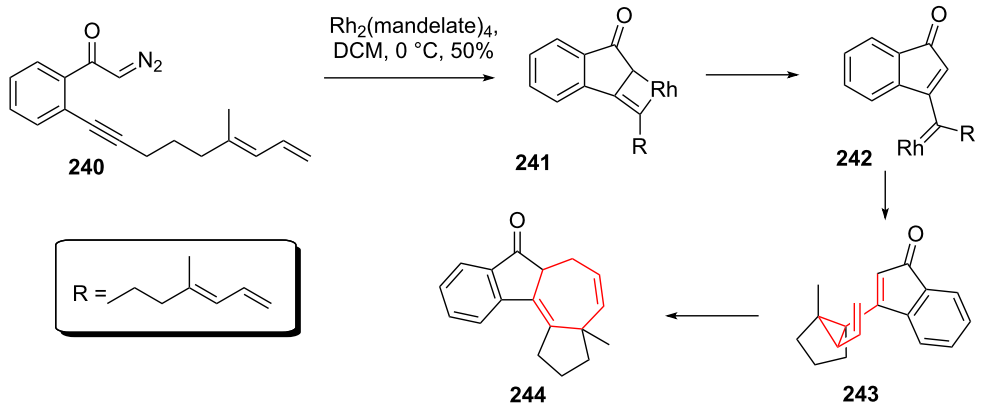
Scheme 28: Stoltz's tandem Wolff/DVCPR rearrangement.

Padwa and coworkers [201] discovered an intermediate DVCPR during their investigation of rhodium-catalyzed cyclizations of alkynyl substituted α-diazo ketones. Transition metal-catalyzed diazo-decomposition of compound **240** (see Scheme 30) resulted in the formation of metallacyclobutene **241**, followed by rapid metallacycloreversion to give carbenoid species **242**. Intramolecular cyclopropanation furnished divinylcyclopropane **243**, which underwent DVCPR under these conditions to give tetracycle **244** in 50% yield.

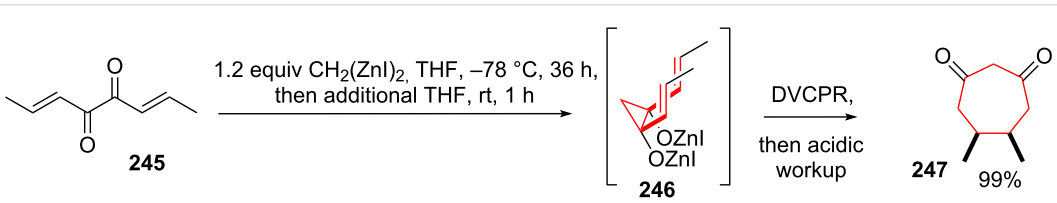
Matsubara and coworkers [202] investigated the formation of cyclohepta-1,3-diones from 1,2-diketone starting materials. Treatment of **245** with *bis*(iodozincio)methane resulted in the formation of *cis*-divinylcyclopropane **246** as the corresponding *bis*-zinc-enolate species. DVCPR occurred at ambient temperature, final acidic workup provided cycloheptadione **247** in excellent yield (see Scheme 31).



Scheme 29: Stephenson's tandem photocatalysis/arylvinylcyclopropane rearrangement.



Scheme 30: Padwa's rhodium cascade involving a DVCPR.

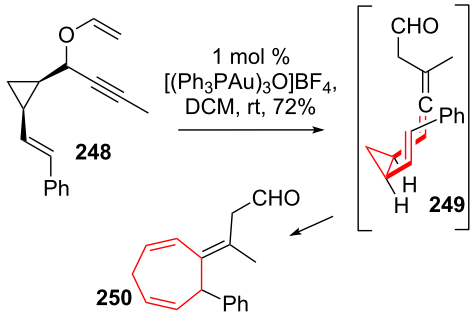


Scheme 31: Matsubara's version of a DVCPR.

Toste and coworkers [203] reported a tandem gold-catalyzed Claisen rearrangement from popargyl vinyl ether **248** (see Scheme 32) to give intermediate vinyl-allenecyclopropane **249**, followed by a DVCPR to furnish cycloheptadiene **250**.

1,2-Shift and vinyl-carbenoid formation sequences

Two major pathways to generate divinylcyclopropanes using transition metal catalysis have been developed. Uemura and coworkers [204] were the first to apply the transition metal catalyzed 1,2-acyl shift with subsequent vinyl carbenoid formation. Propargylic acetate **251** (see Scheme 33) has been shown to undergo 5-*exo*-*dig* cyclization via **252** to give zwitterionic intermediate **253.** A concomitant fragmentation reaction yielded vinyl-carbenoid **254**. Uemura and coworkers used this chemistry with propargylic acetate **255** to achieve cyclopropanation with various dienes, for example cyclopentadiene, to generate a *cis*/*trans*-mixture of divinylcyclopropanes **256**. Heating of this mixture of compounds resulted in the formation of bridged tricycle **257** in good yield. Toste and coworkers [205] discovered a 1,2-pivaloyl shift and cyclopropanation of the resulting



Scheme 32: Toste's tandem gold-catalyzed Claisen-rearrangement/DVCPR.

gold-carbenoid from **258** with enyne **259** to yield vinylalkynecyclopropane **260**. This compound was shown to undergo a gold catalyzed DVCPR to yield **261**. Note that this reaction does most likely proceed via a step wise mechanism and involves charged intermediates.

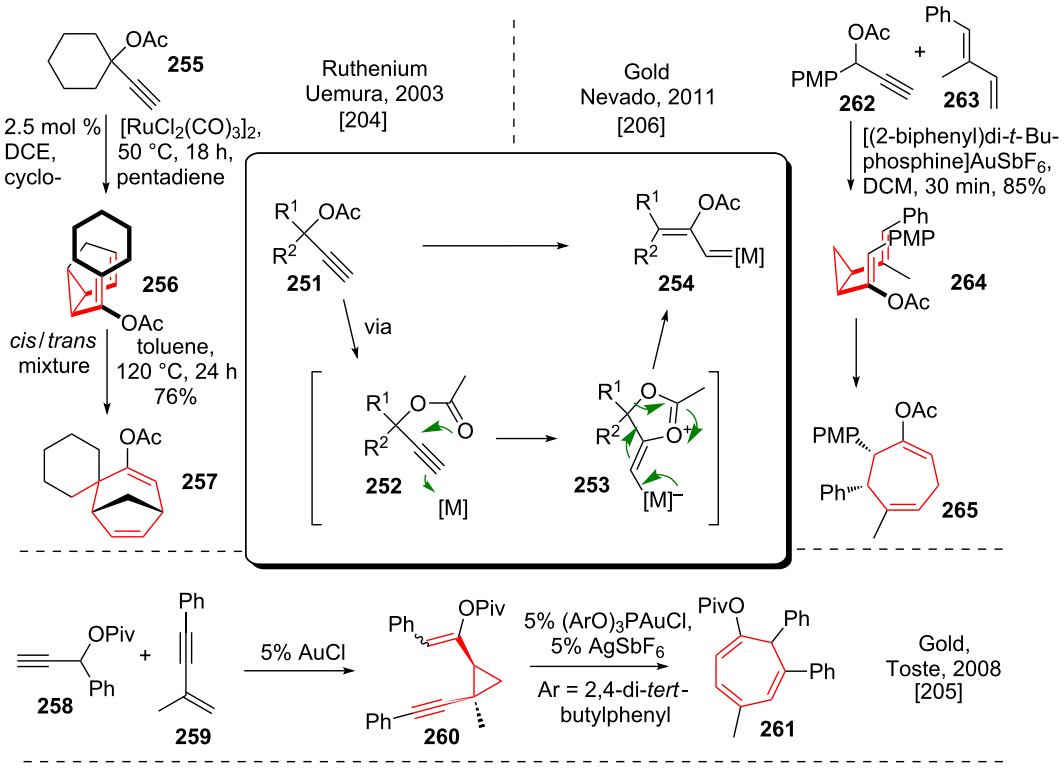
Nevado and coworkers [206] applied a closely related reaction to propargylic acetate **262** using a cationic gold(I) catalyst, which was used to selectively cyclopropanate the less hindered double bond of dienes like **263**. Spontaneous DVCPR provided cycloheptadiene **265** via **264** in good yields.

Further contributions to the topic have been put forward by the group of Echavarren [207] and Gung [208].

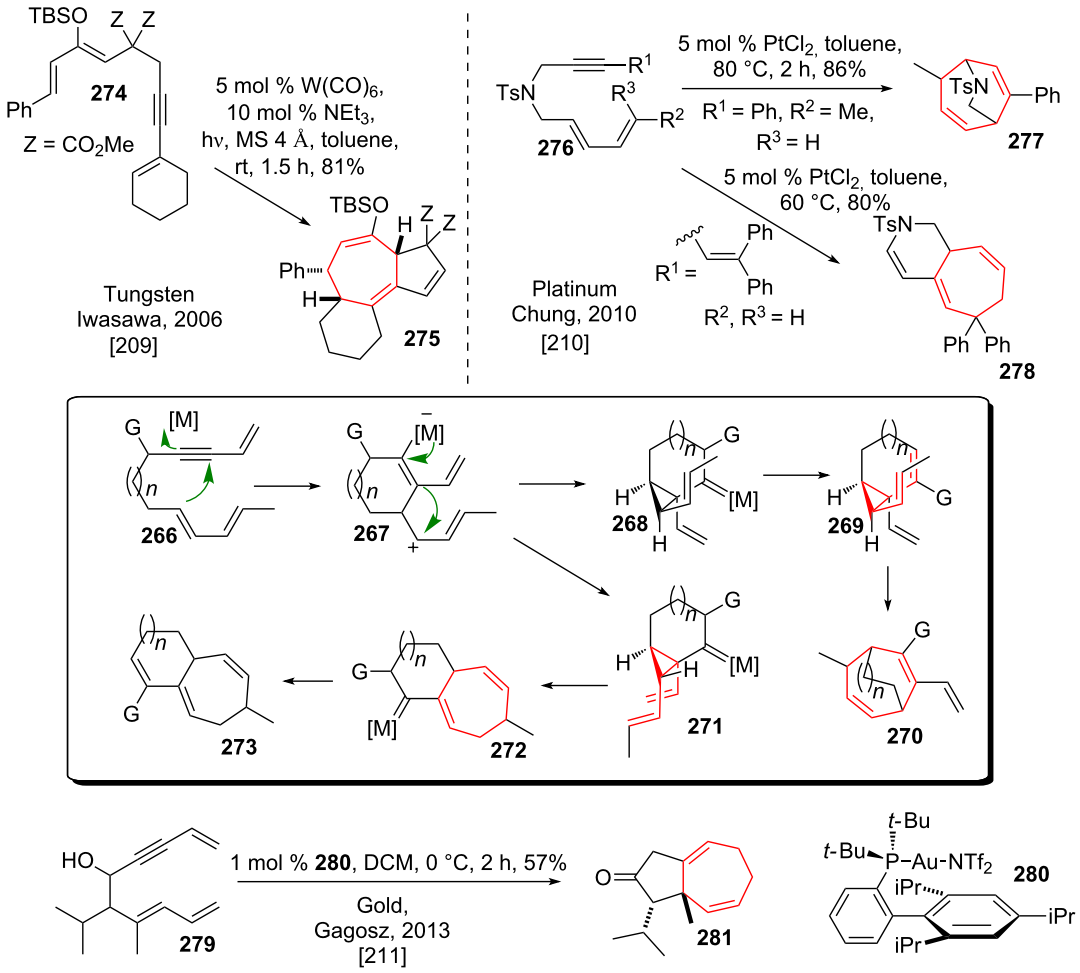
Cycloisomerization involving DVCPR

Iwasawa and coworkers [209] discovered a cyclopropanation/DVCPR sequence of alkyne-substituted silyl enol ethers (for example **274**, see Scheme 34) catalyzed by in situ formed $W(CO)_5$(tol) upon irradiation to give annulated tricycle **275**. The common mechanism for this type of reaction proceeds via *endo-dig* cyclization of enynes like **266** to give zwitterionic intermediate **267**. Metal-carbenoid formation with subsequent cyclopropane formation gives rise to either *cis*- or *trans*-divinylcyclopropanes **268**/**271**. *cis*-Divinylcyclopropane **271** can readily undergo DVCPR to give bicycle **272**. 1,2-Migration of the migrating group G leads to final bicycle **273** after regeneration of the catalyst. *Trans*-divinylcyclopropane **268** can undergo DVCPR after 1,2-migration and subsequent formation of *cis*-divinylcyclopropane **269** yielding bridged bicycle **270**.

Chung and coworkers [210] discovered a related reaction pattern using platinum(II) as the catalyst. Depending on the at-



Scheme 33: Ruthenium- and gold-catalyzed versions of tandem reactions involving a DVCPR.



Scheme 34: Tungsten, platinum and gold catalysed cycloisomerizations leading to a DVCPR.

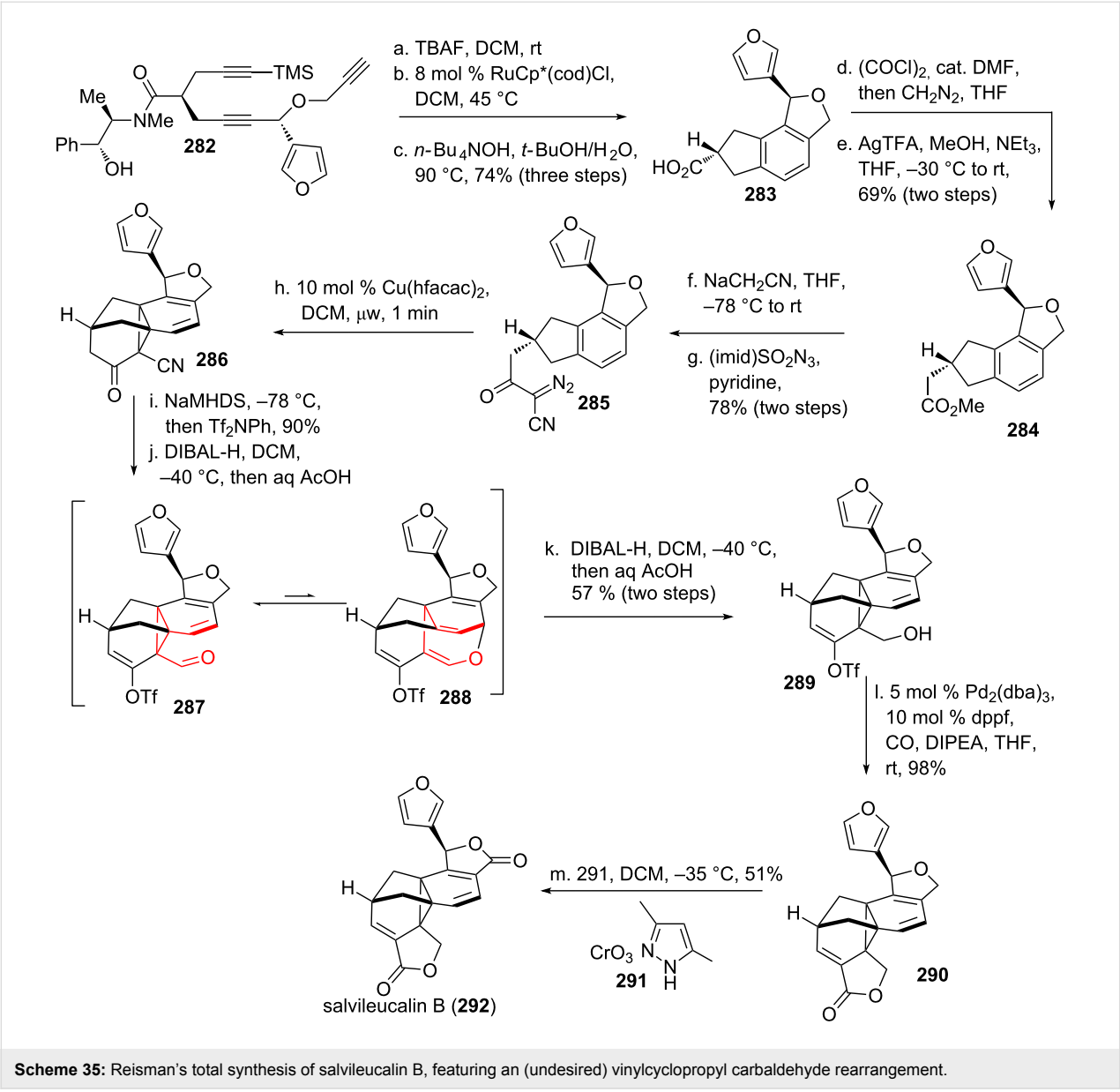
tached rests on enyne **276** both possible cycloheptadienes (bridged **277** or annulated **278**) could be accessed. The selective formation of annulated bicycle **278** in preference of the possible bridged variant underlined the prefered reactivity of their enyne system.

Gagosz and coworkers [211] recently showed that the cycloisomerization of enynes can be catalyzed by gold(I) catalysts. In a particular striking example propargylic alcohol **279** could be converted into bicyclic ketone **281** in good yields.

Heteroatom variants

The oxygen substituted versions of the DVCPR have been subject to more intense research in the covered time period than the corresponding nitrogen variants. In general there are two different modes for the heteroatom incorporation into the DVCPR, as part of the cyclopropane moiety or as part of one of the vinyl moieties. All variants are covered in the following.

The Reisman group [12,212] observed an intermediate vinylcyclopropane carbaldehyde rearrangement on their way towards the total synthesis of salvileucalin B (**292**, see Scheme 35) isolated from the plant *Salvia leucantha* [213]. Starting from enantiopure trialkyne **282**, desilylation was affected using TBAF, followed by ruthenium-catalyzed cycloisomerization [214] and cleavage of the chiral auxiliary to obtain tetracycle **283**. The carboxylic acid was converted into the corresponding acyl chloride, followed by addition of diazomethane and subsequent Arndt–Eistert homologation [215] to obtain methyl ester **284**. Claisen condensation furnished the intermediate β-cyanoketone, which was subjected to diazotransfer conditions [216] to obtain **285**. This compound underwent smooth cyclopropanation with the adjacent benzene moiety to give *cis*-vinylcyclopropane cyanide **286**. Conversion of the ketone to the corresponding triflate followed by mono-reduction of the nitrile furnished *cis*-vinylcyclopropane carbaldehyde **287**, which underwent smooth, but undesired rearrangement to dihydroox-

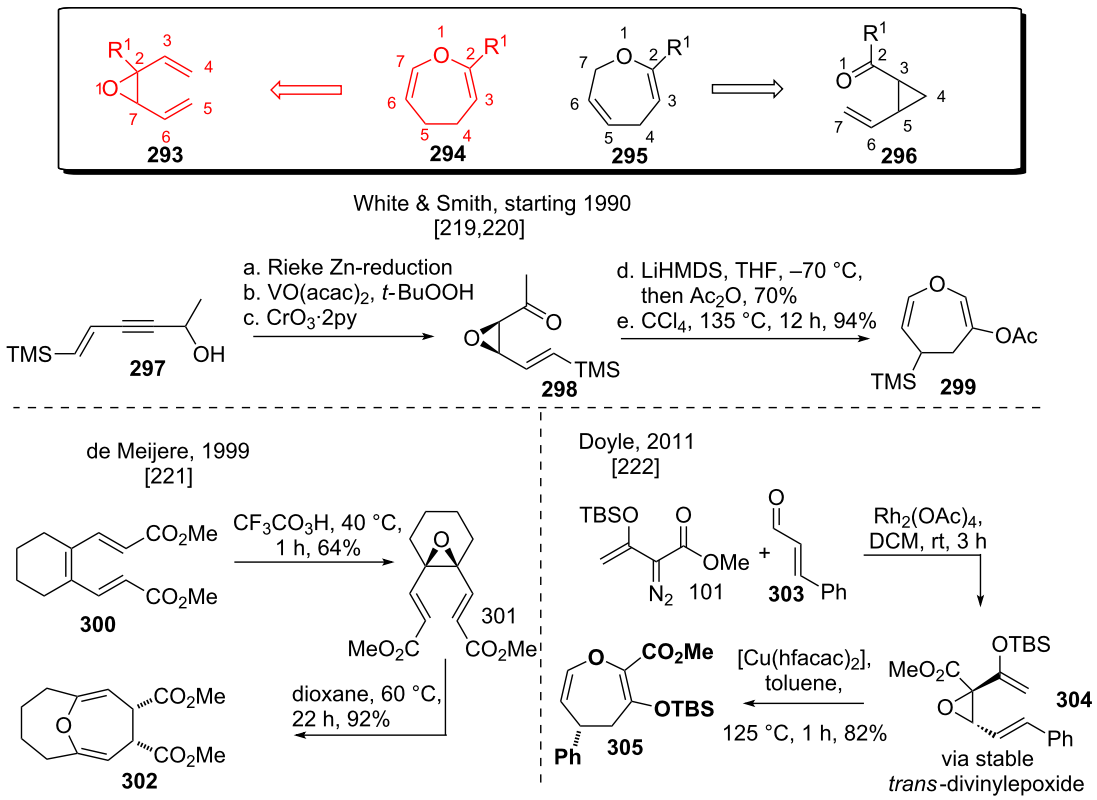


Scheme 35: Reisman's total synthesis of salvileucalin B, featuring an (undesired) vinylcyclopropyl carbaldehyde rearrangement.

epin **288**. This rearrangement has been observed to be reversible [217]. Treatment with DIBAL-H reduced the carbaldehyde moiety selectively to give alcohol **289**. Lactonization was achieved upon Pd-catalyzed CO-insertion to give **290**. The desired natural product was obtained after oxidation of the tetrahydrofuran to the desired natural product salvileucalin B (**292**) using chromium trioxide·3,5-dimethylpyrazole [218].

Oxygen variants overview

The divinyloxirane rearrangement (**293** to **294**, see Scheme 36) has been investigated in detail by the groups of White and Smith [219,220]. The synthesis of the cyclization precursors started from enynes like **297**, beginning with *cis*-selective Rieke-Zn reduction. Epoxidation followed by oxidation furnished *cis*-vinylketone-epoxide **298**. Enolate formation and acetate trapping afforded an intermediate enol-acetate, which underwent high-yielding *cis*-divinylepoxide rearrangement at elevated temperatures to yield dihydrooxepine **299** in good yield. De Meijere and coworkers [221] investigated the selective epoxidation of hexatrienes like **300** to yield *cis*-divinylepoxide **301**. Gentle heating provided bridged bicycle **302**, containing two-*anti*-Bredt olefins in a stereospecific reaction. Doyle and coworkers [222] succeeded in preparing *trans*-divinylcyclopropanes like **304** via rhodium-catalyzed vinyldiazo decomposition (using compound **101**) and subsequent epoxide formation in the presence of cinnamon aldehyde (**303**). These rather stable epoxides (see **304**) were shown to undergo *trans-cis* isomerization followed by divinylepoxide rearrange-

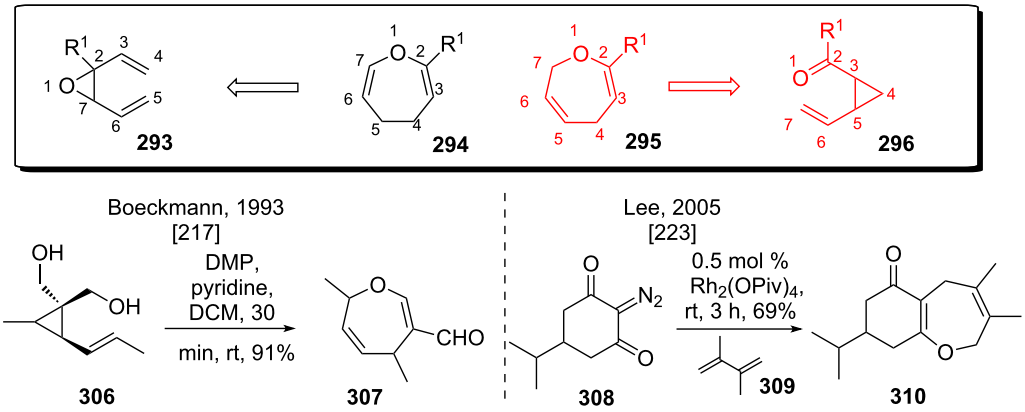


Scheme 36: Studies on the divinylepoxide rearrangement.

ment to give dihydrooxepine **305** at 125 °C. The necessary reaction temperature could be lowered using copper(II) catalysis, accelerating the reaction rate as well.

The vinylepoxide–carbaldehyde rearrangement (**295** to **296**, see Scheme 37) has been investigated early on by the group of Boeckmann [217]. Dess–Martin periodinane oxidation of diol **306** resulted in a smooth rearrangement at ambient temperature, yielding formyldihydrooxepine **307**.

A modified approach has been investigated by the group of Lee, using transition metal mediated diazo decomposition [223]. The in situ generated rhodium-carbenoid formed upon diazo decomposition of **308** underwent cyclopropanation with butadi-



Scheme 37: Studies on the vinylcyclopropanecarbonyl rearrangement.

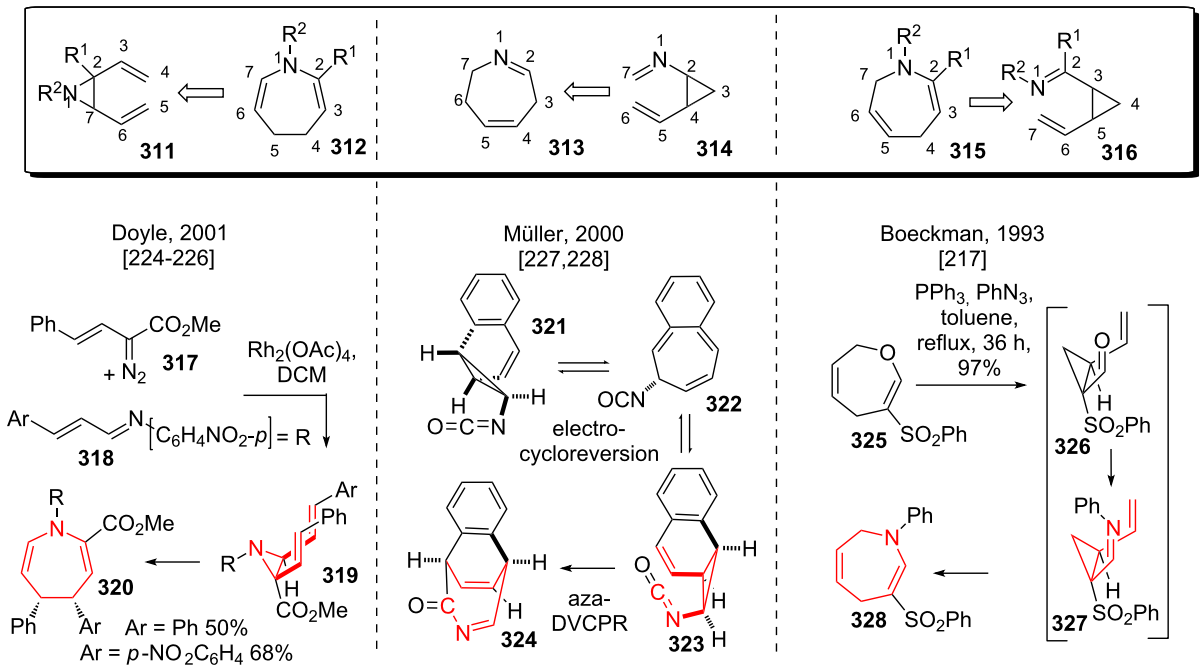
enes like **309**. The resulting vinyl-epoxide ketone underwent rearrangement to give dihydrooxepine **310** in good yield. Vinylcyclopropane–cyclopentene rearrangement [13,14] has been shown to be the major competing side reaction in this case.

Nitrogen variants

Three different approaches can be used to incorporate nitrogen into the DVCPR. The *cis*-divinylaziridine rearrangement (**311** to **312**, see Scheme 38) after rhodium-catalyzed aziridine formation between vinyl-diazo compound **317** and imine **318** has been found by Doyle [224-226]. Rearrangement occurred smoothly to give desired dihydroazepine **320**. Note that the authors suggest a transition state including an opened aziridine zwitterion. Alternatively, a cyclopropylamine can be used in an iminium ion type DVCPR rearrangement (**313** to **314**, see Scheme 38), or a cyclopropylcarbaldehyde can be condensed with an amine to an imine, which then undergoes the DVCPR rearrangement (**315** to **316**, see Scheme 38). Müller and coworkers [227,228] investigated the *trans*-vinylisocyanato–cyclopropyl rearrangement in great detail. Electrocycloreversion of initialy formed nitrene **321** leads to intermediate **322**, which can undergo electrocyclization to give the required *trans*-vinylisocyanatocyclopropane **323**, which underwent the desired rearrangement to give tricycle **324**. The group of Boeckman pioneered the heteroatom variants of the DVCPR, namely the vinylcyclopropane carbaldehyde–dihydrooxepine rearrangement [217], the vinylcyclopropane carbimine–dihydroazepine [217] rearrangement and the corresponding cyclobutane analogues [229-231]. A very stunning application [231] has been achieved using the Claisen reaction of dihydrooxepine **325** (see Scheme 38) to access vinylcyclopropane carbaldehyde **326**, which was in situ converted into the corresponding imine **327** using an aza-Wittig reaction. Subsequent vinylcyclopropane carbimine–dihydroazepine rearrangement furnished cyclic **328** in excellent yield.

Conclusion

The divinylcyclopropane–cycloheptadiene rearrangement has been developed as a versatile method for the construction of seven-membered rings. The utilization in the total synthesis of both sesqui- and diterpenoid natural products as well as in the total synthesis of alkaloids and fatty acid-derived metabolites underlines its robustness and broad applicability. Contribution of the DVCPR as the key step to the solution of some of the most daunting synthetic challenges in present synthetic organic chemistry make it the tool of choice when constrained and highly substituted seven-membered rings are involved. The development of the formal [4 + 3]-cycloaddition (using a tandem cyclopropanation/DVCPR) has largely added to the scope of natural products that were synthesized using a DVCPR and shortened the overall synthetic routes.



Scheme 38: Nitrogen-substituted variants of the divinylcyclopropane rearrangement.

References

1. Vogel, E. *Angew. Chem.* **1960,** *72,* 4–26. doi:10.1002/ange.19600720103
2. Vogel, E.; Ott, K.-H.; Gajek, K. *Justus Liebigs Ann. Chem.* **1961,** *644,* 172–188. doi:10.1002/jlac.19616440121
3. Brown, J. M.; Golding, B. T.; Stofko, J. J. *J. Chem. Soc., Chem. Commun.* **1973,** 319–320. doi:10.1039/C3973000319B
4. Hofmann, K.; Orochena, S. F.; Sax, S. M.; Jeffrey, G. A. *J. Am. Chem. Soc.* **1959,** *81,* 992–997. doi:10.1021/ja01513a059
5. Hudlicky, T.; Fan, R.; Reed, J. W.; Gadamasetti, K. G. *Org. React.* **1992,** *4,* 1–133. doi:10.1002/0471264180.or041.01
6. Piers, E. In *Comprehensive Organic Synthesis;* Trost, B. M.; Fleming, I.; Paquette, L. A., Eds.; Pergamon Press: Oxford, 1991; Vol. 5, pp 971–988. doi:10.1016/B978-0-08-052349-1.00143-8
7. Tang, P.; Qin, Y. *Synthesis* **2012,** *44,* 2969–2984. doi:10.1055/s-0032-1317011
8. Evans, A. P., Ed. *Modern Rhodium Catalyzed Reactions;* Wiley-VCH: Weinheim, 2005. doi:10.1002/3527604693
9. Lin, H.; Danishefsky, S. J. *Angew. Chem., Int. Ed.* **2003,** *42,* 36–51. doi:10.1002/anie.200390048
10. Davies, H. M. L.; Denton, J. R. *Chem. Soc. Rev.* **2009,** *38,* 3061–3071. doi:10.1039/b901170f
11. Buchner, E.; Curtius, T. *Ber. Dtsch. Chem. Ges.* **1885,** *18,* 2377–2379. doi:10.1002/cber.188501802119
12. Reisman, S. E.; Nani, R. R.; Levin, S. *Synlett* **2011,** 2437–2442. doi:10.1055/s-0031-1289520
13. Goldschmidt, Z.; Crammer, B. *Chem. Soc. Rev.* **1988,** *17,* 229–267. doi:10.1039/cs9881700229
14. Hudlicky, T.; Reed, J. W. *Angew. Chem., Int. Ed.* **2010,** *49,* 4864–4876. doi:10.1002/anie.200906001
15. Tantillo, D. J.; Hoffmann, R. *J. Org. Chem.* **2002,** *67,* 1419–1426. doi:10.1021/jo0107002
16. Doering, W. V. E.; Roth, W. R. *Angew. Chem.* **1963,** *75,* 27–35. doi:10.1002/ange.19630750106
17. Özkan, I.; Zora, M. *J. Org. Chem.* **2003,** *68,* 9635–9642. doi:10.1021/jo035173w
18. Zora, M.; Özkan, I.; Danisman, M. F. *J. Mol. Struct.: THEOCHEM* **2003,** *636,* 9–13. doi:10.1016/S0166-1280(03)00478-0
19. Zora, M. *J. Mol. Struct.: THEOCHEM* **2004,** *681,* 113–116. doi:10.1016/j.theochem.2004.05.011
20. Von E. Doering, W.; Roth, W. R. *Tetrahedron* **1963,** *19,* 715–737. doi:10.1016/S0040-4020(01)99207-5
21. Klärner, F.-G.; Jones, M., Jr.; Magid, R. M. *Acc. Chem. Res.* **2009,** *42,* 169–181. doi:10.1021/ar800100h
22. Zora, M. *J. Org. Chem.* **2005,** *70,* 6018–6026. doi:10.1021/jo050711l
23. Zora, M.; Özkan, I. *J. Mol. Struct.: THEOCHEM* **2003,** *625,* 251–256. doi:10.1016/S0166-1280(03)00073-3
24. Sperling, D.; Reißig, H.-U.; Fabian, J. *Liebigs Ann.* **1997,** 2443–2449. doi:10.1002/jlac.199719971207
25. Sperling, D.; Reißig, H.-U.; Fabian, J. *Eur. J. Org. Chem.* **1999,** 1107–1114. doi:10.1002/(SICI)1099-0690(199905)1999:5<1107::AID-EJOC1107>3.0.CO;2-E
26. Schneider, M. P.; Csacsko, B. *J. Chem. Soc., Chem. Commun.* **1977,** 330–331. doi:10.1039/C39770000330
27. Arai, M.; Crawford, R. J. *Can. J. Chem.* **1972,** *50,* 2158–2162. doi:10.1139/v72-348
28. Baldwin, J. E.; Ullenius, C. *J. Am. Chem. Soc.* **1974,** *96,* 1542–1547. doi:10.1021/ja00812a044
29. Baldwin, J. E.; Gilbert, K. E. *J. Am. Chem. Soc.* **1976,** *98,* 8283–8284. doi:10.1021/ja00441a078
30. Pohnert, G.; Boland, W. *Tetrahedron* **1997,** *53,* 13681–13694. doi:10.1016/S0040-4020(97)00886-7
31. Boland, W.; Pohnert, G.; Maier, I. *Angew. Chem., Int. Ed. Engl.* **1995,** *34,* 1602–1604. doi:10.1002/anie.199516021
32. Müller, D. G.; Jaenicke, L.; Donike, M.; Akintobi, T. *Science* **1971,** *171,* 815–817. doi:10.1126/science.171.3973.815
33. Hortmann, A. G. *Tetrahedron Lett.* **1968,** *9,* 5785–5786. doi:10.1016/S0040-4039(00)76350-7
34. Hortmann, A. G.; Danile, D. S.; Martinelli, J. E. *J. Org. Chem.* **1973,** *38,* 728–735. doi:10.1021/jo00944a024
35. Tomita, B.; Hirose, Y. *Tetrahedron Lett.* **1970,** *11,* 235–238. doi:10.1016/0040-4039(70)80034-X
36. Cox, P. J.; Sim, G. A.; Roberts, J. S.; Herz, W. *J. Chem. Soc., Chem. Commun.* **1973,** 428–429. doi:10.1039/C39730000428
37. Sun, H. H.; Waraszkiewicz, S. M.; Erickson, K. L.; Finer, J.; Clardy, J. *J. Am. Chem. Soc.* **1977,** *99,* 3516–3517. doi:10.1021/ja00452a062
38. Schwarzer, D. D.; Gritsch, P. J.; Gaich, T. *Angew. Chem., Int. Ed.* **2012,** *51,* 11514–11516. doi:10.1002/anie.201203586
39. Schwarzer, D. D.; Gritsch, P. J.; Gaich, T. *Synlett* **2013,** *24,* 1025–1031. doi:10.1055/s-0032-1318501
40. Floss, H. G. *Tetrahedron* **1976,** *32,* 873–912. doi:10.1016/0040-4020(76)85047-8
41. Wenkert, E.; Sliwa, H. *Bioorg. Chem.* **1977,** *6,* 443–452. doi:10.1016/0045-2068(77)90043-8
42. Seiler, M. P. Ph.D. Dissertation No. 4574, ETH Zürich, 1970.
43. Marvell, E. N.; Crystal, L. *J. Am. Chem. Soc.* **1978,** *100,* 877–883. doi:10.1021/ja00471a036
44. Ito, H.; Takeguchi, S.; Kawagishi, T.; Iguchi, K. *Org. Lett.* **2006,** *8,* 4883–4885. doi:10.1021/ol061947u
45. Iwashima, M.; Terada, I.; Okamoto, K.; Iguchi, K. *J. Org. Chem.* **2002,** *67,* 2977–2981. doi:10.1021/jo011043g
46. Murga, J.; Garcia-Fortanet, J.; Carda, M.; Marco, J. A. *Synlett* **2004,** 2830–2832. doi:10.1055/s-2004-835653
47. Wender, P. A.; Eissenstat, M. A.; Filosa, M. P. *J. Am. Chem. Soc.* **1979,** *101,* 2196–2198. doi:10.1021/ja00502a042
48. Wender, P. A.; Filosa, M. P. *J. Org. Chem.* **1976,** *41,* 3490–3491. doi:10.1021/jo00883a043
49. Piers, E.; Moss, N. *Tetrahedron Lett.* **1985,** *26,* 2735–2738. doi:10.1016/S0040-4039(00)94898-6
50. Piers, E.; Jung, G. L. *Can. J. Chem.* **1987,** *65,* 1668–1671. doi:10.1139/v87-279
51. Piers, E.; Jean, M.; Marrs, P. S. *Tetrahedron Lett.* **1987,** *28,* 5075–5078. doi:10.1016/S0040-4039(00)95593-X
52. Ranieri, R. L.; Calton, G. J. *Tetrahedron Lett.* **1978,** *19,* 499–502. doi:10.1016/S0040-4039(01)85316-8
53. Calton, G. J.; Ranieri, R. L.; Espenshade, M. A. *J. Antibiot.* **1978,** *31,* 38–42. doi:10.7164/antibiotics.31.38
54. Kubiak, G.; Cook, J. M.; Weiss, U. *J. Org. Chem.* **1984,** *49,* 561–564. doi:10.1021/jo00177a040
    Obtained from monopreotection of the diketone according to this reference.
55. Burke, S. D.; Murtiashaw, C. W.; Saunders, J. O.; Oplinger, J. A.; Dike, M. S. *J. Am. Chem. Soc.* **1984,** *106,* 4558–4566. doi:10.1021/ja00328a043
56. Burke, S. D.; Murtiashaw, C. W.; Oplinger, J. A. *Tetrahedron Lett.* **1983,** *24,* 2949–2952. doi:10.1016/S0040-4039(00)88066-1

57. Burke, S. D.; Murtiashaw, C. W.; Saunders, J. O.; Dike, M. S. *J. Am. Chem. Soc.* **1982,** *104,* 872–874. doi:10.1021/ja00367a049
58. Beechan, C. M.; Djerassi, C.; Finer, J. S.; Clardy, J. *Tetrahedron Lett.* **1977,** *18,* 2395–2398. doi:10.1016/S0040-4039(01)83775-8
59. Andersen, N. H.; Falcone, M. S. *Chem. Ind. (London)* **1971,** 62–63.
60. Carrol, P. J.; Ghisalberti, E. L.; Ralph, D. E. *Phytochemistry* **1976,** *15,* 777–780. doi:10.1016/S0031-9422(00)94442-X
61. Crandall, J. K.; Baker, D. B.; Colyer, R. A.; Watkins, R. J.; Arrington, J. P. *J. Org. Chem.* **1968,** *33,* 423–425. doi:10.1021/jo01265a089
Obtained after TBS-protection of the alcohol.
62. Overman, L. E.; Ricca, D. J.; Tran, V. D. *J. Am. Chem. Soc.* **1993,** *115,* 2042–2044. doi:10.1021/ja00058a064
63. Abelman, M. M.; Overman, L. E. *J. Am. Chem. Soc.* **1988,** *110,* 2328–2329. doi:10.1021/ja00215a068
64. Kucera, D. J.; O'Connor, S. J.; Overman, L. E. *J. Org. Chem.* **1993,** *58,* 5304–5306. doi:10.1021/jo00072a006
65. Overman, L. E.; Ricca, D. J.; Tran, V. D. *J. Am. Chem. Soc.* **1997,** *119,* 12031–12040. doi:10.1021/ja972427k
66. Hayashi, T.; Kishi, M.; Kawasaki, M.; Arisawa, M.; Shimizu, M.; Suzuki, S.; Yoshizaki, M.; Morita, N.; Tezuka, Y.; Kikuchi, T.; Berganza, L. H.; Ferro, E.; Basualdo, I. *Tetrahedron Lett.* **1987,** *28,* 3693–3696. doi:10.1016/S0040-4039(00)96357-3
67. Skattebøl, J. *J. Org. Chem.* **1964,** *29,* 2951–2956. doi:10.1021/jo01033a035
68. Seyferth, D.; Yamazaki, H.; Alleston, D. L. *J. Org. Chem.* **1963,** *28,* 703–706. doi:10.1021/jo01038a025
69. Grigg, R.; Sridharan, V.; Stevenson, P.; Worakun, T. *J. Chem. Soc., Chem. Commun.* **1986,** 1697–1699. doi:10.1039/C39860001697
70. Abelman, M. M.; Oh, T.; Overman, L. E. *J. Org. Chem.* **1987,** *52,* 4130–4133. doi:10.1021/jo00227a038
71. Overman, L. E.; Abelmann, M. M.; Kucera, D. J.; Tran, V. D.; Ricca, D. J. *Pure Appl. Chem.* **1992,** *64,* 1813–1819. doi:10.1351/pac199264121813
72. Osuka, A.; Taka-Oka, K.; Suzuki, H. *Chem. Lett.* **1984,** *13,* 271–272. doi:10.1246/cl.1984.271
73. Solomon, M.; Jamison, W. C. L.; McCormick, M.; Liotta, D.; Cherry, D. A.; Mills, J. E.; Shah, R. D.; Rodgers, J. D.; Maryanoff, C. A. *J. Am. Chem. Soc.* **1988,** *110,* 3702–3704. doi:10.1021/ja00219a079
74. Panetta, C. A.; Dixit, A. S. *Synthesis* **1981,** 59–60. doi:10.1055/s-1981-29337
75. Meyer, N.; Seebach, D. *Chem. Ber.* **1980,** *113,* 1304–1319. doi:10.1002/cber.19801130410
76. Taber, D. F. *J. Org. Chem.* **1976,** *41,* 2649–2650. doi:10.1021/jo00877a033
77. Hook, J. M.; Mander, L. N.; Woolias, M. *Tetrahedron Lett.* **1982,** *23,* 1095–1098. doi:10.1016/S0040-4039(00)87030-6
78. Nagata, W.; Yoshiaka, M. *Org. React.* **1977,** *25,* 255–476.
79. Chong, J. M.; Sharpless, K. B. *J. Org. Chem.* **1985,** *50,* 1560–1563. doi:10.1021/jo00209a048
80. Carlsen, P. H. J.; Katsuki, T.; Martin, V. S.; Sharpless, K. B. *J. Org. Chem.* **1981,** *46,* 3936–3938. doi:10.1021/jo00332a045
81. Fox, M. E.; Li, C.; Marino, J. P., Jr.; Overman, L. E. *J. Am. Chem. Soc.* **1999,** *121,* 5467–5480. doi:10.1021/ja990404v
82. Davies, H. M. L.; Doan, B. D. *J. Org. Chem.* **1998,** *63,* 657–660. doi:10.1021/jo971577a
83. Davies, H. M. L. In *Advances in Cycloadditions;* Hermata, M., Ed.; JAI Press: Greenwich, CT, 1998; Vol. 5, pp 119–164.
84. Ayer, W. A.; Cruz, E. R. *J. Org. Chem.* **1993,** *58,* 7529–7534. doi:10.1021/jo00078a035
85. Fairlie, D. P.; Bosnich, B. *Organometallics* **1988,** *7,* 936–945. doi:10.1021/om00094a025
86. Davies, H. M. L.; Cantrell, W. R.; Romines, K. R.; Baum, J. S. *Org. Synth.* **1992,** *70,* 93–97.
87. Davies, H. M. L. *Tetrahedron* **1993,** *49,* 5203–5223. doi:10.1016/S0040-4020(01)82371-1
88. Davies, H. M. L.; Bruzinski, P. R.; Lake, D. H.; Kong, N.; Fall, M. J. *J. Am. Chem. Soc.* **1996,** *118,* 6897–6907. doi:10.1021/ja9604931
89. Davies, H. M. L.; Doan, B. D. *Tetrahedron Lett.* **1996,** *37,* 3967–3970. doi:10.1016/0040-4039(96)00723-X
90. Osborn, J. A.; Jardine, F. H.; Young, J. F.; Wilkinson, G. *J. Chem. Soc. A* **1966,** 1711–1732. doi:10.1039/j19660001711
91. Olson, J. P.; Davies, H. M. L. *Org. Lett.* **2008,** *10,* 573–576. doi:10.1021/ol702844g
92. Olson, J. P.; Davies, H. M. L. *Org. Lett.* **2010,** *12,* 1144. doi:10.1021/ol100111w
93. Patil, A. D.; Freyer, A. J.; Killmer, L.; Offen, P.; Carte, B.; Jurewicz, A. J.; Johnson, R. K. *Tetrahedron* **1997,** *53,* 5047–5060. doi:10.1016/S0040-4020(97)00205-6
94. Yang, D.; Zhang, C. *J. Org. Chem.* **2001,** *66,* 4814–4818. doi:10.1021/jo010122p
95. Inoue, M.; Frontier, A. J.; Danishefsky, S. J. *Angew. Chem., Int. Ed.* **2000,** *39,* 761–764. doi:10.1002/(SICI)1521-3773(20000218)39:4<761::AID-ANIE761>3.0.CO;2-I
96. Inoue, M.; Carson, M. W.; Frontier, A. J.; Danishefsky, S. J. *J. Am. Chem. Soc.* **2001,** *123,* 1878–1889. doi:10.1021/ja0021060
97. Lian, Y.; Miller, L. C.; Born, S.; Sarpong, R.; Davies, H. M. L. *J. Am. Chem. Soc.* **2010,** *132,* 12422–12425. doi:10.1021/ja103916t
98. Rudi, A.; Kashman, Y. *J. Nat. Prod.* **1992,** *55,* 1408–1414. doi:10.1021/np50088a004
99. Rudi, A.; Shalom, H.; Schleyer, M.; Benayahu, Y.; Kashman, Y. *J. Nat. Prod.* **2004,** *67,* 106–109. doi:10.1021/np030261x
100. Gevorgyan, V.; Rubin, M.; Benson, S.; Liu, J.-X.; Yamamoto, Y. *J. Org. Chem.* **2000,** *65,* 6179–6186. doi:10.1021/jo000726d
101. Schwartz, B. D.; Denton, J. R.; Lian, Y.; Davies, H. M. L.; Williams, C. M. *J. Am. Chem. Soc.* **2009,** *131,* 8329–8332. doi:10.1021/ja9019484
102. Davies, H. M. L.; Loe, Ø.; Stafford, D. G. *Org. Lett.* **2005,** *7,* 5561–5563. doi:10.1021/ol052005c
103. Schwartz, B. D.; Denton, J. R.; Davies, H. M. L.; Williams, C. M. *Aust. J. Chem.* **2009,** *62,* 980–982. doi:10.1071/CH09267
See for the total synthesis of vibsanin E.
104. Fukuyama, Y.; Minami, H.; Matsuo, A.; Kitamura, K.; Akizuki, M.; Kubo, M.; Kodama, M. *Chem. Pharm. Bull.* **2002,** *50,* 368–371. doi:10.1248/cpb.50.368
105. Mander, L. N.; Thomson, R. J. *J. Org. Chem.* **2005,** *70,* 1654–1670. doi:10.1021/jo048199b
106. Anders, E.; Gassner, T. *Angew. Chem., Int. Ed. Engl.* **1982,** *21,* 289–290. doi:10.1002/anie.198202891
107. Anders, E.; Gassner, T. *Angew. Chem. Suppl.* **1982,** 675–685.
108. Anders, E.; Gassner, T. *Angew. Chem., Int. Ed. Engl.* **1983,** *22,* 619–620. doi:10.1002/anie.198306191
109. Schwartz, B. D.; Williams, C. M.; Anders, E.; Bernhardt, P. V. *Tetrahedron* **2008,** *64,* 6482–6487. doi:10.1016/j.tet.2008.04.068
110. Gaydou, M.; Miller, R. E.; Delpont, N.; Ceccon, J.; Echavarren, A. M. *Angew. Chem., Int. Ed.* **2013,** *52,* 6396–6399. doi:10.1002/anie.201302411

111. Ma, W.-H.; Huang, H.; Zhou, P.; Chen, D.-F. *J. Nat. Prod.* **2009,** *72,* 676–678. doi:10.1021/np8007864
112. Davies, H. M. L.; Huby, N. J. S. *Tetrahedron Lett.* **1992,** *33,* 6935–6938. doi:10.1016/S0040-4039(00)60899-7
113. Carrol, F. I.; Lewin, A. H.; Boja, J. W.; Kuhar, M. J. *J. Med. Chem.* **1992,** *35,* 969–981. doi:10.1021/jm00084a001
See for a further reading.
114. Clarke, R. L.; Daum, S. J.; Gambino, A. J.; Aceto, M. D.; Pearl, J.; Levitt, M.; Cumiskey, W. R.; Bogado, E. F. *J. Med. Chem.* **1973,** *16,* 1260–1267. doi:10.1021/jm00269a600
115. Davies, H. M. L.; Saikali, E.; Young, W. B. *J. Org. Chem.* **1991,** *56,* 5696–5700. doi:10.1021/jo00019a044
116. Davies, H. M. L.; Hougland, P. W.; Cantrell, W. R., Jr. *Synth. Commun.* **1992,** *22,* 971–978. doi:10.1080/00397919208019285
117. Davies, H. M. L.; Cantrell, W. R., Jr. *Tetrahedron Lett.* **1991,** *32,* 6509–6512. doi:10.1016/0040-4039(91)80206-L
118. Fukuyama, T.; Gang, L. *J. Am. Chem. Soc.* **1996,** *118,* 7426–7427. doi:10.1021/ja961701s
119. Fukuyama, T.; Liu, G. *Pure Appl. Chem.* **1997,** *69,* 501–506. doi:10.1351/pac199769030501
120. Yokoshima, S.; Tokuyama, H.; Fukuyama, T. *Angew. Chem., Int. Ed.* **2000,** *39,* 4073–4075. doi:10.1002/1521-3773(20001117)39:22<4073::AID-ANIE4073>3.0.CO;2-V
121. Lovell, F. M.; Pepinsky, R.; Wilson, A. J. C. *Tetrahedron Lett.* **1959,** *1,* 1–5. doi:10.1016/S0040-4039(01)82717-9
122. Conroy, H.; Chakrabarti, J. K. *Tetrahedron Lett.* **1959,** *1,* 6–13. doi:10.1016/S0040-4039(01)82718-0
123. Kondo, K.; Umemoto, T.; Yako, Y.; Tunemoto, D. *Tetrahedron Lett.* **1978,** *19,* 3927–3930. doi:10.1016/S0040-4039(01)95100-7
124. Pfitzner, K. E.; Moffat, J. G. *J. Am. Chem. Soc.* **1965,** *87,* 5661–5670. doi:10.1021/ja00952a026
125. Brown, H. C.; Narsimhan, S. *J. Org. Chem.* **1982,** *47,* 1604–1606. doi:10.1021/jo00347a057
126. Deziel, R. *Tetrahedron Lett.* **1987,** *28,* 4371–4372. doi:10.1016/S0040-4039(00)96512-2
127. Tebbe, F. N.; Parshall, G. W.; Reddy, G. S. *J. Am. Chem. Soc.* **1978,** *100,* 3611–3613. doi:10.1021/ja00479a061
128. Newcomb, N. J.; Ya, F.; Vijn, R. J.; Hiemstra, H.; Speckamp, W. N. *J. Chem. Soc., Chem. Commun.* **1994,** 767–768. doi:10.1039/C39940000767
129. Benhamou, M. C.; Etemad-Moghadam, G.; Speziale, V.; Lattes, A. *Synthesis* **1979,** 891–892. doi:10.1055/s-1979-28864
130. Kende, A. S.; Smalley, T. L., Jr.; Huang, H. *J. Am. Chem. Soc.* **1999,** *121,* 7431–7432. doi:10.1021/ja991528a
131. Isostemofoline has been reported to be isolated in the laboratories of Prof. Yang Ye, Insititute of Materia Medica, Chinese Academy of Science in the reference above and has not been published yet.
132. Krapcho, A. P. *Synthesis* **1982,** 893–914. doi:10.1055/s-1982-29991
133. Seebach, D.; Locher, R. *Angew. Chem., Int. Ed. Engl.* **1979,** *18,* 957–958. doi:10.1002/anie.197909571
134. Pelter, A.; Al-Bayati, R. I. H.; Ayoub, M. T.; Lewis, W.; Pardasani, P.; Hansel, R. *J. Chem. Soc., Perkin Trans. 1* **1987,** 717–742. doi:10.1039/P19870000717
135. Knight, D. W.; Pattenden, G. *J. Chem. Soc., Perkin Trans. 1* **1975,** 635–640. doi:10.1039/P19750000635
136. Irie, H.; Masaki, N.; Ohno, R.; Osaki, K.; Taga, T.; Uyeo, S. *J. Chem. Soc. D* **1970,** 1066. doi:10.1039/C29700001066
137. Ng, F. W.; Lin, H.; Danishefsky, S. J. *J. Am. Chem. Soc.* **2002,** *124,* 9812–9824. doi:10.1021/ja0204675
138. Lin, H.; Ng, F. W.; Danishefsky, S. J. *Tetrahedron Lett.* **2002,** *43,* 549–551. doi:10.1016/S0040-4039(01)02213-4
139. Ng, F. W.; Lin, H.; Chiu, P.; Danishefsky, S. J. *J. Am. Chem. Soc.* **2003,** *125,* 13303. doi:10.1021/ja0334558
140. Story, P. R. *J. Org. Chem.* **1961,** *26,* 287–290. doi:10.1021/jo01061a001
141. Klumpp, G. W.; Barnick, J. F. W. K.; Veefkind, A. H.; Bickelhaupt, F. *Recl. Trav. Chim. Pays-Bas* **1969,** *88,* 766–778. doi:10.1002/recl.19690880702
142. Cupas, C.; Watts, W. E.; von R. Schleyer, P. *Tetrahedron Lett.* **1964,** 2503–2507. doi:10.1016/S0040-4039(00)70415-1
143. Luche, J.-L.; Gemal, A. L. *J. Chem. Soc., Chem. Commun.* **1978,** 976–977. doi:10.1039/C39780000976
144. Beyerman, H. C.; Heiszwolf, G. L. *J. Chem. Soc.* **1963,** 755–756.
145. Johnson, W. S.; Werthemann, L.; Bartlett, W. R.; Brocksom, T. J.; Li, T.-T.; Faulkner, D. J.; Perterson, M. R. *J. Am. Chem. Soc.* **1970,** *92,* 741–743. doi:10.1021/ja00706a074
146. Shiori, T.; Ninomiya, K.; Yamada, S. *J. Am. Chem. Soc.* **1972,** *94,* 6203–6205. doi:10.1021/ja00772a052
147. NInomiya, K.; Shiori, T.; Yamada, S. *Tetrahedron* **1974,** *30,* 2151–2157. doi:10.1016/S0040-4020(01)97352-1
148. Felix, D.; Gschwend-Steen, K.; Wick, A. E.; Eschenmoser, A. *Helv. Chim. Acta* **1969,** *52,* 1030–1042. doi:10.1002/hlca.19690520418
149. Pappo, R.; Allen, D. S., Jr.; Lemieux, R. U.; Johnson, W. S. *J. Org. Chem.* **1956,** *21,* 478–479. doi:10.1021/jo01110a606
150. Griffith, W. P.; Ley, S. V.; Whitcombe, G. P.; White, A. D. *J. Chem. Soc., Chem. Commun.* **1987,** 1625–1627. doi:10.1039/C39870001625
151. Confalone, P. N.; Huie, E. M. *J. Org. Chem.* **1987,** *52,* 79–83. doi:10.1021/jo00377a014
152. Lin, L.-Z.; Cordell, G. A.; Ni, C.-Z.; Clardy, J. *Phytochemistry* **1991,** *30,* 1311–1315. doi:10.1016/S0031-9422(00)95223-3
153. Shimokawa, J.; Harada, T.; Yokoshima, S.; Fukuyama, T. *J. Am. Chem. Soc.* **2011,** *133,* 17634–17637. doi:10.1021/ja208617c
154. Shimokawa, J.; Harada, T.; Yokoshima, S.; Fukuyama, T. *Pure Appl. Chem.* **2012,** *84,* 1643–1650. doi:10.1351/PAC-CON-11-10-25
155. Achmatowicz, O., Jr.; Bukowski, P.; Szechner, B.; Zwierzchowska, Z.; Zamojski, A. *Tetrahedron* **1971,** *27,* 1973–1996. doi:10.1016/S0040-4020(01)98229-8
156. van den Heuvel, M.; Cuiper, A. D.; van der Deen, H.; Kellogg, R. M.; Feringa, B. L. *Tetrahedron Lett.* **1997,** *38,* 1655–1658. doi:10.1016/S0040-4039(97)00155-X
157. Kende, A. S.; Luzzio, M. J.; Mendoza, J. S. *J. Org. Chem.* **1990,** *55,* 918–924. doi:10.1021/jo00290a023
158. Yoshida, Y.; Sjimonishi, K.; Sakakura, Y.; Okada, S.; Aso, N.; Tanabe, Y. *Synthesis* **1999,** 1633–1636. doi:10.1055/s-1999-3561
159. Kawabata, H.; Hayashi, M. *Tetrahedron Lett.* **2002,** *43,* 5645–5647. doi:10.1016/S0040-4039(02)01133-4
160. Kobayashi, S.; Tsuchiya, Y.; Mukaiyama, T. *Chem. Lett.* **1991,** *20,* 537–540. doi:10.1246/cl.1991.537
161. Krespki, L. R.; Jensen, K. M.; Heilmann, S. M.; Rasmussen, J. K.; Lynch, L. E. *Synth. Commun.* **1986,** *16,* 617–625. doi:10.1080/00397918608057730
162. Bredereck, H.; Simchen, G.; Rebsdat, S.; Kantlehner, W.; Horn, P.; Wahl, R.; Hoffmann, H.; Grieshaber, P. *Chem. Ber.* **1968,** *101,* 41–50. doi:10.1002/cber.19681010108

163. Arnold, Z.; Zemlicka, J. *Collect. Czech. Chem. Commun.* **1959,** *24,* 2378–2384.
164. Arnold, Z.; Zemlicka, J. *Collect. Czech. Chem. Commun.* **1959,** *24,* 2385–2392.
165. Scott, W. J.; Stille, J. K. *J. Am. Chem. Soc.* **1986,** *108,* 3033–3040. doi:10.1021/ja00271a037
166. Su, Y.; Hu, Y.; Han, J.; Zheng, J.; Qi, J.; Jiang, T.; Pan, X.; She, X. *J. Org. Chem.* **2009,** *74,* 2743–2749. doi:10.1021/jo9000146
167. Jung, M. E.; Lyster, M. A. *J. Chem. Soc., Chem. Commun.* **1978,** 315–316. doi:10.1039/C39780000315
168. Olah, G. A.; Narang, S. C.; Gupta, B. G. B.; Malhotra, R. *Synthesis* **1979,** 61–62. doi:10.1055/s-1979-28558
169. Wender, P. A.; Hillemann, C. L.; Szymonifka, M. J. *Tetrahedron Lett.* **1980,** *21,* 2205–2208. doi:10.1016/0040-4039(80)80003-7
170. Evans, F. J.; Soper, C. J. *Lloydia* **1978,** *41,* 193.
171. Davies, H. M. L.; Calvo, R. L.; Townsend, R. J.; Ren, P.; Churchill, R. M. *J. Org. Chem.* **2000,** *65,* 4261–4268. doi:10.1021/jo991959b
172. Dabrah, T. T.; Kaneko, T.; Massefski, W., Jr.; Whipple, W. B. *J. Am. Chem. Soc.* **1997,** *119,* 1594–1598. doi:10.1021/ja961000v
173. Dabrah, T. T.; Harwood, H. J., Jr.; Huang, L. H.; Jankovich, N. D.; Kaneko, T.; Li, J. C.; Lindsey, S.; Mashier, P.; Subashi, T. A.; Therrien, M.; Watts, P. C. *J. Antibiot.* **1997,** *50,* 1–7. doi:10.7164/antibiotics.50.1
174. Vaswani, R. G.; Day, J. J.; Wood, J. L. *Org. Lett.* **2009,** *11,* 4532–4535. doi:10.1021/ol901746c
175. Caroll, A. R.; Hyde, E.; Smith, J.; Quinn, R. J.; Guymer, G.; Forster, P. I. *J. Org. Chem.* **2005,** *70,* 1096–1099. doi:10.1021/jo048439n
176. Tsuji, J.; Shimizu, I.; Minami, I.; Ohashi, Y. *Tetrahedron Lett.* **1982,** *23,* 4809–4812. doi:10.1016/S0040-4039(00)85719-6
177. Trost, B. M. *Angew. Chem., Int. Ed. Engl.* **1989,** *28,* 1173–1192. doi:10.1002/anie.198911731
178. Furrow, M. E.; Myers, A. G. *J. Am. Chem. Soc.* **2004,** *126,* 5436–5445. doi:10.1021/ja049694s
179. Kobayashi, S.; Hamada, T.; Manabe, K. *Synlett* **2001,** 1140–1142. doi:10.1055/s-2001-15166
180. Takeda, K.; Nakane, D.; Takeda, M. *Org. Lett.* **2000,** *2,* 1903–1905. doi:10.1021/ol0059753
181. Albutt, A. D.; Ayer, W. A.; Brodie, H. J.; Johri, B. N.; Taube, H. *Can. J. Microbiol.* **1971,** *17,* 1401–1407. doi:10.1139/m71-223
182. Ayer, W. A.; Taube, H. *Tetrahedron Lett.* **1972,** *13,* 1917–1920. doi:10.1016/S0040-4039(01)84751-1
183. Ayer, W. A.; Taube, H. *Can. J. Chem.* **1973,** *51,* 3842–3854. doi:10.1139/v73-574
184. Ayer, W. A.; Lee, S. P. *Can. J. Chem.* **1979,** *57,* 3332–3337. doi:10.1139/v79-543
185. Ayer, W. A.; Carstens, L. L. *Can. J. Chem.* **1973,** *51,* 3157–3160. doi:10.1139/v73-470
186. Ayer, W. A.; Browne, L. A.; Mercer, J. R.; Taylor, D. R.; Ward, D. E. *Can. J. Chem.* **1978,** *56,* 717–721. doi:10.1139/v78-118
187. Ayer, W. A.; Yoshida, T.; van Schie, D. M. J. *Can. J. Chem.* **1978,** *56,* 2113–2120. doi:10.1139/v78-345
188. Ayer, W. A.; Nakashima, T. T.; Ward, D. E. *Can. J. Chem.* **1978,** *56,* 2197–2199. doi:10.1139/v78-360
189. Ayer, W. A.; Lee, S. P.; Nakashima, T. T. *Can. J. Chem.* **1979,** *57,* 3338–3343. doi:10.1139/v79-544
190. Swaminathan, S.; Narayanan, K. V. *Chem. Rev.* **1971,** *71,* 429–438. doi:10.1021/cr60273a001
191. Snider, B. B.; Rodini, D. J.; van Straten, J. *J. Am. Chem. Soc.* **1980,** *102,* 5872–5880. doi:10.1021/ja00538a028
192. Takeda, K.; Nakajima, A.; Takeda, M.; Yoshii, E.; Zhang, J.; Boeckmann, R. K., Jr. *Org. Synth.* **1999,** *76,* 199–213.
193. Gone, J. R.; Wallock, N. J.; Lindeman, S.; Donaldson, W. A. *Tetrahedron Lett.* **2009,** *50,* 1023–1025. doi:10.1016/j.tetlet.2008.12.051
194. Zhang, S.; Wang, J.; Xue, H.; Deng, Q.; Xing, F.; Ando, M. *J. Nat. Prod.* **2002,** *65,* 1927–1929. doi:10.1021/np0202632 See for two selected members of the guianolide family.
195. Zhang, S.; Zhao, M.; Bai, L.; Hasegawa, T.; Wang, J.; Wang, L.; Xue, H.; Deng, Q.; Xing, F.; Bai, Y.; Sakai, J.; Bai, J.; Koyanagi, R.; Tsukumo, Y.; Kataoka, R.; Nagai, K.; Hirose, K.; Ando, M. *J. Nat. Prod.* **2006,** *69,* 1425–1428. doi:10.1021/np068015j
196. Sarpong, R.; Su, J. T.; Stoltz, B. M. *J. Am. Chem. Soc.* **2003,** *125,* 13624–13625. doi:10.1021/ja037587c
197. Su, J. T.; Sarpong, R.; Stoltz, B. M.; Goddard, W. A., III. *J. Am. Chem. Soc.* **2004,** *126,* 24–25. doi:10.1021/ja037716p
198. Freeman, P. K.; Kuper, D. G. *Chem. Ind. (London)* **1965,** 424–425.
199. Wolff, L. *Justus Liebigs Ann. Chem.* **1902,** *325,* 129–195. doi:10.1002/jlac.19023250202
200. Tucker, J. W.; Stephenson, C. R. J. *Org. Lett.* **2011,** *13,* 5468–5471. doi:10.1021/ol202178t
201. Padwa, A.; Krumpe, K. E.; Gareau, Y.; Chiacchio, U. *J. Org. Chem.* **1991,** *56,* 2523–2530. doi:10.1021/jo00007a047
202. Takada, Y.; Nomura, K.; Matsubara, S. *Org. Lett.* **2010,** *12,* 5204–5205. doi:10.1021/ol102237b
203. Mauleón, P.; Krinsky, J. L.; Toste, F. D. *J. Am. Chem. Soc.* **2009,** *131,* 4513–4520. doi:10.1021/ja900456m
204. Miki, K.; Ohe, K.; Uemura, S. *J. Org. Chem.* **2003,** *68,* 8505–8513. doi:10.1021/jo034841a
205. Gorin, D. J.; Watson, I. D. G.; Toste, F. D. *J. Am. Chem. Soc.* **2008,** *130,* 3736–3737. doi:10.1021/ja710990d
206. Garayalde, D.; Krüger, K.; Nevado, C. *Angew. Chem., Int. Ed.* **2011,** *50,* 911–915. doi:10.1002/anie.201006105
207. Jiménez-Núñez, E. J.; Raducan, M.; Lauterbach, T.; Molawi, K.; Solorio, C. R.; Echavarren, A. M. *Angew. Chem., Int. Ed.* **2009,** *48,* 6152–6155. doi:10.1002/anie.200902248
208. Gung, B. W.; Bailey, L. N.; Wosner, J. *Tetrahedron Lett.* **2010,** *51,* 2251–2253. doi:10.1016/j.tetlet.2010.02.099
209. Kusama, H.; Onizawa, Y.; Iwasawa, N. *J. Am. Chem. Soc.* **2006,** *128,* 16500–16501. doi:10.1021/ja0671924
210. Kim, S. Y.; Park, Y.; Chung, Y. K. *Angew. Chem., Int. Ed.* **2010,** *49,* 415–418. doi:10.1002/anie.200905361
211. Cao, Z.; Gagosz, F. *Angew. Chem., Int. Ed.* **2013,** *52,* 9014–9018. doi:10.1002/anie.201304497
212. Levin, S.; Nani, R. R.; Reisman, S. E. *J. Am. Chem. Soc.* **2011,** *133,* 774–776. doi:10.1021/ja110192b
213. Aoyagi, Y.; Yamazaki, A.; Nakatsugawa, C.; Fukaya, H.; Takeya, K.; Kawauchi, S.; Izumi, H. *Org. Lett.* **2008,** *10,* 4429–4432. doi:10.1021/ol801620u
214. Yamamoto, Y.; Arakawa, T.; Ogawa, R.; Itoh, K. *J. Am. Chem. Soc.* **2003,** *125,* 12143–12160. doi:10.1021/ja0358697
215. Bachmann, W. E.; Struve, W. S. *Org. React.* **1942,** *1,* 38–62.
216. Goddard-Boger, E. D.; Stick, R. V. *Org. Lett.* **2007,** *9,* 3797–3800. doi:10.1021/ol701581g
217. Boeckman, R. K., Jr.; Shair, M. D.; Vargas, J. R.; Stolz, L. A. *J. Org. Chem.* **1993,** *58,* 1295–1297. doi:10.1021/jo00058a001
218. Salmond, W. G.; Barta, M. A.; Havens, J. L. *J. Org. Chem.* **1978,** *43,* 2057–2059. doi:10.1021/jo00404a049

219. Clark, D. L.; Chou, W. N.; White, J. B. *J. Org. Chem.* **1990,** *55,* 3975–3977. doi:10.1021/jo00300a005
220. Chou, W. N.; White, J. B.; Smith, W. B. *J. Am. Chem. Soc.* **1992,** *114,* 4658–4667. doi:10.1021/ja00038a032
221. von Zezschwitz, P.; Voigt, K.; Lansky, A.; Noltemeyer, M.; de Meijere, A. *J. Org. Chem.* **1999,** *64,* 3806–3812. doi:10.1021/jo981496u
222. Xu, X.; Hu, W.-H.; Zavalij, P. Y.; Doyle, M. P. *Angew. Chem., Int. Ed.* **2011,** *50,* 11152–11155. doi:10.1002/anie.201105557
223. Lee, Y. R.; Hwang, J. C. *Eur. J. Org. Chem.* **2005,** 1568–1577. doi:10.1002/ejoc.200400452
224. Doyle, M. P.; Hu, W.; Timmons, D. J. *Org. Lett.* **2001,** *3,* 3741–3744. doi:10.1021/ol016703i
225. Doyle, M. P.; Hu, W.; Timmons, D. J. *Org. Lett.* **2001,** *3,* 933–935. doi:10.1021/ol015600x
226. Doyle, M. P.; Yan, M.; Hu, W.; Gronenberg, L. S. *J. Am. Chem. Soc.* **2003,** *125,* 4692–4693. doi:10.1021/ja029745q
227. Müller, P.; Toujas, J.-L.; Bernardinelli, G. *Helv. Chim. Acta* **2000,** *83,* 1525–1534. doi:10.1002/1522-2675(20000705)83:7<1525::AID-HLCA1525>3.0.CO;2-1
228. Müller, P.; Imogai, H. *Helv. Chim. Acta* **1999,** *82,* 315–322. doi:10.1002/(SICI)1522-2675(19990310)82:3<315::AID-HLCA315>3.0.CO;2-T
229. Boeckman, R. K., Jr.; Reeder, M. R. *J. Org. Chem.* **1997,** *62,* 6456–6457. doi:10.1021/jo9712254
230. Boeckman, R. K., Jr.; Zhang, J.; Reeder, M. R. *Org. Lett.* **2002,** *4,* 3891–3894. doi:10.1021/ol0267174
231. Boeckman, R. K., Jr.; Genung, N. E.; Chen, K.; Ryder, T. R. *Org. Lett.* **2010,** *12,* 1628–1631. doi:10.1021/ol100397q

License and Terms

This is an Open Access article under the terms of the Creative Commons Attribution License (http://creativecommons.org/licenses/by/2.0), which permits unrestricted use, distribution, and reproduction in any medium, provided the original work is properly cited.

The license is subject to the *Beilstein Journal of Organic Chemistry* terms and conditions: (http://www.beilstein-journals.org/bjoc)

The definitive version of this article is the electronic one which can be found at: doi:10.3762/bjoc.10.14

Beilstein Journal of Organic Chemistry

Synthesis of the B-*seco* limonoid core scaffold

Hanna Bruss[1,2], Hannah Schuster[1,2], Rémi Martinez[1], Markus Kaiser[3], Andrey P. Antonchick[1,2] and Herbert Waldmann[*1,2]

Full Research Paper

Open Access

Address:
[1]Abteilung Chemische Biologie, Max-Planck-Institut für Molekulare Physiologie, Otto-Hahn-Straße 11, 44227 Dortmund, Germany, [2]Fakultät für Chemie und Chemische Biologie, Technische Universität Dortmund, Otto-Hahn-Straße 6, 44227 Dortmund, Germany and [3]Chemical Biology, Zentrum für Medizinische Biotechnologie, Fakultät für Biologie, Universität Duisburg-Essen, Universitätsstraße 2, 45117 Essen, Germany

Email:
Herbert Waldmann* - herbert.waldmann@mpi-dortmund.mpg.de

* Corresponding author

Keywords:
B-*seco* limonoids; biology oriented synthesis; Ireland–Claisen rearrangement; natural products; tetranortriterpenoids

Beilstein J. Org. Chem. **2014,** *10,* 194–208.
doi:10.3762/bjoc.10.15

Received: 30 September 2013
Accepted: 10 December 2013
Published: 16 January 2014

This article is part of the Thematic Series "Natural products in synthesis and biosynthesis".

Guest Editor: J. S. Dickschat

© 2014 Bruss et al; licensee Beilstein-Institut.
License and terms: see end of document.

Abstract

Synthetic investigations towards the structurally complex and highly decorated framework of B-*seco* limonoid natural products by means of a [3,3]-sigmatropic rearrangement are described. Detailed model studies reveal, that an Ireland–Claisen rearrangement can be employed to construct the central C9–C10 bond thereby giving access to the B-*seco* limonoid scaffold. However, application of the developed strategy ended up failing in more complex and sterically demanding systems.

Introduction

B-*seco* limonoids are a family of more than 100 highly oxygenated plant tetranortriterpenoids derived from the 4,4,8-trimethyl-17-furanylsteroid core structure **I** (Figure 1) [1-3]. Members of this natural product class, like 21-hydroxytoonacilide (**1**) [4,5] and prieurianin (**2**) [6-16] display antifeedant [6,7,17-21], antimalaria and anticancer [10,11,22-25] as well as diverse further bioactivities. Recently it was discovered that prieurianin (**2**) impairs the actin cytoskeleton by a mechanism that does not involve direct interaction with actin suggesting that its mode of action differs from previously known modulators [26].

B-*seco* limonoids constitute exceptionally challenging synthesis targets, as the characteristic structural features are a compact, highly oxygenated as well as richly decorated framework and stereochemically dense functionalization. In all B-*seco* limonoids an A ring is linked by a C–C bond to a *trans*-fused bicyclic C–D ring having an *exo*-methylene moiety. The crowded C9–C10 bond bridging the two domains is the main synthetic obstacle.

Taking into account the biology-oriented synthesis (BIOS) concept [27-34], which employs the scaffolds of biologically

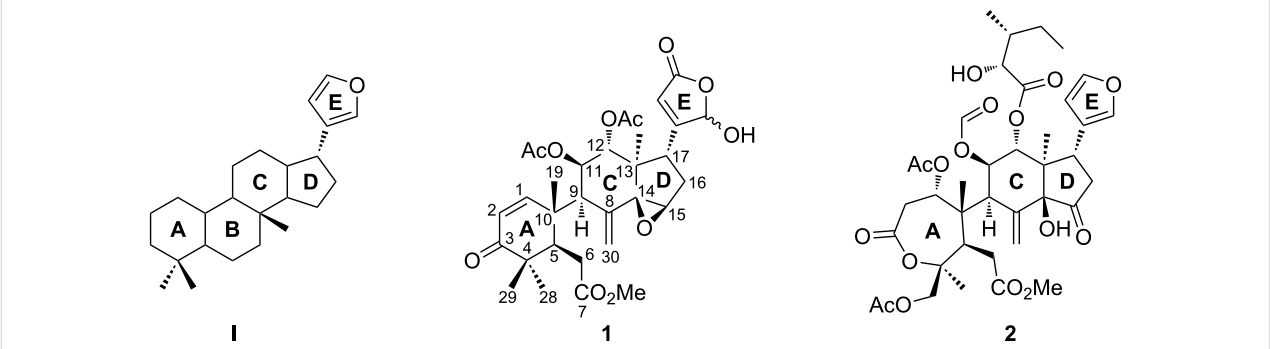


Figure 1: Structures of the 4,4,8-trimethyl-17-furanylsteroid core structure **I** and the representative B-*seco* limonoids 21-hydroxytoonacilide (**1**) and prieurianin (**2**).

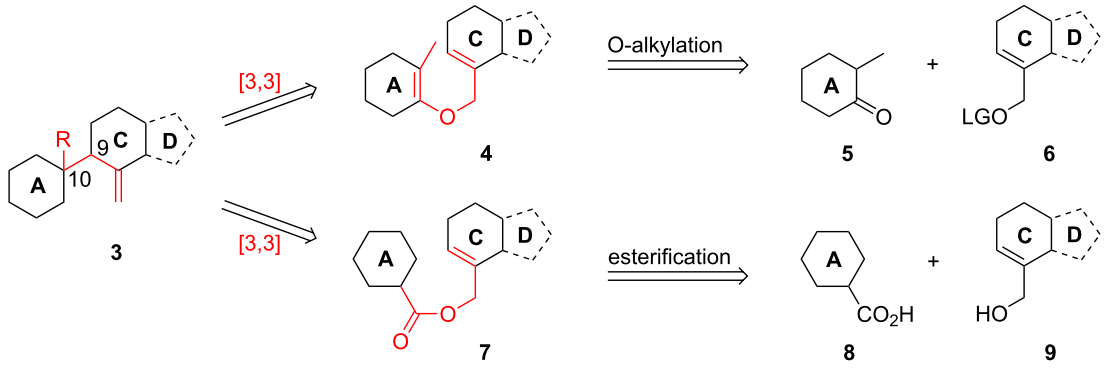
relevant natural product classes to inspire the synthesis of probes and reagents for chemical biology and medicinal chemistry research, we aimed at the development of a synthetic strategy to get access to the B-*seco* limonoid scaffold by means of a [3,3]-sigmatropic rearrangement as key step enabling the formation of the crucial C9–C10 bond (Scheme 1) [35]. In this paper we present a full report on this synthesis [36] as well as further synthetic studies towards the application of the developed strategy to the total synthesis of B-*seco* limonoid natural products.

Results and Discussion

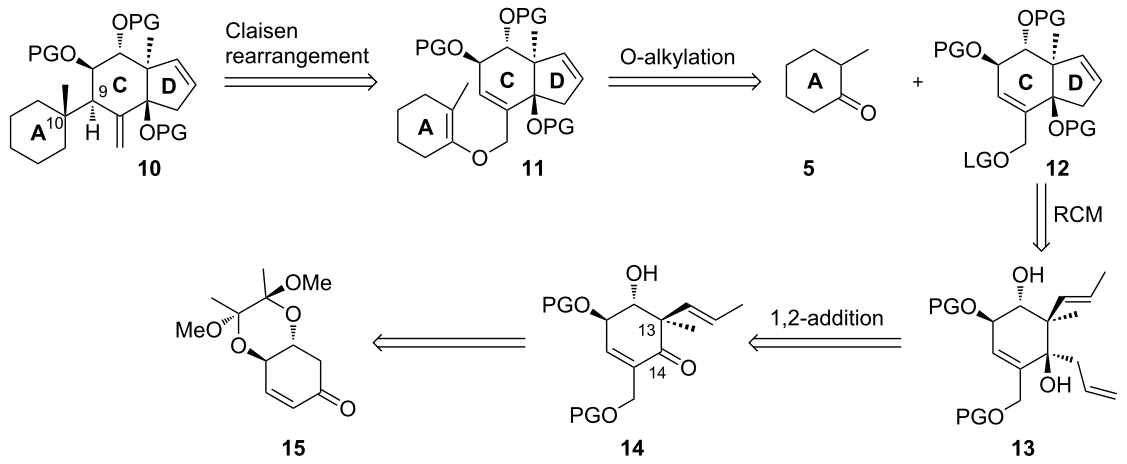
Retrosynthetic analysis: Claisen rearrangement. In planning the synthesis we were inspired by Ley's synthesis of azadirachtin in which a Claisen rearrangement has been successfully employed as key transformation [37,38]. Thus the allyl vinyl ether rearrangement precursor **11** was thought to be obtained from an O-alkylation between the thermodynamic enolate of 2-methylcyclohexanone (**5**) and the bicyclic electrophile **12** (Scheme 2). A challenging synthetic problem appears to be the construction of the stereochemically dense *trans*-fused C–D ring system **12**, which possesses four stereogenic centers including two contiguous asymmetric quaternary centers at the ring junction. We decided to start the sequence with known enone **15** [39] and intended to construct the all-carbon quaternary center at C13 by substrate controlled α-functionalization. The second quaternary center at C14 might be established by 1,2-addition and finally, ring-closing metathesis would give rise to bicyclic system **12**.

Model studies towards the Claisen rearrangement. As the stereochemical substitution on the C ring system will have a major impact on the face selectivity of the planned Claisen rearrangement we defined precursors **19**, **20** and **22** (Scheme 3) as suitable model systems, presenting appropriate stereogenic substitution at the C ring system. After merging these alcohols with an undecorated A ring, the resulting allyl vinyl ethers could serve as suitable rearrangement precursors.

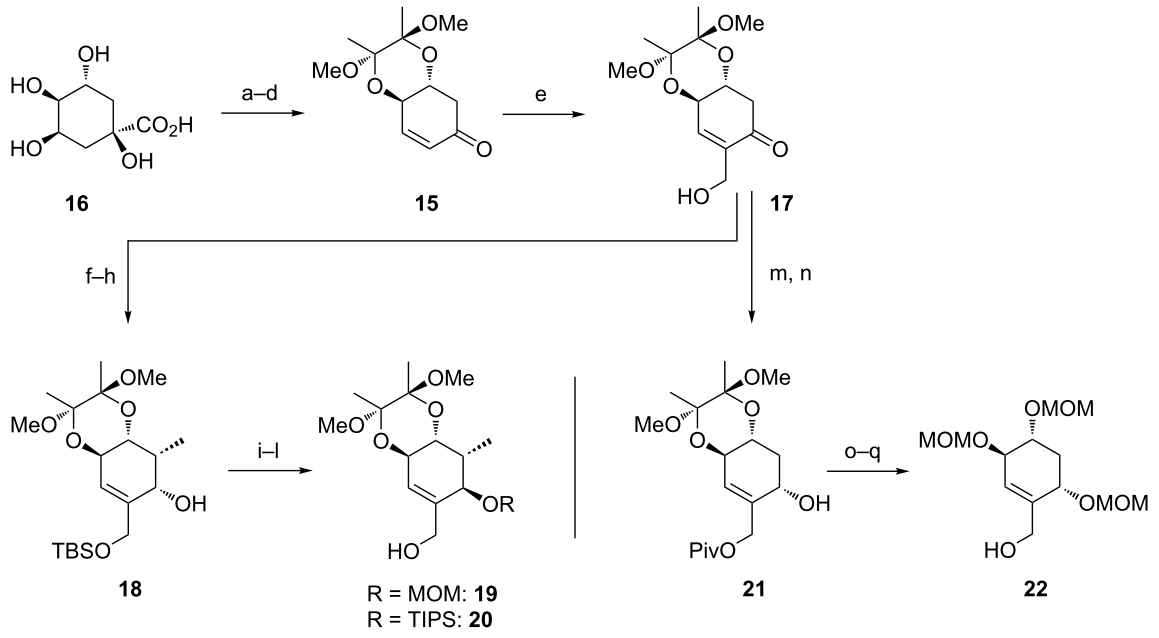
The synthesis of **19** and **20** commenced with enone **15** [39], which was prepared from (−)-quinic acid (**16**) according to the route reported by Arthurs et al. [40] with minor modifications. After Baylis–Hillman reaction and subsequent silylation of the resulting free primary hydroxy group, substrate-controlled



Scheme 1: Retrosynthetic analysis of the B-*seco* limonoid framework employing a [3,3]-sigmatropic rearrangement for formation of the C9–C10 bond. R = Me or CO_2H, LG = leaving group.



Scheme 2: Retrosynthetic analysis of the B-*seco* limonoid scaffold employing a Claisen rearrangement as key step for formation of the C9–C10 bond. PG = protecting group, LG = leaving group.



Scheme 3: Synthesis of alcohols **19**, **20** and **22**. Reagents and conditions: a) CSA, 2,3-butanedione, trimethyl orthoformate, MeOH, reflux, 16 h, 93%; b) $NaBH_4$, MeOH, rt, 0.5 h, quant.; c) silica-gel supported $NaIO_4$, CH_2Cl_2/MeOH (20:1), rt, 3 h, quant.; d) MsCl, NEt_3, CH_2Cl_2, 0 °C to rt, 3 h, quant.; e) paraformaldehyde, imidazole, THF/1 M $NaHCO_3$ (1:1), rt, 2.5 h, 74%; f) TBSOTf, 2,6-lutidine, CH_2Cl_2, 0 °C, 15 min, quant.; g) LiHMDS, MeI, THF/DMPU (5:1), −78 °C to −10 °C, 91%, de = 100%; h) $NaBH_4$, $CeCl_3{\cdot}7H_2O$, MeOH, 0 °C, 15 min, 90%, de = 100%; i) PPh_3, *p*-nitrobenzoic acid, DEAD, toluene, rt, 18 h; j) MeOH, Et_2O, aqueous saturated K_2CO_3 solution, rt, 1 h, 64% (2 steps); for the synthesis of **19**: k) DIPEA, MOMCl, CH_2Cl_2, reflux, 16 h, 99%; l) TBAF, THF, rt, 20 min, 94%; for the synthesis of **20**: k) TIPSOTf, 2,6-lutidine, DMF, 0 °C to rt, 3 h, quant.; l) PTSA, MeOH, THF, rt, 30 h, 77%; m) PivCl, DMAP, pyridine, −15 °C to rt, 2 h, 77%; n) $NaBH_4$, $CeCl_3{\cdot}7H_2O$, MeOH, 0 °C to rt, 30 min, 96%, de = 100%; o) TFA, H_2O, rt, 5 min, 72%; p) DIPEA, MOMCl, CH_2Cl_2, reflux, 15 h, 62%; q) DIBAL-H, CH_2Cl_2, −78 °C to rt, 2 h, quant.

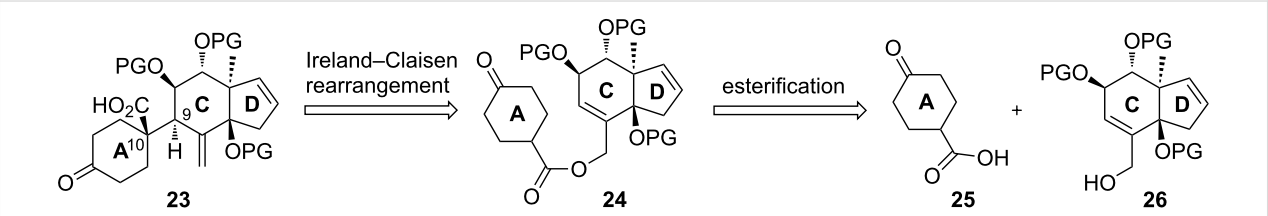
α-methylation of the lithium enolate proceeded with full stereocontrol [41,42], which can be explained by the strong conformational rigidity of the butane-2,3-diacetal (BDA) protected *trans*-diequatorial diols [43] and the stereoelectronic preference for axial attack on the electron-rich C13. Luche reduction with stereoelectronically preferred axial attack of the hydride gave alcohol **18** and Mitsunobu reaction installed the required stereochemistry at C14. The free C14 hydroxy group was masked with protecting groups (MOM and TIPS) of different size and chemical nature to examine the *face*-selectivity of the [3,3]-sigmatropic rearrangement. After selective desilylation, alcohols **19** and **20** were obtained.

In order to synthesize a model substrate without the rigid BDA-protecting group, compound **21** was treated with aqueous TFA to give a triol which was masked with three MOM-protecting groups (Scheme 3). Reductive cleavage of the pivaloyl group furnished alcohol **22**.

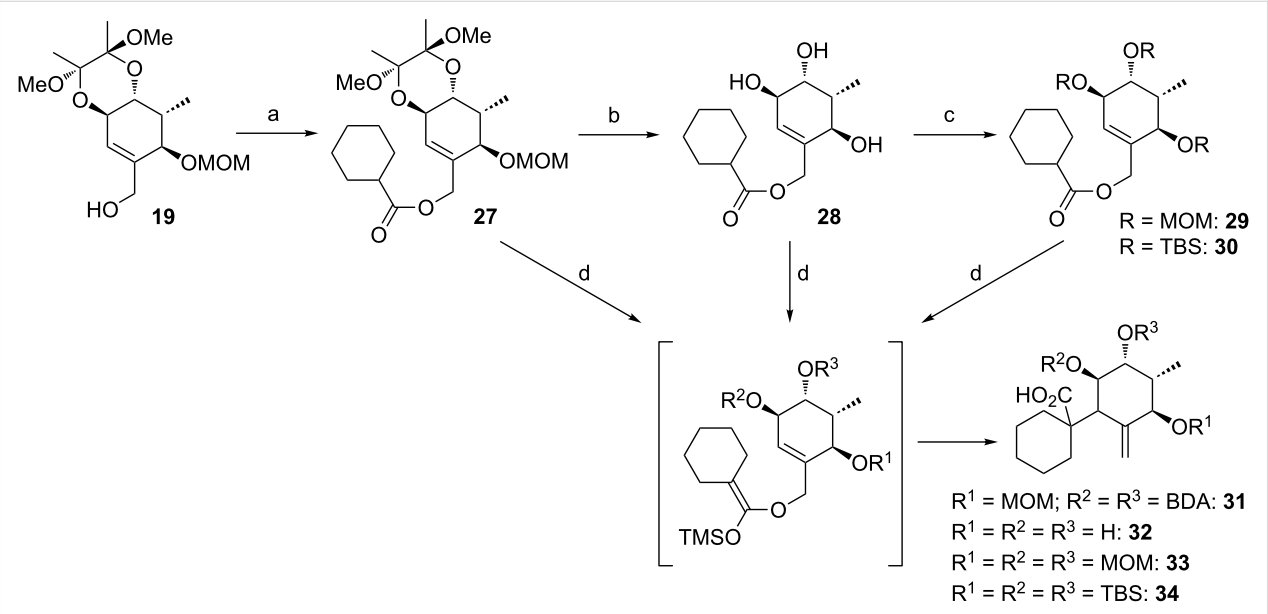
Mesylation or tosylation of the primary alcohols in **19**, **20** and **22** gave suitable electrophiles for the planned O-alkylation with the thermodynamic enolate of 2-methylcyclohexanone. However, under various conditions (NaH/15-crown-5/THF; *t*-BuOK/18-crown-6/THF/DMPU; KHMDS/THF) [44,45], the intended O-alkylation to yield the allyl vinyl ether failed. Equally, copper-catalyzed C–O couplings [46] of the alcohols **19**, **20** and **22** with organotrifluoroborates failed or gave only low yields. Likewise Buchwald's procedure for the copper-catalyzed coupling of primary alcohols with vinyl iodides to yield the allyl vinyl ether or, depending on the reaction conditions, directly the Claisen rearrangement products was not successful [47].

Alternative strategy: Ireland–Claisen rearrangement. As the Claisen rearrangement precursor, the allyl vinyl ether, could not be obtained under various conditions, we had to change the synthetic strategy and employed the Ireland variant of the Claisen rearrangement to construct the crucial C9–C10 bond (Scheme 4). In this strategy the A-ring **25** could be merged with the bicyclic C–D system **26** by esterification in order to obtain the allyl ester rearrangement precursor **24**. Murai et al. [48] showed the utility of an Ireland–Claisen rearrangement in their model studies addressing the limonoid framework of azadirachtin.

Model studies towards the Ireland–Claisen rearrangement. To test the feasibility of this approach, model rearrangement precursor **27** was prepared from alcohol **19** (Scheme 5). Esterification with cyclohexanecarboxylic acid gave the desired allyl ester **27**. Furthermore, to investigate the influence of the protecting groups at C11, C12 and C14 on the stereoselectivity and reaction rate, the allyl esters **28**, **29** and **30** were prepared.



Scheme 4: Retrosynthetic analysis of the B-*seco* limonoid scaffold employing an Ireland–Claisen rearrangement as the key step for the formation of the C9–C10 bond. PG = protecting group.



Scheme 5: Synthesis and Ireland–Claisen rearrangement of the allyl esters **27**, **28**, **29** and **30**. Reagents and conditions: a) DCC, DMAP, cyclohexanecarboxylic acid, CH_2Cl_2, rt, 4 h; b) TFA/H_2O (3:1), rt, 30 min, 73% (2 steps); for the synthesis of **29**: c) DIPEA, MOMCl, CH_2Cl_2, 40 °C, 15 h, 86%; for the synthesis of **30**: c) imidazole, TBSCl, CH_2Cl_2, rt, 21 h, 45%; d) KHMDS, TMSCl, toluene, −78 °C to 85 °C, 18 h. Results: see Table 1.

The four rearrangement precursors **27**, **28**, **29** and **30** were exposed to KHMDS and TMSCl in toluene, in order to induce the Ireland–Claisen rearrangement (Scheme 5, Table 1). The rigid BDA protecting group at C11 and C12 in **27** was not compatible with these conditions, resulting in only cleavage of the ester moiety (Table 1, entry 1). In case of the unprotected rearrangement precursor **28** an excess of base and TMSCl was used for in situ protection of the three free hydroxy groups as TMS ether, but the desired [3,3]-sigmatropic rearrangement could not be induced (Table 1, entry 2). However rearrangement of *tris*-MOM ether **29** as well as *tris*-TBS ether **30** gave the desired carboxylic acids **33** and **34** in high yield and excellent diastereoselectivity (Table 1, entries 3 and 4).

Table 1: Ireland–Claisen rearrangement of model compounds **27**, **28**, **29** and **30**.

entry	rearrangement precursor	result
1	**27**	cleavage of the ester moiety
2	**28**	no conversion
3	**29**	89% yield of **33** (de = 76%)
4	**30**	quant. yield of **34** (de = 100%)

In view of the stereochemistry of the major diastereomers of the products, the rearrangement would occur from the *re*-face (transition state **A**, Figure 2). Thus, assuming the OTBS group in **30** at C14 is pseudo-axial to avoid allylic $A^{1,2}$-strain, the sigmatropic rearrangement occurred via a pseudo-axial attack of the silyl ketene acetal on the double bond in the cyclohexene ring. These results are in accordance with the observations of Ireland et al. [49], who examined the propensity for axial versus equatorial attack in the rearrangement of cyclohexenyl acetates and observed a strong preference for the stereochemically controlled axial approach. The size of the protecting groups had a strong influence on the face-selectivity, furnishing in case of the TBS derivative only one diastereomer. By substitution of C14 with a bulky group (1,2-allylic strain) the ring inversion barrier of the cyclohexene conformations might be increased, resulting in higher de values.

These model studies suggested that an Ireland–Claisen rearrangement is a feasible strategy to construct the C9–C10 bond in B-*seco* limonoids.

In order to perform further model studies, we established a straight forward synthetic access to model substrates without the BDA group (Scheme 6). With the TBDPS- instead of the TBS ether on the primary hydroxy group, the BDA group in alcohol **35** could be selectively cleaved by treatment with TFA

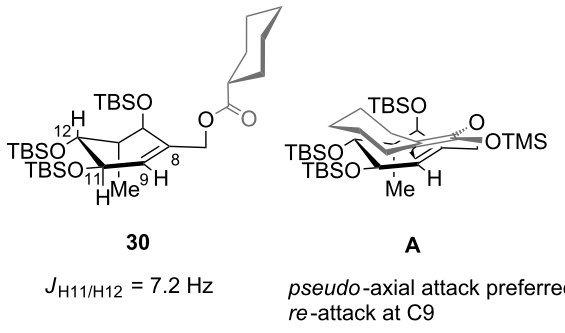
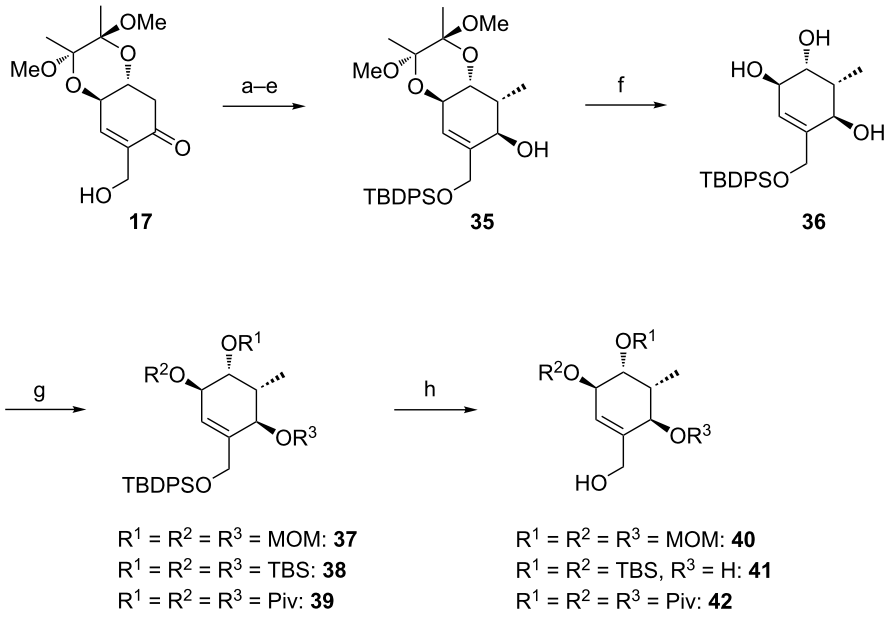


Figure 2: Conformation of rearrangement precursor **30** and possible transition state involved in the Ireland–Claisen rearrangement.

in aqueous CH_2Cl_2 to release triol **36**, which was masked with different protecting groups (MOM, TBS, Piv). After desilylation, the liberated alcohols **40**, **41** and **42** could be esterified with various cyclic and acyclic model A rings to give the targeted rearrangement precursors **A** (Scheme 6, Table 2).

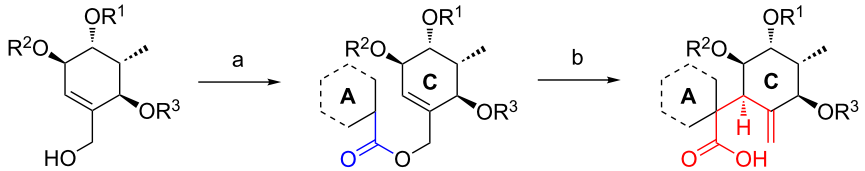
The obtained rearrangement precursors were submitted to the Ireland–Claisen rearrangement conditions and gave the desired carboxylic acids **B** in excellent yield and diastereoselectivity (Scheme 6, Table 2). The presence of the keto functionality in **43** is compatible with the rearrangement conditions (Table 2, entry 1). Intermediary, the silyl enol ether and the silyl ketene acetal are formed. However, after the rearrangement, the keto-functionality can be set free again during an acidic work-up. In terms of yield and diastereoselectivity there was no difference observed between rearrangements with derivatives with a cyclic or acyclic model A ring. Rearrangement precursor **51** containing a free hydroxy group could not be converted into the desired carboxylic acid (Table 2, entry 5). Under the same conditions but by using an excess of base and TMSCl for the in situ protection of the free hydroxy group, only the starting material could be reisolated.

Encouraged by these findings we attempted to perform the [3,3]-sigmatropic rearrangement with C1-substituted A rings, as many B-*seco* limonoids are oxygenated at this position. For this purpose, both the *anti*- and *syn*-substituted β-alkoxy esters **56** and **57** were synthesized (Scheme 7; for experimental procedure see Supporting Information File 1). In the literature [50] not many examples are known in which β-alkoxy esters serve as rearrangement precursors as the β-elimination of the alkoxy group can easily occur under the rearrangement conditions. Indeed, under various conditions by using different bases (LDA, LiHMDS, KHMDS) and solvents (THF, toluene, THF/DMPU) and by carefully controlling the reaction conditions (deprotona-



Scheme 6: Synthesis of model C rings **40**, **41** and **42**. Reagents and conditions: a) TBDPSCl, DMAP, NEt_3, CH_2Cl_2, rt, 18 h, 93%; b) LiHMDS, MeI, THF/DMPU (10:1), −78 °C to 0 °C, 1.5 h, 98%; c) $CeCl_3{\cdot}7H_2O$, $NaBH_4$, MeOH, 0 °C, 15 min, 86%; d) Ph_3P, *p*-nitrobenzoic acid, DEAD, toluene, 15 h; e) MeOH, Et_2O, aqueous saturated K_2CO_3-solution, rt, 2 h, 85% (2 steps); f) CH_2Cl_2/TFA/H_2O (2:1:0.1), rt, 10 min, 85%; for the synthesis of **37**: g) DIPEA, MOMCl, NaI, THF, 65 °C, 4.5 h, 98%; for the synthesis of **38** g) TBSCl, imidazole, DMF, rt, 18 h, 92%; for the synthesis of **39**: PivCl, DMAP, pyridine, rt, 4 d, 78%; for the synthesis of **40**: h) **37**, TBAF, THF, rt, 2 h, 95%; for the synthesis of **41**: h) **38**, 10% NaOH/MeOH, reflux, 6.5 h, 72%; for the synthesis of **42**: h) **39**, HF·pyridine, THF, rt, 24 h, 71%.

Table 2: Esterification of alcohols **40**, **41** and **42** and Ireland–Claisen rearrangement. Reagents and conditions: a) EDC·HCl, DMAP, carboxylic acid, CH_2Cl_2, rt, 15–22 h; for **52**: silylation of the free hydroxy group at C14: imidazole, TBSCl, DMAP, DMF, rt, 40 h; b) KHMDS, TMSCl, toluene, −78 °C to 85 °C, ca. 18 h.



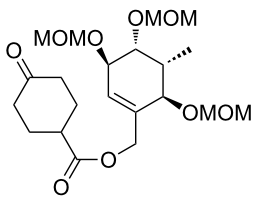
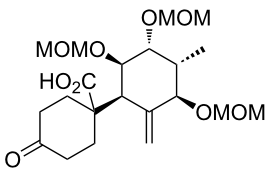
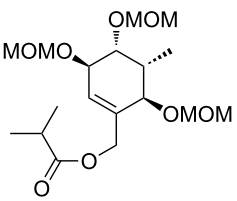
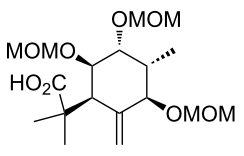
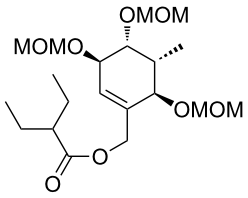
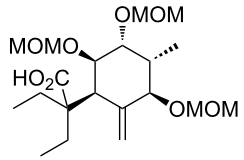
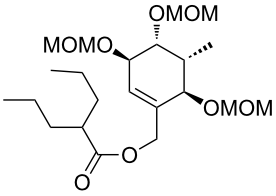
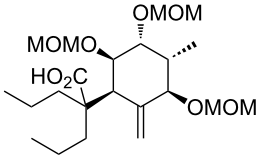
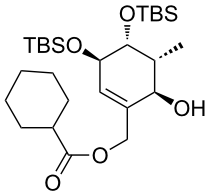
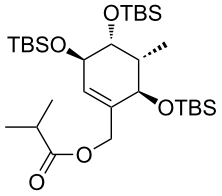
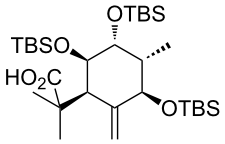
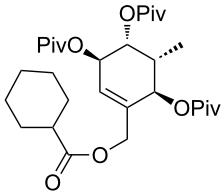
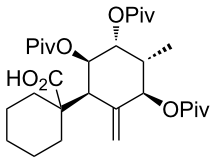
entry	alcohol	allyl ester **A**	carboxylic acid **B**
1	**40**	 **43** (87% yield)	 **44** (75% yield, de = 80%)
2	**40**	 **45** (81% yield)	 **46** (93% yield, de = 78%)

Table 2: Esterification of alcohols **40**, **41** and **42** and Ireland–Claisen rearrangement. Reagents and conditions: a) EDC·HCl, DMAP, carboxylic acid, CH_2Cl_2, rt, 15–22 h; for **52**: silylation of the free hydroxy group at C14: imidazole, TBSCl, DMAP, DMF, rt, 40 h; b) KHMDS, TMSCl, toluene, −78 °C to 85 °C, ca. 18 h. (continued)

3	**40**	 **47** (93% yield)	 **48** (quant. yield, de = 72%)
4	**40**	 **49** (quant. yield)	 **50** (95% yield, de = 72%)
5	**41**	 **51** (79% yield)	–
6	**41**	 **52** (78% yield, 2 steps)	 **53** (quant. yield, de = 94%)
7	**42**	 **54** (95% yield)	 **55** (90% yield, de = 94%)

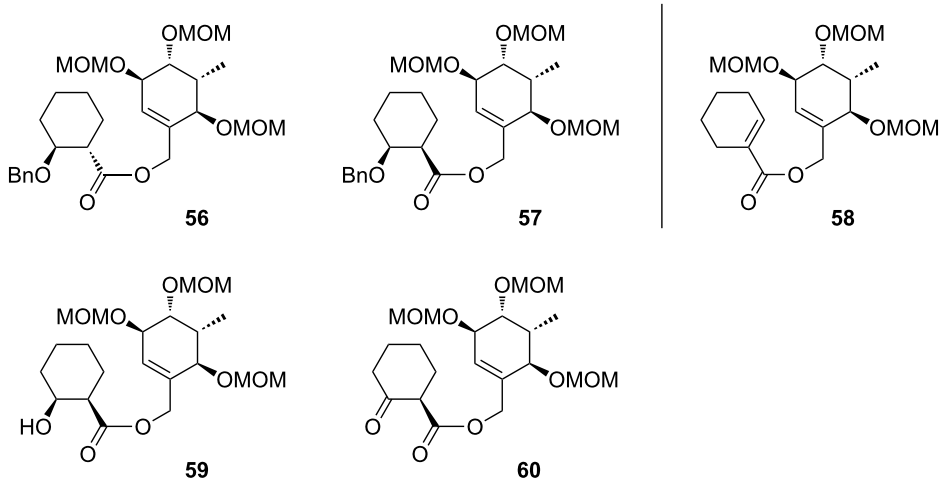
tion at low temperature (−100 °C), gradual warming of the reaction mixture), only the elimination product **58** could be isolated.

Furthermore, a dianionic Ireland–Claisen rearrangement employing β-hydroxy ester **59** was unsuccessful (Scheme 7). Under various conditions, we observed only decomposition of the starting material by cleavage of the ester moiety. Likewise, cleavage of the ester moiety occurred in an attempt to perform a Carroll rearrangement with β-keto ester **60**.

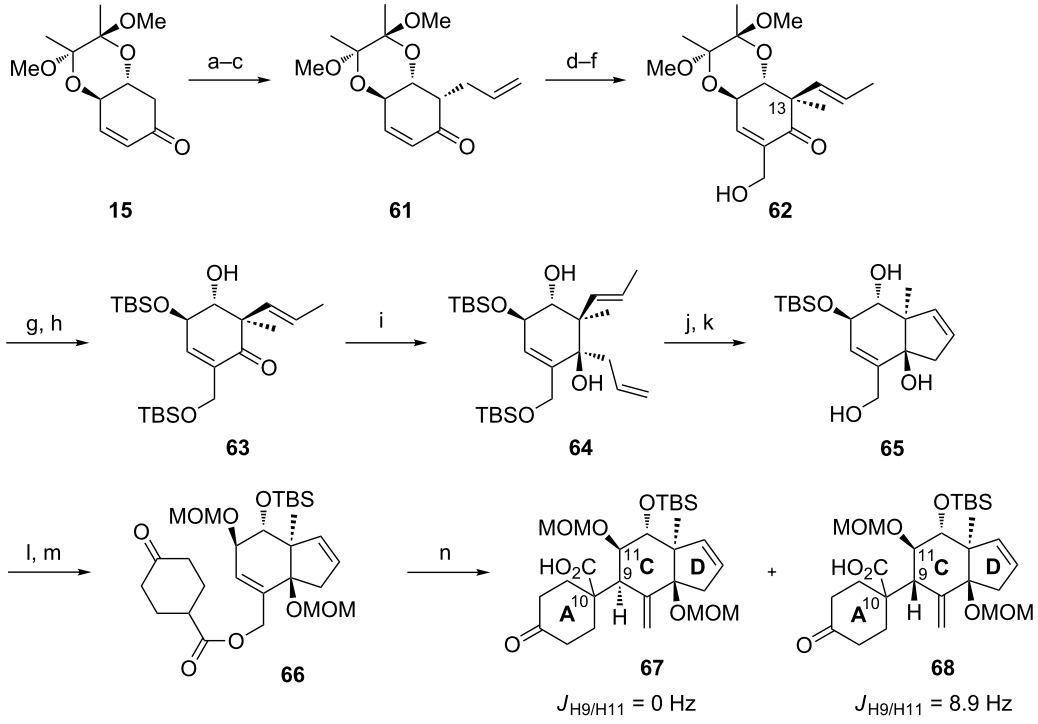
These studies show that it might be necessary to oxygenate at C1 after the sigmatropic rearrangement because the C1 substitution seems to have major impact on the success of the rearrangement.

Synthesis of the B-*seco* limonoid scaffold. Encouraged by the results of the rearrangements of the model substrates with an undecorated A ring, we attempted to access the B-*seco* limonoid scaffold by an analogous rearrangement of bicyclic precursor **66** (Scheme 8).

The elaboration of the required bicyclic system commenced with enone **15** (Scheme 8). Initially, we envisaged an α-vinylation via Buchwald's procedure for the catalytic asymmetric



Scheme 7: β-Substituted allyl esters tested in the Ireland–Claisen and the Carroll rearrangement.



Scheme 8: Synthesis and Ireland–Claisen rearrangement of bicyclic allyl ester precursor **66**. Reagents and conditions: a) LiHMDS, TMSCl, THF, −78 °C to 0 °C, 90 min; b) NBS, THF, 0 °C, 90 min, 68% (2 steps); c) allyltributyltin, AIBN, toluene, 80 °C, 18 h, 81%, de = 80%; d) KHMDS, THF, −78 °C, 1 h, then MeI, rt, 20 min, 74%, de = 100%; e) $PdCl_2(CH_3CN)_2$, toluene, 65 °C, 2 days, 70% (81% brsm); f) paraformaldehyde, imidazole, THF/1 M $NaHCO_3$ (2:1), rt, 19 h, 74%; g) TFA/H_2O (3:1), rt, 30 min, 84%; h) TBSCl, imidazole, DMF, rt, 18 h, 94%; i) tetraallyltin, BuLi, THF, −78 °C to rt, 30 min, 72%, dr = ca. 2:1; j) Grubbs I, CH_2Cl_2, rt, 18 h, 80%; k) HF·pyridine, THF, 0 °C to rt, 20 h, 99%; l) EDC·HCl, 4-oxocyclohexanecarboxylic acid (**25**), DMAP, CH_2Cl_2, rt, 16 h, 80%; m) DIPEA, MOMCl, NaI, THF, 50 °C, 21 h, 62%; n) LiHMDS, supernatant of a centrifuged mixture of TMSCl/NEt_3 (v/v = 1:1) and toluene, toluene, −78 °C to 65 °C in 6 h, 60 h at 65 °C, 88% yield, dr = 1:2 (**67**:**68**).

vinylation of enones [51]. However, the desired vinylated product could not be obtained under the described conditions. An alternative α-formylation/Wittig olefination sequence gave only low yields. O'Brien et al. [41] described the failure of a direct alkylation of the lithium enolate of **15** with alkyl halides under several conditions. They incorporated an α-allyl side chain via an α-bromo-enone, which can be obtained from an initially formed silyl enol ether, and subsequent reaction with NBS.

Keck allylation of the α-bromo-enone using allyltributyltin and AIBN gave the desired α-allylated product **61**. We used the high substrate control to construct the first quaternary center at C13 by trapping the potassium enolate of **61** with MeI, furnishing the desired product as a single diastereomer. Isomerization of the terminal double bond with cat. $PdCl_2(CH_3CN)_2$ and Baylis–Hillman reaction proceeded uneventfully to afford compound **62**. Deprotection of the butane-2,3-diacetal under acidic conditions followed by selective silylation of the primary and the allylic hydroxy groups gave alcohol **63**.

The second quaternary center of the bicyclic C–D system **66** was envisaged to be constructed by 1,2-addition, using the free β-hydroxy functionality in **63** as directing group. Several conditions with allyl boronates, stannanes, silanes, indium, magnesium bromide, cerium, zinc bromide and other reagents have been screened. Finally, the best result was achieved with tetraallyltin and BuLi affording a 2:1 mixture of diastereomers, with the desired diastereomer being the minor product. The stereochemistry was unambiguously confirmed by crystal structure analysis of a derivative of the major diastereomer [36]. Thus, the preference for the axial attack predominates the aimed directing effect of the β-hydroxy group.

Bicyclic system **65** could be obtained by ring-closing metathesis using Grubbs 1st generation catalyst and subsequent selective deprotection of the primary silyl ether. After esterification with 4-oxocyclohexanecarboxylic acid (**25**) and protection of the remaining two free hydroxy groups as MOM ethers, which was accompanied by silyl migration, the synthesis of rearrangement precursor **66** was completed.

Application of the developed reaction conditions for the rearrangement of the model systems was fruitless, resulting in only cleavage of the ester moiety. Crucial for the success of the envisaged Ireland–Claisen rearrangement was a gradual warming of the reaction mixture from −78 °C to 65 °C over a period of 6 h and the addition of the supernatant of a centrifuged mixture of TMSCl, NEt_3 and toluene instead of the addition of unactivated TMSCl. When **66** was exposed to TMSCl/NEt_3 and LiHMDS in toluene, the intended rearrangement occurred smoothly giving rise to **67** and **68** (ca. 1:2 ratio, 88% combined yield) through the desired C9–C10 bond formation (Scheme 8). The configuration of the diastereomers was determined based on the analysis of the coupling constants of H9 and H11 and nOe signal enhancements.

In contrast to the high face-selectivity in the rearrangement of the model systems, the reaction seems to take place from both sides of the bicyclic C–D system. However, in this case the *si*-face approach appears to be favoured (transition state **C**, Figure 3a). This might be explained by the rigidity of the bicyclic system, such that transition states **B** and **C** can compete without preference for a conformation that clearly favours axial attack. Underscored by MM2 conformational calculations, it is furthermore plausible that the C11 oxygen can form an H-bond to the terminal methyl C–H of the C14 MOM group, thus blocking a pseudo-axial approach and leading to the observed reversal in selectivity.

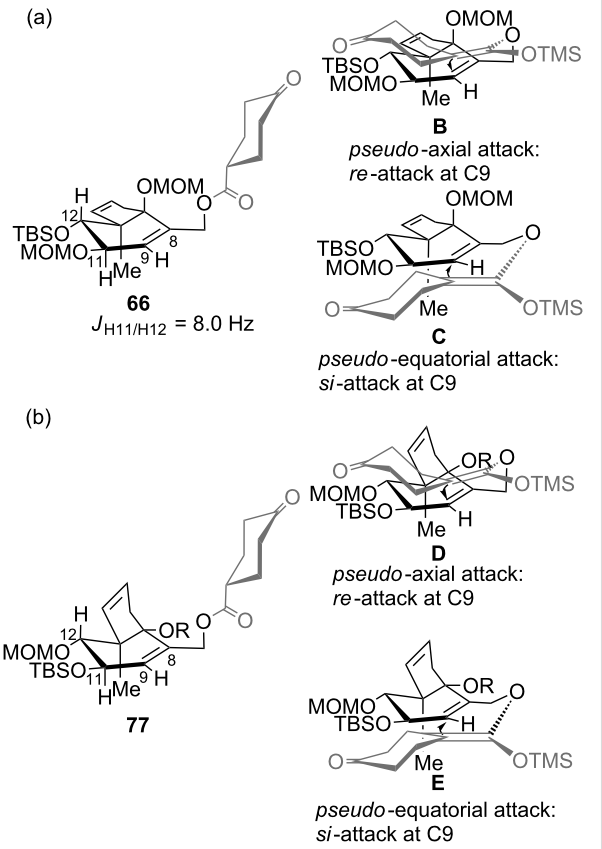
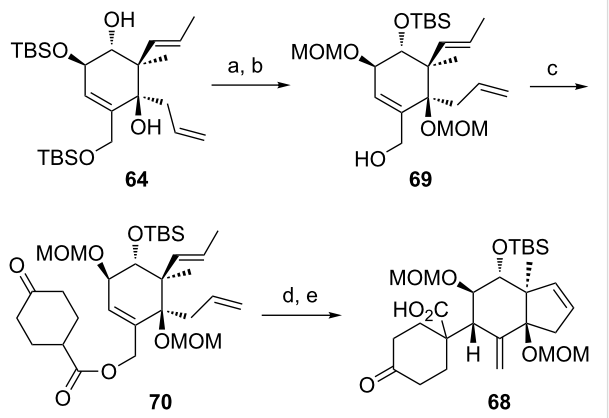


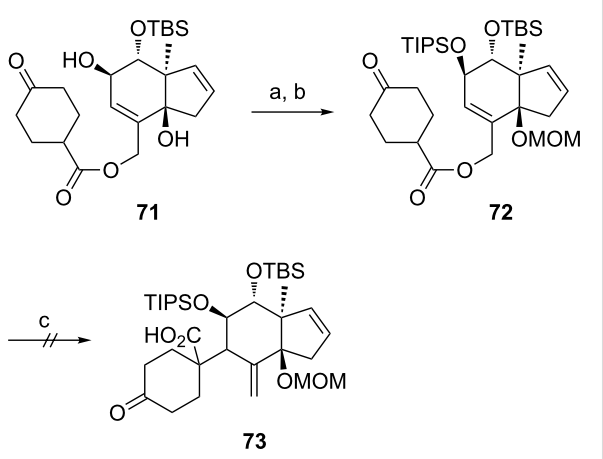
Figure 3: Conformations of rearrangement precursors **66** and **77** and possible transition states involved in the Ireland–Claisen rearrangements. R = MOM.

We hypothesized that the diastereoselectivity could be improved by performing the rearrangement with the open-chain precursor **70** (Scheme 9), which should be less rigid than the bicyclic system **66** and therefore, in analogy to the results of the rearrangements with the model substrates, probably preferably rearrange via a pseudo-axial attack. The open-chain precursor **70** was obtained by MOM protection of diol **64**, selective cleavage of the primary TBS group and subsequent esterification with 4-oxocyclohexanecarboxylic acid (**25**).

However, in this case the [3,3]-sigmatropic rearrangement proceeded exclusively via pseudo-equatorial attack, giving after



Scheme 9: Synthesis and Ireland–Claisen rearrangement of allyl ester **70**. Reagents and conditions: a) DIPEA, MOMCl, NaI, THF, 65 °C, 3 days, 35%; b) HF·pyridine, THF, 20 h, rt, 83%; c) EDC·HCl, DMAP, CH_2Cl_2, 4-oxocyclohexanecarboxylic acid (**25**), rt, 24 h, 83%; d) LiHMDS, TMSCl/NEt_3, toluene, 1 h at −78 °C, then gradual warming to 65 °C within 6 h and 40 h at 65 °C, yield n.d. dr = 1:0; e) Grubbs I, CH_2Cl_2, rt, 20 h, yield n.d.



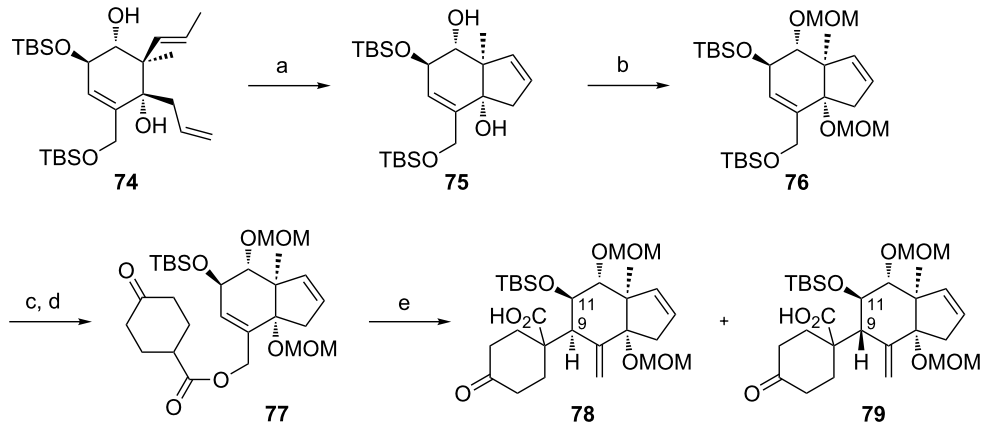
Scheme 10: Synthesis and Ireland–Claisen rearrangement of allyl ester **72**. Reagents and conditions: a) TIPSOTf, pyridine, DMAP, rt, 22 h, 60%; b) DIPEA, MOMCl, THF, 25 h, 50 °C, 29%; c) LiHMDS, TMSCl/NEt_3, toluene, 1 h at −78 °C, then gradual warming to 65 °C within 6 h and stirred for 2 days at 65 °C.

RCM the C9-*epi* limonoid scaffold **68** as single diastereomer. The sterically demanding rearrangement precursor **70** seems to allow only the undesired pseudo-equatorial attack.

We envisaged that protecting the free secondary hydroxy group in **71** with a sterically demanding TIPS group might induce a conformational change of the rearrangement precursor and intended to investigate the influence of this conformational change on the diastereoselectivity of the Ireland–Claisen rearrangement (Scheme 10). However, the allyl ester **72** seems to be too sterically hindered to allow the [3,3]-sigmatropic rearrangement to proceed. After 2 days reaction time, only traces of rearrangement product **73** could be observed.

Moreover, in order to allow the synthetic access to further B-*seco* limonoid analogues, the C14-*epi* B-*seco* limonoid scaffold **78** and C14-*epi*/C9-*epi* scaffold **79** were accessed (Scheme 11). Starting from diol **74**, the C14-*epi* rearrangement precursor **77** was synthesized employing a sequence of ring-closing metathesis, TBS deprotection, esterification and MOM protection. The Ireland–Claisen rearrangement proceeded smoothly and gave a ca. 1.3:1 (**78**:**79**) mixture of diastereomers with the product resulting from the pseudo-axial attack of the silyl ketene acetal being the major diastereomer.

In analogy to the results above the transition states **D** and **E** seem to compete without any preference for a conformation that



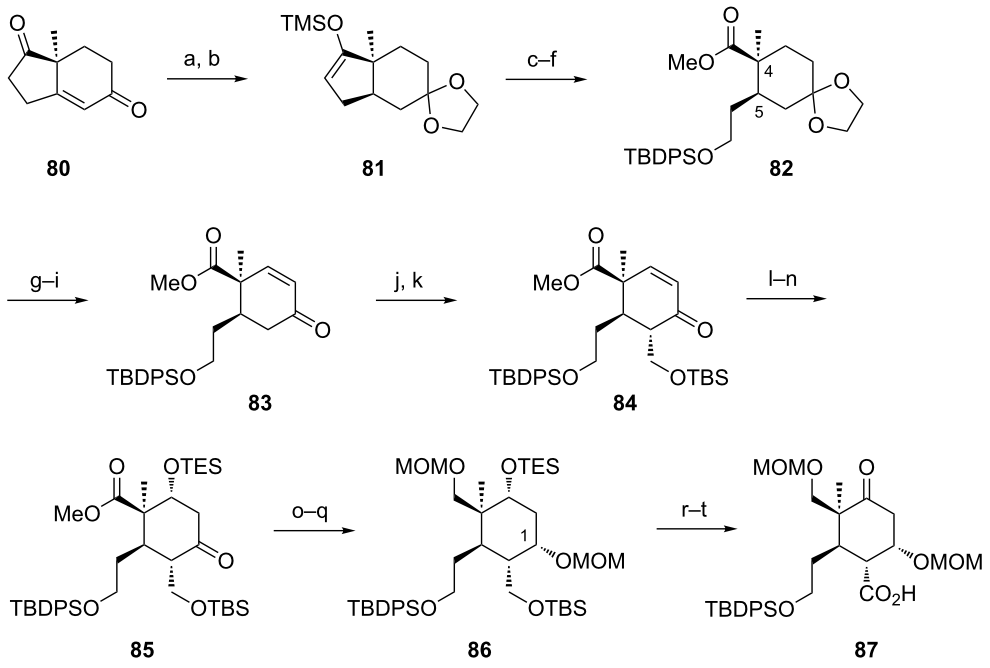
Scheme 11: Synthesis of the C14-*epi* and C14/C9-*epi* B-*seco* limonoid scaffolds **78** and **79**. Reagents and conditions: a) Grubbs I, CH_2Cl_2, rt, 18 h, 86%; b) DIPEA, MOMCl, NaI, THF, 20 h, 65 °C, 89%; c) HF·pyridine, THF, 0 °C to rt, 24 h, 76%; d) EDC·HCl, DMAP, CH_2Cl_2, 4-oxocyclohexane-carboxylic acid (**25**), rt, 19 h, 92%; e) LiHMDS, TMSCl/NEt_3, toluene, 1 h at −78 °C, then gradual warming to 65 °C within 6 h and stirred for 43 h at 65 °C, 78% yield, dr = 1.3:1 (**78**:**79**).

clearly favours axial attack (Figure 3b). Presumably because of the absence of electrostatic interactions in the pseudo-axial attack of the silyl ketene acetal (compare transition state **B** in Figure 3a: electrostatic interaction with -OMOM at C14), this approach is slightly favored.

Synthesis of fully functionalized A ring. Having these extensive studies completed we then focused on the synthesis of a suitable fully functionalized A ring **87** (Scheme 12) that after connection to the bicyclic C–D system and subsequent Ireland–Claisen rearrangement was supposed to give access to the entire framework of B-*seco* limonoids.

Explorations to access this fragment started from Hajos–Parrish ketone **80** [52] (Scheme 12), as we were inspired by a reaction sequence Arseniyadis et al. [53] used in their synthesis of a left-half taxoid building block. Regioselective protection of the less hindered ketone in **80** and diastereoselective hydrogenation of the double bond could be achieved in a known one-pot procedure [54,55] affording the *cis*-hydrindanone and providing the desired stereochemistry at C4 and C5. Ozonolytic cleavage of the corresponding silyl enol ether **81** followed by esterification with $TMSCHN_2$ furnished the ester aldehyde that was reduced to the primary alcohol and protected to give TBDPS ether **82**. After selective cleavage of the acetal group by treatment with perchloric acid, installation of the double bond via Saegusa oxidation [56,57] of the previously formed TMS ether furnished enone **83** as the major regioisomer. Minor amounts of the undesired regioisomer could be separated by column chromatography. Hydroxymethylation of **83** using 1*H*-benzotriazole-1-methanol proceeded diastereoselectively due to substrate control [58]. The configuration was determined by the high coupling constant ($J_{H4/H5}$ = 12.6 Hz) indicating the *trans*-diaxial orientation of H4 and H5. Silylation of the primary hydroxy group afforded compound **84** that was converted into the epoxide with complete stereocontrol [59]. The epoxide underwent regioselective opening [60,61] leading to the β-hydroxyketone that was temporarily masked as a TES ether.

Reduction of ketone **85** with $NaBH_4$ resulted in the formation of two diastereomeric alcohols in 2:1 ratio. To our delight flash chromatography permitted smooth separation of the two compounds. nOe studies revealed that the main product is 1*S*-configurated as in most B-*seco* limonoids suggesting that an equatorial attack of the hydride is slightly preferred over the axial attack. However bearing in mind the elimination issues



Scheme 12: Synthesis of fully functionalized A ring **87**. Reagents and conditions: a) $HO(CH_2)_2OH$, THF, Pd/C, H_2, pH 5, rt, overnight, 97%, de = 100%; b) LDA, TMSCl, THF, −78 °C to rt, 1.5 h, quant.; c) O_3, CH_2Cl_2, −78 °C, then DMS, −78 °C to rt; d) $TMSCHN_2$, CH_2Cl_2/MeOH (1:1), rt, 0.5 h, 59% (2 steps); e) $NaBH_4$, MeOH, 0 °C, 0.5 h; f) TBDPSCl, imidazole, DMAP, CH_2Cl_2, 0.5 h, rt, 78% (2 steps); g) $CH_2Cl_2/H_2O/HClO_4$ (25:5:1), rt, 6 h; h) LiHMDS, TMSCl, THF, −78 °C to rt, 1.5 h; i) $Pd(OAc)_2$, DMSO, O_2, overnight, 72% (3 steps); j) LDA, 1*H*-benzotriazole-1-methanol, THF, −78 °C, 3 h, 67%, de = 100%; k) TBSCl, imidazole, DMF, rt, overnight, 90%; l) H_2O_2, NaOH, MeOH, 0 °C, 1 h, 80%, de = 100%; m) $NaBH_4$, $(PhSe)_2$, EtOH, 0 °C to rt, 10 min, 93%; n) TESCl, imidazole, DMF, 40 °C, 2 h, 99%; o) $NaBH_4$, MeOH, 0 °C, 3 h, 64%; p) $LiBH_4$, THF, 65 °C, 4 days, 67% (92% brsm); q) MOMCl, DIPEA, NaI, THF, 50 °C, 4 days, 96%, dr = 2:1; r) 5% TFA in CH_2Cl_2, rt, 0.5 h, 74%; s) DMP, $NaHCO_3$, CH_2Cl_2, 0 °C, 3 h, 76%; t) $NaClO_2$, NaH_2PO_4, 2-methyl-2-butene, *t*-BuOH/H_2O (4:1), rt, 3.5 h, 91%.

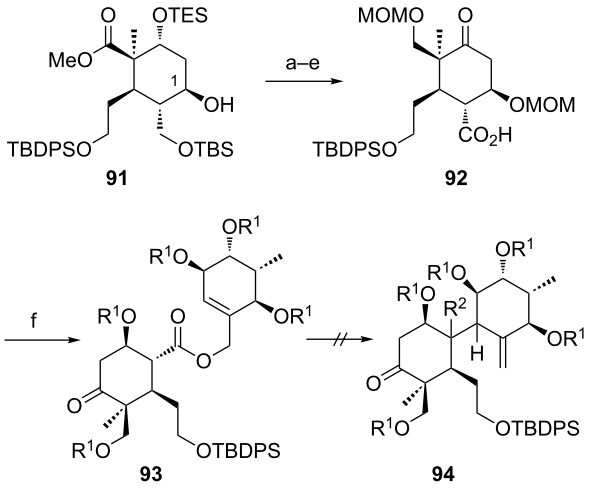
with β-alkoxy esters during Ireland–Claisen rearrangements discussed above we decided to continue the synthesis with both diastereomers as this elimination is expected to proceed faster in *syn*-substituted β-alkoxy esters since the hydrogen and the leaving group are in an antiperiplanar arrangement.

Continuing the synthesis with the 1*S*-isomer (Scheme 12), reduction of the ester moiety could be initiated by $LiBH_4$ but proceeded sluggishly. For the protection of the corresponding diol we were limited to small protecting groups as introduction of the MOM-groups already occurred slowly and required high excess of reagents. Selective deprotection of the TBS and the TES ethers in **86** was achieved under acidic conditions. Oxidation of the resulting diol with Dess–Martin periodinane and subsequent Pinnick oxidation completed the synthesis.

Ireland–Claisen rearrangements with fully decorated A ring. With the suitable substituted fragment **87** in hand, we decided to initially perform the intended rearrangement with one of the model C rings. Thus carboxylic acid **87** was esterified with allylic alcohol **40** to give allyl ester **88** (Scheme 13).

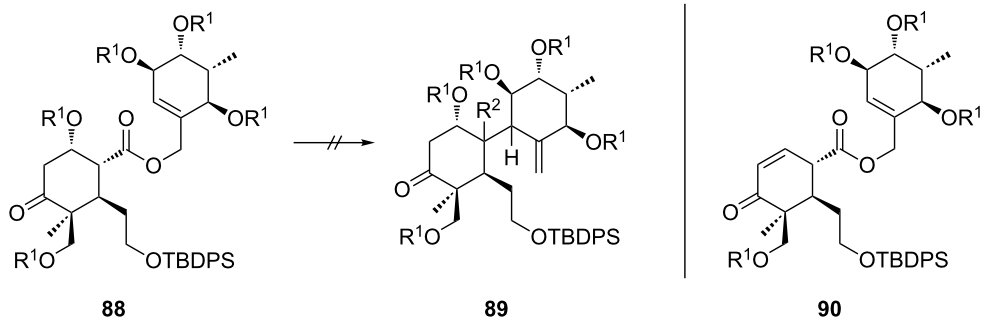
Unfortunately exposure of **88** to the optimized conditions developed for the synthesis of the B-*seco* limonoid scaffold did not initiate the desired Ireland–Claisen rearrangement. Addition of HMPA was also fruitless. Noteworthy elimination of the MOM-protected hydroxy group at C1 occurred only to a minor extent under these conditions, but was not observed at all when HMPA was added. In situ formation of the TMS enol ether of **88** was detected, however as a consequence of the acidic work-up β-elimination of the OMOM group was induced resulting in α,β-unsaturated ketone **90**.

Despite these unsatisfactory results we continued with the synthesis of C1-*epi* allyl ester **93** starting from alcohol **91** employing the same reaction sequence of ester reduction, diol protection, desilylation, oxidation and esterification (Scheme 14). Attempts to rearrange **93** under the optimized conditions were again unsuccessful. As expected, elimination of the OMOM group during the reaction was not detected due to the unfavoured orientation of the hydrogen and the leaving group. Subsequent acidic treatment did again lead to formation of enone **90**.



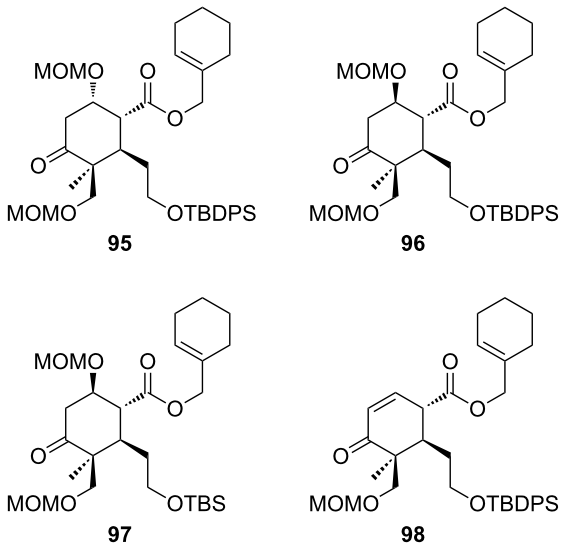
Scheme 14: Synthesis and attempted Ireland–Claisen rearrangement of allyl ester **93**. Reagents and conditions: a) $LiBH_4$, THF, 65 °C, overnight, 84%; b) MOMCl, DIPEA, NaI, THF, 50 °C, overnight, 89%; c) 8% TFA in CH_2Cl_2, rt, 0.5 h, 52%; d) DMP, $NaHCO_3$, CH_2Cl_2, 0 °C, 3 h, 86%; e) $NaClO_2$, NaH_2PO_4, 2-methyl-2-butene, *t*-BuOH/H_2O (4:1), rt, 2.5 h, 99%; f) EDC·HCl, **40**, DMAP, CH_2Cl_2, rt, 2 d, 47%. R^1 = MOM, R^2 = CO_2H.

We assume that the additional substituents as well as the intermediary formed TMS ether cause excessive steric bulk and rigidity that prevent the silyl ketene acetals from adopting the required conformation. Hence, we considered enone **90** as an alternative rearrangement precursor as many B-*seco* limonoids exhibit a double bond in this position (see 21-hydroxytoonacilide (**1**)). However, despite the incapacity to form the silyl enol ether as well as the lack of the C1-substituent allyl ester **90** failed to furnish the corresponding carboxylic acid using the general conditions.



Scheme 13: and Attempted Ireland–Claisen rearrangement of allyl ester **88**. R^1 = MOM, R^2 = CO_2H.

In order to explore whether the whole system or whether the A ring **87** itself is too crowded to allow the rearrangement to proceed, we used a completely undecorated C ring. For this purpose rearrangement precursors **95**, **96**, and **97** were synthesized (see Supporting Information File 1) and investigated with respect to their behavior in the [3,3]-sigmatropic rearrangement (Scheme 15). Unfortunately all attempts to procure this transformation using different bases (LiHMDS, KHMDS, LDA), additives (Et_3N, HMPA), solvents (THF, toluene) and temperatures (up to 110 °C) completely failed. Indeed the results are in accordance with those obtained earlier. All allyl esters were converted to the corresponding TMS ethers under the rearrangement conditions. Formation of the β-elimination product was exclusively observed for the 1*S*-configurated allyl ester **95** in the absence of HMPA. Replacing the sterically demanding TBDPS group by the smaller TBS group in **97** could not initiate the rearrangement either. Furthermore, α,β-unsaturated ketone **98**, that was generated during the acidic work-up, did not show any conversion (Scheme 15).



Scheme 15: Allyl esters tested in the Ireland–Claisen rearrangement.

Conclusion

In view of the results obtained we conclude that an Ireland–Claisen rearrangement is not a suitable method to build up the completely decorated scaffold of the B-*seco* limonoid natural products, as it failed when a fully substituted A ring is used. Presumably steric constraints in combination with the rigidity caused by the intermediary formed silyl enol ether are responsible for the failure as it has been indicated before for substrates that contain a rigid BDA group or a bulky TIPS group.

Supporting Information

Supporting Information File 1

Experimental procedures and characterisation data.
[http://www.beilstein-journals.org/bjoc/content/supplementary/1860-5397-10-15-S1.pdf]

Acknowledgements

This research was supported by the European Research Council (ERC European Advanced Investigator Grant to H.W.), the Max Planck Society and the Fonds der Chemischen Industrie (Kekulé-stipend to H.S.).

References

1. Mulholland, D. A.; Parel, B.; Coombes, P. H. *Curr. Org. Chem.* **2000,** *4,* 1011–1054. doi:10.2174/1385272003375941
2. Roy, A.; Saraf, S. *Biol. Pharm. Bull.* **2006,** *29,* 191–201. doi:10.1248/bpb.29.191
3. Heasley, B. *Eur. J. Org. Chem.* **2011,** 19–46. doi:10.1002/ejoc.201001218
4. Kraus, W.; Grimminger, W. *Nouv. J. Chim.* **1980,** *4,* 651–655.
5. Cheplogoi, P. K.; Mulholland, D. A. *Phytochemistry* **2003,** *62,* 1173–1178. doi:10.1016/S0031-9422(03)00028-1
6. Lidert, Z.; Taylor, D. A. H.; Thirugnanam, M. *J. Nat. Prod.* **1985,** *48,* 843–845. doi:10.1021/np50041a029
7. Sarker, S. D.; Savchenko, T.; Whiting, P.; Šik, V.; Dinan, L. *Arch. Insect Biochem. Physiol.* **1997,** *35,* 211–217. doi:10.1002/(SICI)1520-6327(1997)35:1/2<211::AID-ARCH19>3.0.CO;2-E
8. Koul, O.; Daniewski, W. M.; Multani, J. S.; Gumulka, M.; Singh, G. *J. Agric. Food Chem.* **2003,** *51,* 7271–7275. doi:10.1021/jf0304223
9. Bray, D. H.; Warhurst, D. C.; Connolly, J. D.; O'Neill, M. J.; Phillipson, J. D. *Phytother. Res.* **1990,** *4,* 29–35. doi:10.1002/ptr.2650040108
10. Lukacova, V.; Polonsky, J.; Moretti, C.; Pettit, G. R.; Schmidt, J. M. *J. Nat. Prod.* **1982,** *45,* 288–294. doi:10.1021/np50021a010
11. Pettit, G. R.; Barton, D. H. R.; Herald, C. L.; Polonsky, J.; Schmidt, J. M.; Connolly, J. D. *J. Nat. Prod.* **1983,** *46,* 379–390. doi:10.1021/np50027a015
12. Musza, L. L.; Killar, L. M.; Speight, P.; McElhiney, S.; Barrow, C. J.; Gillum, A. M.; Cooper, R. *Tetrahedron* **1994,** *50,* 11369–11378. doi:10.1016/S0040-4020(01)89279-6
13. Bevan, C. W. L.; Ekong, D. E. U.; Taylor, D. A. H. *Nature* **1965,** *206,* 1323–1325. doi:10.1038/2061323a0
14. Gullo, V. P.; Miura, I.; Nakanishi, K.; Cameron, A. F.; Connolly, J. D.; Duncanson, F. D.; Harding, A. E.; McCrindle, R.; Taylor, D. A. H. *J. Chem. Soc., Chem. Commun.* **1975,** 345–346. doi:10.1039/c39750000345
15. Cameron, A. F.; Duncanson, F. D. *Acta Crystallogr., Sect. B: Struct. Crystallogr. Cryst. Chem.* **1976,** *32,* 1841–1845. doi:10.1107/S056774087600650X
16. Robert, S.; Chary, S. N.; Drakakaki, G.; Li, S.; Yang, Z.; Raikhel, N. V.; Hicks, G. R. *Proc. Natl. Acad. Sci. U. S. A.* **2008,** *105,* 8464–8469. doi:10.1073/pnas.0711650105
17. Kraus, W.; Grimminger, W.; Sawitzki, G. *Angew. Chem., Int. Ed. Engl.* **1978,** *17,* 452–453. doi:10.1002/anie.197804521

18. Munehiro, N.; Miyako, O.; Takashi, I.; Kosei, M.; Hideo, N.; Tsunao, H. *Heterocycles* **1984,** *22,* 2335–2340. doi:10.3987/R-1984-10-2335
19. Luo, X.-D.; Wu, S.-H.; Wu, D.-G.; Ma, Y.-B.; Qi, S.-H. *Tetrahedron* **2002,** *58,* 7797–7804. doi:10.1016/S0040-4020(02)00944-4
20. Koul, O.; Daniewski, W. M.; Multani, J. S.; Gumulka, M.; Singh, G. *J. Agric. Food Chem.* **2003,** *51,* 7271–7275. doi:10.1021/jf0304223
21. Qi, S.-H.; Chen, L.; Wu, D.-G.; Ma, Y.-B.; Luo, X.-D. *Tetrahedron* **2003,** *59,* 4193–4199. doi:10.1016/S0040-4020(03)00573-8
22. Wang, X.-N.; Yin, S.; Fan, C.-Q.; Wang, F.-D.; Lin, L.-P.; Ding, J.; Yue, J.-M. *Org. Lett.* **2006,** *8,* 3845–3848. doi:10.1021/ol061466a
23. Wang, X.-N.; Yin, S.; Fan, C.-Q.; Lin, L.-P.; Ding, J.; Yue, J.-M. *Tetrahedron* **2007,** *63,* 8234–8241. doi:10.1016/j.tet.2007.05.107
24. Kishore, K. C.; Vijayalakshmi, K.; Bibha, C.; Mridula, N.; Rama Gopal, G.; Sathees, C. R. *FEBS Lett.* **2008,** *582,* 4066–4076. doi:10.1016/j.febslet.2008.11.001
25. Yang, S.-P.; Chen, H.-D.; Liao, S.-G.; Xie, B.-J.; Miao, Z.-H.; Yue, J.-M. *Org. Lett.* **2011,** *13,* 150–153. doi:10.1021/ol102745h
26. Tóth, R.; Gerding-Reimers, C.; Deeks, M. J.; Menninger, S.; Gallegos, R. M.; Tonaco, I. A. N.; Hübel, K.; Hussey, P. J.; Waldmann, H.; Coupland, G. *Plant J.* **2012,** *71,* 338–352. doi:10.1111/j.1365-313X.2012.04991.x
27. Wetzel, S.; Bon, R. S.; Kumar, K.; Waldmann, H. *Angew. Chem., Int. Ed.* **2011,** *50,* 10800–10826. doi:10.1002/anie.201007004
28. Bon, R. S.; Waldmann, H. *Acc. Chem. Res.* **2010,** *43,* 1103–1114. doi:10.1021/ar100014h
29. Kumar, K.; Waldmann, H. *Angew. Chem., Int. Ed.* **2009,** *48,* 3224–3242. doi:10.1002/anie.200803437
30. Nören-Müller, A.; Reis-Correa, I., Jr.; Prinz, H.; Rosenbaum, C.; Saxena, K.; Schwalbe, H. J.; Vestweber, D.; Cagna, G.; Schunk, S.; Schwarz, O.; Schiewe, H.; Waldmann, H. *Proc. Natl. Acad. Sci. U. S. A.* **2006,** *103,* 10606–10611. doi:10.1073/pnas.0601490103
31. Koch, M. A.; Schuffenhauer, A.; Scheck, M.; Wetzel, S.; Casaulta, M.; Odermatt, A.; Ertl, P.; Waldmann, H. *Proc. Natl. Acad. Sci. U. S. A.* **2005,** *102,* 17272–17277. doi:10.1073/pnas.0503647102
32. Koch, M. A.; Wittenberg, L.-O.; Basu, S.; Jeyaraj, D. A.; Gourzoulidou, E.; Reinecke, K.; Odermatt, A.; Waldmann, H. *Proc. Natl. Acad. Sci. U. S. A.* **2004,** *101,* 16721–16726. doi:10.1073/pnas.0404719101
33. Dückert, H.; Pries, V.; Khedkar, V.; Menninger, S.; Bruss, H.; Bird, A. W.; Maliga, Z.; Brockmeyer, A.; Janning, P.; Hyman, A.; Grimme, S.; Schürmann, M.; Preut, H.; Hübel, K.; Ziegler, S.; Kumar, K.; Waldmann, H. *Nat. Chem. Biol.* **2012,** *8,* 179–184. doi:10.1038/nchembio.758
34. Zimmermann, T. J.; Roy, S.; Martinez, N. E.; Ziegler, S.; Hedberg, C.; Waldmann, H. *ChemBioChem* **2013,** *14,* 295–300. doi:10.1002/cbic.201200711
35. In all molecules described in this paper including fragments and model compounds we maintain the numbering of the carbon atoms established for limonoid natural products as it is indicated in Figure 1 for 21-hydroxytoonacilide (**1**).
36. Schuster, H.; Martinez, R.; Bruss, H.; Antonchick, A. P.; Kaiser, M.; Schürmann, M.; Waldmann, H. *Chem. Commun.* **2011,** *47,* 6545–6547. doi:10.1039/c1cc11388g
37. Veitch, G. E.; Beckmann, E.; Burke, B. J.; Boyer, A.; Maslen, S. L.; Ley, S. V. *Angew. Chem., Int. Ed.* **2007,** *46,* 7629–7632. doi:10.1002/anie.200703027
38. Veitch, G. E.; Beckmann, E.; Burke, B. J.; Boyer, A.; Ayats, C.; Ley, S. V. *Angew. Chem., Int. Ed.* **2007,** *46,* 7633–7635. doi:10.1002/anie.200703028
39. Barros, M. T.; Maycock, C. D.; Ventura, M. R. *J. Chem. Soc., Perkin Trans. 1* **2001,** 166–173. doi:10.1039/b002980g
40. Arthurs, C. L.; Lingley, K. F.; Piacenti, M.; Stratford, I. J.; Tatic, T.; Whitehead, R. C.; Wind, N. S. *Tetrahedron Lett.* **2008,** *49,* 2410–2413. doi:10.1016/j.tetlet.2008.02.059
41. Murray, L. M.; O'Brien, P.; Taylor, R. J. K. *Org. Lett.* **2003,** *5,* 1943–1946. doi:10.1021/ol034521d
42. Marchart, S.; Mulzer, J.; Enev, V. S. *Org. Lett.* **2007,** *9,* 813–816. doi:10.1021/ol0630189
43. Lence, E.; Castedo, L.; Gonzalez-Bello, C. *Chem. Soc. Rev.* **2008,** *37,* 1689–1708. doi:10.1039/b717902b
44. Durand-Reville, T.; Gobbi, L. B.; Gray, B. L.; Ley, S. V.; Scott, J. S. *Org. Lett.* **2002,** *4,* 3847–3850. doi:10.1021/ol0201557
45. Ziegler, F. E.; Nangia, A.; Schulte, G. *Tetrahedron Lett.* **1988,** *29,* 1669–1672. doi:10.1016/S0040-4039(00)82013-4
46. Quach, T. D.; Batey, R. A. *Org. Lett.* **2003,** *5,* 1381–1384. doi:10.1021/ol034454n
47. Nordmann, G.; Buchwald, S. L. *J. Am. Chem. Soc.* **2003,** *125,* 4978–4979. doi:10.1021/ja034809y
48. Fukuzaki, T.; Kobayashi, S.; Hibi, T.; Ikuma, Y.; Ishihara, J.; Kanoh, N.; Murai, A. *Org. Lett.* **2002,** *4,* 2877–2880. doi:10.1021/ol026260y
49. Ireland, R. E.; Varney, M. D. *J. Org. Chem.* **1983,** *48,* 1829–1833. doi:10.1021/jo00159a008
50. Hiersemann, M.; Nubbemeyer, U., Eds. *The Claisen Rearrangement;* Wiley-VCH: Weinheim, Germany, 2007.
51. Chieffi, A.; Kamikawa, K.; Åhman, J.; Fox, J. M.; Buchwald, S. L. *Org. Lett.* **2001,** *3,* 1897–1900. doi:10.1021/ol0159470
52. Hajos, Z. G.; Parrish, D. R. *J. Org. Chem.* **1974,** *39,* 1615–1621. doi:10.1021/jo00925a003
53. Arseniyadis, S.; Yashunsky, D. V.; de Freitas, R. P.; Dorado, M. M.; Potier, P.; Toupet, L. *Tetrahedron* **1996,** *52,* 12443–12458. doi:10.1016/0040-4020(96)00735-1
54. Hudson, P.; Parsons, P. J. *Synlett* **1992,** 867–868. doi:10.1055/s-1992-21520
55. Shi, H. *Synth. Commun.* **2006,** *36,* 237–248. doi:10.1080/00397910500334611
56. Ito, Y.; Hirao, T.; Saegusa, T. *J. Org. Chem.* **1978,** *43,* 1011–1013. doi:10.1021/jo00399a052
57. Larock, R. C.; Hightower, T. R.; Kraus, G. A.; Hahn, P.; Zheng, D. *Tetrahedron Lett.* **1995,** *36,* 2423–2426. doi:10.1016/0040-4039(95)00306-W
58. Deguest, G.; Bischoff, L.; Fruit, C.; Marsais, F. *Org. Lett.* **2007,** *9,* 1165–1167. doi:10.1021/ol070145b
59. The configuration of the epoxide was determined *via* Mosher ester analysis of a derivative of the corresponding β-hydroxyketone, that was obtained during the synthetic studies.
60. Miyashita, M.; Suzuki, T.; Yoshikoshi, A. *Tetrahedron Lett.* **1987,** *28,* 4293–4296. doi:10.1016/S0040-4039(00)96488-8
61. Miyashita, M.; Suzuki, T.; Hoshino, M.; Yoshikoshi, A. *Tetrahedron* **1997,** *53,* 12469–12486. doi:10.1016/S0040-4020(97)00781-3

License and Terms

This is an Open Access article under the terms of the Creative Commons Attribution License (http://creativecommons.org/licenses/by/2.0), which permits unrestricted use, distribution, and reproduction in any medium, provided the original work is properly cited.

The license is subject to the *Beilstein Journal of Organic Chemistry* terms and conditions: (http://www.beilstein-journals.org/bjoc)

The definitive version of this article is the electronic one which can be found at: doi:10.3762/bjoc.10.15

Beilstein Journal of Organic Chemistry

Tanzawaic acids I–L: Four new polyketides from *Penicillium* sp. IBWF104-06

Louis P. Sandjo[1], Eckhard Thines[2,3], Till Opatz[*1] and Anja Schüffler[*2]

Full Research Paper

Open Access

Address:
[1]Johannes-Gutenberg-University Mainz, Institute of Organic Chemistry, Duesbergweg 10–14, D-55128 Mainz, Germany, [2]Institute of Biotechnology and Drug Research, Erwin-Schroedinger-Strasse 56, D-67663, Kaiserslautern, Germany and [3]Johannes-Gutenberg-University Mainz, Institute of Biotechnology and Drug Research, Duesbergweg 10–14, D-55128 Mainz, Germany

Email:
Till Opatz[*] - opatz@uni-mainz.de; Anja Schüffler[*] - schueffler@ibwf.de

* Corresponding author

Keywords:
arohynapene; natural products; polyketides; structure elucidation; tanzawaic acid

Beilstein J. Org. Chem. **2014,** *10,* 251–258.
doi:10.3762/bjoc.10.20

Received: 26 September 2013
Accepted: 20 December 2013
Published: 22 January 2014

This article is part of the Thematic Series "Natural products in synthesis and biosynthesis".

Guest Editor: J. S. Dickschat

© 2014 Sandjo et al; licensee Beilstein-Institut.
License and terms: see end of document.

Abstract

Four new polyketides have been identified in culture filtrates of the fungal strain *Penicillium* sp. IBWF104-06 isolated from a soil sample. They are structurally based on the same *trans*-decalinpentanoic acid skeleton as tanzawaic acids A–H. One of the new compounds was found to inhibit the conidial germination in the rice blast fungus *Magnaporthe oryzae* at concentrations of 25 μg/mL.

Introduction

Nature still represents the richest source of new antimicrobials which can be attractive as lead structures or biochemical tools for target identification for medical applications as well as for crop science. In both areas, the omnipresent development of resistance results in a demand for new active principles for which the structural diversity of nature holds an excellent supply. While natural products, their synthesis, evolution, and ecological role are of academic interest, compounds identified might also be relevant for application. In the course of investigations into the secondary metabolism of fungal species for the identification of novel lead structures for agrochemical and pharmaceutical research, we isolated a fungal strain from a soil sample. The culture filtrate extract of this organism was found to inhibit the conidial germination in the rice blast fungus *Magnaporthe oryzae*, one of the most devastating plant diseases on cultivated rice. Bioactivity-guided fractionation of organic extracts led to the isolation of a series of eight pure compounds, the structures of which were elucidated by 2D NMR spectroscopy as well as by mass spectrometry.

Results and Discussion

Structure elucidation. Compound **1** has the molecular formula $C_{18}H_{26}O_4$ determined on the basis of NMR and HRMS-ESI data which gave a pseudo-molecular ion at *m*/*z* 329.1744 (calcd

for $[M + Na]^+$: 329.1729). This composition accounted for six double bond equivalents. The NMR spectra of **1** (Table 1 and Table 2) displayed signals of a (2*E*,4*E*)-penta-2,4-dienoic acid moiety including a carbon of a conjugated carbonyl group at δ_C 170.9 and four olefinic resonances at δ_H 5.86 (d, J = 15.3 Hz)/δ_C 122.0, δ_H 7.28 (dd, J = 11.2, 15.3 Hz)/δ_C 145.9, δ_H 6.45 (dd, J = 11.2, 15.2 Hz)/128.5, and δ_H 6.10 (d, J = 15.2 Hz)/δ_C 144.8. Moreover, these spectra showed signals of three CH_3 groups,

Table 1: ^{1}H NMR data of compounds **1–4** (CD_3OD, 600 MHz).

Position	Compound **1**	Compound **2**	Compound **3**	Compound **4**
1	–	–	–	–
2	5.86 (1H, d, 15.3)	5.83 (1H, d, 15.3)	5.80 (1H, d, 15.3)	5.87 (1H, d, 15.1)
3	7.28 (1H, dd, 11.2, 15.3)	7.28 (1H, dd, 11.2, 15.3)	7.32 (1H, dd, 10.9, 15.3)	7.37 (1H, dd, 11.1, 15.1)
4	6.45 (1H, dd, 11.2, 15.2)	6.45 (1H, dd, 11.2, 15.5)	6.20 (1H, dd, 11.0, 15.0)	6.33 (1H, dd, 11.1, 15.6)
5	6.10 (1H, d, 15.2)	6.16 (1H, d, 15.5)	6.31 (1H, dd, 10.6, 15.0)	6.74 (1H, d,15.6)
6	–	–	2.40 (1H, t, 10.6)	–
7	1.39 (1H, m)	1.52 (1H, d, 11.0)	1.09 (1H, m)	1.56 (1H, m)
8	1.39 (1H, m)	1.75 (1H, m)	1.39 (1H, m)	2.03 (1H, m)
9	0.72 ($1H_{ax}$, q, 11.8) 1.54 ($1H_{eq}$, m)	0.78 ($1H_{ax}$, q, 12.3) 1.57 ($1H_{eq}$, m)	0.77 ($1H_{ax}$, m) 1.65 ($1H_{eq}$, *pseudo*-dd, 3.1, 13.3)	1.06 ($1H_{ax}$, dd, 11.9, 13.9) 1.73 ($1H_{eq}$, m)
10	1.45 (1H, d, 6.6)	1.50 (1H, m)	1.54 (1H, m)	–
11	1.17 ($1H_{ax}$, q, 12.3) 1.54 ($1H_{eq}$, m)	1.17 ($1H_{ax}$, q, 12.4) 1.56 ($1H_{eq}$, m)	0.72 ($1H_{ax}$, m) 1.71 ($1H_{eq}$, *pseudo*-dd, 3.0, 13.0)	1.33 ($1H_{ax}$, t, 13.3) 1.69 ($1H_{eq}$, m)
12	1.59 (1H, m)	1.61 (1H, m)	1.94 (1H, *pseudo*-t, 11.0)	2.36 (1H, m)
13	3.80 (1H, t, 4.4)	3.75 (1H, dd, 2.7, 5.8)	5.41 (1H, d, 10.0)	5.74 (1H, dd, 2.2, 9.2)
14	5.69 (1H, d, 5.2)	5.79 (1H, d, 6.1)	5.48 (1H, dd, 2.4, 10.0)	5.97 (1H, dd, 2.8, 9.2)
15	–	–	–	–
16	1.62 (3H, s)	1.63 (3H, s)	1.18 (3H, s)	1.89 (3H, s)
17	0.90 (3H, d, 6.4)	0.91 (3H, d, 6.4)	0.89 (3H, d, 6.5)	1.20 (3H, s)
18	1.09 (3H, d, 5.3)	0.91 (3H, d, 6.4)	0.98 (3H, d, 6.3)	0.98 (3H, d, 6.2)

Table 2: ^{13}C NMR data of compounds **1–4** (CD_3OD, 150 MHz).

Position	Compound **1**	Compound **2**	Compound **3**	Compound **4**
1	170.9	170.9	170.9	170.9
2	122.0	121.3	120.6	120.8
3	145.9	146.2	146.7	147.1
4	128.5	127.8	130.5	131.0
5	144.8	153.7	147.5	142.3
6	79.0	76.1	58.8	133.4
7	49.8	49.1	51.1	49.9
8	35.3	34.3	37.2	29.1
9	47.1	47.1	48.1	49.3
10	32.9	33.0	33.7	70.1
11	39.1	39.0	42.8	44.0
12	41.4	39.9	44.7	35.9
13	67.6	68.0	132.9	137.3
14	127.0	128.0	135.2	131.0
15	142.9	140.9	74.5	133.8
16	18.1	19.1	24.6	19.8
17	23.1	23.1	22.8	31.3
18	23.0	24.2	23.8	23.4

two CH_2 groups, six CH groups, and two quaternary carbons (Table 1 and Table 2). These data suggested a structural similarity of **1** to the tanzawaic acids, secondary metabolites from *Penicillium citrinum* [1]. COSY and HMBC correlations (Figure 1) revealed the presence of a *trans*-decalin scaffold containing six CH groups, two CH_2 groups and two quaternary carbons as the hydrogen at δ_H 1.39 (H-7) showed correlations with hydrogens at δ_H 1.59 (H-12) and 0.72 (H-9) while the latter correlated with the proton at δ_H 1.45 (H-10). Likewise, the resonance at δ_H 1.45 had a correlation with the proton at δ_H 1.17 (H-11_{ax}) which in turn correlated with those at δ_H 1.54 (H-11_{eq}) and 1.59 (H-12) forming the western part of the bicyclic framework; further homonuclear interactions were revealed from H-12 (δ_H 1.59) to H-13 (δ_H 3.80) and H-14 (δ_H 5.69). The eastern part of the decalin system was established based on HMBC correlations between the olefinic proton at δ_H 5.69 (H-14) and the carbons C-12 (δ_C 41.4), C-13 (δ_C 67.6), and C-6 (δ_C 79.0) while the hydrogen of the oxymethine at δ_H 3.80 (H-13) correlated with the carbons C-7 (δ_C 49.8), C-14 (δ_C 127.0) and C-15 (δ_C 142.9). Based on the COSY and HMBC interactions as well as their 1D multiplicity, the CH_3 groups at δ_H 0.90 (H-17), 1.09 (H-18) and 1.62 (H-16) were attached to the carbons resonating at δ_C 32.9 (C-10), 35.3 (C-8), and 142.9 (C-15) respectively, while the penta-2,4-dienoic acid unit was connected to the carbon at δ_C 79.0 (C-6).

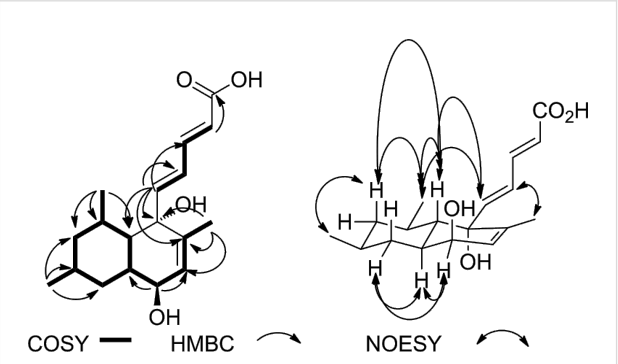


Figure 1: HMBC, COSY and NOESY correlations of compound **1**.

The relative configuration of the stereogenic centers was assigned based on NOESY data (Figure 1) and the previous work reported by Malmstrøm et al. on the stereochemistry of two related compounds, tanzawaic acids E and F [2].

The NOESY spectrum showed contacts (Figure 1) between the proton of the oxymethine group at δ_H 3.80 (H-13) and the protons at δ_H 1.54 (H-11_{eq}) and 1.59 (H-12) suggesting an axial orientation of the OH group at C-13. The proton at δ_H 1.17 (H-11_{ax}) correlated with those at δ_H 0.90 (H-17), 0.72 (H-9_{ax}), and 1.39 (H-8) while H-9_{ax} showed same interactions with the methyl protons at δ_H 1.09 (H-18) and 0.90 (H-17) suggesting them to be oriented equatorially. The same orientation was suggested for the unsaturated side chain since correlations were found between the proton at δ_H 6.10 (H-5) and those at 1.09 (H-18) and 1.39 (H-7).

The foregoing data in conjunction with those of the structurally related tanzawaic acid E [2] led to the identification of **1** as a new member of this compound class and it was given the name tanzawaic acid I (Figure 5).

Compound **2** has the molecular formula $C_{18}H_{26}O_4$ deduced from its NMR and HRMS-ESI data which revealed a pseudomolecular ion at *m*/*z* 329.1736 (calcd for $[M + Na]^+$: 329.1729). As in compound **1**, this composition accounted for six double bond equivalents. The NMR spectra of compound **2** exhibited features similar to those of **1**. Signals of a (2*E*,4*E*)-penta-2,4-dienoic acid moiety (δ_H 5.83 (d, *J* = 15.3 Hz, H-2)/δ_C 121.3, δ_H 7.28 (dd, *J* = 11.2, 15.3 Hz, H-3)/δ_C 146.2, δ_H 6.45 (dd, 11.2, 15.5 Hz, H-4)/δ_C 127.8, and δ_H 6.16 (d, *J* = 15.5 Hz, H-5)/δ_C 153.7 and δ_C 170.9 (C-1)) and a *trans*-decalin bearing three methyl groups (δ_H 0.91 (d, *J* = 6.4 Hz, H-17)/δ_C 23.1, 0.91 (d, *J* = 6.4 Hz, H-18)/δ_C 24.2 and δ_H 1.63 (s, H-16)/δ_C 19.1) were found as well as a trisubstituted double bond (δ_H 5.79 (d, *J* = 6.1 Hz, H-14)/δ_C 128.0 and δ_C 140.9 (C-15)), an oxymethine (δ_H 3.75 (dd, *J* = 2.7, 5.8 Hz, H-13)/δ_C 68.0), and a tertiary alcohol (δ_C 76.1, C-6). A careful inspection of COSY and HMBC data (Figure 2) of compound **2** suggested a diastereomeric relationship with **1** which was substantiated by the different optical rotations of –262 and +73.7 for compounds **1** and **2**, respectively.

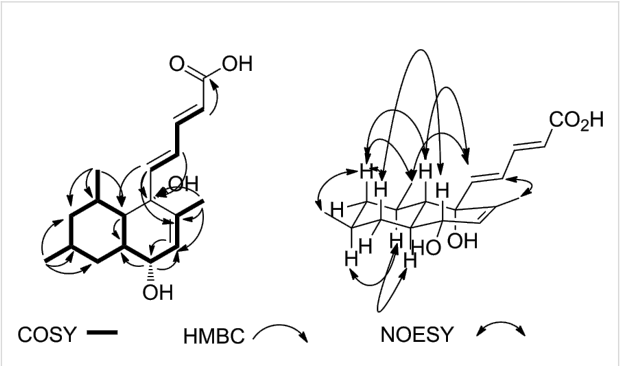


Figure 2: HMBC, COSY and NOESY correlations of compound **2**.

In compound **2**, NOESY correlations (Figure 2) observed between H-11_{ax} (δ_H 1.17) and H-9_{ax} (δ_H 0.78), H-13 (δ_H 3.75) and H-7 (δ_H 1.52) revealed the oxymethine at δ_H 3.75 (dd, *J* = 2.7, 6.0 Hz)/δ_C 68.0 to be responsible for the diastereomery between **1** and **2** due to inversion of the configuration at C-13.

Further NOESY correlations were observed between the proton resonating at δ_H 0.78 (H-9_{ax}) and the methyl protons at δ_H 0.91 (Me-17 and Me-18) while H-18 showed the same interactions with the olefinic protons at δ_H 6.16 (H-5) and 6.45 (H-4). This observation suggested **2** to have the same relative configuration as **1** at C-6, C-7, C-8, and C-10. The above-mentioned data allowed to identify compound **2** as another member of the tanzawaic acid family and was given the name tanzawaic acid J.

The molecular formula of compound **3**, $C_{18}H_{26}O_3$ was established by NMR in conjunction with HRMS-ESI which gave a pseudo-molecular ion at *m*/*z* 313.1788 (calcd for $[M + Na]^+$: 313.1780). This composition required six double bond equivalents and differed from those of compounds **1** and **2** by one oxygen atom. This observation was supported by the absence of oxymethine signals in the NMR spectra. However, features similar to those of the (2*E*,4*E*)-penta-2,4-dienoic acid moiety of compounds **1** and **2** and some signal patterns of the *trans*-decalin part different from those of the two other compounds were observed. The resonance of H-5 (δ_H 6.31, *J* = 10.6, 15.0 Hz) was found as a doublet of doublets suggesting the side chain to be attached to a methine carbon in the bicyclic portion. This conclusion was confirmed by a COSY-correlation to H-6 [δ_H 2.40 (t, *J* = 10.6 Hz)]. Furthermore, two signals of a *cis* olefin were unveiled at δ_H 5.41 (d, *J* = 10.0 Hz)/δ_C 132.9 and δ_H 5.48 (dd, *J* = 2.4, 10.0 Hz)/δ_C 135.2 and originated from the protons bound to C-13 and C-14. This supposition was consistent with diagnostic HMBC correlations connecting the protons [δ_H 1.18 (s)] of the C-16 methyl group to C-6 (δ_C 58.8), C-15 (δ_C 74.5) as well as C-14 (δ_C 135.2) (Figure 3).

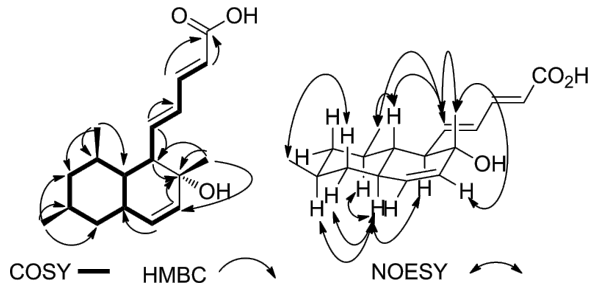


Figure 3: HMBC, COSY and NOESY correlations of compound **3**.

The NOESY spectrum of compound **3** revealed similar correlations as in its analogues **1** and **2** between the olefinic proton H-5 (δ_H 6.31) and the CH_3 group attached to C-8 suggesting the same relative orientation of the side chain and the CH_3 group (Figure 3) which is supported by a correlation between H-5 and the CH_3 (C-16) group (δ_H 1.18). The complete assignment led to structure **3** as shown in Figure 5. The compound was named tanzawaic acid K.

The molecular formula of compound **4**, $C_{18}H_{24}O_3$ was determined based on its NMR and HRMS-ESI data which gave a pseudo-molecular ion at *m*/*z* 311.1630 (calcd for $[M + Na]^+$: 311.1623). This composition required seven double bond equivalents. It differed from compound **3** by two hydrogen atoms suggesting one additional carbon–carbon double bond. This assumption was justified by the presence of four olefinic signals (δ_H 5.74 (dd, *J* = 2.2, 9.2 Hz, H-13)/δ_C 137.3, δ_H 5.97 (dd, *J* = 2.8, 9.2, H-14)/δ_C 131.0, δ_C 133.4 (C-6), and 133.8 (C-15)) in the 1D NMR spectra. The two latter signals were attributed to a tetrasubstituted olefin which was unique for compound **4**, along with only one CH_3 group appearing as a doublet at δ_H 0.98 (d, *J* = 6.2 Hz, H-18)/δ_C 23.4. The second CH_3 group observed as a doublet in compounds **1**–**3** appeared in the ^1H NMR spectrum of **4** as a singlet (δ_H 1.20, H-17) and showed a HMBC correlation with the quaternary carbon at δ_C 70.1 (C-10) (Figure 4). As in compounds **1**–**3**, resonances of a (2*E*,4*E*)-penta-2,4-dienoic acid moiety as well as three additional CH groups, two CH_2 groups and one CH_3 for the completion of the decalin part were observed.

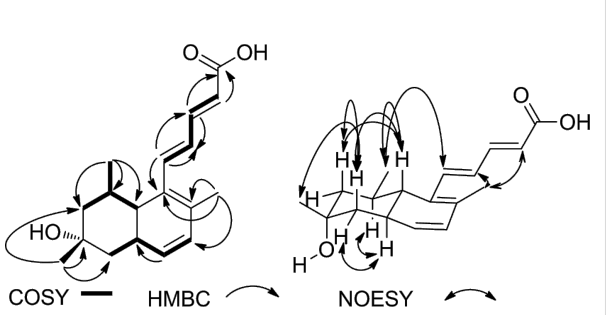


Figure 4: HMBC, COSY and NOESY correlations of compound **4**.

The relative configuration of the stereogenic centers was determined by NOESY (Figure 4). Correlations were observed between H-7 (δ_H 1.56) and H-9_{ax} (δ_H 1.06), H-11_{ax} (δ_H 1.33), and the C-18 methyl protons (δ_H 0.98). An additional correlation was found between H-11_{ax} (δ_H 1.33) and the C-17 methyl protons (H-17, δ_H 1.20) suggesting an equatorial orientation of the latter. From the complete spectral assignment, the structure of compound **4** was established as shown in Figure 5. The fourth member of the series was consequently named tanzawaic acid L (Figure 5).

Along with compounds **1**–**4**, four known polyketides were isolated and identified (Figure 5) as arohynapene A (**5**) [3], arohynapene B (**6**) [3], tanzawaic acid A (**7**) [1], and tanzawaic acid E (**8**) [2]. Their structures were established based on NMR data and by comparison with those reported in the literature. The structures of arohynapene A and tanzawaic acid E were

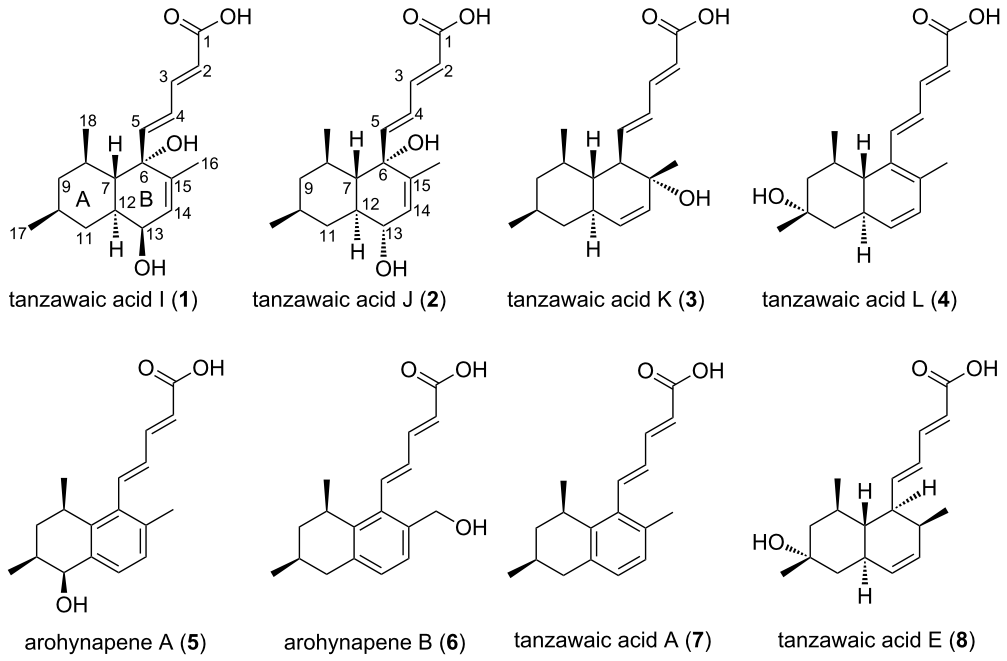


Figure 5: Structures of the isolated compounds.

furthermore supported by X-ray crystallography (Figure 6). In the latter case, the absolute configuration could be determined even though no heavy atom is present in the unit cell. The result confirms the synthetic work of Arimoto et al. who determined the configuration of tanzawaic acid A to be 8*R*,10*S* [4] and suggests the other tanzawaic acids to have the same absolute configuration.

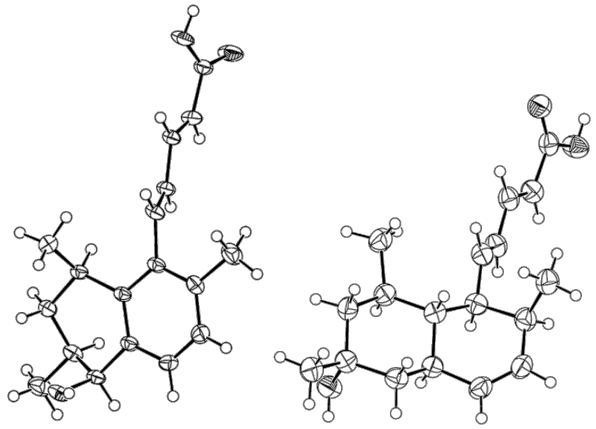


Figure 6: Crystal structures (ORTEP plot) of arohynapene A (**5**, left) and tanzawaic acid E (**8**, right). Thermal ellipsoids are drawn at the 50% probability level.

Tanzawaic acids were found in different *Penicillium* species, especially tanzawaic acid A which seems to be omnipresent in *Penicillium citrinum* [1,2]. Tanzawaic acids E and F were isolated from a marine-derived *Penicillium steckii* and were detected in at least 16 culture collection strains of the same species in a secondary metabolite study [2].

Recently, El-Neketi et al. [5] described the isolation of two new tanzawaic acids G and H, as well as tanzawaic acids B and F and arohynapene D from an endophytic *Penicillium citrinum* species. Therefore, *Penicillium* sp. IBWF104-06 appears to be related by its secondary metabolites to the aforementioned strains which do belong to the *Penicillium* section *Citrina* [6]. Tanzawaic acid E differs from tanzawaic acid L by two more hydrogen atoms at C-6 and C-15 and has the same elemental composition as tanzawaic acid K, the structural difference being the position of the OH group located at C-15 of tanzawaic acid K instead of C-10 in tanzawaic acid E [2]. Tanzawaic acids I and J have an 18 amu lower mass than hynapene A [7]. In contrast to the latter compound, both tanzawaic acids contain a double bond at C-14/15 instead of an OH group at C-14.

Biological activity. The isolated compounds were tested for their bioactivity in a series of antimicrobial and antiproliferative assays. We found that apart from compounds **1** and **2**, the other isolates (**3**–**8**) inhibited the conidial germination in

Magnaporthe oryzae at concentrations of 50 µg/mL or less (Table 3) whereas the germination of the grey mold *Botrytis cinerea* and the potato blight caused by the oomycete *Phytophthora infestans* were not affected at comparable concentrations. Even though several biological activities have been found for the known compounds **5**–**8**, an inhibition of fungal spore germination of *Magnaporthe oryzae* was not reported to date. The structurally related hynapenes B and C showed antimicrobial activity against *Pyricularia oryzae* [8] whereas arohynapenes A, B, and D [3,9] were not active in agar diffusion assays. However, arohynapenes A and B inhibited the spore germination at 25 µg/mL (IC_{90}). In addition, tanzawaic acid A (**7**) showed weak activity in agar diffusion assays at 50 µg/filter dics against *Bacillus brevis*, *Mucor miehei*, and *Paecilomyces variotii*, as well as cytotoxic effects against HeLaS3 cells at a concentration of 50 µg/mL. However, none of the other compounds showed bioactivity in these assays up to 50 µg/mL.

Table 3: Inhibition of germination in *Magnaporthe oryzae* (IC_{90} represents the concentration at which 90% inhibition of conidial germination was observed).

Compound	*M. oryzae* IC_{90} [µg/mL]
tanzawaic acid I (**1**)	–
tanzawaic acid J (**2**)	–
tanzawaic acid K (**3**)	25
tanzawaic acid L (**4**)	50
arohynapene A (**5**)	25
arohynapene B (**6**)	25
tanzawaic acid A (**7**)	10
tanzawaic acid E (**8**)	25

Experimental

General experimental procedures. Optical rotations were measured on a Perkin Elmer polarimeter model 241 at 546 and 578 nm and were extrapolated to 589 nm using Drude's equation [10]. ^{1}H, ^{13}C and 2D NMR spectra were recorded on a Bruker AVANCE III 600 MHz spectrometer equipped with a 5 mm TCI cryogenic inverse probe head (*z*-gradient) using standard pulse sequences. APCI-MS spectra were measured from a solution of the analyte in $MeCN/H_2O$ with a Hewlett Packard MSD 1100 using an evaporator temperature of 400 °C and a drying gas temperature of 350 °C at a flow of 6 L/h (N_2). In positive ionization mode, the capillary voltage amounted to 3.5 kV, the corona discharge current was 4 µA. In negative ionization mode, the capillary voltage amounted to 2.2 kV, the corona discharge current was 6 µA. HRMS-ESI data were recorded on a Q-ToF ULTIMA-III (Waters) equipped with a LockSpray-interface. A Bruker IFS48 FTIR spectrometer and a Perkin-Elmer Lambda-16 spectrophotometer were used to measure the IR and UV spectra, respectively.

Producing organism. The producing fungus IBWF104-06 was isolated from a soil sample. The strain was determined as a *Penicillium* species by morphology. Strain IBWF104-06 has been deposited in the culture collection of the Institute of Biotechnology and Drug Research (IBWF e.V.), Kaiserslautern, Germany. For maintenance, the fungus was grown on agar slants on YMG agar (yeast extract 4.0 g/L, malt extract 10 g/L, glucose 10 g/L, the pH value was adjusted to 5.5 before sterilisation). Solid media contained 2.0% agar.

Fermentation and isolation. The fermentation was carried out according to the method described by Schüffler et al. [11]. The fungus was grown in YMG medium in a 20 L fermenter (Braun, Melsungen) at 22–24 °C with agitation (120 rpm) and aeration (3 L/min). For inoculation, a well-grown shake culture (YMG medium, 250 mL) was used. During fermentation, the bioactive principles were quantified by HPLC and 13 days after inoculation the production was pronounced and the fermentation was stopped. The culture fluid (14.5 L) was separated from the mycelium by filtration and extracted with ethyl acetate (10 L). The solvent was evaporated and the oily crude extract (2.2 g) was applied onto a column filled with silica gel (Merck 60, 0.063–0.2 mm). Elution with a mixture of cyclohexane/ethyl acetate (3:2 v/v) yielded the oily fraction 1 (700 mg), 2:3 cyclohexane/ethyl acetate eluted oily fraction 2 (560 mg), and 1:4 cyclohexane/ethyl acetate eluted oily fraction 3 (100 mg). Further work-up of fraction 1 by solid-phase extraction (Macherey-Nagel, Chromabond C18ec) with 1:1 acetonitrile/water generated intermediate A (600 mg) and with 1:4 acetonitrile/water intermediate B (50 mg). Preparative HPLC of intermediate A (Waters SunFire, Prep C18 OBD, 5 µm, 19 × 250 mm, 17 mL/min, isocratic conditions, 1:1 acetonitrile/0.1% formic acid) resulted in arohynapene A (**5**, 173 mg, t_R 9 min) and tanzawaic acid E (**8**, 143 mg, t_R 13 min). Preparative HPLC of intermediate B resulted in tanzawaic acid A (**7**, 20 mg, t_R 24 min; Waters SunFire, Prep C18 OBD, 5 µm, 19 × 250 mm, 17 mL/min, isocratic conditions, 13:7 acetonitrile/0.1% formic acid). Work-up of fraction 2 by preparative HPLC (Waters SunFire, Prep C18 OBD, 5 µm, 19 × 250 mm, 17 mL/min, isocratic conditions, 11:9 acetonitrile/0.1% formic acid) generated tanzawaic acid K (**3**, 54 mg, t_R 16.5 min) and intermediate C (t_R 7–13 min, 320 mg). Intermediate C yielded tanzawaic acid L (**4**, 29 mg, t_R 25.5 min) and arohynapene B (**6**, 14 mg, t_R 31 min) by a second preparative HPLC (Agilent PrepHT, Zorbax, XDB-C8, 21.2 × 150 mm, 5 µm, 21 mL/min, isocratic conditions, 7:13 acetonitrile/0.1% formic acid). Fraction 3 was applied onto a solid-phase extraction column (Macherey-Nagel, Chromabond C18ec) and extraction with 2:3 acetonitrile/0.1% formic acid gave intermediate D (87 mg) which was used for preparative HPLC (Waters SunFire, Prep C18 OBD, 5 µm, 19 × 250 mm, 16 mL/min, isocratic condi-

tions, 2:3 acetonitrile/0.1% formic acid) to yield tanzawaic acid I (**1**, 7.7 mg, t_R 9 min) and tanzawaic acid J (**2**, 12.6 mg, t_R 10.5 min).

Bioactivity assays. Antimicrobial activities against bacteria and fungi were determined in the agar plate diffusion assay as described previously [12]. Cytotoxicity was assayed as described previously [13]. The cell line HelaS3 was grown in DMEM medium (Invitrogen). The medium was supplemented with 10% heat-inactivated fetal calf serum (Invitrogen), 65 mg/L of penicillin G and 100 mg/L of streptomycin sulfate. The viability was evaluated by microscopy after 72 h. The spore germination was tested with *M. oryzae* as described previously [14]. This method was adapted for the spore germination assay with *Phytophthora infestans* and *Botrytis cinerea*.

Tanzawaic acid I (1). Yellow oil; UV (MeOH) (λ_{max}, log ε): 261 (4.45); $[\alpha]_D^{20}$ −262 (0.4, MeOH); IR (ν, cm^{-1}): 3414, 2950, 2923, 1689, 1640, 1457, 1380, 1248; HRMS-ESI *m/z*: $[M + Na]^+$ calcd for $C_{18}H_{26}O_4Na$, 329.1729; found, 329.1744; APCI-MS (neg) *m/z*: 305.1 $[M - H]^-$; APCI-MS (pos) *m/z*: 289.2 $[M - H_2O + H]^+$, 271.2 $[M - 2H_2O + H]^+$.

Tanzawaic acid J (2). Yellow oil; UV (MeOH) (λ_{max}, log ε): 261 (4.45); $[\alpha]_D^{20}$ +73.7 (0.4, MeOH); IR (ν, cm^{-1}): 3369, 2947, 2835, 1638, 1451, 1032; HRMS-ESI *m/z*: $[M + Na]^+$ calcd for $C_{18}H_{26}O_4Na$, 329.1729; found, 329.1744; APCI-MS (neg) *m/z*: 305.1 $[M - H]^-$; APCI-MS (pos) *m/z*: 289.2 $[M - H_2O + H]^+$, 271.2 $[M - 2H_2O + H]^+$.

Tanzawaic acid K (3). Yellow oil; UV (MeOH) (λ_{max}, log ε): 257 (4.59); $[\alpha]_D^{20}$ −20.1 (0.38, MeOH); IR (ν, cm^{-1}): 3432, 2909, 1688, 1638, 1456, 1275; HRMS-ESI *m/z*: $[M + Na]^+$ calcd for $C_{18}H_{26}O_3Na$, 313.1780; found, 313.1788; APCI-MS (neg) *m/z*: 289.1 $[M - H]^-$; APCI-MS (pos) *m/z*: 273.2 $[M - H_2O + H]^+$.

Tanzawaic acid L (4). Yellow oil; UV (MeOH) (λ_{max}, log ε): 255 (3.70), 286 (3.68); $[\alpha]_D^{20}$ −126.7 (0.32, MeOH); IR (ν, cm^{-1}): 3409, 2961, 2965, 1698, 1638, 1377, 1247; HRMS-ESI *m/z*: $[M + Na]^+$ calcd for $C_{18}H_{24}O_3Na$, 311.1623; found, 311.1630; APCI-MS (neg) *m/z*: 287.1 $[M - H]^-$; APCI-MS (pos) *m/z*: 271.1 $[M - H_2O + H]^+$, 253.1 $[M - 2H_2O + H]^+$.

CCDC 962065 and 962066 contain crystallographic data for arohynapene A and tanzawaic acid E, respectively. A copy of the data can be obtained free of charge from the Cambridge Crystallographic Data Centre, on application to CCDC, 12 Union Road, Cambridge CB2 1EZ, UK, (fax: +44-(0)1223-336033 or e-mail:deposit@ccdc.cam.ac.uk).

Supporting Information

Supporting Information File 1

NMR spectra and crystallographic data.
[http://www.beilstein-journals.org/bjoc/content/supplementary/1860-5397-10-20-S1.pdf]

Acknowledgements

We thank the Rhineland Palatinate Center for Natural Product Research for financial support, Prof. Dr. H. Anke (IBWF, Kaiserslautern) for providing the strain IBWF104-06, Nina Wolff and Anja Meffert (both Kaiserslautern) for expert technical assistance, Dr. Johannes C. Liermann (Mainz) for NMR spectroscopy, Dr. N. Hanold (Mainz) for mass spectrometry, and Dr. D. Schollmeyer (Mainz) for X-ray crystallography.

References

1. Kuramoto, M.; Yamada, K.; Shikano, M.; Yazawa, K.; Arimoto, H.; Okamura, T.; Uemura, D. *Chem. Lett.* **1997,** *26,* 885–886. doi:10.1246/cl.1997.885
2. Malmstrøm, J.; Christophersen, C.; Frisvad, J. C. *Phytochemistry* **2000,** *54,* 301–309. doi:10.1016/S0031-9422(00)00106-0
3. Masuma, R.; Tabata, N.; Tomoda, H.; Haneda, K.; Iwai, Y.; Omura, S. *J. Antibiot.* **1994,** *47,* 46–53. doi:10.7164/antibiotics.47.46
4. Arimoto, H.; Nishimura, K.; Kuramoto, M.; Uemura, D. *Tetrahedron Lett.* **1998,** *39,* 9513–9516. doi:10.1016/S0040-4039(98)02226-6
5. El-Neketi, M.; Ebrahim, W.; Lin, W.; Gedara, S.; Badria, F.; Saad, H.-E. A.; Lai, D.; Proksch, P. *J. Nat. Prod.* **2013,** *76,* 1099–1104. doi:10.1021/np4001366
6. Houbraken, J.; Frisvad, J. C.; Samson, R. A. *Stud. Mycol.* **2011,** *70,* 53–138. doi:10.3114/sim.2011.70.02
7. Tabata, N.; Tomoda, H.; Iwai, Y.; Omura, S. *J. Antibiot.* **1993,** *46,* 1854–1858. doi:10.7164/antibiotics.46.1854
8. Tabata, N.; Tomoda, H.; Masuma, R.; Haneda, K.; Iwai, Y.; Omura, S. *J. Antibiot.* **1993,** *46,* 1849–1853. doi:10.7164/antibiotics.46.1849
9. Tabata, N.; Tomoda, H.; Iwai, Y.; Omura, S. *J. Antibiot.* **1995,** *48,* 83–84. doi:10.7164/antibiotics.48.83
10. Lippke, G.; Thaler, H. *Starch/Staerke* **1970,** *22,* 344–351. doi:10.1002/star.19700221005
11. Schüffler, A.; Kautz, D.; Liermann, J. C.; Opatz, T.; Anke, T. *J. Antibiot.* **2009,** *62,* 119–121. doi:10.1038/ja.2008.21
12. Anke, H.; Bergendorff, O.; Sterner, O. *Food Chem. Toxicol.* **1989,** *27,* 393–397. doi:10.1016/0278-6915(89)90145-2
13. Zapf, S.; Hoßfeld, M.; Anke, H.; Velten, R.; Steglich, W. *J. Antibiot.* **1995,** *48,* 36–41. doi:10.7164/antibiotics.48.36
14. Kettering, M.; Valdivia, C.; Sterner, O.; Anke, H.; Thines, E. *J. Antibiot.* **2005,** *58,* 390–396. doi:10.1038/ja.2005.49

License and Terms

This is an Open Access article under the terms of the Creative Commons Attribution License (http://creativecommons.org/licenses/by/2.0), which permits unrestricted use, distribution, and reproduction in any medium, provided the original work is properly cited.

The license is subject to the *Beilstein Journal of Organic Chemistry* terms and conditions: (http://www.beilstein-journals.org/bjoc)

The definitive version of this article is the electronic one which can be found at: doi:10.3762/bjoc.10.20

Beilstein Journal of Organic Chemistry

Decandrinin, an unprecedented C_9-spiro-fused 7,8-*seco*-*ent*-abietane from the Godavari mangrove *Ceriops decandra*

Hui Wang[1,2], Min-Yi Li[3], Félix Zongwe Katele[4], Tirumani Satyanandamurty[5], Jun Wu[*3] and Gerhard Bringmann[*4]

Full Research Paper

Open Access

Address:
[1]Key Laboratory of Marine Bio-resources Sustainable Utilization, South China Sea Institute of Oceanology, Chinese Academy of Sciences, 164 West Xingang Road, Guangzhou 510301, P. R. China, [2]Hubei Key Laboratory of Natural Products Research and Development, College of Chemistry and Life Science, China Three Gorges University, Yichang 443002, P. R. China, [3]Marine Drugs Research Center, College of Pharmacy, Jinan University, 601 Huangpu Avenue West, Guangzhou 510632, P. R. China, [4]Institute of Organic Chemistry, University of Würzburg, Am Hubland, Würzburg 97074, Germany and [5]Government Degree College at Amadala valasa, Srikakulam District, Andhra Pradesh 532185, India

Email:
Jun Wu[*] - wwujun2003@yahoo.com; Gerhard Bringmann[*] - bringmann@chemie.uni-wuerzburg.de

* Corresponding author

Keywords:
abietane; absolute configuration; *Ceriops decandra*; circular dichroism; decandrinin; Rhizophoraceae

Beilstein J. Org. Chem. **2014,** *10,* 276–281.
doi:10.3762/bjoc.10.23

Received: 16 October 2013
Accepted: 18 December 2013
Published: 27 January 2014

This article is part of the Thematic Series "Natural products in synthesis and biosynthesis".

Guest Editor: J. S. Dickschat

© 2014 Wang et al; licensee Beilstein-Institut.
License and terms: see end of document.

Abstract

Decandrinin (**1**), an unprecedented C_9-spiro-fused 7,8-*seco*-*ent*-abietane, was obtained from the bark of an Indian mangrove, *Ceriops decandra*, collected in the estuary of Godavari, Andhra Pradesh. The constitution and the relative configuration of **1** were determined by HRMS (ESI) and extensive NMR investigations, and the absolute configuration by circular dichroism (CD) and optical-rotatory dispersion (ORD) spectroscopy in combination with quantum-chemical calculations. Decandrinin is the first 7,8-*seco*-*ent*-abietane.

Introduction

Ceriops decandra is a mangrove of the family Rhizophoraceae. It is widely distributed along the sea coasts of South Asia down to the southern pacific islands, and of Africa and Madagascar. The genus *Ceriops* only consists of five mangrove plant species. Besides *C. decandra*, these are *C. australis*, *C. pseudodecandra*, *C. tagal*, and *C. zippeliana* [1-4]. In Indian traditional medicine,

the bark of *C. decandra* have been used for the treatment of amoebiasis, diarrhea, hemorrhage, and malignant ulcers [5], making it rewarding to screen the bioactive compounds of this plant. Before our work, already 28 compounds had been isolated from *C. decandra* [6] (three pimaranes, four beyeranes, five kauranes, and 16 lupanes). Recently, some of us have reported on the isolation of eleven new diterpenes from this plant, named decandrins A–K [7], of which nine belong to the group of abietanes.

S*eco*-abietane diterpenoids are a small group of natural products. To date, a total of 58 such compounds have been reported from plants of the genera *Abies*, *Cephalotaxus*, *Colus*, *Cordia*, *Hyptis*, *Isodon*, *Pinus*, *Premna*, *Salvia*, *Taiwania*, *Thuja*, and *Vitex*, including a 1,2-*seco*-abietane [8], a 1,10-*seco*-abietane [9,10], three 2,3-*seco*-abietanes [8,11-13], three 3,4-*seco*-abietanes [8,14], 31 4,5-*seco*-abietanes [8,15,16], ten 6,7-*seco*-abietanes [8,17-19], two 7,8-*seco*-abietanes [8,20], two 8,14-*seco*-abietanes [21,22], three 9,10-*seco*-abietanes [22,23], and two 9,11-*seco*-abietanes [24,25]. Among the above *seco*-abietanes, only laxiflorin V is a *seco*-*ent*-abietane [14]. Herein, we report on the isolation and structural elucidation of an unprecedented C_9-spiro-fused 7,8-*seco*-*ent*-abietane, named decandrinin (**1**) (Figure 1), from the bark of an Indian mangrove, *C. decandra*, collected in the estuary of Godavari, Andhra Pradesh. The absolute stereostructure of **1** was established by HRMS (ESI), extensive NMR investigations, and by circular dichroism (CD) and optical-rotatory dispersion (ORD) spectroscopy in combination with quantum-chemical calculations.

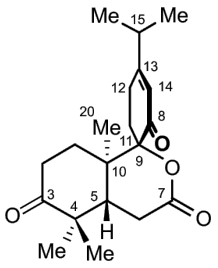


Figure 1: Structure of decandrinin (**1**).

Results and Discussion

Decandrinin (**1**) was obtained as a colorless solid. Its molecular formula was established as $C_{20}H_{28}O_4$ by HRMS (ESI) (*m*/*z* 333.2053, calcd for $[M + H]^+$, 333.2060). From this formula, it was suggested that **1** has seven degrees of unsaturation, of which four could be ascribed to one carbon–carbon double bond, one lactone carbonyl group, and two ketone groups, according to its ^1H and ^{13}C NMR data (Table 1); the molecule should thus be tricyclic.

Table 1: ^1H (400 MHz) and ^{13}C (100 MHz) NMR spectroscopic data for **1** in $CDCl_3$ (δ ppm).

Position	δ_H (*J* in Hz)	δ_C
1α	1.87, m	31.5, CH_2
1β	2.03, m	
2α	2.33, m	33.8, CH_2
2β	2.68, m	
3		213.1, C
4		47.1, C
5	2.47, m	43.1, CH
6α	2.66, m	28.8, CH_2
6β	2.47, m	
7		170.9, C
8		195.9, C
9		88.3, C
10		39.0, C
11α	2.59, m	30.1, CH_2
11β	2.23, m	
12	2.52, m	26.6, CH_2
	2.52, m	
13		172.0, C
14	6.03, br s	124.1, CH
15	2.45, m	35.4, CH
16	1.11, d (6.9)	20.6, CH_3
17	1.11, d (6.9)	20.8, CH_3
18	1.06, s	25.4, CH_3
19	1.13, s	21.6, CH_3
20	1.37, s	14.9, CH_3

The NMR data and a DEPT experiment (Table 1) indicated the presence of an olefinic methine group [δ_H 6.03 (br s), δ_C 124.1], two aliphatic methine groups [δ_H 2.47 (m), δ_C 43.1; δ_H 2.45 (m), δ_C 35.4], five methylene groups [δ_H 2.33 (m), 2.68 (m), δ_C 33.8; δ_H 1.87 (m), 2.03 (m), δ_C 31.5; δ_H 2.59 (m), 2.23 (m), δ_C 30.1; δ_H 2.66 (m), 2.47 (m), δ_C 28.8; δ_H 2.52 (2H, m), δ_C 26.6], five methyl groups [δ_H 1.06 (3H, s), δ_C 25.4; δ_H 1.13 (3H, s), δ_C 21.6; δ_H 1.11 (d, J = 6.9 Hz, 3H), δ_C 20.8; δ_H 1.11 (d, J = 6.9 Hz, 3H), δ_C 20.6; δ_H 1.37 (3H, s), δ_C 14.9], two keto groups (δ_C 213.1, 195.9), and a lactone carbonyl group (δ_C 170.9). The NMR spectroscopic data indicated that **1** was a rearranged abietane.

The existence of an isopropyl group was suggested by $^1H,^1H$-COSY correlations between H-15 and protons of two methyl groups [δ_H 1.11 (d, J = 6.9 Hz, 3H), 1.11 (d, J = 6.9 Hz, 3H)]. From $^1H,^1H$-COSY correlations, three further proton–proton spin systems, viz. H_2-1–H_2-2, H_2-11–H_2-12, and H-5–H_2-6, were deduced (Figure 2).

HMBC correlations between H_3-16/C-13, H_3-17/C-13, and H-14/C-15 placed the above isopropyl group at C-13, while

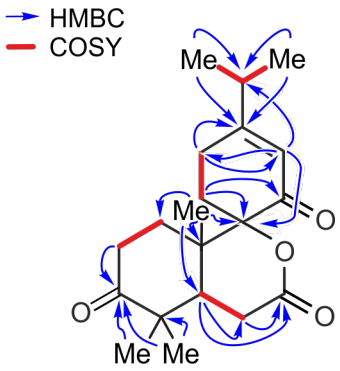


Figure 2: Selected ^{1}H–^{1}H COSY and HMBC correlations for decandrinin (**1**).

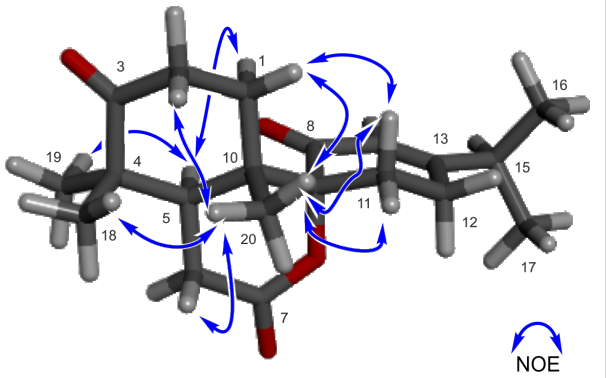


Figure 3: Diagnostic NOE interactions for decandrinin (**1**, B97D/TZVP-optimized structure): arbitrarily the 5*R*,9*R*,10*S*-enantiomer is shown.

those from H-14 to C-9 and C-12 indicated the presence of a $\Delta^{13,14}$ double bond. HMBC correlations from H_3-18, H_3-19, and H_2-2 to the carbon at δ_C 213.1 suggested the location of a keto group at C-3, whereas those from H_2-11 to the carbon at δ_C 195.9 indicated that there was another keto group at C-8 (Figure 2).

HMBC correlations from H-5 and H_2-6 to the carbonyl carbon (δ_C 170.9) of a δ-lactone suggested its location at C-7, while those from H_2-11, H-14, and H_3-20 to the quaternary carbon (δ_C 88.3) placed it at C-9 (Figure 2).

The NOE interactions for the two methyl groups at C-4 suggested that one methyl group is located at the same side as H-5, while the other one has the same orientation as Me-20. The NOEs between the two protons of the methylene at C-11 and Me-20 led to the conclusion that the carbonyl at C-8 is opposite to Me-20 (Figure 3). If the carbonyl at C-8 was oriented in the same direction as Me-20 these NOEs would not be observed because there would be several atoms between the concerned protons (Figure S9 in Supporting Information File 1). Therefore, the relative configuration of **1** was identified as shown in Figure 1.

The absolute configuration of **1** was assigned by CD and ORD spectroscopy in combination with quantum-chemical calculations. The conformational analysis of **1** by using RI-SCS-MP2/def2-TZVP//B97D/TZVP yielded six relevant conformers within the energetical range of 3 kcal/mol above the global minimum. For each of the six conformers thus identified, TDB2PLYP/def2-TZVP calculations were performed providing single UV and CD spectra, which were then summed up with Boltzmann weighting. The resulting averaged CD spectrum was corrected by a UV shift [26] of 13 nm and compared with the experimental CD curve (Figure 4). While the CD curve predicted for the 5*R*,9*R*,10*S*-configuration was nearly opposite to the one experimentally observed, the spectrum calculated for the 5*S*,9*S*,10*R*-enantiomer showed a good fitting with a moderate Δ_{ESI} value of 58% [27]. To further corroborate the assignment of the absolute configuration of **1**, ORD calculations were performed using the PBE0/cc-pVDZ//B97D/TZVP method. The ORD calculated for the 5*S*,9*S*,10*R*-configuration in the non-resonant region matched with the one observed experimentally (Figure S10 in Supporting Information File 1). The good agreement of the experimental CD and ORD spectra with the ones calculated for the 5*S*,9*S*,10*R*-enantiomer revealed the absolute configuration of **1** to be as shown in Figure 4.

A plausible biogenetic precursor of decandrinin (**1**) might be the naturally more common β-diastereomer of 7,13-*ent*-abietadien-3-ol (**2**). Accordingly, its 3β-OH group would be oxidized to yield **int A**, whose C-9 would then be hydroxylated to afford **int B**. Oxidative cleavage at the $\Delta^{7,8}$ double bond of **int B** could yield **int C**. Finally, the lactonization of **int C** would give decandrinin (**1**) (Scheme 1).

Experimental

General methods

Optical rotation values were recorded on a JASCO P-1020 polarimeter. CD spectra were recorded on a J-715 spectropolarimeter (JASCO, Gross-Umstadt, Germany). UV spectra were obtained on a Beckman DU-640 UV spectrophotometer. NMR spectra were recorded on a Bruker Avance 400 NMR spectrometer in $CDCl_3$. High-resolution ESI mass spectra were performed on a Bruker maXis UHR-TOF mass spectrometer in positive ion mode. For column chromatography, silica gel (200–300 mesh, Qingdao Mar. Chem. Ind. Co. Ltd.) and RP C_{18} gel (YMC) were used. High-performance liquid chromatography (HPLC) was performed on a Shimadzu LC-6AD controller with an SPD-20A UV–vis detector equipped with YMC-Pack ODS-A columns (250 × 10 mm i.d., 5 µm and 250 × 4.6 mm i.d., 5 µm).

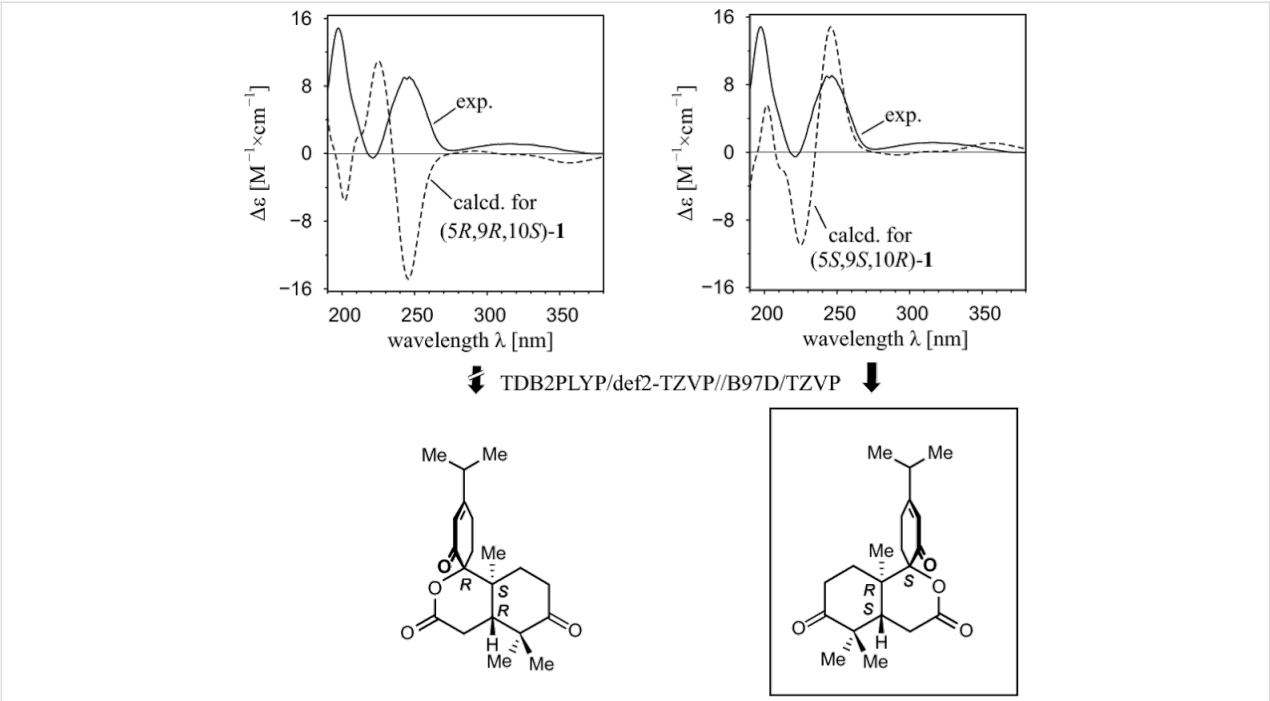
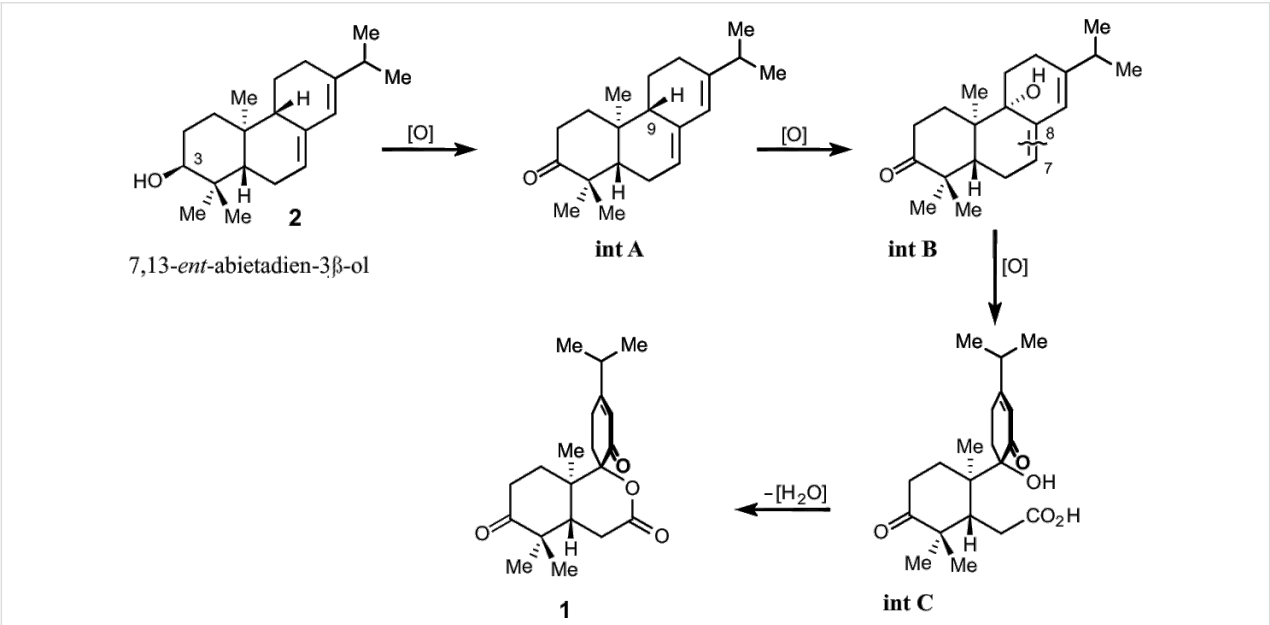


Figure 4: Determination of the absolute configuration of decandrinin (**1**) by comparing the calculated CD spectra with the experimental one.



Scheme 1: Proposed biosynthetic pathway for decandrinin (**1**).

Plant material

As described previously [7] the bark of *Ceriops decandra* were collected in September 2009 in the estuary of Godavari, Andhra Pradesh, India. The identification of the plant was performed by one of the authors (T.S.). A voucher sample (No. CD-001) is maintained at the Marine Drugs Research Center, College of Pharmacy, Jinan University.

Extraction and isolation

The extraction and isolation procedures were in part identical to those described recently [7]: The chloroform extract (65.2 g) from air-dried bark (7.4 kg) of *C. decandra* was subjected to silica-gel column chromatography (200−300 mesh, 3.0 kg) and eluted with petroleum ether/acetone (100:0 to 1:2) to yield 285 fractions. Fractions 173 to 204 were combined and further

purified using RP C_{18} column chromatography eluted with acetone/H_2O (30:70 to 100:0) to give 57 subfractions. Subfractions 8–13 were combined and subjected to preparative HPLC (YMC-Pack 250 × 10 mm i.d., MeCN/H_2O, 32:68) to afford eight subfractions. Then the sixth subfraction was further purified by HPLC (YMC-Pack 250 × 4.6 mm i.d., MeOH/H_2O, 40:60) to provide **1** (1.9 mg).

Characterization

Decandrinin (**1**): Colorless solid; $[\alpha]_D^{25}$ +242.0 (*c* 0.12, Me_2CO); UV (MeCN) λ_{max} 246.9 nm; For ^1H and ^{13}C NMR spectroscopic data (see Table 1); HRMS (ESI) *m*/*z*: $[M + H]^+$ calcd for $C_{20}H_{29}O_4$, 333.2060; found 333.2053.

Computational details

The B97D/TZVP [28,29] method was used to perform the conformational analysis of **1** with Gaussian 09 [30]. Single-point energy calculations at the RI-SCS-MP2/def2-TZVP [31,32] level and TDB2PLYP/def2-TZVP [33-35] calculations in combination with the COSMO solvation model with acetonitrile as a solvent and the chain-of-spheres approximations [35-37] were done using ORCA [38]. The optical rotatory dispersion (ORD) was calculated at the PBE0/cc-pVDZ [39,40] level using Gaussian 09. The Boltzmann weighting of single UV and CD spectra, UV shift, the determination of Δ_{ESI} values in the wavelength region between 190 nm and 380 nm (13 nm UV shift, σ = 0.22 eV), and the comparison of the calculated CD (σ = 0.22 eV) and ORD spectra with those observed experimentally were done with SpecDis 1.61 [41].

Supporting Information

Supporting Information File 1

HRMS (ESI) and NMR spectra of decandrinin (**1**), NOE interactions for the B97D/TZVP-optimized structure diagnostic for the 9-epimer of decandrinin (**1**), and comparison of the calculated ORD with the experimental one.
[http://www.beilstein-journals.org/bjoc/content/supplementary/1860-5397-10-23-S1.pdf]

Acknowledgements

This work was financially supported by NSFC (31100258, 31170331, and 81125022), the Guangdong Key Science and Technology Special Project (2011A080403020), and the Special Financial Fund of Innovative Development of Marine Economic Demonstration Project (GD2012-D01-001). The authors thank Franziska Witterauf for the experimental CD and ORD measurements. F.Z.K. is grateful to the BEBUC Excellence Scholarship System and the Else-Kröner-Fresenius-Stiftung for the support of his master studies.

References

1. Wu, J.; Xiao, Q.; Xu, J.; Li, M.-Y.; Pan, J.-Y.; Yang, M.-H. *Nat. Prod. Rep.* **2008,** *25,* 955–981. doi:10.1039/b807365a
2. Huang, Y.; Tan, F.; Su, G.; Deng, S.; He, H.; Shi, S. *Genetica* **2008,** *133,* 47–56. doi:10.1007/s10709-007-9182-1
3. Sheue, C.-R.; Liu, H.-Y.; Tsai, C.-C.; Rashid, S. M. A.; Yong, J. W. H.; Yang, Y.-P. *Blumea* **2009,** *54,* 220–227. doi:10.3767/000651909X476193
4. Sheue, C.-R.; Liu, H.-Y.; Tsai, C.-C.; Yang, Y.-P. *Bot. Stud.* **2010,** *51,* 237–248.
5. Rastogi, R. P.; Mehrotra, B. N. *Compendium of Indian Plants;* New Delhi, 1991.
6. Wang, H.; Li, M.-Y.; Wu, J. *Chem. Biodiversity* **2012,** *9,* 1–11. doi:10.1002/cbdv.201000299
7. Wang, H.; Li, M.-Y.; Satyanandamurty, T.; Wu, J. *Planta Med.* **2013,** *79,* 666–672. doi:10.1055/s-0032-1328459
8. Kabouche, A.; Kabouche, Z. *Stud. Nat. Prod. Chem.* **2008,** *35,* 753–833. doi:10.1016/S1572-5995(08)80017-8
9. Baxter, R. L.; Blake, A. J.; Gould, R. O. *Phytochemistry* **1995,** *38,* 195–197. doi:10.1016/0031-9422(94)00588-K
10. Hanson, J. R. *Nat. Prod. Rep.* **1997,** *14,* 245–258. doi:10.1039/NP9971400245
11. Siddiqui, B. S.; Perwaiz, S.; Begum, S. *Tetrahedron* **2006,** *62,* 10087–10090. doi:10.1016/j.tet.2006.08.043
12. Hanson, J. R. *Nat. Prod. Rep.* **2002,** *19,* 125–132. doi:10.1039/b009027l
13. Hanson, J. R. *Nat. Prod. Rep.* **2007,** *24,* 1332–1341. doi:10.1039/b705951p
14. Wang, W.-G.; Du, X.; Li, X.-N.; Yan, B.-C.; Zhou, M.; Wu, H.-Y.; Zhan, R.; Dong, K.; Pu, J.-X.; Sun, H.-D. *Nat. Prod. Bioprospect.* **2013,** *3,* 145–149. doi:10.1007/s13659-013-0057-0
15. Xu, X.-H.; Zhang, W.; Cao, X.-P.; Xue, S. *Phytochem. Lett.* **2011,** *4,* 52–55. doi:10.1016/j.phytol.2010.12.003
16. Hanson, J. R. *Nat. Prod. Rep.* **2004,** *21,* 785–793. doi:10.1039/b414026p
17. Kelecom, A.; Dos Santos, T. C.; Medeiros, W. L. B. *Phytochemistry* **1987,** *26,* 2337–2340. doi:10.1016/S0031-9422(00)84714-7
18. Ohtsu, H.; Iwamoto, M.; Ohishi, H.; Matsunaga, S.; Tanaka, R. *Tetrahedron Lett.* **1999,** *40,* 6419–6422. doi:10.1016/S0040-4039(99)01191-0
19. Salae, A. W.; Rodjun, A.; Karalai, C.; Ponglimanont, C.; Chantrapromma, S.; Kanjana-Opas, A.; Tewtrakul, S.; Fun, H.-K. *Tetrahedron* **2012,** *68,* 819–829. doi:10.1016/j.tet.2011.11.058
20. da Cruz Araújo, E. C.; Lima, M. A. S.; Silveira, E. R. *Magn. Reson. Chem.* **2004,** *42,* 1049–1052. doi:10.1002/mrc.1489
21. Yang, N.-Y.; Tao, W.-W.; Duan, J.-A.; Tian, L.-J. *Phytochemistry* **2010,** *71,* 1528–1533. doi:10.1016/j.phytochem.2010.06.008
22. Yang, X.-W.; Feng, L.; Li, S.-M.; Liu, X.-H.; Li, Y.-L.; Wu, L.; Shen, Y.-H.; Tian, J.-M.; Zhang, X.; Liu, X.-R.; Wang, N.; Liu, Y.; Zhang, W.-D. *Bioorg. Med. Chem.* **2010,** *18,* 744–754. doi:10.1016/j.bmc.2009.11.055
23. Zheng, C.-J.; Huang, B.-K.; Wang, Y.; Ye, Q.; Han, T.; Zhang, Q.-Y.; Zhang, H.; Qin, L.-P. *Bioorg. Med. Chem.* **2010,** *18,* 175–181. doi:10.1016/j.bmc.2009.11.004
24. Chyu, C.-F.; Chiang, Y.-M.; Lin, H.-C.; Kuo, Y.-H. *Tetrahedron Lett.* **2004,** *45,* 641–643. doi:10.1016/j.tetlet.2003.07.008

25. Hanson, J. R. *Nat. Prod. Rep.* **2005,** *22,* 594–602. doi:10.1039/b501834j
26. Bringmann, G.; Bruhn, T.; Maksimenka, K.; Hemberger, Y. *Eur. J. Org. Chem.* **2009,** 2717–2727. doi:10.1002/ejoc.200801121
27. Bruhn, T.; Hemberger, Y.; Schaumlöffel, A.; Bringmann, G. *Chirality* **2013,** *25,* 243–249. doi:10.1002/chir.22138
28. Grimme, S. *J. Comput. Chem.* **2006,** *27,* 1787–1799. doi:10.1002/jcc.20495
29. Schäfer, A.; Horn, H.; Ahlrichs, R. *J. Chem. Phys.* **1992,** *97,* 2571–2577. doi:10.1063/1.463096
30. Frisch, M. J.; Trucks, G. W.; Schlegel, H. B.; Scuseria, G. E.; Robb, M. A.; Cheeseman, J. R.; Scalmani, G.; Barone, V.; Mennucci, B.; Petersson, G. A.; Nakatsuji, H.; Caricato, M.; Li, X.; Hratchian, H. P.; Izmaylov, A. F.; Bloino, J.; Zheng, G.; Sonnenberg, J. L.; Hada, M.; Ehara, M.; Toyota, K.; Fukuda, R.; Hasegawa, J.; Ishida, M.; Nakajima, T.; Honda, Y.; Kitao, O.; Nakai, H.; Vreven, T.; Montgomery, J. A.; Peralta, J. E., Jr.; Ogliaro, F.; Bearpark, M.; Heyd, J. J.; Brothers, E.; Kudin, K. N.; Staroverov, V. N.; Keith, T.; Kobayashi, R.; Normand, J.; Raghavachari, K.; Rendell, A.; Burant, J. C.; Iyengar, S. S.; Tomasi, J.; Cossi, M.; Rega, N.; Millam, J. M.; Klene, M.; Knox, J. E.; Cross, J. B.; Bakken, V.; Adamo, C.; Jaramillo, J.; Gomperts, R.; Stratmann, R. E.; Yazyev, O.; Austin, A. J.; Cammi, R.; Pomelli, C.; Ochterski, J. W.; Martin, R. L.; Morokuma, K.; Zakrzewski, V. G.; Voth, G. A.; Salvador, P.; Dannenberg, J. J.; Dapprich, S.; Daniels, A. D.; Farkas, O.; Foresman, J. B.; Ortiz, J. V.; Cioslowski, J.; Fox D. J. in *Gaussian 09, revision B.01*, Gaussian, Inc., Wallingford CT, 2010.
31. Grimme, S. *J. Chem. Phys.* **2003,** *118,* 9095–9102. doi:10.1063/1.1569242
32. Weigend, F.; Ahlrichs, R. *Phys. Chem. Chem. Phys.* **2005,** *7,* 3297–3305. doi:10.1039/b508541a
33. Grimme, S. *J. Chem. Phys.* **2006,** *124,* 034108. doi:10.1063/1.2148954
34. Grimme, S.; Neese, F. *J. Chem. Phys.* **2007,** *127,* 154116. doi:10.1063/1.2772854
35. Petrenko, T.; Kossmann, S.; Neese, F. *J. Chem. Phys.* **2011,** *134,* 054116. doi:10.1063/1.3533441
36. Neese, F.; Wennmohs, F.; Hansen, A.; Becker, U. *Chem. Phys.* **2009,** *356,* 98–109. doi:10.1016/j.chemphys.2008.10.036
37. Kossmann, S.; Neese, F. *J. Chem. Theory Comput.* **2010,** *6,* 2325–2338. doi:10.1021/ct100199k
38. Neese, F.; Becker, U.; Ganyushin, D.; Hansen, A.; Liakos, D.; Kollmar, C.; Koβmann, S.; Petrenko, T.; Reimann, C.; Riplinger, C.; Sivalingam, K.; Wezista, B.; Wennmohs, F. *ORCA – an ab initio, density functional and semiempirical program package, version 2.9.1*, Max Planck Institute for Bioinorganic Chemistry, Germany, 2012.
39. Adamo, C.; Barone, V. *J. Chem. Phys.* **1999,** *110,* 6158–6170. doi:10.1063/1.478522
40. Dunning, T. H., Jr. *J. Chem. Phys.* **1989,** *90,* 1007–1023. doi:10.1063/1.456153
41. Bruhn, T.; Schaumlöffel, A.; Hemberger, Y.; Bringmann, G. *SpecDis*, version 1.61, University of Würzburg, Germany, 2013.

License and Terms

This is an Open Access article under the terms of the Creative Commons Attribution License (http://creativecommons.org/licenses/by/2.0), which permits unrestricted use, distribution, and reproduction in any medium, provided the original work is properly cited.

The license is subject to the *Beilstein Journal of Organic Chemistry* terms and conditions: (http://www.beilstein-journals.org/bjoc)

The definitive version of this article is the electronic one which can be found at: doi:10.3762/bjoc.10.23

Beilstein Journal of Organic Chemistry

Total synthesis and cytotoxicity of the marine natural product malevamide D and a photoreactive analog

Werner Telle[1], Gerhard Kelter[2], Heinz-Herbert Fiebig[2], Peter G. Jones[3] and Thomas Lindel[*1]

Full Research Paper

Open Access

Address:
[1]Institute of Organic Chemistry, TU Braunschweig, Hagenring 30, 38106 Braunschweig, Germany, [2]Oncotest Institute for Experimental Oncology GmbH, Am Flughafen 12–14, 79108 Freiburg, Germany and [3]Institute of Inorganic and Analytical Chemistry, TU Braunschweig, Hagenring 30, 38106 Braunschweig, Germany

Email:
Thomas Lindel[*] - th.lindel@tu-braunschweig.de

* Corresponding author

Keywords:
cytotoxicity; diazirines; dolastatin analogs; marine natural products; peptides; total synthesis

Beilstein J. Org. Chem. **2014,** *10,* 316–322.
doi:10.3762/bjoc.10.29

Received: 17 October 2013
Accepted: 03 January 2014
Published: 03 February 2014

This article is part of the Thematic Series "Natural products in synthesis and biosynthesis".

Guest Editor: J. S. Dickschat

© 2014 Telle et al; licensee Beilstein-Institut.
License and terms: see end of document.

Abstract

The marine natural product malevamide D from the cyanobacterium *Symploca hydnoides* was synthesized for the first time. The final peptide coupling linked the dolaisoleuine and dolaproine subunits. The phenyl group of malevamide D was also functionalized with a photoreactive diazirine moiety, which was carried through seven reaction steps. Comprehensive assessment of the cytotoxicity in a panel of 42 human cancer cell lines revealed a geomean IC_{70} value of 1.5 nM (IC_{50} 0.7 nM) for malevamide D, whereas the photoreactive derivative proved to be less active by a factor of at least 200. COMPARE analysis indicated tubulin interaction as likely mode of action of malevamide D.

Introduction

The depsipeptide malevamide D (**1**, Figure 1) belongs to the dolastatin class of marine natural products and has been isolated from the cyanobacterium *Symploca hydnoides* by Scheuer and co-workers in 2002 (7.5 mg, 0.014% of the dry weight) [1]. Malevamide D (**1**) was reported to exhibit in vitro cytotoxicity in the subnanomolar range (IC_{50} values about 0.7 nM). Closely related to malevamide D (**1**) is isodolastatin H (**2**), which is also active in vivo, but slightly weaker than dolastatin 10 (**3**) [2]. Although there has been no study regarding the mode of action, it can be assumed that malevamide D (**1**) acts similarly to dolastatin 10 (**3**) by inhibiting the formation of microtubuli from tubulin and, thereby, cell division. Dolastatin-type natural products continue to be tested in clinical trials for cancer therapy [3]. This includes an antibody conjugate of monomethylauristatin E (MMAE), which has been approved for the treatment of Hodgkin lymphoma (Brentuximab vedotin) [4].

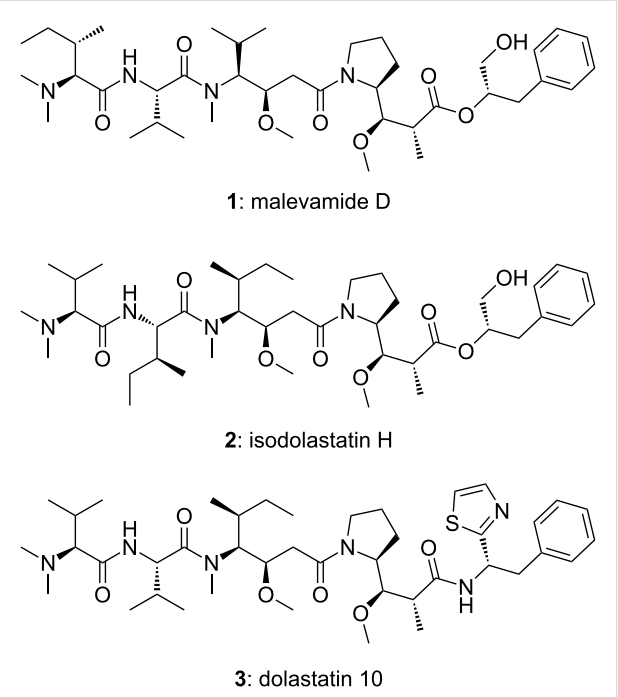


Figure 1: Structures of the strongly cytotoxic marine natural products malevamide D (**1**), isodolastatin H (**2**), and dolastatin 10 (**3**).

In this paper, we report the first total synthesis of malevamide D (**1**) and an assessment of its in vitro cytotoxicity in a panel of 42 cell lines. We also synthesized a diazirinylated analog of **1**, which, by photocrosslinking, might contribute to the understanding of the binding of **1** to tubulin.

Results and Discussion

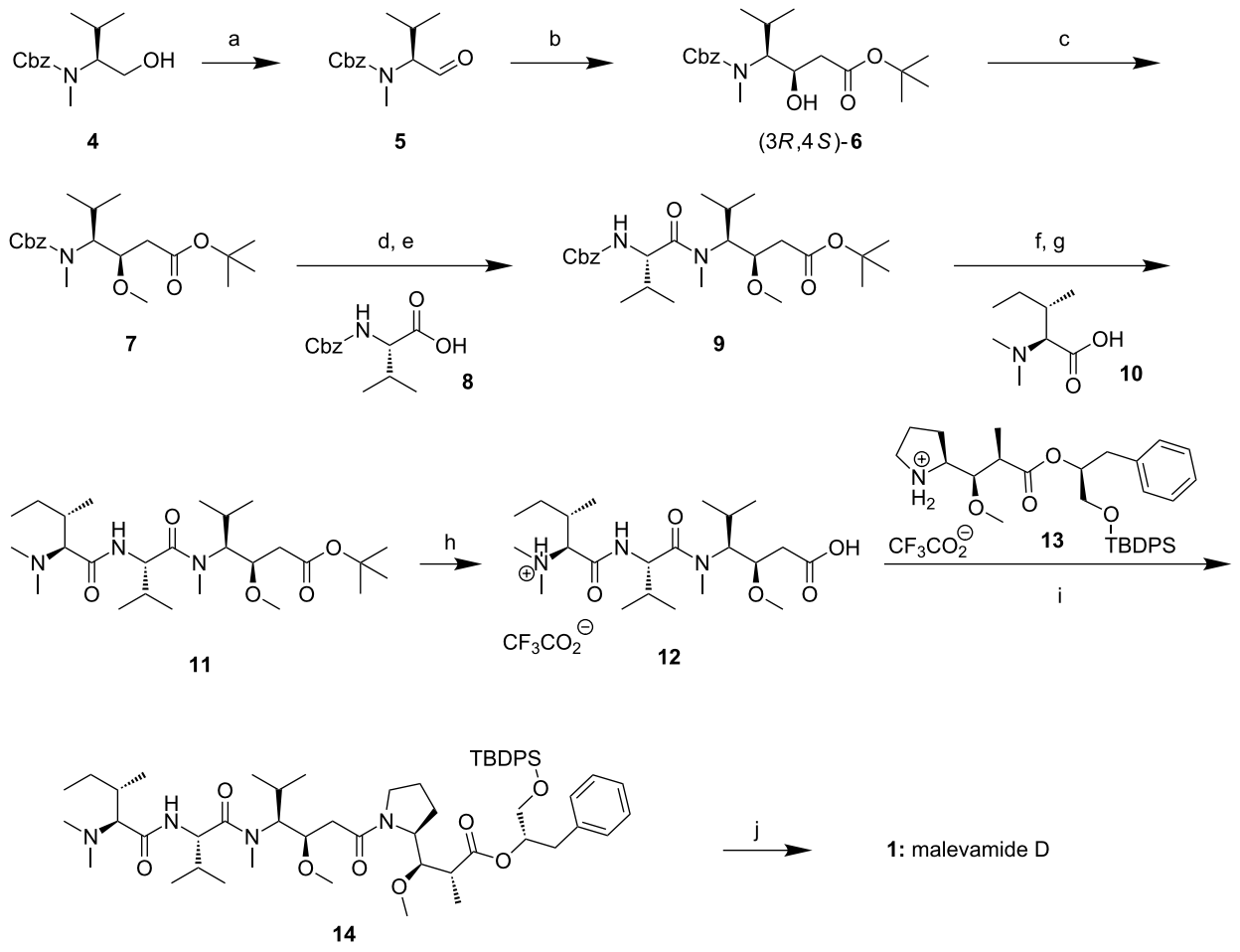
Total synthesis of malevamide D

The natural products malevamide D (**1**), isodolastatin H (**2**), and dolastatin 10 (**3**) share two β-methoxy-γ-amino acid building blocks. The closest structural analog of malevamide D (**1**) is isodolastatin H (**2**) with an identical ester section composed of dolaproine and (2*S*)-3-phenylpropan-1,2-diol. On the N-terminal side, the isopropyl and two *sec*-butyl side chains of isodolastatin H (**2**) are replaced by one *sec*-butyl and two isopropyl side chains, respectively, in the case of malevamide D (**1**).

The total synthesis of **1** adopts the strategy by Yamada and co-workers in their total synthesis of **2**, which sets the first retro cut at the tertiary amide bond between dolaisoleuine and dolaproine [2]. The *tert*-butyl ester **7** of Cbz-protected 3-methoxy-5-methyl-4-(methylamino)hexanoic acid (MMMAH) was obtained in multigram quantities within five steps from Cbz-valine (**8**), adapting a convenient sequence developed for dolaisoleuine by Pettit and co-workers [5]. Cbz-protected *N*-methylvalinol (**4**) [6] was oxidized to the aldehyde **5** under Parikh–Doering conditions, followed by aldol addition of the lithium enolate of *t*-BuOAc (Scheme 1). β-Hydroxyhexanoate **6** was obtained as a mixture of diastereomers (5:4), which was separated by column chromatography (silica) on a multigram scale. Treatment of (3*R*,4*S*)-**6** with Meerwein's salt in presence of proton sponge afforded Cbz-protected MMMAH *tert*-butyl ester **7** in 87% yield. There are also other, enantioselective syntheses of **7** [7] and Boc-protected versions of MMMAH [8,9], but we intended to also have the (3*S*)-epimer of **7** at our disposal.

After hydrogenation of **7**, the resulting secondary amine was coupled with Cbz-valine (**8**) affording dipeptide **9** (DEPCl, diethyl phosphorochloridate), 80% over two steps, Scheme 1). *N*,*N*-Dimethylisoleucine (**10**), obtained by reductive dimethylation of isoleucine with aqueous formaldehyde and H_2 on Pd/C [10,11], was appended at the N-terminus (DEPC, diethyl phosphorocyanidate) affording tripeptide *tert*-butyl ester **11**. Treatment with TFA liberated the free acid **12**, which was coupled with the trifluoroacetate of dolaproine ester **13**, liberated from the *N*-Boc-protected analog [2].

With the subsequent coupling step affording TBDPS-protected malevamide D (**14**), we initially had difficulties. It proved to be crucial to remove excess of TFA from both coupling partners **12** and **13** completely, by repeated evaporation of DCM solutions. Finally, a coupling yield of 68% was reached following the DEPC protocol. Desilylation (TBAF in THF/H_2O) afforded **1** (HRESIMS found 755.49257, calcd. for $C_{40}H_{68}NaN_4O_8$ 755.49294) in 12% yield after 10 steps from valinol **4** (longest linear sequence). The optical rotation of the synthesized material ($[\alpha]_D^{28}$ −37, *c* 0.09, MeOH) is a little smaller than reported for the isolated natural product ($[\alpha]_D^{26}$ −55, *c* 0.10, MeOH) [1]. The ^{1}H and ^{13}C NMR spectra of **1** shows two sets of signals in a ratio of ca. 1:1. Clearly separated in the ^{13}C NMR spectrum are, for instance, the ester carbonyl signals of the conformers (174.0 and 173.3 ppm), the carbonyl signals of the pyrrolidine amide (170.5 and 170.6 ppm), and all phenyl carbon signals. Of the eastern section, only three of the four pyrrolidine carbon signals are broad. Most of the carbon signals of the western tripeptide of malevamide D are broadened (see Supporting Information File 1). The ^{1}H NMR spectrum shows many broad and overlapping signals, the assignment of which was only possible by careful interpretation of the 2D NMR data set. The only isolated signals belonging to different signal sets are located at δ_H 3.84 (one of the diastereotopic OCH_2 signals) and 5.21 ppm (acylated carbinol). The two sets of signals are probably caused by the presence of both conformers of the acyl pyrrolidine. An assignment of the data sets to either of the two conformers was not possible. The occurrence of conformers has been mentioned by Scheuer and co-workers and is also known for dolastatin 10 [12] and symplostatin 1 [13].

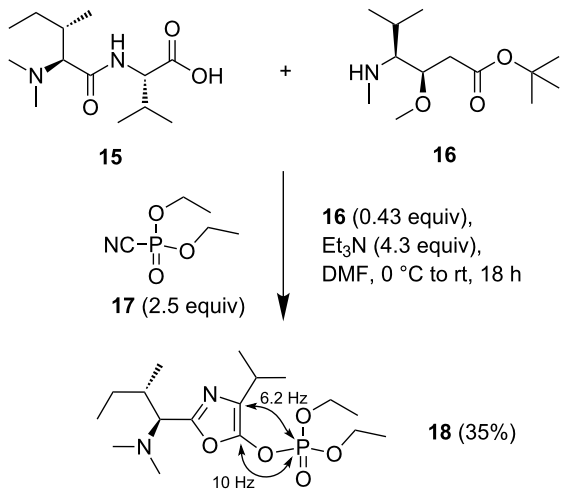


Scheme 1: Total synthesis of malevamide D (**1**). a) DMSO (16 equiv), NEt_3 (5 equiv), pyridine·SO_3 (5 equiv), 0 °C, 1 h, 91%. b) LDA (2.5 equiv), *t*-BuOAc (1.3 equiv), THF, −78 °C, 1 h; separation of diastereomers, (3*R*,4*S*)-**6**: 47%. c) 1,8-bis(dimethylamino)naphthalene (2.5 equiv), Me_3OBF_4 (2.6 equiv), 4 Å MS, 1,2-DCE, 0 °C, 2 h, rt, 16 h, 87%. d) H_2, Pd/C (5%), MeOH, rt, 1 h. e) **8** (3 equiv), NEt_3 (4 equiv), DEPCl (2 equiv), DCM, 0 °C, 2 h, rt, 16 h, 80% from **7**. f) H_2, Pd/C (5%), MeOH, rt, 90 min. g) **10** (3 equiv), NEt_3 (4 equiv), DEPC (1.5 equiv), DCM, 0 °C, 2 h, rt, 16 h, 83% from **9**. h) TFA, DCM, 0 °C, 90 min, quant. i) **13** (1 equiv), NEt_3 (6 equiv), DEPC (1.3 equiv), DCM, 0 °C to rt, 16 h, 68%. j) TBAF·$3H_2O$ (5 equiv), THF/H_2O 19:1, rt, 3 h, 71%. DEPCl: diethyl phosphorochloridate; DEPC: diethyl phosphorocyanidate.

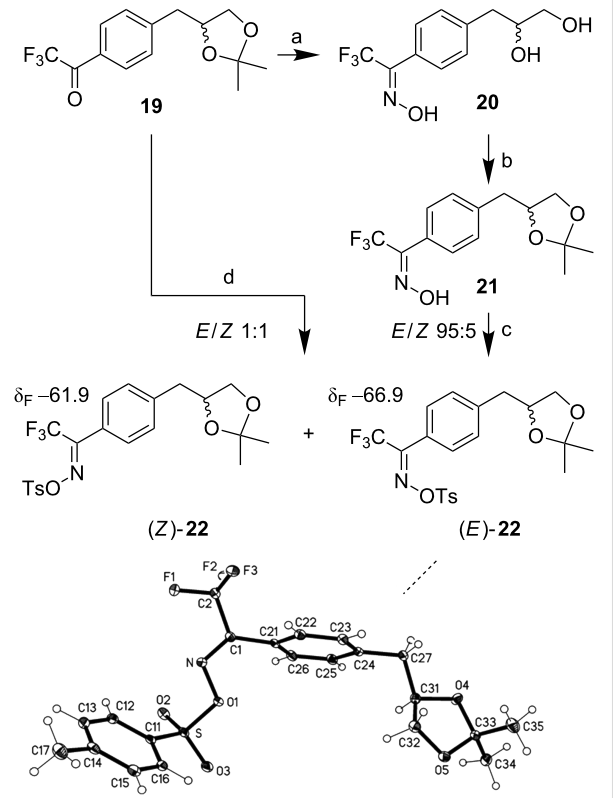
As an alternative route to the N-terminal tripeptide **11**, we also investigated the coupling of the N-terminal dipeptide **15** with MMMAH *tert*-butyl ester (**16**, Scheme 2). However, after treatment of dipeptide **15** with secondary amine **16** (0.43 equiv) and DEPC (**17**, 2.5 equiv), the only isolable product was oxazolylphosphate **18** (35%) without any amide formation occurring. The structure elucidation of **18** required C–P coupling constant analysis, which showed doublet ^{13}C NMR signals of oxazole C-5 (10 Hz) and C-4 (6.2 Hz). To the best of our knowledge, this is only the second time that a peptide-derived oxazol-5-ylphosphate has been characterized. Earlier, Boyd and co-workers had converted an oxazolone to an oxazolyl phosphate by treatment with excess diphenyl chlorophosphate [14]. In our case, a similar pathway is to be assumed with the oxazolone being formed first. The secondary amine **16** appears to react too slowly to be able to compete with oxazolone formation.

Diazirinyl-substituted malevamide D

Encouraged by the strong cytotoxicity of **1**, we addressed the synthesis of a photoactivatable analog. The question was whether such a derivative would still be cytotoxic. The phenyl ring of **1** was chosen as location of a trifluoromethyldiazirinyl substituent. Pettit and co-workers have shown that introduction of a phosphate moiety at the *p*-position of the phenyl ring of auristatin PE did not lead to loss of cytotoxicity [3]. Recently, we have synthesized a hemiasterlin derivative with a diazirinylated indole moiety by incorporation of a thermally stable L-phototryptophan carrying a 1-azi-2,2,2-trifluoroethyl unit [15].



Scheme 2: Formation of oxazolylphosphate **18** on attempted DEPC-mediated coupling of dipeptide **15**.



Scheme 3: Synthesis of tosyloximes (*Z*)-**22** and (*E*)-**22**, X-ray structure of (*E*)-**22**. a) $NH_2OH·HCl$ (1.5 equiv), pyridine, reflux, 2 h, 80%. b) 2,2-dimethoxypropane (12.4 equiv), *p*-TsOH·H_2O (5 mol %), DMF, rt, 1 h, 95%. c) *p*-TsCl (1.05 equiv), NEt_3 (1.3 equiv), DCM, 0 °C to rt, 18 h, 83%. d) (i) $NH_2OH·HCl$, NaOH, EtOH, pyridine, reflux (for details see Supporting Information File 1); (ii) *p*-TsCl (1.05 equiv), NEt_3 (1.3 equiv), DCM, 0 °C to rt, 18 h, 74%. ^{19}F NMR chemical shifts (ppm) in $CDCl_3$.

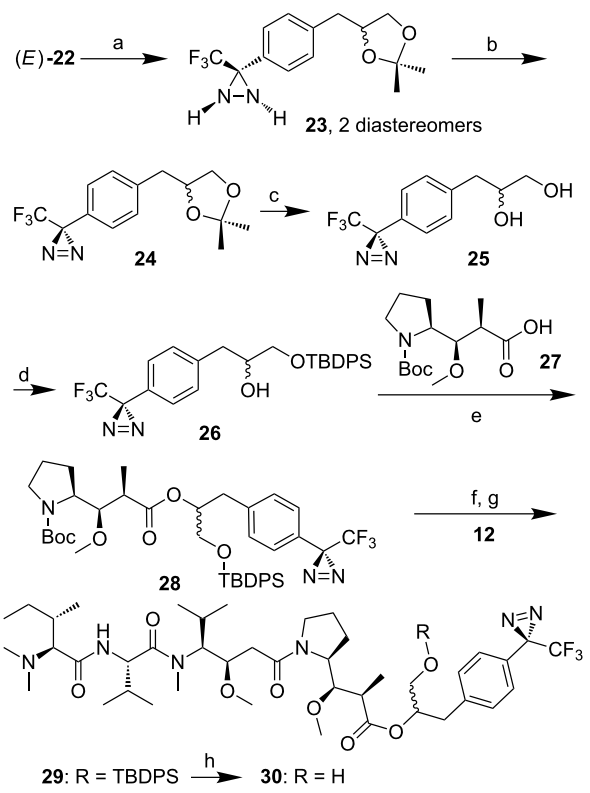
Racemic photo phenylpropanediol **25** was obtained starting from aryl(trifluoromethyl)ketone **19** (Scheme 3), which itself was synthesized via Grignard monoallylation of 1,4-dibromobenzene, followed by dihydroxylation, dioxolane protection and trifluoroacetylation of the remaining brominated position [16]. Refluxing of ketone **19** with $NH_2OH·HCl$ in pyridine led to nearly quantitative hydrolysis of the dioxolane affording diol oxime **20** as 95:5 mixture of *E*- and *Z*-isomers. However, if solid NaOH was added to the reaction mixture and heated for several hours, the dioxolane survived, affording a 1:1 mixture of *E*/*Z*-oximes, which were tosylated after short work-up to (*E*)- and (*Z*)-**22**.

Reprotection of the diol unit of **20** and tosylation of **21** afforded tosyloxime (*E*)-**22**, which crystallized overnight from the neat mixture and was analyzed by X-ray crystallography [17]. Thus, it became possible to assign the ^{19}F NMR chemical shifts of both isomers ((*E*)-**22**: δ_F −66.9; (*Z*)-**22**: δ_F −61.9).

Conversion of (*E*)-**22** to diaziridine **23** (colorless solid, δ_F −75.96, −75.93) was performed quantitatively (liquid NH_3 in *t*-BuOMe, Scheme 4). As expected, the NMR spectra of the colorless solid **23** showed two sets of signals. Oxidation of **23** with I_2/NEt_3 to diazirine **24** (δ_F −65.7) and acidic deprotection afforded diazirine diol **25**. Figure 2 shows the DSC (differential scanning calorimetry) profile of **25**, which melts at 54 °C and starts to decompose above 80 °C, indicating sufficient thermal stability for biological studies. Monosilylation of the primary hydroxy group of **25** afforded building block **26**. Coupling with Boc-protected dolaproine (**27**, DCC/DMAP/CSA) yielded ester **28** as a mixture of two diastereomers. After deprotection of the pyrrolidine, coupling with tripeptide **12** afforded *O*-silylated diazirinyl-substituted malevamide D (**29**, 68%). Desilylation (TBAF, THF/H_2O 19:1) led to a product mixture, the separation of which required semipreparative HPLC (RP-18, MeOH/H_2O 9:1). Diazirinyl-substituted malevamide **30** was obtained in 33% isolated yield as a mixture of two epimers differing at the carbinol center (HRESIMS found 863.48644, calcd. for $C_{42}H_{67}NaF_3N_6O_8$, 863.48647). In the NMR spectra, four sets of signals were observed because of additional *cis*/*trans* isomerism of the acyl pyrrolidine moiety. As in the case of **1**, the tripeptidic western half showed mostly broad signals, whereas the signals of the phenyl carbons are resolved better, even if not fully separated.

Cytotoxicity studies of malevamide D and diazirinyl-substituted malevamide D

The synthesized **1** proved to be potently cytotoxic with a geomean IC_{70} value of 1.5 nM (IC_{50} 0.7 nM) in a panel of



Scheme 4: Synthesis of photo malevamide D **30**. a) NH_3(l), *t*-BuOMe, −40 °C, 2 h, rt, 16 h, quant. b) I_2 (1.2 equiv), NEt_3 (2.2 equiv), Et_2O, 0 °C, 15 min, rt, 1 h, 99%. c) THF, 2 N HCl, rt, 3 h, 97%. d) TBDPSCl (1.1 equiv), imidazole (2.2 equiv), DMF, 0 °C, 1 h, 80%. e) **27** (0.97 equiv), DMAP (0.41 equiv), DCC (1 equiv), CSA (0.23 equiv), 0 °C to rt, 16 h, 69%. f) TFA, DCM, 0 °C, 90 min. g) **12** (1 equiv), NEt_3 (6 equiv), DEPC (2.14 equiv), DCM, 0 °C, 150 min, 68%. h) TBAF·$3H_2O$ (5 equiv), THF/H_2O 19:1, 0 °C, 2 h, 33%.

42 human cancer cell lines (see Table 1 and Supporting Information File 1). The cytotoxicity was about 10-fold higher than that of paclitaxel. The breast cancer cell lines MAXF-401 (IC_{70} 0.2 nM) and MCF-7 (0.5 nM), the colon cancer cell lines HT-29 (0.3 nM) and RKO (0.5 nM), the lung cancer cell line H460 (0.7 nM), the liver cancer cell line LIXF-575 (0.6 nM), and the renal cancer cell line RXF-393 (0.4 nM) all proved to be very sensitive. Against 36 of the 42 cell lines, IC_{70} values of below 10 nM were determined. The most resistant cell lines were shown to be RXF-1781 (kidney), CXF-269 (colon), MEXF-276

Table 1: Cytotoxicities (IC_{70}, IC_{50}, nM) of malevamide D (**1**) against selected human cancer cell lines.[a]

histotype	cell line	IC_{70}	IC_{50}
Colon	HT-29	0.3	0.2
Stomach	GXF-251	5.0	0.6
Lung, adeno	LXFA-629	0.7	0.4
Lung, large cell	LXFL-529	0.4	0.3
Breast	MAXF-401	0.2	0.2
Melanoma	MEXF-462	0.6	0.4
Ovary	OVXF-899	1.0	0.7
Pancreas	PAXF-1657	4.0	1.0
Prostate	PRXF-22Rv1	0.8	0.6
Mesothelioma	PXF-1752	0.4	0.3
Kidney	RXF-486L	0.7	0.5
Uterus	UXF-1138L	0.5	0.4

[a]For complete results in the panel of 42 human cancer cell lines and a COMPARE analysis, see Supporting Information File 1.

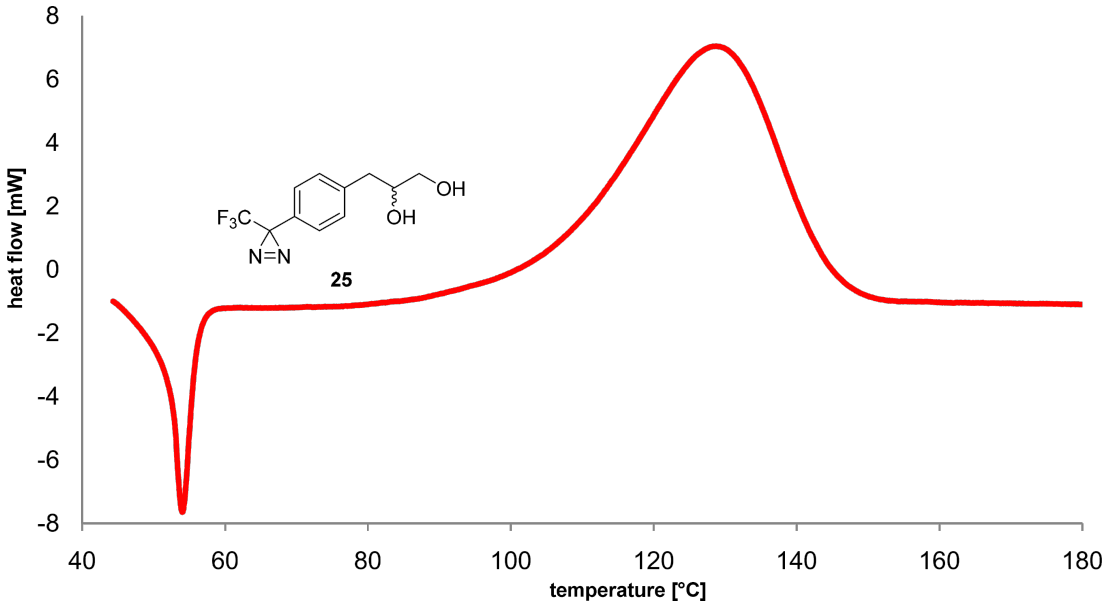


Figure 2: DSC curve of diazirine **25**, heating rate 5 °C/min.

(melanoma, IC_{70} about 50 nM, each), and in particular LXFA-289 (lung, adenocarcinoma), PAXF-546L (pancreas), and PXF-1118 (pleuramesothelioma, IC_{70} > 100 nM, IC_{50} about 50 nM, each). Diazirinyl-substituted malevamide D **30** was about 200 times less cytotoxic than **1**.

To obtain clues on the likely mode of action of **1** and **30**, the in vitro activity data were compared with those of 177 reference compounds by COMPARE analysis. Individual IC_{50} values of a test compound were correlated with those of 177 reference compounds as determined for Oncotest's 42 cell line panel and expressed quantitatively as Spearman correlation coefficients (see Supporting Information File 1). Furthermore, **1** and **30** were correlated to each other. For compound **30**, COMPARE analysis revealed the highest similarities towards tubulin interacting compounds like the vinca alkaloids vinfluine, vincristine, vindesine and the taxoid compound docetaxel. Furthermore, good correlations were detected towards PLK-1 inhibitors. Similar results were obtained for **1**. Determining a Spearman coefficient of 0.742 between **1** and **30** suggested that these compounds share the same mode of action, most probably antimitotic activity based on tubulin interaction.

Conclusion

Our cytotoxicity test results for **1** confirm those obtained by Scheuer and co-workers who determined IC_{50} values of about 0.7 nM against four cell lines (mouse lymphoma P-388, human lung carcinoma A-549, human colon carcinoma HT-29, human melanoma MEL-28) [1]. We had hoped that introduction of a Brunner-type diazirine unit in the *para*-position of the phenyl ring of **1** could lead to an analog that was still active, because it had been shown in several SAR studies that limited variation of the amine or alcohol component at the C-terminal amide or ester moieties of the dolastatin family members can be tolerated without much loss of cytotoxicity. This includes epimerization of the thiazole-carrying stereocenter of **3** [18], replacement of the phenyl by a methyl group, or removal of the thiazole ring [7]. Auristatins, of which some undergo clinical trials, are characterized by lacking the thiazole ring of **3** [19]. Pettit and co-workers prepared auristatin TP, which carries a phosphate unit in the *para*-position of the phenyl ring, and also two aminoquinoline derivatives that were as cytotoxic as dolastatin 10 [3]. Antibody conjugates of monomethylauristatin E functionalized on the C-terminal side have also shown promising pharmacological profiles [20,21]. However, compound **30** is at least 200 times less active than the natural product **1**. Lower cytotoxicity may be associated with solubility problems. We will now search for more water-soluble, photoactivatable analogs of **1**. Nunes and coworkers had synthesized a benzophenone-labelled derivative of the analog HTI-286, which competes with **3**, and were able to identify α-tubulin as binding partner [22].

Supporting Information

Supporting Information File 1

Procedures of synthesis and biotest, X-ray data and ^1H, ^{13}C NMR spectra of selected compounds.
[http://www.beilstein-journals.org/bjoc/content/supplementary/1860-5397-10-29-S1.pdf]

Acknowledgements

We thank Merck KGaA (Darmstadt, Germany) for the generous gift of chromatography materials. The BASF Group (Ludwigshafen, Germany) and Honeywell Specialty Chemicals Seelze GmbH (Seelze, Germany) are thanked for the donation of solvents.

References

1. Horgen, F. D.; Kazmierski, E. B.; Westenburg, H. E.; Yoshida, W. Y.; Scheuer, P. J. *J. Nat. Prod.* **2002,** *65,* 487–491. doi:10.1021/np010560r
2. Sone, H.; Shibata, T.; Fujita, T.; Ojika, M.; Yamada, K. *J. Am. Chem. Soc.* **1996,** *118,* 1874–1880. doi:10.1021/ja9519086
3. Pettit, G. R.; Hogan, F.; Toms, S. *J. Nat. Prod.* **2011,** *74,* 962–968. doi:10.1021/np1007334
4. Bradley, A. M.; Devine, M.; DeRemer, D. *Am. J. Health-Syst. Pharm.* **2013,** *70,* 589–597. doi:10.2146/ajhp110608
5. Pettit, G. R.; Sing, S. B.; Srirangam, J. K.; Hogan-Pierson, F.; Williams, M. D. *J. Org. Chem.* **1994,** *59,* 1796–1800. doi:10.1021/jo00086a034
6. Reddy, G. V.; Rao, G. V.; Sreevani, V.; Iyngar, D. S. *Tetrahedron Lett.* **2000,** *41,* 949–951. doi:10.1016/S0040-4039(99)02105-X
7. Miyazaki, K.; Kobayashi, M.; Natsume, T.; Gondo, M.; Mikami, T.; Sakakibara, K.; Tsukagoshi, S. *Chem. Pharm. Bull.* **1995,** *43,* 1706–1718. doi:10.1248/cpb.43.1706
8. Maugras, I.; Poncet, J.; Jouin, P. *Tetrahedron* **1990,** *46,* 2807–2816. doi:10.1016/S0040-4020(01)88373-3
9. Cella, R.; Venturoso, R. C.; Stefani, H. A. *Tetrahedron Lett.* **2008,** *49,* 16–19. doi:10.1016/j.tetlet.2007.11.031
10. Bowman, R. E.; Stroud, H. H. *J. Chem. Soc.* **1950,** 1342–1345. doi:10.1039/jr9500001342
11. Aurelio, L.; Box, J. S.; Brownlee, R. T. C.; Hughes, A. B.; Sleebs, M. M. *J. Org. Chem.* **2003,** *68,* 2652–2667. doi:10.1021/jo026722l
12. Benedetti, E.; Carlomagno, T.; Fraternali, F.; Hamada, Y.; Hayashi, K.; Paolillo, L.; Shioiri, T. *Biopolymers* **1995,** *36,* 525–538. doi:10.1002/bip.360360414
13. Harrigan, G. G.; Luesch, H.; Yoshida, W. Y.; Moore, R. E.; Nagle, D. G.; Paul, V. J.; Mooberry, S. L.; Corbett, T. H.; Valeriote, F. A. *J. Nat. Prod.* **1998,** *61,* 1075–1077. doi:10.1021/np980321c
14. Boyd, V. L.; Bozzini, M.; Guga, P. J.; DeFranco, R. J.; Yuan, P.-M.; Loudon, G. M.; Nguyen, D. *J. Org. Chem.* **1995,** *60,* 2581–2587. doi:10.1021/jo00113a042
15. Wartmann, T.; Lindel, T. *Eur. J. Org. Chem.* **2013,** 1649–1652. doi:10.1002/ejoc.201201726
16. Bolli, M.; Lehmann, D.; Mathys, B.; Müller, C.; Nayler, O.; Velker, J.; Weller, T. Novel thiophene derivatives. WO Patent WO 2006/100635 A2, Sept 28, 2006.

17. CCDC 956232 contains the supplementary crystallographic data of compound (*E*)-**22**, which can be obtained free of charge from the Cambridge Crystallographic Data Centre via http://www.ccdc.cam.ac.uk/data_request/cif (12, Union Road, Cambridge CB21EZ, UK; fax: (+44) 1223-336-033; or deposit@ccdc.cam.ac.uk).
18. Bai, R.; Roach, M. C.; Jayaram, S. K.; Barkoczy, J.; Pettit, G. R.; Ludueña, R. F.; Hamel, E. *Biochem. Pharmacol.* **1993,** *45,* 1503–1515. doi:10.1016/0006-2952(93)90051-W
19. Shnyder, S. D.; Cooper, P. A.; Millington, N. J.; Pettit, G. R.; Bibby, M. C. *Int. J. Oncol.* **2007,** *31,* 353–360.
20. Doronina, S. O.; Bovee, T. D.; Meyer, D. W.; Miyamoto, J. B.; Anderson, M. E.; Morris-Tilden, C. A.; Senter, P. D. *Bioconjugate Chem.* **2008,** *19,* 1960–1963. doi:10.1021/bc800289a
21. Axup, J. Y.; Bajjuri, K. M.; Ritland, M.; Hutchins, B. M.; Kim, C. H.; Kazane, S. A.; Halder, R.; Forsyth, J. S.; Santidrian, A. F.; Stafin, K.; Lu, Y.; Tran, H.; Seller, A. J.; Biroc, S. L.; Szydlik, A.; Pinkstaff, J. K.; Tian, F.; Sinha, S. C.; Felding-Habermann, B.; Smider, V. V.; Schultz, P. G. *Proc. Natl. Acad. Sci. U. S. A.* **2012,** *109,* 16101–16106. doi:10.1073/pnas.1211023109
22. Nunes, M.; Kaplan, J.; Wooters, J.; Hari, M.; Minnick, A. A., Jr.; May, M. K.; Shi, C.; Musto, S.; Beyer, C.; Krishnamurthy, G.; Qiu, Y.; Loganzo, F.; Ayral-Kaloustian, S.; Zask, A.; Greenberger, L. M. *Biochemistry* **2005,** *44,* 6844–6857. doi:10.1021/bi0474766

License and Terms

This is an Open Access article under the terms of the Creative Commons Attribution License (http://creativecommons.org/licenses/by/2.0), which permits unrestricted use, distribution, and reproduction in any medium, provided the original work is properly cited.

The license is subject to the *Beilstein Journal of Organic Chemistry* terms and conditions: (http://www.beilstein-journals.org/bjoc)

The definitive version of this article is the electronic one which can be found at: doi:10.3762/bjoc.10.29

Beilstein Journal of Organic Chemistry

Intermediates in monensin biosynthesis: A late step in biosynthesis of the polyether ionophore monensin is crucial for the integrity of cation binding

Wolfgang Hüttel[*1,2], Jonathan B. Spencer[3,§] and Peter F. Leadlay[1]

Letter

Open Access

Address:
[1]Department of Biochemistry, University of Cambridge, 80 Tennis Court Road, Cambridge CB2 1GA, UK, Fax: (+44)1223-766002, [2]Institute for Pharmaceutical Sciences, Universität Freiburg, Albertstr. 25, 79104 Freiburg, Germany and [3]Department of Chemistry, University of Cambridge, Lensfield Road, Cambridge CB2 1QW, UK

Email:
Wolfgang Hüttel[*] - wolfgang.huettel@pharmazie.uni-freiburg.de;
Peter F. Leadlay - pfl10@cam.ac.uk

* Corresponding author
§ Deceased

Keywords:
antibiotics; biosynthesis; natural products; polyketides; *Streptomyces*; synthetic biology

Beilstein J. Org. Chem. **2014,** *10,* 361–368.
doi:10.3762/bjoc.10.34

Received: 17 October 2013
Accepted: 30 December 2013
Published: 10 February 2014

This article is part of the Thematic Series "Natural products in synthesis and biosynthesis".

Guest Editor: J. S. Dickschat

© 2014 Hüttel et al; licensee Beilstein-Institut.
License and terms: see end of document.

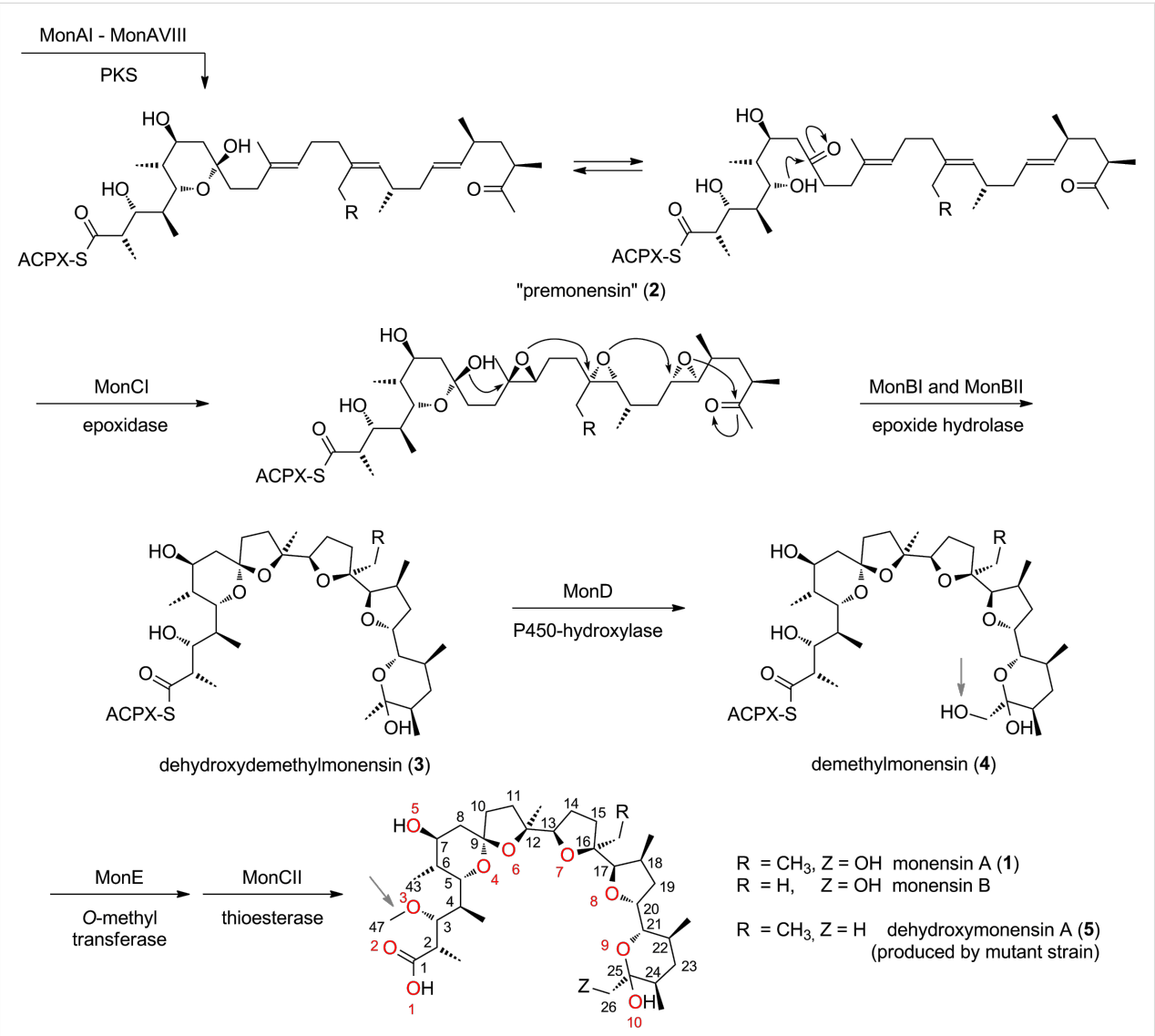
Abstract

Polyether antibiotics such as monensin are biosynthesised via a cascade of directed ring expansions operating on a putative polyepoxide precursor. The resulting structures containing fused cyclic ethers and a lipophilic backbone can form strong ionophoric complexes with certain metal cations. In this work, we demonstrate for monensin biosynthesis that, as well as ether formation, a late-stage hydroxylation step is crucial for the correct formation of the sodium monensin complex. We have investigated the last two steps in monensin biosynthesis, namely hydroxylation catalysed by the P450 monooxygenase MonD and *O*-methylation catalysed by the methyl-transferase MonE. The corresponding genes were deleted in-frame in a monensin-overproducing strain of *Streptomyces cinnamonensis*. The mutants produced the expected monensin derivatives in excellent yields (ΔmonD: 1.13 g L^{-1} dehydroxymonensin; ΔmonE: 0.50 g L^{-1} demethylmonensin; and double mutant ΔmonDΔmonE: 0.34 g L^{-1} dehydroxydemethylmonensin). Single crystals were obtained from purified fractions of dehydroxymonensin and demethylmonensin. X-ray structure analysis revealed that the conformation of sodium dimethylmonensin is very similar to that of sodium monensin. In contrast, the coordination of the sodium ion is significantly different in the sodium dehydroxymonensin complex. This shows that the final constitution of the sodium monensin complex requires this tailoring step as well as polyether formation.

Introduction

Monensin A (**1**) from *Streptomyces cinnamonensis* is one of the most prominent and best-studied of the polyether class of complex polyketides, an important and extensive group of natural products including a large number of antibiotic ionophores [1-5] as well as remarkable marine toxins such as the brevetoxins [6,7]. The antibiotic polyethers adopt a characteristic con-

formation in which multiple oxygen atoms provide ligands for a centrally-held specific cation (sodium in the case of monensin A) while the external surface is exclusively non-polar. This confers the ability to transport the cation across cell membranes leading to dissipation of the membrane potential and cell death. The toxicity of polyethers has limited their clinical use except in animal husbandry, but they are attracting renewed interest for their antimalarial [8,9], antiviral [10,11] and novel anticancer [12,13] activities. In turn, this has given impetus to current attempts to engineer polyether biosynthetic pathways to provide novel analogues with potentially improved therapeutic properties. We report here fresh insight into the order of the final steps of monensin biosynthesis, facilitated by genetic manipulation of an industrial strain of *S. cinnamonensis*. Further, the crystal structures of two of the monensin analogues obtained reveal the structural basis for the key role of late-stage hydroxylation at C-26 of the monensin molecule. Like other polyether ionophores, monensin is assembled by the polyketide biosynthetic pathway on a modular polyketide synthase (PKS) multienzyme [14]. A model has been proposed [14] for monensin biosynthesis in which an initially-formed (*E*,*E*,*E*)-triene undergoes stereospecific epoxidation to a tri-epoxide and subsequent ring-opening and cyclisation to generate the polyether rings. This model has been confirmed and extended (Scheme 1) by the results of more recent work in which specific genes have been disrupted or deleted in *S. cinnamonensis* [15-



Scheme 1: The proposed pathway for monensin biosynthesis in *Streptomyces cinnamonensis*. The polyketide synthase (PKS) initially produces an enzyme-bound triene, which is transferred to a discrete acylcarrier protein (ACPX) to give **2**. After oxidative cyclisation via **3** and **4** the ACP-bound product is finally hydrolysed by MonCII to the free monensin A (**1**, R = CH_3, Z = OH). Monensin B is a minor product of fermentation. For the final product the atom numbering of the central carbon chain and oxygen atoms (red) is shown.

20], but much remains to be learned about the timing of the various steps of oxidative ring formation (and hence the true nature of the enzyme-bound intermediates) and about the exact role of the enzymes involved in these late steps. As shown in Scheme 1, the monensin PKS (MonAI-MonAVIII) assembles the carbon skeleton of monensin A from five acetate, one butyrate and seven propionate units. The butyrate unit may be substituted by a further propionate unit, producing monensin B, which bears a methyl instead of an ethyl group at C-16.

It appears that oxidative cyclisation is not initiated before the full-length chain is produced, and that the initial product of the PKS is a linear enzyme-bound (*E*,*E*,*E*)-triene, "premonensin" (**2**) [19]. The monensin PKS does not have a conventional C-terminal thioesterase domain that would catalyse polyketide chain release, and instead a transferase (MonKSX) transfers the chain to a discrete acyl carrier protein (MonACPX) [20], both of these proteins being encoded within the monensin gene cluster [16]. The flavin-dependent epoxidase MonCI then catalyses three stereospecific epoxidations to give the tri-epoxide **3**, which then undergoes a cascade of ring opening/closing catalysed by the combined action of the unusual epoxide hydrolases MonBI and MonBII, to give the putative protein-bound intermediate dehydroxydemethylmonensin. The next steps, catalysed respectively by the cytochrome P450 hydroxylase MonD and the methyltransferase MonE, are hydroxylation at C-26 and O-methylation of the hydroxy group at C-3. Although hydroxylation is shown as preceding methylation in Scheme 1, the preferred order of these events has not been established. The final catalysed step in biosynthesis is the release of mature monensins A and B from the MonACPX, catalysed by the unusual thioesterase MonCII [20].

The evidently tight coupling between PKS-mediated chain assembly and oxidative cyclisation has hampered efforts to unravel the exact sequence and mechanism of events in the late stages of the biosynthesis. Indirect but suggestive evidence for the formation of the presumed tri-epoxide species has been obtained from the analysis of mutants blocked in either or both of the *monBI* and *monBII* genes [17]. These species, after HPLC isolation, were shown to be chemically competent to be isomerised into authentic monensins by the action of dilute acid. Further progress has been hampered by the instability of the various epoxide species as well as by the complexity of the product mixtures, containing both monensin A-related and monensin B-related compounds. Nevertheless, the structural characterisation of one of the products of such blocked mutants as an epimer of monensin A at C-9 [17] has provided clear evidence that both MonD and MonE are capable of acting on altered substrates, which is encouraging for future engineering experiments aimed at production of novel derivatives.

To help to provide a platform for such experiments, and to further elucidate the timing of catalysis of the post-PKS steps in monensin biosynthesis, we have undertaken the specific deletion of *monD* and *monE*, both individually and in combination, and have structurally characterised the principal compounds produced in each case. We report here that the hydroxylation at C-26 has a decisive effect on the three-dimensional structure of the ionophore-cation complex, as revealed by X-ray crystal structure analysis of both dehydroxymonensin A and demethylmonensin A, each in complex with a sodium ion.

Results and Discussion

PCR-targetted in-frame deletions using the ReDirect [21] version of the RedET recombineering technology [22] were designed to create specific *monD* and *monE* mutants, and also a double mutant ΔmonD ΔmonE (see Experimental). Genetic manipulations were carried out in an industrial monensin-producing strain of *S. cinnamonensis* [19] which routinely produced 3–4 g L^{-1} of product in unoptimised 50 mL shake flask cultures, over 100-fold more than the wild type strain. This overproduction greatly facilitated the characterisation of the products of the ΔmonD and ΔmonE mutants. For polyether production the mutant strains were initially cultivated in the SM-16 medium used for the *S. cinnamonensis* wild type strain [16]. However, in this medium the mutants gave highly variable amounts of products, as judged by LC–MS (data not shown). Therefore, a production medium containing large amounts of oil was used, and a short silica column was used to pretreat the initial extract to remove the large excess of oil before HPLC purification. Analysis by LC–MS revealed that the predicted monensin-related metabolites were indeed produced at elevated levels (see typical results in Figure 1 and Table 1) compared to monensin production in the wild type strain, on either SM-16 or the oil-based medium. The yield of isolated dehydroxydemethylmonensin (**3**) from the double mutant is an order of magnitude lower than the production of monensin from the parent industrial strain, but clearly this precursor, as its ACPX-thioester, is accepted as a substrate by the chain-releasing thioesterase MonCII. The results from the single mutants show that **3** is also a substrate for both MonD and MonE. In the ΔmonD strain substantial amounts of dehydroxydemethylmonensin (**3**) remain unconverted by MonE to dehydroxymonensin (**5**). In contrast, compound **3** was not detected in crude extracts of the ΔmonE strain. These results lend support to the idea that the preferred order of events is hydroxylation at C-26 catalysed by MonD, followed by *O*-methylation at the hydroxy group borne at C-3 catalysed by MonE, as shown in Scheme 1. The amount of dehydroxymonensin A isolated from the MonE mutant was substantially higher than the amount of demethylmonensins obtained from the MonD mutant (Table 1). This can be rationalised if the

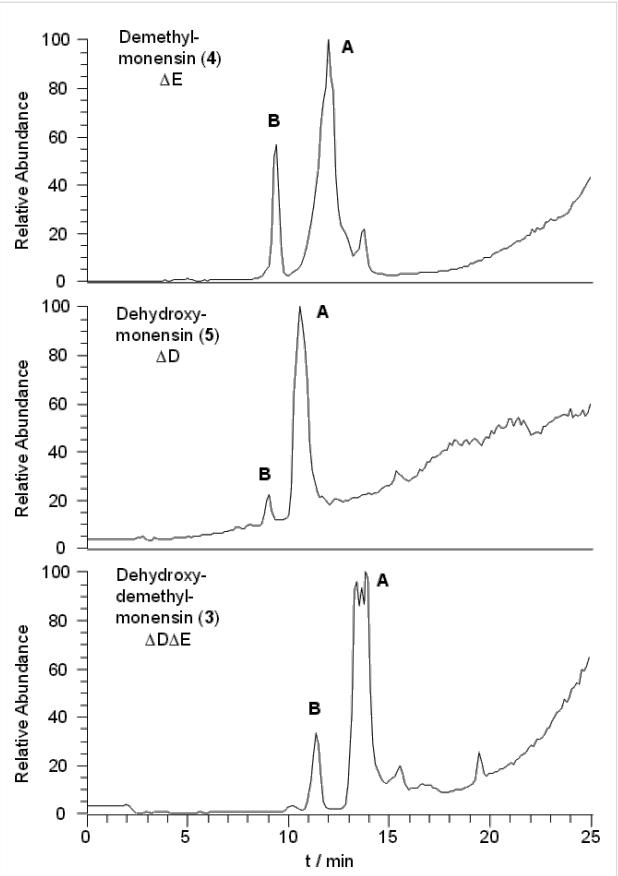


Figure 1: LC–MS-analysis of purified monensin-related metabolites. Monensin B derivatives (peaks marked with B) were identified as minor components of the product mixture. The triple peak for dehydroxy-demethylmonensin A (**3**) is due to an enrichment of disodium-species at the start and the end of the fraction. The chromatograms are uncorrected.

activity of MonCII is more strongly affected by the lack of a methoxy group at C-3 than by lack of the distal hydroxy group at C-26.

Monensin A-related species were predominant in the product mixtures obtained, with monensin B-related compounds produced only in small amounts (Figure 1). This was not unexpected as the parent strain A519 had been selected and optimised for monensin A production [19]. The spectroscopic properties of the purified 3-*O*-demethylmonensin A were in complete agreement with those previously reported for this compound, isolated as a minor component of a wild-type *S. cinnamonensis* strain [23]. Similarly, the spectroscopic properties of the isolated 26-dehydroxymonensin A were identical with those described for this compound obtained either from a specifically-blocked mutant of wild-type *S. cinnamonensis* [24] or from a wild-type fermentation conducted in the presence of the potent methyltransferase inhibitor metapyrone [25].

To gain further insight into the metal-binding properties of demethylmonensin A and dehydroxymonensin A, they were each crystallised as their monosodium salts from an isohexane/ethyl acetate mixture and single crystals were subjected to X-ray structural analysis (Figure 2). Dehydroxydemethylmonensin A did not form crystals under any conditions tested. When the demethylmonensin A structure is overlaid on the structure of the monosodium complex of monensin A [26-29] the conformations of these complexes are revealed to be almost identical (Figure 2b). The obvious difference is that the hydroxy group at C-3 in demethylmonensin A lies on the otherwise wholly non-polar external surface of the complex, a feature that likely accounts for its lower effectiveness as an ionophore antibiotic [7]. Otherwise, both show a highly rigid structure in which the sodium cation is enveloped by the polyether and coordinated by four oxygen atoms in ether rings (O-6, O-7, O-8 and O-9), and by the oxygen atoms (O-5 and O-11, respectively) of the hydroxy groups at C-7 and C-26 (Figure 2a). The oxygen atoms of the carboxylic acid form two hydrogen bonds to, respectively, the oxygen atoms O-10 and O-11 at the other end of the carbon chain (Figure 2a), locking the conformation of the ligand into place around the cation. The importance of such hydrogen bonds for the stability of the complex is underlined by the conservation of this feature in the crystal structures of the polyether ionophores nigericin [30,31] and dianemycin (nanchangmycin) [32], where a carboxylic acid oxygen atom likewise form hydrogen bonds to the distal hydroxy groups equivalent to positions O-10 and O-11 in monensin A. Unlike monensin, these larger polyethers also show direct coordination

Table 1: Monensin derivatives isolated from 250 mL culture medium of *S. cinnamonensis* deletion mutants.

Mutant	Compound[a]	Amount[b]	Crystals
monD	dehydroxymonensin (**5**)	284 mg	yes
	dehydroxydemethylmonensin (**3**)	46 mg	no
monE	demethylmonensin (**4**)	125 mg	yes
monD+ *monE*	dehydroxydemethylmonensin (**3**)	86 mg	no

[a]All products were obtained either as a colourless oil or a colourless solid. [b]For comparison: 750–1000 mg monensin per 250 mL culture of *S. cinnamonensis* A519 were detected in crude extracts by using the vanillin colorimetric assay [19].

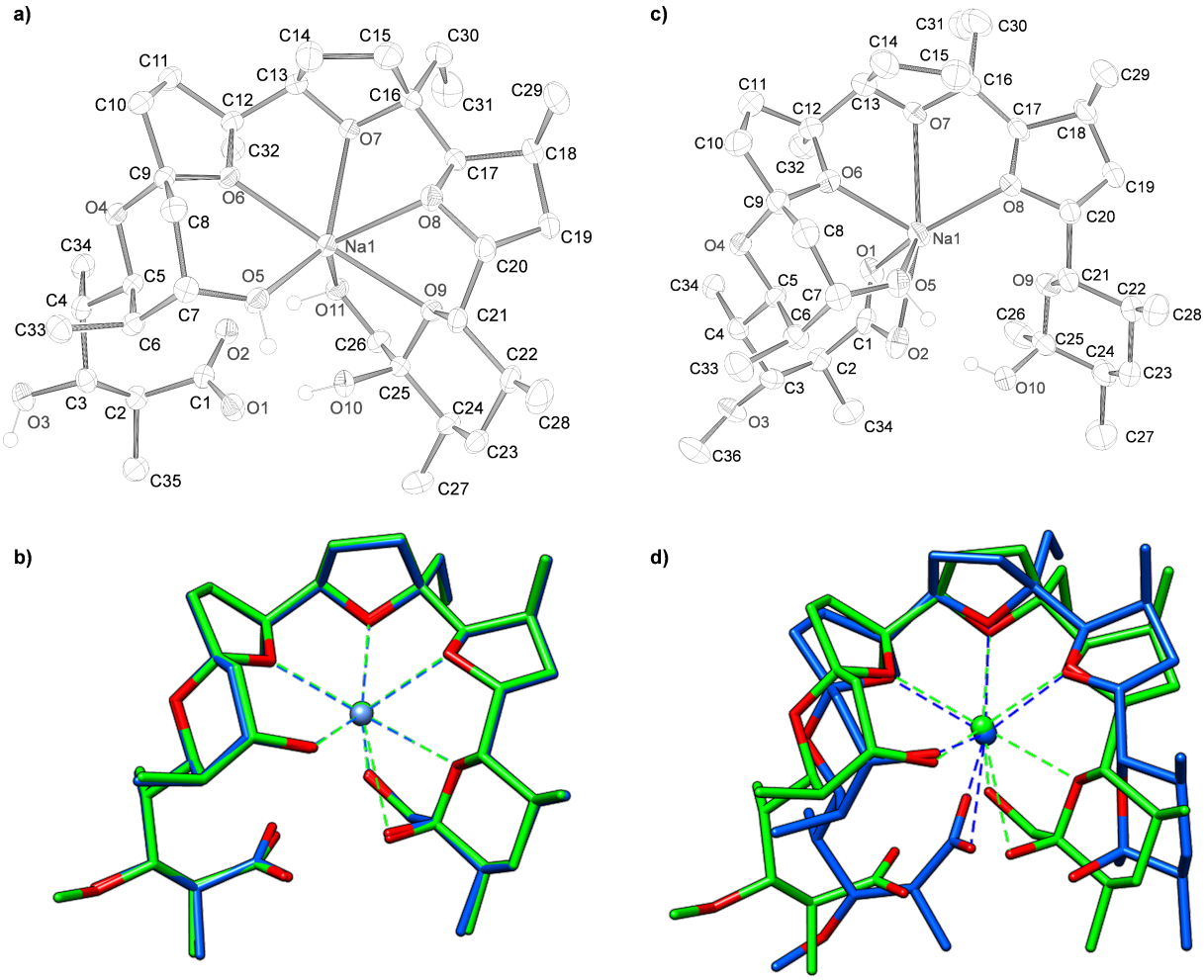


Figure 2: (a) Crystal structure of sodium demethylmonensin A (**4**) (ellipsoid probability = 50%); (b) overlay of **4** (blue) with the structure of sodium monensin A (**1,** green), oxygen atoms are coloured red); (c) crystal structure of sodium dehydroxymonensin A (**5**) and (d) the overlay of **5** (blue) with sodium monensin (**1**) (green).

of a carboxylic acid atom to the cation, as does grisoxin (30-dehydroxynigericin) in which the equivalent of the O-11 atom in monensin A is missing [33]. These differences have been ascribed to the increasing flexibility of the ligand in the larger polyethers, which also permits them to coordinate a wider selection of cations [34].

The structure of 26-dehydroxymonensin A complexed to a sodium ion proved to be remarkably different to that of monensin A (Figure 2a and 2d).

Here, both carboxylic oxygen atoms bind directly to the sodium ion, and the other end of the polyether (C-21–C-28) is fully released from coordination. Apparently, the loss of the H-bonds between the carboxylate (C-1) oxygen atom and the C-26 hydroxy group significantly compromises the integrity of the polyether shell surrounding the sodium ion. It has previously been shown that chemical modifications at the C-25 and/or C-26 hydroxy groups of monensin A lower both cation binding and antibiotic activity [35,36], presumably by the same mechanism. However, not all derivatives at C-26 behave in the same way: both natural and semisynthetic urethane derivatives of monensin A show maintained or even improved antibacterial activity [37-39]. The recently-determined crystal structure of the C-26-*O*-phenylurethane of monensin A sodium salt shows that although one of the carboxylate oxygen atoms coordinates the cation, this atom is also engaged in hydrogen bonding to the secondary alcohol borne at C-25, while the other carboxylate atom is engaged in an H-bond to the NH group of the urethane, thus maintaining the stability of the pseudocyclic structure [39]. The very different metal coordination pattern seen in dehydroxymonensin A and demethylmonensin A, although it

highlights the importance of the C-26 *O*-hydroxylation for the integrity of the ionophore structure, is not directly relevant to the (evolution of) the biosynthetic pathway. As discussed above, the final steps leading to formation of the polyether rings take place with the polyketide in thioester linkage to a discrete acyl carrier protein (MonACPX) [20], and therefore the terminal carboxylate is not available as an alternative ligand for the bound cation until all the tailoring steps have been accomplished and the mature antibiotic is released by thioesterase action. It remains to be established whether the sodium cation is recruited into the ACP-bound polyether even before monensin is released.

Meanwhile, the convenient production of large amounts of advanced monensin-related metabolites by an engineered industrial strain now opens the way to the synthesis of the ACPX-thioesters of these compounds and a detailed study of the final steps of monensin biosynthesis using authentic substrates and recombinant MonD, MonE and MonCII [40,41].

Experimental

Construction of deletion strains: For generation of the deletion mutants *ΔmonE*, *ΔmonD* and *ΔmonDΔmonE* of the *S. cinnamonensis* strain A519 [19] Redirect©-PCR-targeting technology was used according to the supplier's instructions [21,42]. The disruption cassettes were amplified from a *Hin*DIII-*Eco*RI-fragment of pIJ773 with the following primers (5' to 3') *monD*: oD1for: CGGCCGCCACATTCCCCGACCTGGT CGACCCGTCGTTCTAATTCCGGGGATCCGTCGACC; oD2rev:TCGTGAGCGCACATGCGCAGAGGGAAGCGTATGTGCTCATGTAGGCTGGAGCTGCTTC. *monE:* oE1for: CCCTT GTGCTGGGGGAGGAAAGCGGGGGCGGCACGCTCAATTCCGGGGCCGTCGACC; oE2rev: GTGACGAAGAACGCGACG ACCAAGAAGCCCCCGACGGTGTGTAGGCTGGAGCTGCTC. The DNA cassette used for reinsertion of *oriT* into the cosmid backbone: SCAT1for: CGCGAATTCTCATGTTTGACCGCTTA TCATCGATAAGCTTTCCCGCCAGCCTCGCAGAG; SCAT2rev: CACCGGAAGGAGCTGACTGGGTTGAAGGCTC TCAAGGGCGAAGTTCCTATACTTTCTA. The cosmids Cos2 (*monE*) and Cos11 (*monD*) from a cosmid library of *S. cinnamonensis* [16] were used as templates for PCR. All mutants were verified by sequencing on both forward and reverse strands with the following primers (5' to 3'): oE3rev: CGTTCCGTATGGAACGCGTCAAGAGCAGCTCC. oE4for: CGTCCGCGGGCCGGTACCTGACATTGAGG. oD3rev: CGC TCCAGGAGCTGCAGCGGGCCATACTCG. oD4for: GTCGCC CGTGCCGTGCCCGTGCGGTCGGTGGGCCTGACC. SCAT3for: CCTCGTACTGGAACGCCTCTC. SCAT4rev: CCTGTCCTACGAGTTGCATG. The subsequent sequencing revealed that the ΔmonD mutant contained an 82 bp "scar" instead of the expected in-frame 81 bp (traced to an error in one of the PCR primers) but since there is no downstream gene that might be subject to polar effects this mutant could still be used as though it were in-frame.

Fermentation conditions: Monensin (**1**) and the related metabolites **3**, **4** and **5** were produced as follows: 25 mL germination medium (soya flour (15.0 g L^{-1}), dry yeast (1.5 g L^{-1}), glucose (5 g L^{-1}), dextrin (20 g L^{-1}), $CaCO_3$ (1 g L^{-1}), pH 6.4) were inoculated with either *S. cinnamonensis* overproducer strain A519 or a mutant derived from it, and incubated for 48 h (30 °C, 140 rpm). Production medium (soya flour (32.6 g L^{-1}), soya oil (3.0%), methyl oleate (1.0%), glucose (20.0 g L^{-1}), Na_2SO_4 (2.2 g L^{-1}), $CaCO_3$ (2.0 g L^{-1}), $MnCl_2{\cdot}4H_2O$ (330 mg L^{-1}), $FeSO_4{\cdot}7H_2O$ (110 mg L^{-1}), $Al_2(SO_4)_3{\cdot}16H_2O$ (705 mg L^{-1}), $K_2HPO_4{\cdot}3H_2O$ (75 mg L^{-1}), $MnCl_2{\cdot}4H_2O$ (330 mg L^{-1}), L-ascorbic acid (19 mg L^{-1}), antifoam A (0.02%), pH 6.6–6.9), in portions of 50 mL (in 250 mL flasks) or 75 mL (in 500 mL flasks), was inoculated with the preculture (2.5 mL and 3.75 mL, respectively). The cultures were grown for 10 d at 30 °C and 120 rpm. Additional soya oil (3.0%) was supplemented on day 8.

Product isolation and purification: Polyether production was verified for each flask by TLC analysis of 0.5 mL samples of culture. For purification of polyethers, the 50 mL cultures of each mutant were extracted with ethyl acetate (3 × 100 mL). The combined organic layers were dried ($MgSO_4$) and the solvent was evaporated, yielding 11–13 g of an oily residue. Most of the oil was separated by using a short silica column. A gradient (isohexane/ethyl acetate/isopropanol 20:20:(0–4) by volume) was used for elution, depending on the polarity of the ionophore. Triethylamine (0.1% by volume) was added to all eluents. The crude polyethers were obtained as brownish oils or solids. Further purification was performed by silica gel column chromatography (gradient: 1. isohexane/ethyl acetate 1:1 (0.1% NEt_3), 2. isohexane/ethyl acetate/isopropanol 20:20:1 (0.1% NEt_3), 3. ethyl acetate/isopropanol 20:1). For the less polar polyether **5** an additional gradient (isohexane/ethyl acetate 10:1 → 1:1) was used to separate side-products before elution with the above solvents.

Analysis of monensin-related metabolites: Monensin (**1**) and metabolites **3**, **4** and **5** were detected by TLC on silica gel as red spots after staining with (vanillin (6%), H_2SO_4 (1%) in ethanol). R_f values were ((isohexane/ethyl acetate/methanol 10:10:1)/acetic acid 80:1) **1**: 0.37, **3**: 0.29, **4**: 0.14, and **5**: 0.43. Monensin (**1**) and dehydroxymonensin (**5**) were quantified colorimetrically after vanillin staining (vanillin (3%), H_2SO_4 (0.5%), in methanol) [43]. Staining solution (100 µL) was added to 900 µL sample and incubated for 30 min at 55 °C.

After cooling to room temperature, the absorption at 518 nm was measured and compared to reference samples. LC–MS: Crude extracts and purified compounds were analysed by ESI LC–MS/MS^2/MS^3 using a Phenomenex Prodigy 5 µm ODS3 100 Å column (250 × 4.6 mm) fitted to a Finnegan MAT LCQ mass spectrometer. The column was equilibrated in 20% 20 mM ammonium acetate buffer/80% methanol and compounds were eluted on a gradient to 100% methanol over 25 min. The mass spectrometer was set to record positive and negative ion scans between *m*/*z* 300 to 1000.

Crystal structure data: The crystal structures have been deposited at the Cambridge Crystallographic Data Centre and allocated the deposition numbers CCDC-793152(sp0601) for **4** and CCDC-793153(sp0602) for **5**. These crystallographic data can be obtained free of charge at http://www.ccdc.cam.ac.uk.

Sodium demethylmonensin A (**4**) crystallised from ethyl acetate/hexane as colourless needles, $C_{35}H_{59}NaO_{11}$ (M_r = 678.83), empirical formula: $C_{36}H_{64}NaO_{10}{\cdot}2H_2O$ (M_r = 714.82), crystal size 0.23 × 0.18 × 0.12 mm^3, orthorhombic, a = 8.36180(10) Å, b = 21.0283(3) Å, c = 21.1481(3) Å, V = 3718.56(9) Å^3, Z = 4, ρ_{calcd} = 1.1277 Mg m^{-3}, space group $P2_12_12_1$, Mo Kα radiation (λ = 0.71073 Å), $\mu(Mo_{K\alpha})$ = 0.105 mm^{-1}, F(000) = 1552. Sodium dehydroxy-monensin A (**5**) crystallised from ethyl acetate/hexane as colourless needles, $C_{36}H_{61}NaO_{10}$ (M_r = 676.85), empirical formula: $C_{36}H_{64}NaO_{10}{\cdot}1.5H_2O$ (M_r = 703.87, solvent estimated), crystal size 0.46 × 0.42 × 0.35 mm^3, orthorhombic, a = 8.04150(10) Å, b = 21.3058(3) Å, c = 24.1816(3) Å, V = 4143.05(9) Å^3, Z = 4, ρ_{calcd} = 1.128 Mg m^{-3}, space group $P2_12_12_1$, Mo Kα radiation (λ = 0.71073 Å), $\mu(Mo_{K\alpha})$ = 0.091 mm^{-1}, F(000) = 1532.

Acknowledgements

We thank Drs Yuliya Demydchuk, Barbara Harvey, Andrew Gallimore and Hui Hong for helpful discussions and Dr J. E. Davies for X-ray structure determinations. This work was supported by the Biotechnology and Biological Sciences Research Council UK (BBSRC) through a project grant to P.F.L. (BB/I002513/1), by the Engineering and Physical Sciences Research Council for financial assistance to J.E.D. towards the purchase of the Nonius Kappa CCD X-ray diffractometer, and by the Deutscher Akademische Austauschdienst (DAAD) through a Postdoctoral Fellowship to W.H.

References

1. Westley, J. W. Polyether Antibiotics — Biosynthesis. In *Biosynthesis;* Corcoran, J., Ed.; Springer: Berlin, Heidelberg, 1981; Vol. 4, pp 41–73. doi:10.1007/978-3-642-67724-3_3
2. Hill, A. M. In *Wiley Encyclopedia of Chemical Biolology;* Begley, T. P., Ed.; Wiley Interscience, 2008; pp 1–12.
3. Gallimore, A. R. *Nat. Prod. Rep.* **2009,** *26,* 266–280. doi:10.1039/b807902c
4. Liu, T.; Cane, D. E.; Deng, Z. *Methods Enzymol.* **2009,** *459,* 187–214. doi:10.1016/S0076-6879(09)04609-6
5. Rutkowski, J.; Brzezinski, B. *BioMed Res. Int.* **2013,** No. 162513. doi:10.1155/2013/162513
6. Gallimore, A. R.; Spencer, J. B. *Angew. Chem., Int. Ed.* **2006,** *45,* 4406–4413. doi:10.1002/anie.200504284
   Angew. Chem. **2006,** *118,* 4514–4521. doi:10.1002/ange.200504284
7. Kellmann, R.; Stüken, A.; Orr, R. J. S.; Svendsen, H. M.; Jakobsen, K. S. *Mar. Drugs* **2010,** *8,* 1011–1048. doi:10.3390/md8041011
8. Gumila, C.; Ancelin, M. L.; Delort, A. M.; Jeminet, G.; Vial, H. J. *Antimicrob. Agents Chemother.* **1997,** *41,* 523–529.
9. Otoguro, K.; Kohana, A.; Manabe, C.; Ishiyama, A.; Ui, H.; Shiomi, K.; Yamada, H.; Omura, S. *J. Antibiot.* **2001,** *54,* 658–663. doi:10.7164/antibiotics.54.658
10. Nakamura, M.; Kunimoto, S.; Takahashi, Y.; Naganawa, H.; Sakaue, M.; Inoue, S.; Ohno, T.; Takeuchi, T. *Antimicrob. Agents Chemother.* **1992,** *36,* 492–494. doi:10.1128/AAC.36.2.492
11. Yamagishi, Y.; Ueno, M.; Ueno, C.; Kato, A.; Kanasaki, R.; Sato, B.; Takakura, K.; Fujie, A.; Nakajima, H.; Fujii, T.; Hino, M.; Tsujii, E. *J. Antibiot.* **2009,** *62,* 95–98. doi:10.1038/ja.2008.18
12. Gupta, P. B.; Onder, T. T.; Jiang, G.; Tao, K.; Kuperwasser, C.; Weinberg, R. A.; Lander, E. S. *Cell* **2009,** *138,* 645–659. doi:10.1016/j.cell.2009.06.034
13. Fuchs, D.; Daniel, V.; Sadeghi, M.; Opelz, G.; Naujokat, C. *Biochem. Biophys. Res. Commun.* **2010,** *394,* 1098–1104. doi:10.1016/j.bbrc.2010.03.138
14. Cane, D. E.; Celmer, W. D.; Westley, J. W. *J. Am. Chem. Soc.* **1983,** *105,* 3594–3600. doi:10.1021/ja00349a040
15. Leadlay, P. F.; Staunton, J.; Oliynyk, M.; Bisang, C.; Cortés, J.; Frost, E.; Hughes-Thomas, Z. A.; Jones, M. A.; Kendrew, S. G.; Lester, J. B.; Long, P. F.; McArthur, H. A.; McCormick, E. L.; Oliynyk, Z.; Stark, C. B. W.; Wilkinson, C. J. *J. Ind. Microbiol. Biotechnol.* **2001,** *27,* 360–367. doi:10.1038/sj.jim.7000204
16. Oliynyk, M.; Stark, C. B. W.; Bhatt, A.; Jones, M. A.; Hughes-Thomas, Z. A.; Wilkinson, C.; Oliynyk, Z.; Demydchuk, Y.; Staunton, J.; Leadlay, P. F. *Mol. Microbiol.* **2003,** *49,* 1179–1190. doi:10.1046/j.1365-2958.2003.03571.x
17. Gallimore, A. R.; Stark, C. B. W.; Bhatt, A.; Harvey, B. M.; Demydchuk, Y.; Bolanos-Garcia, V.; Fowler, D. J.; Staunton, J.; Leadlay, P. F.; Spencer, J. B. *Chem. Biol.* **2006,** *13,* 453–460. doi:10.1016/j.chembiol.2006.01.013
18. Hughes-Thomas, Z. A.; Stark, C. B. W.; Böhm, I. U.; Staunton, J.; Leadlay, P. F. *Angew. Chem., Int. Ed.* **2003,** *42,* 4475–4478. doi:10.1002/anie.200351375
19. Bhatt, A.; Stark, C. B. W.; Harvey, B. M.; Gallimore, A. R.; Demydchuk, Y.; Spencer, J. B.; Staunton, J.; Leadlay, P. F. *Angew. Chem., Int. Ed.* **2005,** *44,* 7075–7078. doi:10.1002/anie.200501757
20. Harvey, B. M.; Mironenko, T.; Sun, Y.; Hong, H.; Deng, Z.; Leadlay, P. F.; Weissman, K. J.; Haydock, S. F. *Chem. Biol.* **2007,** *14,* 703–714. doi:10.1016/j.chembiol.2007.05.011
21. Gust, B.; Challis, G. L.; Fowler, K.; Kieser, T.; Chater, K. F. *Proc. Natl. Acad. Sci. U. S. A.* **2003,** *100,* 1541–1546. doi:10.1073/pnas.0337542100

22. Zhang, Y.; Muyrers, J. P. P.; Testa, G.; Stewart, A. F. *Nat. Biotechnol.* **2000,** *18,* 1314–1317. doi:10.1038/82449
23. Pospísil, S.; Sedmera, P.; Vokoun, J.; Vaněk, Z.; Buděsínský, M. *J. Antibiot.* **1987,** *40,* 555–557. doi:10.7164/antibiotics.40.555
24. Ashworth, D. M.; Holmes, D. S.; Robinson, J. A.; Oikawa, H.; Cane, D. E. *J. Antibiot.* **1989,** *42,* 1088–1099. doi:10.7164/antibiotics.42.1088
25. Pospísil, S.; Sedmera, P.; Havlícek, V.; Tax, J. *Appl. Environ. Microbiol.* **1994,** *60,* 1561–1564.
26. Agtarap, A.; Chamberlin, J. W.; Pinkerton, M.; Steinrauf, L. K. *J. Am. Chem. Soc.* **1967,** *89,* 5737–5739. doi:10.1021/ja00998a062
27. Pinkerton, M.; Steinrauf, L. K. *J. Mol. Biol.* **1970,** *49,* 533–546. doi:10.1016/0022-2836(70)90279-2
28. Duax, W. L.; Smith, G. D.; Strong, P. D. *J. Am. Chem. Soc.* **1980,** *102,* 6725–6729. doi:10.1021/ja00542a010
29. Adam, H.; Małgorzata, R.-S.; Andrzej, K.; Bogumil, B. *J. Mol. Struct.* **2007,** 832.
30. Steinrauf, L. K.; Pinkerton, M.; Chamberlin, J. W. *Biochem. Biophys. Res. Commun.* **1968,** *33,* 29–31. doi:10.1016/0006-291X(68)90249-0
31. Shiro, M.; Koyama, H. *J. Chem. Soc. B* **1970,** 243–253.
32. Czerwinski, E. W.; Steinrauf, L. K. *Biochem. Biophys. Res. Commun.* **1971,** *45,* 1284–1287. doi:10.1016/0006-291X(71)90157-4
33. Alleaume, M.; Hickel, D. *J. Chem. Soc., Chem. Commun.* **1972,** 175–176. doi:10.1039/c39720000175
34. Steinrauf, L. K.; Czerwinski, E. W.; Pinkerton, M. *Biochem. Biophys. Res. Commun.* **1971,** *45,* 1279–1283. doi:10.1016/0006-291X(71)90156-2
35. Gaboyard, C.; Dauphin, G.; Vaufrey, F.; Jeminet, G. *Agric. Biol. Chem.* **1990,** *54,* 1149–1155. doi:10.1271/bbb1961.54.1149
36. Tanaka, R.; Nagatsu, A.; Mizukami, H.; Ogihara, Y.; Sakakibara, J. *Chem. Pharm. Bull.* **2001,** *49,* 711–715. doi:10.1248/cpb.49.711
37. Westley, J. W.; Evans, R. H., Jr.; Sello, L. H.; Troupe, N.; Liu, C.-M.; Miller, P. A. *J. Antibiot.* **1981,** *34,* 1248–1252.
38. Westley, J. W.; Liu, C.-M.; Evans, R. H., Jr.; Sello, L. H.; Troupe, N.; Hermann, T. *J. Antibiot.* **1983,** *36,* 1195–1200.
39. Huczyński, A.; Ratajczak-Sitarz, M.; Stefańska, J.; Katrusiak, A.; Brzezinski, B.; Bartl, F. *J. Antibiot.* **2011,** *64,* 249–256. doi:10.1038/ja.2010.167
40. Harvey, B. M.; Hong, H.; Jones, M. A.; Hughes-Thomas, Z. A.; Goss, R. M.; Heathcote, M. L.; Bolanos-Garcia, V. M.; Kroutil, W.; Staunton, J.; Leadlay, P. F.; Spencer, J. B. *ChemBioChem* **2006,** *7,* 1435–1442. doi:10.1002/cbic.200500474
41. Liu, T.; Lin, X.; Zhou, X.; Deng, Z.; Cane, D. E. *Chem. Biol.* **2008,** *15,* 449–458. doi:10.1016/j.chembiol.2008.04.006
42. Gust, B.; Kieser, T.; Chater, K.; John Innes Centre: Norwich, 2002.
43. Golab, T.; Barton, S.; Scroggs, R. *J. – Assoc. Off. Anal. Chem.* **1973,** *56,* 171–173.

License and Terms

This is an Open Access article under the terms of the Creative Commons Attribution License (http://creativecommons.org/licenses/by/2.0), which permits unrestricted use, distribution, and reproduction in any medium, provided the original work is properly cited.

The license is subject to the *Beilstein Journal of Organic Chemistry* terms and conditions: (http://www.beilstein-journals.org/bjoc)

The definitive version of this article is the electronic one which can be found at:
doi:10.3762/bjoc.10.34

Beilstein Journal of Organic Chemistry

Concise, stereodivergent and highly stereoselective synthesis of *cis*- and *trans*-2-substituted 3-hydroxypiperidines – development of a phosphite-driven cyclodehydration

Peter H. Huy[*1,§], Julia C. Westphal[2] and Ari M. P. Koskinen[*1]

Full Research Paper

Open Access

Address:
[1]Aalto University, School of Chemical Technology, Laboratory of Organic Chemistry, Kemistintie 1, 02015 Espoo, Finland and
[2]University of Cologne, Department of Chemistry, Organic Chemistry, Greinstrasse 4, 50939 Cologne, Germany

Email:
Peter H. Huy[*] - peter.huy@uni-saarland.de; Ari M. P. Koskinen[*] - ari.koskinen@aalto.fi

* Corresponding author
§ Current Address: Saarland University, Institute of Organic Chemistry, Mailbox 151150, 66041 Saarbrücken, Germany

Keywords:
amino acids; asymmetric synthesis; cyclodehydration; hydroxypiperidines; natural products; one-pot

Beilstein J. Org. Chem. **2014,** *10,* 369–383.
doi:10.3762/bjoc.10.35

Received: 18 November 2013
Accepted: 16 January 2014
Published: 11 February 2014

This article is part of the Thematic Series "Natural products in synthesis and biosynthesis".

Guest Editor: J. S. Dickschat

© 2014 Huy et al; licensee Beilstein-Institut.
License and terms: see end of document.

Abstract

A concise (5 to 6 steps), stereodivergent, highly diastereoselective (dr up to >19:1 for both stereoisomers) and scalable synthesis (up to 14 g) of *cis*- and *trans*-2-substituted 3-piperidinols, a core motif in numerous bioactive compounds, is presented. This sequence allowed an efficient synthesis of the NK-1 inhibitor L-733,060 in 8 steps. Additionally, a cyclodehydration-realizing simple triethylphosphite as a substitute for triphenylphosphine is developed. Here the stoichiometric oxidized P(V)-byproduct (triethylphosphate) is easily removed during the work up through saponification overcoming separation difficulties usually associated to triphenylphosphine oxide.

Introduction

1,2-Amino alcohols of the type **A** (Figure 1) represent a frequent core motif of many pharmacologically active natural products [1-9], chiral auxiliaries [10,11] and catalysts for asymmetric synthesis [12-14]. Especially the 2-substituted 3-hydroxypiperidine scaffold of the general structure **B** (as one type of an 1,2-amino alcohol) can be found in numerous natural products and other bioactive compounds [1-7]. Selected examples are given in Figure 1: The non-peptidic human neurokinin-1 (NK1) substance P receptor antagonists L-733,060 [15,16] and CP-99,994 [17-19], the natural product febrifugine (antimalarial) [20,21] and antiprotozoal agent halofuginone (commercial trade names Halocur® (lactate salt) and Stenorol® (hydro-

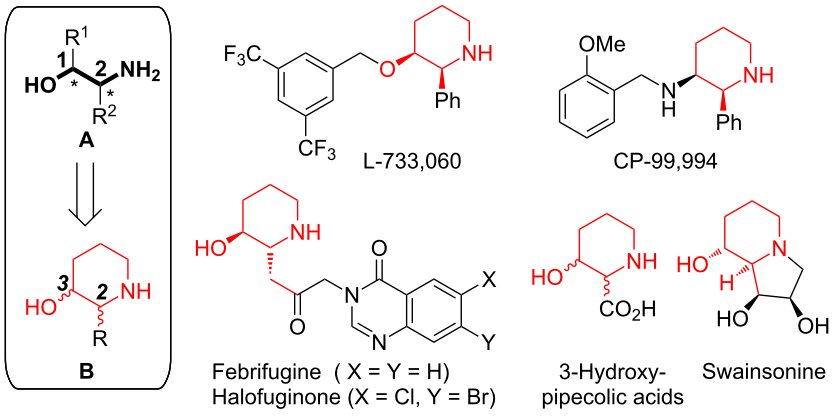


Figure 1: Natural products and other bioactive piperidine derivatives of type **B**.

bromide salt)) [22]. Other relevant examples are 3-hydroxypipecolic acids, which serve as (conformationally restricted) substitutes of proline and serine [23,24] and have been incorporated into diverse bioactive peptidomimetics [25,26], and the iminosugar swainsonine, a new potential chemotherapeutic agent [27,28]. Recently, analogs of halofuginone were discovered as inhibitors of tRNA synthetases [29-31].

The majority of the reported syntheses [2-4,32-35] are elaborate (far more than 10 steps), specific on one of the targets depicted in Figure 1 and therefore on one relative configuration (either *cis*- or *trans*), and have not been proven to be scalable. In our opinion the following examples represent the most efficient synthesis of 3-piperidinols of type **B** in terms of step-economy (<10 steps to establish the core motif **B**): 1. Charette [36] prepared the less bioactive enantiomers of L-733,060 and CP-99,994 through nucleophilic additions to chiral pyridylium salts and subsequent hydrogenation. 2. Cossy and Pardo [37,38] synthesized L-733,060 (formal total synthesis) and two (epimeric) hydroxypipecolic acid through ring expansions of 2-(α-hydroxyalkyl)pyrrolidines deduced to proline. 3. Based on the ring expansion of Cossy and Pardo [37], O´Brien [39] realized the synthesis of L-733,060 (80% ee). The 2-(α-hydroxyalkyl)pyrrolidine precursor was prepared from a protected pyrrolidine through sparteine-mediated enantioselective lithiation and subsequent hydroxyalkylation. 4. Recently, Pansare [40] reported the synthesis of L-733,060, CP-99,994 and a hydroxypipecolic acid through asymmetric organocatalytic vinylogous aldol addition as the key step.

While the syntheses by Charette [38] and Pansare [40] are restricted to piperidinols **B** in *cis*-configuration (dr >19:1 and 8:1, respectively), the sequences of Cossy and Pardo [35] and O´Brien [39] are stereodivergent. Nevertheless, the observed diastereomeric ratios are low (1:1 and 2.3:1 for *trans*-**B**, respectively) at least for one of the epimers. Considering the versatile pharmacological activities of compounds based on the 3-piperidinol scaffold, a step-economic, scalable and stereodivergent synthesis of both *cis*- and *trans*-diastereomers of **B** in good diastereoselectivities is highly desirable.

In the syntheses of potentially new drug candidates scalability is a significant factor to provide sufficient substance amounts for clinical tests [41,42]. Additionally, alternatives in reactions driven by the formation of phosphine oxides from phosphines (e.g. the Appel and Mitsunobu reaction) are highly desired to improve atom economy (reduced waste amounts) and to circumvent difficulties in the separation of these by-products as demonstrated by a number of reviews [43-45]. Numerous protocols have been developed to improve these issues, mostly based on polymer supported or otherwise modified (more complex) phosphines [43-45]. Surprisingly, in this context simple and inexpensive phosphites ($P(OR)_3$) have only been applied as phosphine substitutes in one single example: Beal [46] utilized tri-isopropylphosphite in a Mitsunobu condensation of a guanine-derived nucleoside analog with benzylic alcohols providing simplified byproduct separation through improved water solubility (of $O{=}P(OiPr)_3$). In our case we were not able to remove stoichiometric amounts of $OP(OEt)_3$ (which is more hydrophilic than $OP(OiPr)_3$) through an aqueous work up (without saponification). Moreover, pentavalent $P(OEt)_5$ prepared from $P(OEt)_3$ with diethylperoxide and ethylbenzenesulfonate, respectively, in an additional step, was reported to effect cyclodehydration of diols to furans and pyrans [47,48] (for recent examples for cyclodehydration protocols see [49,50]). Thereby, the volatile products were separated from $O{=}P(OEt)_3$ through distillation.

After our initial short communication [51] about the step-economic and stereodivergent synthesis of *trans*- and *cis*-2-substituted 3-piperidinols **B**, we want to report the development of this sequence in more detail with a focus on the phosphite-

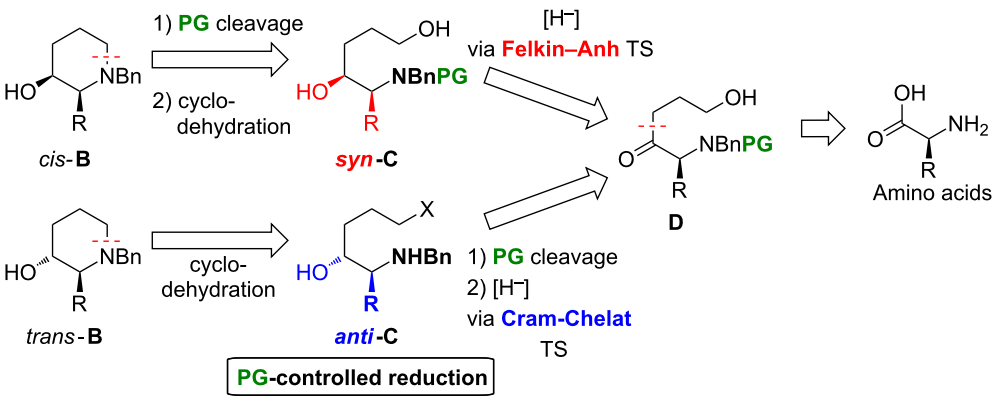


Figure 2: Retrosynthetic analysis of piperidines **B** (X = OH or leaving group, PG = protecting group).

mediated cyclodehydration. Additionally, the synthesis of a side chain functionalized piperidinol derived from methionine and studies towards the preparation of glutamic and aspartic acid derived heterocycles are presented.

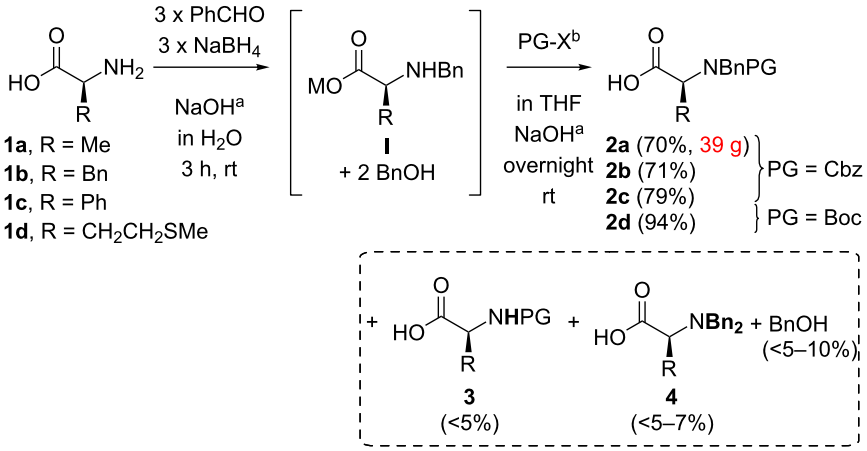
Following the retrosynthetic analysis in Figure 2 the relative configuration of **B** (*cis*/*trans*) should be controlled through targeted protecting group (PG) manipulation: Reduction of the common precursor ketone **D** (derived from commercial available amino acids) should deliver the *syn*-amino alcohol **C** proceeding though a Felkin–Anh transition state [52,53] (due to the sterically demanding –NBnPG function). Further PG cleavage and cyclodehydration would give rise to *cis*-**B**. On the other hand, initial deprotection of **D** (to liberate the Lewis-basic –NHBn moiety) and subsequent reduction passing through a Cram-chelate transition state [54] should deliver the *anti*-amino alcohol **C**.

After subsequent cyclisation *trans*-**B** would result. Noteworthy, this strategy would completely circumvent configurationally labile amino aldehyde intermediates [55,56]. Basically any carbamate or amide protecting group (= PG) orthogonal to the benzyl moiety would be suitable for this strategy. Furthermore, we decided to surrender protection of the OH functions in the synthesis of intermediates **D** and **C** in order to minimize the number of steps of the sequence. Thus far only four examples following a related strategy to establish the *syn*- and *anti*-configuration of 1,2-aminoalcohol motifs have been reported [57-60].

Results and Discussion

Synthesis of hydroxyketone intermediates D

In the first step L-alanine, phenylalanine, phenylglycine and methionine **1a–d** were converted to their *N*-benzyl-*N*-carbamate-protected derivatives **2a–d** (PG = Cbz, Boc) in a practical one pot procedure through combination of Quitt´s reductive benzylation protocol [61] and a Schotten–Baumann acylation [62,63] in 70–95% yield (Scheme 1). While we choose a Cbz protecting group for the amino acids **1a–c** due to the mild cleavage conditions (hydrogenolysis), we decided to introduce a



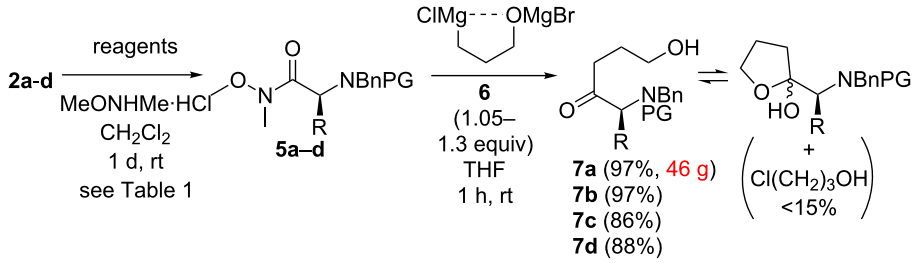
Scheme 1: Synthesis of the protected amino acids **2**. (a) KOH for **1b**. b) PG–X = Cbz–Cl (**1a–c**), Boc_2O (**1d**).

Boc group at the *N*-terminus of methionine **1d** to avoid desulfuration (–EtSMe → –Et) in the later deprotection.

In order to suppress the formation of the only carbamate protected amino acid derivatives **3** (remaining as impurity in the isolated products **2**), quantitative benzylation (**1**→**I**) was ensured by successive addition of three portions of benzaldehyde/$NaBH_4$ (Quitt´s procedure [61] → two portions) and by maintaining the pH at a value of 10–11. The extractive separation (washing of a basic aqueous solution of the acids **2**) of the two equivalents of BnOH formed during the reductive amination (**1**→**I**) proved to be challenging: Due to the high amphiphilicity of carboxylate salts of **2**, mixtures in water and an organic solvent tend to form three distinct phases separating poorly. Nevertheless, washing of an aqueous solution of the polar lithium salts of **2** (crude **2** in aq. LiOH) with organic solvents of increasing polarity (Et_2O→EtOAc) allowed to remove BnOH almost completely (<10% of BnOH referred to **2**). Residual benzyl alcohol diminished the yield in the following amidation (**2**→**5**) due to competitive formation of the corresponding benzyl esters. Depending on the $NaBH_4$ batch the dibenzyl-protected derivatives **4** formed as side products (<10% referred to **2**). The residual impurities (BnOH and **4**) were separated either through work up (of amide **5a**) or chromatographic purification (of amides **5b–d**) after the following amidation (**2**→**5**).

Importantly, through this procedure not only one isolation step was avoided, but also the overall yield was improved significantly: For the transformation from **1a** to **2a** (**I** isolated as free acid) under (optimized) literature conditions we achieved a yield of 44% over two steps (59% and 74%, respectively) compared to 70% according to our direct conversion from **1a** to **2a**.

Next the carboxylic acids **2** were transformed to the Weinreb amides **5** with DCC and MeONHMe in 77–91% yield (Scheme 2). While no racemisation occurred with substrates **2a**, **2b** and **2d** (Et_3N/DMAP or NMM as bases; Table 1, entries 1 and 2), the protected phenylglycine derivative **2c** showed high configurational lability: Under standard conditions (DCC/Et_3N/0.3 equiv DMAP) the amide **5c** was obtained in a diminished ee



Scheme 2: Synthesis of hydroxy ketones **7** (R = Me (**a**), Bn (**b**), Ph (**c**) and EtSMe (**d**); PG = Cbz (**a–c**), Boc (**d**)).

Table 1: Ees and isolated yields of Weinreb amides **5**.

entry	substrate	R	reagents	ee[a]	yield
1	**2a**	–Me	DCC, NMM	99%	91%[b]
2	**2b**	–Bn	DCC, Et_3N, DMAP (cat.)[d]	99%	77%[c]
3			DCC, Et_3N, DMAP (cat.)[d]	49%	n.d.
4			DCC, Et_3N, HOBt (cat.)[d]	5%	n.d.
5	**2c**	–Ph	DCC, NMM, DMAP (cat.)[d]	75%	n.d.
6			DCC, NMM	95%	81%[b]
7			T3P, pyridine[e]	74%	n.d.
8	**2d**	–EtSMe	DCC, NMM	99%[f]	91%[b]

[a]The ee was determined via HPLC on a chiral stationary phase. [b]Isolated crude yield, purity >90% according ^1H NMR. [c]Isolated yield after chromatography. [d]cat. = 0.3 equiv. [e]Solvent EtOAc instead of CH_2Cl_2. [f]The ee was determined to be ≥99% at the later stage the piperidinol *cis*-**11d**. DCC = *N,N´*-dicyclohexylcarbodiimide; NMM = *N*-methylmorpholine; DMAP = *N,N*-dimethylaminopyridine, HOBt = 1-hydroxybenzotriazole; T3P = *n*-propylphosphonic acid anhydride; n.d. = not determined.

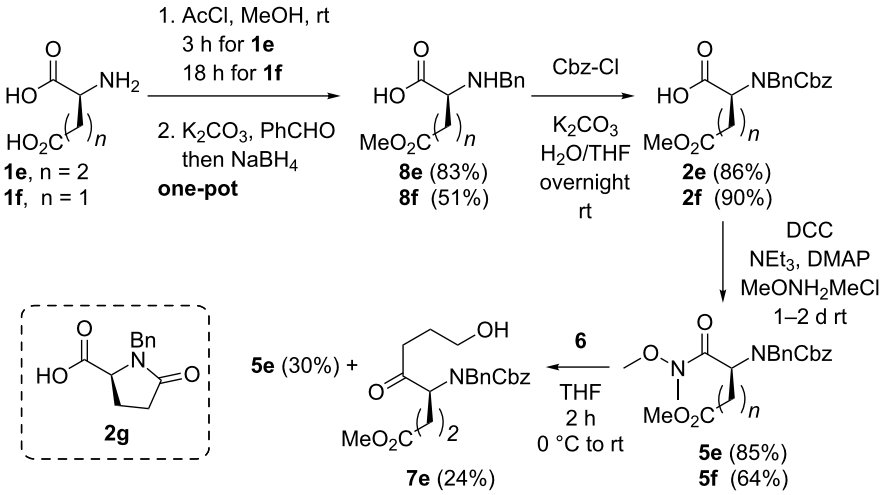
of 49% (Table 1, entry 3). HOBt as nucleophilic catalyst proved to be even worse than DMAP, because under otherwise identical conditions the product **5c** was isolated almost as a racemate (5% ee, entry 4). By replacing Et_3N with the less basic NMM (in the presence of DMAP) the ee increased clearly (49→75%, entry 5). However, without any nucleophilic catalyst the desired amide **5c** was isolated with a very good ee of 95% (entry 6) [64].

The high racemisation sensitivity of **2c** is further underlined by a T3P/pyridine (*n*-propylphosphonic acid anhydride) [65,66] mediated amidation, which has been reported to suppress racemisation [67]. With substrate **2c** the condensation product **5c** was formed in a moderate ee of 74% (Table 1, entry 7). The configurational lability of the phenylglycine derivative was not surprising, as phenylglycine itself is 60 times more prone to racemisation than alanine [68]. The optical purity of amides **5a–c**, hydroxyketone **7c** and piperidins *cis*-**11a–d** and *trans*-**11a** (Table 2, Scheme 6 and 7) was determined with HPLC on a chiral stationary phase and comparison with racemic samples (alanine **1a** and phenylglycine **1c** derived substrates) or in analogy to the aforementioned amino acid derivatives (phenylalanine **1b** and methionine **1d** deduced substrates).

In the next step, addition of a slight excess of the 3-chloropropanol-derived Grignard reagent **6** (final concentration 0.25–0.3 mol/L), which was found to be superior in the final concentration to the reported ClMg*n*PrOMgCl derivative (0.1–0.2 mol/L in our hands) [69], to amides **5a–d** resulted in ketones **7a–d** in good to excellent yields (86–97%, Scheme 2). In contrast to the reported procedure (2–3 h of reflux) [69], short reflux times to form **6** (20–30 min) were crucial to avoid decomposition of this dianionic reagent. Furthermore, a slight excess of MeMgBr in the deprotonation step of 3-chloropropanol was found to assist the Grignard formation. Notably, with this strategy we saved additional protection and deprotection steps of the free hydroxy group of **7**. Thereby, only the phenylglycine derivative **7c** displayed a slight decrease of ee (95→92%), the other hydroxy ketones **7a**, **7b** and **7d** did not show any racemisation at all, not even after a longer time of storage. For the latter three the enantiomeric excess was not determined on this step: Further conversion as depicted in Scheme 4 and Table 2 delivered piperidinols **11a**, **11b** and **11d** in ≥99% ee. As no intermediate in the conversion of **7** to **11** was crystallized, the ketones **7a**, **7b** and **7d** must have been enantiopure.

Residual 3-chloropropanol (<15 mol % referred to **7**), which was difficult to separate chromatographically, was removed after the next step either during the work up (diols **9**) or chromatographically (on the sequence leading to **15a**). Interestingly, the ketones **7a–d** existed in an equilibrium with their cyclic hemiacetal tautomers as shown in Scheme 2. The predominant keto form possessed a clear singlet around 205–210 ppm for the quaternary carbonyl carbon and the furan form was indicated by two weak signals at 105–110 ppm for the hemiacetal carbon (two diastereomers) in the ^{13}C NMR.

Additionally, a short 3 step route to the functionalized glutamic and aspartic acid derived Weinreb amides **5e** and **5f** was coined as outlined in Scheme 3: At the outset both amino acids (**1e** and **1f**) were subjected to esterification of the sterically less hindered side chain carboxyl function with acetyl chloride in MeOH [70-72]. Neutralization of the reaction mixture with K_2CO_3 and reductive benzylation [73] in one-pot then delivered the benzyl amines **8e** and **8f**. While glutamic acid showed



Scheme 3: Synthesis of amides **5e** and **5f** and ketone **7e**.

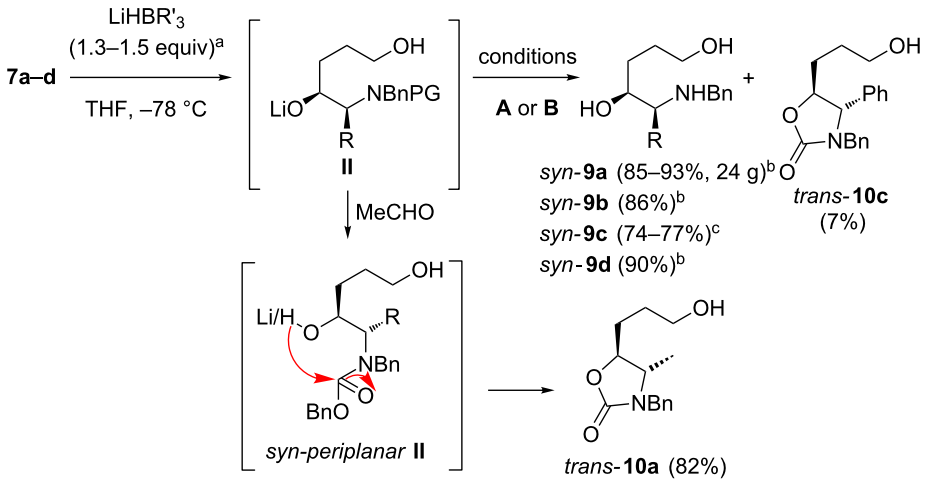
selective mono esterification after 3 h at room temperature, the aspartic acid mono ester was obtained in a 5:1 ratio with the diester (not shown) after approximately 18 h of reaction time. Shorter reaction times in the esterification step of **1f** decreased the yield of **8f**.

The amines **8e** and **8f** were converted in a straightforward manner to the carbamates **2e** and **2f** under Schotten–Baumann conditions [62,63]. Thus, K_2CO_3 (→ pH = 10) as the base prevented saponification of the side chain methyl ester functions (as observed with hydroxide salts). Nevertheless, in the acylation of the glutamic acid derivative **8e** the corresponding pyroglutamic acid derivative **2g** resulting from lactamisation of the ester function was observed as a side product in traces (<5%). Next, amidation of the acids **2e** and **2f** gave the amides **5e** and **5f** in good yields under standard coupling conditions. Unfortunately, the ketone **7e** was obtained in only 24% yield through addition of the Grignard reagent **6** to amide **5e** (along with 30% of reisolated starting material), illustrating the tendency of reagent **6** to attack the side chain ester moiety.

Synthesis of *syn*-amino alcohols C

Already the $NaBH_4$ reduction (in MeOH at −40/0 °C) of ketones **7a** and **7b** and subsequent hydrogenolysis of the Cbz-group in one-pot delivered the *syn*-amino alcohols **9a** and **9b** in good diastereomeric ratios (around 11:1 *syn*/*anti*, compare Scheme 4). In contrast the $NaBH_4$ reduction of ketone **7c** under identical conditions gave diol **9c** without any selectivity (dr = 1.3:1). To our delight, reduction of the ketones **7a** and **7b** with L-Selectride [74] (or N-Selectride) and subsequent hydrogenolysis of the Cbz-group in one-pot delivered the benzyl amines *syn*-**9a** and **9b** in accordance with the Felkin–Anh model in excellent yields and as pure diastereomers as indicated by 400 MHz ^{1}H NMR (Scheme 4). Unfortunately, L-Selectride proved to be too unreactive at low temperatures towards the phenylglycine derived ketone **7c**, at higher temperatures mainly decomposition of the starting material was observed. Nevertheless, Superhydride [75,76] reduction and successive Cbz-cleavage gave the desired amino alcohol *syn*-**9c** in useful diastereomeric ratios of 3.7–4:1 *syn*/*anti*. The slightly diminished yield of **9c** (74–77%) compared to **9a** and **9b** (85–93%) is rationalized by formation of the oxazolidinone **10c** as side-product. This cyclic carbamate results from the condensation of the alcoholate moiety of **II** with the Cbz-function passing the *syn-periplanar* conformation indicated in Scheme 4. With a bulky phenyl substituent (= R) this conformation is higher populated than with smaller R groups (e.g. Me and Bn) due to increased steric repulsion between the *n*-PrOH and R moiety. This explains the more facile formation of oxazolidinones of type **10** with the phenylglycine derived carbamate **7c**. Indeed, if the excess of Selectride was quenched with acetaldehyde after reduction of **7a**, the oxazolidine **10a** was obtained (under the basic reaction conditions) as the major product.

The outcome of the Cbz-cleavage strongly depended on the activity of the commercial Pd/C batch: While an active catalyst led to a quantitative cleavage after 3 h (all substrates), less reactive batches led to considerably increased reaction times (2 d for **7a**). For **7b** and **7c** the isolated yields of the amines **9** even dropped to 10–20% after 2 d reaction time due to incomplete Cbz-cleavage. However, Pd/C freshly prepared from $Pd(OAc)_2$ and activated charcoal according to Felpin [77] delivered consistent results (reaction time < 3 h). Although the Cbz-cleavage beside a benzyl moiety in alcohols as solvent is known



Scheme 4: Synthesis of amino alcohols *syn*-**9a–d** and oxazolidinone **10a**. (for **7a–c** conditions **A**: H_2 (1 atm), Pd/C, HCl, MeOH (THF/MeOH 1:1), rt, 3 h; for **7d** conditions **B**: HCl (aq.; 4 N HCl in THF/H_2O), rt, 6 h) [a]R´= *s*Bu for **7a**, **7b** and **7d** (L-Selectride); R´= Et for **7c** (Superhydride). [b]dr ≥ 19:1. [c]dr = 3.7–4:1.)

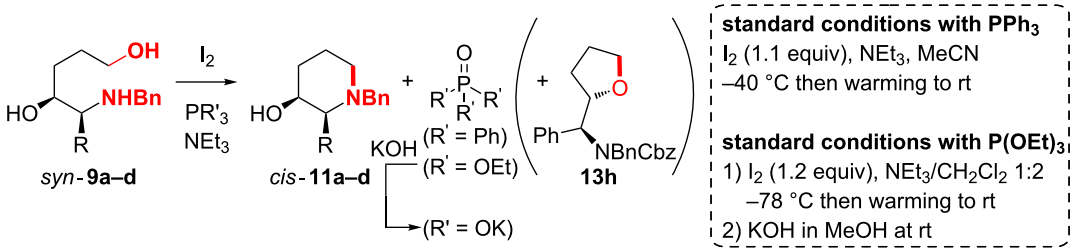
(for selected examples of the chemoselective Cbz-cleavage of Bn, Cbz-protected amines see [78-80]), we only achieved high chemoselectivities in the presence of an excess of HCl.

In a similar manner the methionine derived Boc-protected ketone **7d** was converted through L-Selectride reduction and Boc-cleavage induced by aqueous HCl solution in one pot to the *syn*-aminoalcohol **9d** as a single diastereomer according to ^{1}H NMR. Importantly for up-scaling, only a slight excess of L-Selectride (1.3 equiv) or Superhydride (1.5 equiv), respectively, was required for the quantitative conversion of **7a–d** to the intermediate **II**. Therefore the deprotonation of the free OH-group of **7** must be significantly slower than the desired reduction of the carbonyl function. Practically, the residual 3-chloropropanol remaining from the prior Grignard addition **5**→**7** step (vide supra) and *sec*-Bu_3B/BEt_3 from the reduction were easily separated through washing with Et_2O of an (HCl) acidic, aqueous phase of the products **9** resulting in the crude diols **9a–d** in a circa 90% purity according ^{1}H NMR. Hence, the crude amino alcohols **9** were not further purified before the following cyclodehydration.

Synthesis of *cis*-piperidinols B

Cyclodehydration of amino alcohol *syn*-**9a** to piperidinol *cis*-**11a** under Appel conditions (I_2, PPh_3) [81,82] surpassed by far Mitsunobu conditions and sulfonation (with MsCl, TsCl) induced cyclisations (see Supporting Information File 1 for more details): Under optimized conditions (1.1 equiv I_2, Et_3N in MeCN at −40 °C) the cyclic products **11a–c** were isolated in 68–77% yield and 90–99% ee (Table 2 entry 1, 10, 12). For work up the reaction mixture was simply absorbed on silica gel (ca. 9 fold amount of starting material **9**) through evaporation of the solvent and directly subjected to chromatographic purification.

Table 2: Cyclodehydration of amino alcohols **9a–d** to piperidinols **11a–d**.



entry	substrate	R	PR_3	deviation from standard conditions	yield
1	*syn*-**9a**	–Me	PPh_3	–	77%[a,b,c]
2			$P(OEt)_3$	–	82%[a,b,c] (14 g)
3			$P(OEt)_3$	reflux instead of rt in saponification	52%[a,c]
4			$P(OEt)_3$	DIPEA instead of Et_3N[e]	57%[c,d]
5			$P(OEt)_3$	lutidine instead of Et_3N[e]	50%[c,d]
6			$P(OEt)_3$	imidazole instead of Et_3N[e]	30%[c,d]
7			$P(OEt)_3$	Et_3N/CH_2Cl_2 1:10	79%[c,d]
8			$P(OEt)_3$	THF instead of CH_2Cl_2[e]	58%[c,d]
9			$P(OEt)_3$	−20 °C then warming to 0 °C	41%[a,c]
10	*syn*-**9b**	–Bn	PPh_3	–	68%[a,b,c]
11			$P(OEt)_3$	–	74%[a,b,c]
12	*syn*-**9c**	–Ph	PPh_3	–	77%[a,e,f] (2.3 g)
13			$P(OEt)_3$	Et_3N/CH_2Cl_2 1:1.3	68%[a,e,f]
14			$P(OEt)_3$	–	49%[a,f]
15			$P(OEt)_3$	Et_3N/CH_2Cl_2 1:3	22%[a,f]
16	*syn*-**9d**	–EtSMe	$P(OEt)_3$	–	74%[a,b,c]

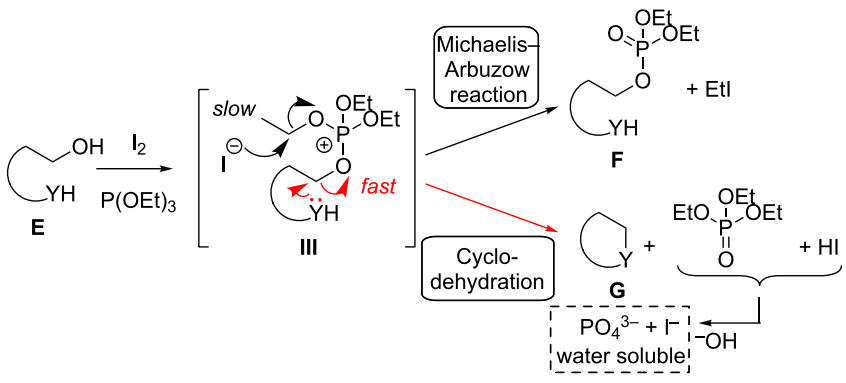
[a]Isolated yield after chromatographic purification. [b]ee ≥ 99%, determined by HPLC on a chiral stationary phase. [c]dr >19:1 *cis/trans*. [d]Yield determined with naphthalene as NMR-standard. [e]Ratio base/solvent 1:10. [f]ee = 90%; dr = 4.0:1 (entry 12), 5.3:1 (entry 13), 3.7.1 (entry 14), 3.0:1 (entry 15) *cis/trans*. DIPEA = di-isopropylethylamine; lutidine = 2,6-dimethylpyridine. All reactions were run until full conversion of the starting material **9**.

Unfortunately, the stoichiometric byproduct triphenyl phosphine oxide was only separable by chromatography requiring significantly increased amounts of silica gel (the crude product weight usually obtained 300–400% of the theoretical yield after aqueous work up). Attempts to crystallize $OPPh_3$ beside the piperidine **11a** or of the fumaric acid salt of **11a** for instance failed, only an oily mixture of **11a** and $OPPh_3$ precipitated. Separation of $OPPh_3$ through washing of an aqueous solution of hydrochlorides of **11** led to a significant loss of piperidines **11** (especially with **11b** and **11c** bearing lipophilic side chains R).

In general, the reaction of alcohols with alkyl phosphites ($P(OR)_3$), activated through oxidants such as iodine, have been reported to give the corresponding phosphates in a Michaelis–Arbuzow type reaction [83-85] (Scheme 5). In order to improve atom economy and side product separation, we rationalized that in the phosphonium intermediate **III** (originating from activation of the diol/amino alcohol **E**) the intramolecular substitution by the amino function (delivering the desired heterocycles of type **G**) should be significantly faster than the bimolecular reaction of the iodide ion with intermediate **III** as indicated (resulting in the formation of the corresponding undesired phosphates **F**). The formation of heterocycles **G** passing phosphates **F** through substitution of the phosphate leaving group by the nucleophilic YH moiety would be in principal also a plausible explanation for the formation of **F**, but can most likely be excluded (see Supporting Information File 1).

Indeed, under optimized conditions (1.2 equiv I_2, $P(OEt)_3$, Et_3N (5–6 equiv)/CH_2Cl_2 1:2; −78 °C then warming to rt) the piperidinols **11a–d** were isolated after saponification (during work up) of triethylphosphate and chromatographic purification in 68–82% yield and high enantiomeric excess (90–99%) (Table 2, entries 2, 11, 13 and 16).

For both cyclodehydration methods (with PPh_3 and $P(OEt)_3$) neat iodine was simply added to a solution of the amino alcohols **9a–d**, the phosphorus reagent and Et_3N in the reaction solvent at the indicated temperature (−40 °C and −78 °C, respectively) and stirred at this temperature, until I_2 had dissolved completely (1–2 h with PPh_3 and 2–5 h with $P(OEt)_3$). Then the usually heterogeneous mixture (through precipitated $Et_3NH^+Cl^-$) was allowed to warm to room temperature to reach full conversion of the starting material **9**. Due to the ammonium salt precipitation and the solid iodine for the large scale preparation of piperidinol **11a** (14 g, Table 2, entry 2) mechanical stirring was preferred. For saponification, saturated KOH solution in MeOH (ca. 4 N) was chosen, because aqueous KOH or NaOH solution would result in biphasic mixtures. A quantitative hydrolysis of the triethylphosphate side product required evaporation of CH_2Cl_2 and Et_3N (and MeOH) after the addition of the methanolic KOH-solution in vacuo, dilution with MeOH, stirring at room temperature for ca. 1 h, and a second concentration under reduced pressure. Most likely, the solubility of KOH in the CH_2Cl_2/Et_3N/MeOH mixture is too low resulting in incomplete hydrolysis of the phosphate without evaporation of the solvent. Saponification at reflux on the other hand (in order to circumvent the solvent evaporations) led to partial decomposition of the product **11a** (isolated yield 52% after several hours of reflux, see Table 2, entry 3). Chromatographic purification of the crude piperidinols **11a–d**, which were already isolated in 85–90% purity (from the phosphite cyclodehydration), was best achieved with halogen free iPrOH/Et_3N/hexane eluent mixtures (ratio 0.8–3:2–4:100 depending on the polarity of the product). Although the diastereomers of piperidinol **11c** (dr ca. 4:1 *cis*/*trans*) were chromatographically separable, we decided to separate them after protecting group exchange at the stage of the Boc carbamate **16c** (see Scheme 8), because the epimers of the latter one were much easier to isolate.



Scheme 5: Competition between the Michaelis–Arbuzow process and the desired cyclodehydration of amino alcohols and diols **E** (Y = e.g. O, NBn).

Interestingly, we observed a high specificity in the base: With pyridine, NMM, DMAP and DBU (1,8-diaza[5.4.0]bicycloundec-7-ene), respectively, (instead of Et_3N) the desired heterocycle **11a** was only formed in traces. DIPEA, lutidine and imidazole delivered **11a** in clearly diminished yields of 30–57% (Table 2, entries 4–6) compared to Et_3N (79%, entry 7). For comparison we ran the condensation of amino alcohol **9a** to piperidinol **11a** in the same concentration as in Table 2, entries 4–6 and 8 (as opposed to the standard conditions) and determined the yield also through NMR-standard: The yield assigned in that way (79%, entry 7) shows a decent match to the 82% isolated yield obtained under standard conditions (entry 2). Hence, the comparability of Table 2 entry 2 to entries 4–8 is established. In conclusion NMM, pyridine and imidazole might be too weak bases, DBU might be too strong and a base favoring other reaction pathways then the desired cyclodehydration. DIPEA and lutidine could be sterically too hindered and DMAP too nucleophilic inducing side reactions.

Moreover, we observed a strong influence of the ratio of Et_3N/CH_2Cl_2 with substrate **9c**: The phenylglycine-derived hydroxypiperidine **11c** was obtained in 68% yield in Et_3N/CH_2Cl_2 in a 1:1.3 ratio, while a 1:3 solvent mixture gave **11c** in only 22% yield (Table 2, entries 13–15). Indeed, the furan **13h** (see Table 2) resulting from nucleophilic substitution of the primary (activated) OH-function through the secondary hydroxy group of **9c** formed in significant amounts in the cyclisation of amino diol **9c**. This is explained by steric shielding of the amino function (→ decreased nucleophilicity) through the bulky phenyl group in α-position (compared to the less demanding Me and Bn side chains R of substrates **9a** and **9c**). As the R-substituent is in the β-position of the secondary OH-function of diols **9**, this hydroxy moiety is less shielded. For substrate **9c** the yield could not be improved further, because in higher ratios Et_3N/CH_2Cl_2 iodine did not completely dissolve (react) at −78 °C in a reasonable time (<12 h).

This strong influence of the ratio of Et_3N/CH_2Cl_2 can be attributed to the lower solubility of iodine in Et_3N (which leads to a slower and thus more selective reaction) and general base catalysis: Simultaneous deprotonation (through Et_3N) in the cyclisation step strongly favours the desired reaction pathway to piperidines **11**. Due to this effect we chose a ratio of Et_3N/CH_2Cl_2 1:2 as standard conditions for the phosphite mediated cyclodehydration. Typically, 5 to 6 equivalents of Et_3N resulting in a reasonable concentration of the substrates **11** and **12** (see Table 3) of 0.4–0.5 mol/L (in Et_3N/CH_2Cl_2) were sufficient enough to guarantee magnetically stirring, as the viscosity of the reaction mixture increases through ammonium salt precipitation during the preceding reaction. Noteworthy, Et_3N is as cheap as common solvents such as THF and CH_2Cl_2.

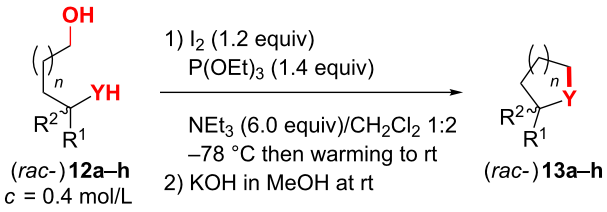
Furthermore, in THF the yield of **11a** decreased to 58% (Table 2, entry 8), whereas in MeCN low conversions were observed most likely through reaction of the solvent with the I–$P(OEt)_3^+$ intermediate and in Et_3N as the sole solvent the solubility of iodine is too low. Even at room temperature iodine did not dissolve (= react) completely. Also a larger excess of iodine (>1.2 equiv) has a negative effect on the yield, because the secondary hydroxy function probably is activated as well. With the more atom economic $P(OMe)_3$ complex product mixtures were obtained (in the case of substrate **9a**). Most likely the differentiation between the Michaelis–Arbuzow and cyclodehydration pathway (see Scheme 5) is declined. Moreover, the reaction temperature has a strong influence: When the condensation of **9a** had been performed at −20 °C for instance, piperidine **11a** was isolated in only 41% yield (Table 2, entry 9). Interestingly, the activation of the primary OH function of substrates **9** in the presence of the secondary OH group proceeded (with PPh_3 and $P(OEt)_3$) in very high chemoselectivity most likely due to steric effects. The corresponding aziridine of **9a** clearly resulting from activation of the secondary hydroxy group and subsequent fast 3-*exo*-*trig* cyclisation was only obtained as a sideproduct at higher temperatures (I_2, PPh_3, imidazole, CH_2Cl_2 at 0 °C; see Supporting Information File 1 for more details).

Significantly, 14 g of alanine derivative *cis*-**11a** were obtained (cyclodehydration with $P(OEt)_3$) in one batch with no purification of the intermediates (**2a**, **5a**, **7a** and *syn*-**9a**) at all and an overall yield of 44%, demonstrating the scalability and high practicability of our sequence. The relative configurations of compounds **9** and **11** were proven by NOE spectroscopy of piperidinols *cis*-**11a–d**, *trans*-**11a**, *cis*- and *trans*-**16c**, L-733,060·HCl and of oxazolidinones *trans*-**10a** and *trans*-**10c** (see Supporting Information File 1 for more details).

Synthesis of other heterocycles through phosphite-mediated cyclodehydration

We next wanted to demonstrate the generality of the phosphite-mediated cyclodehydration (Table 3). Towards this end, a range of amino alcohols and diols **12a,b** and **12d–h** were converted in usually very good yields (>80%) to pyrrolidines, piperidines and furans **13a,b** and **13d–h**. The established cyclodehydration procedure only had to be slightly modified regarding the work up: As most of the products **13a**,**b** and **13d–h** are volatile, the crude reaction mixture was concentrated under reduced pressure (50 mbar) after quenching with the methanolic KOH solution and kept at this pressure at the rotatory evaporator for ca. 0.5 h. Then the residue was portioned between water and *n*-pentane (high volatility and low solubility of $OP(OEt)_3$!) and the organic phase was washed with five portions of water to remove the remaining phosphate (after saponification **13**

Table 3: Cyclodehydration of amino alcohols and diols **12a–h** to heterocycles **13a–h**.



entry	substrate	YH	R^1	R^2	*n*	deviation from standard conditions	yield
1	**12a**	NBn	H	H	1	–	80%[a]
2						washing of **13-HCl** (aq.) with EtOAc instead of saponification	81%[b]
3	**12b**	NBn	H	H	2	washing **13b-HCl** (aq.) with EtOAc instead of saponification	63%[b]
4	**12c**	NBoc	H	H	2	2 d at rt	n. r.
5	*rac*-**12d**	OH	Ph	H	1	–	92%[b]
6	*rac*-**12e**	OH	*o*-ClPh	H	1	–	85%[b]
7	*rac*-**12f**	OH	*p*-BrPh	H	1	–	83%[b]
8						$P(OiPr)_3$ instead of $P(OEt)_3$	67%[a]
9						$P(OPh)_3$ instead of $P(OEt)_3$	83%[a]
10	*rac*-**12g**	OH	Mes	H	1	–	84%[b]
11	**12h**	OH	Ph	Ph	1	–	82%[b]
12						PPh_3/MeCN instead of $P(OEt)_3/CH_2Cl_2$	75%[a]

[a]Yield determined with naphthalene as NMR-standard. [b]Isolated yields, purity >90% according to crude ^{1}H NMR.

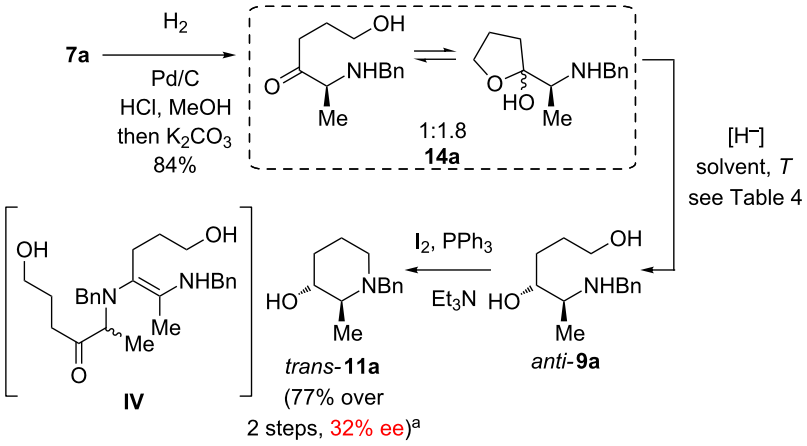
contained 20–30 mol % of the phosphate). Finally, the heterocycles **13** were isolated without a trace of the phosphoric acid ester ("traceless cyclodehydration") in >90% purity according to ^{1}H NMR.

We first investigated the amino alcohols **12a–c**: Pyrrolidine **13a** was formed in 80% yield after hydrolysis of the phosphate and in 81% yield after extraction of triethylphosphate with EtOAc (×5) while keeping the product **13a** as the hydrochloride salt in the aqueous phase (Table 3, entries 1 and 2). Surprisingly, with the higher homologue **12b** the piperidine **13b** was obtained in only 63% yield (entry 3). The lower yield compared to the hydroxypiperidines **11a**,**b** and **11d** (≥74%, see Table 2) might be explained by the preference of a conformation of the phosphonium intermediate **III** of **11a**,**b** and **11d** (Scheme 5), which is favourable for the cyclisation. This arrangement might be stabilized through a hydrogen bridge between the NH proton and the O atom of the secondary OH group and a (weak) Thorpe–Ingold effect by the substituent R. The much less nucleophilic Boc-carbamate **12c** was not converted to the desired piperidine **13c** (entry 4). Here only starting material was re-isolated (probably originating from hydrolysis of the corresponding phosphate of alcohol **12c**).

The α-aryl furans **13d–f** were formed in excellent yields (83–92%, Table 3, entries 5–7). Interestingly, the cyclodehydration of *rac*-**12f** was also mediated by $P(OiPr)_3$ and $P(OPh)_3$ in 67% and 83% yield, respectively (entries 8–9). Whereas $OP(OiPr)_3$ was hydrolyzed in the work up, $OP(OPh)_3$ was not saponified and therefore still remained in the isolated product **13f**. However, considering the atom economy these phosphites do not represent an alternative to $P(OEt)_3$. Even the diols *rac*-**12g** and **12h** with a sterically demanding mesityl and two phenyl substituents, respectively, gave cleanly the furans *rac*-**13g** and **13h** in good yields (Table 3, entries 10 and 11). Also in terms of isolated yield the phosphite-mediated cyclodehydration of substrate **12h** was superior (82%, Table 3, entry 11) to the phosphine driven conditions (75%, entry 12).

Synthesis of a *trans*-piperidinol B

We initially investigated the diastereoselectivity of the reduction of the secondary benzylamino ketone **14a**, which was synthesized from hydroxyketone **7a** through Cbz-cleavage and basic work up (Scheme 6 and Table 4). According to ^{1}H NMR the hemiacetal of **14a** (ca. 1:1 ratio of its epimers) forms an equilibrium with its ketone tautomer in a 1.8:1 ratio. In contrast to hydroxyketones **7a–d** the furan tautomer of **14a** is thermody-



Scheme 6: Initial synthesis of the *trans*-piperidinol **11a** in diminished enantiopurity. [a]The amino alcohol **9a** obtained through L-Selectride reduction according to entry 6 in Table 4 (dr = 25:1) was subjected to cyclodehydration.

namically more stable than the keto form. This might be rationalized by a lower steric strain in the heterocyclic form due to the smaller NHBn side chain (compared to NBnCbz in **7a–d**).

Disappointingly, in the reduction with $NaBH_4$ no selectivity was observed at all (dr = 1:1 *anti*/*syn*, Table 4, entry 1). However, in the presence of one equivalent of HCl the diol **9a** was isolated in a moderate dr of 2.6:1 (entry 2), which demonstrated the formation of a Cram chelate transition state stabilized through a hydrogen bond of the hydrochloride of **14a**. Under Luche conditions ($NaBH_4$, $CeCl_3$) [86] a similar result was attained (dr = 2.9:1, Table 4, entry 3).

DIBALH delivered amino alcohol **9a** (various solvents tested) only in poor selectivities (dr up 2.6:1, Table 4, entry 4), which is in harsh contrast to previously reported reductions of related *para*-methoxybenzylamino and benzylamino ketones with DIBALH giving rise of the best diastereoselectivities [59,60]). Albeit up to four equivalents of DIBALH were utilized, only 40–60% conversion of **14a** was reached. Here the complexation by –$AliBu_2$ after the initial deprotonation of the OH and NH function of **14a** might shield the carbonyl group and encumber reduction.

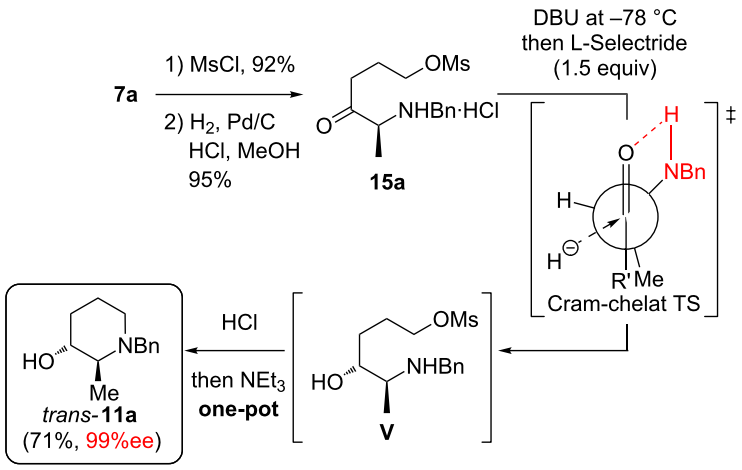
Table 4: Diastereoselectivity in the reduction of ketone **14a**.

entry	[H–]	solvent	*T* [°C]	dr (*anti*/*syn*)
1	$NaBH_4$	MeOH	0	1:1[a]
2	$NaBH_4$, HCl	MeOH	0	2.6:1[a]
3	$NaBH_4$, $CeCl_3$	MeOH	−78	2.9:1[a]
4	DIBALH	divers[b]	−78	1.4–2.6:1[c]
5	L-Selectride	THF	−78	6:1[d]
6	L-Selectride	CH_2Cl_2/THF[d]	−78	25:1[e]
7	N-Selectride	THF	−78	>50:1[e]

[a]The amino alcohol **9a** was isolated in 87% (entry 1), 85% (entry 2), 93% (entry 3) yield and >90% purity according to ^{1}H NMR. [b]CH_2Cl_2, *n*-Hex/THF or *n*-Hex/CH_2Cl_2. [c]40–60% conversion were achieved, starting material was not separated. [d]A solution of the starting material **14a** in CH_2Cl_2 was treated with a commercial solution of L-Selectride in THF. [e]60–80% conversion were achieved, starting material was not separated.

However, L-Selectride reduction resulted in better stereoselectivities with dr = 6:1 *anti*/*syn* (Table 4, entry 5). If the starting material **14a** was dissolved in the less polar CH_2Cl_2 (rather than THF), the dr further increased to >19:1 (entry 6). Moreover, N-Selectride provided the product **9a** almost as a pure diastereomer (entry 7, solvent THF), only a very small trace of the *syn*-diastereomer was visible in the ^{1}H NMR (400 MHz). Nevertheless, even with 4 equivalents of Selectride conversions of only up to 80% were observed. Unfortunately, subsequent Appel reaction of the diol *anti*-**9a** (dr = 25:1), synthesized through L-Selectride reduction in THF/CH_2Cl_2 (Table 4, entry 6), gave piperidinol **11a** in a significantly diminished ee of 32% (determined via HPLC on a chiral stationary phase and comparison with a racemic sample). This racemisation might be rationalized by an intermolecular enamine formation of the secondary amino ketone **14b** as depicted in the intermediate **IV**, Scheme 6.

At this point we realized that a hydrochloride of the secondary amino ketone **14a** or a derivative should be unable to racemise through autocatalytic enamine formation (due to the protonation of the amino function). However, the hydrochloride of amine **14a** was poorly soluble in organic solvents, so that its isolation proved to be difficult. Straightforward, mesylation of hydroxyketone **7a** and subsequent Cbz-cleavage (H_2, Pd/C) in

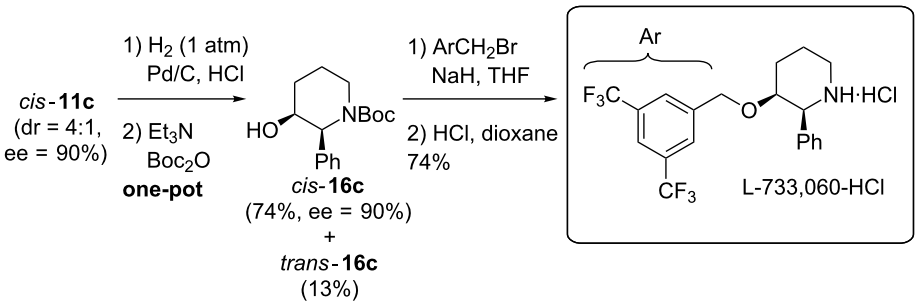


Scheme 7: Synthesis of *trans*-piperidinol **11a** in excellent ee.

the presence of HCl delivered the hydrochloride salt **15a**, which was easily isolated through filtration and solvent evaporation (Scheme 7). To our delight, subsequent liberation of the free amine through DBU at low temperature, immediate L-Selectride reduction (giving intermediate **V**), HCl quenching and Et_3N-induced cyclisation afforded the piperidine *trans*-**11a** in an excellent ee (≥99%) and as a single diastereomer according to crude ^1H NMR. Although the reduction is performed in the presence of a secondary amino function bearing an N–H-proton and one equivalent of DBU-H^+, only 1.5 equivalents of L-Selectride were required for a quantitative conversion. Thus we assume the Cram chelate transition state is formed through an amine N–H proton rather than an amide N–Li lithium cation as shown in Scheme 7 (which would result from deprotonation of the amino group by L-Selectride and would thus consume at least 2 equivalents of the reducing agent).

Synthesis of L-733,060

In order to probe the practicability of our sequence we synthesized L-733,060 as shown in Scheme 8. After cleavage of the Bn-group under 1 atm of hydrogen and subsequent Boc-protection in one pot, the diastereomers *cis*- and *trans*-**16c** were easily separated by flash chromatography. Thereby, we found it advantageous to perform the hydrogenolysis in the presence of HCl to protonate the released amine and then induce Boc protection after neutralisation of the acid by Et_3N rather than to run the hydrogenolysis in the presence of Boc_2O. As already observed in the reduction/Cbz-cleavage **7**→**9** (Scheme 4) the quality of the Pd/C batch had a high influence on the hydrogenolysis: No Bn cleavage was observed with Pd/C charges of a low activity, more catalytically active batches and freshly prepared Pd/C [77] led to quantitative conversion within 1–2 d (1 atm H_2). The resulting alcohol *cis*-**16c** was subjected to Williamson etherification and subsequently the Boc-group was cleaved under acidic conditions (HCl in dioxane). We decided to isolate L-733,060 as its hydrochloride salt, because it is a non-hygroscopic solid (rather than an oil) and can be easily extracted with organic solvents (e.g. EtOAc) from an aqueous phase. With 8 steps, our sequence represents one of the shortest syntheses reported to date [38-40]. Additionally, with the carbamate *cis*-**16c** (synthesized in 6 rather than 8 steps) we also achieved a formal total synthesis of CP-99,994 [87].



Scheme 8: Synthesis of L-733,060·HCl.

Although the phenylalanine and phenylglycine-derived piperidinols **11b** and **11c** bear "unfunctionalized" side chains, phenyl groups represent masked carboxylic acid functions. For instance, the enantiomers of piperidine *cis*-**11c** and its *N*-deprotected derivative were converted to (2*S*,3*R*)-3-hydroxypipecolic acid through protecting group manipulation and oxidative cleavage of the phenyl group with $RuCl_3$ and $NaIO_4$ [38,40].

Conclusion

Herein we presented a highly stereodivergent (dr up to 19:1), scalable and practical (up to 14 g of *cis*-**11a** without any purification of intermediates) synthesis of *cis*- and *trans*-configured 3-piperidinols **11**, which represent a key structural motive in various natural products and other bioactive target compounds. Moreover, a high step-economy (5–6 steps) was guaranteed by several novel one-pot procedures (**1**→**2**, **7**→*syn*-**9**, **15a**→*trans*-**11a**) and surrendering any protection of OH functions. To probe the efficiency of this sequence piperidinol **11c** was converted to the NK-1 inhibitor L-733,060 in three further steps. Additionally, a unique cyclodehydration procedure replacing PPh_3 through $P(OEt)_3$ to improve atom economy (166 compared to 262 g/mol) and to allow separation of the oxidized side product ($OP(OEt)_3$) by saponification (no similar literature precedents known) was implemented. Ongoing research is focusing on the transformation of the methionine-derived piperidinol **11d** to other pharmacologically relevant targets on a gram scale.

Supporting Information

Supporting Information File 1

Experimental and characterisation data.
[http://www.beilstein-journals.org/bjoc/content/supplementary/1860-5397-10-35-S1.pdf]

Acknowledgements

We want to thank the German Academic Exchange Service (DAAD) for a generous scholarship for P. H., and Prof. Dr. H.-G. Schmalz for the very kind opportunity to perform a part of the project at the University of Cologne. Additionally, we want to thank Christopher Lood (Aalto University) for recording analytical data.

References

1. Karjalainen, O. K.; Koskinen, A. M. P. *Org. Biomol. Chem.* **2012,** *10,* 4311–4326. doi:10.1039/c2ob25357g
2. Wijdeven, M. A.; Willemsen, J.; Rutjes, F. P. J. T. *Eur. J. Org. Chem.* **2010,** 2831–2844. doi:10.1002/ejoc.200901494
3. Huang, P.-Q. *Synlett* **2006,** 1133–1149. doi:10.1055/s-2006-941565
4. Nemr, A. L. *Tetrahedron* **2000,** *56,* 8579–8629. doi:10.1016/S0040-4020(00)00790-0
5. Bergmeier, S. C. *Tetrahedron* **2000,** *56,* 2561–2576. doi:10.1016/S0040-4020(00)00149-6
6. Horne, G.; Wilson, F. X.; Tinsley, J.; Williams, D. H.; Storer, R. *Drug Discovery Today* **2011,** *16,* 107–118. doi:10.1016/j.drudis.2010.08.017
7. Winchester, B. G. *Tetrahedron: Asymmetry* **2009,** *20,* 645–651. doi:10.1016/j.tetasy.2009.02.048
8. Pruett, S. T.; Bushnev, A.; Hagedorn, K.; Adiga, M.; Haynes, C. A.; Sullards, M. C.; Liotta, D. C.; Merrill, A. H., Jr. *J. Lipid Res.* **2008,** *49,* 1621–1639. doi:10.1194/jlr.R800012-JLR200
9. Brunner, M.; Koskinen, A. M. P. *Curr. Org. Chem.* **2004,** *8,* 1629–1645. doi:10.2174/1385272043369638
10. Zappia, G.; Cancelliere, G.; Gacs-Baitz, E.; Delle Monache, G.; Misiti, D.; Nevolam, L.; Botta, B. *Curr. Org. Synth.* **2007,** *4,* 238–307. doi:10.2174/157017907781369306
11. Ager, D. J.; Prakash, I.; Schaad, D. R. *Chem. Rev.* **1996,** *96,* 835–875. doi:10.1021/cr9500038
12. Singh, P. K.; Singh, V. K. *Pure Appl. Chem.* **2012,** *84,* 1651–1657. doi:10.1351/PAC-CON-11-10-16
13. Nishiyama, H.; Ito, J.-i. *Chem. Commun.* **2010,** *46,* 203–212. doi:10.1039/b918923h
14. Desimoni, G.; Faita, G.; Jørgensen, K. A. *Chem. Rev.* **2006,** *106,* 3561–3651. doi:10.1021/cr0505324
15. Baker, R.; Harrison, T.; Swain, C. J.; Williams, B. J. J. Eur. Patent 0528495A1, 1993.
16. Harrison, T.; Williams, B. J.; Swain, C. J.; Ball, R. G. *Bioorg. Med. Chem. Lett.* **1994,** *4,* 2545–2550. doi:10.1016/S0960-894X(01)80280-8
17. Desai, M. C.; Lefkowitz, S. L.; Thadeio, P. F.; Longo, K. P.; Snider, R. M. *J. Med. Chem.* **1992,** *35,* 4911–4913. doi:10.1021/jm00104a018
18. Rosen, T.; Seeger, T. F.; McLean, S.; Desai, M. C.; Guarino, K. J.; Bryce, D.; Pratt, K.; Heym, J. *J. Med. Chem.* **1993,** *36,* 3197–3201. doi:10.1021/jm00073a022
19. Data, P.; Srivastava, S.; Coutinho, E.; Govil, G. *Curr. Top. Med. Chem.* **2004,** *4,* 75–103. doi:10.2174/1568026043451636
20. Koepfli, J. B.; Mead, J. F.; Brockman, J. A., Jr. *J. Am. Chem. Soc.* **1947,** *69,* 1837. doi:10.1021/ja01199a513
21. Koepfli, J. B.; Mead, J. F.; Brockman, J. A., Jr. *J. Am. Chem. Soc.* **1949,** *71,* 1048–1054. doi:10.1021/ja01171a080
22. Linder, M. R.; Heckeroth, A. R.; Najdrowski, M.; Daugschies, A.; Schollmeyer, D.; Miculka, C. *Bioorg. Med. Chem. Lett.* **2007,** *17,* 4140–4143. doi:10.1016/j.bmcl.2007.05.053
23. Grauer, A.; König, B. *Eur. J. Org. Chem.* **2009,** 5099–5111. doi:10.1002/ejoc.200900599
24. Hanessian, S.; McNaughton-Smith, G.; Lombart, H.-G.; Lubell, W. D. *Tetrahedron* **1997,** *53,* 12789–12854. doi:10.1016/S0040-4020(97)00476-6
25. Maillard, M. C.; Brookfield, F. A.; Courtney, S. M.; Eustache, F. M.; Gemkow, M. J.; Handel, R. K.; Johnson, L. C.; Johnson, P. D.; Kerry, M. A.; Krieger, F.; Meniconi, M.; Muñoz-Sanjuán, I.; Palfrey, J. J.; Park, H.; Schaertl, S.; Taylor, M. G.; Weddell, D.; Dominguez, C. *Bioorg. Med. Chem.* **2011,** *19,* 5833–5851. doi:10.1016/j.bmc.2011.08.020
26. Quibell, M.; Benn, A.; Flinn, N.; Monk, T.; Ramjee, M.; Wang, Y.; Watts, J. *Bioorg. Med. Chem.* **2004,** *12,* 5689–5710. doi:10.1016/j.bmc.2004.07.054
27. Guengerich, F. P.; DiMari, S. J.; Broquist, H. P. *J. Am. Chem. Soc.* **1973,** *95,* 2055–2056. doi:10.1021/ja00787a080
28. Elbein, A. D. *FASEB J.* **1991,** *5,* 3055–3063.

29. Teitelbaum, S. L.; Deselm, C. J. U.S. Pat. Appl. Publ. US 20110311519 A1, 2011.
30. Keller, T.; Mazitschek, R.; Whitman, M.; Lee, J. US Patent 2011/0263532 A1, 2011.
31. Keller, T.; Mazitschek, R.; Whitman, M. *PCT Int. Appl.* WO 2010019210 A2, 2010.
32. Cochi, A.; Pardo, D. G.; Cossy, J. *Heterocycles* **2012,** *86,* 89–116. doi:10.3987/REV-12-SR(N)2
Review on the synthesis of L-733,060 and L-733,061.
33. Cochi, A.; Pardo, D. G.; Cossy, J. *Eur. J. Org. Chem.* **2013,** 809–829. doi:10.1002/ejoc.201201415
Reviews on the synthesis of (3-hydroxy)pipecolic acid derivatives.
34. Cant, A. A.; Sutherland, A. *Synthesis* **2012,** *44,* 1935–1950. doi:10.1055/s-0031-1289767
Reviews on the synthesis of (3-hydroxy)pipecolic acid derivatives.
35. Kadouri-Puchot, C.; Comesse, S. *Amino Acids* **2005,** *29,* 101–130. doi:10.1007/s00726-005-0193-x
Reviews on the synthesis of (3-hydroxy)pipecolic acid derivatives.
36. Lemire, A.; Grenon, M.; Pourashraf, M.; Charette, A. B. *Org. Lett.* **2004,** *6,* 3517–3520. doi:10.1021/ol048624n
37. Cossy, J.; Dumas, C.; Pardo, D. G. *Eur. J. Org. Chem.* **1999,** 1693–1699. doi:10.1002/(SICI)1099-0690(199907)1999:7<1693::AID-EJOC1693>3.0.CO;2-J
38. Cochi, A.; Burger, B.; Navarro, C.; Pardo, D. G.; Cossy, J.; Zhao, Y.; Cohen, T. *Synlett* **2009,** 2157–2161. doi:10.1055/s-0029-1217568
39. Bilke, J. L.; Moore, S. P.; O'Brien, P.; Gilday, J. *Org. Lett.* **2009,** *11,* 1935–1938. doi:10.1021/ol900366m
40. Pansare, S. A.; Paul, E. K. *Org. Biomol. Chem.* **2012,** *10,* 2119–2125. doi:10.1039/c2ob06644k
41. Shioiri, T.; Izawa, K.; Konoike, T.; Karpf, M. *Pharmaceutical Process Chemistry;* Wiley-VCH: Weinheim, Germany, 2010; pp 1–37.
42. Roberge, D. M. *Org. Process Res. Dev.* **2004,** *8,* 1049–1053. doi:10.1021/op0400160
43. Constable, D. J. C.; Dunn, P. J.; Hayler, J. D.; Humphrey, G. R.; Leazer, J. L., Jr.; Linderman, R. J.; Lorenz, K.; Manley, J.; Pearlman, B. A.; Wells, A.; Zaks, A.; Zhang, T. Y. *Green Chem.* **2007,** *9,* 411–420. doi:10.1039/b703488c
44. Dandapani, S.; Curran, D. P. *Chem.–Eur. J.* **2004,** *10,* 3130–3138. doi:10.1002/chem.200400363
45. Dembinski, R. *Eur. J. Org. Chem.* **2004,** 2763–2772. doi:10.1002/ejoc.200400003
46. Véliz, E. A.; Beal, P. A. *Tetrahedron Lett.* **2006,** *47,* 3153–3156. doi:10.1016/j.tetlet.2006.02.138
47. Chang, B. C.; Conrad, W. E.; Denney, D. B.; Denney, D. Z.; Edelman, R.; Powell, R. L.; White, D. W. *J. Am. Chem. Soc.* **1971,** *93,* 4004–4009. doi:10.1021/ja00745a031
48. Denney, D. B.; Denney, D. Z.; Gigantino, J. J. *J. Org. Chem.* **1984,** *49,* 2831–2832. doi:10.1021/jo00189a044
49. Kelly, B. D.; Lambert, T. H. *Org. Lett.* **2011,** *13,* 740–743. doi:10.1021/ol102980t
50. Flamme, E. M.; Roush, W. R. *Beilstein J. Org. Chem.* **2005,** *1,* No. 7. doi:10.1186/1860-5397-1-7
51. Huy, P. H.; Koskinen, A. M. P. *Org. Lett.* **2013,** *15,* 5178–5181. doi:10.1021/ol4026588
52. Cherest, M.; Felkin, H.; Prudent, N. *Tetrahedron Lett.* **1968,** *9,* 2199–2204. doi:10.1016/S0040-4039(00)89719-1
Introduction of Felkin–Anh model.
53. Stevens, C. L.; TerBeek, K. J.; Pillai, P. M. *J. Org. Chem.* **1974,** *39,* 3943–3946. doi:10.1021/jo00940a035
An early example of diastereodiscriminating reductions of amino ketones.
54. Cram, D. J.; Wilson, D. R. *J. Am. Chem. Soc.* **1963,** *85,* 1245–1249. doi:10.1021/ja00892a008
Introduction of Cram chelate model.
55. Rittle, K. E.; Homnick, C. F.; Ponticello, G. S.; Evans, B. E. *J. Org. Chem.* **1982,** *47,* 3016–3018. doi:10.1021/jo00136a045
56. Lubell, W. D.; Rapoport, H. *J. Am. Chem. Soc.* **1987,** *109,* 236–239. doi:10.1021/ja00235a035
57. Reyes, E.; Ruiz, N.; Vicario, J. L.; Badia, D.; Carrillo, L. *Synthesis* **2011,** 443–450. doi:10.1055/s-0030-1258390
58. Fraser, D. S.; Park, S. B.; Chong, J. M. *Can. J. Chem.* **2004,** *82,* 87–101. doi:10.1139/V03-165
59. Chung, S.-K.; Lee, J.-M. *Tetrahedron: Asymmetry* **1999,** 1441–1444. doi:10.1016/S0957-4166(99)00147-0
60. Dondoni, A.; Perrone, A. *Synthesis* **1993,** 1162–1176. doi:10.1055/s-1993-26021
61. Quitt, P.; Hellerbach, J.; Vogler, K. *Helv. Chim. Acta* **1963,** *46,* 327–333. doi:10.1002/hlca.19630460133
62. Schotten, C. *Ber. Dtsch. Chem. Ges.* **1884,** *17,* 2544–2547. doi:10.1002/cber.188401702178
63. Baumann, E. *Ber. Dtsch. Chem. Ges.* **1886,** *19,* 3218–3222. doi:10.1002/cber.188601902348
64. Anderson, G. W.; Zimmerman, J. E.; Callaha, F. M. *J. Am. Chem. Soc.* **1967,** *89,* 5012–5017. doi:10.1021/ja00995a032
Report about NMM preventing racemisation during peptide coupling due to its low basicity.
65. Wissmann, H.; Kleiner, H.-J. *Angew. Chem., Int. Ed. Engl.* **1980,** *19,* 133–134. doi:10.1002/anie.198001331
66. Wissmann, H. *Phosphorus Sulfur Relat. Elem.* **1987,** *30,* 645–648. doi:10.1080/03086648708079147
67. Dunetz, J. R.; Xiang, Y.; Baldwin, A.; Ringling, J. *Org. Lett.* **2012,** *13,* 5048–5051. doi:10.1021/ol201875q
A recent study towards the amidation of an racemisation sensitive amino acid derivative.
68. Smith, G. G.; Sivakua, T. *J. Org. Chem.* **1983,** *48,* 627–634. doi:10.1021/jo00153a001
69. Cahiez, G.; Alexakis, A.; Normant, J. F. *Tetrahedron Lett.* **1978,** *33,* 3013–3014. doi:10.1016/S0040-4039(01)94926-3
70. Hanby, W. E.; Waley, S. G.; Watson, J. *J. Chem. Soc.* **1950,** 3239–3249. doi:10.1039/JR9500003239
Selective monoesterification of glutamic acid.
71. Gmeiner, P.; Feldman, P. F.; Chu-Moyer, M. Y.; Rapoport, H. *J. Org. Chem.* **1990,** *55,* 3068–3074. doi:10.1021/jo00297a023
Selective side chain monoesterifications of aspartic acid.
72. Schwarz, H.; Bumpus, F. M.; Page, I. H. *J. Am. Chem. Soc.* **1957,** *79,* 5697–5703. doi:10.1021/ja01578a030
73. Hannachi, J.-C.; Vidal, J.; Mulatier, J.-C.; Collet, A. *J. Org. Chem.* **2004,** *69,* 2367–2373. doi:10.1021/jo035700b
Reductive benzylation of amino acids with PhCHO and $NaBH_4$ in MeOH.
74. Brown, H. C.; Krishnamurthy, S. *J. Am. Chem. Soc.* **1972,** *94,* 7159–7161. doi:10.1021/ja00775a053
Initial discovery of L-Selectride.
75. Brown, H. C.; Krishnamurthy, S. *J. Am. Chem. Soc.* **1973,** *95,* 1669–1671. doi:10.1021/ja00786a057
Initial development of Superhydride.

76. Brown, H. C.; Kim, S. C.; Krishnamurthy, S. *J. Org. Chem.* **1980,** *45,* 1–12. doi:10.1021/jo01289a001
Initial development of Superhydride.
77. Felpin, F.-X.; Fouquet, E. *Chem.–Eur. J.* **2010,** *16,* 12440–12445. doi:10.1002/chem.201001377
78. Khan, I. A.; Saxena, A. K. *Tetrahedron* **2012,** *68,* 1272–1279. doi:10.1016/j.tet.2011.11.047
79. Kobrzycka, E.; Gryko, D.; Jurczak, J. *Tetrahedron: Asymmetry* **2002,** *13,* 2133–2139. doi:10.1016/S0957-4166(02)00545-1
80. Griengl, H.; Hayden, W.; Schindler, E.; Wanek, E. *Arch. Pharm.* **1983,** *316,* 146–153. doi:10.1002/ardp.19833160211
81. Appel, R.; Kleinstück, R. *Chem. Ber.* **1974,** *107,* 5–12. doi:10.1002/cber.19741070102
82. Lange, G. L.; Gottardo, C. *Synth. Commun.* **1990,** *20,* 1473–1479. doi:10.1080/00397919008052864
Cyclodehydration with I_2 and PPh_3.
83. Stowell, J. K.; Widlanski, T. S. *Tetrahedron Lett.* **1995,** *36,* 1825–1826. doi:10.1016/0040-4039(95)00153-4
84. Oza, V. B.; Corcoran, R. C. *J. Org. Chem.* **1995,** *60,* 3680–3684. doi:10.1021/jo00117a018
85. Watanabe, Y.; Inada, E.; Jinno, M.; Ozaki, S. *Tetrahedron Lett.* **1993,** *34,* 497–500. doi:10.1016/0040-4039(93)85111-9
86. Gemal, A. L.; Luche, J. L. *J. Am. Chem. Soc.* **1981,** *103,* 5454–5459. doi:10.1021/ja00408a029
87. Huang, P.-Q.; Liu, L.-X.; Wei, B.-G.; Ruan, Y.-P. *Org. Lett.* **2003,** *5,* 1927–1929. doi:10.1021/ol034505g

License and Terms

This is an Open Access article under the terms of the Creative Commons Attribution License (http://creativecommons.org/licenses/by/2.0), which permits unrestricted use, distribution, and reproduction in any medium, provided the original work is properly cited.

The license is subject to the *Beilstein Journal of Organic Chemistry* terms and conditions: (http://www.beilstein-journals.org/bjoc)

The definitive version of this article is the electronic one which can be found at: doi:10.3762/bjoc.10.35

Beilstein Journal of Organic Chemistry

Preparation of new alkyne-modified ansamitocins by mutasynthesis

Kirsten Harmrolfs[1], Lena Mancuso[1], Binia Drung[1], Florenz Sasse[2] and Andreas Kirschning[*1]

Full Research Paper

Open Access

Address:
[1]Institute of Organic Chemistry and Center of Biomolecular Drug Research (BMWZ), Leibniz University Hannover, Schneiderberg 1b, 30167 Hannover, Germany and [2]Department of Chemical Biology, Helmholtz Center for Infectious Research (HZI), Inhoffenstraße 7, D-38124 Braunschweig, Germany

Email:
Andreas Kirschning[*] - andreas.kirschning@oci.uni-hannover.de

* Corresponding author

Keywords:
ansamitocins; antibiotics; antitumor agents; click chemistry; mutasynthesis; natural products

Beilstein J. Org. Chem. **2014,** *10,* 535–543.
doi:10.3762/bjoc.10.49

Received: 30 November 2013
Accepted: 29 January 2014
Published: 03 March 2014

This article is part of the Thematic Series "Natural products in synthesis and biosynthesis".

Guest Editor: J. S. Dickschat

© 2014 Harmrolfs et al; licensee Beilstein-Institut.
License and terms: see end of document.

Abstract

The preparation of alkyne-modified ansamitocins by mutasynthetic supplementation of *Actinosynnema pretiosum* mutants with alkyne-substituted aminobenzoic acids is described. This modification paved the way to introduce a thiol linker by Huisgen-type cycloaddition which can principally be utilized to create tumor targeting conjugates. In bioactivity tests, only those new ansamitocin derivatives showed strong antiproliferative activity that bear an ester side chain at C-3.

Introduction

Although natural products and analogues cover a large portion of the drug market particularly in the treatment of cancer as well as bacterial and viral infections their role in pharmaceutical research has decreased over the past two decades. In part, this development is due to their often limited accessibility as well as their structural complexity. This situation hampers their use as lead structures for which access to small compound libraries is essential in order to perform structure–activity relationship studies. Besides semisynthetic and total synthesis approaches the combination of chemical synthesis with biotechnological strategies has seen increased interest lately [1-3]. The concepts either rely on a concise understanding of the biosynthesis of natural products or simply individual enzymes for in vitro applications [4]. In this context, producer strains that are genetically engineered in the biosynthesis of important and complex natural products have shown to be powerful synthetic tools, e.g., knock out mutants are key players in mutational biosynthesis, or in short mutasynthesis. This technique relies on the cellular uptake of modified biosynthetic intermediates. Processing of these intermediates, sometimes called mutasyn-

thons, can provide complex secondary metabolites specifically modified as planned by choice of the synthetic modification incorporated into the mutasynthon [5-7].

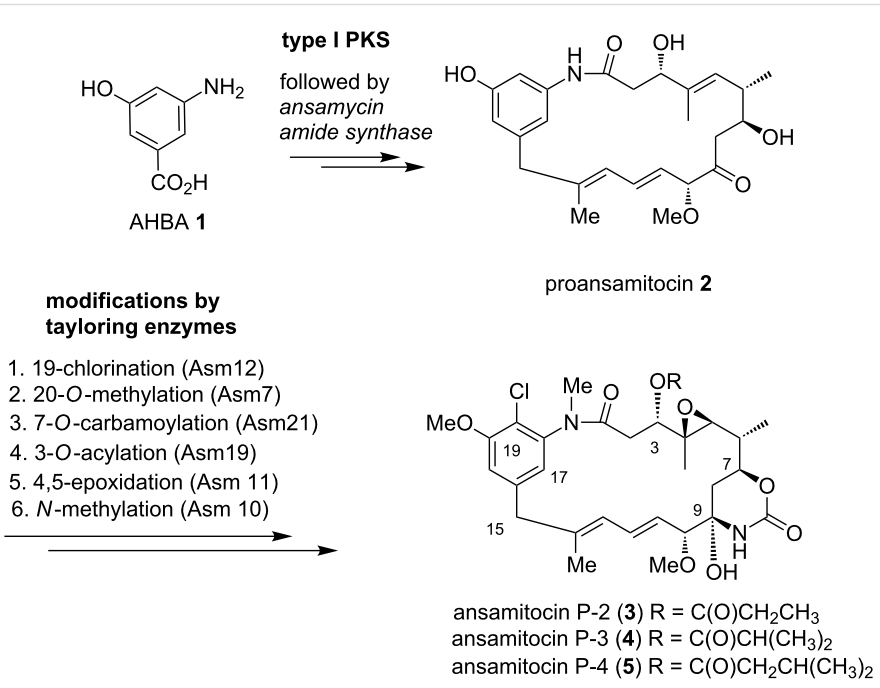
In earlier work, we demonstrated that the ansamitocins (maytansinoids) **3**–**5** are an ideal showcase for creating small libraries by mutasynthesis [8-10]. These secondary metabolites exert strong antiproliferative activity towards different leukemia cell lines as well as human solid tumors. Inhibitory concentrations were as low as 10^{-3} to 10^{-7} μg/mL [11] which resulted from binding to β-tubulin monomers [12]. The ansamitocins are produced by *Actinosynnema pretiosum*. For our mutasynthetic studies we utilized an AHBA blocked mutant of *A. pretiosum* [13-21]. 3-Amino-5-hydroxybenzoic acid (**1**, AHBA) is the starter building block of the PKS type I that is responsible for the biosynthesis of the ansamitocin backbone [22]. This PKS is a well studied megaenzyme complex and after the action of tailoring enzymes succeeding the PKS machinery ansamitocins **3**–**5** are formed [23-27].

In the present case, **1** is loaded on the starter module of the polyketide synthase (Scheme 1). The last PKS module releases and cyclizes *seco*-proansamitocin, likely by an ansamycin amide synthase (gene *asm9*) [23-27], that generates the 19-membered macrocyclic lactam proansamitocin (**2**). From here a set of tailoring enzymes transform proansamitocin into the bioactive final metabolites **3**–**5** following a predetermined logic that is only flexible in part (Scheme 1).

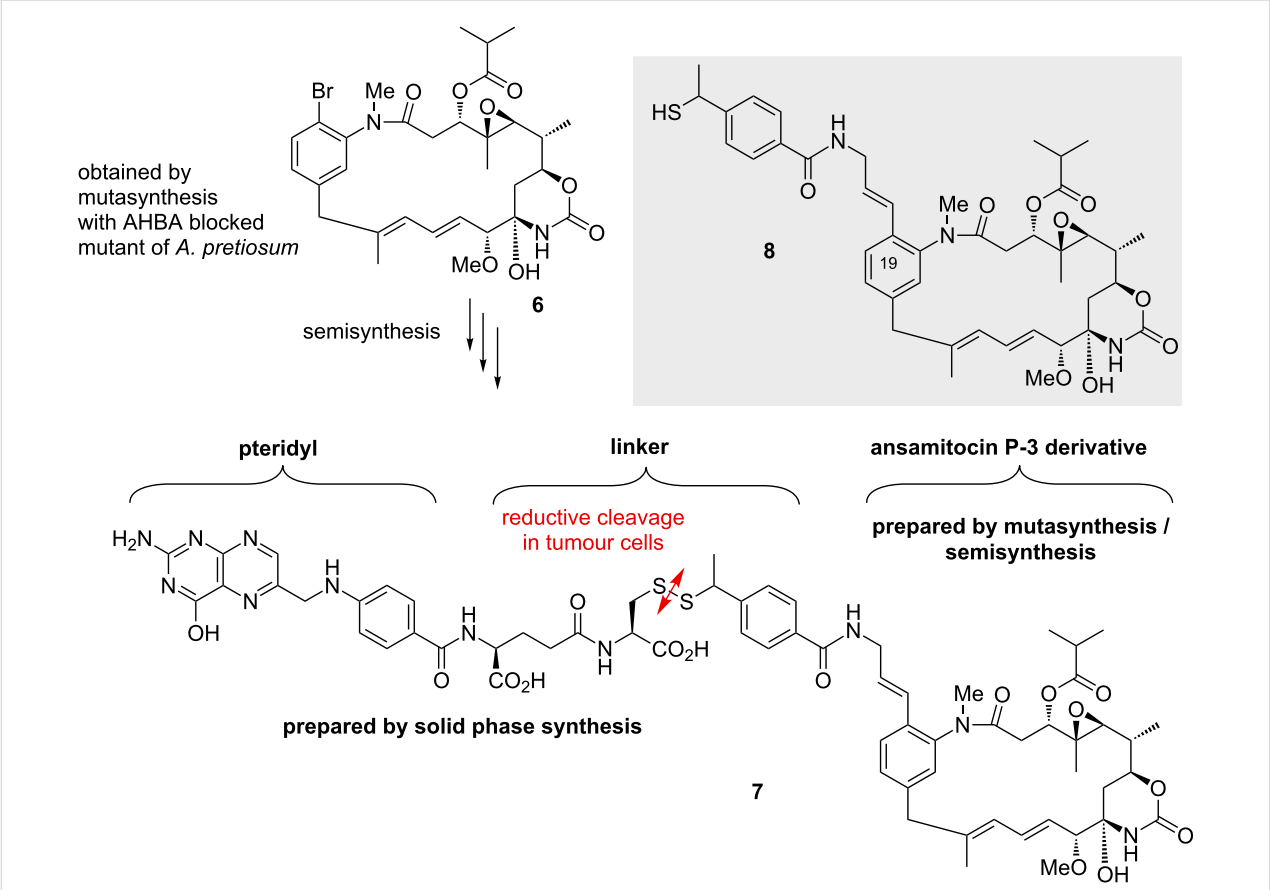
We extended these studies by combining mutasynthesis and semisynthesis and thus accessed four new tumor specific folic acid/ansamitocin conjugates [28] (Scheme 2). Bromo-ansamitocin **6** was obtained by mutasynthesis and was synthetically modified to the complex folic acid/drug conjugate **7**. The vitamin folic acid has become a promising ligand for selectively targeting the folate receptor (FR) in cancer tissues where the FR is known to be overexpressed [29,30]. Folic acid has a high affinity for the FR ($K_d = 10^{-10}$ M), even when conjugated to a cytotoxin such as maytansin. An important feature of these conjugates is the linker concept that connects the drug to the tumor-specific ligand. The linker is commonly designed in a way that a release mechanism of the cytotoxin is part of the molecular architecture of the conjugate [31].

Disulfide linkers have shown to be well suited when utilizing the reducing power between extra- and intracellular milieus which results in cleavage and liberation of the drug. Mitomycin conjugates [32] were one of the earliest examples of folate disulfide–drug conjugates and after the conjugate is internalized by endocytosis, it was demonstrated that the endosomes exert reductive cleavage.

For conjugate **7** we found that disulfide cleavage provided a thiol derivative of ansamitocin P-3 (**4**, AP-3) **8** with still strong antiproliferative activity (IC_{50} < 10 nM) for different cancer cell lines. Importantly, the intact conjugate showed strong antiproliferative activity for a FR+ cancer cell line but was inactive



Scheme 1: Short representation of ansamitocin biosynthesis.



Scheme 2: Structures of bromo-ansamitocin derivative **6**, folate-ansamitocin P-3 conjugate **7** and thiol **8**.

against a FR− cell line. Indeed, despite the substantial size of the substituent remaining at C19 after reductive cleavage, ansamitocin derivative **8** still showed sufficient antiproliferative activity. This is in line with our observation that structural changes at the aromatic ring do not affect the biological properties of the ansamitocins to a great extent [13-21].

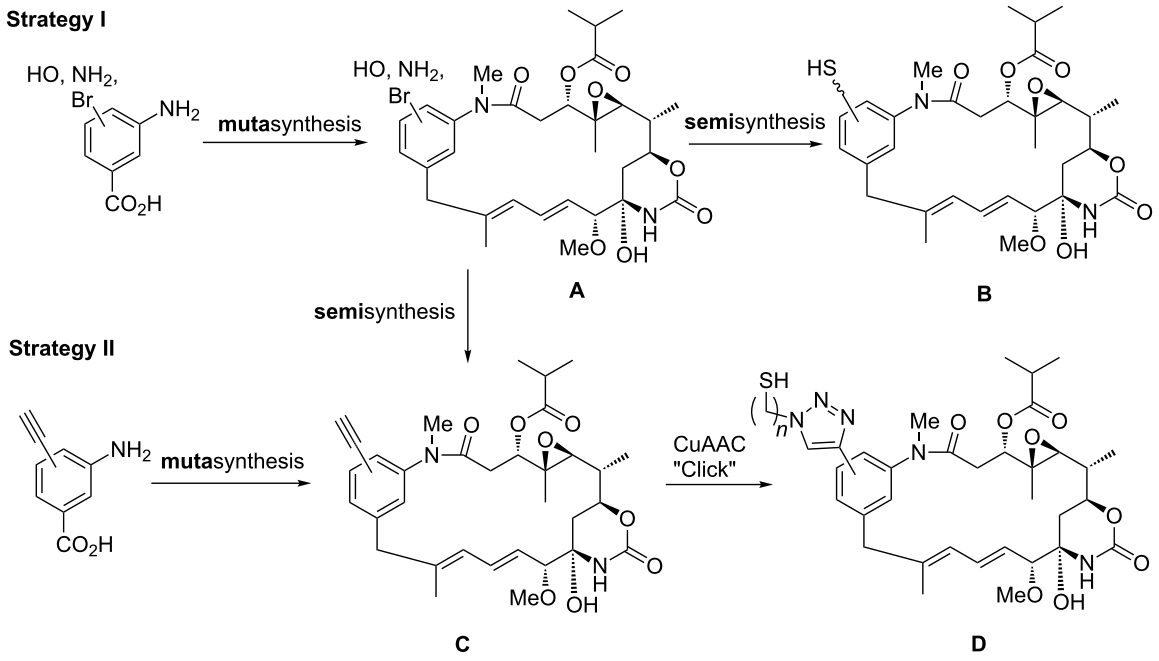
In order to broaden the opportunities of this approach for the ansamitocins, we now describe alternative accesses towards disulfide linked conjugates that are based on thiol-functionalized AP-3 derivatives. These are planned to be obtained by a combined muta- and semisynthetic strategy using different aminobenzoic acids as mutasynthons.

Results and Discussion

Mutasynthetic experiments

As potential groups for introducing linker systems bound to the aromatic moiety that contain terminal thiol groups (**B** and **D**, Scheme 3), we envisaged several activated functional groups (Hal, OH, NH_2). Activation was planned to be achieved by benzylic positioning as well as by choosing aryl bromides **A** (Scheme 3) that can be modified to the corresponding aryl alkynes **C** by cross coupling chemistry. Previously, we successfully utilized this combination of mutasynthesis and semisynthesis for 19-brominated ansamitocin derivatives [13]. Alternatively, also alkyne-, vinyl- and allyl-substituted aminobenzoic acids can serve as mutasynthons so that the corresponding alkynyl- or respectively alkenyl-substituted ansamitocin derivatives can be accessed directly after fermentation. Alkynes can be further used for Huisgen-type cycloadditions better known as “copper mediated Click-chemistry” while alkenes, especially vinyl- and allylbenzoic systems, are predestined for being utilized in cross metathesis reactions.

Therefore a series of aminobenzoic acids **9**–**20** (Figure 1) were prepared (see Supporting Information File 1). We expected them to serve our purposes, when fully processed after being fed to the mutant strain of *A. pretiosum* blocked in the biosynthesis of the PKS starter unit AHBA (**1**). We found that several of these aminobenzoic acids, namely **10**, **14** and **16**–**20** were either not loaded onto the PKS or not processed by the polyketide synthase in *A. pretiosum* and thus no formation of new ansamitocin derivatives was encountered in these cases.



Scheme 3: Strategies for introducing linker-based thiol groups to the aromatic moiety of ansamitocin P-3 for accessing tumor targeting conjugates (CuAAC; Cu-mediated azide–alkyne cycloaddition).

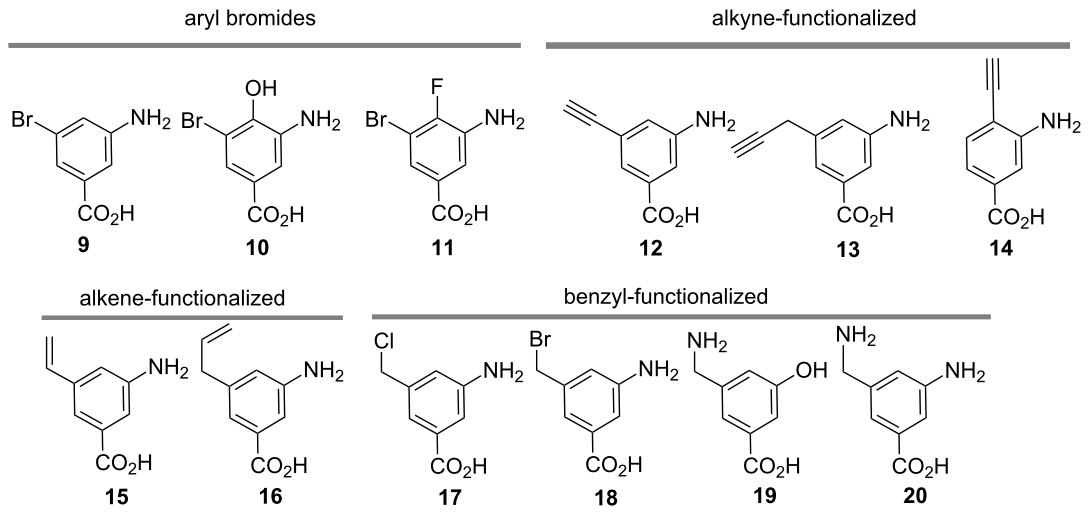
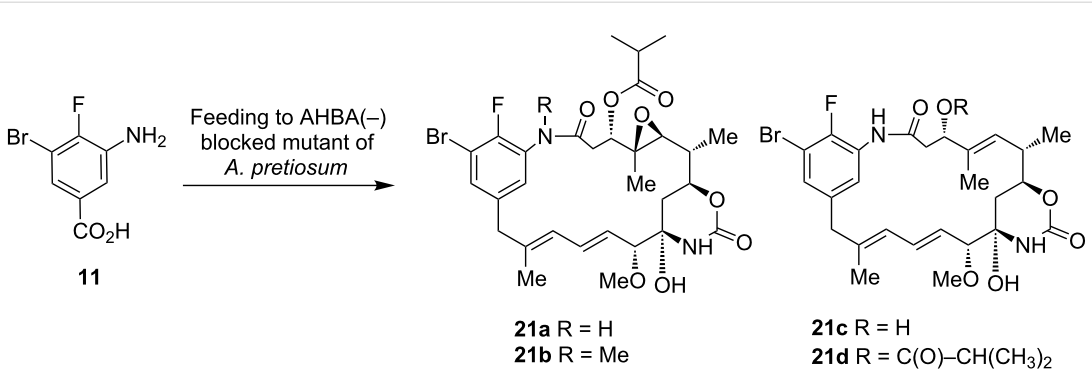


Figure 1: *m*-Aminobenzoic acid derivatives **9**–**20** tested as mutasynthons.

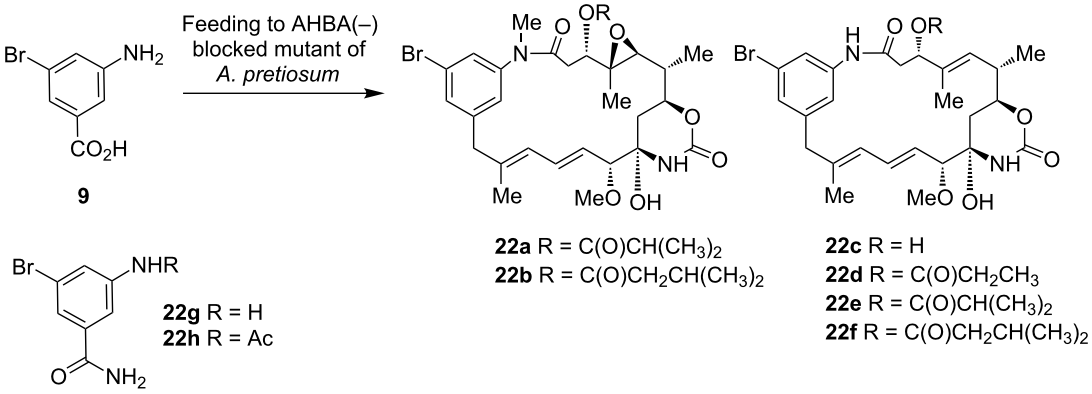
In contrast, benzoic acid **11** provided Br-F-ansamitocin derivatives **21a**–**d** after being fed to a growing culture of the mutant strain as judged by HRMS (Scheme 4). The retention times in LC and MS experiments clearly showed common patterns for ansamitocins. Additionally, the isotopic pattern provided evidence for the incorporation of the bromo functionality (see Supporting Information File 1). However, yields for each of the four ansamitocins were too small for practical scale-up.

To evaluate the sterical and electronical properties of mutasynthon **11** with respect to bioprocessing, 3-amino-5-bromobenzoic acid (**9**) was next employed in feeding experiments. It was well processed to a series of new ansamitocin derivatives **22a**–**f** (Scheme 5).

Again, all derivatives showed common fragmentation patterns and isotopic composition in the MS. Bromo-ansamitocin deriva-



Scheme 4: Mutasynthetic transformation of aminobenzoic acid **11** with AHBA(−)-mutant of *A. pretiosum*; putative structures of ansamitocin-derivatives **21a–d** as judged from HRMS analysis.

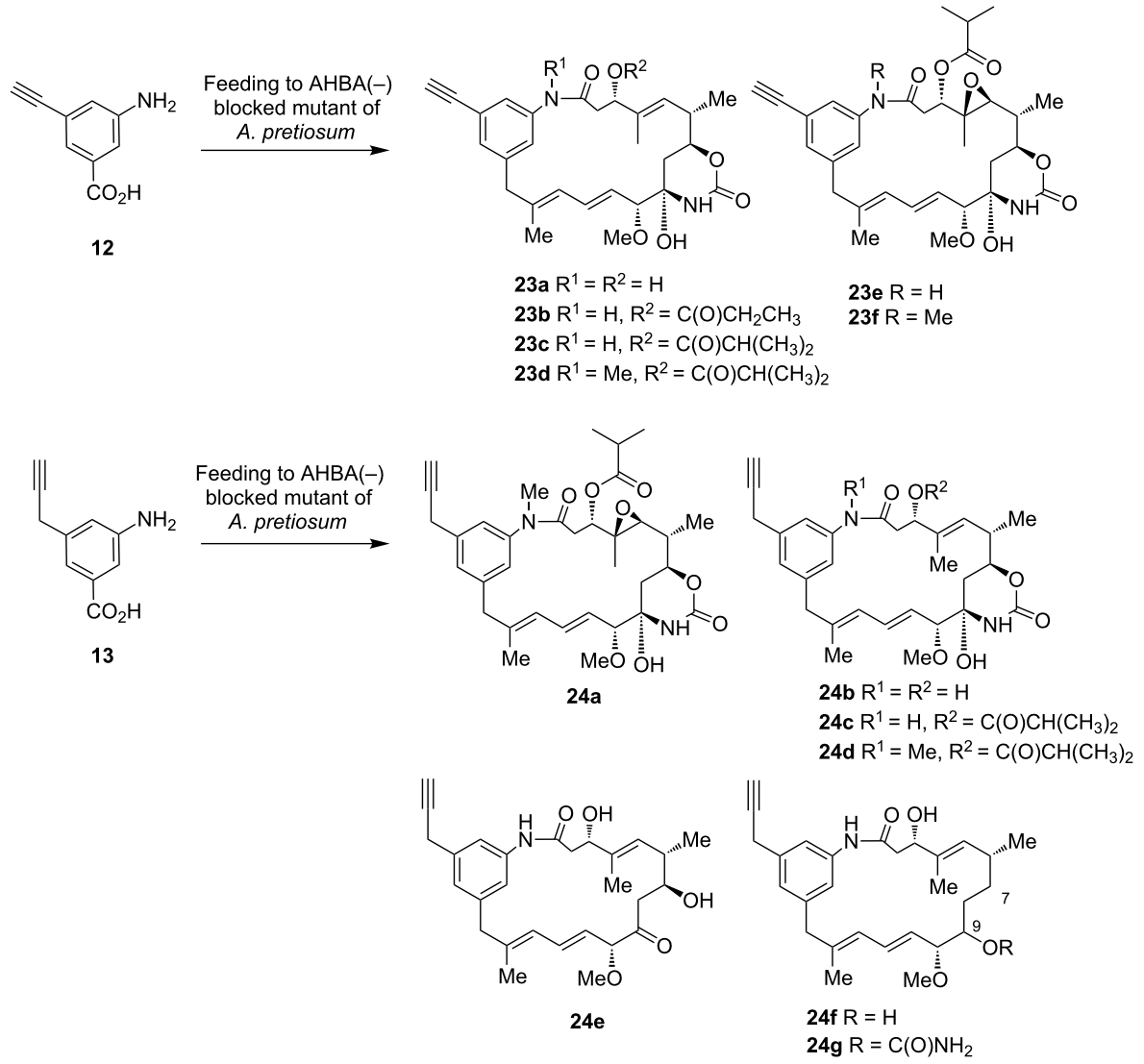


Scheme 5: Mutasynthetic transformation of aminobenzoic acid **9** with AHBA(−)-mutant of *A. pretiosum* to bromo-ansamitocins **22a–f** and detoxification products **22g** and **22h**.

tives **22a**, **22c** and **22e** were isolated after scale up to a 1000 mL culture broth. Structures, expected from HRMS analysis, were corroborated by NMR spectroscopy. Yields were determined to be in the low mg/L range or 0.01% yield based on compound **9** (see Supporting Information File 1 for further details). In addition to the formation of the bromo-ansamitocin derivatives, also the detoxification products **22g** and **22h** were isolated in 0.1% yield. The bromo-ansamitocins can be regarded to be an ideal starting material for transition metal-catalyzed coupling reactions. Due to the low product yield obtained with mutasynthon **9**, for which the steric demand of the bromo substituent can likely be made responsible, we switched the strategy towards the direct introduction of an alkyne moiety by a mutasynthetic approach. Feeding of alkynyl(amino)benzoic acid **12** to cultures of the AHBA(−)-mutant of *A. pretiosum* yielded six new alkynyl-modified ansamitocin derivatives **23a–f** in yields in the lower mg/L range (Scheme 6). Among them, the major compound **23f** was obtained in 0.34% yield based on compound **12**, furnishing enough mutasynthetic material (15 mg) for further chemical transformations (see below).

Likewise, also feeding of propargyl-substituted aminobenzoic acid **13** furnished new propargyl-modified ansamitocins **24a–g**. Besides the expected AP-3 derivative **24a**, also the formation of the corresponding *N*-desmethyl ansamitocins **24b** and **24c** and/or desepoxy-derivatives **24b–d** were encountered. Finally, also the propargyl-modified proansamitocin **24e** and two truncated derivatives **24f** and **24g** were obtained. We had observed this unprecendeted defunctionalization at C7 in proansamitocin and the possible biotransformation before for the mutasynthon 5-chloro-3-aminobenzoic acid [30]. Again, reduction of the keto group at C9 occurred; but the relative configuration of C9 also remains unknown in the present example. All derivatives, which could be isolated in preparative scale (**24b–d**, **24f** and **24g**) were formed in 0.1% scale.

In essence, the loading module of the ansamitocin PKS shows excellent flexibility towards aminobenzoic acids that bear the slim alkynyl or propargyl substituent at C5. After upscaling of the fermentation alkynyl-ansamitocins **23c**, **23f**, **24b–d** and **24f** and **24g** were isolated and the structures were corroborated by



Scheme 6: Mutasynthetic transformation of aminobenzoic acids **12** and **13** with AHBA(−)-mutant of *A. pretiosum*.

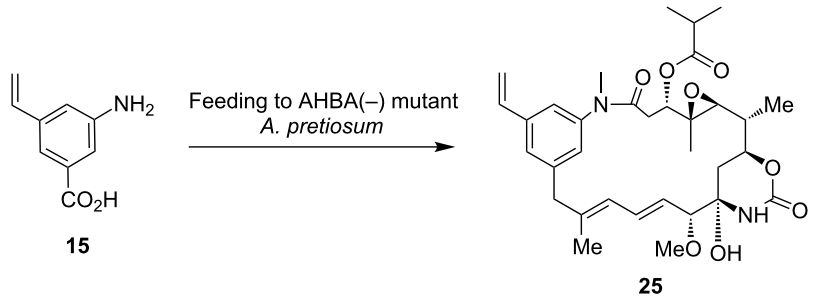
analysis of NMR and MS spectra. Derivatives **23a**, **23b**, **23d**, **23e** and **24a**, **24e** were detected only by HRMS–MS analysis of the crude extract.

Mutasynthetic experiments with vinyl(amino)benzoic acid **15** supposedly provided ansamitocin derivative **25** as judged by HRMS–MS analysis of the crude extract (Scheme 7). However, yields were too low for practical upscaling.

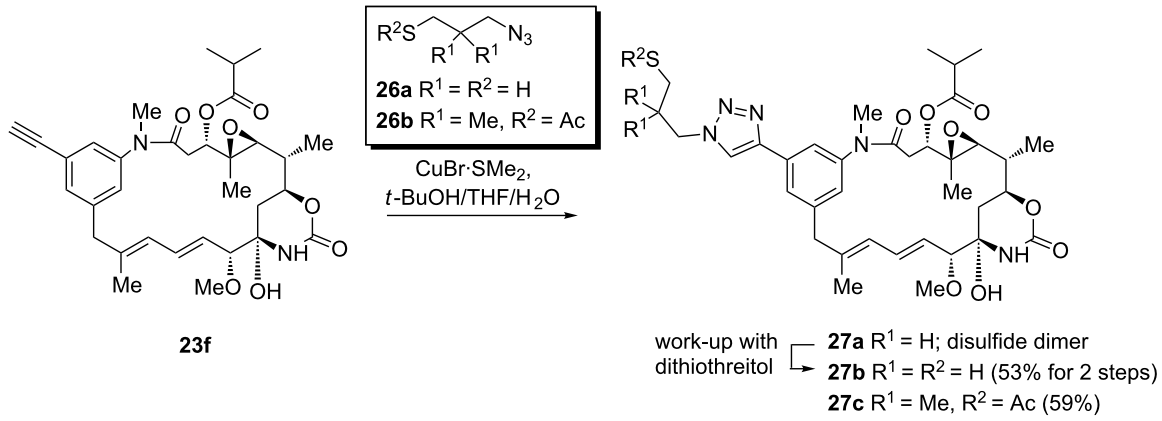
As mutasynthetic experiments with alkynyl- and propargyl-(amino)benzoic acids gave best results, we decided to test the Huisgen-type cycloaddition with alkynyl derivative **23f** bearing the biologically relevant ester side chain, the oxirane moiety and the carbamoyl group for introducing a thiol moiety that would be suited for further conjugation. Two linker elements **26a** and **26b** were prepared (see Supporting Information File 1) and coupled with ansamitocin derivative **23f** to yield the disulfide dimer **27a** and the thioacetate **27c** (Scheme 8). The former could be transformed into the thiol monomer **27b** by dithiothreitol reduction.

Biological testing

New ansamitocin derivatives **22a**, **22c**, **22e**, **23c**, **23f**, **24b–d**, **24f**, **24g**, **27b** and **27c** were subjected to in vitro biological testing with different human cell lines and one murine cell line derived from tumors or from connective tissue, respectively. The results are listed in Table 1 and are provided as values for the half-maximal inhibitory concentration of the respective ansamitocin derivatives. The most active derivatives were **23f** and **27c**. Expectedly, **24b** and **24f** are inactive, as they lack the



Scheme 7: Mutasynthetic transformation of vinyl(amino)benzoic acid **15** with AHBA(−)-mutant of *A. pretiosum*.



Scheme 8: Preparation of thiofunctionalized ansamitocin derivatives **27** by Huisgen-type copper-mediated cycloaddition.

Table 1: Antiproliferative activity IC_{50} [ng/mL] of **22a**, **22c**, **22e**, **23c**, **23f**, **24b–d**, **24f**, **24g**, **27b** and **27c** in comparison to AP-3 (**4**). Values shown are means of two determinations in parallel; human cell lines: KB-3-1 (cervix carcinoma), A-431 (epidermoid carcinoma), SK-OV-3 (ovary adenocarcinoma), PC-3 (prostate adenocarcinoma), L-929 (connective tissue of a mouse).

cell line / compound	KB-3-1	A-431	SK-OV-3	PC-3	L-929
AP-3 **4**	0.11	0.050	0.030	0.035	0.1
22a	2.1	0.31	0.34	0.26	4.1
22c	0.28	0.65	3.1	4.0	78
22e	7.5	5.1	1.8	0.80	8.7
23c	2.2	0.77	0.46	0.28	1.9
23f	0.38	0.074	0.099	0.14	0.81
24b	>10000	>10000	>10000	>10000	>10000
24c	7.8	5.5	9.0	18	220
24d	6.0	70	8.0	95	580
24f	1800	2200	2500	3500	>10000
24g	50	0.85	70	3.8	100
27b	2200	>10000	2800	>10000	>10000
27c	0.09	0.25	0.09	0.28	0.33

ester side chain at C3, the key pharmacophore of the maytansinoids. All other derivatives show strong to moderate antiproliferative activity, irrespective whether the lack of the *N*-methyl group, and or the oxirane groups or not. This is in line with the view obtained from structure–activity relationship studies that these tailoring modifications only modulate the biological

activity of the maytansinoids. In the present study, the human cancer cell lines were more sensitive than the mouse fibroblasts. Some derivatives also seem to exert a specificity towards certain cell lines, e.g. A-431 showed particular sensitivity for **24g**.

The high antiproliferative activity of the "click" product **27c** is remarkable as it demonstrates that substantial structural changes at C20 of the ansamitocins are tolerated and thus alkyne substituents open up diverse opportunities to diversify that position as reported including the introduction of tumor targeting ligands. Noteworthy **27b** is inactive which we ascribe to the fact that it may have dimerized back to **27a**.

Conclusion

The combination of mutasynthesis and semisynthesis has great potential for the production of more selective ansamitocin derivatives. In this work we pursued different options to prepare ansamitocin derivatives by mutasynthesis that are set for introducing linker systems to the aromatic moiety suited to create conjugates composed of ansamitocin and tumor-specific ligands.

Supporting Information

The supporting information provide the synthesis of building blocks, mutasynthetic experiments as well as purification protocols after fermentations, a short description of the cell proliferation assay, analytical descriptions of new metabolites and copies of ^{1}H and ^{13}C NMR spectra.

Supporting Information File 1

Additional experimental details and NMR spectra.
[http://www.beilstein-journals.org/bjoc/content/supplementary/1860-5397-10-49-S1.pdf]

Acknowledgements

This work was supported by the Deutsche Forschungsgemeinschaft (grant Ki-397, 13-1) and the Fonds der Chemischen Industrie.

References

1. Cragg, G. M.; Grothaus, P. G.; Newman, D. J. *Chem. Rev.* **2009,** *109,* 3012–3043. doi:10.1021/cr900019j
2. Newman, D. J.; Cragg, G. M. *J. Nat. Prod.* **2007,** *70,* 461–477. doi:10.1021/np068054v
3. von Nussbaum, F.; Brands, M.; Hinzen, B.; Weigand, S.; Häbich, D. *Angew. Chem.* **2006,** *118,* 5194–5254. doi:10.1002/ange.200600350
Angew. Chem., Int. Ed. **2006,** *45,* 5072–5129. doi:10.1002/anie.200600350
4. Kirschning, A.; Hahn, F. *Angew. Chem.* **2012,** *124,* 4086–4096. doi:10.1002/ange.201107386
Angew. Chem., Int. Ed. **2012,** *51,* 4012–4022. doi:10.1002/anie.201107386
5. Weist, S.; Süssmuth, R. D. *Appl. Microbiol. Biotechnol.* **2005,** *68,* 141–150. doi:10.1007/s00253-005-1891-8
6. Kirschning, A.; Taft, F.; Knobloch, T. *Org. Biomol. Chem.* **2007,** *5,* 3245–3259. doi:10.1039/b709549j
7. Kennedy, J. *Nat. Prod. Rep.* **2008,** *25,* 25–34. doi:10.1039/B707678A
8. Cassady, J. M.; Chan, K. K.; Floss, H. G.; Leistner, E. *Chem. Pharm. Bull.* **2004,** *52,* 1–26. doi:10.1248/cpb.52.1
9. Kirschning, A.; Harmrolfs, K.; Knobloch, T. *C. R. Chim.* **2008,** *11,* 1523–1543. doi:10.1016/j.crci.2008.02.006
10. Floss, H. G.; Yu, T.-W.; Arakawa, K. *J. Antibiot.* **2011,** *64,* 35–44. doi:10.1038/ja.2010.139
11. Funayama, S.; Cordell, G. A. In *Studies in Natural Product Chemistry;* Rahman, A.-U., Ed.; Elsevier Science B. V.: Amsterdam, 2000; Vol. 23, pp 51–106. doi:10.1016/S1572-5995(00)80127-1
12. Hamel, E. *Pharmacol. Ther.* **1992,** *55,* 31–51. doi:10.1016/0163-7258(92)90028-X
13. Taft, F.; Brünjes, M.; Floss, H. G.; Czempinski, N.; Grond, S.; Sasse, F.; Kirschning, A. *ChemBioChem* **2008,** *9,* 1057–1060. doi:10.1002/cbic.200700742
14. Kubota, T.; Brünjes, M.; Frenzel, T.; Xu, J.; Kirschning, A.; Floss, H. G. *ChemBioChem* **2006,** *7,* 1221–1225. doi:10.1002/cbic.200500506
15. Taft, F.; Brünjes, M.; Knobloch, T.; Floss, H. G.; Kirschning, A. *J. Am. Chem. Soc.* **2009,** *131,* 3812–3813. doi:10.1021/ja8088923
16. Knobloch, T.; Harmrolfs, K.; Taft, F.; Thomaszewski, B.; Sasse, F.; Kirschning, A. *ChemBioChem* **2011,** *12,* 540–547. doi:10.1002/cbic.201000608
17. Eichner, S.; Knobloch, T.; Floss, H. G.; Fohrer, J.; Harmrolfs, K.; Hermane, J.; Schulz, A.; Sasse, F.; Spiteller, P.; Taft, F.; Kirschning, A. *Angew. Chem.* **2012,** *124,* 776–781. doi:10.1002/ange.201106249
Angew. Chem., Int. Ed. **2012,** *51,* 752–757. doi:10.1002/anie.201106249
18. Meyer, A.; Brünjes, M.; Taft, F.; Frenzel, T.; Sasse, F.; Kirschning, A. *Org. Lett.* **2007,** *9,* 1489–1492. doi:10.1021/ol0702270
19. Frenzel, T.; Brünjes, M.; Quitschalle, M.; Kirschning, A. *Org. Lett.* **2006,** *8,* 135–138. doi:10.1021/ol052588q
20. Harmrolfs, K.; Brünjes, M.; Dräger, G.; Floss, H. G.; Sasse, F.; Taft, F.; Kirschning, A. *ChemBioChem* **2010,** *11,* 2517–2520. doi:10.1002/cbic.201000422
21. Knobloch, T.; Dräger, G.; Collisi, W.; Sasse, F.; Kirschning, A. *Beilstein J. Org. Chem.* **2012,** *8,* 861–869. doi:10.3762/bjoc.8.96
22. Walsh, C. T.; Haynes, S. W.; Ames, B. D. *Nat. Prod. Rep.* **2012,** *29,* 37–59. doi:10.1039/c1np00072a
23. Spiteller, P.; Bai, L.; Shang, G.; Carroll, B. J.; Yu, T.-W.; Floss, H. G. *J. Am. Chem. Soc.* **2003,** *125,* 14236–14237. doi:10.1021/ja038166y
24. Yu, T.-W.; Bai, L.; Clade, D.; Hoffmann, D.; Toelzer, S.; Trinh, K. Q.; Xu, J.; Moss, S. J.; Leistner, E.; Floss, H. G. *Proc. Natl. Acad. Sci. U. S. A.* **2002,** *99,* 7968–7973. doi:10.1073/pnas.092697199
25. Arakawa, K.; Müller, R.; Mahmud, T.; Yu, T.-W.; Floss, H. G. *J. Am. Chem. Soc.* **2002,** *124,* 10644–10645. doi:10.1021/ja0206339
26. Yu, T.-W.; Müller, R.; Müller, M.; Zhang, X.; Dräger, G.; Kim, C.-G.; Leistner, E.; Floss, H. G. *J. Biol. Chem.* **2001,** *276,* 12546–12555. doi:10.1074/jbc.M009667200
27. Moss, S. J.; Bai, L.; Toelzer, S.; Caroll, B. J.; Mahmud, T.; Yu, T.-W.; Floss, H. G. *J. Am. Chem. Soc.* **2002,** *124,* 6544–6545. doi:10.1021/ja020214b

28. Taft, F.; Harmrolfs, K.; Nickeleit, I.; Heutling, A.; Kiene, M.; Malek, N.; Sasse, F.; Kirschning, A. *Chem.–Eur. J.* **2012,** *18,* 880–886. doi:10.1002/chem.201101640
29. D'Alincourt Salazar, M.; Ratnam, M. *Cancer Metastasis Rev.* **2007,** *26,* 141–152. doi:10.1007/s10555-007-9048-0
30. Low, P. S.; Antony, A. C. *Adv. Drug Delivery Rev.* **2004,** *56,* 1055–1058. doi:10.1016/j.addr.2004.02.003
31. Lee, R. J.; Wang, S.; Low, P. S. *Biochim. Biophys. Acta* **1996,** *1312,* 237–242. doi:10.1016/0167-4889(96)00041-9
32. Reddy, J. A.; Westrick, E.; Vlahov, I.; Howard, S. J.; Santhapuram, H. K.; Leamon, C. P. *Cancer Chemother. Pharmacol.* **2006,** *58,* 229–236. doi:10.1007/s00280-005-0151-z

License and Terms

This is an Open Access article under the terms of the Creative Commons Attribution License (http://creativecommons.org/licenses/by/2.0), which permits unrestricted use, distribution, and reproduction in any medium, provided the original work is properly cited.

The license is subject to the *Beilstein Journal of Organic Chemistry* terms and conditions: (http://www.beilstein-journals.org/bjoc)

The definitive version of this article is the electronic one which can be found at: doi:10.3762/bjoc.10.49

Beilstein Journal of Organic Chemistry

New sesquiterpene hydroquinones from the Caribbean sponge *Aka coralliphagum*

Qun Göthel and Matthias Köck*

Full Research Paper

Open Access

Address:
Alfred-Wegener-Institut, Helmholtz-Zentrum für Polar- und Meeresforschung, Am Handelshafen 12, 27570 Bremerhaven, Germany

Email:
Matthias Köck* - mkoeck@awi.de

* Corresponding author

Keywords:
Aka coralliphagum; bioassay; natural products; NMR; sesquiterpene hydroquinone; structure elucidation

Beilstein J. Org. Chem. **2014,** *10,* 613–621.
doi:10.3762/bjoc.10.52

Received: 06 December 2013
Accepted: 23 December 2013
Published: 06 March 2014

This article is part of the Thematic Series "Natural products in synthesis and biosynthesis".

Guest Editor: J. S. Dickschat

© 2014 Göthel and Köck; licensee Beilstein-Institut.
License and terms: see end of document.

Abstract

Four new sulfated sesquiterpene hydroquinones siphonodictyals E1–E4 (**1**–**4**) and cyclosiphonodictyol A (**5**) were isolated from a sample of the Caribbean sponge *Aka coralliphagum* collected off the coast of San Salvador in the Bahamas. The structures of the new compounds were elucidated on the basis of mass spectrometric and NMR spectroscopic analysis. Compounds **1**–**4** are derivatives of siphonodictyal E (**9**). Siphonodictyal E4 (**4**) exhibited mild antiproliferation activity against L929 mouse fibroblast, KB-31 epidermoid carcinoma, and MCF-7 breast cancer cell lines, while siphondictyal E3 (**3**) and cyclosiphonodictyol A (**5**) showed moderate activity against Gram-positive bacteria.

Introduction

Aka coralliphagum (*Siphonodictyon coralliphagum*) is known to have four distinct morphological forms: forma *typica*, f. *tubulosa*, f. *obruta*, and f. *incrustans* [1]. This sponge has the ability to burrow into live coral heads, leaving only the oscular chimney protruding (*typica*) or the flat crusts (*incrustans*) exposed. The oscular chimneys or the flat crusts are encircled by a so-called "dead zone" which protects the sponge from overgrowth [2]. Sullivan and Faulkner have proposed that the coral polyps are killed by the viscous mucus containing the toxic secondary metabolites which are produced by the sponge tissue [3]. This ecological observation inspired the chemical investigation of this sponge by different research groups. Thus many secondary metabolites have been reported, such as the sesquiterpene phenolic aldehydes, siphonodictyals B, C, D, E, the monosulfated siphonodictyols G and H, the disulfated siphonodictyal B3, and siphonodictyoic acid [2,4,5]. The sponge under our investigation is of the growth form *incrustans*, which was collected off the coast of San Salvador in the Bahamas. Fractionation of the aqueous *n*-BuOH extract yielded the new compounds siphonodictyals E1–E4 (**1**–**4**) and

cyclosiphonodictyol A (**5**). In this article, we describe the isolation, structural elucidation, and bioactivity of compounds **1**–**5** from the *Aka* growth form *incrustans*, as well as discuss the biosynthetic pathway of related compounds.

Results and Discussion

The aqueous *n*-BuOH extract from *Aka coralliphagum* was subjected to solvent partitioning, followed by gel chromatography and reversed phase (C18) HPLC to yield siphonodictyals E1–E4 (**1**–**4**) and cyclosiphonodictyol A (**5**) (Figure 1). The structure elucidation was based on 1D and 2D NMR as well as HRMS-ESI(−) experiments. The ^{1}H and ^{13}C NMR chemical shifts for the five new compounds are given in Table 1.

Siphonodictyal E1 (**1**) was identified by NMR data and its accurate mass of 598.1338 [M + Na − 2H]$^{-}$ which indicated the molecular formula $C_{24}H_{35}NO_{11}S_2$. Comparison of the NMR data of **1** and siphonodictyal E (**9**, Figure 2) [2] revealed the presence of the identical sesquiterpene acyclic chain with one of the terminal methyl groups oxidized to a carboxylic acid. Moreover, the diagnostic values for C-14 (δ 15.7) and C-15 (δ 15.9) confirmed a common 6*E*, 10*E* double-bond geometry [6,7]. The NMR spectral data also suggested a similar aromatic ring system as in siphonodictyal E (**9**). Moreover, the ^{1}H,^{1}H-COSY correlation between the two methylene groups CH_2-23 and CH_2-24 as well as the ^{1}H,^{13}C-HMBC correlations from H-22 (δ 8.67) to C-18 (δ 144.0), C-19 (δ 156.4), C-20 (δ 110.9), C-21 (δ 141.8), and C-23 (δ 51.2) further indicated that an iminoethanesulfonic acid is connected to the aromatic ring system in **1** (Figure 3), as in siphonodictyal B1 (**6**, Figure 2) [5].

Examination of the NMR data for siphonodictyal E2 (**2**) revealed a high degree of similarity with the data reported for siphonodictyal E (**9**). However, the molecular ion peak of compound **2** was shown at *m*/*z* 469.1534 ([M − H]$^{-}$ $C_{22}H_{29}O_9S$), which has 80 amu more than that of **9**, indicating an additional sulfate ester group in compound **2**. The ^{1}H,^{13}C-HMBC correlations from 18-OH to C-17 (δ 122.8), C-18 (δ 141.8), and C-19 (δ 147.8) as well as from 19-OH to C-18 (δ 141.8), C-19 (δ 147.8), and C-20 (δ 115.5) indicated that C-18 and C-19 are

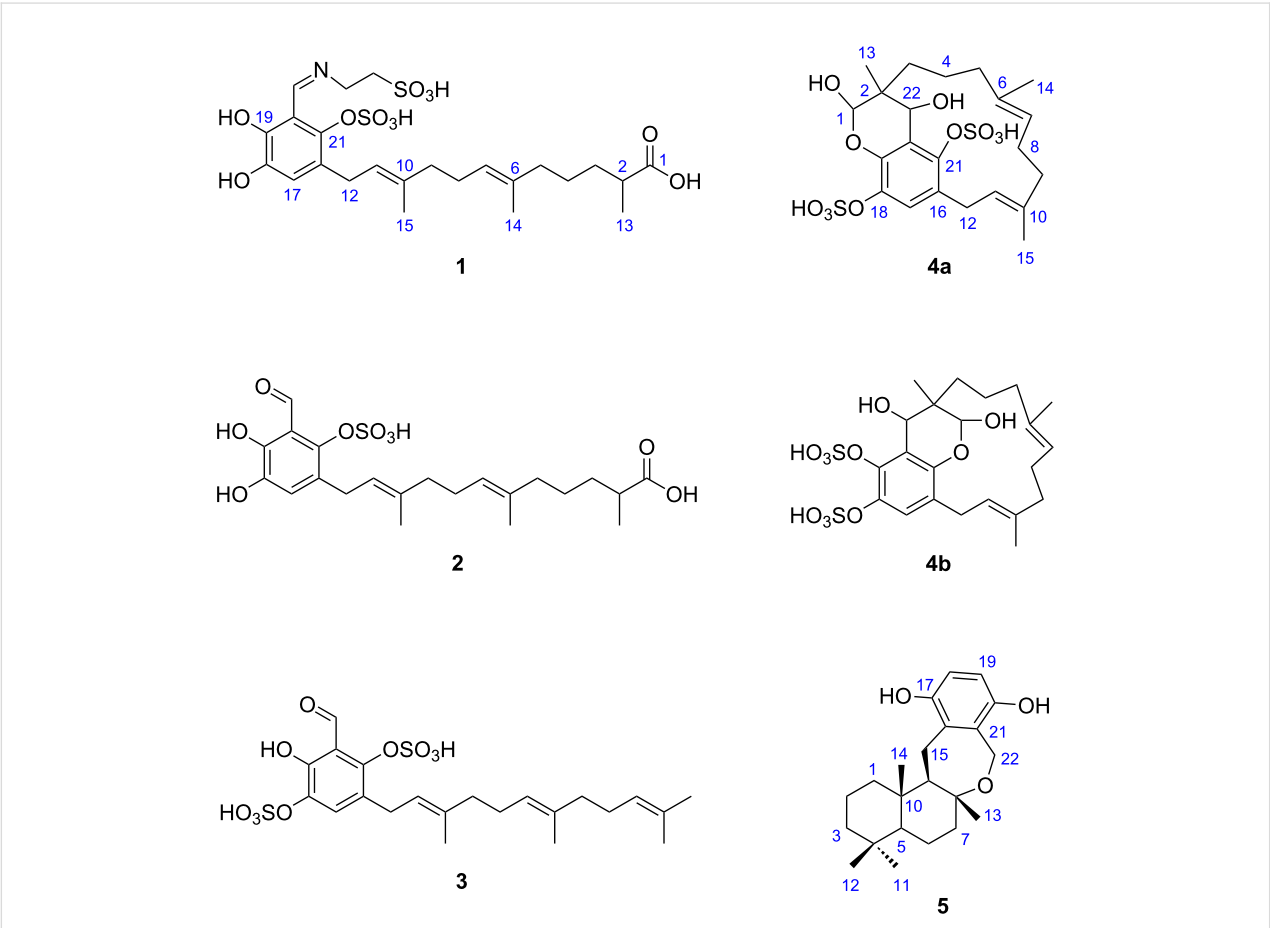


Figure 1: Structures of the new compounds siphonodictyals E1–E4 (**1**–**4**) and cyclosiphonodictyol A (**5**) isolated from the sponge *Aka coralliphagum*. Since the structure of siphonodictyal E4 (**4**) could not be unambiguously assigned, the two possible constitutional isomers (**4a** and **4b**) are shown.

Table 1: NMR data of compounds **1**–**5** (δ_C 150 MHz, δ_H 600 MHz in DMSO-d_6).[a]

No.	**1**		**2**		**3**		**4**		**5**	
	δ_C	δ_H	δ_C	δ_H	δ_C	δ_H	δ_C	δ_H	δ_C	δ_H
1	177.8	–	177.5	–	25.5	1.62 (s)	96.2	5.42 (s)	39.4	0.76 (m)
										1.91 (m)
2	38.7	2.28 (m)	38.6	2.28 (m)	130.6	–	37.3	–	18.2	1.38 (m)
										1.60 (m)
3	32.9	1.25 (m)	32.8	1.25 (m)	124.2	5.05 (t, 7.1)	31.4	1.03 (m)	41.6	1.08 (dt, 4.0, 13.5)
		1.47 (m)		1.47 (m)				1.13 (m)		1.33 (m)
4	24.9	1.32 (m)	24.9	1.31 (m)	26.3	2.00 (m)	22.1	0.56 (m)	33.1	–
								1.11 (m)		
5	38.9	1.91 (m)	39.4	1.91 (t, 6.9)	39.3	1.92 (m)	39.3	1.28 (m)	55.4	0.83 (m)
								1.75 (m)		
6	134.4	–	134.4	–	134.4	–	134.9	–	19.8	1.58 (m)
										1.60 (m)
7	124.0	5.09 (t, 6.5)	124.0	5.09 (t, 6.8)	124.0	5.09 (t, 7.1)	121.7	4.52 (t, 5.9)	40.1	1.43 (m)
										1.60 (m)
8	26.2	2.06 (m)	26.2	2.06 (m)	26.2	2.06 (m)	23.8	1.89 (m)	78.5	–
								2.01 (m)		
9	40.1	1.98 (m)	39.8	1.99 (t, 7.2)	40.1	1.97 (m)	39.0	1.92 (m)	58.1	1.32 (m)
10	134.5	–	135.4	–	135.5	–	131.9	–	38.2	–
11	123.7	5.19 (t, 7.2)	122.9	5.21 (t, 7.2)	122.6	5.21 (t, 7.0)	125.7	5.10 (t, 7.9)	33.1	0.83 (s)
12	27.2	3.25 (d, 3.4)	26.9	3.33[b,c]	27.1	3.35[b,c]	29.8	2.58 (dd, 6.8, 12.6)	21.2	0.78 (s)
								3.99 (dd, 9.6, 12.4)		
13	17.0	1.01 (d, 6.6)	17.0	1.01 (d, 6.9)	17.6	1.54 (s)	19.9	1.04 (s)	21.6	1.31 (s)
14	15.7	1.53 (s)	15.6	1.53 (s)	16.0	1.55 (s)	17.2	1.36 (s)	15.3	0.79 (s)
15	15.9	1.65 (s)	15.9	1.66 (s)	15.8	1.66 (s)	15.1	1.62 (s)	20.8	2.33 (dd, 9.6, 15.5)
										3.06 (d, 15.5)
16	120.5	–	125.9	–	125.5	–	126.5	–	129.9	–
17	117.7	6.50 (s)	122.8	6.84 (s)	129.5	7.48 (s)	120.8	7.19 (s)	146.4	–
18	144.0	–	141.8	–	137.7	–	137.2	–	113.7	6.45 (d, 8.6)
19	156.4[c]	–	147.8	–	151.3	–	143.2	–	112.4	6.38 (d, 8.6)
20	110.9[c]	–	115.5	–	115.9	–	120.3	–	146.5	–
21	141.8[c]	–	144.5	–	148.2	–	142.9	–	127.7	–
22	164.6	8.67 (s)	197.2	10.10 (s)	196.6	10.11 (s)	65.3	4.44 (s)	56.7	4.50 (d, 15.0)
										4.64 (d, 15.0)
23	51.2[d]	3.83 (t, 6.5)								
24	51.2[d]	2.82 (t, 6.2)								
1-OH								7.07 (bs)		
18-OH				9.09						
19-OH				11.37						
22-OH								5.09 (bs)		

[a]δ are given in ppm (reference: DMSO-d_6, 2.50 ppm, 39.52 ppm), coupling constants are given in Hz; assignments were confirmed by 2D NMR experiments (COSY, HSQC, HMBC). [b]Overlap with water peak. [c]Chemical shifts were obtained from HMBC spectra. [d]Overlap with each other.

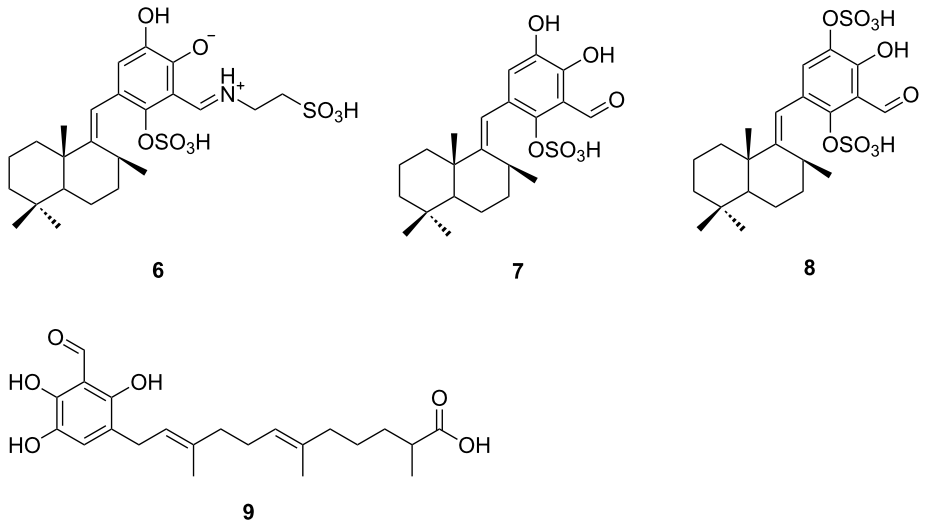


Figure 2: Structures of the related known compounds siphonodictyal B1 (**6**), siphonodictyal B2 (**7**), siphonodictyal B3 (**8**), and siphonodictyal E (**9**) from the sponge *Aka coralliphagum*.

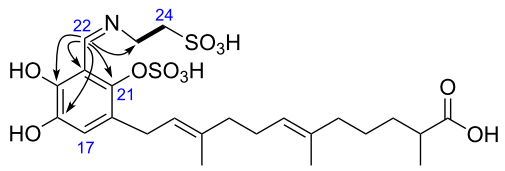


Figure 3: Selected ^{1}H,^{13}C-HMBC correlations (H → C) and ^{1}H,^{1}H-COSY correlation (bold line) observed for siphonodictyal E1 (**1**).

Table 2: ^{13}C substituent effects Δδ in monosubstituted benzenes relative to the benzene carbon at 128.5 ppm [9].

Functional group	*i* [ppm]	*o* [ppm]	*m* [ppm]	*p* [ppm]
CHO	8.4	1.2	0.5	5.7
OH	26.9	−12.8	1.4	−7.4
Allyl	15.3	0	0.2	−2.4
OSO_3H	22.0	−7.0	1.5	−2.0

connected to hydroxy groups rather than sulfate ester groups (Figure 4). Thus, the sulfate ester group should be at position C-21. Furthermore, the ^{13}C NMR chemical shifts of the three constitutional isomers **2**-I to **2**-III were calculated using an increment system (Table 2) with additional values for sulfate esters published by Ragan [8]. These calculations (Table 3) allowed us to confirm the position of the sulfate moiety (**2**-I, Figure 5). The comparison of the NMR data of **2** and siphonodictyal B2 (**7**, Figure 2) [5] further confirmed the identity of the aromatic moiety of both compounds.

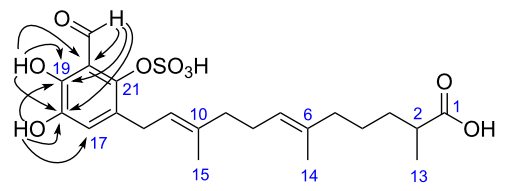


Figure 4: Selected ^{1}H,^{13}C-HMBC correlations (H → C) observed for siphonodictyal E2 (**2**).

The HRMS-ESI(−) spectrum for siphonodictyal E3 (**3**) displayed the pseudomolecular ion peak $[M + Na - 2H]^-$ at *m*/*z* 539.1046, indicating the molecular formula $C_{22}H_{30}O_{10}S_2$. The ^{13}C NMR spectrum contained six olefinic signals in addition to the aromatic signals, and the ^{1}H NMR spectrum contained four olefinic methyl signals at δ 1.62 (s), δ 1.54 (s), δ 1.55 (s), and δ 1.66 (s), which suggested a sesquiterpene side chain containing three trisubstituted olefinic bonds. The two sulfate ester groups were assigned to attach to C-18 and C-21 after comparison of the NMR data of the aromatic moieties of **3** with those of siphonodictyal B3 (**8**, Figure 2). Nevertheless, the results of the increment calculations using the values for sulfate esters from Ragan [8] clearly favours the isomer **3**-I (Figure 5), which further supports our proposed structure.

The HRMS-ESI(−) spectrum for siphonodictyal E4 (**4**) showed the pseudomolecular ion peak $[M + Na - 2H]^-$ at *m*/*z* 555.0954, confirmed its molecular formula as $C_{22}H_{30}O_{11}S_2$, corresponding to eight double bond equivalents. The sesquiterpenoid moiety of the molecule contained two trisubstituted olefinic

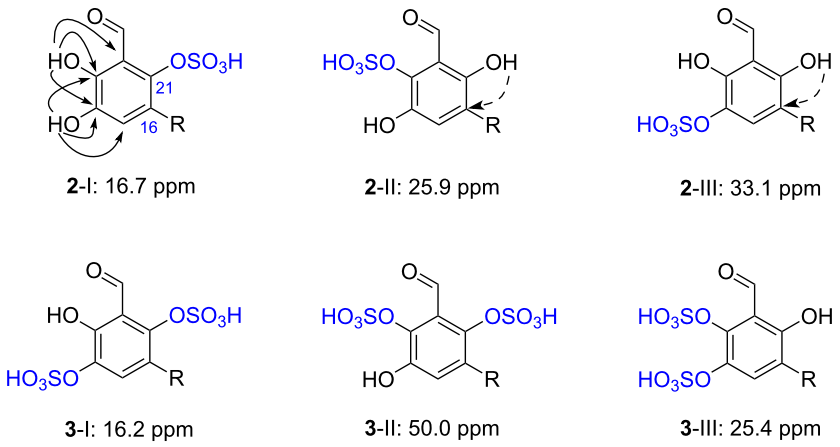


Figure 5: Possible constitutions for the aromatic moieties of siphonodictyals E2 (**2**) and E3 (**3**) (sum over all $\Delta\delta(^{13}C)$): **2**-I 16.7 ppm, **2**-II 25.9 ppm, **2**-III 33.1 ppm, **3**-I 16.2 ppm, **3**-II 50.0 ppm, **3**-III 25.4 ppm); plain arrows in **2**-I showed the HMBC correlations from 18-OH and 19-OH to the aromatic carbons; dashed arrows in **2**-II and **2**-III indicate HMBC correlations which would be expected.

Table 3: Results of the increment calculations for the aromatic moiety of the three constitutional proposals of siphonodictyal E2 (**2**) and siphonodictyal E3 (**3**).

Carbon No.	Siphonodictyal E2 (**2**)	**2**-I	**2**-II	**2**-III
16	125.9	131.3 (5.4)	130.9 (5.0)	125.6 (0.3)
17	122.8	124.3 (1.5)	124.3 (1.5)	130.0 (7.2)
18	141.8	141.3 (0.5)	141.7 (0.1)	131.0 (10.8)
19	147.8	142.9 (4.9)	137.9 (9.9)	148.6 (0.8)
20	115.5	118.7 (3.2)	118.7 (3.2)	113.0 (2.5)
21	144.5	145.7 (1.2)	150.7 (6.2)	156.0 (11.5)
Σ [ppm]		16.7	25.9	33.1
Carbon No.	Siphonodictyal E3 (**3**)	**3**-I	**3**-II	**3**-III
16	125.5	131.4 (5.9)	136.7 (11.2)	131.0 (5.5)
17	129.5	130.1 (0.6)	124.4 (5.1)	130.1 (0.6)
18	137.7	136.4 (1.3)	147.1 (9.4)	136.8 (0.9)
19	151.3	148.7 (2.6)	138.0 (13.3)	143.7 (7.6)
20	115.9	118.8 (2.9)	124.5 (8.6)	118.8 (2.9)
21	148.2	151.1 (2.9)	145.8 (2.4)	156.1 (7.9)
Σ [ppm]		16.2	50.0	25.4

bonds (δ 121.7, δ 125.7, δ 131.9, δ 134.9) and a hemiacetal carbon (δ 96.2) at one terminus which differed from the acyclic side chain in **1** and **2**. The remaining six carbon signals in the downfield region of the ^{13}C NMR spectrum belonged to the tetrasubstituted aromatic ring system. In contrast to **1** and **2**, compound **4** contained an oxymethine group (CH-22, δ_C 65.3, δ_H 4.44) which connected the sesquiterpene chain with the aromatic ring. This is supported by the six/seven HMBC correlations from H-22 to C-1 (δ 96.2), C-2 (δ 37.3), C-3 (δ 31.4), C-13 (δ 19.9), C-19 (δ 143.2) / C-21 (δ 142.9), and C-20 (δ 120.3). The HMBC correlations from H-12 (δ 2.58, 3.99) to C-17 (δ 120.8) and C-21 and from H-17 (δ 7.19) to C-18 (δ 137.2) confirmed the position of the unsubstituted CH-17 as shown in the proposed structure (Figure 6). Since the very weak HMBC correlation from H-1 to C-19 or C-21 could not be unambiguously assigned, the constitutional isomers with respect to the position of the oxygen bridge **4a** and **4b** (Figure 1) are in accordance with the NMR data. This is the first compound

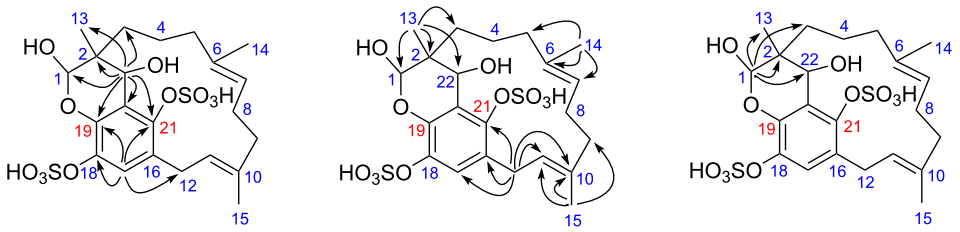


Figure 6: Selected $^{1}H,^{13}C$-HMBC correlations (H → C) observed for siphonodictyal E4 (**4a**).

isolated from this sponge which contains a macrocycle. Moreover, this macrocycle could probably be formed by an aldol addition from a precursor with an acyclic sesquiterpene side chain (Figure 7). The aromatic ring system of proposed precursor **3**-ox in Figure 7 also appeared in the known compound siphonodictyal B3 (**8**) [5] isolated from the same sponge source as well as the newly identified compound **3**. There are no similar compounds known which contained the aromatic ring system with two adjacent sulfate ester groups. Therefore, we assumed that the constitutional isomer **4a** is more likely. The δ values of methyl carbons C-14 and C-15 below 20 ppm indicated the *E* configuration of the double bonds C-6/C-7 and C-10/C-11 of the isoprenoid chain [6,7]. Additionally, in the NOESY spectrum we could observe a weak correlation between H-22 (δ 4.44) and H-3 (δ 1.03) as well as between H-22 (δ 4.44) and H-13 (δ 1.04). Because of the overlapping of the proton signals of H-3 and H-13, this assignment is not unambiguous. Due to the flexibility of the macrocycle of **4** it was not possible to analyse the conformation of the pyrane. Therefore, the configurations at the centers C-1, C-2, and C-22 could not be assigned. Further investigations are hindered by the fact that compound **4** easily degrades.

The HRMS-ESI(−) spectrum for cyclosiphonodictyol A (**5**) showed the pseudomolecular ion peak $[M + Na - 2H]^-$ at *m*/*z* 343.2292, confirmed its molecular formula as $C_{22}H_{32}O_3$. The ^{13}C NMR spectrum displayed six signals in the area of aromatic carbon atoms and 16 signals in the aliphatic region. The $^{1}H,^{13}C$-HSQC spectrum indicated four methyl and seven methylene groups. Two of these methylene groups connected directly to the aromatic ring system indicated by the $^{1}H,^{13}C$-HMBC correlations H-15 (δ 2.33, 3.06) → C-16 (δ 129.9), C-17(δ 146.4), and C-21 (δ 127.7) as well as H-22 (δ 4.50, 4.64) → C-16, C-20 (δ 146.5), and C-21. The sesquiterpene unit of **5** was identified by $^{1}H,^{1}H$-COSY and $^{1}H,^{13}C$-HMBC experiments. Furthermore, the HMBC correlations H-15 → C-8 (δ 78.5), C-9 (δ 58.1), and C-10 (δ 38.2) confirmed the connection between C-15 and C-9 and the HMBC correlation H-22 → C-8 indicated the existence of the oxygen bridge between C-22 and C-8. The *p*-hydroquinone moiety was established on the basis of the ^{1}H and ^{13}C NMR chemical shifts as well as the HMBC correlations mentioned above, namely, H-15 → C-16, C-17, C-21; H-22 → C-16, C-20, C-21. The relative configuration was confirmed by a ROESY experiment. The observed ROESY correlations between H-12 and H-13, H-13 and H-15,

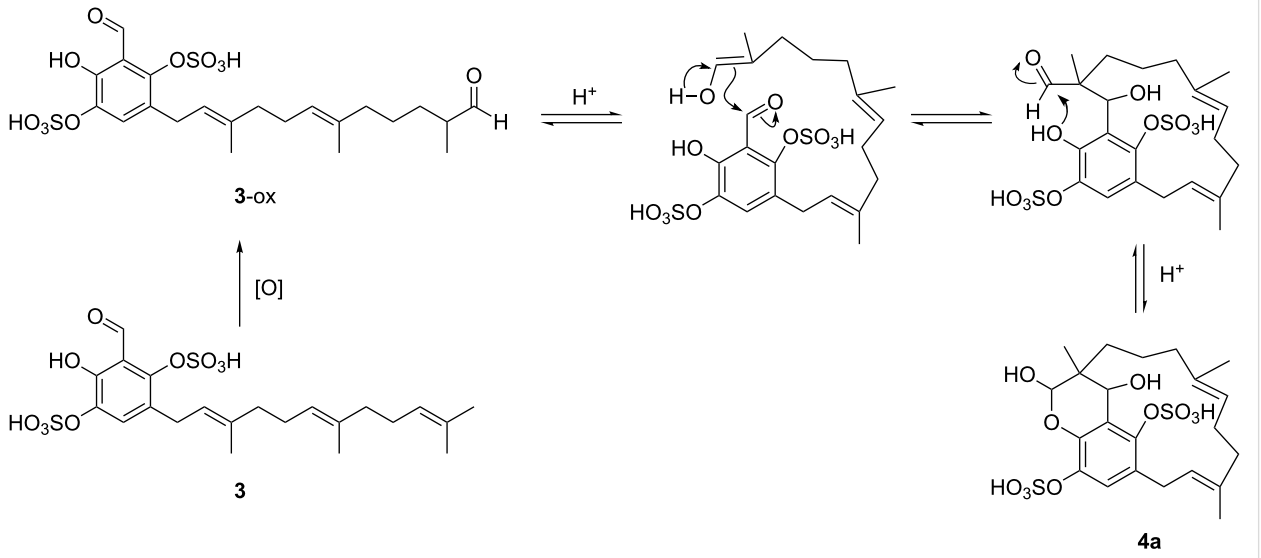


Figure 7: Proposed biogenesis of **4a** starting from the hypothetical precursor **3**-ox with an acyclic sesquiterpenoid part.

H-14 and H-15 suggested that the three methyl groups as well as CH_2-15 are axial. Examination of the NMR data for **5** revealed a high degree of similarity with data reported for bis(sulfato)cyclosiphonodictyol A [10]. The difference concerned the absence of the two sulfate ester groups. Compound **5** could be the precursor of bis(sulfato)cyclosiphonodictyol A. Another possibility is that bis(sulfato)cyclosiphonodictyol A lost its sulfate ester group during the isolation procedure.

The new compounds were tested for antimicrobial activity against different Gram-positive and Gram-negative bacteria, fungi, and for antiproliferative activity. The results given in Table 4 show that siphonodictyal E3 (**3**) and cyclosiphonodictyol A (**5**) exhibited mild activity against the Gram-positive bacteria *Staphylococcus aureus* and *Micrococcus luteus*, while siphonodictyal E4 (**4**) show cytotoxic activity against the L929 mouse fibroblasts, KB-31 epidermoid carcinoma, and the breast cancer cell line MCF7, although none of them showed activity in the antimicrobial assays against Gram-negative bacteria and the fungus *Candida albicans*.

Many of the isolated compounds from *Aka coralliphagum* are bicyclic sesquiterpene hydroquinones. However, in the course of our investigation, three linear sesquiterpenes were isolated. From a biosynthetical point of view [11], we propose that the linear sesquiterpenes are the precursors of the bicyclic sesquiterpenes (Figure 8). Therefore, siphonodictyals B1–B3 (**6**–**8**) could be derived from siphonodictyals E1–E3 (**1**–**3**), respectively.

Table 4: Results of the antimicrobial and antiproliferation assays of compounds **1**–**5**. Minimum inhibiting concentrations (MIC) for the antimicrobial assays and the IC_{50} values for the antiproliferation assays are given in μM.

		1	**2**	**3**	**4**	**5**
Gram-negative bacteria	*Pseudomonas aeruginosa*	–	–	–	–	–
	Klebsiella pneumonia	–	–	–	–	–
Gram-positive bacteria	*Staphylococcus aureus* (MRSA)	–	–	37	–	117
	Staphylococcus aureus (MSSA)	–	–	74	–	117
	Micrococcus luteus	–	–	74	–	58
Fungi	*Candida albicans*	–	–	–	–	–
Cytotoxic activity	L929 mouse fibroblasts	–	–	–	27	–
	KB31 epidermoid carcinoma	–	–	–	108	–
	MCF7 breast cancer	–	–	–	54	175
	FS4-LTM conditional immortalization human fibroblasts	–	–	–	–	–

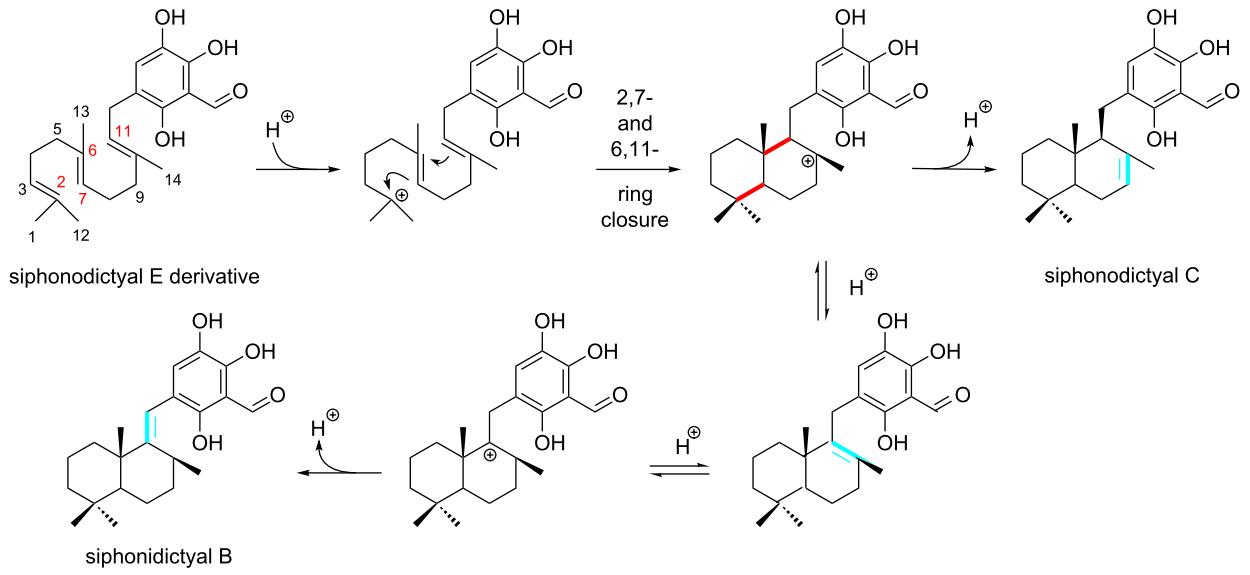


Figure 8: Hypothetical biogenesis of the bicyclic sesquiterpenoid moiety from the acyclic precursor of the siphonodictyals in the sponge *Aka coralliphagum* [11]. The newly formed bonds from the acyclic to the bicyclic sesquiterpenoid moiety are drawn in red. The isomerizing double bond is drawn in blue.

Aromatic sulfates occur in a wide range of higher plants and animals, particularly those growing in marine, estuarine, or freshwater environments. This is probably due to the high content of inorganic sulfate in aquatic environments (both limnic and marine environments – seawater contains an average of 28.7 mM inorganic sulfate [12]). Jensen and Ragan have demonstrated the presence of the natural product 1,2,3,5-tetrahydroxybenzene-2,5-disulfate in the marine brown alga *Ascophyllum nodosum* [13]. Kobayashi et al. isolated halenaquinol sulfate from the marine sponge *Xestospongia sapra* [14].

In the course of our investigation on the sponge *Aka coralliphagum*, we isolated a number of compounds containing sulfated phenols. These sulfated metabolites are labile [5], and easily loose the sulfate ester groups by hydrolysis in water [15]. Moreover, the influence of the sulfate esters on the bioactivity has been proven by activity tests: the desulfated compounds tend to be more active [5]. Therefore, we propose that the sulfate esters act as hydroxy protecting groups. The sponges excrete the sesquiterpene hydroquinones primarily in the sulfated form and their activities get increased by hydrolysis of these labile groups. This would lead to a prolonged bioactivity of these metabolites and therefore to a more efficient defense against predators or pathogens.

Experimental

^{1}H and ^{13}C NMR spectra were recorded on a Bruker Avance 600 MHz NMR spectrometer equipped with a cryo platform and a Bruker Avance 400 MHz NMR spectrometer. All experiments were measured at 303 K. HPLC separation was achieved by a Kromasil RP-18 column (16 mm × 250 mm, 5 µm) applying a H_2O (5 mM NH_4OAc)/MeCN/MeOH gradient. UV spectra were recorded during HPLC separation with a DAD detector (Jasco MD-2010 Plus). Accurate mass spectra were acquired using a Bruker micrOTOF$_{LC}$ mass spectrometer equipped with an ESI source. Mass calibration was performed using a sodium formate cluster prior each experiment.

The sponges were collected by SCUBA diving at a depth of 29 m off the coast of San Salvador in the Bahamas in June 2008. The samples were immediately frozen after collection and kept at −20 °C until extraction. A voucher specimen of this species is deposited in our lab (voucher number: *AKA* 08/45). The freeze-dried sponge sample (107.6 g) was extracted three times at room temperature with DCM/MeOH (1:1). After filtration, the filtrate was evaporated to yield 35.5 g crude extract which was further partitioned between *n*-hexane and methanol. The methanol extract was dried and followed with the partitioning between *n*-BuOH and H_2O. The resulting *n*-BuOH phase was concentrated (9.2 g) and purified by liquid chromatography using RP-18 silica gel with a stepwise gradient from H_2O/MeOH (100:0), (85:15), (50:50) to (0:100) yielding fractions A, B, C, and D, respectively. The fraction B was further purified by HPLC using an RP-18 column yielding compounds **1** (2.2 mg, HPLC gradient flow: H_2O (5 mM NH_4OAc)/MeCN: 0 min 81:19, 40 min 75:25), **2** (3.1 mg, HPLC isocratic flow: H_2O (5 mM NH_4OAc)/MeCN: 87:13 40 min), **4** (1.3 mg, HPLC gradient flow: H_2O (5 mM NH_4OAc)/MeCN: 0 min 85:15, 40 min 83:17, 60 min 80:20), and **5** (3.0 mg, HPLC gradient flow: H_2O (5 mM NH_4OAc)/MeCN: 0 min 85:15, 40 min 83:17, 60 min 80:20). The fraction C was also further purified by HPLC using the same RP-18 column yielding **3** (2.5 mg, HPLC gradient flow: H_2O (5 mM NH_4OAc)/MeCN: 0 min 76:24, 40 min 74:26, 45 min 70:30)

Antimicrobial assay

Determination of antimicrobial activities was carried out by the Helmholtz Center for Infection Research (HZI), and was based on the microdilution test, using 96-well micro titration plates. The MIC was defined as 50% growth inhibition after 24 hour incubation compared to that in the growth control well.

Cytotoxic assay

The cytotoxicity was determined using WST-1 assays, targeting cell lines L929 mouse fibroblasts, KB-31 epidermoid carcinoma, MCF-7 breast cancer, and FS4-LTM conditional immortalization human fibroblasts, respectively. The FS4-LTM cell line was incubated for 24 hours with the tested substances. The other cell lines were incubated for 5 days with the tested substances.

Experimental data

Siphonodictyal E1 (**1**): yellow powder; ^{1}H NMR (DMSO-d_6, 600 MHz) and ^{13}C NMR (DMSO-d_6, 150 MHz) see Table 1; HRMS-ESI(−) *m/z*: $[M + Na - 2H]^-$ calcd for $C_{24}H_{33}NO_{11}S_2Na$, 598.1398; found, 598.1338.

Siphonodictyal E2 (**2**): yellow powder; ^{1}H NMR (DMSO-d_6, 600 MHz) and ^{13}C NMR (DMSO-d_6, 150 MHz) see Table 1; HRMS-ESI(−) *m/z*: $[M - H]^-$ calcd for $C_{22}H_{29}O_9S$, 469.1538; found, 469.1561.

Siphonodictyal E3 (**3**): yellow powder; ^{1}H NMR (DMSO-d_6, 600 MHz) and ^{13}C NMR (DMSO-d_6, 150 MHz) see Table 1; HRMS-ESI(−) *m/z*: $[M + Na - 2H]^-$ calcd for $C_{22}H_{28}O_{10}S_2Na$, 539.1027; found, 539.1046.

Siphonodictyal E4 (**4**): yellow powder; CD data {(MeOH) $[\theta]_{291}^{max} = +37$}; ^{1}H NMR (DMSO-$d_6$, 600 MHz) and ^{13}C NMR (DMSO-d_6, 150 MHz) see Table 1; HRMS-ESI(−) *m/z*: [M +

Na − 2H]$^-$ calcd for $C_{22}H_{28}O_{11}S_2Na$, 555.0976; found, 555.0954.

Cyclosiphonodictyol A (**5**): colorless powder; CD data {(MeOH) $[\theta]^{max}_{295}$ = +163}; ^{1}H NMR (DMSO-d_6, 600 MHz) and ^{13}C NMR (DMSO-d_6, 150 MHz) see Table 1; HRMS-ESI(−) *m/z*: [M − H]$^-$ calcd for $C_{22}H_{31}O_3$, 343.2279; found, 343.2292.

Supporting Information

Supporting Information File 1

1D and 2D NMR spectra of the isolated compounds.
[http://www.beilstein-journals.org/bjoc/content/supplementary/1860-5397-10-52-S1.pdf]

Acknowledgements

Financial support from the Deutsche Forschungsgemeinschaft (DFG) under grants Ko 1314/5-1 and 5-2 (DFG research unit FOR 934) is gratefully acknowledged. Sponge collection was carried out by Dr. Gesine Schmidt and Dr. Achim Grube during a scientific expedition to the Bahamas in 2008. We would like to acknowledge the support of Prof. Dr. Joseph R. Pawlik (University of North Carolina, Wilmington, USA) who gave members of the Köck research group the opportunity to participate in the research trips to the Bahamas for the time period from 1998 to 2008. We further thank Dr. Sven Zea (Universidad Nacional de Colombia) for identification of the sponge samples as well as Dr. Florenz Sasse and Dr. Galina Sergeev (HZI Braunschweig) for carrying out the bioassays.

References

1. Rützler, K. *Smithsonian Contrib. Zool.* **1971,** *77,* 1–37. doi:10.5479/si.00810282.77
2. Sullivan, B. W.; Faulkner, D. J.; Matsumoto, G. K.; He, C. H.; Clardy, J. *J. Org. Chem.* **1986,** *51,* 4568–4573. doi:10.1021/jo00374a015
3. Sullivan, B. W.; Faulkner, D. J. New Perspectives in Sponge Biology. Third International Sponge Conference, Woods Hole, Massachusetts, Nov 17–23, 1985; Smithsonian Institution Press: Washington, DC, 1985; pp 45–50.
4. Sullivan, B.; Djura, P.; Mcintyre, D. E.; Faulkner, D. J. *Tetrahedron* **1981,** *37,* 979–982. doi:10.1016/S0040-4020(01)97672-0
5. Grube, A.; Assmann, M.; Lichte, E.; Sasse, F.; Pawlik, J. R.; Köck, M. *J. Nat. Prod.* **2007,** *70,* 504–509. doi:10.1021/np0603018
6. Couperus, P. A.; Clague, A. D. H.; van Dongen, J. P. C. M. *Org. Magn. Reson.* **1976,** *8,* 426–431. doi:10.1002/mrc.1270080807
7. Coates, R. M.; Ley, D. A.; Cavender, P. L. *J. Org. Chem.* **1978,** *43,* 4915–4922. doi:10.1021/jo00420a003
8. Ragan, M. A. *Can. J. Chem.* **1978,** *56,* 2681–2685. doi:10.1139/v78-441
9. Kalinowski, H.-O.; Berger, S.; Braun, S. *^{13}C NMR-Spektroskopie;* Georg Thieme Verlag: Stuttgart, 1984; pp 685 ff.
10. Killday, K. B.; Wright, A. E.; Jackson, R. H.; Sills, M. A. *J. Nat. Prod.* **1995,** *58,* 958–960. doi:10.1021/np50120a024
11. Fontana, A.; Tramice, A.; Cutignano, A.; d'Ippolito, G.; Gavagnin, M.; Cimino, G. *J. Org. Chem.* **2003,** *68,* 2405–2409. doi:10.1021/jo026131v
12. Zehnder, A. J. B.; Zinder, S. H. The Sulfur Cycle. In *The Handbook of Environmental Chemistry;* Hutzinger, O., Ed.; Springer: Berlin, 1980; Vol. 1A, pp 105–145.
13. Jensen, A.; Ragan, M. A. *Tetrahedron Lett.* **1978,** *19,* 847–850. doi:10.1016/S0040-4039(01)85415-0
14. Kobayashi, M.; Shimizu, N.; Kyogoku, Y.; Kitagawa, I. *Chem. Pharm. Bull.* **1985,** *33,* 1305–1308. doi:10.1248/cpb.33.1305
15. Benkovic, S. J. *J. Am. Chem. Soc.* **1966,** *88,* 5511–5515. doi:10.1021/ja00975a027

License and Terms

This is an Open Access article under the terms of the Creative Commons Attribution License (http://creativecommons.org/licenses/by/2.0), which permits unrestricted use, distribution, and reproduction in any medium, provided the original work is properly cited.

The license is subject to the *Beilstein Journal of Organic Chemistry* terms and conditions: (http://www.beilstein-journals.org/bjoc)

The definitive version of this article is the electronic one which can be found at:
doi:10.3762/bjoc.10.52

Beilstein Journal of Organic Chemistry

Synthesis of complex intermediates for the study of a dehydratase from borrelidin biosynthesis

Frank Hahn[*,‡1,2], Nadine Kandziora[‡1], Steffen Friedrich[1] and Peter F. Leadlay[2]

Full Research Paper

Open Access

Address:
[1]Institut für Organische Chemie und Biomolekulares Wirkstoffzentrum, Leibniz Universität Hannover, Schneiderberg 1B, 30167 Hannover, Germany and [2]Department of Biochemistry, University of Cambridge, 80 Tennis Court Road, Cambridge CB2 1GA, United Kingdom

Email:
Frank Hahn[*] - frank.hahn@oci.uni-hannover.de

* Corresponding author ‡ Equal contributors

Keywords:
aldol reaction; coenzyme A; natural products; pig liver esterase; polyketide biosynthesis; protection groups

Beilstein J. Org. Chem. **2014,** *10,* 634–640.
doi:10.3762/bjoc.10.55

Received: 30 August 2013
Accepted: 30 January 2014
Published: 11 March 2014

This article is part of the Thematic Series "Natural products in synthesis and biosynthesis".

Guest Editor: J. S. Dickschat

© 2014 Hahn et al; licensee Beilstein-Institut.
License and terms: see end of document.

Abstract

Herein, we describe the syntheses of a complex biosynthesis-intermediate analogue of the potent antitumor polyketide borrelidin and of reference molecules to determine the stereoselectivity of the dehydratase of borrelidin polyketide synthase module 3. The target molecules were obtained from a common precursor aldehyde in the form of *N*-acetylcysteamine (SNAc) thioesters and methyl esters in 13 to 15 steps. Key steps for the assembly of the polyketide backbone of the dehydratase substrate analogue were a Yamamoto asymmetric carbocyclisation and a Sakurai allylation as well as an *anti*-selective aldol reaction. Reference compounds representing the *E*- and *Z*-configured double bond isomers as potential products of the dehydratase reaction were obtained from a common precursor aldehyde by Wittig olefination and Still–Gennari olefination. The final deprotection of TBS ethers and methyl esters was performed under mildly acidic conditions followed by pig liver esterase-mediated chemoselective hydrolysis. These conditions are compatible with the presence of a coenzyme A or a SNAc thioester, suggesting that they are generally applicable to the synthesis of complex polyketide-derived thioesters suited for biosynthesis studies.

Introduction

Borrelidin (**1**) is a macrolactone polyketide natural product with promising antibacterial, antimalarial, anticancer and anti-angiogenesis activities, which are probably caused by the inhibition of threonyl-tRNA synthetase and apoptosis induction by caspase activation [1-4]. It bears several unusual structural elements like a cyclopentane ring and a carbonitrile (Figure 1a), which are built-up by unconventional biosynthesis mechanisms [5,6]. The carbonitrile for example is probably formed by allylic oxidation of the 12-methyl group in 12-desnitrile-12-methylborrelidin to the corresponding aldehyde and transamination to the amine followed by oxidation [6]. In the course of our studies on borrelidin biosynthesis, we became interested in the formation

of the (12*Z*,14*E*)-diene [7]. *Z*-configured double bonds are much rarer in polyketides than their *E*-configured counterparts, and their biosynthesis has not been thoroughly investigated yet [7-9].

Gene cluster analysis suggested that the double bond at position 12 in **1** is installed by the dehydratase of polyketide synthase (PKS) module 3 (BorDH3). Characteristic residues in the active site of the preceding ketoreductase point towards a 3D configuration of the BorDH3 precursor **3** [10,11]. Furthermore, we have shown in a previous study that BorDH3 preferentially accepts the 2D,3D-configured precursor, if all four potential stereoisomers of 3-hydroxy-2-methyl-SNAc-pentanoate model substrates are presented [7].

A commonly accepted model suggests that DHs from PKS I systems catalyze the removal of water by *syn*-dehydration and that a 2D,3D-configured precursor should lead to an *E*-configured BorDH3 product [10]. However, in the case of borrelidin this is in contradiction to the structure of the natural product in which a *Z*-configured double bond is present at position 12. In the borrelidin gene cluster, there is no obvious gene coding for an isomerase, which might be able to catalyze the inversion of a double bond configuration. Consequently, the *Z*-configured double bond must be installed either directly by BorDH3 or by *E*/*Z*-isomerisation of an initially formed *E*-configured double bond via a not yet elucidated mechanism in downstream biosynthetic processes.

Our aim was to assay the stereochemical course of the dehydratase of polyketide synthase (PKS) module 3 (BorDH3) in vitro. Therefore, the surrogate **5a** for BorDH3 as well as reference molecules such as **6a** and **6b** and the corresponding methyl esters **7a** and **7b**, which resemble the potential assay products or easily accessible derivatives of it, are required (Figure 1c, Scheme 1).

During chain elongation and reductive processing by PKSs, their intermediates are bound to acetyl carrier proteins (ACPs) via a 4'-phosphopantetheine arm (Figure 1b). It has been shown for other PKS domains that the recognition of this prosthetic group is essential for proper substrate orientation in the active site and catalysis with natural stereoselectivity [13]. To mimic the ACP-bound state of PKS intermediates, their analogues, free SNAc thioesters, are used in enzyme assays.

Alternatively, ACP-bound substrates can be conveniently obtained by loading coenzyme A (CoA) thioesters onto active site serine residues of recombinant ACPs by using 4'-phosphopantetheinyl transferases [12,14]. However, coenzyme A thioesters are synthetically hard to access, especially if the substrate structure is complex.

Results and Discussion

Retrosynthetic analysis of target molecules

One common feature of activated biosynthesis intermediate analogues such as **5a** is their relative low stability. In the natural

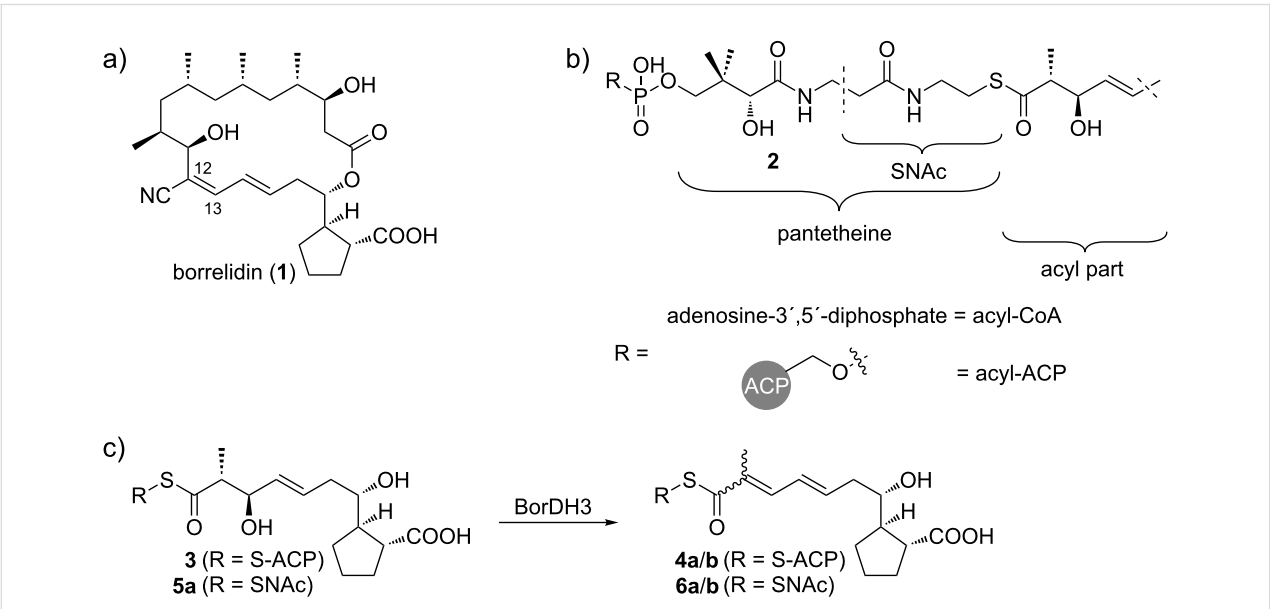
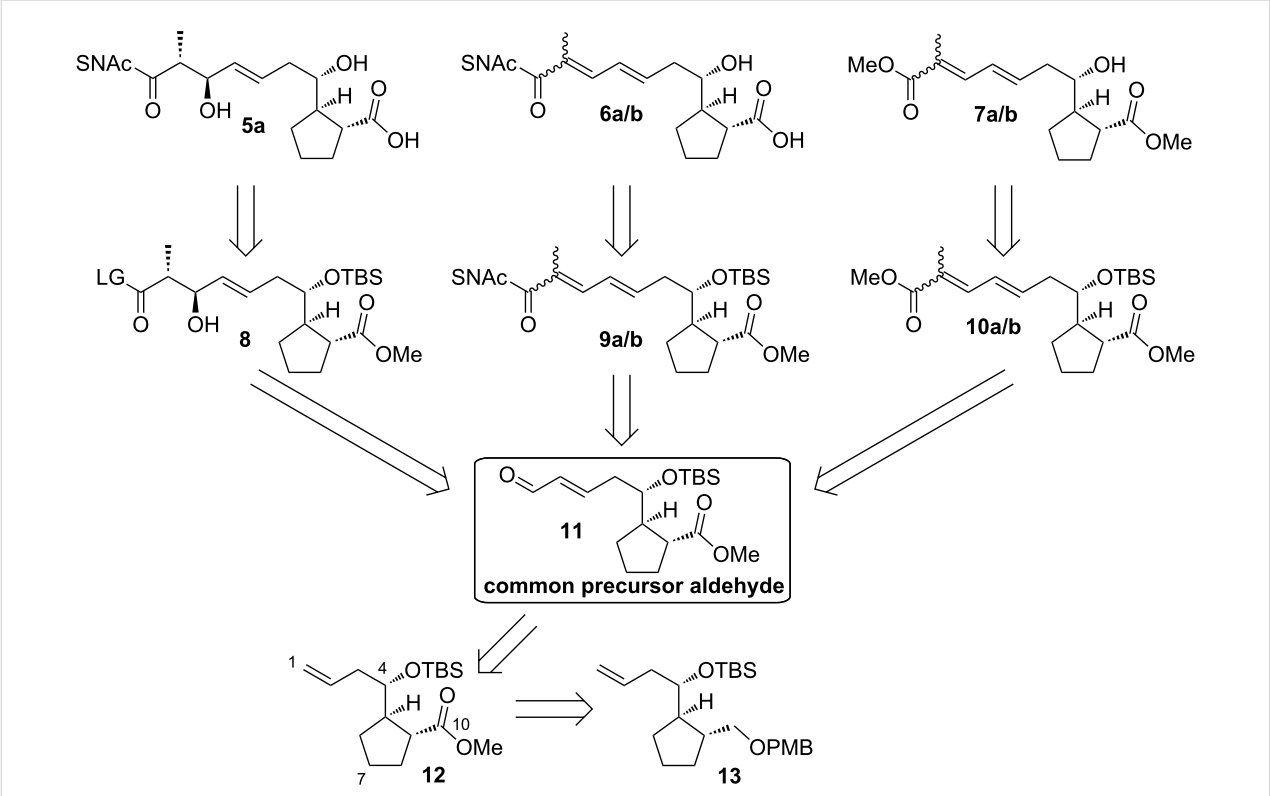


Figure 1: a) Structure of borrelidin (**1**); b) PKS intermediates are attached to an acyl carrier protein domain (ACP) via a 4'-phosphopantetheine linker, giving acyl-ACPs (**2**); c) BorDH3 catalyzes the dehydration of ACP-bound 3-hydroxyacylate **3** to one of the ACP-bound enoates **4a** or **4b**. The configuration of the double bond in the dehydration product is presently unknown. In a previous study, we have shown that BorDH3 only accepts surrogates with the shown 2D,3D-configuration if incubated with simple 3-hydroxy-2-methyl-SNAc pentanoates [7,12].



Scheme 1: Retrosynthetic analysis of surrogate substrates for BorDH3 and reference molecules for enzyme assays (**5a**, **6a**, **6b**, **7a** and **7b**); TBS = *tert*-butyldimethylsilyl, PMB = *p*-methoxybenzyl, LG = leaving group.

context, PKS intermediates are quickly processed by downstream domains or tailoring enzymes. However, if analogues are synthesized chemically and isolated, it has to be taken into account that they often tend to undergo destructive side reactions. Therefore, mild reaction conditions are required, and the synthetic routes to them should preferably be organized in a divergent fashion that allows flexible access to all target compounds from a stable late-stage synthetic intermediate. For the synthesis of the target compounds presented in this study, a strategy via the common precursor aldehyde **11** was envisaged (Scheme 1).

The situation is additionally complicated by the fact that the polyketide part contains a cyclopentyl carboxylate, which necessitates differentiation of the carboxyl groups at the termini to permit regioselective thioester formation. We decided to avoid late redox transformations. Instead, we achieved differentiation by choice of a chemoselective protection group strategy with removal conditions that are compatible for SNAc thioesters (Scheme 1).

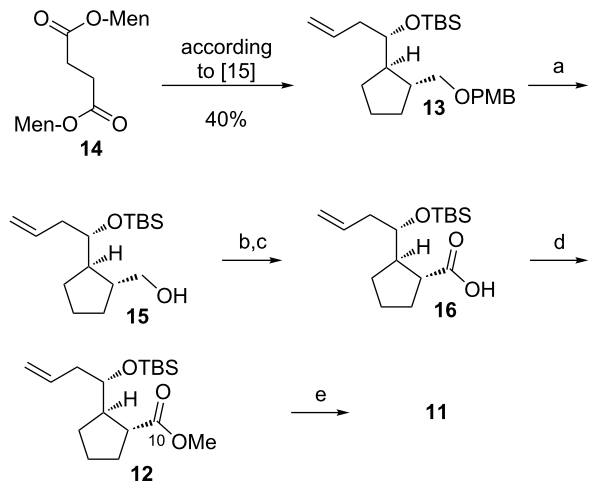
We envisaged the usage of TBS ether for the protection of the secondary hydroxy group and to protect the carboxylic acid as its methyl ester in the precursors **8**, **9a**, **9b**, **10a** and **10b**. These groups should be cleavable under mildly acidic or esterase-catalyzed conditions. As the presence of a methyl ester would prevent the selective introduction of one thioester into **5a** by saponification–thioesterification, we planned transesterification from a suitably activated carboxylic acid derivative **8**. Alternatively, direct introduction into **11** with appropriate SNAc thioester building blocks was planned for the synthesis of **6a** and **6b**.

Starting from aldehyde **11**, a common precursor for all molecules required in this study, aldol reaction and following transesterification should lead to thioester **8**. The bismethyl esters **7a** and **7b** as well as the SNAc thioesters **6a** and **6b** should be accessible from aldehyde **11** through a Horner–Wadsworth–Emmons reaction and the Still–Gennari olefination as well as by a Wittig olefination with stabilised phosphoranes, respectively. The aldehyde **11** should be accessible from the known molecule **13** via **12** [15].

Synthesis of the common precursor aldehyde **11**

The synthesis of the common precursor aldehyde **11** was accomplished from di(menth-1-yl)succinate (**14**) through a known route described by Omura et al. (Scheme 2) [15-17]. The

final oxidation state at C10 in **12** was installed after protective group removal to primary alcohol **15** followed by Dess–Martin oxidation, Pinnick oxidation and methylation. Methyl ester **12** was obtained in 10 steps with a good overall yield of 20%. Olefin cross metathesis of alkene **12** with crotonaldehyde in the presence of a second generation Grubbs catalyst required only a short filter column to isolate α,β-unsaturated aldehyde **11** in a pure form.



Scheme 2: Synthesis of the common precursor aldehyde **11**. Compound **13** was prepared in six steps and with an overall yield of 40% via a known route by Omura et al. [15]. a) DDQ, CH_2Cl_2, rt, 30 min (85%); b) DMP, CH_2Cl_2, rt, 2 h; c) NaOCl, 2-methyl-2-butene, *t*-BuOH, phosphate buffer, rt, 16 h; d) TMS-CHN_2, toluene/MeOH 2:3, rt, 40 min (58% over three steps); e) second generation Grubbs catalyst, crotonaldehyde, CH_2Cl_2, 40 °C, 120 min (88%); DDQ = 2,3-dichloro-5,6-dicyano-1,4-benzoquinone, Men = (*l*)-menthyl, DMP = Dess–Martin periodinane, TMS = trimethylsilyl.

Synthesis of DH substrate surrogate

For the synthesis of the DH substrate surrogate **5a** we aimed at an *anti*-selective aldol reaction, which permits efficient access to the desired 2D,3D-stereoisomer followed by a smooth transformation into the SNAc thioester in the presence of a methyl ester function. Amongst others, we tested Paterson's lactate-derived benzoyl auxiliary, Evans' magnesium-catalyzed direct aldol reaction, and an Abiko–Masamune-like aldol reaction by using a thiodesoxy variant of the norephedrine-derived auxiliary on simplified model aldehydes as well as on aldehyde **11** [18-21]. However, in all these cases either the aldol reaction itself proved to be low yielding (<20%) or removal conditions of chiral auxiliaries were destructive to the molecule.

The best results were obtained for an *anti*-selective variant, in which aldehyde **11** was reacted with an (*E*)-boron enolate formed by the reaction of thiophenol propionate with chlorodicyclohexylborane and dimethylethylamine, similar to the conditions described by Paterson et al. for lactate-derived auxiliaries [18]. In this way, the aldol product was conveniently obtained as an inseparable 1:1 mixture of both 2,3-*anti* diastereomers **17a** and **17b** in 57% yield over two steps [22]. Such thiophenol esters readily undergo thiol-exchange reactions and are therefore suitable precursors for SNAc, pantetheine and CoA thioesters [14]. Accordingly, when we treated the mixture of thiophenol esters **17a** and **17b** with HSNAc and triethylamine in DMF, they underwent clean transesterification furnishing SNAc thioesters **18a** and **18b** in 70% combined yield [20] (Scheme 3).

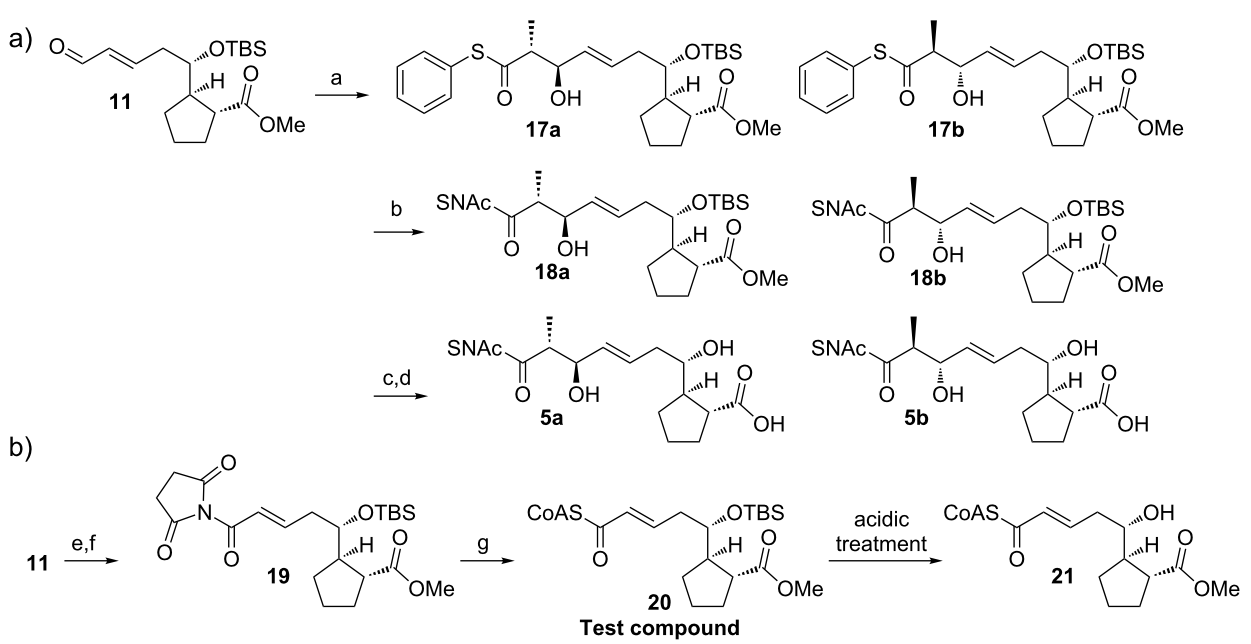
With the mixture of **18a** and **18b** in hand, we turned to the mild removal of the protection groups. For TBS cleavage, we focused on conditions previously described by us for the removal of an acid-sensitive dioxolane protection group from a CoA thioester [23]. We evaluated the exposure of the model CoA ester **20**, synthesized from **11** by Pinnick oxidation and CoA thioesterification via an intermediate activation as *N*-hydroxysuccinimide ester, to several acids in H_2O/THF mixed solvent systems. In **20** the acyl part is similarly functionalized as in the protected SNAc thioesters **18a** and **18b**. However, the CoA thioester can be regarded as more demanding in terms of sensitivity.

The progress of the reaction was followed by mass spectrometry. While the use of strong acids like *p*-toluenesulfonic acid or hydrochloric acid led to the decomposition of **20**, weaker acids like acetic acid did not lead to any detectable product formation, even after reaction times of up to 20 h. Gratifyingly, treatment with a mixture of THF/HCOOH/H_2O (6:3:1), gave a slow conversion into the desired product **21** (see Figure S1 and Figure S2 in Supporting Information File 1). Complete deprotection was achieved after 2 days.

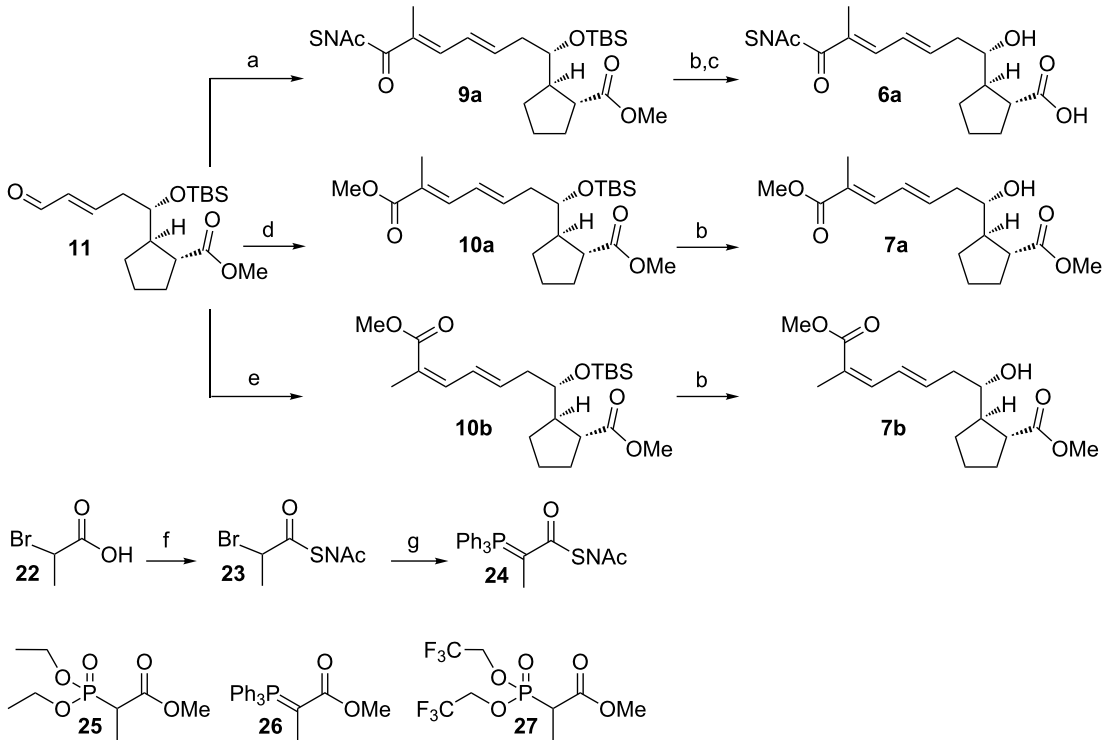
The mixture of SNAc esters **18a** and **18b** was exposed to the established acidic deprotection conditions and the progress of the reaction was monitored by mass spectrometry. After two days, complete TBS removal was obtained. The crude product was subjected to selective methyl ester cleavage by using pig liver esterase (PLE) [24]. The target molecule was obtained as a mixture of both *anti*-diastereomers **5a** and **5b** after 15 steps in 7% overall yield.

Synthesis of reference compounds

We exploited a Wittig reaction with a suitable stabilized phosphorane for the synthesis of (*E,E*)-diene **6a** (Scheme 4). The Wittig compound **24** was obtained in two steps from 2-bromopropionic acid following synthetic procedures described for its acetic acid analogue and the respective methyl ester ylide **26** [25,26]. The reaction of phosphorane **24** with **11** under neutral conditions at 50 °C gave the desired diene **9a** in very good 88%



Scheme 3: Synthesis of the BorDH3 substrates. a) Thiophenolpropionate, Cy_2BCl, Me_2EtN, Et_2O, −78 °C to −20 °C, 16 h (57% over two steps from **12**); b) HSNAc, Et_3N, DMF, rt, 16 h (70%); c) THF/HCOOH/H_2O (6:3:1), rt, 2 d; d) pig liver esterase, phosphate buffer, rt, 5 d (81% over two steps); e) NaOCl, 2-methyl-2-butene, *t*-BuOH, phosphate buffer (pH 7.0), rt, 16 h; f) *N*-hydroxysuccinimide, *N*,*N*′-dicyclohexylcarbodiimide, THF, rt, 16 h (50% over three steps from **12**); g) HSCoA·3Li, THF/H_2O (2:1) adjusted to pH 8.0 by phosphate buffer, 35 °C, 18 h; DMF = *N*,*N*-dimethylformamide.



Scheme 4: Synthesis of reference compounds for the BorDH3 assay. a) **24**, CH_2Cl_2, 50 °C, 3 h (88% over two steps); b) THF/HCOOH/H_2O (6:3:1), rt, 2 d (62% for **7a**, 57% for **7b**); c) pig liver esterase, phosphate buffer, rt, 3 d (67% over two steps from **9a**); d) **25,** NaH, THF, 0 °C, 3 h (18% over two steps from **12**) or **26**, CH_2Cl_2, 50 °C, 21 h (64% over two steps from **12**); e) **27**, 18-crown-6, K_2CO_3, THF, −20 °C then 0 °C for 5 h (47% over two steps from **12**); f) HSNAc, EDC, DMAP, CH_2Cl_2, rt, 16 h (78%); g) PPh_3, H_2O, 70 °C, 11 h, then NaOH, rt (64%).

yield and in nearly perfect *E*-selectivity. The protection groups were removed from **9a** under the previously established conditions to finally give target SNAc thioester **6a** in a total yield of 12% over 14 steps. Alternative attempts to synthesize **9a** and **9b** by Horner–Wadsworth–Emmons olefination and Still–Gennari olefination with the respective phosphonates gave no reaction product at all (Horner–Wadsworth–Emmons olefination) or only the (*E*,*E)*-diene **10a** instead of the desired *E,Z*-configured product **10b** (Still–Gennari olefination).

In order to obtain alternative reference compounds for both potential products of the BorDH3 enzyme assay, we synthesized double bond isomers **7a** and **7b**. To be able to compare them to the products in the crude BorDH3 assay mixture, the latter will be transformed into their corresponding methyl esters by saponification and following methylation with trimethylsilyldiazomethane.

The fully protected *E*-isomer **10a** was obtained in 18% yield by a Horner–Wadsworth–Emmons reaction with phosphonate **25** or, alternatively, in 64% yield by a Wittig reaction with stabilized phosphorane **26**. The *Z*-isomer **10b** was synthesized by Still–Gennari olefination using phosphonate **27** in 47% yield. The yield for the deprotection step was satisfying (61% for **7a** and 57% for **7b**) in both cases, indicating that both isomers are configurationally stable under these conditions. The overall yield over 13 steps was 8% for **7a** and 5% for **7b**.

(*E,E*)-diene **6a** will find application in the comparative NMR evaluation of a large scale BorDH3 enzyme assay of substrates **5a** and **5b**. Together with the successful synthesis of **5a** and **5b** and the availability of the isomers **7a** and **7b**, this sets the stage to determine the stereoselectivity of BorDH3.

Conclusion

We reported on the synthesis of a complex substrate and appropriate reference compounds for assaying the activity of the dehydratase in module 3 of the borrelidin polyketide synthase. All the target molecules **5a**, **6a**, **7a** and **7b** were obtained in 13 to 15 step sequences with overall yields of up to 12%. The routes diverged from a common precursor aldehyde **11**, which had been prepared in 18% yield over 11 steps, and had exploited the Yamamoto asymmetric carbocyclization and $MgBr_2$-mediated Sakurai reaction to set up the three stereogenic centres.

The construction of the backbone was accomplished by *anti*-selective aldol reaction or olefination by using the respective phosphonates or phosphoranes. A notable achievement was the development of a chemoselective, mild protection strategy, which is based on an acidic treatment to cleave a silyl ether and a highly efficient and less common late stage ester hydrolysis by using pig liver esterase. Preliminary tests suggest the compatibility of these conditions with coenzyme A thioesters, indicating that the chosen strategy has broad potential in the future synthesis of similarly (or even more) complex polyketide-derived coenzyme A thioesters.

Thus, the presented strategy enables for the first time the in vitro assaying of a potential *Z*-selective dehydratase domain from a polyketide synthase with suitable precursor molecules. These experiments are currently ongoing in our lab.

Supporting Information

The supporting information provides reaction details, analytical data, and copies of ^1H and ^{13}C NMR spectra.

Supporting Information File 1

Procedures.
[http://www.beilstein-journals.org/bjoc/content/supplementary/1860-5397-10-55-S1.pdf]

Supporting Information File 2

NMR spectra.
[http://www.beilstein-journals.org/bjoc/content/supplementary/1860-5397-10-55-S2.pdf]

Acknowledgements

We thank the Marie Curie program of the European Union and the Emmy Noether program of the DFG for funding. We would also like to thank the NMR facility and the mass facility of the OCI Hanover as well as Prof. Andreas Kirschning and his group for general support and helpful discussion.

References

1. Berger, J.; Jampolsky, L. M.; Goldberg, M. *Arch. Biochem.* **1949,** *22,* 476–478.
2. Keller-Schierlein, W. *Helv. Chim. Acta* **1967,** *50,* 731–753. doi:10.1002/hlca.19670500303
3. Otoguro, K.; Ui, H.; Ishiyama, A.; Kobayashi, M.; Togashi, H.; Takahashi, Y.; Masuma, R.; Tanaka, H.; Tomoda, H.; Yamada, H.; Omura, S. *J. Antibiot.* **2003,** *56,* 727–729. doi:10.7164/antibiotics.56.727
4. Kawamura, T.; Liu, D.; Towle, M. J.; Kageyama, R.; Tsukahara, N.; Wakabayashi, T.; Littlefield, B. A. *J. Antibiot.* **2003,** *56,* 709–715. doi:10.7164/antibiotics.56.709
5. Olano, C.; Wilkinson, B.; Sánchez, C.; Moss, S. J.; Sheridan, R.; Math, V.; Weston, A. J.; Braña, A. F.; Martin, C. J.; Oliynyk, M.; Méndez, C.; Leadlay, P. F.; Salas, J. A. *Chem. Biol.* **2004,** *11,* 87–97. doi:10.1016/j.chembiol.2003.12.018

6. Olano, C.; Moss, S. J.; Braña, A. F.; Sheridan, R. M.; Math, V.; Weston, A. J.; Méndez, C.; Leadlay, P. F.; Wilkinson, B.; Salas, J. A. *Mol. Microbiol.* **2004,** *52,* 1745–1756. doi:10.1111/j.1365-2958.2004.04090.x
7. Vergnolle, O.; Hahn, F.; Baerga-Ortiz, A.; Leadlay, P. F.; Andexer, J. N. *ChemBioChem* **2011,** *12,* 1011–1014. doi:10.1002/cbic.201100011
8. Valenzano, C. R.; You, Y.-O.; Garg, A.; Keatinge-Clay, A.; Khosla, C.; Cane, D. E. *J. Am. Chem. Soc.* **2010,** *132,* 14697–14699. doi:10.1021/ja107344h
9. Guo, X.; Liu, T.; Valenzano, C. R.; Deng, Z.; Cane, D. E. *J. Am. Chem. Soc.* **2010,** *132,* 14694–14696. doi:10.1021/ja1073432
10. Reid, R.; Piagentini, M.; Rodriguez, E.; Ashley, G.; Viswanathan, N.; Carney, J.; Santi, D. V.; Hutchinson, C. R.; McDaniel, R. *Biochemistry* **2003,** *42,* 72–79. doi:10.1021/bi0268706
11. Caffrey, P. *ChemBioChem* **2003,** *4,* 654–657. doi:10.1002/cbic.200300581
12. Carreras, C. W.; Gehring, A. M.; Walsh, C. T.; Khosla, C. *Biochemistry* **1997,** *36,* 11757–11761. doi:10.1021/bi971350+
13. Bali, S.; Weissman, K. S. *ChemBioChem* **2006,** *7,* 1935–1942. doi:10.1002/cbic.200600285
14. Mishra, P. K.; Drueckhammer, D. G. *Chem. Rev.* **2000,** *100,* 3283–3310. doi:10.1021/cr990010m
15. Nagamitsu, T.; Takano, D.; Fukuda, T.; Otoguro, K.; Kuwajima, I.; Harigaya, Y.; Omura, S. *Org. Lett.* **2004,** *6,* 1865–1867. doi:10.1021/ol049356w
16. Misumi, A.; Iwanaga, K.; Furuta, K.; Yamamoto, H. *J. Am. Chem. Soc.* **1985,** *107,* 3343–3345. doi:10.1021/ja00297a048
17. Compound **14** was prepared in quantitative yield by refluxing succinic acid and (*l*)-menthol for 4 h in toluene at 120 °C under Dean–Stark conditions.
18. Paterson, I.; Wallace, D. J.; Cowden, C. J. *Synthesis* **1998,** 639–652. doi:10.1055/s-1998-5929
19. Evans, D. A.; Tedrow, J. S.; Shaw, J. T.; Downey, C. W. *J. Am. Chem. Soc.* **2002,** *124,* 392–393. doi:10.1021/ja0119548
20. Fanjul, S.; Hulme, A. N.; White, J. W. *Org. Lett.* **2006,** *8,* 4219–4222. doi:10.1021/ol0614774
21. Heathcock, C. H.; Pirrung, M. C.; Montgomery, S. H.; Lampe, J. *Tetrahedron* **1981,** *37,* 4087–4095. doi:10.1016/S0040-4020(01)93284-3
22. The relative stereochemistry was determined from the characteristic ^{3}J coupling constant of 7.5 Hz between the protons at positions 2 (dq at 2.87 ppm) and 3 (dd at 4.26 ppm) in the ^{1}H NMR spectrum. HPLC–MS analysis of the mixture of **17a** and **17b** suggested an approximate 1:1 mixture of both diastereomers.
23. Sun, Y.; Hahn, F.; Demydchuk, Y.; Chettle, J.; Tosin, M.; Osada, H.; Leadlay, P. F. *Nat. Chem. Biol.* **2010,** *6,* 99–101. doi:10.1038/nchembio.285
24. Morimoto, Y.; Terao, Y.; Achiwa, K. *Chem. Pharm. Bull.* **1987,** *35,* 2266–2271. doi:10.1248/cpb.35.2266
25. Gilbert, I. H.; Ginty, M.; O'Neill, J. A.; Simpson, T. J.; Staunton, J.; Willis, C. L. *Bioorg. Med. Chem. Lett.* **1995,** *5,* 1587–1590. doi:10.1016/0960-894X(95)00276-Y
26. Handa, M.; Scheidt, K. A.; Bossart, M.; Zheng, N.; Roush, W. A. *J. Org. Chem.* **2008,** *73,* 1031–1035. doi:10.1021/jo702250z

License and Terms

This is an Open Access article under the terms of the Creative Commons Attribution License (http://creativecommons.org/licenses/by/2.0), which permits unrestricted use, distribution, and reproduction in any medium, provided the original work is properly cited.

The license is subject to the *Beilstein Journal of Organic Chemistry* terms and conditions: (http://www.beilstein-journals.org/bjoc)

The definitive version of this article is the electronic one which can be found at: doi:10.3762/bjoc.10.55

Beilstein Journal of Organic Chemistry

Synthesis of (2*S*,3*R*)-3-amino-2-hydroxydecanoic acid and its enantiomer: a non-proteinogenic amino acid segment of the linear pentapeptide microginin

Rajendra S. Rohokale and Dilip D. Dhavale*

Full Research Paper

Open Access

Address:
Department of Chemistry, Garware Research Centre, University of Pune, Pune - 411 007, India

Email:
Dilip D. Dhavale* - ddd@chem.unipune.ac.in

* Corresponding author

Keywords:
AHDA; carbohydrate; chiron approach; enantioselective; natural products; non-proteinogenic amino acid

Beilstein J. Org. Chem. **2014,** *10,* 667–671.
doi:10.3762/bjoc.10.59

Received: 19 November 2013
Accepted: 10 February 2014
Published: 17 March 2014

This article is part of the Thematic Series "Natural products in synthesis and biosynthesis".

Guest Editor: J. S. Dickschat

© 2014 Rohokale and Dhavale; licensee Beilstein-Institut.
License and terms: see end of document.

Abstract

A directed manipulation of the functional groups at C3 and C4 of D-glucose was demonstrated to synthesize naturally occurring (2*S*,3*R*)-α-hydroxy-β-aminodecanoic acid (AHDA, **2a**) and its enantiomer **2b**. The enantiomer of **2a** is the N-terminal part of the natural linear pentapeptide microginin, which is used as an antihypertensive agent.

Introduction

Microginin **1** (Figure 1), isolated from the cyanobacterium *Microcystis aeruginosa,* is a linear pentapeptide consisting of L-Tyr-L-*N*-Me-Tyr-L-Val-L-Ala and (2*S*,3*R*)-α-hydroxy-β-aminodecanoic acid ((2*S*,3*R*)-AHDA, **2a**) [1]. Microginin is used as a hypertensive agent based on its biological activity against angiotensin converting enzyme, which is responsible for the vasoconstriction of blood vessels [2-4]. Amongst different amino acids present in microginin, (2*S*,3*R*)-AHDA (**2a**) is a non-proteinogenic natural amino acid attached at the N-terminal part of the peptide chain. The α-hydroxy-β-amino acid fragment in AHDA **2a** is also present in linear peptides such as bestatin and valinoctin [5-8], which are isolated from the same species. In addition, the chiral α-hydroxy-β-amino acid constituent is an important component of protein kinase inhibitor compounds like balanol and the anticancer drug taxol [9].

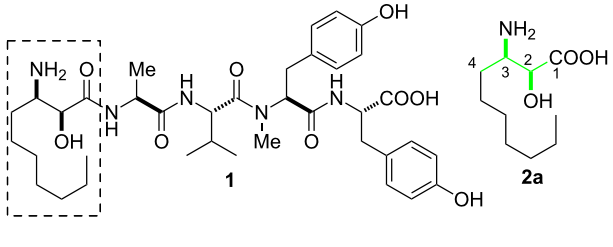


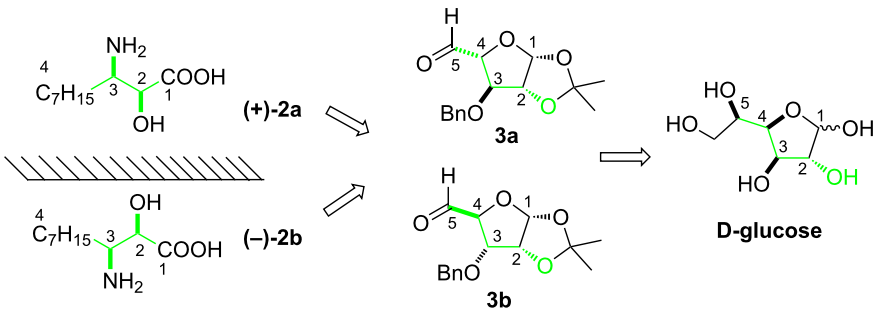
Figure 1: Microginin (**1**) and (2*S*,3*R*)-AHDA (**2a**).

Due to the biological importance of (2*S*,3*R*)-AHDA, the enantioselective synthesis of its chiral core is a challenge task. This fact led to several approaches for the stereoselective synthesis of (2*S*,3*R*)-AHDA including (i) the enantioselective introduction of amino- and hydroxy-groups to olefinic acid by either asymmetric epoxidation, dihydroxylation or aminohydroxylation [10-15], (ii) the asymmetric synthesis of β-lactams by a Staudinger reaction between ketene and imine to give the corresponding amino acids [16], and (iii) the Lewis acid catalyzed multicomponent condensation reactions of aldehyde, an amine and ketene silyl acetal derivatives to get the vicinal hydroxylamino acids [17]. In addition, a few strategies employ a chiral pool approach. For example, Wee et al. utilized the zinc-silver-mediated reductive elimination of α-D-lyxofuranosyl phenylsulfone to get (4*S*,5*S*)-4-formyl-5-vinyl-2-oxazolidone, which was converted into **2a** [18]. Merrer and co-workers used D-isoascorbic acid, which was transformed via (2*R*)-amino-1,3,4-triol to **2a** [19]. Bergmeier et al. synthesized a chiral allyl alcohol from D-mannitol, which is converted to the azidoformate and thermally cyclized to a bicyclic aziridine. The opening of the aziridine with organocuprate led to a corresponding chiral hydroxylated amino acid core [20]. Although a number of chiron approaches are known [21], there is no report from D-glucose towards the synthesis of (2*S*,3*R*)-AHDA (**2a**) and its enantiomer (2*R*,3*S*)-AHDA (**2b**). As a part of our continuous interest in the synthesis of chiral amino acids [22,23] and their utility in the synthesis of iminosugars [24-29], we report here an efficient and practical approach for the synthesis of both enantiomers of AHDA (**2a** and **2b**) from the same precursor D-glucose by simple manipulation of the functional groups.

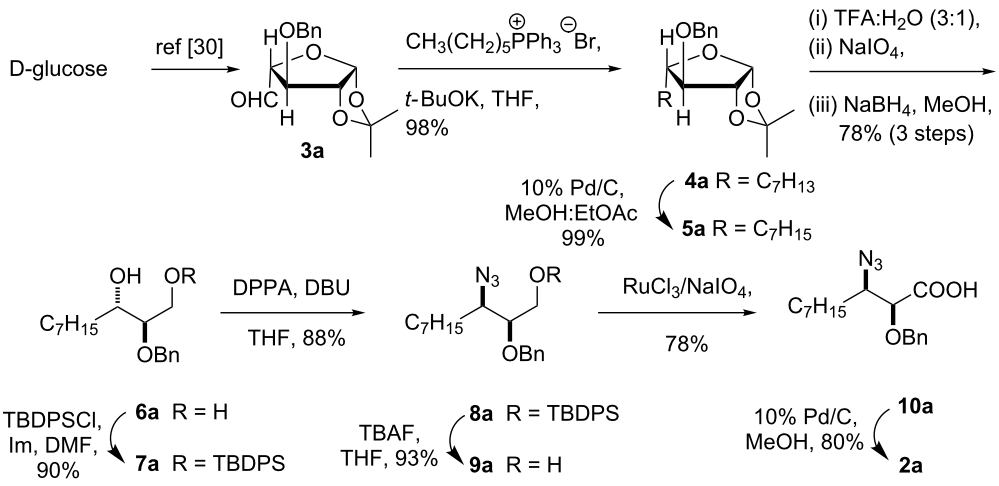
We visualized that the structural and the stereochemical symmetry of both enantiomers (**2a**/**2b**) is present in D-glucose. The C1-carboxyl carbon atom of **2a** is present at the C2 of the D-glucose, and the C4 carbon atom with an alkyl chain in **2a** could be built on C5 of the D-glucose (Scheme 1). The required relative stereochemistry of the vicinal hydroxyamino functionality in **2a** at C2 and C3 is embedded at the C3 and C4 of D-glucose, respectively, and needs to be manipulated by usual functional group transformations. Thus, for the synthesis of enantiomers **2a** and **2b** the corresponding sugar precursors were found to be suitably protected β-L-arabino-pentodialdo-1,4-furanose **3a** [30,31] and α-D-ribo-pentodialdo-1,4-furanose **3b** [32]. There exists a distinct possibility to synthesize these chiron synthons **3a** and **3b** from the easily available and cheap starting material D-glucose. Our results of the synthesis of both enantiomers **2a** and **2b** are described herein.

Results and Discussion

As reported earlier, D-glucose was converted to the 3-*O*-benzyl-1,2-*O*-isopropylidene-β-L-arabino-pentodialdo-1,4-furanose (**3a**) in 72% yield (Scheme 2) [30]. While targeting the synthesis of **2a**, the Wittig olefination of **3a** with *n*-hexyltriphenylphosphonium bromide and *t*-BuOK gave olefin **4a** as a diasteromeric mixture of *Z* and *E*-isomers in the ratio 9.5:0.5 as shown by ^{1}H NMR of the crude product. The catalytic hydrogenation of alkene **4a** with 10% Pd/C in methanol:ethyl acetate (3:2) at balloon pressure gave 4-heptyl-L-threose derivative **5a** as a viscous oil in 99% yield [33]. Removal of the 1,2-acetonide group with TFA–water in **5a** provided an anomeric mixture of the hemiacetal, which was directly subjected to oxidative cleavage by using sodium metaperiodate in acetone–water (to cleave the anomeric carbon) followed by a treatment with sodium borohydride to give triol **6a** as a viscous oil in 78% overall yield in three steps [34]. The primary hydroxy group of triol **6a** was selectively monosilylated with *t*-butyldiphenylsilyl chloride to give **7a**. Subsequently, the secondary hydroxy group in **7a** was converted to azido derivative **8a** with an inversion of the configuration by using diphenylphosphoryl azide in the presence of DBU in 88% yield [35]. Cleavage of the silyl functionality in **8a** with *n*-tetrabutylammonium fluoride offered azido alcohol **9a** as a viscous oil. The azido alcohol **9a** was oxidized to the corresponding acid by using $RuCl_3{\cdot}3H_2O/NaIO_4$ to give **10a** [36].



Scheme 1: Retrosynthetic analysis of AHDA.



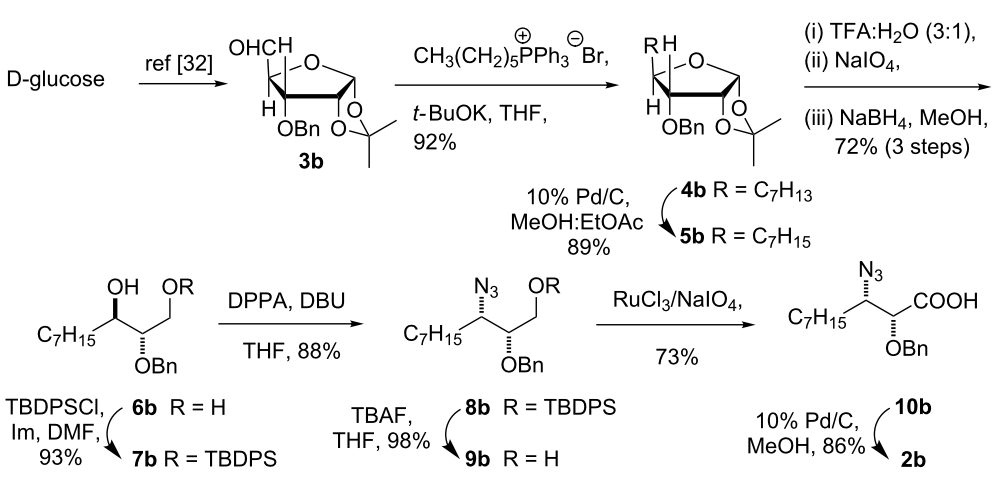
Scheme 2: Synthesis of AHDA **2a**.

Finally, cleavage of the 2-*O*-benzyl ether and reduction of the 3-azido group to the corresponding amine in one step with 10% Pd/C in methanol provided (−)-α-hydroxy-β-aminodecanoic acid (AHDA, **2a**) in 80% yield as a white solid. The spectral and analytical data of **2a** was found to be in good agreement with published data ($[\alpha]_D^{25}$ +5.6 (*c* 0.51, 1 M HCl). $[\alpha]_D^{22}$ +7.3 (*c* 0.37, 1 M HCl)) [18].

The synthesis of AHDA enantiomer **2b** was accomplished starting from 3-*O*-benzyl-1,2-*O*-isopropylidene-α-D-ribo-pentodialdo-1,4-furanose (**3b**) which was obtained from D-glucose in good yield as reported earlier [33]. Thus, the Wittig reaction of **3b** followed by hydrogenation (10% Pd/C) gave 4-heptyl-D-threose derivative **5b** (Scheme 3). Hydrolysis of 1,2-*O*-isopropylidene (TFA:H_2O) followed by oxidative cleavage of the hemiacetal with $NaIO_4$ and reduction with $NaBH_4$ gave triol **6b**,which was monosilylated with TBDPSCl to give **7b**. Conversion of the secondary hydroxy group in **7b** to azide **8b** according to the Mitsunobu protocol, and deprotection followed by oxidation of the primary hydroxy group gave azido acid **10b**. Finally, hydrogenolysis of the benzyl group and reduction of the azido group by using 10% Pd/C, in one pot, gave **2b** in 30.1% overall yield from **3b**. The spectral and analytical data was found to be in good agreement with reported data ($[\alpha]_D^{30}$ −5.1(*c* 0.51, 1 M HCl). $[\alpha]_D^{30}$ −6.2 (*c* 0.4, 1 M HCl)) [21].

Conclusion

In conclusion, we demonstrated a practical approach for the synthesis of both enantiomers of AHDA (**2a** and **2b**) to obtain the stereochemistry required for the α-hydroxy-β-amino acid. Our method starts from D-glucose by an easy manipulation of



Scheme 3: Synthesis of *ent*-AHDA **2b**.

its functional groups at C3 and C4. In addition, the chiral core (α-hydroxy-β-amino acid) in **2a** is present in several biologically active compounds such as taxol, balanol and bestatin. Therefore, this methodology could be potentially exploited for the synthesis of the chiral segment of these compounds.

Supporting Information

Supporting Information File 1

Experimental procedures.
[http://www.beilstein-journals.org/bjoc/content/supplementary/1860-5397-10-59-S1.pdf]

Supporting Information File 2

Copies of NMR spectra.
[http://www.beilstein-journals.org/bjoc/content/supplementary/1860-5397-10-59-S2.pdf]

Acknowledgements

We are thankful to the Department of Science and Technology, New Delhi (Project File No. SR/S1/OC-20/2010) for providing financial support. R.S.R. is thankful to CSIR, New Delhi for providing a Junior Research Fellowship.

References

1. Okino, T.; Matsuda, H.; Murakami, M.; Yamaguchi, K. *Tetrahedron Lett.* **1993,** *34,* 501–504. doi:10.1016/0040-4039(93)85112-A
2. Wyvratt, M. J.; Patchett, A. A. *Med. Res. Rev.* **1985,** *5,* 483–531. doi:10.1002/med.2610050405
3. Moore, R. E.; Banarjee, S.; Bomemann, V.; Caplan, F. R.; Chen, J. L.; Corley, D. G.; Larsen, L. K.; Moore, B. S.; Patterson, G. M. L.; Paul, V. J.; Stewart, J. B.; Williams, D. E. *Pure Appl. Chem.* **1989,** *61,* 521–524. doi:10.1351/pac198961030521
4. Carmichael W. W. *Handbook of Natural Toxins*; Tu, A. T.; Ed.; Marcel Dekker: New York, 1988; pp. 121 ff.
5. Umezawa, H.; Aoyagi, T.; Suda, H.; Hamada, M.; Takeuchi, T. *J. Antibiot.* **1976,** *29,* 97–99. doi:10.7164/antibiotics.29.97
6. Nakamura, H.; Suda, H.; Takita, T.; Aoyagi, T.; Umezawa, H. *J. Antibiot.* **1976,** *29,* 102–103. doi:10.7164/antibiotics.29.102
7. Sekizawa, R.; Iinuma, H.; Muraoka, Y.; Naganawa, H.; Kinoshita, N.; Nakamura, H.; Hamada, M.; Takeuchi, T.; Umezawa, K. *J. Nat. Prod.* **1996,** *59,* 232–236. doi:10.1021/np960067t
8. Tsuda, M.; Muraoka, Y.; Takeuchi, T. *J. Antibiot.* **1996,** *49,* 1031–1035. doi:10.7164/antibiotics.49.1031
9. Nicolau, K. C.; Dai, W.-M.; Guy, R. K. *Angew. Chem., Int. Ed.* **1994,** *33,* 15–44. doi:10.1002/anie.199400151
10. Bunnage, M. E.; Burke, A. J.; Davies, S. G.; Goodwin, C. J. *Tetrahedron: Asymmetry* **1994,** *5,* 203–206. doi:10.1016/S0957-4166(00)86173-X
11. Li, G.; Chang, H.-T.; Sharpless, K. B. *Angew. Chem., Int. Ed.* **1996,** *35,* 451–454. doi:10.1002/anie.199604511
12. Chandrasekhar, S.; Mohapatra, S.; Yadav, J. S. *Tetrahedron* **1997,** *8,* 4089–4099. doi:10.1016/S0957-4166(97)00595-8
13. Sugimura, H.; Miura, M.; Yamada, N. *Tetrahedron: Asymmetry* **1997,** *8,* 4089–4099. doi:10.1016/S0957-4166(97)00595-8
14. Righi, G.; Chionne, A.; D'Achille, R.; Bonini, C. *Tetrahedron: Asymmetry* **1997,** *8,* 903–907. doi:10.1016/S0957-4166(97)00056-6
15. Jeffords, C. W.; Mcnulty, J.; Lu, Z. H.; Wang, J. B. *Helv. Chim. Acta* **1996,** *79,* 1203–1216. doi:10.1002/hlca.19960790426
16. Ha, H. J.; Ahn, Y. G.; Woo, J. S.; Lee, G. S.; Lee, W. K. *Bull. Chem. Soc. Jpn.* **2001,** *74,* 1667–1672. doi:10.1246/bcsj.74.1667
17. Gassa, F.; Contini, A.; Fontana, G.; Pellegrino, S.; Gelmi, M. L. *J. Org. Chem.* **2010,** *75,* 7099–7106. doi:10.1021/jo1011762
18. Wee, A. G. H.; McLeod, D. D. *J. Org. Chem.* **2003,** *68,* 6268–6273. doi:10.1021/jo034334t
19. Tuch, A.; Saniere, M.; Merrer, Y. L.; Depezay, J.-C. *Tetrahedron: Asymmetry* **1996,** *7,* 2901–2909. doi:10.1016/0957-4166(96)00381-3
20. Bergmeier, S. C.; Stanchina, D. M. *J. Org. Chem.* **1999,** *64,* 2852–2859. doi:10.1021/jo9823893
21. Shirode, N. M.; Deshmukh, A. R. A. S. *Tetrahedron* **2006,** *62,* 4615–4621. doi:10.1016/j.tet.2006.01.082
22. Kalamkar, N. B.; Kasture, V. M.; Dhavale, D. D. *Tetrahedron Lett.* **2010,** *51,* 6745–6747. doi:10.1016/j.tetlet.2010.10.086
23. Kalamkar, N. B.; Kasture, V. M.; Dhavale, D. D. *J. Org. Chem.* **2008,** *73,* 3619–3622. doi:10.1021/jo702749r
24. Dhavale, D. D.; Markad, S. D.; Karanjule, N. S.; Prakasha Reddy, J. *J. Org. Chem.* **2004,** *69,* 4760–4766. doi:10.1021/jo049509t
25. Karanjule, N. S.; Markad, S. D.; Dhavale, D. D. *J. Org. Chem.* **2006,** *71,* 6273–6276. doi:10.1021/jo060823s
26. Karanjule, N. S.; Markad, S. D.; Shinde, V. S.; Dhavale, D. D. *J. Org. Chem.* **2006,** *71,* 4667–4670. doi:10.1021/jo0601617
27. Dhavale, D. D.; Ajish Kumar, K. S.; Chaudhari, V. D.; Sharma, T.; Sabharwal, S. G.; Prakasha, R. *Org. Biomol. Chem.* **2005,** *3,* 3720–3726. doi:10.1039/b509216g
28. Ajish Kumar, K. S.; Chaudhari, V. D.; Puranik, V. G.; Dhavale, D. D. *Eur. J. Org. Chem.* **2007,** 4895–4901. doi:10.1002/ejoc.200700461
29. Pawar, N. J.; Parihar, V.; Chavan, S.; Joshi, R.; Joshi, P. V.; Sabharwal, S. G.; Puranik, V. G.; Dhavale, D. D. *J. Org. Chem.* **2012,** *77,* 7873–7882. doi:10.1021/jo3009534
30. Sato, K.-i.; Akai, S.; Sakuma, M.; Kojima, M.; Suzuki, K.-j. *Tetrahedron Lett.* **2003,** *44,* 4903–4907. doi:10.1016/S0040-4039(03)01098-0
31. Hanessian, S. *Total Synthesis of Natural Products: The "Chiron" Approach;* Pergamon Press: Oxford, 1983.
32. Patil, N. T.; John, S.; Sabharwal, S. G.; Dhavale, D. D. *Bioorg. Med. Chem.* **2002,** *10,* 2155–2160. doi:10.1016/S0968-0896(02)00073-1
33. Bindra, J.; Grodski, A. *J. Org. Chem.* **1978,** *43,* 3240. doi:10.1021/jo00410a031
34. Mane, R. S.; Ajish Kumar, K. S.; Dhavale, D. D. *J. Org. Chem.* **2008,** *73,* 3284–3287. doi:10.1021/jo800044r
35. Thompson, A. S.; Humphrey, G. R.; DeMarco, A. M.; Marthe, D. J.; Grabowaski, E. J. J. *J. Org. Chem.* **1993,** *58,* 5886–5888. doi:10.1021/jo00074a008
36. Carlsen, P. J. H.; Katsuki, T.; Martin, V. S.; Sharpless, K. B. *J. Org. Chem.* **1981,** *46,* 3936–3938. doi:10.1021/jo00332a045

License and Terms

This is an Open Access article under the terms of the Creative Commons Attribution License (http://creativecommons.org/licenses/by/2.0), which permits unrestricted use, distribution, and reproduction in any medium, provided the original work is properly cited.

The license is subject to the *Beilstein Journal of Organic Chemistry* terms and conditions: (http://www.beilstein-journals.org/bjoc)

The definitive version of this article is the electronic one which can be found at: doi:10.3762/bjoc.10.59

Beilstein Journal of Organic Chemistry

Asymmetric total synthesis of a putative sex pheromone component from the parasitoid wasp *Trichogramma turkestanica*

Danny Geerdink[1], Jeffrey Buter[1], Teris A. van Beek[2] and Adriaan J. Minnaard[*1]

Full Research Paper

Open Access

Address:
[1]Stratingh Institute for Chemistry, University of Groningen, Nijenborgh 7, 9747 AG, Groningen, The Netherlands and [2]Natural Products Chemistry Group, Laboratory of Organic Chemistry, Wageningen University, Dreijenplein 8, 6703 HB Wageningen, The Netherlands

Email:
Adriaan J. Minnaard* - a.j.minnaard@rug.nl

* Corresponding author

Keywords:
asymmetric catalysis; copper; deoxypropionates; natural products; sex pheromone; *Trichogramma turkestanica*

Beilstein J. Org. Chem. **2014,** *10,* 761–766.
doi:10.3762/bjoc.10.71

Received: 17 December 2013
Accepted: 04 March 2014
Published: 02 April 2014

This article is part of the Thematic Series "Natural products in synthesis and biosynthesis".

Guest Editor: J. S. Dickschat

© 2014 Geerdink et al; licensee Beilstein-Institut.
License and terms: see end of document.

Abstract

Virgin females of the parasitoid wasp *Trichogramma turkestanica* produce minute amounts of a sex pheromone, the identity of which has not been fully established. The enantioselective synthesis of a putative component of this pheromone, (6*S*,8*S*,10*S*)-4,6,8,10-tetramethyltrideca-2*E*,4*E*-dien-1-ol (**2**), is reported as a contribution to this identification. Catalytic asymmetric conjugate addition of methylmagnesium bromide and stereoselective Horner–Wadsworth–Emmons olefinations are used as the key steps, and **2** was obtained in 16 steps with an overall yield of 4.4%.

Introduction

Communication by means of pheromones is common in many animal species. For instance, many insects secrete air-borne volatiles to attract a mate for generating offspring [1,2]. In 2005, one of us reported the isolation and partial characterization of the putative sex pheromone of *Trichogramma turkestanica*, a parasitoid wasp [3]. These wasps, belonging to the large Trichogrammatidae family, are minute in size (0.5 mm, 8 µg adult weight) as well as morphologically similar making a taxonomic characterization at the species level difficult [4]. A classification on the basis of sex pheromones might help in this respect.

Apart from the above reason and the scientific challenge to elucidate the identity of a complex pheromone at the low nanogram level, an additional reason to study these tiny wasps is their possible application in an environmentally friendly way of crop protection [5]. After copulation, the female wasp deposits the fertilized eggs inside the eggs of a host insect,

which is used as a food source for the hatched wasps. Biological studies have revealed that only virgin females are able to trigger casting behavior in males, which has led to the assumption that virgin females of *Trichogramma turkestanica* produce a sex pheromone. Analysis of headspace volatiles of virgin females, collected via solid-phase microextraction, showed the presence of two sex specific components which were regarded to play an important role in this sex pheromone. After extensive analysis by mass spectrometry and derivatisation studies, the natural products were postulated to be 2,6,8,12-tetrametyltrideca-2,4-diene (**A**) and 2,6,8,12-tetramethyltrideca-2,4-dien-1-ol (**B**) (Figure 1) [3]. Stereochemical assignments were lacking. Subsequent synthesis of reference compounds led to revision of the structures, and as a result, the compounds were unambiguously identified to be (2*E*,4*E*)-*syn*,*syn*-4,6,8,10-tetramethyltrideca-2,4-diene (**1**) and (2*E*,4*E*)-*syn*,*syn*-4,6,8,10-tetramethyltrideca-2,4-dien-1-ol (**2**, Figure 1) [6]. The absolute configurations of the putative pheromone components, however, remained unknown. To solve this problem we undertook the stereoselective synthesis of **2**, thereby arbitrarily choosing the all-*S* configuration.

Results and Discussion

Nowadays, a number of efficient strategies is available for the synthesis of deoxypropionates [7-15]. Our approach [16] is based on copper-catalyzed asymmetric conjugate addition of methylmagnesium bromide to α,β-unsaturated thioesters and has proven its versatility [17-19]. Arrays of up to eight methyl substituents have been constructed [20]. Starting from **3**, the first conjugate addition using *(R,S*$_{Fe}$*)*-**L1** afforded **4**, as expected in high yield and excellent enantiomeric excess (Scheme 1). Reduction with DIBALH, followed by Horner–Wadsworth–Emmons olefination and again asymmetric conjugate addition gave **6** in 77% yield over three steps. To ultimately remove the carbonyl function, we introduced the third methyl ramification in α,β-unsaturated ketone **7**, preparation of which was straightforward [21]. Conjugate addition to **7** using the conditions from step A proved clearcut and gave **8**

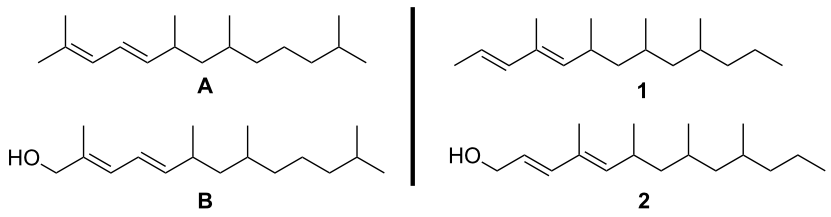
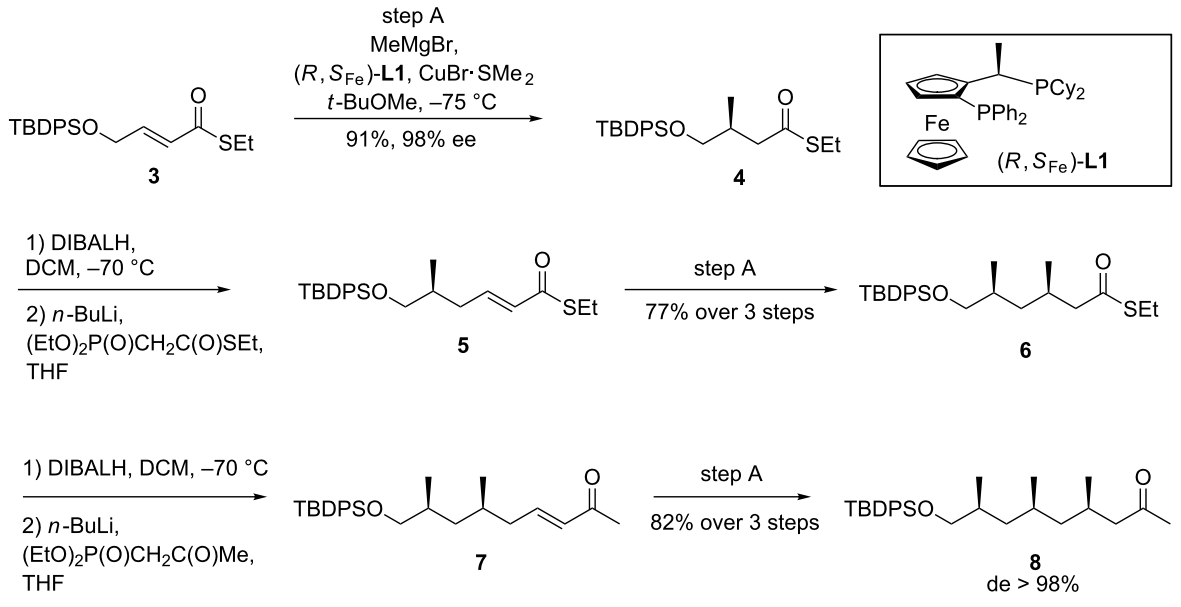


Figure 1: Originally proposed structures **A** and **B** and revised structures **1** and **2** of putative sex pheromone components of *Trichogramma turkestanica*.

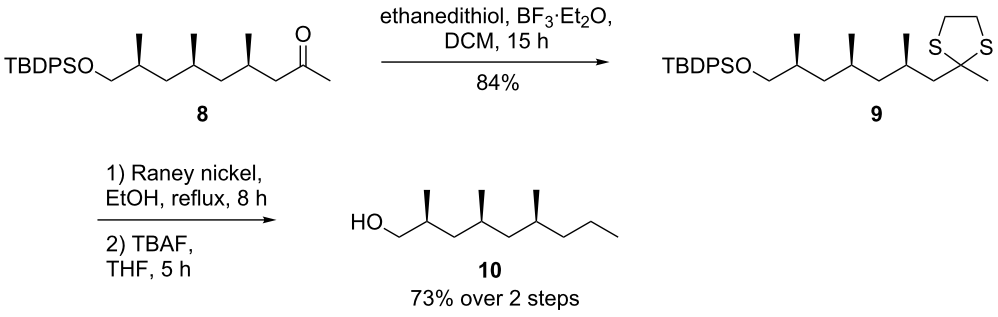


Scheme 1: Application of the iterative conjugate addition protocol for the preparation of **8**.

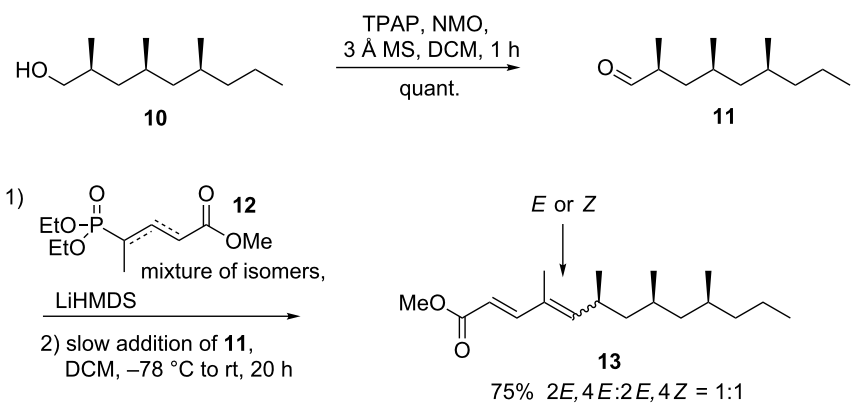
in 82% yield over three steps from **6**. Both the enantiomeric excess and the diastereomeric excess of **8** were excellent which is important as the response of insects to their pheromones can be highly sensitive to the stereoisomeric composition.

A number of procedures exist to reduce ketones to their corresponding methylene groups. Initial attempts focused on the formation and subsequent removal of the corresponding hydrazones. Regrettably, the Myers modification of the Wolf–Kishner reduction did not afford detectable amounts of **10** [22]. Also the modification of Caglioti proved only moderately successful with 30% isolated yield of **10** over two steps [23]. As an alternative deoxygenation procedure, we relied on the so-called Mozingo reduction. Although the procedure for dithiane formation has been reported to be catalytic in Lewis acid, we found a linear correlation between the amount of $BF_3{\cdot}Et_2O$ used and the conversion (Scheme 2) [24]. The use of 1.2 equiv of $BF_3{\cdot}Et_2O$ led to **9** in 84% isolated yield. Reduction of **9** with freshly prepared Raney nickel and subsequent desilylation afforded **10** over two steps in 73% yield.

To introduce the desired *E,E*-diene present in **2** and **1**, we realized that the procedure reported by Markiewicz, comprising a vinylogous Horner–Wadsworth–Emmons olefination, offered in principle a very efficient procedure to obtain dienoate **13** (Scheme 3), and would leave only a single step in the synthesis of **2** [25]. Therefore, reagent **12** was prepared in two steps. After quantitative conversion of **10** into **11** using Ley–Griffith oxidation, its reaction with **12**, using LiHMDS as the base, afforded **13** in 75% yield, though as a 1:1 mixture of 2*E*,4*E*- and 2*E*,4*Z*-isomers. Moreover, the ^{1}H NMR spectra indicated the presence of an impurity, which appeared as a multiplet between 5.00 and 5.45 ppm. Although minimal amounts of 2*E*,4*Z*-**13** could be isolated, 2*E*,4*E*-**13** was inseparable from this impurity. We decided to continue the synthesis with impure **13**, which was reduced with DIBALH at low temperature to give crude **1** in 96% yield. TLC analysis indicated the presence of two major, separable, products. Purification by flash-column chromatography over either silica gel or neutral aluminium oxide, however, led to rapid degradation of **2**. In the process, we were unable to isolate a pure sample of either isomer. This approach was ultimately abandoned, and only delivered the knowledge that **2** is unstable upon purification by column chromatography. This sensitivity to acid has been reported before for similar compounds [26], and can be explained by the readily formed dienyl cation.



Scheme 2: Deoxygenation and desilylation of **8**.

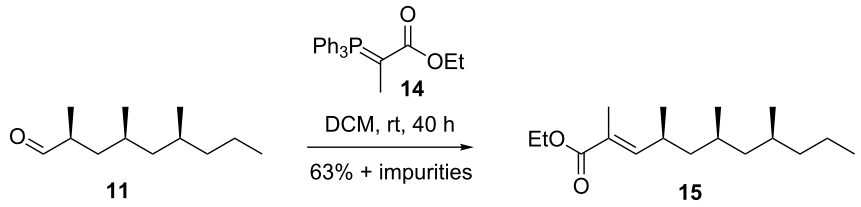


Scheme 3: Vinylogous Horner–Wadsworth–Emmons olefination.

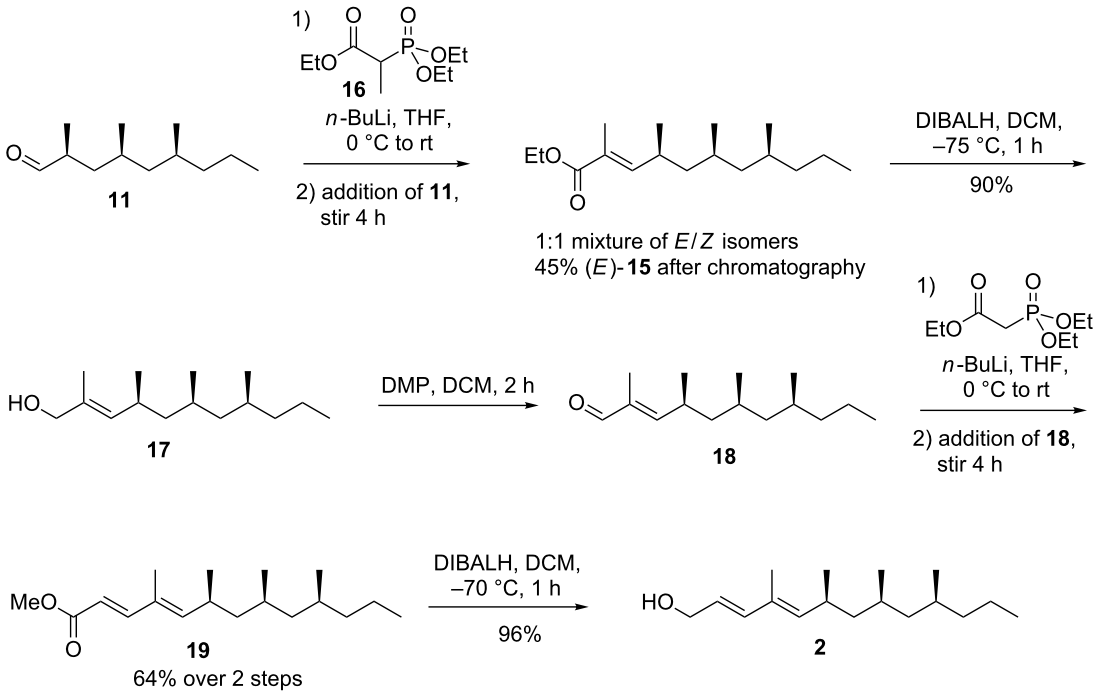
We realized that, in order to obtain a pure sample of **2**, it was essential to avoid chromatographic purification after the final step. As the reduction of **13** with DIBALH is a clean reaction, affording essentially pure **2** after work-up, the preparation of pure **13** was highly desirable. A stepwise olefination approach was therefore considered.

Wittig reaction of aldehyde **11** with phosphorane **14** to give **15** was carried out first (Scheme 4) [27]. Next to ~60% of the desired product, around 40% of the mass balance consisted of an inseparable impurity. ^{1}H NMR spectroscopy again showed a set of multiplets between 4.95–5.00 ppm. Although repeated recrystallization of commercial reagent **14** reduced the impurity to 6%, pure **15** could not be obtained, not even with freshly prepared **14**. Moreover, in none of the successive steps the impurity could be separated and therefore also this approach was abandoned. Although NMR and GC–MS analysis of the mixture gave no conclusive evidence for the nature of the impurity, double bond isomers of **15** could account for the observed ^{1}H NMR signals.

As the Wittig reaction of **11** did afford **15**, although with the simultaneous formation of an inseparable side-product, we were curious to see how the analogous Horner–Wadsworth–Emmons olefination towards **15** would perform. Thus, aldehyde **11** was freshly prepared and subjected to the conjugate base of **16** (Scheme 5). This olefination proved to be much faster, but afforded **15** as a 1:1 mixture of *E*- and *Z*-isomers as determined by ^{1}H NMR spectroscopy. This is attributed to a destabilizing interaction of the α-methyl moiety of the HWE reagent in the transient four-centered intermediate, leading to a mixture of double bond isomers. The impurity previously observed as a result of the Wittig reaction was not present. In addition, the *E*- and *Z*-isomers could be separated using column chromatog-



Scheme 4: Synthesis of α,β-unsaturated ester **15** using a Wittig reaction.



Scheme 5: Completion of the synthesis of the putative sex pheromone **2**.

raphy affording pure *E*-**15** in 45% yield. Reduction of **15** was achieved using DIBALH, affording allylic alcohol **17** in 90% yield, which in turn was oxidized to aldehyde **18** using Dess–Martin periodinane. Given that the conversion of **18** into **19** using a Wittig reaction had proven to be sluggish, we switched again to a Horner–Wadsworth–Emmons olefination, expecting to observe high *E*-selectivity. Indeed, **19** was obtained in 64% yield over two steps, as the pure *E,E*-isomer. Reduction of pure **19** with DIBALH finally afforded **2** in 96% yield after work-up. The compound showed to be identical to the natural product and *rac*-**2** prepared in the accompanying paper [6] on the basis of two GC retention times (polar and nonpolar column) and mass spectrum.

Conclusion

In summary, after two unsuccessful attempts, (*E,E,S,S,S*)-**2** has been obtained in a linear sequence of 16 steps and 4.4% overall yield. As the absolute configuration of natural **2** is yet unknown, comparison of natural **2** with now available synthetic enantiopure and racemic **2** will be the next step. Separation of racemic **2** by chiral GC has up till now shown impossible, however. The preparation of deoxy analogue **1** is currently part of our investigations.

Supporting Information

Supporting Information File 1

Detailed experimental procedures and spectral data of all new compounds.
[http://www.beilstein-journals.org/bjoc/content/supplementary/1860-5397-10-71-S1.pdf]

Acknowledgements

This work was financially supported by The Netherlands Organization for Scientific Research (NWO-CW). Mr. K. Ward of Ward Illustration is acknowledged for providing artwork.

References

1. Wyatt, T. D. *Pheromones and animal behaviour: communication by smell and taste;* Cambridge University Press: Cambridge, 2003; p 371. doi:10.1017/CBO9780511615061
2. Schulz, S., Ed. *The Chemistry of Pheromones and other Semiochemicals, part I & II;* Springer Verlag: Berlin Heidelberg, 2004.
3. van Beek, T. A.; Silva, I. M. M. S.; Posthumus, M. A.; Melo, R. *J. Chromatogr., A* **2005,** *1067,* 311–321. doi:10.1016/j.chroma.2004.09.030
4. Silva, I. M. M. S.; Honda, J.; van Kan, F.; Hu, J.; Neto, L.; Pintureau, B.; Stouthamer, R. *Biol. Control* **1999,** *16,* 177–184. doi:10.1006/bcon.1999.0755
5. Smith, S. M. *Annu. Rev. Entomol.* **1996,** *41,* 375–406. doi:10.1146/annurev.en.41.010196.002111
6. Tröger, A.; van Beek, T. A.; Huigens, M. E.; Silva, I. M. M. S.; Posthumus, M. A.; Francke, W. *Beilstein J. Org. Chem.* **2014,** *10,* 767–773. doi:10.3762/bjoc.10.72
7. ter Horst, B.; Feringa, B. L.; Minnaard, A. J. *Chem. Commun.* **2010,** *15,* 2535–2547. doi:10.1039/b926265b
8. Barroso, S.; Minnaard, A. J. *Asymmetric Catalysis in the total synthesis of Lipids and polyketides*. In *Asymmetric Synthesis II: More Methods and Applications;* Christmann, M.; Bräse, S., Eds.; Wiley-VCH: Weinheim, Germany, 2012; pp 213–219. doi:10.1002/9783527652235.ch27
9. Nakamura, T.; Harachi, M.; Kano, T.; Mukaeda, Y.; Hosokawa, S. *Org. Lett.* **2013,** *15,* 3170–3173. doi:10.1021/ol401406m
10. Diez, P. S.; Micalizio, G. C. *Angew. Chem., Int. Ed.* **2012,** *51,* 5152–5156. doi:10.1002/anie.201200035
11. Weise, C. F.; Pischl, M. C.; Pfaltz, A.; Schneider, C. *J. Org. Chem.* **2012,** *77,* 1477–1488. doi:10.1021/jo202330b
12. Weise, C. F.; Pischl, M. C.; Pfaltz, A.; Schneider, C. *Chem. Commun.* **2011,** *47,* 3248–3250. doi:10.1039/c0cc05215a
13. Pischl, M. C.; Weise, C. F.; Mueller, M.-A.; Pfaltz, A.; Schneider, C. *Angew. Chem., Int. Ed.* **2013,** *52,* 8968–8972. doi:10.1002/anie.201303776
14. Herber, C.; Breit, B. *Angew. Chem., Int. Ed.* **2005,** *44,* 5267–5269. doi:10.1002/anie.200501612
15. Schmidt, Y.; Breit, B. *Org. Lett.* **2009,** *11,* 4767–4769. doi:10.1021/ol901591t
16. Des Mazery, R.; Pullez, M.; López, F.; Harutyunyan, S. R.; Minnaard, A. J.; Feringa, B. L. *J. Am. Chem. Soc.* **2005,** *127,* 9966–9967. doi:10.1021/ja053020f
17. Barroso, S.; Castelli, R.; Baggelaar, M. P.; Geerdink, D.; ter Horst, B.; Casas-Arce, E.; Overkleeft, H. S.; van der Marel, G. A.; Codée, J. D. C.; Minnaard, A. J. *Angew. Chem., Int. Ed.* **2012,** *51,* 11774–11777. doi:10.1002/anie.201206221
18. ter Horst, B.; Feringa, B. L.; Minnaard, A. J. *Org. Lett.* **2007,** *9,* 3013–3015. doi:10.1021/ol071078o
19. Barroso, S.; Geerdink, D.; ter Horst, B.; Casas-Arce, E.; Minnaard, A. J. *Eur. J. Org. Chem.* **2013,** 4642–4654. doi:10.1002/ejoc.201300437
20. Geerdink, D.; ter Horst, B.; Lepore, M.; Mori, L.; Puzo, G.; Hirsch, A. K. H.; Gilleron, M.; de Libero, G.; Minnaard, A. J. *Chem. Sci.* **2013,** *4,* 709–716. doi:10.1039/c2sc21620e
21. Matcha, K.; Madduri, A. V. R.; Roy, S.; Ziegler, S.; Waldmann, H.; Hirsch, A. K. H.; Minnaard, A. J. *ChemBioChem* **2012,** *13,* 2537–2548. doi:10.1002/cbic.201200512
22. Furrow, M. E.; Myers, A. G. *J. Am. Chem. Soc.* **2004,** *126,* 5436–5445. doi:10.1021/ja049694s
23. Caglioti, L. *Tetrahedron* **1966,** *22,* 487–493. doi:10.1016/0040-4020(66)80015-7
24. Srikrishna, A.; Ravi, G.; Satyanarayana, G. *Tetrahedron Lett.* **2007,** *48,* 73–76. doi:10.1016/j.tetlet.2006.11.011
25. Markiewicz, J. T.; Schauer, D. J.; Löfstedt, J.; Corden, S. J.; Wiest, O.; Helquist, P. *J. Org. Chem.* **2010,** *75,* 2061–2064. doi:10.1021/jo902422y
26. Hoecker, J.; Gademann, K. *Org. Lett.* **2013,** *15,* 670–673. doi:10.1021/ol303502a
27. Jessen, H. J.; Schumacher, A.; Shaw, T.; Pfaltz, A.; Gademann, K. *Angew. Chem., Int. Ed.* **2011,** *50,* 4222–4226. doi:10.1002/anie.201007671

License and Terms

This is an Open Access article under the terms of the Creative Commons Attribution License (http://creativecommons.org/licenses/by/2.0), which permits unrestricted use, distribution, and reproduction in any medium, provided the original work is properly cited.

The license is subject to the *Beilstein Journal of Organic Chemistry* terms and conditions: (http://www.beilstein-journals.org/bjoc)

The definitive version of this article is the electronic one which can be found at: doi:10.3762/bjoc.10.71

Beilstein Journal of Organic Chemistry

Structure elucidation of female-specific volatiles released by the parasitoid wasp *Trichogramma turkestanica* (Hymenoptera: Trichogrammatidae)

Armin Tröger[1], Teris A. van Beek[2], Martinus E. Huigens[3], Isabel M. M. S. Silva[3], Maarten A. Posthumus[2] and Wittko Francke[*1]

Full Research Paper

Open Access

Address:
[1]Institute of Organic Chemistry, University of Hamburg, Martin-Luther-King Platz 6, D-20146 Hamburg, Germany, [2]Laboratory of Organic Chemistry, Wageningen University, Dreijenplein 8, 6703 HB Wageningen, The Netherlands and [3]Laboratory of Entomology, Wageningen University, P.O. Box 8031, 6700 EH Wageningen, The Netherlands

Email:
Wittko Francke[*] - francke@chemie.uni-hamburg.de

* Corresponding author

Keywords:
natural products; structure elucidation; sex specific; *Trichogramma turkestanica*; volatile deoxypropionates

Beilstein J. Org. Chem. **2014,** *10,* 767–773.
doi:10.3762/bjoc.10.72

Received: 17 December 2013
Accepted: 07 March 2014
Published: 02 April 2014

This article is part of the Thematic Series "Natural products in synthesis and biosynthesis".

Guest Editor: J. S. Dickschat

© 2014 Tröger et al; licensee Beilstein-Institut.
License and terms: see end of document.

Abstract

Females of the parasitoid wasp *Trichogramma turkestanica* produce the putative polydeoxypropionates (2*E*,4*E*,6*S*,8*S*,10*S*)-4,6,8,10-tetramethyltrideca-2,4-diene and (2*E*,4*E*,6*S*,8*S*,10*S*)-4,6,8,10-tetramethyltrideca-2,4-dien-1-ol or their enantiomers as sex specific volatiles. The structures were assigned on the basis of GC–MS investigations using synthetic reference compounds.

Introduction

Wasps of the genus *Trichogramma* (Hymenoptera: Trichogrammatidae) are egg parasitoids of insect eggs [1]. They are commercially used as biological control agents against many insect pests, worldwide [2]. The taxonomy of *Trichogramma* wasps is hampered by their particularly small size and by strong morphological similarities between the species. Several attempts, including chemotaxonomic approaches, have been made to solve this problem [3-5]. While it is generally accepted that parasitoid wasps use chemical cues for host location [6], little is known about (volatile) semiochemicals playing a role in intraspecific communication [7-11].

Based on bioassays with *Trichogramma turkestanica* and extensive analytical investigations, two female-specific volatile compounds have been described as possible pheromone components and were tentatively identified as the hydrocarbon 2,6,8,12-tetramethyltrideca-2,4-diene (**A**) and the corresponding allylic alcohol 2,6,8,12-tetramethyltrideca-2,4-diene-1-

ol (**B**) [12]. Since the two proposed structures were deduced from analytical data only, the aim of the present study was to scrutinize these suggestions by unambiguous synthesis.

Results and Discussion

The 70 eV EI mass spectra of the two natural products **A** and **B** are depicted in Figure 1 [12]. Because the carbon skeleton had been reported to be the same in both compounds, we used the hydrocarbon **A** as the first target for the preparation of a reference sample. As an initial approach we aimed at the synthesis of a library of stereoisomers of **A** (Figure 2).

The commercially available racemic *anti*-dimethyl 2,4-dimethylglutarate (**1**) was reduced to the corresponding racemate of 2,4-dimethylpentan-1,5-diol (**2**) [13], which was further transformed to the monosilyl ether **3** and subsequently to the corresponding tosylate **4**. Using 3-methylbutylmagnesium bromide and applying cuprate chemistry [14], **4** was chain elongated to **5**, which was deprotected to yield *anti*-2,4,8-trimethylnonanol (**6**). After oxidation to the corresponding aldehyde, the stereogenic center at position 2 underwent ca. 6% epimerization to yield **7** as a mixture of 4 stereoisomers. The synthesis of 2,6,8,12-tetramethyltrideca-2,4-diene (**8**) was completed by Wittig reaction using (3-methylbut-2-en-1-yl)triphenylphosphonium bromide [15]. As expected, the obtained mixture of all possible stereoisomers of **8** showed an *E*/*Z*-ratio of ca. 2:1 and was highly dominated by the *anti*-isomers (see Supporting Information File 1, Figure S1). The *E*/*Z*-isomers of the two pairs of diastereomers could be separated by gas chromatography. Analysis by coupled gas chromatography/mass spectrometry (GC–MS) showed the 70 eV EI mass spectra of the synthetic compounds to be almost identical. Though the mass spectra of **8** (Figure 3) and that of the natural product **A** (Figure 1) showed strong similarities, small but decisive qualitative and quantitative differences in the fragmentation pattern were obvious. In contrast to the mass spectrum of **A**, those of **8** showed an additional signal at *m*/*z* 180 (loss of isobutene), whereas the signal at *m*/*z* 153, present in the spectrum of **A** was absent. In addition, the pair at *m*/*z* 67 and *m*/*z* 69 showed different relative abundances.

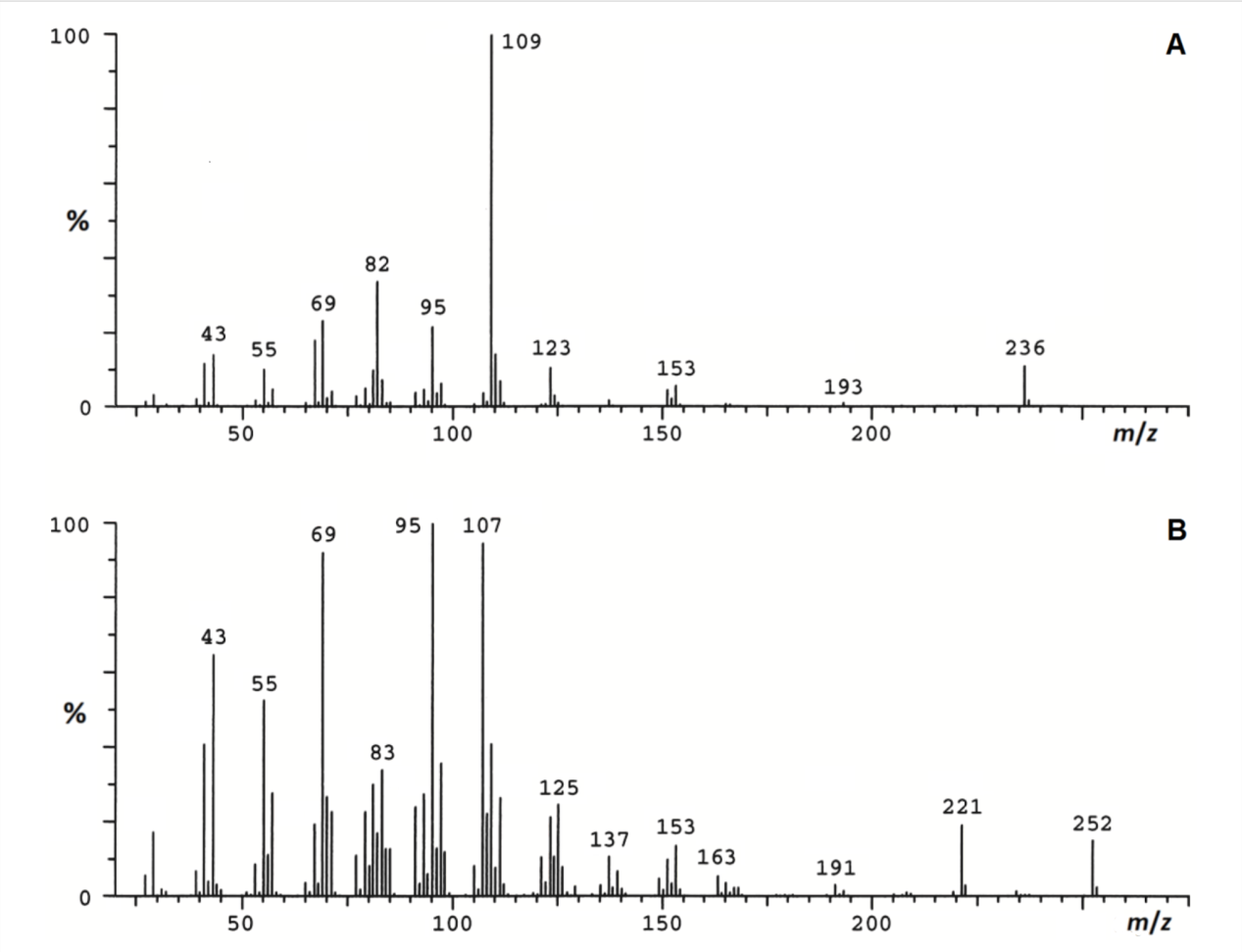


Figure 1: Published 70 eV EI mass spectra of the naturally occurring compounds **A** and **B** [12].

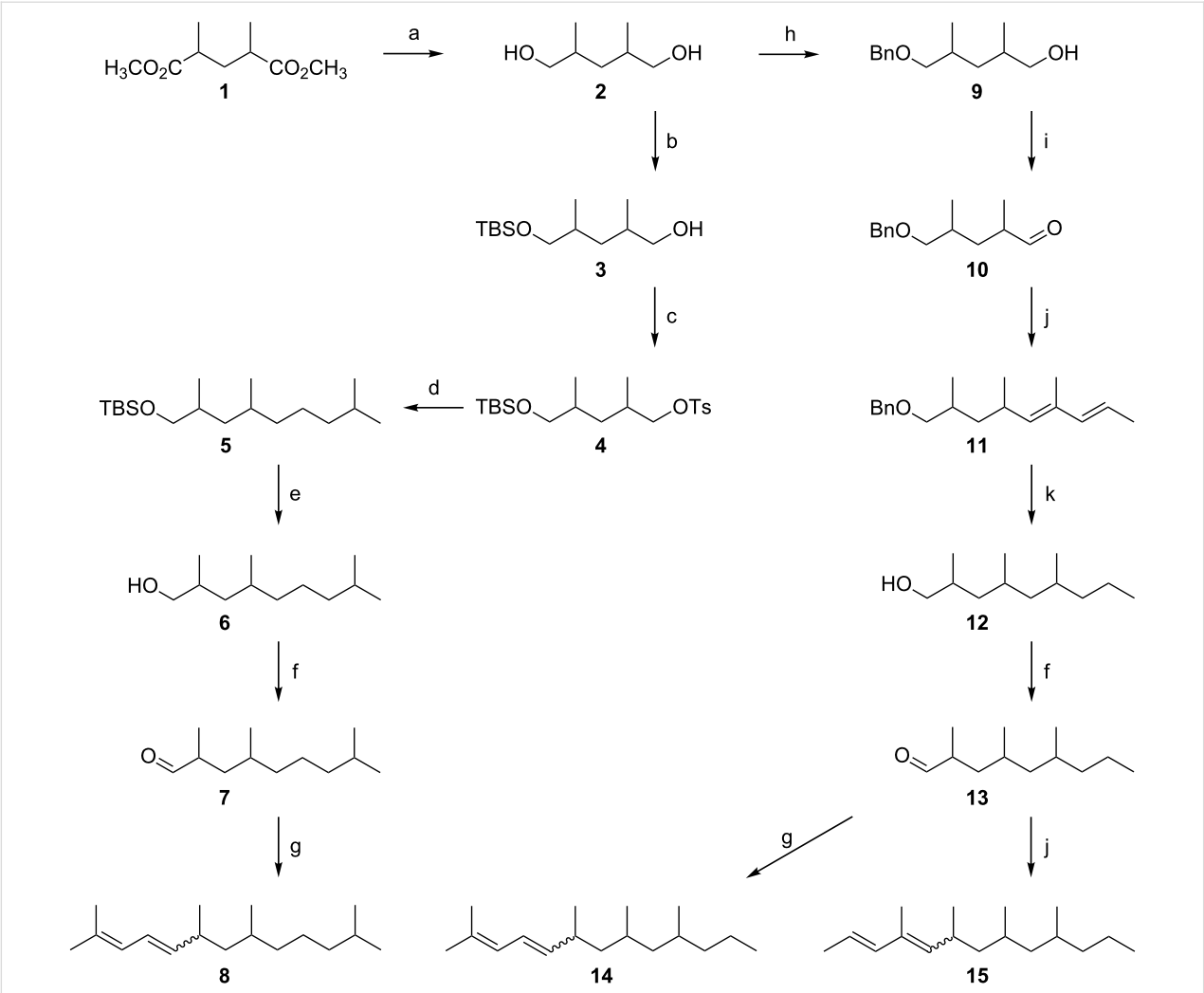


Figure 2: Synthesis of tetramethyltrideca-2,4-dienes **8**, **14** and **15**. Conditions: a: $LiAlH_4$, Et_2O, −30 °C to rt, 12 h; b: 1) NaH, THF, −20 °C to rt 1 h; 2) TBDMSCl (1 equiv), rt, 10 h; c: *p*-TsCl, DMAP, TEA, DCM, −20 °C to rt, 12 h; d: (3-methylbutyl)magnesium bromide, CuI, THF, −90 °C to rt, 16 h; e: TBAF, THF, rt, 14 h; f: PDC, MS 4 Å, DCM, −20 °C, 90 min; g: (3-methylbut-2-en-1-yl)triphenylphosphonium bromide, *n*-BuLi, THF, −40 °C to rt 16 h; h: 1) NaH, THF, −20 °C to rt, 1 h; 2) BnBr (1 equiv), *n*-Bu_4NI, 0 °C to rt, 16 h; i: PCC, MS 4 Å, DCM, −20°C, 90 min; j: [(*E*)-1-methylbut-2-en-1-yl]triphenylphosphonium bromide, *n*-BuLi, THF, −40 °C, 14 h; k: H_2, 20 bar, 10% Pd/C, pentane, rt, 18 h.

Thus, it was obvious that the structures published for the natural products needed modification. Sticking to the basic carbon skeleton proposed for **A** and **B** [12], we looked for a plausible biogenetic way providing an alternative structure for **A** from reasonable building blocks without too much changing of **8**. Methyl branching at positions 6 and 8 was indicated by pronounced signals at *m*/*z* 123 = M^+ − 113 and *m*/*z* 151 = M^+ − 85 in the mass spectrum of **A** [12] (Figure 1), which we regarded to result from loss of the last eight or six carbons, respectively. Therefore, we kept this feature in the structure of the next candidate. Leaving the dienic system unchanged, we consequently decided to shift the methyl group from position 12 in **8** to position 10. As a result, our next candidate was 2,6,8,10-tetramethyltrideca-2,4-diene (**14**), because the formation of such a polydeoxypropionate by condensation of four units of methylmalonate, followed by chain elongation with malonate and another methylmalonate (including deoxygenation steps) seemed to be plausible [16]. These biogenetic considerations excluded methyl groups at positions 9 and 11.

To prepare a mixture of all stereoisomers of **14**, we again used **2** as the starting material (Figure 2). Monobenzylation to **9**, followed by oxidation, yielded the aldehyde **10**, which was chain elongated by Wittig reaction with [(2*E*)-1-methylbut-2-en-1-yl]triphenylphosphonium bromide [17] to afford the protected dienol **11** as a mixture of 4 racemates. This was due to partial epimerization at position 2 of the aldehyde **10** and the less selective Wittig coupling. Consequently, hydrogenation of **11** yielded a mixture of all 8 possible stereoisomers of the saturated alcohol **12**; for relative proportions, see Supporting Infor-

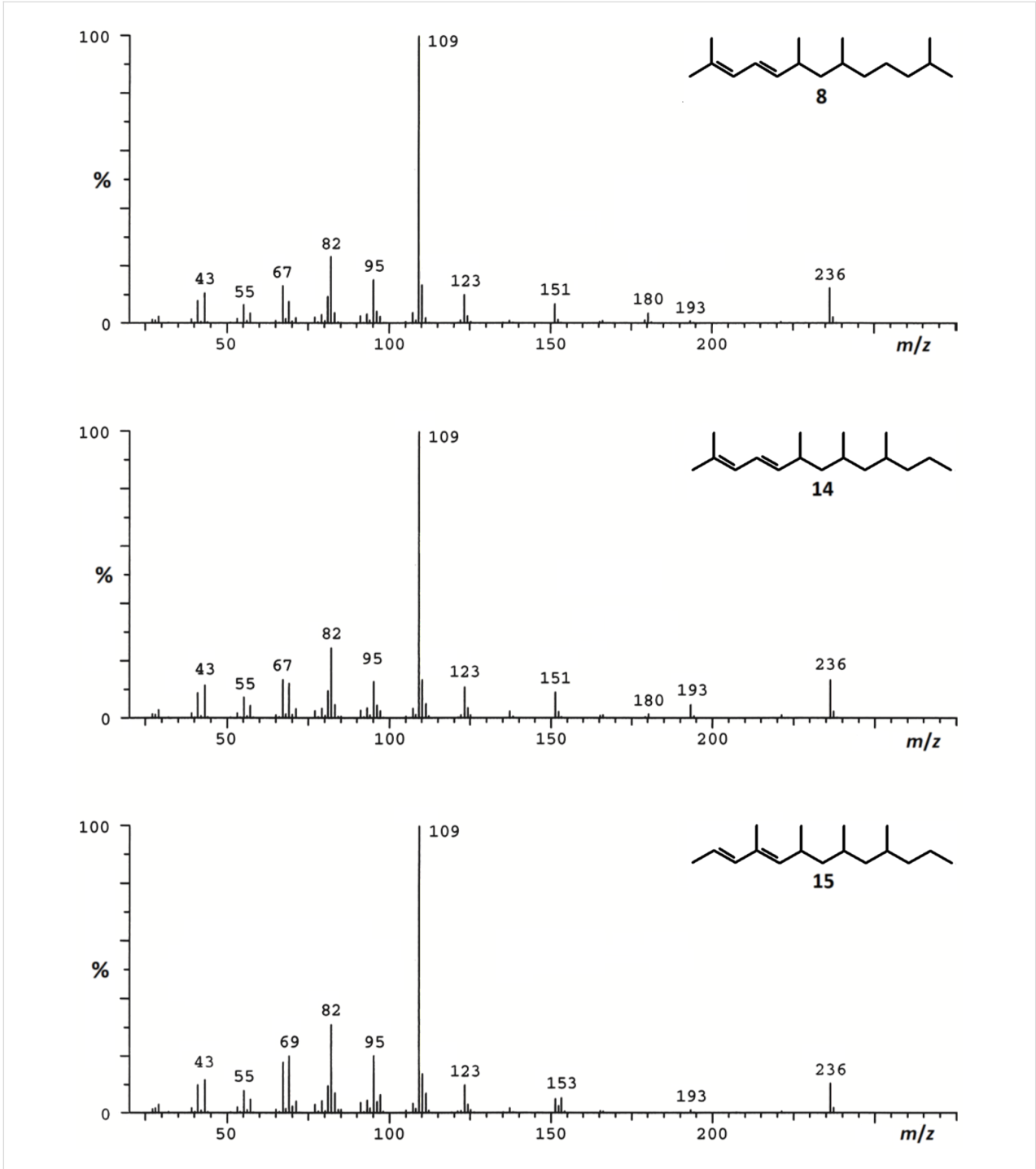


Figure 3: 70 eV EIMS of synthetic tetramethyltrideca-2,4-dienes **8**, **14** and **15**. These spectra were run under the same analytical conditions as described in the original paper [12].

mation File 1. Starting from **12** and following the sequence described for the transformation of **6** to **8**, a mixture of the stereoisomers of the target diene **14** was obtained via 2,4,6-trimethylnonanal (**13**) [15]. GC–MS-analysis of this mixture revealed a 3:1 dominance of the *E*-configurated racemates over the earlier eluting *Z*-series. The chromatogram showed seven well-separated peaks, indicating that only two isomers co-eluted (see Supporting Information File 1, Figure S1). However, it soon became clear that the natural product was not among the synthetic compounds **14**, because their mass spectra basically showed the same differences to that of **A** (presence of *m*/*z* 180, absence of *m*/*z* 153) as did the 2,6,8,12-tetramethyltrideca-2,4-

dienes (**8**) (Figure 1 and Figure 3). In the next approach we considered a structural change in the dienic system of **14** as an additional modification of the published structure of **A**.

As indicated above, the formation of the signal at *m*/*z* 180 in the mass spectra of **8** and **14** may be due to the loss of isobutene – which would be avoided by a shift of the methyl group from carbon 2 to positions 4 or 5. Results of derivatization reactions of the natural product by Diels–Alder reaction with 4-methyl-1,2,4-triazolin-3,5-dione left room for the positioning of a methyl group at carbons 2, 3, 4, or 5 of the chain [12]. Location at position 2 would provide **14**, which was already ruled out. According to a conceivable biosynthesis of the natural product from methylmalonate and acetate, positions 3 and 5 would be less favourable [16]. However, linear condensation of five methylmalonate units and a final malonate (and again corresponding deoxygenation steps) would produce the carbon skeleton of a 4,6,8,10-tetramethyltrideca-2,4-diene (**15**). Thus, from a biosynthetic point of view, the structure would be reasonable and follow established principles.

To test the validity of our assumption, we transformed **13** into **15** by Wittig reaction using [(*E*)-1-methylbut-2-en-1-yl]triphenylphosphonium bromide [17] in the chain elongation step (Figure 2). The reaction yielded a mixture of products representing two quantitatively different series of eight racemic stereoisomers of **15**. According to the *E*-configuration of the double bond in the starting phosphorane and the known *E*-selectivity of the reaction [17], we assigned the (2*E*,4*E*)-configuration to the more abundant and later eluting series of stereoisomers and the (2*E*,4*Z*)-configuration to the less abundant one. The diastereomers could be well separated by GC, and only two members of the less abundant 4*Z*-series co-eluted (see Supporting Information File 1, Figure S1). The mass spectra of **15** were the same as that of the natural product (Figure 1 and Figure 3). Gas chromatographic properties on a non-polar DB-1 and a polar Stabilwax (for conditions see ref. [12]) of the first eluting racemate of the more abundant 4*E*-series matched those of the natural product, strongly indicating (2*E*,4*E*)-configuration of the conjugated double system in the target compound (see Supporting Information File 1, Figure S2).

After the gross structure of the natural product had been found to very likely be (2*E*,4*E*)-4,6,8,10-tetramethyltrideca-2,4-diene (**15**), we had to assign the relative stereochemistry at the three stereogenic centers. Actually, we had to decide between 4 structures: *syn*,*syn*-, *syn*,*anti*-, *anti*,*syn*-, and *anti*,*anti*-configuration of the methyl groups at carbons 6, 8, and 10. Since semiochemicals representing saturated polydeoxypropionates typically show *syn*-configuration, suggesting general principles in enzymatic chain elongation [16,18], we hypothesized (2*E*,4*E*,6*S*,8*S*,10*S*)-tetramethyltrideca-2,4-diene or its enantiomer to be the natural product.

To establish a *syn*,*syn*-configuration of the three chiral centers in our target compound, we followed the way used by Mori and Kuwahara for the synthesis of the mite pheromone lardolure [19], which we had successfully adopted in the synthesis of vittatalactone [20]. Commercially available 2,4,6-trimethylphenol was hydrogenated to form all-*cis*-2,4,6-trimethylcyclohexanone. Subsequent Baeyer–Villiger oxidation, followed by reduction of the obtained lactone, yielded *syn*,*syn*-2,4-dimethylheptan-1,6-diol **16** (Figure 4). Protection of the primary hydroxy group gave **17** followed by a Mitsunobu sequence involving the secondary hydroxy group, afforded **18**. Chain elongation of **18** by applying cuprate chemistry [14] to its mesylate gave **19** which was deprotected to give **20**, which, in turn was oxidized to *syn*,*syn*-2,4,6-trimethylnonanal (**21**). As described for the transformation of **13** into **15** (Figure 2), **21** was chain-elongated to a 1:3-mixture of (2*E*,4*Z*)-*syn*,*syn*- and (2*E*,4*E*)-*syn*,*syn*-4,6,8,10-tetramethyltrideca-2,4-diene (**22**). The stereochemical composition of this defined mixture of stereoisomers of **15** (see Supporting Information File 1, Figure S2) was assigned by NMR spectroscopy, matching respective data reported in the literature [21,22].

The mass spectrum of (2*E*,4*E*)-*syn*,*syn*-4,6,8,10-tetramethyltrideca-2,4-diene (Figure 1 and Figure 3) and its gas-chromatographic properties perfectly matched the corresponding data of the natural product **A** (linear retention index on DB1 = 1511 and on Stabilwax = 1579) [12]. The structure closely resembles those of the oligomethylpolyenes known as pheromones of nitidulid beetles [24]. The 4-methyl-2*E*,4*E*-diene motif has been known as a substructure of pheromones of beetles, cockroaches and scale insects [16]. Whether these compounds are insect-produced or products of (endo)symbionts will need further investigations.

In analogy to the structure of **A**, compound **B** was assigned to be (2*E*,4*E*,6*S*,8*S*,10*S*)-4,6,8,10-tetramethyltrideca-2,4-dien-1-ol (**23**) or its enantiomer. According to the procedure described by Markiewicz et al. [23], racemic **23** was prepared by vinylogous Horner–Wadsworth–Emmons reaction of the aldehyde **21** with the anion of diethyl [(2*E*)-3-methoxycarbonyl-1-methyl-2-en-1-yl]phosphonate, followed by reduction of the resulting methyl ester (Figure 4). The obtained product proved to be a mixture of **23** and its (2*E*,4*Z*)-isomer (**23a**) in a ratio of about 1:1. For an unambiguous gas-chromatographic discrimination of **23** and **23a** we also synthesized a mixture of the two series of stereoisomers by applying "salt-free" conditions. As expected, the blend was strongly biased by the (*Z*)-series **23a** (see Supporting Information File 1, Figure S3A). The mass spec-

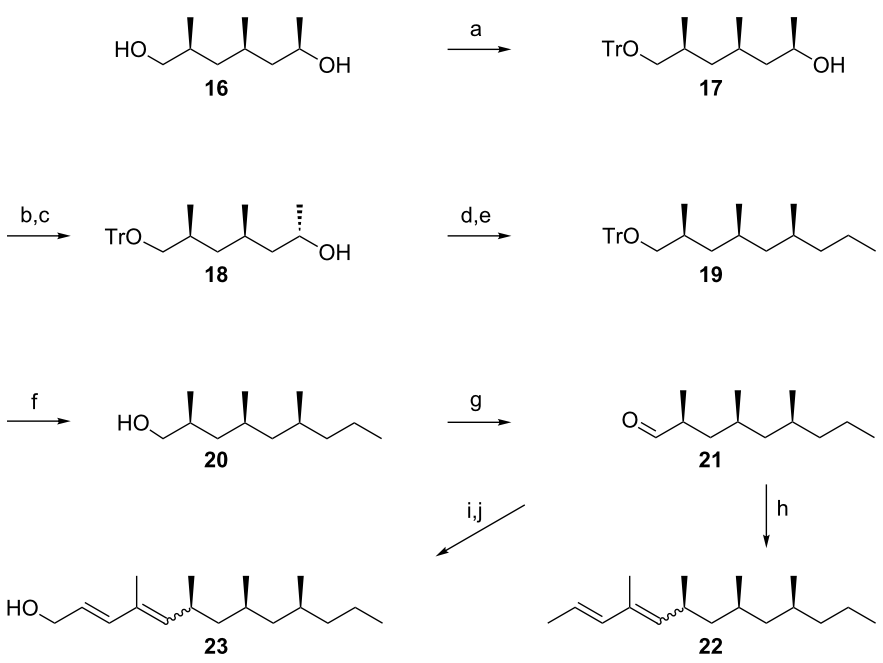


Figure 4: Synthesis of (2*E*,4*EZ*)-*syn*,*syn*-4,6,8,10-tetramethyltrideca-2,4-diene (**22**), as well as (2*E*,4*E*)- and (2*E*,4*Z*)- *syn*,*syn*-4,6,8,10-tetramethyltrideca-2,4-dien-1-ol (**23** and **23a**). Conditions: a: TrCl, DMAP, TEA, DCM, rt, 16 h; b: 1) DIAD, TPP, THF, −20 °C, 30 min; 2) 3,5-DNBA, rt, 40 min; 3) **17**, rt, 17 h; c: 2 N NaOH aq, THF/MeOH, rt, 45 min; d: MsCl, TEA, DCM, −80 °C, 2 h; e: *n*-propylmagnesium bromide, CuI, THF, −90 °C to rt, 48 h; f: *p*-TsOH, MeOH/THF/H_2O, rt, 2 h; g: PDC, MS 4 Å, DCM, −20 °C, 90 min; h: [(*E*)-1-methylbut-2-en-1-yl]triphenylphosphonium bromide, *n*-BuLi, LiBr, THF, −40 °C, 12 h; i: 1) diethyl [(1/2*EZ*)-3-(methoxycarbonyl)-1-methylprop-1/2-en-1-yl]phosphonate (as a mixture of isomers [23]), NaHMDS, LiBr, THF, −90 °C, 1 h; 2) **21**, −70 °C to rt, 16 h; j: DIBAlH, DCM, −80 °C to rt, 2.5 h.

trum of the (2*E*,4*E*)-configured 2,4-dien-1-ol **23** (Figure 1), and its gas-chromatographic properties perfectly matched the corresponding data of the natural product **B** (linear retention index on DB1 = 1766 and a Stabilwax = 2317) [12].

Since the preparation of enantiomerically pure *syn*,*syn*-2,4,6-trimethylnonanal has been described [25-28], our approach includes a formal synthesis of optically active **A** and **B**. Until now, we did not find suitable conditions to separate the enantiomers of the tetramethyldiene **22** and the respective allyl alcohol **23** (or corresponding derivatives thereof) in order to assign the absolute configuration of the natural products by enantioselective gas chromatography. However, ozonolysis of a natural sample [29] containing the two compounds, followed by reductive work-up, would yield *syn*,*syn*-2,4,6-trimethylnonanol, the enantiomers of which can be easily separated by using heptakis-[2,3-di-*O*-methyl-6-*O*-(*tert*-butyldimethylsilyl)]-β-cyclodextrin (50% in OV1701) as the stationary GC phase, operated at 100 °C. Under these conditions, the (2*S*,4*S*,6*S*)-enantiomer [30] is the later eluting stereoisomer, giving an α-value of (tr_2:tr_1) = 1.019 (see Supporting Information File 1, Figure S4).

As a result of our investigations we corrected the structures of the initially published *Trichogramma* compounds and showed a way to determine the enantiomeric composition of the natural products. Details including the assignment of the absolute configuration of the compounds will be published separately. As yet, the biological significance of the two female-produced compounds is unclear, however, Pompanon et al. [31] showed the presence of a sex specific pheromone released by females of *Trichogramma brassicae*. Future bioassays with the two new polydeoxypropionates will scrutinize whether they induce courtship behavior in males of *Trichogramma turkestanica*, as did the extract of females [12].

Supporting Information

Supporting Information File 1

Experimental details and characterization data for synthesized compounds.
[http://www.beilstein-journals.org/bjoc/content/supplementary/1860-5397-10-72-S1.pdf]

References

1. Flanders, S. E.; Quednau, W. *Entomophaga* **1960,** *5,* 285–294. doi:10.1007/BF02372951
2. Smith, S. M. *Annu. Rev. Entomol.* **1996,** *41,* 375–406. doi:10.1146/annurev.en.41.010196.002111

3. Pinto, J. D. *Systematics of the North American Species of Trichogramma Westwood (Hymenoptera: Trichogrammatidae; Memoirs of the Entomological Society of Washington*, Vol. 22; Entomological Society: Washington, U.S.A, 1999; pp 1–287.
4. Stouthamer, R.; Hu, J.; van Kan, F. J. P. M.; Platner, G. R.; Pinto, J. D. *BioControl* **1999,** *43,* 421–440. doi:10.1023/A:1009937108715
5. Rohi, L.; Pintureau, B. *J. Appl. Entomol.* **2003,** *127,* 265–268. doi:10.1046/j.1439-0418.2003.00753.x
6. Milonas, P. G.; Martinou, A. F.; Kontodimas, D. C.; Karamaouna, F.; Konstantopoulou, M. A. *Ann. Entomol. Soc. Am.* **2009,** *102,* 1145–1150. doi:10.1603/008.102.0624
7. Kainoh, Y. In *Pheromones of non-leptidopteran insects associated with agricultural plants;* Hardie, J.; Minks, A., Eds.; CABI Publishing: Wallingford, UK, 1999; pp 383–404.
8. Ruther, J. In *Chemical ecology of insect parasitoids;* Wajnberg, E.; Colazza, S., Eds.; John Wiley & Sons: Chichester, UK, 2013; pp 112–144.
9. Ruther, J.; Thal, K.; Steiner, S. *J. Chem. Ecol.* **2011,** *37,* 161–165. doi:10.1007/s10886-010-9898-8
10. Kühbandner, S.; Sperling, S.; Mori, K.; Ruther, J. *J. Exp. Biol.* **2012,** *215,* 2471–2478. doi:10.1242/jeb.071217
11. Keeling, C. I.; Plettner, E.; Slessor, K. N. *Top. Curr. Chem.* **2004,** *239,* 133–177. doi:10.1007/b95452
12. van Beek, T. A.; Silva, I. M. M. S.; Posthumus, M. A.; Melo, R. *J. Chromatogr., A* **2005,** *1067,* 311–321. doi:10.1016/j.chroma.2004.09.030
13. Ukaji, Y.; Narasaka, K. *Bull. Chem. Soc. Jpn.* **1988,** *61,* 571–573. doi:10.1246/bcsj.61.571
14. Fouquet, G.; Schlosser, M. *Angew. Chem., Int. Ed. Engl.* **1974,** *13,* 82–83. doi:10.1002/anie.197400821
15. Haag, G.; Luu, B.; Hetru, C. *J. Chem. Soc., Perkin Trans. 1* **1988,** 2353–2363. doi:10.1039/p19880002353
16. Francke, W.; Schulz, S. *Pheromones of Terrestrial Invertebrates.* In *Comprehensive Natural Products II - Chemistry and Biology;* Mander, L.; Lui, H.-W.; Mori, K., Eds.; Elsevier: Oxford, 2010; Vol. 4, pp 153–223. doi:10.1016/B978-008045382-8.00095-2
17. Bartelt, R. J.; Dowd, P. F.; Plattner, R. D.; Weisleder, D. *J. Chem. Ecol.* **1990,** *16,* 1015–1039. doi:10.1007/BF01021008
18. Morris, B. D.; Smyth, R. R.; Foster, S. P.; Hoffmann, M. P.; Roelofs, W. L.; Franke, S.; Francke, W. *J. Nat. Prod.* **2005,** *68,* 26–30. doi:10.1021/np049751v
19. Mori, K.; Kuwahara, S. *Tetrahedron* **1986,** *42,* 5545–5550. doi:10.1016/S0040-4020(01)88158-8
20. Titze, J. *Identifizierung und Synthese von Signalstoffen aus Insekten*. Ph.D. Thesis, Universität Hamburg, Hamburg, Germany, 2007.
21. Chow, S.; Fletcher, M. T.; Lambert, L. K.; Gallagher, O. P.; Moore, C. J.; Cribb, B. W.; Allsopp, P. G.; Kitching, W. *J. Org. Chem.* **2005,** *70,* 1808–1827. doi:10.1021/jo0481093
22. Schmidt, Y.; Lehr, K.; Colas, L.; Breit, B. *Chem.–Eur. J.* **2012,** *18,* 7071–7081. doi:10.1002/chem.201103988
23. Markiewicz, J. T.; Schauer, D. J.; Löfstedt, J.; Corden, S. J.; Wiest, O.; Helquist, P. *J. Org. Chem.* **2010,** *75,* 2061–2064. doi:10.1021/jo902422y
24. Francke, W.; Dettner, K. *Top. Curr. Chem.* **2005,** *240,* 85–166. doi:10.1007/b98316
25. Akibo, A.; Masamune, S. *Tetrahedron Lett.* **1996,** *37,* 1081–1084. doi:10.1016/0040-4039(95)02353-4
26. Magnin-Lachaux, M.; Tan, Z.; Liang, B.; Negishi, E. *Org. Lett.* **2004,** *6,* 1425–1427. doi:10.1021/ol0497483
27. Lum, T.-K.; Wang, S.-Y.; Loh, T.-P. *Org. Lett.* **2008,** *10,* 761–764. doi:10.1021/ol702715q
28. Weise, C. F.; Pischl, M. C.; Pfaltz, A.; Schneider, C. *J. Org. Chem.* **2012,** *77,* 1477–1488. doi:10.1021/jo202330b
29. Schulz, C. M.; Lehmann, L.; Blatrix, R.; Jaisson, P.; Hefetz, A.; Francke, W. *J. Chem. Ecol.* **2002,** *28,* 2541–2555. doi:10.1023/A:1021492204400
30. Geerdink, D.; Buter, J.; van Beek, T.; Minnaard, A. J. *Beilstein J. Org. Chem.* **2014,** *10,* 761–766. doi:10.3762/bjoc.10.71
31. Pompanon, F.; De Schepper, B.; Mourer, Y.; Fouillet, P.; Bouletreau, M. *J. Chem. Ecol.* **1997,** *23,* 1349–1360. doi:10.1023/B:JOEC.0000006468.19993.70

License and Terms

This is an Open Access article under the terms of the Creative Commons Attribution License (http://creativecommons.org/licenses/by/2.0), which permits unrestricted use, distribution, and reproduction in any medium, provided the original work is properly cited.

The license is subject to the *Beilstein Journal of Organic Chemistry* terms and conditions: (http://www.beilstein-journals.org/bjoc)

The definitive version of this article is the electronic one which can be found at: doi:10.3762/bjoc.10.72

Beilstein Journal of Organic Chemistry

Amino acid motifs in natural products: synthesis of *O*-acylated derivatives of (2*S*,3*S*)-3-hydroxyleucine

Oliver Ries[1], Martin Büschleb[1], Markus Granitzka[2], Dietmar Stalke[2] and Christian Ducho*[1,3]

Full Research Paper

Open Access

Address:
[1]Department of Chemistry, Institute of Organic and Biomolecular Chemistry, Georg-August-University Göttingen, Tammannstr. 2, 37077 Göttingen, Germany, [2]Department of Chemistry, Institute of Inorganic Chemistry, Georg-August-University Göttingen, Tammannstr. 4, 37077 Göttingen, Germany and [3]Department of Pharmacy, Pharmaceutical and Medicinal Chemistry, Saarland University, Campus C2 3, 66123 Saarbrücken, Germany

Email:
Christian Ducho* - christian.ducho@uni-saarland.de

* Corresponding author

Keywords:
chiral pool; cross metathesis; esterification; β-hydroxy-α-amino acids; natural products

Beilstein J. Org. Chem. **2014,** *10,* 1135–1142.
doi:10.3762/bjoc.10.113

Received: 16 December 2013
Accepted: 04 April 2014
Published: 16 May 2014

This article is part of the Thematic Series "Natural products in synthesis and biosynthesis".

Guest Editor: J. S. Dickschat

© 2014 Ries et al; licensee Beilstein-Institut.
License and terms: see end of document.

Abstract

(2*S*,3*S*)-3-Hydroxyleucine can be found in an increasing number of bioactive natural products. Within the context of our work regarding the total synthesis of muraymycin nucleoside antibiotics, we have developed a synthetic approach towards (2*S*,3*S*)-3-hydroxyleucine building blocks. Application of different protecting group patterns led to building blocks suitable for *C*- or *N*-terminal derivatization as well as for solid-phase peptide synthesis. With respect to according motifs occurring in natural products, we have converted these building blocks into 3-*O*-acylated structures. Utilizing an esterification and cross-metathesis protocol, (2*S*,3*S*)-3-hydroxyleucine derivatives were synthesized, thus opening up an excellent approach for the synthesis of bioactive natural products and derivatives thereof for structure activity relationship (SAR) studies.

Introduction

Besides the proteinogenic β-hydroxy-α-amino acids serine and threonine, (2*S*,3*S*)-3-hydroxyleucine can be found as a substructure of several bioactive natural products. This structural motif often serves as a 'three-way-junction', as for instance in azinothricin [1], citropeptin [2], kettapeptin [3], pipalamycin [4], dentigerumycin [5], as monosulfuric acid ester [6] or as potential acylation site for fatty acid side chains such as in A- and B-series muraymycin nucleoside antibiotics (Figure 1) [7-9]. In the case of these muraymycin congeners, acylation of the 3-hydroxy position with fatty acid side chains, which are ω-functionalized in the A-series, leads to a significant increase in biological activity. While non-acylated muraymycins C1 (**1c**)

and D1 (**1d**) showed a minimal inhibitory concentration (MIC) value of 1 μg/mL (*E. coli*), the attached unfunctionalized acyl side chain present in muraymycin B6 (**1b**) led to an increase of potency up to MIC = 0.06 μg/mL, which was therefore nearly as active as the most active naturally occurring muraymycin A1 (**1a**, MIC = 0.03 μg/mL). For other bacteria such as *S. aureus*, the presence of the 3-*O*-acyl motif can even turn biologically inactive C- and D-series muraymycins **1c**,**d** into active derivatives **1a**,**b** of the A- and B-series, respectively (Figure 1) [7]. This significant change in potency might be owed to increased lipophilicity and thus to improved cellular uptake, as muraymycins inhibit the transmembrane protein MraY (translocase I), an enzyme involved in peptidoglycan formation with its active site located on the cytosolic side of the membrane [10-14]. For previously reported SAR studies on muraymycins and their analogues, the fatty acid side chain was either neglegted or replaced with a structurally distinct lipophilic mimic [15-17]. Mansour and co-workers found a direct relation of the lipophilicity of semi-synthetic muraymycin C1 analogues and their biological activity [18]. They thus also postulated that the lipid structure might be involved in transporting the molecule to the active site of the target enzyme. The most recent SAR investigation on synthetic muraymycin analogues conducted by Ichikawa et al. also supported the proposal of increased membrane penetration resulting from the lipophilic moiety [17]. However, they employed simple lipophilic amino acids as surrogates of the naturally occurring *O*-acylated (2*S*,3*S*)-3-hydroxyleucine motif. This led to antibacterially active compounds, but one of it showed a ca. 30-fold reduction of inhibitory potency towards the target enzyme MraY as compared to non-lipidated muraymycin D2 containing L-leucine instead of (2*S*,3*S*)-3-hydroxyleucine. This result highlighted the significance of the native linkage of the lipophilic moiety to the muraymycin scaffold.

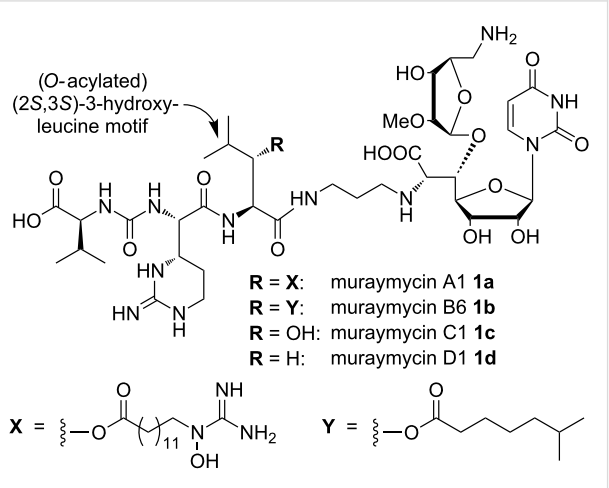


Figure 1: Structures of muraymycins A1, B6, C1 and D1 **1a–d**.

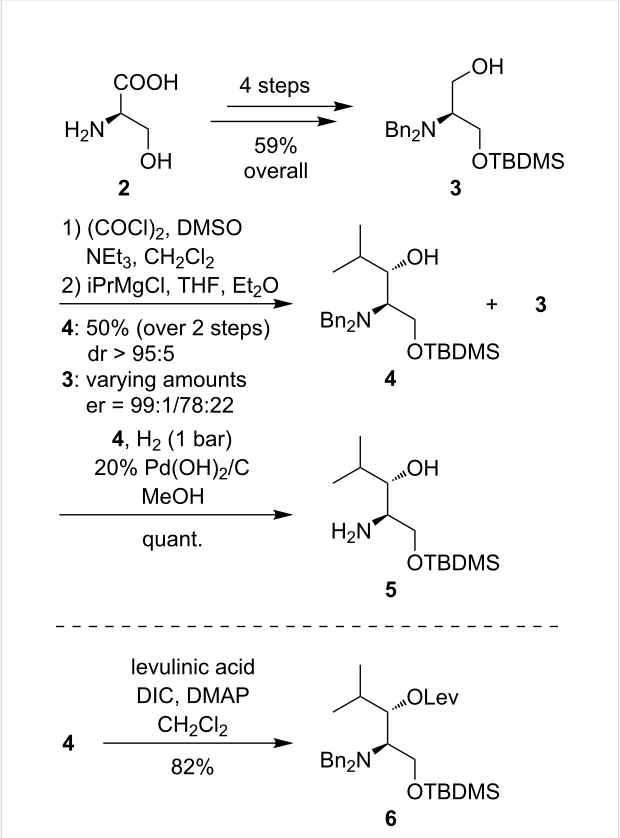
As part of our synthetic studies on muraymycins and their analogues [19-24], including investigations on the unusual ω-functionalized fatty acid motif found in muraymycin A1 (**1a**) [25], we identified the need for a highly stereoselective synthesis of (2*S*,3*S*)-3-hydroxyleucine and its *O*-acylated derivatives. Efficient synthetic access to such compounds will enable the unprecedented preparation of lipidated muraymycins bearing the native linkage of the fatty acid moieties, thus potentially leading to novel congeners with improved biological activity. It will also be useful for the synthesis of other natural products containing this amino acid.

Several synthetic approaches towards (2*S*,3*S*)-3-hydroxyleucine have been established utilizing for instance diastereoselective aldol reactions [26-28], Sharpless epoxidation [29], asymmetric hydrogenation [30] and dynamic kinetic resolution [31]. However, in contrast to these routes, we desired to develop a synthesis of *O*-acylated (2*S*,3*S*)-3-hydroxyleucine derivatives which should be easily scalable and would enable *O*-acylation after construction of the stereocenters with only few changes in the protecting group pattern. The most promising strategy to achieve these goals appeared to be a variation of the ex-chiral pool synthesis developed by Zhu and co-workers [32]. They have utilized the stereocenter of D-serine in a diastereoselective Grignard addition to protected D-serinal as the key step of their route. In addition, we also envisaged to establish a facile strategy to introduce structural diversity in the *O*-acyl moiety, ideally by the late-stage derivatization of an according precursor.

Results and Discussion

Utilizing the aforementioned synthetic strategy developed by Zhu and co-workers [32], we have employed their 7-step synthesis of a stereoisomerically pure amino alcohol as the key intermediate. According to the previously reported protocol, D-serine (**2**) was transformed into protected derivative **3** (4 steps, 59% overall yield, Scheme 1). Alcohol **3** was then oxidized to a D-serinal derivative with limited stability, which was immediately converted into alcohol **4** by diastereoselective Felkin–Anh type Grignard addition with isopropyl magnesium chloride (50% yield over 2 steps from **3**, dr > 95:5). However, we could not confirm that the use of diethyl ether as co-solvent in the Grignard reaction would suppress the reformation of alcohol **3** as the competing Grignard reduction product, as it had been claimed by Zhu and co-workers in their initial report [32]. It was therefore decided to attempt the recycling of alcohol **3**, which was obtained in varying amounts, for another round of oxidation and Grignard addition. The enantiomeric purity of reisolated **3** was determined by HPLC analysis as its racemization can readily occur via silyl migration under the basic reaction conditions (see Supporting Information File 2 for HPLC

chromatograms and for the synthesis of the racemic reference). After one oxidation–addition sequence we could isolate **3** with an enantiomeric purity of er = 99:1. Use of the obtained alcohol in a second oxidation–addition sequence followed by subsequent HPLC analysis of reduction product **3** demonstrated a decrease in enantiomeric purity to er = 78:22 though. On the basis of these results, we desisted from the use of this alcohol in a third oxidation–addition cycle. It was concluded that the recycling of the Grignard reduction product is in principle feasible, but that one should always check its enantiomeric purity prior to a repetition of the oxidation–addition sequence. Finally, the previously reported hydrogenolytic debenzylation of **4** [32] provided amino alcohol key intermediate **5** in quantitative yield for the deprotection step and in 29% overall yield over 7 steps from D-serine (**2**, Scheme 1). It should be noted that Garner's aldehyde is often used instead of acyclic D-serinal derivatives for the addition of nucleophiles to amino acid-derived aldehydes [33,34]. However, Zhu and co-workers have pointed out that Garner's aldehyde surprisingly furnishes the *syn* diastereomer as the major product from its reaction with isopropyl magnesium chloride [32], thus discouraging its use for the preparation of *anti*-configured (2*S*,3*S*)-3-hydroxyleucine.



Scheme 1: Synthesis of stereoisomerically pure amino alcohol **5** [32] and of derivative **6** suitable for X-ray crystallography.

Zhu and co-workers had based their stereochemical assignment of **5** on the ^{1}H NMR coupling constants of a cyclic derivative of this amino alcohol. We were able to confirm the postulated stereochemical outcome of the Grignard addition by X-ray crystallography as (2*R*,3*S*) for the amino alcohol and thus, due to altered priorities, (2*S*,3*S*) for the corresponding amino acid, respectively. The absolute configuration was deduced assuming the integrity of the stereocenter at the 2-position, which had been derived from D-serine (**2**). As neither **4** nor **5** gave crystals suitable for X-ray analysis, the 3-hydroxy group of **4** was acylated with levulinic acid, leading to ester **6** in 82% yield (Scheme 1) which crystallized upon removal of residual solvent under reduced pressure. Hence, a single crystal of **6** was obtained, and X-ray crystal structure analysis unambiguously confirmed the relative configuration (Figure 2; see Supporting Information File 1 for crystallographic data). Levulinyl ester **6** crystallizes in the orthorhombic space group $P2_12_12_1$ with one molecule in the asymmetric unit. The Flack parameter [35] refined to x = −0.05(8) and confirmes the stereocenters to have the proposed (2*R*,3*S*)-configuration.

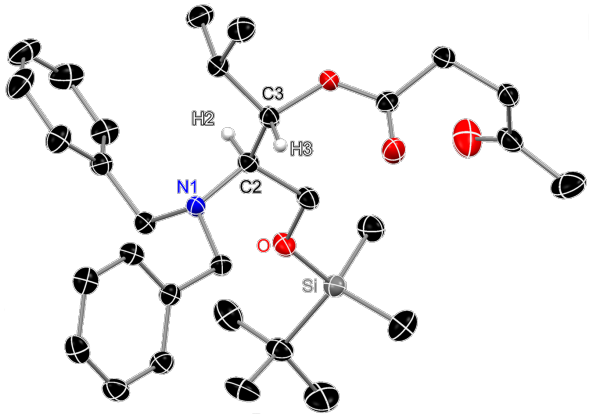
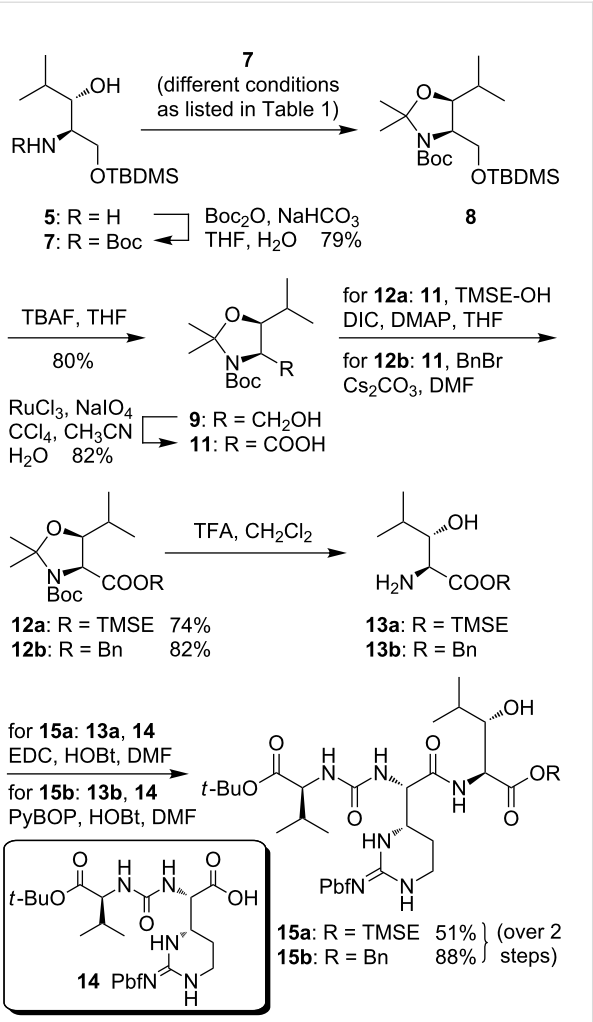


Figure 2: Molecular structure of levulinyl ester **6**. Anisotropic displacement parameters are depicted at the 50% probability level. Atom color code: carbon = black, oxygen = red, nitrogen = blue, silicon = grey, and hydrogen = white. The other hydrogen atoms are omitted for clarity.

In their synthesis of (2*S*,3*S*)-3-hydroxyleucine, Zhu and co-workers cyclized amino alcohol **5** towards an oxazolidinone, with the carbonyl group simultaneously providing *O*- and *N*-protection [32]. Removal of this protecting group required harsh reaction conditions though (conc. HCl, reflux, 40 h) and yielded the unprotected amino acid as the hydrochloric salt. However, in the case of our envisaged synthesis of 3-hydroxyleucine building blocks suitable for further derivatization as well as incorporation into natural products and their analogues, we were in need for a more versatile protecting group pattern. We therefore investigated different carbamates as protecting

groups for the amino functionality, leading to the secondary alcohol functionality being selectively accessible for further conversions. We discovered that we were in need for a protecting group reducing the basic character of the amino group as an oxidation of the silyl-deprotected amino alcohol to the corresponding acid was not possible, probably due to the basicity of the amino group (reactions not displayed).

For the synthesis of a *C*-protected building block, **5** was converted with Boc anhydride to yield Boc-protected amino alcohol **7** in 79% yield (Scheme 2). After removal of the silyl group, a selective oxidation of the primary alcohol in presence of the unprotected 3-hydroxy group unfortunately could not be achieved (reactions not displayed). It was therefore decided to introduce an *N*,*O*-acetal moiety by transformation of **7** into the dimethyloxazolidine **8**, a reaction which required careful optimization though (Scheme 2, Table 1). Using boron trifluoride and 2,2-dimethoxypropane (2,2-DiMP), as known from the synthesis of the structurally related Garner's aldehyde [33,34], led to an unwanted cleavage of the silyl ether and furnished a mixture of the desired product **8**, the TBDMS cleavage product **9** and the corresponding *O*,*O*-acetal **10** (Table 1, entry 1). Hence, further reaction conditions using different acid catalysts and solvents were investigated. Changing the catalyst to pyridinium *p*-toluenesulfonate (PPTS) only led to small amounts of the product after prolonged reaction times and could not suppress the formation of the *O*,*O*-acetal (Table 1, entries 2 and 3). The use of racemic camphorsulfonic acid (CSA) in toluene and acetone, respectively, resulted in the formation of **8** in moderate to good yields (Table 1, entries 4–6). Finally, when 2,2-DiMP was used as solvent with catalytic amounts of CSA in the presence of magnesium sulfate, **8** could be isolated in a very good yield of 93% (Table 1, entry 7). After TBAF-mediated cleavage of the silyl ether, the resultant primary alcohol **9** (obtained in 80%

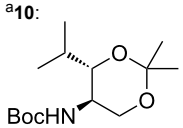


Scheme 2: Synthesis of (2*S*,3*S*)-3-hydroxyleucine building blocks **13a**,**b** useful for *N*-derivatization and of the protected muraymycin tripeptide unit **15a**,**b**.

Table 1: Optimization of the reaction of **7** to dimethyloxazolidine **8**.

Entry	Reaction conditions	Yield [%] (compound)
1	9 equiv 2,2-DiMP, 0.1 equiv $BF_3{\cdot}Et_2O$, acetone, rt, 23 h	19 (**8**), 19 (**9**), 30 (**10**)[a]
2	9 equiv 2,2-DiMP, 0.1 equiv PPTS, acetone, rt, 4 d	76 (**7**), 21 (**8**)
3	10 equiv 2,2-DiMP, 0.3 equiv PPTS, THF, rt, 17 h	mixture (**8**)/(**9**)[b], 9 (**10**)
4	26 equiv 2,2-DiMP[c], 0.02 equiv CSA, MS 3 Å, toluene, 80 °C, 17 h	79 (**8**)
5	20 equiv 2,2-DiMP[d], 0.02 equiv CSA, MS 3 Å, toluene, 80 °C, 15 h	74 (**7**), 20 (**8**)
6	30 equiv 2,2-DiMP, 0.03 equiv CSA, acetone, reflux, 16 h	60 (**8**)
7	0.15 equiv CSA, $MgSO_4$, 2,2-DiMP, 50 °C, 24 h	93 (**8**)

[a]**10**:

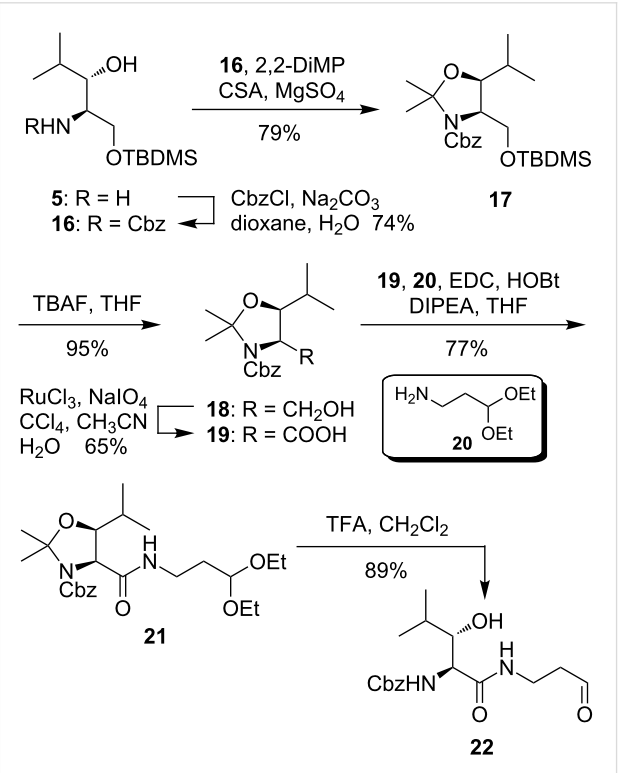


[b]not separated; [c]2,2-dimethoxypropane (2,2-DiMP) was added in two portions; [d]2,2-DiMP was added at once.

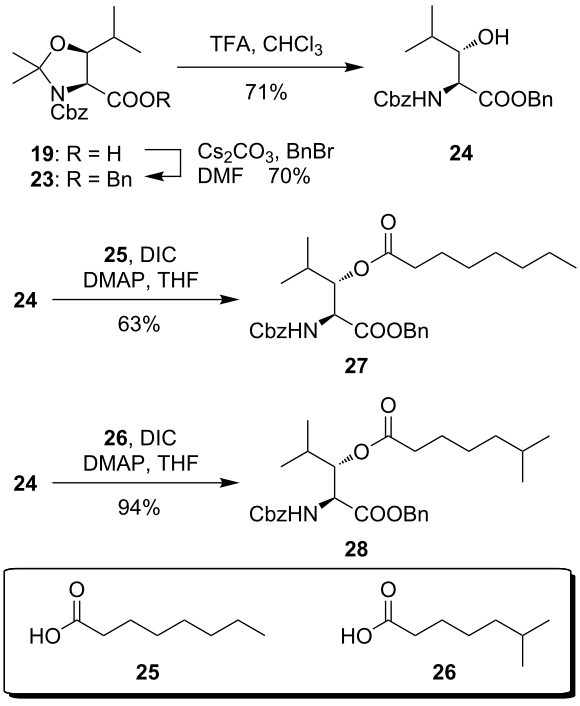
yield) was oxidized to carboxylic acid **11** by ruthenium(III)-catalyzed periodate oxidation in 82% yield. Subsequent protection of the acid functionality furnished 2-(trimethylsilyl)ethyl (TMSE) and benzyl esters **12a** and **12b** (yields 72% and 84%, respectively). Finally, acidic deprotection afforded the desired building blocks **13a**,**b** suitable for *N*-derivatization, with the compounds not being fully purified. In order to demonstrate the synthetic versatility of these 3-hydroxyleucine derivatives, they were coupled with urea dipeptide **14** [36], thus providing protected derivatives **15a**,**b** of the full-length peptide unit of C-series muraymycins in yields of 51% and 88%, respectively, over 2 steps from **12a**,**b**. It is expected that **15a**,**b** can serve as useful building blocks in the total synthesis of muraymycins and their analogues.

Following the synthesis of building blocks **13a**,**b** suitable for *N*-derivatization, it was also desired to obtain (2*S*,3*S*)-3-hydroxyleucine derivatives suitable for *C*-terminal coupling reactions. We therefore chose a Cbz group as amino protecting group. Treatment of amino alcohol **5** with Cbz chloride furnished protected derivative **16** in 74% yield (Scheme 3). In analogy to the aforementioned synthetic route, **16** was then cyclized with 2,2-DiMP to the corresponding dimethyloxazolidine **17** (79% yield), followed by TBAF-mediated cleavage of the silyl ether (product **18**, 95% yield) and oxidation of the primary alcohol to carboxylic acid **19** in 65% yield (49% over 3 steps from **17**). The potential of **19** to serve as a universal building block for *C*-terminal derivatization was demonstrated by the following transformations. Acid **19** was reacted with 1,1-diethoxy-3-aminopropane (**20**) under standard EDC/HOBt coupling conditions to afford amide **21** in 77% yield, followed by concomitant acidic cleavage of the *N*,*O*- and *O*,*O*-acetal protecting groups leading to building block **22** in 89% yield (Scheme 3). Aldehyde **22** can be used for the connection of the (2*S*,3*S*)-3-hydroxyleucine motif of C-series muraymycins (such as muraymycin C1 (**1c**), Figure 1) to the nucleoside moiety by reductive amination (reactions not displayed), as demonstrated before in our syntheses of simplified muraymycin analogues [21,22].

N-Cbz-protected acid **19** was also used for a methodical study regarding the acylation of the 3-hydroxy group. Therefore, **19** was converted into benzyl ester **23** (70% yield) followed by acidic cleavage of the acetonide to yield building block **24** in 71% yield (Scheme 4). Acylation reactions were carried out with DIC as coupling reagent and catalytic amounts of DMAP. Based on this protocol, esterification reactions with octanoic acid (**25**) and 6-methylheptanoic acid (**26**, vide infra) yielded the acylated (2*S*,3*S*)-3-hydroxyleucine derivatives **27** and **28** in 63% and 94% yield, respectively. The latter compound might



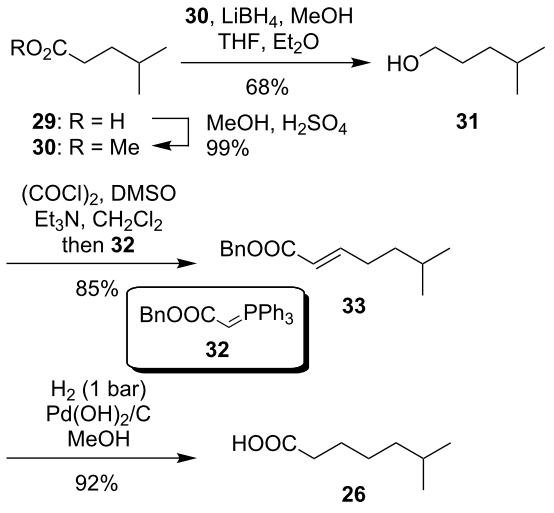
Scheme 3: Synthesis of (2*S*,3*S*)-3-hydroxyleucine building block **19** useful for *C*-derivatization and of aldehyde **22**, a synthetic building block for C-series muraymycins.



Scheme 4: Synthesis of *O*-acylated (2*S*,3*S*)-3-hydroxyleucine derivatives **27** and **28**.

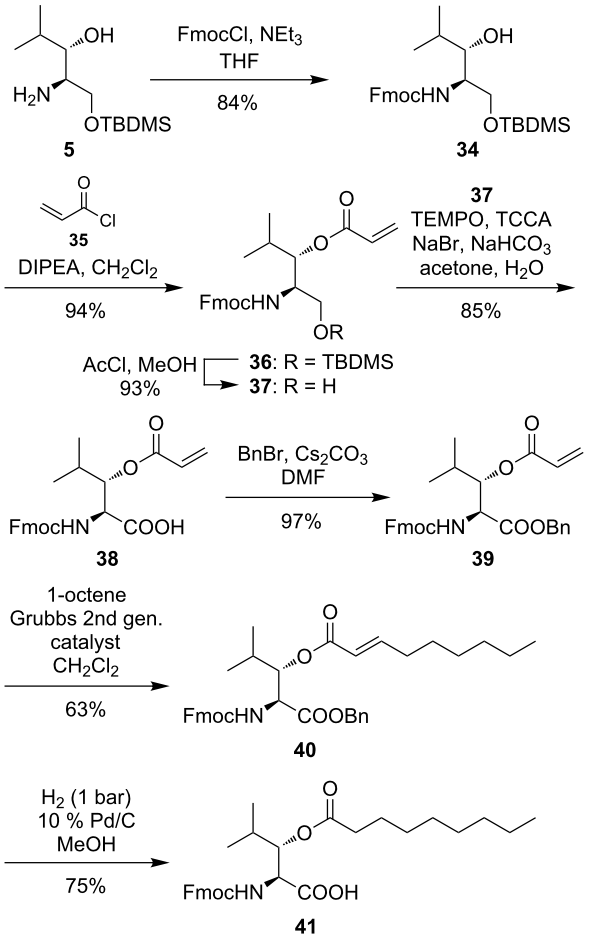
serve as a building block for the synthesis of muraymycin B6 (**1b**) and also muraymycin B7 (as well as derivatives thereof) as the 6-methylheptanoyl moiety is a constituent of these natural products. It represents the first example of a synthetically obtained *O*-acylated 3-hydroxyleucine moiety of a naturally occurring muraymycin.

The preparation of *O*-acylated derivative **28** required the synthesis of 6-methylheptanoic acid (**26**) though. This branched carboxylic acid was obtained starting from commercially available 4-methylpentanoic acid (**29**, Scheme 5). Esterification with methanol (product **30**, 99% yield) and reduction of the ester with lithium borohydride afforded primary alcohol **31** in 68% yield. A direct reduction of acid **29** with lithium aluminum hydride was also investigated, but resulted in a moderate yield of 32% only (reaction not displayed). One-pot Swern oxidation to the corresponding aldehyde and subsequent Wittig reaction with stabilized Wittig reagent **32** led to α,β-unsaturated ester **33** in 85% yield. After simultaneous reduction of the double bond and cleavage of the benzyl ester by catalytic hydrogenation, 6-methylheptanoic acid (**26**) could be obtained in 92% yield for the final step (Scheme 5).



Scheme 5: Synthesis of 6-methylheptanoic acid (**26**).

With respect to the (2*S*,3*S*)-3-hydroxyleucine motif occurring in several different peptidic natural products (vide supra), we also investigated the synthesis of *N*-Fmoc-protected building blocks potentially suitable for solid-phase peptide synthesis (SPPS). It is well established that *O*-acylated β-hydroxy-α-amino acids can be used in Fmoc-strategy peptide syntheses without migration of the acyl unit [37-39]. Based on these findings, we have desired to develop a method for the modification of the acyl side chain of a previously incorporated *O*-acylated β-hydroxy-α-amino acid building block at a very late stage and under mild conditions, e.g., by olefin cross metathesis. Therefore, amino alcohol **5** was Fmoc-protected (product **34**, 84% yield), followed by esterification of the 3-hydroxy group with acryloyl chloride (**35**), thus furnishing acrylate **36** in 94% yield (Scheme 6). After acidic cleavage of the silyl ether in 93% yield [40], the resultant primary alcohol **37** was oxidized using catalytic amounts of TEMPO and trichlorocyanuric acid (TCCA) as stoichiometric oxidant to provide (2*S*,3*S*)-3-hydroxyleucine derivative **38**, a potential building block for SPPS and post-synthetic modification of the peptide, in 85% yield.



Scheme 6: Synthesis of Fmoc-protected building blocks **38** and **41** suitable for SPPS, with late-stage side chain diversification by olefin metathesis.

In order to demonstrate the feasibility of the olefin cross metathesis approach for the late-stage diversification of the acyl side chain, acid **38** was transformed into benzyl ester **39** in 97% yield (Scheme 6). Subsequent treatment with commercially available 1-octene and Grubbs 2nd generation catalyst [41] afforded lipidated (2*S*,3*S*)-3-hydroxyleucine derivative **40** in 63% yield without any observed homo-coupling of the amino

acid. Amino acid **40** was then debenzylated under standard hydrogenation conditions with concomitant reduction of the double bond, thus leading to lipidated amino acid building block **41** suitable for SPPS in 75% yield for the final step.

Conclusion

In summary, we have developed a divergent approach for the synthesis of several (2*S*,3*S*)-3-hydroxyleucine building blocks employing stereoisomerically pure amino alcohol **5** [32]. Applying different protecting group strategies, we were able to prepare (2*S*,3*S*)-3-hydroxyleucine derivatives suitable for further modification both at the carboxy and the amino moiety, as well as for solid-phase peptide synthesis (SPPS). Furthermore, we have employed such building blocks for the synthesis of protected analogues **15a**,**b** of the tripeptide unit of naturally occurring muraymycin nucleoside antibiotics.

We have also established unprecedented protocols for early- and late-stage derivatizations of the 3-hydroxy group of the (2*S*,3*S*)-3-hydroxyleucine scaffold by esterification of the alcohol or cross metathesis of the corresponding acryloyl ester, respectively. This led to an efficient and versatile access towards acylated (2*S*,3*S*)-3-hydroxyleucine derivatives, thus enabling the preparation of according natural products and analogues thereof. As a first proof-of-principle experiment, the lipidated (2*S*,3*S*)-3-hydroxyleucine subunit of antibacterially active muraymycins B6 and B7 was synthesized in protected form. Overall, our results thus contribute to the methodology for the synthesis of unusual non-proteinogenic amino acid motifs for synthetic natural product chemistry.

Supporting Information

The Supporting Information features the preparation, analytical data and copies of ^{1}H and ^{13}C NMR spectra of compounds **6**–**9**, **11**–**13**, **15**–**19**, **21**–**24**, **26**–**28**, **30**, **31**, **33**, **34**, **36**–**41** and racemic HPLC reference **S1** as well as crystallographic data for compound **6**.

Supporting Information File 1

Crystallographic data for compound **6**.
[http://www.beilstein-journals.org/bjoc/content/supplementary/1860-5397-10-113-S1.cif]

Supporting Information File 2

Experimental procedures and NMR spectra of compounds **6**–**9**, **11**–**13**, **15**–**19**, **21**–**24**, **26**–**28**, **30**, **31**, **33**, **34**, **36**–**41** and **S1**.
[http://www.beilstein-journals.org/bjoc/content/supplementary/1860-5397-10-113-S2.pdf]

Acknowledgements

O. R., M. B. and C. D. thank the Deutsche Forschungsgemeinschaft (DFG, SFB 803 "Functionality controlled by organization in and between membranes") and the Fonds der Chemischen Industrie (FCI, Sachkostenzuschuss) for financial support. M. G. and D. S. thank the Danish National Research Foundation (DNRF)-funded Center for Materials Crystallography (CMC).

References

1. Maehr, H.; Liu, C.-M.; Palleroni, N. J.; Smallheer, J.; Todaro, L.; Williams, T. H.; Blount, J. F. *J. Antibiot.* **1986,** *39,* 17–25. doi:10.7164/antibiotics.39.17
2. Nakagawa, M.; Hayakawa, Y.; Furihata, K.; Seto, H. *J. Antibiot.* **1990,** *43,* 477–484. doi:10.7164/antibiotics.43.477
3. Maskey, R. P.; Fotso, S.; Sevvana, M.; Usón, I.; Grün-Wollny, I.; Laatsch, H. *J. Antibiot.* **2006,** *59,* 309–314. doi:10.1038/ja.2006.44
4. Uchihata, Y.; Ando, N.; Ikeda, Y.; Kondo, S.; Hamada, M.; Umezawa, K. *J. Antibiot.* **2002,** *55,* 1–5. doi:10.7164/antibiotics.55.1
5. Oh, D.-C.; Poulsen, M.; Currie, C. R.; Clardy, J. *Nat. Chem. Biol.* **2009,** *5,* 391–393. doi:10.1038/nchembio.159
6. Augustiniak, H.; Forche, E.; Reichenbach, H.; Wray, V.; Gräfe, U.; Höfle, G. *Liebigs Ann. Chem.* **1991,** 361–366. doi:10.1002/jlac.199119910163
7. McDonald, L. A.; Barbieri, L. R.; Carter, G. T.; Lenoy, E.; Lotvin, J.; Petersen, P. J.; Siegel, M. M.; Singh, G.; Williamson, R. T. *J. Am. Chem. Soc.* **2002,** *124,* 10260–10261. doi:10.1021/ja017748h
8. Kimura, K.-i.; Bugg, T. D. H. *Nat. Prod. Rep.* **2003,** *20,* 252–273. doi:10.1039/b202149h
9. Winn, M.; Goss, R. J. M.; Kimura, K.-i.; Bugg, T. D. H. *Nat. Prod. Rep.* **2010,** *27,* 279–304. doi:10.1039/b816215h
10. Ikeda, M.; Wachi, M.; Jung, H. K.; Ishino, F. M. M. *J. Bacteriol.* **1991,** *173,* 1021–1026.
11. Bouhss, A.; Mengin-Lecreulx, D.; Le Beller, D.; van Heijenoort, J. *Mol. Microbiol.* **1999,** *34,* 576–585. doi:10.1046/j.1365-2958.1999.01623.x
12. Dini, C. *Curr. Top. Med. Chem.* **2005,** *5,* 1221–1236. doi:10.2174/156802605774463042
13. Bugg, T. D. H.; Lloyd, A. J.; Roper, D. I. *Infect. Disord.: Drug Targets* **2006,** *6,* 85–106. doi:10.2174/187152606784112128
14. Chung, B. C.; Zhao, J.; Gillespie, R. A.; Kwon, D.-Y.; Guan, Z.; Hong, J.; Zhou, P.; Lee, S.-Y. *Science* **2013,** *341,* 1012–1016. doi:10.1126/science.1236501
15. Yamashita, A.; Norton, E.; Petersen, P. J.; Rasmussen, B. A.; Singh, G.; Yang, Y.; Mansour, T. S.; Ho, D. M. *Bioorg. Med. Chem. Lett.* **2003,** *13,* 3345–3350. doi:10.1016/S0960-894X(03)00671-1
16. Tanino, T.; Ichikawa, S.; Al-Dabbagh, B.; Bouhss, A.; Oyama, H.; Matsuda, A. *ACS Med. Chem. Lett.* **2010,** *1,* 258–262. doi:10.1021/ml100057z
17. Tanino, T.; Al-Dabbagh, B.; Mengin-Lecreulx, D.; Bouhss, A.; Oyama, H.; Ichikawa, S.; Matsuda, A. *J. Med. Chem.* **2011,** *54,* 8421–8439. doi:10.1021/jm200906r
18. Lin, Y.-I.; Li, Z.; Francisco, G. D.; McDonald, L. A.; Davis, R. A.; Singh, G.; Yang, Y.; Mansour, T. S. *Bioorg. Med. Chem. Lett.* **2002,** *12,* 2341–2344. doi:10.1016/S0960-894X(02)00469-9
19. Spork, A. P.; Koppermann, S.; Ducho, C. *Synlett* **2009,** 2503–2507. doi:10.1055/s-0029-1217742

20. Spork, A. P.; Koppermann, S.; Dittrich, B.; Herbst-Irmer, R.; Ducho, C. *Tetrahedron: Asymmetry* **2010,** *21,* 763–766. doi:10.1016/j.tetasy.2010.03.037
21. Spork, A. P.; Ducho, C. *Org. Biomol. Chem.* **2010,** *8,* 2323–2326. doi:10.1039/c003092a
22. Spork, A. P.; Wiegmann, D.; Granitzka, M.; Stalke, D.; Ducho, C. *J. Org. Chem.* **2011,** *76,* 10083–10098. doi:10.1021/jo201935w
23. Büschleb, M.; Granitzka, M.; Stalke, D.; Ducho, C. *Amino Acids* **2012,** *43,* 2313–2328. doi:10.1007/s00726-012-1309-8
24. Spork, A. P.; Ducho, C. *Synlett* **2013,** *24,* 343–346. doi:10.1055/s-0032-1318117
25. Ries, O.; Ochmann, A.; Ducho, C. *Synthesis* **2011,** 2357–2368. doi:10.1055/s-0030-1260100
26. Seebach, D.; Juaristi, E.; Miller, D. D.; Schickli, C.; Weber, T. *Helv. Chim. Acta* **1987,** *70,* 237–261. doi:10.1002/hlca.19870700129
27. Corey, E. J.; Lee, D.-H.; Choi, S. *Tetrahedron Lett.* **1992,** *33,* 6735–6738. doi:10.1016/S0040-4039(00)61763-X
28. Panek, J. S.; Masse, C. E. *J. Org. Chem.* **1998,** *63,* 2382–2384. doi:10.1021/jo972013+
29. Schmidt, U.; Respondek, M.; Lieberknecht, A.; Werner, J.; Fischer, P. *Synthesis* **1989,** 256–261. doi:10.1055/s-1989-27216
30. Makino, K.; Okamoto, N.; Hara, O.; Hamada, Y. *Tetrahedron: Asymmetry* **2001,** *12,* 1757–1762. doi:10.1016/S0957-4166(01)00306-8
31. Makino, K.; Goto, T.; Hiroki, Y.; Hamada, Y. *Angew. Chem., Int. Ed.* **2004,** *43,* 882–884. doi:10.1002/anie.200353072
Angew. Chem. **2004,** *116,* 900–902. doi:10.1002/ange.200353072
32. Laïb, T.; Chastanet, J.; Zhu, J. *J. Org. Chem.* **1998,** *63,* 1709–1713. doi:10.1021/jo971468w
33. Garner, P.; Park, J. M. *J. Org. Chem.* **1987,** *52,* 2361–2364. doi:10.1021/jo00388a004
34. Dondoni, A.; Perrone, D. *Org. Synth.* **2000,** *77,* 64–77.
35. Flack, H. D. *Acta Crystallogr., Sect. A* **1983,** *39,* 876–881. doi:10.1107/S0108767383001762
36. The stereocontrolled synthesis of compound **14** will be reported in full detail elsewhere.
37. Branton, W. D.; Fields, C. G.; VanDrisse, V. L.; Fields, G. B. *Tetrahedron Lett.* **1993,** *34,* 4885–4888. doi:10.1016/S0040-4039(00)74037-8
38. Portella, G.; Polupanow, T.; Zocher, F.; Boytsov, D. A.; Pohl, P.; Diederichsen, U.; de Groot, B. *Biophys. J.* **2012,** *103,* 1698–1705. doi:10.1016/j.bpj.2012.08.059
39. Agarwal, H. K.; Chhikara, B. S.; Quiterio, M.; Doncel, G. F.; Parang, K. *J. Med. Chem.* **2012,** *55,* 2672–2687. doi:10.1021/jm201551m
40. Khan, A. T.; Mondal, E. *Synlett* **2003,** 694–698. doi:10.1055/s-2003-38360
41. Trnka, T. M.; Grubbs, R. H. *Acc. Chem. Res.* **2001,** *34,* 18–29. doi:10.1021/ar000114f

License and Terms

This is an Open Access article under the terms of the Creative Commons Attribution License (http://creativecommons.org/licenses/by/2.0), which permits unrestricted use, distribution, and reproduction in any medium, provided the original work is properly cited.

The license is subject to the *Beilstein Journal of Organic Chemistry* terms and conditions: (http://www.beilstein-journals.org/bjoc)

The definitive version of this article is the electronic one which can be found at: doi:10.3762/bjoc.10.113

Beilstein Journal of Organic Chemistry

Heronapyrrole D: A case of co-inspiration of natural product biosynthesis, total synthesis and biodiscovery

Jens Schmidt[1], Zeinab Khalil[2], Robert J. Capon[*2] and Christian B. W. Stark[*1]

Letter

Open Access

Address:
[1]Fachbereich Chemie, Institut für Organische Chemie, Universität Hamburg, Martin-Luther-King-Platz 6, 20146 Hamburg, Germany and [2]Institute for Molecular Bioscience, The University of Queensland, St. Lucia, QLD 4072, Australia

Email:
Robert J. Capon[*] - r.capon@uq.edu.au; Christian B. W. Stark[*] - stark@chemie.uni-hamburg.de

* Corresponding author

Keywords:
biomimetic synthesis; biosynthesis; heronapyrroles; microbial biodiscovery; natural products; nitropyrroloterpenes

Beilstein J. Org. Chem. **2014,** *10,* 1228–1232.
doi:10.3762/bjoc.10.121

Received: 05 February 2014
Accepted: 26 March 2014
Published: 26 May 2014

This article is part of the Thematic Series "Natural products in synthesis and biosynthesis".

Guest Editor: J. S. Dickschat

© 2014 Schmidt et al; licensee Beilstein-Institut.
License and terms: see end of document.

Abstract

The heronapyrroles A–C have first been isolated from a marine-derived *Streptomyces* sp. (CMB-0423) in 2010. Structurally, these natural products feature an unusual nitropyrrole system to which a partially oxidized farnesyl chain is attached. The varying degree of oxidation of the sesquiterpenyl subunit in heronapyrroles A–C provoked the hypothesis that there might exist other hitherto unidentified metabolites. On biosynthetic grounds a mono-tetrahydrofuran-diol named heronapyrrole D appeared a possible candidate. We here describe a short asymmetric synthesis of heronapyrrole D, its detection in cultivations of CMB-0423 and finally the evaluation of its antibacterial activity. We thus demonstrate that biosynthetic considerations and the joint effort of synthetic and natural product chemists can result in the identification of new members of a rare class of natural products.

Introduction

Heronapyrroles A–C (Figure 1) were first reported in 2010 by Capon et al. from a marine-derived *Streptomyces* sp. (CMB-M0423) obtained from a shallow water sand sample collected near Heron Island, Queensland, Australia (Figure 1) [1]. As first in class examples of natural products featuring a 2-nitropyrrole, further elaborated by a farnesyl side chain, the heronapyrroles exhibited promising antibacterial activity against *Staphylococcus aureus* (ATCC 2593 and 9144) and *Bacillus subtilis* (ATCC 6051 and 6633). Publication of the heronapyrroles was rapidly followed by an account of the biosynthetically related nitropyrrolins A–E, obtained from a different marine-derived actinomycete strain (CNQ-509) (Figure 1) [2]. Of note, the heronapyrroles and nitropyrrolins both feature the same unprecedented heterocyclic core (2-nitro-4-farnesylpyrrole)

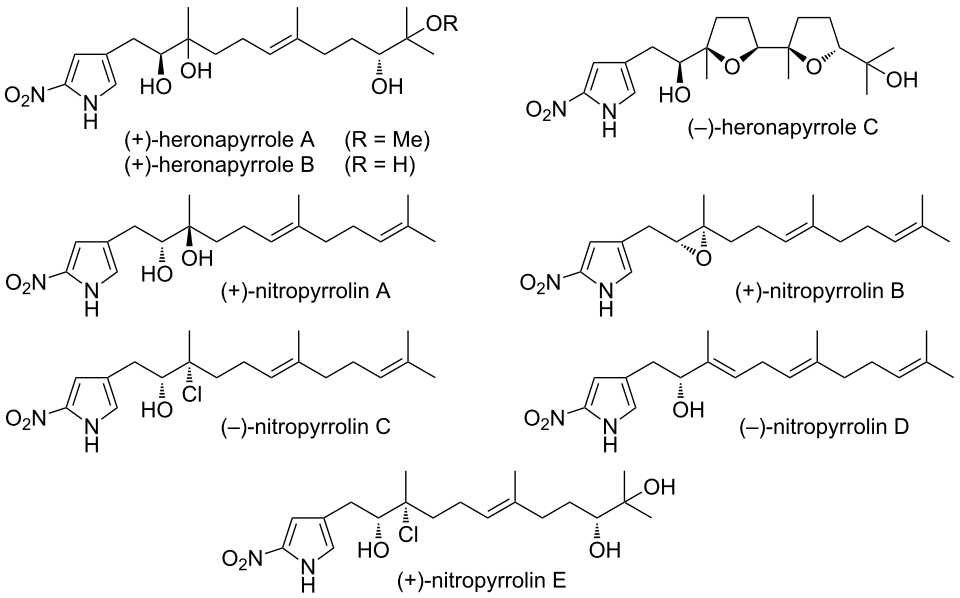
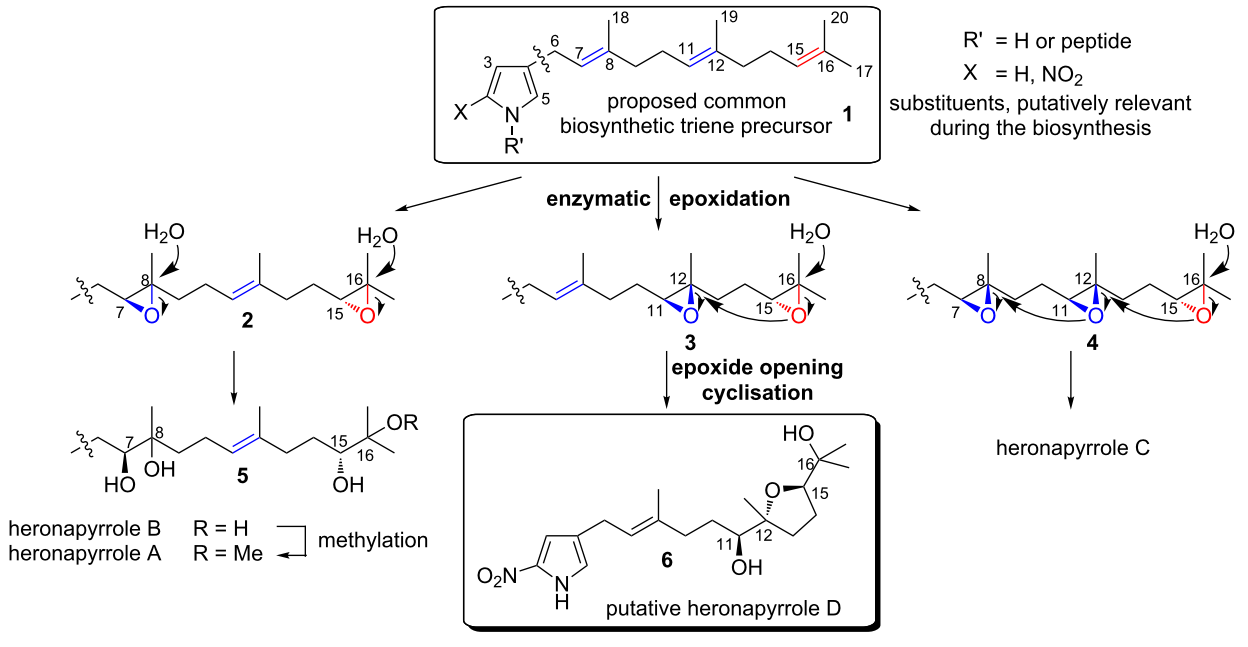


Figure 1: Known heronapyrroles A–C and nitropyrrolins A–E.

with closely related levels of oxidative functionalization of the farnesyl side chain.

In 2012 Stark et al. employed a biomimetic strategy to deliver the first asymmetric total synthesis of heronapyrrole C, confirming its constitution and establishing the relative as well as the absolute configuration [3,4] (recently, verified by Brimble et al. [5]). Building on these achievements, and in a departure from traditional natural products discovery, this report describes an innovative collaborative strategy that employed biosynthetic considerations, along with synthetic (Stark group) and natural products (Capon group) chemistry, to speculate on the likely existence of a hitherto unidentified heronapyrrole. This strategy culminated in the synthesis, detection and confirmation that heronapyrrole D (Scheme 1) was indeed a natural product.

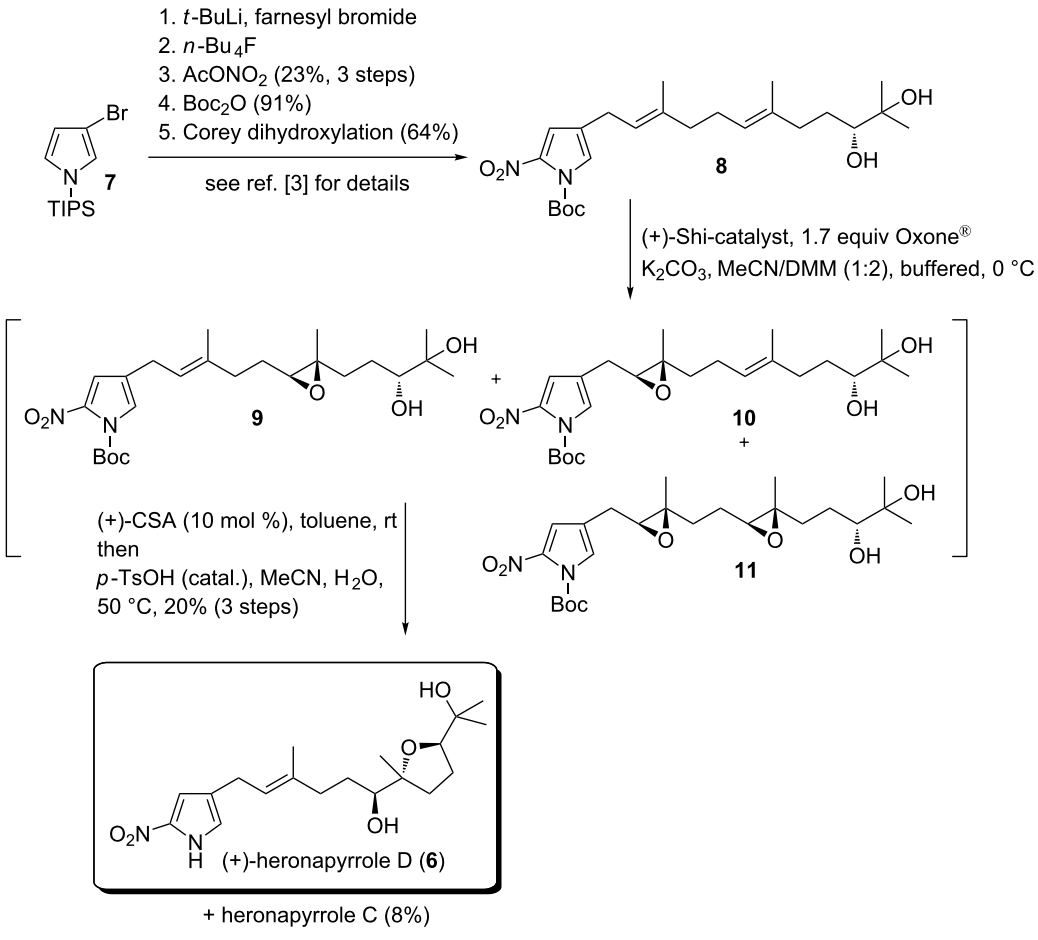


Scheme 1: Plausible biosynthesis of heronapyrroles A–D.

Results and Discussion

Although the genes responsible for heronapyrrole biosynthesis have not been identified yet, it is nevertheless possible to speculate on key aspects of this biosynthetic pathway, particularly those oxidative transformations that generate structural diversity [6-9] in the farnesyl side chain. For example, it is reasonable to conclude that 4-farnesylated 2-nitropyrrole **1** (Scheme 1) – arising from the action of a farnesyl transferase [10,11] on a suitable 2-nitropyrrole precursor – is a highly plausible common precursor for all heronapyrroles. Bisepoxidation of the Δ^7 and Δ^{15} double bond in the farnesyl residue (for atom numbering see Scheme 1), followed by regio- and stereoselective nucleophilic addition of water (and methylation) would deliver heronapyrroles A and B. Similarly, regio- and stereoselective nucleophilic addition of water to a *tris*-epoxy farnesyl intermediate **4** could initiate a cyclization cascade [1,3,8] that would provide the *bis*-tetrahydrofuran heronapyrrole C (Scheme 1), via a mechanism that closely resembles polyether antibiotic biosynthesis [12-17]. This biosynthetic hypothesis raises the possibility that *Streptomyces* sp. (CMB-M0423) may produce an alternative *bis*-epoxy intermediate **3** that can deliver a hitherto undetected *mono*-tetrahydrofuran heronapyrrole (e.g., heronapyrrole D, Scheme 1). To test this hypothesis we completed an asymmetric synthesis of the putative natural product heronapyrrole D, and used this material to probe *Streptomyces* sp. (CMB-M0423) cultivations to test whether heronapyrrole D is indeed a natural product.

The asymmetric synthesis of heronapyrrole D commenced with enantiomerically pure diol **8** (Scheme 2) synthesized in five steps from commercially available TIPS-protected 3-bromopyrrole **7** [3]. This reaction sequence, which incorporates a regioselective pyrrole alkylation, an electrophilic aromatic nitration and a regio- and stereoselective Corey–Noe–Lin dihydroxylation [18], has previously been described (in the total synthesis of heronapyrrole C) [3]. The procedure of Shi et al. [19-21] was then used to effect an epoxidation of **8**. Application of substoichiometric amounts of oxidant (Oxone®) delivered the isomeric *mono*-epoxides **9** and **10** as the main constituents, along with minor amounts of the *bis*-epoxide **11**. Of note, on work-up **9**



Scheme 2: Synthesis of heronapyrrole D.

was observed to undergo partial cyclization to the desired tetrahydrofuran framework, a cyclization event that was driven to completion by treatment with camphorsulfonic acid under non-aqueous conditions. Subsequent heating in H_2O/MeCN containing catalytic amounts of *p*-TsOH led to quantitative *N*-deprotection, while chromatographic purification of the resulting mixture provided heronapyrrole D (with an overall yield of 20% along with 8% of the previously known heronapyrrole C).

Cultivation and detection of heronapyrrole D: Saline broth inoculated with *Streptomyces* sp. (CMB-M0423) was cultivated and extracted as previously reported [1], after which it was analyzed by HPLC–DAD–MS–ESI(±) (Zorbax C_8, gradient elution 90% to 10% H_2O/MeCN with a constant 0.05% formic acid modifier). This analysis, supported by co-injection with authentic natural product standards, confirmed the presence of heronapyrroles A–C, and also detected an unidentified peak exhibiting the characteristic heronapyrrole (2-nitropyrrole) chromophore. HPLC–HRMS–ESI(+) analysis established a molecular formula ($C_{19}H_{30}N_2NaO_5$, Δmmu −0.2) for this unidentified heronapyrrole, consistent with that predicted for heronapyrrole D. Although semi-preparative HPLC fractionation returned a pure sample of this new heronapyrrole, the quantity available was insufficient for in depth structure elucidation. Fortunately, analytical HPLC–DAD comparisons between natural and synthetic samples of heronapyrrole D (see the Supporting Information File 1), together with optical rotation measurements [natural $[\alpha]_D^{22}$ +7.5 (*c* 0.003, MeOH); synthetic $[\alpha]_D^{22}$ +3.9 (*c* 0.1, MeOH)], established that heronapyrrole D was indeed a natural product, and that it possessed the structure and absolute configuration as proposed (see Supporting Information File 1, Figure S2). As with the known heronapyrroles A–C [1], heronapyrrole D exhibited growth inhibitory activity against the Gram-positive bacteria *Staphylococcus aureus* ATCC 25923 (IC_{50} 1.8 μM), *Staphylococcus epidermidis* ATCC 12228 (IC_{50} 0.9 μM) and *Bacillus subtilis* ATCC 6633 (IC_{50} 1.8 μM), but was inactive (IC_{50} > 30 μM) against the Gram-negative bacteria *Pseudomonas aeruginosa* ATCC 10145 and *Escherichia coli* ATCC 25922, and the fungus *Candida albicans* ATCC 90028.

Conclusion

In conclusion, this study illustrates the importance of biosynthetic considerations to both natural products and synthetic chemistry. Biosynthetic hypotheses provide natural product chemists with a framework to challenge the plausibility of assigned structures, and inform and inspire synthetic chemists to develop novel biomimetic transformations and total syntheses. In this study we demonstrate a less well-appreciated benefit that arises from biosynthetic considerations, the ability to predict the occurrence of a new member of a rare class of natural product [22]. The initial discovery of the heronapyrroles A–C [1] prompted a successful biomimetic synthesis of heronapyrrole C [3], which in turn lead to speculation regarding the existence of heronapyrrole D. A biomimetic synthesis of heronapyrrole D was critical to establishing its status as a natural product, and to evaluating its antibacterial properties.

Supporting Information

Supporting Information File 1

Experimental part and additional figures.
[http://www.beilstein-journals.org/bjoc/content/supplementary/1860-5397-10-121-S1.pdf]

Acknowledgements

We thank the Fonds der Chemischen Industrie (FCI) for financial support of this project (Stark group). This work was partially funded (Capon group) by the Institute for Molecular Bioscience, The University of Queensland, and the Australian Research Council (ARC DP120100183).

References

1. Raju, R.; Piggott, A. M.; Barrientos Diaz, L. X.; Khalil, Z.; Capon, R. J. *Org. Lett.* **2010,** *12,* 5158–5161. doi:10.1021/ol102162d
2. Kwon, H. C.; Espindola, A. P. D. M.; Park, J.-S.; Prieto-Davó, A.; Rose, M.; Jensen, P. R.; Fenical, W. *J. Nat. Prod.* **2010,** *73,* 2047–2052. doi:10.1021/np1006229
3. Schmidt, J.; Stark, C. B. W. *Org. Lett.* **2012,** *14,* 4042–4045. doi:10.1021/ol300954s
4. Schmidt, J.; Stark, C. B. W. *J. Org. Chem.* **2014,** *79,* 1920–1928. doi:10.1021/jo402240g
5. Ding, X.-B.; Furkert, D. P.; Capon, R. J.; Brimble, M. A. *Org. Lett.* **2014,** *16,* 378–381. doi:10.1021/ol403246j
6. Chen, B.; Kawazoe, K.; Takaishi, Y.; Honda, G.; Itoh, M.; Takeda, Y.; Kodzhimatov, O. K.; Ashurmetov, O. *J. Nat. Prod.* **2000,** *63,* 362–365. doi:10.1021/np990338a
7. Macherla, V. R.; Liu, J.; Bellows, C.; Teisan, S.; Nicholson, B.; Lam, K. S.; Potts, B. C. M. *J. Nat. Prod.* **2005,** *68,* 780–783. doi:10.1021/np049597c
8. Göhler, S.; Stark, C. B. W. *Org. Biomol. Chem.* **2007,** *5,* 1605–1614. doi:10.1039/b702877f
9. Riclea, R.; Dickschat, J. S. *Chem.–Eur. J.* **2011,** *17,* 11930–11934. doi:10.1002/chem.201101139
10. Wessjohann, L. A.; Sontag, B. *Angew. Chem., Int. Ed. Engl.* **1996,** *35,* 1697–1699. doi:10.1002/anie.199616971
Angew. Chem. **1996,** *108,* 1821–1823. doi:10.1002/ange.19961081527
11. Wessjohann, L.; Sontag, B.; Dessoy, M. A. In *Organic Chemistry Highlights IV;* Schmalz, H.-G., Ed.; Wiley-VCH: Weinheim, 1999; pp 79 ff.
12. Koert, U. *Angew. Chem., Int. Ed. Engl.* **1995,** *34,* 298–300. doi:10.1002/anie.199502981
Angew. Chem. **1995,** *107,* 326–328. doi:10.1002/ange.19951070307

13. Fernández, J. J.; Souto, M. L.; Norte, M. *Nat. Prod. Rep.* **2000,** *17,* 235–246. doi:10.1039/a909496b
14. Gallimore, A. R.; Spencer, J. B. *Angew. Chem., Int. Ed.* **2006,** *44,* 4406–4413. doi:10.1002/anie.200504284
Angew. Chem. **2006,** *118,* 4514-4521. doi:10.1002/ange.200504284
15. de María, P. D.; van Gemert, R. W.; Straathof, A. J. J.; Hanefeld, U. *Nat. Prod. Rep.* **2010,** *27,* 370–392. doi:10.1039/b809416k
16. Ueberbacher, B. T.; Hall, M.; Faber, K. *Nat. Prod. Rep.* **2012,** *29,* 337–350. doi:10.1039/c2np00078d
17. Vilotijevic, I.; Jamison, T. F. *Angew. Chem., Int. Ed.* **2009,** *48,* 5250–5281. doi:10.1002/anie.200900600
Angew. Chem. **2009,** *121,* 5352–5385. doi:10.1002/ange.200900600
18. Corey, E. J.; Noe, M. C.; Lin, S. *Tetrahedron Lett.* **1995,** *36,* 8741–8744. doi:10.1016/0040-4039(95)01920-D
19. Zhao, M.-X.; Shi, Y. *J. Org. Chem.* **2006,** *71,* 5377–5379. doi:10.1021/jo060335k
20. Shi, Y. *Acc. Chem. Res.* **2004,** *37,* 488–496. doi:10.1021/ar030063x
21. Wang, Z.-X.; Tu, Y.; Frohn, M.; Zhang, J.-R.; Shi, Y. *J. Am. Chem. Soc.* **1997,** *119,* 11224–11235. doi:10.1021/ja972272g
22. Löbermann, F.; Mayer, P.; Trauner, D. *Angew. Chem., Int. Ed.* **2010,** *49,* 6199–6202. doi:10.1002/anie.201001862
Angew. Chem. **2010,** *122,* 6335–6338. doi:10.1002/ange.201001862

License and Terms

This is an Open Access article under the terms of the Creative Commons Attribution License (http://creativecommons.org/licenses/by/2.0), which permits unrestricted use, distribution, and reproduction in any medium, provided the original work is properly cited.

The license is subject to the *Beilstein Journal of Organic Chemistry* terms and conditions: (http://www.beilstein-journals.org/bjoc)

The definitive version of this article is the electronic one which can be found at: doi:10.3762/bjoc.10.121

Beilstein Journal of Organic Chemistry

Selective allylic hydroxylation of acyclic terpenoids by CYP154E1 from *Thermobifida fusca* YX

Anna M. Bogazkaya[‡1], Clemens J. von Bühler[‡2], Sebastian Kriening[3], Alexandrine Busch[3], Alexander Seifert[1], Jürgen Pleiss[1], Sabine Laschat[3] and Vlada B. Urlacher[*2]

Full Research Paper

Open Access

Address:
[1]Institute of Technical Biochemistry, University of Stuttgart, Allmandring 31, 70569 Stuttgart, Germany, [2]Institute of Biochemistry, Heinrich-Heine University Düsseldorf, Universitätsstr. 1, 40225 Düsseldorf and [3]Institute of Organic Chemistry, University of Stuttgart, Pfaffenwaldring 55, 70569 Stuttgart, Germany

Email:
Vlada B. Urlacher[*] - vlada.urlacher@uni-duesseldorf.de

* Corresponding author ‡ Equal contributors

Keywords:
allylic hydroxylation; cytochrome P450; natural products; protein engineering; regiochemistry; terpenoids

Beilstein J. Org. Chem. **2014,** *10,* 1347–1353.
doi:10.3762/bjoc.10.137

Received: 23 March 2014
Accepted: 20 May 2014
Published: 13 June 2014

This article is part of the Thematic Series "Natural products in synthesis and biosynthesis".

Guest Editor: J. S. Dickschat

© 2014 Bogazkaya et al; licensee Beilstein-Institut.
License and terms: see end of document.

Abstract

Allylic alcohols are valuable precursors in the synthesis of pharmaceutical intermediates, agrochemicals and natural products. Regioselective oxidation of parental alkenes is a challenging task for chemical catalysts and requires several steps including protection and deprotection. Many cytochrome P450 enzymes are known to catalyse selective allylic hydroxylation under mild conditions. Here, we describe CYP154E1 from *Thermobifida fusca* YX that enables this type of oxidation. Several acyclic terpenoids were tested as possible substrates for CYP154E1, and the regio- and chemoselectivity of their oxidation was investigated. Using a previously established bioinformatics approach we identified position 286 in the active site of CYP154E1 which is putatively involved in substrate binding and thereby might have an effect on enzyme selectivity. To tune regio- and chemoselectivity of the enzyme three mutants at position 286 were constructed and used for substrate oxidation. All formed products were analysed with GC–MS and identified using chemically synthesised authentic samples and known compounds as references. Best regioselectivity towards geraniol and nerol was observed with the wild type enzyme mainly leading to 8-hydroxy derivatives (8-hydroxygeraniol or 8-hydroxynerol) with high selectivity (100% and 96% respectively). Highest selectivities during the oxidation of geranylacetone and nerylacetone were observed with the following variants: V286F led mainly to 7-hydroxygeranylacetone (60% of the total product) and V286A produced predominantly 12-hydroxynerylacetone (75% of total product). Thus, CYP154E1 and its mutants expand the tool-box for allylic hydroxylation in synthetic chemistry.

Introduction

Direct allylic hydroxylation yielding highly valuable allylic alcohols has been recognised for a while as one of the most oxyfunctionalizations [1]. Allylic alcohols can further be exploited for the synthesis of pharmaceutical intermediates, agrochemicals and natural products [2-4]. Various chemical catalysts including enzyme mimetica have been designed, characterised and applied for catalytic allylic hydroxylation reactions leading to synthetically relevant intermediates [5-11]. In addition to chemical catalysts a range of enzymes has been studied for selective allylic hydroxylation of alkenes [12,13]. Among biosynthetic routes selective allylic hydroxylation of monoterpene olefines to terpenoids in plants represents the most prominent example [14]. Heme-containing cytochrome P450 monooxygenases (P450 or CYP) are predominantly responsible for structural and functional diversity of terpenoids: allylic hydroxylation of parental monoterpenes leads to further diversification via sequential oxidation, reduction, isomerisation or conjugation reactions [14]. Furthermore, in some bacteria assimilating terpenes as carbon sources, the first oxidation step is a P450-mediated allylic hydroxylation or allylic rearrangement reaction [15]. In vitro investigations demonstrated that P450 enzymes can catalyse either the allylic hydroxylation of alkenes or the epoxidation of the corresponding C=C double bond or produce a mixture of the respective allylic alcohols and epoxides. Chemo- and regioselectivity of such reactions depend on the structure of the substrate and P450 used [16]. Different P450 enzymes produce different ratios of epoxidised and hydroxylated products [17-19]. The exact factors that govern the regiochemistry of P450 enzymes remain not completely understood [16]. In our previous studies we demonstrated the effects of the substrate stereochemistry on enzyme regio- and chemoselectivity [19]. The *E*-isomer geranylacetone was converted with a mutant of CYP102A1 from *Bacillus megaterium* (also referred to as P450 BM-3) with high activity and enantioselectivity to a single product 9,10-epoxygeranylacetone, while the oxidation of the *Z*-isomer nerylacetone yielded a mixture of several products, mainly epoxides but also allylic alcohols [19]. Later a CYP102A1 double mutant F87V/A328L was identified producing 80% allylic alcohols starting with geranylacetone [20]. These hydroxylated products are useful building blocks for the total syntheses of several natural compounds including smenochromene D [21], pseudopteranes, furanocembranes [22], indole alkaloids [23], and antitumor cembrane lactones crassin and isolobophytolide [24,25]. Obviously, there is a need for P450s with changed chemoselectivity.

Previously a systematic analysis of 31 P450 crystal structures and more than 6300 P450 sequences allowed us to derive rules on how to identify positions in the substrate binding cavity of P450s which is owing to its close proximity to the heme centre preferentially involved in substrate binding and thus in regioselectivity control [26]. Starting from two selectivity-determining positions, a minimal CYP102A1 library of only 24 variants was constructed and screened with four terpene substrates [20]. 11 variants demonstrated either a strong shift or improved regio- or chemoselectivity during oxidation of at least one substrate as compared to CYP102A1 wild type. This library was the starting point for engineering a highly selective CYP102A1 variant for terminal hydroxylation of (4*R*)-limonene at allylic C7 leading to perillyl alcohol. While the wild type did not hydroxylate (4*R*)-limonene at the C7 position, the triple mutant A264V/A238V/L437F converted (4*R*)-limonene to perillyl alcohol with a selectivity of 97% [27]. In a subsequent study, the effect of the two hotspot positions on regioselectivity towards cyclic and acyclic alkanes was investigated [28]. Among others, the double mutant F87V/A328F hydroxylated *n*-octane to 2-octanol with higher regioselectivity (92%) than the wild type (15%). To assess whether the concept of regioselectivity hotspots near the heme was transferable, residues that are equivalent to the two hotspot positions in CYP102A1 were mutated in CYP153A from *Marinobacter aquaeolei*. In the fatty acid ω-hydroxylase CYP153A, L354 corresponds to A328 in CYP102A1. While the wild type enzyme was highly ω-selective towards nonanoic acid with a ratio between the ω and the ω−1 product of 97:3, the variant L354I preferably hydroxylated nonanoic acid at the ω−1 position (24:76) [29].

Recently we reported on CYP154E1 from *Thermobifida fusca YX* that accepts a broad range of substrates including geraniol which is converted to 8-hydroxygeraniol [30]. In the present work several further acyclic terpenoids were screened as possible substrates for CYP154E1 and the regio- and chemoselectivity of their oxidation was investigated.

Results

Selection of the biocatalysts

According to the previously elaborated aforementioned sequence analysis, the residue at position 5 after the conserved ExxR motif is closest to the heme centre and therefore putatively interacting with any substrate in all P450s. In CYP154E1 V286 corresponds to position 5 after ExxR (Figure 1). The systematic analysis further revealed that residues at this position are predominantly hydrophobic. Hence, we substituted valine at position 286 by alanine, leucine and phenylalanine to change the orientation of substrates close to the heme centre.

After soluble protein expression in *E. coli* and subsequent purification, catalytically active P450 systems were reconstituted by addition of putidaredoxin (Pdx) and putidaredoxin reductase (PdR) from *Pseudomonas putida* as well as the pyri-

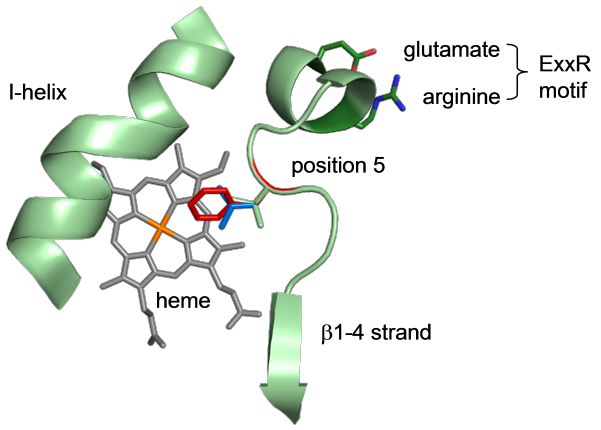
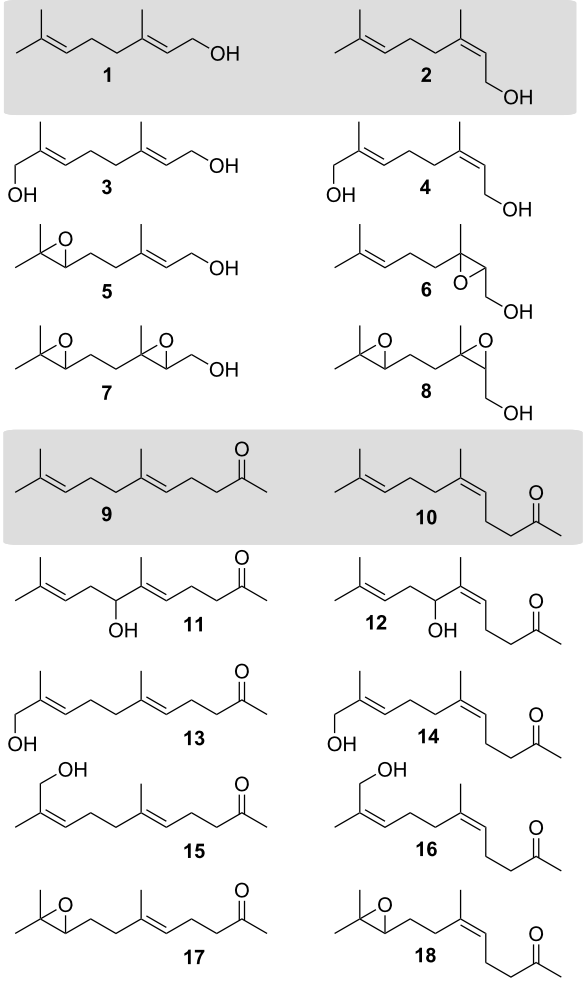


Figure 1: Immediate heme surroundings shown for the nearest relative of CYP154E1 with available crystal structure (CYP154A1, from *Streptomyces coelicolor*, PDB entry 1ODO). The residue in position 5 after the conserved ExxR motif (V286 in CYP154E1, green) reaches close to the heme centre (orange) in almost all P450s and was therefore substituted by phenylalanine (red), leucine (blue), and alanine (not visible). Based on the structure 1ODO point mutations were constructed using the software PyMol (DeLano Scientific LLC). From the rotamer library the candidates with the smallest sterical hindrance were selected.

dine cofactor NADH. Reactions were performed in 500 µL reaction volume. In order to avoid the stoichiometric addition of NADH enzymatic regeneration of this expensive cofactor by glucose dehydrogenase was performed [31]. Reactions run for 4 h. Substrate conversion and product distribution were analysed by GC–MS (see Supporting Information File 1). Products were identified using chemically synthesised authentic samples and known compounds as references (Scheme 1).



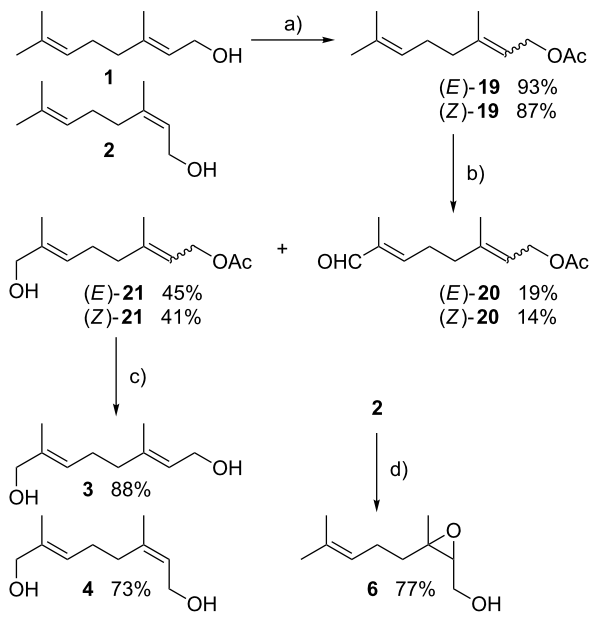
Scheme 1: Terpene substrates (grey background) and their oxidised derivatives.

Chemical synthesis of the oxidation products

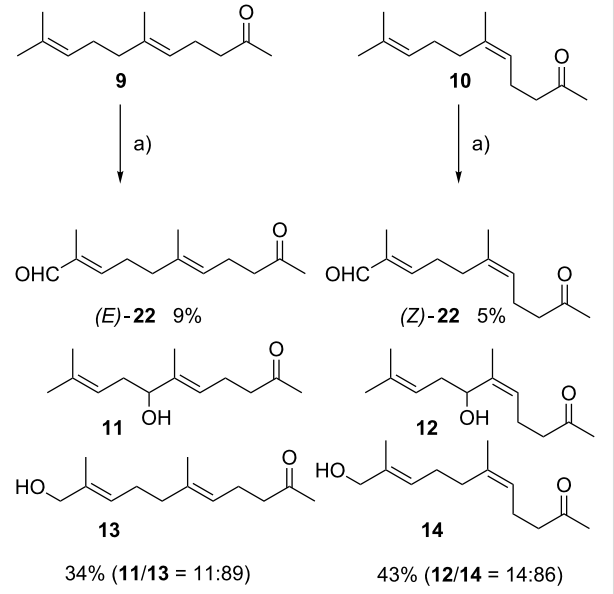
In order to identify the biocatalytic oxidation products synthetic routes to compounds **3**, **4**, **11**, **12**, **13** and **14** have been developed. The syntheses of compounds **5**, **7**, **8** [19] and **15**–**18** [20] have already been described before (see Supporting Information File 1).

There is no literature procedure for the synthesis of alcohol derivatives of geraniol (**1**) or nerol (**2**) by direct allylic oxidation. However, various conditions have been reported for geranyl acetate [32-34]. Following a modified procedure by Li [33], geranyl acetate ((*E*)-**19**), which was prepared from geraniol (**1**) in 93% yield [35] was treated under modified Sharpless conditions [36] with a catalytic amount of SeO_2 in the presence of *t*-BuOOH in dichloromethane at 0 °C, to give enal (*E*)-**20** and allylic alcohol (*E*)-**21** in 19% and 45% yield, respectively, which were separated by column chromatography. The cleavage of the acetyl group was performed with potassium carbonate in methanol at room temperature [37]. Purification by chromatography led to the desired 8-hydroxygeraniol (**3**) in 88% yield (Scheme 2). A similar sequence was applied to nerol (**2**), which was converted into neryl acetate ((*Z*)-**19**) in 87%, followed by allylic oxidation [38], to provide enal (*Z*)-**20** and allylic alcohol (*Z*)-**21** in 14% and 41% yield, respectively. Saponification of 8-hydroxyneryl acetate ((*Z*)-**21**) under the above mentioned conditions gave 8-hydroxynerol (**4**) in 73% yield (Scheme 2). Following a procedure by Fringuelli et al. [39] nerol (**2**) was treated with magnesium monoperoxyphthalate (MPPA) in the presence of NaOH to give 2,3-epoxynerol (**6**) in 77% yield together with 20% of reisolated starting material **2** (see Supporting Information File 1).

According to a method by McMurry [24], modified Sharpless conditions [36] for the allylic oxidation of geranylacetone (**9**) were used. Purification of the crude product by chromatography yielded the enal (*E*)-**22** (9%) and a 11:89 mixture of the alcohols 7-hydroxygeranylacetone (**11**) and 11-hydroxygeranyl-



Scheme 2: a) Ac_2O, pyridine, room temperature, 24 h; b) SeO_2, *t*-BuOOH, CH_2Cl_2, 0 °C, 5 h; c) K_2CO_3, MeOH, room temperature, 2.5 h; d) MPPA, NaOH, H_2O, room temperature, 5 h (MPPA = magnesium monoperoxyphthalate).



Scheme 3: a) SeO_2, *t*-BuOOH, CH_2Cl_2, 0 °C, 3.5 h.

acetone (**13**) in 34% yield and 11% of starting material **9** [24,25] (Scheme 3). The same procedure was employed for the oxidation of nerylacetone (**10**) providing after chromatography the enal (*Z*)-**22** (5% yield) and a 14:86 mixture of 7-hydroxynerylacetone (**12**) and 11-hydroxynerylacetone (**14**) in 43% yield and 4% **10** (see Supporting Information File 1).

Oxidation of geraniol (**1**) and nerol (**2**)

The *E*- and *Z*-isomers geraniol (**1**) and nerol (**2**) were oxidised by CYP154E1 wild type and mutants. Geraniol (**1**) was oxidised by CYP154E1 (98% conversion) regio- and chemoselectively to a single product, which was identified as 8-hydroxygeraniol (**3**). Conversion of nerol (**2**) reached 77%, but was less selective than that of geraniol (**1**) resulting in the allylic alcohol 8-hydroxynerol (**4**, 96%) and 2,3-epoxynerol (**6**, 4%) as byproduct (Table 1).

As expected, amino acid substitutions at position 286 changed both regio- and chemoselectivity of the wild type significantly. All three mutants V286L, V286A, and V286F showed strong preference for epoxides when starting with geraniol (**1**) and nerol (**2**), respectively. Mutant V286L was able to oxidise geraniol (**1**) to a mixture of 6,7-epoxygeraniol (**5**, 26%) and diepoxygeraniol **7** (74%) with 11% conversion, while nerol (**2**) was converted only up to 4% to get a mixture of 2,3-epoxynerol (**6**) and diepoxynerol (**8**) at a ratio of 58:42.

V286A and V286F catalysed the oxidation of geraniol (**1**) to a mixture of epoxides **5** and **7** as in the case of V286L. Two epoxide products appeared at a ratio of 59:41 (V286A), and only 6% substrate conversion was observed. The V286F mutant

Table 1: Comparison of geraniol (**1**) and nerol (**2**) oxidation catalysed by CYP154E1 wild type and three variants.

	Product distribution: Peak area[a]				Conversion	
	geraniol (**1**)		nerol (**2**)		**1**	**2**
CYP154E1		**3** (100%)	**4** (96%)	**6** (4%)	98%	77%
V286L	**5** (26%)	**7** (74%)	**8** (42%)	**6** (58%)	11%	4%
V286A	**5** (59%)	**7** (41%)	**8** (49%)	**6** (51%)	6%	3%
V286F	**5** (58%)	**7** (42%)	**8** (52%)	**6** (48%)	45%	22%

[a]Determined by GC–MS.

produced the same epoxides at a ratio of 58:42, however with a higher activity leading to substrate conversion of 45%.

Nerol (**2**) was oxidised by V286A and V286F again to epoxides **8** and **6**. In both cases conversions were rather low and reached 3 and 22%, respectively (Table 1).

Oxidation of geranylacetone (**9**) and nerylacetone (**10**)

Geranylacetone (**9**) was oxidised by CYP154E1 wild type to four products with 98% conversion (Table 2). The main product was identified as 12-hydroxygeranylacetone (**15**, 42%). The other products were 11-hydroxygeranylacetone (**13**, 41%), 7-hydroxygeranylacetone (**11**, 8%) and the epoxide 9,10-epoxygeranylacetone (**17**, 9%). Similar to the conversion of geraniol (**1**), the regio- and chemoselectivity of geranylacetone oxidation catalysed by the mutants was different compared to the wild type enzyme. The product analysis revealed a strong preference of all three mutants for the formation of C7-hydroxylated compound **11** as the main product.

Table 2: Comparison of geranylacetone (**9**) and nerylacetone (**10**) oxidation catalysed by CYP154E1 wild type and three variants.

	Product distribution: Peak area[a]		Conversion	
	geranylacetone (**9**)	nerylacetone (**10**)	**9**	**10**
CYP154E1	**11** (8%) **13** (41%) **15** (42%) **17** (9%)	**12** (12%) **14** (32%) **16** (56%)	98%	97%
V286L	**11** (44%) **13** (18%) **15** (35%) **17** (3%)	**12** (28%) **16** (72%)	20%	19%
V286A	**11** (46%) **13** (16%) **15** (15%) **17** (23%)	**12** (25%) **16** (75%)	25%	42%
V286F	**11** (60%) **13** (9%) **15** (31%)	**12** (24%) **14**(13%) **16** (63%)	75%	90%

[a]Determined by GC–MS.

Variant V286L produced 44% of 7-hydroxygeranylactone (**11**) as well as the compounds **13** (18%) and **15** (35%). Substrate epoxidation leading to the epoxide **17** was much slower compared to the wild type: this product accounted to less than 3% (substrate conversion was 20%). Variant V286A catalysed the hydroxylation of geranylacetone (**9**) to 7-hydroxygeranylacetone (**11**, 46%), 9,10-epoxygeranylacetone (**17**, 23%), 12-hydroxygeranylacetone (**15**, 15%) and 11-hydroxygeranylacetone (**13**, 16%) with a substrate conversion of 25%.

Variant V286F showed the strongest shift in regio- and chemoselectivity and converted geranylacetone (**9**) to a mixture of allylic alcohols without formation of epoxides. Substrate conversion was 75%, which is similar to that of the wild type. V286F led in this reaction to three allylic alcohols, again with a strong preference for C7 position (**11**, 60%) over C12 (**15**, 31%) and C11 (**13**, 9%).

The *Z*-isomer nerylacetone (**10**) was oxidised by CYP154E1 wild type and its mutants more selectively than the *E*-isomer geranylacetone (**9**) (Table 2). Three products were identified as a mixture of allylic alcohols with hydroxy groups incorporated at positions C7 (**12**, 12%), C11 (**14**, 32%) and C12 (**16**, 56%) with 97% conversion.

The product analysis of nerylacetone (**10**) oxidation catalysed with the mutants revealed a preference for the formation of hydroxylated products with 12-hydroxynerylacetone (**16**) as the main product. V286F oxidised nerylacetone (**10**) with high activity (90% conversion) leading to the same three allylic alcohols as the wild type enzyme, but with a shifted ratio towards 12-hydroxynerylacetone (**16**, 63%). Variants V286L and V286A showed even a stronger shift in regioselectivity and oxidised nerylacetone (**10**) almost exclusively to two allylic alcohols with a notable preference for 12-hydroxynerylacetone (**16**, 72% and 75%, respectively) (Table 2).

Discussion

As mentioned in the introduction a large number of regioselective hydroxylation reactions occur in plants. Recently a geraniol 10-hydroxylase from the plant *Catharanthus roseus* [40] has been cloned and heterologously expressed in baculovirus-infected insect cells [41]. This cytochrome P450 monooxygenase belonging to the CYP76B family has been demonstrated to be involved into the biosynthesis of the alkaloid secologanin, and produced 8-hydroxynerol. It should be noted, that the enzyme used by the authors produced 8-hydroxynerol rather than 10-hydroxynerol according to their Figure 3 [41]. The use of this monooxygenase in biocatalysis is however not feasible because this enzyme is membrane bound, relies on a membrane associated cytochrome P450 reductase (CPR) and could only be produced in insect cells at low concentrations. Bacterial P450s have several advantages over their eukaryotic counterparts. They are soluble cytosolic enzymes interacting with soluble redox partner proteins. Thus, CYP154E1 from *T. fusca* is a valuable alternative for plant CYP76B because it is soluble and thermostable with a T_{50} of 63 °C. It interacts with also soluble redox partners and can be expressed in *E. coli* at a level of up to 50 mg/L. CYP154E1 is able to catalyse the regioselective hydroxylation of geraniol (**1**) to 8-hydroxygeraniol (**3**) and of nerol (**2**) mainly to 8-hydroxynerol (**4**). The chemical synthesis

of these compounds requires 3 steps including protection/deprotection of the terminal hydroxy group.

Altering regio-, chemo- and stereoselectivity of P450-catalysed reactions remain a challenging task for protein engineering. In the recent years significant achievements have been made in this field. By using an iterative mutagenesis approach "combinatorial active-site saturation test (CAST)" Reetz and colleagues constructed several variants of CYP102A1 which demonstrate high regio- and stereoselectivity for testosterone and progesterone oxidation [42]. The parent F87A variant of CYP102A1 catalysed the hydroxylation of testosterone at both positions 2β and 15β. Simultaneous substitutions at three positions in the substrate binding pocket R47, T49, Y51 provided a variant yielding up to 94% of 2β-hydroxytestosterone. Combined mutations in the sites V78 and A82 favoured the 15β-position for hydroxylation and increased the enzyme selectivity towards 15β-hydroxylation finally up to 96% [42]. In another study Commandeur and colleagues tested a library of CYP102A1 variants for their ability to produce regio- and stereoselectively different diastereomers of 3-hydroxy-α-ionone. Several variants were identified with high selectivity for *trans*-3-hydroxy-α-ionone for both substrate enantiomers. They produced (3*R*,6*R*)-hydroxy-α-ionone and (3*S*,6*S*)-hydroxy-α-ionone. Other CYP102A1 mutants demonstrated opposite stereoselectivity and produced not only the trans-isomer (3*S*,6*S*)-hydroxy-α-ionone but also the *cis*-diastereomer (3*S*,6*R*)-hydroxy-α-ionone [43].

The identification of the position 286 in CYP154E1 that obviously influences the regioselectivity of the enzyme and subsequent replacing of valine at this position by three other hydrophobic amino acids of different size allowed for the production of epoxides. Although in this case both substrates, geraniol (**1**) and nerol (**2**) were epoxidised into two products respectively, variant V286F seems to be more promising as it produced 6,7-epoxygeraniol (**5**) at a product ratio of 58% with high activity.

Less selective was CYP154E1 during oxidation of geranylacetone (**9**) and nerylacetone (**10**). With geranylacetone as substrate three allylic alcohols and only 9% epoxide were formed. In the case of nerylacetone (**10**) the reaction catalysed by the wild type enzyme yielded three allylic alcohols. Though being less active, all three mutants were more regio- and chemoselective (except for V286A with geranylacetone (**9**)). Highest selectivities were observed with the following variants: V286F led mainly to 7-hydroxygeranylacetone (**11**, 60% of the total product) and V286A produced predominantly 12-hydroxynerylacetone (**16**, 75% of total product). Thus, to our knowledge for the first time P450s were engineered that catalyse the allylic hydroxylation of geranylacetone (**9**) mainly to 7-hydroxygeranylacetone (**11**) and nerylacetone (**10**) preferentially to 12-hydroxynerylacetone (**16**).

Interestingly, altered regioselectivity and high catalytic activity are not mutually exclusive properties. While for geraniol (**1**) and nerol (**2**) the mutants showed lower conversions than the wild type, for geranylacetone (**9**) and nerylacetone (**10**) the more selective mutant V286F had a catalytic activity similar to that of the wild type. A similar observation was made also during mutagenesis of CYP102A1 where high regioselectivity and high catalytic activity are not mutually exclusive properties. While for geranylacetone (**9**) the most selective mutant showed only 2% of the wild type activity, for limonene the most selective mutant had more than threefold wild type activity [20].

Conclusion

Finally, in this study we investigated the application of CYP154E1 as regio- and chemoselective biocatalyst for the synthesis of allylic alcohols of acyclic terpenoids. Highest regioselectivity towards geraniol (**1**) and nerol (**2**) was observed with the wild type enzyme leading to mainly 8-hydroxy derivatives.

Moreover, by bioinformatics analysis position 286 was identified and a simple point mutation changed the geometry of the active site of this P450 enzyme to shift the product spectrum for the selective oxidation of geranylacetone (**9**) and nerylacetone (**10**) to yield only allylic alcohols.

Supporting Information

Supporting Information File 1

Experimental and analytical data.
[http://www.beilstein-journals.org/bjoc/content/supplementary/1860-5397-10-137-S1.pdf]

Acknowledgements

Generous financial support by the Ministerium für Wissenschaft, Forschung und Kunst des Landes Baden-Württemberg, the Deutsche Forschungsgemeinschaft (SFB 706) and the Fonds der Chemischen Industrie is gratefully acknowledged.

References

1. Gärtner, M.; Mader, S.; Seehafer, K.; Helmchen, G. *J. Am. Chem. Soc.* **2011,** *133,* 2072–2075. doi:10.1021/ja109953v
2. Fraunhoffer, K. J.; Bachovchin, D. A.; White, M. C. *Org. Lett.* **2005,** *7,* 223–226. doi:10.1021/ol047800p

3. Fraunhoffer, K. J.; Prabagaran, N.; Sirois, L. E.; White, M. C. *J. Am. Chem. Soc.* **2006,** *128,* 9032–9033. doi:10.1021/ja063096r
4. Stang, E. M.; White, C. M. *Nat. Chem.* **2009,** *1,* 547–551. doi:10.1038/nchem.351
5. Andrus, M. B.; Lashley, J. C. *Tetrahedron* **2002,** *58,* 845–866. doi:10.1016/S0040-4020(01)01172-3
6. Barry, S. M.; Rutledge, P. J. *Synlett* **2008,** 2172–2174. doi:10.1055/s-2008-1078248
7. Barry, S. M.; Mueller-Bunz, H.; Rutledge, P. J. *Org. Biomol. Chem.* **2012,** *10,* 7372–7381. doi:10.1039/c2ob25834j
8. Che, C.-M.; Lo, V. K.-Y.; Zhou, C.-Y.; Huang, J.-S. *Chem. Soc. Rev.* **2011,** *40,* 1950–1975. doi:10.1039/c0cs00142b
9. Kanbayashi, N.; Onitsuka, K. *Angew. Chem.* **2011,** *123,* 5303–5305. doi:10.1002/ange.201101078 *Angew. Chem., Int. Ed.* **2011,** 50, 5197–5199. doi:10.1002/anie.201101078
10. Moiseev, I. I.; Vargaftik, M. N. *Coord. Chem. Rev.* **2004,** *248,* 2381–2391. doi:10.1016/j.ccr.2004.05.020
11. Nakamura, A.; Nakada, M. *Synthesis* **2013,** *45,* 1421–1451. doi:10.1055/s-0033-1338426
12. Boeglin, W. E.; Brash, A. R. *J. Biol. Chem.* **2012,** *287,* 24139–24147. doi:10.1074/jbc.M112.364216
13. Ortiz de Montellano, P. R. *Chem. Rev.* **2010,** *110,* 932–948. doi:10.1021/cr9002193
14. Mau, C. J. D.; Croteau, R. *Phytochem. Rev.* **2006,** *5,* 373–383. doi:10.1007/s11101-006-9008-2
15. Ortiz de Montellano, P. R.; Nelson, S. D. *Arch. Biochem. Biophys.* **2011,** *507,* 95–110. doi:10.1016/j.abb.2010.10.016
16. Cohen, S.; Kozuch, S.; Hazan, C.; Shaik, S. *J. Am. Chem. Soc.* **2006,** *128,* 11028–11029. doi:10.1021/ja063269c
17. Roduner, E.; Kaim, W.; Sarkar, B.; Urlacher, V. B.; Pleiss, J.; Gläser, R.; Einicke, W.-D.; Sprenger, G. A.; Beifuß, U.; Klemm, E.; Liebner, C.; Hieronymus, H.; Hsu, S.-F.; Plietker, B.; Laschat, S. *ChemCatChem* **2013,** *5,* 82–112. doi:10.1002/cctc.201200266
18. Sowden, R. J.; Yasmin, S.; Rees, N. H.; Bell, S. G.; Wong, L.-L. *Org. Biomol. Chem.* **2005,** *3,* 57–64. doi:10.1039/b413068e
19. Watanabe, Y.; Laschat, S.; Budde, M.; Affolter, O.; Shimada, Y.; Urlacher, V. B. *Tetrahedron* **2007,** *63,* 9413–9422. doi:10.1016/j.tet.2007.06.104
20. Seifert, A.; Vomund, S.; Grohmann, K.; Kriening, S.; Urlacher, V. B.; Laschat, S.; Pleiss, J. *ChemBioChem* **2009,** *10,* 853–861. doi:10.1002/cbic.200800799
21. Bruder, M.; Moody, C. J. *Synlett* **2008,** 575–577. doi:10.1055/s-2008-1032090
22. Marshall, J. A.; DuBay, W. J. *J. Org. Chem.* **1994,** *59,* 1703–1708. doi:10.1021/jo00086a018
23. Clark, V. C.; Raxworthy, C. J.; Rakotomalala, V.; Sierwald, P.; Fisher, B. L. *Proc. Natl. Acad. Sci. U. S. A.* **2005,** *102,* 11617–11622. doi:10.1073/pnas.0503502102
24. McMurry, J. E.; Dushin, R. G. *J. Am. Chem. Soc.* **1990,** *112,* 6942–6949. doi:10.1021/ja00175a031
25. McMurry, J. E.; Matz, J. R.; Kees, K. L. *Tetrahedron* **1987,** *43,* 5489–5498. doi:10.1016/S0040-4020(01)87732-2
26. Seifert, A.; Pleiss, J. *Proteins: Struct., Funct., Bioinf.* **2009,** *74,* 1028–1035. doi:10.1002/prot.22242
27. Seifert, A.; Antonovici, M.; Hauer, B.; Pleiss, J. *ChemBioChem* **2011,** *12,* 1346–1351. doi:10.1002/cbic.201100067
28. Weber, E.; Seifert, A.; Antonovici, M.; Geinitz, C.; Pleiss, J.; Urlacher, V. B. *Chem. Commun.* **2011,** *47,* 944–946. doi:10.1039/c0cc02924f
29. Honda Malca, S.; Scheps, D.; Kühnel, L.; Venegas-Venegas, E.; Seifert, A.; Nestl, B. M.; Hauer, B. *Chem. Commun.* **2012,** *48,* 5115–5117. doi:10.1039/c2cc18103g
30. von Bühler, C.; Le-Huu, P.; Urlacher, V. B. *ChemBioChem* **2013,** *14,* 2189–2198. doi:10.1002/cbic.201300271
31. Truppo, M. D. Cofactor recycling for enzyme catalyzed processes. In *Comprehensive Chirality;* Carreira, E. M.; Yamamoto, H., Eds.; Elsevier Ltd.: Amsterdam, 2012; Vol. 7, pp 46–70. doi:10.1016/B978-0-08-095167-6.00704-7
32. Inouye, H.; Ueda, S.; Uesato, S.; Kobayashi, K. *Chem. Pharm. Bull.* **1978,** *26,* 3384–3394. doi:10.1248/cpb.26.3384
33. Li, W.; Li, Y.; Li, Y. *Synthesis* **1994,** 267–269. doi:10.1055/s-1994-25455
34. Meinwald, J.; Thompson, W. R.; Eisner, T.; Owen, D. F. *Tetrahedron Lett.* **1971,** *12,* 3485–3488. doi:10.1016/S0040-4039(01)97212-0
35. Fretz, H.; Woggon, W.-D. *Helv. Chim. Acta* **1986,** *69,* 1959–1970. doi:10.1002/hlca.19860690822
36. Umbreit, M. A.; Sharpless, K. B. *J. Am. Chem. Soc.* **1977,** *99,* 5526–5528. doi:10.1021/ja00458a072
37. Nakai, T.; Yajima, A.; Akasaka, K.; Kaihoku, T.; Ohtaki, M.; Nukada, T.; Ohrui, H.; Yabuta, G. *Biosci., Biotechnol., Biochem.* **2005,** *69,* 2401–2408. doi:10.1271/bbb.69.2401
38. Marshall, J. A.; Lebreton, J. *J. Org. Chem.* **1988,** *53,* 4108–4112. doi:10.1021/jo00252a044
39. Fringuelli, F.; Germani, R.; Pizzo, F.; Santinelli, F.; Savelli, G. *J. Org. Chem.* **1992,** *57,* 1198–1202. doi:10.1021/jo00030a029
40. Collu, G.; Unver, N.; Peltenburg-Looman, A. M. G.; van der Heijden, R.; Verpoorte, R.; Memelink, J. *FEBS Lett.* **2001,** *508,* 215–220. doi:10.1016/S0014-5793(01)03045-9
41. Sung, P.-H.; Huang, F.-C.; Do, Y.-Y.; Huang, P.-L. *J. Agric. Food Chem.* **2011,** *59,* 4637–4643. doi:10.1021/jf200259n
42. Kille, S.; Zilly, F. E.; Acevedo, J. P.; Reetz, M. T. *Nat. Chem.* **2011,** *3,* 738–743. doi:10.1038/nchem.1113
43. Venkataraman, H.; de Beer, S. B. A.; Geerke, D. P.; Vermeulen, N. P. E.; Commandeur, J. N. M. *Adv. Synth. Catal.* **2012,** *354,* 2172–2184. doi:10.1002/adsc.201200067

License and Terms

This is an Open Access article under the terms of the Creative Commons Attribution License (http://creativecommons.org/licenses/by/2.0), which permits unrestricted use, distribution, and reproduction in any medium, provided the original work is properly cited.

The license is subject to the *Beilstein Journal of Organic Chemistry* terms and conditions: (http://www.beilstein-journals.org/bjoc)

The definitive version of this article is the electronic one which can be found at: doi:10.3762/bjoc.10.137

Beilstein Journal of Organic Chemistry

Streptopyridines, volatile pyridine alkaloids produced by *Streptomyces* sp. FORM5

Ulrike Groenhagen, Michael Maczka, Jeroen S. Dickschat and Stefan Schulz*

Full Research Paper

Open Access

Address:
Institut für Organische Chemie, Technische Universität Braunschweig, Hagenring 30, 38106 Braunschweig, Germany

Email:
Stefan Schulz* - stefan.schulz@tu-braunschweig.de

* Corresponding author

Keywords:
headspace analysis; natural products; polyketide biosynthesis; pyridine derivatives; streptazolin; volatile compounds

Beilstein J. Org. Chem. **2014,** *10,* 1421–1432.
doi:10.3762/bjoc.10.146

Received: 07 February 2014
Accepted: 28 May 2014
Published: 24 June 2014

This article is part of the Thematic Series "Natural products in synthesis and biosynthesis".

Associate Editor: A. Kirschning

© 2014 Groenhagen et al; licensee Beilstein-Institut.
License and terms: see end of document.

Abstract

Streptomyces sp. FORM5 is a bacterium that is known to produce the antibiotic streptazolin and related compounds. We investigated the strain for the production of volatiles using the CLSA (closed-loop stripping analysis) method. Liquid and agar plate cultures revealed the formation of new 2-alkylpyridines (streptopyridines), structurally closely related to the already known 2-pentadienylpiperidines. The structures of the streptopyridines A to E were confirmed by total synthesis. The analysis of the liquid phase by solvent extraction or extraction with an Oasis adsorbent showed that streptazolin and 2-pentadienylpiperidine are the major compounds, while the streptopyridines are only minor components. In the gas phase, only the streptopyridines could be detected. Therefore, an orthogonal set of analysis is needed to assess the metabolic profile of bacteria, because volatile compounds are obviously overlooked by traditional analytical methods. The streptopyridines are strain specific volatiles that are accompanied by a broad range of headspace constituents that occur in many actinomycetes. Volatiles might be of ecological importance for the producing organism, and, as biosynthetic intermediates or shunt products, they can be useful as indicators of antibiotic production in a bacterium.

Introduction

Actinomycetes are excellent producers of diverse and bioactive secondary metabolites. These metabolites belong to many different structural classes including polyketides, nonribosomal peptides, terpenoids, alkaloids, lipids and others. Such compounds became a major source of biologically active natural products as antibiotics, cytotoxic compounds, immunosuppressants etc. In addition, actinomycetes are also able to produce and release a wide variety of volatile compounds with bouquets composed of up to 100 different compounds [1-6]. Major volatile classes comprise aliphatic compounds derived from

fatty acid metabolism, terpenes, aromatic compounds, sulfur compounds, and pyrazines [1]. Apart from pyrazines, indole, and a few strain specific compounds [2] such as methyl pyrrole-2-carboxylate, emitted by *Stackebrandtia nassauensis*, or 2-acetylpyrrole from *Saccharopolyspora erythraea*, volatile alkaloids are rarely produced by actinomycetes.

We became interested in the strain *Streptomyces* sp. FORM5 to elucidate whether volatile formation is linked to the production of other, usually less volatile secondary metabolites and whether different compounds can be detected by headspace analysis [7] compared to commonly used solvent extraction or adsorption/extraction procedures. Strain FORM5 has been reported to produce the tetrahydrocyclopenta[*b*]pyridine derivatives streptazones B_1 (**1**), B_2 (**2**), C (**3**), the 4-pyridone derivative streptazone D (**4**) with a pentadienyl side chain, and streptazolin (**5**) (Figure 1) [8]. Streptazolin is produced by several streptomycetes [8-12], and is formed biosynthetically by a polyketide mechanism [13]. The respective polyketide synthase gene cluster has not been identified yet.

The streptazones are relatively small compounds suggesting that they may be volatile enough to find them in the headspace above bacterial cultures, although the presence of hydrogen bond donor and acceptor sites hints to good solubility in the aqueous phase.

In our study the volatile bouquet of the actinomycete *Streptomyces* sp. FORM5 was investigated and several new 2-alkylated pyridines were identified using the closed-loop stripping analysis (CLSA) [7] headspace technique followed by GC–MS analysis and synthesis of the target compounds for structure verification. Agar plate cultures and liquid cultures were investigated and the liquid phase analyzed for the presence of secondary metabolites. The results showed that by headspace analysis new secondary metabolites can be found that eluded earlier analysis. The separate analysis of headspace and liquid phase is complementary and in combination allows better evaluation of the metabolic potential of an investigated microorganism.

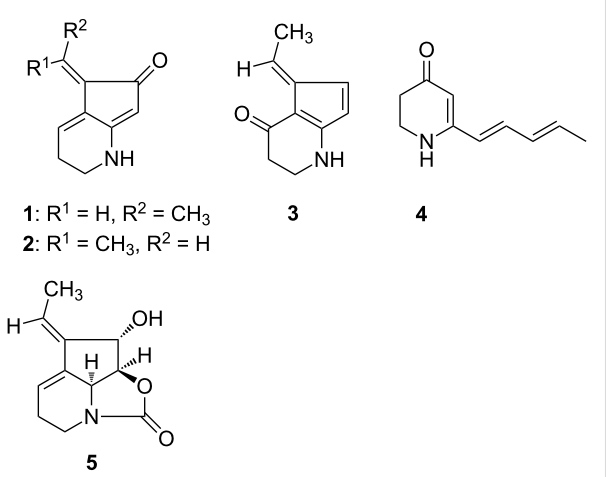


Figure 1: Alkaloids produced by *Streptomyces* strain FORM5.

Results and Discussion

The volatiles released by agar plate cultures of strain *Streptomyces* sp. FORM5 were collected by CLSA for one day on a charcoal filter and eluted with dichloromethane. The extract was then analyzed using GC–MS. More than 40 different compounds were identified in the headspace extract (Table 1, Figure 2, and Figure S1 in Supporting Information File 1). Nevertheless, the major compounds (compounds **8**, **9**, **11**, and **12** in Figure 2) attracted our interest, because they were unknown, thus giving room for the discovery of new volatile secondary metabolites. High resolution GC–MS revealed a molecular composition of $C_{10}H_{11}N$ (found 145.09136, calcd

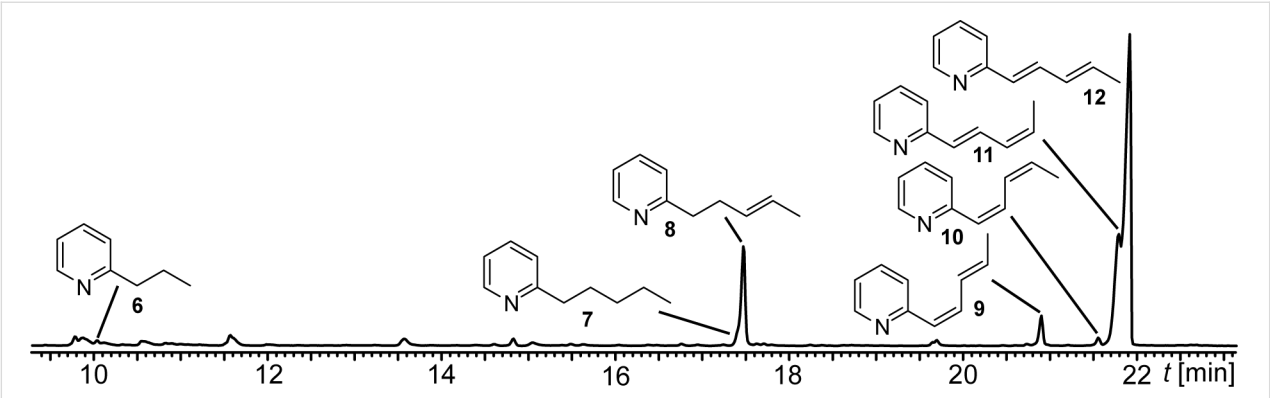


Figure 2: Part of the total ion chromatogram of the headspace extract of *Streptomyces* sp. FORM5 with the structures of 2-propylpyridine (**6**), 2-pentylpyridine (**7**), (*E*)-2-(pent-3-en-1-yl)pyridine (**8**), 2-((1*Z*,3*E*)-penta-1,3-dien-1-yl)pyridine (**9**), 2-((1*Z*,3*Z*)-penta-1,3-dien-1-yl)pyridine (**10**), 2-((1*E*,3*Z*)-penta-1,3-dien-1-yl)pyridine (**11**), 2-((1*E*,3*E*)-penta-1,3-dien-1-yl)pyridine (**12**).

145.08910) for the major compound **12** and $C_{10}H_{13}N$ (found 147.10428, calcd 147.10475) for the minor component **8**. The mass spectrum (Figure 3) of the major compound pointed to the presence of an extended aromatic and conjugated π-system and the formation of a stable $[M - 1]^+$ ion. The methyl loss to form the base peak $[M - 15]^+$ indicated the presence of a methyl group in the compound. Careful analysis of the extract revealed that a small peak (**7**) eluted slightly earlier than compound **8**. The mass spectrum of compound **7** matched that of 2-pentylpyridine, present in public databases [14]. From these data we concluded that the unknown compound **12** might be a 2-(pentadienyl)pyridine with conjugated side chain and that the compounds **9**–**12** might be diastereomers. Compound **8** should carry a pentenyl side chain, while compound **6** showed a mass spectrum identical to the known one of 2-propylpyridine.

The target compounds were then synthesized to prove the structural proposal. Pentadienylpyridines **9**–**12** were synthesized by Wittig reaction using different conditions (Scheme 1). A Wittig–Schlosser reaction [15] starting from a commercially available 5:1 *E*/*Z*-mixture of 1-bromobut-2-ene (**17**) led to preferentially (1*E*)-configured products. After conversion of **17** into the respective Wittig salt **18** and reaction with 2-pyridinecarbaldehyde (**19**) a mixture of four diastereoisomers of 2-(1,3-pentadienyl)pyridine was formed (Figure 4), all showing similar mass spectra. These four diastereomers proved to be identical to the natural compounds **9** to **12** by comparison of mass spectra and GC retention. The major compound, 2-((1*E*,3*E*)-penta-1,3-dienyl)pyridine (**12**), and the 1*Z*,3*E*-isomer **9** could be isolated in almost pure form, but a large amount of material was lost during the purification process (17% yield for compound **12** and 3% yield for compound **9** after purification). The large coupling constants ^3J around 15 Hz between H-1 and H-2 (15.8 Hz) as well as H-3 and H-4 (15.1 Hz) in the side chain indicated the *E*-configuration of both double bonds for compound **12**. The mass spectrum and retention time proved to be identical to compound **12**, the major compound of the natural extract. We propose the name streptopyridine A for this new natural compound. The minor product isolated pure under these conditions was 2-((1*Z*,3*E*)-penta-1,3-dienyl)pyridine (**9**, streptopyridine B), indicated by the coupling constants $^3J_{1,2}$ = 11.8 Hz and $^3J_{3,4}$ = 15.1 Hz.

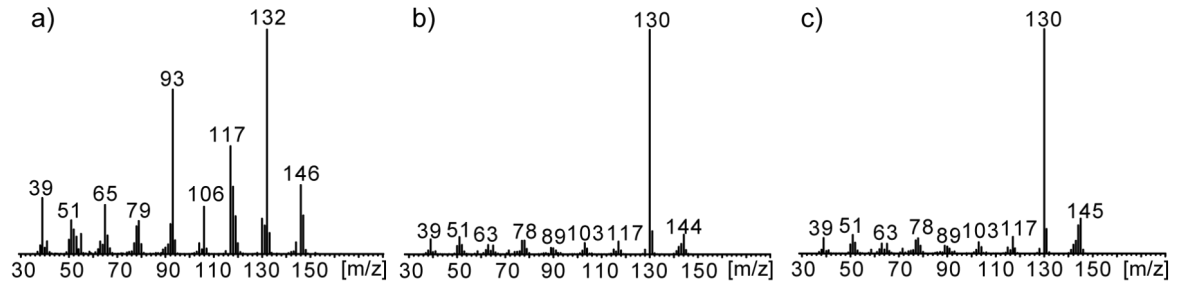
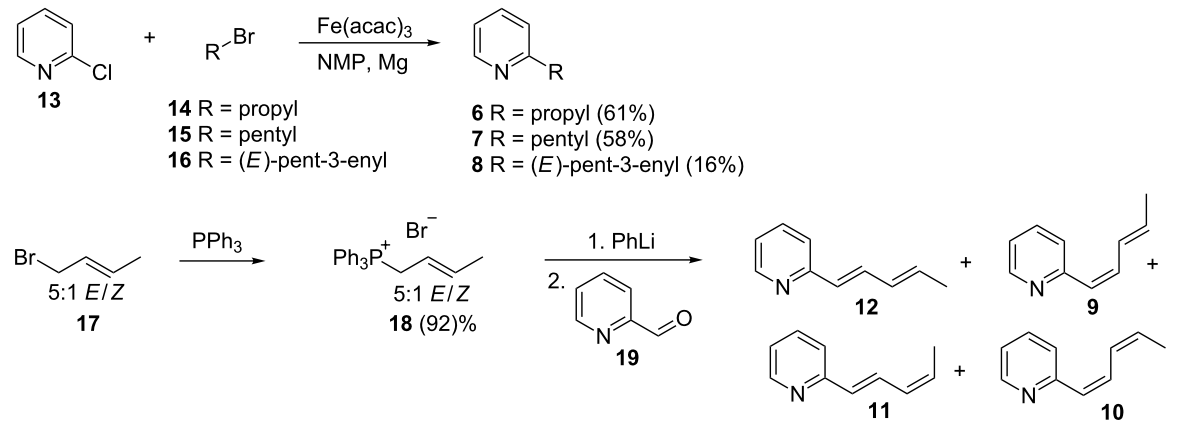


Figure 3: Mass spectra of a) (*E*)-2-(pent-3-en-1-yl)pyridine (streptopyridine E, **8**), b) (1*Z*,3*E*)-penta-1,3-dien-1-yl)pyridine (streptopyridine A, **9**), c) 2-((1*E*,3*E*)-penta-1,3-dien-1-yl)pyridine (streptopyridine B, **12**).



Scheme 1: Synthesis of streptopyridines A to E (**8**–**12**) and the 2-alkylpyridines **6** and **7**.

To delineate the stereochemistry of the other two isomers **10** and **11**, the conditions of the Wittig reaction were changed to favor *Z*-configured products by using NaHMDS as base. Again, all four diastereomers were formed (Figure 4). Together with knowledge of the structures of **9** and **12**, the product ratio in the *Z*-selective reaction indicates that compound **10** (streptopyridine C) is 2-((1*Z*,3*Z*)-penta-1,3-dienyl)pyridine, while compound **11** is 2-((1*E*,3*Z*)-penta-1,3-dienyl)pyridine (streptopyridine D): The formation of only small amounts of **11** indicates that this compound is 1*E*,3*Z*-configured, because it is disfavored by the 1*Z*-selective reaction conditions and the minor amounts of the *Z*-configured isomer in the diastereomeric mixture of Wittig salts. Conclusively, **10** must be the last possible 1*Z*,3*Z*-stereoisomer. Both compounds **10** and **11** could not be isolated in pure form, but their mass spectra and retention times were identical to those of the natural products.

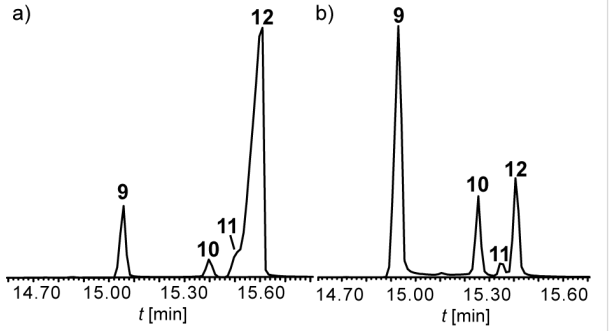


Figure 4: Total ion chromatograms of the product mixtures of isomers **9–12** synthesized under *E*-selective (a) and *Z*-selective Wittig reaction conditions (b).

The mass spectrum of compound **8** indicated that the side chain contained only one double bond, the position of which had to be determined. A 1-pentenyl side chain seemed unlikely because of the high abundance of the *m*/*z* 93 ion in the mass spectrum of **8**, which we assumed is a McLafferty ion that is commonly observed in 2-alkylpyridines [16]. Basing on the structure of streptopyridine A, a 3-pentenyl side chain seemed to be most likely. Coupling of (*E*)-3-pentenylmagnesium bromide with 2-chloropyridine under Fürstner conditions with iron(III) acetylacetonate as catalyst [17] yielded (*E*)-2-(pent-3-enyl)pyridine (**8**) that proved to be identical to the natural compound, now called streptopyridine E. The mass spectra of 2-(pent-1-enyl)pyridine and 2-(pent-2-enyl)pyridine, compounds synthesized for comparison, are shown in Supporting Information File 1 and differ from that of **8**. Finally, pyridines **6** and **7** were synthesized also by Fürstner cross-coupling and proved to be identical to the natural products.

2-Alkylpyridines have been reported earlier as aroma components, like 2-butylpyridine or 2-pentylpyridine (**7**) identified in fried chicken [18], or 2-propylpyridine (**6**), present in sesame seed oil [19], but are not known from bacteria. Natural products of bacteria containing a pyridine ring are rare. As an example, 1-(2-pyridinyl)ethanone was identified as a volatile of *Enterobacter agglomerans* [20]. Highly substituted pyridine derivatives can be found in bacterial thiopeptide antibiotics [21].

The streptopyridines of *Streptomyces* sp. FORM5 are structurally related to known secondary metabolites by *Streptomyces*. The piperidine derivatives 2-((1*E*,3*E*)-1,3-pentadienyl)piperidine (**20**) and 2-((1*E*,3*E*)-1,3-pentadienyl)-piperidin-4-ol (SS20846A, **21**, Figure 5) have been reported from other streptomycetes [8,22,23]. They constitute hydrogenated analogs of the streptopyridines and occur together with streptazolin (**5**).

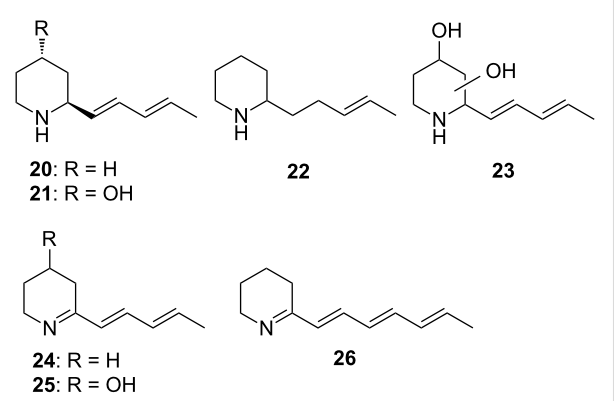


Figure 5: Structures of piperidine derivatives **20**–**26**.

We then tested whether the streptopyridines can also be detected under conventional cultivation and isolation procedures. Therefore, strain FORM5 was grown as liquid culture. Headspace analysis revealed the production of the streptopyridines also under these conditions. The liquid cultures were either extracted with ethyl acetate (E-extract) or filtered over Oasis adsorption material. The latter was than extracted with ethyl acetate (O-extract). These extracts were analyzed by GC–MS. While the E-extract did not show the presence of any streptopyridine, they were present as trace components in the O-extract. Both extracts showed two major constituents, one with a molecular mass of 151 u ($C_{10}H_{17}N$, HRMS found 151.13656, calcd 151.13605), and the other with a molecular mass of 207 u ($C_{11}H_{13}NO_3$, HRMS found 207.09056, calcd 207.08949). Although the compounds were not isolated, the mass spectral data and the previous reports of this class of compounds from *Streptomyces* led us to conclude that these compounds are indeed streptazolin (**5**, molecular mass 207) and 2-(penta-1,3-dien-1-yl)piperidine (**20**, molecular mass 151,

mass spectra and high resolution data see Supporting Information File 1). Both compounds are accompanied by diastereomers exhibiting the same mass spectrum but different retention times. Minor components of the extracts could be tentatively assigned by their mass spectra to be the hydroxypiperidine **21**, occurring again as a pair of diastereomers, and streptazone D (**4**). The mass spectrum of **4** matches the published data [8]. Streptazone B_1/B_2 and/or C elute as broad peak from the GC column; a discrimination basing on the mass spectrum is not possible.

Several additional N-containing compounds occur in the extracts, some of them can be tentatively identified basing on their mass spectra. Two compounds exhibiting a small molecular ion at *m/z* 153 and a dominating base peak at *m/z* 84 are likely 2-(3-pentenyl)piperidines (**22**, mass spectrum see Supporting Information File 1). The ion *m/z* 84 is typical for 2-alkylpiperidines [24] and cannot be formed in piperidine **20** because of the adjacent double bond. The 3-pentenyl side chain is also supported by a small ion series at *m/z* 94 and 108 and present in streptopyridine E (**8**) and streptenols A (**28**) and B, biosynthetic precursors of this compound family (see below). Another compound, only present in the O-extract exhibits a molecular mass of 149 u, 2 units less than the major compound **20**. The mass spectrum (see Supporting Information File 1) resembles that of **20**. The additional double bond resides most likely at the nitrogen, arriving at the 1-piperideine structure **24**. A similar structure has the antibiotic nigrifactin (**26**), a hexaketide produced by *S. nigrifaciens*, differing only in the length of the side chain [25]. Piperideine **24** lacks a N–H and might get lost during work-up of the E-extract, contrary to the other alkylpiperidines. It can be detected as trace component in the headspace extract as well (see Table 1). As with piperidines **20** and **21**, a hydroxypiperideine **25** seems to be present (Figure 5, mass spectrum see Supporting Information File 1). Its oxidation product is streptazone D (**4**) in which the ring double bond moves into conjugation with the carbonyl group by imine–enamine tautomerisation. Finally compound **23** is produced, a derivative of piperidine **21** with an additional hydroxy group with unknown location in the ring. Compounds **22**–**25** (Figure 5) as well as the streptazolin isomer have not been reported from nature before.

We then tested whether the streptopyridines are biosynthetically produced via a polyketide sequence similar to that reported for streptazolin, involving a pentaketide precursor [13], or whether a specific pyridine precursor, e.g., pipecolic acid, with chain elongation was used. Feeding experiments with $^{13}C_2$-sodium acetate showed incorporation of up to five acetate units by GC–MS, indicated by a mass shift of 10 amu for the molecular ion, from *m/z* 145 to *m/z* 155 (Figure 6a and 6b). Because of the dilution with unlabelled acetate the $^{13}C_{10}$ isotopomer is of low abundance (Figure 6c). Nevertheless, the dose dependent incorporation of the acetate units clearly showed the presence of this isotopomer. Feeding of 2 mM sodium $^{13}C_2$-acetate to agar plate cultures showed double incorporation compared to 1 mM sodium $^{13}C_2$-acetate (Figure 6d). The results hint to a biosynthesis of the streptopyridines via the polyketide pathway.

The proposed biosynthesis of the streptopyridines is shown in Scheme 2. The streptopyridines might be as well as the streptazones, streptenols (**27**) and piperidinols (**20**, **21**) [8,9] precursors or side products in the biosynthesis of streptazolin (**5**) [8]. The biosynthesis of **5** has been investigated earlier [13]. Mayer and Thiericke proposed a pentaketide precursor **34** that is transformed into the amine **33**. This amine is *N*-carboxylated, cyclized, and further processed to form **5** [13].

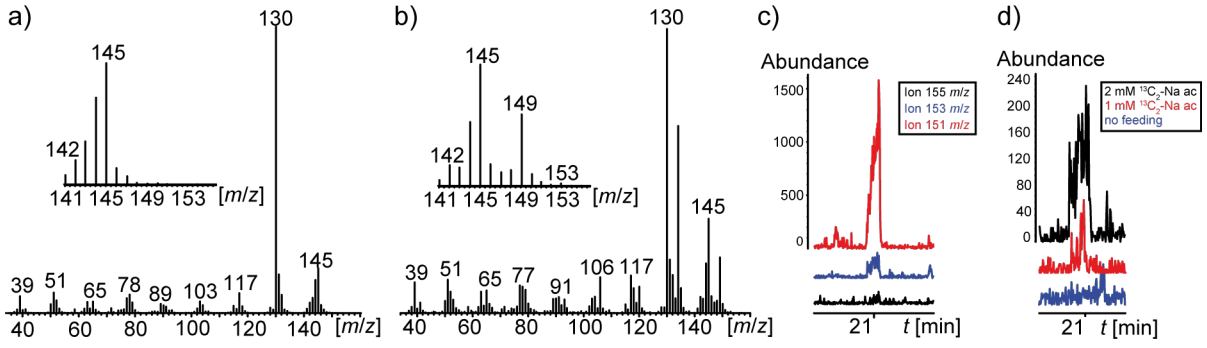
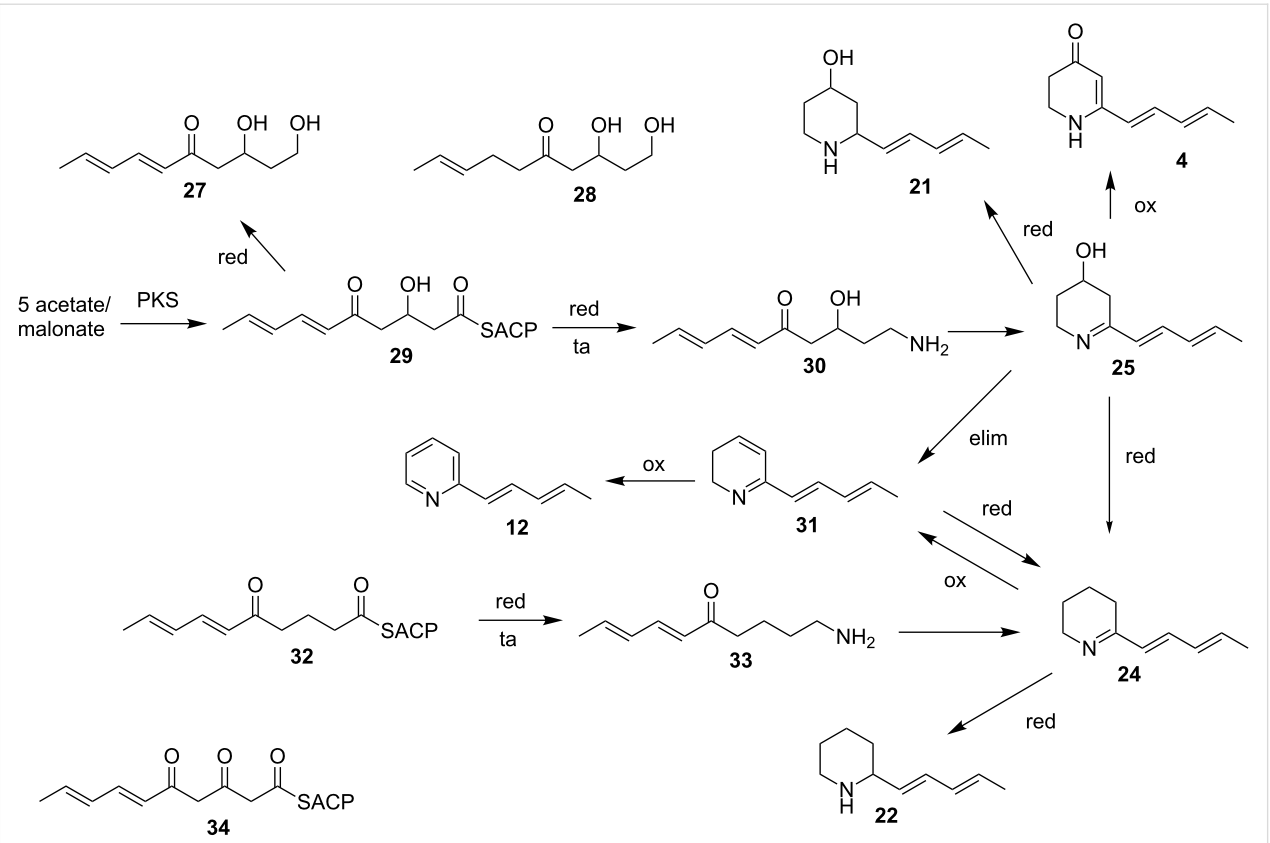


Figure 6: a) Mass spectrum of streptopyridine A (**12**), b) mass spectrum of **12** after feeding of 2 mM $^{13}C_2$-sodium acetate, c) single ion chromatogram of 151, 153, 155 *m/z* after feeding with 2 mM $^{13}C_2$-sodium acetate; d) single ion chromatogram of the 153 *m/z* molecular ion after feeding with 2 mM $^{13}C_2$-acetate, 1 mM sodium $^{13}C_2$-acetate, and a non fed culture as comparison. The ions at *m/z* 151, 153, and 155 indicate the incorporation of three, four, or five $^{13}C_2$-acetate units.



Scheme 2: Proposed biosynthesis of the streptopyridines. PKS: polyketide synthase; red: reduction; ta: transamination; ox: oxidation; elim: elimination.

The streptopyridines might similarly be formed from the pentaketide **29**, showing the reduction status occurring in the previously isolated streptenols A and C (**27**) [9]. Reduction and transamination leads to the amine **30** that cyclizes to the piperideine **25**. Elimination of water leads to the dihydropyridine **31** that is oxidized to the major streptopyridine **12** possibly by spontaneous autoxidation in air. Isomerization of the double bonds during this pathway may lead to the isomers **9**–**11**. Reduction of **25** would lead to piperidine SS 20846A (**21**) [9,23]. Oxidation of intermediate **25** can also form streptazone D (**4**) by oxidation which would concomitantly shift the double bond into conjugation to the carbonyl group. Reductive removal of the hydroxy group, e.g., via **31** followed by double bond reduction may lead to piperideine **24**, a precursor of the major liquid phase component **22**. Alternatively, this compound might originate from the reduced PKS precursor **32** that is transformed via **33** into **24**. Piperidine **22** is then obtained via imine reduction as described. On the other hand, this pathway may also be the entry into the streptopyridine formation by oxidation of **24** to, e.g., **31**, followed by final oxidation.

A 3-pentenyl side chain as found in streptopyridine **8** and other derivatives occurs also in streptenol A (**28**), isolated from *S. luteogriseus* FH-S 1307 [9], *S. fimbriatus* [26], *S. cirratus* [27], and *Streptomyces* sp. HS-HY-045 [28]. This might indicate that the double bond hydrogenation occurs already during the pentaketide biosynthesis in these cases. Similarly, additional hydrogenation leads to the saturated alkylpyridine **7** and a tetraketide to propylpyridine (**6**).

In the bouquet of the headspace extract of *Streptomyces* strain FORM5 several other compounds besides the pyridines **6**–**12** were identified (Figure 7, Table 1). The most abundant of these were dimethyl disulfide (**35**), accompanied by other sulfur components as dimethyl trisulfide (**36**), dimethyl tetrasulfide (**37**), and *S*-methyl methanethiosulfonate (**50**). The hydroxyketones acetoin (**40**), and longer variants **38**, **39**, **41**, and **42** occur often in bacteria and are precursors of alkylated pyrazines [29] like 2,5-dimethylpyrazine (**44**). Aldehydes, ketones, and aromatic compounds commonly found as volatiles from bacteria were present in trace amounts: 5-hepten-2-one (**43**), 2-acetylfuran (**45**), 3-octanone (**48**), nonanal (**54**), decanal (**55**), 1-phenyl-2-propanone (**57**), 1-phenyl-1,2-propandione (**59**), benzaldehyde (**46**), methyl benzoate (**51**), 2-phenylethanol (**56**), 1-phenyl-2-propanol (**58**), ethyl benzoate (**52**), and methyl 2-phenylacetate (**53**) [2]. Of special interest is 5-hepten-2-one

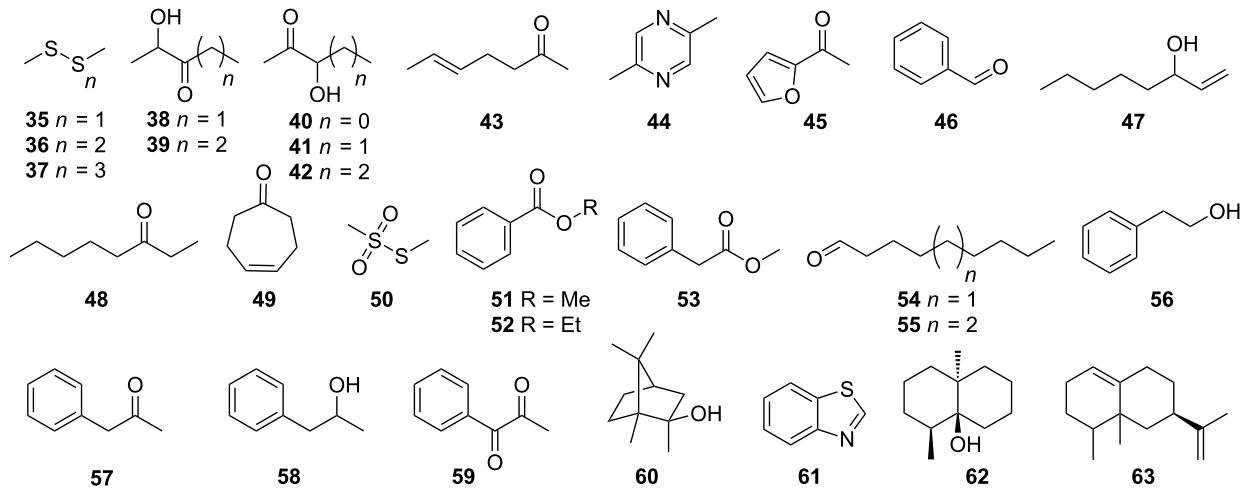


Figure 7: Compounds detected in the headspace of *Streptomyces* sp. FORM5.

Table 1: Volatile compounds identified in the headspace extract of *Streptomyces* strain FORM5. The amounts of the compounds are given as 0–2% (x), 2–8% (xx), >8% (xxx) relative to the largest peak area in the total ion chromatogram. The identification of the compound based on comparison of mass spectrum to a data base spectrum (ms), comparison of retention index to a published retention index on the same or similar GC fused silica capillary column (ri), and/or based on comparison to a synthetic or commercially available reference compound (std).

GC[a]	compound[b]	*I* (exp.)	*I* (lit.)[c]	Ident.	FORM5
	acetoin (**40**)	n.d.[d]		ms, std	xx
a	dimethyl disulfide (**35**)	n.d.		ms, std	xx
b	2-hydroxypentan-3-one (**38**)	829	822*	ms, ri	xx
	3-hydroxypentan-2-one (**41**)	833	838	ms, ri	x
c	5-hepten-2-one (**43**)	909		ms	x
d	2-hydroxyhexan-3-one (**39**)	910		ms	x
	3-hydroxyhexan-2-one (**42**)	914		ms	x
e	2,5-dimethylpyrazine (**44**)	925	925	ms, ri, std	x
f	2-acetylfuran (**45**)	925	923	ms, ri, std	x
g	benzaldehyde (**46**)	977	978	ms, ri, std	x
h	dimethyl trisulfide (**36**)	979	978	ms, ri, std	x
i	1-octen-3-ol (**47**)	987	987	ms, ri, std	x
j	3-octanone (**48**)	994	994	ms, ri, std	x
k	2-propylpyridine (**6**)	1000	1001	ms, ri, std	x
l	cyclohept-4-enone (**49**)	1023	1024	ms, ri, std	x
n	*m/z* = 118, 105, 77, 51, 39	1082			x
o	*S*-methyl methanethiosulphonate (**50**)	1083	1083	ms, ri	x
	methyl benzoate (**51**)	1108	1104	ms, ri, std	x
p	nonanal (**54**)	1116	1116	ms, ri, std	x
	m/z = 106, 135, 79	1128			x
q	2-phenylethanol (**56**)	1129	1129	ms, ri, std	x
	1-phenyl-2-propanone (**57**)	1143		ms	x
	1-phenyl-2-propanol (**58**)	1147		ms	x
	1-phenyl-1,2-propandione (**59**)	1183	1186	ms, ri,	x
	methyl 2-phenylacetate (**53**)	1189	1187	ms	x
	2-methylisoborneol (**60**)	1199	1201	ms, ri, std	x
r	2-pentylpyridine (**7**)	1205	1205	ms, ri, std	x

Table 1: Volatile compounds identified in the headspace extract of *Streptomyces* strain FORM5. The amounts of the compounds are given as 0–2% (x), 2–8% (xx), >8% (xxx) relative to the largest peak area in the total ion chromatogram. The identification of the compound based on comparison of mass spectrum to a data base spectrum (ms), comparison of retention index to a published retention index on the same or similar GC fused silica capillary column (ri), and/or based on comparison to a synthetic or commercially available reference compound (std). (continued)

s	(*E*)-2-(pent-3-enyl)pyridine (**8**)	1207	1208	ms, ri, std	xxx
t	*m/z* = 132, 93, 118, 41, 106	1212			x
u	decanal (**55**)	1216	1216	ms, ri, std	x
v	*m/z* = 118, 93, 46, 130, 52	1219			x
	dimethyl tetrasulfide (**37**)	1233	1234	ms, ri, std	x
	benzothiazole (**61**)	1246	1246	ms, ri, std	x
	ethyl 2-phenylacetate	1256	1252	ms	x
w	*m/z* = 118, 147, 132, 91, 51	1283			x
x	*m/z* = 79, 104, 133, 51, 117	1321			x
y	2-((1*Z*,3*E*)-penta-1,3-dienyl)pyridine (**9**)	1327	1334	ms, ri, std	xx
z	2-((1*Z*,3*Z*)-penta-1,3-dienyl)pyridine (**10**)	1352	1358	ms, ri, std	xxx
aa	2-((1*E*,3*Z*)-penta-1,3-dienyl)pyridine (**11**)	1362	1363	ms, ri, std	xx
ab	2-((1*E*,3*E*)-penta-1,3-dienyl)pyridine (**12**)	1366	1368	ms, ri, std	xxx
ac	geosmin (**62**)	1429	1430	ms, ri, std	x
ad	*m/z* = 105, 120, 91, 204, 176	1465			x
ae	valencene (**63**)	1499	1498	ms, ri, std	x
af	*m/z* = 148, 163, 120	1529		ms	x

[a]Compound assignment refers to Figure S2 (Supporting Information File 1), [b]artefacts found in both control and inoculated samples are not listed, [c]taken from NIST Chemistry WebBook [14] or our own data base, [*]DB-5, A: artifact; [d]not determined.

(**43**) that may be a shunt product of the streptopyridine E biosynthesis: It contains a 3-pentenyl chain motif adjacent to a carbonyl group, thus resembling the structural requirements of a possible streptopyridine E biosynthesis that follows the logic as presented in Scheme 2. Cyclohept-4-enone (**49**) has recently been reported from several actinomycetes [2]. Some terpenes could be identified as well. 2-Methylisoborneol (**60**) and geosmin (**62**) are commonly produced by *Streptomyces* and other actinomycetes [3,30]. In addition, the sesquiterpene valencene (**63**) was found, but the amount of terpenes released is quite low compared to other streptomycetes. Some nitrogen containing trace components could not be identified. In the E- and O-extracts similarly other nitrogen containing trace components occurred, although the small amounts excluded their identification.

The streptopyridines showed only weak antibacterial and cytostatic activity (R. Müller, pers. commun.), similar to that described earlier by us for 2-pentylpyridine [31]. The analysis of the 16S-RNA revealed strain FORM5 to be a *Streptomyces*. It showed 99% sequence similarity to *Streptomyces griseosporus* (R. Müller, pers. commun.).

The two analytical methods used in the current work are obviously orthogonal to each other. They can be used on the same culture. After initial sampling of the headspace of a liquid culture, the culture can be separated from the cells and extracted as described. This consecutive approach allows a broad overview on the metabolites. The E- or O-extracts can be analyzed by HPLC–MS and GC–MS. Small, basic compounds as the piperidines are released from the liquid medium and can be detected only by the extraction methods. Their basicity and/or their ability to interact by hydrogen bonding with water obviously prevent release from the water phase in substantial amounts. Volatile compounds like the streptopyridines are less soluble, have a lower basicity and can be detected as major compounds in the headspace. Both analytical methods have a different analytical window and complement each other.

The detected volatiles fall into different groups. Most of the compounds listed in Table 1 can be regarded as volatiles commonly produced by various bacteria. That does not imply that most bacteria release them, but that these volatiles often occur when bacteria are analyzed. These compounds form a chemical structure space of volatiles released by bacteria and their number is limited, although this space is certainly only partially explored. Another group of volatile compounds forming a structure space is already known from the green part of plants (excluding flowery parts). The plant structure space is different from that emerging for bacteria. The bacterial structure space includes acetoins and aromatic aldehydes, esters and ketones, aliphatic compounds, sulfur compounds, but also 4-cycloheptenone that we found in several other bacteria (unpublished results). The terpenes geosmin and methylisobor-

neol are typical terpenes of the actinomycetes. Various sesquiterpene cyclases occur in the streptomycetes [3,30,32] and give rise to a wide variety of sesquiterpenes, in this case valencene.

The only strain specific compounds are the streptopyridines. They have not been reported from other strains and their biosynthesis seems tightly connected to the biosynthesis of streptazolin. A similar case has been reported for specific volatile butenolides released by streptomycetes producing the antibiotic antimycin [33] and for other strains investigated by us. The analysis of volatiles and detection of unique compounds may thus be used as a method to select microbial strains for the detection of non-volatile biologically active compounds. Alternatively, two independent gene clusters may be responsible for streptazolin and streptopyridines.

The production of strain specific compounds connected to, e.g., antibiotic biosynthesis might also have important ecological consequences. As an example, streptazolin producing streptomycetes have been isolated from mud-dauber wasps [34]. They have been postulated as antibiotic-producing symbionts of the wasps. If this is true, they should also produce specific volatiles as the streptopyridines and add to the odor of the insect. Given the many different bacteria living on the insect, a specific odor bouquet of the insect would arise, assembled by insect derived compounds and bacterial volatiles, finally carrying information on the individual symbiont composition. The symbiont composition might affect the fitness and, if it can be perceived by interacting partners, may in the end influence the behavior of the insects, e.g., mate choice or aggression.

Conclusion

In conclusion, the investigation of the headspace extract of *Streptomyces* strain FORM5 revealed the occurrence of new 2-alkylpyridines that are structurally related to streptazolin and 2-pentadienylpiperidines produced by this strain. While they are the major compounds in the volatile bouquet, they occur only in minor amounts in the liquid phase. In contrast, the major compounds streptazolin and 2-pentadienylpiperidine do not occur in the headspace, thus proving the necessity to use orthogonal analytical methods to assess the full metabolic potential of a microorganism.

Experimental

General experimental procedures

Reagents and solvents were purchased from Sigma-Aldrich Chemie GmbH (Steinheim, Germany) and Acros Organics (Geel, Belgium) and used without further purification. Solvents were distilled before use and, if necessary, dried using standard procedures. All non aqueous reactions were performed under an inert atmosphere (N_2) in flame-dried flasks. Purification of the synthetic products was carried out by flash chromatography using Merck silica gel 60 (70–200 mesh). Thin-layer chromatography was performed with 0.2 mm pre-coated polyester sheets (Polygram SIL (G/UV254), Macherey-Nagel). NMR spectra were obtained on either a Bruker DRX-400 (400 MHz) or an AV III-400 (400 MHz) spectrometer and were referenced against TMS (δ = 0.00 ppm) for ^{1}H NMR and $CHCl_3$ (δ = 77.16 ppm) for ^{13}C NMR. GC–MS analysis were performed on an Agilent 7890A gas chromatograph connected to an Agilent 6975 C inert mass detector fitted with a BPX-5 fused silica capillary column (25 m, 0.25 mm i.d., 0.25 µm film). Conditions were as follows: inlet pressure 67 kPa, He 23.3 mL/min, injection volume 1 µL, transfer line 300 °C, injector 250 °C, electron energy 70 eV. The gas chromatograph was programmed as follows: 5 min at 50 °C, then increasing with 5 °C/min to 320 °C. Linear retention indices were determined from a homologous series of *n*-alkanes (C8–C32). Compounds were identified by comparison of mass spectra to database spectra (Wiley 7, NIST 08 and our own created from synthesized reference compounds), by comparison of the retention index data to standards (own database and NIST Chemistry WebBook (2013) [14]) and by synthesis of reference compounds.

Organism and analysis

Streptomyces strain FORM5 was isolated from a soil sample collected in Formentera (Spain) and is deposited at the Institute of Organic Chemistry in Göttingen [8]. It was cultivated in 10 mL SM-media (20 g/L mannitol, 20g/L soy flour, 4 mL/L 2.5 M magnesium chloride solution, 20 g/L agar only for plates) at 28 °C for 3 days. SM-agar plates were then inoculated with 300 µL of the preculture and cultivated for 6 days at 28 °C. Then the culture was analyzed by closed-loop stripping analysis at room temperature [7]. In this system, air is continuously pumped (MB-21E, Senior Flextronics, USA) through the closed system that contains an activated charcoal filter (Chromtech GmbH, Idstein, Precision Charcoal Filter, 5 mg) and the agar plate or liquid culture for 24 hours. The filter was then extracted by rinsing 3× with 15 µL dichloromethane (≥99.8%, Merck, Germany) and the resulting headspace extract was analyzed by GC–MS. The experiment was repeated at least three times. The SM-medium was analyzed without inoculation as control. Liquid cultures were analyzed similarly by the CLSA method. After the collection of volatiles the liquid phase was analyzed by two different methods. E-extract: The culture media was centrifuged for 20 min at 4 °C and the supernatant was extracted 3 times with 50 mL CH_2Cl_2. The extracts were dried with $MgSO_4$, concentrated under reduced pressure and analyzed by GC–MS. O-extract A Oasis® HLB cartridge (Waters) was prewashed with 2 column volumes ethyl acetate and condi-

tioned with 2 column volumes water. The culture media was centrifuged for 20 min at 4 °C and the supernatant (100 mL) filtered through the cartridge. The cartridge was extracted with 3 column volumes ethyl acetate, the eluent was dried with $MgSO_4$, concentrated under reduced pressure, and finally subjected to GC–MS analysis. For feeding experiments on the biosynthesis of compound **7** the SM-media was enriched with sodium $^{13}C_2$-acetate (ISOTEC) in 1 mM (1.7 mg, 0.02 mmol, in 20 mL medium) and 2 mM (3.4 mg, 0.04 mmol, in 20 mL medium) followed by collection of the volatiles by CLSA.

Synthesis of reference compounds

The compounds **6**–**8** were synthesized after the standard procedure for iron-catalyzed aryl–alkyl cross-coupling described by Fürstner et al [17].

2-Propylpyridine (**6**): Yield (1.01 g, 8.35 mmol, 61%); R_f (pentane/Et_2O 5:1) 0.2; UV (CH_2Cl_2) λ_{max} (log ε): 257 (5.77), 262 (5.78) nm; IR (diamond) ν_{max}: 2960, 2832, 2871, 1590, 1569, 1472, 1434, 1149, 1051, 993, 751 cm^{-1}; ^1H NMR ($CDCl_3$, 400 MHz) δ ppm 0.97 (t, J = 7.4 Hz, 3H, CH_3), 1.76 (sxt, J = 7.5 Hz, 2H, CH_2), 2.74–2.79 (m, 2H, CH_2), 7.07–7.11 (m, 1H, CH), 7.14 (dd, J = 7.8, 0.5 Hz, 1H, CH), 7.58 (tdd, J = 7.6, 1.9, 0.9 Hz, 1H, CH), 8.52 (dt, J = 4.89, 0.94 Hz, 1H, CH); ^{13}C NMR ($CDCl_3$, 100 MHz) δ ppm 13.8 (CH_3), 23.1 (CH_2), 40.4 (CH_2), 120.8 (CH), 122.7 (CH), 136.1 (CH), 149.2 (CH), 162.3 (C); EIMS *m*/*z*: 121 $[M]^+$ (2), 120 (9), 106 (29), 93 (100), 78 (12), 65 (18), 51 (15), 39 (18); HREIMS *m*/*z*: calcd for $C_8H_{11}N$, 121.0891; found, 121.0888; GC (BPX-5) I = 1001.

2-Pentylpyridine (**7**): Yield (827 mg, 5.6 mmol, 56%); R_f (pentane/Et_2O 5:1) 0.2; UV (CH_2Cl_2) λ_{max} (log ε): 257 (6.28), 262 (6.29) nm; IR (diamond) ν_{max}: 2955, 2928, 2858, 1590, 1472, 1434, 1148, 993 cm^{-1}; ^1H NMR ($CDCl_3$, 400 MHz) δ ppm 0.86–0.93 (m, 3H, CH_3), 1.29–1.40 (m, 4H, 2× CH_2), 1.68–1.78 (m, 2H, CH_2), 2.74–2.82 (m, 2H, CH_2), 7.08 (ddd, J = 7.5, 4.9, 1.1 Hz, 1H, CH), 7.13 (dd, J = 7.8, 1.0 Hz, 1H, CH), 7.53–7.60 (m, 1H, CH), 8.50–8.55 (m, 1H, CH); ^{13}C NMR ($CDCl_3$, 100 MHz) δ ppm 13.9 (CH_3), 22.5 (CH_2), 29.5 (CH_2), 31.5 (CH_2), 38.4 (CH_2), 120.7 (CH), 122.6 (CH), 136.1 (CH), 149.1 (CH), 162.5 (C); EIMS *m*/*z*: 149 $[M]^+$ (2), 93 (100), 120 (25), 106 (30), 92 (14), 78 (14), 65 (16), 51 (10), 39 (14); HREIMS *m*/*z*: calcd for $C_{10}H_{15}N$, 149.1204; found, 149.1203; GC (BPX-5) I = 1205.

2-((*E*)-Pent-3-en-1-yl)pyridine (**8**): Yield (326 mg, 2.2 mmol, 16%); R_f (pentane/Et_2O 5:1) 0.24; UV (CH_2Cl_2) λ_{max} (log ε): 257 (5.73), 262 (5.74) nm; IR (diamond) ν_{max}: 3009, 2918, 2854, 1590, 1569, 1474, 1434, 1148, 1051, 966, 750 cm^{-1}; ^1H NMR ($CDCl_3$, 400 MHz) δ ppm 1.62–1.64 (m, 3H, CH_3), 2.38–2.44 (m, 2H, CH_2), 2.82–2.85 (m, 2H, CH_2), 5.41–5.52 (m, 2H, 2× CH), 7.07–7.10 (m, 1H, CH), 7.13 (d, J = 7.8 Hz, 1H, CH), 7.57 (td, J = 7.6, 1.9 Hz, 1H, CH), 8.51–8.53 (m, 1H, CH); ^{13}C NMR ($CDCl_3$, 100 MHz) δ ppm 17.5 (CH_3), 32.4 (CH_2), 38.1 (CH_2), 120.6 (CH_2), 122.4 (CH_2), 125.2 (CH), 129.9 (CH), 135.8 (CH), 148.8 (CH), 161.4 (C); EIMS *m*/*z*: 147 $[M]^+$ (17), 146 (29), 133 (11), 132 (100), 119 (17), 118 (30), 117 (47), 106 (25), 93 (77), 79 (17), 78 /14), 65 (18), 51 (13), 39 (19); HREIMS *m*/*z*: calcd for $C_{10}H_{13}N$, 147.1048; found, 147.1054; GC (BPX-5) I = 1208.

The synthesis of compounds **9** and **12** was achieved by Wittig reaction starting with the synthesis of crotyltriphenylphosphonium bromide (**18**). Crotyl bromide (**17**, 2.23 g, 16.52 mmol) was added to a mixture of triphenylphosphine (3.67 g, 14 mmol) in THF and stirred under reflux overnight. THF was removed under reduced pressure and the resulting solid was dissolved in a mixture of CH_2Cl_2/MeOH (10:1). Column chromatography on silica gel with CH_2Cl_2/MeOH (15:1, R_f = 0.25) yielded **18** (5.12 g, 12.9 mmol, 92%) as a white solid. ^1H NMR ($CDCl_3$, 200 MHz) δ ppm 1.35–1.42 (m, 3H, CH_3), 1.58–1.65 (m, 3H, CH_3), 4.54–4.69 (m, 4H, 2× CH_2), 5.24–5.39 (m, 2H, 2× CH), 5.87–6.04 (m, 2H, 2× CH), 7.65–7.92 (m, 30H, 30× CH); ^{13}C NMR ($CDCl_3$, 50 MHz) δ ppm 18.1 (CH_3), 18.2 (CH_3), 27.2 (CH_2), 28.2 (CH_2), 114.6 (CH), 114.8 (CH), 117.0 (3× C), 118.7 (3× C), 130.0 (6× CH), 130.3 (6× CH), 133.6 (6× CH), 133.8 (6× CH), 134.8 (3× CH), 134.9 (3× CH), 137.4 (CH), 137.7 (CH); ^{31}P NMR ($CDCl_3$, 80 MHz) δ ppm 21.4 (s), 21.6 (s). At room temperature an ethereal phenyllithium solution (1.63 mL, 15.5 mmol) was added to a mixture of **18** (6.15 g, 15.5 mmol) in 30 mL dry THF and 45 mL dry diethyl ether. After stirring for 20 min at rt the mixture was cooled down to −78 °C and pyridine-2-carbaldehyde (**19**, 1.66 g, 15.5 mmol) was added. Afterwards the mixture was allowed to warm to −30 °C in 2 h and again phenyllithium solution (1.63 mL, 15.5 mmol) was added. Then the mixture was cooled down again to −78 °C and potassium *tert*-butoxide (2.61 g, 23.25 mmol) was added. Overnight the mixture was allowed to warm to rt and quenched with dest. water. The aqueous layer was extracted two times with diethyl ether. The combined organic layers were dried with $MgSO_4$ and the solvent was removed under reduced pressure. Column chromatography on silica gel with pentane/diethyl ether (5:1) yielded **9** (0.36 mmol, 53 mg, R_f = 0.3, 3%) and **12** (2.22 mmol, 322 mg, R_f = 0.25, 14%) as yellow oils (crude yield was 62%).

2-((1*Z*,3*E*)-Penta-1,3-dien-1-yl)pyridine (**9**): UV (CH_2Cl_2) λ_{max} (log ε): 271 (6.66), 300 (6.71), 308 (6.72) nm; IR (diamond) ν_{max}: 3006, 2962, 2911, 1641, 1582, 1558, 1469, 1431, 1149, 990, 833, 797, 741 cm^{-1}; ^1H NMR ($CDCl_3$, 400 MHz) δ ppm 1.85 (dd, J = 6.8, 1.7 Hz, 3H, CH_3), 5.96 (dq, J = 15.2, 6.8 Hz, 1H, CH), 6.23 (d, J = 11.8 Hz, 1H, CH), 6.34 (dd, J = 11.5, 11.2

Hz, 1H, CH), 7.07 (dd, J = 7.5, 5.0 Hz, 1H, CH), 7.21 (d, J = 7.9 Hz, 1H, CH), 7.40 (dd, J = 15.2, 11.0 Hz, 1H, CH), 7.61 (td, J = 7.7, 1.9 Hz, 1H, CH), 8.60–8.62 (m, 1H, CH); ^{13}C NMR ($CDCl_3$, 100 MHz) δ ppm 18.5 (CH_3), 121.0 (CH), 124.1 (CH), 125.5 (CH), 128.8 (CH), 134.1 (CH), 135.2 (CH), 136.0 (CH), 149.3 (CH), 156.9 (C); EIMS m/z: 145 $[M]^+$ (9), 144 (12), 143 (6), 142 (5), 131 (10), 130 (100), 117 (5), 103 (4), 89 (3), 78 (5), 77 (4), 65 (3), 51 (4), 39 (3); HREIMS m/z: calcd for $C_{10}H_{13}N$, 145.0892; found, 145.0912; GC (BPX-5) I = 1334.

2-((1*E*,3*E*)-penta-1,3-dien-1-yl)pyridine (**12**): UV (CH_2Cl_2) λ_{max} (log ε): 272 (6.55), 300 (6.60), 308 (6.61) nm; IR (diamond) ν_{max}: 3008, 2962, 2911, 1644, 1582, 1561, 1467, 1429, 1145, 989, 796, 755, 740 cm^{-1}; ^{1}H NMR ($CDCl_3$, 400 MHz) δ ppm 1.82 (dd, J = 6.8, 2 Hz, 3H, CH_3), 5.96 (dq, J = 15.7, 6.8 Hz, 1H, CH), 6.26 (dd, J = 15.1, 10.8 Hz, 1H, CH), 6.48 (d, J = 15.8 Hz, 1H, CH), 7.04 (dd, J = 7.5, 5.0 Hz, 1H, CH), 7.21 (dd, J = 15.1, 11.3 Hz, 1H, CH), 7.21 (d, J = 7.8 Hz, 1H, CH), 7.66 (td, J = 7.7, 1.9 Hz, 1H, CH), 8.51–8.53 (m, 1H, CH); ^{13}C NMR ($CDCl_3$, 100 MHz) δ ppm 18.3 (CH_3), 121.3 (CH), 121.4 (CH), 128.9 (CH), 131.3 (CH), 133.0 (CH), 133.2 (CH), 136.1 (CH), 149.3 (CH), 155.8 (C); EIMS m/z: 145 (18) $[M]^+$, 144 (14), 143 (6), 142 (5), 131 (10), 130 (100), 117 (6), 103 (4), 78 (5), 77 (4), 65 (3), 51 (5), 39 (3); HREIMS m/z: calcd for $C_{10}H_{13}N$, 145.0892; found, 145.0912; GC (BPX-5) I = 1368.

Supporting Information

Supporting Information File 1

Total ion chromatograms of strain *Streptomyces* sp. FORM5, mass spectra, 16S-RNA data, and ^{1}H and ^{13}C NMR spectra of the synthetic compounds.
[http://www.beilstein-journals.org/bjoc/content/supplementary/1860-5397-10-146-S1.pdf]

Acknowledgements

We thank Silke Wenzel and Jennifer Herrmann from the work-group of Rolf Müller, HIPS, Saarbrücken, Germany, for performing 16S-RNA classification and bioassays. We also thank Axel Zeeck, Göttingen, for the strain FORM5.

References

1. Schulz, S.; Dickschat, J. S. *Nat. Prod. Rep.* **2007,** *24,* 814–842. doi:10.1039/b507392h
2. Citron, C. A.; Rabe, P.; Dickschat, J. S. *J. Nat. Prod.* **2012,** *75,* 1765–1776. doi:10.1021/np300468h
3. Citron, C. A.; Gleitzmann, J.; Laurenzano, G.; Pukall, R.; Dickschat, J. S. *ChemBioChem* **2012,** *13,* 202–214. doi:10.1002/cbic.201100641
4. Schöller, C. E. G.; Gürtler, H.; Pedersen, R.; Molin, S.; Wilkins, K. *J. Agric. Food Chem.* **2002,** *50,* 2615–2621. doi:10.1021/jf0116754
5. Gerber, N. N. *J. Chem. Ecol.* **1977,** *3,* 475–482. doi:10.1007/BF00988190
6. Wilkins, K. *Chemosphere* **1996,** *32,* 1427–1434. doi:10.1016/0045-6535(96)00051-3
7. Schulz, S.; Fuhlendorff, J.; Reichenbach, H. *Tetrahedron* **2004,** *60,* 3863–3872. doi:10.1016/j.tet.2004.03.005
8. Puder, C.; Krastel, P.; Zeeck, A. *J. Nat. Prod.* **2000,** *63,* 1258–1260. doi:10.1021/np0001373
9. Grabley, S.; Hammann, P.; Kluge, H.; Wink, J.; Kricke, P.; Zeeck, A. *J. Antibiot.* **1991,** *44,* 797–800. doi:10.7164/antibiotics.44.797
10. Drautz, H.; Zähner, H.; Kupfer, E.; Keller-Schierlein, W. *Helv. Chim. Acta* **1981,** *64,* 1752–1765. doi:10.1002/hlca.19810640605
11. Thiericke, R.; Zerlin, M. *Nat. Prod. Lett.* **1996,** *8,* 163–167. doi:10.1080/10575639608044889
12. Maskey, R. P.; Pusecker, K.; Speitling, M.; Monecke, P.; Helmke, E.; Laatsch, H. *Z. Naturforsch., B* **2002,** *57,* 823–829.
13. Mayer, M.; Thiericke, R. *J. Org. Chem.* **1993,** *58,* 3486–3489. doi:10.1021/jo00065a006
14. NIST Chemistry WebBook. http://webbook.nist.gov/chemistry/ (accessed Jan 15, 2014).
15. Schlosser, M.; Christmann, K. F. *Angew. Chem.* **1966,** *78,* 115. doi:10.1002/ange.19660780118
16. Budzikiewicz, H.; Besler, U. *Org. Mass Spectrom.* **1976,** *11,* 398–405. doi:10.1002/oms.1210110411
17. Fürstner, A.; Leitner, A.; Méndez, M.; Krause, H. *J. Am. Chem. Soc.* **2002,** *124,* 13856–13863. doi:10.1021/ja027190t
18. Tang, J.; Jan, Q. Z.; Shen, G.-H.; Ho, C.-T.; Chang, S. S. *J. Agric. Food Chem.* **1983,** *31,* 1287–1292. doi:10.1021/jf00120a035
19. Shimoda, M.; Shiratsuchi, H.; Nakada, Y.; Wu, Y.; Osajima, Y. *J. Agric. Food Chem.* **1996,** *44,* 3909–3912. doi:10.1021/jf960115f
20. Kiviranta, H.; Tuomainen, A.; Reiman, M.; Laitinen, S.; Liesivuori, J.; Nevalainen, A. *Cent. Eur. J. Public Health* **1998,** *6,* 296–299.
21. Bagley, M. C.; Dale, J. W.; Merritt, E. A.; Xiong, X. *Chem. Rev.* **2005,** *105,* 685–714. doi:10.1021/cr0300441
22. Yang, X.-Q.; Yang, Y.-B.; Zhou, H.; He, G.-W.; Zhao, L.-X.; Xu, L.-H.; Ding, Z.-T. *Nat. Prod. Res.* **2013,** *27,* 1191–1196. doi:10.1080/14786419.2012.718776
23. Komoto, T.; Yano, K.; Ono, J.; Okawa, J.; Nakajima, T. Physiologically active substance SS20846A by fermentation. JP Patent 61035788, Feb 20, 1986.
24. Jones, T. H.; Blum, M. S.; Fales, H. M. *Tetrahedron* **1982,** *38,* 1949–1958. doi:10.1016/0040-4020(82)80044-6
25. Terashima, T.; Idaka, R.; Kishi, Y.; Goto, T. *J. Chem. Soc., Chem. Commun.* **1973,** 75–76. doi:10.1039/c39730000075
26. Keller-Schierlein, W.; Wuthier, D.; Drautz, H. *Helv. Chim. Acta* **1983,** *66,* 1253–1261. doi:10.1002/hlca.19830660425
27. Mizutani, S.; Odai, H.; Masuda, T.; Iijima, M.; Osono, M.; Hamada, M.; Naganawa, H.; Ishizuka, M.; Takeuchi, T. *J. Antibiot.* **1989,** *42,* 952–959. doi:10.7164/antibiotics.42.952
28. Liu, N.; Zhang, H.; Luo, W.-j.; Zheng, W.; Wang, H.-b.; Huang, Y. *Tianran Chanwu Yanjiu Yu Kaifa* **2007,** *19,* 897.
29. Dickschat, J. S.; Wickel, S.; Bolten, C. J.; Nawrath, T.; Schulz, S.; Wittmann, C. *Eur. J. Org. Chem.* **2010,** 2687–2695. doi:10.1002/ejoc.201000155
30. Rabe, P.; Citron, C. A.; Dickschat, J. S. *ChemBioChem* **2013,** *14,* 2345–2354. doi:10.1002/cbic.201300329

31. Schulz, S.; Dickschat, J. S.; Kunze, B.; Wagner-Dobler, I.; Diestel, R.; Sasse, F. *Mar. Drugs* **2010,** *8,* 2976–2987. doi:10.3390/md8122976
32. Rabe, P.; Dickschat, J. S. *Angew. Chem.* **2013,** *125,* 1855–1857. doi:10.1002/ange.201209103
Angew. Chem. Int. Ed. 2013, 52, 1810-1812. doi:10.1002/anie.201209103
33. Riclea, R.; Aigle, B.; Leblond, P.; Schoenian, I.; Spiteller, D.; Dickschat, J. S. *ChemBioChem* **2012,** *13,* 1635–1644. doi:10.1002/cbic.201200260
34. Poulsen, M.; Oh, D.-C.; Clardy, J.; Currie, C. R. *PLoS One* **2011,** *6,* e16763. doi:10.1371/journal.pone.0016763

License and Terms

This is an Open Access article under the terms of the Creative Commons Attribution License (http://creativecommons.org/licenses/by/2.0), which permits unrestricted use, distribution, and reproduction in any medium, provided the original work is properly cited.

The license is subject to the *Beilstein Journal of Organic Chemistry* terms and conditions: (http://www.beilstein-journals.org/bjoc)

The definitive version of this article is the electronic one which can be found at: doi:10.3762/bjoc.10.146

BEILSTEIN JOURNAL OF ORGANIC CHEMISTRY

C–H-Functionalization logic guides the synthesis of a carbacyclopamine analog

Sebastian Rabe[1], Johann Moschner[1], Marina Bantzi[1], Philipp Heretsch[*2] and Athanassios Giannis[*1]

Full Research Paper

Open Access

Address:
[1]Universität Leipzig, Institut für Organische Chemie, Johannisallee 29, D-04103 Leipzig, Germany and [2]Rice University, Department of Chemistry, BioScience Research Collaborative, 6100 Main St., Houston, Texas 77005, United States

Email:
Philipp Heretsch[*] - heretsch@rice.edu; Athanassios Giannis[*] - giannis@uni-leipzig.de

* Corresponding author

Keywords:
cyclopamine; C–H-functionalization; hedgehog signaling pathway; natural products; steroidal alkaloids

Beilstein J. Org. Chem. **2014,** *10,* 1564–1569.
doi:10.3762/bjoc.10.161

Received: 16 April 2014
Accepted: 23 June 2014
Published: 09 July 2014

This article is part of the Thematic Series "Natural products in synthesis and biosynthesis".

Guest Editor: J. S. Dickschat

© 2014 Rabe et al; licensee Beilstein-Institut.
License and terms: see end of document.

Abstract

The chemical synthesis of carbacyclopamine analog **2**, a cyclopamine analog with an all-carbon E-ring, is reported. The use of C–H-functionalization logic and further metal-catalyzed transformations allows for a concise entry to this new class of acid-stable cyclopamine analogs.

Introduction

The isolation of cyclopamine (**1**, Figure 1) nearly 50 years ago followed by the determination of its biological target and pharmacological profile has drawn considerable interest from research groups in biology, chemistry and medicine [1-4]. As the first identified hedgehog signaling inhibitor, cyclopamine exerts its anticancer activity through a novel mechanism of action, which manifests itself in its remarkable activity against several types of human cancer, including medulloblastoma, basal cell carcinoma, and rhabdomyosarcoma [5-10]. The impressive biological activity combined with a unique molecular architecture and the synthetic challenge it poses already let to the first synthesis of cyclopamine by this laboratory employing C–H-functionalization logic [11]. In addition, the rational design and chemical synthesis of several analogs and derivatives by this [12,13] and other groups [14-17] have been disclosed. Here, we report the synthesis of a carbacyclopamine analog (**2**, Figure 1), an analog of the natural product with an all-carbon E-ring and a pyridine F-ring.

Cyclopamine inhibits the 7-transmembrane protein smoothened from converting into its active form [18,19]. Without active smoothened, protein kinases like PKA, GSK3β, and CK1ε phosphorylate the transcription factors Gli2 and Gli3, thereby creating binding sites for the adapter protein β-TrCP [20]. The

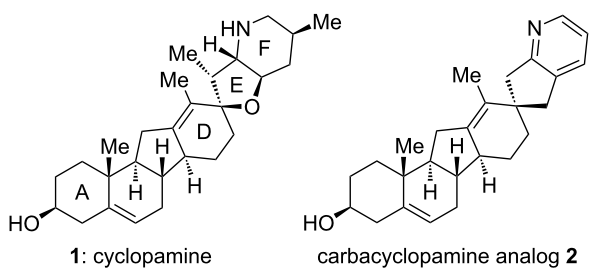


Figure 1: Structures of cyclopamine (**1**) and carbacyclopamine analog **2**.

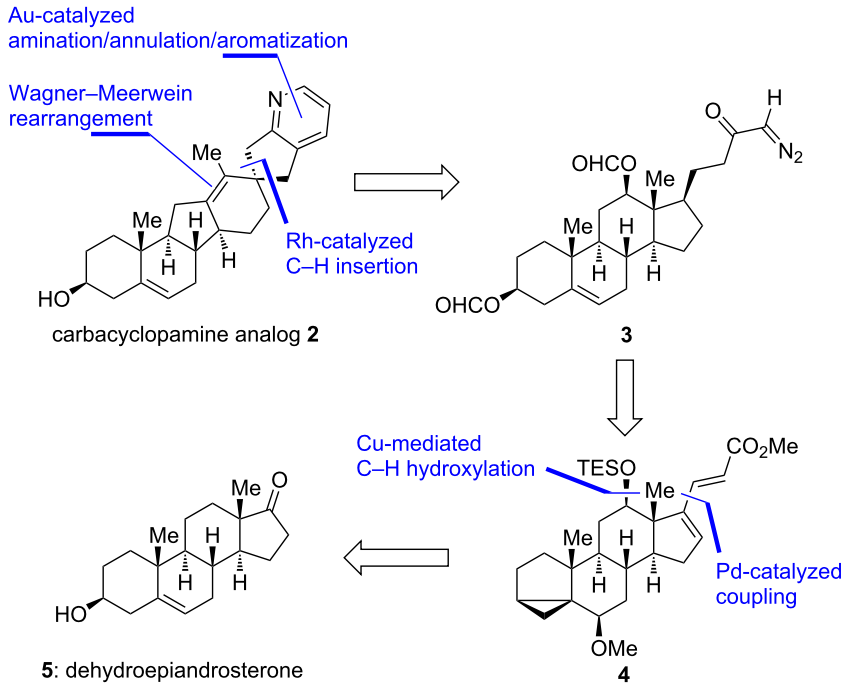
Gli family of transcription factors acts as an effector of the hedgehog signaling pathway and thus, is associated with a wide array of physiological effects, including cell fate determination, proliferation and patterning. The so-formed Gli/β-TrCP complex becomes subject to ubiquitinylation, mediated by the Cul1-based E3 ligase. Eventually, this results in partial proteosomal degradation to form Gli3-R [21], or in the case of Gli2 [22,23], in complete degradation. In addition, the Gli3-R factor acts as a transcription inhibitor of hedgehog-response genes [10].

As part of our continuing work on acid-stable cyclopamine analogs [12,13] we have now focused on the role of the allylic ether oxygen in the acid-mediated E-ring cleavage and decomposition of cyclopamine [24]. We envisioned that its replacement by a methylene group would create an acid-stable cyclopamine analog that still exhibits similar inhibitory activity on hedgehog-signaling. For the sake of brevity of the overall synthetic sequence we defined carbacyclopamine analog **2** (see Figure 1) as our primary target.

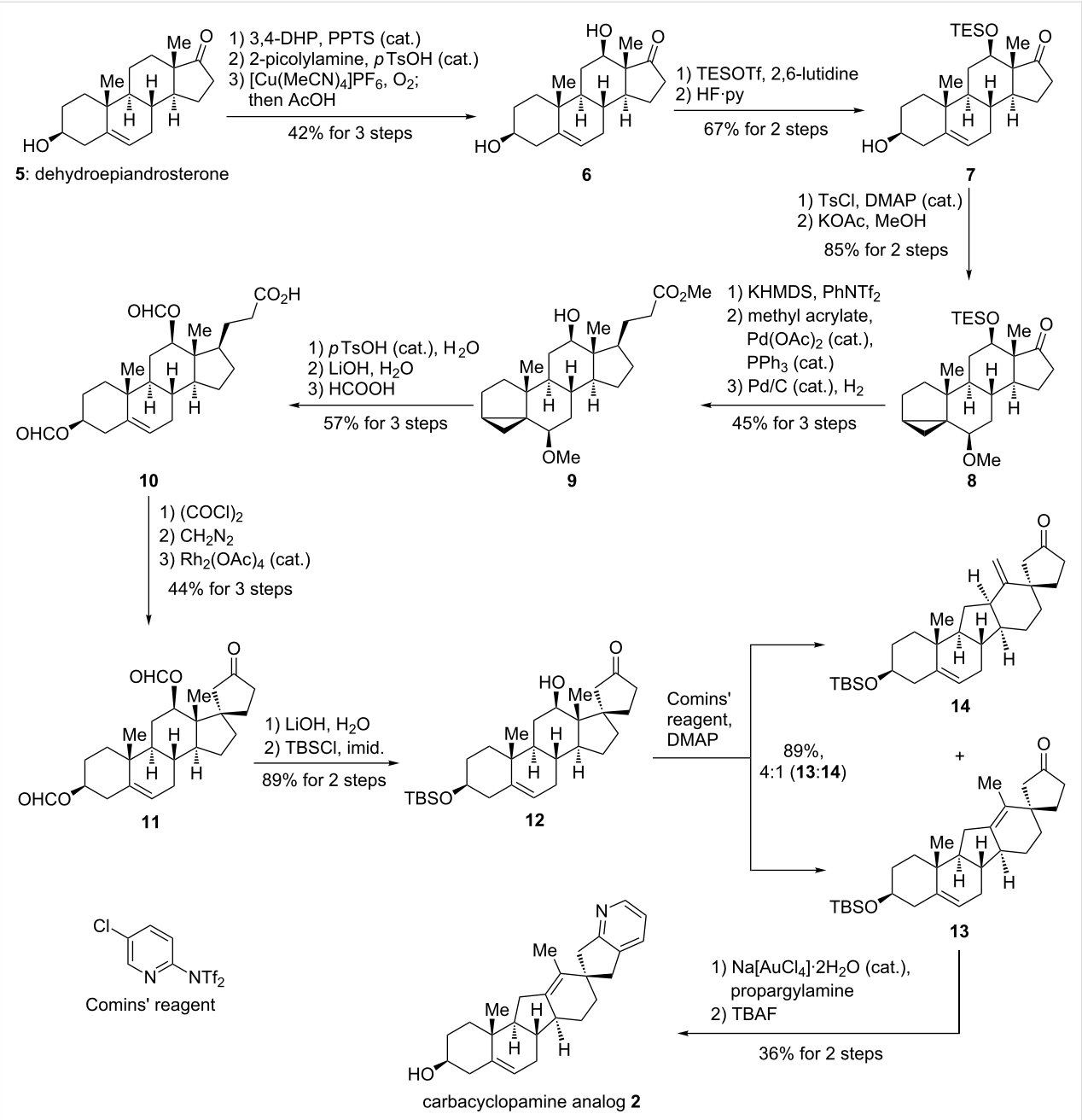
Results and Discussion

A retrosynthetic analysis identified diazo compound **3** as a key intermediate in the synthesis of **2** (see Scheme 1). We envisioned a rhodium-catalyzed C–H-insertion into the C17–H bond to occur with a high degree of selectivity (both regio- and stereoselectivity) to form the all-carbon E-ring (for its structure see **11**, Scheme 2). Furthermore, a Wagner–Meerwein rearrangement was thought to establish the C-*nor*-D-*homo* steroid system, and a gold-catalyzed amination/annulation/aromatization sequence was planned to install the pyridine F-ring. Diazo compound **3** originates from diene **4** through standard transformations, the latter being accessible from commercially available and inexpensive dehydroepiandrosterone (**5**) by the means of a copper-mediated C–H hydroxylation in the 12-position and a palladium-catalyzed coupling of methyl acrylate to an activated enol ether in the 17-position.

In synthetic direction (Scheme 2), dehydroepiandrosterone (**5**) was protected as its tetrahydropyranyl ether (3,4-dihydro-2*H*-pyran, cat. pyridinium *para*-toluenesulfonate, CH_2Cl_2, 25 °C, quantiative, inconsequential mixture of diastereoisomers), and the C17 carbonyl group was transformed into its 2-picolylimine



Scheme 1: Retrosynthetic analysis of carbacyclopamine analog **2**.



Scheme 2: Synthesis of carbacyclopamine analog **2**.

(2-picolylamine, cat. *para*-toluenesulfonic acid, toluene, 111 °C, 92% yield). Subjecting the latter to modified Schönecker conditions ($[Cu(MeCN)_4]PF_6$, O_2, acetone, 25 °C) [25-27], gave, after acidic work-up (AcOH/MeOH, 1:1, 90 °C), diol **6** in 46% yield as the only isolable product. Protection of the newly installed 12β-hydroxy group as a triethylsilyl ether via the bis-protected intermediate (not shown, triethylsilyl trifluoromethanesulfonate, 2,6-lutidine, CH_2Cl_2, 0 °C; then HF·pyridine, THF, 0 °C, 67% yield for the two steps) [28] gave hydroxy ketone **7**.

The remaining homoallylic alcohol was then masked as an *i*-steroid [29,30] (*para*-toluenesulfonyl chloride, cat. 4-dimethylaminopyridine, pyridine, 25 °C; then KOAc, MeOH, 64 °C, 85% yield for the two steps) to give **8**. Generation of an enol triflate from the carbonyl group in **8** (potassium hexamethyldisilazide, phenyl bis-triflimide, THF, −20 → −10 °C, 85% yield) set stage for a Heck-reaction with methyl acrylate (cat. $Pd(OAc)_2$, cat. PPh_3, Et_3N, DMF, 70 °C, 64% yield). The hydrogenation of the so-obtained diene **4** (for its structure see Scheme 1) proceeded smoothly (H_2, cat. Pd/C, MeOH, 25 °C,

82% yield) under concomitant removal of the triethylsilyl ether [31] in 12-position to give methyl ester **9** as a single diastereoisomer. At this point, extensive experimentation suggested a change of protecting groups to enable the pending C–H insertion reaction at C17.

Therefore, the *i*-steroid was reverted to the homoallylic alcohol (cat. *para*-toluenesulfonic acid, 1,4-dioxane/H_2O, 10:1, 65 °C), the methyl ester was hydrolyzed under basic conditions (LiOH, THF/H_2O, 1:1, 68% yield for the two steps), and the alcohol moieties were protected as formyl esters (formic acid, 50 °C, 85% yield) to give key intermediate **10**.

Employing the formyl protecting groups [32], diazoketone **3** (for its structure see Scheme 1) was readily obtained from acid **10** via the corresponding acid chloride (oxalyl chloride, CH_2Cl_2, 25 °C; then diazomethane, THF, 25 °C, 85% yield for the two steps) [33]. The anticipated C–H insertion then proceeded uneventfully under oxygen-free conditions (cat. $Rh_2(OAc)_4$, CH_2Cl_2, 41 °C) [34,35] to give cyclopentanone **11** in 52% yield as a single isomer. Removal of the formyl ester protecting groups (LiOH, THF/H_2O, 1:1, 30 °C, 94% yield) and selective protection of the 3-hydroxy group as a *tert*-butyldimethylsilyl ether (*tert*-butyldimethylsilyl chloride, imidazole, DMF, 25 °C, 95% yield) furnished alcohol **12**.

Treatment of the latter under our previously reported conditions [36] (Comins' reagent, 4-dimethylaminopyridine, toluene, 111 °C) gave an inseparable mixture of the rearranged olefin products, with the desired *endo*-product **13** as the major constituent (89% combined yield, *endo*-product **13**:*exo*-product **14**, 4:1). Isolation of desired product **13** by chromatography was then achieved after selective hydrogenation of only the exocyclic olefin in **14** (H_2, cat. Rh/C, EtOAc, 25 °C, structure of hydrogenation product not shown) employing the mixture of the isomers **13** and **14** from the previous step.

Finally, a gold-catalyzed amination/annulation/aromatization sequence (propargylamine, cat. $Na[AuCl_4]\cdot 2H_2O$, EtOH, 100 °C) [37,38] furnished, after removal of the *tert*-butyldimethylsilyl ether (tetrabutylammonium fluoride, THF, 25 °C), carbacyclopamine analog **2** in 36% overall yield for the two steps [39].

Carbacyclopamine analog **2** was then tested for its stability towards acid. Therefore, **2** was treated with a mixture of aqueous HCl/THF (pH of approx. 0.3) for 1 h and ^{1}H NMR spectra were recorded before and afterwards. While at this pH natural cyclopamine (**1**) was shown to decompose rapidly [12], carbacyclopamine analog **2** showed no signs of decomposition. This result was in full agreement with our initial considerations.

To determine the ability of carbacyclopamine analog **2** to inhibit Gli1-dependent luciferase expression, we employed Shh-LIGHTII cells, a clonal mouse fibroblast cell line which stably incorporates a Gli-dependent firefly luciferase reporter and a constitutive *Renilla* luciferase reporter [18]. The analog was tested in a concentration range from 0.01 μM to 100 μM but showed no activity (data not shown).

Conclusion

We have reported the synthesis of a new, acid stable cyclopamine analog. The implementation of C–H-functionalization logic in the synthetic planning and further metal-catalyzed transformations allows for a fast access to carbocyclopamine analog **2**. At the same time, these investigations strongly suggest the role the ether oxygen plays in the acid-catalyzed decomposition of cyclopamine. This study may find further application in the rational design of new hedgehog inhibitors based on lead structure **2**. Future work will focus on the synthesis of carbacyclopamine analogs with a piperidine F-ring and their biological investigation.

Supporting Information

Supporting Information File 1

Experimental procedures, characterization data, and copies of ^{1}H and ^{13}C NMR spectra for new compounds.
[http://www.beilstein-journals.org/bjoc/content/supplementary/1860-5397-10-161-S1.pdf]

Acknowledgements

We thank Dr. Lothar Hennig, Universität Leipzig, for his help with recording and interpreting the 2D NMR spectra.

References

1. Keeler, R. F. *Phytochemistry* **1968,** *7,* 303–306. doi:10.1016/S0031-9422(00)86328-1
2. Keeler, R. F. *Teratology* **1970,** *3,* 169–174. doi:10.1002/tera.1420030209
3. Beachy, P. A.; Karhadkar, S. S.; Berman, D. M. *Nature* **2004,** *432,* 324–331. doi:10.1038/nature03100
4. Taipale, J.; Beachy, P. A. *Nature* **2001,** *411,* 349–354. doi:10.1038/35077219
5. Hidalgo, M.; Maitra, A. *N. Engl. J. Med.* **2009,** *361,* 2094–2096. doi:10.1056/NEJMcibr0905857
6. Dierks, C.; Grbic, J.; Zirlik, K.; Beigi, R.; Englund, N. P.; Guo, G.-R.; Veelken, H.; Engelhardt, M.; Mertelsmann, R.; Kelleher, J. F.; Schultz, P.; Warmuth, M. *Nat. Med.* **2007,** *13,* 944–951. doi:10.1038/nm1614
7. Hedge, G. V.; Munger, C. M.; Emanuel, K.; Joshi, A. D.; Greiner, T. C.; Weisenburger, D. D.; Vose, J. M.; Joshi, S. S. *Mol. Cancer Ther.* **2008,** *7,* 1450–1460. doi:10.1158/1535-7163.MCT-07-2118

8. Kawahara, T.; Kawaguchi-Ihara, N.; Okuhashi, Y.; Itoh, M.; Nara, N.; Tohda, S. *Anticancer Res.* **2009,** *29,* 4629–4632.
9. Heretsch, P.; Tzagkaroulaki, L.; Giannis, A. *Angew. Chem., Int. Ed.* **2010,** *49,* 3418–3427. doi:10.1002/anie.200906967
10. Heretsch, P.; Tzagkaroulaki, L.; Giannis, A. *Bioorg. Med. Chem.* **2010,** *18,* 6613–6624. doi:10.1016/j.bmc.2010.07.038
    And references cited therein.
11. Giannis, A.; Heretsch, P.; Sarli, V.; Stößel, A. *Angew. Chem., Int. Ed.* **2009,** *48,* 7911–7914. doi:10.1002/anie.200902520
12. Heretsch, P.; Büttner, A.; Tzagkaroulaki, L.; Zahn, S.; Kirchner, B.; Giannis, A. *Chem. Commun.* **2011,** *47,* 7362–7364. doi:10.1039/C1CC11782C
13. Moschner, J.; Chentsova, A.; Eilert, N.; Rovardi, I.; Heretsch, P.; Giannis, A. *Beilstein J. Org. Chem.* **2013,** *9,* 2328–2335. doi:10.3762/bjoc.9.267
14. Tremblay, M. R.; Nevalainen, M.; Nair, S. J.; Porter, J. R.; Castro, A. C.; Behnke, M. L.; Yu, L.-C.; Hagel, M.; White, K.; Faia, K.; Grenier, L.; Campbell, M. J.; Cushing, J.; Woodward, C. N.; Hoyt, J.; Foley, M. A.; Read, M. A.; Sydor, J. R.; Tong, J. K.; Palombella, V. J.; McGovern, K.; Adams, J. *J. Med. Chem.* **2008,** *51,* 6646–6649. doi:10.1021/jm8008508
15. Tremblay, M. R.; Lescarbeau, A.; Grogan, M. J.; Tan, E.; Lin, G.; Austad, B. C.; Yu, L.-C.; Behnke, M. L.; Nair, S. J.; Hagel, M.; White, K.; Conley, J.; Manna, J. D.; Alvarez-Diez, T. M.; Hoyt, J.; Woodward, C. N.; Sydor, J. R.; Pink, M.; MacDougall, J.; Campbell, M. J.; Cushing, J.; Ferguson, J.; Curtis, M. S.; McGovern, K.; Read, M. A.; Palombella, V. J.; Adams, J.; Castro, A. C. *J. Med. Chem.* **2009,** *52,* 4400–4418. doi:10.1021/jm900305z
16. Zhang, Z.; Baubet, V.; Ventocilla, C.; Xiang, C.; Dahmane, N.; Winkler, J. D. *Org. Lett.* **2011,** *13,* 4786–4789. doi:10.1021/ol2017966
17. Winkler, J. D.; Isaacs, A.; Holderbaum, L.; Tatard, V.; Dahmane, N. *Org. Lett.* **2009,** *11,* 2824–2827. doi:10.1021/ol900974u
18. Taipale, J.; Chen, J. K.; Cooper, M. K.; Wang, B.; Mann, R. K.; Milenkovic, L.; Scott, M. P.; Beachy, P. A. *Nature* **2000,** *406,* 1005–1009. doi:10.1038/35023008
19. Wang, Y.; Zhou, Z.; Walsh, C. T.; McMahon, A. P. *Proc. Natl. Acad. Sci. U. S. A.* **2009,** *106,* 2623–2628. doi:10.1073/pnas.0812110106
20. Pearse, R. V., II; Collier, L.S.; Scott, M. P.; Tabin, C. J. *Dev. Biol.* **1999,** *212,* 323–336. doi:10.1006/dbio.1999.9335
21. Wen, X.; Lai, C. K.; Evangelista, M.; Hongo, J.-A.; de Sauvage, F. J.; Scales, S. J. *Mol. Cell. Biol.* **2010,** *30,* 1910–1922. doi:10.1128/MCB.01089-09
22. Pan, Y.; Bai, C. B.; Joyner, A. L.; Wang, B. *Mol. Cell. Biol.* **2006,** *26,* 3365–3377. doi:10.1128/MCB.26.9.3365-3377.2006
23. Wang, B.; Fallon, J. F.; Beachy, P. A. *Cell* **2000,** *100,* 423–434. doi:10.1016/S0092-8674(00)80678-9
24. Wilson, S. R.; Strand, M. F.; Krapp, A.; Rise, F.; Petersen, D.; Krauss, S. *J. Pharm. Biomed. Anal.* **2010,** *52,* 707–713. doi:10.1016/j.jpba.2010.02.017
    See for a proposed mechanism of the decomposition of cyclopamine. For a discussion of the molecular orbitals involved in the process, see ref. [12.]
25. Schönecker, B.; Zheldakova, T.; Lange, C.; Günther, W.; Görls, H.; Bohl, M. *Chem.–Eur. J.* **2004,** *10,* 6029–6042. doi:10.1002/chem.200306054
26. Schönecker, B.; Zheldakova, T.; Liu, Y.; Kötteritzsch, M.; Günther, W.; Görls, H. *Angew. Chem., Int. Ed.* **2003,** *42,* 3240–3244. doi:10.1002/anie.200250815
27. Schönecker, B.; Lange, C.; Zheldakova, T.; Günther, W.; Görls, H.; Vaughan, G. *Tetrahedron* **2005,** *61,* 103–114. doi:10.1016/j.tet.2004.10.055
28. Ojima, I.; Chen, J.; Sun, L.; Borella, C. P.; Wang, T.; Miller, M. L.; Lin, S.; Geng, X.; Kuznetsova, L.; Qu, C.; Gallager, D.; Zhao, X.; Zanardi, I.; Xia, S.; Horwitz, S. B.; Mallen-St. Clair, J.; Guerriero, J. L.; Bar-Sagi, D.; Veith, J. M.; Pera, P.; Bernacki, R. J. *J. Med. Chem.* **2008,** *51,* 3203–3221. doi:10.1021/jm800086e
29. Fernholz, E.; Ruigh, W. L. *J. Am. Chem. Soc.* **1940,** *62,* 3346–3348. doi:10.1021/ja01869a022
30. Wallis, E. S.; Fernholz, E.; Gephart, F. T. *J. Am. Chem. Soc.* **1937,** *59,* 137–140. doi:10.1021/ja01280a034
31. Rotulo-Sims, D.; Prunet, J. *Org. Lett.* **2002,** *4,* 4701–4704. doi:10.1021/ol0271382
32. The formyl groups were chosen both for the ease of their installation, and a considerably lower sterical demand in the pending cyclization event when compared to other protective groups. Using triethylsilyl ethers or allyl ethers instead did not allow for the generation of the desired diazo-compound. The use of acetyl protecting groups led to the formation of seven-membered lactone **25** (for experimental details see Supporting Information File 1).
33. A similar reaction employing diazoethane instead of diazomethane gave the methyl homolog of compound **10**. All attempts to effect the C–H insertion were met with failure, though (see Supporting Information File 1 for experimental details).
34. Nakamura, E.; Yoshikai, N.; Yamanaka, M. *J. Am. Chem. Soc.* **2002,** *124,* 7181–7192. doi:10.1021/ja017823o
35. Doyle, M. P.; Duffy, R.; Ratnikov, M.; Zhou, L. *Chem. Rev.* **2010,** *110,* 704–724. doi:10.1021/cr900239n
36. Heretsch, P.; Rabe, S.; Giannis, A. *J. Am. Chem. Soc.* **2010,** *132,* 9968–9969. doi:10.1021/ja103152k
37. Abbiati, G.; Arcadi, A.; Bianchi, G.; Di Giuseppe, S.; Marinelli, F.; Rossi, E. *J. Org. Chem.* **2003,** *68,* 6959–6966. doi:10.1021/jo0347260
38. The regioisomeric cyclization product (theoretically obtainable by fusion with the C20 methylene) was not detected in the crude reaction mixture.
39. After chromatographic purification the final product was obtained in ca. 90% purity (judged by ^{1}H NMR, see Supporting Information File 1). We were not able to determine the structures of the impurities or completely remove them. The yield reported takes this into account; the biological assay and the stability assay were run with this material.

License and Terms

This is an Open Access article under the terms of the Creative Commons Attribution License (http://creativecommons.org/licenses/by/2.0), which permits unrestricted use, distribution, and reproduction in any medium, provided the original work is properly cited.

The license is subject to the *Beilstein Journal of Organic Chemistry* terms and conditions: (http://www.beilstein-journals.org/bjoc)

The definitive version of this article is the electronic one which can be found at: doi:10.3762/bjoc.10.161

BEILSTEIN JOURNAL OF ORGANIC CHEMISTRY

Synthesis and bioactivity of analogues of the marine antibiotic tropodithietic acid

Patrick Rabe[1], Tim A. Klapschinski[1], Nelson L. Brock[1], Christian A. Citron[1], Paul D'Alvise[2], Lone Gram[2] and Jeroen S. Dickschat[*1]

Letter

Open Access

Address:
[1]Kekulé-Institut für Organische Chemie, Rheinische Friedrich-Wilhelms-Universität Bonn, Gerhard-Domagk-Straße 1, 53121 Bonn, Germany and [2]Department of Systems Biology, Technical University of Denmark, Matematiktorvet bldg. 301, 2800 Kongens Lyngby, Denmark

Email:
Jeroen S. Dickschat[*] - dickschat@uni-bonn.de

* Corresponding author

Keywords:
antibiotics; natural products; *Roseobacter*; SAR study; tropodithietic acid; tropone

Beilstein J. Org. Chem. **2014,** *10,* 1796–1801.
doi:10.3762/bjoc.10.188

Received: 17 April 2014
Accepted: 22 July 2014
Published: 06 August 2014

This article is part of the Thematic Series "Natural products in synthesis and biosynthesis".

Associate Editor: K. N. Ganesh

© 2014 Rabe et al; licensee Beilstein-Institut.
License and terms: see end of document.

Abstract

Tropodithietic acid (TDA) is a structurally unique sulfur-containing antibiotic from the *Roseobacter* clade bacterium *Phaeobacter inhibens* DSM 17395 and a few other related species. We have synthesised several structural analogues of TDA and used them in bioactivity tests against *Staphylococcus aureus* and *Vibrio anguillarum* for a structure–activity relationship (SAR) study, revealing that the sulfur-free analogue of TDA, tropone-2-carboxylic acid, has an antibiotic activity that is even stronger than the bioactivity of the natural product. The synthesis of this compound and of several analogues is presented and the bioactivity of the synthetic compounds is discussed.

Introduction

Tropodithietic acid (TDA, **1a**) is an antibiotic produced by the marine bacterium *Phaeobacter inhibens*. It has an unusual structure that is made up by a dithiet moiety fused to tropone-2-carboxylic acid (Figure 1) [1]. In *Phaeobacter* the compound is accompanied by hydroxy-TDA **2**, while its tautomer thiotropocin (**1b**) was previously reported from *Pseudomonas* [2,3]. The biosynthesis of **1** starts from phenylalanine and requires the *paaABCDE* and *paaG* genes of the upper phenylacetic acid (PAA) catabolon [4,5], the six genes *tdaABCDEF* that are located on a plasmid [6,7], and the adjacent *paaZ2* gene [8], a mutated copy of *paaZ* from the PAA catabolon. Particularly interesting is the mechanism of sulfur introduction that we have recently investigated in a study combining gene knockouts and feeding experiments with ^{34}S-labelled amino acids [8]. In this study we could show that *S*-thiocysteine is the direct sulfur precursor of TDA. The introduction of sulfur proceeds via nucleophilic attack of *S*-thiocysteine to the Michael acceptor of tropone-2-carboxylic acid coenzyme A ester and oxidative

elimination of cysteine. The second sulfur atom is introduced by analogous attack to the vinylogous Michael acceptor. The volatiles tropone (**3**) and tropone hydrate **4** can also be detected in *P. inhibens* headspace extracts and are shunt products of the TDA biosynthetic pathway [9]. Clardy and coworkers have recently reported on a series of structurally related compounds with algicidal activity, represented by roseobacticide A (**5**), but their biosynthesis is unknown [10].

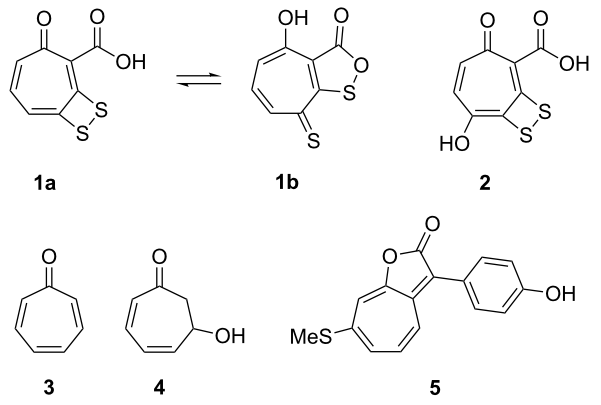


Figure 1: TDA and related natural products from *Phaeobacter inhibens*.

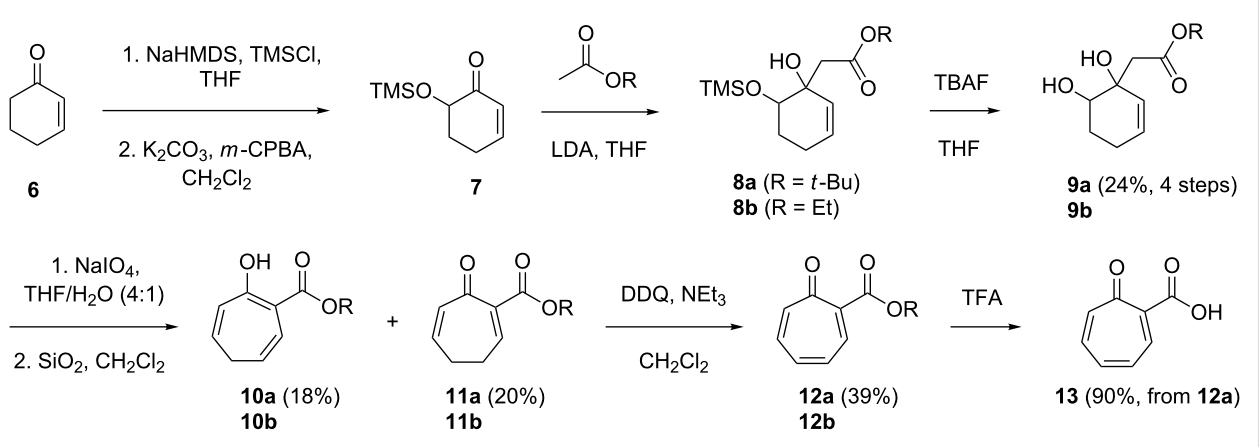
TDA exhibits a strong antibiotic activity against a broad spectrum of bacteria including alpha- and gammaproteobacteria, flavobacteria and actinobacteria [11], but not against the eukaryotic model organisms *Artemia* sp. and *Caenorhabditis elegans*, suggesting *P. inhibens* or other TDA-producing bacteria from the *Roseobacter* clade as promising candidates to be used as probiotics in aquacultures [12]. The mode of action of TDA is unknown, but it is difficult to select resistant and tolerant strains from long-term exposures to sub inhibitory concentrations of TDA, suggesting that TDA may interact with several targets [13]. Here we report on the synthesis and bioactivity of several TDA analogues for investigating the structure–activity relationship (SAR) of this unique marine antibiotic.

Results and Discussion

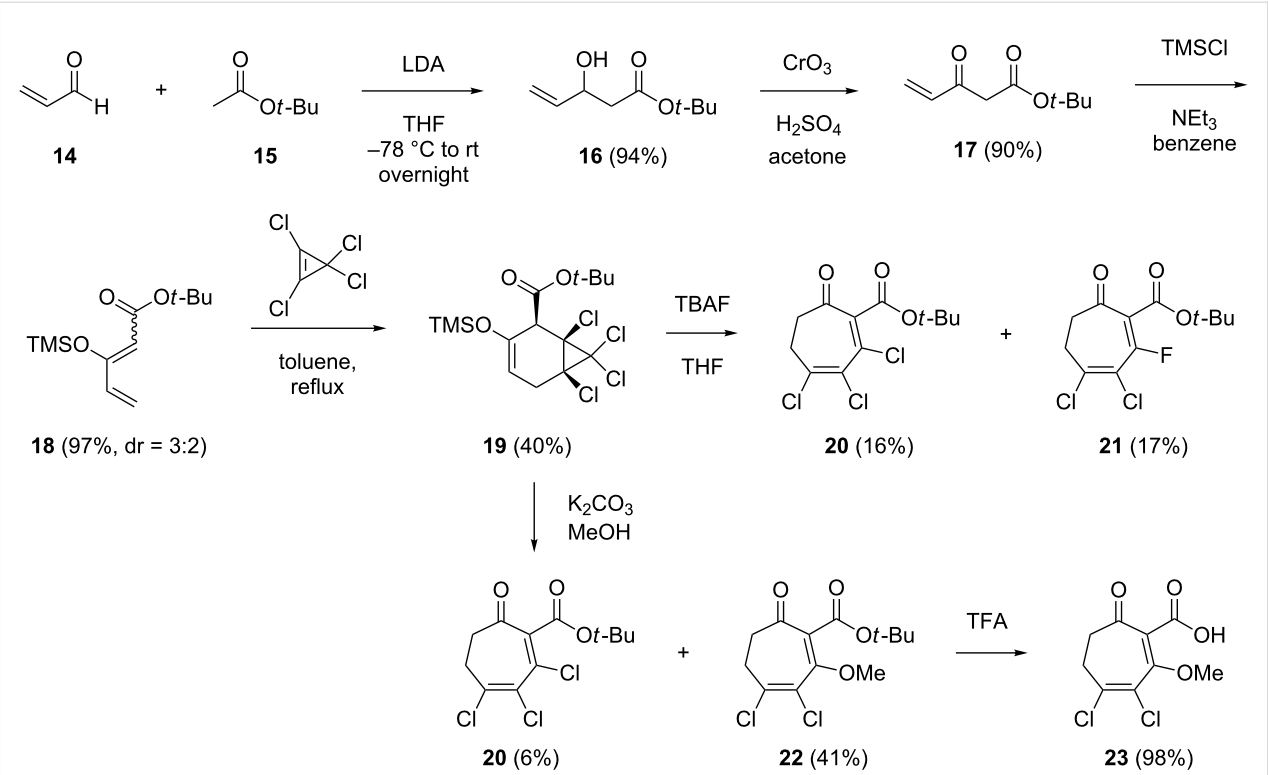
Synthesis of analogues of tropodithietic acid

For a detailed SAR study we first aimed at a series of compounds with a seven-membered carbocyclic core and an overall simplified structure as compared to the antibiotic TDA. Therefore, tropone-2-carboxylic acid (**13**), lacking the unprecedented dithiet moiety of TDA, was synthesised according to Scheme 1. Cyclohexenone **6** was first converted with NaHMDS and TMSCl into the corresponding silylenol ether that upon oxidation with *m*-CPBA under migration of the TMS group yielded the protected hydroxy ketone **7**. Aldol reaction with *tert*-butyl acetate to **8a** and deprotection with TBAF gave **9a** in 24% yield over four steps. Oxidative cleavage of the glycol with $NaIO_4$ resulted in a β-ketoester aldehyde that upon treatment with silica gel underwent an intramolecular aldol condensation to a mixture of **10a** and **11a** that were separable by column chromatography. Oxidation with DDQ gave *tert*-butyl tropone-2-carboxylate (**12a**) that was efficiently converted into **13** by stirring in TFA. The synthesis of **12a** followed a previously published route for ethyl tropone-2-carboxylate (**12b**) [14], but saponification of this ester led to decomposition, and therefore, the *tert*-butyl ester **12a** was prepared that allowed for a conversion into **13** under acidic conditions.

Furthermore, a series of TDA analogues all with a seven-membered carbocyclic core bearing a carbonyl function, a carboxylic acid or ester function in 2-position, and various functional groups such as halogen atoms and methoxy groups was synthesised (Scheme 2). Acrolein (**14**) was reacted with *tert*-butyl acetate (**15**) and LDA to yield the aldol product **16** that



Scheme 1: Synthesis of tropone-2-carboxylic acid (**13**).



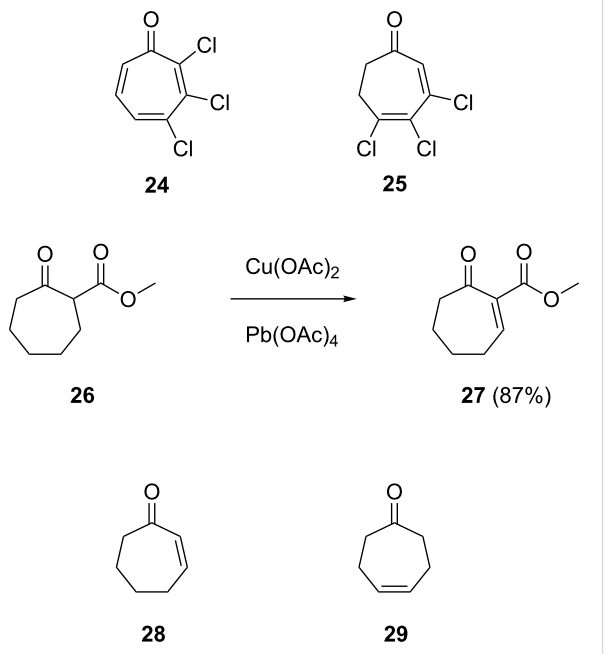
Scheme 2: Synthesis of halogenated TDA analogues.

was subsequently oxidised to the β-keto ester **17** in a Jones oxidation. Treatment of the latter with TMSCl, imidazole and DMAP resulted in **18** as a 3:2 mixture of two diastereomers that proved to be unstable. However, the crude product was sufficiently pure for its direct usage in a Diels–Alder reaction with tetrachlorocyclopropene, resulting in the adduct **19** as a single stereoisomer. The formation of only one stereoisomer is explainable by an *E*/*Z* isomerisation of **18** and a Diels–Alder reaction that only proceeds from (*Z*)-**18**, but not from (*E*)-**18**. Treatment of **19** with TBAF resulted in cleavage of the TMS protecting group followed by instantaneous elimination of HCl under cyclopropane ring opening to **20** with 16% yield. Furthermore, similar amounts of the fluorinated derivative **21** (17%) were isolated. Its formation is explained by the nucleophilic attack of fluoride to the Michael acceptor in **20** followed by elimination of chloride. In contrast, treatment of **19** with potassium carbonate in MeOH yielded only minor amounts of **20** and the substitution product, methoxy derivative **22**, as main product. All three compounds **20**–**22** were treated under various oxidation conditions (including DDQ, IBX, SeO_2, and MnO_2) to install the tropone moiety by dehydrogenation, but unfortunately all these reaction conditions failed. Compound **22** was subsequently converted into the free acid **23** by treatment with TFA, while similar conversions of **20** and **21** were unsuccessful due to the instability of the products.

Two structurally related halogenated compounds lacking the carboxylic acid function as in TDA, 2,3,4-trichlorotropone (**24**) and 3,4,5-trichloro-6,7-dihydrotropone (**25**), were prepared through a known route (Scheme 3) [15]. Finally, a few cycloheptanone derivatives with rigorously simplified structures as compared to TDA were included in this study. The β-ketoester **27** containing a Michael acceptor was synthesised from methyl cycloheptanone-2-carboxylate (**26**) by oxidation with $Cu(OAc)_2$ and $Pb(OAc)_2$ according to a known procedure [16]. The compound cyclohept-2-en-1-one (**28**) is commercially available, while we have previously reported the synthesis of cyclohept-4-en-1-one (**29**) that was identified in headspace extracts from streptomycetes [17].

Bioactivity tests

All synthetic compounds were screened in bioactivity tests towards two bacterial strains, the Gram-positive *Staphylococcus aureus* 8325 and the Gram-negative *Vibrio anguillarum* 90-11-287 (Table 1). These organisms were selected for our bioactivity tests, because *S. aureus* is a clinically important human pathogen and strains with resistances against multiple antibiotic drugs cause severe problems with nosocomial infections. The bioactivity against *V. anguillarum* is interesting from an ecological point of view, because *P. inhibens* was originally isolated from scallop rearings [18-20], suggesting that the



Scheme 3: Further compounds included in this SAR study.

natural function of *P. inhibens* may be to prevent molluscs from *Vibrio* infections.

Most of the compounds tested had minimal inhibitory concentrations (MICs) exceeding that of TDA, however, two compounds were of equal or even better antibiotic activity. Compound **25** was as effective, and tropone-2-carboxylic acid (**13**), closely resembling the structure of TDA, but lacking its sulfur atoms, was even more effective with a MIC corresponding to half the MIC of TDA (MIC against *S. aureus* was 26 μM versus 39 μM, while the MIC against *V. anguillarum* was 6.5 μM versus 19 μM). This indicates that the dithiet moiety of TDA is not essential for the direct antibacterial effect of the compound, and may have other physiological or ecological functions. This result is particularly surprising, because the coenzyme A ester of **13** is an intermediate along the biosynthetic pathway to TDA, so the question arises what may have been the evolutionary advantages of extending the biosynthetic pathway from the coenzyme A ester of **13** to TDA by the introduction of two sulfur atoms. A possible answer may be that TDA has more or other targets than **13** which may have the consequence that the development of resistances against TDA is prevented, thus offering an evolutionary advantage.

Conclusion

We have synthesised a series of compounds with seven-membered carbocyclic rings. Their structures were inspired by the antibiotic TDA from the marine bacterium *P. inhibens*. One compound, 3,4,5-trichloro-5,6-dihydrotropone (**25**), showed a strong antibiotic activity against *S. aureus* and *V. anguillarum* that is similar to the activity of TDA, while tropone-2-carboxylic acid (**13**) had an even stronger antibiotic effect. This

Table 1: Bioactivity tests with TDA and TDA analogues.

Compound[a]	*Staphylococcus aureus* 8325		*Vibrio anguillarum* 90-11-287	
	MIC/mg L^{-1}	MIC/μM	MIC/mg L^{-1}	MIC/μM
1	7.8	39	3.9	19
10a	inactive		125	600
10b	125	700	125	700
11a	inactive		125	600
12a	125	600	125	600
12b	125	700	125	700
13	3.9	26	1.0	6.5
20	inactive		inactive	
21	125	430	125	430
22	inactive		inactive	
23	inactive		inactive	
24	inactive		125	720
25	7.8	45	15.6	89
26	inactive		inactive	
27	62.5	370	46.9	280
28	62.5	570	31.3	280
29	62.5	570	31.3	570

[a]MICs were determined using the microdilution method according to guidelines of the Clinical and Laboratory Standards Institute [21]. Compounds with MICs > 125 mg L^{-1} were regarded as inactive.

suggests that the sulfur atoms in TDA are not essential for bioactivity, but different modes of action for TDA and its sulfur-free analogue cannot be excluded.

Experimental

Bioactivity testing. All synthetic compounds were used in bioactivity tests towards two bacterial strains, *Staphylococcus aureus* 8325 [22] and *Vibrio anguillarum* 90-11-287 [23] (Table 1). The two strains were grown as precultures overnight with agitation at 25 °C in 20 mL cation-adjusted Mueller Hinton II Broth (Cat. No. 297963, Becton, Dickinson and Company, Sparks, MD, USA). The minimum inhibitory concentration (MIC) of the compounds was determined using the microdilution method according to the guidelines of the Clinical and Laboratory Standards Institute (CLSI 2006) [21]. All compounds were dissolved in DMSO to stock solutions of 1.5 g L^{-1} and further diluted in the bacterial growth medium, Mueller Hinton II Broth. Final concentrations ranging from 500 to 0.5 mg L^{-1} were tested and solvent controls were included.

Supporting Information

Supporting Information File 1

Synthetic procedures, compound characterisation data and copies of NMR spectra.
[http://www.beilstein-journals.org/bjoc/content/supplementary/1860-5397-10-188-S1.pdf]

Acknowledgements

This work was funded by the Deutsche Forschungsgemeinschaft as part of the Transregional Collaborative Research Centre SFB-TR 51 ("*Roseobacter*"), by a PhD scholarship of the Beilstein-Institut zur Förderung der Chemischen Wissenschaften (to P.R.), and by a PhD scholarship of the Fonds der Chemischen Industrie (to N.L.B.).

References

1. Liang, L. Ph.D. Thesis, University of Göttingen, Germany, 2003.
2. Cane, D. E.; Wu, Z.; Van Epp, J. E. *J. Am. Chem. Soc.* **1992,** *114,* 8479–8483. doi:10.1021/ja00048a019
3. Greer, E. M.; Aebisher, D.; Greer, A.; Bentley, R. *J. Org. Chem.* **2008,** *73,* 280–283. doi:10.1021/jo7018416
4. Berger, M.; Brock, N. L.; Liesegang, H.; Dogs, M.; Preuth, I.; Simon, M.; Dickschat, J. S.; Brinkhoff, T. *Appl. Environ. Microbiol.* **2012,** *78,* 3539–3551. doi:10.1128/AEM.07657-11
5. Teufel, R.; Gantert, C.; Voss, M.; Eisenreich, W.; Haehnel, W.; Fuchs, G. *J. Biol. Chem.* **2011,** *286,* 11021–11034. doi:10.1074/jbc.M110.196667
6. Geng, H.; Bruhn, J. B.; Nielsen, K. F.; Gram, L.; Belas, L. *Appl. Environ. Microbiol.* **2008,** *74,* 1535–1545. doi:10.1128/AEM.02339-07
7. Thole, S.; Kalhoefer, D.; Voget, S.; Berger, M.; Engelhardt, T.; Liesegang, H.; Wollherr, A.; Kjelleberg, S.; Daniel, R.; Simon, M.; Thomas, T.; Brinkhoff, T. *ISME J.* **2012,** *6,* 2229–2244. doi:10.1038/ismej.2012.62
8. Brock, N. L.; Nikolay, A.; Dickschat, J. S. *Chem. Commun.* **2014,** *50,* 5487–5489. doi:10.1039/c4cc01924e
9. Thiel, V.; Brinkhoff, T.; Dickschat, J. S.; Wickel, S.; Grunenberg, J.; Wagner-Döbler, I.; Simon, M.; Schulz, S. *Org. Biomol. Chem.* **2010,** *8,* 234–246. doi:10.1039/b909133e
10. Seyedsayamdost, M. R.; Case, R. J.; Kolter, R.; Clardy, J. *Nat. Chem.* **2011,** *3,* 331–335. doi:10.1038/nchem.1002
11. Brinkhoff, T.; Bach, G.; Heidorn, T.; Liang, L.; Schlingloff, A.; Simon, M. *Appl. Environ. Microbiol.* **2004,** *70,* 2560–2565. doi:10.1128/AEM.70.4.2560-2565.2003
12. Neu, A. K.; Månsson, M.; Gram, L.; Prol-García, M. J. *Appl. Environ. Microbiol.* **2014,** *80,* 146–153. doi:10.1128/AEM.02717-13
13. Porsby, C. H.; Webber, M. A.; Nielsen, K. F.; Piddock, L. J. V.; Gram, L. *Antimicrob. Agents Chemother.* **2011,** *55,* 1332–1337. doi:10.1128/AAC.01222-10
14. Do, Y.-S.; Sun, R.; Kim, H. J.; Yeo, J. E.; Bae, S.-H.; Koo, S. *J. Org. Chem.* **2009,** *74,* 917–920. doi:10.1021/jo802064c
15. Seitz, G.; van Gemmern, R. *Synthesis* **1987,** 953–956. doi:10.1055/s-1987-28139
16. Schultz, A. G.; Holoboski, M. A. *Tetrahedron Lett.* **1993,** *34,* 3021–3024. doi:10.1016/S0040-4039(00)93368-9
17. Citron, C. A.; Rabe, P.; Dickschat, J. S. *J. Nat. Prod.* **2012,** *75,* 1765–1776. doi:10.1021/np300468h
18. Ruiz-Ponte, C.; Cilia, V.; Lambert, C.; Nicolas, J. L. *Int. J. Syst. Bacteriol.* **1998,** *48,* 537–542. doi:10.1099/00207713-48-2-537
19. Martens, T.; Heidorn, T.; Pukall, R.; Simon, M.; Tindall, B. J.; Brinkhoff, T. *Int. J. Syst. Evol. Microbiol.* **2006,** *56,* 1293–1304. doi:10.1099/ijs.0.63724-0
20. Buddruhs, N.; Pradella, S.; Göker, M.; Päuker, O.; Pukall, R.; Spröer, C.; Schumann, P.; Petersen, J.; Brinkhoff, T. *Int. J. Syst. Evol. Microbiol.* **2013,** *63,* 4340–4349. doi:10.1099/ijs.0.053900-0
21. Wikler, M. A.; Cockerill, F. A.; Craig, W. A.; Dudley, M. N.; Eliopoulos, G. M.; Hecht, D. W.; Hindler, J. F.; Ferraro, M. J.; Swenson, J. M.; Low, D. E.; Sheehan, D. J.; Tenover, F. C.; Turnidge, J. D.; Weinstein, M. P.; Zimmer, B. L. *Guideline M7-A7: Methods for dilution antimicrobial susceptibility tests for bacteria that grow aerobically; Approved Standard–Seventh Edition;* Clinical Laboratory Standards Institute: Wayne, 2006.
22. Novick, R. *Virology* **1967,** *33,* 155–166. doi:10.1016/0042-6822(67)90105-5
23. Skov, M. N.; Pedersen, K.; Larsen, J. L. *Appl. Environ. Microbiol.* **1995,** *61,* 1540–1545.

License and Terms

This is an Open Access article under the terms of the Creative Commons Attribution License (http://creativecommons.org/licenses/by/2.0), which permits unrestricted use, distribution, and reproduction in any medium, provided the original work is properly cited.

The license is subject to the *Beilstein Journal of Organic Chemistry* terms and conditions: (http://www.beilstein-journals.org/bjoc)

The definitive version of this article is the electronic one which can be found at: doi:10.3762/bjoc.10.188

BEILSTEIN JOURNAL OF ORGANIC CHEMISTRY

Sacrolide A, a new antimicrobial and cytotoxic oxylipin macrolide from the edible cyanobacterium *Aphanothece sacrum*

Naoya Oku[1], Miyako Matsumoto[1], Kohsuke Yonejima[1], Keijiroh Tansei[2] and Yasuhiro Igarashi[*1]

Full Research Paper

Open Access

Address:
[1]Biotechnology Research Center and Department of Biotechnology, Toyama Prefectural University, 5180 Kurokawa, Imizu, Toyama 939-0398, Japan and [2]Suizenjinori-Hompo Tanseidoh, 5-13-3 Tsuboi, Chuo-ku, Kumamoto, Kumamoto 860-0863, Japan

Email:
Yasuhiro Igarashi[*] - yas@pu-toyama.ac.jp

* Corresponding author

Keywords:
Aphanothece sacrum; cyanobacterium; food intoxication; natural products; sacrolide A; *suizenji-nori*

Beilstein J. Org. Chem. **2014,** *10,* 1808–1816.
doi:10.3762/bjoc.10.190

Received: 21 April 2014
Accepted: 14 July 2014
Published: 07 August 2014

This article is part of the Thematic Series "Natural products in synthesis and biosynthesis".

Guest Editor: J. S. Dickschat

© 2014 Oku et al; licensee Beilstein-Institut.
License and terms: see end of document.

Abstract

Macroscopic gelatinous colonies of freshwater cyanobacterium *Aphanothece sacrum*, a luxury ingredient for Japanese cuisine, were found to contain a new oxylipin-derived macrolide, sacrolide A (**1**), as an antimicrobial component. The configuration of two chiral centers in **1** was determined by a combination of chiral anisotropy analysis and conformational analysis of different ring-opened derivatives. Compound **1** inhibited the growth of some species of Gram-positive bacteria, yeast *Saccharomyces cerevisiae* and fungus *Penicillium chrysogenum*, and was also cytotoxic to 3Y1 rat fibroblasts. Concern about potential food intoxication caused by accidental massive ingestion of *A. sacrum* was dispelled by the absence of **1** in commercial products. A manual procedure for degrading **1** in raw colonies was also developed, enabling a convenient on-site detoxification at restaurants or for personal consumption.

Introduction

Cyanobacteria continue to be core sources for bioactive secondary metabolites [1,2], and their significance in drug discovery has increased for the past two decades [3]. Some cyanobacteria form macroscopic colonies and are harvested for human consumption in many parts of the world [4].

As a part of our program to exploit untapped microbes for drug discovery, we focus on cyanobacteria that are eaten in Japan, and previously reported the isolation of an unusual ω-1 fatty acid (9*Z*,12*Z*)-9,12,15-hexadecatrienoic acid from a freshwater periphytic cyanobacterium *Nostoc verrucosum* [4].

Aphanothece sacrum is also an edible cyanobacterium, which is an endemic species in the Aso water system in the Kyushu District, Japan. It inhabits oligotrophic but mineral-rich freshwater such as spring-fed ponds with a narrow temperature range of 18 °C–20 °C [5] and forms thin crispate gelatinous floating colonies. The first record of this alga being consumed as food appeared 250 years ago. Various laver sheets, such as *suizenji-nori*, *akizuki-nori*, *jusentai*, or *shikintai*, were developed and designated as regional specialty goods by the local lords [6]. These products have also been presented as a tribute to the shogun family, and because of its economic value, the feudal domains protected habitats from overharvesting and water pollution. In 1924, the government designated the habitat in Kamiezuko Pond as a national treasure. However, with the increasing urbanization in this region, the supply of underground water has decreased significantly, which further narrowed the originally limited distribution of this species [7]. The only remaining natural habitat is reportedly in the Koganegawa Stream, a 2 km-long shallow stream where two companies engage in aquaculture [8]. *A. sacrum* is officially catalogued as a Class IA endangered species by the Ministry of Environment [9].

The aquaculture industry has supported chemical investigations of this rare alga. However, to date, only two substances have been reported: pseudovitamin B_{12} [10] and sulfated polysaccharide sacran [11].

We evaluated the antimicrobial activity of this alga and found that a lipophilic fraction of an ethanolic extract showed inhibitory activity against several microbes. Activity-guided fractionation resulted in the discovery of a new macrolactonic oxylipin, sacrolide A (**1**, Figure 1).

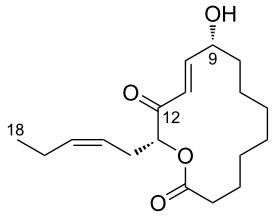


Figure 1: Structure of sacrolide A (**1**).

Results and Discussion

A. sacrum (500 g) was extracted with EtOH, and the combined extract was fractionated by solvent partitioning into *n*-hexane-, 10% aqueous MeOH-, 1-BuOH-, and water-soluble fractions. Antimicrobial testing against four Gram-positive bacteria (*Bacillus subtilis*, *Micrococcus luteus*, *Staphylococcus aureus*, and *Streptomyces lividans*), one Gram-negative bacterium (*Escherichia coli*), two yeasts (*Candida albicans* and *Saccharomyces cerevisiae*), and two fungi (*Aspergillus oryzae* and *Penicillum chrysogenum*) revealed that all these layers varied in the extent of activity against certain test organism(s). Especially intriguing was the antifungal activity exhibited by the *n*-hexane-soluble fraction, which, in most cases, comprises lipids. To identify the responsible constituent, the fraction was successively purified by silica gel chromatography, gel filtration on Sephadex LH-20, and finally by ODS HPLC to yield **1** (1.5 mg, 3.0×10^{-4}% w/w). In addition, the antifungal principle in the aqueous MeOH fraction was isolated and identified as the same substance (6.0 mg, 1.2×10^{-3}% w/w).

The molecular formula $C_{18}H_{28}O_4$ was assigned to **1** based on a molecular ion *m/z* 331.1889 $[M + Na]^+$ observed by HRMS (ESI) (calcd for $C_{18}H_{28}NaO_4$, 331.1880). Of the five degrees of unsaturation calculated from the molecular formula, four were accounted for shielded carbonyl (δ_C 196.7, Table 1) and carboxyl (δ_C 172.9) groups, and two double bonds (δ_C 149.3, 135.6, 124.5, and 121.9) as observed in the ^{13}C NMR spectrum. Thus, the remaining one degree of unsaturation is attributed to a cyclic structure. Because a resonance for a formyl proton (δ_H 9–10) was not observed in the ^1H NMR spectrum, the carbonyl group must be part of a conjugated ketone. Other structural pieces were deduced from an HSQC spectrum to be two oxymethines (δ_H/δ_C 5.23/77.3 and 4.50/71.1), nine methylenes (δ_H/δ_C 1.74/33.81; 2.36, 2.50/33.82; 2.61, 2.56/28.7; 1.50/26.5; 1.35/26.4; 1.34/25.8; 1.68/24.3; 1.28/21.7; 2.06/20.8), and a methyl group (δ_H/δ_C 0.97/14.1), which indicated that a lactone linkage is the only possible cyclization topology. The analysis of the COSY spectrum (Figure 2) helped trace six-carbon and ten-carbon spin systems, both of which include an oxymethine (H9: δ_H 4.50, H13: δ_H 5.23) and a disubstitued olefin. The geometry of the olefins was determined as *E* for Δ^{10} and *Z* for Δ^{15} based on the coupling constants $J_{H10,H11} \sim 15.8$ Hz and $J_{H15,H16} \sim 10$ Hz, respectively. The former spin system (O-H13-$H_2$14-H15=H16-$H_2$17-$H_3$18) had a methyl group at one end and was therefore deemed to constitute a side chain group, whereas the latter (-$H_2$2-$H_2$3-$H_2$4-$H_2$5-$H_2$6-$H_2$7-H28-H9(-O-)-H10=H11-) were bidirectionally opened by a methylene and a double bond at the termini and should constitute a body of the macrocycle core. The connectivity of the two fragments was verified by HMBC correlations from H10 (δ_H 6.93), H11 (δ_H 6.56), H13 (δ_H 5.23), and $H_2$14 (δ_H 2.61, 2.56) to C12 (δ_C 196.7), forming an α,β-unsaturated α'-acyloxy ketone functionality, and from $H_2$2 (δ_H 2.50, 2.36), H3 (δ_H 1.68), and H13 to C1 (δ_C 173.1), bridging a lactone linkage. The structure assembled to this point used up $C_{18}H_{27}O_4$ of the molecular formula $C_{18}H_{28}O_4$ and a remaining proton, not observed in the

^{1}H spectrum, was assigned to a hydroxy proton (9-OH). Thus, the planar structure of **1** was determined to be a new 14-membered macrolide.

Table 1: ^{1}H (500 MHz) and ^{13}C (125 MHz) NMR data for sacrolide A (**1**) in $CDCl_3$ (δ in ppm).

Position	δ_C	δ_H, mult. (*J* in Hz), integr.	HMBC (^{1}H to ^{13}C)
1	172.9		
2	33.81	2.36, m, 1H	1
		2.50, m, 1H	1
3	24.3	1.68, m, 2H	1, 2, 4, 5
4	25.8	1.34, m, 2H	2, 5
5	26.4	1.35, m, 2H	6
6	26.5	1.50, m, 2H	4, 5
7	21.7	1.28, m, 2H	4, 5, 6, 8, 9
8	33.82	1.74, m, 2H	5, 7, 9, 10
9	71.1	4.50, dt (4.7, 4.5), 1H	7, 8, 11
10	149.3	6.93, dd (4.7, 15.8), 1H	8, 9, 11, 12
11	124.5	6.56, d (15.8), 1H	9, 12
12	196.7		
13	77.3	5.23, dd (6.0, 7.6), 1H	1, 12, 14, 15
14	28.7	2.61, m, 2H	12, 13, 15, 16
		2.56, m, 1H	12, 13, 15, 16
15	121.9	5.30, td (7.9, 9.8), 1H	
16	135.6	5.54, td (7.6, 10.0), 1H	
17	20.6	2.06, qd (7.6, 7.4), 2H	15, 16, 18
18	14.1	0.97, t (7.6), 3H	16, 17

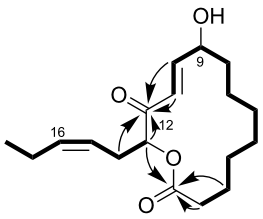
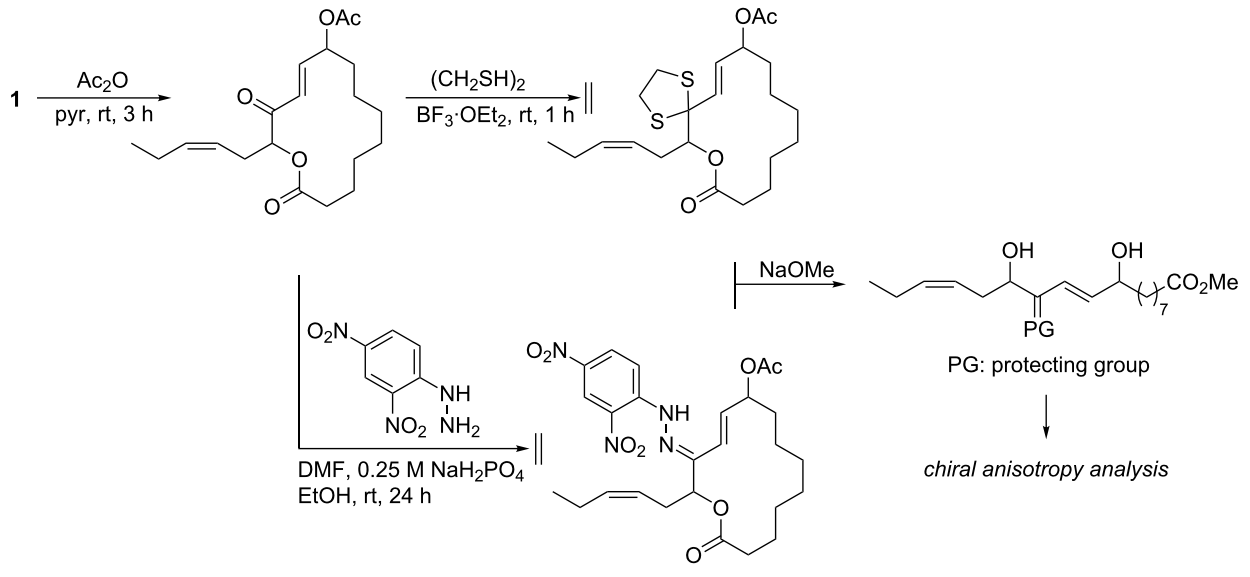
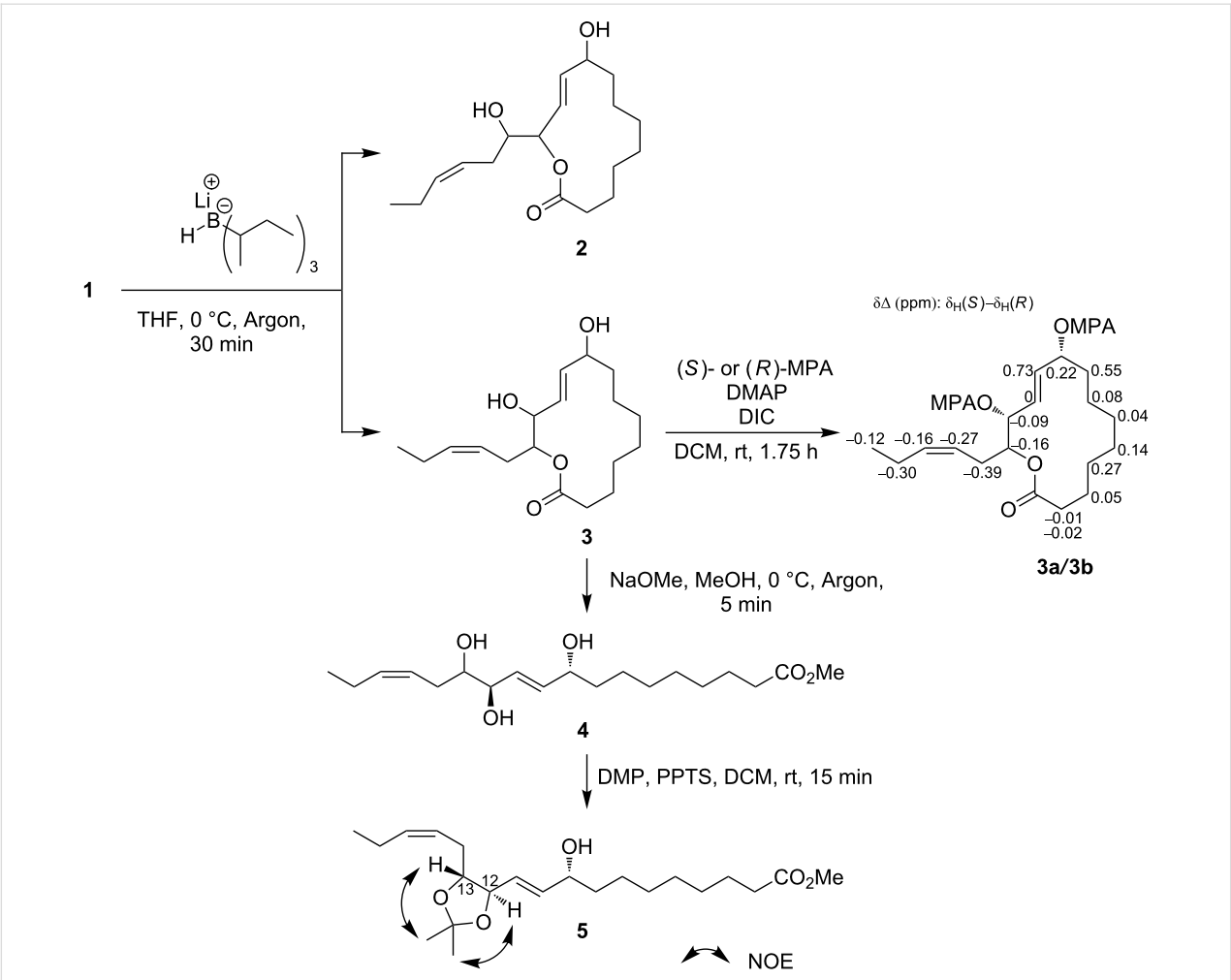


Figure 2: Selected COSY (bold lines) and HMBC (arrows) correlations for sacrolide A (**1**).

The stereogenic center C13 constitutes an α-acyloxy ketone moiety and deacylation catalyzed by a base may result in the loss of chirality because of epimerization [12]. To circumvent this problem, we initially attempted to protect the ketone group prior to chemical conversion (Scheme 1). Compound **1** was acetylated (Supporting Information File 1) and subjected to protection as 1,3-dithiane [13] or 1,4-dinitrophenylhydrazone [14]; however, neither of them resulted in the desired products. Then a strategy without protection was explored (Scheme 2). Reduction with L-selectride (lithium tri-*sec*-butylborohydride) gave the desired alcohol **3** and its ester-exchanged isomer **2** with a ratio of 2:1. To facilitate chiral anisotropy analysis at C9 and C12, the more abundant **3** was condensed either with (*S*)- or (*R*)-α-methoxyphenylacetic acid (MPA) [15] to give bis-MPA esters **3a** and **3b**. The δΔ values for the 2-en-1,4-diol moiety do not hold a diagnostic value because this region is under the influence of overlapping anisotropic effects by the flanking of two MPA residues. However, the consistent distribution of positive and negative values at the right half and on the side chain



Scheme 1: Initial derivatization strategy for the stereochemical analysis of sacrolide A (**1**).



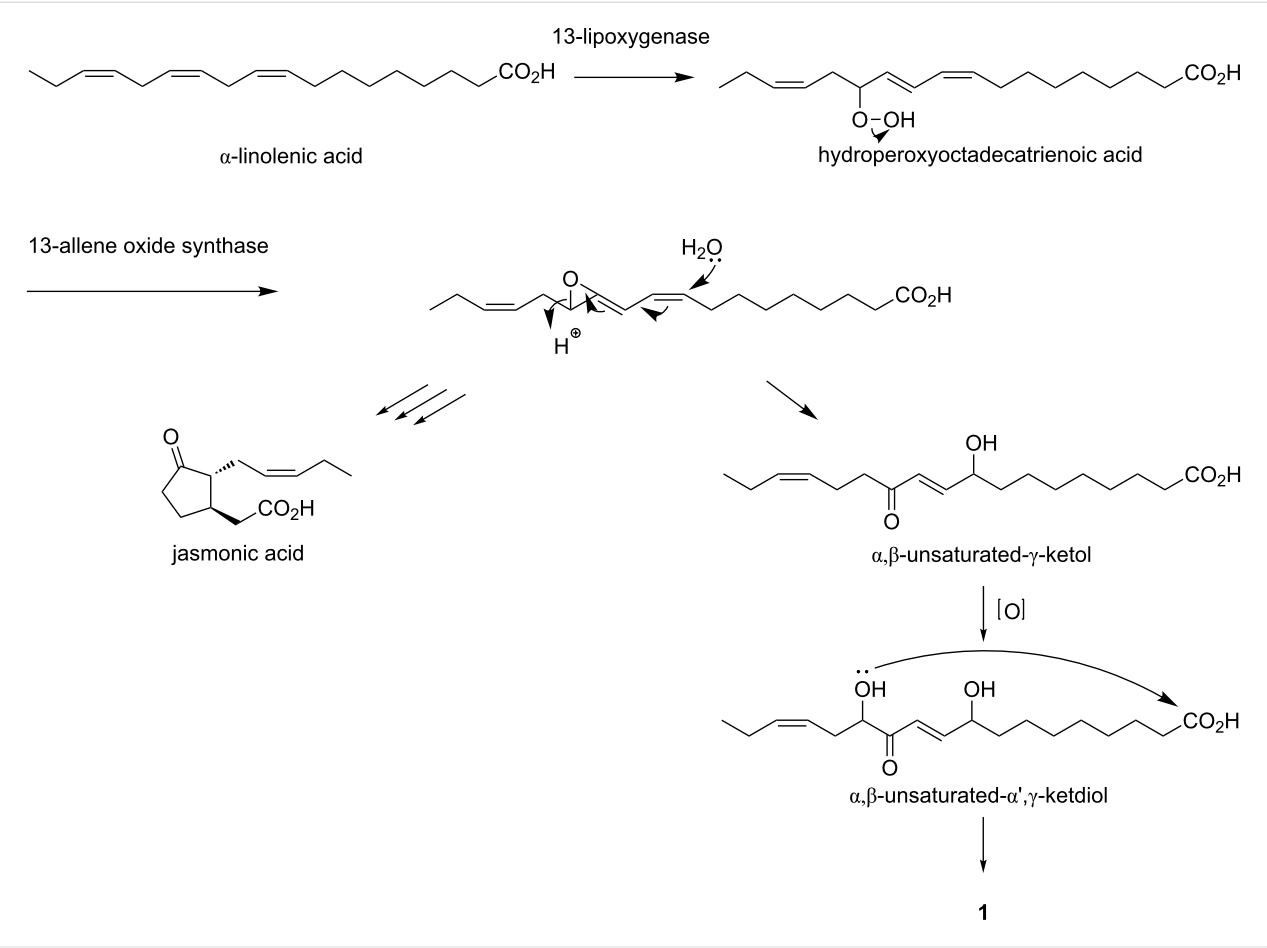
Scheme 2: Determination of the stereochemistry of sacrolide A (**1**).

of the molecule was most reasonably explained by *R*-configurations for both the chiral centers. Thus, the (9*R*,12*R*)-configuration was established for **3**.

To correlate the *R*-configuration of C12 to the chirality of C13, **3** was treated with NaOMe in methanol, and the obtained product triol **4** was converted to acetonide **5**. The conformation of the 2,2-dimethyl-1,3-dioxolane ring in **5** was analyzed by NOESY and HSQC experiments, both of which confirmed a *trans* relationship of H12 and H13 as evidenced by one-to-one NOE correlations between the acetonide methyl groups and oxymethine protons. Therefore, it was concluded that C13 has an *R*-configuration.

Sacrolide A (**1**) is apparently a member of the oxylipins, lipid oxidation products reported from all organisms, and its biosynthesis should be routed through α-linolenic acid-derived allene oxide (Scheme 3) [16]. The addition of H_2O to this intermediate gives α,β-unsaturated-γ-ketol, which accepts further oxidation at the α'-position, and macrolactonization of the resulting α',γ-ketodiol would yield **1**. Similar, but rather simpler metabolites were found from corn [17,18]. However, they comprise a pair of enantiomers and thus should be generated non-enzymatically from α-linoleic acid-derived allene oxide. In contrast, **1** is optically active and is more likely to be produced by a sequence of enzymatic reactions.

Sacrolide A (**1**) inhibited the growth of Gram-positive bacteria (*Micrococcus luteus*, *Streptomyces lividans*, *Staphylococcus aureus*, *Bacillus subtilis*), a yeast (*Saccharomyces cerevisiae*) and a fungus (*Penicillium chrysogenum*) (Table 2). Moreover, **1** was cytotoxic to 3Y1 rat fibroblasts (GI_{50} 4.5 μM). Under microscopic observation, cells exposed to 13 μM of **1** rapidly lost anchorage to the substratum. Blebs developed on the cellular surface (Figure 3B) and the cells eventually detached from the substratum and died (Figure 3C). Because this series of changes occurred within a time frame which was much shorter than the doubling time of the cells, **1** is is not expected



Scheme 3: Plausible biosynthesis of sacrolide A (**1**).

to target cell cycle-associated events, such as the synthesis of proteins, DNA, or RNA. Despite their structural diversity, many oxylipins induce a common stress response in plants and animal cells, and this activity is attributed to their ability to modify the cysteinyl residues in proteins, thereby affecting redox-controlled signal transduction pathways [19]. The induction of membrane blebbing has been reported for lipophilic inhibitors of protein phosphatase 2A, which is a cysteine-dependent phosphatase [20,21]. However, **1** did not inhibit this enzyme (data not shown).

In Japanese cuisine, *A. sacrum* is used as an ingredient in soups and marinades or as a garnish for *sashimi* (thin sliced raw fish). It is sold dry or brined for nationwide distribution or as a fresh food item directly to local restaurants. Although a massive ingestion is rare to happen, the cytotoxicity of **1** raised concerns about potential food intoxication. To evaluate the presence of **1** in these products, extracts were prepared and examined by antifungal testing and LC–MS analysis. The products were softened or desalted by soaking in water and then subjected to the same extraction and fractionation scheme used at the initial antimicrobial screening. The aqueous 90% MeOH fraction of the raw sample exhibited significant antifungal activity (12 mm/6 mm Φ disk) against *Penicillium chrysogenum* at 200 μg/disk and an intense molecular ion of **1** at *m/z* 307 $[M - H]^-$ in nega-

Table 2: Antimicrobial activity of sacrolide A (**1**).

	microbe	MIC[a] value (μg/mL)
Gram-positive	*Bacillus subtilis*	>8.0
	Micrococcus luteus	>8.0
	Staphylococcus aureus	0.5
	Streptomyces lividans	1.0
Gram-negative	*Escherichia coli*	>8.0
yeast	*Candida albicans*	8.0
	Saccharomyces cerevisiae	>8.0
fungus	*Penicillium chrysogenum*	1.0

[a]Minimum inhibitory concentration.

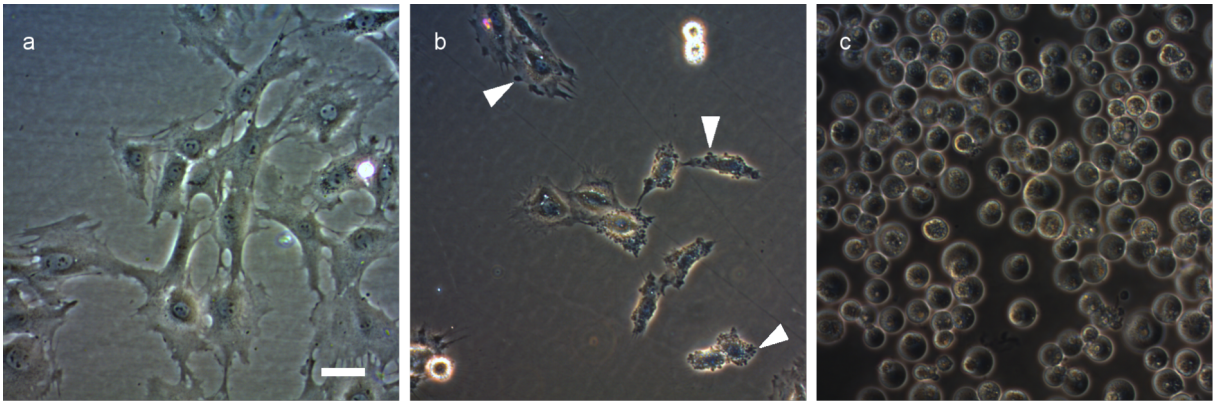


Figure 3: The effect of sacrolide A (**1**) on 3Y1 rat fibroblastic cells. (a) Control. (b) 45 min after exposure to 13 μM of **1**. (c) 20 h after exposure to 13 μM of **1**. Arrowheads indicate blebs on the cell surface. The magnification is identical in (a), (b) and (c), the bar represents 100 μm.

tive mode LC–MS analysis (Figure 4). In contrast, the same fractions from the commercial products were both inactive and devoid of a peak corresponding to **1**, which dispelled the concern about food intoxication for processed *A. sacrum*.

To eliminate the uncertainty with regard to the safety of eating substantial amounts of raw alga, a precooking treatment to manually deactivate **1** was desired. We hypothesized that the modification of the reactive enone functionality or the degradation of the cyclic structure may eliminate the bioactivity of **1,** and envisioned that the treatment with an alkaline solution may serve this purpose. In fact, by boiling the alga in 3% aqueous $NaHCO_3$ for 1 min prior to extraction, the antifungal activity and a peak for **1** in the LC–MS analysis completely disappeared (Figure 4). Although the exact degradation pathway of **1** was not identified during this treatment, a facile deactivation of **1** in the raw alga was achieved in a fast, simple, and inexpensive manner, which offers a useful option when consumers wish to enjoy the crispy texture of fresh alga, but feel uneasy about the possibility of food intoxication.

Conclusion

We explored a bioactive secondary metabolite from the very rare but edible cyanobacterium *A. sacrum* for the first time. *A. sacrum* is endemic to the Aso water system in Japan. As a result, we discovered a new oxylipin-derived macrolide **1** with a

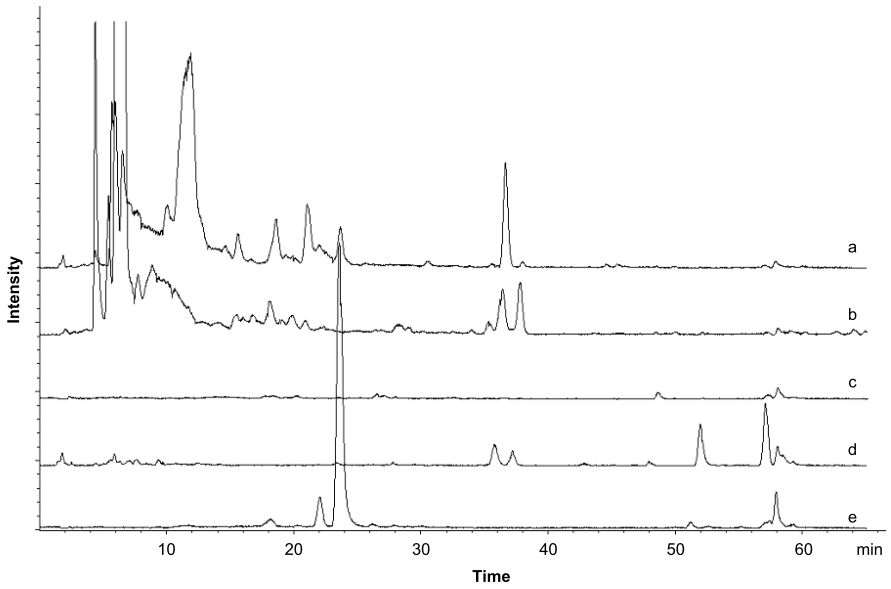


Figure 4: Extracted ion chromatograms for sacrolide A (**1**) molecular ion at *m/z* 307 $[M - H]^-$ in the LC–MS analysis of aqueous 90% MeOH fractions from the ethanolic extracts of (a) raw alga, (b) dry product, (c) brined product, and (d) raw alga boiled in 3% $NaHCO_3$ for 1 min. Chromatogram (e) shows the elution of purified sacrolide A (**1**) at t_R 23.6 min.

broad antimicrobial spectrum and cytotoxicity. Although the safety of this alga as food is secured by 250 years of consumption as a premium delicacy and the lack of a single episode of food intoxication, safety was reconfirmed by checking the absence of **1** in the commercial products. Moreover, a convenient precooking treatment was developed to deactivate **1** in the raw alga, which prevents food intoxication caused by a high-dose intake of **1** and allows for the consumption of a substantial amount of unprocessed alga.

In conclusion, the present study illustrates the importance of exploring untapped biological resources for the discovery of new bioactive molecules, and also encourages the careful conservation of a variety of habitats to maximize the availability of genetic resources.

Experimental

General methods

Cosmosil 75C18-PREP (Nacalai Tesque Inc., 75 μm) was used for ODS flash chromatography. NMR spectra were obtained by a Bruker AVANCE 500 spectrometer at 500 MHz for ^{1}H. Residual solvent peaks at δ_H/δ_C 7.27/77.0 ppm in $CDCl_3$ were used as chemical shift reference signals. HRMS–ESI–TOF and LC–MS analyses were carried out by an Agilent 1200 HPLC-DAD system coupled with a Bruker micrOTOF mass spectrometer. Optical rotation and UV spectra were recorded on a JASCO DIP-3000 polarimeter and a Hitachi U-3210 spectrophotometer, respectively.

Biological material

A. sacrum is commercially cultured by one of the authors (K. T.) in a groundwater-irrigated aquaculture pond located in Kumamoto, Kyushu District. The algal mass collected in a sieve basket was immediately frozen at −20 °C and shipped to the laboratory in October, 2012. Both the dry and brined *A. sacrum* products were purchased from Kisendo Ltd. (Fukuoka, Japan) in January 2014.

Extraction and isolation

500 g of a water-thawed specimen of the alga was ground with an equal amount of Celite in EtOH (1 L). The resulting slurry was paper-filtered to separate an ethanolic extract and an algal cake, and the latter was extracted three more times with the same amount of alcohol. The combined extract (1.5 g) was partitioned between aqueous 60% MeOH (400 mL) and dichloromethane (400 mL × 3), the former of which was further separated between aqueous 90% MeOH and *n*-hexane, whereas the latter was further separated between H_2O (200 mL) and *n*-BuOH (200 mL × 3). The most active aqueous MeOH layer (422.9 mg) was subjected to silica gel chromatography with a stepwise elution by *n*-hexane/EtOAc 4:1, 2:1, 1:1, 1:2, 1:4, chloroform/MeOH 99:1, 97:3, 95:5, 9:1, and chloroform/MeOH/H_2O 6:4:1 to give ten fractions. The second fraction, the one with the highest activity, was gel-filtered on Sephadex LH-20 (chloroform/MeOH 1:1) followed by silica gel HPLC (Cosmosil 5SL-II 1 × 25 cm) eluted with *n*-hexane/Et_2O (2:1) to yield **1** (6.0 mg). Starting with the second most active *n*-hexane layer (380.1 mg) and following the same procedure gave 1.5 mg of **1**.

Sacrolide A (**1**): yellow solid; soluble in MeOH, $CHCl_3$, MeCN, EtOAc, and Et_2O, and insoluble in H_2O. $[\alpha]_D^{24.5}$ +41.4 (*c* 0.115, MeCN); UV (MeCN) λ_{max}, nm (ε) 232 (8000), 283 (320), 331 (160); HRMS–ESI (*m*/*z*): $[M + Na]^+$ calcd for $C_{18}H_{28}NaO_4$, 331.1880; found, 331.1889.

Paper disk agar diffusion method

The antimicrobial potency of the chromatographic fractions was evaluated by a paper-disk agar diffusion method. Fractions at each stage of the purification were diluted to the same concentration with MeOH, and 10 μL aliquots were loaded on paper disks with 6 mm diameter, which were left until completely dried. A loop of the test organism, suspended in a small amount water, was mixed with liquefied agar medium precooled to nearly body temperature, and the inoculated medium was quickly poured into a sterile plastic dish. The medium was composed of 0.5% yeast extract, 1.0% tryptone, 1.0% NaCl, 0.5% glucose, and 1.5% agar. After the agar solidified, the drug-loaded disks were placed on the plate, and the test cultures were incubated at 32 °C for a day or two until the diameters of inhibitory haloes turned measurable.

Microculture antimicrobial testing

100 μL of Mueller–Hinton broth supplemented with $CaCl_2{\cdot}2H_2O$ (5% w/v) and $MgCl_2{\cdot}6H_2O$ (2.5% w/v) were transferred to the wells of a sterilized 96 well microtiter plate. The test samples were dissolved in DMSO and diluted 20 times with the same broth medium. For a two-fold serial dilution along the columns each 100 μL aliquot of the test solution was added to the top row, mixed with the pre-dispensed medium, and the same amount was then transferred to the second row. The same operation was repeated until reaching the bottom row, where the last transfer was discarded to equalize the volume of the medium. The indication strains were grown on agar media (*Staphylococcus aureus* FDA209P JC-1, *Micrococcus luteus* ATCC9341, *Escherichia coli* NIHJ JC-2, *Saccharomyces cerevisiae* S100, and *Candida albicans* A9540) or in Sabouraud broth (*Penicillum chrysogenum* NBRC4626, *Streptomyces lividans* TK23) overnight and then diluted with sterile saline or the same broth to 0.5 McFarland (~10^8 cfu/mL). Two μL of these suspensions were immediately inoculated to the microcultures, and the plates were incubated at 32 °C for 18–24 h. The concen-

tration required to completely inhibit the growth of the microbes was defined as the minimum inhibitory concentration (MIC).

Cytotoxicity testing and cell morphology observation

The cytotoxicity against 3Y1-B clone 1-6 rat fibroblasts and the action of sacrolide A (**1**) on the morphology of the same cell line were evaluated by the procedures described in [22].

Method to precook raw alga for the elimination of sacrolide A (1): A tablespoon of $NaHCO_3$ (15 g) was added to a pot containing 500 mL of water, and the solution was boiled at high temperature. Then 40 g of raw *A. sacrum* was added and boiled with occasional stirring for 1 min. The boiled alga was drained in a colander, washed three times with cold water, and then subjected to the extraction and fractionation procedure described in the next section.

Evaluation of the presence of sacrolide A (1) in two commercial products and precooked sample of *A. sacrum*: Dry or brined alga was soaked in water for 30 min and weighed prior to extraction. A 20 g portion from each product, precooked or raw alga, was extracted with EtOH, and the extracts were separated by solvent partitioning into four fractions soluble in *n*-hexane, aqueous 90% MeOH, 1-BuOH, and water. The yields were: 33.2 mg, 12.0 mg, 12.7 mg, and 51.2 mg from dry alga; 10.9 mg, 8.1 mg, 9.8 mg, and 25.3 mg from brined alga; 10.6 mg, 5.0 mg, 16.4 mg, and 80.6 mg from precooked alga; and 19.6 mg, 17.8 mg, 12.7 mg, and 22.6 mg from raw alga. The fractions were subjected to antifungal susceptibility testing by using the paper-disk agar diffusion method and LC–MS analysis to evaluate the presence of **1**. Given a dose of 200 μg/disk none of the fractions from the commercial products or precooked sample exhibited an activity against *Penicillium chrysogenum*, whereas the aqueous 90% MeOH fraction from raw alga exhibited an inhibition circle with a diameter of 12.0 mm, which indicates the presence of **1**. The LC–MS analysis was conducted with a Cosmosil AR-II column (Nacalai Tesque, 2.0 mm × 150 mm) under the elution program of 40% MeCN for 5 min, 1%/min MeCN concentration ramped to 100%. The concentration was held for 10 min at a flow rate of 0.2 mL/min at 35 °C. Ten μL aliquots from 10 μg/mL DMSO solution of authentic **1** and 1 mg/mL DMSO solution of the aqueous 90% MeOH fraction from each algal sample were injected, and negative ESI was employed for mass spectral detection. The authentic **1** eluted at 23.6 min, showing a negative molecular ion at *m/z* 307. Based on this result, total ion chromatograms for the analytes were edited by extracting an *m/z* 307 ± 0.5 signal, which presented elution of **1** from the raw alga sample. In contrast, other samples were devoid of **1**.

Supporting Information

Supporting Information File 1

Procedures for chemical conversion/derivatization, NMR assignments, copies of NMR, MS and UV spectra for **1**, NMR spectra for **2**, **3**, **3a** and **3b**.
[http://www.beilstein-journals.org/bjoc/content/supplementary/1860-5397-10-190-S1.pdf]

Acknowledgements

This work was supported in part by the President's Fund Initiative at the Toyama Prefectural University. 3Y1-B clone 1-6 rat fibroblastic cells (resource number JCRB0734) were obtained from the Health Science Research Resources Bank.

References

1. Chlipala, G. E.; Mo, S.; Orjala, J. *Curr. Drug Targets* **2011,** *12,* 1654–1673. doi:10.2174/138945011798109455
2. Tan, L. T. *Phytochemistry* **2007,** *68,* 954–979. doi:10.1016/j.phytochem.2007.01.012
3. Bérdy, J. *J. Antibiot.* **2012,** *65,* 385–395. doi:10.1038/ja.2012.27
4. Oku, N.; Yonejima, K.; Sugawa, T.; Igarashi, Y. *Biosci., Biotechnol., Biochem.* **2014,** *78,* 1147–1150. doi:10.1080/09168451.2014.918484
5. Kabata, K.; Okamoto, C.; Sasada, N.; Ono, M.; Igoshi, K.; Kobayashi, K.; Masuoka, C.; Ito, Y. *Proc. Fac. Agric., Kyushu Tokai Univ.* **2005,** *24,* 37–43.
6. Kabata, K.; Okamoto, C.; Odahara, T.; Nakazono, T.; Osumi, K.; Sasada, N.; Ichikawa, T.; Kaneko, Y.; Aramaki, S. *Proc. Fac. Agric., Kyushu Tokai Univ.* **2007,** *26,* 1–6.
7. Kabata, K. Suizenji-nori. In *Shokuhin Kako Soran;* Nohbunkyo, Ed.; Nohsangyosonbunkakyokai: Tokyo, Japan, 2002; Vol. 12, pp 563–569.
8. Uchihira, T.; Naito, S.; Masuoka, C.; Okamoto, C.; Yasuda, S. *Proc. Fac. Agric., Kyushu Tokai Univ.* **2013,** *32,* 7–11.
9. Search system of Japanese red data. http://www.jpnrdb.com/ (accessed April 10, 2014).
10. Watanabe, F.; Miyamoto, E.; Fujita, T.; Tanioka, Y.; Nakano, Y. *Biosci., Biotechnol., Biochem.* **2006,** *70,* 3066–3068. doi:10.1271/bbb.60395
11. Ngatu, N. R.; Okajima, M. K.; Yokogawa, M.; Hirota, R.; Eitoku, M.; Muzembo, B. A.; Dumavibhat, N.; Takaishi, M.; Sano, S.; Kaneko, T.; Tanaka, T.; Nakamura, H.; Suganuma, N. *Ann. Allergy, Asthma, Immunol.* **2012,** *108,* 117–122. doi:10.1016/j.anai.2011.10.013
12. Ödman, P.; Wessjohann, L. A.; Bornscheuer, U. T. *J. Org. Chem.* **2005,** *70,* 9551–9555. doi:10.1021/jo051661n
13. Hatch, R. P.; Shringerpure, J.; Weinreb, S. M. *J. Org. Chem.* **1978,** *43,* 4172–4177. doi:10.1021/jo00415a041
14. Oku, N.; Takada, K.; Fuller, R. W.; Wilson, J. A.; Peach, M. L.; Pannell, L. K.; McMahon, J. B.; Gustafson, K. R. *J. Am. Chem. Soc.* **2010,** *132,* 10278–10285. doi:10.1021/ja1016766
15. Trost, B. M.; Belletire, J. L.; Godleski, S.; McDougal, P. G.; Balkovec, J. M.; Baldwin, J. J.; Christy, M. E.; Ponticello, G. S.; Varga, S. L.; Springer, J. P. *J. Org. Chem.* **1986,** *51,* 2370–2374. doi:10.1021/jo00362a036

16. Andreou, A.; Brodhun, F.; Feussner, I. *Prog. Lipid Res.* **2009,** *48,* 148–170. doi:10.1016/j.plipres.2009.02.002
17. Hayashi, Y.; Ishihara, N.; Takahashi, M.; Fujii, E.; Uenakai, K.; Masada, S.; Ichimoto, I. *Biosci., Biotechnol., Biochem.* **1996,** *60,* 1115–1117. doi:10.1271/bbb.60.1115
18. Hayashi, Y.; Nishikawa, Y.; Mori, H.; Matsushita, Y.; Sugamoto, K.; Matsui, T. *Biosci., Biotechnol., Biochem.* **1998,** *62,* 1771–1773. doi:10.1271/bbb.62.1771
19. Mueller, M. J.; Berger, S. *Phytochemistry* **2009,** *70,* 1511–1521. doi:10.1016/j.phytochem.2009.05.018
20. Barros, L. F.; Kanaseki, T.; Sabirov, R.; Morishima, S.; Castro, J.; Bittner, C. X.; Maeno, E.; Ando-Akatsuka, Y.; Okada, Y. *Cell Death Differ.* **2003,** *10,* 687–697. doi:10.1038/sj.cdd.4401236
21. Bøe, R.; Gjertsen, B. T.; Vintermyr, O. K.; Houge, G.; Lanotte, M.; Døskeland, S. O. *Exp. Cell Res.* **1991,** *195,* 237–246. doi:10.1016/0014-4827(91)90523-W
22. Oku, N.; Matsunaga, S.; Wada, S.; Watabe, S.; Fusetani, N. *J. Nat. Prod.* **2000,** *63,* 205–209. doi:10.1021/np990333d

License and Terms

This is an Open Access article under the terms of the Creative Commons Attribution License (http://creativecommons.org/licenses/by/2.0), which permits unrestricted use, distribution, and reproduction in any medium, provided the original work is properly cited.

The license is subject to the *Beilstein Journal of Organic Chemistry* terms and conditions: (http://www.beilstein-journals.org/bjoc)

The definitive version of this article is the electronic one which can be found at: doi:10.3762/bjoc.10.190